RISK ASSESSMENT OF HYDROGEN STORAGE IN A CONGLOMERATE OF SALT CAVERNS IN THE NETHERLANDS

KEM-28 – FINAL REPORT – November 2023

Pierre Bérest†
Tobias Baumann
Benoit Brouard
Boris Kaus
Jop Klaver
Maximilian Kottwitz
Anton Popov
Joyce Schmatz
Janos L. Urai†
René Vreugdenhil
Vassily Zakharov

Cavern H_2 Conglomerate Combination

smart Tectonics

BROUARD CONSULTING

MAP Microstructure and Pores

PONDERA

GeoStructures Consultancy for Structural Geology and Geomechanics

RISK ASSESSMENT OF HYDROGEN STORAGE IN A CONGLOMERATE OF SALT CAVERNS IN THE NETHERLANDS

Reference: KEM-28 – FINAL REPORT

Version: 231121

21 November 2023

by

H2C^3

H2 Cavern Conglomerate Combination

Prof. Dr. Pierre Bérest[1†], Dr. Tobias Baumann[2], Dr. Benoit Brouard[1], Prof. Dr. Boris Kaus[2],

Dr. Jop Klaver[3], Dr. Maximilian Kottwitz[2], Dr. Anton Popov[2], Dr. Joyce Schmatz[3],

Prof. Dr. Janos L. Urai[5†], Ir. René Vreugdenhil[4], Dr. Vassily Zakharov[1],

[1]Brouard Consulting, Paris, France

[2]smartTectonics GmbH, Mainz, Germany

[3]MaP – Microstructures and Pores GmbH, Aachen, Germany

[4]Pondera Geo Energy, Arnhem, Netherlands

[5]**Geo**Structures Consultancy for Structural Geology and Geomechanics, Maastricht, Netherlands

Dedications

We dedicate this report to the memory of our colleagues Professor Pierre Bérest and Professor Janos L. Urai who both sadly and unexpectedly passed away during this project. Without these world-renowned salt geomechanics experts we would never have been able to start this project. Unfortunately, we cannot finish together what we started.

Pierre passed away shortly before the literature review was completed. His essential and major contributions to this review are a demonstration of his wide knowledge and deep insight in this field of science and engineering. We are grateful for the opportunity of learning from him and will miss his clear and elegant explanations and sense of humour. Our thoughts are with his family, friends, and colleagues. How unfortunate it is that 10 months later we also had to say goodbye to Janos. It is thanks to Janos that we all started working together. With his extraordinary geoscience knowledge on all scales and wide network, Janos was a vital part of our team. It is a great loss for all of us, with his expertise, enthusiasm, and creativity, but especially as a human being. We wish family and friends much strength with this great loss.

Content

Dedications 3
Content 4
Executive summary 13
Part 1: Literature review 13
Part 2: Geomechanical study 14
Part 3 & 4: Risk analyses and recommendations 16
Take home messages 18
General introduction 19
PART 1 – Literature review 21
Summary 22
1 Introduction 29
1.1 Reading guide 29
2 Salt cavern thermodynamics and tightness 30
2.1 Thermodynamics 31
2.1.1 Hydrogen purity 31
2.1.2 Convection in brine-filled and gas-filled caverns 31
2.1.3 Heat transfer in a gas storage cavern 34
2.1.4 Gas purity, the role of water vapor 39
2.2 Tightness of salt caverns 41
2.2.1 Introduction 41
2.2.2 Oil and Gas well tightness. Statistical analyses 41
2.2.3 Case Stories 42
2.2.4 Lessons learned 61
2.2.5 Prevention of a gas leak 68
2.2.6 Conclusion 70
2.3 Blowout 71
2.3.1 Introduction 71
2.3.2 Case histories 71
2.3.3 Blowout model 78
2.3.4 SSSV (Underground automatic safety valve) 82
3 Salt cavern structural stability 84
3.1 Rock-salt behaviour 84
3.1.1 Introduction 84
3.1.2 Laboratory tests 84
3.1.3 Constitutive laws 90
3.1.4 Cavern creep closure 91

3.1.5 Remarkable volume losses 98
3.1.6 Creep closure in a cycled cavern 100
3.1.7 Creep closure in a hydrogen storage cavern 101
3.2 Subsidence 102
3.2.1 Introduction 102
3.2.2 Geometrical characteristics of the subsidence bowl 102
3.2.3 Case histories 104
3.3 Casing overstretching 108
3.3.1 Introduction 108
3.3.2 Case stories 108
3.3.3 Researches dedicated to overstretching 115
3.4 Brittle failure 116
3.4.1 Introduction 116
3.4.2 Failure criteria (laboratory) 116
3.4.3 Thermal stresses (tensile failure) 121
3.4.4 Cratering (overburden failure) 127
3.4.5 Roof Fall 133
3.4.6 Case histories (tensile effective stress) 145
3.4.7 Block Falls 146
3.5 Conglomerates 162
3.5.1 Introduction 162
3.5.2 Case histories 163
3.5.3 The tributary area (elastic behaviour) 164
3.5.4 Pillar progressive unloading (visco-plastic behaviour) 165
3.5.5 Interaction between various storage products 168
3.5.6 Conclusions 168
3.6 Cavern abandonment 171
4 Salt cavern testing 172
4.1 Permeability tests in caverns and boreholes 172
4.1.1 Maximum operating pressure (in a salt cavern) 172
4.1.2 Permeability measurement in a wellbore 175
4.1.3 Permeability measurement in a full-size cavern 177
4.2 Tightness tests 179
4.2.1 Introduction 179
4.2.2 Maximum pressure in gas caverns 179
4.2.3 Tightness tests, an historical perspective 182
4.2.4 Different types of MIT: POT, NLT, LLI and PD 183

4.2.5 The pressure differential method 186
4.2.6 Fail/pass criteria 189
4.2.7 Tightness tests in a hydrogen storage cavern 190
5 Zechstein Salt in the Netherlands 192
5.1 The Dutch subsurface (onshore and offshore) and potential Salt caverns 192
5.2 Salt seismicity in general and Dutch situation 197
Appendix: Local magnitude M_L 203
5.3 Durability: The evolving rheology, transport properties, damage and healing of salt around a cluster of hydrogen storage caverns 204
5.3.1 Rock salt creep rheology, uncertainties in creep rates and upscaling properties of heterogeneous rock salt 204
5.3.2 Interaction of damage, microcracking, recrystallization and crack healing around Hydrogen caverns during pressure cycling 206
5.3.3 The special case of *Kristallbrockensalz* (Barabasch et al., 2023) 206
5.4 Durability: Geochemical processes 208
5.4.1 Introduction 208
5.4.2 The reactants and reactions 209
5.4.3 Microbial reactions 212
5.4.4 Abiotic processes 215
5.4.5 The role of permeability and transport 216
5.4.6 Mechanic durability 217
5.4.7 Concluding Remarks and Recommendations 219
6 Database of (near-) accidents occurred 221
Appendix: Risk assessment 231
General 231
Modelling of risks 231
Risk assessment of H_2-storage in salt caverns 231
Use of Risk based working 235
Proposed structure for Phase 2 238
Bibliography 239
PART 2 – Geomechanical study 240
Summary 241
Introduction 247
Nomenclature 248
1 Geomechanical analysis 251
1.1 Introduction 251
1.1.1 Selection of a reference configuration 251
1.1.2 Cavern thermodynamics 251

1.1.3 Rock-salt mechanical behaviour 251
1.1.4 Mechanical stability of a salt cavern 252
1.1.5 Wellbore modelling for the reference case 252
1.1.6 Creation of parametrized 2D finite element models of hydrogen caverns 252
1.1.7 Cavern modelling for the reference case 252
1.1.8 Sensitivity analysis in 2D 252
1.1.9 Worst case scenarios 252
1.1.10 Conglomerates 252
1.2 Selection of a reference case (volume, geology, material parameters) 253
1.2.1 Introduction 253
1.2.2 Cavern volume and shape 253
1.2.3 Selection a typical geological configuration for the Netherlands 254
1.2.4 Selection of a depth for the last cemented casing shoe 256
1.2.5 Setting of cavern height and maximum radii 256
1.2.6 Selection of loading scenarios 256
1.3 Wellbore/Cavern thermodynamics modelling 258
1.3.1 Introduction 258
1.3.2 Wellbore completion 258
1.3.3 Hydrogen thermodynamics properties 259
1.3.4 Pressure losses 259
1.3.5 Cavern thermodynamics 259
1.3.6 Geothermal temperature 260
1.3.7 Onset of convection in a gas-filled cavern 263
1.3.8 Heat flux at cavern wall 263
1.3.9 Developed powers and energies 264
1.3.10 Gas purity, the role of water vapor 265
1.3.11 Selection of thermal parameters for the rocks 267
1.4 Geomechanical modelling 267
1.4.1 Introduction 267
1.4.2 Selection of mechanical for the rocks 267
1.4.3 Geostatic pressure 272
1.4.4 Coupling between hydrogen thermodynamics and rock-salt rock mechanics 272
1.5 Cavern stability analysis 275
1.5.1 Introduction 275
1.5.2 Creep closure 276
1.5.3 Casing overstretching 276
1.5.4 Subsidence 277

1.5.5 Onset of dilatancy 277
1.5.6 Stresses generated by creep closure and temperature changes 278
1.5.7 Onset of tensile stresses 278
1.5.8 Onset of tensile effective stresses 278
1.5.9 Worst case scenarios 279
1.6 Wellbore modeling – Reference case 281
1.6.1 Introduction 281
1.6.2 Input for wellbore modelling: hydrogen inventory 281
1.6.3 Output: gas properties in the wellbore and in the cavern 281
1.7 Creation of parametrized 2D finite element models of hydrogen caverns 288
1.7.1 Introduction 288
1.7.2 Boundary conditions 288
1.7.3 Meshing 288
1.7.4 Loading 288
1.7.5 Computation outcomes 292
1.7.6 Outputs 292
1.7.7 Evolution at a particular point on the wall 296
1.7.8 Evolution along the wall 296
1.7.9 Analysis of cavern stability 296
1.8 FEM cavern modelling – Reference case 299
1.8.1 Introduction 299
1.8.2 Trends over time 299
1.9 2D Numerical computations - Sensitivity analysis 326
1.9.1 Introduction 326
1.9.2 Selected combinations of parameters 326
1.9.3 Calculation results 326
1.9.4 Analysis of results by smartTectonics 331
1.10 Additional sensitivity case: faster steady-state creep 341
1.10.1 Introduction 341
1.10.2 Computation results 341
1.11 Blowout modelling 346
1.11.1 Introduction 346
1.11.2 Thermodynamics of a blowout 346
1.11.3 Modelling the blowout in the reference case 347
1.12 Workover modelling 361
1.12.1 Introduction 361
1.12.2 Modelling assumptions 361

1.13 Non-halite layer intersecting the cavern 369
1.13.1 Introduction 369
1.13.2 Considered configuration 369
1.14 3D Computations 378
1.14.1 Introduction 378
1.14.2 Background 378
1.14.3 Considered configuration 378
1.14.4 Meshing in 3D 379
1.14.5 3D computations outcomes....379
1.15 Conclusions 402
2 Seismicity: Thermomechanical modelling 405
2.1 Introduction 405
2.2 Generic model of a 3D salt dome 405
2.2.1 Stratigraphy and model geometry....405
2.2.2 Thermomechanical model and “Ist-Zustand” 407
2.3 3D THM dome-scale simulations to assess the potential for seismicity in the vicinity of a salt dome 407
2.3.1 Hydrogen cavern field boundary conditions 407
2.3.2 The influence of hydrogen cavern operation on the stress state of the salt dome and the degree of induced brittle deformation in the overburden.....409
2.4 Conclusions 414
3 Durability: The effective long-term creep properties of heterogeneous rock salt 415
3.1 Introduction 415
3.2 Method: Numerical uniaxial deformation experiments 417
3.2.1 Mathematical model....417
3.2.2 Numerical modeling scheme 419
3.2.3 Workflow of numerical creep tests 421
3.2.4 Pure halite benchmark....423
3.3 Creep properties of *KB rock salt* 424
3.3.1 Synthetic 2D models 424
3.3.2 Effective long term creep of KB rock salt....426
3.3.3 Analysis & interpretation....427
3.3.4 General & site-specific recommendations 430
3.4 Discussion: Influence of anhydrite rheology 434
3.5 Summary & conclusions....436
4 Durability: Microstructural analyses of geochemical and microbial processes 437
4.1 Introduction 437
4.2 Microbial induced microstructural changes anhydrite....438

4.2.1 Problem statement microstructural changes anhydrite....438
4.2.2 Materials and Methods anhydrite....439
4.2.3 Results and Discussion anhydrite....442
4.3 Concluding remarks anhydrite....454
PART 3 & 4 – Risk Analyses and recommended strategy for risk management and mitigation....456
Summary....457
1 Introduction....459
1.1 General....459
1.2 Disclaimer....465
2 List of stakeholders and their objectives....468
3 List of risks....471
4 Risk assessment form....473
4.1 Stakeholder: Operator....474
4.2 Stakeholder: SODM....475
4.3 Stakeholder: Ministry of Economic Affairs and Climate....477
4.4 Bibliography....478
5 Risk management and mitigation....479
5.1 Additional research....479
5.1.1 Well integrity and materials....479
5.1.2 Geology and Cavern integrity....481
5.1.3 Generic research....482
5.2 Preventive measures....483
5.2.1 Preventive measures regarding the well design to reduce risk....483
5.2.2 Preventive measures regarding the cavern design to reduce risk....484
5.2.3 Generic preventive measures to reduce risk (external source)....485
5.3 Corrective measures....487
5.3.1 Corrective measures (operational)....487
5.3.2 Corrective measures (organizational)....487
5.3.3 Corrective measures (repair / restore)....487
5.3.4 Generic corrective measures....488
5.4 Description and classification residual risk matrix....489
6 Recommendations....490
6.1 General....490
6.2 Preferred location....490
6.2.1 Site specific research....490
6.2.2 Surroundings....491
6.2.3 Affected stakeholders....491

6.3 Main research topics and measures (preventive and corrective) 492
6.4 Specific recommendations following research Part 2 492
6.5 Cavern field development and strategy 494
6.5.1 Continued risk assessment 494
References 496
Appendix A: Munson-Dawson Creep Law 528
A.1 Munson-Dawson Creep Law 528
A.2 Munson-Dawson Creep Law Parameters 530
Appendix B: Salt Dilation Criteria 531
B.1 Introduction 531
B.2 Dilation Criterion #1 (Ratigan criterion) 531
B.3 Dilation Criterion #2 (DeVries or RD criterion) 532
Appendix C: Sensitivity Analysis Additional Tables 533
Appendix D: Risk assessment 540
D.1 Stakeholder: Operator 540
D.2 Stakeholder: SODM 566
D.3 Stakeholder: Ministry of Economic Affairs and Climate 573
D.4 Stakeholder: Ministry of Infrastructure and Water Management (Rijkswaterstaat) 577
D.5 Stakeholder: Ministry of Agriculture, Nature and Food Quality (Natuurnetwerk) 582
D.6 Stakeholder: Provincial states (I) 587
D.7 Stakeholder: Provincial states (II) 592
D.8 Stakeholder: Municipalities 597
D.9 Stakeholder: Energie Beheer Nederland 605
D.10 Stakeholder: Water Boards 613
D.11 Stakeholder: Safety region (Veiligheidsregio) 619
D.12 Stakeholder: Gasunie New Energy / Hystock 628
D.13 Stakeholder: Gasunie Transport Services (nitrogen storage) 636
D.14 Stakeholder: Gasunie / Energystock 644
D.15 Stakeholder: Water Company Groningen 652
D.16 Stakeholder: Water Company Drenthe 656
D.17 Stakeholder: Railinfratrust / ProRail 660
D.18 Stakeholder: Railway companies (passengers) 665
D.19 Stakeholder: Railway companies (freight) 670
D.20 Stakeholder: Gasunie Transport Services (gas network) 675
D.21 Stakeholder: TenneT 682
D.22 Stakeholder: NAM 688
D.23 Stakeholder: Corre Energy (CAES) 691

D.24 Stakeholder: Water consuming companies (production) 701
D.25 Stakeholder: Water consuming companies (cooling) 705
D.26 Stakeholder: Nobian salt production (I) 708
D.27 Stakeholder: Nobian salt production (II) 715
D.28 Stakeholder: Data storage facilities (effected by ground vibrations) 725
D.29 Stakeholder: Greenpeace 727
D.30 Stakeholder: Wadden Sea Association (“Waddenvereniging”) 734
D.31 Stakeholder: Wadden Academy 739
D.32 Stakeholder: Private landowner above/close to salt caverns (I) 744
D.33 Stakeholder: Private landowner above/close to salt caverns (II) 749
D.34 Stakeholder: Private landowner above/close to salt caverns (III) 755
D.35 Stakeholder: Private landowner in the vicinity 765

Executive summary

The objective of the KEM-28 project is to increase our knowledge and further quantify and research risks associated with underground hydrogen storage (UHS) in a conglomerate of salt caverns in the Netherlands. This report describes the results of the research project which consisted of four parts:

• Part 1 Literature review

• Part 2 Geomechanical study

• Part 3 Risk analyses

• Part 4 Recommended strategy for risk management and mitigation

Overall, we aimed to answer the main research question: 'What are the risks and their likelihood associated with underground hydrogen storage in a conglomerate of salt caverns for hydrogen storage in the Netherlands, either by using existing salt caverns, by developing new ones or by a combination of both options and what is the recommended strategy for risk management and mitigation?'. More specifically, the study aimed to addresses the following research questions:

- *What are the incremental effects of having conglomerates of salt caverns for UHS in the Northern and North-eastern Netherlands on the current levels of induced seismicity and subsidence, and how do they affect the stability of the existing and new to construct salt cavern field(s)?* Answers to this question can be found in Part 1, the Literature review in sections 3.2, 3.5, 5.2 and in Part 2 the Geomechanical study in sections 1.9, 1.14 and 2.3.
- *What are the effects on the long-term durability (deformation and transport properties) of rocks surrounding the caverns and well materials in contact with hydrogen under an alternating pressure regime and what are associated risks?* These topics are addressed in Part 1, the Literature review in sections 5.3 and 5.4 and in Part 2 the Geomechanical study in section 3.3.
- *What are potential interactions between the stored hydrogen with the salt cavern itself, caprock, and the well infrastructure?* Answers to this question can be found in Part 1, the Literature review in section 2.2, 5.3, 5.4 and in Part 2 the Geomechanical study in sections 1.5, 1.6 and 4.2.
- *What are the possible interactions of the conglomerates with other nearby underground storage and/or production facilities, such as producing gas fields, salt caverns for compressed air energy storage (CAES) and gas fields used for CO2 storage?* See case studies in the Literature review sections 3.5.5 and 2.2.3.1.4 in Part 1. A modelling example is given in section 1.14.5.5 in the geomechanical analyses of Part 2.
- *What are recommendations for risk management and mitigation? This will include design criteria for dimensions, shape and depth of new caverns, distance between caverns, surface installation considerations, interaction with other underground storage facilities such as CAES and CO2-storage, brine processing, etc.* Chapter 5 and 6 of the last part present all recommendations and measures to mitigate the risks.

As underground hydrogen storage (UHS) in a conglomerate of salt caverns is not yet a fully mature technology and the study was intended as a generic study, a direct answer to the above questions is not feasible. However, this report provides a comprehensive overview of the risks associated with salt caverns, in particular hydrogen storage in particular, and presents the state-of-the-art modelling and experimental work that can help answering or mitigate the risks as presented in the following parts.

Part 1: Literature review

Large scale UHS is a key element of the energy transition. This is not a mature technology, and the objective of KEM-28 is to increase our knowledge of relevant processes and risks associated with UHS in the Netherlands, focusing on a conglomerate of caverns in Zechstein salt, and recommend strategy for

risk management and mitigation. Here we present a literature review on relevant processes, geological and material properties, engineering experience and risks of UHS. The review accordingly has the following parts:

- a comprehensive overview of existing experience with the more than 2000 salt caverns in operation worldwide, with description, discussion and interpretation of processes and problems in this large knowledge base. Much can be learned from experience with storing different fluids and gases, and to a lesser amount from experience with storing hydrogen, and the review therefore provides a solid basis for the work in Phase 2 (Part 2, 3 and 4).
- together with this overview, a database of (near-)accidents is presented that forms an important part of the risk analysis in Phase 2.
- geological knowledge of the location, structure, and composition of potential sites for UHS in salt caverns. Here we show that much is still unknown about this - we review modern methods to reduce this uncertainty.
- mechanical and transport properties ("durability") of salt rocks surrounding salt caverns (including biochemical processes) and building on our work in KEM-17 we present the state of the art of knowledge in these properties and processes, together with the uncertainties. In part 2 of the report, these uncertainties will be further investigated to use the best possible parameters in the multi-cavern numerical models and field tests to certify caverns for UHS.
- a review of existing risk assessment methodologies for UHS in salt caverns. We show that all existing analyses are qualitative and build on analyses for natural gas storage.

Part 2: Geomechanical study

A generic geomechanical study includes an unlimited number of variables, however within this part we aimed to perform realistic thermodynamical and geomechanical modelling based on the "*average*" Dutch situation. We also investigated durability in relation to creep rheology and the effects of microbial activity of the heterogenous Zechstein rock salt.

Chapter 1 is an extensive geomechanical analysis of hydrogen cavern stability that includes modelling of well thermodynamics, creation of 2D and 3D parameterized finite element models, numerical calculations including sensitivity analysis, blowout modelling and workover of a reference case. For the sensitivity analysis, 54 combinations of parameters were computed and 14 indicators were defined to characterise the mechanical stability of a cavern and its energy efficiency. The stability criteria included the rate of cavern closure due to creep, associated subsidence, the possibility of fractures opening in the cavern wall as a result of the high thermoelastic stresses generated during the production phases, and damage to the rock salt due to dilation at low cavern pressure. The sensitivity study shows that certain configurations are favourable to hydrogen storage, while other configurations are highly unfavourable. For a given geological configuration, there is generally a combination of parameters (cavern characteristics and/or mode of operation) that ensures acceptable mechanical stability.

A sensitivity study in 3D of the behaviour of a cluster of 9 caverns by varying the extraction ratio between 5% and 30% has been performed. As previous studies have shown, the volume loss of each cavern in a cluster is less than the volume loss of a single cavern. This is due to the fact that a large part of the vertical load above the cluster is progressively transferred to the abutment, which reduces the deviatoric stresses in the pillar that cause the loss of volume. In the cases considered, the difference between an extraction ratio of 5% and 10% rate is small, for both cavern volume loss and maximum subsidence. By increasing the extraction ratio from 5% to 10%, the spacing between wellheads is reduced by approximately 50 m (from 160 m to 110 m) and the surface area occupied by a cluster of 9 caverns is halved. Such a reduction in the size of the pillars between caverns does not generate any additional dilatant zone in the pillars.

It should be noted that the conclusions presented in this report are valid given the assumptions that have been made, both for the geometry and for the thermal and mechanical properties of the rocks. This study is generic and not site specific. In the case of a real project, the geology and properties of the rocks will have to be precisely defined, both through studies on a microscopic scale (characterisation of the different types of salt and the average grain size, for example) and on a dome scale. Finally, realistic modelling on the scale of the caverns can be carried out to optimise the characteristics of the caverns, their positioning, and the operating method (minimum pressure, maximum rate of pressure change, etc.).

Chapter 2 involves large-scale 3D thermomechanical modelling of a generic salt dome to investigate whether a cavern field under cyclic loading conditions influences the stress state of the overburden and leads to induced seismicity. For this purpose, we tested the impact of an optimised cavern field on the dynamics of a typical salt dome and the adjacent overburden under different conditions. Using the recommended cavern field design and pressure cycle conditions from Chapter 1, a series of coupled, high-resolution 3D models with and without cavern fields were computed, for which the stress state and degree of brittle deformation were compared. The comparison showed that (1) the degree to which the stress field is perturbed depends on the creep rheology of the rock salt and the dome internal stratigraphy with distinct mechanical properties. (2) In terms of location, a cavern field in the centre of the dome has the least impact on the brittle deformation in the overburden, although the stress within a few hundred meters is significantly disturbed. (3) If the cavern field is located close to the salt-sediment interface and in the immediate vicinity of faults, induced brittle deformation can be observed in the pre-existing fault zones. (4) Several locations close to the dome flanks were tested and not all scenarios lead to the same level of stress perturbation, suggesting that general dome dynamics also play an important role.

Chapter 3 describes a study on the long-term rock salt creep rheology with respect to heterogeneities such as mega grains and anhydrites. Based on a comprehensive analysis with numerical creep tests, we investigated the effect of this structural variability on the effective long-term creep properties of heterogeneous rock salt. At halite matrix volume fractions below 80%, non-matrix phases (e.g., mega grains and anhydrite) have a significant influence on the creep behaviour at low stress (1-3 orders of magnitude). The results show that if the volume fraction of the halite matrix is above 80%, the creep properties of the halite matrix dominate the overall creep behaviour of the rock salt multi-phase aggregate. If the volume fraction of the non-matrix phases is about 60 % or more, there is a high probability that the non-matrix phases form a skeleton that dominates the effective creep behaviour of the rock salt conglomerate, which is then less predictable and follows the individual and (uncertain) creep properties of the mega grains and the second-phase impurities. Furthermore, we have established a general empirical constitutive law that parameterises the strain rate of the heterogeneous rock salt based on the applied stress, the known halite creep properties, and its volume fraction. In the expected stress range and for the expected halite matrix volume fractions of natural salt domes, it can predict our synthetic dataset with an uncertainty of 20 %. It is important to note that this only reflects the average creep behaviour and should be adjusted to site-specific conditions. However, the results and conclusions of this study provide the basis for integrating the creep of a highly heterogeneous multi-phase rock salt into thermomechanical simulations, which ultimately supports the risk assessments of UHS in salt caverns.

Chapter 4 explores into the assessment of salt durability concerning geochemical processes related to second phases and microbes, employing imaging techniques. The challenging subsurface boundary conditions—such as accessibility, depth, and p-T conditions—render in situ examinations of the geochemical processes associated with underground hydrogen storage nearly impractical. Furthermore, laboratory investigations involving actual reactants are constrained; transporting substances (rock samples and fluids) to the surface induces immediate alterations due to shifting p-T conditions and potential changes from contact with drilling fluids, groundwater, surface fluids, or atmospheric gases. State-of-the-art analysis methods, like (cryo)-Scanning Electron Microscopy or µ- or nano-Computer

Tomography, offer the capability to visualize processes both ex-situ and in-situ during laboratory tests. These methods could yield valuable insights for better constraining the rate-controlling processes during subsurface storage, particularly concerning the involved rock phases, such as porous anhydrite, and casing materials like cement and steel. The research investigates microbial alteration of anhydrite involving H_2, CO_2, and H_2S, emphasizing the significance of comprehending the extent and kinetics of reactions within the context of hydrogen storage in salt caverns. Microstructural examinations play a pivotal role in understanding these processes at submicron pore scales, facilitating upscaling and the implementation of preventive measures. Key findings include the impact of impurities and grain size on reaction kinetics, the influence of salt concentrations on sulphate-reducing bacteria and H_2S production, and the identification of dolomite formation through microbial activity. The study also highlights that anhydrite can permit the passage of aqueous solutions, thereby increasing porosity. The solubility of anhydrite in water and its hydration to gypsum are noted to be influenced by various factors, with potential consequences for the mechanical and hydrogeological properties of salt formations. The research underlines the importance of site-specific investigations to comprehend the biological and chemical impacts during hydrogen storage in diverse salt formations. In essence, the research aims to provide insights into the intricate processes involved in hydrogen storage within salt caverns and identifies areas requiring further study to mitigate potential risks.

Part 3 & 4: Risk analyses and recommendations

The last two parts are combined and describe the risk analyses and present three risk assessments – all others can be found in Appendix D – followed by the recommendations in the final paragraphs, including the recommended strategy for risk management and mitigation.

The risk analyses was generic at the request of the Ministry of Economic Affairs and Climate (EZK), resulting in a maximum of combinations of stakeholders and risks that had to be considered. In total 31 stakeholders and 26 risks have been assessed using the method of “Risk-based Working” during various workshops. The performed semi-quantitative risk assessment focusses only on the period of hydrogen storage, i.e., the operational phase (the storage of the gas / liquid). However, the results of the risk assessment in terms of research and measures do not solely apply to the operational phase. The results of the generic risk analysis represent a worst-case scenario, also taking into account that probabilities are relatively high as we need to consider dozens of caverns (a cluster). As the current risk analysis is generic, all site-specific information still needs to be gathered and subsequently processed in the actual risk assessment for any salt cavern planned for future H_2 storage once a location is known.

After mitigation of all preventive and corrective measures the main residual risk concerns the “Threat for future (underground) energy storage”. Overall, social acceptance of hydrogen storage is an important part of the success or failure of hydrogen storage and should receive attention from the government. Secondly, hydrogen storage in a conglomerate of salt caverns in the Netherlands is technically feasible, though many preventive and corrective measures have to be implemented and additional research has to be performed to minimize risks.

The main topic for additional research, based on the research in Part 2 and the risk analyses done, are:

- An improved characterization of the salt dome internal structure, including anomalous zones, using borehole logging and testing and site-specific integrated multi-scale modelling. This includes improving specific tools for the investigation of internal salt stratigraphy and heterogeneities;
- Creep research (e.g., effect of grainsize and impurities; calibration of a transient creep law for Dutch salt) and durability of the salt, including transport properties, damage and healing of salt;
- Analysis of the stability of a cluster of caverns that could be leached asynchronously;

- Validation of the existence of a heat exchange coefficient on the cavern wall and possible calibration of this parameter in the case of hydrogen;
- Analyse the possible development of fractures when effective tensile effective stresses appear on the cavern wall;
- Analysis of the surface effects of a blowout (jet fire, flash fire and unconfined vapor explosion), evolution of the hydrogen plume formed by a leak for several atmospheric conditions, calculation of the distance of effects for several scenarios;
- Research on prevention of micro annuli at the casing / cement / rock interfaces;
- Research of materials interacting with hydrogen and/or H_2S;
- Development of high-quality mechanical integrity tests (MIT) including clear success criteria.

The main preventive measures are:

- Select the best location and configuration for caverns (shape and depth);
- Use of H_2 and H_2S certified material (including packers and valves);
- Minimum preconditions for H_2 storage cavern (well test / acceptance criteria);
- Open, pro-active communication with stakeholders (public, politics and press) and other operators;
- Regular cavern and well tests, including sonar measurements, high quality Mechanical Integrity Tests (MIT) and cement bonding log (frequency to be determined) and safety valve tests (SSV);
- Implement strict regulations (e.g., with respect to stacked mining) and strengthen the role of the regulator;

The main corrective measures are:

- Actions according to the (to be developed and implemented) rapid response plan;
- Adaptation of the storage properties (e.g., pressures (min/max), max. yield);
- (micro-annuli and material) treatment with special materials (resins, silicates etc., biological treatment);
- Controlled production / flaring of H_2;
- Open communication with stakeholders (public, politics and press) and other operators.

Due to the generic nature a relevant part of the risks cannot be easily quantified as a result of lacking information. This results in the need for site specific risk assessments for each location and/or field on:

- Site specific geological information
- The surroundings of the location / field with respect to activities, infrastructure, inhabitants etc.
- The relevant stakeholders

The development of a cavern (field) starts with selecting the right location and should be first based on the geology and then on the minimum number of stakeholders. Preferably construct new caverns and avoid old wells and caverns and start with a relatively small design with low frequency operation while continuing the research. A part of the research strategy includes evaluation of the risk measures and report to all relevant stakeholders and update the risk analyses. The additional research can build upon the findings of Part 2.

Take home messages

- Transparency, strict regulations and a strong regulator are key to minimising risk and gaining support from all stakeholders, especially the local population.
- Technically, hydrogen storage in salt caverns is feasible, although there are still many research questions that should be addressed to reduce the risks.
- Field-scale experiments are essential to test, validate and calibrate existing and newly developed models.
- Finally, the selection of a site based on geological constraints and minimum number of stakeholders should take place as soon as possible to perform a site-specific risk analysis and sensitivity modelling to "*get things started*".

General introduction

This report contains a literature review, generic research, and risk assessment on hydrogen storage in a conglomerate of salt caverns in the Netherlands following the *'Request for Proposal: Risk assessment of hydrogen storage in a conglomerate of salt caverns in The Netherlands'* (Reference: KEM-28 | 202111034), dated 17 February 2022, (a.k.a. RfP) by the Dutch Ministry of Economic Affairs and Climate (Ministerie van Economische Zaken en Klimaat; EZK). To fulfil the scope of this project we expanded the cavern closure consortium (CCC) with Pondera Geo-Energy to bring in world class expertise on risk analysis to form the H2 Cavern Conglomerate Combination (H2C3). The members of the CCC (including Brouard Consulting, GeoStructures Consultancy for Structural geology and Geomechanics, MaP - Microstructure and Pores GmbH and smartTectonics GmbH) have a long and extensive, world class experience with all aspects of this project. Our cooperation started with the KEM-17 project (KEM-17, 2019) and is continuing in a large integrated project aimed at salt cavern abandonment (Baumann et al., 2022a).

It is clear that large-scale energy storage is a key element of the energy transition. For hydrogen to become an essential energy carrier, large scale underground hydrogen storage in salt caverns is a key necessity in the Netherlands (van Gessel et al., 2021c) and internationally (e.g., Smith et al., 2023). Because this is not yet a fully mature technology, the objective of KEM-28 is to increase our knowledge and further assess and research risks associated with underground hydrogen storage (UHS) in a conglomerate of salt caverns.

In our project we aimed to answer the main research question: '*What are the risks and their likelihood associated with underground hydrogen storage in a conglomerate of salt caverns for hydrogen storage in the Netherlands, either by using existing salt caverns, by developing new ones or by a combination of both options and what is the recommended strategy for risk management and mitigation*?' As the study was meant to be generic, so not site-specific, and the number of caverns was unknown risks were evaluated in a semi-quantitively way. Moreover, considering the relatively low number of accidents associated with storage caverns over more than several decades, while technology advanced and regulations got stricter, a robust statistical analysis is not realistic. However, knowledge of risks associated with natural gas and oil storage in conglomerates of salt caverns should be used as the starting point for a better understanding of hydrogen storage and are presented in the extensive literature review. Our research and risk assessment aimed to tackle risks based on various failure scenarios, considering the relative likelihood of their occurrence and their effects, and identifying measures to mitigate those risks and to outline where additional research is necessary.

This project consisted of four parts divided over 2 phases in time, see also Figure 1. Part 3 and 4 are merged in this report to enhance the readability.

Phase 1 (3 months):

- Part 1 Literature review

Phase 2 (12 months):

- Part 2 Geomechanical study
- Part 3 Risk analyses
- Part 4 Recommended strategy for risk management and mitigation

By the end of Phase 1 we delivered a comprehensive literature review (Part 1) on hazards and risks of storage in salt caverns. Additionally, the Zechstein salt in the Northern and North-eastern Netherlands was assessed with a special focus on seismicity and the durability of salt, in particular the creep properties of heterogeneous rock salt and geochemical processes in general. It further includes a database of (near-

) accidents occurred in the construction and operation of salt caverns for oil storage, identifying the causes and consequences. The risk assessment was also introduced.

The deliverables of Phase 2 (also referred as the research phase) consist of the three parts listed in addition to the literature review. The geomechanical study (Part 2) includes a detailed 2D and 3D geomechanical analysis and sensitivity analyses on the stability of a generic cavern field, assuming that a conglomerate of salt caverns is used for storage with various configurations and scenarios and 3D Thermo-hydro-mechanical (THM) dome-scale simulations to assess the potential for seismicity in the vicinity of a salt dome. Additionally, the durability of salt was researched regarding the long-term creep properties of heterogeneous rock salt and microbial processes. These findings, plus the literature review of Phase 1 and expert knowledge provides input parameters for Part 3 of the project which contains a semi-quantitative generic risk analysis of underground hydrogen storage in a conglomerate of salt caverns in the Zechstein salt of the Northern Netherlands following several risk workshops. The last sections (initially Part 4) report on the preventive and corrective measures to be considered. Additionally, a recommendation for further study to better asses the risks of UHS storage in conglomerates of salt caverns is presented.

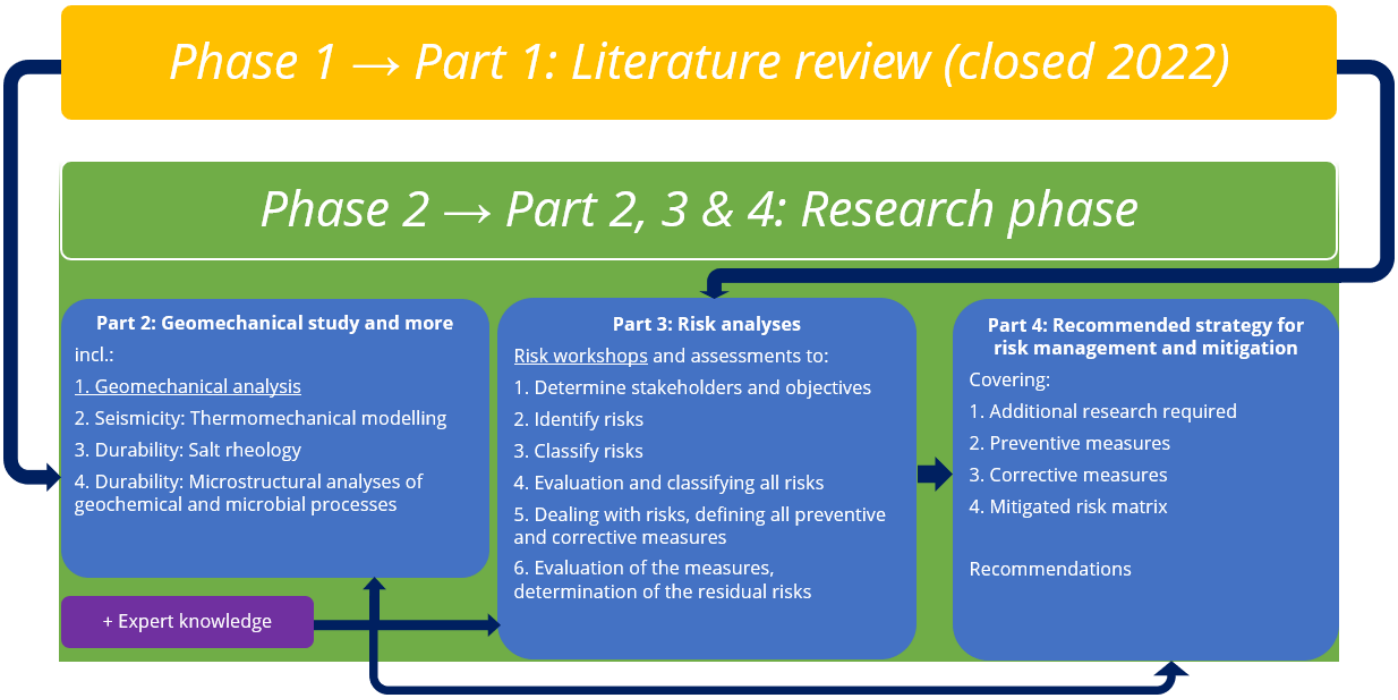

Figure 1. Initial framework of the whole project. Part 3 and 4 were merged in this report to enhance the readability.

Risk assessment of hydrogen storage in a conglomerate of salt caverns in the Netherlands

PART 1 – Literature review

Reference: KEM-28 – Part 1

Summary

In the Netherlands, large scale underground hydrogen storage is a key element of the energy transition. Because this is not yet a fully mature technology, the objective of KEM-28 is to increase our knowledge of relevant processes, further quantify and investigate risks associated with underground hydrogen storage (UHS), focusing especially on a conglomerate of salt caverns, and present a recommended strategy for risk management and mitigation. This is the report of the first phase of the KEM-28 project[1] "Risk assessment of hydrogen storage in a conglomerate of salt caverns in The Netherlands". We present a literature review on relevant processes, engineering experience and risks for underground Hydrogen storage in conglomerates of salt caverns in the Netherlands. We address and integrate a number of aspects of the technology: including an overview of the relevant physical, chemical, and biological processes, we discuss the state of the art of knowledge of geological and geomechanical state (the "Ist-Zustand") of salt diapirs and salt pillows (including a review of associated minor seismicity), with focus on the Dutch subsurface. We discuss methods to efficiently investigate the suitability of candidate structures before deciding to build cavern clusters. Building on our work in KEM-17 we review aspects of the physical properties of the salt surrounding the storage caverns, and identify aspects of their creep-, damage-, and gas tightness properties which are insufficiently known to make reliable predictions of the deformations, subsidence, and tightness in salt cavern clusters over the long periods of their operation. We also review biochemical processes which lead to H_2S formation in the cavern and identify where knowledge is insufficient of reactions and reaction kinetics of H_2S formation. This is integrated with a comprehensive and critical overview of the knowledge of the thermodynamics and engineering aspects of (gas-filled) salt caverns, their tightness along the well and of the salt formation, the pressure permissible in the cavern. Discussion includes analysis of examples of the full range of problems known from the many caverns, illustrated with a database and insights on failure mechanisms based on experience with (near-) accidents from underground storage projects in salt caverns worldwide. This includes experience with gas storage which provides a large knowledge base for those processes which can be compared with H_2 storage. It provides an important contribution to the development of well- and cavern scale tests as a basis for certifying and permitting of a structure for H_2 storage.

We can conclude that many lessons can be drawn from the salt cavern industry. Storage of gaseous and liquid hydrocarbons in salt caverns is a mature technology. More than 2000 caverns are operated worldwide. A lot of experience has been gained which can be transposed – with some changes – to the hydrogen storage case. Especially tightness is a fundamental requisite of hydrogen storage in a salt cavern, due to the small hydrogen molecule size and high flammability of the gas.

Overall, we conclude the following:

- modelling the thermodynamics, tightness, and structural stability of a conglomerate of salt caverns, in particular storing hydrogen and interaction between various storage products, is not comprehensive and requires more work.
- Also, the internal structure of the Dutch subsurface salt structures which are potentially suitable for the construction of hydrogen storage caverns is not well known and determining suitability for caverns needs much more work using available validated methods.
- Yet, it is unclear how characteristic hydrogen cavern parameters affect the exact stress response and corresponding creep processes in the rock salt mass but similarities with other caverns are to be expected. In addition, it is not clear whether natural seismic events, which occur due to the natural creep of the salt dome, can be distinguished from induced micro seismic events, which arise due to increased creep rates from operated caverns.

[1] https://kemprogramma.nl/cms/view/85497703-4743-498f-bd78-13c2e0574691/onderzoeksprojecten

- Moreover, pressure cycles in addition to cavern creep closure poses a much less well-understood problem next to weakening of the (wet) cavern wall by damage, dilatancy, crystal plasticity, dynamic recrystallisation and grainsize-dependent pressure solution.
- Finally, we recommend identifying critical lithologies with sufficient spatial resolution and conduct laboratory and in-situ testing to obtain more reliable kinetic rate data.

In the research phase of this project, we will provide detailed descriptions and recommendations of possible steps to bridge the research gap.

In general, the (near-) accidents are related to thermodynamics, tightness and structural stability of salt caverns and experience on this will be reviewed in detail in chapter 2 and 3, followed by a review on salt cavern testing in Chapter 4. Chapter 5 addresses the Dutch case with respect to the Zechstein salt structures in the subsurface, seismicity and salt durability regarding rheology, transport properties and geochemical processes. All these different aspects are summarized in the following sections below.

CHAPTER 2 SALT CAVERN THERMODYNAMICS AND TIGHTNESS

2.1 Thermodynamics

Salt-cavern thermodynamics is complex, it is influenced by several coupled phenomena. Pressure – cycled gas caverns experience large temperature swings, especially when the cycling period is short. Gas thermodynamic behaviour during cycles is not adiabatic, and the amplitude of the temperature changes strongly depends on the duration of the pressure change and the walls area – cavern volume ratio. In a hydrogen storage, water vapor and other gases (for instance H_2S, when the brine sump contains anhydritic insoluble contents) can be contained in the withdrawn gas. Large pressure drops may generate net tensile stresses at cavern wall. However, the depth of penetration of thermal fractures seems to be relatively small. The upper part of a quiescent gas cavern is stirred by natural convection resulting from the geothermal gradient. In most cases, a temperature gradient inversion is observed in the lower part of the cavern and heat, or mass transfer is impeded above the brine sump, except after a large temperature drop. It seems that the brine sump in a frequently cycled cavern remains perennially cooler than the rock mass, as the gas cavern is a thermo-dynamical device: condensation (after a pressure drop) is spread in the whole gas body and vaporization (after a pressure increase) takes place at the brine-gas interface. These mechanisms do not seem to raise a risk issue; they are important from the standpoint of hydrogen purity and have not been widely discussed in the literature. A simplified model for heat transfer of a cavern is described in the report.

2.2 Tightness of salt caverns

Generally speaking, salt permeability is exceedingly small. However, in-situ tests proved that the overall cavern permeability experiences a significant increase when fluid pressure at cavern depth is larger than 80-85% of the geostatic pressure. Several incidents proved that breaches or conduits can be created or pre-exist between a cavern and a neighbouring cavern, or between a cavern and the boundaries of the salt formation. The origin of most of these incidents is the presence, see below, of Anomalous Zones in the salt formation. However, as in most pressure vessels, it is the “piping” (the access well) that most often is the weakest point. Several incidents are described in this Section. The origin of most of these incidents is the presence of a single casing between the stored product and the rock formation. No tightness loss has been reported from the 6 hydrogen-storage caverns currently operated worldwide, but as hydrogen is a mobile gas, the consequences of a leak reaching ground level might be severe. The analysis of the leak mechanisms identified in 11 cases are described in the report; it enables to identify some common patterns. The onset and nature of a casing breach, the development of a leak, consequences at ground level and monitoring-prevention are discussed. Prevention of a gas leak includes

quality of drilling and cementing job. More specific topics, as pressure monitoring and well completion, are presented.

2.3 Blowout

A blowout is the uncontrolled release of cavern fluid after pressure control systems have failed. Blowouts from salt caverns are not common, only a couple of examples have been described in the literature. The most striking difference between a blowout in a gas reservoir and a blowout in a salt cavern is that the gas inventory in a cavern is relatively small and the blowout is completed within a couple of days. During a blowout, the gas velocity in a borehole typically is a couple hundreds of meters per second (more, when hydrogen is considered). In other words, only a few seconds are needed for gas to travel from the cavern top to ground level. Such a short period of time is insufficient for cavern pressure and temperature to change significantly. Gas flow is adiabatic and turbulent, the effects of friction are confined to a thin boundary layer at the steel casing wall. The gas flow must remain subsonic in the wellbore. At the beginning of the blowout, the flow, which is sonic at ground level, is said to be a “choked flow” and wellhead pressure is larger than atmospheric pressure. Conversely, when the cavern pressure becomes relatively small, the gas flow is said to be “normal”. Even at ground level, the gas rate is significantly slower than the speed of sound, and wellhead pressure is equal to atmospheric pressure. Very low temperatures can be reached in the cavern and at the wellhead during the blowout. In some cases, it can start to rain or even snow in the cavern depending on the initial gas water content.

CHAPTER 3 SALT CAVERN STRUCTURAL STABILITY

Rock salt is a very complex material; since the beginning of the 80’s, ten conferences have been dedicated to its mechanical behaviour. The mechanical behaviour of salt can be studied at various scales: the scale of crystals, at which dislocations climb, glide, and pile up; the scale of grains and interfaces between grains, where micro-cracks can form and pressure-solution is active; and the scale of the salt formation, in which the salt, clay or anhydrite layers generate specific interactions. Rock-salt behaviour is highly non-linear, it is elastic-ductile when considering short-term compression tests, and it is elastic fragile when tensile tests are considered.

3.1 Rock-salt behaviour

In the long term, salt behaves as a fluid in the sense that it flows even under very small deviatoric stresses (i.e., as soon as the state of stress is not purely isotropic). All solution-mined cavities shrink as they gradually, and quite slowly, close. Creep ability strongly depends on the salt formation under consideration. The report describes several aspects of the mechanical behaviour of salt. One section presents the tests that are commonly performed at the lab to determine the transient and steady-state parameters of the dislocation-creep law. The case of small deviatoric stresses, or pressure solution creep, that require special tests performed in a mine is discussed. The most popular constitutive laws are described briefly. Several case histories of spectacular cavern volume losses due to salt creep are presented. Creep closure may also lead to subsidence, casing overstretching and permeability increases at the anhydrite/salt interface. Creep closure in a cycled cavern is discussed.

3.2 Subsidence

Subsidence is an unavoidable consequence of salt cavern creation and cavern creep closure. An abundant literature was dedicated to this topic. It is generally accepted that the volume of the subsidence bowl roughly equals the cavern volume loss. The maximum vertical subsidence is of the order of magnitude of the volume loss divided by the square of the cavern depth; however, the exact figure and, more generally, the shape of the subsidence bowl (the ‘transfer function’) generated by a single cavern are site-specific notions. Subsidence can be computed both through full 3-D computations and through a simpler ‘transfer

function' method. Geometrical characteristics of the subsidence bowl are presented in the report. Several case histories of significant subsidence are also described

3.3 Casing overstretching

Casing overstretching results from large cumulated strains at cavern roof. After a long period of time, in some cases when the steel casing, whose elastic limit is small, is not able to accommodate such deformations, resulting in casing failure and gas leak. The design of the cavern shape and location of the last cemented casing shoe above the cavern roof play a major role, as flat roofs, interlayered formations, large spans, and the absence of a high enough chimney expose the cemented casings to large strains and increases the risk of casing overstretching. Two casing overstretching incidents are described.

3.4 Brittle failure

Even if rock salt behaviour is generally recognized as pre-eminently ductile, it exhibits several brittle features which are important from cavern structural stability. The report describes several examples of brittle failure as observed at the laboratory and in salt caverns. At the laboratory, dilation, tensile failure, hydraulic micro-fracturing, and post-failure behaviour can be observed. At the scale of caverns, examples of the onset of thermal stresses leading to tensile failure are described. These thermal stresses may appear when cavern temperature decreases rapidly, during a blowout for instance. The report also describes the mechanisms that can lead to an overburden failure. Several case histories are presented. Cratering is the most spectacular failure mechanism of a salt cavern: a cylinder of rock drops abruptly by several dozens of meters. However, this phenomenon requires special conditions which have never been met in storage caverns. Roof fall are quite common, and several examples from the literature are analysed. Known examples prove that roof falls occur: in large-spanned, flat-roofed caverns; when interlayers can be found above the roof; and when cavern minimal pressure is small. These three ingredients seem to be mandatory. Block falls from cavern walls is a mundane phenomenon. Evidence of block falls include frequently observed breaks or bending of the inner tubes hit by falling blocks and the observed accumulation of the blocks on the floor of a cavern. Such incidents are typically not reported in literature and belong to the routine operation of many salt caverns. In the following, only incidents that led to large volume displacements or incidents having uncommon mechanisms are reported. Four gas-storage examples and two oil-storage examples are described. Heterogeneities, dome scale anomalies like anomalous zones are mentioned as possible additional factors leading to some instabilities. Several additional examples are provided.

3.5 Conglomerates

The case of 'conglomerates' (large cavern clusters) has not been intensively studied in the literature, probably because it requires heavy computing resources. The mechanical behaviour of a cluster is complex; some computations prove that a large part of the overburden load is transferred to the abutment (the periphery of the cluster), in sharp contrast with the case of an elastic rock mass. Caverns often have been created at the same depth and, from a structural stability standpoint, a major problem is the minimum distance between two neighbouring caverns or, in other words, computation of safe extraction ratio. Some rules can be found in the literature, often based on the dimensioning of room-and-pillar mines. From the literature, it appears that cavern clusters are usually stable. A couple of computation examples are presented. Conglomerates will be studied into detail during the phase 2 of the project.

CHAPTER 4 SALT CAVERN TESTING: Permeability (4.1) and tightness (4.2) tests

The tightness of a cavern and its external well components is a fundamental requirement to ensure that any leak does not cause contamination of drinking water resources or the unreasonable escape of stored

products to the surface. Full-scale testing is necessary to ensure that acceptable tightness exists. A great asset of liquid hydrocarbon storage in salt caverns, when compared to natural gas or CO_2 storage in depleted reservoirs or aquifer layers, is that hydrocarbons occupy a well-defined volume, allowing for precise tightness tests to be performed before commissioning and during the operating life of a cavern. Such tests commonly are referred to as Mechanical Integrity Tests, or MITs. In most countries, conducting an MIT is a regulatory requirement and must be performed at various times during a cavern's life cycle. Every year, hundreds of mechanical integrity tests (MITs) are performed worldwide. A large amount of literature has been dedicated to various technical aspects of MITs. The Solution Mining Research Institute (SMRI) suggested a reference for interpreting the results of an MIT. The report describes the permeability tests that can be performed in a wellbore after drilling and also the determination of cavern average permeability that can be inferred from a test performed in a full-size cavern. The different types of tightness tests that can be performed on an existing cavern are also described in the report. Regarding hydrogen storages, there is no standard procedure for testing the integrity yet. It seems that in the three hydrogen storages in Texas, the caverns were tested through a standard Nitrogen Leak Test (NLT) before debrining the cavern; i.e., before filling the cavern with hydrogen.

CHAPTER 5 ZECHSTEIN SALT IN THE NETHERLANDS

Chapter 5 reviews the Dutch subsurface with respect to the Zechstein salt structures, seismicity, and durability in four sections. The durability encompasses the evolving rheology, transport properties, damage, and healing of salt around a cluster of hydrogen storage caverns and the geochemical processes.

5.1 The Dutch subsurface (onshore and offshore) and potential Salt caverns

Permian Zechstein evaporites are present in large parts of the subsurface of the Netherlands. Layers of rock salt, potassium-magnesium salts and sulphates form a highly complex structure, ranging from thick, tectonically undeformed salt to highly deformed and reworked tectonites in salt pillows and diapirs Although the majority of possible locations have been identified, the internal structure of the Dutch subsurface salt structures which are potentially suitable for the construction of Hydrogen storage caverns is not well known and determining suitability for caverns needs much more work using available validated methods - significant part of this can be done before investing in data acquisition by high resolution seismic and measurements in wells.

5.2 Salt seismicity in general and Dutch situation

In principle, the specific occurrence of induced seismicity due to hydrogen storage in salt caverns is a topic that has not yet been documented much in the literature. This section provides an overview of possible causes of seismicity related to operating and abandoned salt caverns, and salt structures in general. We review the literature articles that describe microseismic events associated with caverns and assess the situation for hydrogen caverns. Compared to other induced seismic events from, for example, depleting gas reservoirs (ML < 3.5), induced seismic microseismic events possibly associated with cavern operations appear to have 100-1000 times smaller amplitudes (ML < 1.3).

5.3 Durability: The evolving rheology, transport properties, damage and healing of salt around a cluster of hydrogen storage caverns

The situation of hydrogen in contact with the cavern wall where pressure is cycled in addition to cavern creep closure poses a much less well-understood problem. In our opinion, it is likely that the cavern walls will be wet when in contact with H2. This poses an interesting and unexplored problem of damage, dilatancy, crystal plasticity, dynamic recrystallisation and pressure solution, which can weaken the cavern walls with the very low viscosity of H2 allowing much more rapid penetration of pore pressure and dilatancy than previously thought, with an as yet unknown depth of penetration. This calls for a much

better understanding of the processes in this complex damage zone over long periods. Additionally, the Z2 Stassfurt salt, which is expected to be the major host of Hydrogen caverns in the Netherlands, shows evidence of grainsize-dependent differences in halite rheology based on microstructural observations. We recommend that this mechanism is included in the constitutive laws describing deformation of engineered structures in rock salt.

5.4 Durability: Geochemical processes

This review on the geochemical process related to the storage of hydrogen in salt caverns comprises: i. a short overview on the physic-chemical properties of the reactive second phases within the Zechstein formation, especially the anhydrite/polyhalite layers, and the related abiotic geochemical reactions and reaction kinetics; ii. the associated biotic processes, reactions and reaction kinetics causing the risk of H_2S formation; and, iii. the material integrity and durability in terms of possible chemical changes of the borehole materials.

Although hydrogen stored in salt caverns is expected to have a major impact on sulphur chemistry, a number of studies suggest that the impact on second-phase lithologies, which contain only small amounts of sulphur, is unlikely to be significant because reactions of hydrogen with minerals become relevant only over time periods much longer than the storage cycles considered. In contrast, however, significant effects of biotic and abiotic processes are expected on sulphur-bearing lithologies such as the anhydrite/polyhalite layers and the brine sump (Dopffel et al., 2021; Hemme and van Berk, 2017; Laban, 2020; Muhammed et al., 2022; Panfilov, 2016). Geochemical models are valuable tools to constrain the long-term behaviour of the reservoir in terms of mineral dissolution and precipitation reactions in the presence of hydrogen, as well as the associated effects on, but reliable data on the kinetic rates of these processes are lacking according to many authors. In the absence of reliable data on the effects of hydrogen on permeability and mechanical integrity in critical lithologies such as anhydrites, sump sediments, or the casing cements, as well as information on the kinetics of abiotic geochemical and microbial reactions in the corresponding pore fluids, predictions on the long-term behaviour of geologic hydrogen storage are limited. To better assess the quality and safety of the potential salt cavern conglomerate storage sites, it is recommended that, in addition to geochemical modelling, (i) subsurface geologic conditions be characterized with sufficient spatial resolution to identify critical lithologies, and (ii) laboratory (analogue and case studies) and in-situ testing be conducted to obtain more reliable kinetic rate data.

CHAPTER 6 DATABASE OF (NEAR-) ACCIDENTS OCCURRED

A database of (near-)accidents, or incidents, occurred in the construction and operation of conglomerates of salt caverns for hydrocarbon storage worldwide is presented in chapter 6. It lists over 50 (near-) accidents with corresponding location, incident date, cause, consequence, and references.

Appendix: Risk assessment

Based on the above, we present in the Appendix an overview of existing risk assessment methodologies for H_2 storage in salt caverns. Although existing methods are quite diverse, focusing on a variety of risks associated with part of or the total life-cycle of the salt cavern, all existing analyses are qualitative. Risk assessment on H_2 storage, however, is scarce and mainly built upon the risk assessment of natural gas storage. For Phase 2 of this project, we propose “Risk based Working” which is semi-quantitative, to determine the risks, the consequences, and the effect of the measures to be taken. This method consists of a structure of 6 steps based on unambiguous working definitions for “uncertainty”, “risk” and “risk perception”. Based on the knowledge described in this review and further developed in Phase 2, we will

develop a general template for the risk assessment of H_2 storage in salt caverns. After that we will build the frame of a generic risk analysis, organize several workshops with our team and will complete the risk analysis based on facts, interpretation of facts and assumptions, all using the inherent expert knowledge. The final risk analysis describes all possible stakeholders, the risks that might influence them and the mitigations that can be taken.

1 Introduction

Large-scale energy storage is a key element of the energy transition. For hydrogen to become an essential energy carrier in the Netherlands, large-scale underground hydrogen storage is crucial. We, the H2 Cavern Conglomerate Combination ($H2C^3$), present a comprehensive literature review on hazards and risks of underground storage in conglomerates of salt caverns relevant for hydrogen storage in the Northern and North-eastern Netherlands (focusing on the Zechstein salt layer). All according to our proposal (Proposal: 'Risk assessment of hydrogen storage in a conglomerate of salt caverns in The Netherlands', version 220328) by the $H2C^3$ following the 'Request for Proposal: Risk assessment of hydrogen storage in a conglomerate of salt caverns in The Netherlands' (Reference: KEM-28 | 202111034), dated 17 February 2022, (a.k.a. RfP). We build on the results of KEM-17 (Baumann et al., 2019; Brouard and Bérest, 2019; Urai et al., 2019) combined with our expertise in risk analysis and on the extensive relevant published work by others (e.g., Groenenberg et al., 2020b, 2020a; Sijm et al., 2020; van Gessel et al., 2018; Winters et al., 2020) and our group.

1.1 Reading guide

Our literature review consists basically of two parts. The first part (Chapter 2, 3 and 4) includes insights on (near-) accidents from underground storage projects in conglomerates of salt caverns worldwide. Next to describing the incidents in detail, the lessons learned, preventive measures, and specific criteria are presented for a selection of failure mechanisms. It includes a database of (near-)accidents that occurred in the construction and operation of conglomerates of salt caverns for gas and/or oil storage, identifying the causes and consequences (Chapter 6 Database of (near-) accidents occurred). The other part, Chapter 5 Zechstein Salt in the Netherlands, includes a literature review on the Dutch subsurface and potential salt caverns followed by a section on salt seismicity in general and Dutch situation. The chapter also contains a section on durability regarding the evolving rheology, transport properties, damage and healing of salt, and geochemical processes. Additionally, a template for the risk analyses of underground hydrogen storage in salt caverns, including a review of the risk analyses already conducted, is presented in Appendix: Risk assessment. The reference list is at the end of the document (p496).

In the following, we list the main author(s) of the relevant sections:

- Chapter 2 Salt cavern thermodynamics and tightness: Prof. Dr. Pierre Bérest
- Chapter 3 Salt cavern structural stability: Prof. Dr. Pierre Bérest
- Chapter 4 Salt cavern testing: Prof. Dr. Pierre Bérest
- Section 5.1 The Dutch subsurface (onshore and offshore) and potential Salt caverns: Prof. Dr. Janos L. Urai
- Section 5.2 Salt seismicity in general and Dutch situation: Dr. Tobias Baumann and Prof. Dr. Janos L. Urai
- Section 5.3 Durability: The evolving rheology, transport properties, damage and healing of salt around a cluster of hydrogen storage caverns: Dr. Tobias Baumann, Prof. Dr. Janos L. Urai and Prof. Dr. Boris Kaus
- Section 5.4 Durability: Geochemical processes: Dr. Joyce Schmatz
- Chapter 6 Database of (near-) accidents occurred: Prof. Dr. Pierre Bérest and Dr. Jop Klaver
- Appendix: Risk assessment: Ir. René Vreugdenhil

2 Salt cavern thermodynamics and tightness

Author: Pierre Bérest – Brouard Consulting

Storage of gaseous and liquid hydrocarbons in salt caverns is a mature technology. More than 2000 caverns are operated worldwide. A lot of experience has been gained which can be transposed – with some changes – to the hydrogen storage case.

Tightness is a fundamental requisite of any storage cavern. However, storing hydrogen raises a couple of new problems, related to the small hydrogen molecule size and high flammability of the gas. Tightness results from (Bérest and Brouard, 2003):

- the properties of the rock formation (KEM-17, 2019),
- the nature of the stored product (density, viscosity)
- the pressure selected for storage operation
- Blowout prevention
- the design of wellbore completion, and
- the quality of the cementing job and steel equipment.

A considerable asset is that much information and experience are available from the 2000+ salt caverns used worldwide for hydrocarbon storage.

2.1 Thermodynamics

2.1.1 Hydrogen purity

From an economic standpoint, gas purity is a more important concern. Existing hydrogen storage caverns are used for industrial uses and a high purity of hydrogen is not required. Hydrogen used for mobility (cars, trucks, or trains), needs much higher requirements. Highlights are provided by natural gas storages. Water vapor amount in the injected gas is low (In France, for instance, water vapor concentration in a mass of gas injected in a cavern must be less than $c_v = 46\ \mathrm{mg/Nm^3}$; $\mathrm{Nm^3}$ stands for "Normal" (standard) $\mathrm{m^3}$). However, after cavern creation, a significant amount of brine is left at cavern bottom (Figure 2), and vapor amount in the gas gradually increases to reach equilibrium with the sump brine. This process is relatively fast as gas is stirred by natural convection in the cavern. When gas is withdrawn from the cavern its temperature and pressure drop and gas is oversaturated with water, there is a risk that gas hydrates form at ground level (Klafki et al., 2003a). Hydrates are a significant hazard for pipes and pumps at ground level (Réveillère et al., 2016). Gas must be dehydrated before being injected in the grid, a costly part of storage operation.

In a hydrogen storage, water vapor and other gases (for instance H_2S, when the brine sump contains anhydritic insoluble contents) can be contained in the withdrawn gas.

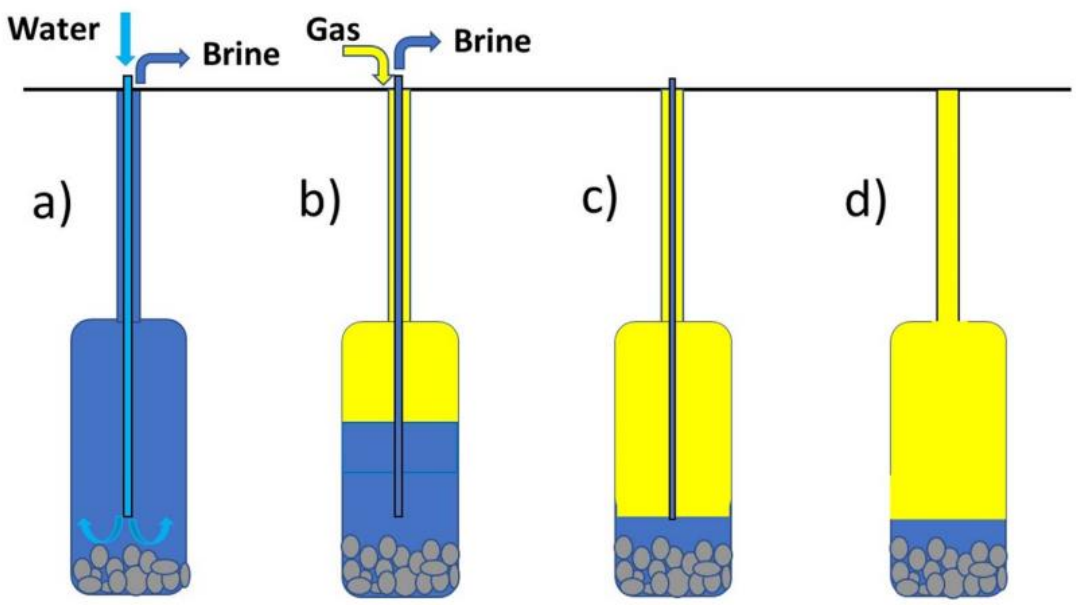

Figure 2. From left to right: (a) solution mining; (b) debrining; (c) end of debrining; (d) before commissioning.

2.1.2 Convection in brine-filled and gas-filled caverns

2.1.2.1 Onset of convection in a brine-filled cavern

Salt caverns often are leached out using soft water from a lake or a shallow aquifer having a low temperature (typically, 10-12 °C). When solution-mining is completed, cavern brine temperature is significantly lower than rock temperature (which typically is 45 °C at a 1000-m depth). The same is true for the brine sump in a gas cavern. Heat transfer through conduction takes place in the rock mass, and the resulting heat flux through the cavern walls (∂V) warms the cavern brine (Bérest, 2019):

$$\rho_b C_b^P V \dot{T}_b = \int_{\partial V} -K_{salt} \frac{\partial T_{salt}}{\partial n} dA \qquad (1)$$

Where $\rho_b C_b^P$ is the volumetric heat capacity of brine; $V$is the cavern volume; T_b is the brine temperature; T_{salt} is the rock-salt temperature at cavern depth; K_{salt} and k_{salt} are the salt thermal conductivity and diffusivity, respectively. From these two equations, as $K_{salt} = \rho_{salt} C_{salt}^P k_{salt}$ is not very different from $\rho_b C_b^P k_{salt}$, it can be inferred that the characteristic time for brine warming in a quiet cavern is $\frac{V^{2/3}}{k_{salt}}$. Typically in a cavern of spheroidal shape, the gap between rock temperature and brine temperature is divided by a factor of 4 after some time (in years), which approximately is $\frac{V^{2/3}}{400}$; V is in m^3 (More precise computations can be found in Karimi-Jafari et al., 2007).

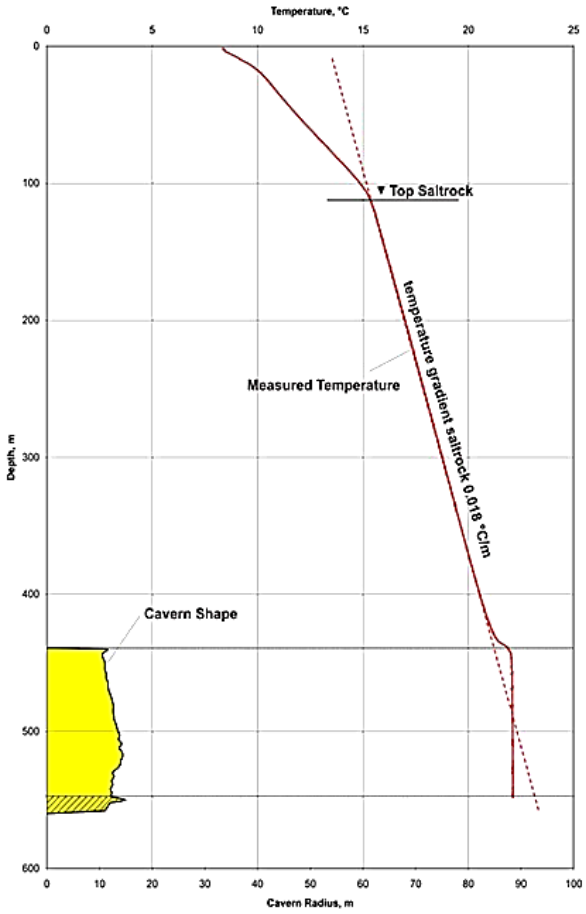

Figure 3. Temperature profile along the vertical axis of symmetry in a brine cavern (Banach and Klafki, 2009).

When thermal equilibrium is reached, after several years or decades, depending on cavern size, brine temperature is almost constant in the cavern, even though the virgin salt mass is the seat of an upward geothermal gradient: $G_{geo} = 1.6 \times 10^{-2}$ °C/m, typically. This is because, in addition to conductive heat transfer, brine is stirred by convective heat transfer. Brine at the bottom of the cavern is warmer than at the top, and equilibrium is unstable. Consider a brine particle that rises by $dz < 0$. Mechanical equilibrium is reached almost instantaneously, and particle pressure decreases by $dP = \rho_b g dz$. Its temperature decreases accordingly. The temperature decrease is larger when the particle does not have enough time to exchange heat with the surrounding brine — i.e., when the thermodynamic transformation is adiabatic, or $dP|_S = \rho_b C_b^P dT$ (i.e., when entropy S remains constant), and $dT|_S = gdz/C_b^P$. The particle keeps rising as long as its temperature is warmer than the temperature of its environment (i.e., when $\frac{g}{C_b^P} < G_{geo}^{cav}$, where G_{geo}^{cav} is the inferred geothermal gradient in the cavern should no convection take place, it is slightly smaller than the geothermal gradient in the rock mass), a condition

that is always met ($C_b^P = 3800\ \mathrm{J/kg/°C}$ is typical, $g = 10\ \mathrm{m/s^2}$). More details can be found in Bérest (2019).

Figure 3 provides an example: the geothermal gradient in the cavern is quite small. There is a second condition for onset of natural convection: the Grasshof number must be sufficiently large, a condition always met in a salt cavern.

Table 1. Thermal properties of brine and several gases. Constants are measured at 25 °C and atmospheric pressure (Air Liquide, 2022).

Fluid	C^p **(J/kg-K)**	K_F **(mW/m-K)**	$G_{ad} = \frac{\alpha T g^p}{C}$ **(°C/km)**
Air	1006	26	9.8
CH_4	2232	34	4.4
H_2	14306	185	0.7
O_2	920	26	10.6
CO_2	851	16	11.5
Brine*	3200	600	0.31

** Manuel pour le Transport et la Distribution du Gaz, 1985.*

2.1.2.2 Onset of convection in a gas-filled cavern

It should be expected that a similar (almost vertical) temperature profile be found in gas caverns, especially in the case of hydrogen and natural gas (methane), as the adiabatic gradient, although larger than brine adiabatic gradient, is smaller the inferred geothermal gradient. The condition for onset of thermal convection in a gas cavern is $G_{ad} = \frac{\alpha T g}{C_g^P} < G_{geo}^{cav}$, where α is the coefficient of thermal expansion of the gas, $\alpha T \simeq 1$, and the heat capacity of the gas, C_g^P, is relatively large (see Table 1). In fact, this is not true, a temperature gradient inversion can be observed at cavern bottom, several dozens of meters above the gas-brine interface (see Figure 4) as will be seen in paragraph 2.1.3.

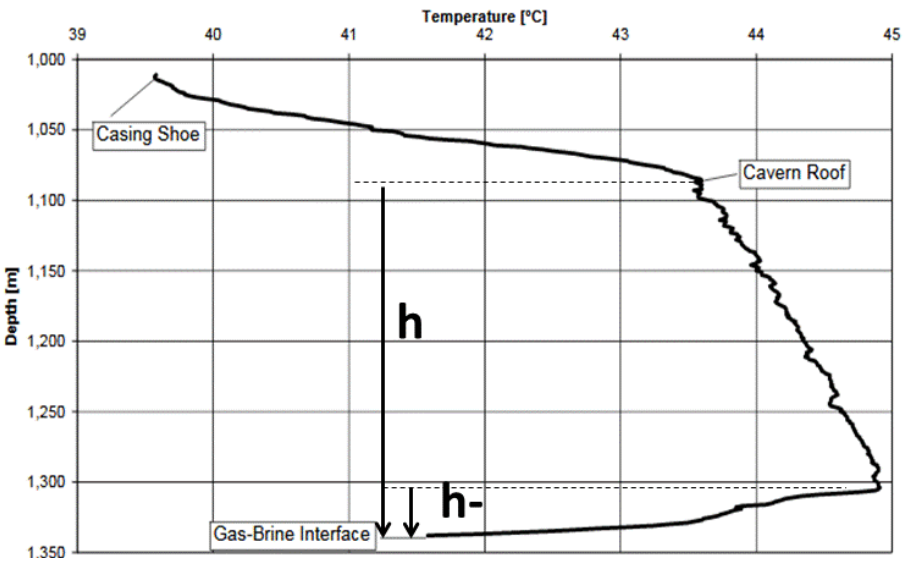

Figure 4. Temperature profile in an anonymous gas cavern: the temperature gradient in the upper part of the cavern is $G = 6\ \mathrm{°C/km}$; it is negative above the sump (After Berger et al., 2002).

2.1.3 Heat transfer in a gas storage cavern

2.1.3.1 A case history

A gas storage cavern is an open system: gas is injected or withdrawn from the cavern. Gas pressure and temperature experience large changes. An example was described by Klafki et al., (2003b). In the Cavern S107 at Stassfurt, Germany, during a 14-day period, three gas withdrawals (60,000 Nm^3/hr over 20 h, 100,000 Nm^3/h over 12 hours, 142,000 Nm^3/hr over 7 hours, followed by a 77-hour standstill) and a 61,000-Nm^3/hr injection over 61 hours were managed (for natural gas, 1 Nm^3 = 0.68 kg). Temperature profiles were measured through a Raman optical fibre (Figure 5); they remain almost vertical during withdrawal, evidence of the perennial effect of thermal convection in the main cavern body, except for the lower part of the cavern (below the gradient inversion depth), which will be addressed later.

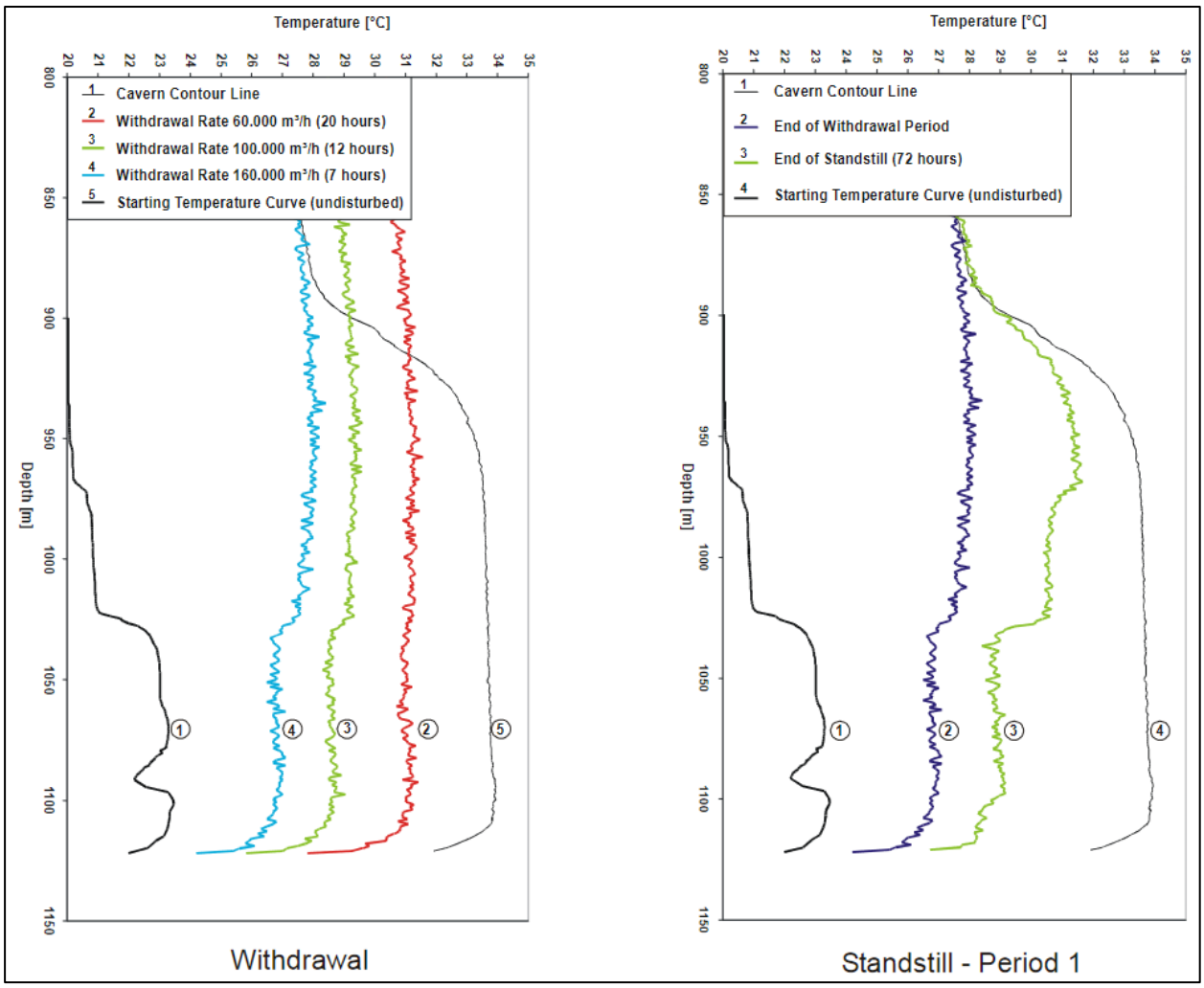

Figure 5. The cavern profile (1) is drawn on the left side of each picture. In the left illustration, temperature profiles before (5) and after (2, 3, 4) three consecutive withdrawals are represented; the right illustration represents how temperature reaches thermal equilibrium after the withdrawals are completed (2, 3) (Klafki et al., 2003b).

2.1.3.2 A simplified model for heat transfer in a cavern

A simplified version of the first principle of thermodynamics can be written as follows:

$$m\left(\dot{h}_c - v_c \dot{P}_c\right) = Q + < \dot{m} > \left(h_{inj} - h_c\right) \qquad (2)$$

The mass of gas in the cavern is $m = m(t)$; h_c is the gas enthalpy per unit of mass), $v_c = \frac{1}{\rho_c}$ is the gas massic volume; $Q = \int_\Sigma K_R \frac{\partial T_R}{\partial n} d\Sigma$ is the heat flux transferred from the rock mass to the gas through the

cavern wall. The system is open, and mass is exchanged with the wellbore through the cavern chimney; $<\dot{m}>=\dot{m}$ when $\dot{m}>0$ and $<\dot{m}>=0$ when $\dot{m}<0$. At the cavern entrance, fluid pressure is continuous. When gas is injected, temperature is not continuous, and a jump in enthalpy must be considered, $h_{inj} - h_c = C_P\left(T_{inj} - T_c\right)$, where T_{inj} is the temperature of the injected fluid. No such term exists when fluid is withdrawn ($\dot{m}<0$). In a gas cavern, gas often is compressed before being injected; however, in most cases, T_{inj} is smaller than 60 °C to prevent excessive thermal expansion of the wellhead and steel casings.

In this simplified version of energy balance, several terms are neglected:

- Heat exchange between brine sump and gas at the bottom of the cavern is not considered
- The effect of water vapor condensation or vaporization is not taken into account
- Gas temperature is assumed constant throughout the cavern.
- Gas temperature equals rock temperature at cavern wall. In fact, many authors (e.g., Kushnir et al., 2012), assume that some surface heat-transfer coefficient ($\bar{H}$) must be taken into account, $K_R(T_R - T_c) = \bar{H}\frac{\partial T_R}{\partial n}$. Selecting the value of this parameter ($\bar{H}$) is difficult.
- (There is a lack of field data, and this value depends strongly on roughness of the cavern wall and convection intensity.) In fact, the turbulent boundary layer at the cavern wall is likely to be thin, making $\bar{H}$ quite small; in this paragraph, it is assumed that temperature is continuous at cavern wall, $T_R = T_c$.

They will be considered in the next paragraph.

Further simplifications are considered below:

- The gas is ideal ($P_c v_c = r_g T_c$ and $h_c = C^p T_c$)
- Precise computation of the heat flux from the rock mass (Q) can be done through numerical computations. However, when rapid injections/withdrawals are considered, simplifications can be made. Consider a $\delta t-$long rapid gas withdrawal — for instance, $\delta t = 4$ days. Pressure and temperature both drop. During such a short period, temperature changes are not given enough time to penetrate into the rock mass much deeper than $d = \sqrt{k_R \delta t}$ where $k_R = 3 \times 10^{-6}\ \mathrm{m^2/s}$ is the thermal diffusivity of salt, or $d \approx 1\mathrm{m}$. From the perspective of thermal conduction, cavern walls, as noted by Crotogino et al., (2001) and Krieter and Gotthardt, (2015), can be considered as the sum, Σ, of small flat surfaces (a simplified description of small surfaces whose radius of curvature is not smaller than d.) Σ is the effective area of cavern walls — a notion that depends on the duration of the gas withdrawal.

  When a constant temperature, T_0, is applied at the flat surface of a semi-infinite space, the heat flux is $Q = \Sigma K_R\left(T_\infty - T_0\right)\Big/\sqrt{\pi k_R t}$. ($T_\infty$ is the temperature at a large distance from the cavern.) When gas temperature is not constant, $T_c = T_c(t)$, the flux can be expressed through a convolution:

$$Q(t) = K_R \Sigma \int_0^t \frac{\dot{T}(\tau)}{\sqrt{\pi k_R (t-\tau)}} \tag{3}$$

  After some algebra, the energy equation can write:

$$\frac{\gamma}{\gamma-1}\frac{P(t)}{T(t)}\dot{T}(t) - \dot{P}(t) = -\frac{\Sigma}{V}\frac{K_R}{\sqrt{\pi k_R}}\int_0^t \frac{\dot{T}(\tau)}{\sqrt{t-\tau}}\, d\tau + \frac{<\dot{m}>}{V} C_P\left(T_{inj} - T\right) \tag{4}$$

2.1.3.3 Factors of influence in gas temperature evolution

When a gas withdrawal is considered ($\dot{m} < 0$), beside initial conditions, P_0 and T_0, only two physical constants appear in this equation, $\gamma = \frac{C_p}{C_v}$ and $\frac{\Sigma K_R}{V\sqrt{\pi k_R}}$.

- The ratio $\frac{V}{\Sigma}$ depends on cavern shape and is proportional to cavern size. This is the parameter susceptible of the largest variations. Following a gas withdrawal, the temperature drop is larger in a bigger cavern (because cavern gas behaviour is closer to adiabatic)**.** Staudtmeister et al., (2011), suggest V/Σ = 8-12 m; larger values are found in a large cavern when the height/diameter ratio is close to 1. In an idealized spherical cavern with radius a, for instance, $V = 525{,}000\ \mathrm{m}^3$, $a = 50\ \mathrm{m}$ and $\frac{V}{\Sigma} = \frac{a}{3} = 17\ \mathrm{m}$. Rokahr et al., (2011), mention that "*the ratio* V/Σ *is usually less than 10 m for caverns in salt domes because they are often shaped long and thin*" (p. 194).
- The ratio $\frac{K_R}{\sqrt{\pi k_R}}$ depends of the thermal properties of the rock formation; it does not vary much from one site to the other. Its value typically is 1800 W.s$^{1/2}$/m^2 (see Table 2). A smaller value was found, 1532 W.s$^{1/2}$/m^2, was found by Brouard and Bérest (2022) from the calibration of field data.

Table 2. Values of $\frac{K_R}{\sqrt{\pi k_R}}$ for rock salt.

	K_{salt} (W/m-°C)	ρ_{salt} (kg/m^3)	C_{salt} (J/kg-K)	k_{salt} (×10^{-6} m^2/s)	$\frac{K_{salt}}{\sqrt{\pi k_{salt}}}$ (W.s$^{1/2}$/m^2)
1	5.2	2174	800	2.99	1700
2	5.5	2180	870	2.90	1820
3	5	2200	860	2.64	1740
4	3.85	2200	886	2.01	1532

(3 = Blanco Martín et al., 2015; 4 = Brouard and Bérest, 2022; 1 = Pellizzaro et al., 2011; 2 = Staudtmeister et al., 2011).

$$\frac{\gamma}{\gamma-1}\frac{P(t)}{T(t)}\dot{T}(t) - \dot{P}(t) = -\frac{\Sigma}{V}\frac{K_R}{\sqrt{\pi k_R}}\int_0^t \frac{\dot{T}(\tau)}{\sqrt{t-\tau}}\,d\tau \qquad (5)$$

- The adiabaticity index, $\gamma = \frac{C_p}{C_v}$, equals $\gamma = 1.4$ (air, hydrogen) or $\gamma = 1.3$ (methane). A comparison of temperature evolution when air, methane or hydrogen is stored can be found in Nieland, (2008), Schlichtenmayer et al., (2015) and Louvet et al., (2017).

An example of the role of the adiabaticity is discussed in Paragraph 2.1.2.2.

2.1.3.4 *Comparison between air, natural gas and hydrogen storages*

This is illustrated by Figure 6 to Figure 8. As expected from equation (5), minimum temperatures are slightly smaller in the case of natural gas (methane) storage.

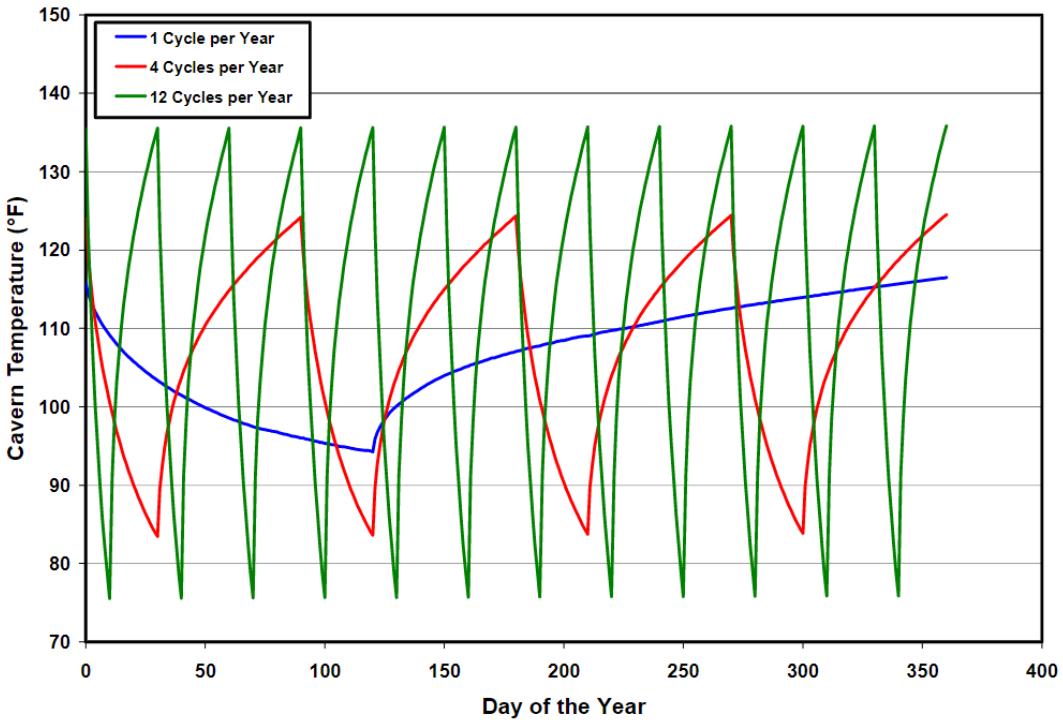

Figure 6. Temperature in a cycled natural gas storage (from Nieland, 2008).

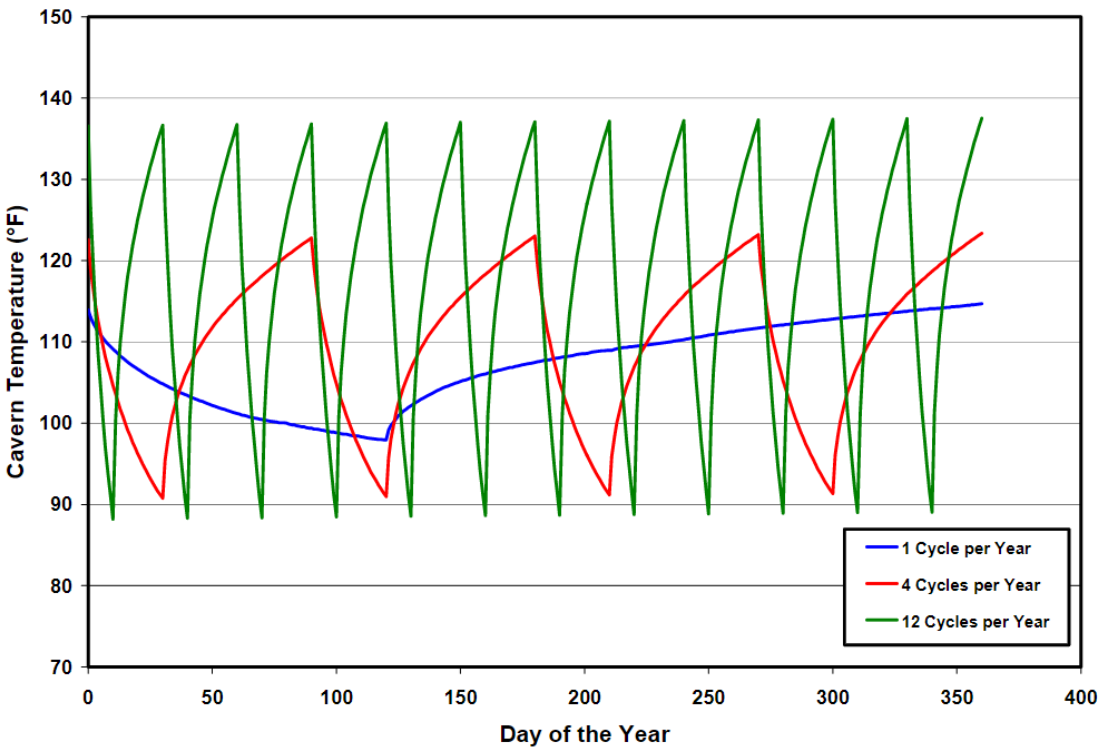

Figure 7. Temperature in a cycled air storage (from Nieland, 2008).

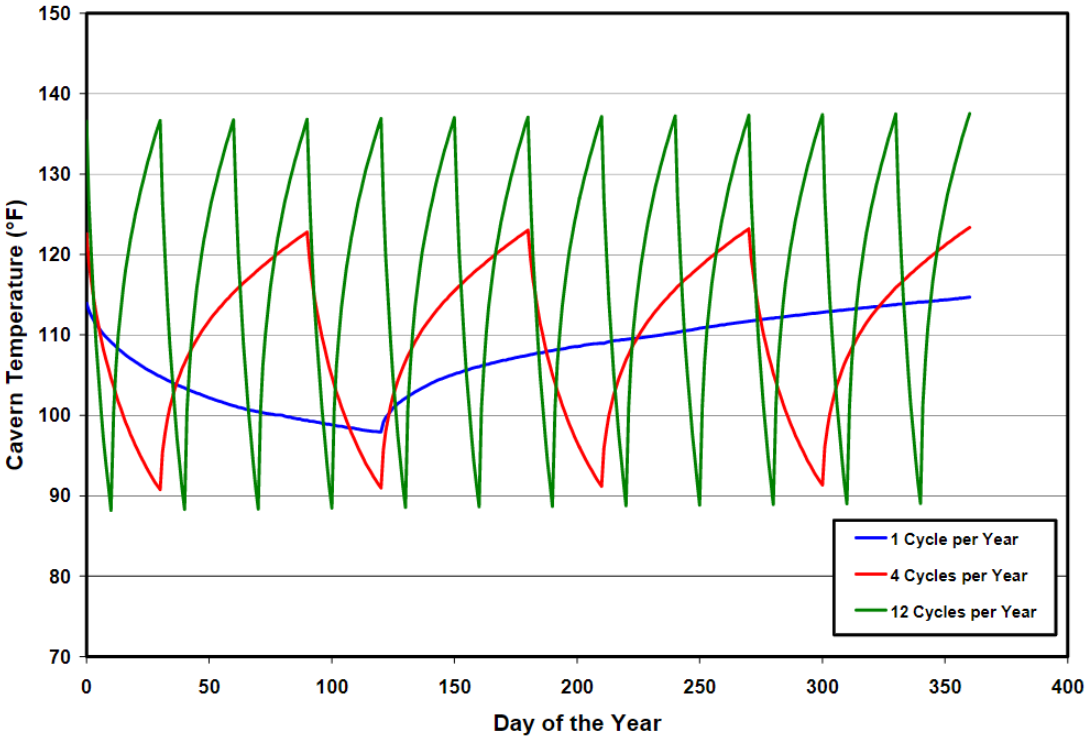

Figure 8. Temperature in a cycled hydrogen storage (from Nieland, 2008).

2.1.3.5 Return to thermal equilibrium after large temperature changes

2.1.3.5.1 A case history

In Figure 4, it can be observed that after a gas withdrawal, when the cavern is kept at standstill for 3 days, thermal disequilibrium reduces by more than 25%. The same can be said of the example described in Figure 9.

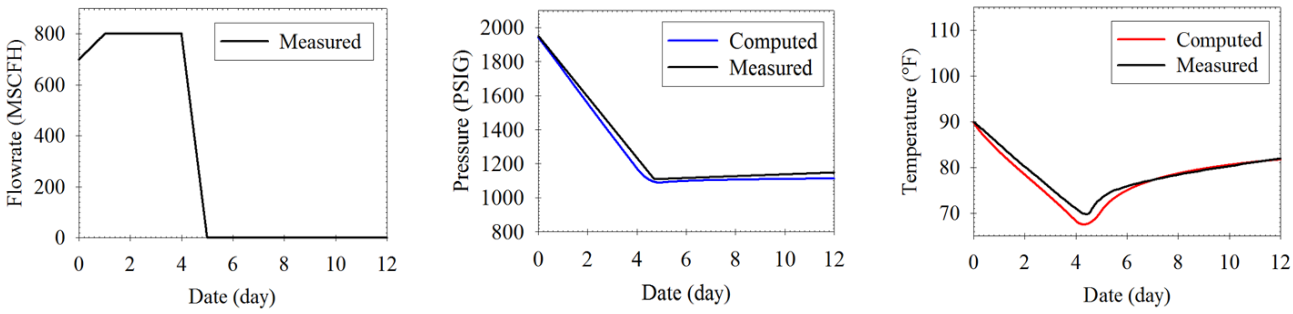

Figure 9. Melville Cavern: Gas withdrawal rate, pressure and temperature evolutions as observed (after Crossley, 1996) and as computed: 1 MSCFH = 28,317 Nm^3/hr, 1 MPa = 145 psi and 20° C = 68° F.

2.1.3.5.2 Gas warming in a shut-in gas cavern

This can be explained as follows. Instead of P, T in equation (5), m and T can be selected as the main variables, $m = \frac{PV_0}{RT}$:

$$mC_v\dot{T} - \dot{m}rT = -\frac{\Sigma K_R}{\sqrt{\pi k_R}}\int_0^t \frac{\dot{T}(\tau)}{\sqrt{t-\tau}}\, d\tau + < \dot{m} > C_P\left(T_{inj} - T\right) \qquad (6)$$

During a standstill, $\dot{m} = 0$, and equation (6) reduces to (7):

$$mC_v\dot{T} = -\frac{\Sigma K_R}{\sqrt{\pi k_R}}\int_0^t \frac{\dot{T}(\tau)}{\sqrt{t-\tau}}\,d\tau \qquad (7)$$

After a large withdrawal of gas, m is small; the volumetric heat capacity of a gas, *or* C_v, is small (when compared to brine, for instance) and the characteristic time for gas warming is short (one week, typically) in short contrast with the case of a brine-filled cavern (years to decades, typically). This explains why the effects of thermal stresses are small (see section 3.4.3).

2.1.4 Gas purity, the role of water vapor

It was mentioned in Paragraph 2.1.3.1 that in most gas caverns the temperature gradient is small, as natural convection stirs cavern gas and homogenizes its temperature. However, at cavern bottom but several dozens of meters above the interface between gas and the brine sump, a temperature gradient inversion is observed (Figure 10). Such an inversion can be expected short after debrining. The brine sump, which contains brine formed during solution-mining from circulating water originating from ground level, is still colder than the rock mass at sump depth (in sharp contrast with cavern gas, whose thermal heat capacity is smaller than brine's, and swiftly reaches thermal equilibrium with the rock mass). However, this temperature difference is still present decades after debrining (Figure 11).

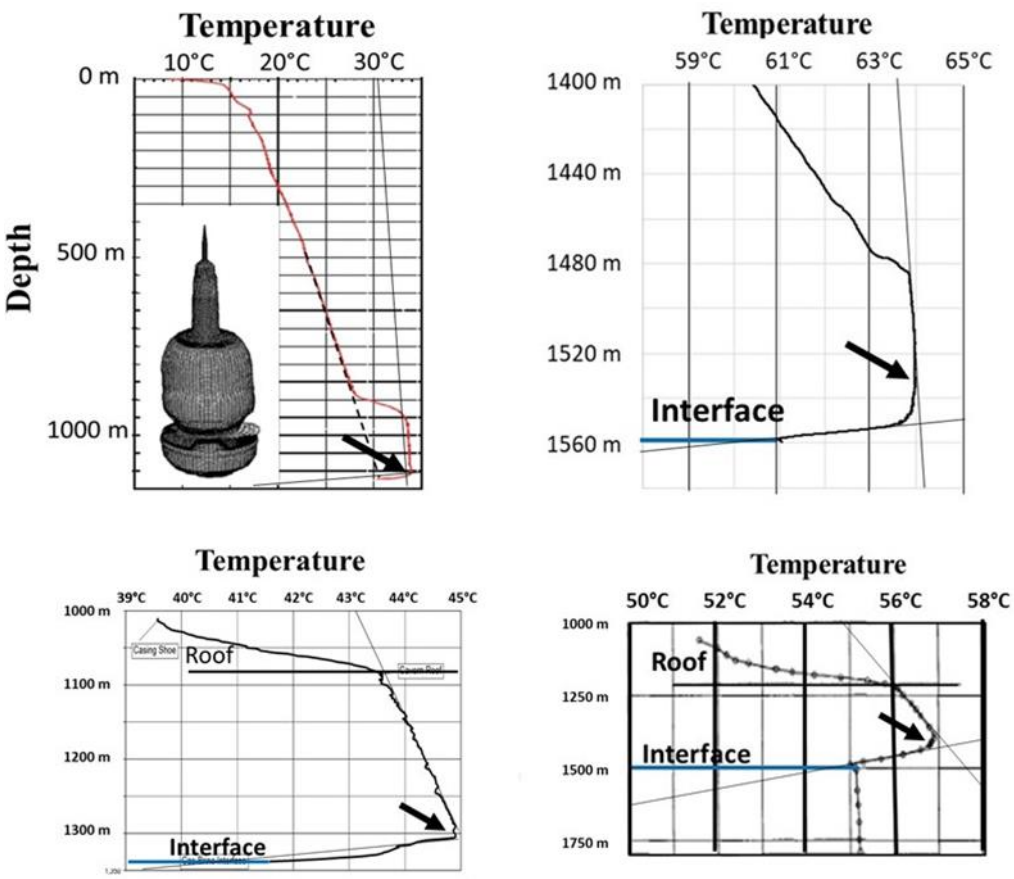

Figure 10. Vertical temperature profiles along the axes of symmetry of gas storage caverns (Bérest and Louvet, 2020; Berger et al., 2002; Klafki et al., 2003b; Thaule and Gentzsch, 1994) showing the temperature-gradient inversion at cavern mid-depth above the gas-brine interface (black arrow).

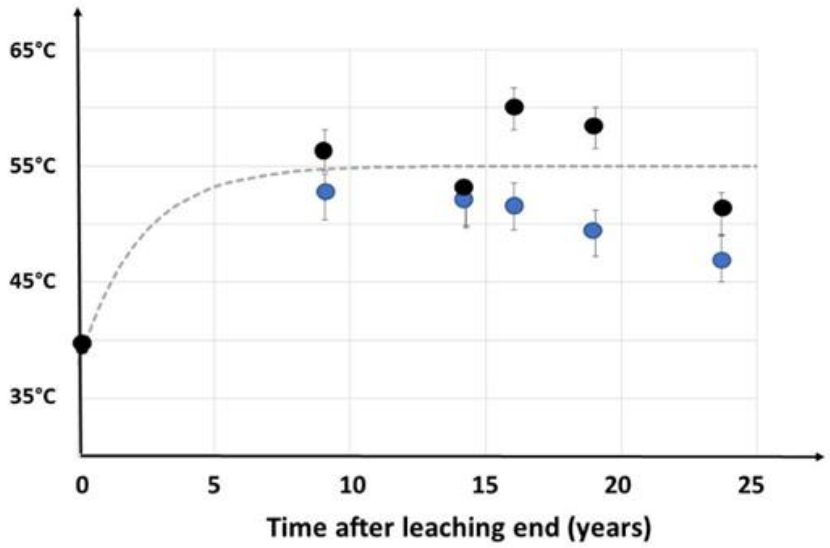

Figure 11. As-observed brine-sump temperature (blue dots), and average gas temperature (black dots) in a Storengy natural gas cavern. The dotted line is the computed brine-sump evolution when a 2.25-year characteristic time is assumed (Bérest and Louvet, 2020).

In this context, vapor content in the cavern is an important parameter during operation of a gas cavern.

Field data gathered in this paper suggest that, in the cavern, gas thermodynamic behaviour (its temperature, pressure and water content) is influenced by several coupled phenomena. During pressure cycles, temperature evolution is dictated by gas expansion-contraction and heat exchange with the rock mass. In addition, water vapor condenses in the entire gas body and evaporates at the brine-gas interface at the cavern bottom, an asymmetrical process leading to cooling of the brine sump, which remains perennially cooler than the rock mass, especially when cycles are frequent. The geothermal gradient generates natural convection in the upper part of the cavern; natural convection is impeded in the lower part of the cavern, above the brine sump, creating a buffer for water vapor diffusion in the cavern. These phenomena are important when purity of the withdrawn gas is required. Qualitative explanations are provided in the paper; more quantitative results can be obtained through numerical computations.

2.2 Tightness of salt caverns

Summary

Generally speaking, salt permeability is exceedingly small. However, in-situ tests proved that the overall cavern permeability experiences a significant increase when fluid pressure at cavern depth is larger than 80-85% of the geostatic pressure. Several incidents proved that breaches or conduits can be created or pre-exist between a cavern and a neighbouring cavern, or between a cavern and the boundaries of the salt formation. The origin of most of these incidents is the presence, see below, of Anomalous Zones (see Section 2.6) in the salt formation. In-situ tests proved that the overall cavern permeability experiences a significant increase when fluid pressure at cavern depth is larger than 80-85% of the geostatic pressure. However, as in most pressure vessels, it is the "piping" (the access well) that most often is the weakest point. Several incidents are described in this Section. The origin of most of these incidents is the presence of a single casing between the stored product and the rock formation.

2.2.1 Introduction

Prompted in part by projects related to carbon dioxide (CO_2) sequestration in which long-term tightness is crucial, and hydrogen (H_2) storage in salt caverns, in which the high flammability of gas is an important concern, there has been an increasing interest in the tightness of hydrocarbon (oil and gas) storage wells. In addition, high profile incidents, such as the 2015 Aliso Canyon blow-out, in California, have raised public awareness. The Aliso Canyon incident involved a massive gas leak from a depleted reservoir natural gas storage facility, the cause of which was a failure of the production tubing in a production well at around 2577 m (8450 ft) and consecutive leak from the well at a shallower (around 134 m, or 440 ft.; Long et al., 2018).

This section focuses on hydrocarbon storage facilities using salt caverns, access to which in most cases is through a single well or, more rarely, through a number of wells. These wells are of similar design and construction to those used in the oil and gas industry.

Tightness is a fundamental requisite of any storage cavern. Tightness results from (Bérest and Brouard, 2003):

1. the properties of the rock formation (2.2.3.1),
2. the nature of the stored product (density, viscosity) (2.2.4 and 4.2),
3. the pressure selected for storage operation (2.2.4.2.2),
4. the design of wellbore completion (2.2.3.2), and
5. the quality of the cementing job and steel equipment (2.2.2).

In most cases, salt caverns walls are almost perfectly tight (several in *situ* tests proving this are discussed in Section 4), at least when the maximum gas pressure P_{max} at the depth of the last casing shoe or H is smaller than $\frac{P_{max}}{H \text{ bar/m}}$. A few exceptions are known (2.2.3.1). For this reason, as in most pressure vessels, the tightness problem is with the ''piping'' connecting the cavern to surface; i.e., the completion (casing and tubing) and cementation of the wells (2.2.3.2).

2.2.2 Oil and Gas well tightness. Statistical analyses

Research and innovation on cementation have been ongoing since the early days of oil and gas production. However, challenging hurdles are still being faced. The effects of a better cement quality, of better cementing procedures or of more stringent regulations cannot be easily checked through simple and unequivocal criteria; in case of an incident or accident, the *post-mortem* analysis, i.e., the statistical analysis of the largest number of cases and identification of correlations is difficult.

In a study of data for 315,000 oil, gas and injection wells held by EUB, the regulatory agency in Alberta, Canada, Watson and Bachu (2009) discussed the results of two mandatory tests for wells, which have

been required since 1995. The tests, undertaken within 60 days of drilling rig release and prior to well abandonment, are the Surface Casing Vent Flow (SCVF) test, and the Gas Migration (GM) test, which provide at least a first indication of well tightness. Watson and Bachu paper focused on abandoned rather than active wells. These results are relative to tests performed at ground level and there is a risk, as for any statistical analysis, that the relation between causes and consequences remains ambiguous. Data analysis shows that there is a correlation between SCVF/GM results and oil price (with higher price comes the incentive to drill more wells, or more difficult wells, although equipment and skilled workforce are scarcer), geographic location, and technology or regulatory changes. Additional influential factors are wellbore deviation, well type (drilled and abandoned wells have leakage occurrence rates smaller than cased and abandoned wells), abandonment method (wells in which a cement plug was placed across completed intervals have better results than bridge-plugged wells). Low cement top and exposed casings were found to be the most important indicator for SCVF/GM poor results.

Nicot (2009) surveyed abandoned oil and gas wells in the Texas Gulf Coast, drawing a list of factors, which are favourable for long-term tightness. The abandonment year is of special significance, as innovations were progressively introduced: Use of centralizers (1930), calliper surveys (1940), tagging of the cement plug, introduction of improved cement additives adapted to temperature, pressure, and chemical-specific conditions (1940), improvement of the quality of material used in well construction and abandonment. Nicot also outlines the promulgation of both specific plugging instructions by the Texas Railroad Commission (In 1934, the RRC promulgated specific plugging instructions, and did so again in 1967.) and the Drinking Water Act, publication of API national standards (starting 1953), increased scrutiny by the State (after 1983) and certification of plugging operators (1997). Nicot (2009) points out that problems lie in the plugging/abandonment performance rather than in the quality of the material used.

In a survey of new gas wells in the US, Miyazaki (2009) suggested that up to 10% of the wells leaked.

More specific to natural gas storages, Marlow (1989) undertook a survey covering some 6953 wells operated by twenty American Gas Association (AGA) member companies. He mentions that: ‘‘*Tests show that even when the most up-to-date cement types and techniques are used, leakage can and will occur in a significant number of cases*’’ (p. 1151). The number of wells with a known operation lifetime duration until the leakage was detected was 426 (6%), among which 77% leaked in less than 30 days (it is likely that they were rapidly repaired). Leak ages at greater than 10 injection/withdrawal cycles occurred in only 2.6% of cases. The only statistically significant correlating variables are depth and bottom-hole pressure. Wells that leak tend to be deeper (>4500 ft, or 1375 m) and have higher pressures (>3000 psig, or 210 barg).

It will be seen that significant improvements were made since the 1990’s, especially when well completion (number and length of the various cemented casings) in storage caverns is concerned (2.2.6).

2.2.3 Case Stories

In this section a different approach is adopted. Much information and experience are available from the 2000+ salt caverns used worldwide for hydrocarbon storage. This section draws on a report prepared by Réveillère et al. (2017) for the Solution Mining Research Institute (SMRI), representing a collaborative effort to gather and explain all wellhead failure, overfilling, or casing leaks incidents in the salt caverns storage industry; provided that public information was available, reliable and precise enough to gain a satisfactory understanding of the event. This analysis builds on 12 cases whereas the SMRI report detailed 21, in order to focus on casing leaks incidents (overfilling and wellhead failure are not considered in this paper). Cases which were not considered in the SMRI report imply breaches at the cavern walls (discussed in Paragraph 2.2.3.1), operational problems or surface piping failure. Two cases in the SMRI report – Conway and Yoder, Kansas – were merged in the present Report. The twelve cases of loss of tightness in salt caverns due to a leak through or along the cemented casing are described briefly in Paragraph 2.2.3.2. Note that two cases (Eminence salt dome and Bolling) will be repeated in Section 3.3, Casing

overstretching, as the origin of the leak is excessive creep closure). The second part, draws general lessons learned from these cases, Paragraph 2.2.4).

2.2.3.1 Case Stories, Cavern breaches (Cavern tightness)

Information on salt caverns used for brine production and hydrocarbon storage in which a breach was detected include some well-known cases. Information of these cases is provided in Figure 12 to Figure 17, and summarized below (More details can be found in Bérest et al., 2019b; Réveillère et al., 2017).

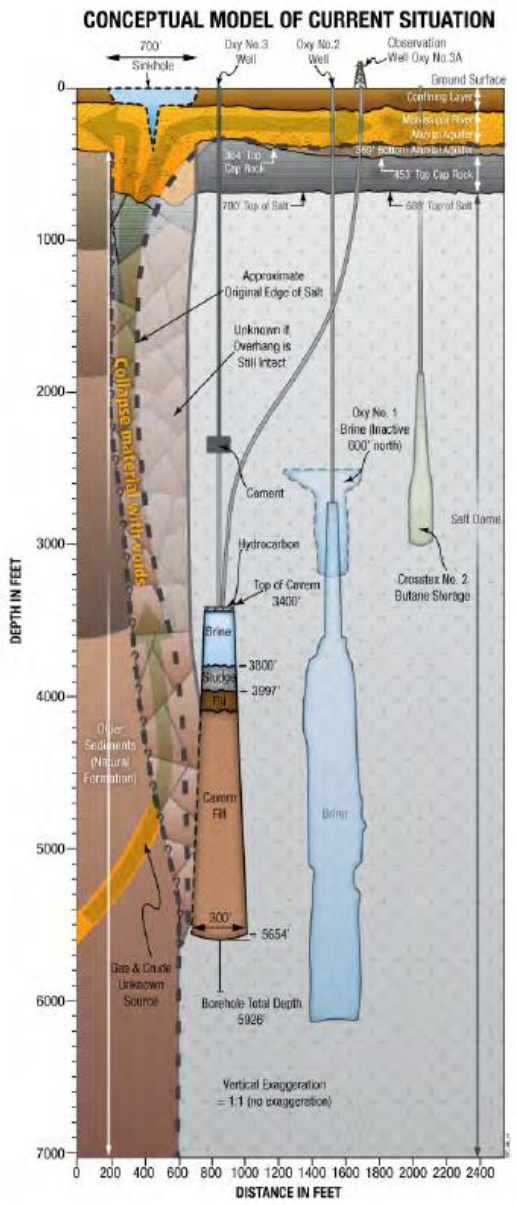

Figure 12. Bayou Corne Oxy 3 conceptual model (Blue Ribbon Commission, 2014).

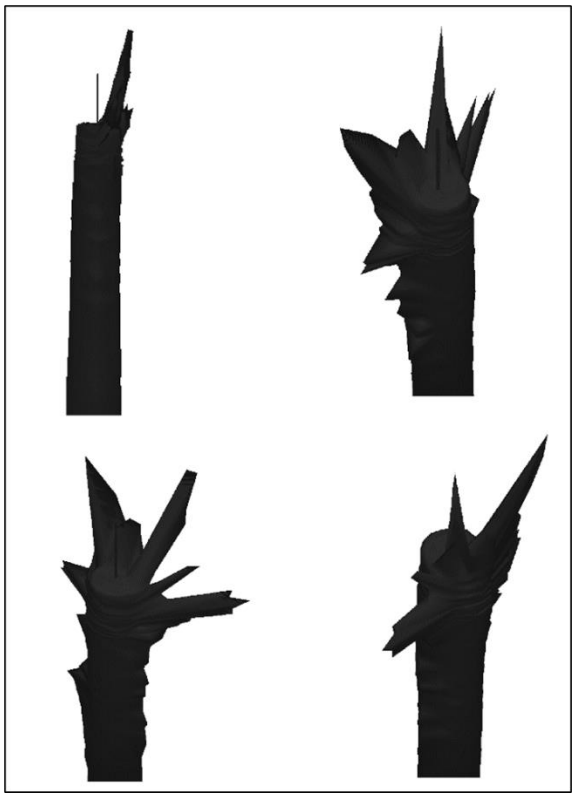

Figure 13. Mont Belvieu Cavern 16E roof area. Isometric Illustrations of cavern roof area sonar survey run in the well without hanging strings (Cartwright and Ratigan, 2005).

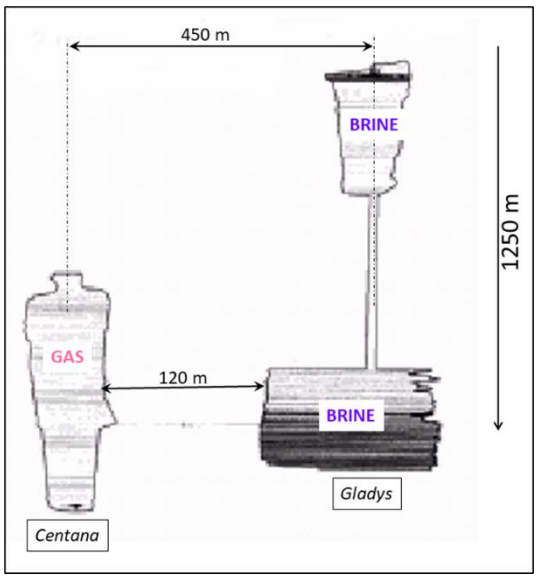

Figure 14. Spindletop Centana 1 and Gladys 2 caverns (after Johnson, 2003).

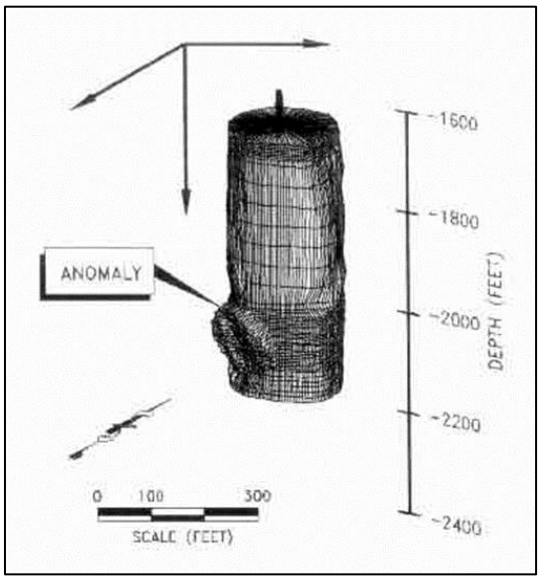

Figure 15. Clovelly Salt Dome Cavern (McCauley et al., 1998).

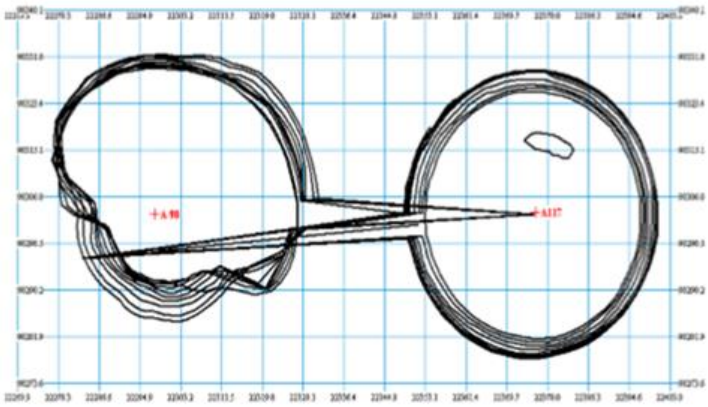

Figure 16. Arabali Caverns a-98 and a-117 (Kirmic and Rałowicz, 2003).

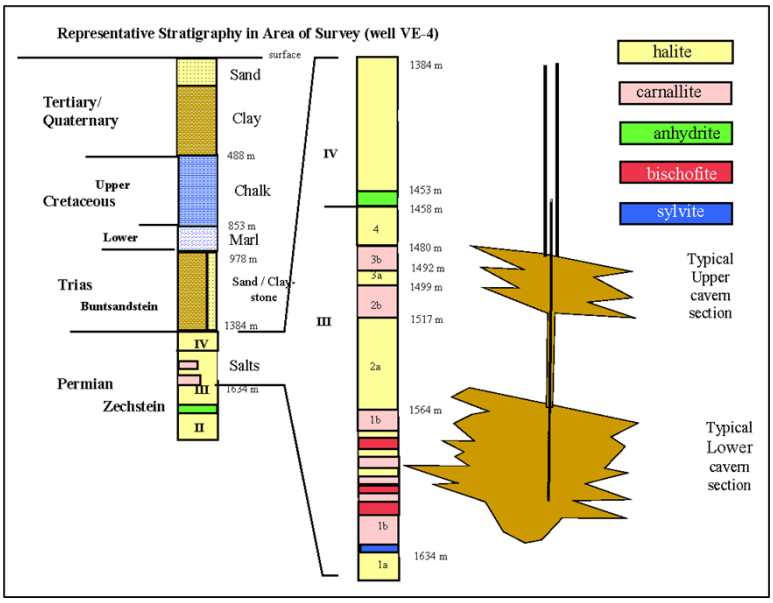

Figure 17. Stratification of salts near Veendam, the Netherlands (Fokker et al., 2004).

2.2.3.1.1 Bayou Corne, Louisiana, 2012

As illustrated in Figure 12, a sinkhole was discovered in the swamp near Bayou Corne, Louisiana, on August 3, 2012. It quickly was suspected that the sinkhole was connected to Oxy3, a brine cavern located near the edge of the Napoleonville salt dome. Oxy3's roof was at a 1050-m depth and its height was 670 m. Further investigation proved that loose and soft sediments flowed along the dome flank from ground level to a breach created in the lower part of the cavern where the salt wall was thin.

2.2.3.1.2 Mont Belvieu, Texas

A Mechanical Integrity Test (MIT) and pressure observations proved that Cavern 16E and neighbouring Cavern 2E, two brine caverns in the Mont Belvieu, Texas, site were connected hydraulically; origin of the breach is likely to be an Anomalous Zone inside the dome

> *("The term "anomalous features" (Afs) has been used by Kupfer (1990) to designate unusual features found in the stocks of Gulf Coast salt domes. Based on observations made in rock-salt mines, he identified ten major groups of Afs, including such items as intense structural folding, the presence of "impurities" (e.g., anhydrite, shales, and sandstones), gas releases, connate brine seeps, exceptionally large crystal size, potash, hydrocarbons, etc. He observed that these unusual features tended to cluster in linear trends through salt stocks; and, if they contained three or more Afs, [he] designated such trends as "anomalous zones (Azs)" (see also Looff, 2017; Thoms and Neal, 1992, p.1).*

More on Anomalous Zones can be found in Section 3.4.

2.2.3.1.3 Spindletop, Texas

Gas originating from the Centana No. 1 natural-gas storage at Spindletop, Texas, leaked to the Gladys No. 2 brine cavern, although the minimum distance between the two caverns is 120 m (Figure 14). Asymmetric growth and brine contamination by sylvite during an earlier enlargement of Centana No. 1 suggest the presence of a heterogeneity.

2.2.3.1.4 Clovelly salt dome, Louisiana, 1992

Clovelly salt dome Cavern No. 14, in Louisiana (see Figure 15), an oil storage cavern, did not pass an MIT. This cavern is close to the side of the dome. Further investigation suggested that brine leaked to the exterior of the dome through a 660-m deep "*inhomogeneity*".

2.2.3.1.5 Arabali brine field, Turkey

In the Arabali brine field, Turkey (Figure 16), a hydraulic connection was detected between Caverns a-98 and a-117. Sonar surveys suggested that a 9-m-high, 30-m-long, 2-m-wide slot was created between the two caverns, exactly coinciding with the vertical plane crossing through the hanging strings of each of the two caverns, a puzzling circumstance.

2.2.3.1.6 Veendam, the Netherlands

Regarding Figure 17, at Veendam (the Netherlands), the mining method consists of selecting a rather high brine pressure (85% of geostatic) in the cavern to allow the Mg-salt to flow (''*squeeze*'') at a rate comparable to the solution-mining rate (Fokker et al., 2004) (Over time, the cavern volume remains roughly constant.) On April 20, 2018, "*a sudden pressure drop occurred in the cluster* [a labyrinth composed of many roughly permeable conduits interconnecting nine caverns.] *Pressure dropped by about 2.5 MPa after 1 day and by about 3 MPa after 2 days, after which the situation stabilized*" (Smit, 2019 p. 2). The brine volume that seeped from the cluster during the first 30 minutes was estimated to be 25 000 m^3. It has been hypothesized that the initial fracture or breach through the relatively thin salt layer (a dozen meters) at the top cluster opened in the overlying Buntsandstein layer, where the state of stresses is suspected to be strongly anisotropic, favouring swift fracture growth.

2.2.3.1.7 Weeks Island, Louisiana

Somewhat related to this theme, the Weeks Island case is typical (Figure 18). This is a two-level room-and-pillar mine with the two levels, measured to the mine floor, 163-m (mined from 1902 to 1955) and 224-m (mined from 1955 to 1976) below the surface, respectively. The rooms height was 22 m to 23 m, the pillars were 30.5-m wide, and the rooms were 15.2-m wide, resulting in an extraction ratio of 55% (Bauer et al., 2000; Neal et al., 1995). Two sinkholes, the first one in 1992, appeared at ground level above the edge of the mine. Evidences suggested that brine was seeping to the mine, which was abandoned in 1995 (Bauer et al., 2000). Sinkhole creation was unexpected because the mine, which was stable during mining operations (Carosella, 1978), had been converted to an oil storage facility in 1981 and contained such (relatively) high fluid pressure in the mine that drastic mechanical evolutions (following conversion) did not seem likely. In fact, numerical computations (Bauer et al., 2000) suggest that the following sequence of events: creation of the mine – redistribution of stresses in the rock mass from 1902 to 1981 – increase of mine pressure resulting from filling with oil – new redistribution of stresses in the rock mass – may lead to the development of tensile stresses in the rock mass and formation of leak path crossing the salt formation from the mine to the edge of the dome. Similar sequences are present in gas caverns and may explain cavern permeability increase when gas pressure is high, see section 3.4 (Brittle Failure).

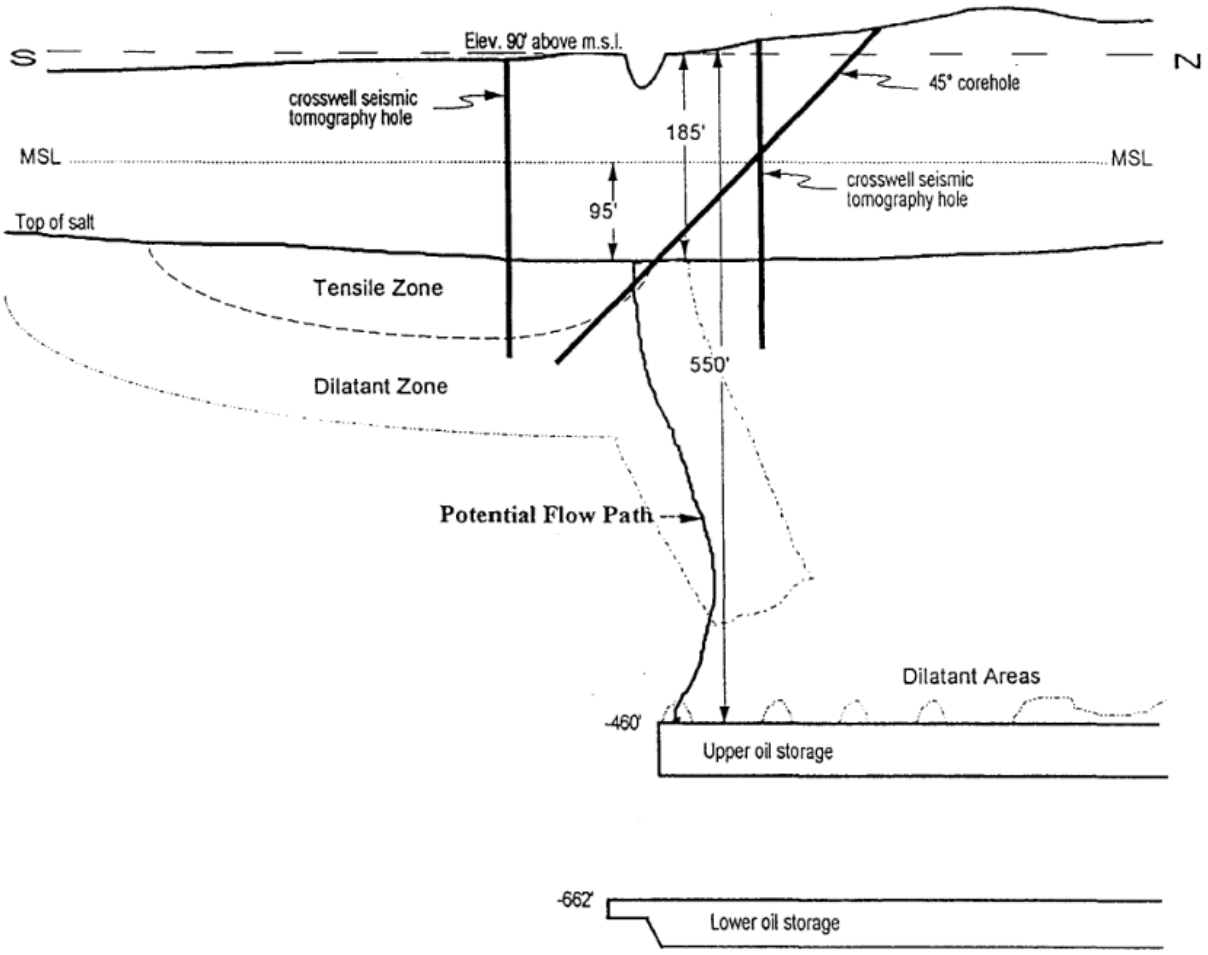

Figure 18. Weeks Island Mine. The mine was converted into an oil storage. Geomechanical modelling by Neal et al. (1995) showed mechanism for crack development in tension that would develop over mined openings after a number of years and progress through weakened dilatant zones (after Bauer et al., 2000).

Except for the last one, these examples prove that tightness can be lost:

1) when a cavern is too close to the salt formation boundaries, or:
2) when a cavern intersects an Anomalous Zone,

two circumstances that can be avoided when geological/geophysical investigations and tightness tests are performed.

2.2.3.2 Case histories, Well leaks

2.2.3.2.1 Eminence salt dome, Mississippi, 1970, 2004 and 2010–2011

The Eminence salt dome is located 20 km (12 miles) northwest of Hattiesburg, Mississippi. The top of the salt is between 730 and 743 m (2400–2440 ft); it is overlain by a 150-m thick cap-rock of limestone and anhydrite. In 1991, this natural gas storage site comprised seven caverns. Caverns #1–#4 were certificated in the early 1970's and caverns 5, 6 and 7 in 1991. These caverns are especially deep, from 1725 m to 2000 m in the case of Cavern #1 (Fig. 3). For those wells drilled in the 1970s, a surface casing was set and cemented at 50 ft. A 2800 hole was then drilled to 2700 ft (823 m) and a 2000 OD cemented casing set, and the last cemented casing shoe, diameter 133 —8 00, was at 1737 m (5700 ft) depth (Allen, 1972, 1971). Cavern #1 was filled with gas at a 70 bars (1000 psi) pressure over a period of 2 months, after which it was increased to 280 bars (or 4000 psi; geostatic stress at cavern depth is 380–450 bars). After a second pressure cycle, the ''*cavity bottom was at 1953 m (6408 ft), showing a loss of 46 m (152 ft) in about two years''* (Baar, 1977; Coates et al., 1981) and cavern volume loss was 40% (Figure 19), see also Section 3.

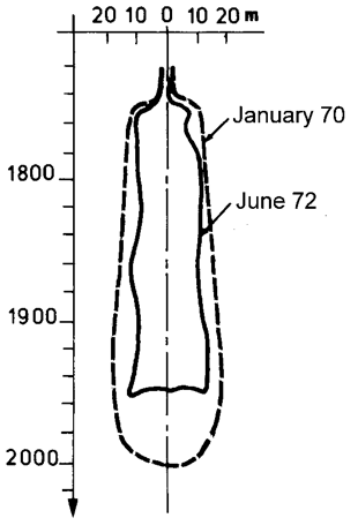

Figure 19. Extent of salt creep and decrease in cavern size for Eminence Cavern #1, as determined from cavern sonar surveys in 1970 and 1972. Based upon and redrawn from Allen (1972); Baar (1977); Coates et al. (1981); Bérest and Brouard (2003).

Once the problem was recognized, reduced losses were achieved through various measures, including maintaining a higher minimum pressure over extended time periods and less dewatering. In 2004, Cavern #4 well casing failed at a depth of 1639.5 m (5379 ft; Wellinghoff et al., 2013); i.e., a few dozens of feet above cavern roof. The company took Cavern #4 out of service, filling it with water and shutting it in. On December 26, 2010, a large, unexpected pressure drop of 25 bars (357 psi) in one minute was detected in Cavern #3. The initial response to the leak was to flow ~8.65 million m^3 (306 MMcf) of gas into the pipeline system. Another gas leak from the wellhead of Cavern #3 was accompanied by water shooting into the air from on-site water wells. On January 4, 2011, the company began flaring gas from Cavern #3, until its production tubing became clogged with debris. Gas was also escaping from the ground around the wellhead of Cavern #1. A large cave-in occurred, sealing off the flow. The company began drilling monitoring wells in the surrounding freshwater zones. By January 24, 2011, the decision was made to

take Caverns #1 and #3 out of service. Later, a leak to the caprock was detected in Cavern #7 and maximum operating pressure was lowered from 248 bars to 191 bars (3600 psi–2775 psi). Investigations revealed that leakage in Cavern #3 well likely arose through salt creep leading to overstretching (see Section 3.2) of the casings above the cavern, where displacements due to creep closure were especially intense (Wellinghoff et al., 2013). These excessive strains led to damage of steel casings and/or steel-cement and cement-rock interfaces, as a result of which, gas migrated up the well to the cap-rock and ultimately to surface.

2.2.3.2.2 Elk City, Oklahoma, 1973

On February 23, 1973, the Oklahoma Geological Survey was informed that a central crater about 10 m by 15 m (30 ft by 50 ft) by 6 m (20 ft) deep, plus 20 m–50 m (160 ft–360 ft) -long pressure cracks radiating from the crater, had appeared in level grassland, about 8 km (5 miles) south of Elk City, Oklahoma. Siltstone blocks of 20–45 kg (50–100 pounds) were thrown as far as 23 m (75 ft.) away, and several 30-ton boulders were lifted to an upright position (Figure 20, left), and 5 m (15 ft.) tall trees in the vicinity were tilted 45°. On March 1, 1973, gas samples were taken at the blow-out site. Analyses revealed 1% total hydrocarbons, of which 75% was propane, a result excluding any natural origin. A leak from a propane salt storage cavern leached out from the upper part of the Permian Blaine formation was suspected. Several investigations and tests were undertaken at that site. A 13-hour observation period with the cavern maintained at constant halmostatic pressure was performed (i.e., with the inner tubing filled with saturated brine and opened at the surface). This test found a 30-gal/day (5 L/h) apparent leak in the cavern (such a test is not fully conclusive as phenomena other than a leak can explain such an outflow, see Section 4.2, Tightness tests). The storage cavern was emptied, with the propane being displaced from the cavern by brine on March 28. The two inner strings were retrieved and checked for flaws (Figure 21).

Figure 20. Central crater (left, from Fay, 1973a) and one of the pressure cracks (right, from Fay, 1973b) discovered on February 23, 1973.

A cement-bond survey was run to assess cementing around the 10-¾" casing string. The survey demonstrated that the lower 60 m (200 ft), from about 341 m to 411 m (1120 ft–1347 ft), in which a special resin cement had been used, was well bonded and that the upper 341 m (1120 ft) was poorly bonded. This strongly suggested that the leak was between 35.5 m and 340 m, a zone in which the well was equipped with a single cemented casing (instead of two casings above 35.5 m). As illustrated in Fig. 5, liquefied gas would have leaked through a weak point in the well casing, migrated upwards in the poorly cemented annulus until it reached the Doxey shales. From there it would have migrated laterally to the blow-out site 700 m away from the wellhead and at 23 m lower elevation. The liquid LPG pressure would have decrease along the migration, triggering LPG vaporization at some point. The mechanical energy

liberated by the vaporization generated the crater and cracks observed at the surface. Both retrieved strings were then run back into the well with a packer added for isolating the annulus at 365 m (1197 ft). This annulus was filled with inert water and tested for leaks (Figure 21). No leak was detected and neither did a pressure test on the cavern prove any leakage. The storage well was returned to service on April 23, 1973. There were no later reported leakages similar to the one that led to the blow-out, suggesting that the breach depth was located above 365 m depth, a zone now covered by two casings and a monitoring annulus.

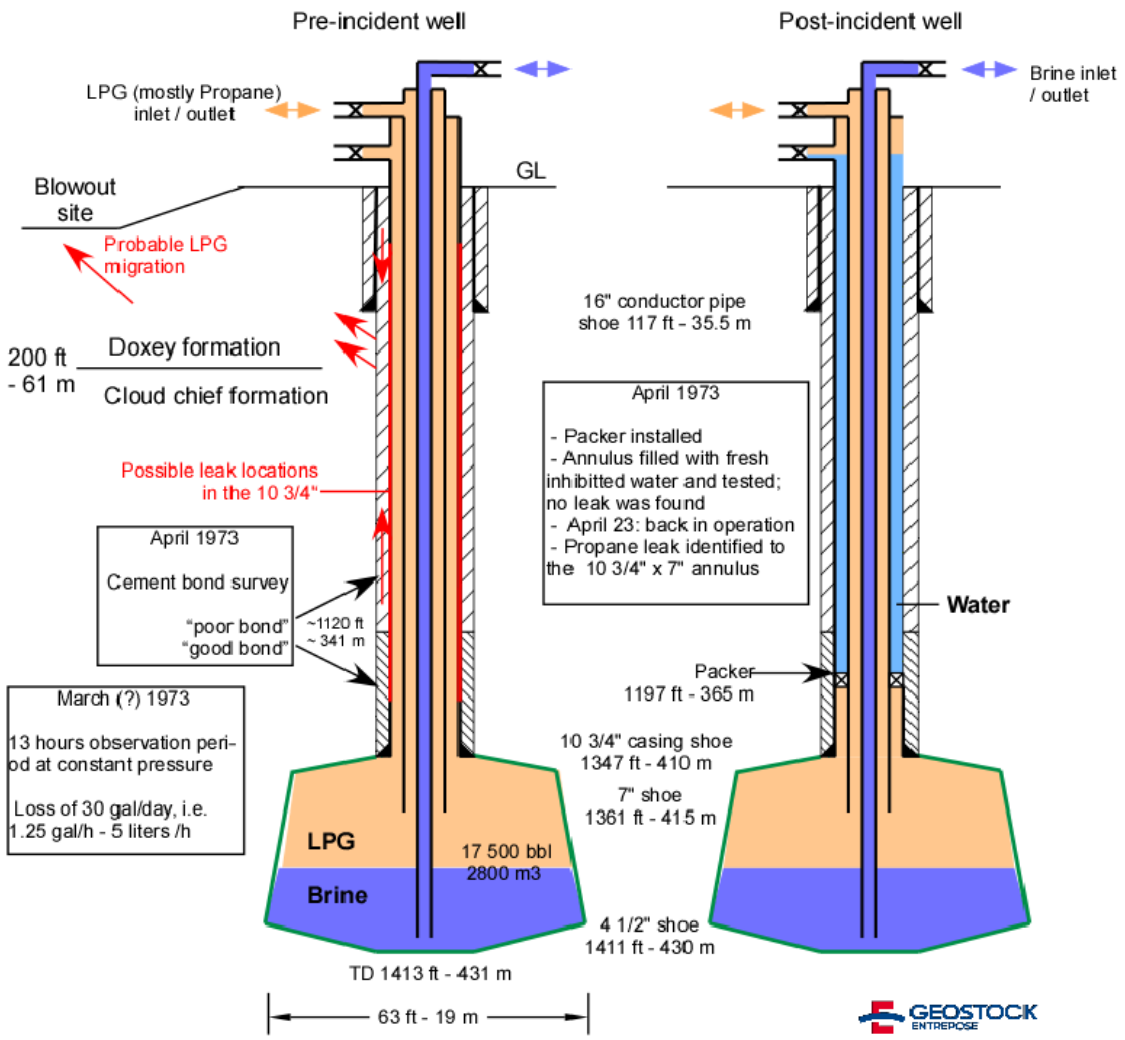

Figure 21. State of the well before and after the incident, probable leak path (in red) and summary of the main investigations (From Réveillère et al., 2017).

2.2.3.2.3 Conway-cavern field (Hutchinson salt formation), Kansas, 2000

Over 600 solution-mined salt storage caverns are located in Kansas. Nearly 50% of these are near Conway, a small town in eastern Kansas, where underground storage of Natural Gas Liquids (NGLs) began in 1951. Evidence of fugitive NGLs was known as early as 1956 (Ratigan et al., 2002). Propane was detected in several operators and domestic wells, ultimately leading to the relocation of residents and demolition of the properties. The Hutchinson Salt Member of the Permian Wellington Formation from which the storage caverns were leached out, is shallow (around 120 m or 400 ft; Figure 22). It is overlain by two impervious shale formations (Ninnescah and Wellington shale formations), above which lies the Quaternary Equus Beds Aquifer, a source of potable water. The eastern boundary of the Hutchinson Salt Member is a dissolution boundary (Figure 22). In December 2000, fugitive NGLs were encountered in a recently drilled

cathodic protection at the Williams Conway Underground East (CUE) storage facility, which includes 71 caverns. Within a 1.6 km (1-mile) radius of this well, all wells (water, oil, observation) were investigated. NGLs were encountered in two more wells near brine recovery wells. The 71 operating wells were evaluated through pressure monitoring and temperature logs. As of March 15, 2002, nearly all the wells have been evaluated and none have been found to be a contributor to the fugitive NLG occurrence. Cement bond logs run in the wells revealed that casing cement-bonds were poor.

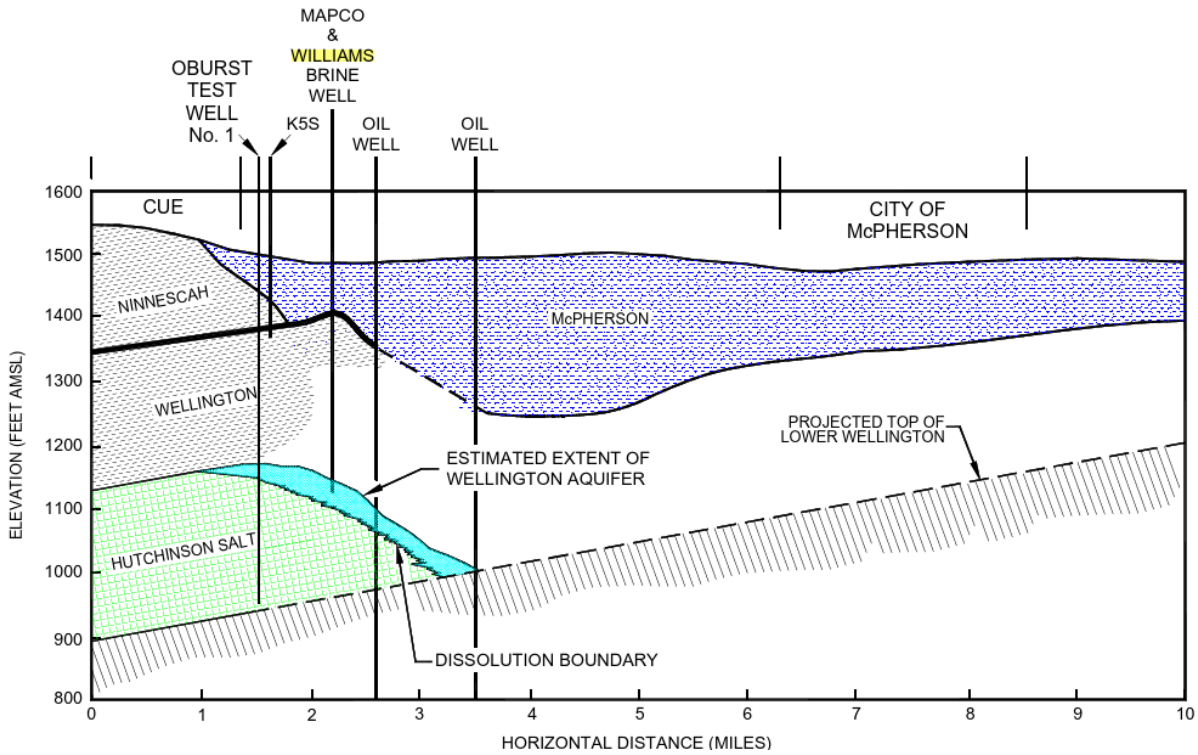

Figure 22. West-East cross-section of the Williams-CUE Facility (after Ratigan et al., 2002).

2.2.3.2.4 Yoder, Kansas, 1980

A similar incident occurred on June 30, 1980 near Yoder, Kansas, 9.7 km (6 miles) south of Hutchinson and 48 km (30 miles) south of Conway. A propane blow-out occurred along the shoulder of a county road. Bryson (1980) reported: ''*Groundwater and sand were blown fifteen to twenty feet into the air. Within twenty-four hours, the pressure of the propane in hole had abated. Within a week, the surface of the water in the blowout conduit was placid, however propane vapors continued to rise up through clay and silt surrounding the hole*''. In 2004, Johnson and Hoffine presented an update of the Conway investigations: ''*The results of the investigation indicated a plume of NGL located east of the Brine Production Test Well Willems No. 1. Geophysical logging of the Brine Production Test Well Willems No. 1 and adjacent Brine Production Well indicated poor cement bond along the casings. Subsequent abandonment of the Brine Production Well Willems No. 1 and recompletion of the Brine Production Test Well Willems No. 1 have resulted in a rapid and significant decrease in the concentration of NGLs in the adjacent shallow Monitoring Well CUE01-6S*'' (Johnson and Hoffine, 2004).

2.2.3.2.5 Mont Belvieu

This accident occurred in 1980 at Barber's Hill, near Mont Belvieu, Texas, where a salt dome was home to 134 solution-mined caverns (and 135 wells) used primarily for Liquefied Petroleum Gas (LPG) storage and distribution and for brine production (Ratigan, 2009). On September 17, 1980 a pressure drop was recorded at the wellhead of one of the salt caverns containing LPG. On October 3, a spark from an electrical appliance ignited gas (70% ethane, 30% propane) that had accumulated in the foundation of a house in the area, causing an explosion; there were no casualties. The cavern in which the pressure had

dropped was emptied and filled with brine. In the days that followed, gas appeared haphazardly around the area, and 50 families had to be evacuated. Holes were spud into the water table above the salt to find and vent the gas. Investigations proved (Figure 23) that gas had leaked through a breach in the well casing – which was 22 years old – at caprock depth. Depths to caprock and to salt are 100 m (350 ft) and 300 m (1000 ft), respectively (Bérest and Brouard, 2003; Pirkle, 1986).

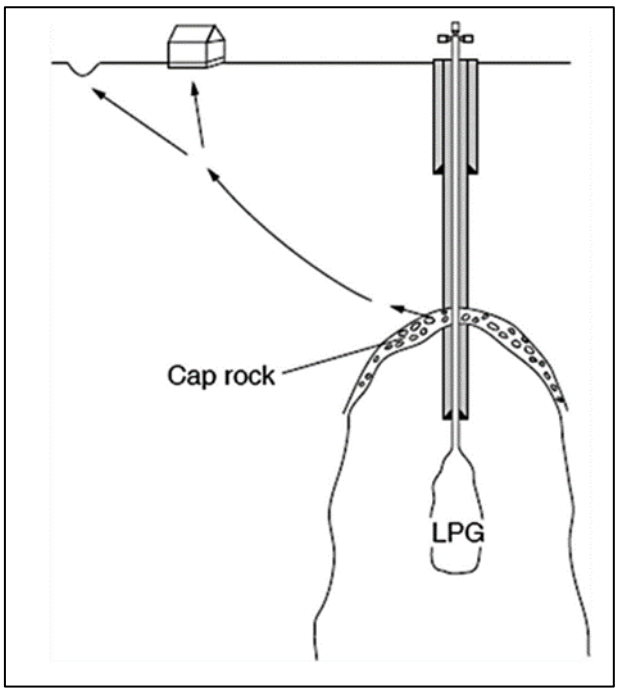

Figure 23. Conceptual sketch of an LPG leak from the Mont Belvieu cavern (from Bérest and Brouard, 2003).

2.2.3.2.6 Teutschenthal/Bad Lauchstädt, Germany, 1988

The Teutschenthal/Bad Lauchstädt storage site is located 40-km west of Leipzig, central Germany (Figure 25), Arnold et al. (2010). Bedded rock salt (halite) deposits lie at a depth of 500 m–1000 m (1500–3000 ft), with the thickness of the halite increasing to the SE, from less than 50 m to more than 500 m. The overburden comprises 300 m (1000 ft) of argillaceous rocks overlain by a 110 m (360 ft) thickness of an alternating sandstone and mudstone sequence (Figure 24). The well Ug Lt 5/71 was drilled and completed in 1971, within which the last cemented 11-⅜" casing shoe was set at 726.4 m depth, and the intermediate 16-⅜" casing shoe depth at 92.1 m (302 ft) (Figure 24). The cavern, with a volume of 40 000 m^3, was used to store ethylene (in a supercritical state). On March 29, 1988, a drop in pressure in the ethylene annulus of cavern Ug Lt 5/71 from 75 bars to 40 bars was observed. One hour later, the first eruption of an ethylene – water mixture took place 50 m (165 ft) away from the well and was followed by additional eruptions in a North-West direction and 250 m (800 ft) southward, close to the neighbouring cavern Ug Lt 6/71 (Figure 25). Elongated chimneys formed, from ejected debris and partly pulsating ethylene-water fountains, aligned along parallel WNW-ESE emission of ethylene continued for several days until an estimated 60–80% of the cavern volume was released. An area of 8 km^2 was evacuated. Ethylene outflow decreased rapidly. Immediately after the start of the eruption, elevation surveys revealed an NW-SE trending ellipsoid uplift of 0.2 m (0.7 ft). Fractures and crevasses, displaced concrete road pads, and fractures were found in a building at the crest of this uplift. This enabled an estimate of uplift prior to the blow-outs as around 0.5 m (1.7 ft). Subsequent downhole surveys found a damaged connection to the 11-¾" casing at a depth of 111.8 m, from which ethylene escaped and accumulated in a sandstone layer between 100 and 140 m depth. The sandstone lies below a 25-m thick impervious layer, which was uplifted and led to overstretching and failure of the 11-¾", ultimately resulting in a massive release of ethylene on March 29th.

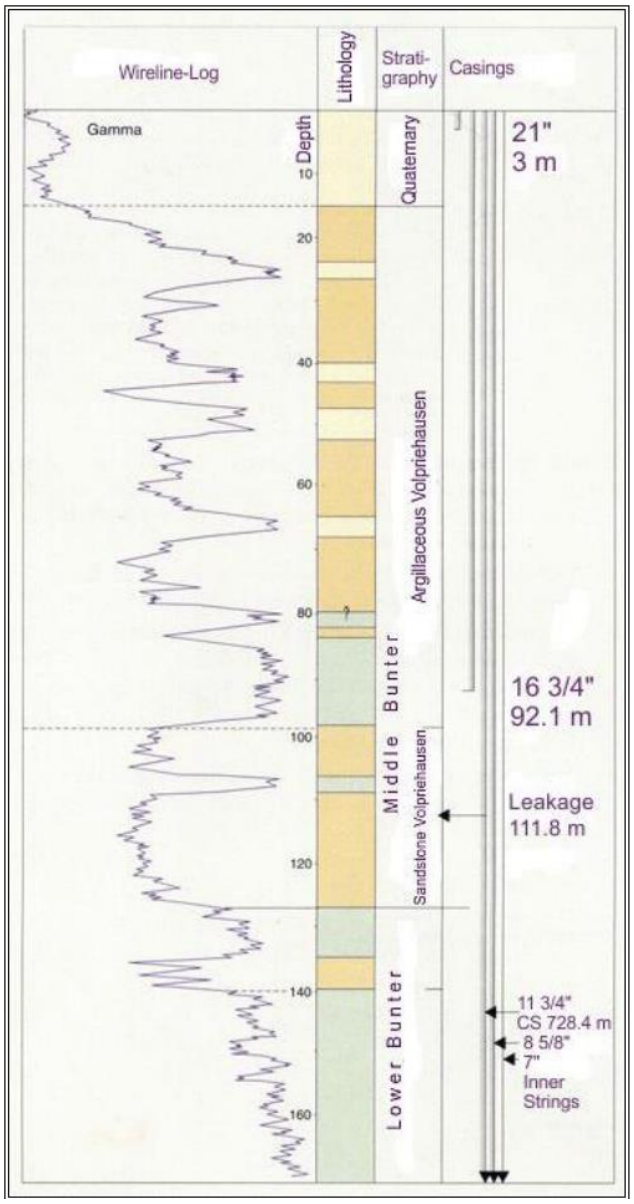

Figure 24. Casing program and top-hole geology of Ug Lt 5/71. Based upon and modified from Katzung et al. (1996).

Figure 25. Aerial photo of the site on April 3rd 1988 showing location of the well, the settlement area of Teutschenthal, alignment of eruptions and close up of main eruption fracture. Right side showing fault zones and area of uplift as dashed lines and elevation measuring points as squares. Based upon and modified from Katzung et al. (1996).

2.2.3.2.7 Clute, Texas, 1988

This storage cavern facility was constructed in the Stratton Ridge Salt Dome about 1.6 km (1 mile) NE of Clute in south Brazoria County, 25 km (15 miles) SSW of Houston, Texas. Several hundred oil and gas wells drilled across the salt diapir have established its shape and structure. The caprock is several hundred feet thick, comprising limestone, gypsum, and anhydrite beds and the diapir shows an unusual geometry, including a large structural depression in the eastern third of the dome. This and the features and problems associated with the caprock, which are most likely caused by active salt movement, indicate that the internal salt structure is complex and still evolving. The internal structure and fabric of the salt is thus likely to influence construction and operation of any storage caverns (Lord et al., 2006).

On December 27, 1988, company officials advised the Railroad Commission of Texas that they were aware ethylene had been lost from a storage cavern. By December 30, it was assessed that the loss amounted to 1850 m^3 (0.5 million gallons). Water wells in the area were tested but found no contamination (Toth, 1989a). It was decided to drill an exploratory well near the site to try and discover the whereabouts of the escaped ethylene and perhaps attempt recovery of some (Toth, 1990, 1989b). The first test well was drilled on March 19th, 1989 and the fugitive ethylene was immediately located. The escaped product was flared off and continued to be so until at least April 1990 (Toth, 1990). Company officials said the casing failure could have been caused by movement in the salt formation with product having escaped at around 396m (1300-ft) depth.

2.2.3.2.8 Mineola, Texas, 1995

This incident occurred in 1995 at the Mineola Storage Terminal about 145 km (90 miles) east of Dallas, Texas (Warren, 2006). Its cause and how the resultant fire at ground level was extinguished was described by Gebhardt et al. (2001). The facility had two storage caverns the wells to which were originally drilled

as oil producers in the late 1950s. One cavern, the volume of which was 49 000 m^3 (13 million gallons) of propane, suffered loss of product. Well completion included an 8-⅝" casing set at 484 m (1584 ft). The shoe of the 5-½" tubing string was 720 m (2400 ft) deep, 30 m (100 ft) above the cavern bottom; it seems that undersaturated water, rather than brine, was used as an injection fluid. The cavern well developed a casing leak at an undetermined depth. According to Gebhardt et al. (2001), the ''*initial*'' theory was that injection of undersaturated water led to dissolution and thinning of the salt pillar (wall) between the caverns; a leak was created when a workover was run on the second cavern, where nitrogen was being used in the workover to ensure that there was no LPG in the tubing. The pressure induced in the workover well caused fracturing in the salt pillar. In this theory, the pressure surge was transmitted to the cavern in LPG causing a breach in its well casing. Propane escaped from the well and migrated upwards, eventually escaping through surface soils to the atmosphere. It collected in low-lying areas around the terminal and surrounding forest and found an ignition source. The water-bearing shallow water sand was filled with LPG. A water well used to supply water for cavern leaching located approximately 50 ft (15 m) from the product withdrawal well was first to ignite and burn. This was followed by the cavern wellhead. Propane escaped through the soil up to 30 m (100 ft) from the well itself. Firefighters inferred from the characteristics of the fire that the casing leak was at shallow depth. Considerable efforts were required to extinguish the fire.

2.2.3.2.9 Hutchinson, Kansas, 2001

On January 17, 2001, at 10:45 am, a sudden release of natural gas burst from the ground under a store and a neighbouring shop in downtown Hutchinson, a town with 40,000 inhabitants in Kansas. Within minutes, the building was ablaze (Figure 26). During the afternoon of the same day, eight brine and natural-gas geysers began bubbling up, 3–5 km (2–3 miles) east of the downtown fire, some reaching 10-m (30-ft) in height, two of the geysers igniting. The next day, natural gas coming up from such a long-forgotten brine well exploded beneath a mobile home, killing two people. Also on January 17, 15 min after the first downtown blast and 13 km (8 miles) northwest of downtown Hutchinson, technicians from the Yaggy natural-gas storage recorded a gas-pressure drop of 7 bars (100 psi) in the S-1 salt cavern, whose casing shoe was 239 m (794 ft) below ground level. The underground storage facility was developed in the 1980s to hold propane. The owner became bankrupt, and the wells were plugged by partially filling them with cement. In the early 1990s the site was converted to a natural-gas storage. A link between the pressure drop and the events in Hutchinson was suspected immediately, even though the distance between the storage and the downtown geysers [10–12 km (7–8 miles)] set a puzzling geological and reservoir engineering problem. A plug was set at the bottom of the S-1 well and a downhole video run. This revealed a large curved slice in the casing at a depth of about 180 m (585 ft). It was suspected that various metal objects, including a steel casing coupler, had been dropped down the well when the former storage was abandoned. During the well re-opening, when the cement and cast-iron plugs were drilled, the system composed of the drill bit and dropped metal objects cut a slice ''*like a kitchen knife cutting into a can*'' in the 900 (23-cm) casing of the S-1 cavern at about the depth (179 m or 595 ft) of the later leak. Gas moved vertically up the outside of the casing from the breach until it reached a fractured gypsiferous/dolomitic horizon (G on Figure 27) at the top of the Wellington Shale Formation.

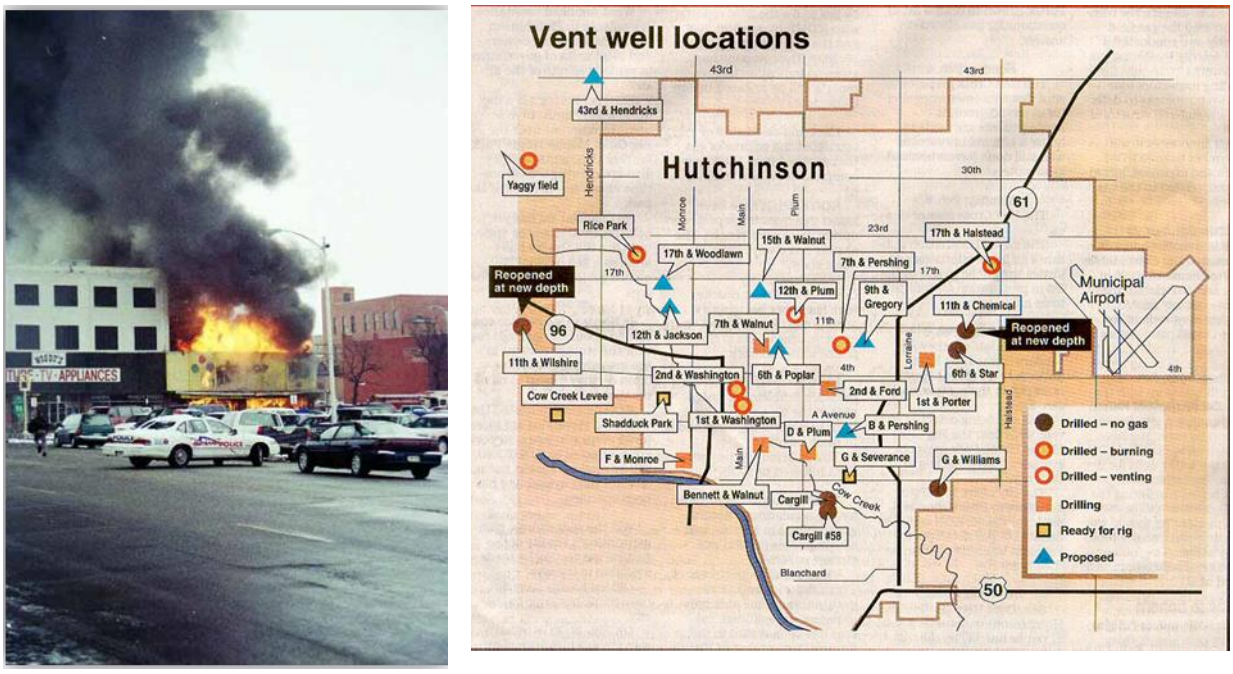

Figure 26. (Left) Initial fire at Hutchinson, Kansas. (Right) Gas venting wells (Kansas Geological Survey).

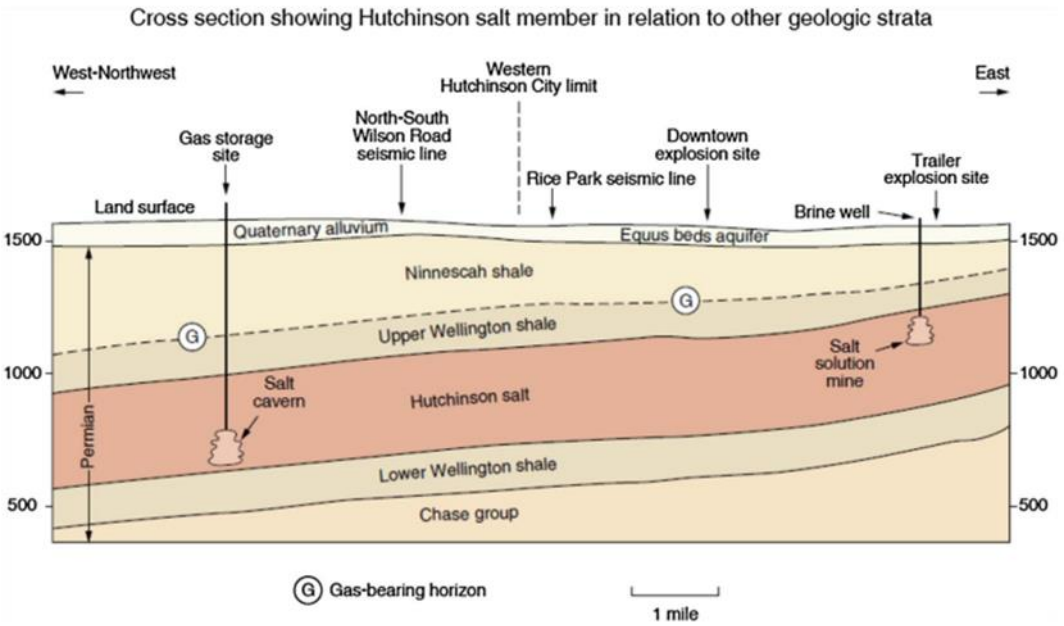

Figure 27. Hutchinson leak pathway. Quaternary alluvions are composed of sands and gravels, 15-m (50-ft) thick. Elevations are in feet. Below are the Permian Ninnescah Shale, the Upper Wellington Shale and the Hutchinson Salt member. The gas-bearing interval ranges from 82-m (270-ft) deep in the east side of the city to 122-m (400-ft) deep several miles northwest of the city; the dip is 6 m (20 ft) per mile. Gas migrated through fractured dolomite layers (G-G). (Kansas Geological Survey, 2001a, 2001b).

At this point the gas migrated laterally up-dip to the east towards Hutchinson, remaining trapped between the two impermeable shale layers, until it encountered the abandoned brine wells. Most of these were only cased down to a shallow aquifer. Clear evidence of the existence of multiple independent channels within the dolomite layer is suggested by the occurrence of a dozen geysers during the 24-h period following the first blow-out. The geysers appeared in the west and then progressively eastwards, and vented the accumulation of gas under the city, until no further gas eruptions occurred. In the following weeks, a number of seismic reflection lines were acquired to try to locate the gas migration path, and 36 venting wells were drilled. Only eight of them hit gas, supporting the view that migration of gas to surface

occurred along narrow pathways or channels within the dolomite layer (Allison, 2001). After 1997, the State had authorized a 17.5% maximum pressure increase, raising the maximum pressure at the casing shoe (239-m, or 794-ft, deep) to 47.8 bars (693 psi). This additional storage capacity remained largely unused for years on Cavern S1. Early in January 2001, gas was injected, and the pressure jumped from 29 bars (426 psi) to 47.6 bars (691 psi) at 6 a.m. on January 14. The pressure gradient was then 0.266 bar/m (1.18 psi/ft) at leak depth on January 14 and gas pressure was above the overburden pressure. The pressure began to drop at the wellhead, a move that, with hindsight, may be interpreted as a clear sign of increasing leak rate. The pressure build-up spread throughout the gas-filled fractured channels, ultimately reaching that of hydrostatic pressure beneath the Hutchinson area. After the accident, poor regulation and, when compared to other states, the small number of inspection staff in Kansas state, were implicated by several experts (e.g., Ratigan, 2001). New sets of regulations were discussed and imposed (Johnson, 2002). These included mandatory double casing in wells, corrosion control, restrictions on well-conversion (salt caverns designed to store LPG could not be converted to store natural gas, and cavern wells that have been plugged cannot be reopened and reused), a maximum pressure gradient of 0.76 psi/ft (0.173 bar/m) at the production casing shoe, and new testing requirements (with a Mechanical Integrity Test (MIT) performed every 5 years).

2.2.3.2.10 Magnolia, Louisiana, 2003

The natural gas storage facility of Magnolia is located at Grand Bayou, Louisiana, where several other storage and brine production caverns are operational. Salt roof is 200 m (600 ft) deep. In 2003, the facility included Caverns #13 and #14, drilled in the 1970's. On November 1, operators started filling the caverns with natural gas. On December 24, an underground gas leak led to the release of about 9.9 MNm^3 (0.35 billion ft^3) in a matter of hours. The gas migrated to an adjacent aquifer and then to the atmosphere. On December 29, cavern operations were suspended, and 30 residents were evacuated. The wells were plugged, and 36 vent wells were installed in the aquifer over the salt dome, of which 17 collected or burned off gas. Downhole videos were run in the wells. Several theories were put forward to explain the gas leak from around 440 m (1450 ft) below the surface. Causes of the leak were considered to be: crushed casings (EIA, 2006), cracks in the casing (Edgar, 2005; Hopper, 2004), separation of three or four casings connections permitting gas to leak behind the casing and then to the surface (Nations, 2005), or improper back-welding that resulted in cracks in the well casing (State of Louisiana, 2017). Video of Well #13 is reported as showing cracks in the casing near a coupling; the well had been plugged at the point of the lowest crack, after which the leakage stopped, which pointed to the cracks as a possible cause of the leaks.

2.2.3.2.11 Boling, Texas, 2005

Four caverns had been solution-mined and filled with natural gas between 1980 and 1983 in the Boling Dome near Boling, Wharton County, Texas. Depth to the caprock is globally about 192 m (630 ft), and the top of the salt occurs at a depth of around 305 m (1000 ft). Cavern roof depths are between 1066 and 1083 m (3497 and 3553 ft), except for Cavern #3, the roof of which is deeper by 45–60 m (150–200 ft). Apart from Cavern #3, casing shoe is close to the cavern roofs, 0–18 m (0–59 ft) above, which are flat (Figure 28). In the Fall of 2005, Cavern #4 was nearly full. An abnormally fast pressure drop was observed, which was monitored over a period of several weeks. Temperature loggings found cold spots in Caverns #1, #2 and #4, raising the possibility of a production casing leak not far above the cavern roof. During gas removal, the three caverns were filled with water.

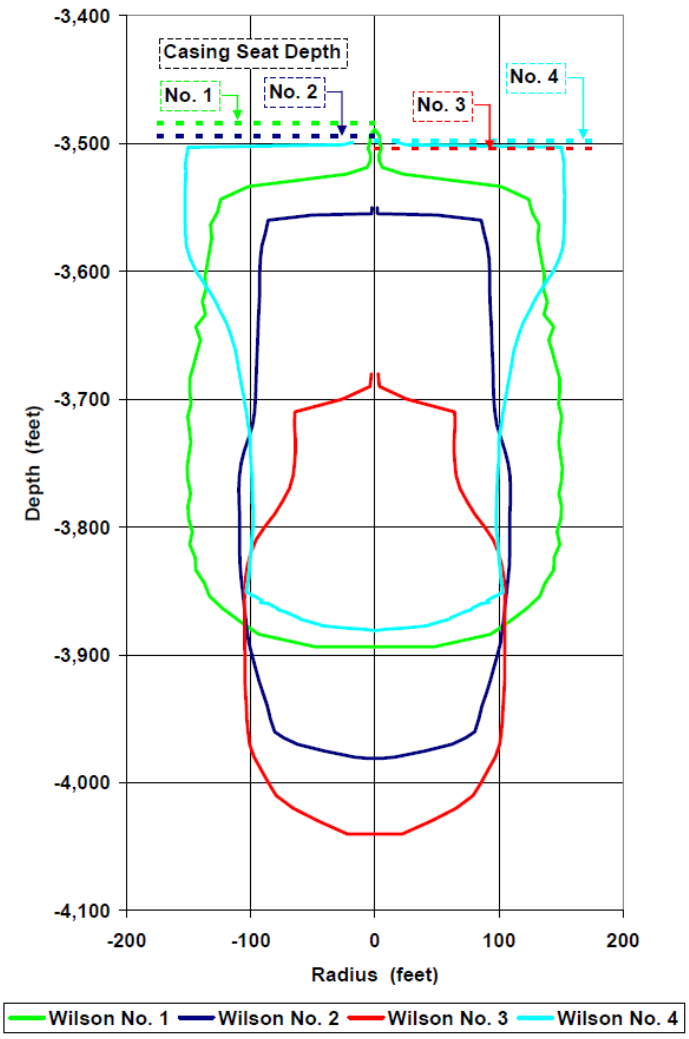

Figure 28. General cross-sections of caverns, based on sonar data. From Osnes et al. (2007).

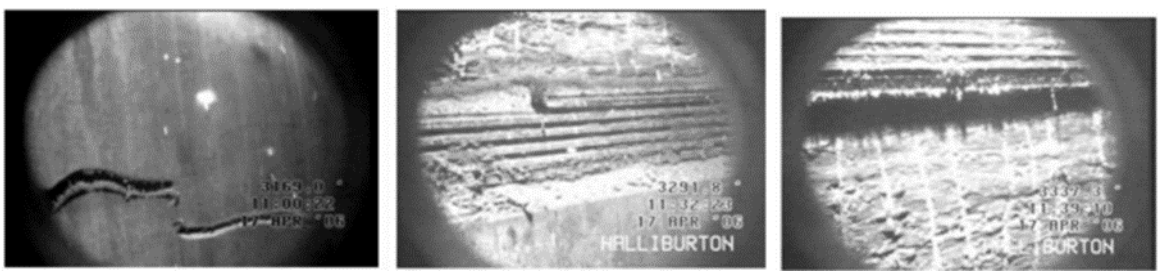

Figure 29. Examples of failures detected by the video inspection. From left to right: circumferential fracture of the pipe body, of the threaded coupling, and thread jump-out. From Osnes et al. (2007).

Detailed investigations into the incident were undertaken, including running downhole video camera logs, which identified casing collar and coupling partings for over 100 m above the casing shoe depth (Figure 29). The video log revealed that the casing had failed at eight different locations, always near or at a connection. Failure often was a circumferential fracture. The casing being dragged down after it fractured, up to 60 cm height of cement could be observed in between the two parts of the fractured casing. Fracture shape, the absence of any failure in Cavern #3 the chimney which was 60-m in height, and flat roofs, strongly suggest that casings were overstretched above cavern roofs and experienced tensile failure. This was confirmed by numerical analyses, that clearly showed the cemented casings of Wells #1, #2 and #4 were not able to accommodate the resulting large tensile salt strains, and their ultimate strength limit was exceeded (Figure 30). The well repair procedure for the three leaking wells included milling a 30 m

(100 ft) section from the original 11-¾" casing and cementing a 10-¾" welded liner. The new casing shoe, 30 m higher than the original one, was therefore in a zone where simulations suggest the strain induced by the salt creep should stay below the casing strength, thanks to this new 30 m long cavern neck.

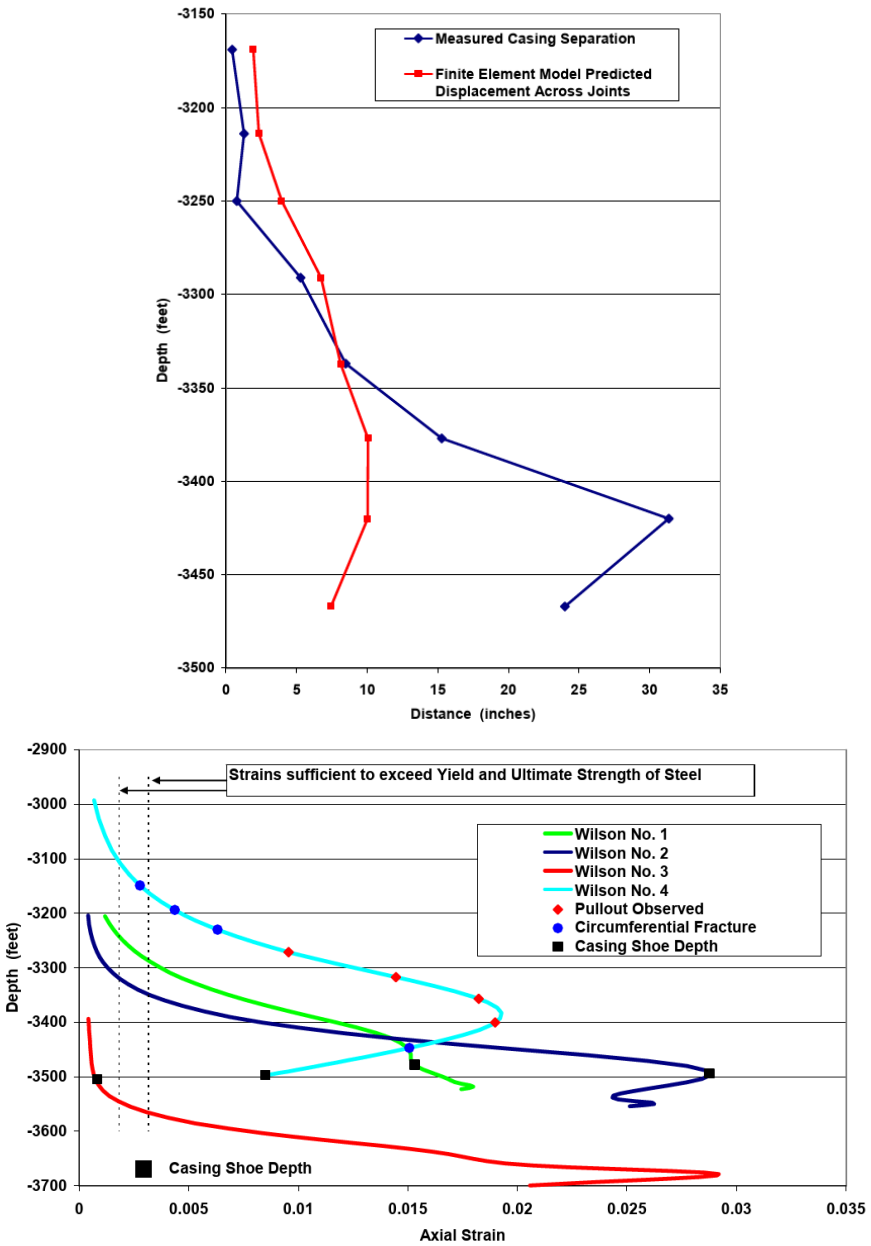

Figure 30. Observed and modelled casing deformations (Osnes et al., 2007). Top: comparison of measured casing separation and predicted relative displacements between casing connections from finite element modelling. Bottom: vertical strains as a function of depth in the salt near the centre lines of the Wilson storage caverns predicted from finite element modelling.

2.2.3.2.12 Epe, Germany, 2014

At the Epe site, 80 km north of Dortmund, Germany, several dozens of salt caverns have been leached-out from a 200–400 m thick sequence of halites overlain by clastic and argillaceous rocks; top of salt can be found at a 1000-m depth. The Epe S5 cavern is 147 m in height, with a diameter of 82 m (269 ft) and volume of approximately 450 000 m^3. In 1980, approximately 408 000 m^3 of oil were injected into storage. The cavern operated in brine compensated mode, with brine injected or produced through a 7-⅝" string to displace the crude oil through the 11-¾" —7-⅝" annulus. The last 11-¾" casing is anchored at a 1086.8-m depth and the penultimate 16" cemented casing at a 212 m depth. Typical of a strategic oil reserve, it

experienced only a small number of withdrawals or injections. On February 23rd and 24th 2014, a pressure drop of 3.6 bars was recorded in the annular space of Cavern S5. The cavern was taken out of operation and a number of inspection runs were performed in the well. These did not indicate any evidence of a leakage. The mining authorities agreed to commence operation again on April 2nd 2014 with restrictions regarding the maximum pressure. On April 12th 2014, an oil seep was discovered at surface in a meadow. On April 15th, two more spills developed close to a farm, inducing a family to leave their home for some days. After first analysis of the locations of the spills, it became clear that the origin of the crude oil was Cavern S5. The cavern was made safe and multiple efforts were undertaken to understand the reasons for the leakage, assess the extent of the leakage, minimize its impact and, ultimately, restore cavern integrity. Investigations and computations suggested that cavern convergence, evidenced by subsidence measurements at ground level, caused movement of the rock mass (salt) surrounding Cavern S5, especially at a depth of 217 m (Figure 31). The calculated vertical strain at a depth of 200 m is approx. 0.1–0.2 mm/m, enough to trigger a significant displacement on the casing connection at 217 m. Above 212 m, the completion, including the 16" casing, is much stiffer and stronger than the one casing section below and it was concluded that the first casing connection below the 16" casing shoe was a critical point for structural damage.

At a depth of 217 m crude oil pressure was 81 bars and capillary entrance pressure of the enclosing argillaceous series (mudstones) was approximately 47 bars. Pre-existing shear zones and fractures in the surrounding rocks re-opened, along which the crude oil migrated as the permeability of the matrix is too low for oil penetration. Upon reaching the base of the Quaternary series, the crude oil migrated into a shallow, groundwater aquifer and ultimately reached the surface. As a result of this incident, and as is already the case in the Netherlands, it is expected that to prevent that kind of incident in future, the regulations for operating storage caverns in Germany will require a double barrier installation for all wells (Bezirksregierung Arnsberg, 2014; Coldewey and Wesche, 2015; Kukla and Urai, 2015).

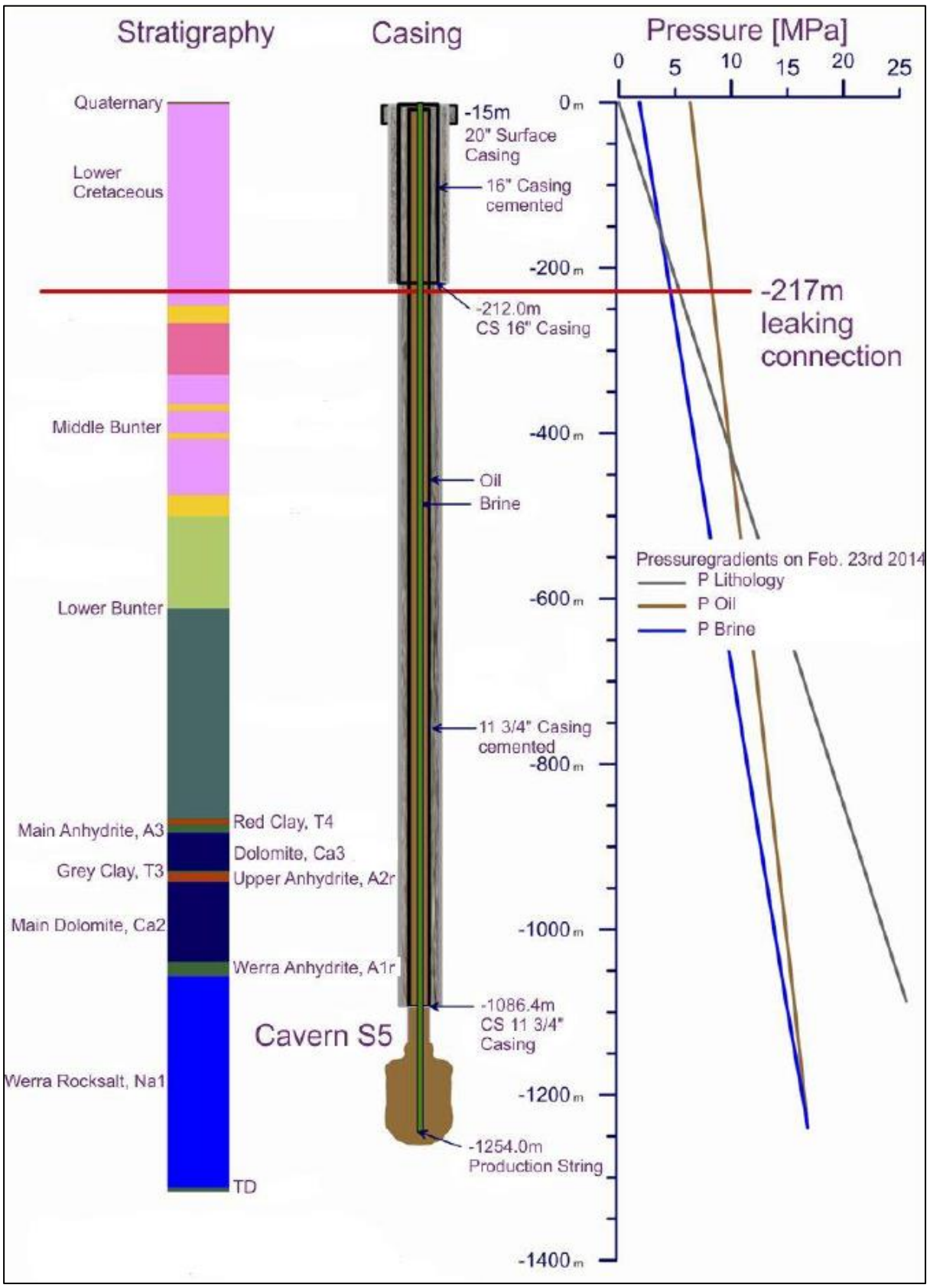

Figure 31. Well scheme and pressure gradients of Epe S5 (Stöwer, in: Réveillère et al., 2017).

2.2.3.2.13 Tightness of hydrogen storage caverns

Four hydrogen storage caverns have been operated worldwide:

- At Teesside in the United Kingdom, for more than 30 years, 3 salt caverns whose geometrical volume is 70 000 m^3 each, have been in operation. Each can store 1 million Nm^3 of almost pure hydrogen (95% H_2 and 3-4% CO_2). These salt caverns are located at an average depth of 370 m. They are operated according to the compensation method (average pressure is halmostatic).
- At Clemens Dome, Lake Jackson in Texas (USA) where, since 1986, Conoco Philips has stored 30.2 Mm^3 of hydrogen from synthetic gas (95% hydrogen) in an 850-m deep salt cavern. The salt cavern has a geometric volume of 580 000 m^3 and is operated between 70 bars and 135 bars.
- At Moss Bluff, Liberty County, Texas, since 2007, Praxair has stored 70.8 Mm^3 of industrial hydrogen in a salt cavern. The cavern has a geometric volume of 566 000 m^3 and is operated between 76 bars and 134 bars.
- At Spindletop Dome, in Beaumont, Texas (USA), Air Liquide commissioned in 2017 a 588 000 m^3 hydrogen storage cavern. The salt cavern is located at a depth of 1,500 m and its diameter is about 70 m.

No tightness loss has been reported from these six caverns which have been operated (in 2022) for a cumulated period of 150 years.

2.2.4 Lessons learned

The analysis of the leak mechanisms identified in the 11 cases previously described enables to identify some common patterns. In the following the onset and nature of a casing breach, the development of a leak, consequences at ground level and monitoring-prevention are discussed. These three successive steps are represented in Figure 32.

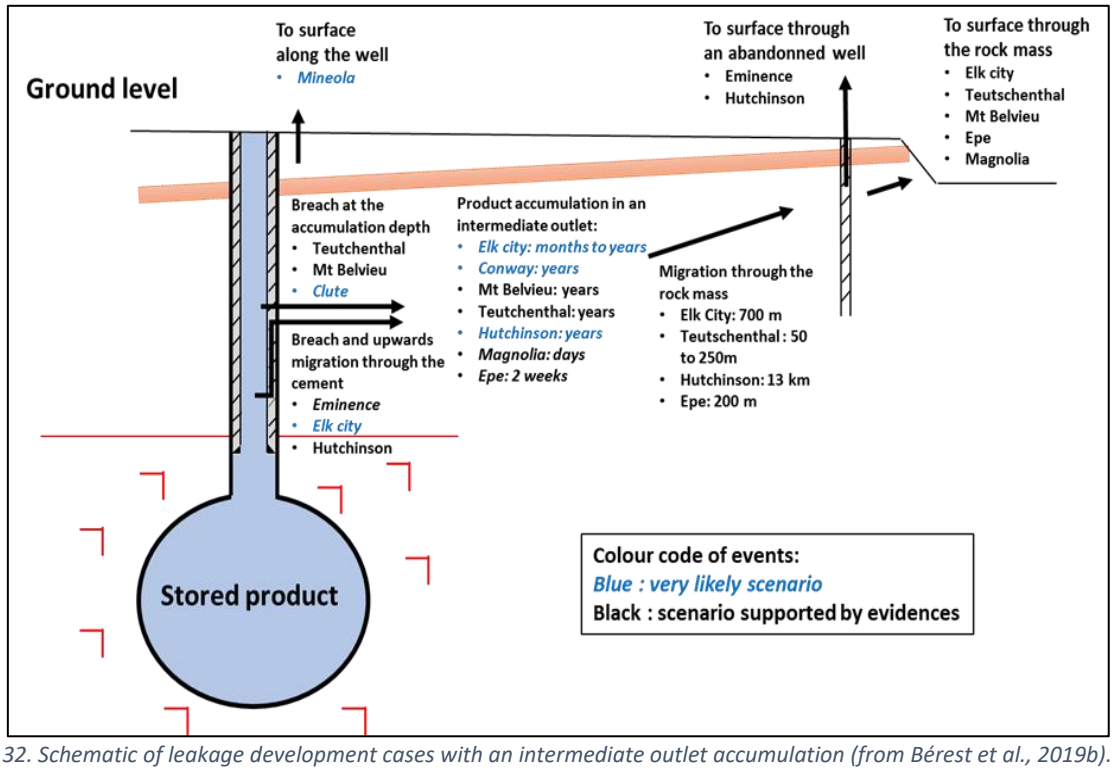

Figure 32. Schematic of leakage development cases with an intermediate outlet accumulation (from Bérest et al., 2019b).

2.2.4.1 *Onset of a breach*

2.2.4.1.1 Leak initiation

In most incidents, a breach (and leakage) is created through a steel casing at a depth where the well completion comprises a single cemented casing (‘‘*single barrier*’’). It is noteworthy that in the oldest wells, the depth of the penultimate casing shoe was shallow, and a single casing formed more than 50% of the total length. In the accidents described here, depths of the two last cemented casings were 35.5 m and 410 m at Mineola; 212 m and 1086.6 m at Epe; 823 m and 1737 m at Eminence; 92.1 m and 728.4 m at Teutschenthal (Figure 33). The breach may result from physico-chemical phenomena (internal and external corrosion), or in faulty screwed or welded connection between two consecutive pipes.

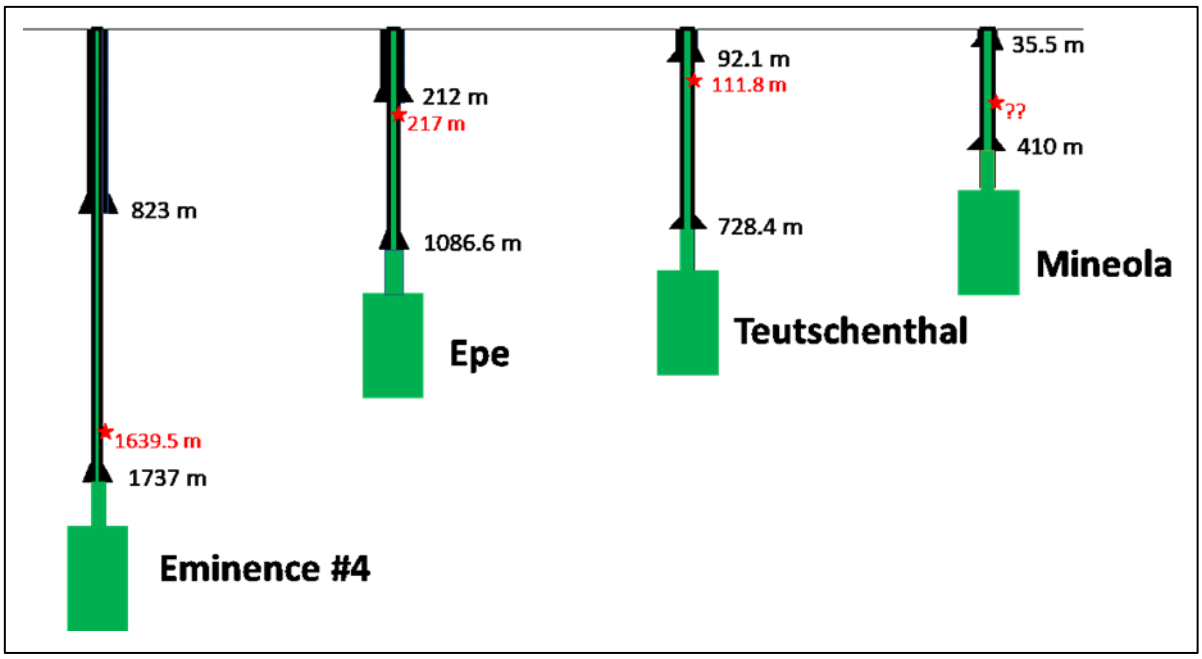

Figure 33. Depths of the two last cemented casings and depth of the breach through the tubing at Eminence, Epe, Teutschenthal and Mineola.

However, external mechanical phenomena may also contribute to the creation of a breach. At Hutchinson, a somewhat exceptional case, an LPG storage well on abandonment was plugged and cemented. When required for later natural gas storage, the well had been drilled-out. A slice was cut in the steel casing during drilling.

Deformation of the salt mass (or, more generally, the rock formation) is a more generic cause. Two basic cases can be distinguished, depending on whether the casing is subject to excessive tensile or shear stresses.

In the first case (see Section 3.3, Casing overstretching) the last cemented casing shoe is close to the cavern roof (the ‘‘chimney’’ or ‘‘neck’’ below the casing shoe is not very tall). In the case of Eminence, cavern creep closure was rapid in this region of the well, because the caverns were deep, and/or because cavern roof was flat, a shape that generates large vertical strains, as in the case of Boling wells #1, 2 and 4. In Boling well #3 the last casing shoe was anchored much higher above the cavern roof and the well experienced no leak (Figure 33). In both the Eminence and Boling cases, large vertical strains led to casing overstretching and failure. To a certain extent, the Epe case also belongs to the tensile failure type, however overstretching took place at much shallower depth. Breach creation is believed to originate in a large overall subsidence, which was initiated by and as a result of cavern convergence. This led to a sharp contrast in vertical deformations above and below the penultimate casing shoe, where the breach appeared.

Teutschenthal exemplifies the second case. Two stages were recognized in the leak development. The initial leak rate was slow, perhaps over many years, or even dozens of years, during which time gas accumulated in a 30-m thick layer whose thickness increased by half a meter; in this layer the casing, strongly bonded to the rock mass, became overstretched and at one point it experienced tensile failure, leading to the formation of a much larger ''secondary'' breach, which allowed higher leak rates. One hour later, ethylene and water mix blew out at ground surface. In the second case, due to tectonic deformation inside a salt dome, large differential movements develop, including horizontal differential (shear) displacements between two levels, the mechanical properties to which are in sharp contrast (for instance, salt top and caprock). The casing, which is strongly bonded to each of these two levels, experiences shear failure (this is likely to have happened also at Clute). This interpretation is confirmed by several incidents (the consequences of which were small) such as the failure of casings at caprock depth at the West-Hackberry oil storage facility (Sobolik and Ehgartner, 2012). There is no well-documented example in which a leak clearly starts at the depth of the last-cemented casing shoe, which often is considered to be a weak point from the perspective of cavern tightness. For instance, at Boling, breach(es) were close to, but above the casing shoe point.

To summarize the main findings, two likely causes – which do not exclude one another, and do not exclude a combination with other causes – appear. In all the cases, a breach is created in a zone where well completion includes a single casing. Except for the Hutchinson case (the breach was created when re-drilling an abandoned well), five cases are related to a structural cause: Eminence, Boling, Clute, Teutschenthal and Epe cases, with proven or suspected excess tensile stress experienced by the casings. In the Eminence, Boling, Clute and Epe cases, this is, or is suspected to be, due to salt creep dragging down the casings. In the Teutschenthal escape, this was due to a small leak that accumulated over a caprock, creating a local uplift. We note that phenomena are relatively slow to occur and if a tightness test had been conducted during commissioning of the caverns, it would not have detected a problem. Therefore, a relationship exists with the ages of the wells.

Influence of well age in Table 3 illustrates that leakage occurrences happen several dozens of years after well creation. This might be the time needed for a breach in the casing to occur through corrosion; or excessive strains, tensile and shear stresses to build up through salt creep. In the US, the last incident occurred in Texas in 2005 (where, since 1993, a double casing anchored in the salt formation has been mandatory for new caverns) at Boling, which had only one casing anchored in the salt formation, and in 2001 in Kansas (where similar regulations were enforced in 2003 following the 2001 Hutchinson incident).

Table 3. Well ages in hydrocarbon storage leakage events (Bérest et al., 2019b).

Site	Date drilled (or debrined)	Incident date	Time span between creation and accident	Comment
Elk City, Oklahoma	Unknown. After 1954??	February 23, 1973	19 years?	Leak likely started as early as November 1972
Conway, Kansas	Beginning 1951	After 1956	5–60 years	The described accident in 2012
Yoder, Kansas	– Idem	June 30, 1980	30 years or more	
Mont Belvieu, Texas	1963	September 17, 1980 (wellhead pressure drop)	17 years	October 3, 1980 (fire)
Mineola, Texas	End of 1950's	2000?	50 years	Paper written in 2001
Hutchinson, Kansas	Drilled in 1980; Re-drilled in 1990	January 19, 2001	20 years	
Epe, Germany	1980	February 23, 2014	34 years	
Magnolia, Louisiana	1970's	December 24, 2003	33 years	6 weeks after repressurization
Eminence, Mississippi	1970–1973	26 December 2010	37–40 years	
Teutschenthal	1971	March 29, 1988	*c.* 17 years	
Boling, Texas	End of January 1983 (de-brined)	Fall 2005	*c.* 22 years	
Clute, Texas	Leached out in 1961	December 1988	*c.* 27 years	

2.2.4.1.2 Leak development

In this section the factors which favour the development of a leak are explored.

2.2.4.1.2.1 An intermediate outlet ("receptor") often is needed

A leak can only develop from a breach in the casing when a pathway to an outlet exists or is created. This outlet may be ground level, or a sufficiently porous and permeable underground layer, or structural zone (e.g., a fault or jointed rock mass). Conversely, where no receptor horizon exists, or when the cementing job was completely successful, leading to a low permeability and a high gas entry pressure, a breach in the casing does not result in a leak. This occurs when, at breach depth, the rock mass is tight or deforms plastically, tightening the bond between rock and the cement job. In this respect, rocksalt (or clays/shales) exhibits very favourable properties; however, it does not mean that no fluid can migrate at the rocksalt-cement-steel interfaces, as witnessed in the Eminence or Boling examples. We also note here that cases exist in both the storage industry and in oil and gas production wells, where a leak built up in the cemented annulus. Generally speaking, however, in spite of many advances, it is difficult to guarantee cementation quality from wellhead to the last cemented casing shoe. In many cases, the leak finds an underground receptor, i.e., a porous and permeable zone whose volume is large enough to accommodate, at least for a period of time, a large quantity of fugitive hydrocarbons. This outlet can be at the same depth as the breach, for instance in the dome caprock (Mont Belvieu, and probably Clute also) or, as in Teutschenthal, in a sandstone layer, 30-m thick, below a tight overburden layer. However, in many other cases, receptor depth, where leaking products accumulate, is shallower than the breach depth itself. When the enclosing rock is tight and well cementation is poor, hydrocarbons can migrate upward in the cemented annulus between the steel casing and the rock, until it encounters a permeable layer: at Hutchinson, the point of escape and lateral migration was a thin, fractured dolomitic horizon between two tight shale layers, into which the gas migrated and moved updip, toward the town. In most cases there is an accumulation phase during which the escaped product progressively fills the receptor: receptor pressure increases to reach equilibrium with cavern pressure. The products may remain in the outlet for a long period (Boling, Eminence where Cavern #7 leaked to the caprock); or product pressure

may build up to a level such that a pathway is created to ground level (the outlet is the Doxey shales at Elk City; and the brine aquifer at salt top in the Conway case). A poorly consolidated caprock above a salt dome, composed of insoluble blocks left by dissolution (of evaporitic minerals), is favourable to the development of a leak (Mont Belvieu), on the one hand because it is the site of differential displacements in the casing and, on the other hand, because the caprock is *per se* a possible outlet. Revision of regulations in Texas took this fact into account. One might infer that leaks should be more frequent associated with salt dome storages rather than those in bedded salts. In fact, among the 12 cases presented above, 7 are related to domal salts and 5 with bedded salt. Both cases are found in sedimentary environment, in which successions of tight and permeable layers commonly occur in the overburden. Mudstones and fine-grained siltstone interbeds are also found within massively bedded halite deposits. Therefore, above a bedded salt formation, as above a salt dome, intermediate aquifer layers (or, at least, more permeable layers, as in the Hutchinson case or at Elk City) overlain by a tighter overburden (Teutschenthal) are potential candidates for hosting an accumulation of leaking hydrocarbons. In addition, in a salt dome, the overburden has been deformed, which can aid fracture enhanced pathway development within the overburden succession; the caprock often is porous and permeable, making drilling and cementing a more difficult job.

2.2.4.1.2.2 A pressure differential is needed (leakage driving force)

In addition to a breach in the casing and a receptor horizon, development of a significant leak requires a driving force, i.e., a pressure differential. At any depth, except maybe in the case of a natural gas storage when inventory is at a minimum, pressure of the stored product is larger than pore pressure in the rock mass (Figure 34). The second condition for leak development, that of a pressure gradient driving the leakage flow, is always fulfilled. Density of the stored product plays a major role: the lighter the fluid, the larger the pressure differential between products pressure in the well and ground water pressure at leak depth; it is larger when the cavern is deeper, and breach is shallower. This is especially true in the case of natural gas (or hydrogen): when the cavern is full and gas pressure is at a maximum, it is higher than geostatic pressure at almost any depth above the casing shoe Figure 35); when a leak through a breach is created, it can find its way to ground level even through low permeability layers. Density also plays a role when considering effects at ground level, see below. When leaking product migrates through the cemented annulus before reaching an outlet, pressure differential must be computed at receptor depth, where it is higher than at breach depth. At Hutchinson, on January 14, 2001, gas pressure was 47.6 bars at casing shoe depth (238 m) and only slightly lower (hence, larger than geostatic) at the depth of the fractured layer through which gas escaped and spread, allowing fast leak rates.

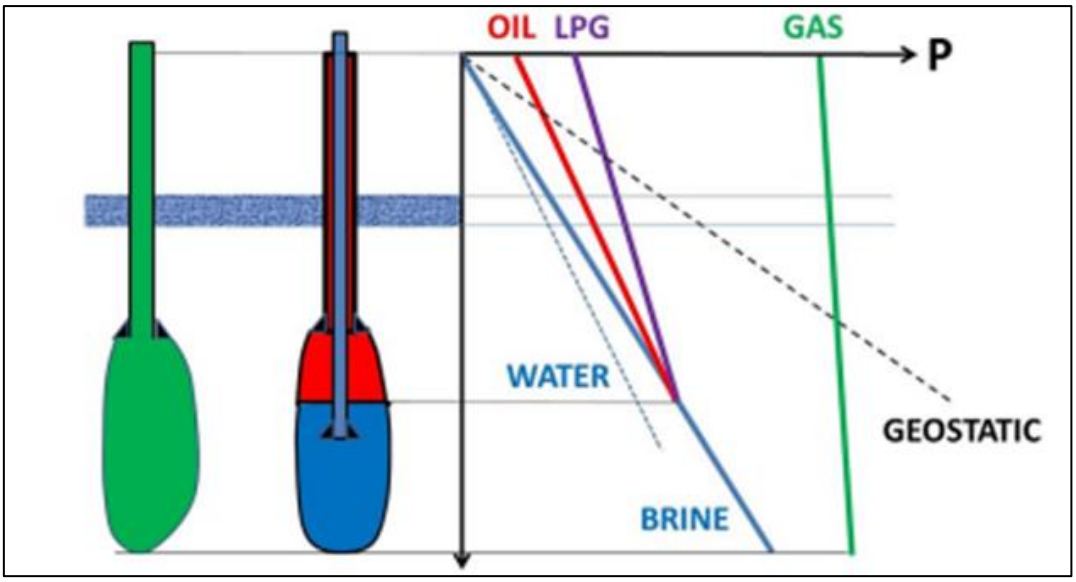

Figure 34. Pressure distribution in the borehole in the case of a natural gas storage (green line) and in the case of an LPG or oil caverns (purple and red lines, respectively). Geostatic pressure and typical water pressure in aquifer layers are also represented.

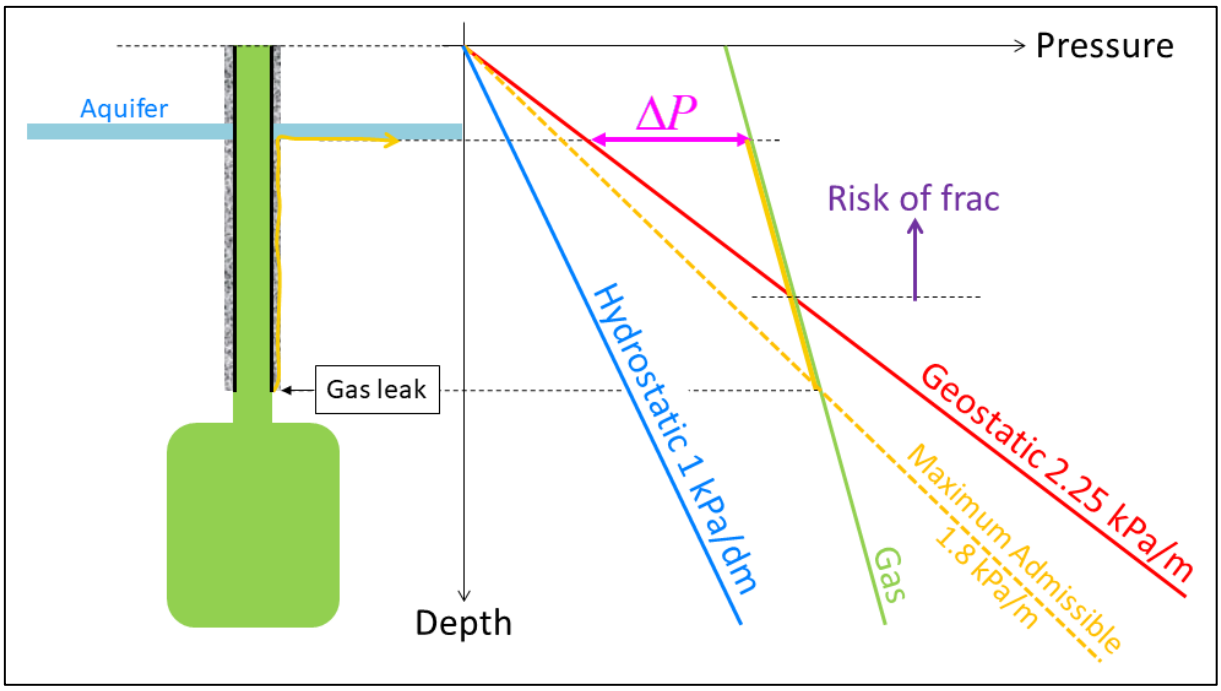

Figure 35. A gas leaks from a breach in the casing. Gas migrates through the cement and reaches a shallower aquifer layer, at which point its pressure is much higher than in situ groundwater pressure and even, in many cases, higher than geostatic pressure.

2.2.4.1.2.3 Wellhead pressure drops

In several occurrences (Epe, Teutschenthal, Eminence, Boling, Mont Belvieu and Hutchinson), a pressure drop was observed at the wellhead: at Epe (an oil storage), wellhead pressure dropped by 3.6 bars 3 weeks before oil appeared at ground surface. At Teutschenthal (an ethylene storage), pressure dropped from 75 bars to 40 bars: and ethylene blew out at ground level 1 h later. At Eminence (a natural gas storage), pressure dropped by 25.6 bars in 1 min. At Boling (a natural gas storage), pressure drop was spread over one week, although natural gas did not appear at ground level, and it is likely that gas found a porous and permeable level in the salt overburden. At Mont Belvieu (an LPG storage) pressure dropped 20 days before an explosion occurred at ground surface. At Hutchinson (natural gas) the pressure drop by 7 bars follows the first blow-out after 15 min; the salty aquifer layer below the city of Hutchinson was an intermediate outlet in which gas accumulated and the pressure drop generated by the blow-out took 15 min to propagate to the S1 cavern, 13 km away. No pressure drop is mentioned in other cases, but one was also observed in Regina South Gas Storage Cavern No. 5 in Saskatchewan (Section 3.4, Brittle failure and 3.4.5, Roof Fall). The volume of this cavern, leached out in 1983–1984, was more than 700 000 bbls (45 000 m^3). ''*Maximum pressure was 3000 psi (205 bars), a relatively low value for a cavern whose roof depth was 5363 ft (1780 m). Roof salt thickness was 50 ft. The final developed roof position was higher than originally planned and located in a structurally unstable area with many thin insoluble bands. In July 1989, a 267-psig pressure drop occurred in this cavern following gas fill up to 3000 psig. A rate of change in pressure decline from the pressure vs. time graphs used to monitor cavern operating condition suggested the cavern roof had a leak away from the well bore).*'' (Crossley, 1998). A block fall generates no perennial gas pressure change; the pressure drop must be due to a gas leak to a porous and permeable layer above the salt roof.

Occurrence of a rapid pressure drop is especially puzzling in the case of a natural gas storage cavern. Gases are much more compressible than liquids and a large gas pressure drop requires the loss of a large fraction of the cavern inventory. When V is the cavern volume, the pressure drop due to a δV inventory loss is $\delta P = \frac{\delta V}{\beta V}$ where β is the coefficient of compressibility of the fluid-filled cavern (Bérest et al., 1999);

for a brine cavern, $\beta = 4 \times 10^{-5}$ /bar; for a propane filled cavern $\beta = 10^{-4}$ /bar; for a gas-filled cavern, $\beta = \frac{1}{P}$ where P is gas pressure, for instance $\beta = 1$ /bar when gas pressure is 1 bar. A $\delta P = 5$ bar pressure drop is generated by a 0.125% inventory loss in a brine cavern; in a gas cavern, the same pressure drop is generated by a 5% inventory loss – a huge value. For this reason, a large pressure drop in a gas cavern is possible only when the casing breach opens in a large, porous and permeable volume (Mont Belvieu); or, long after the breach is created, when the leaking gas reaches ground level or a large porous and permeable receptor.

2.2.4.1.2.4 Products viscosity, capillary effects

Leakage can affect all types of stored fluids, oil, natural gas, ethylene, or LPG. A low viscosity and a low entry pressure in the rock formation favours leakage; as such, natural gas (and*, a fortiori*, hydrogen) may be more likely to leak than liquids. It is difficult to quantify how much more likely to leakage natural gas is, as leak rate depends, in addition to gas viscosity, on the way a leak path develops. Leak flow is likely to be bi-phasic first, with a gas/water front inside which capillary pressures slow down gas migration rate, before a continuous path is created from breach to ground level or to an intermediate receptor. The storage industry (Crotogino, 1996) suggested empirical rules for conversion of a gas leak (which can be easily measured during a tightness test) into a liquid leak. Cases have been observed in which the cavern is found to be somewhat leaky when the testing fluid is a gas, but tight when it contains a liquid hydrocarbon. An example was at Magnolia, where the cavern did not pass a Nitrogen Mechanical Integrity Test, although the cavern had experienced no leakage issue when the annular space was filled with a much more viscous diesel oil (Bennett, 2009).

2.2.4.2 Eruption at ground level

2.2.4.2.1 The path toward ground level

One might think that a leak necessarily appears at ground level near the wellhead; i.e., it follows the shortest path to surface. This was clearly the case at Mineola, from which it was inferred that the breach was shallow (the shoe of the penultimate casing was only 35.5-m deep) and at Eminence in 2011. However, in the general case, and especially when hydrocarbons accumulate first in an intermediate receptor (a porous layer or caprock, e.g., Hutchinson, Teutschenthal, Clute, Elk City, Epe) the path found by the leak can be complex and surface release somewhat distant from the wellhead; it is often governed by geological features at shallow depth and is not always the shallowest path along a vertical line. In such a case, the blow-out can occur abruptly (Hutchinson, Elk City, Teutschenthal) and can be localized at a large horizontal distance from the wellhead (600 m at Elk City, 50–200 m at Teutschenthal, 500 m at Epe, and even up to 14 km in the exceptional case of Hutchinson); and, probably at a point where elevation is low (Mont Belvieu, Elk City). At Hutchinson, general opinion is that a period of 8 years was needed for gas to charge a thin, 13-km long sub-horizontal fractured level before gas erupted in downtown Hutchinson (several experts believe that filling took place over a few days prior to the eruptions, however, this conclusion is not fully substantiated by the (scarce) available information). At Teutschenthal, two distinct steps were observed: first, gas slowly filled an aquifer at 100-m–140-m depth, generating an uplift, and opening a new breach in the severely stretched casing. This led to a significantly increased leak rate, a pressure drop (from 75 bar to 40 bar) in the cavern and, 1 h later, a blow-out at ground level. Both the cavern and the intermediate receptor were vented by gas outflow at ground level, with ground uplift vanishing.

2.2.4.2.2 Effects at ground level

The effects observed at ground level depend on many factors, among which are the nature of the stored gas, the configuration of shallow layers, and local topography. They might be especially severe in the case of a hydrogen leak. Two types of effects can be observed: mechanical effects in case of an abrupt blow-out (Teutschenthal, or Elk City, where 30-tons rock blocks were uplifted; Yoder where, however, the propane/water jet was small) and chemical effects (Mont Belvieu, where the gas exploded; Hutchinson,

where several explosions occurred). Importantly, no asphyxia case has been reported in the incidents discussed here. It is known from other types of incidents (wellhead failures, which often lead to a loss of the full cavern inventory – e.g., Moss Bluff) that a natural gas blow-out, with high gas flow rates (gas velocity is sonic at ground level) is not an extremely severe hazard (except at the very beginning of the process) as natural gas, lighter than air does not spread laterally at ground level. In contrast, oil, and more generally liquids, remain at ground level and generate low-rate leaks (Epe), and do not burn in the absence of an ignition source. This may not be true when hydrocarbons spread over a large area of ground, as, above the liquid phase, a cloud forms containing the most volatile parts, ignition of which is easier. Ethylene, which is stored in a supercritical form, is gaseous at atmospheric pressure; its density is close to that of air, with which it forms an explosive mixture (however ethylene decomposes under the effect of light). At Clute, ethylene remained confined in the caprock. At Teutschenthal, it appeared haphazardly at ground level, however, topography and wind favoured dispersal. LPGs present a more difficult problem. In the cavern, they are liquid, but vaporize, at least partially, on their way to ground level when their pressure becomes lower than their vaporization pressure – at least when the flowrate is not too fast, and enough time is left for the rock mass to provide the heat needed for phase change. In their gaseous state, they are heavier than air and, at ground level, they tend to remain stagnant at low elevation points, or in building foundations (Mont Belvieu, Elk City). At Elk City effects of the blowout were mechanical rather than chemical; measurements proved that gas concentration at ground level was small (less than 1%).

2.2.4.2.3 Actions taken after a leak is found

After the occurrence of a leak is established, its origin must be confirmed (it could result from a breach in a buried pipeline). Gas composition often is a clue. Drilling boreholes to shallow ground water level, or to the level where products circulate, allows venting the gas and understanding the pathways followed by the leak (at Hutchinson, gas underground pathways, which were complex, were identified progressively; it was composed of several branches through which gas flowed toward the city When the leaking cavern is identified, it must be vented, when possible. At Boling, a temperature log identified the depth at which the leak took place, as gas depressurization creates a cold spot. Frequently, a plug is set in the wellbore, as deep as possible and hopefully below the leak level. A video log often assists in detecting this level, especially when the rupture was created by excessive tension on the cemented casing, or re-entry operations during well conversion damaged the casing (Hutchinson).

2.2.5 Prevention of a gas leak

Prevention of a gas leak includes quality of drilling and cementing job. More specific topics are discussed below.

2.2.5.1 Pressure monitoring

Pressure monitoring at cavern wellhead is necessary; at Mont Belvieu, this monitoring provided a warning, 15 days before the blow-out. However, in most cases a pressure drop was not observed, or was observed too late, or even observed after the blow-out (Hutchinson), when the leak path was already fully developed. In principle, careful monitoring of the wellhead pressure over a long period should provide a warning; however, in a natural gas storage, the stored product is so compressible that pressure changes resulting from a leak are exceedingly small, especially when the cavern experiences frequent injection/withdrawal, the cumulative effects of which generate large uncertainties. In a strategic oil storage, the inventory of which changes little, a better resolution can be anticipated but important efforts must be made, in terms of accuracy and interpretation, to reach an acceptable resolution (Colcombet and Nguyen, 2013).

2.2.5.2 Well completion

The role of wellbore completion is extremely important. It was observed that the combination of a flat cavern roof and a short chimney leads to tensional stresses and stretching of the casing, especially when

cavern creep closure is fast. In many of the described cases, a large difference can be observed between the depth of the deepest and penultimate cemented casing. In other words, between the shoes of these two casings, a single ‘‘barrier’’ (i.e., a casing cemented to the rock formation) can be found: a breach through the steel casing opens directly to the rock mass. It is interesting to note that, in most cases, when repairing a leak, an inner steel tube is added to form, with the pre-existing casing, an annular space the bottom to which is closed; this annulus is filled with water whose pressure is monitored at ground level – a way of creating a ‘‘second barrier’’ which did not exist in the initial design. Such a completion (an internal tube delimiting a monitoring annulus plugged at its bottom) has been mandatory in France and Germany for natural gas storages and the trend in Europe is to equip new liquid storage caverns with such a system, it is a requirement under Dutch mining law (Koopmans et al., 2014). For many years in Texas, Louisiana, and Kansas (three states in which can be found the majority of US salt cavern storages), State regulation has required that new caverns have two cemented casings, anchored in the salt formation (Figure 36). In addition, a tightness test is mandatory at least every 5 years, which covers the case of old caverns which are not equipped with a double casing.

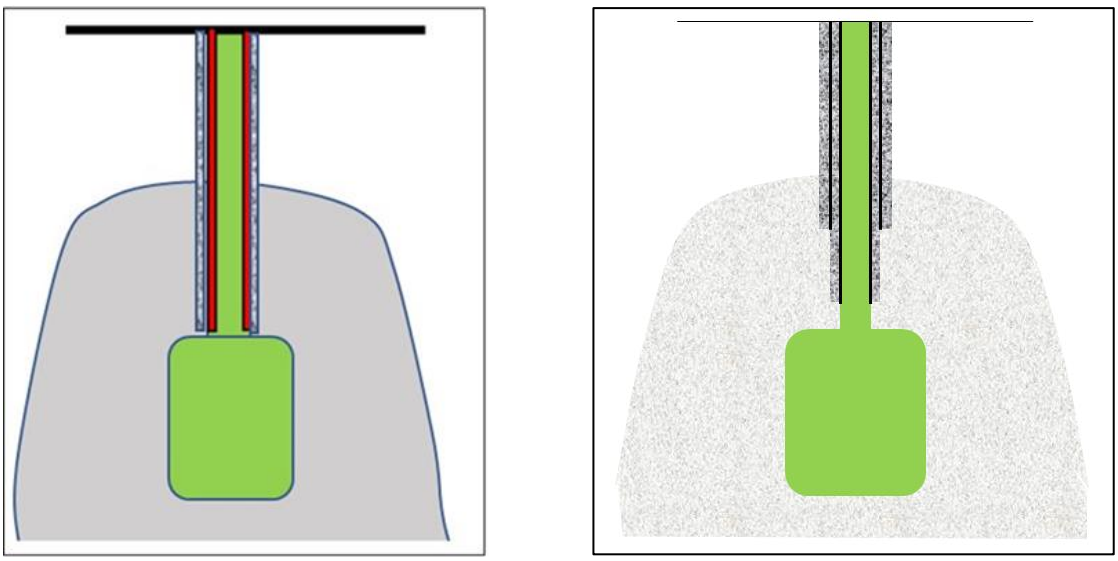

Figure 36. Schematic completion design: (left) in Europe, a water-filled annulus (in red), isolates the casing from the gas; and (right) in the U.S., the two last-cemented casings are anchored to the salt formation.

2.2.5.3 Tightness Tests (MITs)

Although the number of storage caverns in operation increases, fewer and fewer incidents are occurring. Several reasons exist for this.

Recent caverns are equipped with a double casing anchored to the salt formations, or a water/brine-filled annular space. Both new and old caverns are now tested using the Nitrogen Leak Test (NLT) or Liquid Leak Test (LLT) methods. The former consists of injecting nitrogen into the annular space, the latter instead of nitrogen, a liquid hydrocarbon is injected. Salt caverns present a remarkable advantage (when compared to depleted reservoirs or, more generally, oil and gas fields): borehole tightness can be tested, as the borehole opens in a closed ‘‘container’’ (the cavern itself), which is almost perfectly tight. Typically, the NLT consists of injecting nitrogen into the annular space slightly below the last cemented casing shoe. A logging tool is used to measure the brine/nitrogen interface location. At least two measurements, generally separated by 3 days, are undertaken. Upward movement of the interface is deemed to indicate a nitrogen leak. Pressures are measured at ground level, and temperature logs are recorded to allow estimating effects such as thermal expansion and compressibility and enable precise back-calculation of nitrogen seepage. MITs are mandatory every five years in most US states and countries. Fail/Pass criteria

have been proposed by the SMRI (Crotogino, 1996). MITs – and especially NLTs – are the most significant prevention tool in the cavern industry. These notions are discussed in Section 4.2, Tightness tests.

2.2.6 Conclusion

In Bérest et al. (2019b), based on a study funded by the SMRI, 12 incidents involving product leaks through the cemented casing of salt storage cavern wells are described. Their causes have been analysed and general lessons drawn, which are informative for not only storage caverns, but also oil and gas field wells. They prove that experience, dissemination of new techniques and best practices, and advances in well design (double casing) and testing (MITs), leads to an ongoing reduction in the frequency and severity of incidents.

2.3 Blowout

2.3.1 Introduction

Generally speaking, a **blowout** is the uncontrolled release of crude oil and/or natural gas from an oil well or gas well after pressure control systems have failed (for instance, after the wellhead was hit by a heavy truck). This definition applies also to a gas storage cavern. In most cases a blowout from a salt cavern leads to expulsion of the full gas inventory and is completed after one week or so. A gas cloud forms at ground level. Such a cloud can ignite or explode. This incident often is considered as "the worst-case scenario" (van der Valk et al., 2020) for a hydrogen storage. An additional consequence is that, at the end of the blowout, cavern gas pressure is virtually zero, i.e., much smaller than the minimum gas pressure selected for operation, with possible consequences for cavern mechanical stability.

Such an incident may also occur in liquid or liquefied storage caverns. There consequences are less severe, at least in the case of liquid storage, as only a small part of the inventory is lost. A well described case is the West Hackberry oil spill and fire in Louisiana.

2.3.2 Case histories

Several examples of blowouts in gas storage caverns have been described in the literature, such as that in an ethane storage at Fort Saskatchewan, Canada (Alberta Energy and Utilities Board, 2002) or in a natural gas storage at Moss Bluff, Texas (Rittenhour and Heath, 2012). There were no casualties in these instances, as the gas rapidly ignited, although the entire inventory was lost. A somewhat similar accident occurred in a "compressed air storage" (in fact, an abandoned salt mine) at Kanopolis, Kansas; a complete description can be found in Van Sambeek (2009).

In these two cases, initial interpretation of the incident (when the blowout started) proved incomplete.

2.3.2.1 Fort Saskatchewan Ethane Blow-out and Fire (2001)

In 2001, BP Canada Energy Company operated 10 salt caverns at a storage site located about 6 km northeast of Fort Saskatchewan, Alberta, Canada. Ethane was stored in Cavern 103, a two-well storage cavern operated according to the brine compensation method Cavern 103 had been completed in the Lotsberg Salt Formation at a depth of 1850 m. Brine (resp., ethane product) is injected/withdrawn through well 103A (resp., well 103). The two wells are about 20 m apart. Equipment includes a 2-inch horizontal connecting line between the two wellheads, an equalization line which was used during servicing operations and was not necessary for the day-to-day operations. At the time of the incident the ethane volume in the cavern was 76 000 m^3, approximately.

In the early morning hours on August 26, 2001, [Note that this event is different from the event at Prud'homme 2014 presented in the press releases copied below] ethane was being pumped up well 103 as brine was injected into well 103A. At 7:00 am an alarm was received from a detector analyser. A vapor cloud formed above cavern 103. After the incident it was determined that an elbow failed on the 2-inch connecting line. Cavern 103 was shut in. When the Emergency Shutdown (ESD) valve on the well was activated at 7:10, the vapor cloud did not disperse. BP attempted to reduce the leak by opening up the well to a pipeline. This attempt failed. The ethane vapor cloud came into contact with overhead power lines. Electric arcs sparked the plume, creating an explosion and resulting fire (Figure 37), at 9:40, approximately 2 hours after the initial failure. Fire-control experts sprayed water to cool the two wellheads.

In the first 48 hours, black smoke from the fire was significant and observable for many kilometres but did not present any danger to the public. Throughout the incident, the fire was contained entirely on site.

Figure 37. Ethane fire in Fort Saskatchewan, Alberta. Note the hay rolls lying unharmed in the foreground while the fire blazes nearby (Liz Nayowski/Fort Saskatchewan Record photograph).

Figure 38. The first photo (right) was taken right after the fire had been extinguished and the new wellhead lowered in to place. A temporary vent stack has been attached to the top of the wellhead. The second photo is from June 2015 and more clearly shows the new wellhead chained in place. Acknowledgment: Dave Burdeniuk.

Over a period of 6 days, pressure dropped from 207 bars to 44 bars as the cavity slowly emptied. Ongoing fire control, and reduced product flow, resulted in smoke reduction. On August 29 a connecting valve between the two wellheads was closed, reducing the fire. On September 1, the small remaining fire on the brine well was outfitted with a new master valve (Figure 38). On September 3 [or 4?], a plug was set down-hole in the second well, and the emergency was declared over. No injury was reported.

The incident prompted the EUB (Alberta Energy and Utilities Board) to review BP's ignition policy. BP has eliminated the 2-inch line between the two wells. The EUB required that wellhead on its Alberta Natural Gas Caverns be equipped with ESDs.

The EUB Report (Alberta Energy and Utilities Board, 2002) provide interesting insight in crisis management and public information during the incident. An oral presentation was given during a SMRI Meeting (Banff Spring Meeting, 2002), in compliance with the company policy "*to share the findings with the industry in the interest of safety*."

Jug Manocha, a member of the regulatory authority, kindly drew our attention on a media release on July 28, 2015 from SaskEnergy (2015). This release is partly copied below. Investigations were pending. Dave Burdeniuk, Director, Gov't and Media Relations of SaskEnergy/Transgas kindly offered to provide updates. A new media release (SaskEnergy, 2016a) on September 20, 2016 is also copied below.

July 28, 2015 media release

''*SaskEnergy begins next phase of investigation into Prud'homme Cavern Fire SaskEnergy has started the next phase of its investigation into the October 2014 gas release and fire at its Prud'homme natural gas storage facility east of Saskatoon. No one was hurt in the nine-day incident [.]. The remaining caverns were not impacted and provided natural gas service to meet the region's peak 2014/15 winter load. The gas release was safely contained on October 17th with the installation of a new wellhead; safety testing and site clearance were completed two days later. A full investigation was immediately launched to determine the exact cause of the incident and the extent of damage at the site. The original wellhead, which controls the flow of gas into and out of the cavern, was tested at an engineering lab in Calgary and determined the unit was not a contributing factor to the gas release. SaskEnergy, with the assistance of specialized contractors, also began temporary repair work immediately after the incident to assess the heat damage and ensure the facility was back in operation before peak winter months. Permanent above ground repair work, which included thoroughly inspecting and analyzing the affected equipment at the site, began in March 2015 at the beginning of spring thaw with all above ground repairs and replacements now completed. SaskEnergy is currently preparing for an internal investigation within the affected cavern well. Preliminary investigative work had discovered an obstruction 3.5 meters below the surface in the steel well casing, which is the pipe that links the surface with the cavern located a kilometer underground in a deep salt formation.*

SaskEnergy will now use a process of injecting water to remove the remaining gas and transfer it to another cavern at the facility. This injection process maintains the correct internal pressure to preserve the integrity of the cavern. Once the gas is removed, closer inspection of this obstruction will be conducted, with the potential of removing a portion of the well casing for further analysis. This project is expected to take 30 weeks. Pending the results of this work, the cavern will either be repaired and returned to service, or retired from use by utilizing established protocols and safety procedures.''

September 20, 2016 media release (SaskEnergy, 2016b)

"*SaskEnergy has completed the investigation into the October 2014 gas release and fire at its Prud'homme natural gas storage facility east of Saskatoon. The nine-day incident began October 11th, 2014 at one of the seven underground natural gas storage caverns at the facility. No one was hurt in the incident, and no service was lost to any residential, business or industrial customer. The gas release was safely contained*

on October 17th with the installation of a new wellhead; safety testing and site clearance were completed two days later. The remaining caverns at the site were not impacted. SaskEnergy's investigation, using the resources of industry experts, determined the cause of the incident was a failure in the steel casing pipe used to inject and remove natural gas from the underground cavern. A thorough examination of the impacted cavern could only be conducted after the remaining gas was safely removed, and the cavern was filled with water. This process was carefully monitored and took several months to complete.

The failure, located about two meters below ground, allowed natural gas to leak into an external concrete casing protecting the pipe, where it moved up and released through a valve on the side of the cavern wellhead. The force of the high-pressure natural gas release damaged the wellhead building, causing a spark and the resulting fire [.] The affected cavern has been decommissioned with no plans to repair and recertify it for use at this time."

2.3.2.2 Moss Bluff natural gas blow out and Fire (2004)

The information contained in this note is mainly extracted from Brouard Consulting and RESPEC (2013) and Rittenhour and Heath (2012). The text below is a slightly revised version of Réveillère et al. (2017) summary.

2.3.2.2.1 Facility background and pre-incident state

MB #1 salt cavern is located in Liberty County, Texas, approximately 80 km east of Houston, Texas. It is part of a site comprising the natural gas storage caverns MB #1, MB #2, MB #3, MB #4, and a Praxair hydrogen storage cavern. Only the first three caverns were in service at the time of the incident. Cavern #4 went into service in 2011, and the Praxair hydrogen storage cavern in 2007. These caverns are hosted in the northern part of the Moss Bluff salt dome, whose dimensions are approximately 4.5 km by 3.6 km, as shown in Figure 39.

MB #1 was spud on September 30, 1981. The well was drilled to a total depth of 4408 ft (1344 m) with the caprock top encountered at 865 ft (263.7 m) and the salt top encountered at 1185 ft (361 m). Cavern leaching began in May 1982, and occurred by brief leaching periods until the cavern was put into gas storage service in 1990. The cavern volume was 2.16 MMbbls (344 000 m^3) at that time, and its volume was not modified until the cavern Solution Mining Under Gas (SMUG) began in 2000. SMUGing is a special technique such that additional solution mining is performed after a first debrining took place (the cavern is partly filled with gas). Its main advantage is that gas storage operations can start before solution mining is completed. To accommodate SMUG, the well was configured with two hanging strings as exposed in figure 2, during a workover operation that followed the cavern rebrining in 1999. Cavern SMUG progressively increased the cavern volume to 8.21 MMbbls (1.3 million m^3) at the time of the incident, in 2004.

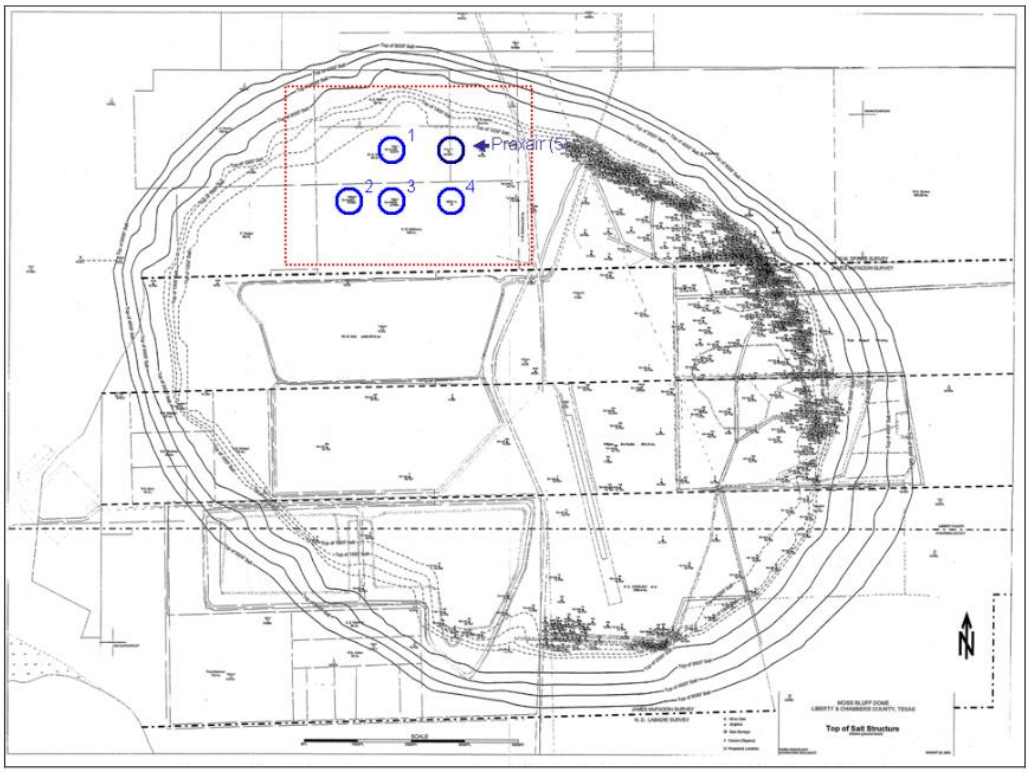

Figure 39. Moss Bluff salt dome overview (from Réveillère et al., 2017; after Rittenhour and Heath, 2012).

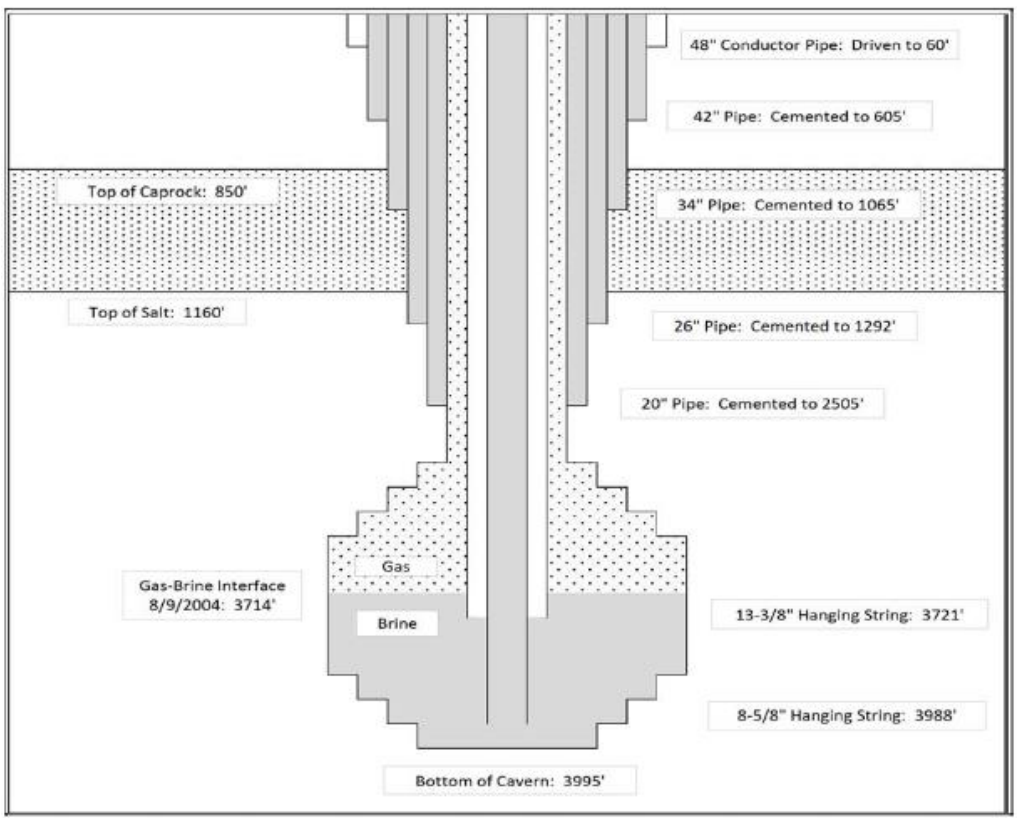

Figure 40. MB #1 well configuration, from the 2000 work-over and SMUG operation beginning to the 2004 incident (after Rittenhour and Heath, 2012).

2.3.2.2.2 Blow-out incident

On August 9, a wireline unit confirmed the gas-brine interface level to be at 3714 ft (1132 m). The tool touched down at 3938 ft (1200 m), and it was concluded that the casing possibly was bent at this location (probably due to a block falling from the cavern walls), approximately 50 ft (15 m) short of where previous logs had indicated the well string shoe.

On August 17, a "normal" de-brining rate was established, and the process was considered to be "on line" (gas being injected/withdrawn through the 13-⅜" × 20" annulus, water injected through the 8-⅝" ×13-⅜" intermediate annulus, and brine produced through the 8-⅝" central string, Figure 40).

At approximately 4:00 a.m. on August 19, 2004, MB #1 experienced a rupture of the 8" brine-outlet piping attached to the wellhead. The gas escaping from the open pipe ignited. The fire initially was directed downward at the base of the wellhead (Figure 41 and Figure 42). The force of the gas flow carved a crater 60-ft (18-m) across and 30-ft (9-m) deep at the vicinity of the wellhead. Well-control experts responded to the scene, but, due to the intensity of the fire, no attempt was made to approach the wellhead and shut off the wing valve.

At approximately 1:30 a.m. on August 20, the fire self-extinguished for a brief period of time. This occurred due to the wellhead assembly separating from the well casings and falling into the crater beside the production casing. The gas re-ignited within a minute, with the flame then being directed upward, fuelled by gas escaping from the 20" production casing.

Figure 41. Blowout and fire at Moss Bluff.

Post-incident logging confirmed that the interface level was far from above the pre-incident depth of the 8-⅝" tubing shoe: the gas did not enter the brine 8-⅝" brine string from its shoe, but from a leak path within this string. The Emergency Shutdown (ESD) valve on the 8-⅝" outlet surface pipe was found in the appropriate position — i.e., fully closed, but was located downstream of the 8-⅝" rupture.

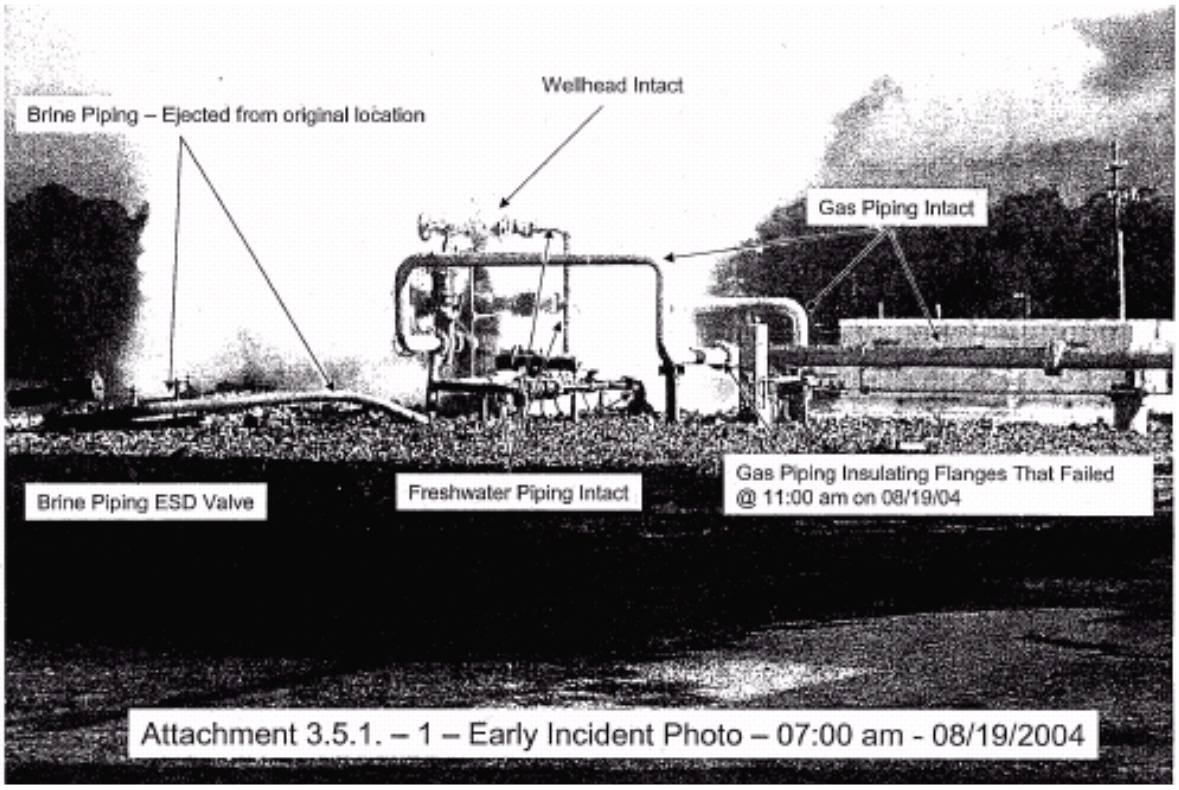

Figure 42. Moss Bluff - Early incident photo.

2.3.2.2.3 Investigation Summary

The incident that occurred at Moss Bluff Cavern 1 beginning on the morning of August 19 and continuing through the morning of August 20, 2004, initiating a blowout that lasted until August 26, can be broken down into three significant events.

1) The first event was the compromise of the 8-⅝" well string that allowed high-pressure gas to fill the string. Although uncommon, these types of events do occur, and safety systems are installed to protect above-ground components from such an event.
2) The second, and most significant, event was the fracture of the 8-⅝" above-ground brine piping. This piping experienced tensional forces beyond its tensile strength limit. It was subjected to an accelerated column of brine being pushed by high-pressure gas, and its integrity was compromised due to internal corrosion that had thinned the pipe significantly. This extremely aggressive internal corrosion and/or erosion resulted in well over a 50% wall loss and was not something the facility had experienced in these systems prior to the incident.
3) The third event was the separation of the wellhead from the 26" and 20" casings. This event was primarily a result of exposure to intense heat and scouring, and is considered a secondary event rather than a primary contributor to the incident.

2.3.2.2.4 Post-incident assessment and return to service

Moss Bluff Cavern 1 was depressurized for approximately three months in late 2004 as the result of a wellhead incident resulting in the loss of the natural gas inventory. An MIT of the cavern after the blowout indicated that the well was not leaking. Similarly, calliper logs performed after the incident showed no evidence of damage to the casing. Also, a cement-bond log indicated good bonding over much of the well except for a micro-annulus from ground surface to a depth of approximately 200 ft (60 m), but whether it happened before or after the blow-out event cannot be determined

The wellhead, hanging strings and surface piping were replaced, design and operational modifications were made to help ensure a similar incident would not occur again. Notably, the ESD valves were set

directly on the wellhead. These modifications were also implemented on all of the caverns of the facility and two other Gulf Coast cavern-storage locations. The cavern has been returned to gas storage and has been operated with proven integrity to date.

Brouard Consulting and RESPEC (2013), in a Report prepared for the SMRI, proved that gas temperature in the cavern experienced a severe drop to -40°C as gas pressure dropped to atmospheric. It is likely that thermal fracturing was initiated at cavern wall. However, at the end of the blowout the amount of gas remaining in the cavern was small, and heat transfer from the rock mass swiftly increased cavern temperature. It was computed that depth of penetration of thermal fractures in the rock mass was small.

2.3.3 Blowout model

2.3.3.1 Underground model

2.3.3.1.1 Gas thermodynamic behaviour in the cavern

A simplified model of cavern gas thermodynamic behaviour was given by Bérest (2013) see Section 2.1, Thermodynamics. Bérest's model integrates the thermodynamics of gas in the well-cavern system to predict the blowout on underground gas storage caverns. Only major assumptions and simplifications of the model are provided- in this Section. The model is widely developed in the papers Bérest et al. (2013), Djizanne et al. (2014b).

Both gas behaviours in the cavern and in the wellbore must be described; they are coupled through the boundary conditions at gas entry at the end of the wellbore (gas temperature and pressure must be continuous). The thermodynamic behaviour of hydrogen exhibits some specific features of interest (in particular, an isenthalpic depressurization can lead to hydrogen warming); so, instead of the standard state equation of an ideal gas, a van der Waals state equation was selected to describe the gas behaviour during the blowout, $P = -a/v^2 + RT/(v-b)$ and $h(v,T) = C_v T - \frac{2a}{v} + \frac{rTv}{(v-b))}$ ($h = e + Pv$ is the gas enthalpy). (However, ideal gas state equation is used for natural gas such as methane or compressed air.) During a gas withdrawal, the energy balance equation can be written $m[\dot{e}(T,v) + P\dot{v}] = Q$ where $m$is the mass of gas in the cavern, *e* is the gas internal energy, *P* and *v* its pressure and specific volume. In addition, cavern volume is constant, or $V = mv$. From thermodynamics, $\dot{e}(T,v) + P\dot{v} = C_v\dot{T} + T(\partial P/\partial T)_v\dot{v}$. Q is the heat flux transferred from the rock mass to the cavern gas through the cavern wall. Blowout in a gas cavern is a rapid process: it is completed within a week or less. During such a short period of time, temperature changes are not given time enough to penetrate deep into the rock mass and, from the perspective of thermal conduction, cavern walls can be considered as the sum of small flat surfaces whose area equals the actual area of the cavern.

When a varying temperature, $T_c = T_c(t)$, is applied on the surface, the heat flux per surface unit can be expressed as $Q = \int_0^t -K\,\dot{T}_c(\tau)d\tau/\sqrt{\pi k(t-\tau)}$ where K and $k$are the thermal conductivity and diffusivity of salt, respectively. When these simplifications are accepted, the heat balance equation can be written:

$$\frac{\dot{T}_c}{v} + (\gamma - 1)\frac{\dot{v}T_c}{v^2} = \frac{-\Sigma_c K}{C_v V\sqrt{k}}\int_0^t \frac{\dot{T}_c(\tau)}{\sqrt{\pi(t-\tau)}}d\tau \qquad (8)$$

Where Σ_c is the (actual) surface of the cavern walls.

2.3.3.1.2 Gas thermodynamic behaviour in the wellbore

The gas rate in the borehole typically is a couple hundreds of meters per second (more when hydrogen is considered). This means that, only a few seconds are needed for gas to travel from the cavern top to ground level. Such a short period of time is insufficient for cavern pressure to experience large pressure changes and steady state can be assumed at each instant. (Obviously, when longer periods of time are considered, cavern pressure slowly decreases). Duct diameter or$D$is assumed to be constant throughout

the well; hence, the cross-sectional area of the well is constant too. Gas massic flowrate is $\dot{m} = \frac{u}{v}$. Enthalpy is such that $\frac{dh}{dz} + \frac{udu}{dz} + g = 0$. The momentum equation can write $\frac{vdP}{dz} + \frac{vdv}{dz} + g = -f(u)$. Head losses per unit of length are described by $f(u) > 0$. During the blowout, the gas flow is turbulent. The average gas velocity is uniform through any cross-sectional area (except, of course, in the boundary layer). The effects of friction are confined to a thin boundary layer at the steel casing wall. Head losses are written $f(u) = Fu^2$ where $F = \frac{f}{2D}$ is the friction coefficient and f is the friction factor. The Colebrook's equation is used, $\frac{1}{\sqrt{f}} = -2\,log_{10}\left(\frac{\varepsilon}{3.71D}\right)$ where ε is the well roughness ($\varepsilon = 0.02$ mm is typical).

Gas pressure and temperature (hence, gas specific volume) at the end of the string are known from the computation of cavern gas thermodynamic behaviour. In principle, gas pressure at the wellhead should be atmospheric, however, when gas flow rate is very high, such an assumption leads to a solution such that gas flow is supersonic in the upper part of the well, which is not compatible with the second principle of thermodynamics ($\frac{dS}{dz} > 0$) [no shock can exist inside the wellbore]. In such a case, it is assumed that the flow rate is sonic at the wellhead ("choked flow"), or $u = c$. No constraint is applied to wellhead gas pressure which, in general, is larger than atmospheric. Conversely, when the cavern pressure is relatively small, the gas flow is said to be "normal" and gas pressure is atmospheric at ground level. These assumptions ("Fanno-flow" model), which are standard (Landau and Lifchitz, 1971, Section 91) are commonly accepted (von Vogel and Marx, 1985).

Note that heat transfer from the rock mass to the wellbore is neglected, and gas flow is considered adiabatic. In the computations, gravity forces (g) are neglected. This model was tested against the Moss Bluff historical case with good results (blowout duration was predicted correctly, Bérest et al., 2013; Djizanne et al., 2014b).

2.3.3.1.3 Computations: subterranean part

A 500 000 m^3 hydrogen storage cavern is considered by Djizanne et al. (2022). Cavern top depth is 1000 m and cavern height is 197 m; tubing diameter is 8-⅝". Gas temperature and pressure in the cavern before the blowout are 45 °C and 176 bars, respectively. Figure 43 and Figure 44 gives evolutions of gas mass, velocities, temperature, and pressure during the blowout.

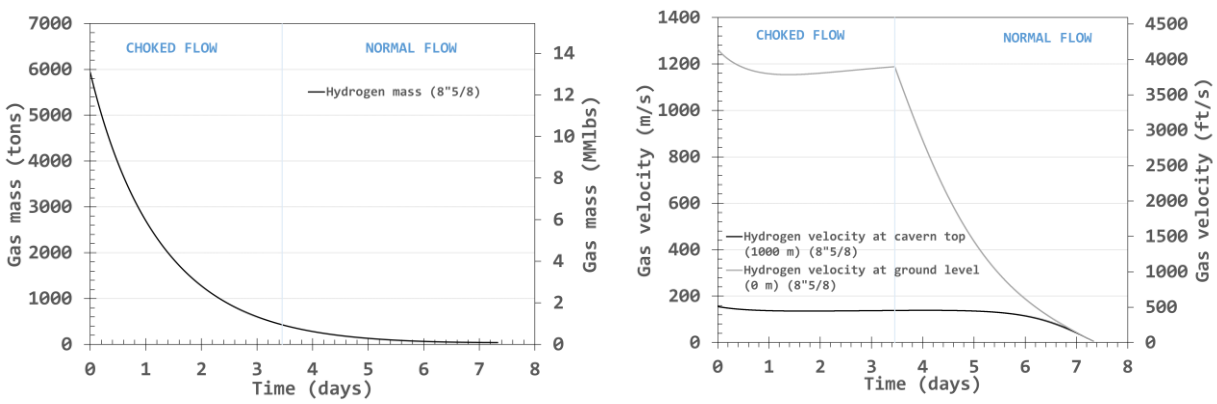

Figure 43. Evolutions of gas mass in the cavern and gas velocities at cavern top and ground level. The blowout is 7.3 day long; the flow is choked (sonic at ground level) during 3.4 days, after which 90% of the hydrogen mass has been expelled from the cavern and gas celerity rapidly drops.

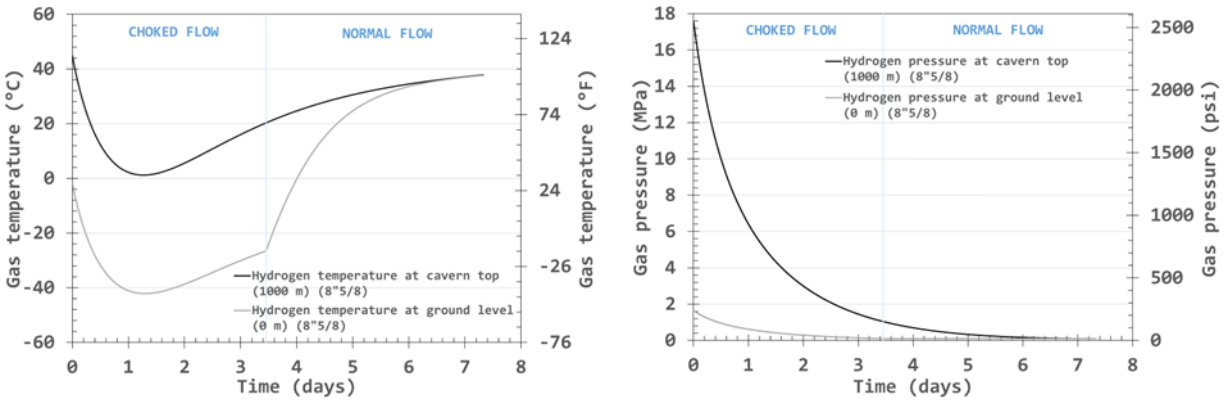

Figure 44. Evolutions of gas temperature and pressure. mass in the cavern and gas velocities at cavern top and ground level.

2.3.3.1.4 Computations: aerial part

The flammability range of hydrogen (a volumetric ratio gas to air between 4% and 75%) is large. In addition, the ignition energy of this mixture is low (0.02 mJ, to be compared to 0.29 mJ for methane). When compared to natural gas, early ignition of a hydrogen-air cloud forming at the wellhead is highly likely (for instance due to electric arcs generated by differences in electric potential of the wellhead and the ground). The worst-case scenario is a vapor cloud which does not ignite immediately (for instance because gas outflow rates are very high) as an explosion with dramatic possible consequences can be expected.

An example of a computation of the aerial part of a blowout was given by Djizanne et al. (2022). When hydrogen is expelled from the cavern, an unconfined cloud, a mixture of air and hydrogen, forms above the wellhead. The cloud is defined by the volume in which the Lower Flammability Limit (40,000 ppm) is reached. The shape and evolution of the cloud is governed by buoyancy (it rises because of low hydrogen density), atmospheric conditions (stability and wind speed – 10 m/s at a 10-m height in the following computations) and hydrogen flowrate from the wellhead (which decreases with time, as described above.) A recent version of the Unified Dispersion Model developed by Woodward et al. (1995) is used.

Three hazardous phenomena mainly associated with the ignition of the dispersing flammable cloud are considered:

1) Flash fire (thermal effects are dominant). This phenomenon is generated by the ignition of a flammable gas/air mixture at a distance from the source. The event is developed as the flame front burns through the pre-mixed vapor cloud and expands its volume. The cloud expansion can push vapours ahead and enlarge the visible flame and burn back to the source to become a jet fire.
2) Unconfined vapor cloud explosions (overpressure effects are dominant). Unconfined Vapor Cloud explosion (UVCE): This phenomenon is generated when the ignition of a flammable gas/air mixture leads to significant overpressure levels. In accordance with this definition, the effects produced by this event can be more severe than those generated by a flash fire. Generation of a UVCE is due to changes in the combustion process that are attributed to a total or partial confinement of the gas/air mixture as well as variations of the turbulence intensity in the environment.
3) Jet fire following the ignition of gas issuing from a pipe or orifice (thermal effects are dominant). This phenomenon is observed if the cloud is ignited at the source location. Thermal radiation is transferred away from the flame's visible boundaries. The effects associated with this event are more severe than those generated by a transient flash fire, especially if the jet impinges on an object.

The occurrence of these events can result into lethal effects on the general public and severe damage to nearby structures due to considerable thermal effects or high overpressures. When compared to natural gas, early ignition of a hydrogen-air cloud forming at the wellhead is highly likely (for instance due to electric arcs generated by differences in electric potential of the wellhead and the ground). The worst-case scenario is a vapor cloud which does not ignite immediately (for instance because gas outflow rates are very high) as an explosion with dramatic possible consequences can be expected.

The lethal distances (see Figure 45) are computed according to the severity of the overpressure or the thermal radiation. The evolution of the dispersion cloud during a blowout of a 500 000 m^3 hydrogen cavern, whose string length and diameter are 1000 m and 8-⅝", respectively (see description of the subterranean part of a blowout, above) is presented in the following figures. For this purpose, the dispersion of hydrogen is predicted for nine atmospheric conditions that describe the stability of the atmosphere as well as the velocity field in the surrounding environment. These conditions are specified by the French Circular of May 10th, 2010. The maximum expansion of the cloud is achieved during the first 120 minutes (Djizanne et al., 2022). The distance from the cloud for which irreversible effects occur (for an ignition at 120 minutes) depend on atmospheric conditions and the type of event. Typically, it is 40 m in the case of a flash fire, from 350 m to 700 m in the case of an unconfined vapor cloud explosion and 55 m to 110 m in the case of a jet fire (the thermal effects are computed at a height of 1.5 m to evaluate the hazardous effects on the general public.)

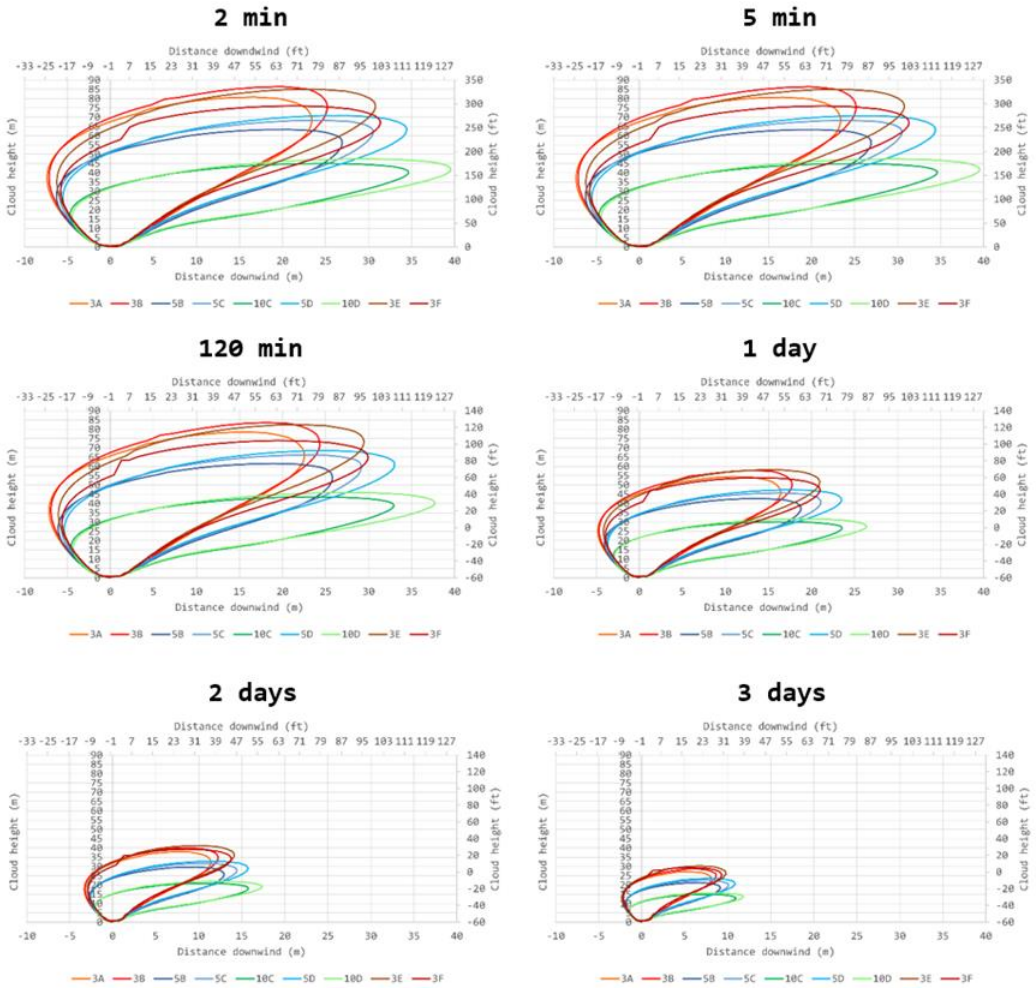

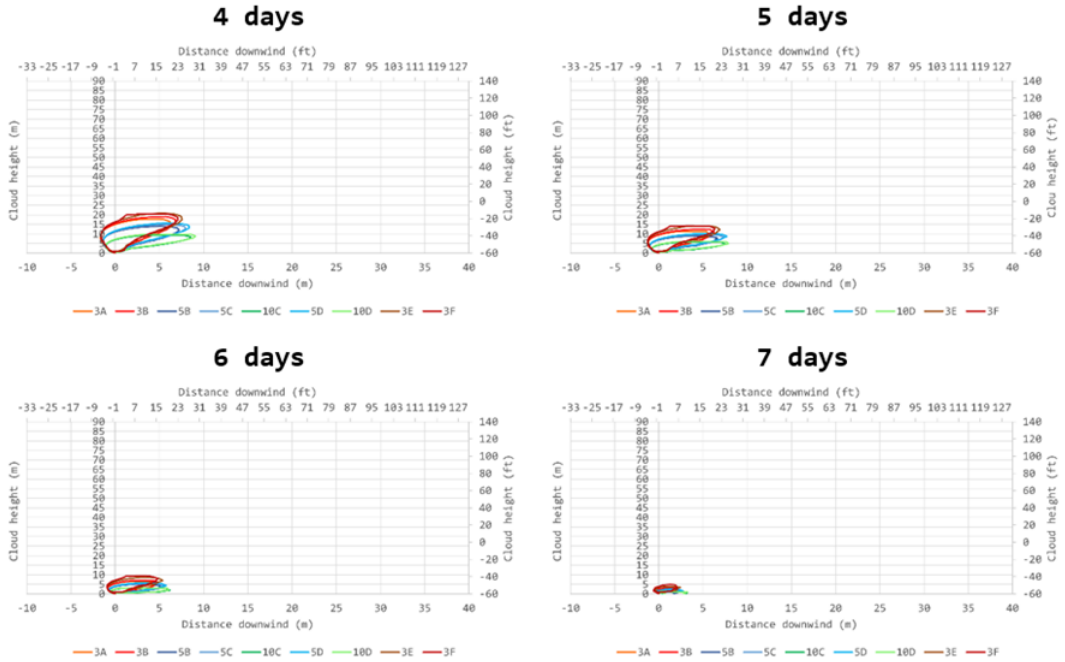

Figure 45. Extension of vapor cloud as a function of time (no ignition). Vertical axis: height above the wellhead. Horizontal axis: downwind distance from the wellhead.

2.3.4 SSSV (Underground automatic safety valve)

A hydrogen blowout must absolutely be prevented. In Europe, all gas storage caverns are equipped with an SSSV (Underground automatic safety valve, also called WRSV), an underground safety valve which is kept open through a pressurized line which is automatically closed in case of a wellhead failure. No blowout occurred in caverns equipped with an SSSV (several hundreds of caverns, sometimes operated for more than 50 years.) It must be noticed that debrining (first gas injection) raises a specific problem as, at this stage, the well is still equipped with a brine string, and an annular valve must be designed. During operation, the safety valve is set in the hydrogen production tubing. A tentative design is suggested in Figure 46 (Storengy, HYPSTER Project).

It seems that no specialized SSSV for hydrogen salt caverns have been designed and tested yet. A high priority should be attached to this issue.

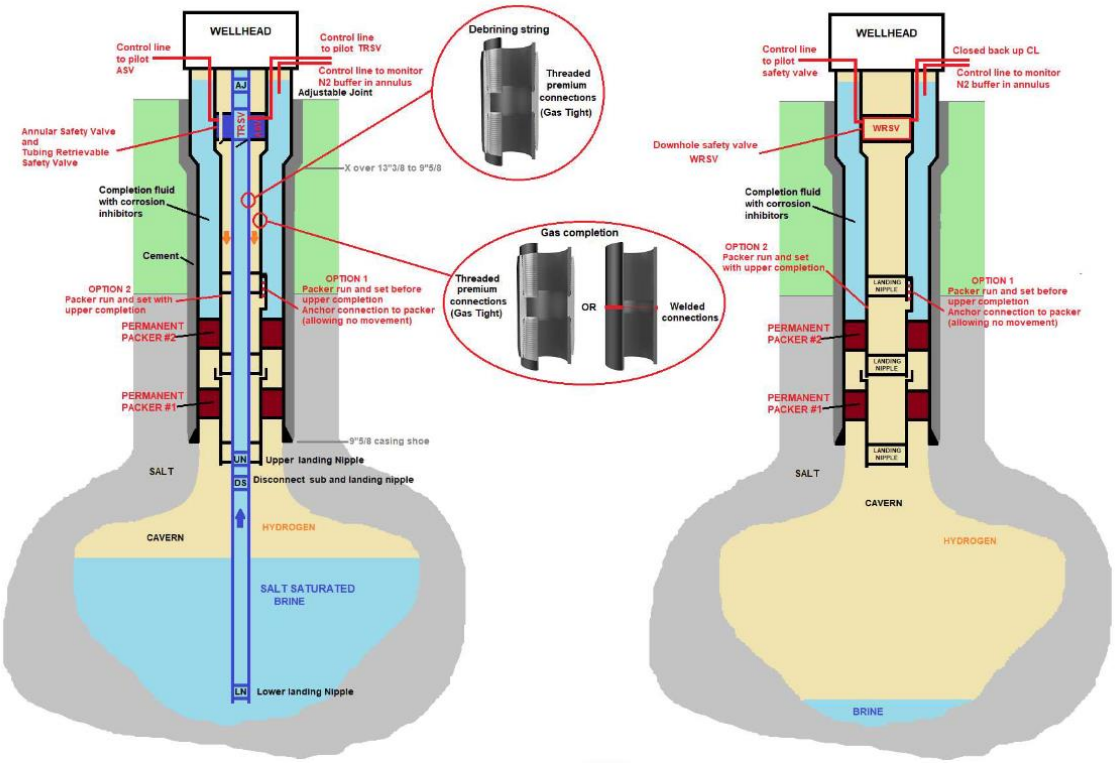

Figure 46. Tentative completion during debrining and storage operation (HYPSTER Project, Storengy).

3 Salt cavern structural stability

Author: Pierre Bérest – Brouard Consulting

3.1 Rock-salt behaviour

NB. the mechanical and transport properties of the host rocks of salt caverns are discussed at different places in this report.

3.1.1 Introduction

The mechanical behaviour of salt can be studied at various scales: the scale of crystals, at which dislocations climb, glide, and pile up; the scale of grains and interfaces between grains, where micro-cracks can form and pressure-solution is active; and the scale of the salt formation, in which the salt, clay or anhydrite layers generate specific interactions. These scales are provided by Nature. Two other scales are man-made. A large part of this Section is dedicated to the scale of the body under study: mine, cavern, or repository. The first paragraph discusses the laboratory scale.

3.1.2 Laboratory tests

Salt behaviour exhibits a fascinating complexity. Few other rocks have given rise to such a comprehensive set of laboratory experiments (see, for instance, the eight Proceedings of the Conferences on the Mechanical Behavior of Salt). While a full description of these efforts is beyond the scope of this paper, the results that are widely accepted by rock mechanics experts are listed below.

3.1.2.1 Steady-state creep

It generally is accepted (e.g., Bérest, 2013) that the axial strain,ε, observed during a creep test performed on a cylindrical-shaped salt specimen in the laboratory, is the sum of three components: the thermoelastic strain, the steady-state viscoplastic strain (ε_{ss}) and the transient viscoplastic strain (ε_{tr}), whose sum is the viscoplastic strain, $\varepsilon^{vp} = \varepsilon_{tr} + \varepsilon_{ss}$, as shown in Figure 47 and Figure 48, and mathematically expressed in one-dimensional rate form as:

$$\dot{\varepsilon} = \frac{\dot{\sigma}}{E} - \alpha\dot{T} + \dot{\varepsilon}_{ss} + \dot{\varepsilon}_{tr} \qquad (9)$$

where contractive strains and compressive stresses are positive, the applied deviatoric stress is $\sigma = \sqrt{3J_2}$ where $J_2 = s_{ij}s_{ji}/2$ is the second invariant of the deviatoric stress tensor, $s_{ij} = \sigma_{ij} - \frac{\sigma_{kk}\delta_{ij}}{3}$; E is Young's modulus; T is the absolute temperature; and α is the thermal expansion coefficient of salt. During a triaxial test, when confining pressure is P, the axial stress is $\sigma + P$ (no "extension test" during which the axial stress is smaller than the confining pressure is considered).

The *steady-state* viscoplastic component contribution to the total deformation is typically defined as a constant strain rate, $\dot{\varepsilon}_{ss}$, reached after several months when the temperature and the deviatoric stress are kept constant. For rock salt, steady-state strain rate is a function of shear stress and temperature. A simple formulation (Norton-Hoff's law, or "power" law) for a steady-state creep is:

$$\dot{\varepsilon}_{ss}^{ij} = \frac{3\dot{\varepsilon}_{ss}s^{ij}}{2\sqrt{3J_2}} \qquad \dot{\varepsilon}_{ss} = A(\Phi)\, exp\left(\frac{-Q}{RT}\right)\sigma^n \qquad (10)$$

where Q and n are two constants, with $n$in commonly the 3-6 range and the thermal constant, $\frac{Q}{R}$, in the 3000 to 10,000 K domain, and $A = A(\Phi)$ is a function of the relative humidity (in %RH). At a deviatoric stress of $\sigma = 10$ MPa and at ambient temperature, the steady-state strain rate for salt is typically about $\dot{\varepsilon}_{ss} = 10^{-10} s^{-1}$.

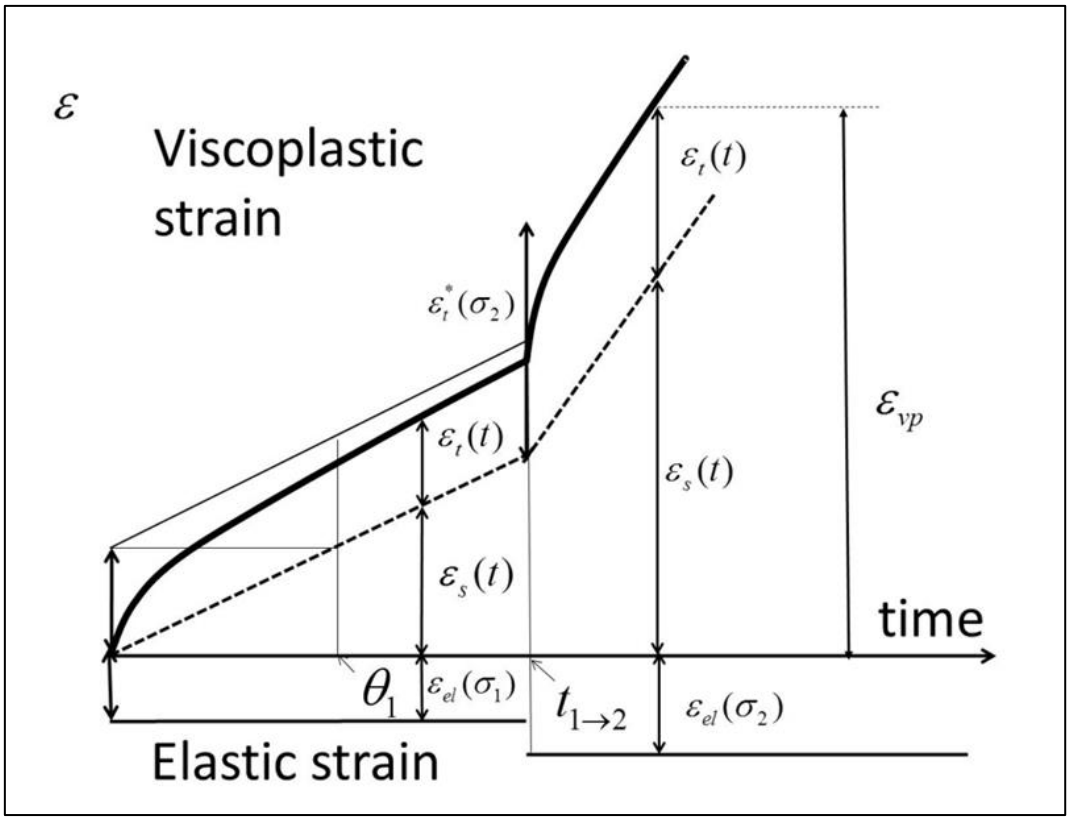

Figure 47. Schematic strain-stress curve during an isothermal uniaxial creep test. Increasing mechanical loading.

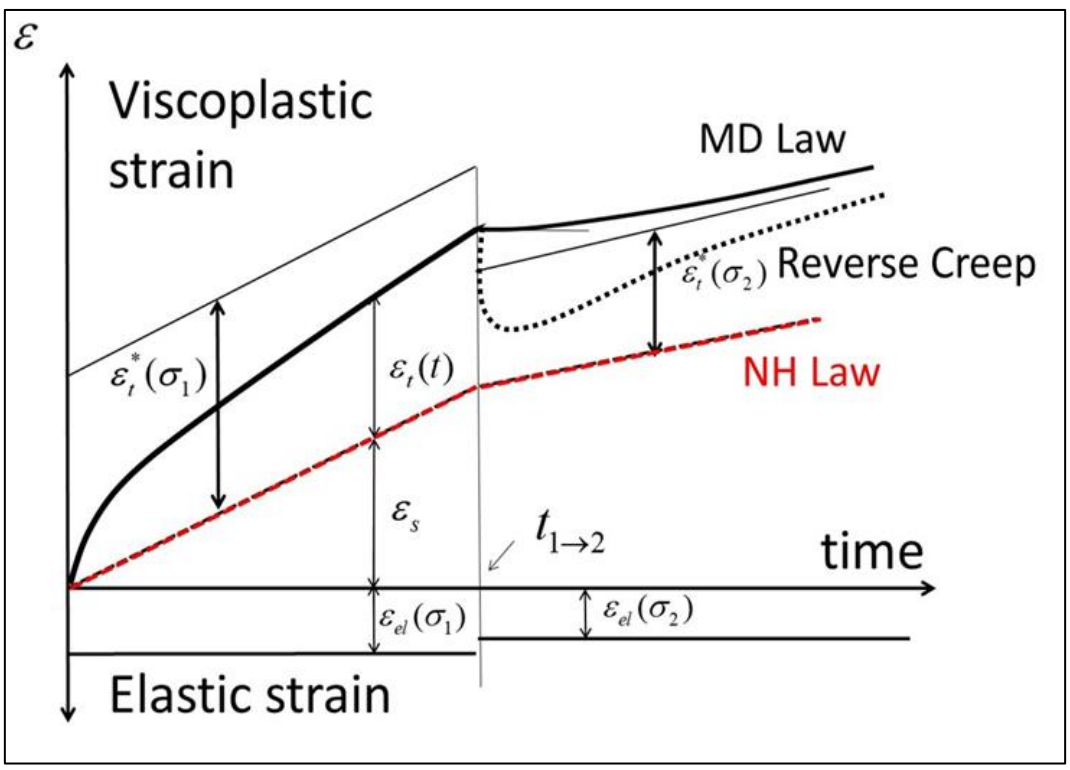

Figure 48. Schematic strain-stress curve during an isothermal uniaxial creep test. Decreasing mechanical loading.

3.1.2.2 Transient creep

The *transient* component describes the rock viscoplastic behaviour before steady state is reached. Any change in applied loading or temperature triggers a transient creep response. Following a compressive load increase ("direct transient creep") or $\sigma = \sigma_1$ when $t < t_{1\to2}$ and $\sigma = \sigma_2 > \sigma_1$ when $t > t_{1\to2}$, transient creep is characterized by faster initial strain rates compared to the steady state strain rates. If the applied stress is kept constant after the stress change, the transient rate slowly decreases until the transient strain exhausts itself (Figure 47), i.e., the total strain rate becomes equal to the steady-state rate and the transient strain reaches an asymptotic value defined as the transient strain limit $\varepsilon_{tr}^* = \varepsilon_{tr}^*(\sigma_2, T)$ that is a function of deviatoric stress and temperature. Munson et al. (1997) suggested:

$$\varepsilon_{tr}^* = K_0 e^{cT} \sigma^m \tag{11}$$

Where $K_0, c,$ and m ($m = 3$ is typical) are three material constants.

Munson et al. (1984) proposed an internal variable, $\zeta(t)$, such that, during a creep test, $\dot{\varepsilon}_{tr} = \dot{\zeta}$, to describe the evolution of the transient strain, which slowly increases to reach the transient strain limit $\varepsilon_{tr}^* = \varepsilon_{tr}^*(\sigma, T)$ when σ and T are kept constant. During a uniaxial creep test:

$$\frac{\zeta}{\varepsilon_{tr}^*} < 1, \frac{\dot{\zeta}}{\dot{\varepsilon}_{ss}} = \Phi(\zeta/\varepsilon_{tr}^*; \Delta) = exp\left[\Delta\left(1 - \frac{\zeta}{\varepsilon_{tr}^*}\right)^2\right] - 1 \tag{12}$$

where Δ is a function of σ (M-D transient law). The case of a load decrease ("stress drop", or $\sigma_2 < \sigma_1$), is addressed in the next paragraph.

Although other formulations can be selected, Norton-Hoff and M-D law constitutive laws capture the main features of both transient direct and steady-state creep behaviour and they will be used for interpretation, at least in a qualitative way, of the main results reported herein.

3.1.2.3 Reverse transient creep

When at $t_{1\to2}$ the applied deviatoric stress is decreased abruptly ($\sigma_2 < \sigma_1$) and kept constant (a "stress drop"), steady-state creep rate will be reached again after a long period of time. This rate is slower than the steady state rate when the load was higher as $\varepsilon_s(\sigma)$ and is an increasing function of σ. In fact two kinds of behaviour can be observed. When the load decrease is small, the transient viscoplastic rate remains contractive (as it was before the load change). When the load decrease is large, the transient viscoplastic rate is expansive: during several weeks or months, sample height increases (strain rate is *negative*) although the applied axial stress is compressive (Figure 48).

3.1.2.4 The case of small deviatoric stresses

It has been suspected for long (Spiers et al., 1990; Urai and Spiers, 2007) that, in the small deviatoric stress domain ($\sigma < 3$ MPa), the governing mechanism for salt creep was pressure solution – rather than dislocation creep (Figure 49). A consequence should be that creep rate in this domain is much faster - by several orders of magnitude - than the rate extrapolated from tests performed in the high-stress domain. In addition, creep rate should be a decreasing function of grain size: it should be a linear function of the applied stress, and the presence of a small amount of brine at the grain interface should be a necessary condition for active creep. These statements were based on theoretical arguments, geological evidence and the results of tests performed on artificial salt.

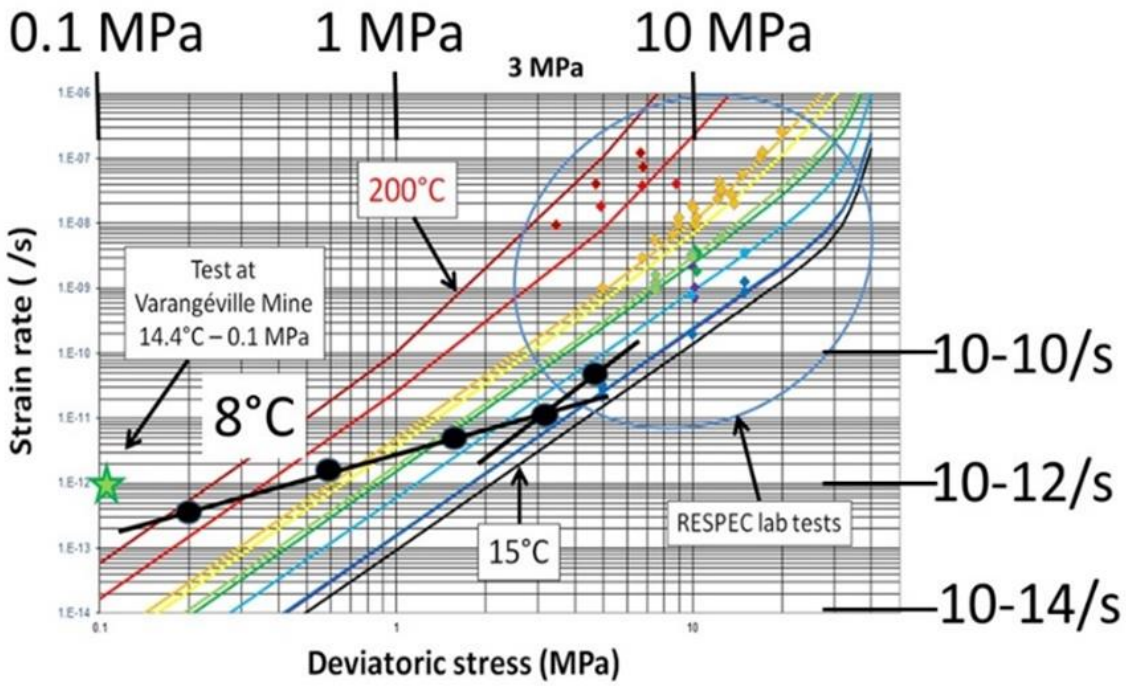

Figure 49. Tests performed on Avery Island samples at high deviatoric stress (coloured dots) at RESPEC laboratory and five tests performed at small deviatoric stress on the same Avery Island salt sample in the Altaussee drift (black dots) (from Bérest et al., 2022).

Several testing campaigns performed on natural salt during which testing devices were set in remote mine drifts (where temperature and humidity are quite constant) confirmed these views (Bérest et al., 2022, 2019a, 2005).

Various authors suggested constitutive laws which take into account this duality (Cornet et al., 2017). A simple example is Marketos et al. (2016) law:

$$\dot{\varepsilon}_S = A_1\, exp\left(\frac{-Q_1}{RT}\right)\left(\frac{\sigma}{\sigma_0}\right)^n + \frac{A_2}{D^3}\, exp\left(\frac{-Q_2}{RT}\right)\left(\frac{\sigma}{\sigma_0}\right) \quad (13)$$

where D is the grain size, $\sigma_0 = 1$ MPa is a reference stress, T is the absolute temperature (in Kelvin). When the applied stress (σ) is low, the power-law term is negligible, and the opposite is true when the applied stress is high.

Such a change in the constitutive has important consequences in shallow caverns, when cavern pressure is close to geostatic (Figure 50), and (Cornet et al., 2017) when the virgin state of stress is not isotropic.

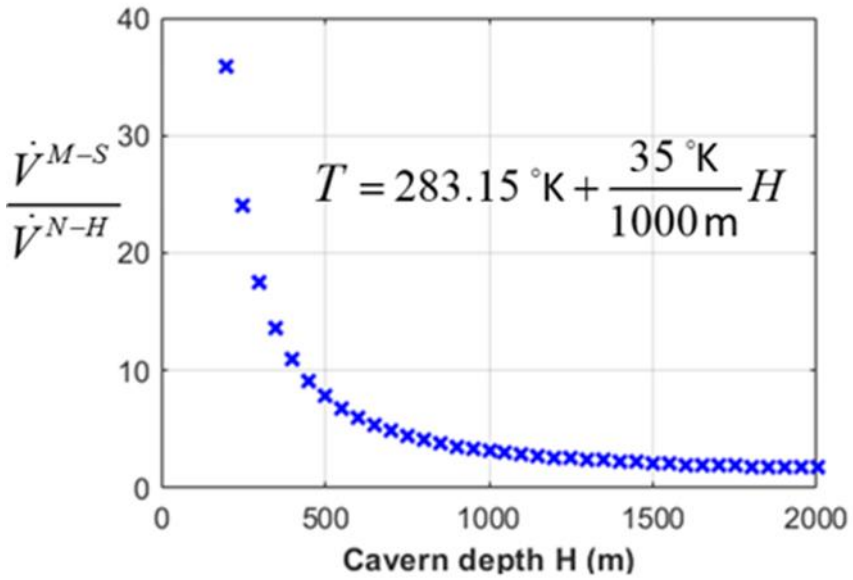

Figure 50. Comparison between steady-state volume loss rates at various cavern depth when Munson-Dawson and Marketos laws are considered (from Gordeliy and Bérest, 2022).

3.1.2.5 Temperature

The role of temperature is two-fold. On one hand, creep rate is a function of the sample temperature; on the other hand, salt warming or cooling generates thermal expansion or contraction.

$$\dot{\varepsilon}_{ij} = \frac{1+\nu}{E}\dot{\sigma}_{ij} - \frac{\nu}{E}\dot{\sigma}_{kk}\delta_{ij} + \alpha_R \dot{T}\delta_{ij} + \frac{3A}{2} exp\left(-\frac{Q}{RT}\right)\left(\sqrt{3J_2}\right)^{n-1} s_{ij} + \dot{\varepsilon}_{ij}^{tr}(T,..) \qquad (14)$$

The influence of temperature on the steady-state strain rate is captured through the term: $exp\left(\frac{-Q}{RT}\right)$, and $\frac{\dot{\varepsilon}_{,T}^{SS}}{\varepsilon^{SS}} = Q/RT^2 \approx 3 - 10 \times 10^{-2}/°\mathrm{C}$ when $T = 300\,\mathrm{K}$. (Transient strain rate is also temperature-dependent.) However, several authors (for instance, Tijani, CEC Cosa Report, 1987, unpublished.) underlined that such a formulation is likely to be too simple. Hunsche (1984) mentioned that for a given testing temperature, the creep rate is slower after a step during which temperature was higher than it was before that step. A possible explanation for this is that some brine is removed from the sample when the temperature is high; this might also be a consequence of "thermal reverse creep". In a cavern, temperature of the stored fluid may change by several dozens of °C, with possible effects on rock temperature and the creep closure rate of the cavern, but this effect does not seem to be large enough to be detected; the same cannot be said of a repository of heat-generating wastes.

The thermo-elastic effect of temperature is captured through the coefficient of thermal expansion, which is larger than for most rocks, $\alpha_{salt} \approx 4 \times 10^{-4}/°\mathrm{C}$. Daily fluctuations in room temperature by ± 1°C, or $\dot{T} \approx 10^{-5} s^{-1}$ can blur the results of a creep test when the steady-state strain rate is slower than $\dot{\varepsilon}_{ss} \approx 10^{-9} s^{-1}$.

It is known that, in an idealized spherical or cylindrical cavern, a change in cavern temperature has no effect on cavern volume — a counter-intuitive result that remains approximately true even when a more realistic cavern shape is considered (Karimi-Jafari et al., 2007). Conversely, tangential stresses, or σ_{tt}, are generated at the cavern wall. Their order of magnitude is large:

$$\frac{\sigma_{tt}}{\Delta T} = \frac{-E_{salt}\alpha_R}{(1-\nu_{salt})} \approx 0.8 \text{ MPa}/^\circ \text{ C}, \quad (15)$$

These tangential stresses are compressive when the cavern fluid is warmed and tensile when the cavern fluid is cooled. Because the tensile strength of salt is low (1-2 MPa), the effect of fluid cooling can be especially important. In fact, prompted by the needs of gas traders, withdrawal rates from gas caverns tend to be faster; cavern gas cools down by several dozens of °C during withdrawal. This effect has been discussed by several authors (Bérest et al., 2012; Lux and Dresen, 2012; Pellizzaro et al., 2011; Wallner and Eickemeier, 2001; Zapf et al., 2012). It was feared that such a temperature drop would generate fractures at the cavern wall. However, computations prove that, in most cases, only a thin salt layer at cavern wall experiences severe temperature drops and tensile stresses (Bérest et al., 2012).

3.1.2.6 Visco-plastic threshold

It has been frequently observed that, in Zechstein salt domes, anhydrite "stringers" float in the salt mass. Anhydrite is significantly denser than salt and dimensional analysis – or more sophisticated numerical computations – strongly suggest that these stringers should sink to the bottom of the dome (Li and Urai, 2016). They do not, and it was suggested that there exists a threshold for deviatoric stress below which viscoplastic behaviour vanishes (Van Oosterhout et al., 2022). The testing campaign mentioned above suggests that, should such a threshold exist, it would be smaller than 0.05 MPa.

3.1.2.7 Humidity

Influence of water vapor on salt creep during laboratory tests has been investigated by several authors, among which are Horseman (1988), Spiers et al. (1990), Le Cléac'h et al. (1996), and Hunsche and Schulze (2002, 1996). Hunsche and Schulze proved that steady-state creep rate increases by a factor of 90 when relative air humidity varies from 0% RH to 75% RH (the limit above which salt dissolves in air water vapor); they also proved that this effect was much more pronounced during uniaxial tests and, more generally, when the sample experienced dilation. Dilation increases salt porosity and permeability; vapor can diffuse through micro-cracks and open grain boundaries; at contact areas, where stresses are high, solubility rises and creep is faster. Van Sambeek (2012) observed a clear correlation between room-closure rate (which was slow) and relative humidity in a 600-m deep salt mine.

One can expect that brine influence be even more significant. Spiers et al. (1990) and Cosenza et al. (2002) proved that, when saturated brine is added at the periphery of a salt sample submitted to a moderate mechanical loading (say, 10 MPa), creep rate immediately accelerates. However, when mines are flooded with brine, it seems, in most cases, that the brine-filled mine is more stable than the dry mine had been. [See Van Sambeek & Thoms (2000), who observed that subsidence rate above the Jefferson Island Mine decreased by a factor of 10 after the mine was flooded, or Feuga (2003), who performed a sonar survey in an old flooded mine at Dieuze to find that actual mine geometry was exactly the same as what was expected from a map drawn by the miners 130 years before.] These results suggest that creep acceleration only exists in a relatively thin damaged zone at pillar walls and that the favourable effect of the increase in mine internal pressure (from atmospheric to halmostatic; i.e., from 0 bar/m to 0.12 bar/m) is much more significant from the perspective of mine stability. This topic clearly is still open to discussion.

3.1.2.8 Triaxiality

It is assumed in most models that viscoplastic strain rate is a function of stress through the second invariant of the stress tensor, or J_2. In fact, most laboratory tests are the so-called "*triaxial*" tests during which the two main stresses are equal, which means that the influence of the third invariant of the stress tensor, or J_3, cannot be investigated. Liu & Hunsche (1988) performed "*true*" triaxial tests on cubic samples and proved that "*within the limits of precision of the measurements, the behaviour is isotropic*" (p.235). Mellegard et al. (2007) performed creep tests under alternating compressive ($0 > \sigma_2 = \sigma_3 > \sigma_1$) and extensive ($0 > \sigma_1 > \sigma_2 = \sigma_3$) states of stresses and observed that while creep rate depends on

$|\sigma_1 - \sigma_2|$ only, "*each time the Lode angle was changed, a significant transient response (not predicted by constitutive models) was observed*" (p.9). Munson et al. (1992), however, proved that closure displacements in a 655-m deep room of the WIPP repository was explained better when, instead of $\sqrt{3J_2}$, the viscoplastic potential was expressed in terms of $|\sigma_1 - \sigma_3| = 2\,cos\,\psi\sqrt{J_2}$ (the Tresca criterion; ψ is the Lode angle). Tests performed on hollow cylinders seem to confirm this choice.

3.1.3 Constitutive laws

Many models were proposed to capture the main features of this behaviour. In simple terms, most of them include a Maxwell model (to describe steady-state creep) and a Kelvin model (to describe transient creep). However, these models are non-linear (the relations between stress and strain rate are non-linear); the parameters strongly depend on temperature; in some models, relative humidity also plays a role. More recently, in addition to dislocation creep, which is the governing mechanism at high deviatoric stress, a second mechanism, pressure solution, which is especially active in the low deviatoric stress (σ < 3-5 MPa) also is taken into account.

A couple of examples are briefly described below, which will be used in the following.

LUBBY2 CREEP LAW

$$\varepsilon = \left[\frac{1}{\bar{\eta}_M} + \frac{1}{\bar{\eta}_K}\left(1 - \frac{\varepsilon_{tr}}{\sigma}\bar{G}_K\right)\right]\cdot\sigma$$

$$\dot{\varepsilon}_{tr} = \frac{\sigma}{\bar{\eta}_K}\left(1 - \frac{\varepsilon_{tr}}{\sigma}\bar{G}_K\right)$$

$$\bar{\eta}_M = 3\eta_{M_o}\exp(\boldsymbol{m}_o\sigma + \boldsymbol{l}_o T)$$

$$\bar{\eta}_K = 3\eta_{K_o}\exp(\boldsymbol{k}_2\sigma)$$

$$\bar{G}_K = 3G_{K_o}\exp(\boldsymbol{k}_1\sigma)$$

6 parameters to be fitted

MUNSON-DAWSON CREEP LAW

$$\dot{\varepsilon}_{ij}^{vp} = \frac{\partial\sigma}{\partial\sigma_{ij}}F\dot{\varepsilon}_{ss} \qquad \begin{cases} F = e^{N(1-\varsigma/\varepsilon_t^*)^2} & \text{when } \varsigma \le \varepsilon_t^* \\ F = e^{-\delta(1-\varsigma/\varepsilon_t^*)^2} & \text{when } \varsigma \ge \varepsilon_t^* \end{cases}$$

$$\dot{\varsigma} = (F-1)\dot{\varepsilon}_{ss} \qquad \dot{\varepsilon}_{ss} = A\exp(-Q/RT)\sigma^n \quad \} \text{ Steady-state}$$

$$\sigma = \sqrt{3J_2} \qquad J_2 = \frac{1}{2}s_{ij}s_{ij}$$

$$\varepsilon_t^* = K_0 e^{cT}(\sigma/\mu)^m$$

$$\mu = \frac{E}{2(1+\nu)} \quad \text{and} \quad \Delta = \alpha_w + \beta_w Log_{10}(\sigma/\mu) \quad \} \text{ Transient}$$

7 parameters to be fitted

LEMAITRE CREEP LAW

$$\varepsilon = A_o\exp\left(-\frac{Q}{RT}\right)\left(\frac{\sigma}{K}\right)^{\beta} t^{\alpha}$$

3 parameters to be fitted

- The Lubby2 creep law (Heusermann et al., 2003; Lux, 1984) is a Kelvin + Maxwell non-linear model which describes both transient and steady state creep.
- The Munson-Dawson model (Munson and Dawson, 1984) is a (non-linear) generalized Kelvin-Maxwell model, including both transient and steady state creep. However, it cannot describe rheological reverse creep, as it is built in such a way that the sum of the transient and steady state creep rate is always positive ($\dot{\varsigma} + \dot{\varepsilon}_{ss} = F\dot{\varepsilon}_{ss} > 0$).
- The Norton-Hoff model is a simplified version of the Munson-Dawson model; it includes steady state creep only (i.e., $F = 1$). As such, it is well adapted to the computation of the long-term behaviour of a cavern submitted to a constant pressure.
- The Lemaitre creep law (Tijani et al., 2009), also called Lemaitre-Menzel-Schreiner creep law, is worth mentioning as it is extremely simple; three parameters only are used. This law allows a good description of the initial transient phase during a several month-long lab test. As such, it is well adapted to the computation of a cavern submitted to pressure cycles. As $\alpha > 1$, it predicts a vanishing creep rate in the long term.

Many other laws, more or less sophisticated, were proposed in the literature, see for instance Günther and Salzer (2012) or Hampel (2012).

3.1.4 Cavern creep closure

3.1.4.1 Consequences of the main features of salt behaviour for cavern behaviour

From laboratory tests performed at the laboratory, a few conclusions can be inferred:

- Rock salt behaves as a non-Newtonian fluid. In the long term, salt cannot withstand without flowing a non-isotropic state of stresses (in which shear stresses are non-zero). A consequence is that all salt caverns shrink when fluid pressure is smaller than geostatic pressure at cavern depth.
- Cavern creep closure rate increases exponentially with cavern depth. The driving force for cavern volume loss is the gap between geostatic pressure and cavern fluid pressure; creep rate is an increasing function of rock temperature; both increase with depth.
- Large (transient) thermal stresses are generated at cavern wall following temperature changes.
- Cavern behaviour depends upon the full history of cavern pressure evolutions since cavern creation

More difficult to anticipate, in a cavern, in addition to transient *rheological* creep described above, transient *geometrical* creep results from the slow redistribution of stresses in the rock mass – an effect which does not exist in a sample tested at the laboratory.

3.1.4.2 Cavern volume and volume loss measurement

Measuring cavern volume loss, or cavern volume loss rate, is not an easy task. A fundamental difference must be made between brine caverns or liquid/liquefied hydrocarbon caverns and gas storage caverns.

Most often, liquid storage caverns are operated through the brine compensation (or “balance”) method. A large amount of brine is available at ground level; the well is equipped with a brine injection string; products are circulated through the annulus; any brine injection (or withdrawal) is balanced by an equivalent withdrawal (or injection) of products, in order that cavern pressure remains approximately constant. In most cases, cavern pressure is kept halmostatic: the operating pressure at casing shoe depth, divided by casing shoe depth; i.e., the gradient at casing shoe depth, is 0.12 bar/m. [However, in some cases, the cavern is shut-in and cavern pressure increases due to liquid warming and cavern creep closure; the cavern is vented when its pressure reaches a pre-definite level, for instance a gradient of 0.18 bar/m. The advantage of this last method, which is used for instance in the US Strategic Petroleum Reserve, is that the average creep closure rate is slower that when the gradient is kept constant and equal to 0.12 bar/m.]

Gas storage caverns, most often, are operated as a pressurized bottle: fluid pressure (P) experiences large swings as it is an increasing function of the gas inventory (m), which is essentially varying, $PV = mrT$. A minimum and a maximum gas pressures are defined. In many cases, the maximum gradient is 0.18 bar/m (Bérest et al., 2020). The minimum gradient is 0.06 bar/m, typically; however, this value is selected according to the specifics of the site. It is less frequent that gas storage caverns be operated according to the brine compensation method (operations require that a large amount of brine be available at ground level). The hydrogen storage caverns at Teesside (UK) and several natural gas caverns in Canada are operated according to the brine compensation method.

Choice of the operating method has profound consequences. High pressures may have detrimental consequences for cavern tightness; low pressures lead to high volume loss rates (which are a highly non-linear function of the gap between geostatic pressure and cavern fluid pressure). Large pressure swings (which generate large temperature swings in gas caverns) raise specific problems. In that sense, the balance method, during which cavern pressure is (most often) constant and moderate, raises less problems. However, in the case of gas caverns, operations are much simpler – and cost-effective – when cavern pressure is cycled, and this method is widely preferred by operators.

Measurement of cavern volume and cavern volume loss rate is not an easy task. *Sonar surveys* provide much information (in addition to cavern volume, cavern shape is measured). However, its accuracy is 3-5% (in the best cases, a resolution of 1% can be achieved. A remarkable example was described by Rokahr et al. (2007), see also Section 3.4, Brittle failure, and in most caverns a clear picture of cavern volume loss rate cannot be reached before several years or more. *Other methods* can be used; cavern volume evolution can be measured; however, these methods do not allow measuring cavern shape changes; in addition, interpretation of tests results is not straightforward, as account must be taken of the effects of phenomena other than creep closure (brine warming and brine thermal expansion; possible leaks through the well casing or cavern walls; additional dissolution following cavern pressure changes, etc.). For this reason, these tests are not routinely performed and must be considered as scientific tests.

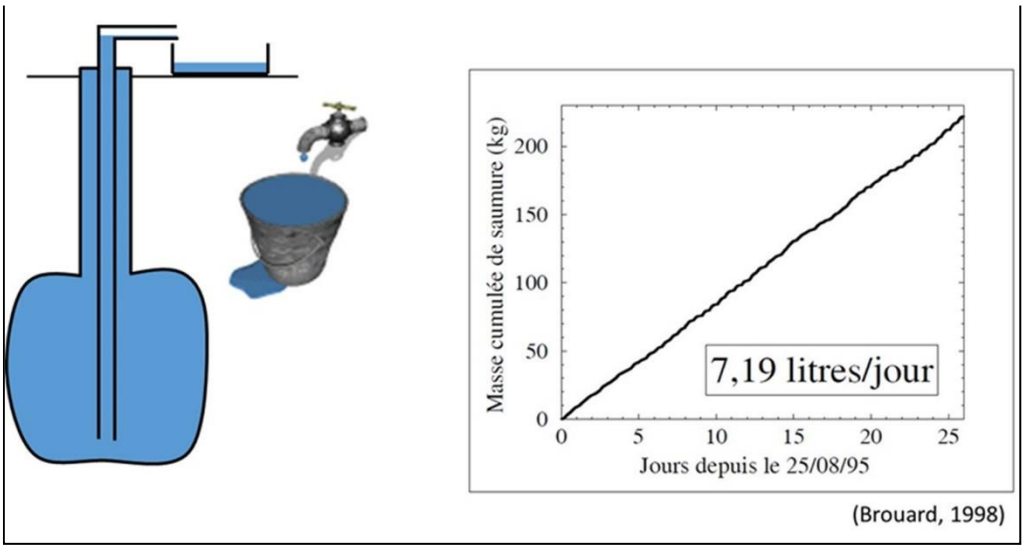

Figure 51. Example of a liquid outflow test.

Among these methods, the *liquid outflow test* (Figure 51) consists of opening the wellhead and recording the flow of liquid expelled from the wellhead as a function of time. The cavern must be equipped with a liquid-filled string (brine, in most cases). Interpretation is not straightforward as, in addition to cavern creep closure, other phenomena (brine warming, additional dissolution) contribute to brine outflow.

The *shut-in pressure test* is the most commonly performed. The wellhead is closed, and wellhead pressure evolution as a function of time is recorded. Interpretation is more difficult as pressure is not kept constant during the test. Dozens of examples were described in the literature.

Such a test is almost impossible in a gas cavern, as gas in a cavern (even when highly pressurized) is more compressible than any liquid by 1 or 2 orders of magnitude. A third method, the interface displacement measurement, which applies to gas storage caverns, consists in measuring vertical displacements of the gas-brine interface during gas injection or withdrawal. This method is not frequently used (a string lowered in the cavern is needed.) An interesting example (Figure 52) was provided by Denzau and Rudolph (1997).

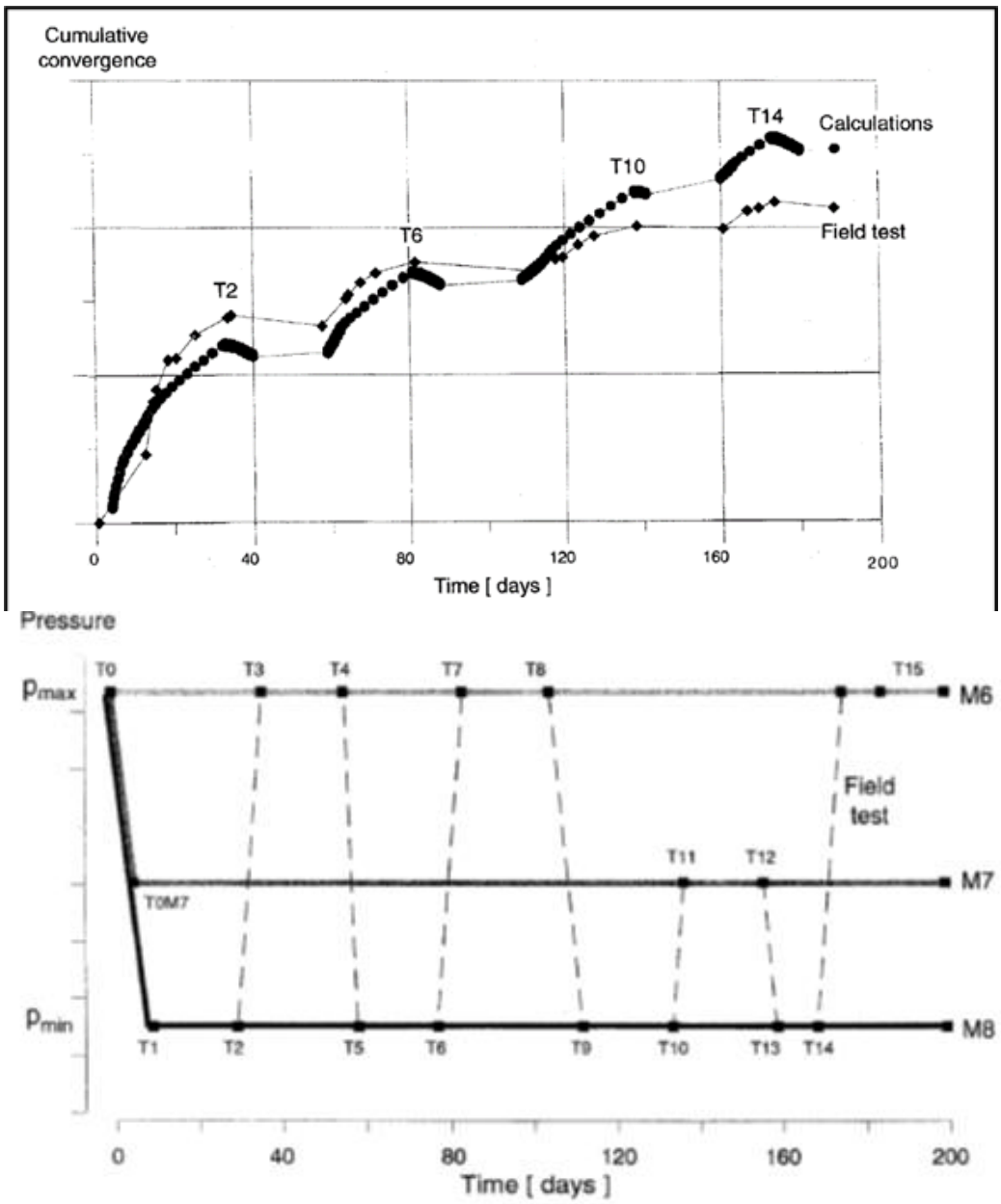

Figure 52. Denzau and Rudolph test (1997). Gas pressure history and cumulated volume loss (no unit is provided) during a four-cycle pressure test in a gas storage cavern ay Epe, Germany (Denzau and Rudolph, 1997).

As a matter of fact, only a dozen of fully documented testing results was published in the literature.

3.1.4.3 The role of cavern depth

A couple of important lessons can be drawn from the simplest model, the Norton Hoff constitutive law, or $\dot{\varepsilon} = \dot{\sigma}/E + A\,exp(-Q/RT)\sigma^n$, which captures a couple of important features of salt behaviour. In the case of an idealized spherical cavern, when cavern pressure (P_c) is kept constant and halmostatic and geostatic pressure is P_∞, the steady state deviatoric stress and the volume loss rate are:

$$S^{ss}(r) = \left(\frac{a_0}{r}\right)^{\frac{3}{n}} \frac{3(P_\infty - P_c)}{2n} \qquad \frac{\dot{V}^{ss}}{V} = -\frac{3}{2} A\, exp\left(-\frac{Q}{RT}\right)\left[\frac{3(P_\infty - P_c)}{2n}\right]^n \qquad (16)$$

A somewhat similar formula can be obtained in the case of an idealized cylindrical cavern:

$$S^{ss}(r) = \left(\frac{a_0}{r}\right)^{\frac{2}{n}} \frac{(P_\infty - P_c)}{n} \qquad \frac{\dot{V}^{ss}}{V_0} = -A\, exp\left(-\frac{Q}{RT}\right)\sqrt{3}^{n+1}\left[\frac{P_\infty - P_c}{n}\right]^n \qquad (17)$$

(The same formula holds for the Munson-Dawson model). Rock mass temperature, brine volumetric weight, halmostatic pressure, geostatic pressure are linear functions of depth, $T = T_0 + Gz$, $G = 18$ °C/km, $P_c = \gamma_b z$, $P_\infty = \gamma_R z$, $\gamma_b = 0.12$ bar/m, $\gamma_R = 0.22$ bar/m. Steady state volume loss rate is an increasing function of depth because both the rock temperature and the gap between geostatic pressure and halmostatic pressure increase with depth. This is clearly confirmed by field observations. Tests at the Vacherie and Rayburn's salt domes in northern Louisiana have been described by Thoms and Gehle (1983). In early 1978, exploratory boreholes were drilled to depths of 5000 ft. (1525 m). The exploratory boreholes were logged several times with 4-arm calliper tools over a period of approximately four years. Borehole pressure was kept constant ("halmostatic", or 0.12 bar/m – 0.52 psi/ft). A final calliper logging of both holes was performed in April 1982 (1465 days and 1438 days, respectively, after boreholes drilling). Below a depth of approximately 3400 ft. (1040 m), hole closure increased drastically (Figure 53), reflecting the non-linear effect of higher temperature and the larger gap between geostatic pressure and brine pressure in the borehole (i.e., the effect of depth below ground level).

Figure 53 dispatches diameter loss as a function of time and depth. Closure rate decreases with time in the lower part of the well, where the closure rate is faster.

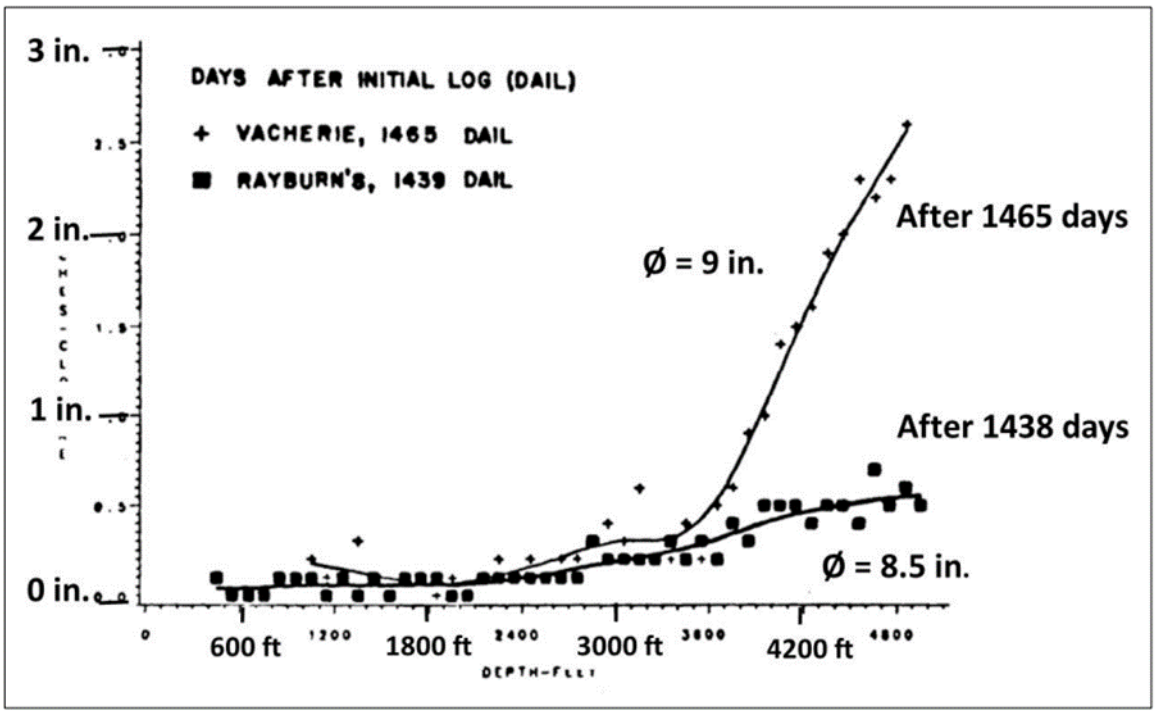

Figure 53. Diameter loss as a function of depth in two boreholes during a 4.5-year period: diameters at Vacherie and Rayburn's are 9" and 8.5", respectively (after Thoms and Gehle, 1983).

3.1.4.4 Transient behaviour in a salt cavern

The role of cavern depth is clearly illustrated by the analysis of steady state. However, steady state does not provide a full picture of cavern behaviour, even in the case when cavern pressure is kept constant. Figure 54 provides diameter loss as a function of depth in Vacherie's borehole at three different instants after the initial log (163 days, 413 days, and 1465 days, respectively). Closure rate is much faster during the first year after borehole creation.

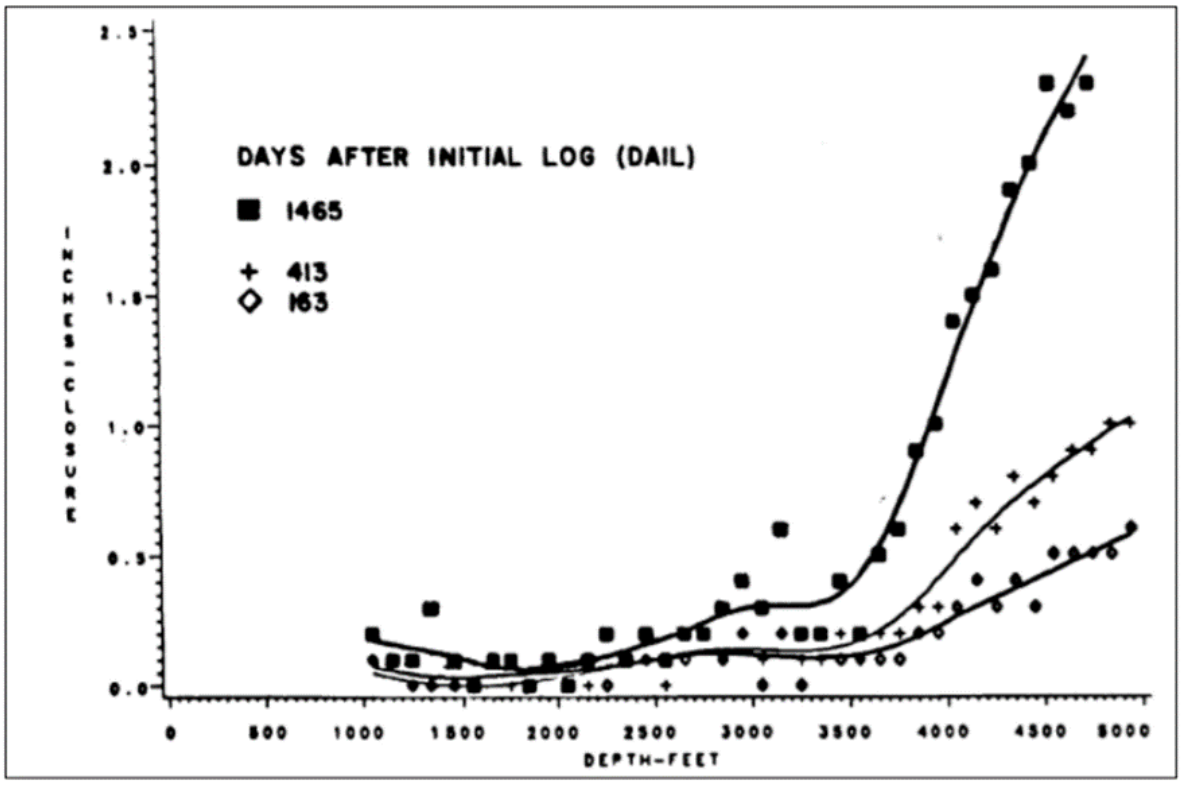

Figure 54. Diameter loss as a function of time in Vacherie's borehole after 163 days, 413 days and 1465 days (4.5 years), DAIL = Days After Initial Logging (after Thoms and Gehle, 1983).

3.1.4.5 Geometrical versus rheological transient creep closures

A couple of theoretical comments are needed at this stage. Consider for instance the case (somewhat sketchy) of a cavern created instantaneously at $t = 0$. Cavern pressure, which was P_∞ before cavern creation, equals P_c after cavern creation (P_c is the halmostatic pressure, typically, and is kept constant after cavern creation, Figure 55).

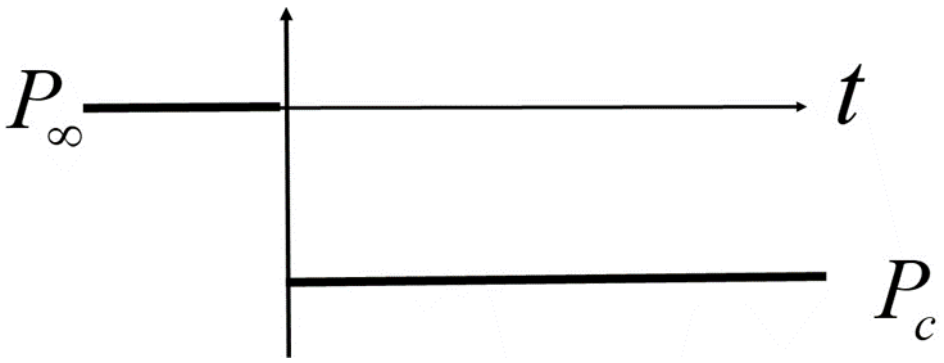

Figure 55. Pressure evolution in a non-cycled cavern.

An idealized spherical cavern and the simplest model (Norton-Hoff) are considered. This model includes no rheological transient creep (the transient creep observed at the laboratory is not included in the numerical model). The initial deviator stress ($S = \sigma_{rr} - \sigma_{\theta\theta}$; $|S|$ is the deviatoric stress) and the initial volume loss can write:

$$S^{ss}(r, t = 0^+) = \left(\frac{a_0}{r}\right) \frac{3(P_\infty - P_c)}{2} \qquad \frac{V^{ss}}{V}(t = 0^+) = -\frac{3(1+\nu)}{2} \frac{(P_\infty - P_c)}{E} \qquad (18)$$

And the derivative of the deviator stress (when the Poisson's coefficient is *v* = 0.5) can write (Gordeliy and Bérest, 2022):

$$\frac{\partial S}{\partial t}(r,0^+) = EA^*\left[\frac{3}{2}(P_\infty - P_c)\right]^n\left[\frac{1}{3n}\left(\frac{a_0}{r}\right)^3 - \left(\frac{a_0}{r}\right)^{3n}\right] \quad (19)$$

From which a couple of important lessons can be drawn:

1. **The initial deviatoric stress is much larger than the steady state deviatoric stress.**

This derivative of the deviator is not zero; after $t = 0$, *cavern evolution is transient*, even though the constitutive equation includes no transient component. Such a transient cavern evolution is said to be *geometrical,* as opposed to the *rheological* transient creep, which results from the constitutive law. The geometrical transient creep is due to the slow redistribution of stresses in the rock mass from its initial to its final steady-state distribution, an effect that does not exist when an idealized triaxial creep test is performed on a rock sample. (Stresses are uniform in the sample.) Note that the deviator decreases at the cavern wall ($\partial S(a_0, 0^+) < 0$) and increases at a large distance from the cavern wall ($\partial S(r, 0^+) > 0$ when $\frac{r}{a_0} > [3n]^{3(n-1)}$). It slowly converges to the steady-state distribution. Failure criteria will be discussed later. However, it can be noted that a "dilatant" criterion, $\sqrt{3J_2} < \bar{a}[I_1]$, or $|S| < \bar{a}|2S + 3P_c|$ (DeVries et al., 2003]) often is used to assess cavern integrity; $I_1$is the first invariant of the Cauchy stress tensor; see Section 3.4, Brittle failure. As $\frac{|S|}{|2S+3P_c|}$ is an increasing function of S, and $S(a_0, t)$ is a decreasing function of time at the cavern wall, this criterion is more demanding immediately after cavern creation rather than later.

2. **The initial volume loss rate is much faster than the steady state volume loss rate**

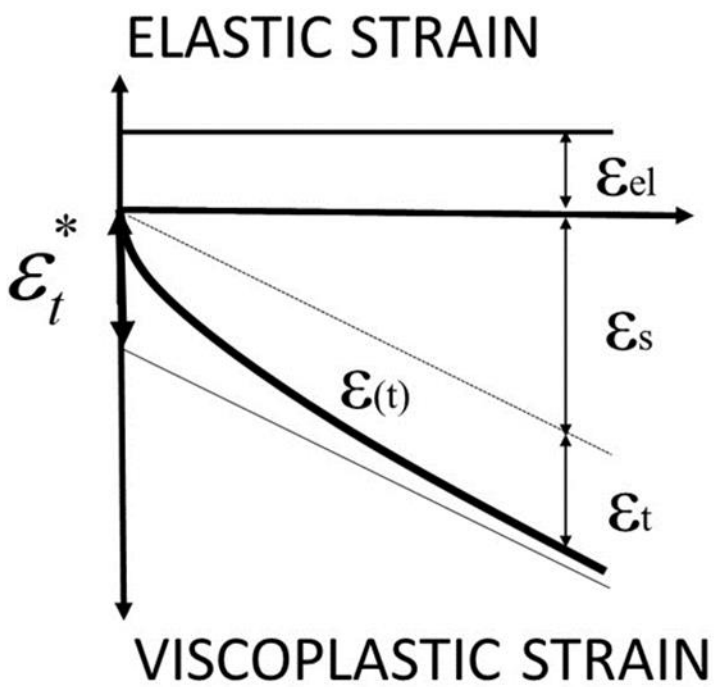

Figure 56. Schematic of Munson-Dawson law.

A more realistic picture can be obtained when considering the Munson-Dawson law (Figure 56) which, opposite to Norton-Hoff law, takes into account transient creep:

$$\dot{\varepsilon} = \frac{\dot{\sigma}}{E} + AF[\sigma, T, \zeta(t)]\, exp\left(\frac{-Q}{RT}\right)\sigma^n \qquad (20)$$

where F is a monotonously decreasing function of an internal parameter $\zeta = |\varepsilon_{tr}|$ (the transient strain) which increases to ε_{tr}^* (the cumulated transient strain rate) when σ and T are kept constant such that $F(\sigma, T, \varepsilon_{tr}^*) = 1$ (transient creep exhausts itself).

Figure 57 displays the evolution of an idealized spherical volume when pressure in a 950-m deep cavern drops abruptly from geostatic pressure ($P_\infty = 20.9$ MPa) to halmostatic pressure (11.4 MPa). Both the NH-law (no rheological transient creep) and the M-D law (rheological transient creep is taken into account) are considered. The geometrical transient loss of volume is active during several centuries. During a short period, the rheological transient loss of volume is extremely active (it is larger than the geometrical transient loss of volume by several orders of magnitude). However, after one year, it becomes negligible and only the geometrical loss of volume must be taken into account.

Figure 57 compares the evolutions of cavern volume loss rate in the case of the Munson-Dawson and Norton-Hoff creep laws.

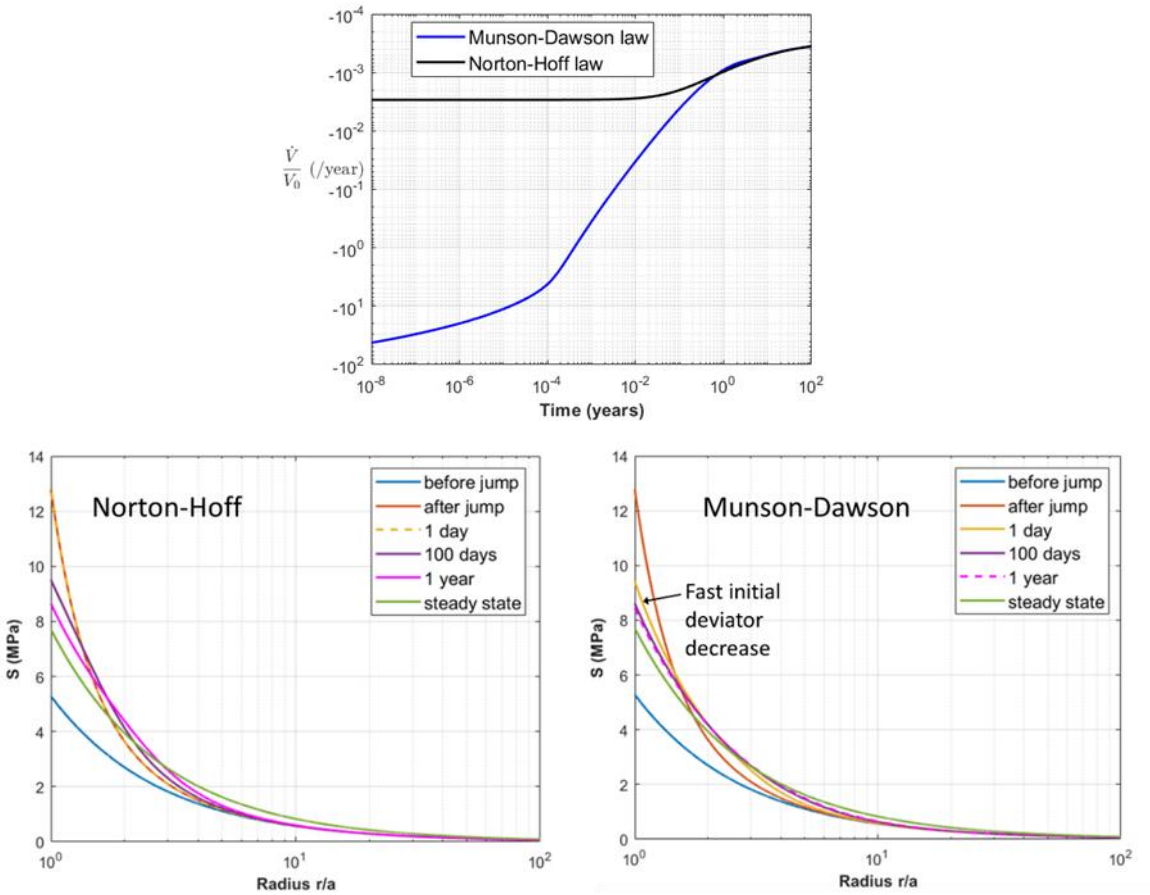

Figure 57. Creep closure rate as a function of time (Above) and Deviatoric Stress distribution in the rock mass when Norton-Hoff and Munson-Dawson laws are considered (from Gordeliy and Bérest, 2022).

Obviously, these notions apply when cavern pressure is kept constant. When cavern pressure is cycled, with a cycle period somewhat similar to the duration during which rheological creep is active, volume loss is much larger than in the case when cavern pressure is constant and equal to the average pressure value during a cycle (see Paragraph 3.1.5). This is due, on one hand, to the fact that the constitutive law is non-linear (volume loss rate is faster when pressure is low than when pressure is high) and, on the other hand, to the effect of rheological creep, which is active during each cycle.

3.1.4.6 Creep closure rate is a site-specific notion

Creep ability strongly depends on the salt formation under consideration. Volume loss rate strongly depend (several orders of magnitude) on the effective mechanical properties of the salt formations (Brouard and Bérest, 1998). In the Table below, a simple index is suggested. Based on laboratory data, steady state cavern volume loss rate of an idealized spherical cavern, 981.5-m deep, is computed. It varies by 5 orders of magnitude.

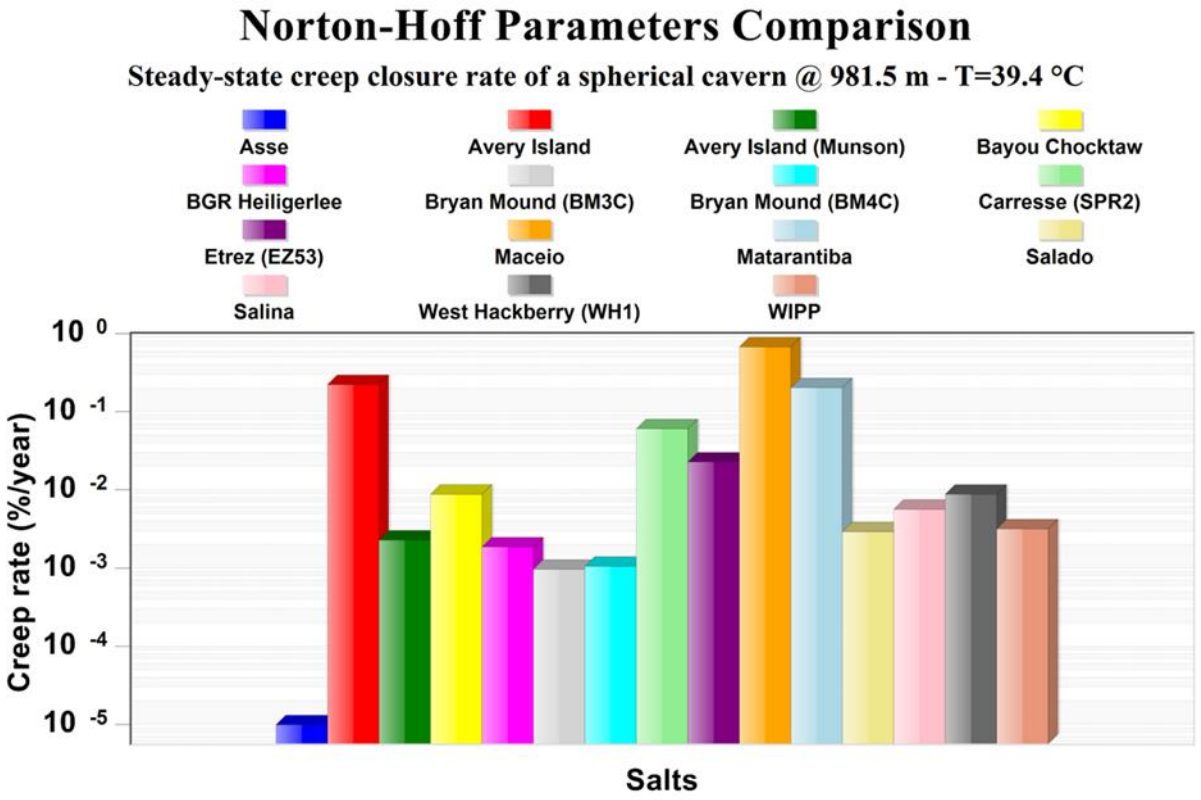

Figure 58. Comparison between different salts (Brouard and Bérest, 1998).

3.1.5 Remarkable volume losses

3.1.5.1 Case histories

As explained above, volume loss rate is a non-linear function of the gap between geostatic pressure and cavern pressure. Based on in situ measurements, when cavern pressure is halmostatic and has been kept at rest for several years, volume loss rate is 10^{-5}/yr at a 250-m depth (Brouard et al., 2017) gap; it is 3×10^{-4}/yr at a 1000-m depth (Brouard, 1998) and 1%/yr at a 1500-m depth (these are orders of magnitude; the actual values may vary by one order of magnitude, depending on the site under consideration and are faster in a cycled cavern). Several remarkable cases are known. For instance, a loss of volume by 60% in 37 years in the Tersanne gas storage site in France, Hévin et al., 2007, where caverns are 1450-m deep (Figure 59). In this gas storage cavern, the minimum pressure was 80 bars. This fast evolution is consistent with what was observed at the laboratory, where experimental creep strains were exceptionally fast.

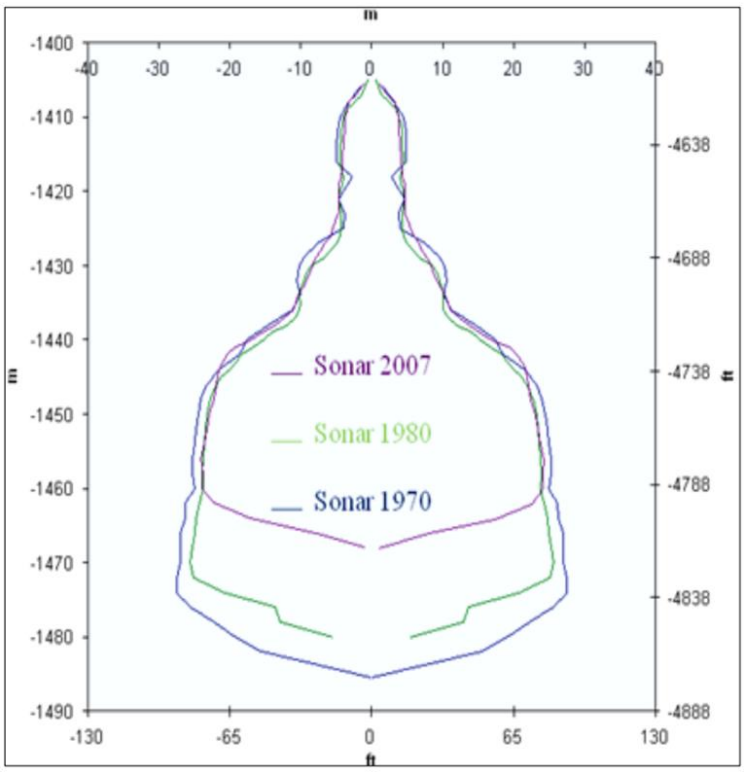

Figure 59. Smoothed TE02 vertical profiles, as measured in 1970, 1980 and 2007 (Acknowledgement: G. Hévin, Storengy).

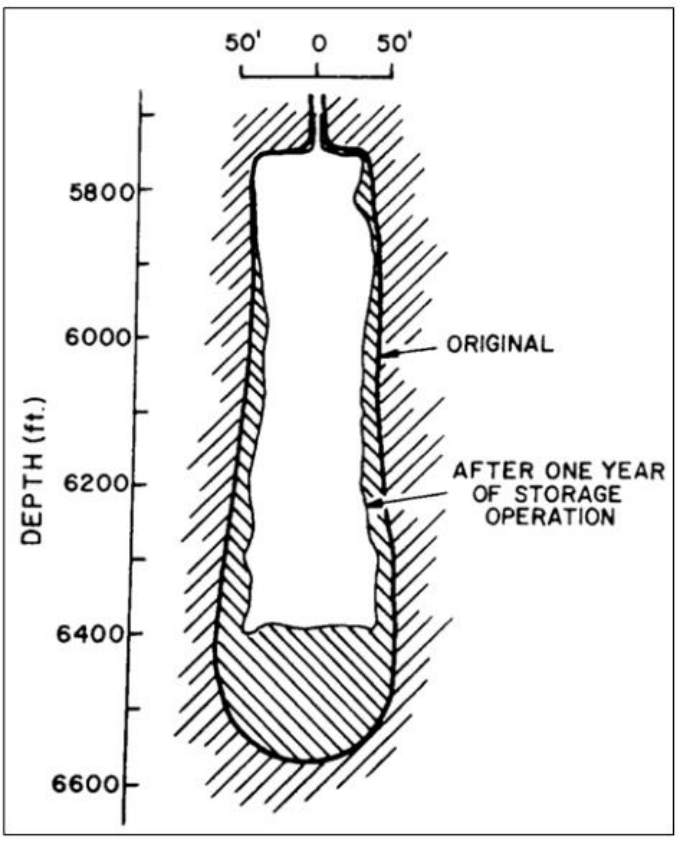

Figure 60. Cavern #1, Eminence Salt Dome, Mississippi, in 1970 and 1972 (Serata and Cundey, 1979, p. 170).

Similar observation was made in the Eminence salt dome 1 cavern (Mississippi) after a much shorter period (1970-1972, Figure 60). This case has been described by Allen (1972, 1971), Baar (1977), Serata

and Cundey (1979), Coates et al. (1983). The following description is partly drawn from Réveillère et al. (2017). The top of the salt is between 730-743 m (2400-2410 ft.); it is overlain by a 150 m-thick (500 ft.) cap rock of limestone and anhydrite. In 1991, this natural-gas storage site comprised seven caverns. Caverns #1 to #4 were certificated in the early 1970s; caverns #5, #6 and #7 were certified in 1991. These caverns are especially deep, from 1725 m to 2000 m (5650 ft. to 6550 ft.) in the case of Cavern #1 (Figure 60). For those wells drilled in the 1970s, the last cemented casing shoe, with a diameter of 13-⅜", was at a depth of 1737 m (5700 ft.) (Allen, 1972, 1971). Salt was cored at the interval of 5700 to 6700 ft. (1740 to 2040 m). The anhydrite average content was 4 % (Coates et al., 1983). Cavern #1 was filled with gas at a 70 bars (1000 psi) pressure over a period of two months, after which it was increased to 280 bars (or 4000 psi; geostatic stress at cavern depth is 38-45 MPa, or 5500-6500 psi). After a second pressure cycle, the "*cavity bottom was at 6408 ft (1953 m), showing a loss of 152 ft (45.6 m) in about two years*" (Baar, 1977 p. 144), and cavern volume loss was 40 % (Figure 60). Once the problem was recognized, reduced losses were achieved through various measures, including less dewatering and maintaining a higher minimum pressure over extended time periods. Fig. 14 exhibits a couple of features of special interest. The cavern bottom rose by 152 ft. (45.6 m) in about two years. However, there is no sign that massive salt blocks fell from the cavern walls to the cavern bottom. Serata and Cundey (1979) note that ''*it was suspected that much of the boundary salt had failed and fallen from the walls to the cavity floor*'' (p. 167); however, Baar (1977) rightly mentions that such a block fall would not lead to a change in the volume available for gas, and that it would make diameter changes smaller than observed in the upper part of the cavern (in sharp contrast, for instance, with the Markham case described in Section 3.4 Brittle failure, characterized by a combination of creep closure and salt-block fall).

3.1.5.2 Bottom upheaval

Creep closure was more intense at the cavern bottom than at the cavern top. This phenomenon, also observed at Tersanne and Markham (see this Section and Section 3.4) is puzzling. It has been hypothesized that both the geothermal temperature and the gap between geostatic pressure and gas pressure were higher at the cavern bottom, resulting in faster creep rate in this region (Bérest et al., 1986). Several years later, gas seepage from several caverns at this site led to decommissioning. It is generally believed that large creep closure led to cemented-casing overstretch over the cavern roofs (see Section 3.3, Casing overstretching).

3.1.6 Creep closure in a cycled cavern

Creep closure is significantly faster in a cavern whose pressure is cycled (rather than constant), Gordeliy and Bérest (2022); volume loss rate is quite sensitive to the value of the minimum pressure.

In this section, the M-D and N-H laws are used to simulate the case of a cyclic pressure change. The elastic moduli are set to $E = 17{,}000$ MPa and $\mu = 5667$ MPa. The parameters of the M-D and N-H laws are taken from in situ tests performed on the Cavern EZ53 of the Etrez site, Gordeliy and Bérest (2022), except that the power law exponent n is set to $n = 3$ in these examples. A constant pressure difference, $P_\infty - P_c^- = 10$ MPa, was maintained at the cavern wall over a long period of time before $t = 0$, such that steady state was reached at $t = 0^-$. At $t = 0^+$, the cavern pressure is cycled according to $P_\infty - P_c^+(t) = P_\infty - \bar{P}_c^{av} - \Delta P \sin\left(\frac{2\pi t}{T}\right)$, where $\bar{P}_c^{av} = P_c^-$ (average cavern pressure during the cycles), ΔP (amplitude of the cycles) and T (period of the cycles) are three constants. On Figure 61 (upper left), the steady-state volume Evolution (when cavern pressure equals average pressure) is drawn for comparison. The M-D law, short cycle periods (1 day and 1 week) and two cycle amplitudes ($\Delta P = 3$ MPa and 6 MPa) are considered; the average pressure difference is $P_\infty - P_c^{av} = 10$ MPa. Volume loss is more than doubled when cycle amplitude is doubled, reflecting the non-linearity of the creep law. Influence of the period is more discreet. Figure 61 (upper right) illustrates the difference between the N-H and M-D (more realistic) creep laws. Volume loss is considerably larger when the M-D law is selected; this is expected, as the M-D law takes into account the rheological transient behaviour of salt, which is activated during each pressure

cycle. Longer periods (a one-year period is typical of the historical operation mode of natural gas caverns) are considered in the lower pictures. Lessons are similar to those drawn when the cycle period is shorter: volume loss is much larger when the M-D law is selected; the influence of the cycle period (1 month and 1 year) is relatively minor. (Note, however, that more time is left to restore cavern volume when cavern pressure is higher.)

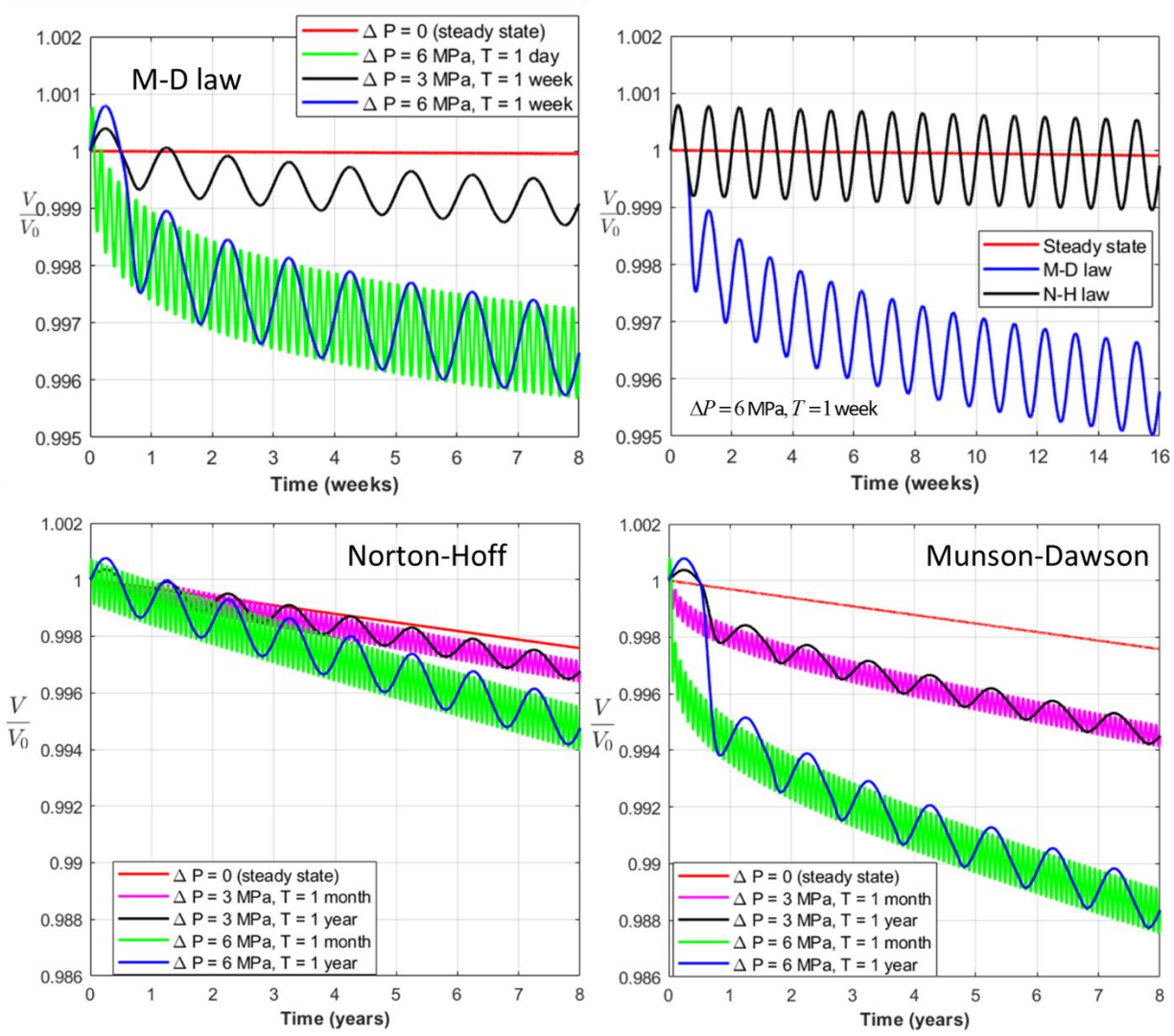

Figure 61. Volume change for a cavern under cyclic pressure. Results are computed with the N-H law or the M-D law for several sets of cycle amplitude ΔP and period T.

3.1.7 Creep closure in a hydrogen storage cavern

Storing hydrogen does not seem to raise specific rock mechanics problems, except that its thermodynamic behaviour (hence, amplitude of the temperature swings) is slightly different from those of methane or compressed air and pressure cycles might be more frequent, see Section 2.1, Thermodynamics.

Creep closure may lead to large volume losses, subsidence (Section 3.2), casing overstretching (Section 3.3), permeability increases at the anhydrite/salt interface.

3.2 Subsidence

3.2.1 Introduction

Subsidence is an unavoidable consequence of salt cavern creation and cavern creep closure. An abundant literature was dedicated to this topic. It is generally accepted that the volume of the subsidence bowl roughly equals the cavern volume loss. The maximum vertical subsidence is of the order of magnitude of the volume loss divided by the square of the cavern depth; however, the exact figure and, more generally, the shape of the subsidence bowl (the 'transfer function') generated by a single cavern are site-specific notions. Subsidence can be computed both through full 3-D computations and through a simpler 'transfer function' method.

3.2.2 Geometrical characteristics of the subsidence bowl

3.2.2.1 Subsidence bowl volume and creep closure volume

From a theoretical standpoint, equality of the volume of the subsidence bowl above a salt cavern and the cavern volume loss can be proven as follows.

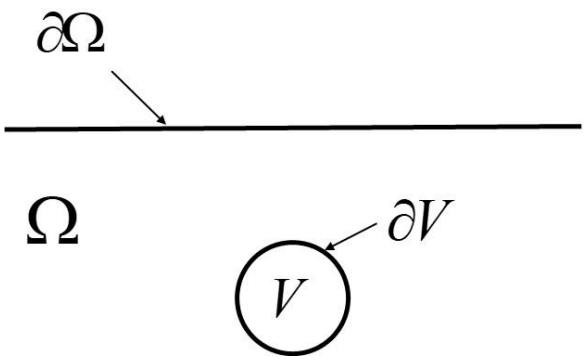

Figure 62. Main notations.

Assume that a cavern, volume V, internal pressure P, is created in an infinite half-space Ω whose boundary (ground level) is $\partial\Omega$ (Figure 62). From the equilibrium condition, $\dot{\sigma}_{ij,j} = 0$, it results that $0 = \int_\Omega x_i\, \dot{\sigma}_{ij,j} d\Omega = -\int_\Omega \dot{\sigma}_{ii}\, d\Omega + \int_{\partial\Omega} x_i\, \dot{\sigma}_{ij} n_j dA$ where $\int_{\partial V} x_i\, \sigma_{ij} n_j dA = -3\dot{P}V$. Furthermore, it can be assumed that rock mass strain rate can be described as the sum of an elastic component plus an isochoric viscoplastic component $\dot{\varepsilon}_{ij} = \frac{(1+\nu)\dot{\sigma}_{ij}}{E} - \frac{\nu\dot{\sigma}_{kk}\delta_{ij}}{E} + \dot{\varepsilon}_{ij}^{vp}, \dot{\varepsilon}_{kk}^{vp} = 0$ (salt dilation is neglected) – a model which, even if simple, captures the main features of salt rheological behaviour. It results that $\int_\Omega \dot{\varepsilon}_{kk}\, d\Omega = \int_{\partial V} \dot{u}_i\, n_i d\Sigma + \int_{\partial\Omega} \dot{u}_i\, n_i dA = \int_\Omega \frac{(1-2\nu)\dot{\sigma}_{kk}}{E}\, d\Omega$ and, after some algebra:

$$\int_{\partial V} \dot{u}_i\, n_i d\Sigma + \int_{\partial\Omega} \dot{u}_i\, n_i dA = -3\,\frac{(1-2\nu)\dot{P}V}{E} \qquad (21)$$

The difference between the growth rate of the subsidence trough (at ground level $\partial\Omega$) and the shrinkage rate of the cavern is zero when cavern pressure is kept constant. Based on field observations, most authors (Eickemeier, 2005; Nguyen Minh et al., 1993; Ratigan, 2014; Reitze, 2000; Shober et al., 1987; van Sambeek, 2000); Ratigan, 2014), agree on this: above a salt cavern, trough volume roughly equals cavern volume loss due to creep closure. In fact, the as-observed value is slightly smaller because vertical subsidence at a large distance from the wellhead often is too small to be measured, although its contribution to the overall trough volume is not negligible.

3.2.2.2 Transfer function

The vertical component of subsidence at ground level often is approximated by a "transfer function", $u_z = v_{loss} f\left(\frac{r}{H}\right)$, where r is the distance from a given point at ground level to the wellhead and v_{loss} is the cavern volume loss. In the case of a cavern cluster, it is generally accepted that the effects of the individual caverns can simply be added, allowing straightforward computation of the overall subsidence. The transfer function is a site-specific notion. Various transfer functions have been proposed in the literature. A popular choice is:

$$f(r) = \frac{\alpha}{H^2} exp\left(-\frac{\pi \alpha r^2}{H^2}\right) \tag{22}$$

where $\alpha = 1$ is typical; note that in this model subsidence trough volume equals cavern loss volume:

$$v_{trough} = \int_0^\infty v_{loss}\, 2\pi r f\left(\frac{r}{H}\right) dr = v_{loss} \tag{23}$$

and the maximum vertical subsidence at ground level equals the cavern volume loss (v_{loss}) divided by the square of cavern depth, $u_z(0) = v_{loss}/H^2$. In the case of an elongated cavern, Schrober-Sroka (1987) proposed

$$f(r, z_b, z_t) = \frac{2a}{(z_b^2 - z_t^2)} (tg\gamma)^2 Log\left(\frac{z_b}{z_t}\right) exp\left[-\pi (tg\gamma)^2 \frac{r^2}{z_b z_t}\right] \tag{24}$$

where γ is the influence angle and z_b and z_t are the depths of cavern bottom and cavern roof, respectively, $0 < a < 1$. When $\gamma = 45°$ and cavern height is small ($z_b = z_t = H$), one gets:

$$f(r, z_b = z_t = H) = a \frac{1}{H^2} exp\left(-\pi \frac{r^2}{H^2}\right) \tag{25}$$

Many more or less empirical formulas have been proposed in the literature, for instance Eickemeier (2005):

$$f\left(r, \sqrt{z_b z_t}\right) = \frac{\psi \delta}{2\pi^{1-2/\delta} R^2 \Gamma\left(\frac{2}{\delta}\right)} exp\left[-\pi \psi^{\delta/2} \left(\frac{r}{R}\right)^2\right] \tag{26}$$

where $R = \sqrt{z_b z_t}\, cot\, \beta$; ψ, δ and β are empirical constants to be fitted on field data.

Fokker et al. (2002) provide the following empirical formula, whose coefficients were back-calculated in the case of the Barradeel brine field (caverns are more than 2500 m deep in this site):

$$f(r) = Z\, exp(-\gamma r^5)_{max} \tag{27}$$

where $\gamma = 4.5 \times 10^{-7}\ \mathrm{m}^{-5}$ and $\delta = 1.97$ (Z_{max} varies with time).

Horizontal stresses are compressive at a short distance from the wellhead (folds can form) and tensile far from the wellhead (crevices can form).

Maruyama (Maruyama, 1964, p.331) considers the case of a loss of volume in a point of an elastic infinite half space and suggests the following formula:

$$f(r, H) = \frac{3}{2\pi} \frac{H^3}{(H^2 + r^2)^{5/2}} \tag{28}$$

which is the exact solution of an elastic problem. However, this solution seems to overestimate the vertical displacement at large distances from the wellhead (see for instance Figure 65).

3.2.2.3 Horizontal displacements

InSAR techniques allow to measure the horizontal displacements due to subsidence. Most often, for computations, it is accepted that the displacement vector points to the centre of the cavern (Figure 63):

$$\vec{u}(r,\theta,z=0) = v_{loss} f(r) \left(\vec{e}_z - \frac{r}{H}\vec{e}_r\right) \quad (29)$$

Allowing to compute strains and stresses at ground level.

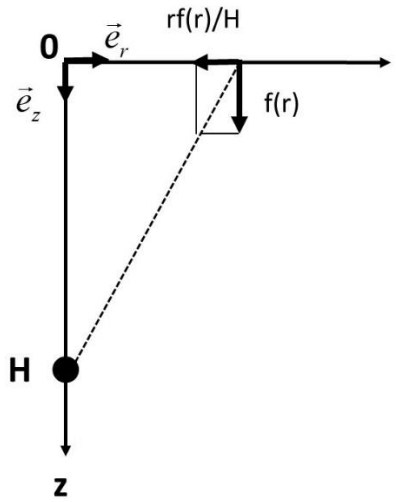

Figure 63. Generally accepted assumption for horizontal displacements.

3.2.3 Case histories

3.2.3.1 Mont Belvieu, Texas

There are several caverns in this site. Caverns depths are 500-650 m; the useful volumes of the caverns are 1-3×10^5 m^3. The shape of the subsidence bowl is conic (Figure 64).

3.2.3.2 Subsidence at Bernburg, Germany

Profile of the subsidence bowl as a function of time is shown in Figure 65.

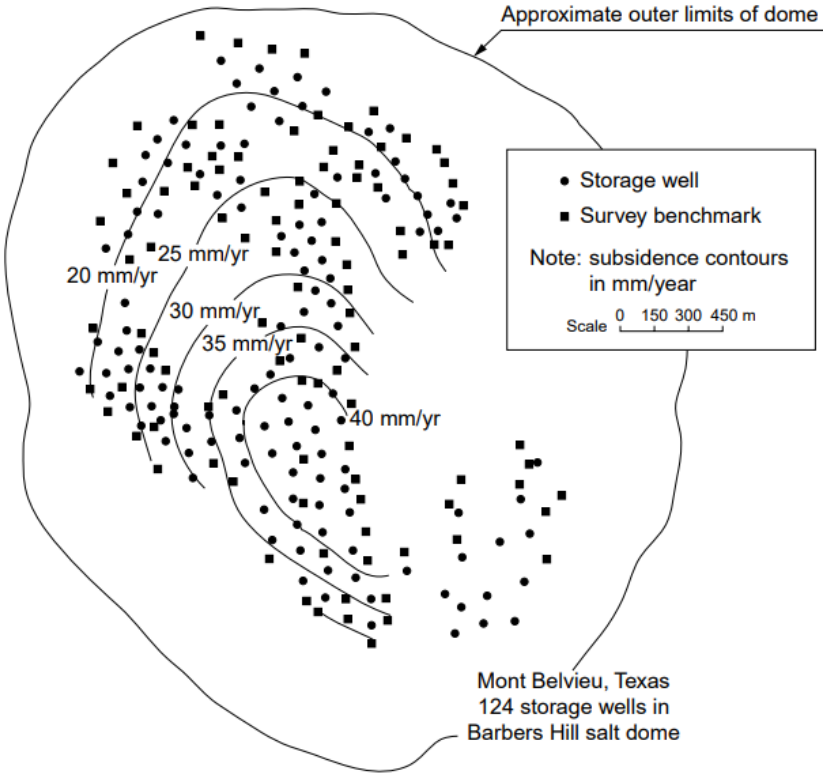

Figure 64. Subsidence in the Mont Belvieu (Texas) site (after Ratigan, 1991). At this site, 124 caverns were operated in 1991.

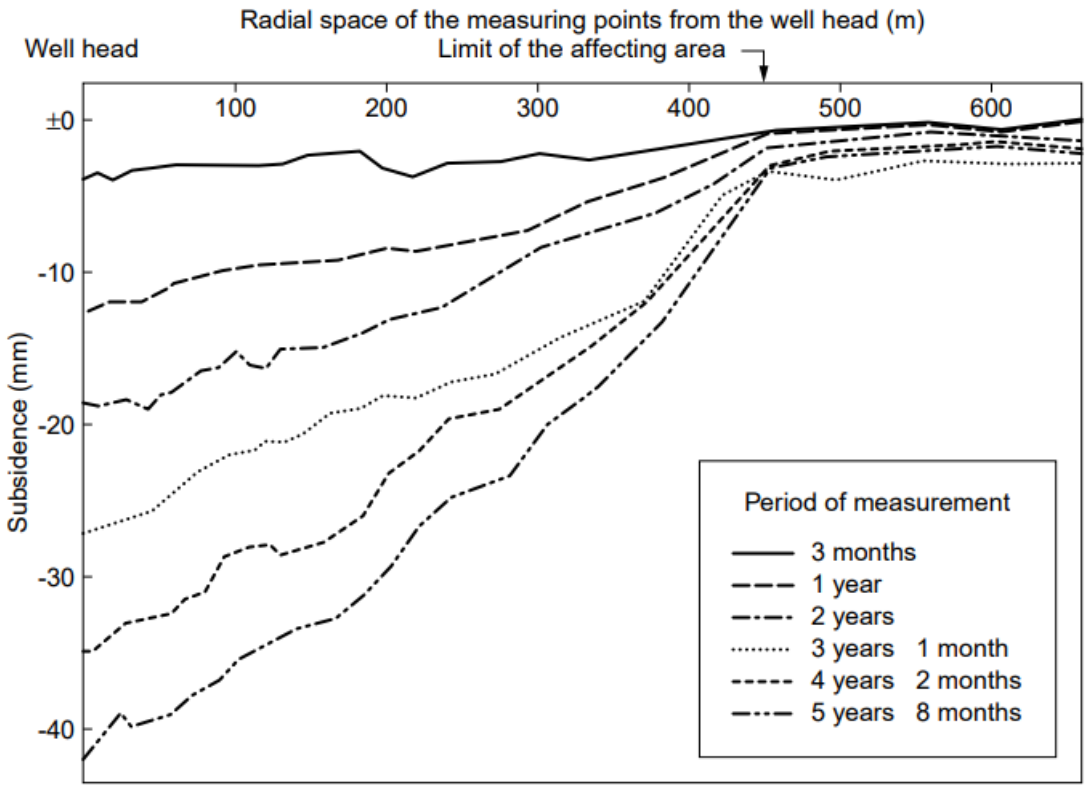

Figure 65. Subsidence in the Bernburg (Germany) site (from Menzel and Schreiner, 1985).

3.2.3.3 Subsidence at Tersanne, France

Creep closure rate above the Tersanne gas caverns cluster is described in Paragraph 3.1.5. Nguyen Minh D. et al. (1993) tried to reconcile subsidence trough volume and cavern volume loss (Figure 66). The former is 60% of the latter, significantly less than predicted by theory. The discrepancy might be due to an underestimation of the far field vertical displacements which are small and difficult to assess.

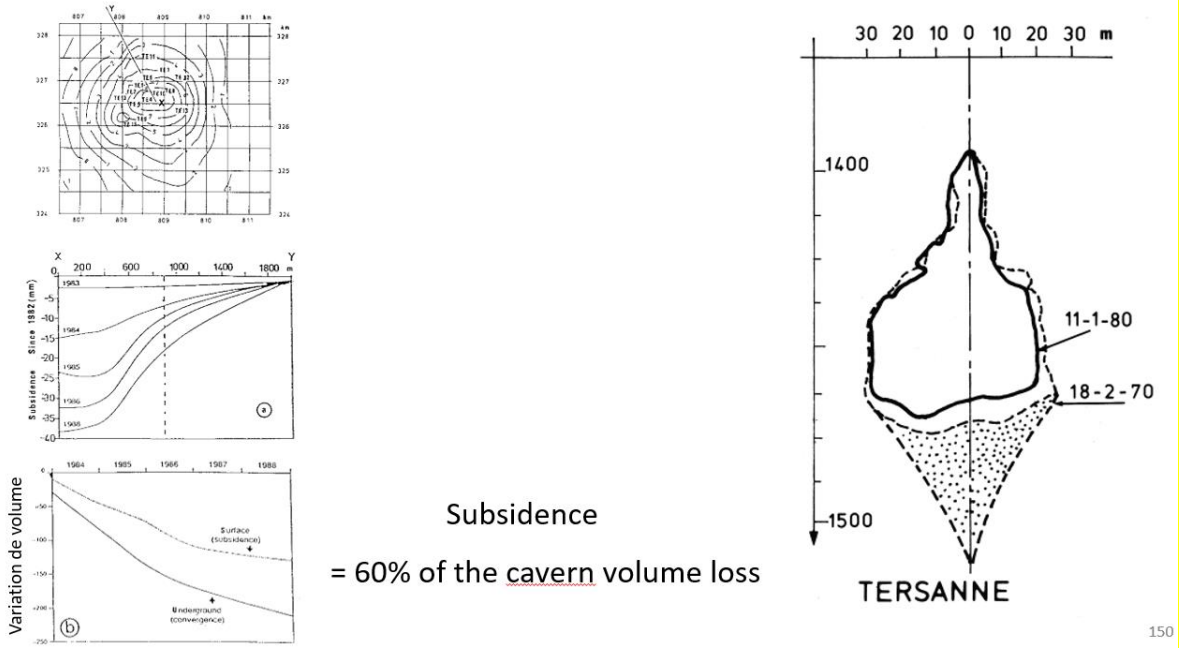

Figure 66. Subsidence above the Tersanne (France) gas cavern cluster (Nguyen Minh et al., 1993).

3.2.3.4 Subsidence at Maceió, Brazil

More recently, a remarkable example was described by Vassileva et al. (2021), published in www.nature.com/scientificreports.

"*Since 1970, a total of 35 brine extraction wells have been installed along the Mundaú Lagoon coast in the urban area of Maceió, Brazil. Maceió, the capital city of the Brazilian state of Alagoas, lies in the Sergipe-Alagoas salt basin, which formed along the Brazilian coast during South Atlantic rifting and was initiated in the Late Jurassic*." Caverns depth is 1000 m, approximately and their volume ranged from 30 000 m^3 to 540 000 m^3. The extraction ratio (the ratio between the cumulated maximum cross-sectional area of the 35 caverns and the area of the cluster footprint) was slightly larger than 25%. In the period 1995-2004, a 6 million m^3 volume (approximately) was excavated and an additional 6 million m^3 volume (approximately) was excavated during the 2004-2019 period.

On Figure 67, InSAR series are represented. On the upper right corner, two vertical subsidence profiles are shown. The maximum vertical subsidence is more than two meters.

"*At the beginning of 2018, fractures on both buildings and roads started to develop.* […]. *A total of 6,356 buildings were classified as risk zones and placed under demolition by the Brazilian authorities, with consequences for 25,000 residents, who had to be relocated to other parts of the city.*"

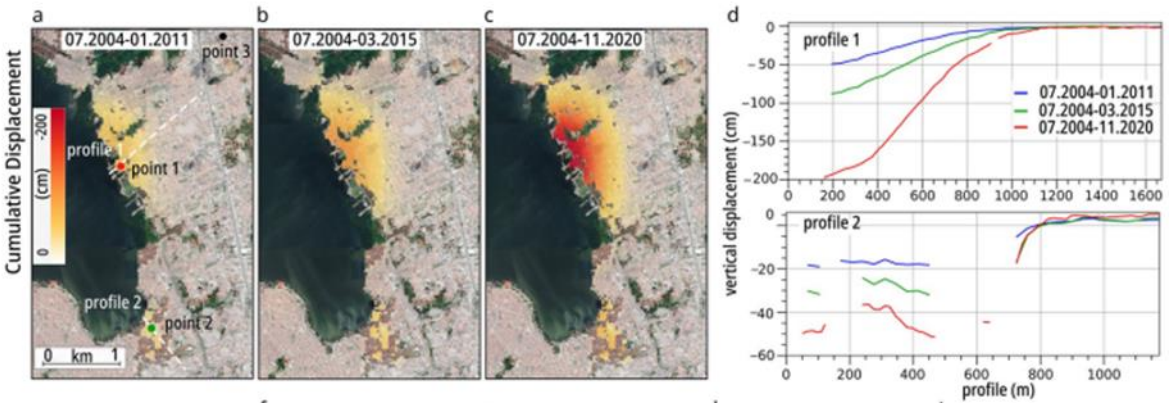

Figure 67. InSAR time series results. (a–c) Cumulative vertical subsidence maps obtained by projecting the LOS component into vertical only and combining in time and space all available displacement datasets. […] Background Google Earth CNES/Airbus imagery. The figures were plotted in QGIS (v. 3.16, https://www.qgis.orgs/en/site/), from Magalena Vassileva et al. (2021).

3.3 Casing overstretching

3.3.1 Introduction

Under many respects, this topic is related to roof fall; however, occurrence of large strains in the cavern roof - rather than failure of interbedded layers - is the primary cause of the incident. As such, its origin cavern creep closure (discussed in Section 3) Casing overstretching results from large cumulated strains at cavern roof (after a long period of time, in some cases when the steel casing, whose elastic limit is small, is not able to accommodate such deformations, resulting in casing failure and gas leak. A couple of cases are known. The design of the cavern shape and location of the last cemented casing shoe above the cavern roof play a major role, as flat roofs, interlayered formations, large spans and the absence of a high enough chimney expose the cemented casings to large strains and increases the risk of casing overstretch.

Note that in dry mines, at a different scale, the same phenomenon occurs when bolts experience tensile failure when they are fully grouted to the salt mass.

3.3.2 Case stories

3.3.2.1 Boling 1, 2, 4, Texas, USA, 2005

This case was described by Osnes et al. (2007). The following summary is reproduced (with small changes) from Bérest et al. (2019c), based on Réveillère et al. (2017). Four caverns ('wells'), Wilson #1 to #4, had been solution-mined and filled with natural gas between 1980 and 1983 in the Boling Dome near Boling, Wharton County, Texas. Depth to the cap rock is generally about 192 m, and the top of the salt occurs at a depth of around 305 m. Cavern roof depths are between 1066 and 1083 m, except for Cavern #3, the roof of which is deeper by 45-60 m. Apart from Cavern #3, 11-⅜" casing shoe is close to the cavern roofs (0 to 18 m above), which, except in the case of cavern #3, are flat (Figure 68). In the Fall of 2005, Cavern #4 was nearly full. An abnormally fast pressure decline, which was monitored over a period of several weeks, was observed after the well was shut-in. Temperature loggings found cold spots in Caverns #1, #2 and #4, raising the possibility of a production casing leak not far above the cavern roof. It was decided to remove gas and the three caverns were filled with water. Detailed investigations into the Cavern #4 incident were undertaken, including running downhole video camera logs, which identified casing collar and coupling partings for over 100 m above the casing shoe depth (Figure 69).

The video log revealed that the casing had failed at eight different locations, always near or at a connection. Failure often was a circumferential fracture. A 60 cm (2 ft.) length of cement was visible between the two last casings. Failure shape, the absence of any failure in Cavern #3 the chimney to which was 60 m in height, and flat roofs, strongly suggest that casings were overstretched above cavern roofs and experienced tensile failure. Above cavern roof, salt experiences large vertical strains and the cemented steel casing, strongly bonded to the rock mass, is stretched until its tensile strength – or tensile strain limit – is exceeded (in Osnes et al. (2007) paper, this strain limit is $\varepsilon = 2 - 3.5 \times 10^{-3}$).

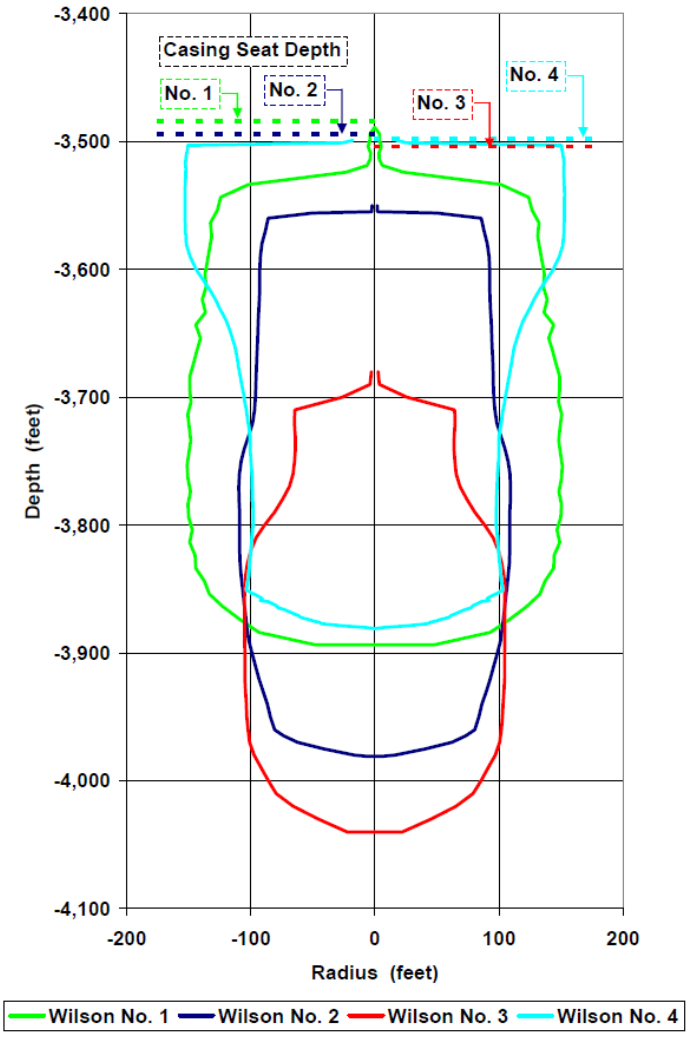

Figure 68. General cross-sections of caverns, based on sonar data. From Osnes et al. (2007).

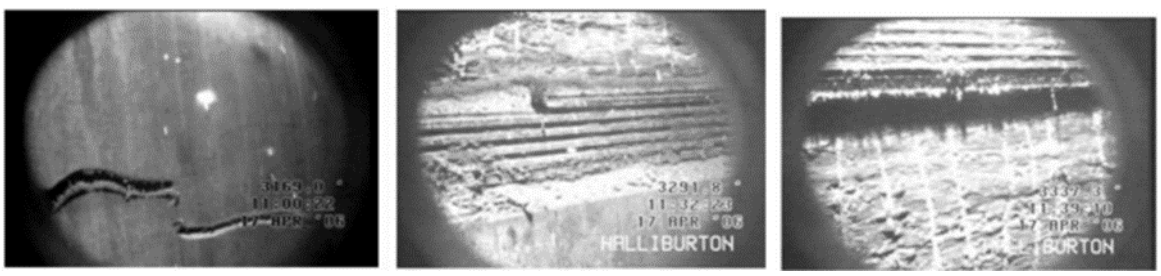

Figure 69. Examples of failures detected by the video inspection. From left to right: Circumferential fracture of the pipe body, of the threaded coupling, and thread jump-out. From Osnes et al. (2007).

This was confirmed by numerical analyses, that clearly showed the cemented casings of Wells #1, #2 and #4 were not able to accommodate the resulting large tensile strains in the salt roof, and their ultimate strength limit was exceeded (Figure 70). [Note that the pressure decline observed at Cavern #4 wellhead is somewhat puzzling. A pressure decline in a gas cavern implies that a significant amount of gas seeped to a pre-existing or newly created void. Was the cement sheath around the steel casing able to accommodate such an amount of gas?]. The well repair procedure for the three leaking wells included milling a 30 m section from the original 11-⅜" casing and cementing a 10-¾" welded liner. The new casing shoe, 30 m higher than the original one, was therefore in a zone where simulations suggested the strain induced by the salt creep should stay below the casing strength, thanks to this new 30 m long cavern chimney.

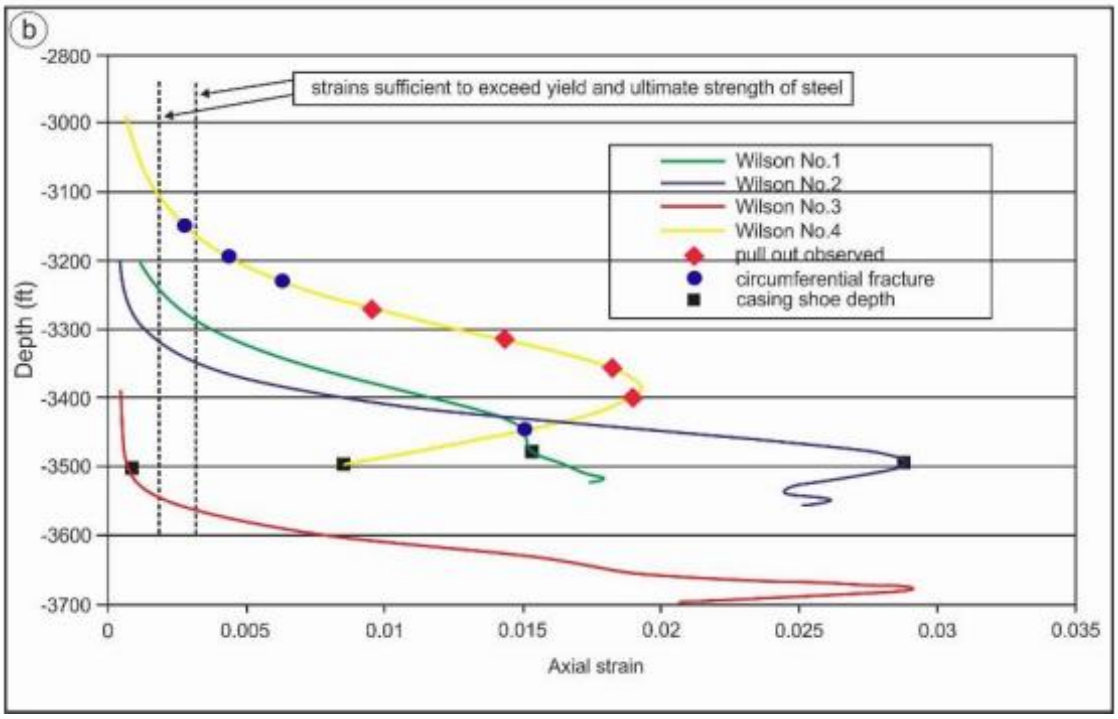

Figure 70. Observed and modelled casing deformations (from Osnes et al., 2007): vertical strains as a function of depth in the salt near the centre lines of the Wilson storage caverns predicted from finite element modelling.

3.3.2.2 Eminence salt dome 1,3, 4, Mississippi, 1972, 2004 and 2010-2011

The following description is drawn from Réveillère et al. (2017), Bérest et al. (2019c) and Wellinghof (2013). The Eminence salt dome is located 20 km northwest of Hattiesburg, Mississippi. The top of the salt is between 730-743-m deep; it is overlain by a 150-m thick cap-rock of limestone and anhydrite. In 1991, this natural gas storage site comprised seven caverns. Caverns #1 to #4 were certificated in the early 1970's and caverns 5, 6 and 7 in 1991. These caverns are especially deep, from 1725 m to 2000 m - in the case of Cavern #1 (Figure 71). For those wells drilled in the 1970s, a 30" surface casing was set and cemented at 50 ft. (15 m). A 28" hole was then drilled to 2700 ft (823 m) and a 20" OD cemented casing set, and the last cemented casing shoe, diameter 13⅜'', was at 1737 m (5700 ft.) depth (Allen, 1971, 1972). Cavern #1 was filled with gas at a 70 bars (1000 psi) pressure over a period of 2 months, after which gas pressure was increased to 280 bars (or 4000 psi; geostatic stress at cavern depth is 38-45 MPa). After a second pressure cycle, the "*cavity bottom was at 1953 m [6408 ft.], showing a loss of 46 m [152 ft.] in about two years*" (Baar, 1977; Coates et al., 1981) and cavern volume loss was 40 %, see also Figure 71. Once the problem was recognized, reduced losses were achieved through various measures, including maintaining a higher minimum pressure over extended time periods and less dewatering. In 2004, Cavern #4 well casing failed at a depth of 1639.5 m (Wellinghoff et al., 2013), i.e., a few dozens of feet above cavern roof. The company took Cavern #4 out of service, filling it with water and shutting it in. On December 26, 2010, a large, unexpected pressure drop of 25 bars (357 psi) in one minute was detected in Cavern #3. The initial response to the leak was to flow ~8.65 mcm (306 MMcf) of gas into the pipeline system. Another gas leak from the wellhead of Cavern #3 was accompanied by water shooting into the air from on-site water wells. On January 4, 2011, the company began flaring gas from Cavern #3, until its production tubing became clogged with debris. Gas was also escaping from the ground around the wellhead of Cavern #1. A large cave-in occurred, sealing off the flow. The company began drilling monitoring wells in the surrounding freshwater zones. By January 24, 2011, the decision was made to take Caverns #1 and #3 out of service. Later, a leak to the caprock was detected in Cavern #7 and maximum operating pressure was lowered from 248 bars to 191 bars (3600 psi to 2775 psi). Investigations revealed that leakage in Cavern #3 well likely arose through salt creep leading to overstretching of the

casings above the cavern, where displacements due to creep closure were especially intense (Wellinghoff et al., 2013). These excessive strains led to damage of steel casings and/or steel-cement and cement-rock interfaces, as a result of which, gas migrated up the well to the cap-rock and ultimately to surface.

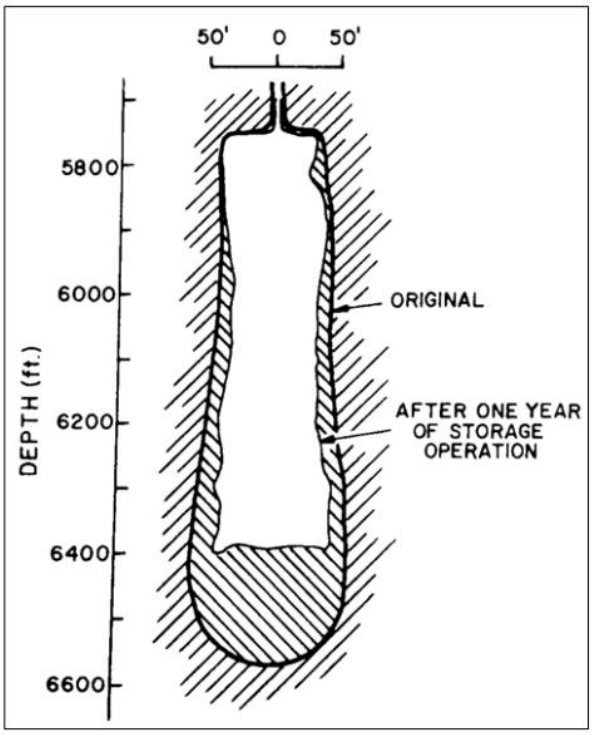

Figure 71. Cavern #1, Eminence Salt Dome, in 1970 and 1972 (Serata and Cundey, 1979, p.170).

3.3.2.3 Dewdney Field, Saskatchewan, Canada, 2015

This case was described by Coleman Hale et al. (2015). The Dewdney field is located in Regina, Saskatchewan. The caverns are completed in the Prairie Evaporate Salt, an extensive bedded salt formation (Figure 72). At Dewdney Field, the salt interval top is 1575-m deep, and base is 1690-m deep, generally. The upper 65 meters of the interval is composed of interbedded salt, potash, and thin mudstone (clay) seams. Eight caverns were developed in the early 1970's (Figure 73) Three of them were used for natural gas storage. In 2015, four LPG storage caverns were active. They were operated in compensated mode (brine is injected when products are withdrawn, and cavern pressure does not vary much over time). The four active caverns have volumes ranging from 103,590 m^3 to 149,862 m^3 and maximum diameters range from 79.7 m to 130.6 m. Cavern roofs are generally flat, and the distance between cavern roof and last casing seat is small. "*Throughout the operational history of the cavern field, this interbedded interval has proven to increase strain on the cemented production string of each cavern well. All of the wells have experienced some degree of cemented casing damage, and four of the eight wells have experienced severe casing separations within the interbedded interval*", p.1, Coleman Hale et al. (2015). A good example is provided by Well 2, which was drilled in 1971 and used for LPG storage. In 2013, casing inspection logs found separated casing at 1602, 1613, 1621 and 1626.5 m. It was decided to install a liner and to drill a second wellbore entry (well 2A) to maintain fluid rates. Well-2A entry is 20 m to the east of Well 2.

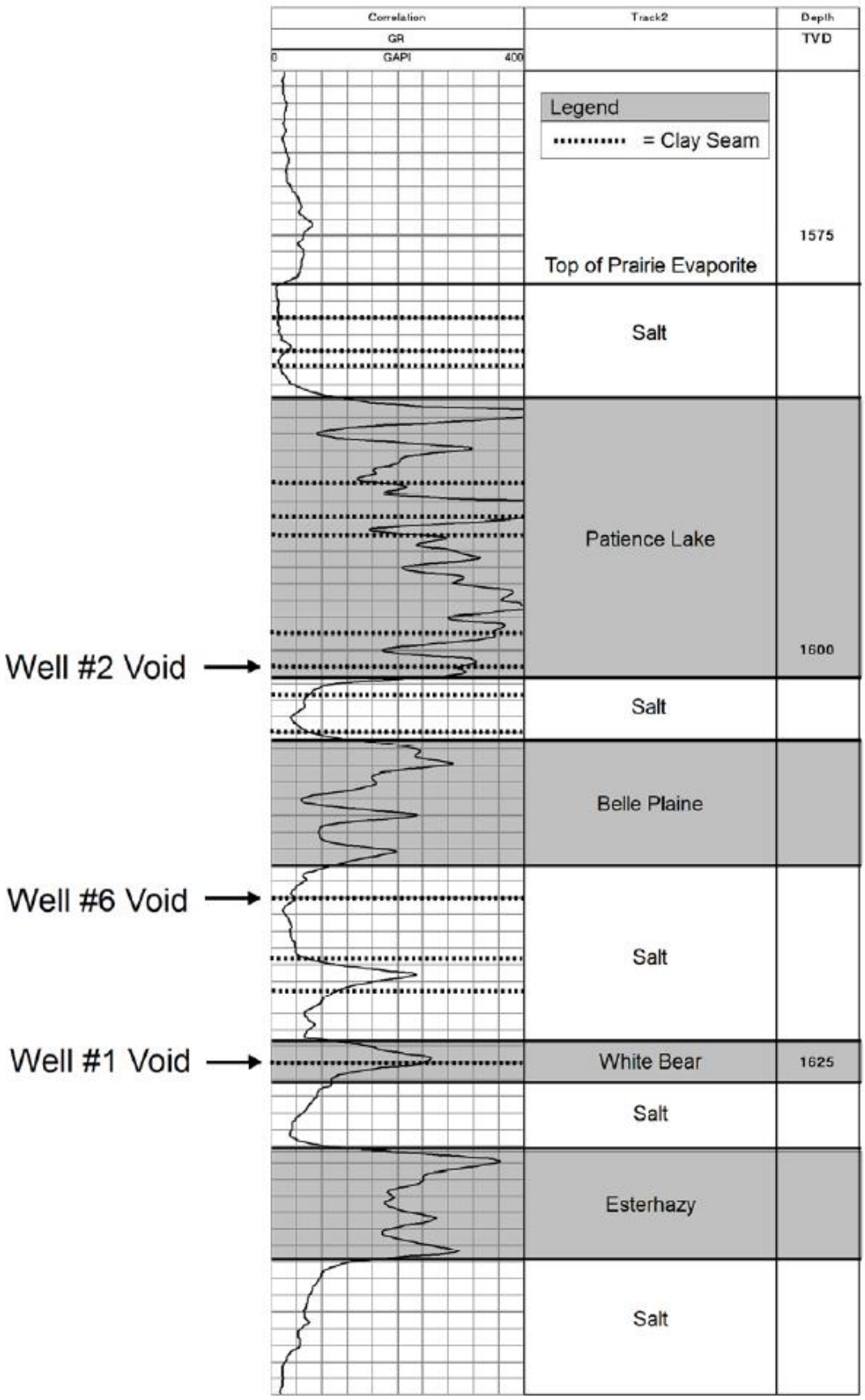

Figure 72. General stratigraphic column of the Prairie evaporates at Dewdney Field (from Coleman Hale et al., 2015, p.13).

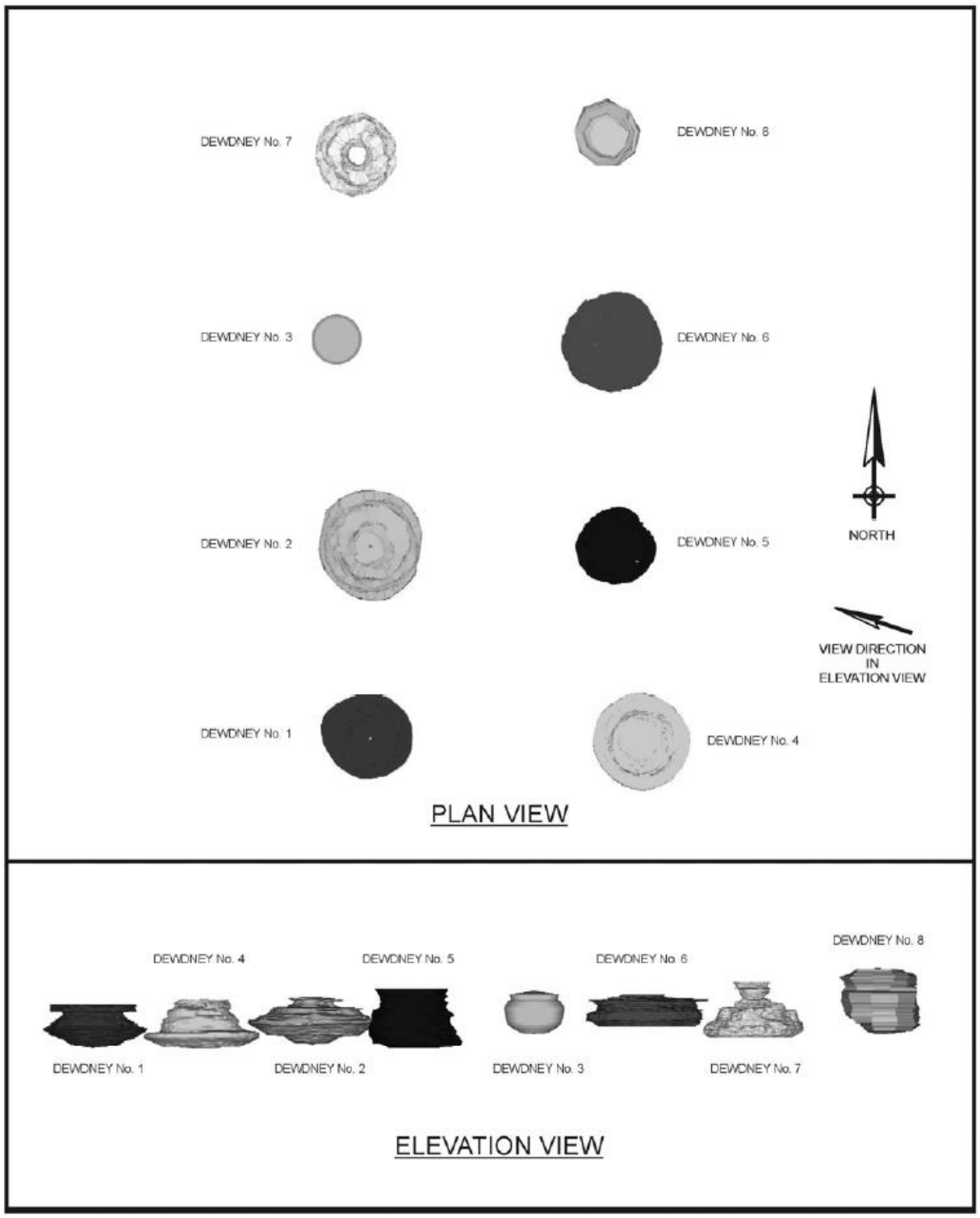

Figure 73. Plan view and Elevation view of the Dewdney Cavern Field (from Coleman Hale et al., 2015).

During Well 2A drilling, much information was gained on the state of Well-2 roof. Well 2A also provided an opportunity for the collection of formation cores and an updated set of wireline logs, which were analysed by RESPEC. The salt is "hard" (very "slow creeping" according to Munson's classification, (1998)). Potash creep rate is 10 times faster and intermediate between "hard" and "soft" salts. In addition, multiple horizontal mudstone (clay) seams, ranging from 3 to 21 cm in thickness were found. The clay is soft ("*it can be scratched with a knife*") and "*it was determined that the clay seams are a plane of weakness*" (Figure 72). During drilling, mud return was lost at 1602 m, where a clay seam exists, proving that a void or path existed with well 2. A Nitrogen test proved that void/path volume was 14.7 m^3. More

generally, nitrogen injections (during MIT) proved that horizontal fractures had been created in the mudstone seams (No cavern-to-cavern communication was detected). Void/path volumes ranged from 9.6 to 38.4 m^3 and the radial extent can be at least 20-m away from the wellbore axis.

RESPEC analysis

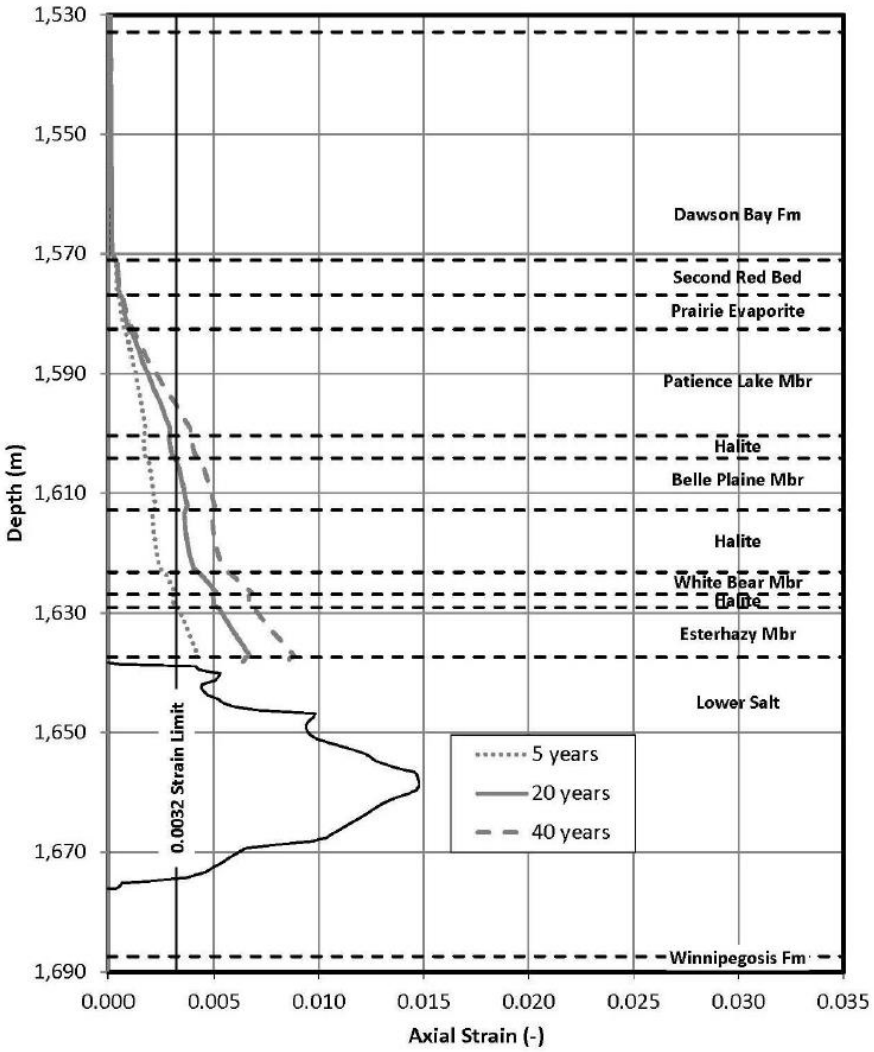

Figure 74. Dewdney Cavern No. 2 Vertical Cavern strains predictions, RESPEC Analysis 2015 (from Coleman Hale et al., 2015, p.14).

RESPEC analysed vertical strains generated by 40-year long operation of several caverns through numerical computations. The steel casing was not explicitly modelled, displacements were assumed to be continuous at cement casing and casing-rock interfaces. The criterion for tensile failure was expressed in terms of a maximal strain of$\varepsilon = 3.2 \times 10^{-3}$. As a conclusion, overtime the vertical strain on the cemented casing exceeded the failure limit. Casings failure have occurred approximately 30 to 35 years after well completion (and less for gas storage caverns operated between 0.15 to 0.70 psi/ft or 0.03 to 0.158 bar/m). Figure 74 shows a typical computation performed by RESPEC: at the bottom of the casing the $\varepsilon = 3.2 \times 10^{-3}$ strain limit is exceeded in less than 5 years after cavern commissioning. The distances between the shoe seat and cavern roof or the maximum cavern diameter affect the magnitude of the vertical strain. RESPEC concluded that caverns are stable (when operated according the brine-compensation method) but that the vertical strain on the cemented casings resulting from potash fast creep and mudstone poor tensile strength exceeds the casing strain limit. These effects are larger when the distances from the casing shoe to the top of the cavern and to the depth of maximal diameter are smaller (such a geometry favours large strain rates in the salt roof).

3.3.3 Researches dedicated to overstretching

It is worth mentioning a paper by Belzer and DeVries (2017) who used numerical modelling to predict tensile casing failure of cemented casings of natural gas storage caverns. In conclusion they state that "*Some aspects of cavern design (such as the cavern depth, diameter, and roof shape) can be controlled and used to limit casing strains and the potential for tensile casing failure. However, the creep rate of the salt cannot be controlled and can have a significant impact on casing strains. Additionally, the location of the casing shoe, minimum pressure, and characteristics of cemented casing completions can also impact casing strain*", p. 1. Also worth mentioning is the paper by Lux et al. (2019) who performed numerical simulations of a system consisting of "*casing, annulus cementation, and contact surfaces in space and time under consideration of a time-dependent cavern convergence*", p.8; and lab tests which suggest that "*strain-based assessment criteria used by Park et al.* (2006)*, [i.e., ε = 0.02 %], available for casing and annulus cementation, seem to be very conservative*", p. 8.

See also further research on this topic in the reference list (i.e., Allen, 1972, 1971; Baar, 1977; Belzer and DeVries, 2017; Bérest et al., 2019b, 2019c; Bérest and Brouard, 2003; Coates et al., 1981; Coleman Hale et al., 2015; Lux et al., 2019; Munson, 1998; Osnes et al., 2007; Park et al., 2006; Réveillère et al., 2017; Thompson et al., 2007; Wellinghoff et al., 2013).

3.4 Brittle failure

NB. the mechanical and transport properties of the host rocks of salt caverns are discussed at different places in this report.

3.4.1 Introduction

Even if rock salt behaviour is generally recognized as pre-eminently ductile, it exhibits several brittle features which are important from cavern structural stability. In this Section, these features, as observed at the laboratory (dilation, tensile failure, effective tensile failure) are described first (3.4.2).

Examples of brittle failure in salt caverns are discussed in Paragraphs 3.4.3-3.4.7.

The first example is related to thermal stresses (Paragraph 3.4.3). Following abrupt pressure changes, cavern gas experiences large temperature changes and thermal stresses develop at cavern wall. In particular, tensile stresses and fractures are generated at cavern wall. In the early 1990's, this topic generated several papers as loss of tightness was feared. These concerns were alleviated by further analyses which proved that after a large withdrawal temperature return to equilibrium is fast and time enough is not left to allow fractures to penetrate deep into the rock mass.

The second example, and most spectacular, is the onset at ground level of a crater, several dozens of meters deep (Paragraph 3.4.4). This example is worth mentioning as it can generate severe concerns in the general public. However, it must be mentioned that, technically speaking, cratering results from overburden failure rather than salt failure; in addition, the main origins of craters are the presence of too large a roof span and the absence of a salt roof above cavern top – two circumstances which, in sharp contrast with brine production caverns, do not apply to salt storage caverns. A dozen of cases are known.

The third example is roof fall (Paragraph 3.4.5) whose origin is relatively well characterized (flat, large-spanned roof set in an interstratified part of the rock formation and, in most cases, cavern pressure drop). Five examples have been described in the literature.

The fourth example is bloc falls from the cavern wall (Paragraph 3.4.7). In most cases, this incident is mundane, and its origin is the redistribution of stresses following cavern creation and operation. A more systematic cause is the presence of Anomalous Zones which are frequent in the Gulf Coast salt domes. Six examples are described.

3.4.2 Failure criteria (laboratory)

3.4.2.1 Dilation

When an increasing deviatoric stress is applied to a salt sample, onset of "dilation" can be observed: (inelastic) volumetric strain rate becomes positive (expansion), a clear sign of the development of multiple micro-fractures in the sample. These micro-fractures are oriented in the direction of the most compressive stress. Onset of dilation is easier when the confining pressure is smaller. Dilation generally is accompanied by a loss of material strength, an increase in permeability and acoustic emission, a decrease in ultrasonic wave velocities (Popp et al., 2012, 2007), and a strong influence of external humidity on strain rate. It is widely accepted that rock dilation is a relevant indicator of damage (Cristescu and Hunsche, 1998; Cristescu and Paraschiv, 1996). Several authors suggest that the onset of dilation characterizes the long-term strength of the rock.

Onset of dilation can be predicted by a stress criterion obtained during short-term tests, often described by: $\eta = \frac{\sqrt{J_2}}{(a|I_1|+b)} < 1$ (Spiers et al., 1990) where η is called the *dilation index* (no dilation before η = 1*)*; $J_2 = \frac{s_{ij}s_{ji}}{2}$; $s_{ij} = \sigma_{ij} - \frac{\sigma_{kk}\delta_{ij}}{3}$; $I_1 = \sigma_{kk}$. For Gulf Coast salt, Van Sambeek et al. (1993) suggest $b = 0, a = 0.27$ (Compressive stresses are negative.)

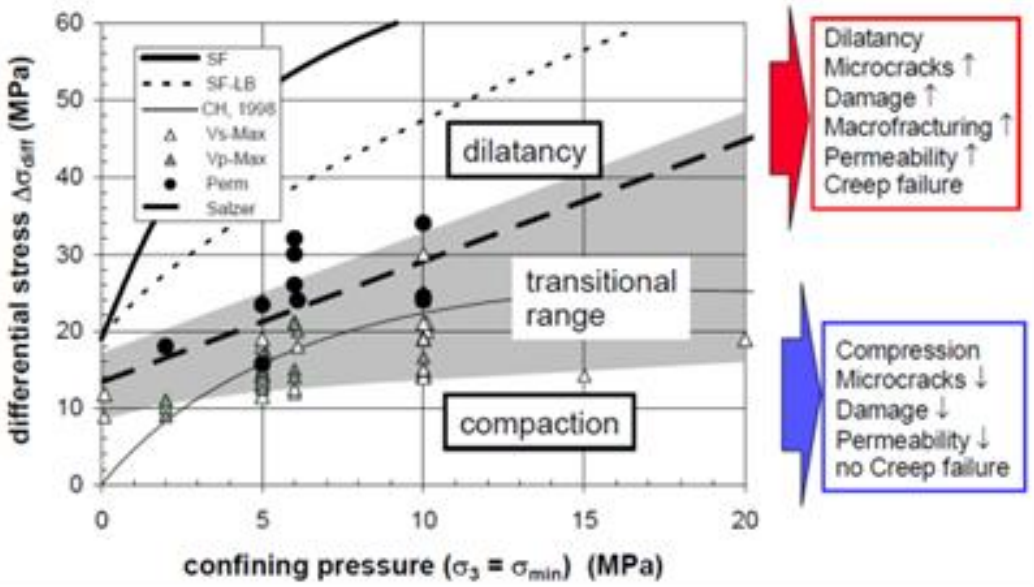

Figure 75. Dilation criterion in the plane (Popp et al., 2007).

DeVries or RD criterion

This criterion is expressed as follows:

$$FOS = \frac{D_1\left|\frac{I_1}{\sigma_0}\right|^n + T_0}{\frac{(\sqrt{3}\cos\psi - D_2\sin\psi)}{\sqrt{J_2}}} > 1, \quad 3\psi = \arcsin\left[-\frac{3\sqrt{3}\,J_2}{2J_3^{3/2}}\right] \qquad (30)$$

where T_0 is the rock tensile strength,

FOS is the Factor Of Safety (no dilation when FOS > 1),

$\sigma_o = 1$ MPa is a reference stress,

ψ is the Lode angle,

I_1 is the mean stress, and

J_2 and J_3 are the second and third invariants of the deviatoric stress tensor, respectively.

Advanced criteria, taking into account stress triaxiality (through Lode's angle) were proposed by DeVries et al. (2006). Generally speaking, as was underlined by Schultze (2007), the dilation criterion must be seen as a band (in the σ-plane) rather than a line, as the onset of volume increase does not coincide with the onset of changes in ultrasonic wave velocities (Popp et al., 2002), and Figure 75.

There is strong evidence that the dilation criterion must be modified when, instead of a single monotonous loading, dozens of cycles are applied to the sample (see Arnold et al., 2011; Düsterloh et al., 2012). DeVries and Mellegard (2010) proved that variability of dilation onset was strongly related to preconditioning procedures.

It must be noted that the dilation criteria mentioned above do not depend on the stress *rate*, a possible flaw when rapid stress changes are discussed. Schultze (2007) noted that at this time no author mentioned such a dependency when the dilation index is concerned. However, Wallner (1984), speaking

of rock strength rather than dilation criterion, stated that "*the strength besides the well-known dependence on the stress also depends on the strain rate*" (p.745), a concept that should be revised in the new context of rapid pressure changes in salt caverns. However, during a blowout, cavern pressure drops from $P_1 = 200$ bar to $P_2 = 0$ bar in 8 days, typically. The amplitude of the deviatoric stress variation at cavern wall during this period is $\frac{3(P_2-P_1)}{2}$ or 15 bar/hr, a relatively small stress rate.

3.4.2.2 Tensile failure

It is known that most rocks exhibit poor tensile strength. Tensile strength can be measured through direst methods or through the Brazilian test. The tensile strength of salt typically is T_0 =1-2 MPa (Hansen et al., 1984), smaller than uniaxial compressive stress by one order of magnitude. In most cases, contrary to the case of a mine gallery, no tensile stresses are generated at a cavern wall. Even in a gas cavern, when the gas inventory is small, stresses at cavern wall are compressive, except perhaps at some specific locations such as overhanging parts or a flat roof. Blocks may fall, and cavern shape is rearranged; overall cavern stability is not at stake. However, when high-amplitude rapid cycles are conducted, gas temperature experiences large changes, and tensile "thermal stresses" are generated at the cavern wall. This topic is addressed in Paragraph 3.4.3.

3.4.2.3 Tensile effective stress — Hydraulic micro-fracturing

When, at the wall of a borehole, gas — or brine — pressure (P) is larger than the least compressive stress σ_{max} by, say, $T_0 = 2$ MPa or, $\sigma 0_{max}$, a fracture is created. The onset of such a fracture allows the assessment of *in situ* stresses in rock formations (Doe and Osnes, 2006; Durup, 1994a; Rummel et al., 1996). The pioneering works of Kenter et al. (1990) and Fokker (1995), however, proved that, before the onset of such a discrete fracture in the pressure domain: $-t_0 < \sigma 0_{max}$ (tensile failure criterion, t_0 is small or null*),* micro-fractures develop, and salt permeability increases significantly. This mechanism has important practical consequences. It is known that when a tight, brine-filled cavern is abandoned, cavern pressure increases to geostatic pressure and above (Wallner and Paar, 1997), raising fears of tightness loss and brine migration. Micro-fracturing allows pressure release and brine seepage in the immediate vicinity of the cavern — a much less severe scenario. The SMRI has put this problem at the centre of its research program (Bérest, 2007; Ratigan, 2003; Rokahr et al., 2003). In the long term, a similar problem is raised in a radioactive waste repository, when anaerobic corrosion generates gases whose pressure increases (the "gas-frac scenario", Popp et al., 2012, 2007). An abundant literature has been dedicated to laboratory experiments (see for instance Alkan and Pusch, 2002; Peach, C.J., 1991), and studies raise experimental difficulties. Bérest et al. (2001b) performed tests on hollow spheres and proved that permeability starts increasing slightly before the condition σ_{max} is met. It was observed that such micro-fracturing is accompanied by small, or no, acoustic emission and a small increase in salt porosity (Popp et al., 2012). The micro-fractured zone develops in a direction perpendicular to the minimum compressive stress (Wolters et al., 2012), and "*micro-cracks and associated permeability develop anisotropically with strain*" (Popp et al., 2002, p. 109).

When these notions are applied to an actual salt cavern, two additional problems appear. The first problem lays in the computation of the least compressive stress. This stress is low (making the onset of micro-fractures easier) in two circumstances: (1) in a gas or liquid-filled cavern after a rapid pressure increase following a long period of time during which the cavern was kept idle (2) in the case of a flat roof raises specific problems, as the vertical stress is such that: $(\sigma_{zz} + P)_{,z} = (\rho_{salt} - \rho_{fluid})g > 0$, and the effective stress is larger in the rock mass than it is at cavern wall]. This idea was mentioned by Wallner (1988) and Wawersik & Stone (1989); a comprehensive discussion can be found in Brouard et al. (2007) and Djizanne et al. (2012). The second problem is the modelling of the post-micro-fracturing behaviour.

3.4.2.4 Post failure behaviour

In the previous sections, the onset of dilation or hydro-mechanical fracturing was discussed. How these notions can be applied to the dimensioning of a cavern or a mine raise difficult problems. The simplest approach consists of simply drawing the zone in which the dilation criterion or the tensile failure criterion is met, without attempting to model the rock behaviour after the onset of damage. This approach was applied successfully to back-calculate the behaviour of salt mines in which collapse or loss of tightness had been observed (Bauer et al., 2000; Bérest et al., 2008a) or to design salt caverns (DeVries, 2006). It should be noted that, in a cavern with constant pressure, delayed onset of dilation is not expected. A typical constitutive law can be written: $\dot{\varepsilon} = \dot{\varepsilon}^{el} + \dot{\varepsilon}^{vp} = M \cdot \dot{\sigma} + \dot{\Phi}$, where $\Phi = A\, exp\left(\frac{-Q}{RT}\right)\frac{\left(\sqrt{3J_2}\right)^{n+1}}{(n+1)}$ is an increasing function of J_2. In the rock mass, $div(\dot{\sigma}) = 0 \text{ in } \Omega \text{ and } \dot{\sigma} \cdot n = 0 \text{ on } \partial\Omega$, typical: when averaged throughout the entire rock mass, the deviatoric stress, J_2, is a decreasing function of time, and the dilation criterion will never be met when it is not met from the start.

It must be said that at this time, however, that there is no consistent theoretical basis that allows for predicting failure through a dilation criterion. (Such a basis exists, for instance, when a perfect plastic criterion is used). The adopted approach is more empirical: a dilated zone may appear at the wall of a cavern or a dry mine pillar, but to prevent generalized failure, the dilated zone must remain confined inside a non-dilated zone. In a dry mine, for example, a significant part of the core of the pillars must remain non-dilated. Such a prudent approach seems to provide a conservative assessment. This approach was adopted successfully in a couple of post-mortem analyses.

Figure 76 shows the case of the Saint-Maximilien panel at Varangéville, France. From the central pillar (on the left), 9 rooms are created, progressively and the increase of the dilatant zone is represented. When rooms 7, 8, 9 are created, a continuous dilatant zone is generated when the 9th room is excavated – i.e., when the panel collapsed.

Various attempts were made to describe the "post-dilation" behaviour of salt mathematically. Several modelling strategies can be used to account for volume increase. Thorel and Ghoreychi (1993), Serata and Fuekenjorn (1993) and Brückner et al. (2012) treat the dilation criterion as a plastic-like criterion: the flow rule can be associated, or not. Pudewills (2012) introduces a second viscoplastic potential that, in addition to the second invariantJ_2, depends on the first invariantI_1.

Volume increase is related to porosity increase (Pusch and Alkan, 2002; Stormont and Daemen, 1992), which, in turn, is related to permeability change through a modified Kozeny-Carman relation (Popp et al., 2012). However, this approach might be too simple, as the "secondary" permeability clearly is not anisotropic. In addition, the material loses some strength (weakening), and viscoplastic strain rates are faster. Chan et al. (1996), and Thorel and Ghoreychi (1993) use Kachanov's damage theory, in which the constitutive law is a function of Kachanov's "effective stress",$\tilde{\sigma} = \sigma/(1 - D)$, strain where D is a damage parameter increasing from 0 (virgin state) to 1. In such a context localization is likely and may raise difficult numerical problems. Strain softening is an alternative modelling strategy, successfully used by Kamlot et al. (2007) to compute dilatancy in the Asse II salt mine in Germany. A remarkable dynamic analysis was provided by Minkley and Menzel (1996) in the case of mine excavated in a salt formation with brittle behaviour.

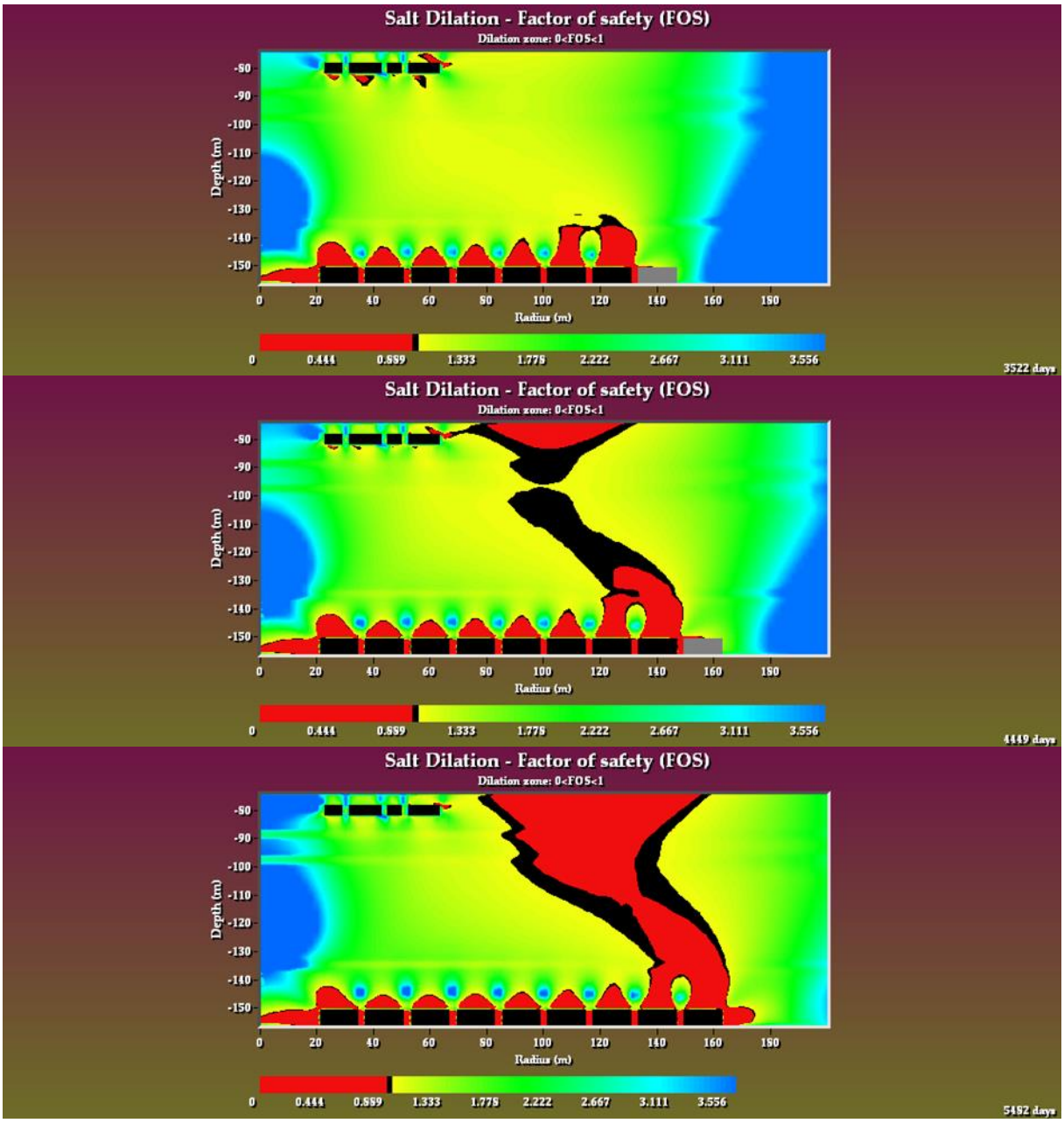

Figure 76. Varangéville salt mine. Progression of the zone in which the dilation criterion is met during excavation of galleries n°7, 8 and 9 (after Bérest et al., 2008b).

When gas or brine can enter the micro-fractures, the poro-mechanical problem is fully coupled. Whether the notions of Darcy flow and Biot's coefficient (classical notions in Reservoir Engineering) apply is an open question (see Cosenza et al., 2002; Pfeifle and Hurtado, 2000). When gas is concerned, the notion of a capillary pressure (two-phase flow) does not apply, as micro-fracturing creates new voids (Brine must not be removed by gas.), which provides a possible explanation for the results of a micro-fracturing test performed in a wellbore by Durup (1994a). Most of these comments also apply to post-tensile micro-fracturing and dilation as well. Interpretation of laboratory tests becomes more difficult, because the development of dilation and fluid permeation cause the state of stress in the sample to be non-uniform. In addition, it is believed that, to some extent, a dilated material can "heal" and restore its initial strength (Chan et al., 1996; Popp et al., 2012; Wolters et al., 2012). In this sense, one must distinguish between *compaction*, which refers to permeability decrease observed when an isotropic stress is applied, and true *healing*, which means that any memory of past damage has been lost. These research fields are being pursued actively, and new developments are expected.

3.4.3 Thermal stresses (tensile failure)

3.4.3.1 Onset of thermal stresses

This topic was briefly addressed in Paragraph 3.4.1; the onset of tangential thermal stresses at cavern wall was predicted. More details are discussed in this paragraph.

Especially in the case of the N-H law, during several days after an initial abrupt pressure drop from P_c^- to P_c^+, rock mass response is almost perfectly elastic (deviatoric stress change is slow). Consider for instance an idealized spherical cavern. Principal stresses are $\sigma_{rr}, \sigma_{\theta\theta} = \sigma_{\varphi\varphi}; S = \sigma_{rr} - \sigma_{\theta\theta}$ is the "deviator", $|S| = \sqrt{3J_2}$. The deviator jump is:

$$[S^{EL}]_-^+ = -\frac{3}{2}\left(\frac{a_0}{r}\right)^3 (P_c^+ - P_c^-) \tag{31}$$

However, in the case of a gas-filled cavern, gas experiences a severe temperature drop during a rapid (a few days) depressurization, as gas heat capacity is low (much lower than brine's, for instance). Rock temperature change can be written $\tau(r,t) < 0$. Thermal stresses must be taken into account (when cooled, rocks at cavern wall contract. Deeper rock layers, whose temperature remain constant, do not contract. Generated strains are not compatible and thermal stresses are created. These stresses are tensile, as superficial layers at cavern wall are stretched in the tangential direction). They are compressive when the rock is heated instead of cooled. When temperature changes are large, rock failure at cavern wall takes place.

These stresses are especially large in the case of rock salt, whose thermal expansion coefficient α_{salt} is large. The thermoelastic constitutive equations for displacement (u^{TH}) and stresses (σ^{TH}) of purely thermal origin can be written:

$$\frac{\partial u^{TH}}{\partial r} = \frac{\sigma_{rr}^{TH} - 2\nu_{salt}\sigma_{\theta\theta}^{TH}}{E_{salt}} + \alpha_{salt}\tau \tag{32}$$

$$\frac{u^{TH}}{r} = \frac{(1-\nu_{salt})\sigma_{\theta\theta}^{TH} - \nu\sigma_{rr}^{TH}}{E_{salt}} + \alpha_{salt}\tau \tag{33}$$

where α_{salt} is the thermal expansion coefficient of the rock mass. Boundary conditions are $\sigma_{rr}^{TH}(a_0) = 0$, $\sigma_{rr}^{TH}(\infty) = 0$ and $r^3 u^{TH}(r) \to 0$ when $r \to \infty$. The second equation can be subtracted from the first one, the resulting equation can be divided by *r* and integrated with respect to *r* between $r = a_0$ and $r = b_0 = \infty$, leading to $\frac{u^{TH}(r)}{r} + (1+\nu_{salt})\frac{\sigma_{rr}^{TH}(r)}{2E_{salt}} = 0$, from which $u^{TH}(a_0) = 0$: thermal stresses generate no cavern volume change, and $\sigma_{\theta\theta}^{TH} + \frac{E_{salt}\alpha_{salt}\tau}{(1-\nu_{salt})} = 0$. The overall deviator stress change is:

$$[S^{EL}(a_0,t) + S^{TH}(a_0,t)]_-^+ = -\frac{3}{2}(P_c^+ - P_c^-) + 2\frac{E_{salt}\alpha_{salt}\tau(a_0,t)}{1-\nu_{salt}} \tag{34}$$

In the right-hand side of this equation, the first quantity is positive, for instance $\frac{-3(P_c^+ - P_c^-)}{2} = 7.5$ MPa, the second quantity is negative, for instance, for instance $E_{salt} = 17{,}000$ MPa, $\nu_{salt} = 0.3, \tau = 9$ °C and $2E_{salt}\alpha_{salt}\frac{\tau(a_0,t)}{(1-\nu_{salt})} = -21.8$ MPa. (Various values of this quantity from the literature are given in Table 4).

The overall deviator is negative (the effective stress is tensile) when the thermal stress is large enough; i.e., when the thermodynamic Evolution is fast enough, as explained in Bérest et al. (2012), hydro-fracturing is likely.

Table 4. Thermal stresses coefficients for various salts.

	E_{salt} **(GPa)**	ν_{salt}	α_{salt} **(×10^{-5}/°C)**	$\frac{E_{salt}\alpha_{salt}}{(1-\nu_{salt})}$ **(MPa/°C)**
Pellizzaro et al. (2011)	27.05	0.3	3.2	1.237
Staudtmeister et al. (2017)	18	0.2	4	0.9
Argüello and Rath (2012)	31	0.25	4.5	1.86
Tijani et al. (2012)	25	0.3	3.5	1.25

3.4.3.2 Case histories

3.4.3.2.1 A salt cavern solution-mined below a mine drift

Dreyer (1978) solution-mined a small (2.5-m high) cavern underneath a mine drift and filled the cavern with liquid nitrogen, lowering cavern temperature by $\tau = -200$ °C. After several days, nitrogen was withdrawn from the cavern. It was observed that the huge tensile stresses generated by cavern filling had left four main fractures, 50-cm deep, which were not fully closed (Figure 77).

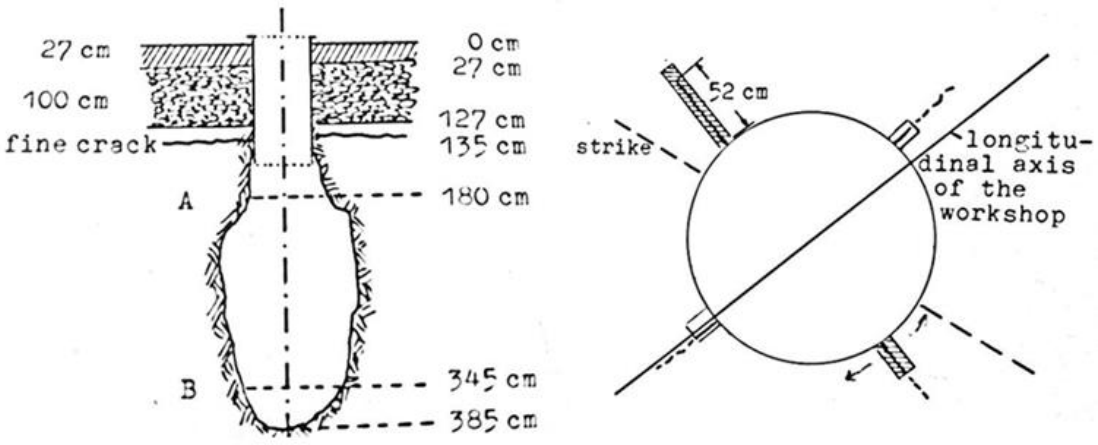

Figure 77. Thermal fractures in a salt cavern leached out underneath a 600-m mine drift, the temperature drop is -200°C (from Dreyer, 1978).

3.4.3.2.2 A gallery in which hot exhaust gases circulate

Lee et al. (1982) describe a drift, 1.8-m high, 150-m deep, in a granitic paragneiss rock mass in which hot exhaust gases from an underground power plant circulate. Virgin stresses are not known.

Gas temperature was 315 °C (τ = 300 °C) generated spalling. Roof rose by 1.8 m. environ. Scales were 2.5 cm thick; their diameter was 0.3 to 0.6 m (Figure 78). Rupture surface was generally parallel to the wall. As mentioned by Gray (1965): « *the course of the fracture seemed to be determined mainly by the pattern of thermal stresses surrounding the opening, and not by the gneissic structure of the rock* »… A test proved that spalling started when gas temperature was 61 °C.

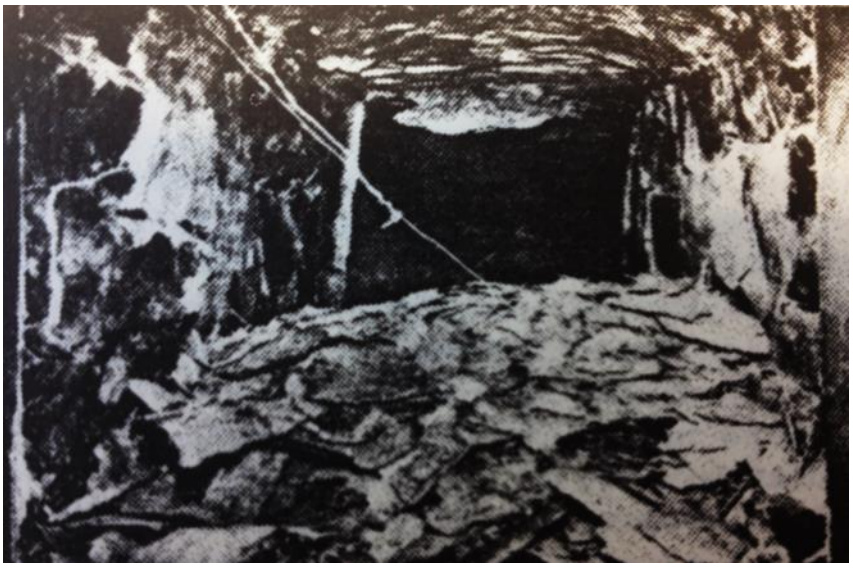

Figure 78. Thermal spalling in an exhaust gas drift at North Bay, Ontario (Lee et al., 1982, p. 964).

3.4.3.2.3 A test in a salt mine

In 2014-2015 a scientific consortium, led by Storengy, a storage company, performed a cooling test in a gallery of the Varangéville salt mine in France. This test was supported by the Solution Mining Research Institute (SMRI). A horizontal cold airflow was blown along a 10 m² salt surface at gallery floor for 28 days. Mine temperature is 14 °C and cold air temperature was –6 °C. Each cold phase was followed by a 28-day warming phase (a "cycle"). During the first cycle, after 2 hours, cracks appeared on the surface and a large number of acoustic events were recorded. Four cycles were managed. During each cycle, cracks opened and closed, and new cracks were generated (Figure 79). From acoustic emission and post-mortem analysis of cores, it was inferred that cracks depth was 1 m. The horizontal distance between two main cracks also was s = 1 m, approximately. Crack aperture was from o = 0.3 to 1 mm (Balland et al., 2016).

Figure 79. A thermal fracture during the SMRI test at Varangéville. The wall was cooled by τ = -20°C (Acknowledgements: G. Hévin, Storengy).

3.4.3.2.4 A mine ventilation shaft in the Gorleben mine

In the case of an idealized cylindrical cavern (or a borehole, or a mine shaft), thermos-elastic stresses at cavern wall can write:

$$\begin{cases} \sigma_{rr}^{TH}(a) = P_c^+ - P_c^- \\ \sigma_{\varphi\varphi}(a) = -(P_c^+ - P_c^-) - \frac{E_{salt}\alpha_{salt}\tau}{(1-\upsilon_{salt})} \\ \sigma_{zz}(a) = -E_{salt}\alpha_{salt}\tau/(1-\upsilon_{salt}) \end{cases} \quad (35)$$

Figure 80 shows a South-South map of a mine ventilation shaft wall between 370-m and 380-m depths. During winter, ventilation air drops by $\tau = -20$ °C; air pressure does not change, drop from $P_c^- = P_c^+$, rock. Additional thermal stresses by 20 MPa generate horizontal fractures (red dots).

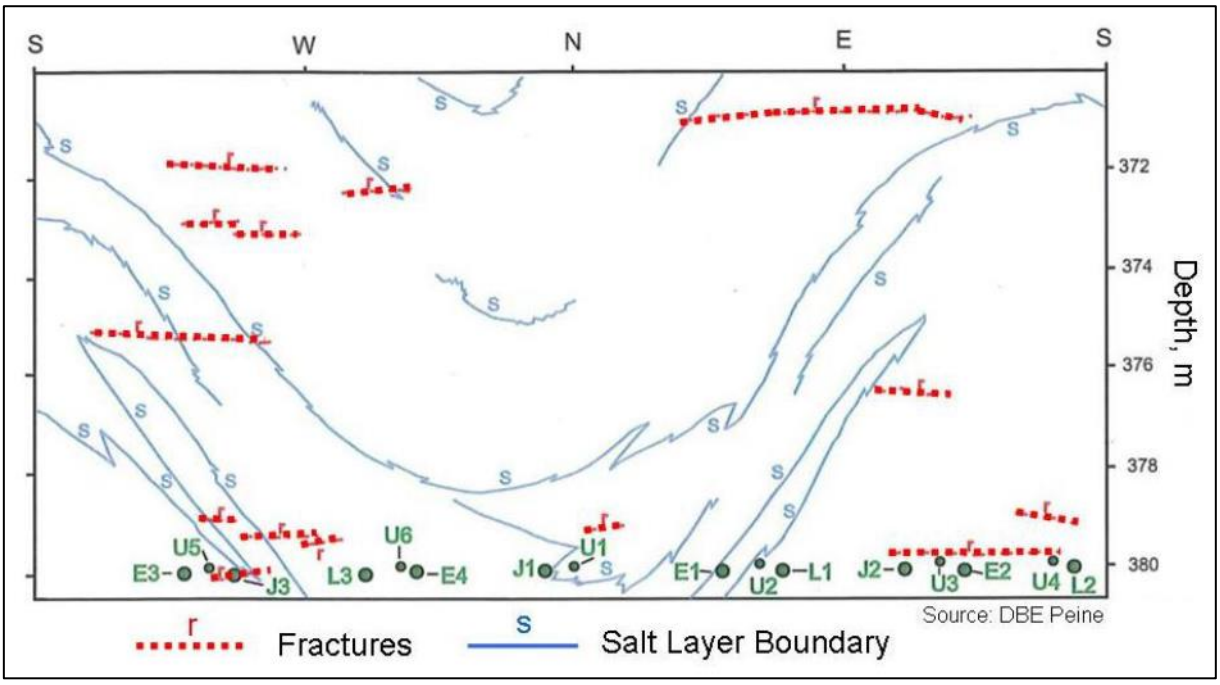

Figure 80. Thermal fractures at the wall of a ventilation shaft of the Gorleben Mine (Wallner and Eickemeier, 2001; Zapf et al., 2012).

One may ask why thermal fractures are horizontal (rather than vertical) in a cylindrical cavern (or borehole). In simple terms, the thermal stresses must be added to the visco-plastic stresses. When the cavern has been at rest before the temperature drop, steady state stress distribution is reached (Wang et al., 2015):

$$\sigma_{rr}^{SS}(a) = -P_c;\ \ \sigma_{\varphi\varphi}^{SS}(a) = -P_\infty - \left(1 - \frac{2}{n}\right)P_c;\ \ \sigma_{zz}^{SS}(a) = -P_\infty - \left(1 - \frac{1}{n}\right)P_c;$$
$$I_1(a) = -3P_\infty - 3\left(1 - \frac{1}{n}\right)P_c;\ \sqrt{J_2(a)} = \frac{(P_\infty - P_c)}{n} \quad (36)$$

And the least compressive (tangential) stress is the vertical one; after cooling it becomes the most tensile.

3.4.3.3 *Growth of fractures at cavern wall*

Sicsic and Bérest (2014) computed the theoretical example of a cavern in which a low temperature ($\tau = -40$ °C) following a blow-out is kept constant in the cavern during a 6 month-long period (In fact, gas temperature rapidly increases after one week.) Many thin fractures, perpendicular to the cavern wall, develop first (Figure 81). As temperature is kept low, fractures grow; their length is the thickness of the zone in which the vertical stress is tensile; however, they are smaller and smaller. A kind of selection takes place, some fractures keep growing. The geometry has very little influence on the position and spacing of cracks. Although the surface of the rock wall is neither perfectly flat nor smooth, the global picture is that of a parallel array of cracks.

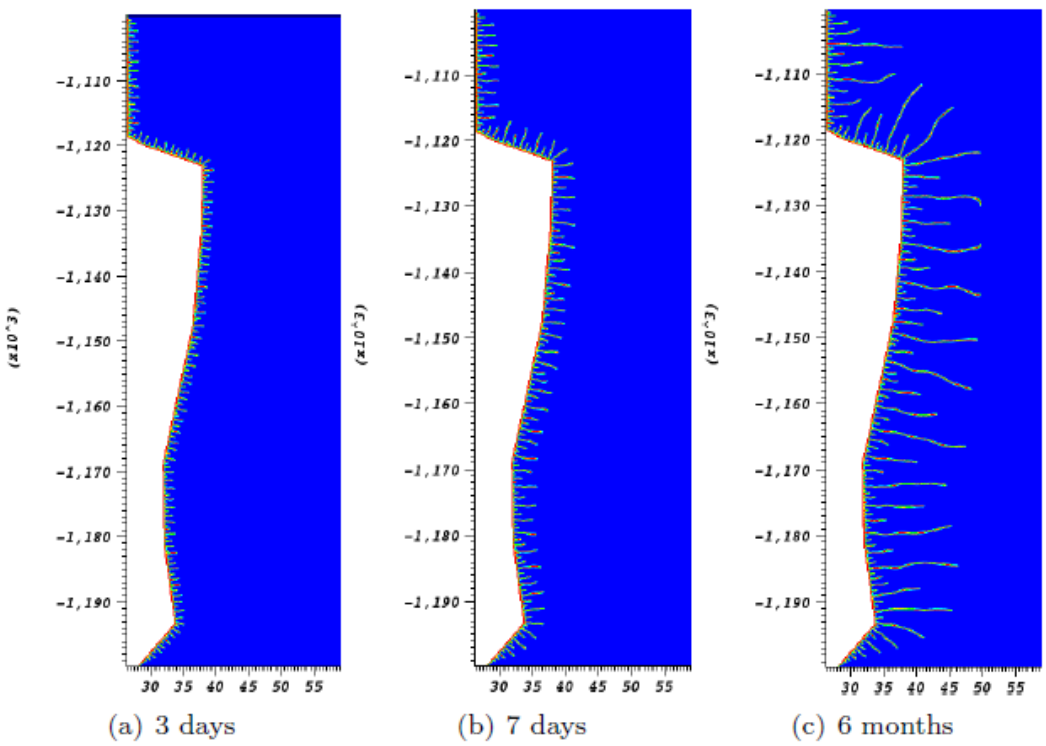

Figure 81. Fracture growth as a function of time when a low temperature is kept (artificially) constant at cavern wall.

3.4.3.4 *Factors mitigating the concerns raised by thermal fractures*

These analysis and computations raised concerns in the early 2010's. It was feared that, after large pressure drops, thermal fractures be created and caverns loss tightness. These computations may seem concerning: they predict that fractures can be created at cavern wall. They must be taken with a pinch of salt.

3.4.3.4.1 Rapid warming of the cooled gas

First, in sharp contrast with the theoretical example described in Paragraph 3.4.3.1 for that matter, cold temperature is not applied for a long time at the walls of a salt cavern: when pressure drop comes to an end, gas warms rapidly (see Paragraph 2.1.3.5: in the Melville cavern, temperature started warming before the end of the gas withdrawal It is known from experience that fracture depth equals the depth of the zone in which tensile stresses (perpendicular to the cavern wall) were computed. This depth is determined by the depth of the zone in which rock temperature significantly dropped. In general, this depth is small in a cycled cavern. Not enough time is left for cold temperature to penetrate deep into the rock mass at cavern wall and the tensile zone is thin.)

3.4.3.4.2 Thermo-elasto-viscoplastic stresses in an actual cavern

Second, tensile stresses are slightly lessened in a visco-plastic medium (when compared to an elastic medium).

In an actual salt cavern stresses evolutions are more complex as, in addition to the purely thermos-elastic stresses whose order of magnitude was computed in the previous section, pressure changes generate viscoplastic strains and additional stresses. Numerical computations are required. Fig. 8 shows the results of such computations in an elongated cylindrical cavern. The effects of pressure cycling in a point of the cavern wall is represented. Temperature evolution (red line) is the same for the three examples; however, the thermo-elastic, thermo-visco-plastic (Norton-Hoff and Munson-Dawson) are discussed successively. The three principal stresses, the deviatoric stress and the mean stress are represented.

On Figure 82, the upper picture shows temperature evolution during gas pressure cycles. The middle picture shows that, at cavern mid-depth, the vertical stress is tensile (and high) following large pressure drops (phases 4-5 and 8-9), a consequence of the development of thermal stresses (see the Gorleben example above). The lower picture represents the deviatoric stress (more precisely, $\sqrt{J_2}$) and the mean stress ($|I_1|$) multiplied by 0.27. Dilation occurs when $\sqrt{J_2} > 0.27|I_1|$; i.e., at cavern mid-depth, the vertical stress is tensile (and high) following large pressure drops (phases 4-5 and 8-9).

Figure 82 shows that these effects (onset of tensile stresses and dilation) are slightly mitigated when the Norton-Hoff law (instead of the thermoelastic law) is considered, as viscous effects allow some stress redistribution, making deviatoric stresses smaller.

This is all the truer when Munson-Dawson law (Figure 82, bottom) is taken into account, as viscous effects are exacerbated.

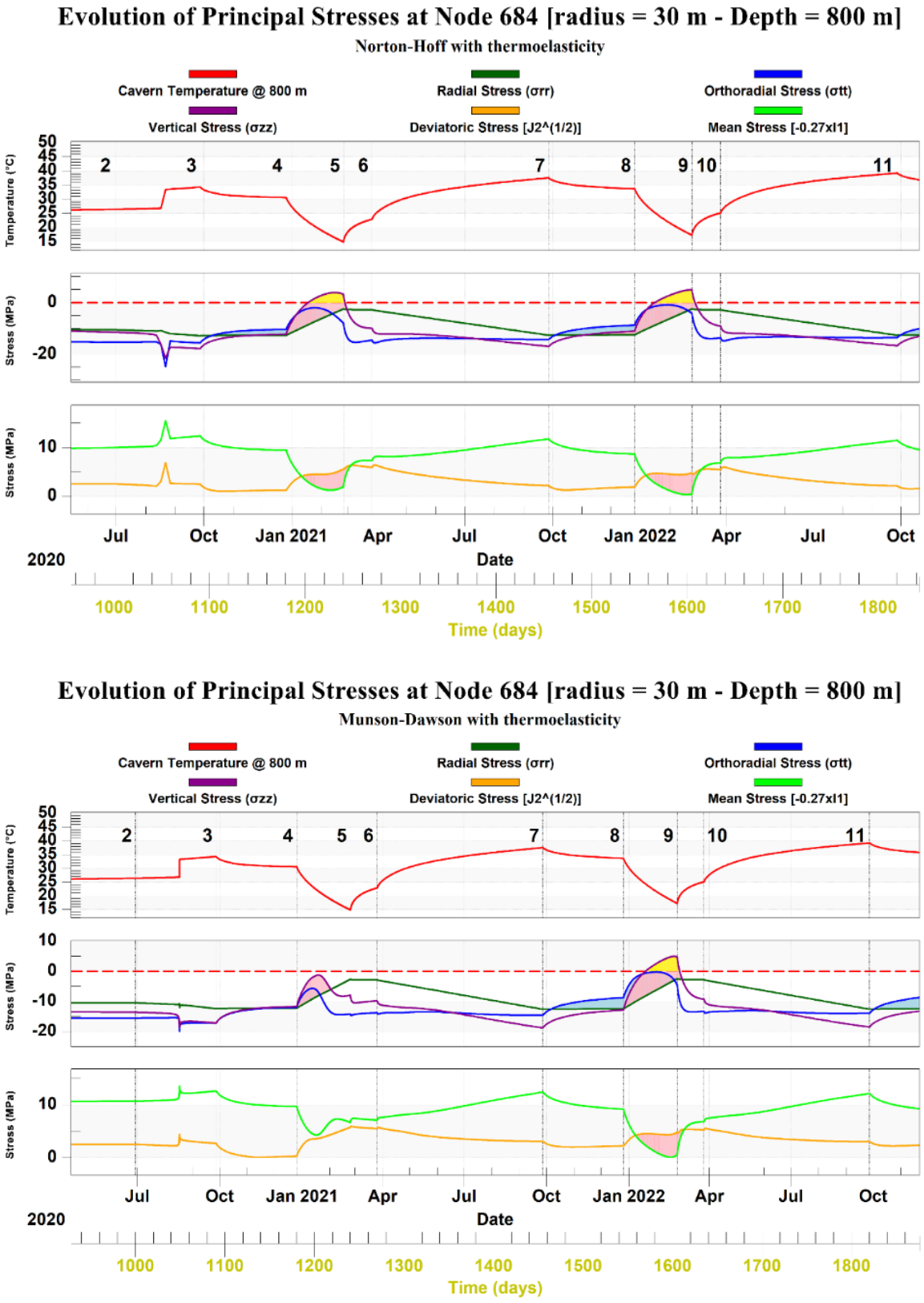

Figure 82. Stresses Evolution at the wall of a pressure-cycled cavern (top: Norton-Hoff model; bottom: Munson-Dawson model).

3.4.4 Cratering (overburden failure)

Cratering is the most spectacular failure mechanism of a salt cavern: a cylinder of rock drops abruptly by several dozens of meters (Figure 83). However, this phenomenon requires special conditions which have never been met in storage caverns.

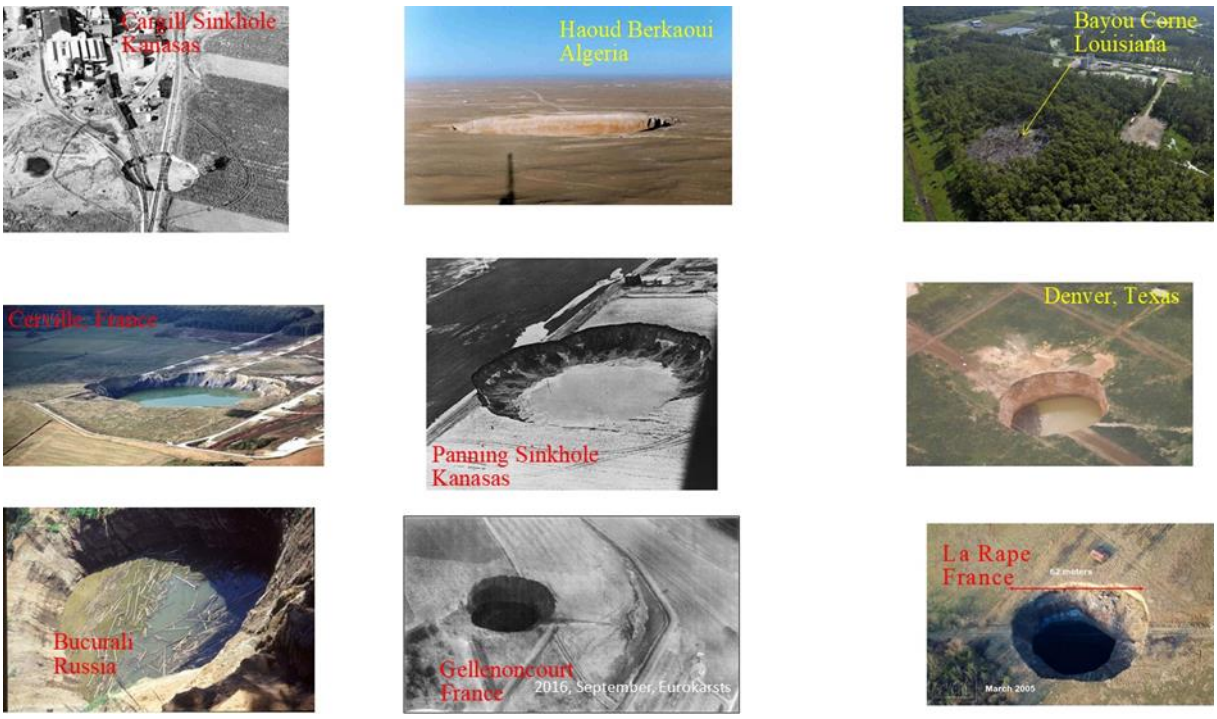

Figure 83. Craters formed above salt caverns above.

3.4.4.1 Case histories: a summary

A few introductory definitions are needed. A *subsidence bowl* is a trough observed at ground level above any underground opening. Its vertical profile is smooth, and its slope is several mm/m or less. In some instances, folds and vertical fractures, implying a discontinuity in horizontal displacements, can be observed at ground level. A *crater* (Figure 84, Above) is generated by downward vertical displacement of a piece of rock (the "*piston*" model, Figure 84, Below) or an inward horizontal displacement of loose materials toward a central hole at the roof of a cavern (the "hourglass" model). A discontinuity in vertical displacements by several meters or dozens of meters (a "step") can be observed at the edge of a crater. A *sinkhole* is defined less clearly: a sinkhole is a crater or a subsidence bowl deep enough to generate safety issues for buildings, mains, roads, ground water flow etc.

Millions of craters or sinkholes have been created worldwide during geological times. Natural sinkholes result from the collapse of overburden rocks above karstic voids created through the dissolution of limestone (sometimes of gypsum or chalk) by swift running water; or through the washing of loose shallow materials through fissures and caves, a process named suffusion. A similar classification ("piston" and "hourglass") applies to sinkholes created above caverns leached out from salt formations for brine production or hydrocarbon storage. If crater formation – deliberate or not – is not exceptional above caverns operated for brine production, no case is known of a crater formed above a gas or liquid storage cavern. The reason is that brine producers search for a high extraction ratio of the salt formation, which may lead to horizontal dimensions of the cavern too large from the standpoint of structural stability, hydrocarbon storages must absolutely be stable, as hydrocarbons are much more valuable than brine, and large safety margins are selected.

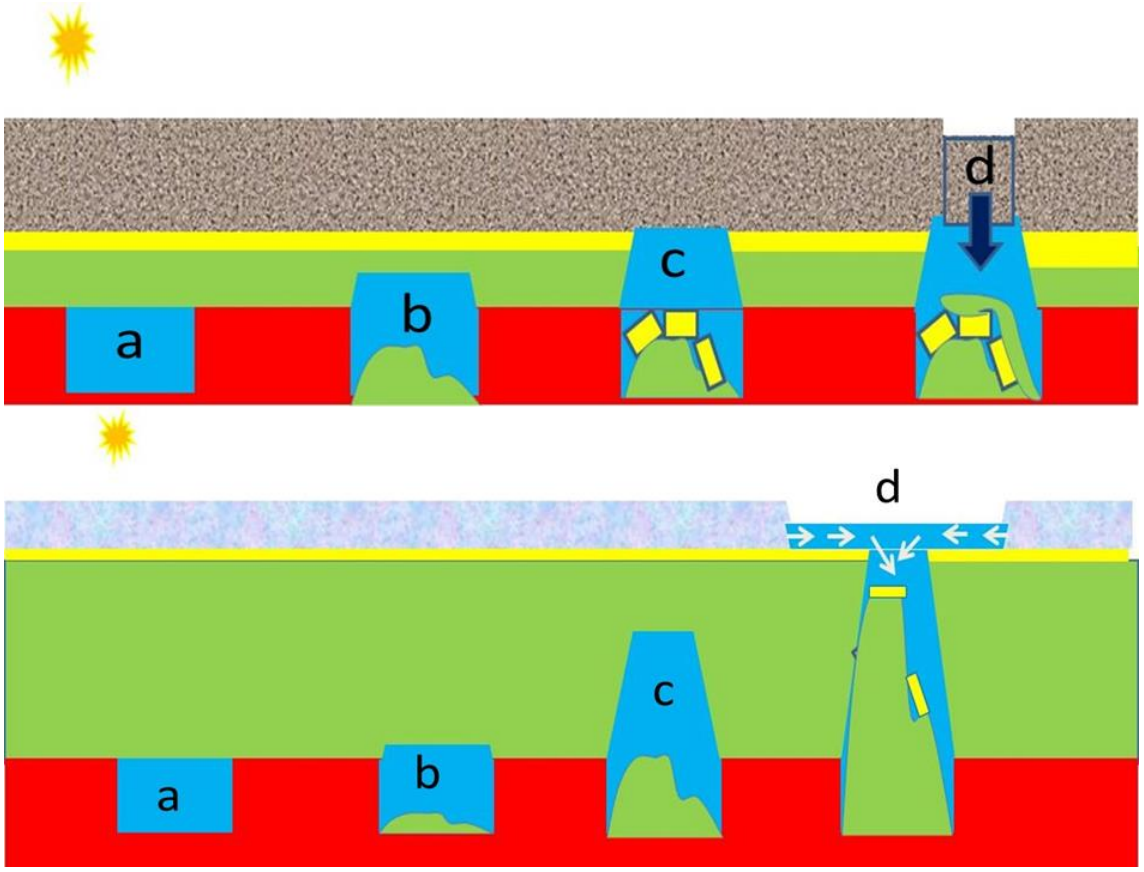

Figure 84. Cratering: cavern roof reaches the top of the salt formation and rises in the overburden through progressive weathering of the clayey layers (stoping), until (Above) a piston drops in the cavern by several meters or dozens of meters without experiencing deformation or (Below) water-saturated sands or gravels flow toward a central hole created at the top of a cavern (hourglass) which rose in the overburden through stoping.

Formation of twenty-odd craters were described in the literature (Bérest, 2017). None was associated with a cavern deeper than$H = 500$ m. Two lines of reasoning can explain this.

The rock cylinder above the cavern can fall only if its weight, $\pi R^2 H \gamma_R$, minus the force resulting from the pressure applied by cavern brine at cylinder bottom, $\pi R^2 H \gamma_b$, is larger than the sum of the shear forces which apply to the lateral surface of the cylinder, $\int_0^H 2\pi R \tau_{rz}\,(z) dz$. Overburden rocks are assumed to satisfy a Coulomb criterion ($\tau_{rz}(z) < C + tg\varphi\ \sigma_{rr}(z)$, cohesion C, friction angle φ) and $\sigma_{rr}(z) = \gamma_R z$. (The maximum admissible shear stress increases with depth). The condition writes:

$$(\gamma_R - \gamma_b) R > 2C + \gamma_R\ H\ tg\varphi \qquad (37)$$

Where H is the cavern roof depth, R is the radius of the cylinder, γ_R is the volumetric weight of the rock mass (0.23 bar/m), γ_s is the volumetric weight of brine (0.12 bar/m). When cohesion C is neglected, to err on the safe side, it can be inferred from known cases that a crater cannot form when the ratio between cavern radius and cavern roof depth is significantly smaller than $\frac{R}{H} = \frac{1}{3}$. – a condition met by all storage caverns.

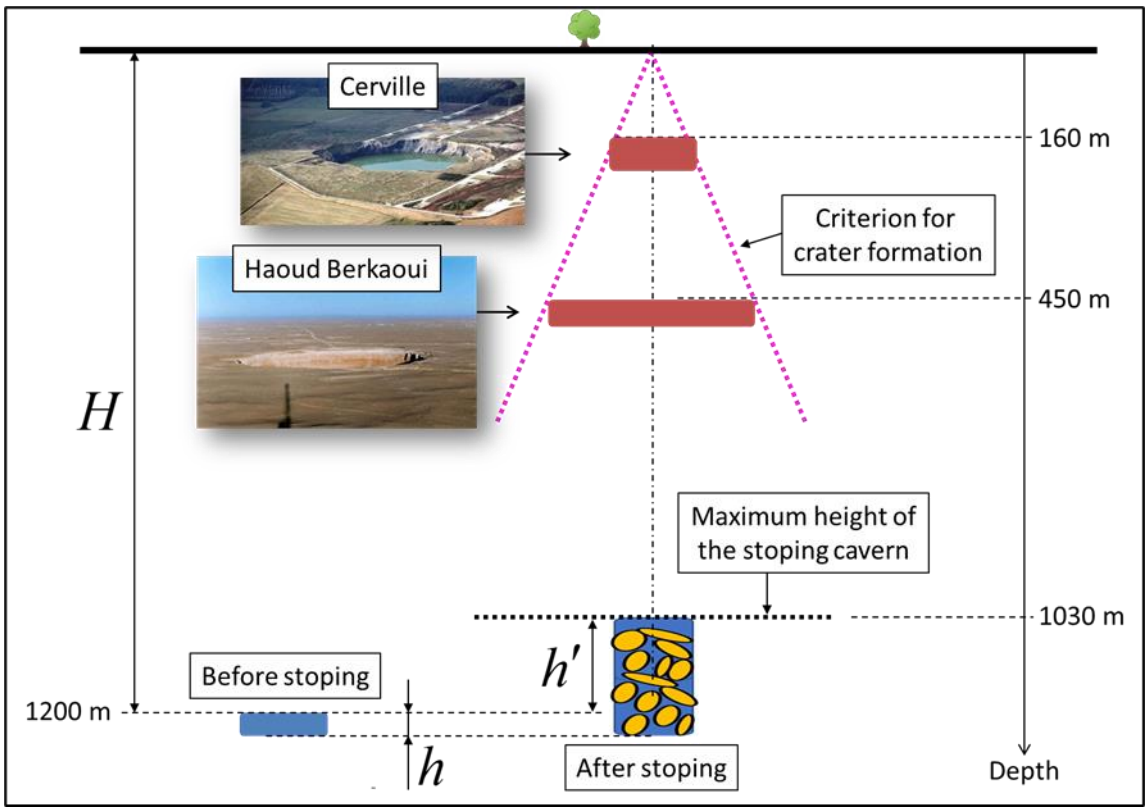

Figure 85. (Above) Two caverns that experienced cratering. (Below) Stabilization of a cavern through bulking.

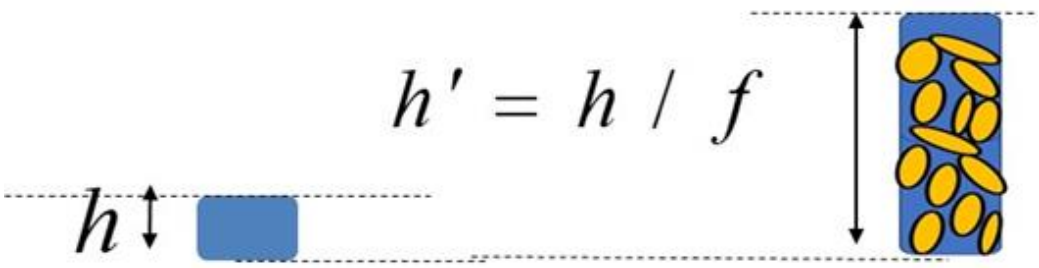

Figure 86. Cavern filling through debris and blocks fallen from cavern roof.

It could be feared, however, that a cavern rises in the overburden without experiencing any radius decrease (« *chimneying* ») as shown in Figure 85. The criterion would be met before stoping occurs, but it should be violated after a sufficient rise of the roof (this occurred in the Lorraine and Kansas caverns mentioned in Figure 83). However, this can only occur after cavern roof reaches the top of the salt formation. In addition, during stoping, blocks fall at the bottom cavern and bulk (the volume of the blocks assembly at the bottom of the cavern is larger than the sum of the individual blocks volume): their volume equals $(1 + f)$times their initial volume. The bulking factor f is site-specific. $f = 50\ \%$ is often suggested. From the analysis of block falls in the 62 caverns of the U.S. Strategic Petroleum Reserve, Munson et al. (1998) suggest $f = 55\ \%$. Guarascio et al. (1999) propose $1 + f = 1.7$ to 1.85 for hard rocks (limestone) and $1 + f = 1.3$ to 1.5 for soils or soft rocks (marls, shales). However, at Twente-Rijn in the Netherlands, Dortland (2003), Dortland et al. (2005) and Mensen and Paar (2002), suggest $f = 7 - 14\ \%$ [a small value]. It is easy to check that a cylindrical cavern whose roof rises in the overburden through stoping and chimneying is fully filled by accumulated blocks when its actual height equals its initial height divided by f (Figure 86). When cavern depth then is sufficiently high, there is no risk of crater formation. Several cases are known in Lorraine, France.

3.4.4.2 A puzzling example (Matarandiba Island, Brazil, 2018)

The following information was taken from Réveillère, Bérest and Jeronimo, (2021), whose main source is the CPRM (Brazil Geological Survey) Preliminary Report, by Guimarães et al. (2018).

The Matarandiba Island, 30-km west of Salvador/Bahia – Brazil, belongs to a humid and dense forest region with many lagoons. Matarandiba Island belongs to the Recôncavo Basin, which was formed from the fragmentation of the Pangea Supercontinent during the Cretaceous. Its basic architecture is a half-graben, with normal faults at the edges: at the east, Salvador's fault system (oriented NE-SW) and, at the west, Maragogipe's Fault System (oriented NNE-SSW). The salt deposit is located 1200-1300 m below the surface. It has a stratified, continuous, and horizontal geometry, with a thickness varying from 20 to 60 meters; it is composed 92% NaCl (halite).

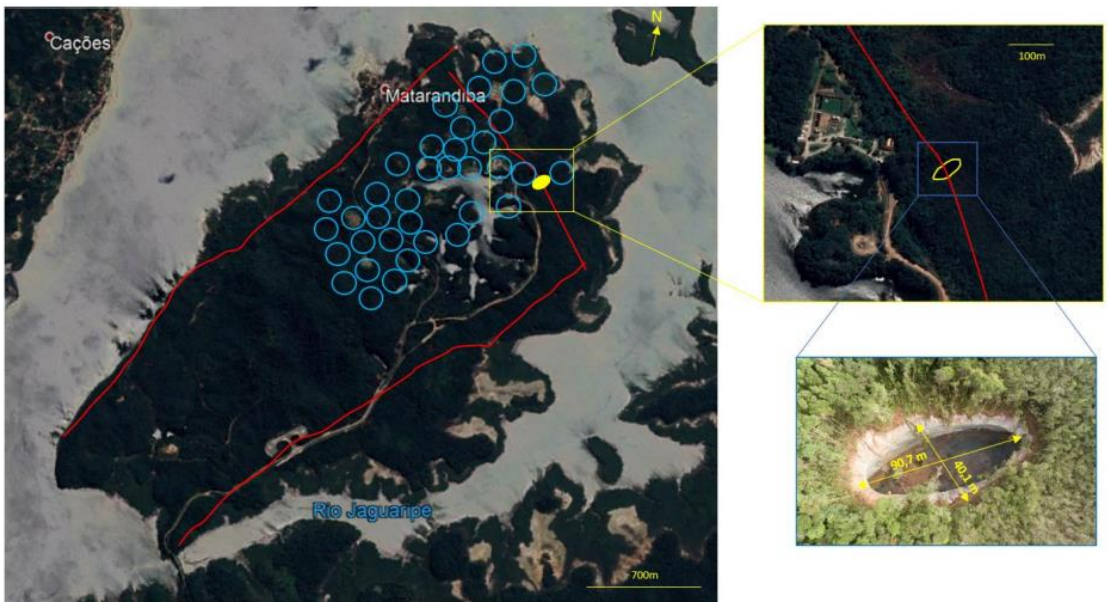

Figure 87. Location of geological faults (red lines), salt cavities (blue circles) and sinkhole (yellow ellipse) at Matarandiba Island (based on CPRM Preliminary Report information, Guimarães et al., 2018).

In 1976 the first well was drilled, and the salt production started in 1977. 51 wells were spud for brine extraction and an equal number of cavities was created. The cavities have diameters of 150 m and several of them formed a cluster of interconnected caverns (Figure 87). In 2018, 10 of the 51 wells were active (Guimarães et al., 2018). In the island, four water production wells are used to feed the salt extraction system. An artificial lake ("*Lago*") (Figure 88) occupies a large part of the island and its water is also used for salt recovery. Studies have revealed a quasi-orthogonal system of faults with general orientation N40°E and N45°W. It coincides with the major and minor axes of the sinkhole formed in 2018 (Guimarães et al., 2018).

Figure 88. Sinkhole location in Matarandiba Island (from G1, 2018).


Figure 89. Drone view of the sinkhole location in Matarandiba Island (from G1, 2018).

The crater was discovered on May 30, 2018 during routine rounds (Figure 89). The exact day on which the crater appeared is not known, nor whether the collapse was sudden or progressive. The crater had an elliptical shape when it formed, its dimensions being 69-m long, 29-m wide and 45-m deep. Its dimensions have increased over time, reaching 90 m × 41 m and 36-m deep in February 2019. In May 2020, the dimensions were 110-m long, 47-m wide, and 33-m deep (G1, 2020). The sinkhole is located more than 200-m away from a well that was put out of operation in 1985 and, therefore, no activity has been carried

out in this well for more than 30 years (G1, 2020). Since the discovery of this sinkhole, more than $ 1 million were invested in studies and monitoring technologies (sobregeologia.com.br5). According to a geomechanical study carried out in 2019, the region around Dow the mining installations in Matarandiba Island is stable and a new crater is unlikely to occur (G1, 2019).

Origin of the crater is still a controversial issue. According to g1.globo.com, a cavern may have appeared leached out at relatively shallow depth due to a fast flow of underground water (possibly triggered by pumping and creation of the artificial lake) and the presence of geological faults in the region. One must be assumed that this process was fast. Other experts believe that the crater originates in the drop of a cylinder to the caverns cluster. However, the sinkhole diameter/cluster depth is very large (when compared to the criterion suggested above) and a 100-200 m offset is observed between the sinkhole and the cluster. Compelling evidences are missing.

3.4.5 Roof Fall

3.4.5.1 Case histories

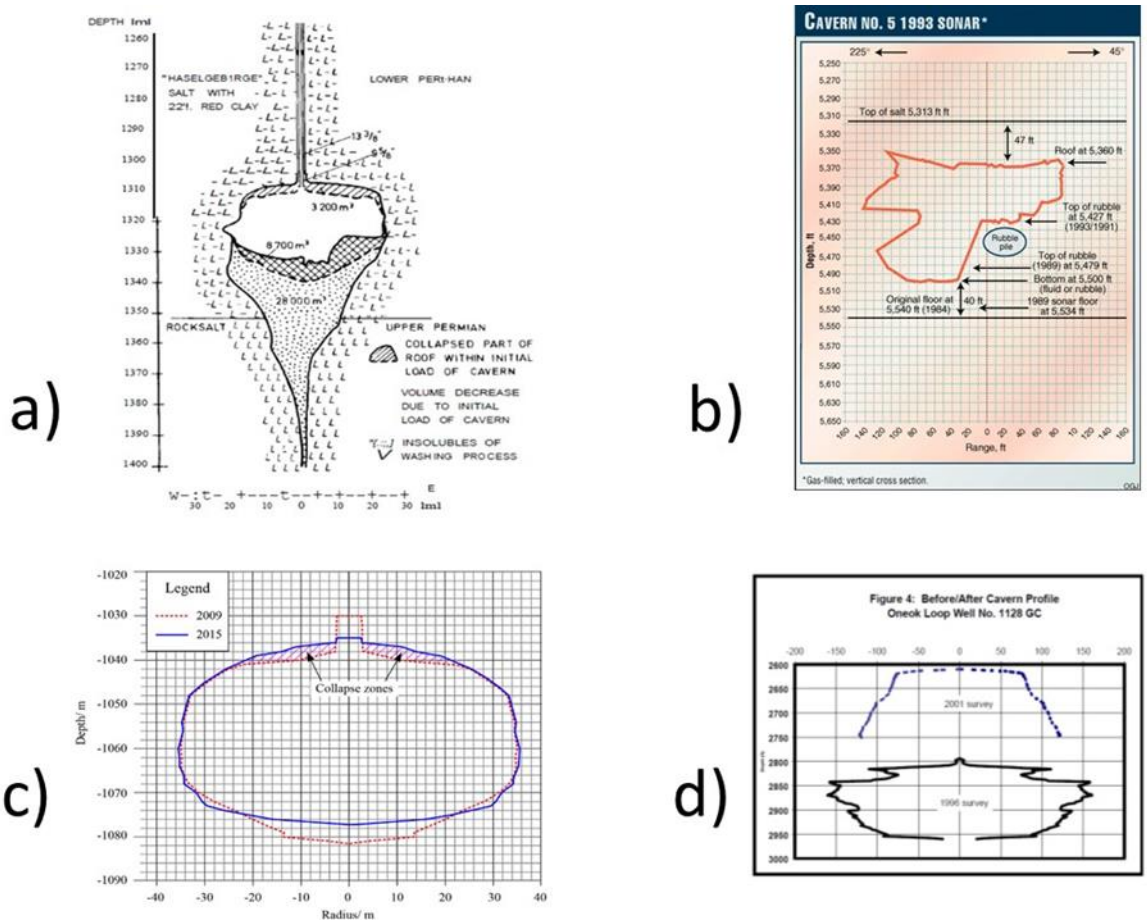

Figure 90. a. Kiel 101 (Baar, 1977; Rohr, 1974) b. Regina South No. 5 (Crossley, 1998, 1996) (Crossley, 1996 et 1998) ; c. Jintan JK-A (Wang et al., 2018); d. Oneok No. 1128 (Istvan et al., 1997; Johnson, 2003).

3.4.5.1.1 Kiel K 101, Germany

This case was described by Dreyer (1978), Röhr (1974) and Baar (1977). Cavern Kiel 101 (Figure 91) had been leached out between 1305 m and 1400 m, Röhr, (1974). The horizontal line (at a depth of 1352 m) corresponds to the limit between the Lower Permian (above) composed of ''*Haselgebirge*'' salt, containing 22 % red clay, and the Upper Permian (below), which is purer. The high insoluble content in the Lower Permian had resulted in a high sump at the cavern bottom. The leached-out volume was 68 000 m^3, the sump volume was 28 000 m^3, and only 60 % (39,600 m^3) of the leached-out volume was available for gas storage. Kiel K 101 was one of the first gas-storage caverns in Europe. It had been

decided, before de-brining the cavern, to lower cavern pressure using an immerged pump in order to investigate cavern behaviour at low internal pressure. Cavern pressure during the test results from the brine/air (or water/air) interface height above the pump. A sonar survey was run before cavern decompression. The first pump lowered in the wellbore was revealed to be under-dimensioned. When a certain depth was reached, cavern creep closure was so fast that the pump was no longer able to lower interface depth: the creep closure rate equalled the pumping rate. On January 11, 1967, cavern pressure was lowered from 156 bars at casing-shoe depth to practically zero through a more powerful pump.

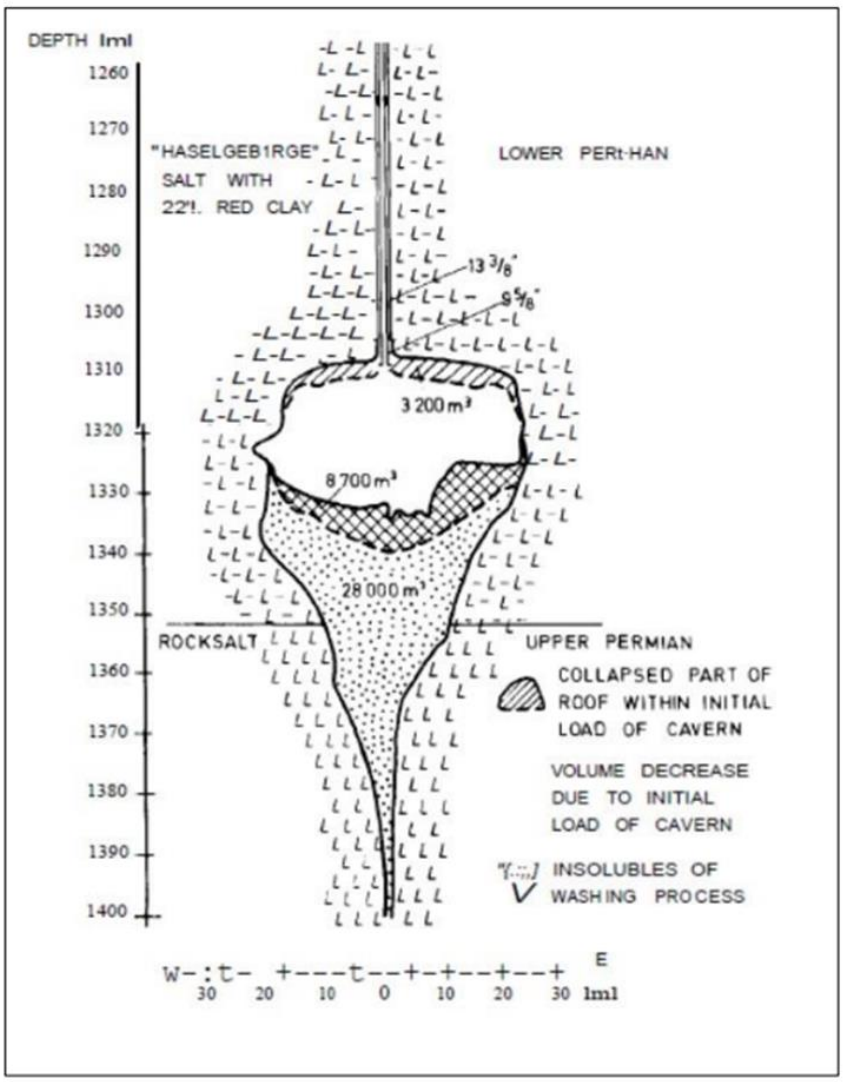

Figure 91. Kiel K 101 Cavern vertical cross-section before and after the first depressurization test (Rohr, 1974, p. 94).

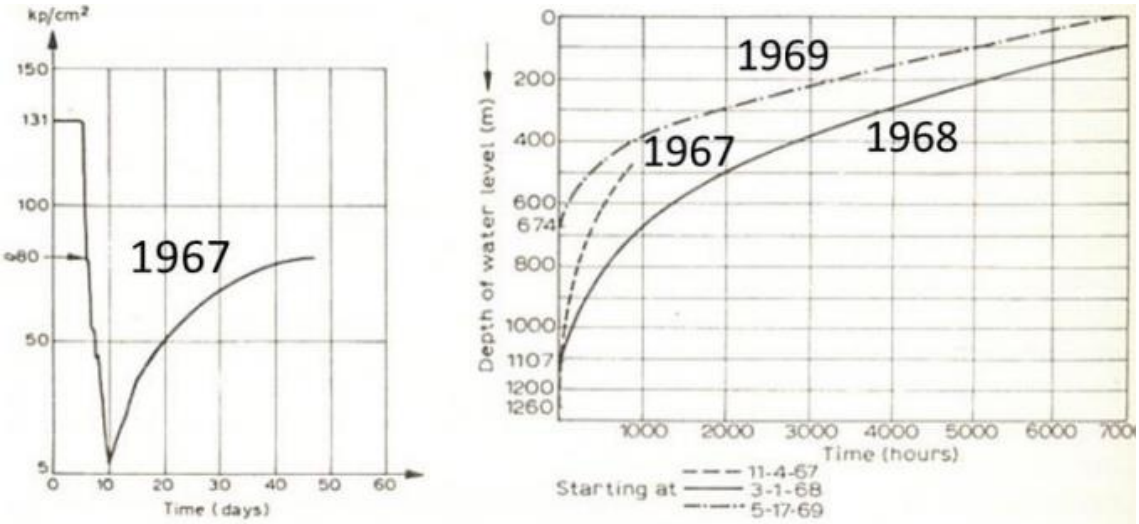

Fig. 4-10. Internal pressure at the roof of the Kiel 101 cavern. (After Dreyer, 1972.)
Pressure drop due to dewatering of the access well. Initial depths of cavern top and bottom approximately 1305 m and 1400 m, respectively; maximum diameter about 40 m. The lower part of the cavern was filled with insoluble residues; the vertical diameter of the brine-filled cavern is given as about 30 m.

Fig. 4-11. Rise of brine levels, Kiel 101 cavern. (After Röhr, 1974.)
Brine levels in the access well were lowered at the indicated times to the indicated levels. The curves reflect the cavern closure due to stress relief rather than "cavern loading".

Figure 92. Pressure evolution in the K 101 cavern during the three depressurization tests (right) and during the first depressurization test (left) (after Baar, 1977, p. 148).

It can be observed that, when pumping stops, the air/brine interface rises, and the rise rate decreases with time (Figure 92). Rate decrease results, on one hand, from the transient character of creep closure (Creep closure rate would decrease even if interface depth remained constant.) and, on the other hand, from the increase in cavern pressure due to interface rise. The test was repeated twice, on March 1st, 1968, and May 17, 1969 (Figure 92, right). The 1969 test is not directly comparable to the two first tests (smaller initial cavern-pressure drop). However, it seems that, during the three consecutive tests, transient closure rates are smaller and smaller. After the 1967 pressure drop, the roof fell, and the volume indicated by the sonar had decreased from 36,600 m^3 to 32,100 m^3, a volume loss of 18.5 % (11 % when the overall volume of the cavern is considered, see Figure 91). Note that the apparent volume loss is the sum of the actual cavern-creep closure and the volume increase ("bulking") of the salt blocks that fell from the roof to the bottom of the cavern. An additional volume loss of 1900 m^3 was observed five months later, when the third sonar survey was run. A 3-m-thick layer at the cavern roof fell immediately or, more precisely, before the second sonar survey run 45 days after the decompression began (or 900 hours after the decompression ended) according to that seen in Figure 92 (Baar, 1977, Figure 4-10). Among the factors explaining this massive roof fall are: presence of a relatively large roof span and a somewhat flat roof, and heterogeneity of the salt formation (especially at the cavern roof). In the K 101 cavern case, however, the magnitude (and rate) of the pressure drop must be highlighted: more than 2 MPa/day during six consecutive days. At the end of cavern decompression, the gap between geostatic pressure P_∞ and cavern pressure$P$at casing shoe depth was $P_\infty - P = 313$ bar (Rohr, 1974), a considerable value. During such a fast pressure drop, theoretical considerations show that the rock mass at the vicinity of cavern walls experiences a response that is mainly elastic: high deviatoric stresses develop at the cavern walls. Later, these deviatoric stresses slowly decrease at the cavern wall, because of the viscoplastic redistribution of stresses in the rock mass. For this reason, the first cavern pressure drop is critical for cavern structural integrity. In addition, in the particular case of a flat roof (The Kiel 101 roof can be said

to be somewhat flat.), the drop in cavern pressure generates high additional horizontal stresses. When, above the roof, the salt formation is interlayered, and the tensile and shear strengths at the interface between layers are low, failure is highly likely. Although no description of the salt formation above cavern roof is available, it is known that the insoluble content in the clayey Lower Permian salt was high, see Figure 91. It must be mentioned that, in contrast to the case of a gas-filled cavern, a rapid brine-pressure drop results in a very slow temperature drop (0.03 °C/MPa) and thermal stresses at the cavern wall are not large enough to contribute to roof failure.

3.4.5.1.2 Regina South No. 4 and No. 5, Saskatchewan, Canada

This case was described by Crossley (1998, 1996) and was mentioned in Réveillère et al.'s (2017) report for the SMRI. Two massive roof falls occurred in the natural-gas storage at Regina South (Saskatchewan, Canada) in caverns No. 5, Figure 92 (and No. 4, Figure 93) after the fifth (respectively, fourth) year of operation. Yearly pressure cycles were applied. These two falls led to gas seepage to non-salt overlying layers.

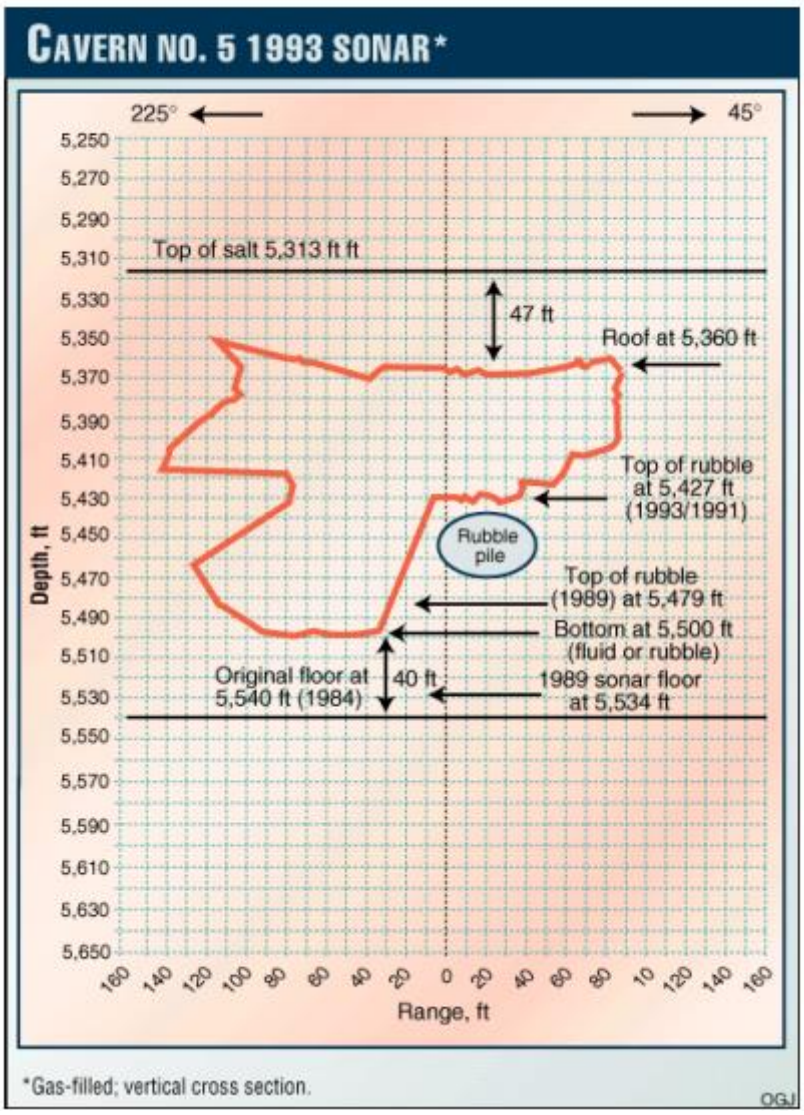

Figure 93. Cavern No. 5 vertical cross-section after the second roof fall (Crossley, 1998, Fig. 3).

At the time of these incidents, TransGas Ltd operated 24 caverns in the Prairie Evaporite formation, a bedded salt formation of the Elk Point evaporitic basin in western Canada. Cavern development occurs

3,000-5,000 ft [900-1500 m] below surface with 2,000-4,000 psig [140 – 280 bar] wellhead pressures. Usual salt thickness varies 300-500 ft [90 -165 m]. A single cavern is typically designed for a spatial volume of around 900,000 bbls [150 000 m^3] or a usable gas volume of 800 MMcf [23 million Nm^3] with withdrawal rates of 40-200 MMcfd [1 to 5 million Nm^3 /day].

3.4.5.1.2.1 Incident in Cavern No. 5

At Regina South Gas Storage Cavern No. 5, "Cavern washing […] started in April 1983 and was completed in August 1984. Cavern debrining (first gas filling) was completed in December 1984". The final spatial volume was 706,000-736,000 bbls (112 000-117 000 m^3), depending on the calculation method. "The cavern had a somewhat irregular shape: more than 300 ft [90 m] wide at the bottom and 70-80 ft [21-24 m] high before the cavern diameter came back to a more reasonable diameter of around 100 ft [30 m] with the smallest section of around 20 ft at the final roof location. The cavern roof depth was 5,363 ft [1636 m]. The maximum cavern height was 180 ft [55 m]. The floor salt thickness was 102 ft [31 m], while the roof salt thickness was 50 ft [15 m]. Several unmined insoluble ledges and fingers were left jutting into the cavern void space in the top half to one-third of the cavern … The maximum allowable wellhead pressure was set at 3,000 psig [210 bar] with a usable gas storage volume of 900 MMcf. The minimum wellhead pressure was 600 psig." [41 bar, a low value]. The cavern was cycled once a year. [Note that maximum wellhead pressure (3,000 psi) is a low value for a cavern whose roof is 1636 m (5,363 ft.) deep — i.e., a gradient at the cavern roof of 3000 psi/5363 ft. = 0.56 psi/ft. (0.127 bar/m); generally speaking, a typical maximum admissible gradient is 0.8 psi/ft. (Bérest et al., 2015). "The final developed roof position was higher than originally planned and located in a structurally unstable area with many thin insoluble bands which threatened future stability. In July 1989, a 267 psig [18 bar] pressure drop occurred in this cavern following gas fill up to 3,000 psig [207 bar]. A rate of change in pressure decline from the pressure-vs-time graphs used to monitor cavern operating condition suggested the cavern roof had a leak away from the well bore [A block fall generates no perennial cavern pressure change when the cavern remains tight after the fall.] In September 1989, the cavern was gamma ray/neutron logged. An 8-16 ft [2.4-4.8 m] roof fall was indicated at the well bore area, and 60 ft [18 m] of new material lay in the cavern bottom, suggesting possible side-wall ledge falls. […] Special logs were run to check for gas loss (accumulation) above the cavern roof; no presence of hydrocarbons was found. The 7-in. production-casing-cement bond appeared sound at the roof. In November 1989, a special gas-sonar survey was run by French Well Surveys Inc., Houston, in a dry (gas-filled) cavern environment. The sonar indicated that a massive roof fall of 27 ft [8.1 m] had occurred over a radial distance of 90-100 ft [27-30 m] and that a 65-80 ft [20-24 m] pyramidal rubble pile lay on the cavern bottom. The roof salt thickness was then only 31 ft [9.2 m]." Such a large pressure drop is remarkable. Gases are compressible: a very large leak is needed for pressure to drop significantly. Roughly speaking, the lost mass is 267/3000, or 9 %, of the total gas inventory. This is possible only when the leak opens in a porous and permeable layer (a "receptor" in the terminology of Bérest et al. (2019c) and Section 2) whose pressure is significantly lower than cavern pressure. In October 1991 another salt collapse was identified, although there had been no noticeable cavern operating problems from 1989 to 1992. Logging at 2,300-2,400 psig [15.8-16.6 MPa] found the rubble pile 60 ft [18 m] higher than identified in 1989 which meant there was now a total of approximately 120 ft [36 m] of rubble in the bottom of this cavern. The cavern roof showed no change, still registering 30 ft [10 m] of salt at the well bore. TransGas concluded that "the roof fall likely occurred in early 1991 when the cavern was cycled down to low pressure and an abnormal pressure rise was observed, most likely the result of fluid re-entry." Highly pressurized gas accumulated in the porous and permeable non-salt layer above cavern roof. When cavern pressure drops, gas flows back swiftly to the cavern, possibly leading to further damage of the porous medium at cavern roof. "In May 1993, the cavern spatial volume was recalculated and found to be reduced to 400 000 bbls [65 000 m^3] or more, or a 45 % loss of space from the original volume". This loss of space is due to the combined effect of creep closure and fallen blocks bulking. "In June 1993, a second special dry-gas sonar was run at 2,250 psig [155 bar] wellhead pressure by Sonar wire to identify the new roof shape [Figure 92]The sonar tool looked down along the

slope of the rubble pile to the bottom. The height of the rubble pile was confirmed at 120 ft [36 m]. The cavern floor may have come up by 40 ft [12 m] from the original floor position. No major change in roof position was recorded. Although the roof had sagged 10 ft [3 m] since 1989, there still should have been a minimum of 31 ft [9.4 m] of salt above the cavern roof. The southern half of the roof area [left side of Fig. 19] was not well defined on the sonar. It could not be determined, therefore, whether any salt was left there or if the roof breached up into the overlying formation. At present, it appears the entire upper portion of the cavern roof and sidewall areas have changed significantly from the original brine sonar in 1984 and the gas-sonar survey in 1989. The cavern roof area is fairly flat and approximately 230 ft [70 m] wide. Since 1989, this cavern has been used only sparingly and is still classified as "emergency use only." The exact location 170 of the cavern leak point is still unknown. The maximum operating pressure was further reduced to the 2,250 psig [155 bar] level to curtail the risk of additional possible gas loss".

3.4.5.1.2.2 Incident in Cavern No. 4

Quotations found in this section, are taken from Crossley (1998). "*Cavern washing began in January 1976, was completed in October 1979, and the cavern was used for partial gas storage during 1978-1979 […] Following cavern development in 1979, the final spatial volume was calculated at 916,906 bbls [*150 000 m^3*], based on brine-displacement metering during gas injection". "The widest section of the cavern was 208 ft [*63.4 m*] and the maximum cavern height was 197 ft [60 m]. The cavern roof depth was 5,349 ft [1631 m] with the floor at 5,546 ft [*1692 m*]. The roof salt back thickness was 15-32 ft [*<u>4.6-9.8 m</u>*] (gamma ray-neutron log vs. sonar survey at well bore location), while the floor salt thickness was 102 ft [31 m]. At 20 ft [*6 m*] below the roof, the cavern walls necked-in to about 62 ft [*19 m*] in diameter because of an insoluble layer. The maximum allowable wellhead pressure was set at 3,200 psig [220 bar]. [The cavern roof was 5349 ft. deep, and the gradient there was 0.6 psi/ft, a low value.] with a usable gas-storage volume of 1,100 MMcf [31 million Nm^3] […] the minimum wellhead pressure was 600 psig [40 bar]"* [0.11 psi/ft, a very small minimum gradient] A temperature logging at a low-pressure level of 800 psig [*55 bar*] wellhead indicated that the inner casing string was damaged in the mid-cavern area. This was the first indication that a cavern roof fall had probably occurred during the 1992-93 production season. There was a rapid pressure drawdown in February 1993. A gamma-ray/neutron log confirmed the roof fall and indicated that the cavern roof position may have risen by 23 ft [*7 m*] or a 23 ft [*7 m*] roof fall had occurred. This meant that now no salt remained above the roof of the cavern. The cavern roof was up by 6 ft [1.8 m] into the overlying carbonates and anhydrites of the Red Beds formation and just below the Dawson Bay limestone and dolomites formation. It was believed the Red Beds would provide an effective seal to natural gas if it remained undisturbed. Drill stem tests on the Dawson Bay formation indicated it to have low permeability. The low cavern pressure experienced was greater than the minimum established pressure for cavern stability concerns (0.15 psi/1 ft of depth to the top of the cavern roof). A review of the cavern salt core data from the Regina caverns indicated that the current cavern roof position was located in competent rock that is neither porous nor fluid-bearing. There should be no concern of gas loss through the cavern roof in the cavern's current status. A decision was made to run a special gas sonar survey to determine the condition of the cavern roof and general cavern condition to verify the future suitability of this cavern to hold and store gas. In May 1993, the inner casing was cut off in mid-cavern with a chemical cutter. The cavern floor was also tagged and subsequently indicated that the cavern bottom had 40 ft [*12 m*] of additional material. In May 1996, SonarWire successfully ran a special gas sonar survey tool under wellhead pressure conditions of 2,080 psig [*143 bar*]. There was approximately 3 ft [1 m] of viscous mud and approximately 7.5-8.5 ft [*2-3 m*] of fluid on the cavern bottom [Figure 94] *…The 1996 sonar indicated that there must have been 31-40 ft [*9.5-12 m*] of roof salt fall which occurred in 1993 and possibly up to 50 ft [*15 m*] of roof fall on the south side. This was more than originally determined from well bore logging. The new cavern roof was actually up into the overlying rock of the Red Beds by approximately 14 ft [*4.5 m] *and up approximately 24 ft [*7.3 m*] on the south side […]".*

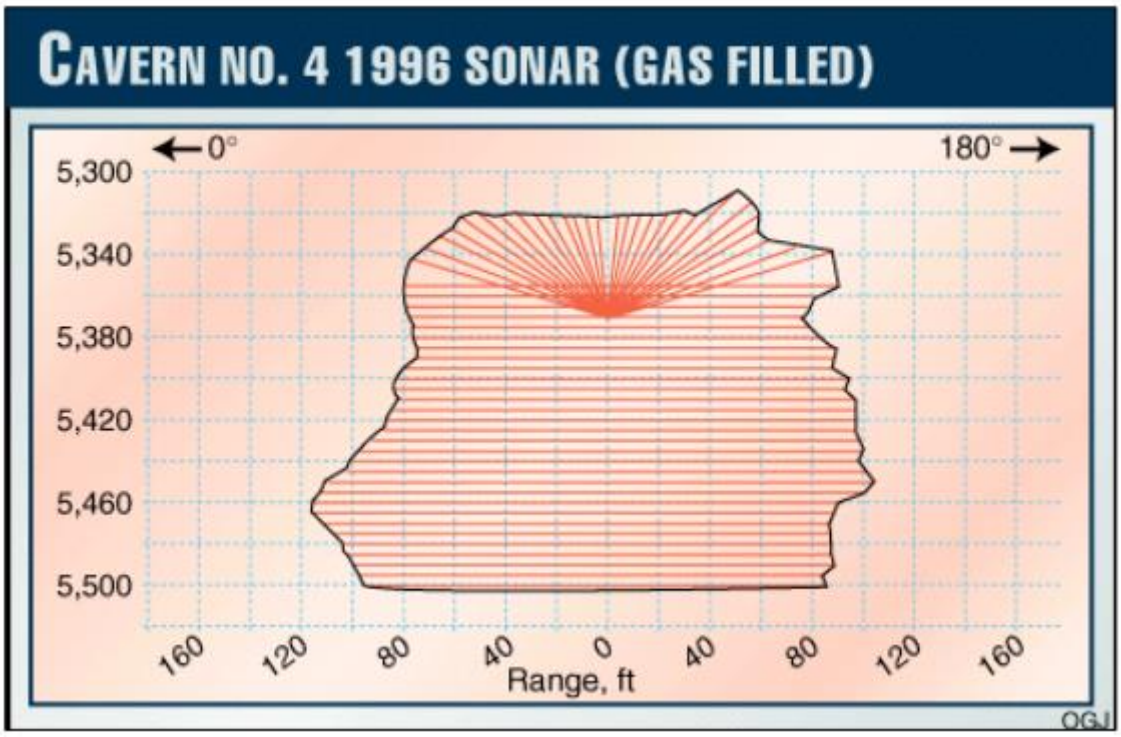

Figure 94. Cavern No. 4 vertical cross-section: the brine-gas interface is 5500 ft. (1677 m) deep (Crossley, 1998).

In these two gas storage caverns, which were more than 5300 ft (1600 m) deep, minimum pressures were quite low. It is tempting to infer that the creep-closure rate was fast; however, there was not much salt available above or beneath the cavern. Salt blocks fell. At least in the case of Cavern No. 5, the cavern roof had been set too high, in a zone in which the insoluble content was high.

3.4.5.1.3 Jintan JK-A, China

As noted by Wang et al. (2018), the first natural gas cavern in China, JK-A, in Jintan, Jiangsu province, was de-brined in November 2010. In several respects (long leaching period, low maximum-admissible gas pressure), this cavern is experimental, and operations were prudent. The July 2009 sonar survey (Figure 95), run after leaching was completed, shows a 116 000 m^3 cavern, with a diameter of 80 m and a height of 40 m. The cavern span is large (50 m), but the roof is not perfectly flat. Salt roof, chimney top and cavern roof depths are 978 m, 1032 m, and 1040 m, respectively. The last casing shoe depth is 1016 m. The sonar survey profile reveals "many overhanging blocks at the wall" (p. 60). In fact, these overhangs are not clearly visible on Figure 95, perhaps because the left-hand illustration in Figure 95 does not focus on the NW part of the cavern in which a significant number of ledges can be seen. In fact, this bedded salt formation contains many "interlayers with high insoluble contents", composed of poorly soluble anhydrite, clayey dolomite, and glauberite. The numerical model described below, takes into account four such layers, with depths and thicknesses of (a) 1036 m and 2.1 m, (b) 1050 m and 3.2 m, (c) 1059 m and 2.5 m (d) 1076 m and 2.8 m, respectively. The most significant layer, for what follows, is the first layer: 2.1-m thick, whose bottom is 2 m above the cavern top.

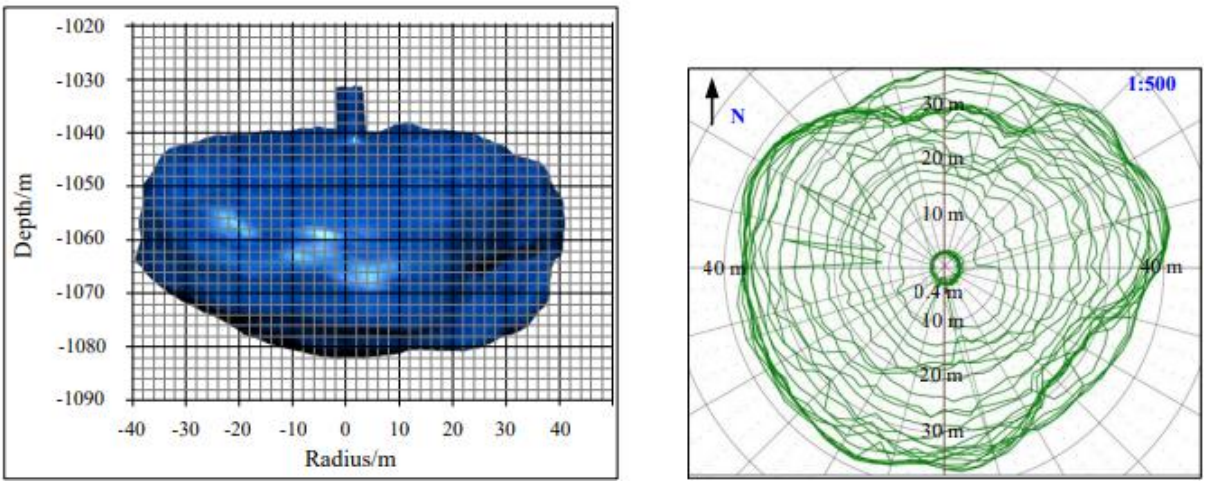

Figure 95. Shape and dimensions of JK-A obtained by the July 2009 sonar survey (Wang et al., 2018, p. 60).

The first gas injection was in November 2010. In principle, minimum and maximum pressures were 70 bars and 158 bars or, when divided by cavern-shoe depth, 0.069 bar/m and 0.156 bar/m (As measured pressures seem to be higher, Figure 96). Maximum gas flowrate was 1.25 million Nm^3/day. Comparison of a 2015 sonar survey to the 2009 survey displays a "notable collapse" (see Figure 97). The cavern volume was still 116 000 m^3, and the volume of the collapsed zone is 3300 m^3. A part of the roof, 50 m in diameter, with a thickness of 2-4 m, fell to the cavern bottom. It included the salt roof and at least a part of the insoluble interlayer.

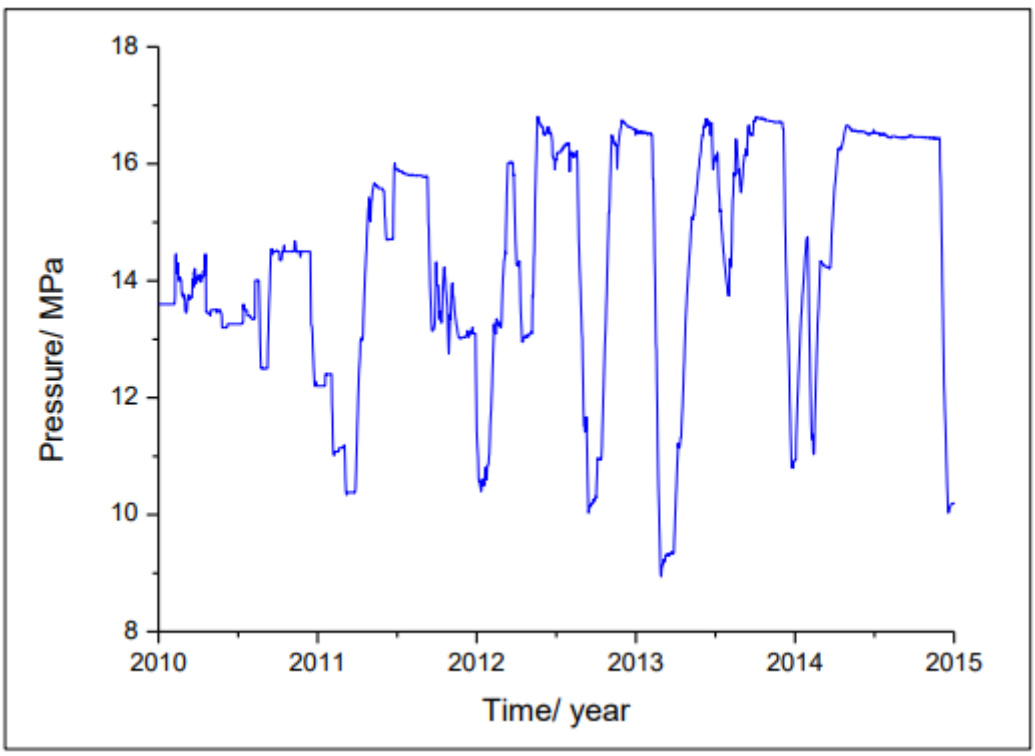

Figure 96. As-measured gas pressure from 2010 to 2015 (Wang et al., 2018, p. 61).

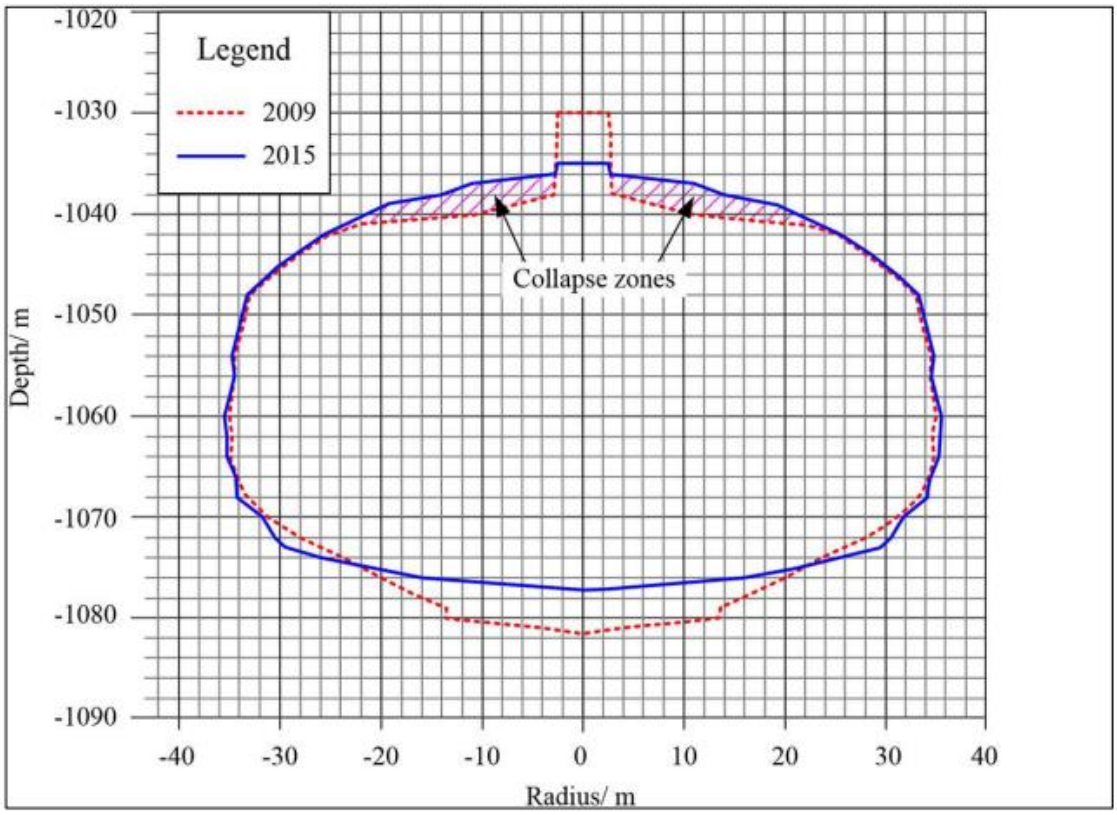

Figure 97. Average profiles of JK-A, 2009 and 2015 sonar surveys (Wang et al., 2018).

Cavern bottom heave was 5 m and the additional insoluble volume at cavern bottom was 3900 m^3. The cavern volume increase at cavern roof was 3300 m^3. These two figures are consistent: the difference can be attributed to bulking, for instance. The authors mention that creep closure was exceedingly slow. More puzzling, cavern volume increased by 3200 m^3. In fact, the 2009 sonar was run immediately after leaching stopped, when the brine was not yet saturated fully (it was 280 g/l, see Wang et al., 2018), and additional dissolution took place.

The authors performed numerical computations using FLAC (Itasca Consulting Group, Inc.) A Norton-Hoff law was selected, and low-creep salt parameters were chosen. Gas pressure history, if slightly smoothed, is taken into account fully. The roof interlayer is described as a "*weak*" material, whose elastic modulus is low. Computation results are compared to five criteria: volume loss, walls displacement, vertical stress, equivalent strain, and dilatancy safety factor (SF). The dilatancy safety factor, also called FOS (van Sambeek et al., 1993), is defined as $FOS = \frac{|I_1|}{0.27\sqrt{J_2}}$ where I_1 is the computed first invariant of the stress tensor and $\sqrt{J_2} = \frac{s_{ij}s_{ji}}{2}$, $s_{ij} = \sigma_{ij} - \frac{\sigma_{kk}\delta_{ij}}{3}$ is the computed deviatoric stress at a given point (see Paragraph 3.1.2.1 for a definition.) The safety margin (to dilatancy onset) is larger when *FOS* is larger than 1. Figure 98 shows that *FOS*, which is larger than 1 before the cavern is operated, decreases and reaches critical values, especially at the cavern roof, occurring in seven instances marked as T1–T7 on Figure 98 that coincided with the lowest pressure periods. The dilatant zone then is widespread, and SF is smaller than 0.6, a low value. Analysis of vertical stresses evolution is consistent with this result. Cavern-wall displacements are small, less than 5 cm at the cavern bottom, as are cavern volume loss and equivalent strain. With regard to strains and displacements, cavern evolution is benign.

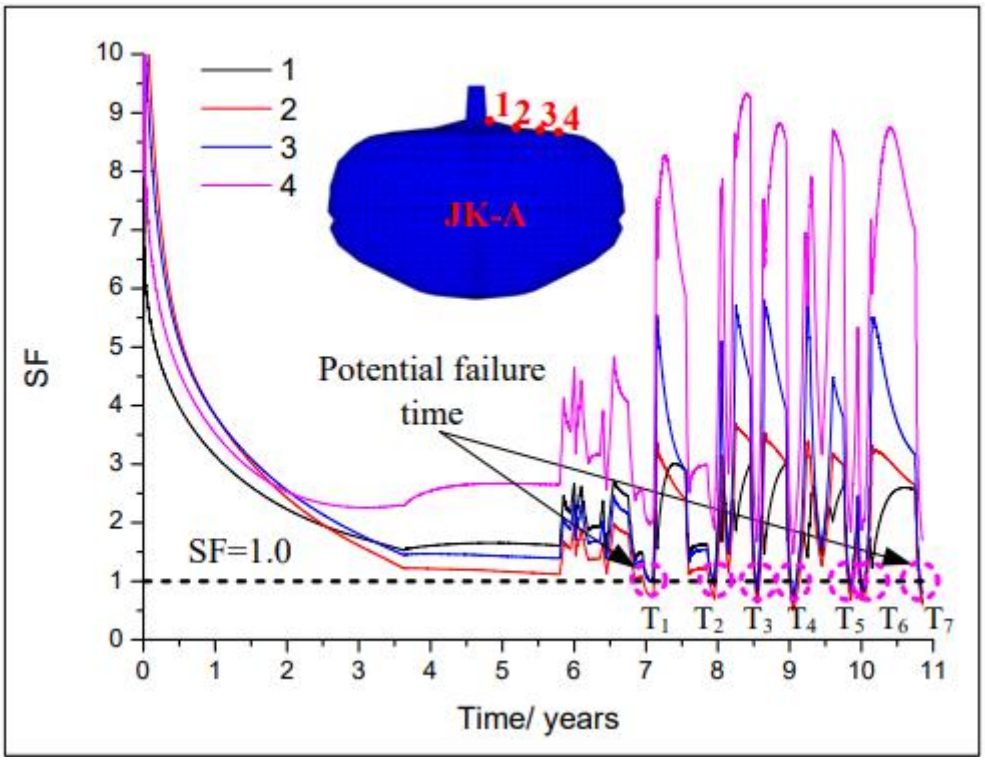

Figure 98. Evolution of the dilatancy factor (SF or FOS) at four points of the cavern roof (Wang et al., 2018, p. 64).

The authors try to infer from computational results the instant when the roof fell. They spot a period (T1) during which pressure dropped from 158 bars to 104 bars in 18 days. They conclude that the main factors explaining roof fall include:

1) a rapid pressure drop,
2) low final value of the pressure at the end of the drop,
3) a flat roof, and
4) the presence of the interlayer immediately above cavern roof.

It can be hypothesized that the thin (2 m) large-span (50 m) salt layer at the cavern roof, poorly bound to the softer overlying interlayer, experienced bending, and buckling-like failure. The role of the interlayer is likely to be decisive.

3.4.5.1.4 Oneok (Loop) 1128 GC, Gaines County, Texas

As described by Johnson (2003), the LOOP Facility was developed in Gaines County, West Texas: ''*The site was permitted in 1992 and gas storage operations commenced in 1993. There are three storage caverns at the site, all initially completed in a similar manner. Each of the caverns was initially developed within the Salado formation from approximately 2800 to 3000 ft. Each well was completed similarly with 13$^{3/8}$" casing set to a depth of approximately 2700 ft]" (p. 2).* During the summer of 2001*,''[I]t was determined that the newest of the three caverns (Well No. 1128 GC) had experienced […] sometime during its five years of gas storage service […] cavern roof migration of approximately 200 ft [60 m] and the loss of the last 80 ft of cemented casing*" (Johnson (2003, p. 3), see Figure 99 and Figure 100). "*Because this cavern is situated approximately midway between the two other caverns, it was feared that additional subsidence caused inacceptable deformation of the cavern casings. It was agreed with the regulatory body that subsidence be monitored, and that a new Mechanical Integrity Test (MIT) and a casing-inspection log be performed. The inspection log showed that the 13-3/8'' casing had not been damaged above the level from where it parted*" (Johnson, 2003, p. 6). Istvan et al. (1997) provide additional details in a paper

written after the roof collapse. With regard to cavern tightness, they mention "*sophisticated mechanical properties logging of the well"* (p. 2.), which determined that the average fracture gradient was 0.65 psi/ft (a very low value) and that a test lasting a few hours at a 1.25 psi/ft gradient performed before brining showed "*no obvious leakage*" (Istvan et al., 1997, p. 2).

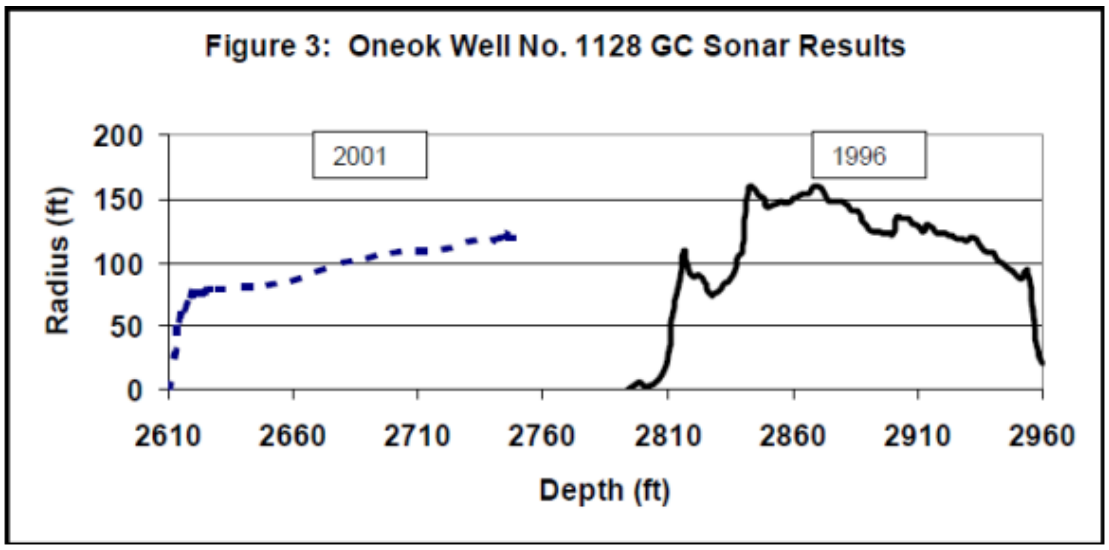

Figure 99. Average radius of Oneok Well No. 1128 as a function of depth (Johnson, 2003).

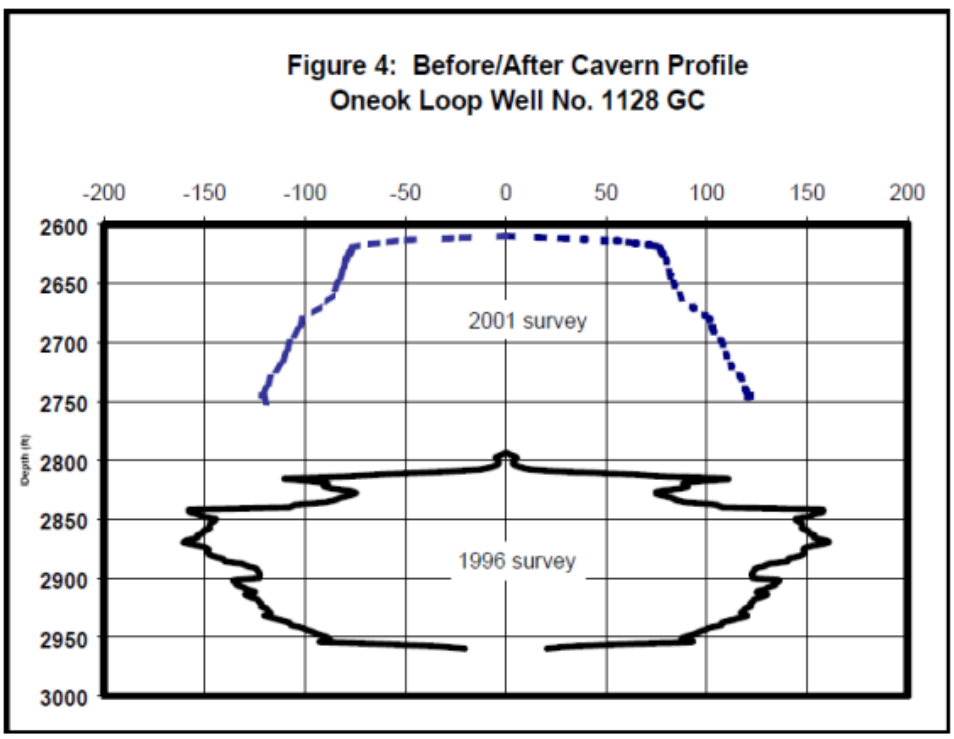

Figure 100. Oneok Well No. 1128 vertical cross-sections in 1996 and 2001 (Johnson, 2003).

Four core runs were made: at 2680 ft., 12 ft. (were recovered; at 2715 ft., 60 ft. were recovered; at 3100 ft., 49 ft. were recovered); and immediately below the third core, 60 ft. (18 m) were recovered. How these depths were selected is not explained. "*Virtually all salt in the cored interval contains impurities. Impurities consist, on the basis of visual observation, to be anhydrite and red clay. The anhydrite is either dispersed throughout the salt core or occurs in thin beds, which are not continuous across the area. Anhydrite was also observed in moderately thick (about 1.5 ft horizontal beds with inclusions of salt.)*

Anhydrite is moderately abundant near the base of core 3. Mud is dispersed throughout a portion of the salt core and alternates with the salt." (Istvan et al., 1997, p. 2). Brazilian tests, UCS tests and creep tests were performed on samples cut from core 2 (5 samples), core 3 (6 samples) and core 4 (13 samples). Tensile strengths were usual; UCS values were scattered, from 850 psi (5.9 MPa) to 3565 psi (24.6 MPa); lower values were associated with a higher insoluble amount. Three creep tests (with axial stress of 30 MPa (4350 psi) and confining pressure of 15 MPa (2175 psi) were performed, one of them ending after 20 minutes, as strains became too large; the other two lasted 20 days, with axial and lateral cumulated strains being larger and smaller, respectively, than "*comparable creep strains from other areas*" (Istvan et al., 1997, p. 5).

3.4.5.2 Lessons drawn

3.4.5.2.1 Roof falls and cavern pressure

It must be reminded that monitoring cavern shape (by sonar survey, brine-gas interface or sump tagging) is not a continuous process. When a roof fall is observed, it is difficult to know exactly when the fall took place (during a pressure drop or at the end? Or several days or weeks later?). Theoretical arguments suggest that roof fall is more likely to occur when cavern pressure is low and, more specifically, during a fast and large pressure drop. Minimum gas pressure was low at Regina South No. 4 and No. 5. [Minimum pressure at the cavern roof was P_{min} = 600 psig (41 bar), and roof depth was 5363 ft. (1636 m, or $P_\infty = 360$ bar; P_∞ is the geostatic pressure at cavern-roof depth when a geostatic gradient of 0.22 bar/m is assumed). At Jintan JK-A, P bar, $_{min}$ and the roof depth was 1040 m ($P_\infty = 230$ bar); at Oneok Well No. 1128 GC, P_{min} is unknown, and the roof depth was 2800 ft. (854 m, or $P_\infty = 190$ bar). Kiel K 101 was filled with brine during the depressurization tests: the minimum pressure was practically zero (Figure 92 suggests it was 0.5 MPa.), and the roof depth was 1305 m ($P_\infty = 290$ bar). Pressure rate was fast during the first depressurization at K 101 (more than 20 bar/day, or 360 psi/day, according to Fig. 13), and a roof fall was established after the sonar survey conducted 45 days later. In the case of Regina South No. 5, a 267 psig (18.5 bar) pressure drop occurred following a gas fill to 3000 psig (The cavern had been debrined in December 1984), and a roof fall was tagged in September 1989. It is difficult to infer from these data when the roof fall occurred. (It may have been long before the pressure drop). In the case of Jintan JK-A, a sonar survey was run in 2015, five years after de-brining. Wang et al. (2018) used an imaginative method, based on numerical computations, to predict when the fall took place; they suggest that this was during or at the end of a pressure drop from 158 bars to 104 bars over 18 days. At Oneok Well No. 11128 GC, Johnson (2003) simply states that "*Well No. 1128 GC … had experienced … sometime during its five years of gas storage service … cavern roof migration of 200 ft [*60 m*]*" (p. 3). In other words, the cavern roof seems to be more prone to fall when cavern pressure is low — especially after a fast and large pressure drop. (However, this does not seem to be true in the case of the Regina South No. 5 Cavern). For this reason, gas caverns are especially prone to roof fall. However, even if this assertion is consistent with what is known from salt behaviour and failure, definite proof is scarce.

3.4.5.2.2 Roof falls and large-span roof

Roof span seems to be an important factor in the occurrence of roof falls. In the four examples, it must be noted that cavern roof was somewhat flat; its span was relatively large (more than 50 meters). (Here, again, Regina South No. 5 Cavern is an exception.) However, at West Hackberry, Louisiana, in Cavern 6, used for oil storage, the roof diameter was 1200 ft (360 m), the largest among all the examples mentioned in this chapter, and it never failed. This might be due to the fact that this cavern never experienced very low pressures; in addition, the salt formation seems to be fairly homogeneous. It should be mentioned that caverns shape is important when assessing stability: in a cavern with a domal-shaped roof, stresses are distributed in a manner that is favourable for roof stability. Conversely, a flat roof is unfavourable. In principle, cavern size plays no role (except that the probability of crossing heterogeneities of the salt formation is higher in a larger cavern).

3.4.5.2.3 Roof fall and interstratified roof

A third ingredient with regard to roof fall is decisive: roof falls occur when, above the cavern roof, a horizontal layer (or horizontal layers) can be found whose mechanical properties strongly contrast with salt properties: a weak layer, or a thin stiff layer, or a layer having an elastic modulus very different from that of salt.

3.4.5.2.4 Conclusion

In summary, known examples prove that roof falls occur: in large-spanned, flat-roofed caverns; when interlayers can be found above the roof; and when cavern minimal pressure is small. These three ingredients seem to be mandatory.

3.4.6 Case histories (tensile effective stress)

Visco-plastic behaviour of the rock mass – as opposed to elastic behaviour – generates a couple of specific failure modes. Possible effects of an abrupt pressure increase are an example of this. During a Pressure Observation Test in a brine-filled cavern, brine is injected during a short period in a cavern to increase its pressure to the maximum operating pressure. Further evolution of the pressure is monitored. In principle, a fast pressure decrease is a clear sign of a leak. Consider for instance an idealized spherical cavern. Principal stresses are $\sigma_{rr}, \sigma_{\theta\theta} = \sigma_{\varphi\varphi}; S = \sigma_{rr} - \sigma_{\theta\theta}$ is the "deviator", $|S| = \sqrt{3J_2}$. At cavern wall, the radial stress is the opposite of the cavern pressure; $\sigma_{rr}(a) = -P_c$. It is assumed that cavern pressure, or P_c^-, had been kept constant during a long period of time before the test. Steady state was reached before the test,

$$S^{ss-}(r) = \left(\frac{a_0}{r}\right)^{\frac{3}{n}} \frac{3(P_\infty - P_c^-)}{2n} \tag{38}$$

At *t* = 0, cavern pressure is increased abruptly to P_c^+, $P_c^- < P_c^+ < P_\infty$, P_∞ is the geostatic pressure at cavern depth. The deviator experiences a jump to:

$$S^+(r) = \left(\frac{a_0}{r}\right)^{\frac{3}{n}} \frac{3(P_\infty - P_c^-)}{2n} + \left(\frac{a_0}{r}\right)^3 \frac{3(P_c^- - P_c^+)}{2} \tag{39}$$

And at cavern wall ($r = a_0$) the deviator is:

$$S^+(a_0) = -P_c^+ + \sigma_{\theta\theta}(a_0) = \frac{3}{2}\left[\frac{P_\infty - P_c^-}{n} + P_c^- - P_c^+\right] \tag{40}$$

And this quantity can be negative (the effective stress at cavern wall, or $-P_c^+ + \sigma_{\theta\theta}(a_0)$ is tensile), especially when the exponent of the power law (n) is high: there is a risk of hydro-fracturing and tightness loss, even when cavern pressure is smaller than geostatic pressure. This may explain why the apparent compressibility of a cavern increases significantly after a rapid pressure increase (Figure 101), as was shown by Djizanne et al. (2012) in the case of the Etzel K-102 Test (Rokahr et al., 2000).

Note that in a gas-filled cavern this effect is mitigated by the temperature increase which accompanies any fast pressure increase (in a brine-filled cavern, such a temperature increase also exists; in fact, it is very small). Temperature increase generates compressive tangential thermal stresses, as mentioned above. Numerical computations are needed to assess the overall resulting stresses.

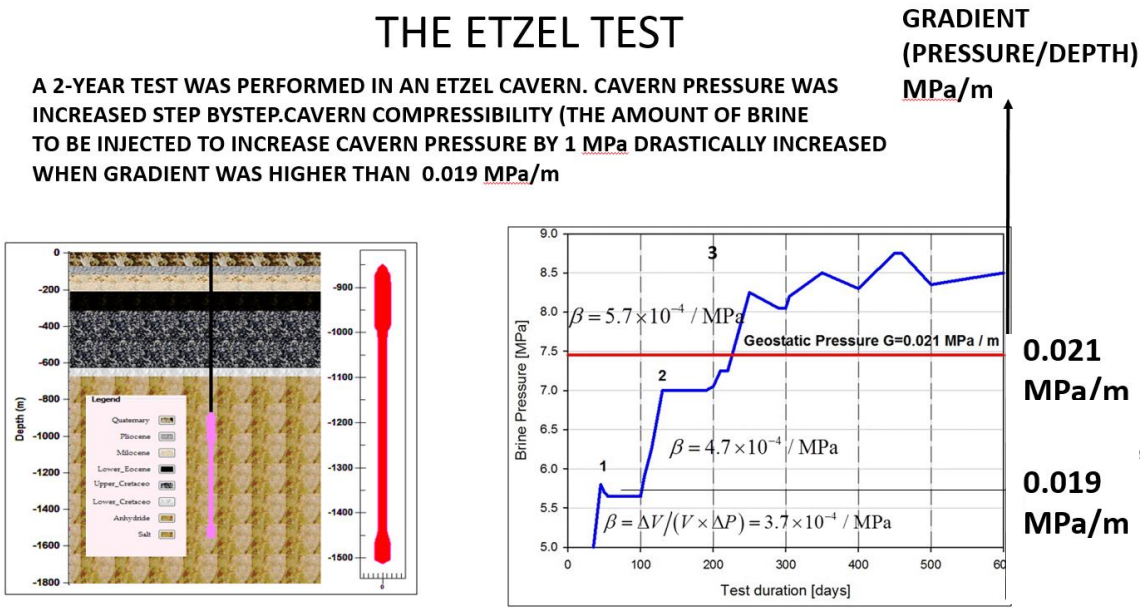

Figure 101. Pressure history during the Etzel K-102 test (After Rokahr et al., 2000).

3.4.7 Block Falls

Block fall from cavern walls is a mundane phenomenon. Evidence of block falls include frequently observed breaks or bending of the inner tubes hit by falling blocks and the observed accumulation of the blocks on the floor of a cavern. Such incidents are typically not reported in literature and belong to the routine operation of many salt caverns. In the following, only incidents that led to large volume displacements or incidents having uncommon mechanisms are reported. Four gas-storage examples and two oil-storage examples are described.

Cases located in Huntorf (Quast, 1983) and Jintan (Wang et al., 2017) are representative of ledge falls. A fall was documented at the Markham salt dome (Cole, 2002) that epitomized the combination of creep sluffing and bulking. Munson et al. (1998) paper emphasized the possible significance of the insoluble content on rock falls in the SPR caverns; however, Thoms and Neal paper (1992) and Munson et al. paper (2004), which described the SPR sites at the Bryan Mound and Big Hill salt domes, respectively, bring the role of anomalous zones in salt domes dome to light. The mechanism leading to block falls is diverse and often poorly understood.

3.4.7.1 Case histories

3.4.7.1.1 Lille-Torup

Rokahr et al. (2007) described a remarkable rock-mechanics test performed in a cavern of the Lille-Torup (Denmark) gas-storage facility. A depressurization test was performed on Cavern TO6. The idea of the test was to reduce the internal pressure of cavern TO6 to $P_c = 60$ bar at a reference depth of 1460 m, see Figure 102, and ''*to observe the cavern convergence as well as to check the stability of the cavern wall. This was planned to be realized by two [*high precision*] sonar surveys [*run in the specific test interval: 1458-1462 m*], the first at the beginning of the test, before pressure was released to 60 bar, and the second at the end of the test, after 30 days at an internal cavern pressure of 60 bar*" (p. 3). As-measured wellhead pressures, computed pressures at reference depth (1460 m) and temperature during the test are represented on Figure 102, right. Cavern pressure decreased from 210 bars (a pressure gradient of 210 bar/1460 m = 0.18 bar/m) to 60 bars (a pressure gradient of 0.041 bar/m.) in three months and four steps. After each withdrawal step, gas temperature decreases significantly (by 15 °C during the last depressurization) before slowly increasing when no gas is injected. The two high-precision sonar surveys were run on January 16, 2005 (blue, or black line), when gas pressure was 14 MPa and on March 31, 2005

(in green, or grey) after a 1-month period at minimum pressure. For each sonar survey, five 360° scans were performed for redundancy; in principle, "every determined cavity volume is associated with a mean relative error of about 1 %. Measurements in oil and gas filled cavities have errors of the same order." (Denzau and Rudolph, 1997). At the end of the test a spall, 1000 to 2000 m^3 in volume, had fallen to cavern bottom. The spall was parallel to cavern wall (hence, it is likely that it did not originate in a heterogeneity of the rock mass). Formation of a spall was confirmed by a rise of the brine-gas interface at cavern bottom (obviously, cavern creep closure may also be influential in interface rise.) Two high-resolution (laser) sonar surveys were performed on January 16, 2005, and March 31, 2005, a period of time over which the cavern gas pressure dropped from $P_c = 140$ bar to $P_c = 60$ bar. The increase in cavern cross-section is clearly visible on Figure 103: *"The enlargement of the cavern in this sector is interpreted as a consequence of local failure of the rock salt at the cavern wall, that means that spalling had occurred locally."* (Rokahr et al., 2007, p. 137).

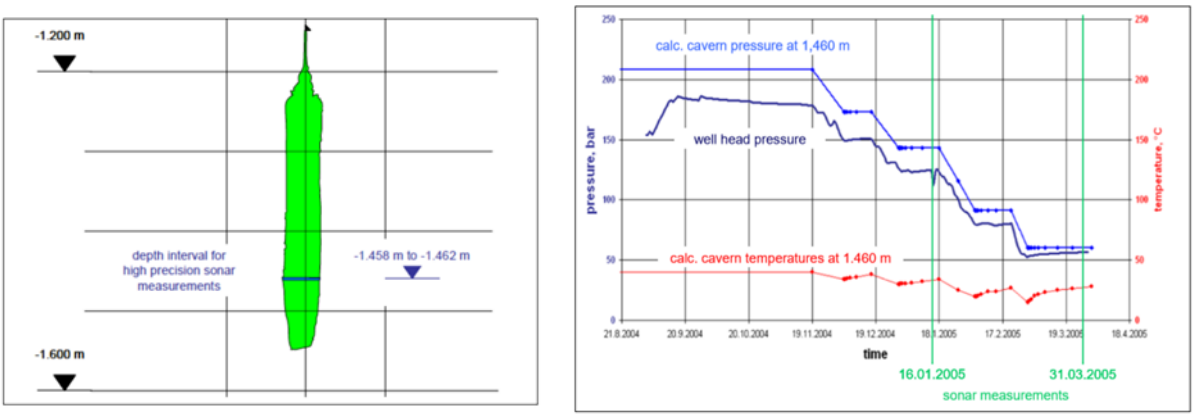

Figure 102. Vertical cross-section of TO6 cavern, indicating the high-resolution test interval (Rokahr et al., 2007).

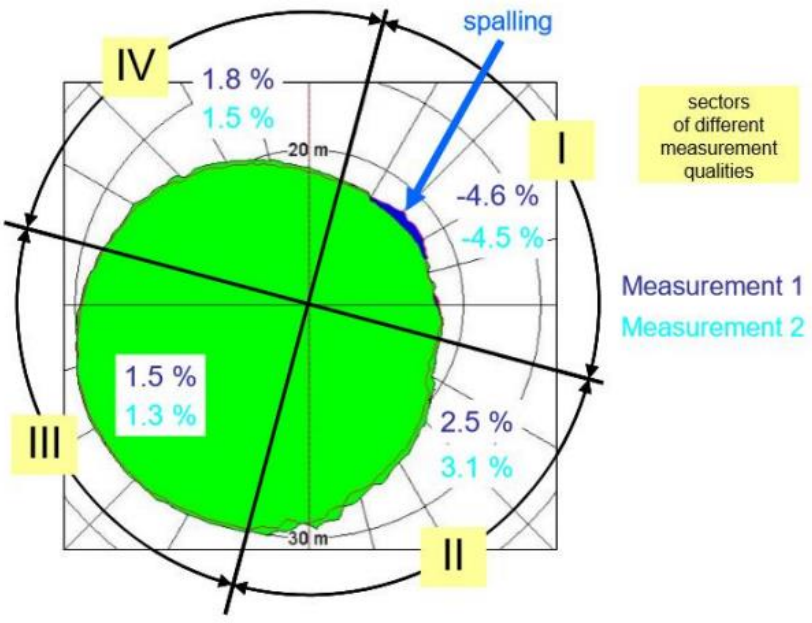

Figure 103. Test Results (Rokahr et al., 2007).

3.4.7.1.2 Huntorf, Germany

Crotogino et al. (2001) described "*more than 20 years of successful operation*" of the CAES storage facility at Huntorf (Germany). Two caverns with depths between 650 m ($P_\infty = 145$ bar) and 800 m, NK1 and

NK2, were operated. Air pressure varied between $P_c = 43$ bar and $P_c = 70$ bar. The fastest depressurization rate was 50 bar/hr. Between 1978 and 1986, there were 200 starts/yr (i.e., cycles/yr), and less than 100 starts/yr in the 1990s. Quast (1983) compared two vertical cross-sections of the NK1 cavern, which had been run in 1976 and in 1980, i.e., before and after the first gas injection (Figure 104). Salt "curtains", still present in 1976 when the cavern was filled with brine, broke, and fell to cavern bottom during the first gas injection (during which the cavern bottom rose by 16 m). Later, the depth of the brine-air interface remained almost constant, and Crotogino et al. (2001) state that "*evaluation over the whole operational period shows practically no changes that can be attributed to roof falls"* (p. 356). Djizanne et al. (2014a) suggested that salt curtains fall originated in the change in Archimedes' thrust when, during debrining, brine was substituted by gas, whose density is much lower.

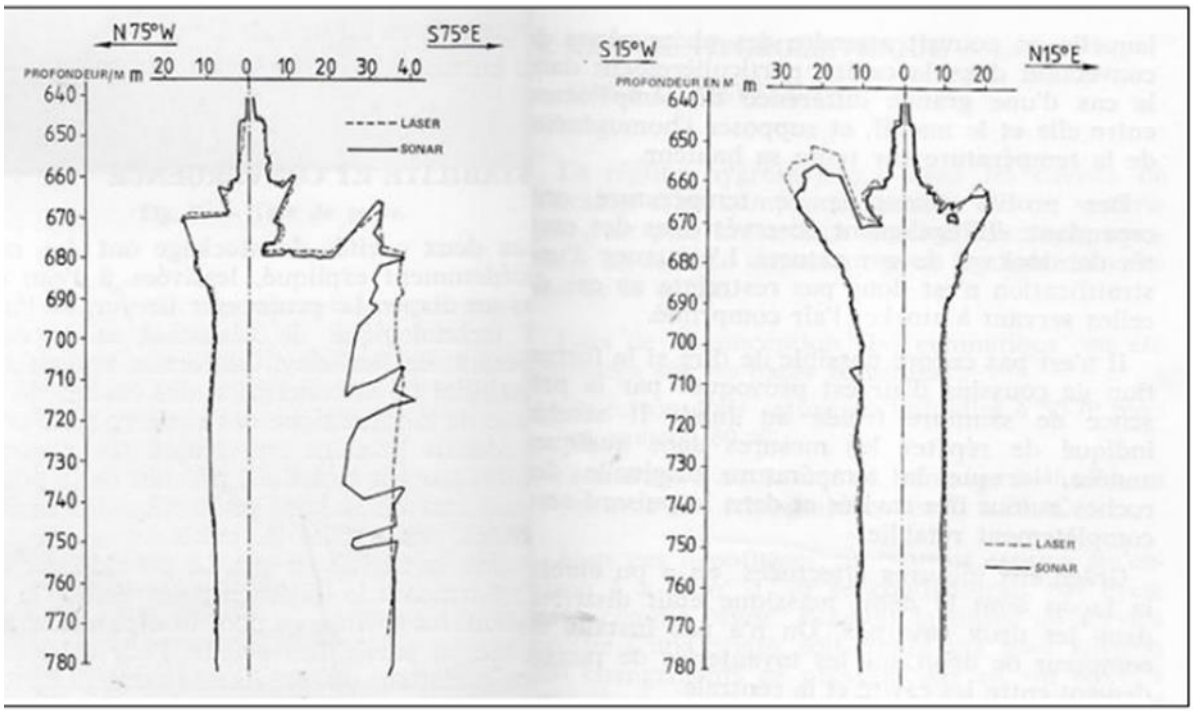

Figure 104. Two vertical cross-sections of Cavern NK1 from a 1976 brine sonar survey (dotted line) and a 1980 laser sonar survey (Quast, 1983).

3.4.7.1.3 Jintan JJKK-D cavern, China

Jintan bedded rock salt hosts the fourth salt section of the Tertiary Fu-Ning group (Wang et al., 2017). The salt body has an E-N strike with a length of 11.75 km and a width of 5.6 km; it shows bedded structure, or bed-like structure, with tens of rock salt and non-salt layers (Figure 105). The layers with the same property are continuous and have stable plane distribution with a dip of less than 10°. The total thickness of the core body is about 143-173 m. Solution mining of the JJKK-D cavern began on July 2, 2006, and was completed on September 12, 2011. A sonar survey performed on September 13, 2011, showed that the volume of the cavern was 214,358 m^3 (Figure 105). During solution mining, many irregular overhanging ledges (anhydrite, mudstone, and glauberite) form on the cavern wall. Even after long immersion in brine, these blocks are strong; however, they are not always stable and can break cavern strings when falling. De-brining started on June 21, 2013, and ended on September 20, 2014. A sonar survey was carried out on November 29, 2015. The cavern total volume was 217,801 m^3 (this increase is likely to be due complementary dissolution, see 3.4.5.1.3 Jintan JK-A, China). Between 2011 and 2015, few changes in cavern shape were observed, except at -1070 m, where spalling took place. Wang et al. (2017) suggest that changes in buoyancy (i.e., in Archimedes' thrust) applied to cantilever beam-like overhangs during de-brining might be responsible for their fall [an idea reminiscent of that by Djizanne et al. (2014a), about the Huntorf case].

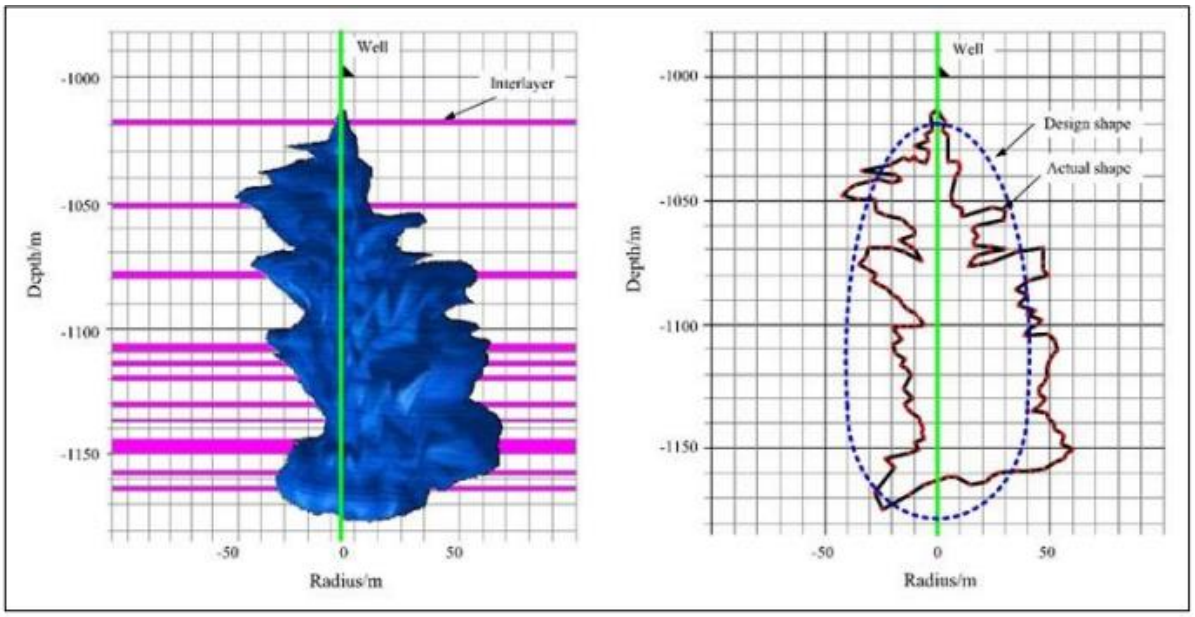

Figure 105. Vertical cross section of the Jintan JJKK-D cavern (Wang et al., 2017).

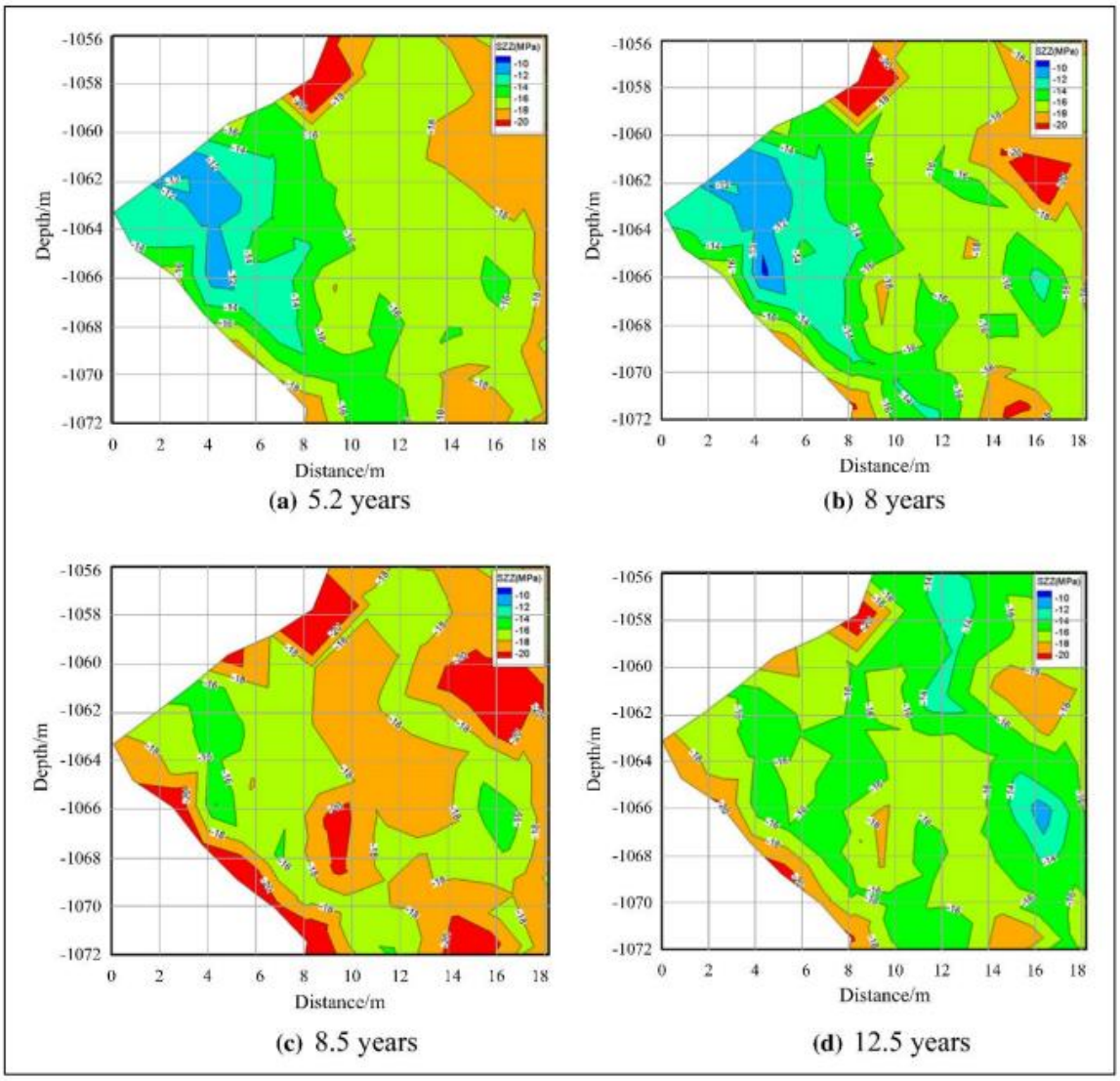

Figure 106. Contours of the vertical stress in the overhanging blocks at different times (Tensile stresses are negative?)

When interpreting computation results, emphasis is put on end of leaching (5.2 years), before and after debrining (8 and 8.5 years; pressure at the casing shoe is 120 bars) and after 4 years of operation (12.5 years). The authors discuss the evolution of five parameters: displacement, equivalent strain, vertical stress, safety factor (in the sense of Van Sambeek et al., (1993) and plastic zone (a variant of the safety factor) in the overhang at a 1070 m (3508 ft.) depth. The two first parameters are not fully relevant for a discussion of buoyancy weight influence (as they increase with time). Vertical stress evolution is considered a better stability indicator (see Figure 106). Vertical stresses are high and negative (tensile). [It is somewhat surprising that stresses are tensile and high in the whole ledge]. The authors suggest that tensile failure is likely.

3.4.7.1.4 A comment on Anomalous zones

"Anomalous zones" were mentioned in Munson et al. (1998) as a "possible second factor" considered in the evaluation of SPR block falls. In fact, heterogeneities in the salt formation were already mentioned as a possible explanation in the case of Huntorf (Section 3.4.7.1.2) or in the case of Markham (Section 3.4.7.1.7) and a definition is needed. Thoms and Neal (1992) note: *"The term "anomalous features" (AFs) has been used by Kupfer (1990) to designate unusual features found in the stocks of Gulf Coast salt domes. Based on observations made in rock- salt mines, he identified ten major groups of AFs, including such items as: intense structural folding, the presence of "impurities" (e.g., anhydrite, shales, and sandstones), gas releases, connate brine seeps, exceptionally large crystal size, potash, hydrocarbons, etc. He observed that these unusual features tended to cluster in linear trends through salt stocks; and, if they contained three or more AFs, [he] designated such trends as "anomalous zones (AZs)"* (Thoms and Neal, 1992, p. 1). Kupfer (1990) also noted that "shear zones" in salt stocks were often subsets of AZs. In Gulf Coast domal salt, three groups of AFs have been reported to impact caverns:

1) insolubles (anhydrite, shale, sandstone etc.);
2) gas releases (flows or outbursts of CH_4, CO_2 and, occasionally, H_2S); and
3) potash (sylvite and, more rarely, carnallite).

"The presence of insolubles was associated with occurrences of "salt falls" within caverns. The falls damaged "hanging strings" (tubing) used in solutioning and product withdrawal. The damage was caused by direct "hits" of falling blocks of insolubles, or indirectly by fluid pressure waves that tended to swing the hanging strings into the cavern walls. In any case, the tubing was damaged to the extent that it had to be replaced. [p.2] … Salt falls tend to occur more frequently in "dry" (no compensated) compressed natural gas (CNG) storage caverns during periods of low cavern pressures following rapid depressurization (drawdown)." (Thoms and Neal, 1992, p. 5). These notions also were explained by Looff (2017): "The concept of anomalous salt and BSZ [Boundary Shear Zone] was primarily developed by Kupfer and others from the 1950's based upon the experience of conventional mining operations in Gulf Coast salt domes. A brief discussion is provided below and more information in the context of salt caverns can be found in Looff et. al., (2010a and 2010b) […]" "Anomalous Salt: Salt quality and geomechanical properties can be expected to be degraded for anomalous salt and anomalous zones often making their occurrence problematic for drilling and cavern development and operations. Kupfer (1990) considered typical Gulf Coast salt to be reasonably pure halite (about 97 %), of uniform grainsize of about 3-10 mm in diameter and either massive (structureless) or banded white to grey. Anomalous salt is any salt that is considered to be atypical such as salt with significant entrained gas, brine, shale, anhydrite, potash, sand, etc.; sheared, brecciated, or faulted salt; coarse or fine-grained salt and voids in the salt. In its original form, this concept was applied only to Gulf Coast domal salt but has now been expanded to include other deformed salt structures, bedded salt and potash deposits (Warren, 2017). Major groups of anomalous salt include but are not limited to the following:

- Unusual colour - Generally not an issue except where this indicates problematic impurities or staining by fluid flow,
- K/MG salts - Highly soluble and creep prone salts that can result in planes of preferred dissolution or anomalous creep closure
- Coarse-grained salt or veins of pure recrystallized salt - May tend to be weaker or creep faster
- Sheared/Faulted/Dilated salt - Generally an indicator of weak and friable salt or differential salt movement - Increased potential for spalling and roof falls, loss of containment or potential leak zones, planes of preferred dissolution and potential for casing shear
- Voids and vugs - Indicates potential for highly soluble salts or active fluid flow within the salt
- Insoluble impurities - Distribution and type of insoluble impurities may influence strength and dissolution properties of the rock salt; increase potential for slabbing, irregular cavern shape, and roof falls; allow migration pathways for gas, liquid hydrocarbons, cavern product, and brine
- Hydrocarbons and gas - Contaminate product and an indicator of weak salt or permeable salt.

Anomalous Zones: An anomalous zone (AZ) is a non-genetic term used to describe a zone within the salt that can be hundreds to thousands of feet in length that contains three or more dissimilar anomalous salt features. These zones "*although highly variable, lenticular, and discontinuous in detail*" are "*commonly predictable in trend*" (Kupfer, 1990). Edge zones (EZ) and BSZ are specific cases of anomalous zones that have a genetic connotation. EZ occur at the edge of a diapir where there is increased strain and where non-salt entrained impurities can be encountered at the salt-sediment interface. BSZ occur between differentially moving salt spines. Higher geologic risk is attached to both EZ and BSZ as they also are likely to be areas of active shearing within the salt. EZ also have the added risk of uncertainty associated with locating the exact edge of salt. Salt domes generally move upward over time episodically as a series of salt spines. The salt tends to go through continuous cycles of deformation and recrystallization, with an overprinting of older zones. It is important to realize that the current internal salt characteristics and dome geometry are a mosaic of current geologic processes overprinted upon relict features. AZ and BSZ can be identified by analysing top of salt and caprock maps. Other useful information is derived from sonars, surface topography, well logs, core, and drilling records. Caprock maps are important as there are usually more caprock well penetrations (data points) and it is generally easier to identify top of caprock on electric logs, which are the primary source of data for mapping Gulf Coast salt domes. As previously mentioned, due to limited data availability or other factors, when making top of salt maps, there is a common tendency to smooth the contours and draw a "*bullseye*". However, these types of maps are not very useful for identifying BSZ. Mapping the details is important. Care must be taken to determine if such details are geologically meaningful or are the result of errors or inconsistencies in well locations, correlations, etc. Geologic Risk Associated with Anomalous Salt and Anomalous Zones: Zones of weak or porous salt:

- Cavern shape anomalies - trapped product - difficulty controlling leaching - difficulty maintaining buffers to the edge of salt, other caverns, property boundaries, etc.
- Increased potential for a migration pathway - product contamination (i.e., methane) - loss of integrity/product Impure salt
- Increased potential for roof falls and rock falls - cavern bottom moves up and loss of effective cavern volume - damage to hanging strings
- Shape anomalies like wings, attic space and preferred planes of dissolution − increased potential for degraded geomechanical properties
- Increased potential for anomalous creep characteristics such as differential salt movement
- Increased potential for casing shear or deformation (in salt, caprock or overburden)
- Increased potential for sheared, weak and porous salt that creeps at a higher rate
- Higher cavern closure rates − Increased potential for surface subsidence" (Looff, 2017, pp. 3–4).

There is no doubt that anomalous zones are closely related with a propensity to block falls, as the two following examples will describe. However, the precise mechanism explaining the onset of block falls in anomalous zones is unclear.

3.4.7.1.5 Bryan Mound

The case at Bryan Mound was described by Thoms and Neal in 1992 — i.e., before Munson et al.'s 1998 paper. Thoms and Neal summarized data gathered by interviewing operators of storage caverns in Gulf Coast salt domes. Thoms and Neal also selected the Bryan Mound dome located in Brazoria County, Texas, to illustrate effects of Anomalous Features (AFs) on storage caverns. Caverns 1 to 5, whose shapes are irregular, were leached out during Phase I. The dotted lines on Figure 107 represent trends of AFs based on features observed during Phase I cavern development and cores from Phase 2 wells. Insolubles, potash and gas noticed during drilling are denoted respectively by magenta-, gold-, and green-line segments within cavern circles in Figure 107. Falls, potash percentage in brine returns, and abundance of gas during and following cavern solutioning are denoted respectively by the stars, and by gold and green symbols on the right-outside of cavern circles. ''*[S]ignificant numbers of falls have occurred in some Bryan Mound caverns (e.g., seven in #106*). *Falls are probably due to a number of factors including: amount and distribution of insolubles, gas, and cavern solutioning technique. The "worst case" scenario for falls would include: concentrated insolubles at the tops of caverns, ongoing gas releases, and "parallel" cavern development from two or more wells. Concentrated insolubles would tend to break off in blocks and falls from high in the cavern would be more likely to damage hanging strings. Gas releases would tend to disaggregate salt and increase numbers of falls. The parallel development of caverns with multiple wells would result in vertical ridges of unconfined salt projecting from well intersections.*'' (Thoms and Neal, 1992). Cavern BM 106, in which seven falls were observed (before 1992), had two of the characteristics of the "worst case scenario" for falls: "spikes" of anhydrite were identified near the top of the cavern from the well logs. Three wells were used in the development of the cavern, and three vertical ridges of projecting salt can be seen in the #106 cavern sonar logs.

Cavern 1 appears to show irregular leaching angled upward toward the northeast (Neal et al., 1994) and numerous caverns show vertical channelling or grooves (Munson, 2008). Impurity content (distribution and type) may also influence both cavern shape and salt creep properties (Looff et al., 2010a, 2010b; Munson, 2008). While having a similar total insoluble content as other SPR facilities, Bryan Mound has a higher fraction of disseminated black shale as opposed to anhydrite (Munson, 2008). Two bands of sylvite have been found on the southwest side of the dome (Neal et al., 1994). At Bryan Mound, 10 caverns show marginal to excessive gas in oil ratios. Caverns 2, BM5, BM103, BM 111, BM 112, BM114 and BM116 have the highest historical gas intrusion rates (Neal et al., 1994). Of these caverns, BM 103 and BM112 also have a history of apparent salt falls and casing loss (Neal et al., 1994). It appears that anomalous salt and BSZ play a role. Frequency of salt falls has been related to proximity to anomalous salt and BSZ (Looff and Looff, 1998; Looff et al., 2010a; Neal et al., 1994) or shale content (Munson, 2008). Figure 108 shows the occurrence of salt falls and gas related to BSZ identified by Sobolik and Ehgartner (2009). There is a definite pattern; however, it is unclear if the trend is due more to BSZ or different salt spines. Slight adjustment of the BSZ shown in Figure 107 would place most of the salt fall activity and gas occurrence in BSZ. Looking at the salt contours, a case can be made for such adjustment. SPR Caverns, Louisiana and Texas Munson et al. (1998), describe hanging-string damage and pipe-loss events recorded prior to November 1997 at the 62 oil-storage caverns of the four SPR cavern facilities at Bryan Mound and Big Hill (Texas), and West Hackberry and Bayou Choctaw (Louisiana). They include 13 caverns (called Phase I caverns) purchased from developers, most of which are irregular in diameter, size and depth, and 49 caverns (Phases II and III) designed especially for the SPR Program, which are roughly cylindrical, 2000 ft. (600 m) high and 200 ft. (60 m) in diameter. Depths to cavern roofs are all about 2000 ft. (600 m). These caverns contain at least one hanging string, and they are typically in a quiescent condition, except during workovers, when a cavern is depressurized to accommodate damaged hanging strings. Hanging-string

damage is a primary “witness gage” (Munson, 1998, p. 11) of the amplitude and frequency of salt falls — a gauge that does not exist in many gas caverns, equipped with no hanging string. Prior to November 1997, more than 33,435 ft (10,200 m) of casings had been lost. From Figure 108, 71 events (and 54 string failures) were recorded. (While only event was recorded at Big Hill, significant events at Big Hill are described by Munson et al. (2004) in a later paper.) They are detected through the appearance of oil in the brine pond or by wireline logs. When a casing damage event (or loss) is identified, the string is pulled from the cavern. In many instances, distinct abrasions and indentations are observed, coupled with a general bending, suggesting impact and block fall. Ehgartner (1997) computed that a 1 × 5 × 5 ft^3 salt slab falling in a viscous oil media would attain a velocity of 40 miles/hr (18 m/s) within 150 ft (45 m) and 130 miles/hr (60 m/s) after 2000 ft (600 m), providing a substantial kinetic energy for string bending/failure.

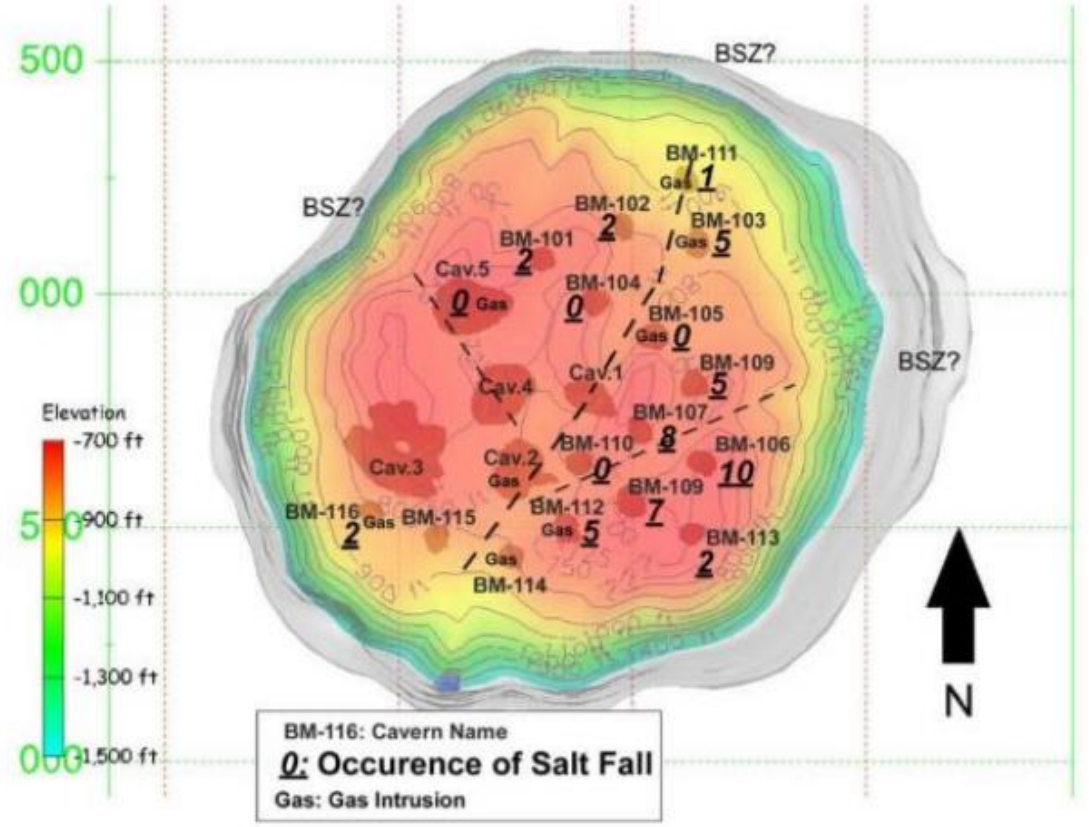

Figure 107. Top of salt map from Bryan Mound salt dome with inferred boundary shear zones and salt spines with cavern locations and occurrence of salt falls (Looff, 2017, p. 13; modified from Sobolik and Ehgartner, 2009; see also Thoms and Neal, 1992, p. 9).

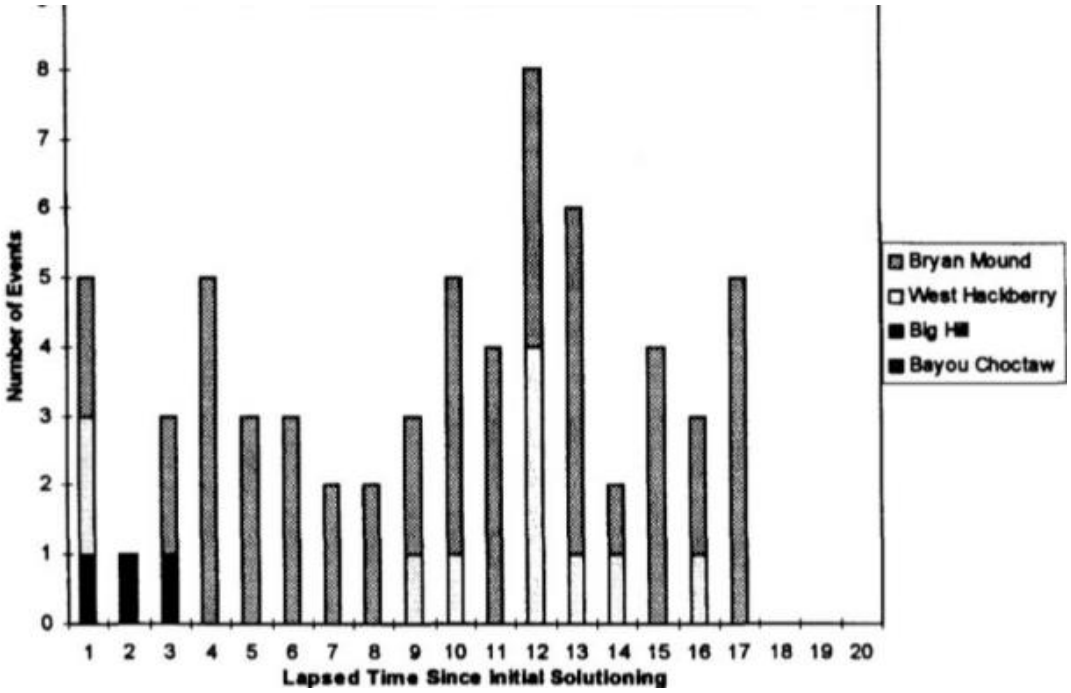

Figure 108. Distribution of Hanging-String Casing Damage and Loss Events in the SPR Caverns (Munson et al., 1998).

Munson et al. (1998) also listed various factors capable of causing damage (Table 5). Material fracture, as influenced by concentration of local impurities, was thought to explain higher propensity for events in some domes or caverns in a given dome. The greatest concentration of events is in the lower half for all sites (except for the single event observed at Big Hill). Munson et al. suggest that "generation of salt falls is a function of overburden depth" [p. 6; in fact, one may assume that the travel time needed to impact the vertical string can also be a factor]. The operator routinely obtains wireline surveys, including cavern-bottom tagging, which (together with sonar surveys) allow calculation of the volume of salt accumulation at the cavern bottom. A 55 % bulking factor (see Paragraph 3.4.4) was taken into account. In the case of Bryan Mound, an accumulation of 10,000 tons/yr. was computed. (Large uncertainty is possible.) A reasonable correlation between the amount of salt fall and casing-damage events can be observed. However, comparison between amounts of accumulation and the number of damaging impacts suggests that "the general spall size of any salt fall is quite small." (Munson et al., 1998, p. 7) .

Table 5. Major Factors Considered in Evaluation Process (Munson et al., 1998).

Factor	Condition	Application	Comments	Cause
Anomalous Zones	Natural	General	Possibly a secondary factor.	Secondary
Crude Type	Imposed	General	Possibly a secondary factor.	Secondary
Leaching Method	Imposed	Local	Linked to geometry irregularities.	Secondary
Operating Pressure	Imposed	Local	Linked to stress.	Secondary
Depressuring				
Cycling of Crude				
Location in Dome	Imposed	Local	Cavern spacing, dome edges.	Secondary
Cavern Depth	Imposed	Local	Linked to stress magnitude.	Secondary
Cavern Geometry	Imposed	Local	Roof span, geometry irregularities.	Secondary
Creep Properties	Natural	General/Local	Deformation processes.	Secondary
Fracture Properties	Natural	General/Local	Salt fracture, link to impurities.	Primary

Even if not very accurate (a factor of 2), local impurity content, which varies between cavern and facility sites, can be determined from solution-mining data (e.g., successive sonar survey, volume balance).

Munson et al. (1998) conclude that the primary factor for the propensity of salt falls is the creep and fracture response of the salt formation. They suggest a conceptual model, inspired from studies performed at the WIPP facility, such that the fracture criterion is highly dependent on the content of impurities. Numerical computations were performed in the case of a vertical 2100 ft. deep shaft; damage at the shaft walls was small, meaning that other factors that affect impurity content play a role: "[U]ndoubtly, the necessary additional feature is probably comparatively small geometric irregularities in the cavern wall […]" (p. 11), because stress concentration may occur there. This 1998 paper was the first attempt by Munson's group to identify the main factors responsible for block falls in SPR caverns. In a later paper, Munson emphasizes the significance of geological features, also mentioned in Thoms and Neal (1992).

3.4.7.1.6 Big Hill, Texas

Munson et al. (2004) examined a major block fall that occurred in Cavern 103, one of the 14 caverns of the SPR oil storage field at Big Hill, Texas. As mentioned above, these caverns, created during Phase II of the SPR Program, are of cylindrical shapes and have nearly the same dimensions: 200 ft (60 m) in diameter and 2000 ft (600 m) high. The *"cylinders taper slightly inward at the bottom to give a smaller diameter. The cavern roofs are nearly 600 ft [180 m] below top of salt, or about 2300 ft. [690 m] below ground surface. Consequently, the current cavern bottoms are at roughly a depth of 4300 ft [1300 m] below ground surface.*'' (Munson et al., 1998, p. 2). Because of their regular geometry, the caverns were thought to be quite stable. Only one identifiable event of damage to a brine hanging string, attributed to a salt fall, which had occurred previously in 1990 at the Big Hill site, in Cavern 114.

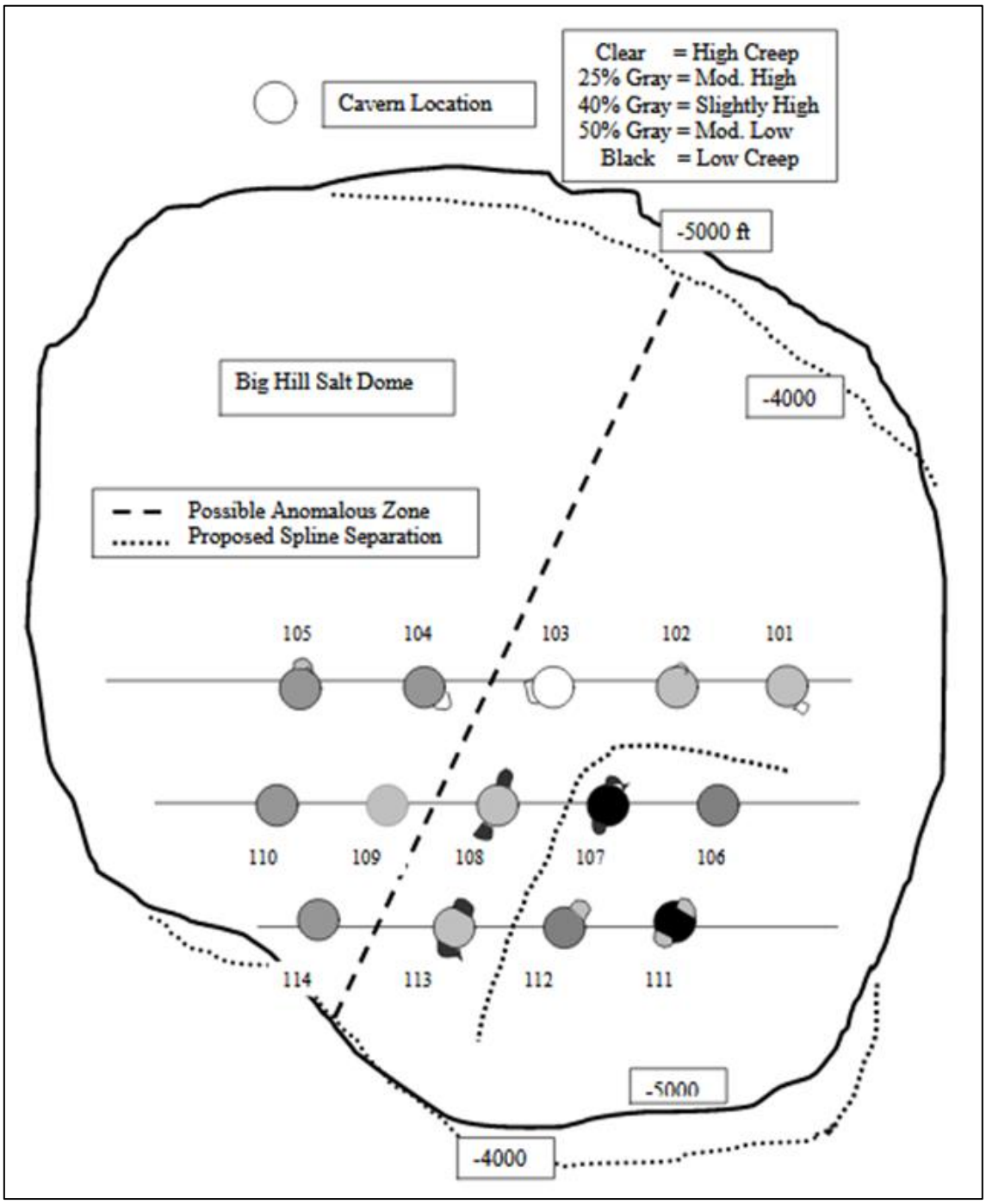

Figure 109. Schematic of Big Hill dome and SPR caverns with relative closure rates. The caverns are shaded according to their respective closure rates, where black = low rates and white = high rates. Leaching anomalies are also represented, and a division of the dome by salt splines is also illustrated (Munson et al., 2004). A more recent interpretation can be found in Looff (2017).

Cavern 103, a two-well cavern, is located near the centre of the Dome (Figure 109). Well B contains the hanging string. Well A does not contain a hanging string and is used for oil injection and withdrawal. Cavern roof and bottom depths are 2250 ft (685 m) and 4095 ft (1250 m), respectively, making cavern height 1845 ft (565 m). Cavern creation was completed in November 1990. During solution mining, the cavern floor rose because of the accumulation of insoluble fractions contained in the salt. After the mining was completed, during routine cavern operation, the floor continued to rise slowly because of the sloughing of salt from the cavern walls (the amount of insoluble fractions in the rock formation is 2.9 %). There was a gradual increase in floor elevation between January 1992 and May 2000 of about 7 ft (2 m), an accumulation of 212,000 ft^3 (7,800 m^3) of salt. On March 7, 2002, a wireline log showed a marked

increase (when compared to an earlier log on July 26) in floor elevation (Figure 110). After the March event, cavern bottom elevations increased markedly. A directional survey deduced that the bottom of the brine hanging string was displaced toward the southeast by nearly 30 ft (9 m). However, there was no evidence of damage to the hanging string. A study of the wellhead pressures (recorded every minute) showed no significant changes during this period [block falls generate pressure oscillations that typical have periods of 20 s — typically, too short to be detected (see Bérest et al., 2017)]. A sonar was conducted in an attempt to characterize the cavern geometry.

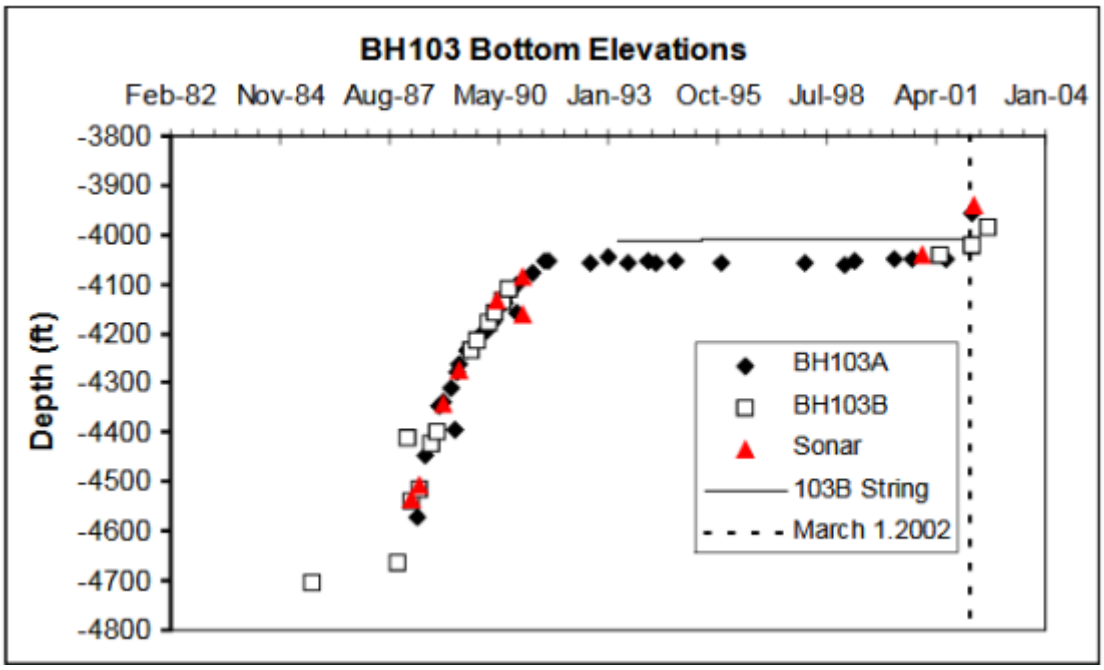

Figure 110. Depths of cavern 103 bottom (as seen by sonar surveys and tags) and depths of strings A and B shoes.

The March 2002 sonar (Figure 111) showed that the brine string was buried in debris from a salt fall event. In addition, debris from the fall also produced a marked upward slope in the cavern bottom toward the east, directly opposite from the wall that produced the salt fall. [A large amount of kinetic energy was needed.] The string bottom is buried ‘‘i*n perhaps as much as 100 feet of debris*” (Munson et al., 2004, p. 8). Comparison of 1990, 2000 and 2002 surveys provided additional information. Application of a three-dimensional graphics method (Rautman and Stein, 2003) yields grey-scale images of the sonar survey data and displays a resolution of features not possible with earlier graphical methods (Figure 112).

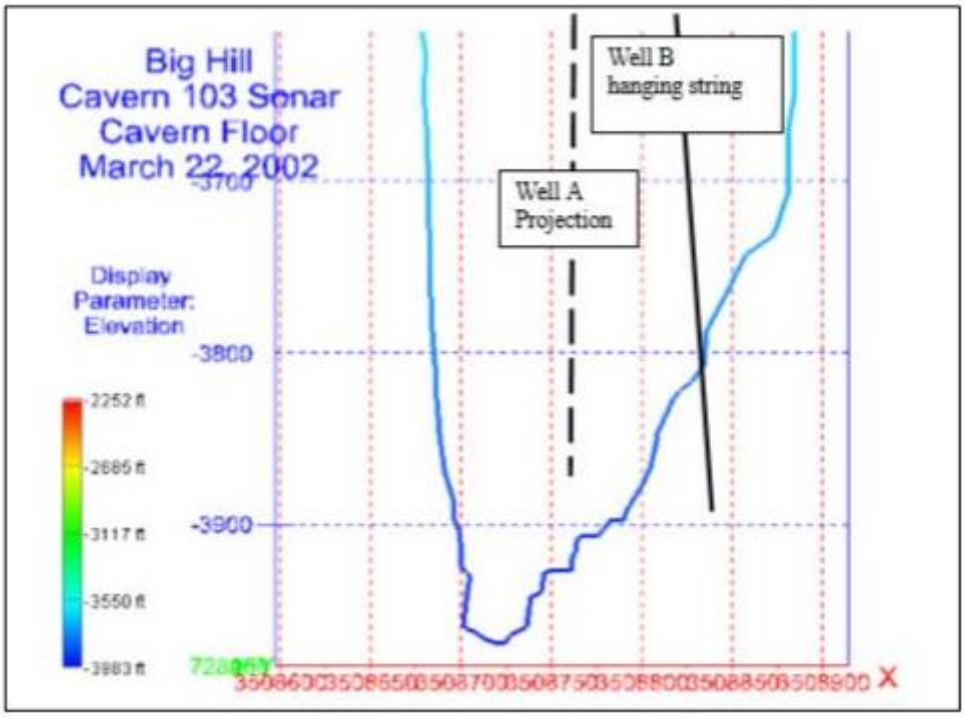

Figure 111. The Well B hanging string is buried in debris that accumulated on the east wall (Munson et al., 2004).

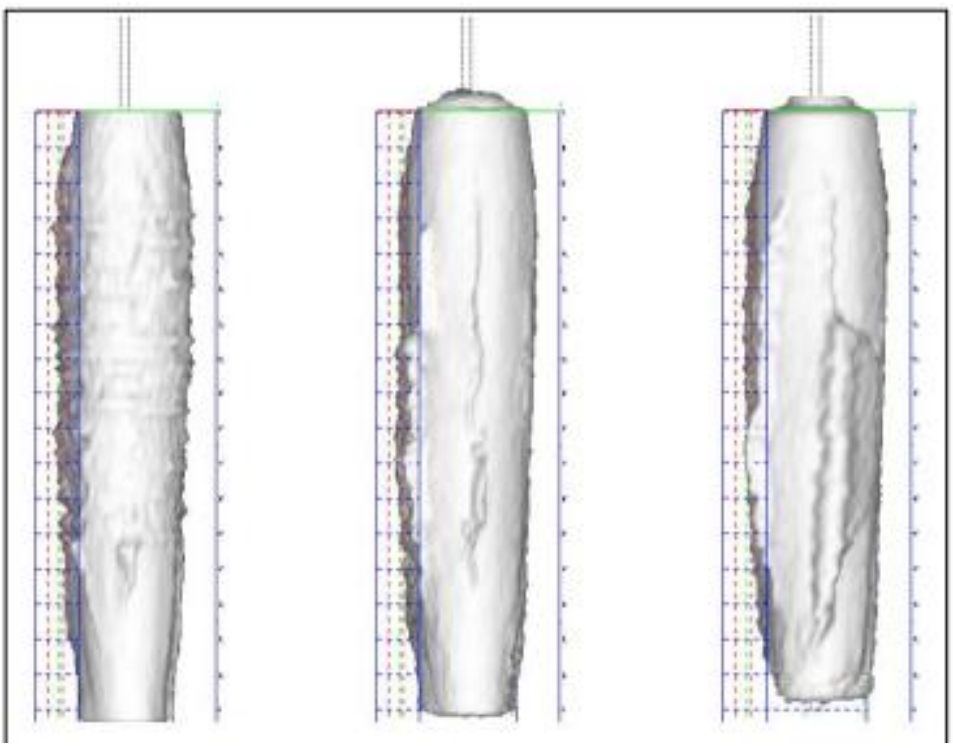

Figure 112. Comparison of the 1990, 2000 and 2002 views of Cavern 103 from the compass direction of 285°, showing evolution of a feature initially located at a depth of 1300 ft. below the cavern roof (Scale: 100 ft. Vertical and 50 ft. Horizontal). From Munson et al., (2004, p. 7).

In 1990 (Figure 112, left), a feature appeared at a vertical cavern depth (below the cavern roof) of 1300 ft. (400 m); it was 100 ft (30 m) in length and in the form of a wedge with the apex pointed downward, suggesting a salt fall. In 2000 (Figure 112, centre), this initial indentation had extended vertically more than 250 ft (75 m), and a linear groove now extended upward nearly 400 ft (120 m) from the top of the

indentation. The orientation of the groove is N75°W. In 2002 (Figure 112, right), it was apparent that ''*a large volume of material that once was in the cavern wall fell to the cavern bottom''* (Munson et al., 2004, p. 8). The feature had grown to almost 1000 ft (300 m) in height, becoming about 30 ft (9 m) wide and 57 ft (17 m) thick. The angular extent of the void is some 45°, or about 80 ft, beginning on the west and extending around toward the south to an angle of about S45oW. The approximate salt-fall volume is 2 Mft^3 (57 000 m^3). The evaluation determined that a large volume of material fell from the western cavern wall. The debris was cast up in a sloping pile against the opposite, or eastern, side of the cavern (rather than rained down to produce a mound of debris directly beneath the western wall). It was posited (Munson et al., 2004) that the bulk of the salt-fall mass fell as a unit, essentially straight downward, disintegrating progressively as it hit the bottom of cavern and throwing the debris to the eastern side of the crater.

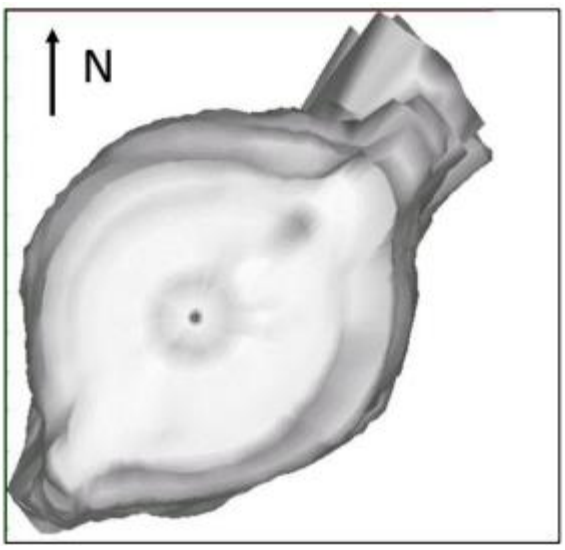

Figure 113. Top View of the Cavern 108 Sonar Contours, Exhibiting Wings (Munson et al., 2004).

The Big Hill 103 Cavern event prompted a comprehensive review of the sonar surveys run in all the caverns of the site, together with cavern closure rates, accumulation of material at cavern bottoms and material deformation properties. Ehgartner used CAVEMAN (Ehgartner et al., 1995), a cavern management tool, to compare cavern-creep closures. In Figure 109, grey-scale shadings provide the relative creep rates of the individual caverns. The four caverns with the lowest closure rates (which include Cavern 103) are grouped together in the SE quadrant of the dome, suggesting that the group belongs to a spline composed of material different from the rest of the dome. The following two categories of preferential solutioning can be observed: Linear preferential solutioning, nearly vertical, especially marked in Cavern 108 (Figure 113, which show horizontal cross sections superimposed on each other) — There are “marked” wings in the NE and SW directions, suggesting that a more easily dissolved layer cuts diametrically across the cavern. Caverns 107, 112 and 113 exhibit the same trend. Caverns 105, 111, 112 and 113 exhibit a different linear preferential solutioning, a foot-shaped lobe at the very bottom of the cavern, oriented NE-SWW, except for Cavern 105. General preferential solutioning, analogous to very large pits in cavern walls, whose vertical extent is a hundred feet (30 meters) or larger — Cavern 110 (Figure 114) is an extreme example of this. A third category is believed to be the result of loss rock fall through mechanical failure. Cavern 103 obviously belongs to this category. Cavern 101 (Figure 114) presents a similar feature at a 3200 ft (975 m) below ground surface. ”*Here the edges of the indentation appear sharp, typical of material fracture, rather than the rounded edges typical of preferential solutioning.”* (Munson et al., 2004, p. 13).

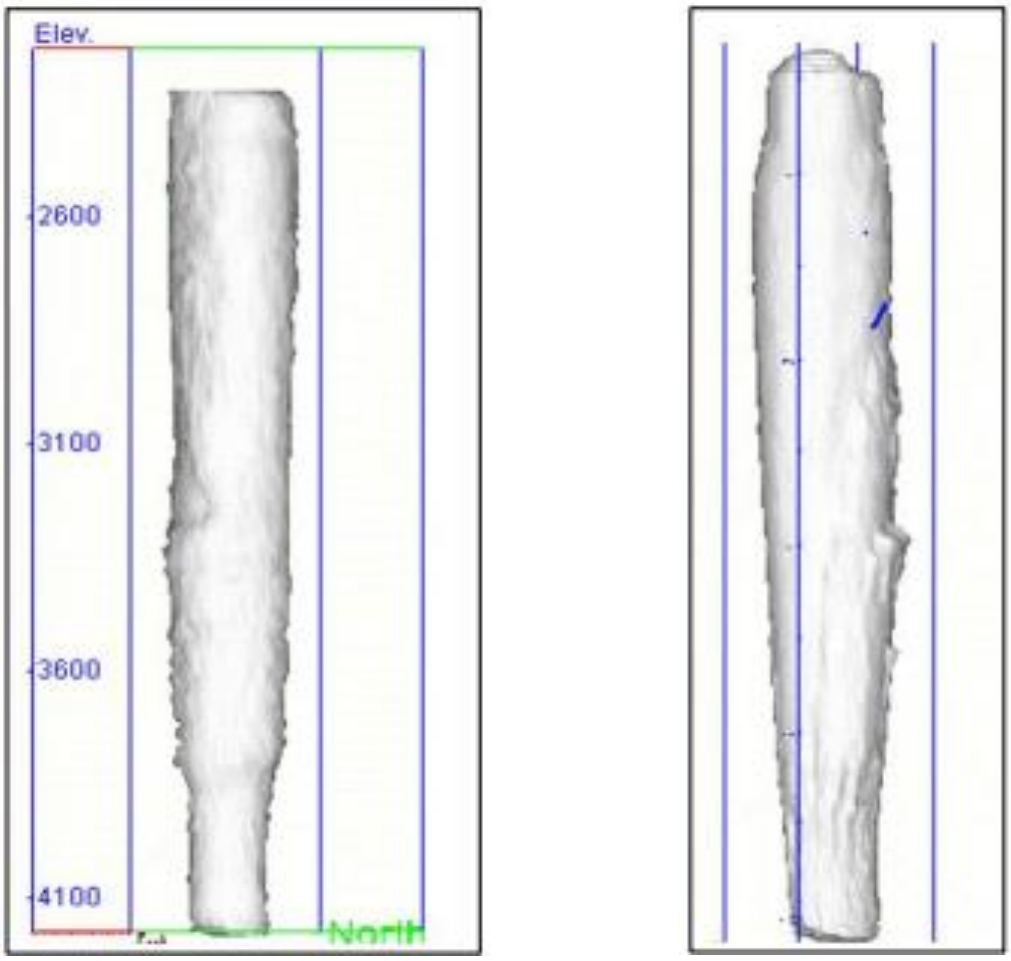

Figure 114. Cavern with solutioning pits (a) Cavern 110, 109; 2000 and Cavern with Mechanical Salt Fall Pits (b) Cavern 101, 210; 2000. From Munson et al., (2004).

3.4.7.1.7 Markham, Texas

Cole (2002) describes two gas caverns in the Markham storage field in Texas. These caverns were cycled 8 to 10 times per year, and withdrawal rates were 3-4 times faster than injection rates. The cavern tops are at 1050 m and 1075 m ($P_\infty = 230$ bar), and the original cavern heights were 530 m and 696 m, respectively. The first gas injections were in June 1992 (Cavern #2) and October 1995 (Cavern #5). Cavern operation resulted in cavern-volume loss, and salt sluffing from the walls and roof of the cavern. Brine-gas interface surveys were run every year. As of January 2002, the caverns had lost 89 m and 128 m of their depths. A "material balance" test also had been performed in 2001 to assess the cavern "free" volume, and natural gas sonars were run in January 2002. Comparison of these various methods suggests that cavern closure was approximately 5% of the initial volume; however, a similar volume of salt had fallen from the walls to the bottom of the caverns. Comparison of sonar profiles shows vertical profile overlay of sonars performed in June 1992 and January 2002; and May 1995 and January 2002, respectively (Figure 115). Note the bottom heave and possible break-outs at the cavern wall. However, "no large sections of salt from one area of the caverns fell to the bottom creating the fill ... the salt was removed in thin layers over large areas of the caverns ... horizontal cavern closure occurred ... thus closing in part of the area created by the salt falling." (Cole, 2002, p. 82).

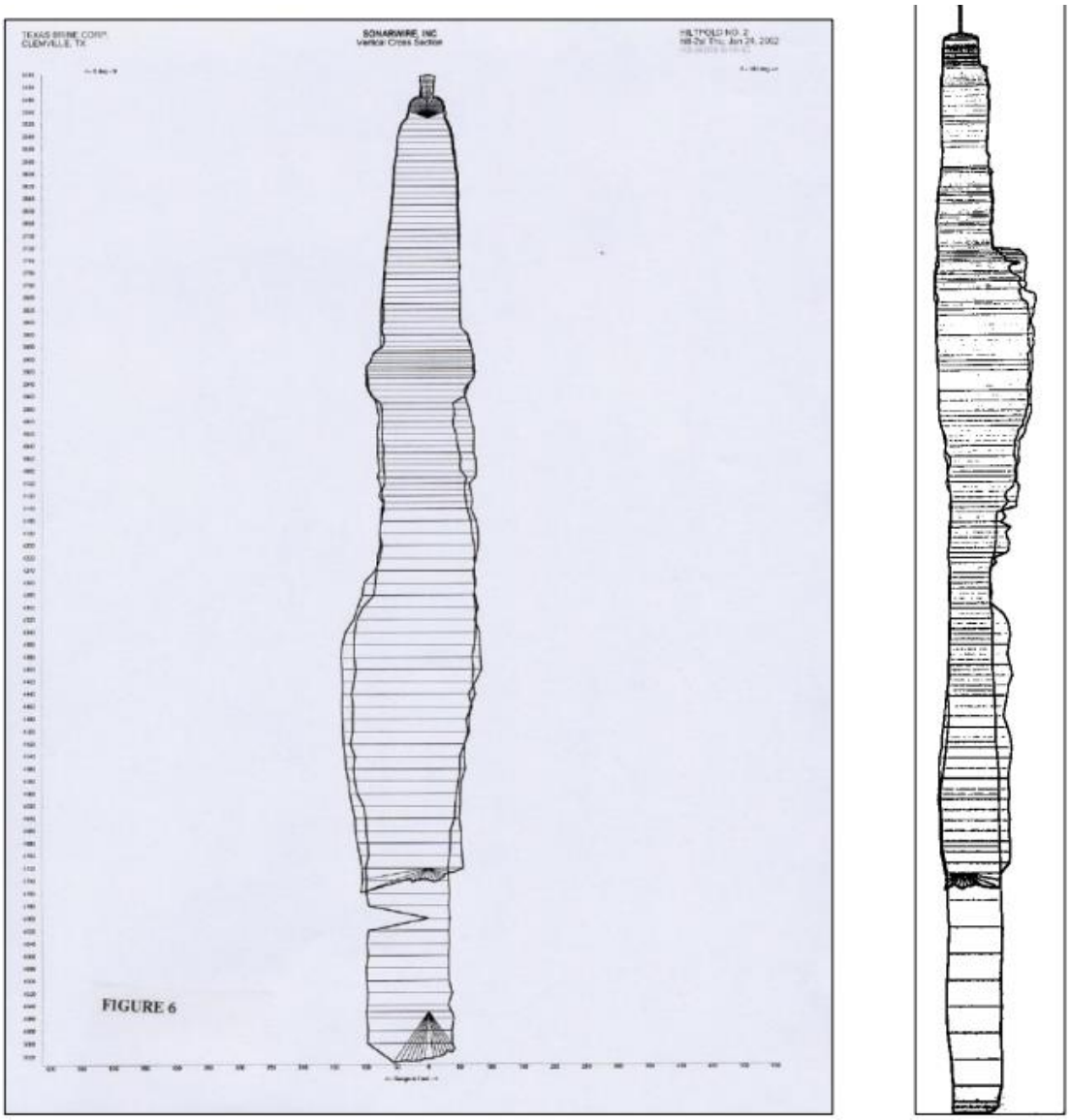

Figure 115. Markham: (left) Cavern 2, June 1992 brine-sonar profile and January 24, 2002 gas-sonar profile; (right) Cavern 5, May 1995 brine-sonar profile and January 25, 2002 gas-sonar profile (Cole, 2002).

3.4.7.2 Lessons learned

It is difficult to draw lessons from the above-described cases. It seems that several different mechanisms are involved. In some cases, local heterogeneities play a major role (Huntorf); in other cases, dome-scale anomalies are to be incriminated (Big Hill); significant pressure changes might have been instrumental (Markham, Lille Torup).

3.5 Conglomerates

The case of '*conglomerates*' (large cavern clusters) has not been intensively studied in the literature, probably because it requires heavy computing resources. The mechanical behaviour of a cluster is complex; computations prove that a large part of the overburden load is transferred to the abutment (the periphery of the cluster), in sharp contrast with the case of an elastic rock mass (Brouard et al., 2021a, 2021b). It is proposed to study conglomerates more in detail in this project.

3.5.1 Introduction

Most considerations in the previous sections addressed the case of single caverns. In fact, in most cases, a storage site is a cluster in which dozens of caverns are implemented, Figure 116. Caverns often have been created at the same depth and, from a structural stability standpoint, a major problem is the minimum distance between two neighbouring caverns or, in other words, computation of safe extraction ratio.

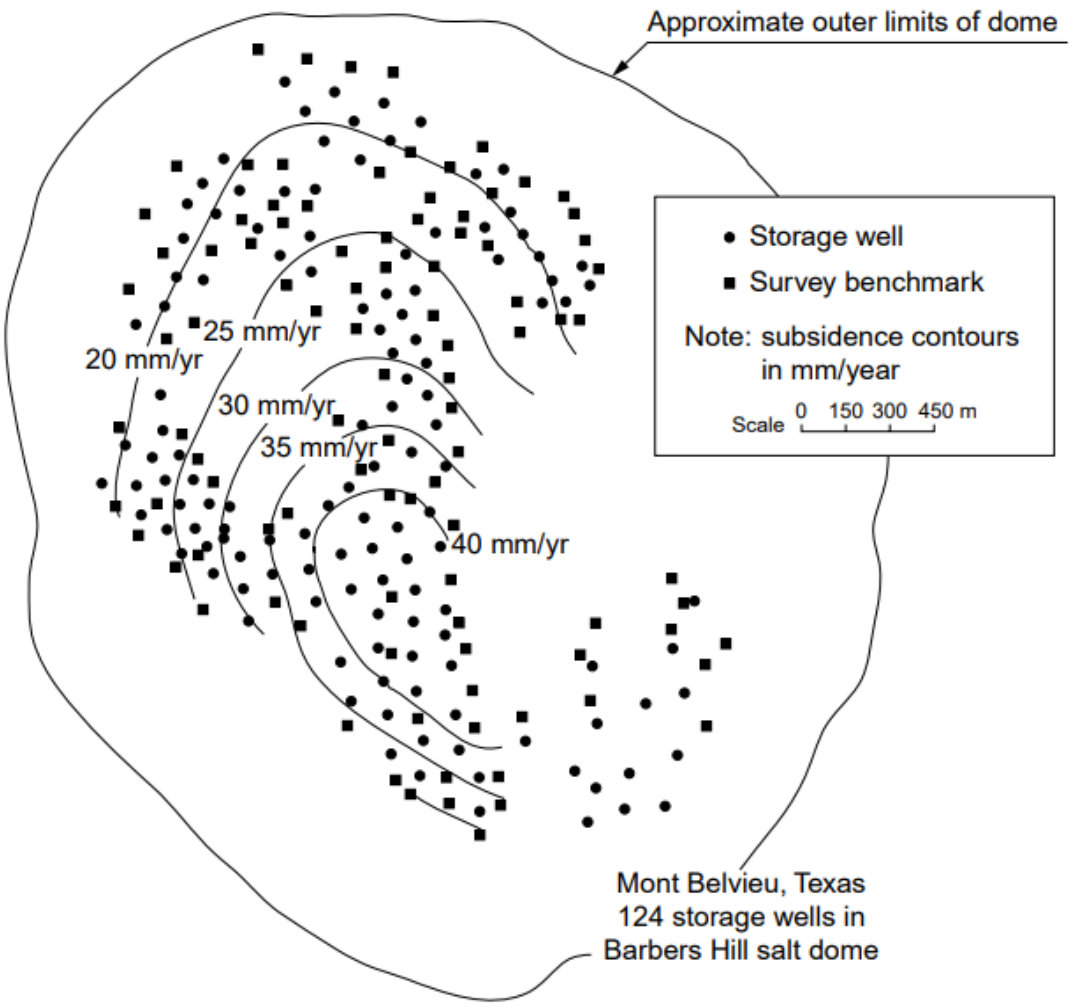

Figure 116. Subsidence in the Mont Belvieu (Texas) site(after Ratigan, 1991). At this site, 124 caverns were operated in 1991.

In the past, no 3-D computation tool was available and the cluster problem was approximated as follows. The cluster was assumed to be infinite in the two horizontal directions and it was assumed that, at any given instant, fluid pressure was the same in all the caverns. Any cavern was a "cell" in an infinite array of caverns and could be treated as a single cavern such that the radial displacement was zero at a distance from the cavern axis equal to half the distance between two neighbouring cavern wellheads. The criterion for stability, typically, was that the computed dilatant zone at the wall of a cavern did not reach the boundary of the cylindrical cell in which the cavern was included.

An example of this method, based on elastoplastic computation is provided by Ineris (the French National Agency for the Study of Industrial Risks)

The risk of a generalized collapse of a cavern cluster can be excluded when caverns number is smaller than three or when the extraction ratio is smaller than a critical value τ_{cr} *= 1 / [2 * exp (0,00125*P - 0,5) - 1]; where P is the cavern roof depth (in meters).* [i.e., 79%, 31% et 15% when cavern roof depth is P = 500, 1000 et 1500m, respectively].

This method suffered from two flaws. First, there is no strong theoretical basis for a description of the behaviour of a dilatant zone joining two neighbouring caverns (see Section 3.4, Brittle failure). Second, this method missed an important point which is the progressive transfer of the overburden weight from the centre of the cluster to the abutment.

This problem shares some similarity with the dimensioning of room-and-pillar mines

3.5.2 Case histories

Many salt clusters are stable. A remarkable example is shown on Figure 117.

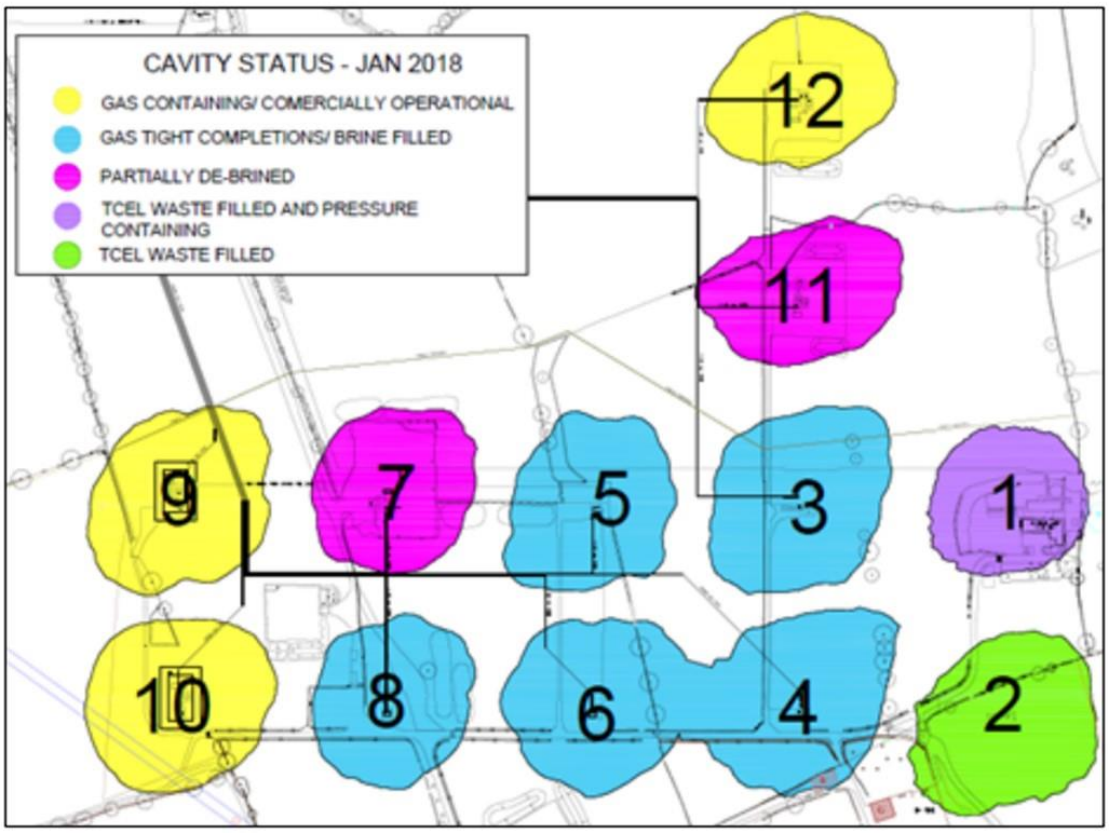

Figure 117. A cavity cluster (Europe).

A somewhat extreme example of a “stable” cavity cluster is represented on Figure 117. This cluster had been operated for brine production before being converted to a natural gas storage. Two caverns coalesced (#4 and #6). The minimum distance between two neighbouring caverns is 19 m, much smaller than the distance between the wellheads of two neighbouring caverns. Cavern depths are between 250 m and 400 m, typically. Caverns 9, 10, 12 have been operated as gas storage caverns since 2001 up to now (2022). Gas pressure has been cycled between 35 bars and 45 bars (these values are higher than halmostatic pressure at cavern depth, because of mechanical stability concerns.) For the same reason, pressure change rates are smaller than 1 bar/day and gas pressures are kept equal in #9 and #10. Somewhat surprisingly, the cluster has remained stable, though the extraction ratio is extremely high.

The behaviour of the salt pillar between neighbouring caverns is an important issue in this context. The elastic theory predicts that the vertical load on the pillar is significantly larger than the virgin (geostatic) stress when the distance between neighbouring caverns is small. In some cases, the pillars cannot bear the load excess generated by a high extraction ratio, as proved by several examples of mine collapses (Minkley and Menzel, 1996). However, when the mechanical behaviour of the rock mass is visco-plastic, a significant part of the load excess is transferred to the abutment; i.e., outside the footprint of the mine (Bérest et al., 2008b). The state of stresses in the pillars is less critical than in the elastic case.

3.5.3 The tributary area (elastic behaviour)

A simplistic model allows capturing a couple of features of the mine problem (Figure 118).

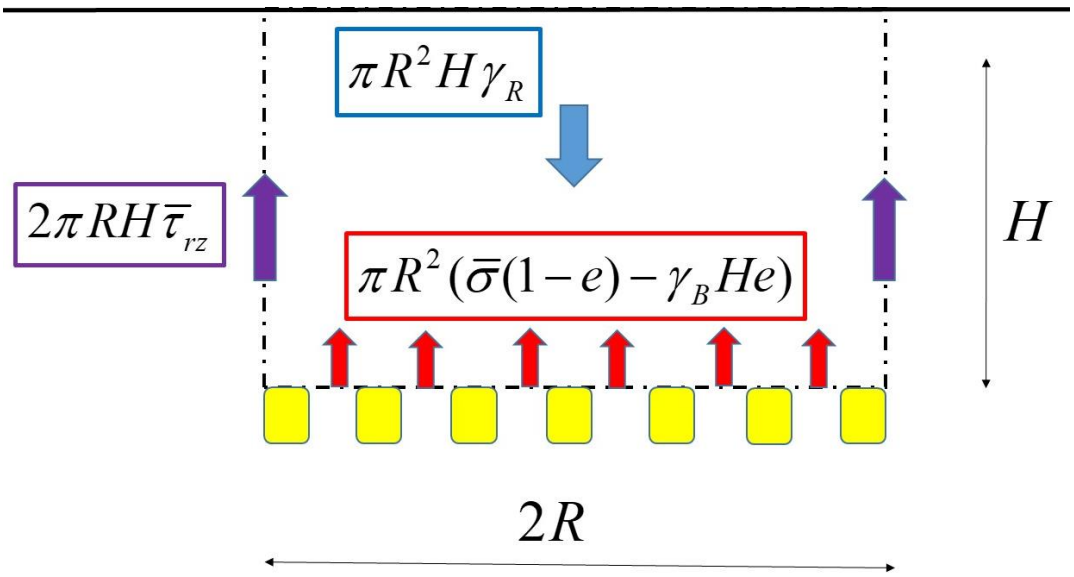

Figure 118. Equilibrium of the forces applying on the overburden of a cluster or a dry mine.

For simplicity, mine (or cluster) footprint is assumed to be a circle, radius R. Cluster depth is H. The extraction ratio is e. The mine is assumed to grow (R increases). Mechanical equilibrium of the cylinder of rock above the cluster can write:

$$\pi R^2 \gamma_R H < \pi R^2 \gamma_b He + \pi R^2 \bar{\sigma}(1-e) + 2\pi RH\bar{\tau}_{rz} \quad (41)$$

The weight of the overburden, or $\pi R^2 \gamma_R H$ ($\gamma_R = 0.023$ MPa/m is the volumetric weigh of the rock formation) must be larger than the sum of:

- The force applied by brine pressure (in a caverns cluster) on the bottom of the cylinder, ($\pi R^2 \gamma_B He$); $\gamma_B = 0.012$ MPa/m is the volumetric weight of brine); in a dry mine, this force is zero.
- The force applied by the pillars on the bottom of the cylinder, $\pi R^2 \bar{\sigma}(1-e)$; $\bar{\sigma} > 0$ is the average vertical stress in the pillar.
- The vertical force resulting from the cumulated shear forces applied on the cylinder contour, $2\pi RH\bar{\tau}_{zr}$; $H\bar{\tau}_{zr} = \int_0^z \tau_{zr}(z)dz$)

In addition, two failure criteria can be used:

- **Salt pillar strength**: the average stress in the pillar must be smaller than ultimate strength of the pillar or R'_{cr} (taking into account the confining pressure provided by cavern brine).

- **Overburden shear failure**: the overburden satisfies a Coulomb criterion, $\tau_{rz}(z) < C + tg\varphi\ \sigma_h(z)$, a simple assumption is $\sigma_h(z) = \gamma_R z$, from which:

$$H\bar{\tau}_{cr} = \int_0^z \tau(z)dz = CH + \frac{tg\varphi H^2}{2} \quad (42)$$

After some algebra, the problem can write:

$$R\gamma_R < R\gamma_b e + \frac{R(1-e)\bar{\sigma}}{H} + 2\bar{\tau}_{rz}(H) \quad (43)$$

$$0 < \bar{\sigma} < \bar{\sigma}_{cr} \quad (44)$$

$$0 < \bar{\tau}_{rz} < \bar{\tau}_{cr}(H) \quad (45)$$

In the $\bar{\sigma}, \bar{\tau}$ plane (Figure 119), equation (43) can be represented as a straight line which is a function of R (the radius of the cluster) crossing through the "tributary" point $\bar{\sigma} = \frac{\gamma_R H}{(1-e)}, \bar{\tau} = 0$ (for simplicity, the case of a dry mine is represented). Consider first the case of an elastic material.

On Figure 119, left, rock strength $\bar{\sigma}_{cr}$ is high [larger than the tributary stress, $\bar{\sigma}_{cr} > \frac{\gamma_R H}{(1-e)}$]. When the mine is still small but grows (R increases), the pillars bear a slightly larger and increasing part of the overburden weight and shear stresses develop above the mine external contour. After the critical radius is reached, the stress in the pillar slowly converges to the tributary stress, the shear stresses decrease and the mine is stable.

On Figure 119, right, rock strength $\bar{\sigma}_{cr}$ is small (smaller than the tributary stress) When the mine grows, equation (43) together with inequalities (44) and (45) cannot be satisfied. The mine fails: pillars break or a crater forms.

A complete model, including a description of the salt roof and how the overburden load can or cannot be transmitted to the abutment, is needed to determine which can of failure occurs.

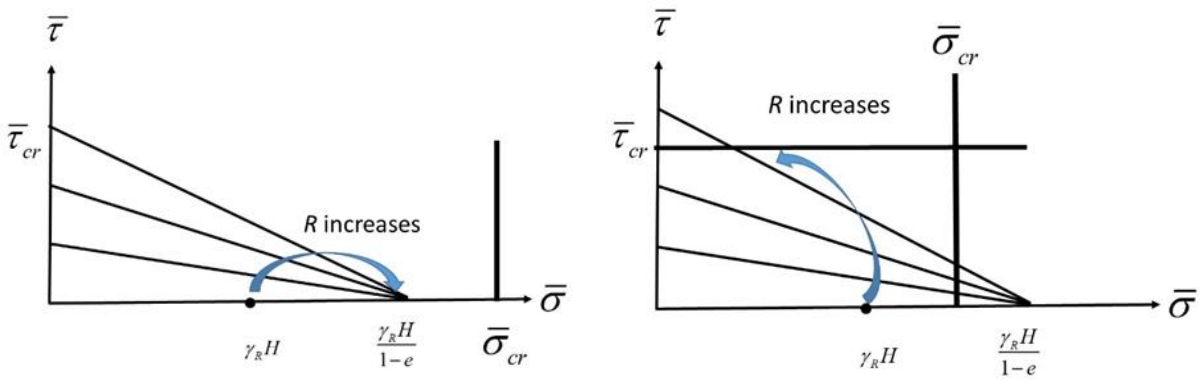

Figure 119. Stability of a room-and-pillar mine.

3.5.4 Pillar progressive unloading (visco-plastic behaviour)

An example of this is provided by Figure 120 and Figure 121. The central pillar of the dry mine is on the left (Figure 121). Nine rooms are created progressively. When a pillar is created, the vertical load on the pillar increases during one year to 5 MPa, approximately (like in the elastic approach) before decreasing to 2.5 MPa after a several year period. A significant part of the overburden weight is transferred to the abutment The ability to transfer weight outside cluster footprint is a characteristic feature of a visco-plastic material.

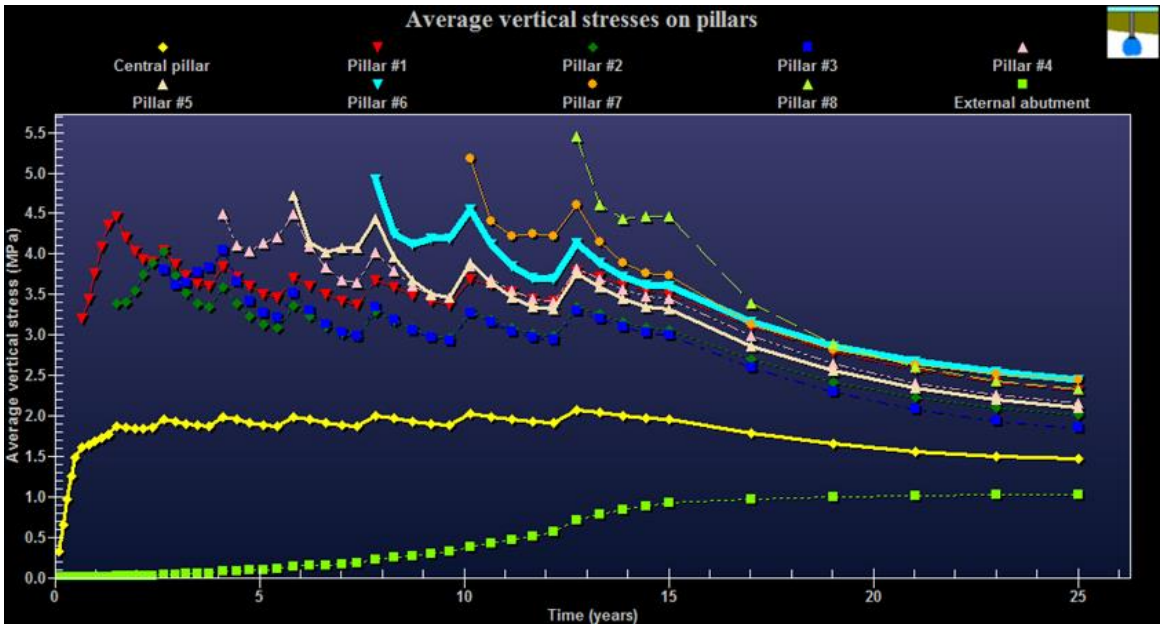

Figure 120. Additional vertical loads on the pillars and external abutment as a function of time. A 3.5 MPa initial geostatic stress must be added to obtain the actual stress (after Bérest et al., 2008b).

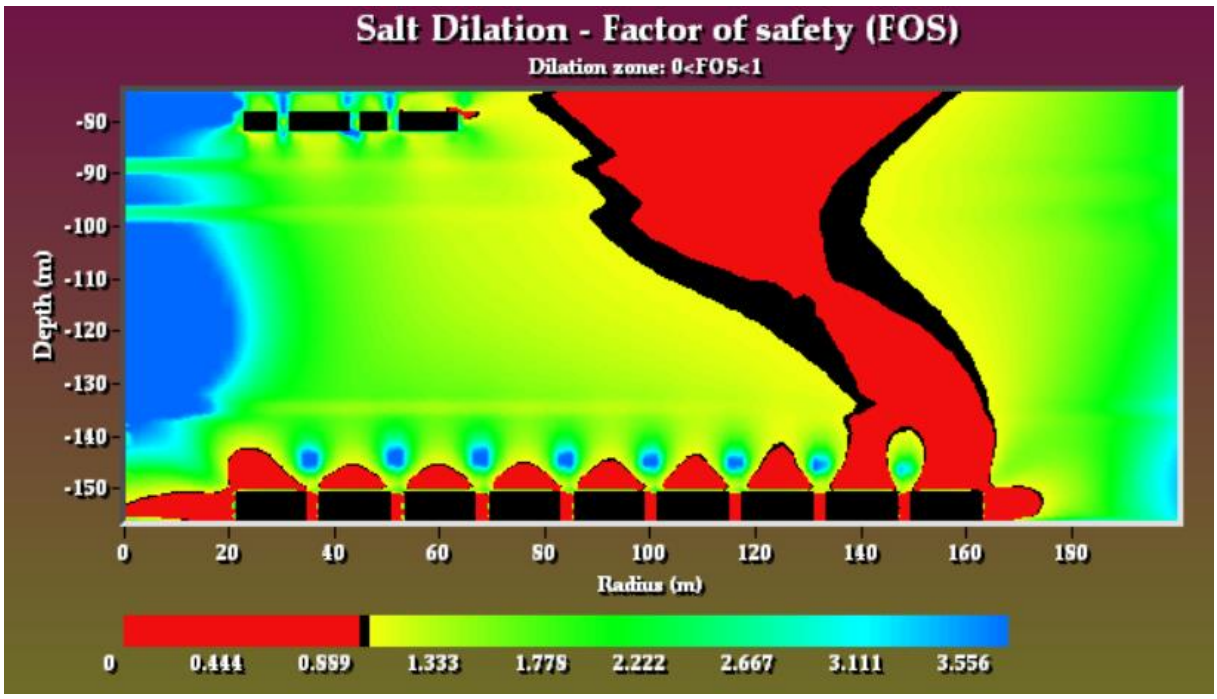

Figure 121. Extension of the dilatant zone (after Bérest et al., 2008b).

Brouard et al. (2021a) discussed the theoretical case of a 4 or 9 caverns cluster, in which a similar phenomenon (transfer of a part of the overburden weight to the abutment) takes place. Several extraction ratios (i.e., several distances between the caverns, Figure 122) were considered (e = 20%, 40% and 60%). It was shown that, opposite to the case of an elastic rock mass, in the case of a visco-plastic rock mass (a salt formation), a few years after the end of mining, the vertical stress in the pillar is smaller than the virgin stress. This effect is more pronounced still when the extraction ratio is larger.

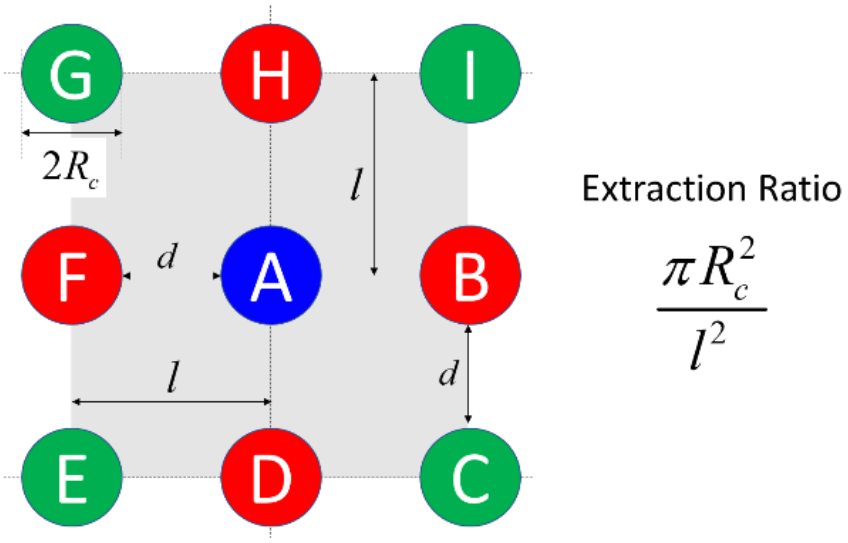

Figure 122. Definition of the extraction ratio.

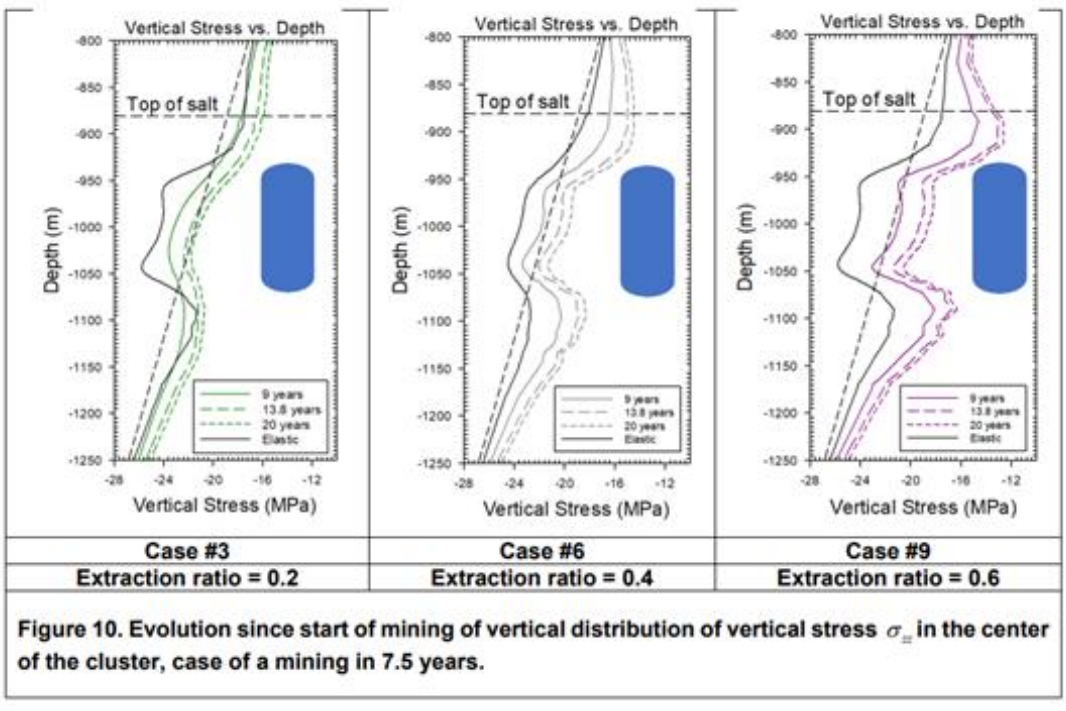

Figure 10. Evolution since start of mining of vertical distribution of vertical stress σ_{zz} in the center of the cluster, case of a mining in 7.5 years.

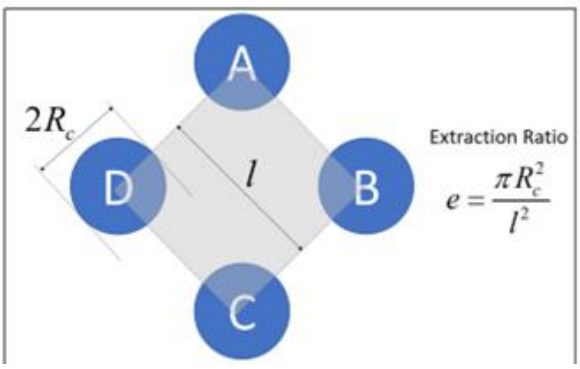

Figure 123. A four-cavern cluster.

An example is provided on Figure 123. Three different extraction ratios are considered and the vertical distribution of the vertical stress at the middle of the pillar is represented. In the elastic case, at pillar depths, vertical stresses are significantly larger than the virgin stress. In the visco-plastic case, vertical stresses slowly decrease (they are less and less compressive), become smaller than the virgin stress, as a part of the overburden load is transferred to the abutment.

In this example the creep closure in a cluster of 9 caverns with extraction ratios of 20% and 40% is analysed more into details. Comparison of Figure 124 and Figure 125 (vertical stress distribution at cavern mid-depth when solution-mining is completed, and 18 years later) shows again that a significant part of the overburden weight has been transferred to the abutment. More generally, main results are as follows (Brouard et al., 2021b):

1) At the end of mining the central pillars are overloaded, but, a few years later, a large part of this overstress has been transferred outside the footprint of the cluster.
2) At the end of mining the central pillars are overloaded, but, a few years later, a large part of this overstress has been transferred outside the footprint of the cluster.
3) For elongated caverns, at cavern wall, vertical stress is less compressive than natural stress, this may induce tensile effective stresses and micro-cracks when cavern pressure is quickly increased, even at a cavern pressure significantly lower than geostatic pressure.
4) The average volume loss in a cluster is only slightly larger than the volume loss of a single cavern.
5) Rise of cavern bottom is faster than descent of cavern roof. The larger the extraction ratio, the larger the ratio between bottom rise and roof descent.

Computed maximum subsidence at ground level is very sensitive to the selected boundary conditions (size of the meshed domain, etc.).

3.5.5 Interaction between various storage products

A few examples of interactions between various storage products are reported in the literature. The example of Clovelly salt dome in Louisiana was shortly described in Paragraph 2.2.3.1.4.

3.5.6 Conclusions

Most caverns cluster seem to be stable. No example of crater creation above a cluster of storage caverns is known. This phenomenon is understood. Transfer of a part of the overburden weight to the abutment is at least a partial explanation. More researches are required to reach a complete understanding. The availability of 3-D computations will be an important tool in this context.

Caverns at a 1000-m or 3280-ft mid depth

End of Mining

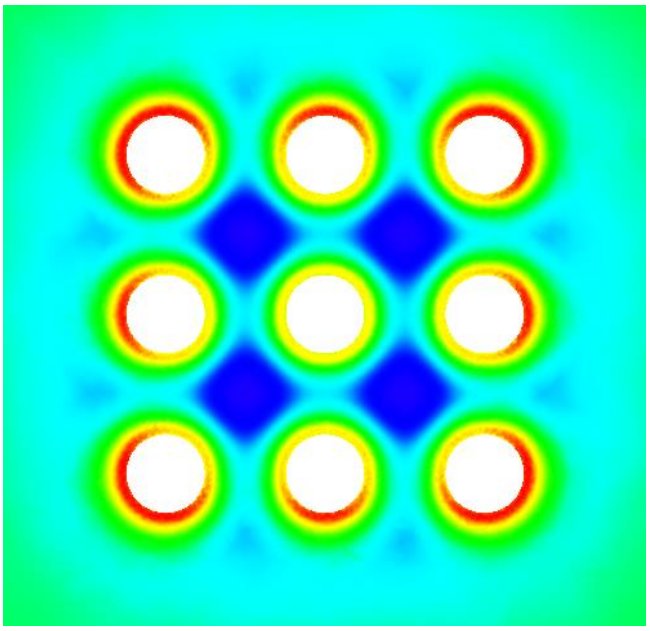

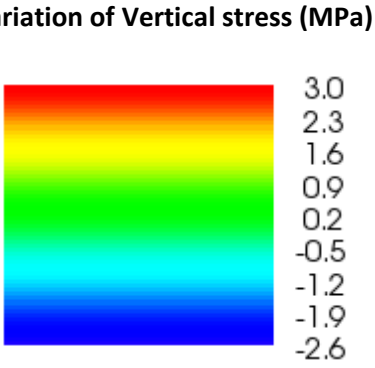

Extraction ratio: 20%

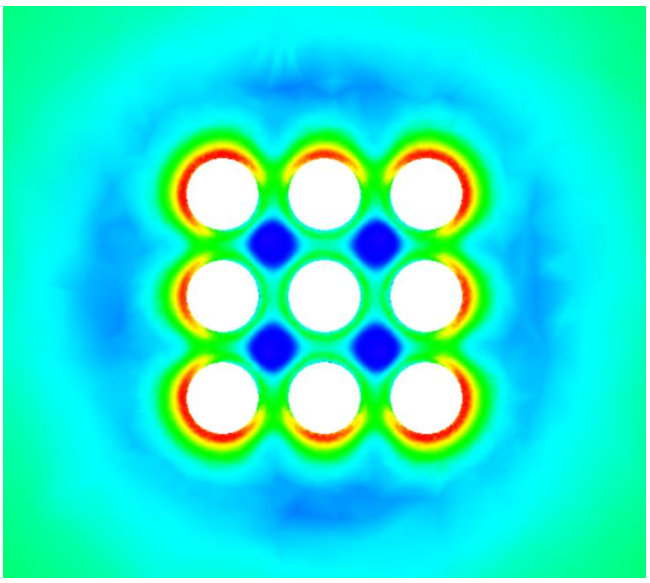

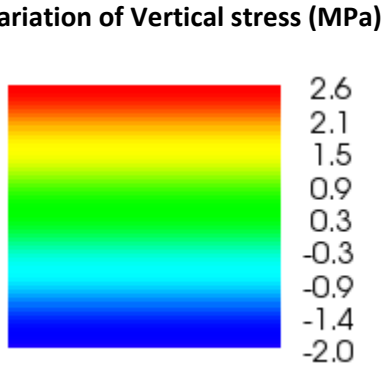

Extraction ratio: 40%

Figure 124. Variation of vertical stress at caverns mid depth, 1000 m or 3280 ft, at the end of mining for two extraction ratios.

Caverns at a 1000-m or 3280-ft mid depth

18 years after the end of mining

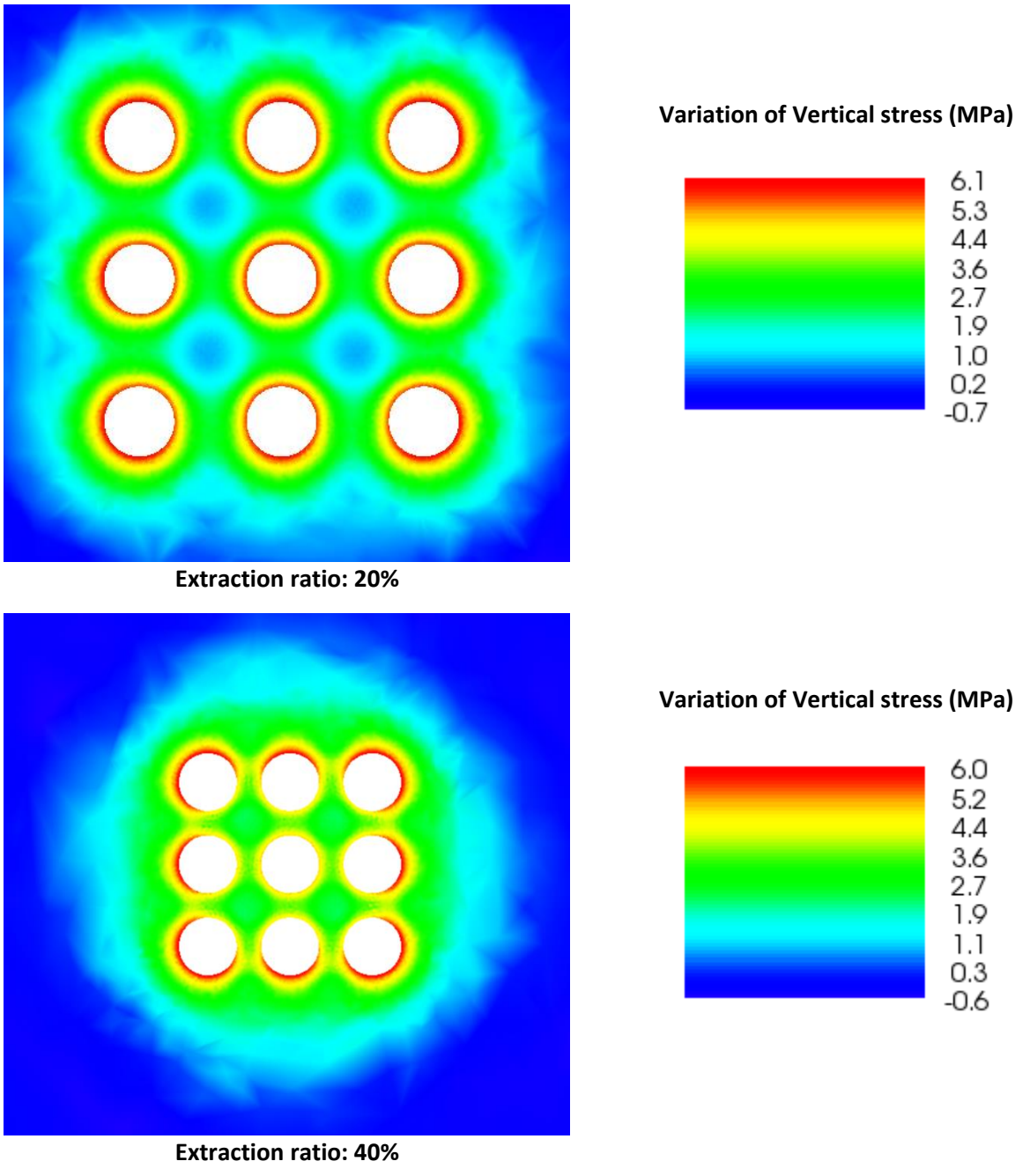

Figure 125. Variation of vertical stress at caverns mid depth, 1000 m or 3280 ft, 18 years after the end of mining for two extraction ratios.

3.6 Cavern abandonment

A thorough integrated study on cavern abandonment was carried out in the frame of KEM-17 covering the dome, cavern and microscale (respectively Baumann et al., 2019; Brouard and Bérest, 2019; Urai et al., 2019). The next summary is from the conclusions and recommendations of the project (KEM-17, 2019).

"In summary then, using the present state of engineering practice, it is not possible to say with sufficient reliability if a deep abandoned cavern will evolve by localized brine flow, hydraulic fracturing and major loss of containment, or with a pressure build-up that is moderate with leak-off by diffuse permeation and no hydraulic fracturing.

We see a clear opportunity to improve predictions of the evolution of abandoned caverns, by integrating existing knowledge in the geoscience and materials science with engineering practice, at the micro, cavern, and salt-dome scale.

The consortium strongly recommends that further researches be performed to get a better understanding of the notions for which uncertainties remain. In particular, the required integration level between engineering and materials science domains has not been reached yet.

When permeation rate equals creep closure rate, an equilibrium pressure can be reached as proved by in-situ tests performed in various salt formations. In shallow caverns, this equilibrium pressure is much lower than geostatic. In a deep cavern, uncertainties are larger: cavern permeability increases as effective stresses are less and less compressive; fluid-assisted creep closure (rather than dislocation creep) becomes preeminent; the notion of a "geostatic pressure" blurs, as the state of stresses at cavern roof depends on cavern pressure history and far-field virgin stress.

When equilibrium pressure is computed at cavern mid-depth, "Wallner's margin" must be added to this equilibrium pressure to assess fracturing risk."

For further reading on this project and (extensive) bibliography we refer to the individual reports available at the website of the SODM[1].

[1] https://www.sodm.nl/documenten/rapporten/2020/02/11/onderzoek-langetermijnrisicos-afsluiten-zoutcavernes

4 Salt cavern testing

Author: Pierre Bérest – Brouard Consulting

4.1 Permeability tests in caverns and boreholes

4.1.1 Maximum operating pressure (in a salt cavern)

4.1.1.1 Evidence of cavern compressibility increase at high pressure

There are strong indications that overall cavern compressibility apparently increases when the pressure gradient at the casing shoe is larger than 0.18-0.19 bar/m; i.e., 80-85 % of the geostatic gradient, which typically is 0.22-0.25 bar/m. [Cavern compressibility during a brine injection test, or βV, in m^3/bar, is the ratio between the injected flow rate, Q_{in}, and the concomitant cavern pressure increase, $\dot{P}$, or $Q_{in} = \beta V \times \dot{P}$. An increase of the cavern compressibility is a clear sign of a leak, or Q_{out}, as $\beta V \times \dot{P} = Q_{in} - Q_{out}$ and $\beta_{app} = \beta + \frac{Q_{out}}{V\dot{P}}$].

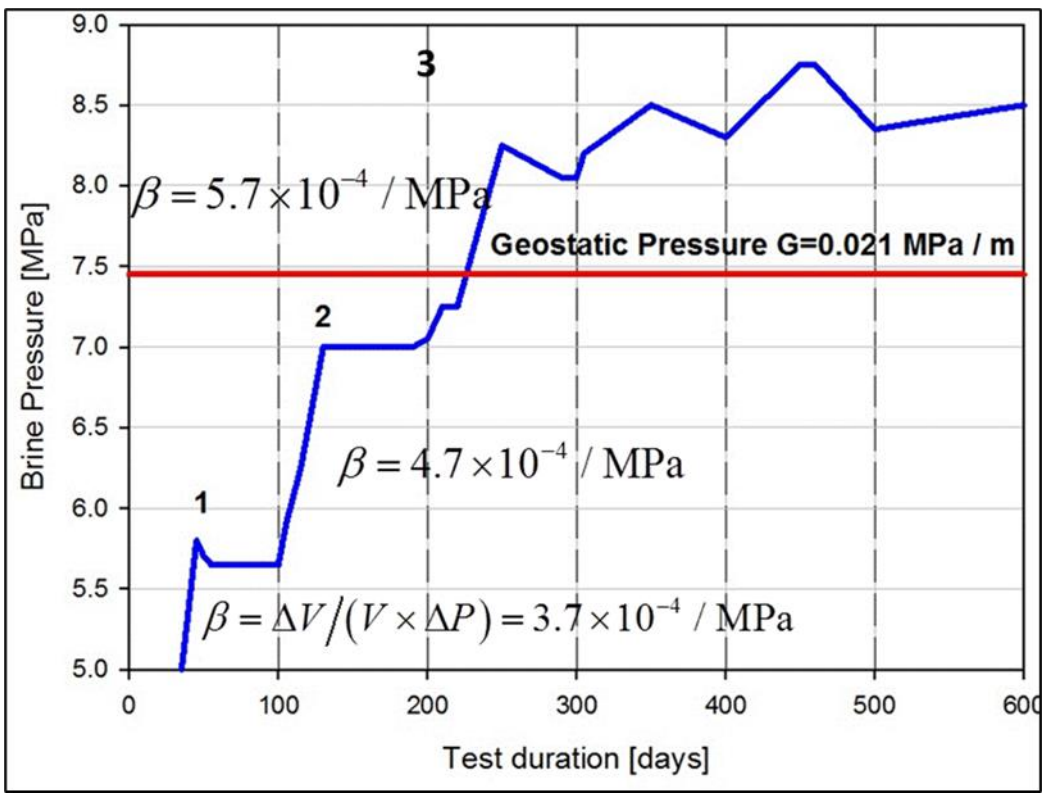

Figure 126. Etzel test (after Rokahr et al., 2000).

A high-pressure test was performed in a brine-filled cavern at Etzel (Germany) in 1990-1992 (Rokahr et al., 2000). It was observed (Figure 126) that the cavern coefficient of compressibility, β, *apparently* increased significantly, from $\beta = 3.7 \times 10^{-5}$ /bar (when the cavern-pressure gradient was 0.19 bar/m) to $\beta = 4.7 \times 10^{-5}$ /bar (when it was 0.205 bar/m.)

Durup, 1990, 1994, performed a pressure build-up test in a wellbore at Etrez (France) in which the pressure was increased through step-by-step brine injections. The open-hole length was 198 m. The test lasted six hours.

On Figure 127, the pressure at well-bottom depth (871 m) is plotted against the cumulated injected volume (The slope of this curve is $1/\beta V$). When pressure increased from 145 bars to 205 bars (from 0.17 bar/m to 0.23 bar/m at a depth of 871 m), wellbore apparent compressibility increased from $\beta V = 0.97$ liters/bar to $\beta V = 2.4$ liters/bar.

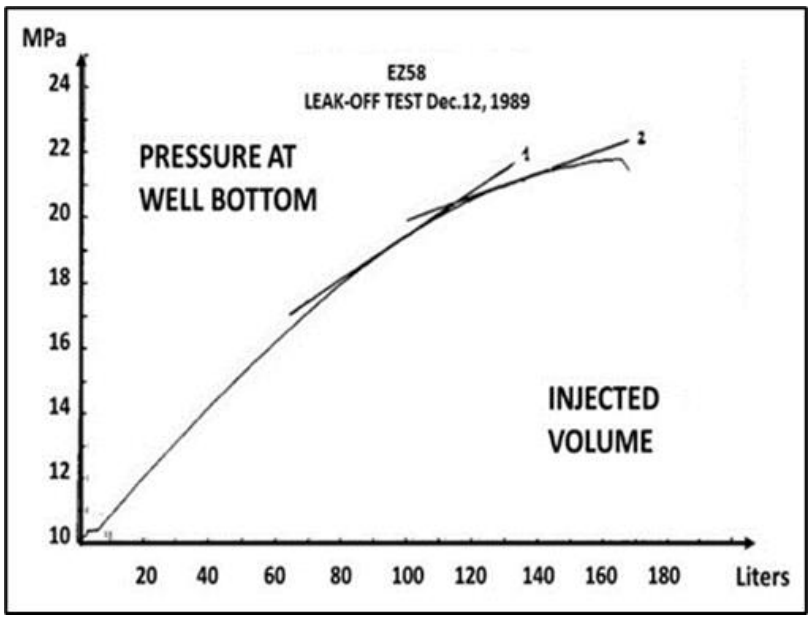

Figure 127. Etrez build-up test (after Durup, 1994b, 1990).

This notion was confirmed by Van Heekeren et al. (2009) who measured cavern compressibility as a function of cavern pressure during four pressure build-up tests. Results of these tests are shown on Figure 128 (No scale is provided in the paper by van Heekeren et al., 2009). At low pressure, apparent compressibility is a slowly increasing function of wellhead pressure; a pressure threshold can be observed above which apparent compressibility drastically increases. This threshold seems to be significantly smaller than the virgin geostatic pressure. In fact, when successive tests are considered, compressibility is smaller and smaller, and the threshold is higher and higher.

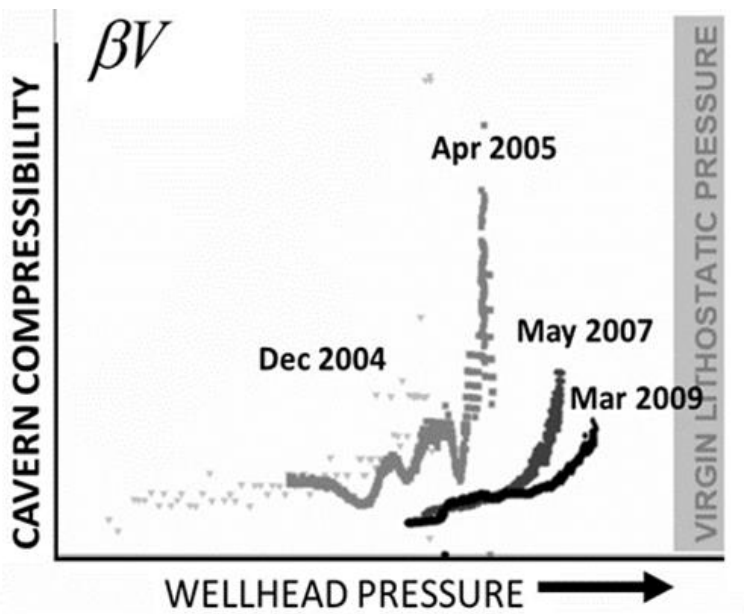

Figure 128. Frisia test (after van Heekeren et al., 2009).

Brückner et al. (2003), described a test performed in a 22-m^3 cavern leached out at a 448-m depth from a drift at the Bernburg Mine in Germany. In this test, cavern pressure was increased incrementally from zero. At the beginning of the test, 8.8 litres of brine were injected in the cavern: pressure increased by 10 bars, from which it can be inferred that cavern compressibility was $\beta V = 0.88\,\text{liters/bar}$ $(\beta = 4 \times 10^{-5}\ /\text{bar})$. Cavern compressibility increased over the next steps, becoming $\beta = 4.7 \times 10^{-5}/\text{bar}$ when pressure increased from 14.8 bar to 44.8 bar (a gradient of 44.8/448 = 0.1 bar/m). During the last step, when pressure increased to 92.5 bars (a gradient of 0.21 bar/m), an "*exponential*" increase in compressibility was observed.

The origin of such early micro-fracturing, not observed during standard frac tests, is not understood fully. The (macroscopic) state of stresses generated by a swift pressure increase (following a long idle period at low pressure) at the wall of a cavern excavated from a visco-plastic medium (Djizanne et al., 2012) and the (microscopic) state of stresses at the boundaries between salt grains have been implicated.

4.1.1.2 Maximum operating pressure in a gas storage cavern

In Table 6, the maximum gas pressure in 24 sites worldwide is represented (Bérest et al., 2020). In most cases, the pressure gradient at casing shoe depth is 0.18 bar/m, a value which, although being of empirical origin, is consistent with what was described in Paragraph 3.4.2.3 (a significant permeability increase is observed when the gradient is higher than 0.19 bar/m.)

Table 6. Maximum pressures in selected gas storage caverns (from Bérest et al., 2020 and references herein).

Gas storage	Authors	CCS depth (m)	Pmax (MPa)	Maximum gradient (MPa/m)	Maximum gradient (psi/ft)
Aldbrough	Slingsby et al., 2011	1800	27	0.015	0.66
Carriço	Colcombet et al., 2008	1000	18	0.018	0.8
Etzel	Schweinsburg & Schneider, 2010	1150	20	0.017	0.76
Holford	Fawthrope et al., 2013	≈ 550	10	0.018	0.8
Krummhörn	Rummel et al., 1996	≈1500	27	0.018	0.8
Nuttermoor	Bernhardt & Steijn, 2013	≈ 1000	17	0.017	0.76
Teesside	Mullaly, 1982	≈ 350	4.5	0.013	0.58
Zuidwending	Hoelen et al., 2010	1000	18	0.018	0.8
Manosque	de Laguérie & Durup, 1994	1000	18	0.018	0.8
Stublach	Pellizzaro et al., 2011	≈ 550	10	0.018	0.8
Egan	Chabannes, 2005	1125	23	0.0204	0.9
Kansas	Itsvan, 1998	NA	12		
China	Fansheng et al., 2010	≈ 2000	17	0.016-0.017	0.72
Aldbrough	McLeod et al., 2011	≈1500	27	0.0155	0.66
Nüttermoor	Bernhardt & Steijn, 2013	≈ 1020	17	0.017	0.8
Germany	Wagler & Draijer, 2013	≈ 648	12.2	0.0188	0.83
Torup	Johansen, 2010			0.0184	0.81
Huai'an	Zhao et al., 2013	1493	26.0	0.0175	0.77
Jintan (Xi-2#)	Yang et al., 2015	937	13.5 15.0	0.144 0.0160	0.64 0.7
Jintan (PetroChina)	Hongling Ma, Institute of Soil and Rock Mechanics, Wuhan, pers.com. (May 2018)	≈1000	17.0 18.0	0.0170 0.0180	0.76 0.8
Jintan (Sinopec)		900	17.0	0.0188	0.83
Qianjiang		1980	32.0	0.0160	0.7

4.1.1.3 Maximum pressure in a hydrogen storage

Scarce data collected for hydrogen storage caverns has been provided in the literature (Laban, 2020). The Teesside hydrogen storage caverns in the UK are operated according to the brine compensation method; pressure in the caverns is constant and low (0.12 bar/m). According to Laban (2020), the maximum pressure gradient at mean cavern depth is 0.135 bar/m at Clemens Dome in Texas, 0.127 bar/m at Moss Bluff and 0.151 bar/m (?) at Spindletop. These figures underestimate slightly the gradient at casing-shoe depth (rather than mean depth) – which is the notion generally preferred to compare maximum pressures in different caverns. In addition, Laban (2020), is likely to underestimate the maximum gas pressure at Spindletop which, according to Jallais (2018), is 202 bars at a 1340-m depth, or a pressure gradient of 0.173 bar/m at the cavern-top depth. The reasons for the apparently low gradients selected at Moss Bluff and Clemens Dome are unknown.

4.1.2 Permeability measurement in a wellbore

4.1.2.1 Methodology

It has been recognized for long that pressure evolution in a shut-in cavern or wellbore is influenced by 4 main factors: creep closure, fluid thermal expansion, fluid permeation and hole compressibility. Creep closure rate (in %/yr) is independent of cavern size; fluid permeation rate (in %/yr) is inversely proportional to the cavern volume/cavern walls surface area, which is $\frac{V}{\Sigma} = 0.1$ m in a wellbore, typically, and larger by two orders of magnitude in a full-size cavern; thermal equilibrium is reached within a few weeks in a borehole (after several years or decades in a full-size cavern); borehole stiffness is larger by several orders of magnitude than cavern stiffness. Testing salt formation in a borehole is much more accurate than in a cavern.

Permeation rate is a function of wellbore pressure and virgin pore pressure (P_0). Natural brine pressure in the interconnected pores or cracks cannot be measured directly. Durup (1994b, 1990), proved that a linear relation did exist between the steady-state brine seepage rate and the pressure build-up in the EZ58 well (Figure 127). Extrapolating this relation proves that no flow takes place when cavern pressure is equal to halmostatic pressure, which strongly suggests that natural pore pressure is equal to halmostatic pressure. Even if no clear physical argument can be made, this hypothesis seems to be widely accepted. The distribution of pore pressure in the formation is, then, $P_h\ (\text{bar}) = 0.12 \times H\ (m)$ where H is the cavity depth. [However, test performed at the WIPP mine excavated in the Salado formation have provided higher figures, $P_0 = 0.14 \times H$; see Howarth et al. (1991).]

As an example, Bérest et al. (2001) describe the GDF tightness testing method.

One month (or more) after drilling is completed, a string is set inside the cemented casing. A packer is set a dozen of meters above the casing shoe (Figure 129). In a first step, water is injected in the central string and in the annulus in such a way that the testing gradient, 0.146 bar/m, is the same in the two volumes. The daily amount of water injected in the annular space is called the "*casing seepage rate*", and the daily amount of water injected in the central tubing is called the "*rock-formation seepage rate*". The test is considered to be satisfactory when the casing seepage rate is smaller than q = 1 litre per day. The second step consists of the "casing-shoe+plus-rock-formation" test. The testing gradient in the annular space is 0.146 bar/m, as it was during the first step. The testing gradient in the central tubing and in the unlined part of the well ranges from 0.18 to 0.22 bar/m. Pressure evolution is then monitored in both the annular space and in the central tubing; soft water is withdrawn or injected twice a day to keep the pressures (or gradients) fairly constant during the entire test. The daily fluid loss is then computed as follows: Daily injected water volume in the central tubing + Daily injected water volume in the annular space - Daily observed casing seepage rate during the first test = Apparent daily fluid loss. The observed daily fluid loss will be used later to back-calculate the equivalent permeability of the salt rock formation.

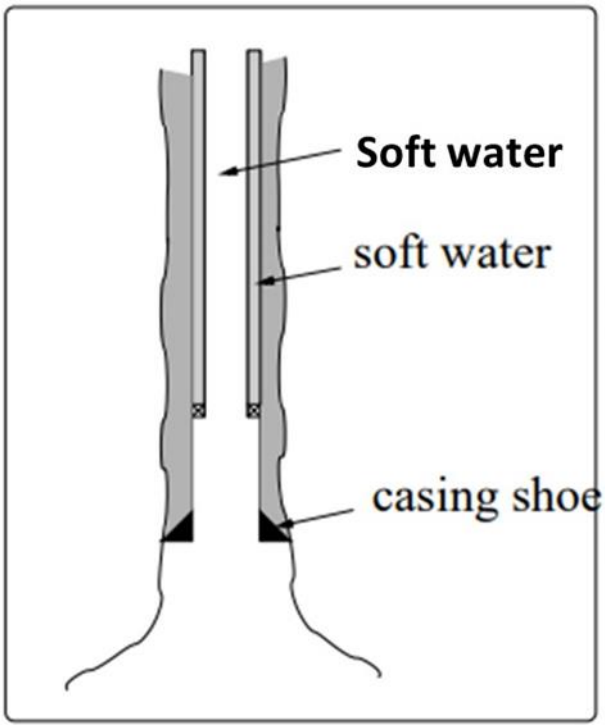

Figure 129. Schematic of wellbore completion during a tightness test.

4.1.2.2 Test results

Two different storage sites have been examined, Tersanne (Table 7) and Etrez (Table 8), in France (Brouard et al., 2001).

Table 7. Tersanne tests results (Daily volume loss is measured at the end of the test).

Well #	Testing Gradient	Test Duration (days)	Daily Volume Loss (liters/day)	Back-calculated Permeability (m^2)
Te01	1.89	6	0.65	1.6×10^{-21}
Te02	1.77	7	0.65	1.8×10^{-21}
Te03	1.73	305	0.57	3.2×10^{-21}
Te04	1.74	10	0.60	1.9×10^{-21}
Te05	1.73	10	0.58	1.1×10^{-21}
Te06	1.77	4	0.56	8.6×10^{-22}
Te07	1.77	20	0.57	1.4×10^{-21}
Te15	1.77	30	0.89	3.0×10^{-21}

Table 8. Etrez tests results (Daily volume loss is measured at the end of the test).

Well #	Testing Gradient	Test Duration (days)	Daily Volume Loss (liters/day)	Back-calculated Permeability (m^2)
Ez11	1.8	5	4.50	1.3×10^{-20}
Ez12	1.8	4	2.08	4.6×10^{-21}
Ez12	2	5	4.66	9.2×10^{-21}
Ez17	2	42	7.8	1.9×10^{-20}
Ez18	2	126	6.24	1.4×10^{-20}
Ez18	2.2	84	9.15	1.6×10^{-20}

A couple of comments can be made. Etrez salt permeability is larger by one order of magnitude; it is worth mentioning that Tersanne salt ability to creep is much higher. In the case of Etrez salt, a jump in permeability is observed when the testing gradient increases from 0.18 bar/m to 0.20 bar/m.

4.1.3 Permeability measurement in a full-size cavern

Cavern average permeability can be inferred from a "trial & error" abandonment test (Figure 130, Section 3.6).

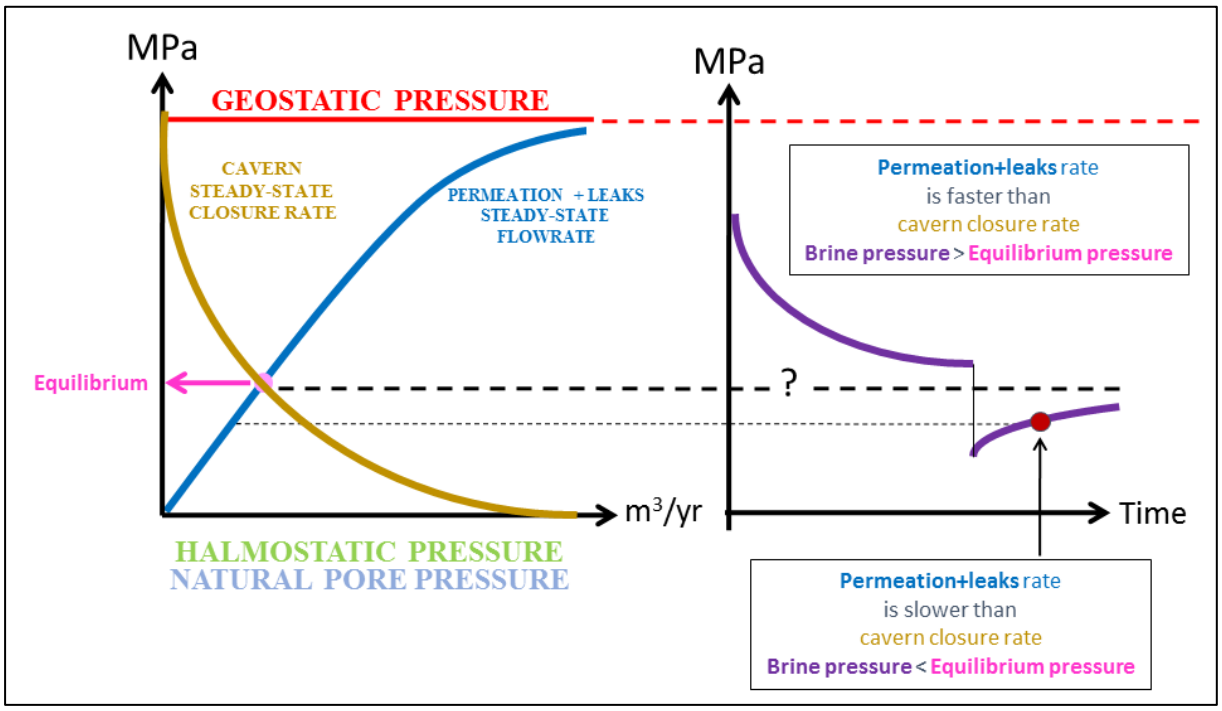

Figure 130. Cavern closure rate is a decreasing function of cavern pressure: it vanishes to zero when cavern fluid pressure equals geostatic pressure. Brine permeation (+ leak) flow-rate is an increasing function of cavern pressure; it vanishes to zero when cavern fluid pressure equals virgin pore pressure. When the two curves cross (left), the equilibrium pressure is reached. The trial-and-error method consists of successively testing several cavern pressures to obtain lower and upper bounds for the equilibrium pressure.

The steady-state closure rate curve (closure rate Q vs. wellhead pressure P) can be reasonably well drawn (Figure 131) before the test is performed as two points of the curve are known: O is the zero-closure point, reached when cavern pressure equals geostatic pressure (P_∞); OFT is the maximum closure rate point, which can be measured through an outflow test; the curve satisfies the relation $Q = A(P_\infty - P)^n$ where n is the exponent of the power law (at least in the case of an idealized spherical or cylindrical cavern) which is known from laboratory test. From the abandonment test and the equilibrium pressure, the equilibrium point (E) can be computed. From the equilibrium point (E), the slope (χ) of the steady-state permeation + leaks curve is obtained, and the average permeability can be inferred through a numerical computation.

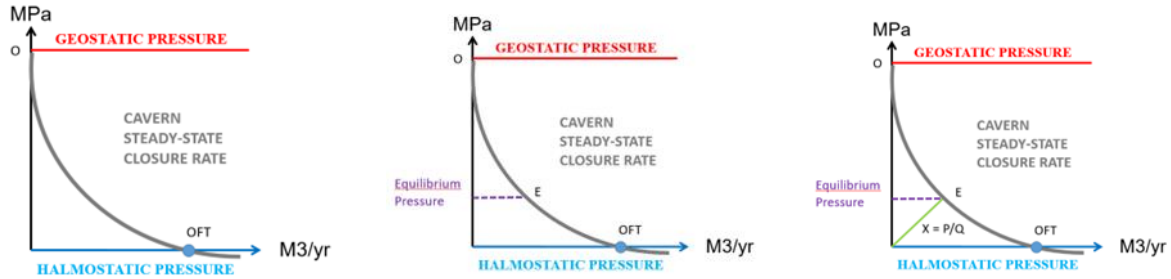

Figure 131. Determining cavern average permeability from the results of an abandonment test.

This method was used by Bérest et al. (2001a) to assess the average permeability of the EZ53 cavern at Etrez, France and found that "*it can be* $K = 2 \times 10^{-19} m^2$"; i.e., larger by one order of magnitude than the average permeability inferred from permeability tests performed in Etrez wellbores (see Table 8). This difference is consistent with Brace (1980).

4.2 Tightness tests

NB. the mechanical and transport properties of the host rocks of salt caverns are discussed at different places in this report.

4.2.1 Introduction

Salt caverns are deep cavities (from 300 m to 2000 m) that are connected to the ground level through a cased and cemented well. One to several strings are set in the well to allow injection or withdrawal of fluids into or from the cavern. These caverns are created in both bedded and domal salt formations by solution mining; they range in volume from 5000 m^3 to 5 000 000 m^3. They provide chemical plants with brine (mineral production) or, more commonly, are used to store hydrocarbons, compressed air, or waste. The tightness of a cavern and its external well components is a fundamental requirement to ensure that any leak does not cause contamination of drinking water resources or the unreasonable escape of stored products to the surface. Full-scale testing is necessary to ensure that acceptable tightness exists.

A great asset of hydrocarbon storage in salt caverns, when compared to natural gas or CO_2 storage in depleted reservoirs or aquifer layers, is that hydrocarbons occupy a well-defined volume, allowing for precise tightness tests to be performed before commissioning and during the operating life of a cavern. Such tests commonly are referred to as Mechanical Integrity Tests, or MITs. In most countries, conducting an MIT is a regulatory requirement and must be performed at various times during a cavern's life cycle. Every year, hundreds of mechanical integrity tests (MITs) are performed worldwide. A large amount of literature has been dedicated to various technical aspects of MITs. The Solution Mining Research Institute (SMRI) suggested a reference for interpreting the results of an MIT (Crotogino, 1996).

4.2.2 Maximum pressure in gas caverns

4.2.2.1 Introduction

A tightness test (Mechanical Integrity Test [MIT]) must be performed before commissioning a cavern. A tightness test consists of increasing cavern pressure to the maximum operating pressure (or slightly more) and monitoring cavern evolution over several days. The best method (Nitrogen Leak Test [NLT]) consists of lowering a nitrogen column to develop a brine-nitrogen interface below the last casing shoe in the cavern neck and monitoring the interface location over a couple of days: in a nutshell, too fast an interface rise is a sign of poor tightness. Monitoring wellhead pressures during the test provides additional information. When the cavern has no neck, lowering a light hydrocarbon column (instead of a nitrogen column) can provide good results. In some countries, tightness tests are performed periodically during the entire operating life of a cavern. Acceptance criteria were proposed by Crotogino (1996) (resolution of the testing system must be smaller than 50 kg/day and the maximum admissible leak rate is 150 kg/day) and by Thiel (1993) (the computed leak rate must be smaller than 1000 bbls/yr). In most cases, the results of the test performed before commissioning a cavern meet these criteria. (This is a remarkable achievement: when Thiel's fail/pass criterion is selected, the leak rate is smaller than 0.03%/yr in a 3-MMbbls cavern.) When they do not, various techniques allow identification of the weak zones of the cement column and repair of the well before performing a second tightness test (see, for instance, McLeod et al., 2011).

4.2.2.2 Selection of the testing pressure

The testing pressure must be selected carefully. It must be equal to or larger than the maximum operating pressure. Several companies prefer that the testing pressure equal the maximum operating pressure (Quintanilha de Menezes et al., 2001), as testing the well above the operating pressure can be harmful for future well integrity. Conversely, other companies prefer selecting a higher pressure, which provides additional confidence. One advantage of this second option is that, after several years of satisfactory operation, increasing maximum pressure is easier, as the cavern already has been tested for pressures higher than those used in operation. Maximum testing pressure must be smaller than the vertical stress

(0.22–0.23 bar/m, typically), which can be assessed through density logs and/or frac-tests. However, some safety margin must be left. There are two reasons for this: on one hand, the least compressive stress is not always the vertical stress – even if they often are equal; on the other hand, the cement behind the last steel casing often is weaker than the rock mass itself.

4.2.2.3 Margin of safety

The empirical, or pragmatic, approach consists of (1) estimating the weight of the overburden at cavern-shoe depth using density logs (density-based vertical stress), assuming that it equals the vertical stress, and (2) selecting a maximum admissible pressure that is a fraction (80–85%) of the vertical stress. This 15–20% margin of safety takes into account such factors as geological uncertainties, imperfectly known physical or mechanical processes (secondary stresses), and possible cement weaknesses, as explained above. Note that the tensile strength of the rock, which equals 5–10% of the vertical stress, typically, is not taken into account, which errs on the safe side. This method is robust, as it is based on simple mechanical principles and reliable measurements (density logs). In addition, performing frac tests can be useful, as they provide the value (an upper bound, in fact) of the least compressive stress (shut-in pressure). The maximum operating pressure must be re-assessed in the (rare) case that the shut-in pressure is smaller than the vertical stress, computed as explained above. Research on cementation (its evolution with time, fracturing mechanisms, logs) must be fostered, but it is doubtful that this research affects, in the short term, the rule mentioned above, which relies primarily on experience.

4.2.2.4 Assessing rock-mass volumetric weight

The SI unit for rock density (ρ) is kg/m^3. The unit for volumetric weight, $\gamma = \rho g$, is bar/m. Determining the actual density of the rock formations above the caverns is important in such a context. Pereira (2012) states that "*typical values of the overburden stress gradient may range from a low of 21.5 kPa/m (0.92 psi/foot) for a domal salt overlain by soft sediments, to a high of about 26 kPa/m (1.14 psi/foot) for a bedded salt largely overlain by dense limestone and anhydrite layers*" (p. 6-2) (see also Schreiner et al., 2010). Misinterpretation is possible, as explained by Rokahr et al. (2000). Before the Etzel test, described in Paragraph 3.4.6, it was assumed that the lithostatic gradient was 0.241 bar/m (1.06 psi/ft). Additional investigations from a newly referenced borehole, and three existing boreholes, led to a revised value of 0.204–0.211 bar/m (0.9–0.93 psi/ft) – a significantly smaller figure. Litho-density logs are convenient to use. Density measurements at the laboratory also can be used; they provide a lower bound of the in-situ rock density, which errs on the safe side.

4.2.2.5 Pressure gradient

Density, which is a site-specific notion, must be measured on a case-by-case basis. However, regulators often prefer rules that can be applied uniformly state-wide and define a maximum allowable pressure gradient, $\frac{dP_{max}}{dz}$ (e.g., in bar/m, or psi/ft), independently of local overburden densities values. This rule generally is accepted in the U.S. For instance, Texas Administrative Code § 3.97(k)(2) stipulates that "*The maximum operating pressure at the casing seat shall not exceed 0.85 psi/ft of depth*". In 2003, the Kansas Department of Health & Environment stated that: "*The maximum allowable operating pressure for underground natural gas storage wells shall not exceed 0.75 psi/ft*", or 0.17 bar/m (Poyer and Cochran, 2003, p. 199; note that in Kansas, storage caverns are 200- to 300-m deep). In a report prepared for the SMRI, Pereira (2012) indicates that "*the maximum regulated pressure gradient is 0.9 psi/ft (0.204 bar/m) in Louisiana and Mississippi and 80% of fracture pressure or 0.8 psi/ft in Canada*". In France, Germany and the UK, the maximum admissible pressure is "negotiated case by case" (J.C Pereira, 2012, pp. 6–14).

Research on cementation (its evolution with time, fracturing mechanisms, logs) must be fostered, but it is doubtful that this research affects, in the short term, the rule mentioned above, which relies primarily on experience.

4.2.2.6 Typical values of maximum pressure gradient in gas caverns

Most caverns meet this criterion (Table 6, page 174). Rummel et al. (1996) describe frac tests performed at Krummhörn, Germany, where three caverns had been leached out: casing shoe depths were about 1500 m, and the selected maximum pressure was 270 bar – an 0.18 bar/m (0.8 psi/ft) gradient. Istvan (1998) mentions a cavern under construction in Kansas in which the maximum gas-storage pressure was 1760 psi, a gradient of 0.88 psi/ft at 2000 ft (cavern depth not mentioned). Bruno and Dusseault (2002) discussed the case of pressure limits for thin, bedded salt caverns: the maximum pressure for such caverns must not exceed the estimated fracture pressure for the weakest lithology (margins of safety not specified). Chabannes (2005) mentions a cavern at Egan (Jennings salt dome, Louisiana) in which the maximum pressure gradient was 0.9 psi/ft. Colcombet et al. (2008) describe the Carriço Project, in Portugal: the maximum pressure was 180 bar, and the last cemented casing was around 1000 m (a 0.18-bar/m gradient). Schweinsburg and Schneider (2010) present a cavern at Etzel, Germany, where the casing-shoe depth is 1150 m and the maximum gas pressure is 200 bar–0.17 bar/m. (More recently, 208 bar was accepted.) Hoelen et al. (2010) dimensioned a four-cavern project at Zuidwending in the Netherlands. The caverns were to be operated between 90 bar and 180 bar, and the casing-shoe depth was 980–1028 m (an approximate gradient of 0.18 bar/m). In China, Fansheng et al. (2010) indicate "*gas injection-production pressure is [...] 170 bar to 320 bar for gas storage constructed in about 2000–m deep salt bed, and from 70 bar to 170 bar in about 1000-m deep salt bed*" (p. 190) – a maximum gradient of 0.16–0.17-bar/m. McLeod et al. (2011) describe a nine-cavern gas-storage facility at Aldbrough, Yorkshire (UK), in which the casing-shoe depth was 1500 m and the maximum pressure was 270 bar (a gradient of 0.15 bar/m). Bernhardt and Steijn (2013) discussed two cavern projects at Nüttermoor, Germany. There, the cavern-roof depths and maximum pressures at the casing shoe were, respectively, 1020 m and 945 m, and 170 bars and 160 bars. In Germany, Wagler and Draijer (2013) discuss a nitrogen-storage project in which the last casing-shoe depth is 648.2 m. The maximum pressure initially considered was 122 bars (a 0.188 bar/m, 0.83 psi/ft, gradient). Installing a new casing at a depth of 984 m led to a maximum pressure of 177 bars (a 0.18-bar/m, 0.8 psi/ft, gradient). Fawthrope et al. (2013) discuss construction of eight caverns at Holford, Cheshire (UK), in which the casing-shoe depth was 550 m and the maximum pressure was 100 bars, a gradient of 0.18 bar/m (0.8 psi/ft). In China, IRSM (Institute for Rock and Soil Mechanics, Wuhan) dimensioned new caverns, in which the gradient ranged from 0.16 bar/m to 0.188 bar/m (0.71–0.89 psi/ft), with the smallest value associated with the deepest site (Hongling Ma, personal communication, May 2018).

4.2.2.7 Higher values of the maximum operating pressure

It is tempting to select a maximum operating pressure larger than those suggested above (80–85% of the overburden pressure) to increase the amount of gas that can be stored in the cavern. For instance, Igoshin et al. (2010) describe three gas-storage caverns under construction at Kaliningrad, Russia. The cavern volume is 400000 m^3, and the maximum and minimum admissible cavern pressures are 180 bars and 52 bars, respectively. There, cavern depth is from 880 to 1020 m (casing-shoe depth not provided), making the gradient at the cavern top equal to 0.2 bar/m. Based on pneumatic tests, Schreiner et al. (2004) suggest a storage-pressure gradient of 0.19–0.205 bar/m or 0.84–0.91 psi/ft (around 85% of the geostatic pressure) for bedded salt formations and 0.18 bar/m in domal salt, as densities of the overburden are lower. The risk of a significant leak is greater when fluid pressure is higher, and that must be considered carefully. A high admissible pressure can be accepted when a large amount of information is available to increase confidence in the outcome. For instance, Arnold et al. (2014) mentioned that: "*The storage site Bernburg is operated since the early 1970's […] the rock mechanical dimensioning of caverns has been developed and enhanced continuously using comprehensive investigations [...] the most recently approved rock mechanical dimensioning includes a Pmax of 100 bars casing shoe depth is 490 m (gradient 2.04*)" (0.204 bar/m, 0.9 psi/ft) (p. 138). Johansen (2010) describes the Torup gas storage in Denmark. When the first caverns were created in 1981, the maximum pressure gradient was 0.175 bar/m (0.77 psi/ft). When

the last cavern was leached out in 1992, the accepted gradient was 0.184 bar/m (0.81 psi/ft). In these two cases, the increase in maximum admissible pressure was vindicated by the experience drawn from decades of satisfactory operation of existing caverns.

In our opinion, setting the maximum admissible pressure above the standard value (80–85% of the overburden weight) must be justified through a specific "*safety file*" that contains discussions of such topics as local sensitivity of the storage site (a layer of salt or plastic clay several hundreds of meters thick above the cavern roof is favourable, and a permeable cap rock within a small distance from the cavern roof is unfavourable), along with density log files, results of the MITs, etc.

4.2.3 Tightness tests, an historical perspective

Many kinds of tightness tests have been designed. The literature addressing cavern-well testing is relatively abundant. Van Fossan (1985) and Van Fossan and Whelply (1985) discuss both the legal and technical aspects of cavern-well testing and strongly support the Nitrogen Leak Test (NLT). They point out the significance of the minimum detectable leak rate (MDLR), or the accuracy of the test method. The ATG Manual (1985) describes a method in which a light hydrocarbon is injected into the annular space to a depth of 15 m below the last cemented casing shoe. The test pressure is 110% of the maximum operating pressure. The pass/fail criterion is a hydrocarbon loss rate smaller than 250 litres/day (85 m^3 /year; leak rates are computed in the pressure and temperature conditions prevailing at cavern depth). Heitman (1987) presents a set of case histories that illustrate several difficulties encountered when testing real caverns. Vrakas (1988) discusses the cavern-integrity program used by the US Strategic Petroleum Reserve, which includes both the NLT and the Pressure Observation Test (POT, or Liquid Leak Test, LLT). During a POT, results are somewhat erratic; in several cases, the wellhead pressure rises instead of decreases. (In hindsight, these results may be attributed to the effects of brine thermal expansion; see below). Diamond (1989) and Diamond et al. (1993) propose the ''*water– brine interface method*'', which originally was designed to test multiple-well caverns operated for brine production. These caverns are filled with brine, and the wells are shut-in. Soft water then is injected into one well. Because of the difference between water and brine densities, any upward displacement of the water–brine interface results in a pressure drop at the wellhead, which can be compared to the pressure evolution in a reference brine-filled well. Brasier (1990) strongly supports the interface method described by Diamond rather than the standard POT. Thiel (1993) describes several test methods based on the measurement of cavern compressibility. He suggests a 1000 bbls/yr (160 m^3/yr) MALR. Bérest et al. (2000) suggest distinguishing between the ''*apparent leak*'', the ''*corrected leak*'' and the ''*actual leak*''. They performed an NLT and simulated artificial leaks by withdrawing calibrated amounts of fluid from the closed cavern to assess NLT accuracy. Remizov et al. (2000) propose two pass/fail criteria: (1) the leak rate must be smaller than 20–27 litres/day when testing with a liquid or 50 kg/day when testing with gas; and (2) the pressure drop rate during an LLT must become constant and be smaller than 0.05% (of the test pressure) per hour. Branka et al. (2002) and Edler et al. (2003) describe innovative methods in which the central string is equipped with a weep hole: a testing fluid is injected into the annular space, and periodic searches for overflow are conducted to assess changes in the volume of the testing fluid. Thiel and Russel (2004) propose an LLT method for testing caverns in the state of Kansas, where the salt formation is thin and shallow, preventing a well-defined cavern neck—a prerequisite for any NLT method. The Solution Mining Research Institute (SMRI), an association of companies and consultants involved with salt caverns, has promoted research in the MIT field, including: the CH2 M HILL report (1995), which provides a practical description of the NLT; a report by Crotogino (1996) who proposes standards for the MDLR and the MALR (150 kg of nitrogen per day); a report by Nelson and Van Sambeek (2003) that addresses the issue of MIT techniques that can be implemented for gas-filled storage caverns; and a report by Van Sambeek et al. (2005). More recently, Skaug et al. (2011), Lampe and Ratigan (2014), Manivannan et al. (2015) have discussed the influence of transient disequilibrium in the vertical distribution of temperature in the wellbore. An historical perspective has been provided by Réveillère et al. (2017; 2021).

4.2.4 Different types of MIT: POT, NLT, LLI and PD

Several types of MIT will be discussed in more detail in the following: the Pressure Observation Test (POT), the (nitrogen) Mechanical Integrity Test (MIT), the Liquid-Liquid Interface test (LLI) and the Pressure Differential (PD) method.

4.2.4.1 The Pressure Observation Test (POT)

The Pressure Observation Test (POT) is the simplest (and coarsest) testing method. The cavern is filled with liquid (brine, in most cases); cavern pressure is increased to the testing pressure through liquid injection; after injection, wellhead pressure evolution is monitored for several days. A rapid pressure-drop rate is deemed to be a clear sign of poor tightness. More precisely, if βV is the cavern compressibility, during a rapid injection, $\beta V \dot{P} = \dot{v}$ and βV is the ratio between the volume of liquid injected in the cavern $(\dot{v})$ and the resulting pressure increase $(\dot{P})$. Cavern compressibility equals the cavern volume (V) multiplied by the cavern compressibility factor (β), which is the sum of the compressibility factor of brine plus the compressibility factor of the "hole", typically, $\beta = 4 - 5 \times 10^{-5}$ /bar. When the pressure-drop rate (in bar/day, for instance) is $\dot{P}$, the leak rate is deemed to be $\dot{v}_{leak} = \beta V \dot{P}$, negative in most cases. This test is too coarse, as many other factors (other than an actual leak), or "apparent leaks", contribute to the observed pressure-drop rate, including pre-existing brine warming $(\alpha V \dot{T} > 0)$, creep closure $(\dot{V}_{creep} < 0)$, additional dissolution, "reverse" creep, (van Sambeek et al., 2005), $\beta V \dot{P} = \dot{v}_{leak}(< 0) + \alpha V \dot{T}(> 0) - \dot{V}_{creep}(< 0) + \ldots$ Cases were reported in which wellhead pressure increased during the test (Vrakas, 1988), suggesting that the leak was negative! In addition – this comment is true for any kind of tightness tests – the initial pressure build-up at the beginning of a test triggers various transient effects which can hide the actual leak during several days or weeks.

Figure 132 and Figure 133 (Brouard Consulting et al., 2006) provide an example of this. Wellhead pressure is increased by 16.77 bar at the beginning of the test. During several days after the pressure increase, (Figure 132) wellhead pressure drops, suggesting a brine leak from the cavern. In fact, after one month (Figure 133) wellhead pressure increases. During the first weeks, transient effects govern well head pressure evolution. After one month more perennial effects (cavern creep closure, brine thermal expansion) become predominant.

For instance, Brasier (1990) correctly explained that

> *The theory* […] *is if the salt cavity is "shut in" and a leak develops* […] *a pressure decrease can be observed at the surface. This test was deemed inappropriate for two reasons* […] *given the enormous size of* […] *the cavities, a massive leak would have to be present in order to detect any pressure decrease. Any uncalculated pressure changes in the "shut in" cavity due to temperature fluctuations of cavity fluid, further dissolution of salt and salt heaving will interfere with the interpretation of the results making the test unreliable*. (p. 6).

A quantitative estimate of these "*uncalculated pressure changes*" can be found in Van Sambeek et al. (2005).

However, the main drawback of the POT is that it does not distinguish between apparent leaks from the cavern and leaks from the wellbore.

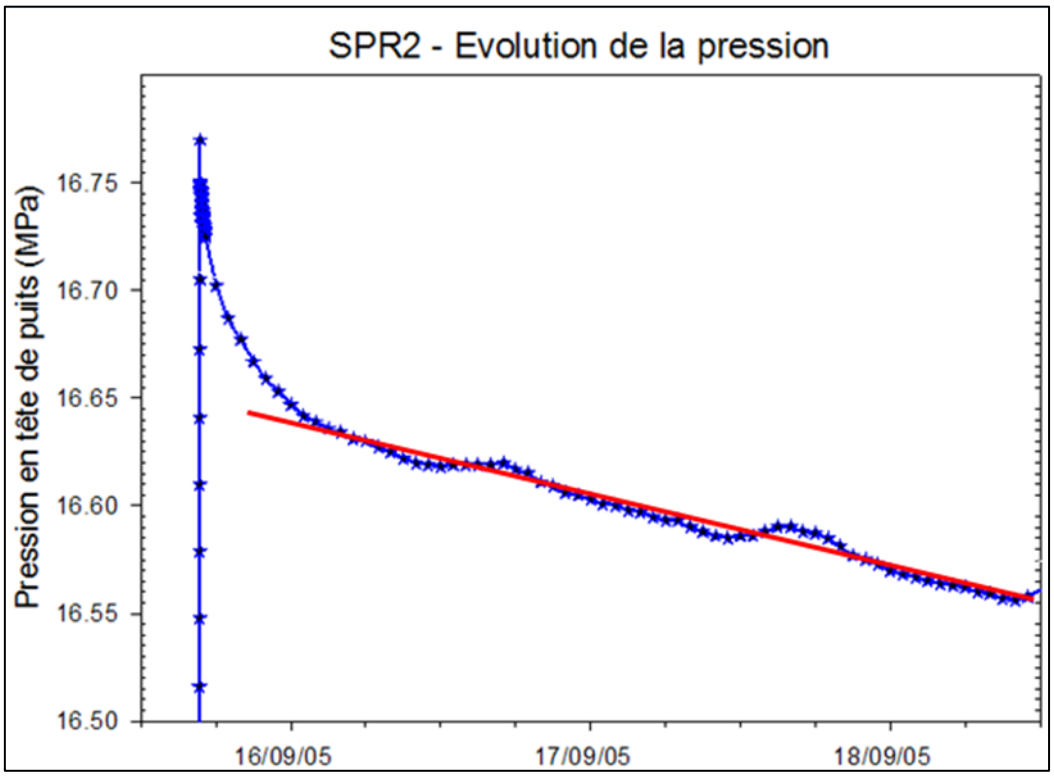

Figure 132. Wellhead pressure evolution during a 3-day test in Cavern SPR2, Carresse site in France. At the beginning of the test, well head pressure was increased by 1.677 MPa (16.77 bar).

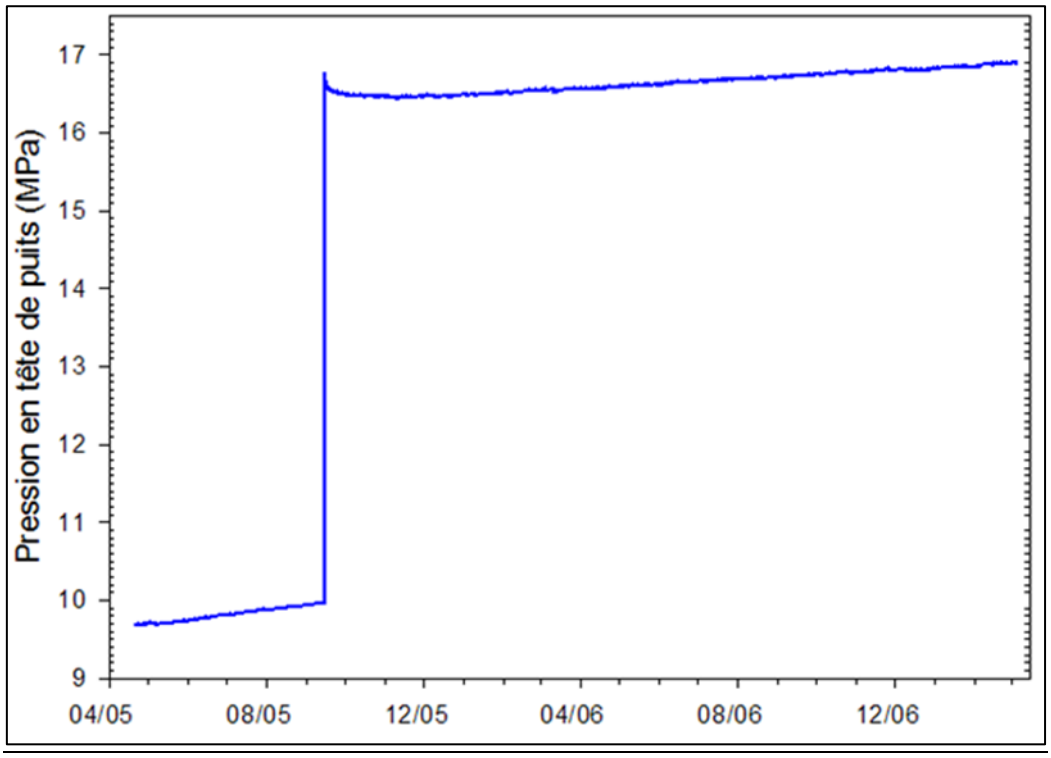

Figure 133. Follow-up of Figure 20. Pressure was measured during one year.

4.2.4.2 Nitrogen Leak Test (NLT) and Liquid-Liquid Interface Test (LLI)

In the early 1980s (Lampe and Ratigan, 2014), a much more reliable testing method was developed and implemented by the cavern industry, the Nitrogen Leak Test (NLT). In general, testing a pressure vessel

involves increasing the pressure in the vessel above the maximum operating pressure and detecting leaks through record of pressure evolution. A slightly different test procedure is possible in deep salt caverns. The cavern-plus-well system is similar to the ball-plus-tube system used in a standard barometer or thermometer. Compared to a huge cavern, the well appears as a very thin capillary tube, and tracking movements of a fluid-fluid interface in the well allows highly sensitive records of cavern fluid-volume changes.

The gas leak can be computed when multiplying the interface rise (The accuracy typically is $\delta h = 6''$, or 15 cm) by the cross-sectional area of the chimney at interface depth (or Σ, typically a fraction of a m^2). Correction can be made to take into account possible T, P changes during the test. Changes in gas mass can be computed quite accurately. This method is much better than the historical PV method, as it focuses on wellbore tightness (the topic of concern, see Section 2) rather than on the complex behaviour of the whole cavern. Because it is based on gas-mass balance, it is independent of all the phenomena described by Brasier (1990), and Van Sambeek et al. (2005), which blur the interpretation of pressure changes in the PV method.

The NLT consists of injecting nitrogen into the annular space formed by the last casing and the central string to develop a nitrogen/liquid interface in the cavern neck, below the last cemented casing and above the cavern roof. The central string and the cavern remain filled with brine, and a logging tool is used to measure the brine/nitrogen interface depth, or h. Two or three measurements, generally separated by 24 hours, are performed. Upward movement of the interface is deemed to indicate a nitrogen leak. Pressures are measured at ground level, and temperature logs are recorded to allow precise back-calculation of nitrogen seepage. The computed leak rate $\dot{v}_{leak} < 0$ is related to the interface rise rate $(\dot{h} < 0)$ by the simple relation leak $\dot{v}_{leak} = \Sigma \dot{h}$ where $\Sigma(h)$ is the annular cross-sectional area at interface depth. It sometimes is accepted that the duration of the MIT, Δt, and the accuracy of the interface displacement measurement, Δh, must be such that $\Sigma(h)\dot{h} = 1000$ bbls/yr = 450 liters/day The usual accuracy of standard logging tools is 15 cm (6 in), making $\Delta h = 0.3$ m (Two measurements are needed.); $\Sigma(h) = 1\ \mathrm{m}^2$ is typical. In such a context, uncertainties with magnitudes of a few dozens of liters are not significant. The test is more sensitive when the annular cross-sectional area is smaller and the test duration longer.

However, in some cases, a higher resolution and more accurate tools are needed. Meinecke et al. (2013) describe a case in which the interface was monitored continuously with an ultrasonic logging tool, providing an accuracy rating of 25.8 litres/day; Langlinais and Moran (2008) used a downhole camera to monitor the nitrogen/brine interface during an MIT, resulting in a minimum detectable leak rate of 58 bbls/yr or 25 litres/day. In the spirit of the SMRI standardization effort achieved by Crotogino (1996), Geostock (personal communication) considers that the accuracy of MITs should be better than 50 kg/day (≈ 65 litres/day) for gasoil and 150 kg/day for nitrogen.

Nitrogen is the preferred testing fluid when performing an MIT. However, in some instances, a liquid testing fluid is used (Liquid-Liquid Interface test, LLI or LLMIT), when, for example, the wellhead was not designed to withstand the high gas pressures involved during a nitrogen MIT or when cavern neck is not consistent, making difficult to set the interface at a precise location Figure 134.

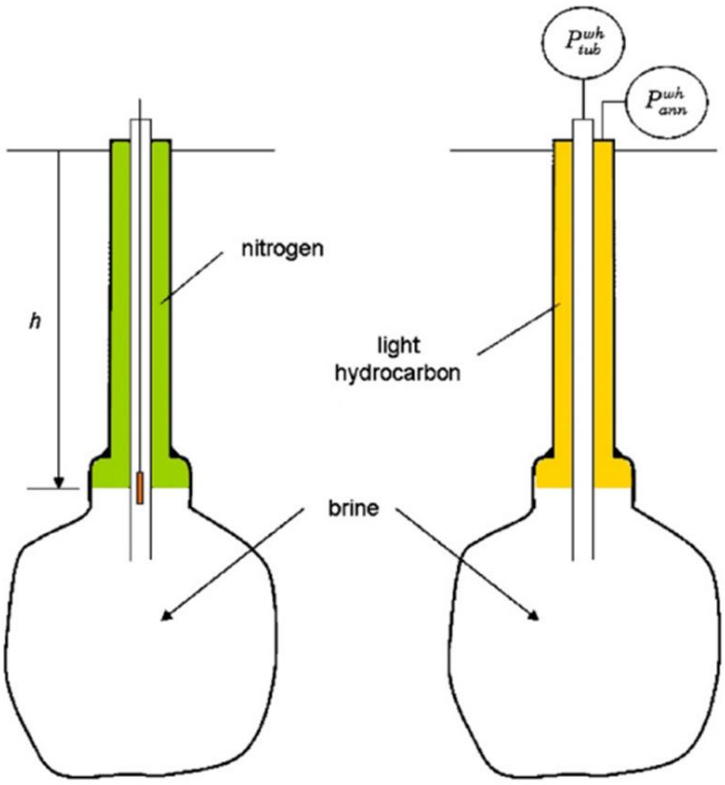

Figure 134. Tightness tests.

4.2.5 The pressure differential method

This method, first suggested by Diamond et al. (1993), applies to the NLT and LLI tests. The difference lays in the interpretation method. The Pressure Differential (PD) method is applied in addition to interface logging. This method (Figure 134 right) is based on wellhead pressure measurements (Bérest et al., 2021a, 2021b); and is explained below.

4.2.5.1 Testing Pressure

The test pressure (P_t) must be higher than the maximum operating pressure (P_M) and is proportional to casing shoe depth, or H. The ratio $\frac{P_t}{H}$ is the test gradient (in bar/m). For liquid or liquefied storage, the current operating gradient is 0.12 bar/m (*halmostatic* gradient, see below), and the test gradient typically is $\frac{P_t}{H} = 0.15\ \mathrm{bar/m}$. For natural gas storage, the maximum operating gradient typically is 0.18 bar/m, and the test gradient is $\frac{P_t}{H} = 0.2\ \mathrm{bar/m}$ — i.e., smaller than the geostatic gradient, which is $\frac{P_\infty}{H} = 0.22\ \mathrm{bar/m}$.

In most cases, the cavern pressure is *halmostatic* before the test.

4.2.5.2 Test Interpretation

Interpretation of the PV test is straightforward. A cavern is a compressible body. Any brine withdrawal (Q_{out}) generates a pressure drop, $Q_{out} = \beta V \times \dot{P}$, where V is the cavern volume, and β is the compressibility factor, which is the sum of (1) the adiabatic compressibility of brine, $\beta_b = 2.57 \times 10^{-5}$ /bar [which is related to wave speed in brine (c), $\beta_b \rho_b c^2 = 1$], (2) the compressibility of the cavern (the elastic "box" that contains brine, β_c), and (3) the effect of additional dissolution, β_{diss}. (Salt concentration in brine is a function of pressure.) A typical value is $\beta = \beta_b + \beta_c + \beta_{diss} = 4 - 5 \times 10^{-5}$ /bar is typical; larger values are found in "flat" caverns (Bérest et al., 1999). These figures explain why accuracy of the PV tests is poor. In the U.S., it is often accepted that the maximum admissible leak rate is 1000 bbls/yr, or 160 m^3/yr. When the cavern volume is $V = 300{,}000\ \mathrm{m}^3$, cavern

compressibility is $\beta V = 16\ \frac{m^3}{\text{bar}}$. When the accuracy of the pressure sensor is $\delta P = 1\ \text{kPa}$, the tightness test accuracy (i.e., the Minimum Detectable Leak Rate, or MDLR) during a test lasting $\delta t = 3\text{-day}$ is $2\beta V \times \frac{\delta P}{\delta t} = 300\ \text{liters/day}$.

The simplest interpretation of the NLT is as follows: the chimney cross-sectional area at interface depth is Σ ($\Sigma = 0.03\ \text{m}^2$ is typical), the interface rise rate is $\dot{h} < 0$, and the gas leak rate is assumed to be $Q_g = -\Sigma\dot{h}$. Accuracy of the interface tracking tool is $\delta h = 15\ \text{cm}$; when two consecutive measurements are separated by $\delta t = 3\ \text{days}$, the resolution is $2\ \Sigma\ \frac{\delta h}{\delta t} = 3\ \text{liters/day}$ — much smaller than the PV resolution. However, this interpretation is a little too simple: when the interface rises, brine pressure increases accordingly, and the cavern expands, hiding some of the actual leak.

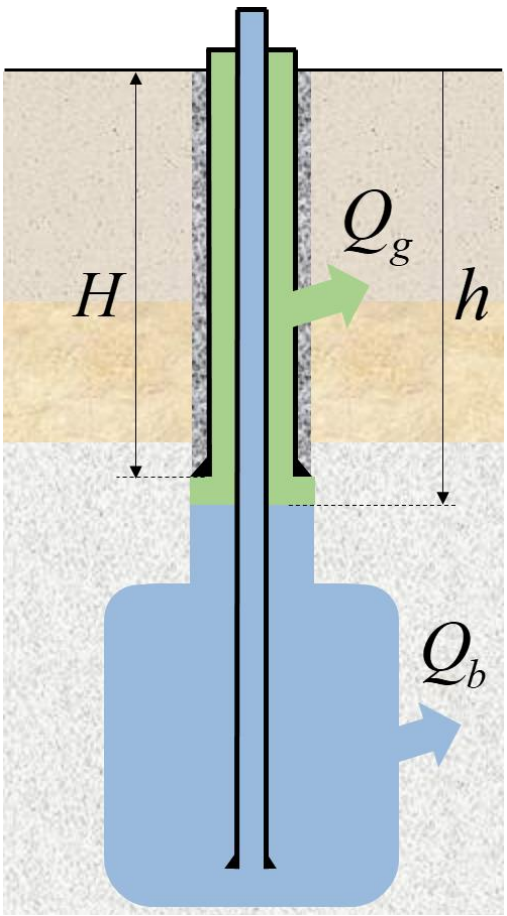

Figure 135. Gas Leak Test (H is the casing-shoe depth; h is the interface depth; Q_g is the gas-leak rate; and Q_b is the brine-leak rate.

A better interpretation requires modelling. The gas-state equation is $P = \rho\ rT$; the three variables are functions of depth (*z*, oriented downward) and

$$\frac{\rho_z^{'}}{\rho} = \frac{P_z^{'}}{P} - \frac{T_z^{'}}{T} = \frac{\rho g}{P} - \frac{G_{geo}}{T} = \frac{1}{T}\left(\frac{g}{r} - G_{geo}\right) \tag{46}$$

where G_{geo} is the geothermal gradient, and *g* is the gravity acceleration. For nitrogen, $r_{N2} = 260\ \text{J/kg/°C}$ and $\frac{g}{r_{N2}} = 0.038\ \text{°C/m}$ for hydrogen, $r_{H2} = 4200\ \text{J/kg/°C}$ and $\frac{g}{r_{N2}} = 0.0023\ \text{°C/m}$. The average geothermal gradient is $G_{geo}^{salt} = 0.016\text{°C/m}$ in the salt formation, and $G_{geo}^{rock} = 0.03\ \text{°C/m}$ above the salt formation, or $G_{geo}^{av} = 0.02\ \text{°C/m}$, as an average, from which, when $T = 300\ \text{K}$, $\frac{\rho_z'}{\rho} = 5 \times 10^{-5}\ \text{/m}$ for

nitrogen, and 6×10^{-5} /m for hydrogen. When the interface depth is $h = 700$ m, the relative error made when assuming that density is uniform is 1-2 %. (Obviously, gas density is a function of time.) Gas pressure distribution in the annular space is

$$P_g(z) = P_g^{wh}(t) + \gamma_g(t)z \tag{47}$$

where $\gamma_g(t) = \rho_g(t)g$ and $P_g^{wh}(t)$ is the wellhead gas pressure. For the brine column in the central string,

$$P_b(z) = P_b^{wh}(t) + \gamma_b z \tag{48}$$

where $P_b^{wh}(t)$ is the wellhead brine pressure. The gas mass is $m_g = \rho_g(h)V_g$, where V_g is the volume of gas in the annular space above the interface. Its derivative with respect to time equals the gas leak rate:

$$\Sigma\dot{h} + \beta_g V_g \dot{P}_g^{wh} + Q_g = 0 \tag{49}$$

where $\beta_g = \frac{1}{P_g^{wh}}$ is the isothermal coefficient of compressibility of nitrogen. (It is assumed that thermal equilibrium with the rock mass is reached, as the wellbore diameter is small.) For brine, a similar equation can be found:

$$-\Sigma\dot{h} + \beta V \dot{P}_b^{wh} + Q_b = 0 \tag{50}$$

where Q_b is the brine leak rate. (In fact, this term includes all the phenomena which, together with the actual brine leak, contribute to brine volume changes, such as thermal expansion.) Finally, gas and brine pressures are equal at interface depth:

$$(1+\delta)\dot{P}_g^{wh} - \dot{P}_s^{wh} + \Delta\gamma\dot{h} = 0 \tag{51}$$

where $\delta = \frac{gh}{r_g T}$ and $\Delta\gamma = \gamma_s - \gamma_g$. The interface compressibility, $\frac{\Sigma}{\Delta\gamma}$ (in m^3/bar), must be compared to the compressibility of the brine-filled cavern, βV, and the compressibility of the gas-filled annular space, $\beta_g V_g$. Using algebra, these formulas can be written

$$\begin{bmatrix} \beta_g V_g + \frac{(1+\delta)\Sigma}{\Delta\gamma} & \frac{-\Sigma}{\Delta\gamma} \\ \frac{-(1+\delta)\Sigma}{\Delta\gamma} & \beta V + \frac{\Sigma}{\Delta\gamma} \end{bmatrix} \begin{bmatrix} \dot{P}_g^{wh} \\ \dot{P}_b^{wh} \end{bmatrix} + \begin{bmatrix} Q_g \\ Q_b \end{bmatrix} = \begin{bmatrix} 0 \\ 0 \end{bmatrix} \tag{52}$$

$$\frac{1}{D}\begin{bmatrix} \beta V + \frac{\Sigma}{\Delta\gamma} & \frac{\Sigma}{\Delta\gamma} \\ (1+\delta)\frac{\Sigma}{\Delta\gamma} & \beta_g V_g + (1+\delta)\frac{\Sigma}{\Delta\gamma} \end{bmatrix} \begin{bmatrix} Q_g \\ Q_b \end{bmatrix} + \begin{bmatrix} \dot{P}_g^{wh} \\ \dot{P}_b^{wh} \end{bmatrix} = \begin{bmatrix} 0 \\ 0 \end{bmatrix} \tag{53}$$

$$-\frac{1+\delta}{\beta_b V_g} Q_g + \frac{1}{\beta V} Q_b - \left(\frac{1+\delta}{\beta_b V_g} + \frac{1}{\beta V} + \frac{\Delta\gamma}{\Sigma}\right)\Sigma\dot{h} = 0 \tag{54}$$

where $D = \beta V \beta_g V_g + \left(\frac{\Sigma}{\Delta\gamma}\right)\left[\beta_g V_g + (1+\delta)\beta V\right]$. For hydrogen, in a 1000-m deep cavern, $\delta = \frac{gh}{r_{H_2} T} = 0.0073$ (when $T = 320$ K) is very small when compared to 1. (It is less true for nitrogen, as $r_{N2} = 260$ J/kg/°C instead of $r_{H2} = 4200$ J/kg/°C).

Three "compressibilities" play a role:

1) cavern compressibility, $\beta V = 20$ m^3 with cavern volume $V = 50{,}000$ m^3;
2) compressibility of hydrogen in the annular space ($\beta_g V_g$) [A simple estimate can be reached as follows. Assuming that the chimney and the annular space cross-sectional area are not very different — for instance, $\Sigma = 0.024$ m^2. The hydrogen volume is $V_g = \Sigma h$. The pressure gradient

at the casing shoe during an MIT typically is $\gamma_t = 0.18$ bar/m, and $P_g = \gamma_t h = 180$ bar, from which $\beta_g V_g = \frac{\Sigma}{\gamma_t} = 0.133 \frac{m^3}{\text{bar}}$.]; and

3) interface compressibility, $\frac{\Sigma}{\Delta\gamma}$. (When gas pressure and temperature are 300 K and 180 bars, respectively, the hydrogen density is $\rho_{H2} = \frac{P_g}{r_{H_2} T = 14 \frac{\text{kg}}{m^3}}$, $\Delta\gamma = \gamma_b - \gamma_{H2} = 0.11 \frac{\text{bar}}{m}$, and $\frac{\Sigma}{\Delta\gamma} = 0.22\ \text{m}^3/\text{bar}$.);

and the relation between leak rates and wellhead-pressure rates can be written

$$\begin{bmatrix} 3.53 & -2.2 \\ -2.2 & 22.2 \end{bmatrix} \begin{bmatrix} \dot{P}_g^{wh} \\ \dot{P}_b^{wh} \end{bmatrix} + \begin{bmatrix} Q_g \\ Q_b \end{bmatrix} = \begin{bmatrix} 0 \\ 0 \end{bmatrix}$$

where units are m^3/day and MPa/day (or litres/day and kPa/day).

Two lessons can be drawn from these formulas.

1) The simplest interpretation of the NLT-type test, ($Q_g = -\Sigma\dot{h}$), can be wrong. When the gas leak rate is zero, the gas-brine interface can move when a brine leak is present, $Q_s - \left(1 + \frac{\beta V}{\beta_b V_g} + \beta V \frac{\Delta\gamma}{\Sigma}\right)\Sigma\dot{h} = 0$, giving the illusion of a "negative" leak, or $Q_g < 0$.
2) The gas-leak can be inferred from wellhead pressure evolutions. In the example discussed above, $Q_g[\text{L/day}] = 3.53\ \dot{P}_g^{wh}[\text{kPa/day}] - 2.2\dot{P}_b^{wh}[\text{kPa/day}]$. A good accuracy value is reached when the minimum detectable flow rate is much smaller than the maximum admissible leak rate, which is 500 litres/day. This condition is met when the accuracy of the pressure gages is 1 kPa.

This is important, as tracking the brine-gas interface with a logging tool is expensive. In the following, we suggest performing several tightness tests, with the interface being at several depths in the borehole. The method presented here allows continuous measurement of the leak rate at a low cost.

4.2.6 Fail/pass criteria

Two methods can be used to assess tightness test results. The first method, used widely in the nuclear industry, consists of building a safety case. A safety case includes leak scenarios and consequences, variants, worst cases, computations, and statistical analyses. Such a method is not used in the underground storage industry, as the occurrence of leak paths below ground are practically unpredictable, leading to unrealistic scenarios. The second method is more empirical; it is based on experience, analysis of past incidents and accidents, and collection of data on good practices in the industry.

The first fail/pass criteria for tightness tests were discussed by Van Fossan (1985) and by Van Fossan and Whelply (1985). These researchers introduced a fundamental distinction between the Minimum Detectable Leak Rate (MDLR), or test resolution, which results from analysis of the various uncertainties of the testing method, and the Maximum Admissible Leak Rate (MALR), which results from *a priori* economic and safety considerations. (This was a considerable breakthrough; at that time, it often was considered sufficient that the as-measured leak rate be smaller than the MDLR —not a big incentive to thorough uncertainties tracking.) In 1995 Crotogino (1996), in a report for the Solution Mining Research Institute (SMRI), suggested that, for a Nitrogen Leak Test, the MDLR and the MALR be 50 kg/day and 150 kg/day, respectively. (When it is assumed that, at cavern-shoe depth, pressure and temperature are 170 bars and 300 K, respectively, 150 kg/day is equivalent to 0.8 m^3/day, or 300 m^3/yr). In U.S., 1000 bbls/yr (160 m^3/yr) is somewhat of a standard for the MALR. (The value of 160 m^3/yr in a 320,000-m^3 cavern means that the relative leak rate is 5×10^{-4} /yr, a remarkable achievement.)

Crotogino's figures apply to a Nitrogen Test; for other fluids, he suggests taking fluid viscosity into account. Hydrogen is 15 times lighter than nitrogen and its viscosity is twice as low as that for nitrogen. Schlichtenmayer and Bannach (2015) measured salt permeability to nitrogen, hydrogen and natural gas at the laboratory and concluded that "*The main result of the measurements is that practically no difference in the permeability of rock salt for natural gas, hydrogen and air could be observed. Any difference in the permeation rates of the gases through a portion of rock salt (given that there are permeation paths existing) results only from their different viscosities*" (p. iv). It is noted that this might not be true for the steel casings.

An MALR of 50 kg/day (three times smaller than the leakage flowrate in kg/day, five times larger than the leakage flow rate in m^3/day suggested by Crotogino for nitrogen) can be considered as a provisional initial reference, open to discussion, and to be revised when additional experience (from tightness tests) becomes available.

4.2.7 Tightness tests in a hydrogen storage cavern

4.2.7.1 Not much experience is available

Several hydrogen storage facilities in salt caverns are planned to be created and operated in Europe. They will be the firsts of their kind (except for "compensated" caverns in Teesside, UK, commissioned in the 1970s). Hydrogen is a mobile gas, and the consequences of a leak reaching ground level might be severe. For these reasons, checking tightness is especially important, as adhesion to such projects by the regulatory authorities and the public is required. The case of a hydrogen storage cavern raises a couple of new problems, as hydrogen molecule is much smaller than methane molecule, for instance. Not much experience is available, and additional research and experimentation will be required. It seems (personal communication) that in the three hydrogen storages in Texas, the caverns were tested through a standard NLT before debrining the cavern (i.e., before filling the cavern with hydrogen.)

4.2.7.2 A proposal for a tightness test in a hydrogen storage in salt caverns

A testing methodology has been proposed by Bérest et al. (2021a, 2021b) suggested that, at least for the first hydrogen caverns to be created, four tightness tests be performed, as described below.

1) After drilling and before starting solution mining, a wellbore tightness test (leak-off test) is performed. Brine pressure during the test is the maximum admissible pressure. This test lasts for a few days.
2) Before commissioning, an NLT test is performed (Figure 136). Monitoring wellhead pressures and interface tracking with a logging tool are used to interpret the tests. The gas-brine interface in the annular space is set at different depths, successively (Figure 137); at borehole mid-depth (to check the accuracy of the measurement system through small deliberate gas withdrawal); above the casing shoe; and below the casing shoe (to identify possible leak locations).
3) The same test is repeated with hydrogen.
4) Tightness of the water-filled annular space is tested.

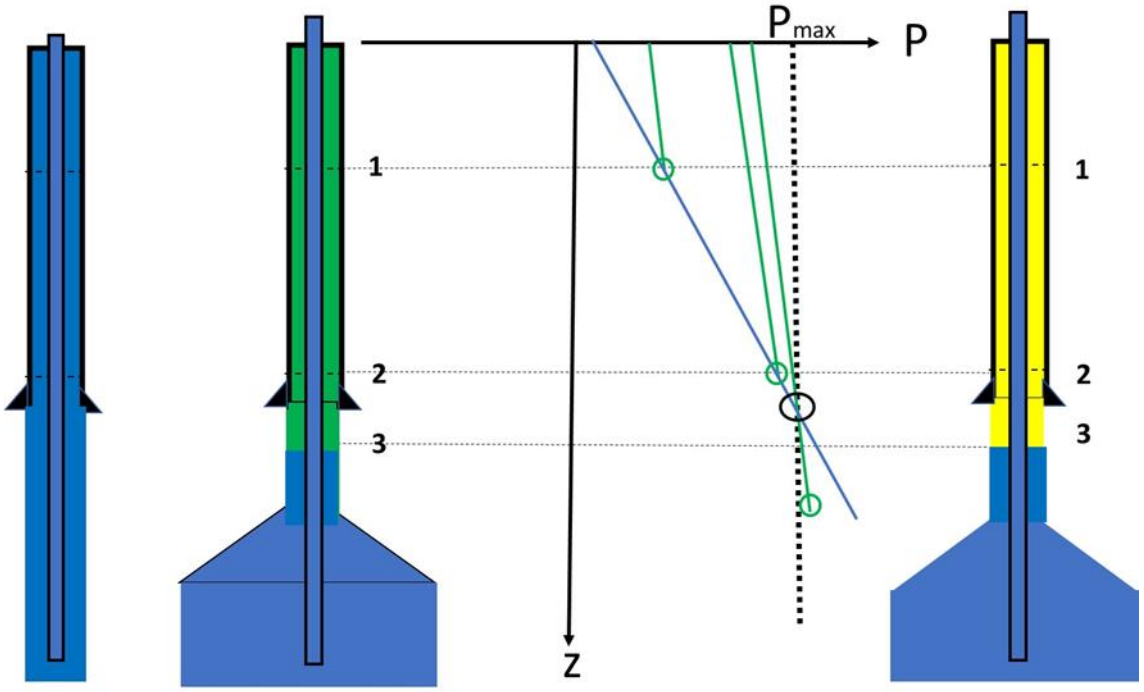

Figure 136. Test after drilling the borehole (left), Tests with nitrogen and hydrogen; the gas-brine interface is set at three different depths (centre), Test of the water-filled annular (right).

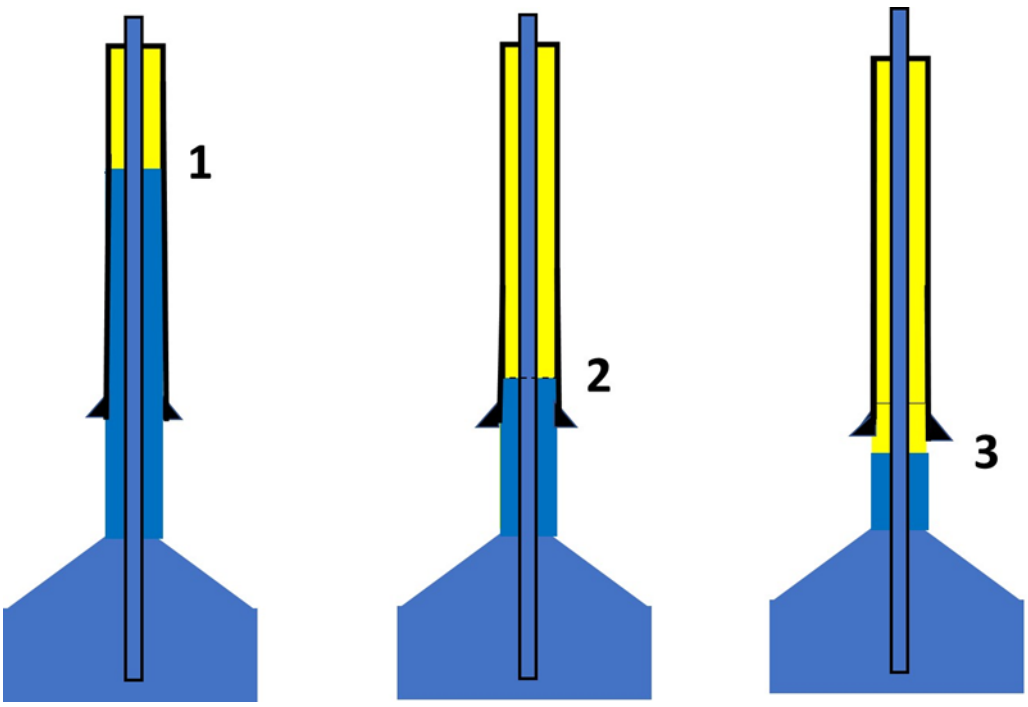

Figure 137. Different interface depths during the tests with gas.

5 Zechstein Salt in the Netherlands

5.1 The Dutch subsurface (onshore and offshore) and potential Salt caverns

Author: Janos L. Urai – GeoStructures Consultancy for Structural geology and Geomechanics

Permian Zechstein evaporites present in large parts of the subsurface of the Netherlands. Layers of rock salt, potassium-magnesium salts and sulphates form a highly complex structure, ranging from thick, tectonically undeformed salt to highly deformed and reworked tectonites in salt pillows and diapirs (Figure 138). In addition, salt from the Permian Upper Rotliegend Group, and the Triassic Röt, Muschelkalk and Keuper formations is also present (Geluk et al., 2007). Zechstein salt in the subsurface has a large effect on basin evolution as shown by areas with and without salt. Evaporites form regional seals for oil and gas, are mined for the chemical industry, and used to store materials and energy in the subsurface. When sufficiently shallow, sufficiently pure and massive, solution-mined caverns can be used to store natural gas, compressed air, liquid hydrocarbons and also hydrogen (Minister Blok (EZK) informed the House of Representatives about the deep underground as the storage room of the energy transition[1]). In most of the Netherlands the rock salt is too deep for these applications, as the creep of salt increases with temperature and pressure. Therefore, targets for salt cavern clusters are located in places where the salt is closer to the surface, in pillow and diapir structures. However, very little is known of the internal structure of these targeted structures (Figure 139).

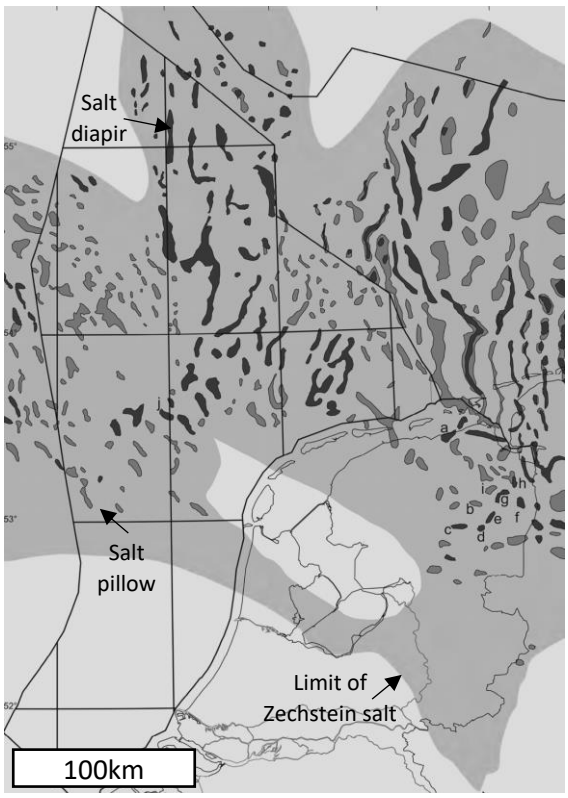

Figure 138. An inventory of salt structures (salt pillow is dark grey, salt is diapir black) in the subsurface of the Netherlands based on knowledge in 2007 (slightly modified after Geluk et al. 2007).

[1] https://open.overheid.nl/repository/ronl-a73cbf7f-755d-419e-b5cd-edfa98090b03/1/pdf/de-diepe-ondergrond-als-de-voorraadkamer-van-de-energietransitie.pdf

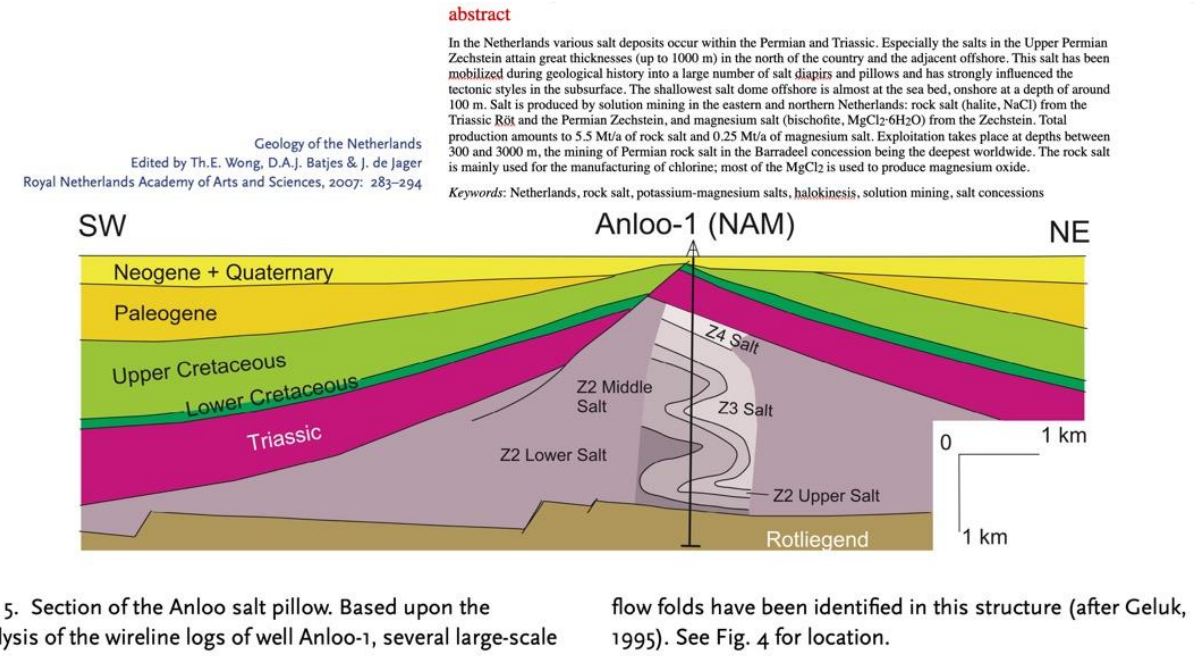

Figure 139. An attempt to understand the internal structure of the Anloo salt pillow, anno 1995 by Marc Geluk (after Geluk et al., 2007).

Onshore salt structures which are sufficiently shallow and sufficiently close to surface have been mapped in the past decades (Figure 140), and this information was used in several studies (Groenenberg et al., 2020b; Juez-Larré et al., 2019; Remmelts, 2011; van Gessel et al., 2021a, 2021b, 2018). In much less detail, a preliminary map of offshore structures was also presented in van Gessel et al. (2018). Caverns in offshore salt structures may become important in the future in combination with wind farms and locally generated green hydrogen.

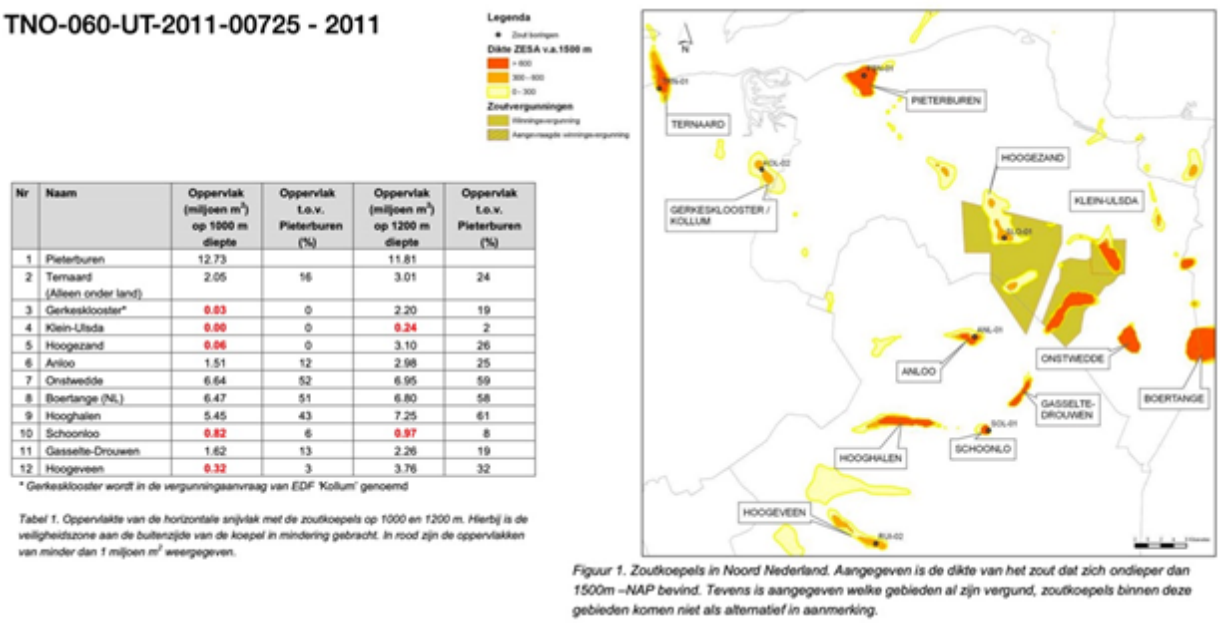

Figure 140. An inventory of salt structures in the North of the Netherlands made in 2011, with a first look at salt volumes at suitable depth for salt caverns (after Remmelts, 2011).

For the TNO reports, the salt structures have been explored including seismic (only partly depth-converted or 3D) and some exploration wells. Based on this data, an overview of all the potentially

suitable structures have been identified and documented (https://www.nlog.nl/steenzout) based on the limited data available, and reasonable assumptions about the spatial extent of the salt (top salt), a first assessment of the large number of potential caverns and their energy storage capacity was presented in TNO-report R11372 (van Gessel et al., 2018) (Figure 141 and Figure 142).

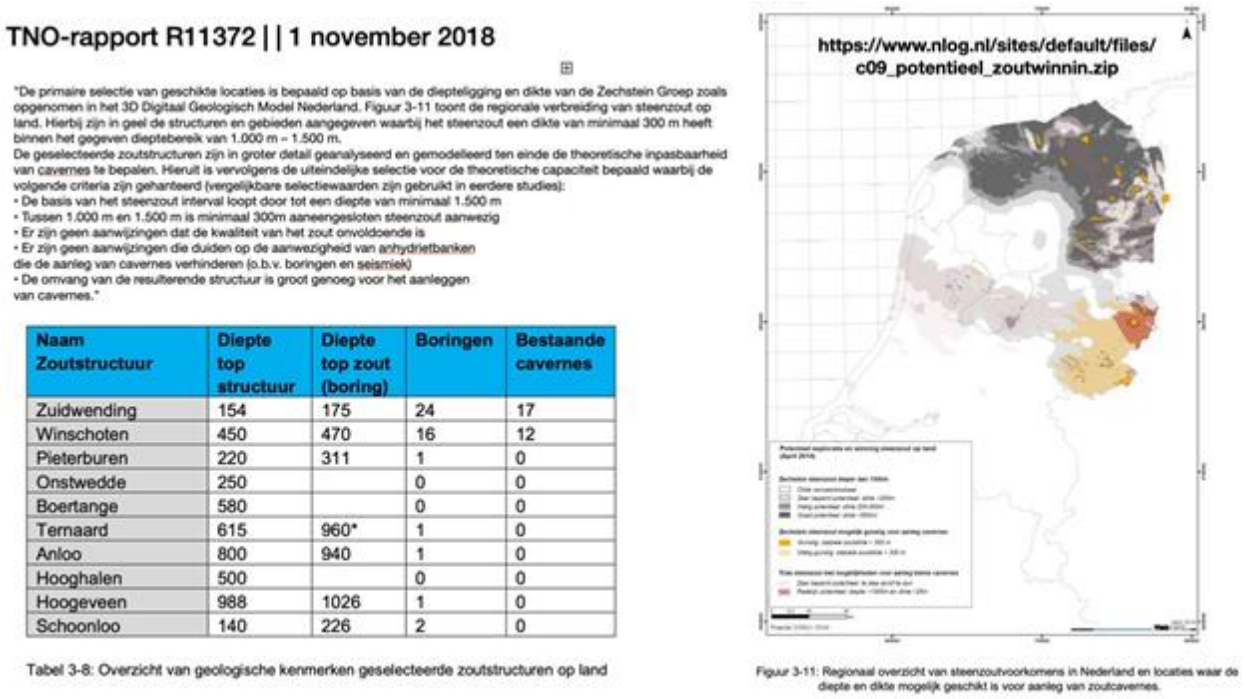

TNO-rapport R11372 | | 1 november 2018

"De primaire selectie van geschikte locaties is bepaald op basis van de diepteligging en dikte van de Zechstein Groep zoals opgenomen in het 3D Digitaal Geologisch Model Nederland. Figuur 3-11 toont de regionale verbreiding van steenzout op land. Hierbij zijn in geel de structuren en gebieden aangegeven waarbij het steenzout een dikte van minimaal 300 m heeft binnen het gegeven dieptebereik van 1.000 m – 1.500 m.
De geselecteerde zoutstructuren zijn in groter detail geanalyseerd en gemodelleerd ten einde de theoretische inpasbaarheid van cavernes te bepalen. Hieruit is vervolgens de uiteindelijke selectie voor de theoretische capaciteit bepaald waarbij de volgende criteria zijn gehanteerd (vergelijkbare selectiewaarden zijn gebruikt in eerdere studies):
- De basis van het steenzout interval loopt door tot een diepte van minimaal 1.500 m
- Tussen 1.000 m en 1.500 m is minimaal 300m aaneengesloten steenzout aanwezig
- Er zijn geen aanwijzingen dat de kwaliteit van het zout onvoldoende is
- Er zijn geen aanwijzingen die duiden op de aanwezigheid van anhydrietbanken die de aanleg van cavernes verhinderen (o.b.v. boringen en seismiek)
- De omvang van de resulterende structuur is groot genoeg voor het aanleggen van cavernes."

Naam Zoutstructuur	Diepte top structuur	Diepte top zout (boring)	Boringen	Bestaande cavernes
Zuidwending	154	175	24	17
Winschoten	450	470	16	12
Pieterburen	220	311	1	0
Onstwedde	250		0	0
Boertange	580		0	0
Ternaard	615	960*	1	0
Anloo	800	940	1	0
Hooghalen	500		0	0
Hoogeveen	988	1026	1	0
Schoonloo	140	226	2	0

Tabel 3-8: Overzicht van geologische kenmerken geselecteerde zoutstructuren op land

Figuur 3-11: Regionaal overzicht van steenzoutvoorkomens in Nederland en locaties waar de diepte en dikte mogelijk geschikt is voor aanleg van zoutcavernes.

Figure 141. 2018 map of possible locations onshore the Netherlands, for storage of Hydrogen in salt caverns. Map was made using the 3D Digitaal Geologisch Model Nederland, with a limited amount of new data since 2007. Note that only two of these salt structures have been explored in any detail internally (after van Gessel et al., 2018).

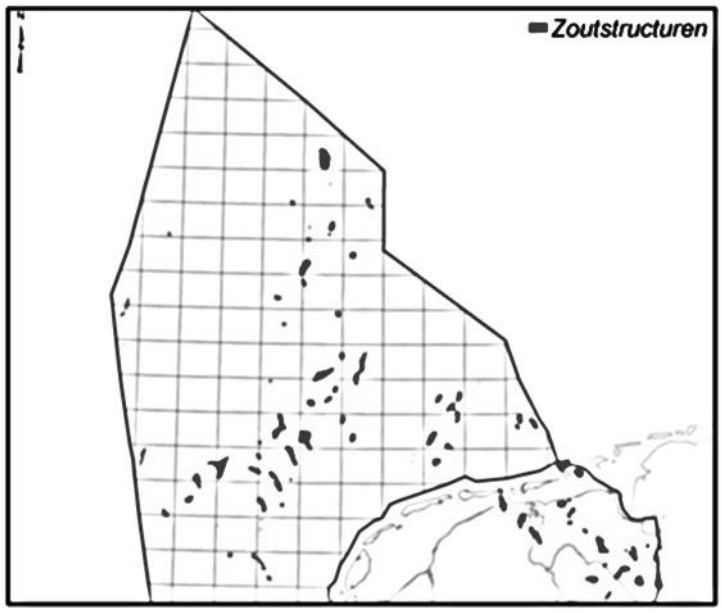

Figure 142. First look using a 2018 map of possible locations offshore the Netherlands, for storage of Hydrogen in salt caverns. Note that very few of these salt structures have been explored in any detail internally (after van Gessel et al., 2018).

In summary, the present state of reporting identifies the main potential locations, and provides a useful first look at the potential number of caverns which may be developed in these (Juez-Larré et al., 2019). The level of detail and approach fits well with the regional estimate for Europe (Caglayan et al., 2020).

On the other hand, although the existing reports clearly recommend further work to better constrain the external and internal structure, there does exist a range of methods which can be applied to learn more, before investing in drilling wells and acquiring new 3D seismic, and it is perhaps surprising that these studies have not been done until now.

Although usually described as rather homogeneous in solution mining, salt pillows and salt diapirs are heterogenous rock volumes with a complex internal structure evolved during deposition and large tectonic deformations (Rowan et al., 2019). A range of evaporitic and clastic lithologies, internal structures like folds, shear zones define smaller scale structures, with heterogeneous rock rheology, variable textures, and inclusions of fluids and gases. One of the challenges facing the solution mining industry is to accurately predict the geometry and properties of internal heterogeneities of salt formations so that the placement of salt caverns can be optimized and their stability understood and predicted, Figure 143 (Duffy et al., In review; Strozyk et al., 2014). More collaboration of the salt tectonic community and the solution mining industry is key in this process. Developing knowledge and improving our predictive capabilities will improve drilling, allow better control on cavern geometry, and reduce risks of cavern placement. Below we briefly describe some modern approaches which can be useful in the Dutch situation.

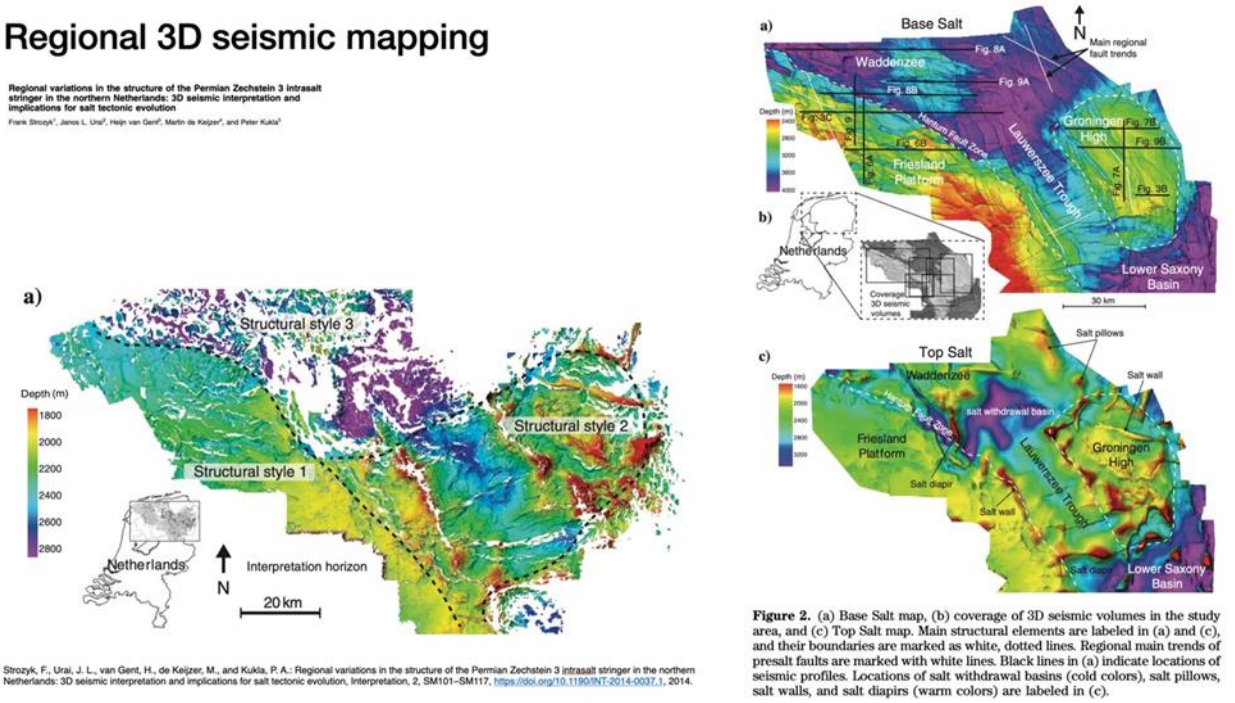

Figure 143. Regional analysis (Strozyk et al., 2014) of the external and internal structure of Zechstein based on high resolution PSDM 3D seismic. This analysis can be extended to understand in much more detail the potential sites for Hydrogen Caverns, as a basis for further location-specific investigations.

Firstly, using the pre-stack depth migrated 3D seismic available for most of the NE Netherlands, the evolution of each salt structure can be reconstructed (Mohr et al., 2005; Trusheim, 1957) from the sedimentary record, providing clues about the internal structure. Using the same 3D seismic, the local structure of the well-known Zechstein III Anhydrite stringers which can cause drilling problems and major problems with cavern construction and stability (Barabasch et al., 2019; Kukla et al., 2019; Strozyk et al., 2014, 2012; van Gent et al., 2011), can be estimated. Secondly, there is a major issue with cavern

construction is the presence of K-Mg salts (Raith et al., 2017, 2016) which can cause problems with cavern development and stability; the regional and local distribution of these is not well known but can be studied using the wealth of well data available.

Finally, our understanding of the internal geometry of salt structures has made rapid developments in the past decade, integrating knowledge from salt mines, 3D seismic, numerical modelling and understanding of the complex, layered rheology of evaporites (Rowan et al., 2019). With the rapid development of 3D geomechanical modelling it is becoming possible to perform 3D geologically constrained forward models of specific salt structures, as a basis of a better understanding of internal structure and integration with 3D seismic, GPR measurements in wells and positioning of wells in future cavern clusters (See smartTectonics contributions, this report).

In summary, although the majority of possible locations have been identified, the internal structure of the Dutch subsurface salt structures which are potentially suitable for the construction of Hydrogen storage caverns is not well known and determining suitability for caverns needs much more work using available validated methods – a significant part of this can be done before investing in data acquisition by high resolution seismic and measurements in wells. In the research part of this project, we aim to provide detailed descriptions and recommendations of possible steps in this direction. Carrying out this research can significantly reduce the risks of cavern development and operation in future Hydrogen Storage in the Netherlands.

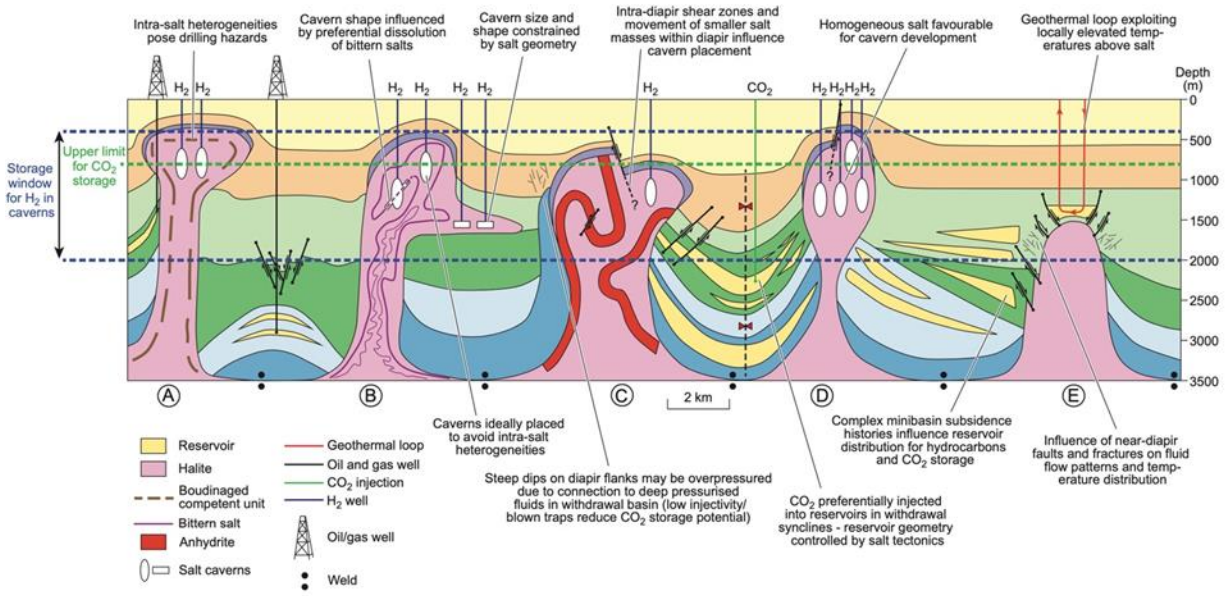

Figure 144. Illustration of the multitude of internal structures which can cause problems with cavern development and operation for Hydrogen storage (from Duffy et al., 2022).

5.2 Salt seismicity in general and Dutch situation

Authors: Tobias Baumann – smartTectonics GmbH and Janos L. Urai – GeoStructures
Consultancy for Structural geology and Geomechanics

"Induced seismicity and subsidence have increasingly become important risks that the wider public in the Netherlands is aware of, especially because of the issues with the Groningen gas field." (van der Valk et al., 2020). However, to our knowledge, no example of damage generated by an external earthquake (for example generated in the underlying Groningen Gas field below) on a salt cavern has been described in the literature. Accelerations are much smaller underground than at ground level – which is a zero-stress surface, hence a maximum-displacement surface. Wavelengths that are of the same order of magnitude as cavern radius can be harmful. In the vicinity of caverns, microseismic events are triggered by block falls and rock mass rearrangement at cavern wall. They become extremely frequent before the onset of a crater (Contrucci et al., 2011); however, their magnitude seems to be relatively small. Caverns may induce seismicity in the overburden and in the caprock of salt structures. Compared to the induced seismicity and subsidence related to the depletion of conventional gas reservoirs, the seismicity and subsidence induced by (conglomerates of) salt caverns for UHS primarily relate to the salt creep as a response to cavern operation, i.e., induced pressure and temperature changes. A recent example is described in Muntendam-Bos (2022), where a series of seismic events was monitored at the Heiligerlee cavern field in the Winschoten salt diapir and a significant number of them was localized at the salt overburden interface, possibly on pre-existing faults.

In principle, the specific occurrence of induced seismicity due to hydrogen storage in salt caverns is a topic that has not yet been documented much in the literature. This section provides an overview of possible causes of seismicity related to operating and abandoned salt caverns, and salt structures in general. We review the literature articles that describe microseismic events associated with caverns and assess the situation for hydrogen caverns.

5.2.1.1 Natural and induced seismicity

Natural seismicity in the Netherlands is mostly restricted to the fault systems in the southern parts of the Netherlands, which can be seen as the north-western extension of the Rhine rift system. Here, earthquakes have normal faulting and strike slip faulting source characteristics. In history, the damage to urban infrastructure has been rather moderate. The maximum expected magnitude based on historic seismicity data scales to M_L= 6.3 or even M_L=7.3 (Dost and Haak, 2007). According to (Dost and Haak, 2007), no significant natural seismicity has been detected for the Northern part of the Netherlands. Since 1986, events coincide with the location of producing gas fields at relatively shallow depths (1-3 km), https://www.parlement.com/id/vlc2ot26wbwc/parlementaire_enquete_aardgaswinning.

5.2.1.2 Induced seismicity in the Netherlands

In the Netherlands, the vast majority of induced seismic events is caused by seismic slip on reactivated faults in producing gas fields. See also https://www.nlog.nl/en/induced-seismicity and Muntendam-Bos et al. (2022).

5.2.1.3 Seismicity related to salt structures and induced seismicity related to salt caverns

Mechanically, salt rocks deform in a ductile manner also on relatively short time scales unlike most sedimentary rocks (e.g., Jackson & Hudec, 2017). Due to the relatively low density, salt rocks are buoyant and evolve in pillows or domes depending on the tectonic regimes they have experienced in their geological history. Overall, the dynamics of the salt structures is a complex geodynamical process with a

variety of different driving mechanisms. However, locally, most salt domes in the Netherlands are associated with a local extensional regime in the overburden above the salt structure, in which typical normal faults have developed in during the geological history. These faults are remnants of the active Halokinesis periods in the Netherlands, predominantly dating back to the Triassic (Geluk, 2005). Although it cannot be ruled out completely, they are not generally known to be active at present. In terms of seismicity, these existing fault systems are possible hypocentres for seismic events associated with the natural dynamics of salt domes and denote characteristic weak zones (Baumann et al., 2022b; Schultz-Ela et al., 1993; Schultz-Ela and Jackson, 1996).

The dynamics of salt structures are controlled in large part by the rate at which the salt structure creeps. The creep of salt rocks is based on microstructural deformation mechanisms of the granular rock salt structure (e.g., Urai et al., 2008), and leads to strain rates that can locally vary by orders of magnitude depending on the local state of stress (Bérest et al., 2019a; Spiers et al., 1990; Urai et al., 2008), depending on the associated dominant creep mechanism and the degree of heterogeneity (Baumann et al., 2019).

Essentially, a cavern field also represents a thermomechanical heterogeneity that induces stress in the adjacent rock mass as a function of the engineering parameters (cavern pressure and temperature). As a response to the induced stress, the microstructure of the rock salt may change and causes a switch in the dominant creep regime, which in turn accelerates local creep rates as described in other sections (3.6 and 5.3) and ultimately lead to controlled or uncontrolled convergence of the caverns. As a result, various characteristic sources of seismicity appear plausible, which are shown in Figure 145. In general, it seems logical that seismic events induced by salt cavern operation with the largest magnitudes appear to locate in the overburden, caprock and side burden rocks on pre-existing faults adjacent to the salt dome (Muntendam-Bos et al., 2022; Ruigrok et al., 2019, 2018; van der Valk et al., 2020). However, it should be noted that a precise hypocentre location depends on a velocity model that is often biased by the presence of the salt structure and the large variations in the 3D velocity field (Ruigrok et al., 2018). Thus, a regional seismic network leads to inaccurate hypocentre localizations, which can be improved by certain optimizations in the localization workflow (Ruigrok et al., 2018), but remain inaccurate unless a local network, preferably with borehole seismometers, is involved (Muntendam-Bos et al., 2022; Ruigrok et al., 2019, 2018; van der Valk et al., 2020).

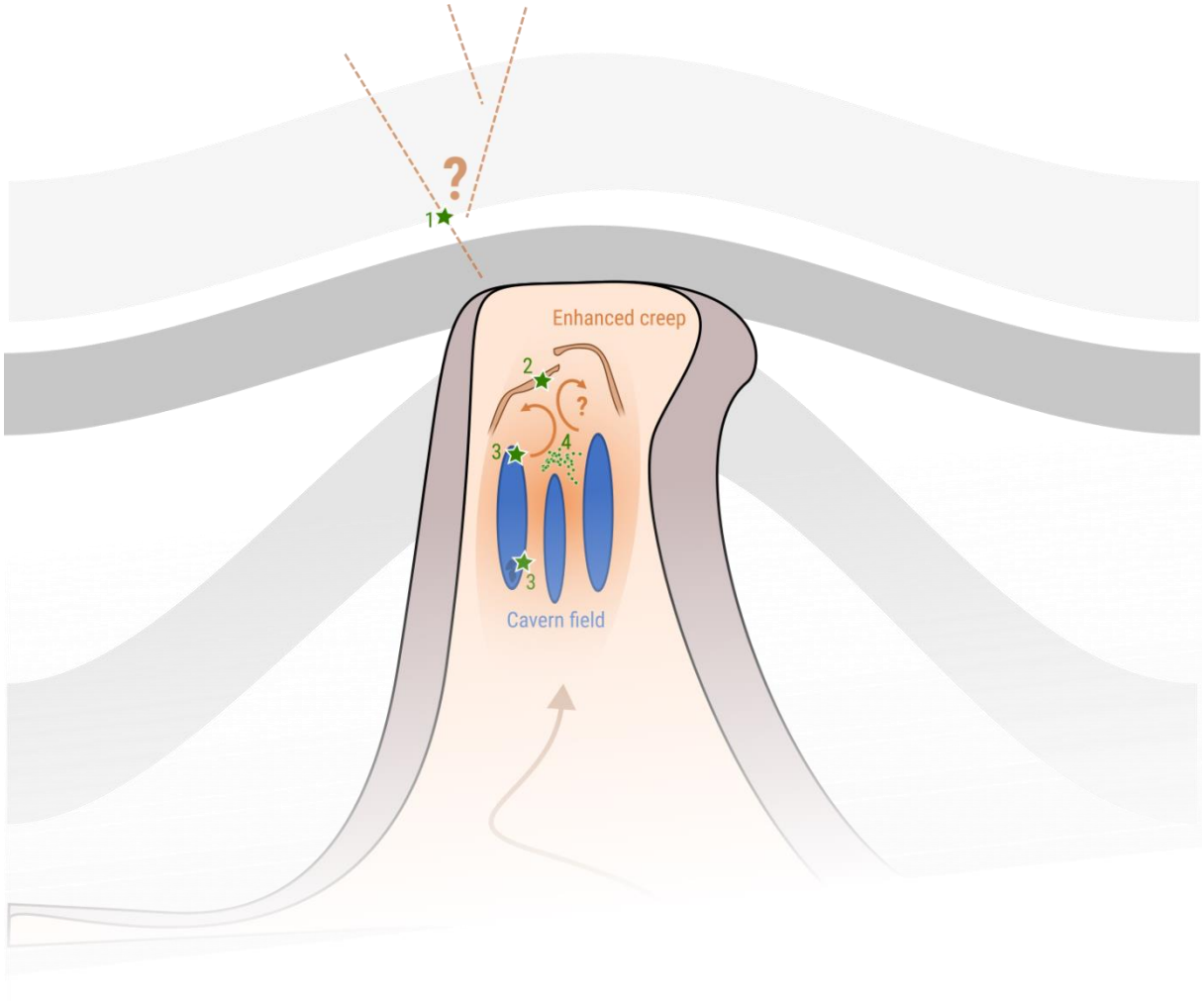

Figure 145. Possible causes of induced seismicity due to the existence of salt caverns. The presence of caverns changes the state of stress in the vicinity of the caverns. Consequently, enhanced creep rates may be induced due to a switch in the rock salt microstructure. Overall, this could ultimately lead to re-activation of supra-salt faults (1). Salt internal heterogeneities will likely amplify this effect. In the context of salt dome heterogeneities, Anhydrite layers have a special role as they accommodate much higher stresses than the rock salt and deform in a brittle manner on short time-scales, thus Anhydrite layers are possible hypocentres for induced seismicity (2). The number of reasons may also lead to instabilities in the roof of caverns (3), which may ultimately lead to rock-fall events of parts of the cavern roof into the cavern (3). These rockfall incidents may come along with a seismic signature but have distinct seismic source mechanisms that are distinguishable from shear-faulting events in (1) and (2) provided a well-equipped micro- or nano-seismic network is available. (4) In addition, it is known from salt mines, that acoustic emissions are present adjacent to cavities at the boundaries of different salt-rock types in salt domes. These acoustic emissions already appear at stresses below the dilatancy boundary where microcracking occurs on the level of grain boundaries.

Figure 146 shows an example of a M_w=1.28 event that occurred at the western flank of the Heiligerlee salt dome on November 19, 2017 as suggested by the localization probability (Ruigrok et al., 2018). However, Figure 146a and b indicate the 95% confidence interval that laterally covers the entire cavern field located in the Heiligerlee salt structure. The event location with the highest probability locates at the interface between the North Sea group and the Chalk group close to the top of the dome. The localization result agrees with a spectral analysis. Ruigrok et al., (2018) argue that a seismic event that originates close to one of the caverns would cause revibrating waves being trapped in the cavern due to the impedance effect (gas or brine and halite) and a resonance effect should be detectable. Their spectral analysis reveals that it is unlikely that the event was close to most of the brine-filled caverns, but a cavern filled with Nitrogen and one out of the 12 brine-filled caverns could explain the resonance pattern in the amplitude spectra. A similar seismic event occurred on January 09, 2019 at the southern flank of the Zuidwending salt dome (Figure 147). As in the case of the 2017 Heiligerlee event, the localization accuracy is not good enough to rule out the hypocentre within the salt dome, but the seismic wave characteristics of both

events have strong similarities such that an origin at the salt dome flank seems most likely (Ruigrok et al., 2019).

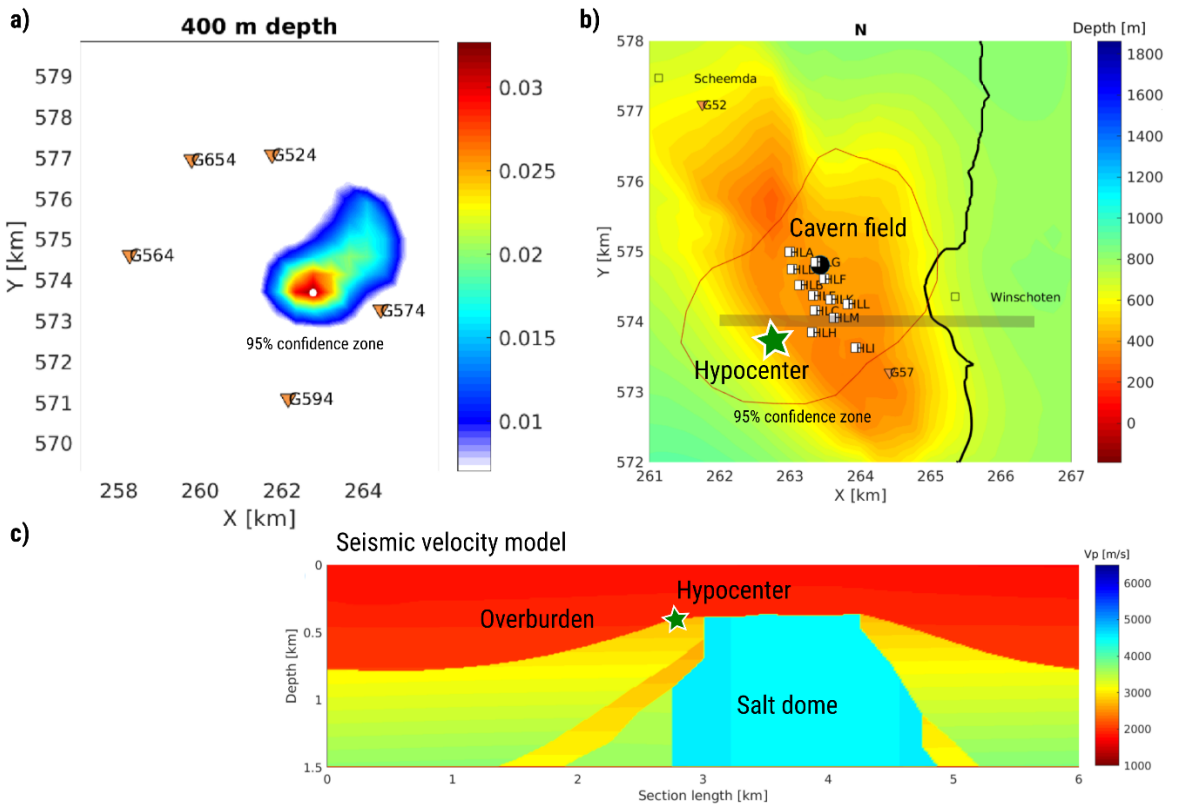

Figure 146. Example of seismic event localization at the Heiligerlee salt dome (2017) with stations of a regional seismic network (modified after Ruigrok et al., 2018). a) Lateral localization accuracy. Colours indicate hypocentre location probabilities. b) Map with depth of Base North Sea Group, and caverns of the Heiligerlee salt dome. Star indicates best matching hypocentre location and line shows the orientation of the cross section shown in c) Solid red line indicates the 95% confidence interval of the hypocentre. c) Cross section with the p-wave velocity model and the hypocentre at the interface between North Sea Group and Chalk Group in the vicinity of the southern flank of the dome.

Another example presented by Muntendam-Bos (2022) refers to events associated to the shallow salt caverns in the Twente area. As a response to a sinkhole event, the operator installed a local micro seismic network to monitor the stability of their caverns between 2016-2017. So far, 59 events with magnitudes ranging between $-2.6 \leq M_L \leq 0.0$ were recorded. Although 10 events were identified to be associated with microcracking events in the vicinity of the caverns, most of the events were related to shear faulting events on known faults in the area.

All these examples demonstrate well that, despite an advanced investigation, it is very difficult to locate such a seismic event with a high precision using a regional seismic network. A local microseismic network is required to detect and locate these events with a higher precision, also because the frequency characteristics are within the range of urban seismic noise (~1-35 Hz e.g., Boese et al., 2015; Groos & Ritter, 2009; Maciel et al., 2021). In addition, an advanced velocity model that accounts for the 3D geometry of the salt dome may be required to achieve the required localization accuracy (e.g., Ruigrok et al., 2018).

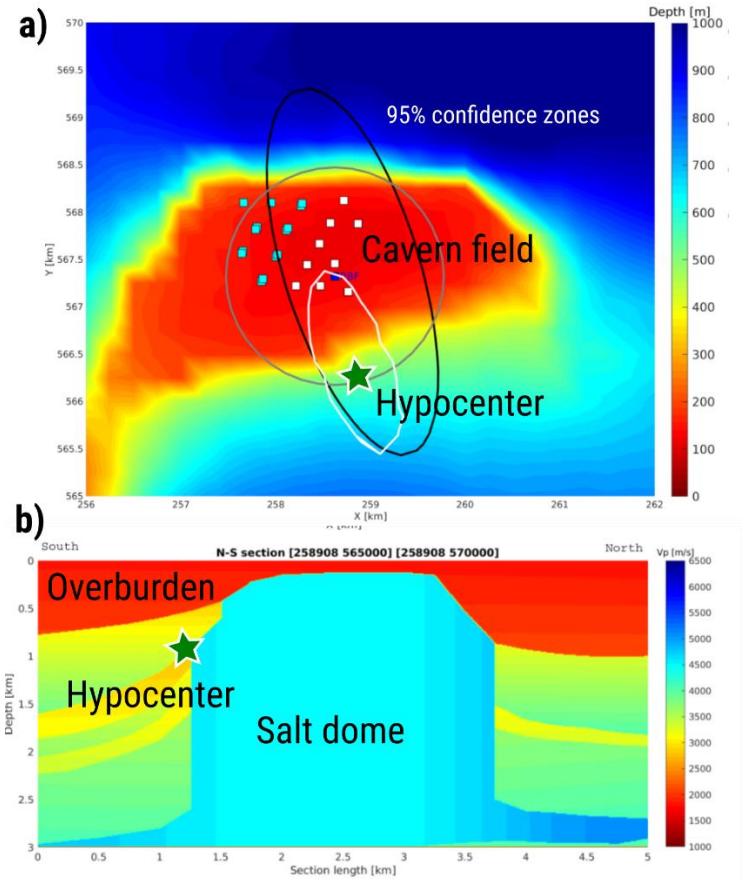

Figure 147. Similar example as in Figure 146, but for an event at the Zuidwending salt dome in 2019 (Ruigrok et al., 2019). a) Lateral event localization with error ellipses and cavern locations in the Northern part of the Zuidwending salt dome. b) Cross section with vp velocity model and the best matching hypocentre location at the southern flank of the Zuidwending salt dome.

In case of Heiligerlee, a local microseismic network with eight (twelve from 2019 onwards) borehole seismometers (50-60 m depths) was installed by the operator in 2018 (Muntendam-Bos et al., 2022). Muntendam-Bos et al. (2022) refer to Bosq et al. (2020), who describes a number of 46 events in a magnitude range $-1.21 \leq M_L \leq 0.65$. 38 events are associated with only two caverns, a significant number of which are likely related to the salt overburden interface and the caprock. Other events were located at the same depths as the caverns and four events indicate clear features of rock fall-events (resonance effects).

Kinscher et al. (2015) and Mercerat et al. (2010) describe a local microseismic monitoring of a salt cavern over a period of two years prior to the collapse of a cavern roof. About 2000 events have been recorded where most events occurred in clusters and were located in the cavern roof. Some of the isolated events had a clear tensile component in their source characteristics showed rock fall- type event properties (Mercerat et al., 2010). Overall, the authors demonstrated that the microseismicity represented the detachment of the cavern roof by tracking a spatial and temporal migration of the microseismicity (Kinscher et al. 2015).

Besides shear fault events in the overburden (Figure 145, no. 1) and isolated rockfall events (Figure 145, no. 3) that may be associated with event clusters in the cavern roof (Figure 145, no. 3), it also seems plausible that seismic events occur in the brittle deforming anhydrite stringers if present in the salt dome stratigraphy (Figure 145, no.2). Compared to the adjacent rock salt the Anhydrite layers accommodate much higher stresses, which could be enhanced due to cavern operation and induced creep and lead to shear faulting events. However, these events are likely to have smaller fault surfaces than shear faulting

events on pre-existing overburden weak zones and would be expected to have smaller magnitudes. In addition to microseismic events, acoustic emissions are reported around backfilled cavities and salt mines.

5.2.1.4 Acoustic emissions around salt cavities and salt mines

Acoustic emissions adjacent to caverns and cavities in salt mines are reported to locate along boundaries of different rock salts (Manthei and Plenkers, 2018) and at the interfaces between Halite and Anhydrite blocks (Köhler et al., 2009). This coincides with locations of higher differential stress (Baumann et al., 2019) of heterogeneous salt structures.

5.2.1.5 Possible damage due to the occurrence of induced seismicity related to salt caverns

Historically, underground structures are affected less by earthquakes than structures at the surface. In very large (M > 6) earthquakes, underground structures may develop some damage but much less than surface structures. Damage tends to decrease with increasing overburden depth. Underground facilities constructed in soils tend to have more damage compared to those constructed in rock.

The first reason for this is that there are two kinds of seismic waves: body waves (P and S) and surface waves (L and R). Surface waves only develop near the Earth's surface and play a negligible role in the subsurface. Seismic waves are described by the following equation: Velocity = Frequency x Wavelength. For example, wavelength of seismic wave in rock when Velocity = 4000 m/s and Frequency 1/s = 4000 meters or 10/s = 400 m. Damage (strains) to underground constructions can be important when the facility size is larger than 1/4 of the Wavelength. Thus, a 1km size construction will be more damaged than a 100 m facility. In other words, the wave just passes through the structure, often unnoticed.

Underground structures are confined by the surrounding rock and its support, but surface structures are free to respond horizontally and develop much stronger motions. More in detail, seismic design for underground structures is done in terms of the deformations and strains imposed on the structure, while surface structures are designed for the inertial forces caused by ground accelerations.

In Pratt et al. (1978) the following summary is given: "In general, the performance of wells during earthquakes is quite good, with the major damage resulting from bending, crushing, or shearing of the casing due to differential movement of the surrounding rock. In general, the major damage appears to be to shallow wells that are in unconsolidated sediments and near the surface. There is very little damage to wells deeper than about 100 m except where the well cross a fault plane along which movement occurs." Because of the logarithmic basis of the scale for earthquake magnitude, each whole number increase in the magnitude corresponds to the release of about 31 times more energy. In the case of salt caverns, the more significant earthquakes occur below the salt in the gas reservoir and they are much smaller than the ones discussed in Pratt et al. (1978).

5.2.1.6 Final remarks and conclusions related to hydrogen caverns

Compared to other induced seismic events from, for example, depleting gas reservoirs ($M_L < 3.6$), induced microseismic events possibly associated with cavern operations appear to have 100-1000 times smaller amplitudes ($M_L < 1.3$). Besides rock-fall type events of the cavern roof, cavern induced events are connected to the induced creep in the rock salt. Enhanced creep rates occur in response to stress changes, which are a function of cavern operation parameters (e.g., frequency of pressure and temperature changes), the microstructure of the dominant rock salt and local heterogeneities in the rock salt stratigraphy. Yet, it is unclear how characteristic Hydrogen cavern parameters affect the exact stress response and corresponding creep processes in the rock salt mass, but similarities with other caverns are to be expected. In addition, it is not clear whether natural seismic events, which occur due to the natural creep of the salt dome, can be distinguished from induced microseismic events, which arise due to increased creep rates from operated caverns.

Appendix: Local magnitude M_L

M_L is referred to the local magnitude, where L stands for local. As other magnitude measures, it is a logarithmic scale and can therefore also be negative for small events. A M_L=0 event corresponds to a 100 times smaller amplitude than M_L=1, and a M_L=-1 event has a 1000 times smaller amplitude than M_L=1. M_L refers back to the well-known Richter magnitude, the original magnitude relationship defined by Richter and Gutenberg in 1935 for local earthquakes. *"It is based on the maximum amplitude of a seismogram recorded on a Wood-Anderson torsion seismograph. Although these instruments are no longer widely in use, M_L values are calculated using modern instrumentation with appropriate adjustments."*[1]

https://www.usgs.gov/faqs/moment-magnitude-richter-scale-what-are-different-magnitude-scales-and-why-are-there-so-manyhttps://www.usgs.gov/programs/earthquake-hazards/magnitude-types

[1] https://www.usgs.gov/programs/earthquake-hazards/magnitude-types

5.3 Durability: The evolving rheology, transport properties, damage and healing of salt around a cluster of hydrogen storage caverns

Authors: Tobias Baumann, Boris Kaus – smartTectonics GmbH and Janos L. Urai – GeoStructures Consultancy for Structural Geology and Geomechanics

In KEM-17 (KEM-17, 2019) we proposed a microphysics-based model for deformation and flow properties of evaporites. This was essential for the salt-brine system, and for this, we proposed models of creep and permeation which provide a strong improvement of existing models because the microstructural analysis and identification of mechanisms allow a much better extrapolation of constitutive equations to long-term creep over long periods at low differential stress.

The situation of hydrogen in contact with the cavern wall where pressure is cycled in addition to cavern creep closure poses a much less well-understood problem (see also the discussion in 2.1). For example, in a recent paper presenting the Dutch state of the art on geomechanical modelling of Hydrogen caverns, Ramesh Kumar et al. (2021) incorporate damage mechanics of the rock salt consistent with earlier work by Khaledi (2016), but do not include pressure solution and related grain boundary brine dissolution-precipitation mechanisms, based on considerations of solubility of water in H2 gas. We disagree with this assumption based on the presence of a brine pool at the bottom of the hydrogen-filled cavern and the thermodynamics of the water – H2 system, see also 2.1.4 and Rahbari et al. (2019). In our opinion, it is more likely that the cavern walls will be wet and maybe even dissolve periodically when in contact with H2 in a storage cavern. This poses an interesting and unexplored problem of damage, dilatancy, crystal plasticity, dynamic recrystallisation and pressure solution, which can weaken the cavern walls (Baumann et al., 2022b) with the very low viscosity of H2 allowing much more rapid penetration of pore pressure and dilatancy than previously thought, with an as yet unknown depth of penetration.

5.3.1 Rock salt creep rheology, uncertainties in creep rates and upscaling properties of heterogeneous rock salt

Constitutive laws of rock salt are required for the prediction of long-term deformation of solution mined caverns which play an important role in the energy transition. Much of this deformation is at differential stresses of a few MPa. Most laboratory measurements of salt creep are at much higher differential stress and require extrapolation over many orders of magnitude. This extrapolation can be made more reliable by including microphysical information on the deformation mechanisms in the laboratory samples integrated with microstructural analysis of samples deformed in natural laboratories at low differential stress. Because of the arguments discussed above, we propose that both in the far field and near field of hydrogen caverns, microcracking, dissolution-precipitation and dislocation creep processes will be all active (see section 3.1.2.4).

It is generally accepted that steady state creep can be described as an additive creep with a strain rate component that depends linearly on stress and a second part that depends on the stress in a non-linear manner. Following microphysical considerations, often the following descriptions are used:

1. Dislocation creep: (e.g., Bräuer et al., 2011; Spiers et al., 1990):

$$\dot{\varepsilon}^{dc} = A_{dc} \exp\left(-\frac{Q_{dc}}{RT}\right) \sigma^{n_{dc}},$$

2. Pressure solution creep (e.g., Spiers et al., 1990):

$$\dot{\varepsilon}^{ps} = A_{ps} \exp\left(-\frac{Q_{ps}}{RT}\right) \frac{\sigma}{TD^{m}}.$$

In the above equations, A_{ps} and A_{dc} denote pre-factors of the creep mechanisms, Q_{ps} and Q_{dc} are the corresponding activation energy parameters, R is the gas constant, T is the temperature, D is the grain size, σ is the effective differential stress, n and m are the dislocation creep and grain size dependence exponents, respectively.

In this additive creep formulation, the pressure solution creep with linear stress dependence is dominant in the low-stress regime (e.g., Urai and Spiers, 2007), see Figure 148. A linear stress dependence in the low-stress domain has been validated experimentally by Bérest et al. (2019a) with long-term creep tests on natural salt samples.

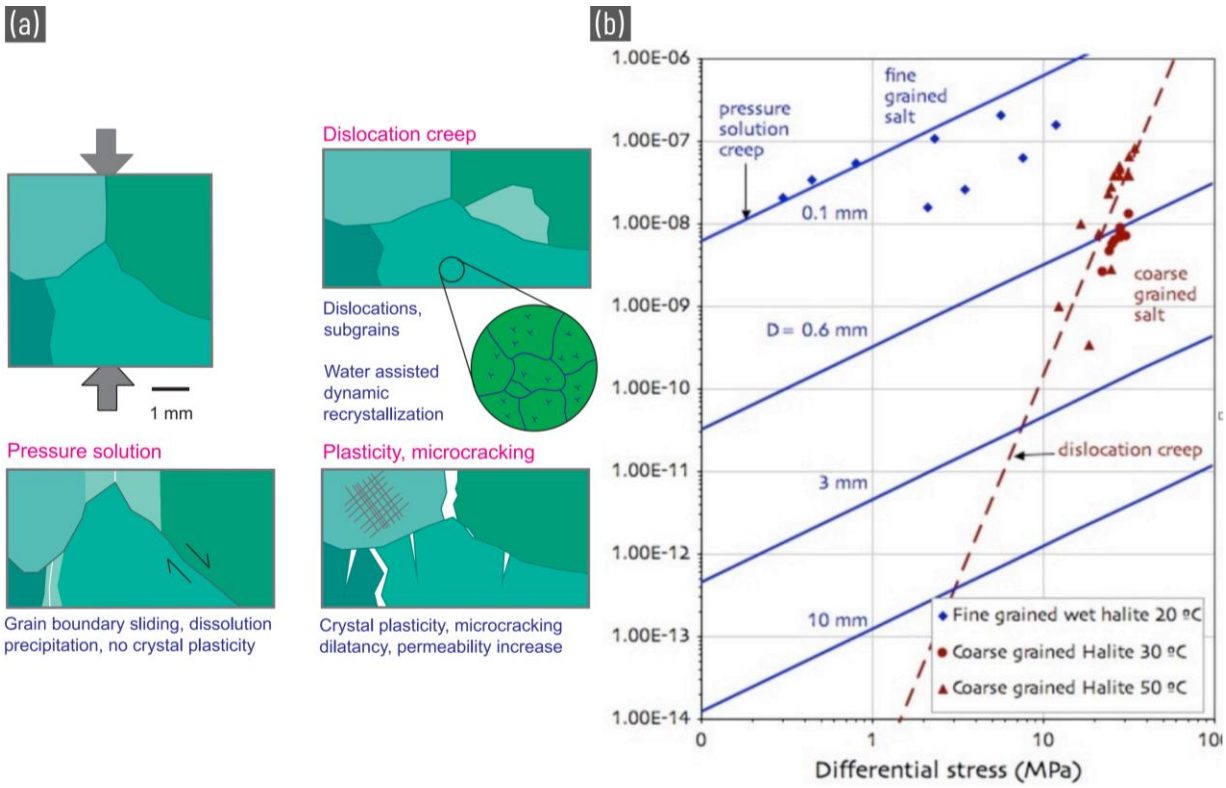

Figure 148. Illustration of the relationship between microphysical processes and bulk constitutive models for the deformation of rock salt in the presence of brine (modified from Urai et al., 2019).

Theoretical models (van Noort et al., 2008) and microstructural observations of grain boundary activity (e.g., Urai et al., 2008) suggest that pressure solution only operates if the grain boundaries are mobile, which requires connected fluid films on the grain boundaries. It is suggested that a lower critical stress exists at which the fluid films on the grain boundaries disintegrate and the pressure solution deformation process stops. Yet, it remains unclear at which critical stress the fluid film disintegration process occurs. A recent theoretical study suggests a stress range between 0.07 and 0.7 MPa (Van Oosterhout et al., 2022). It has been shown that if this additional complexity is integrated into constitutive relations ships of numerical models, the effects on the creep can be significant (Baumann et al., 2022a; Hunfeld et al., 2022).

In addition to the grain boundary activity, the grain size evolution (kinetics) is another complexity that may affect the rock salt creep in a significant manner (e.g., Urai and Spiers, 2007). Experiments show that the grain size always tends to evolve towards the equilibrium between the pressure solution and dislocation creep where the strain rate is partitioned equally between the mechanisms (De Bresser et al., 2001, 1998; J.H. Ter Heege et al., 2005). Integrated into numerical models, this adds an additional non-linear behaviour with respect to the grain-size evolution to the additive creep.

As described in 5.1, rock salt is not homogeneous but usually consists of layers of different salt types that may have very distinct thermomechanical properties depending on their microstructure. Thus, the creep rates of the heterogenous salt layers inside the salt dome may vary several orders of magnitude. Depending on the type of the salt structure, these heterogeneous layers are folded on various length-scales, which reflects the internal geodynamics of the salt formation (e.g., Baumann et al., 2019). In the Netherlands, large volume fractions of the salt structures belong to the Zechstein 2 group, which is characterised by a high frequency of occurrence of mega grains, which span up to several centimetres (see 5.1), also known as *Kristallbrockensalz* and well documented in German Zechstein (e.g., Bräuer et al., 2011).

While creep properties of moderately fine-grained and homogeneous salt can be upscaled to meter and multi-meter scales within the uncertainty limits (Baumann et al., 2022b, 2022a). It is more challenging to upscale the creep properties of *Kristallbrockensalz* from laboratory sample conditions to cavern- and dome-scale conditions. A recent paper on this topic is Barabasch et al. (2023), which is summarized in the following section.

In the geodynamics community, numerical deformation experiments with different loading conditions are well established techniques to determine the effective creep properties of heterogeneous rocks with large crystals (e.g., Deubelbeiss et al., 2011, 2010; Deubelbeiss and Kaus, 2008) or stratified compositions (e.g., Schmalholz and Schmid, 2012). In analogy, it seems feasible to use representative slabs of selected salt cores of *Kristallbrockensalz* to establish numerical deformation experiments on the laboratory sample scale and expand the model domain artificially to a centimetre-, meter- and multi-meter scale, in order to develop a better understanding of the upscaling behaviour of the effective creep properties of *Kristallbrockensalz*. A research chapter on this topic will be included in this report.

5.3.2 Interaction of damage, microcracking, recrystallization and crack healing around Hydrogen caverns during pressure cycling

Khaledi (2016) presented an overview of damage models which claim to describe deformation and dilatancy around salt caverns filled with gas under conditions of cyclic pressure. These models can be implemented in numerical models of deformation over the lifetime and abandonment of caverns. In the research phase of this project, we will discuss this in detail, but at this point, it is important to note that little is known about the details of the processes here. Numerical models do not include much detail of the pressure of the hydrogen in the pore space created in the damage zone around the cavern, most models define operating conditions such that stresses remain below dilatancy boundary. However, the boundary conditions of a salt cavern wall in contact with brine and hydrogen gas have not been fully implemented.

Gabrielli et al. (2020) considered the flow of hydrogen gas in the damage zone around the cavern. Gas flow was assumed to be single-phase and single-component. This is one of the few models to do this, but also here, the mechanical interaction with deforming salt was neglected.

This calls for a much better understanding of the processes in this complex damage zone over long periods. One can, for example, hypothesize of a self-propagating damage zone in the salt, being the product of stress changes due to cavern pressure, creation and destruction of porosity by microcracking, recrystallization, and fracture healing, the effect of effective pressure on deformation of salt and that of gas pressure gradients causing additional deformation. Little is known about these processes.

5.3.3 The special case of *Kristallbrockensalz* (Barabasch et al., 2023)

Barabasch et al. (2023) have demonstrated that the deformation of rock salt can significantly vary at identical temperatures and deviatoric stress. This variation is influenced by factors such as grain size, solid solution, second phase impurities, crystallographic preferred orientation, water content, and grain boundary structure.

They note that both dislocation creep and dissolution-precipitation processes are prevalent, but dissolution-precipitation creep (pressure solution) is often overlooked in current engineering forecasts.

The study focuses the Z2 Stassfurt salt, as it is the primary host of Hydrogen caverns in the Netherlands. There, evidence of substantial grain size-dependent variations in halite rheology, based on microstructural observations from rock salt cores from the Zechstein of Northern Netherlands, which underwent varying degrees of tectonic deformation, is presented. The relatively undeformed Z2 (Stassfurt Formation) layered salt from Barradeel is examined and contrasted with the significantly more deformed equivalent in diapiric salt from Heiligerlee, Zuidwending, and Pieterburen. Sub-grain size piezometry of the data indicates that the deformation during halokinesis occurred at differential stress between 0.5 and 2 MPa, providing a natural constraint on the creep processes. The domal salt samples, characteristic of the well-known "Kristallbrocken" salt, are analysed. These samples feature cm-thick megacrystals alternating with fine-grained halite and thin anhydrite layers in Barradeel, and cm-sized tectonically disrupted megacrystals encircled by fine-grained halite with a grain size of a few mm in the diapiric salt. Significantly higher strains in fine-grained halite are demonstrated by folding and boudinage of thin anhydrite layers in contrast to the megacrystals, which are internally less deformed and develop subgrains during dislocation creep.

They conclude that the fine-grained matrix salt is considerably weaker than Kristallbrocken due to differing dominant deformation mechanisms. This aligns with microphysical models demonstrating that grain size significantly impacts strain rate at these low differential stress levels, providing evidence for the operation of pressure solution creep in rock salt at differential stress of a few Megapascals. The study demonstrates that incorporating results of microstructural analysis can greatly enhance constitutive models of rock salt at low differential stresses relevant in most salt tectonic settings. Subsequently, they recommend including this mechanism into constitutive laws of engineering models of rock salt deformation.

5.4 Durability: Geochemical processes

Author: Joyce Schmatz – MaP – Microstructures and Pores GmbH

5.4.1 Introduction

This review on the geochemical process related to the storage of hydrogen in salt caverns comprises: i. a short overview on the physico-chemical properties of the reactive second phases within the Zechstein formation, especially the anhydrite/polyhalite layers, and the related abiotic geochemical reactions and reaction kinetics; ii. the associated biotic processes, reactions and reaction kinetics causing the risk of H_2S formation; and, iii. the material integrity and durability in terms of possible chemical changes of the borehole materials.

Although the chemical properties of hydrogen and other natural gases such as CH_4 or CO_2 are different, some physico-chemical processes that occur during storage, such as the formation of H_2S and transport through the brine and solid cavern materials (salt, anhydrite, cements, and metals), can be compared and the knowledge previously gained in the operation of natural gas caverns can be used to better define the problems to be expected in hydrogen storage. Further, recent advances from laboratory test and geochemical models dealing with hydrogen-brine-rock within porous media (e.g., Hassannayebi et al., 2019; Heinemann et al., 2021) were taken into account.

Due to the complex interaction of hydrogen with the rock and brine, geochemical models are used to describe the effects of biotic and abiotic processes on the long-term development of the storage sites (e.g., Hassannayebi et al., 2019; Hemme and Van Berk, 2018). For this, **knowledge about the volumetric extent and kinetics of the reactions is essential and experimental work together with microstructural analyses is required to determine the input parameters for the geochemical models on the different reaction kinetics.** The associated outcome of the literature review and successive research phase is the narrowing down of these input parameters for geochemical modelling with the aim of describing the impact of over- or underestimated response rates on risk assessment.

"Before injecting hydrogen into a reservoir or cavern, it is recommended to investigate the mineralogical, chemical, physical and microbiological condition of the reservoir" (van der Valk et al., 2020). "*To accurately assess the risk of H_2S formation in hydrogen storage reservoirs it is of the utmost importance* ***to improve the predictive power of the geo- and biochemical models with laboratory experiments"*** (Groenenberg et al., 2020b; see also van Gessel et al., 2018; Warnecke and Röhling, 2021). Although a number of studies have been carried out, especially in recent years (e.g., Hemme and Van Berk, 2018), to evaluate the chemical-physical influences of hydrogen storage in underground salt caverns, many questions still need to be answered. Because of the **lack of reliable data** on the **effect of hydrogen on permeability and mechanical integrity in the critical lithologies, such as anhydrites, sump sediments, or the casing cements**, as well as information on **the kinetics of abiotic geochemical and microbial reactions** in the corresponding pore fluids, predictions on the long-term behaviour of geological hydrogen storage are only possible to a limited extent. Knowledge of hydrogen reaction pathways, reaction kinetics, and transport processes is critical for H_2 storage (Heinemann et al., 2021). However, **more laboratory data are needed to build reliable geochemical models which are essential for predicting long-term reservoir development.** Gillhaus (2007) summarizes that the **integrity of caverns in inhomogeneous salt structures depends not only on the quality of the surrounding salt, but also on the favourable interaction between different geological formations** (Figure 148). In such cases, non-saline formations may be in direct contact with the medium in the cavern or may be in close proximity. In this context, Gillhaus (2007) mentions the following critical geological boundary conditions in the subsurface:

- Salt formations with a high proportion of insolubles (> approx. 15 %).
- Competent insoluble layers (e.g., dolomite, anhydrite, clay) above and/or below the cavern.
- Competent insoluble layers cutting through the cavern zone
- Faulting in non-saline strata near the cavern.

In summary, they point out that exploration and feasibility testing of unfavourable salt formations often involves significantly higher costs for in situ testing, laboratory analysis, and computer modelling because of the site-specific constraints mentioned above.

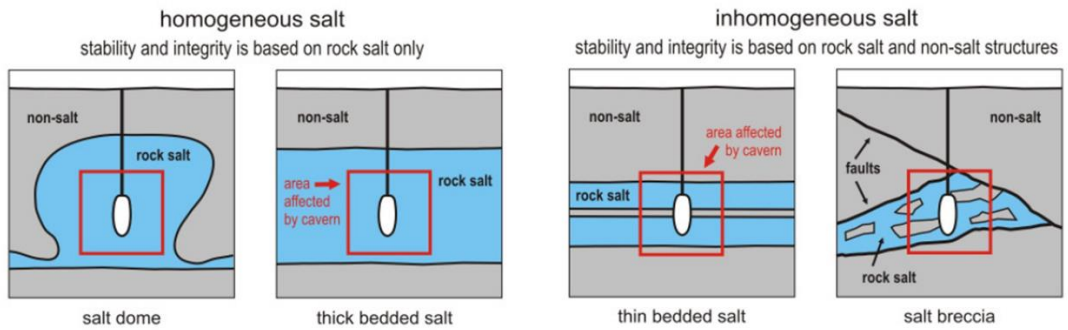

Figure 149. Influence of salt and non-salt on the integrity of caverns in homogenous and inhomogeneous salt formations. From Gillhaus (2007).

5.4.2 The reactants and reactions

In the proximity of salt caverns in Dutch subsurface, the following accompanying lithologies/mineralogies could play a critical role during H_2 storage (Pichat, 2022), see also Figure 150.

- Chlorides: Halite (NaCl), Sylvite (KCl), Carnallite ($KMgCl_3 \cdot 6(H_2O)$) and Kainite ($KMg(SO_4)Cl \cdot 3H_2O$);
- Sulphates and Sulphides: Anhydrite ($CaSO_4$), Gypsum ($CaSO_4 \cdot 2H_2O$), Polyhalite ($K_2Ca_2Mg[SO_4]4 \cdot 2H_2O$), Kieserite ($Mg[SO_4] \cdot H2O$), and FeS;
- Carbonates: limestone (Calcite: $CaCO_3$) and dolostone (Dolomite: $CaMg(CO_3)_2$);
- as well as siliciclastic rocks such as sandstone, claystone, and shale.

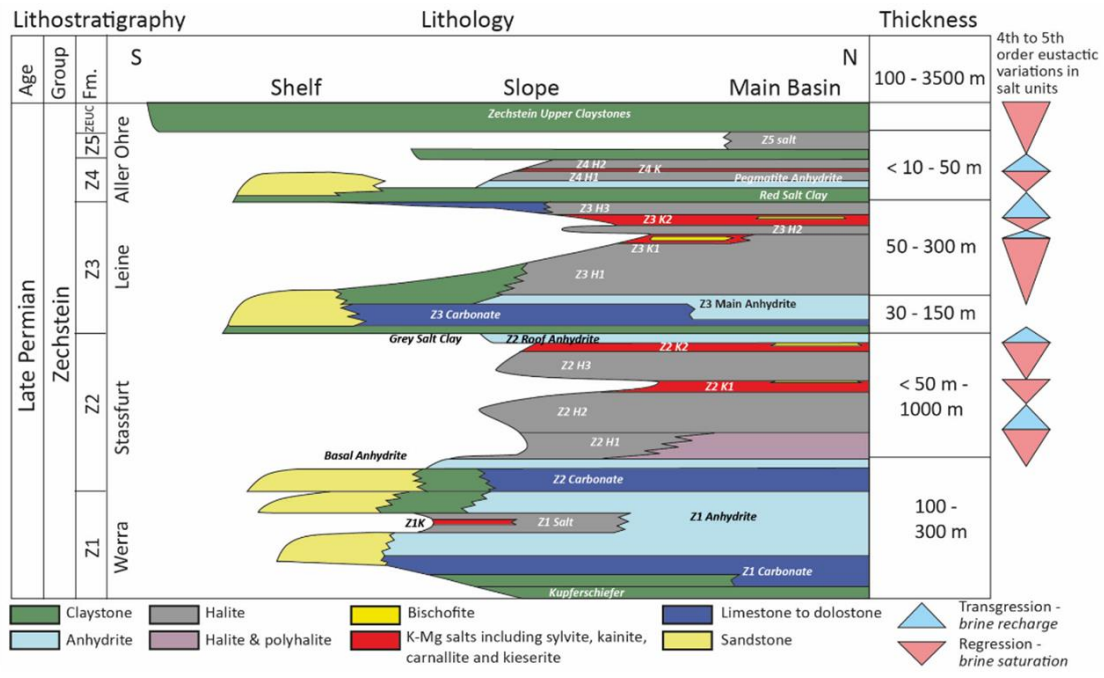

Figure 150 Overview Zechstein lithologies Dutch subsurface. From Pichat (2022).

While the role of halite (NaCl) in the durability of salt caverns during hydrogen storage is discussed elsewhere in this report, this section focuses on the accompanying evaporites and clastic sediments. Because of compositional heterogeneity, a variety of different geochemical processes may occur during storage. Because of the relatively low accessibility of hydrogen to the surrounding reactive lithologies (e.g., clastic sediments), the brine sump, in which the reactants are dissolved during mining, plays a critical role in hydrogen storage. Hemme and van Berk (2017 and authors therein), Figure 152, build their modelling on this fact, describing the division of salt caverns into three parts: the stored gas in the upper part, which occupies the largest volume; the brine in the middle, with a thickness of only a few meters; and the sump in the lower part, which can occupy one-third of the total cavern volume. They describe that the sump is composed of insoluble residue and a residual pore-filling aqueous solution that is not discharged after leaching. The residual brine that is above the sump is in solubility equilibrium with the overlying gas and surrounding mineral phases of the rock salt formation.

Of the above-mentioned solid reactants, anhydrite plays a subordinate role for the storage of hydrogen in salt cavern, i) due to its frequent occurrence in form of layers, layer fragments and as a major component of the sump and ii) as a source of the sulphate anion $[SO_4]^{2-}$. In aqueous conditions, bacterial sulphate reduction causes the formation of H_2S (Figure 151).

Further biogenic induced reactions affecting H_2 storage are methanogenesis, acetogenesis, and iron(III) reduction (Muhammed et al., 2022, see also next section).

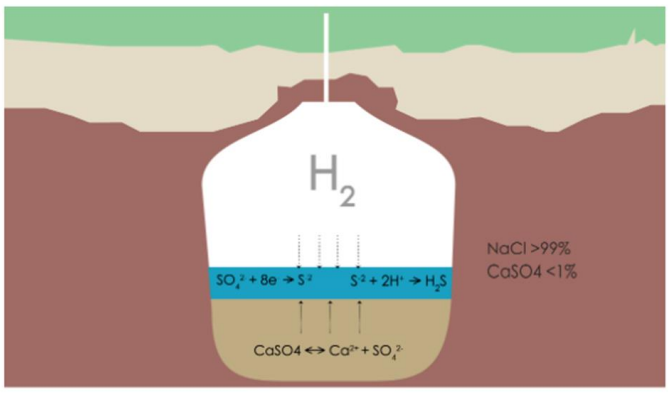

$$H_{2_{aq}} \rightleftharpoons 2H^+ + 2e^-$$

$$4H_{2_{(aq)}} + SO_4^{2-} + 2H^+ \rightarrow H_2S + 4H_2O$$

Figure 4.3: Simplification of reactions important for the production of H2S

Figure 151. H_2S production from Anhydrite source within brine sump. Simplified reactions. From Laban (2020).

Tuche et al. (2020) discuss the reduction of pyrite to pyrrhotite in the context of deep geologic disposal of nuclear waste in a clay-rich host rock. They show the large influence of hydrogen on sulphur chemistry in their kinetic models, but also point out in this context that **no significant effect was found on the other minerals present in the natural rock (clay minerals, quartz, calcite, dolomite, and feldspars)**. A similar conclusion regarding clayey lithologies is reached by Yetka et al. (2018). These and other important reactions were summarized by Hassannayebi et al. (2019) and Laban (2020) against the background of chemical simulations and are shown in Figure 153. However, the majority of these reactions can be considered of little relevance in the context of hydrogen storage in salt caverns, due to the low occurrence of the solid reactants in the immediate vicinity of the salt caverns.

Further, Hassannayebi et al. (2019) present a chemical model based on the actual mineralogy of a Molasse Basin case study: the Underground Sun Storage. They performed a multistep geochemical modelling approach to investigate fluid-rock interactions using equilibrium and batch kinetic simulations (Figure 153). They used the equilibrium approach to estimate the long-term consequences of hydrogen storage,

while kinetic models were used to study the interactions between hydrogen and rock formation on the time scales of typical storage cycles. Their kinetic approach suggests that **reactions of hydrogen with minerals become relevant only over timescales much longer than the storage cycles considered**. Their final kinetic model assumes that both mineral reactions and hydrogen dissolution are kinetically controlled (Hassannayebi et al., 2019), see also Figure 154.

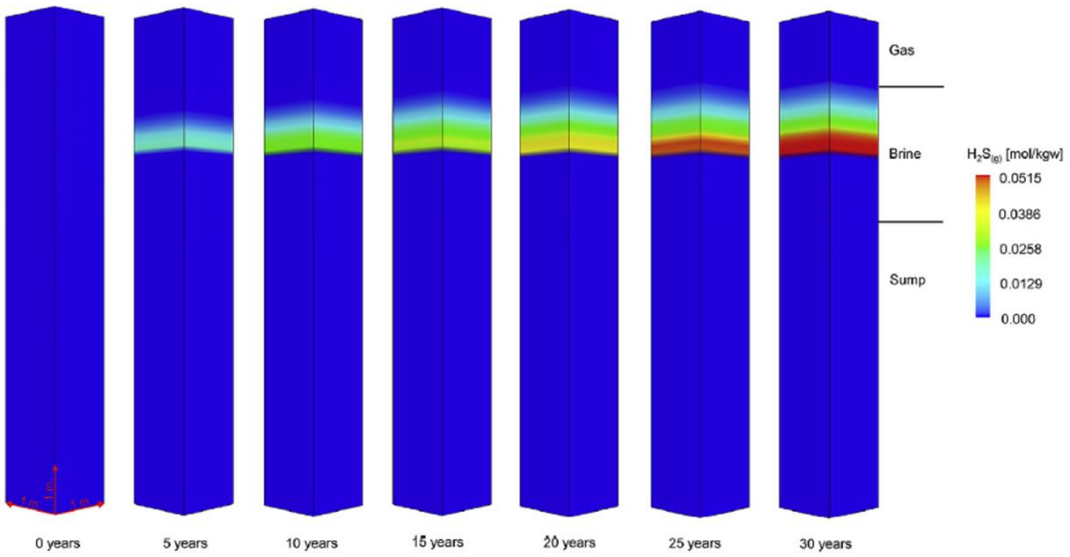

Figure 152 H_2S generation and increasing H_2S amount with ongoing time and bacterial sulphate reduction. From Hemme and van Berk (2017).

Mineral reaction	Precipitation/dissolution	Case study			
		3		4	
Muscovite	$Muscovite + 5H^+ + 5H^+ \leftrightarrow K^+ + 3Al^{+3} + 3SiO_2(aq) + 6H_2O$	*	P	*	P
Dolomite	$Dolomite \leftrightarrow Ca^{+2} + Mg^{+2} + 2CO_3^{2-}$	*	P	*	P
Pyrite	$Pyrite + H_2(aq) \leftrightarrow Fe^{+2} + 2HS^-$	*	P	*	P
Ankerite	$Ankerite + 2H^+ \leftrightarrow Fe^{+2} + Ca^{+2} + 2HCO_3^-$	*	P		
Clinochlore	$Clinochlore + 10H^+ \leftrightarrow 2AlO(OH) + 5Mg^{2+} + 3SiO_2\,(aq) + 8H_2O$	*	S	*	S
Pyrrhotite	$FeS_2 + (1-x)\,H_2 \leftrightarrow FeS_{1+x} + (1-x)H_2S$	*	S	*	S
Daphnite	$Daphnite + 10H^+ \leftrightarrow 2AlO(OH) + Fe^{2+} + 3SiO_2\,(aq) + 8H_2O$			*	S

a) Primary and secondary minerals are indicated by "P" and "S"

Equilibrium phase	Equilibrium reaction	log K
Halite	$NaCl \rightleftharpoons Cl^- + Na^+$	1.570
Anhydrite	$CaSO_4 \rightleftharpoons Ca^{2+} + SO_4^{2-}$	-4.39
Siderite	$FeCO_3 \rightleftharpoons Fe^{2+} + CO_3^{2-}$	-10.89
Goethite	$FeO(OH) + 3H^+ \rightleftharpoons Fe^{+3} + 2H_2O$	-1.0
Pyrite	$FeS_2 + 2H^+ + 2e^- \rightleftharpoons Fe^{+2} + 2HS^-$	-18.479
Mackinawite	$FeS + H^+ \rightleftharpoons Fe^{2+} + HS^-$	-4.648
Sulfur	$S + 2H^+ + 2e^- \rightleftharpoons H_2S$	4.882
Gypsum	$CaSO_4 : 2H_2O \rightleftharpoons Ca^{2+} + SO_4^{2-} + 2H_2O$	-4.58
Calcite	$CaCO_3 \rightleftharpoons CO_3^{2-} + Ca^{2+}$	-8.48
H_2S	$H_2S \rightleftharpoons HS^- + H^+$	-6.994
HS^-	$H_2S \rightleftharpoons S^{-2} + H^+$	-12.918

b)

Figure 153. Important chemical reactions summarized by a) Hassannayebi et al. (2019) and b) Laban (2020).

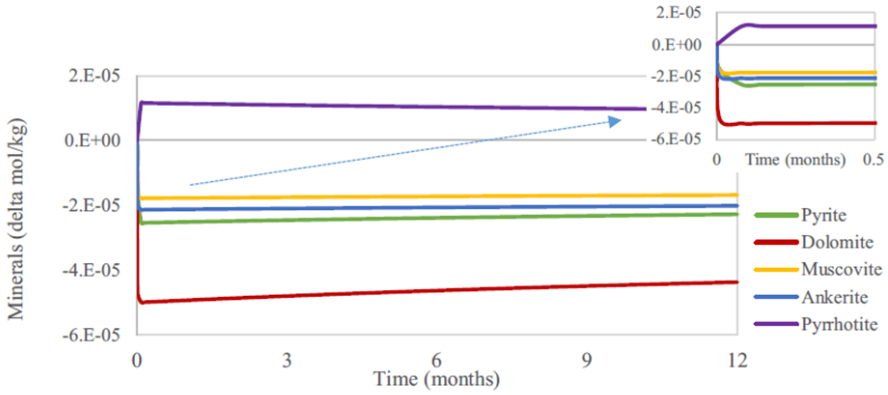

Figure 154. From Hassannayebi et al. (2019): "Finally, hydrogen dissolution kinetics were added to the model. The dissolution kinetic rate is based on a typical storage cycle (12 months) and operational hydrogen partial pressure of 7.5 bars which is derived from many simulations for this specific case study. Owing to a lack of data for kinetic hydrogen dissolution reactions in the literature, we defined several scenarios to understand under which conditions the likelihood of hydrogen loss is considerable. We further compared the same models to cases in which the reactions of redox couples remained at equilibrium. When applying assumptions of both disequilibrium and equilibrium for reactions of redox couples, when the hydrogen reaction rate remains low, the pH increase is minor, and hydrogen behaves like an inert gas. In the case of moderate-to-high hydrogen rate constants, a higher increase in pH is observed; however, this amount remains insignificant when assuming disequilibrium for redox couple reactions and is substantial in the case of the equilibrium assumption for these reactions."

5.4.3 Microbial reactions

In their review, Muhammed et al. (2022) discuss the four main microbial (biotic) processes affecting H_2 geostorage. These processes, methanogenesis, acetogenesis, sulphate reduction, and iron(III) reduction, contributed to H_2 consumption and occur in all types of underground hydrogen storage: caverns and porous media. They indicate that water production by sulphate and iron(III) reducing bacteria is twice the water production per unit mass of H_2 for methanogenesis and acetogenesis (2016). Their summary of studies on microbial activities in subsurface hydrogen storage is shown in Figure 155.

The FLEXg16008 FINAL REPORT (DBI, 2017) summarizes the microbial processes and their effects as follows:

- Corrosion and acidification of the reservoir fluids through accumulation of hydrogen sulphide (H_2S) and organic acids
- Decrease of permeability through iron sulphide (FeS) precipitation, biofilms and extra-cellular substances
- Reduction of gas quality through hydrogen consumption and hydrogen sulphide (H_2S) formation
- Microbial induced corrosion
- Stimulation of microbial processes through additional hydrogen energy potential
- Precipitation respectively solving of matrix-components (carbonates)
- Sedimentation of sulphur / biofilms in surface facilities through increased hydrogen sulphide (H_2S) share in the withdrawn gas

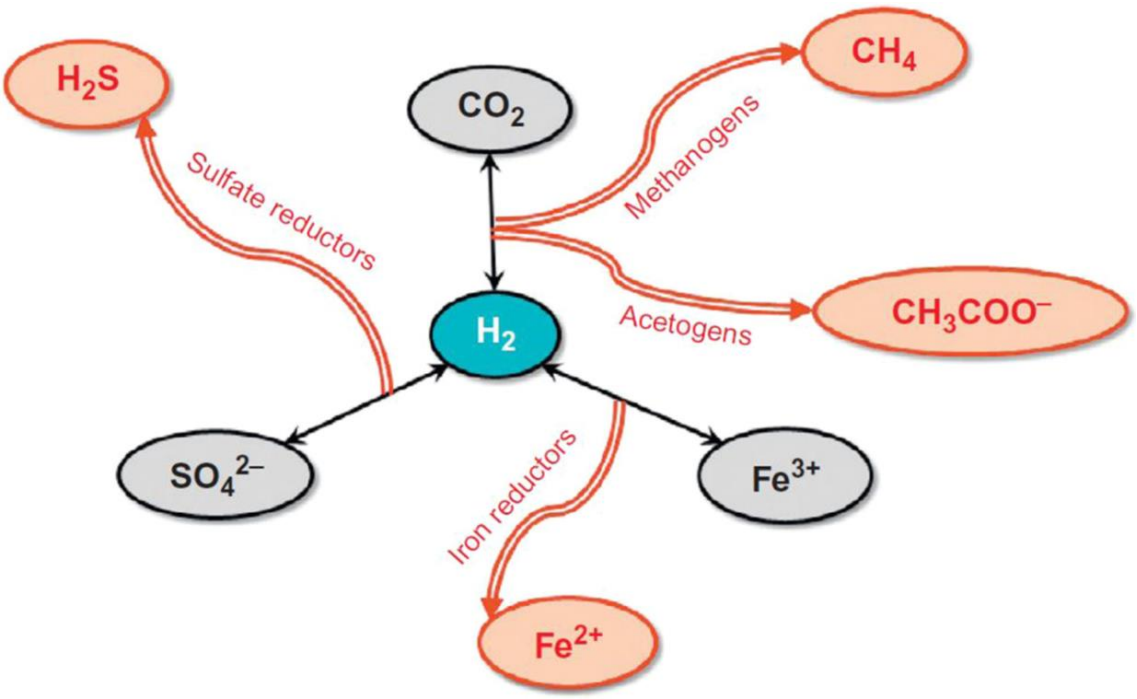

Figure 155. Types of hydrogenotrophic bacteria in subsurface hydrogen storage. From Panfilov (2016).

5.4.3.1 Biotic processes

5.4.3.2 Biotic H_2S formation

It is known that hydrogen is a very reactive gas and can be used as an energy source by many microorganisms. In the presence of aqueous sulphate, **H_2S is produced by bacterial sulphate reduction**, typically thermal regimes from 0 to up to 60-80°C (Machel, 2001). Due to the intercalation of salt with anhydrite, sulphate is always present in the salt formations in varying amounts – both in the anhydrite/polyhalite layers adjacent to the cavern walls as well as in the insoluble sediment and brine sump, which can occur in thick layers at the bottom of the cavern (Bérest and Brouard, 2003; Schwab et al., 2022). H_2 is dissolved in brine. This is a relatively fast process as brine is stirred by natural convection. H_2S can form and interact with rock salt and casing and change the composition of the stored gas. The extent, geometry and physical properties, especially porosity (including fractures) its connectivity and permeability, of the insoluble layers are of particular interest here, since the formation of H_2S depends, among other factors, on the surface area accessible to the microorganisms.

Muhammed et al. (2022) and authors therein note that archaeal microorganisms are bacteria that produce hydrogen sulphide after consuming H_2 in the presence of sulphate-reducing ions. This type of reaction is known mainly from hydrocarbon reservoirs into which incompatible water is injected during flooding due to the activity of sulphate-reducing ions. Their review indicates that the optimum reaction temperature for the bacterial sulphate reduction is about 311 K, but higher temperatures up to 383 K have been reported, for example by Machel (2001).

Parameters that positively influence H_2S production are: high bacterial reduction rate, high pH, high sulphate concentration, relatively high temperature, high pressure and low Fe concentration. Both pH and Fe concentration are parameters that can be adjusted, by injecting either NaOH or Fe-rich solutions to the brine, which could lead to a reduction of H_2S production (Fu et al., 2016; Laban, 2020).

The modelling results of Hemme and van Berk (2017, Figure 152) show that the largest amount of H_2S is formed in the brine, with the amount of $H_2S(g)$ (g=gaseous) generated controlled mainly by the amount of available sulphate(aq) (aq=aqueous) and the diffusion rate, which is coupled to the maximum operating lifetime of the salt caverns. In addition, they show that t**he amount of $H_2S(g)$ produced and released depends on the selected kinetic rate constant**.

5.4.3.3 Biogenic induced pore clogging

Further dominant microbial processes that occur are pore clogging due to the production of biofilms (Ebigbo et al., 2013; Hassannayebi et al., 2021) or e.g., the precipitation of amorphous ferrous sulphide or $CaCO_3$ as a metabolic by-product (Hemme and Van Berk, 2018). These processes are well known from natural gas storage in porous sediments; however, they also play a role, as they can affect the mechanical durability of the cap rocks and the well cements. Fu et al. (2016) indicate that the presence of goethite or other metal hydroxides or oxides can significantly attenuate the acidification intensity of reservoirs and thus delay or even suppress the formation of $H_2S(g)$ due to precipitation of metal(di)sulphides.

5.4.3.4 Risks

To narrow down the potential risks of bacterial activity during hydrogen storage in salt caverns, Warnecke and Röhling (2021) refer to a study by Dopffel et al. (2021), in which it is shown that some halophilic bacteria are able to live in highly concentrated salt solutions, such as those found in salt caverns. However, they weigh that in this case, appropriate bacterial contamination would first have to be introduced into the salt cavern from the outside, e.g., from the purge water, and compare this to pore storage (aquifers and depleted gas reservoirs). However, according to Warnecke and Röhling (2021), the extent of possible **bacterial biofilm formation in salt caverns would be significantly lower compared to pore storage due to the much smaller cavern surface area compared to the accessible surface area in porous media.**

One of the few quantitative studies dealing with the direct risks of hydrogen storage in salt caverns with regard to the biotic reactions was presented by Portarapillo and Di Benedetto (2021). They performed a bow-tie analysis showing all possible causes (base events) as well as consequences (jet fire, UVCE (unconfined vapor cloud explosion) and toxic chemical release). The result of their work is quoted below:

"Underground storage of H2 in salt caverns poses safety problems in terms of fires, explosions, and the release and dispersion of toxic chemicals. Bacterial metabolism converts H2 to CH4. In addition, biotic and abiotic reactions of H2 with sulfates and rocks form H2S. Therefore, the composition of the gas contained in the salt caverns changes over time. ... The impact and risk analyses allowed quantification of risk indices and impact zones, with UVCE identified as the outcome with the highest risk index value. The UVCE impact zone decreases over time due to hydrogen contamination and higher methane and hydrogen sulfide content. This work can be considered a preliminary tool, based on simple models, for understanding the risk associated with large-scale hydrogen storage, which is strongly influenced by time and the microbiological composition of the salt cavern in question. While based on simple models, this risk assessment can be applied to specific salt caverns in the future once the microbiological characteristics and initial composition of the gas to be stored are known. In this way, it will be possible to predict the most appropriate storage strategy and set up a good monitoring system to track and counteract possible microbial side effects, especially in case of leakage." (Portarapillo and Di Benedetto, 2021)

Laban (2020) summarizes that the presence of sulphate-reducing bacteria is strongly influenced by a variety of factors: temperature, saltwater activity, alkalinity, and salinity (% NaCl) of the ecosystem. He points out that some sulphate reducing bacteria tolerate high salt concentrations and that the activity of these species therefore depends on the purity of the salt. The conclusion is that **the location of the caverns plays an important role**: If the cavern is located in a salt layer with lower halite purity or salt layer with lower halite purity or lies within several salt layers, the probability for bacteria increases, due to the fractional decrease of NaCl.

5.4.3.5 Recommendations from Literature

Laban (2020) and Dopffel et al. (2021) emphasize that it is **essential to monitor and analyse the relevant microbiological and chemical processes at each storage site** to determine the most appropriate strategy for safe underground storage.

The results of the geochemical models of Laban (2020) show that the risk of H_2S production is high enough even if the bacterial reduction rate is calculated for the minimum detectable bacterial activity. However, they also show **that low temperature and pressure prevent H_2S production and recommend that this be achieved by reducing the depth of the cavern**. Furthermore, they emphasize that the accessibility of ion donors plays a role and therefore cavern sites with low anhydrite content and preferably high content of iron ion donors (Fe^{2+} and Fe^{3+}) (e.g., pyrite, mackinawite, goethite) should be favoured (see also Fu et al., 2016). In this context, they mention that it would be advisable to monitor the cavern brine for microbial activity, even in a more pure salt environment.

5.4.4 Abiotic processes

5.4.4.1 H_2S formation

Fu et al. (2016), Figure 156, discuss thermal/abiotic sulphate reduction, consumption of anhydrite, and production of H_2S and calcite, allowing for increased porosity. In their modelling approach, they simulate a semigeneric gas reservoir occluded by anhydrite. The calculated diagenetic processes fit observations in TSR-affected (TSR: thermal sulphate reduction) reservoirs (Machel, 2001): Formation of water, precipitation of calcite, metal (di)sulphides, and elemental sulphur to replace dissolved anhydrite at the expense of CH_4(g), and formation of hydrogen sulphide. By varying the input parameters, the critical factors for thermal sulphate reduction (TSR) were identified by Fu et al., and their results show that **reservoir-wide diffusive mass transport is a prerequisite for TSR**. An increase in the rate constant of abiotic sulphate reduction (ASR) and diffusive mass fluxes, as well as a lack of precursor minerals for metal (di)sulphide precipitation, can increase acidification intensity and accelerate H_2S outgassing. Further, Bildstein, et al. (2001) emphasize that during H_2 storage H_2 is readily available for ASR, however, the ASR rate decreases with accessibility of anhydrite surfaces.

Table 1. Main Signals from Selected Thermochemical Sulfate Reduction Case Studies

		Products of TSR*				
Reservoir or Field	Temperature Range	Newly Formed Minerals	Total Concentration of S(–II) Species	H_2S Gas (mol %)	Water	Reference
Nisku Formation (Devonian; western Canada)	125°C–145°C (257°F–293°F)	Calcite, marcasite, pyrite, galena, sphalerite, elemental sulfur		Several percent to 31%		Riciputi et al. (1996), Manzano et al. (1997), Machel (2001)
Smackover Formation (Jurassic; United States)	120°C–150°C (248°F–302°F)	Calcite, elemental sulfur		Up to 78%		Heydari (1997), Machel (2001)
Khuff Formation (Permian; Abu Dhabi)	140°C (284°F)	Calcite, elemental sulfur, pyrite, sphalerite, galena		Several percent to 60%	x[†]	Worden et al. (1996, 1997), Jenden et al. (2015)
Various carbonate reservoirs from the Sichuan Basin (Triassic; southwestern China)	>130°C (266°F)	Calcite, elemental sulfur, pyrite	500–3000 ppm	Mostly 5%, up to 30%	x	Cai et al. (2003, 2004), Hao et al. (2015), Jiang et al. (2015)

Blanks indicate that no data are available.
Abbreviation: TSR = thermochemical sulfate reduction.
*For comparison with modeled data, see Table 3.
[†]Water was proven as one product of TSR.

Figure 156. TSR case studies. From Fu et al. (2016).

5.4.5 The role of permeability and transport

5.4.5.1 Interfacial tension

Though it can be assumed that in-situ pore fluids or fluids related to the mining process saturate the porous rock mass, including the anhydrite/polyhalite layers and the sump sediments, the stored hydrogen will displace them depending on relative permeability. Reciprocal processes during interphase diffusion and advection of the hydrogen with the other fluids present may lead to consumption and contamination of the stored hydrogen, however, high degree of purity is needed, especially for fuel cells.

Technically, underground hydrogen storage involves injecting H_2 into selected storage sites - including salt caverns - for storage and then withdrawing it for use (Pan et al, in press, and authors herein). A number of petrophysical and thermophysical parameters, e.g., porosity, H_2 density and viscosity, H_2-water interfacial tensions, H_2 rock wettability, and H_2 adsorption on rock, play important roles here, and, inter alia, influence permeability. Pan et al, (in press) point out in their study that the interfacial tensions of rock/H_2 and rock/H_2O are also important parameters in this context, as they affect fluid spreading in the reservoir and thus the efficiency of H_2 injection and extraction, storage capacity, and containment safety.

Muhammed et al., (2022) underline that quantifying this effect by **studying the dispersion-diffusion of H_2 in saturated reservoirs and rock types is essential**, since H_2 is considered a very light gas with a higher diffusion tendency at the rock wall, and thus diffusion also occurs at different pore conditions. This becomes clear when one looks at studies on the structural trapping of hydrogen, such as the work of Iglauer (2022). In his analytical models, he describes that the reason that the suspended gases cannot seep into the caprock is the high capillary entry pressure of the caprock, which in turn is related to the very small pores in the caprock. His work evaluates this structural emplacement capacity and shows that an optimal depth of emplacement for H_2 exists at 1100 m depth, where a maximum amount of H_2 can be stored. These findings should be applicable to the evaluation of salt cavern storage structural integrity, particularly with respect to caprock properties. He points out that laboratory experiments have shown that the interfacial tension decreases only slightly with increasing pressure, but decreases sharply with increasing temperature (Chow et al., 2018). Further work in this direction, including possible alteration of the various reactants involved in hydrogen storage, shows additional effects of organic acid and silica nanofluid on interfacial tension rock/fluid (Pan et al., in press). Using their analytical approach, Pan et al. (2021) show that the interfacial tension rock/gas decreases with the increase of pressure, temperature, organic acid concentration, and carbon number, while the interfacial tension rock/H_2O increases with the increase of organic acid concentration and carbon number. With the same thermophysical and surface chemical conditions for the interfacial tension rock/gas, the following order was obtained: $H_2 > CH_4 > CO_2$.

An important note from the review by Muhammed et al. (2022), Figure 157, is that solid, liquid, and solid-fluid properties are important phenomena that govern the simulation, evolution, and prediction of H_2 storage performance and flow behaviour in porous media. **They highlight that in order to achieve this goal, the required information and data are not sufficiently available based on current research**. Their review presents the few available and current data on this aspect.

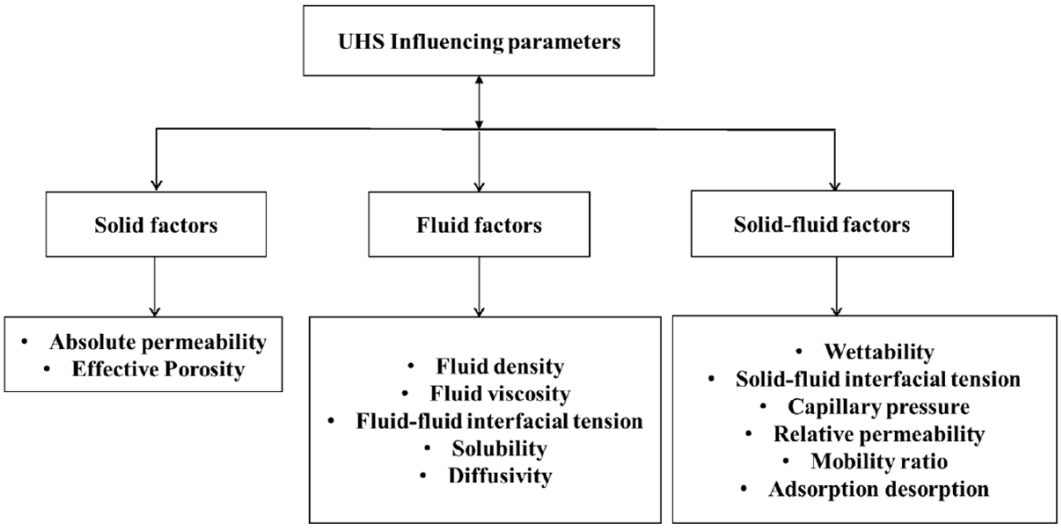

Figure 157. UHS (Underground Hydrogen Storage) and its influencing parameters. From Muhammed et al. (2022).

5.4.5.2 Recommendations from Literature

Regarding the leakage of hydrogen through "second-phase" lithologies, one could draw on the findings from studies on pore storage and restrict this to cap rocks and thick, interlocking lithologies, such as the anhydrite layers that occur in several layers in the Dutch Zechstein sequences. Many authors report that reliable data on hydrogen reactivity and reaction kinetics of hydrogen-mineral reactions are lacking, but are essential for safe subsurface storage (e.g., DBI, 2017; Heinemann et al., 2021; Iglauer, 2022). Similarly, with respect to pore storage, chemical areas suitable for the growth of hydrogen-consuming microbes are discussed to exclude potential storage candidates. These areas are directly related to the poro-perm properties of the lithologies and thus the accessibility of the reaction sites to the microbes (Heinemann et al., 2021).

Of particular interest here are the processes of diffusion and advection, which are triggered by buoyancy forces that exceed capillary forces. With respect to diffusion through the overburden, the FLEXg16008 FINAL REPORT (DBI, 2017) summarizes that the solubility of hydrogen in water is lower than in methane, but diffusivity is four times higher, and that despite the fact that diffusion is a slow process, small initial losses are expected at the beginning of hydrogen storage. Losses are expected to occur until the formation water in the adjacent caprock is saturated with hydrogen, and hydrogen losses on the order of 2% have been reported during the life cycle of a UGS. They mention that this process poses a particular risk if hydrogen lines located in the "second phase" lithologies come into contact with the hydrogen and microbial processes are activated. Regarding advection, Iglauer (Iglauer, 2022) states that the ratio of buoyancy forces and capillary forces depends on the amount of stored H_2 and the vertical H_2 column height h, respectively. He analysed this aspect in more detail and showed that h is not a constant but decreases monotonically with depth, reaching zero at 3700 m depth. Long-term H_2 storage below this sill depth is therefore not advisable because, according to Iglauer's models, H2 would seep up through the surface layer due to the reversal of wettability at this depth.

5.4.6 Mechanic durability

Hydrogen is stored underground in geological formations is injected/produced via wells. Ugarte and Salehi (2021) clearly point out in their review that there is a lack of experience with this technology, as there are only a small number of projects worldwide. They describe that s there are several mechanisms that can compromise the integrity of the wellbore and lead to the leakage of the stored gas. According to Ugarte and Salehi, the mechanisms that can compromise the integrity of the wellbore and lead to leaks include

microbial corrosion, hydrogen bubbling, hydrogen-induced cracking and hydrogen embrittlement, cement degradation, elastomer failure, and caprock seal failure.

5.4.6.1 Mineral alteration

Related changes in microstructure as well as mineral alteration in the geological materials cause the risk of mechanical instability in the respective layers (Heinemann et al., 2021). The structural stability of caverns in salt layers depends on the strength and deformation properties of the salt and non-salt layers surrounding and overlying the cavern (DeVries et al., 2005). Cała et al. (2018) indicate that the presence of intermediate anhydrite layers within the rock salt layers contributed to the reduction in diameter and irregular shape of the caverns they studied. They describe that the contact area between the rock salt layers and the anhydrite interlayers is prone to stress concentration and displacement occurrence. These, in turn, can influence and accelerate geochemical processes.

In the context of hydrogen storage in subsurface porous media, Heinemann et al. (2021) point out the different types of reactions that can be expected during subsurface storage, e.g., hydrogen-driven redox reactions with iron-bearing minerals such as hematite, goethite, or with Fe3+-bearing clays and mica. Such reactions could alter the mechanical strength of the rock matrix when hematite-containing cements or clay cutanes are reduced at grain-to-grain contacts in sandstone deposits. With respect to hydrogen storage in salt caverns, these processes could particularly affect the caprock through dissolution of minerals and the associated formation of leakage pathways. Experimental studies on reservoir sandstones under subsurface conditions (T = 40–100 1C, P = 10–20 MPa) show dissolution of carbonate and sulphate cements, leading to an increase in porosity during hydrogen exposure (Flesch et al., 2018; Heinemann et al., 2021). However, Heinemann et al. (2021) point out that, based on the current state of research, such reactions are likely to be limited in extent.

5.4.6.2 Cement alteration

Though the risk of chemical alteration of the casing cements by the hydrogen itself is considered to be low (van der Valk et al., 2020), processes that lead to microstructural changes in presence of H_2S due to formation of secondary ettringite, which causes molecular expansion is a known problem (Ahmed et al., 2015; Omosebi et al., 2017). Furthermore, it was shown that microbial activity causes chemical, colloidal or physicochemical deterioration and disintegration of cements (Jensen et al., 2009).

5.4.6.3 Steel alteration

Regarding the alteration of steel of metal access shafts, Laban (2020) describes hydrogen embrittlement as a process in which a metal becomes brittle or fractures due to the exposure or diffusion of hydrogen atoms or ions into the metal. In addition, absorption or adsorption of hydrogen in the interstices of the metal lattice play a role in storage, Laban supposed. Here, the hydrogen reacts with impurities or isotopes of the metal to form hydrides or gases, which create an imbalance in the metal structure (Birnbaum and Wert, 1972). The more common form of embrittlement is caused by the diffusion of hydrogen to the metal grain boundaries where it forms bubbles. These bubbles exert pressure on the metal grains. The pressure can build up to a point where the metal has reduced ductility and strength, which in turn can lead to cracking (Laban, 2020; Ugarte and Salehi, 2021).

The constant load and immersion tests with subsequent hydrogen analysis performed by Trautmann et al. (2021) have shown that no cracking occurs in carbon steels at hydrogen pressures up to 100 bar and temperatures of 25°C and 80°C at constant load, since the carbon steels absorb a maximum of 0.54 ppm hydrogen under these conditions, which is well below the embrittlement limit. However, austenitic stainless steels have been shown to absorb much more hydrogen, but these steels also have a higher resistance to hydrogen embrittlement. Furthermore, Trautmann et al. (2021) show that in H_2S-saturated solutions, hydrogen absorption is ten times higher than in hydrogen gas, which has led to fractures in

several steels. The results emphasize that **careful selection of materials for the casing plays a crucial role in the design of an underground storage site to reduce the risk of failure**.

5.4.6.4 Risks

Regarding hydrogen embrittlement, Laban (2020) states that continuous exposure to hydrogen can cause metals to absorb hydrogen, which can lead to material fatigue and cracking. He goes on to state that the greatest risk of leakage is caused by cracks in the steel casing closest to the cavern, which, combined with the porous cementation surrounding the casing, can lead to costly cavern leaks.

"Since the hydrogen molecule is particularly mobile, the major problem is the sealing of the metal access shaft, which is several kilometres long. A number of accidents or incidents from the past are known and well described in the 2,000 or so salt caverns for the storage of liquid or gaseous hydrocarbons in operation around the world. For the most part, these incidents occurred a long time ago, as the industry progressively adopted a principle known as the "double barrier" whereby the pressure is continuously monitored to detect when the gas has breached a first barrier; thereby avoiding the risk of breaching the second." (Pierre Bérest, 2021, https://www.polytechnique-insights.com/en/columns/energy/salt-caverns-the-key-to-storing-hydrogen/)

5.4.7 Concluding Remarks and Recommendations

The boundary conditions in the subsurface (accessibility, depth, p-T conditions) make in situ studies of the geochemical processes involved in underground hydrogen storage nearly impossible. In addition, laboratory work with actual reactants is limited; i.e., because transport of the substances (rock samples and fluids) to the surface results in immediate changes due to changing p-T conditions and possible changes due to contact with drilling fluids, groundwater, surface fluids, or atmospheric gases. In the absence of reliable data on the effects of hydrogen on permeability and mechanical integrity in critical lithologies such as anhydrites, sump sediments, or the casing cements, as well as information on the kinetics of abiotic geochemical and microbial reactions in the corresponding pore fluids, predictions on the long-term behaviour of geologic hydrogen storage are limited.

Although hydrogen stored in salt caverns is expected to have a major impact on sulphur chemistry, a number of studies (Hassannayebi et al., 2019; Laban, 2020; Truche et al., 2010; Yekta et al., 2018) suggest that the impact on second-phase lithologies, which contain only small amounts of sulphur, is unlikely to be significant because reactions of hydrogen with minerals become relevant only over time periods much longer than the storage cycles considered. In contrast, however, significant effects of biotic and abiotic processes are expected on sulphur-bearing lithologies such as the anhydrite/polyhalite layers and the brine sump (Dopffel et al., 2021; Hemme and van Berk, 2017; Laban, 2020; Muhammed et al., 2022; Panfilov, 2016). Geochemical models and simulations (e.g., Bildstein et al., 2001; Bonté et al., 2012; Fu et al., 2016; Gillhaus, 2007; Hassannayebi et al., 2019; Hemme and Van Berk, 2018; Iglauer, 2022) are valuable tools to constrain the long-term behaviour of the reservoir in terms of mineral dissolution and precipitation reactions in the presence of hydrogen, as well as the associated effects on transport (e.g., Heinemann et al., 2021; Iglauer, 2022; Muhammed et al., 2022; Pfeiffer and Bauer, 2015), but reliable data on the kinetic rates of these processes are lacking according to many authors (Groenenberg et al., 2020b; Hassannayebi et al., 2019; Heinemann et al., 2021; van Gessel et al., 2018; Warnecke and Röhling, 2021).

It is advisable to investigate and monitor the mineralogical, chemical, physical, and microbiological condition of the reservoir before injecting hydrogen into a cavern and during storage (Laban, 2020; Schwab et al., 2022; van der Valk et al., 2020) and also to evaluate the quality of the reservoir site in terms of its location in the geological context to avoid unfavourable interactions between the different geological formations (Fu et al., 2016; Gillhaus, 2007; Laban, 2020). It can be assumed that this circumstance is of great importance in the vicinity of a cavern conglomerate. However, there are no specific studies so far dealing with the possible interactions and feedback processes related to biotic and

abiotic chemical reactions in caverns that are close to each other and connected via second-phase lithologies such as anhydrite.

Moreover, few studies to date have used microstructural analyses to determine the nature and effects of various biotic and abiotic processes on THMC properties and thus on the integrity of storage media (rocks and casings) (e.g., Flesch et al., 2018; Gloc et al., 2018). However, it is known from studies dealing with spatial-chemical relationships in porous media that these analyses are essential to better understand and describe the processes that determine reaction kinetics (e.g., Higgs et al., 2022; Jangda et al., 2022). Modern analysis methods, such as cryo-Scanning Electron Microscopy or µ- or nano-Computer Tomography, which can be used to visualize the processes ex-situ but also in-situ during the laboratory tests, are available and could provide valuable insights to better constrain the rate-controlling processes during subsurface storage with respect to the rock phases involved, in particular the porous anhydrite, but also the casing materials such as cement and steel (e.g., Bensing et al., 2022; Pötschke et al., 2022; Schmatz et al., 2015; Viani et al., 2019; Wetzel et al., 2021; Zingg et al., 2008).

As mentioned at the beginning, in situ data on the actual processes in the subsurface are not always easy to obtain. One approach to evaluating parameters relevant to geochemical models is to use analogue models to study specific parameters under well-defined boundary conditions. With known boundary conditions, these models (e.g., Hashemi et al., 2021; Hassannayebi et al., 2021; Iglauer, 2022; Lysyy et al., 2022; Muhammed et al., 2022; van Rooijen et al., 2022). can be used to delineate the actual reaction kinetics in the subsurface and thus provide improved input parameters for the geochemical models or pore network modelling of transport (for pore network models, see, e.g.,: Ebigbo et al., 2013; Joekar-Niasar and Hassanizadeh, 2012).

To better assess the quality and safety of the potential salt cavern conglomerate storage sites, it is recommended that, in addition to geochemical modelling, (i) subsurface geologic conditions be characterized with sufficient spatial resolution to identify critical lithologies, and (ii) laboratory (analogue and case studies) and in-situ testing (e.g., Schwab et al., 2022) be conducted to obtain more reliable kinetic rate data.

6 Database of (near-) accidents occurred

Authors: Pierre Bérest – Brouard Consulting and Jop Klaver – MaP – Microstructures and Pores GmbH

The database in the next pages includes a comprehensive overview of (near-)accidents, or incidents, occurred in the construction and operation of conglomerates of salt caverns for hydrocarbon storage. It lists the date, causes and consequences of the incidents. The associated references are also listed as well as the sections for most of the events, that describe the accidents in more detail in this study together with the main mechanism causing the event.

There are probably 2000 salt storage caverns worldwide. We described 12 leaks cases, so a simple answer is that the probability of an incident is 12/2000 assuming that we do know all the significant cases (which is probably true, except from USSR). However, many technical advances have been made (double barrier, better tightness tests etc), regulations have been implemented and most incidents are relatively old. In this sense, 12/2000 is an overestimation when the current technology is considered. Therefore, the likelihood of occurrence is difficult to assess as many accidents in salt caverns stand on their own with different configurations (e.g., geology, well/casing design, cavern size, etc.) and different root-cause which are sometimes not really clear due to uncertainties in the underground. Also, considering the relatively low number of events and the fact that not all accidents are published (to the full detail), a robust statistical analysis is not realistic. Below we list the frequency of incidents by the main mechanism that are described in detail in chapter 2 (Note that some are incidents are counted more than one as the mechanisms are interrelated, e.g.: creep can lead to cashing overstretch which can lead to a well leak, see also paragraph 3.3.1):

- Well leaks: 12 incidents
- Cavern tightness: 7 incidents
- Blow-out: 6 incidents
- Brittle failure: 13 incidents
- Creep closure and subsidence: 5 incidents
- Cavern creep closure: 2 incidents
- Casing overstretching: 3 incidents

Complementary to the database below, we refer to the work of Réveillère et al. (2021, 2017) and Eising (2021).

Table 9. Database of (near-) accidents occurred.

Place, state/ country	Incident date	Cause	Consequence	Reference	Section Literature review
Elk City, Oklahoma	February 1973	A breach somewhere between 365 m and 35.5 m in the single cemented casing, caused migration upward in the cement and horizontal in the Doxey Formation.	9 x 15 m, 6 m deep crater and pressure cracks radiating from it. Siltstone blocks of 20–45 kg were thrown as far as 23 m and trees were tilted.	(Bérest et al., 2019b and references herein)	2.2.3.2.2 (Well leaks)
Conway, Kansas	NGL detected in wells as early as 1956; fugitive NGLs were encountered in December 2000	Gas leaking from several faulty wells. Cement bond logs run in the wells revealed that casing cement-bonds were poor.	Propane found in shallow wells. Relocation of residents and demolition of the properties	(Bérest et al., 2019b and references herein; Ratigan et al., 2002)	2.2.3.2.3 (Well leaks)
Yoder, Kansas	June 30, 1980	Logging of the brine wells indicated poor cement bond along the casings	A propane blow-out occurred along the shoulder of a county road. Groundwater and sand were blown fifteen to twenty feet into the air and propane vapours continued to rise up through clay and silt surrounding the hole (Bryson 1980).	(Bérest et al., 2019b and references herein; Bryson, 1980)	2.2.3.2.4 (Well leaks)
Mont Belvieu, Texas	September 17, 1980 (pressure drop); gas burst on October 3, 1980	The leak was likely to be at caprock depth in the well casing.	Explosion in a cellar, gas is found in shallow waters. 50 families evacuated.	(Bérest et al., 2019b and references herein; Ratigan, 2009)	2.2.3.2.5 (Well leaks) and 3.2.3.1 (Creep closure and subsidence)
Mineola, Texas	1995	A breach in the casing originating from a pressure surge in a neighbouring cavern.	Gas occurrences near the wellhead and fire at ground level.	(Bérest et al., 2019b; Gebhardt et al., 2001; Warren, 2006)	2.2.3.2.8 (Well leaks)

Place, state/ country	Incident date	Cause	Consequence	Reference	Section Literature review
Hutchinson, Kansas	January 17, 2001	Milling created a breach when re-drilling a cemented abandoned well. Gas migration through fractured channels to the brine aquifer below Hutchinson, and to ground levels through very old and poorly abandoned brine wells.	A building was ablaze and a mobile home exploded. A dozen geysers, gas + brine, two igniting. Two casualties, 1 injured and 250 people evacuated.	(Allison, 2001, p. 200; Bérest et al., 2019b and references herein; Johnson, 2002; Ratigan, 2001)	2.2.3.2.9 (Well leaks)
Epe, Germany	February 23, 2014	Casing overstretching due to caverns convergence.	Oil seeps after April 12, 2014. 10 cows put down; one family displaced for some days.	(Bérest et al., 2019b; Bezirksregierung Arnsberg, 2014; Coldewey and Wesche, 2015; Kukla and Urai, 2015)	2.2.3.2.12 (Well leaks)
Magnolia, Louisiana	December 24, 2003	A flaw in the casing at a 440-m depth, attributed to poor welding job.	During first filling, 107 m3 of gas migrate to an aquifer layer, then to ground level. 30 residents evacuated.	(Bérest et al., 2019b; Edgar, 2005; EIA, 2006; Hopper, 2004; Nations, 2005; State of Louisiana, 2017)	2.2.3.2.10 (Well leaks)
Eminence, Mississippi	December 26, 2010 cavern #3 (Cashing failed in cavern #4 in 2004)	Likely factors: Fast cavern closure rate (40% in one year) frequent re-brining.	Blow-outs in shallow boreholes. Twenty families evacuated during two weeks.	(Bérest et al., 2019b; Wellinghoff et al., 2013)	2.2.3.2.1 (Well leaks) and 3.3.2.2 (Casing over-stretching)
Teutschenthal, Germany	March 29, 1988	Ethylene accumulated in a 100–140-m deep layer overlain by a poorly permeable, 25-m thick layer. Layer uplift led to overstretch of the 11-3/4" casing, which breaks on March 29, followed by a massive leak. Ethylene leakage paths are along existing faults.	One hour after the pressure drop, first ethylene + water blowout, followed by several others, gas production during several days, 60% to 80% of cavern volume is lost. Blow-out spots aligned on parallel lines. Ground uplift by 1.5 m before the eruption. Fractures at ground level. An 8 km^2 zone.	(Bérest et al., 2019b and references herein)	2.2.3.2.6 (Well leaks)

Place, state/ country	Incident date	Cause	Consequence	Reference	Section Literature review
Boling, Texas	Fall 2005	The casing had failed at eight different locations by casing overstretch and tensile failure, dragged down by the salt. This was facilitated by the flat roofs and the absence of cavern necks.	None.	(Bérest et al., 2019b and references herein)	2.2.3.2.11 (Well leaks) and 3.3.2.1 (Cashing over-stretching)
Clute, Texas	December 1988	Effects of dome internal movements?	Gas loss estimated to be 27 000 m^3.	(Bérest et al., 2019b; Toth, 1990, 1989a)	2.2.3.2.7 (Well leaks)
Arabali brine field, Turkey	-	"Sonar surveys suggested that a 9-m-high, 30-m-long, 2-m-wide slot was created between the two caverns, exactly coinciding with the vertical plane crossing through the hanging strings of each of the two caverns (Kirmic and Ralowicz, 2003)." (Bérest et al., 2020)	"A hydraulic connection was detected between Caverns a-98 and a-117." (Bérest et al., 2020)	(Bérest et al., 2019b; Kirmic and Rałowicz, 2003)	2.2.3.1.5 (Cavern Tightness)
Bayou Corne, Louisiana	August 3, 2012	A sheath composed of loose and soft sediments allowed those sediments to flow from ground level to a breach created in the lower part of the cavern.	A sinkhole in the swamp	(Bérest, 2017; Bérest et al., 2020)	2.2.3.1.1 (Cavern Tightness)
Spindletop, Texas	December 19, 2001	Asymmetric growth and brine contamination by sylvite during an earlier enlargement of Centana No. 1 suggest the presence of a heterogeneity.	Cavern integrity loss	(Bérest et al., 2020; Brouard and Bérest, 2019; Caglayan et al., 2020; Horváth and Schneider, 2018; Johnson, 2003; Looff, 2017)	2.2.3.1.3 (Cavern Tightness)
Clovelly salt dome, Louisiana	1992	Investigations suggest that brine leaked to the exterior of the dome through a 660-m deep “inhomogeneity”.	Did not pass MIT	(Bérest et al., 2020; Horváth and Schneider, 2018; McCauley et al., 1998)	2.2.3.1.4 (Cavern Tightness)

Place, state/ country	Incident date	Cause	Consequence	Reference	Section Literature review
Veendam, Netherlands	April 20, 2018	"It has been hypothesized that the initial fracture or breach through the relatively thin salt layer at the top cluster opened in the overlying Buntsandstein layer, where the state of stresses is suspected to be strongly anisotropic." (Bérest et al., 2020). "...via macro-scale (single) fractures. Such a fracture did occur in April 2018 at Nedmag in Veendam." (Fokker et al., 2022)	"Based on cluster compressibility, the brine volume that seeped from the cluster during the 30 first minutes after the pressure drop was estimated to be 25.000 m³." (Bérest et al., 2020). "The fracturing process has driven 100.000 m³ of brine into the overburden" (Fokker et al., 2022)	(Bérest et al., 2020; Fokker et al., 2022)	2.2.3.1.6 (Cavern Tightness)
Weeks Island, Louisiana	1992	"Geomechanical modelling by Neal et al. (1995) showed mechanism for crack development in tension that would develop over mined openings after a number of years and progress through weakened dilatant zones." (Bauer et al., 2000)	Two sinkholes, the first one in 1992, appeared at ground level above the edge of the mine.	(Neal et al., 1995, Bauer et al., 1997; 2000)	2.2.3.1.7 (Cavern Tightness)
Mont Belvieu, Texas	2004	Two brine caverns were connected hydraulically; origin of the breach is likely to be an Anomalous Zone inside the dome	Both wells have been removed from service (Cartwright and Ratigan, 2005; Johnson, 2008)	(Cartwright and Ratigan, 2005; Horvath et al., 2018; Looff, 2017; Bérest et al., 2020)	2.2.3.1.2 (Cavern Tightness) and 3.2.3.1 (Creep closure and subsidence)
Fort Saskatchewan, Alberta	August 26, 2001	Elbow failed on the 2-inch connecting line	Explosion and resulting fire (for days)	(Réveillère et al., 2017)	2.3.2.1 (Blow-out)
Moss Bluff, Texas	August 9, 2004	A rupture of the 8” brine-outlet piping attached to the wellhead (integrity was compromised due to internal corrosion).	The gas escaping from the open pipe ignited. The force of the gas flow carved a crater 60-ft (18-m) across and 30-ft (9-m) deep at the vicinity of the wellhead. 360 people evacuated.	(Réveillère et al., 2017)	2.3.2.2 (Blow-out)

Place, state/ country	Incident date	Cause	Consequence	Reference	Section Literature review
Regina South, Saskatchewan	2013	Vertical strain on the cemented casing exceeded the failure limit.	All of the wells have experienced some degree of cemented casing damage, and four of the eight wells have experienced severe casing separations within the interbedded interval", (p.1, Coleman Hale et al., 2015)	(Coleman Hale et al., 2015)	3.3.2.3 (Casing over-stretching)
Maceió, Brazil	Since 2004	"... both active/pressurized and inactive/ depressurized salt mining conditions led to mechanical instability of the cavities with local upward migration and likely partial to total cavity collapses; and (5) developed from the deforming cavities cracks propagated upward towards the shallower layers." Vassileva et al., 2021	More than 2 m of maximum vertical subsidence. Fractures in roads and buildings of which >6000s were demolished.	(Vassileva et al., 2021)	3.2.3.4 (Creep closure and subsidence)
Etzel, Germany	High-pressure test was performed in a brine-filled cavern at Etzel in 1990–1992	Cavern pressure was increased step by step in a controlled test	Brittle failure	(Rokahr et al., 2000; Rokahr et al., 2003; Djizanne et al., 2012)	3.4.6 (Brittle failure)
Matarandiba Island, Brazil	Discovered May 30, 2018	Brittle failure, but origin controversial, compelling evidences are missing.	69-m long, 29-m wide and 45-m deep crater (sinkhole) since discovery and growing.	(Guimaraes et al., 2018; Réveillère, Bérest and Jeronimo, 2021)	3.4.4.2 (Brittle failure)
Kiel, Germany	1967	Brittle failure of roof due to presence of a relatively large roof span and a somewhat flat roof, and heterogeneity of the salt formation.	Roof fall	(Dreyer 1972; Röhr 1974; and Baar 1977)	3.4.5.1.1 (Brittle failure)

Place, state/ country	Incident date	Cause	Consequence	Reference	Section Literature review
Regina South, Saskatchewan	1989 and after (Cavern No. 5), 1993 (Cavern No.4)	"The exact reason of the rockfalls is unknown; multi-layered overburden and flat roof might be significant factors." Réveillère et al. 2017	Two massive roof falls led to gas seepage to non-salt overlying layer. Cavern pressure was lowered	(Crossley 1988 and 1992; Réveillère et al. 2017)	3.4.5.1.2 (Brittle failure)
Jintan, China	Between 2009-2015	(1) a rapid pressure drop, (2) low final value of the pressure at the end of the drop, (3) a flat roof, and (4) the presence of the interlayer immediately above cavern roof. It can be hypothesized that the thin (2 m) large-span (50 m) salt layer at the cavern roof, poorly bound to the softer overlying interlayer, experienced bending and buckling-like failure.	Roof fall	(Wang et al., 2018)	3.4.5.1.3 (Brittle failure)
Gaines County, Texas	Between 1996-2001	Roof collapse	"Cavern roof migration of approximately 200 ft [60 m] and the loss of the last 80 ft of cemented casing" (Johnson, 2003)	(Johnson 2003)	3.4.5.1.4 (Brittle failure)
Lille Torup, Denmark	2005 (Test)	"Local failure of the rock salt at the cavern wall..." (Rokahr et al., 2007)	Local spalling and block fall	(Rokahr et al. 2007)	3.4.7.1.1 (Brittle failure)
Huntorf, Germany	1978?	Djizanne et al. (2014) suggested that salt curtains fall originated in the change in Archimedes' thrust when, during debrining, brine was substituted by gas, whose density is much lower	Block fall of salt "curtains"	(Crotogino et al. 2001; Djizanne et al. 2014)	3.4.7.1.2 (Brittle failure)

Place, state/ country	Incident date	Cause	Consequence	Reference	Section Literature review
Jintan, China	Between 2011 - 2015	Buoyancy (i.e., in Archimedes' thrust) applied to cantilever beam-like overhangs during de-brining (see also Huntorf case) or tensile failure due to the high vertical stresses in overhangs (Ref?)	Spalling and block fall	(Wang et al., 2017)	3.4.7.1.3 (Brittle failure)
Bryan Mound, Texas	Tens of events since 1980s	Anomalous Features (e.g., anhydrite insolubles, potash and gas) causing brittle failure	Block falls, casing/pipe loss and hanging-string damage.	(Thoms and Neal 1992; Munson et al., 1998)	3.4.7.1.5 (Brittle failure)
Big Hill, Texas	Since 1990	Anomalous Features causing brittle failure	Cavern floor rise and buried string by debris because of block falls and sloughing of salt from the cavern walls in cavern 103. One blockfall damaging hanging string in cavern 114	(Munson et al., 2004)	3.4.7.1.6 (Brittle failure)
Markham, Texas	Since 1992	Significant pressure changes might have been instrumental causing brittle failure	Salt sluffing from the walls and roof of the cavern resulting in cavern-volume loss.	(Cole, 2002)	3.4.7.1.7 (Brittle failure)
West Hackberry, Louisiana	September 21, 1978	"Packer upwards slip during a workover operation. Oil blow out and fire." Réveillère et al., 2017	Blow-out, fire. 1 casualty	(Réveillère et al., 2017 and references herein)	(Blow-out)
Teutschenthal, Germany	November 1984	"Leakage during an operation to recover a logging tool stuck in a wellhead." Réveillère et al., 2017	Gas released to the atmosphere	(Réveillère et al., 2017)	(Blow-out)

Place, state/ country	Incident date	Cause	Consequence	Reference	Section Literature review
Prud'homme, Saskatchewan	October 11, 2014	"A failure in the steel casing, located about 2 m (6 ft) below ground, allowed natural gas to leak into an external concrete casing protecting the pipe, where it moved up and released through a valve on the side of the cavern wellhead. The force of the high pressure natural gas release damaged the wellhead building, causing a spark and the resulting fire." (Réveillère et al., 2017)	Gas blow-out and fire for 9 days	(Réveillère et al., 2017)	2.3.2.1 (Blow-out)
Brenham, Texas	April 7, 1992	"An overfilling occurred during LPG injection, resulting in LPG release in the brine pond and the development of a gas cloud that ignited when an auto entered it." (Réveillère et al., 2017)	"Severe magnitude 3.5 to 4 explosions. 3 dead, 23 injured, 50 evacuated, 26 homes destroyed within 1.5 miles (2 km) of the explosion, damage to further 33 homes." (Réveillère et al., 2017)	(Réveillère et al., 2017)	(Blow-out)
Bernburg, Germany	After 5 years and 8 months	Creep closure and subsidence	Up to 4 cm subsidence	(Menzel and Schreiner, 1983)	3.2.3.2 (Creep closure and subsidence)
Tersanne, France	Since 1982	Creep closure and subsidence	Up to 4 cm subsidence	(Nguyen Minh D. et al., 1993)	3.2.3.3 (Creep closure and subsidence)
Vacherie and Rayburns boreholes, Louisiana	After 4.5 years	Creep closure	Diameter loss as a function of time	(Thoms and Gehle, 1983)	3.1.4.4 (Cavern creep closure)
Gorleben Mine, Germany	-	Brittle failure	Thermal fractures	(Wallner and Eickemeier, 2001; Zapf et al., 2012)	3.4.3.2.4 (Brittle failure)
Te02, France	Over 37 years	Creep closure	Cavern volume loss, subsidence	(Hévin et al., 2007)	3.1.5.1 (Cavern creep closure)

Place, state/ country	Incident date	Cause	Consequence	Reference	Section Literature review
Next incidents are not described in this Literature Review					
Abovyan, Armenia	-	Earthquake and poor maintenance	Well failure and gas leaks	(Energy Charter Secretariat, 2008; Eising, 2021)	-
Manosque, France	-	Brittle failure	Block fall	(Fortier et al., 2006; Mercerat et al., 2010)	-
Viriat, Franc	1986	Failure of compressor unit	Gas leak and cloud	(Eising, 2021; Réveillère et al., 2017)	-
Goodyear, Arizona	-	Corrosion in casing	Gas leak	(Evans, 2007)	-
Bayou Choctaw, Louisiana,	1954	Uncontrolled solutioning	Cavern collapse and abandonment of nearby cavern	(Neal et al., 1993)	-
Petal, Mississippi	August 1974	Cavern overfill due to miscalculation	Flammable cloud, fire, explosions, damaging houses, 24 injured people and 3000 evacuated	(Evans, 2007)	-
Hackberry, Louisiana	1978	Special operations	Oil geyser	(Bérest and Brouard, 2003)	-
Carthage, Missouri	November 16, 1989	Cavern overfill	Ignition of released propane	(Réveillère et al., 2017)	-
Sour lake, Texas	1998	Subsidence and uplift of the salt dome	"…hosting the cavern created cracks and displacement in the concrete cellar, and increased stress to the well casing which ultimately lead to shearing the 16'' cemented casing and to the opening of a leak path." (Réveillère et al., 2017)	(Réveillère et al., 2017)	-
Bad-Lauchstadt / Teutschenthal, Germany	1984	"Leakage during an operation to recover a logging tool stuck in a well" (Réveillère et al., 2017)	Blow-out	(Réveillère et al., 2017)	-

Appendix: Risk assessment

Author: René Vreugdenhil – Pondera Geo Energy

General

For a risk to be relevant it requires:

- a source, the location where the risk originates,
- a path, the way a risk can migrate from the source,
- and a critical object, the vulnerable recipient that will be adversely affected by the risk.

If one of the requirements is not met (e.g., the risk is contained or there is no critical object within the vicinity of the source) there is no actual risk present. This is the basic principle of "Risk based Working", the methodology for risk assessment described by M. van Staveren.

Modelling of risks

Worldwide there are dozens if not hundreds of methods for risk assessment for example to determine the probability of occurrence of a risk or for a comparison between risks. In this case models are schematic representation of reality.

A common model is the bow-tie, referring to the shape the model has: to the left a number of causes, risk as a knot in the middle and a number of consequences or effects at the right. Normally it is a schematization of unilateral risk-effect-relations for one single risk.

There are other models like Ishikawa or fishbone diagram. This model visualises the cause-effect-relations *between* risks but does not show the causes and effects of the individual risks.

A third model is the risk matrix or heat map, most established in the traditional risk management. This model consists of vertical and horizontal axes with the probability of occurrence and the consequences or effects of risks. Risks are plotted in the matrix based upon calculated of guesstimated chances and the effects or consequences of these particular risks. The risk matrices have colours (ranging from green till red, most often 3-4) that represent the seriousness of the individual risks.

Many of the methods focus on the analysis of the risk itself. Others also contain the control of the analysed risks, but none takes the presence or lack of a critical object (represented by a stakeholder) into account. It is not just the building on top that might be impacted. The risk analysis will also comprise stakeholders that are not in the direct neighbourhood, like water companies, private or corporate water wells, geothermal wells etc., that might be affected - directly or in time - by the storage.

Risk assessment of H_2-storage in salt caverns

Risk assessments on storage in salt caverns are well known and describe a wide variety of risks associated with part of or the total life-cycle of the salt cavern. Until now the results are all qualitative analyses. Risk assessment on H_2 storage however is scarce and mainly built upon the risk assessment of natural gas storage. The following two reports have been found, that contain risk assessments concerning H_2 storage in salt caverns.

TNO 2020 (van der Valk et al., 2020)

The risk assessment of TNO (2020, *Inventory of risks associated with underground storage of compressed air (CAES) and hydrogen (UHS), and qualitative comparison of risks of UHS vs. underground storage of natural gas (UGS)*) involves the total life-cycle:

- the process of the design (*pre-execution phase*),
- the salt mining itself (*execution phase*),
- the storage of the gas / liquid (*operation*),
- the abandonment (*decommissioning*)
- and the monitoring afterwards (*post abandonment monitoring*).

TNO bases its assessment on the global experiences with the underground storage of natural gas (methane) adapted to the material differences between hydrogen and methane. A total number of 137 risks (total life cycle) were formulated that apply to hydrogen storage in salt caverns *(NB: as the study of TNO has a wider scope – three different storage types – the total number does not include risks that solely apply to storage in depleted natural gas reservoirs and /or the storage of compressed air (CAES))*.

TNO made a selection of six key risk themes associated with storage of hydrogen:

- material integrity/durability,
- leakage of hydrogen,
- blow-out,
- diffusion and dissolution,
- loss and/or contamination of hydrogen,
- and ground motion (subsidence, induced seismicity)

Risks were inventoried by conducting a literature review and supplemented with expert knowledge. The purpose of the risk inventory was to serve as a starting point and checklist to identify and manage risks in development projects, and to provide guidance on potential mitigation measures to reduce the risks.

A qualitative non-site-specific comparison was made for the risk themes between UHS and underground storage of natural gas. The main conclusions of the report with respect to the material differences between hydrogen and methane are:

- Hydrogen is more prone to ignite when released in air as it has a much wider flammability range and a much lower ignition energy compared to methane. Hydrogen is therefore classified as a high reactive gas;
- When a mixture of hydrogen and air explodes, the higher flame propagation speed potentially generates high pressures that could result in an explosion (a pressure shock wave) with massive burst damage, i.e., damage to buildings or even collapse;
- A catastrophic event on the well pad could lead to uncontrolled outflow of gas (also referred to as a blow-out). A properly installed and operationally tested SSSV (subsurface safety valve) must prevent significant outflow in case of such catastrophic event. The effectiveness of SSSV's in shutting in a flowing hydrogen storage well is yet to be confirmed.

The risks mentioned in the TNO-report will be part of the risk analysis of KEM 28.

Main conclusions of the report with respect to research:

> *"Although the risks associated with UHS are generally known, further research is required in particular on:*
>
> - *the long-term durability of rocks and (well) materials (steel alloys, cement, elastomers, etc.) when subjected to hydrogen under an alternating pressure regime that causes mechanical and thermal stresses, and*

- *interactions of hydrogen with rocks, fluids and microbes in reservoirs and their effects on reservoir performance, quality and retrievability of the stored hydrogen, and integrity and durability of materials subjected to products of such interactions (e.g., H_2S).*"

This – more or less – describes the content of the KEM 28 project.

Eising (2021)

In his report / thesis Eising aims to assess the risks associated with storage of liquids and gasses in salt caverns.

The main research question was:

> *"What can we learn in the Netherlands from the published examples of storage caverns, for liquids and gases, in other countries?"*

In the research an inventory of worldwide storage caverns was conducted and a list of all the published incidents was made. Eising categorized the incidents in 5 different groups, all of them in the "operational" phase:

1. cavern instability, including different top events like roof collapse, block fall and creep closure that influence the shape of the cavern;
2. cavern integrity loss, causing leakage to the overburden, other geological layers, or neighbouring caverns;
3. well integrity loss, caused by mechanical failure of the materials of which the well is composed, like casing, tubing, or other well components (all subterraneous);
4. well control loss, occurring when hydrostatic pressure and formation pressure are not maintained, and outflow of stored liquids / gasses takes place;
5. pipeline integrity loss, damage to the surface installations, like Christmas tree, wellhead, pipelines etc.

Main conclusions / assumptions:

- there have been more incidents in domal salt as opposed to bedded salts, suggesting bedded salts are better suited for cavern storage;
- caverns which are situated relatively shallow (up to 500 m deep) and relatively deep (deeper than 1500 m) have had more incidents, implying cavern storage is safer in-depth ranges between 500 and 1500 m at least;
- preventive measures are important. Cavern design, pressure management, well design and monitoring are basic conditions of the safety of a cavern.

The assumptions were based on a low number of incidents (87 in total) and thus require more research to be confirmed.

For each category Eising made a bow-tie analysis focusing on the event, the causes and escalation factors and the consequences. Furthermore, some primary mitigation factors were mentioned.

One other report / thesis is worthwhile mentioning as it focusses on the characteristics of hydrogen being stored in a salt cavern:

M.P. Laban (2020)

One other report / thesis is worthwhile mentioning as it focusses on the characteristics of hydrogen being stored in a salt cavern, M.P. Laban (2020).

The main research questions were:

What are key cavern conditions that influence the suitability of hydrogen storage in salt caverns and for what purpose can the storage plant be implemented?

The relevant sub-research objectives were:

1. *What are the potential process risks when storing hydrogen in salt caverns?*
2. *Are there substantial risks of contamination with subsurface hydrogen storage? What are the defining variables that contribute to said contamination?*
3. *How do these impurities build up when the salt cavern is used?*

Natural gas storage in salt caverns has proven to be a viable solution for gas storage and might be a suitable option for hydrogen as well. The literature review highlights the largest operating problems with respect to hydrogen, like leakage risks, hydrogen embrittlement, risks of contamination and volumetric density. Furthermore, it concludes that there is a total lack of knowledge with respect to the chemical process in the salt cavern and the contamination with H_2S as a result of bacterial activity.

The thesis of M.P. Laban et al (2020) describes a part of the life-cycle, the *operation* stage with special emphasis on the chemical process of hydrogen within the salt cavern and, more specifically, the effect of H_2S concentrations within the hydrogen gas. In the following figure the specific risks of hydrogen storage are mentioned.

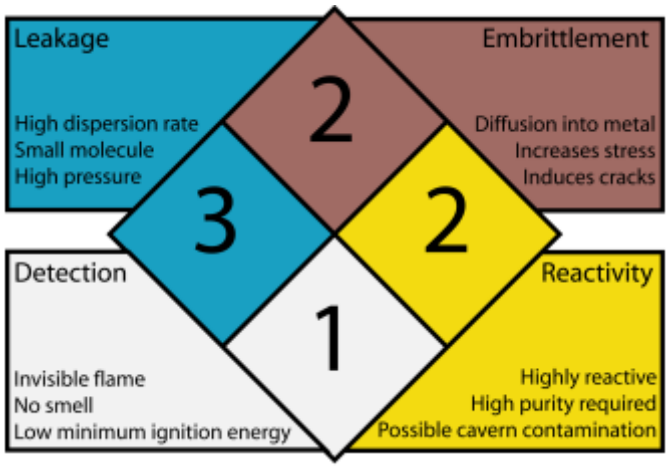

Figure 158. Hazards of the use of high pressure hydrogen gas (Laban, 2020).

The conclusions with respect to the sub-research objectives are:

- *What are potential risks when storing hydrogen in salt caverns*?
  The risks are primarily found when the gas pressure increases. The most important risks when storing high pressure hydrogen in caverns are:
  - Hydrogen gas leakage.
  - Hydrogen diffusion and embrittlement.
  - Hydrogen (auto-)ignition and flame detection.
  - Hydrogen contamination mainly concerning the concentration of H_2S.
- *Are there substantial risks of contamination with subsurface hydrogen storage? What are the defining variables that contribute to said contamination*?
  Results from this research method determine that values that influence the H2S production rate are (sorted by significance):
  - Bacterial growth and reduction rate
  - Brine volume and sulphate concentration.
  - Brine pH and ionic strength.

- Cavern pressure and temperature.
- Fe2+ and Fe3+ concentration.

The cavern pressure, temperature, sulphate and iron concentration and brine volume, are all values that should be taken into account when either building or choosing a cavern that is to be used for hydrogen storage. None are as important as the bacterial presence, the number of sulphate reducing bacteria (SRB) present in the cavern soil.

- *How do these impurities build up when the salt cavern is used*?
  A dynamic model (PHREEQ) was constructed which determines the build-up of H_2S, as a function of time and a cavern demand-curve. In both modelled situations the H_2S build up exceeds the fuel cell guidelines or even, in the worst case, any allowable ISO concentration. The hydrogen probably needs to be purified using gas sweetening.

One sub-research objective was added:

- *What are key cavern conditions that influence the suitability of hydrogen storage in salt caverns and for what purpose can the storage plant be implemented*?
  The key cavern conditions that influence the suitability of hydrogen storage in salt cavern, based on the risk of contamination are the bacterial sulphate reduction rate and the pH of the aqueous environment. Caverns should be tested prior to use on the possibility of sulphate reducing bacteria. It is possible to reduce H_2S production by changing the pH or injecting aqueous iron, or by the way the cavern is used. H_2S in gas outflow is estimated to have large peaks in outflow concentration due to possible H_2S build up in relatively empty caverns.

The risks mentioned in the thesis will be part of the risk analysis.

Use of Risk based working

For the risk analysis “Risk based Working” will be used developed by Martin van Staveren. Risk based working is a semi-quantitative method to determine the risks, the consequences, the effect of the measures to be taken and the residual risks (and consequences) when using the preventive measures and being prepared to commit the corrective measures when needed.

The classification of the risks is presented in a risk matrix (figure 15 of the proposal).

The probability and consequences of occurrence will be rated 0 - 3. The explanation of the different ratings will be described in the template for "Risk based working".

The template for “Risk based Working” consists of a structure of 6 steps of risk-based working. Before starting unambiguous working, definitions are needed for the key terms “uncertainty”, “risk” and “risk perception”. The following definitions are derived from the current definitions in the field of risk management and appear to work well.

- *Working definition “uncertainty”*

  Uncertainty is incomplete certainty caused by (1) inevitable variation and/or (2) lack of information.

  Inevitable variation, like the inherent variation in the composition of salt on a local scale, concerns an uncertainty that cannot be reduced. Lack of information in most cases concerns an uncertainty that can be reduced.

- *Working definition “risk”*

  Risk is an uncertain event with causes, probability of occurrence and impact on objectives.

The definition implies that objectives are needed to determine risks. That means that for each and every stakeholder it must be completely clear what their objectives are in relation to the storage of H_2 in salt caverns. In other words, what is the desired or required situation with respect to H_2 storage.

In the following Figure 159 the relation between objective, risk, causes, consequences and constraining measures is displayed. The figure is based upon the well-known bow-tie scheme in which a risk is a result of causes leading to consequences.

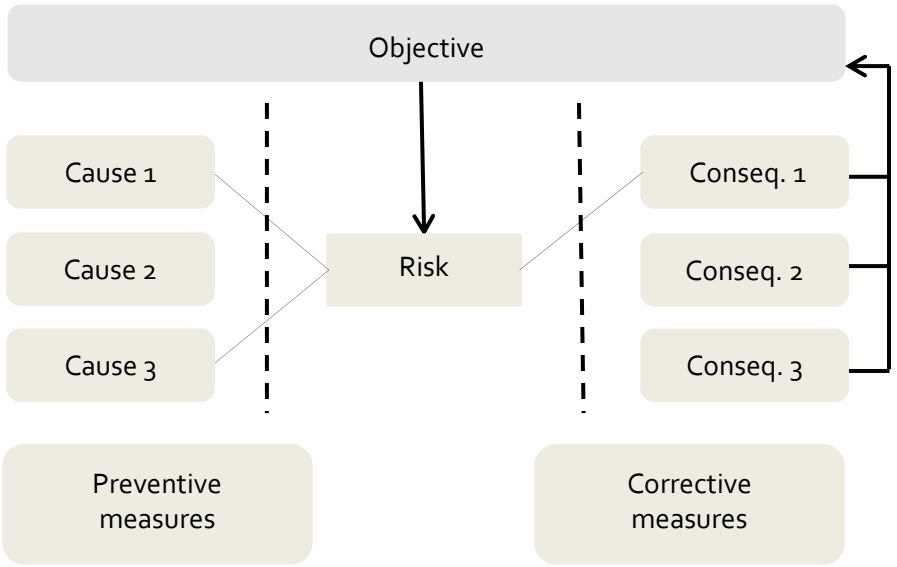

Figure 159. Relation between objective, risk, causes, consequences and constraining measures.

There are two types of measures that can be taken, preventive and corrective. Preventive measures aim at limiting or eliminating the causes, resulting in reduction of the risk itself. Corrective measures reduce or eliminate the consequences of risks. Both types of measures reduce the risk and with it the impact on the objectives.

- *Working definition "risk perception"*

  Risk perception is the unique way in which a person assesses a risk.

  Opportunities and consequences of risks often cannot be determined or calculated objectively. Furthermore, the way in which these opportunities and consequences are (un)acceptable – or: the willingness to take risks - depends strongly on the position, interest, and expectation of the stakeholder. Risk perception is not purely rational, emotions play an important part.

The 6 risk steps are part of each and every risk management approach, as mentioned before. By going through these steps in an explicit and structured way for a specific location of a salt cavern used for the storage of hydrogen one gets (1) insight into the nature and extent of the risks and underlying uncertainties, and (2) insight into the necessity and possibilities for – whether or not – taking measures to contain these risks adequately. This is done in a transparent and therefore understandable and acceptable manner for the stakeholders.

In phase 2 of the KEM 28 project the risk assessment will be composed in multiple steps. It starts with the framework (stakeholders and overall information of the site / region) and ends with a risk matrix before and after the implementation of the preventive and corrective measures.

<u>Risk step 1: Determine stakeholders and their objectives</u>

Determination of all stakeholders and their main or multiple objective(s). The objective of the stakeholders leads to the preferred or required end situation with respect to possible risks related to hydrogen storage in salt caverns.

Risk step 2: Identify risks

Using the objectives (risk step 1) the risks related to hydrogen storage in salt caverns are identified. The risks are described in an unambiguous way as an uncertain event (not an existing problem!) with one or multiple causes and one or multiple consequences.

Causes are classified via HOT-RIP factors. “H” stands for Human cause, “O” for Organisational cause and “T” for Technical cause. The RIP factors may increase the impact of certain risks, with “R” standing for (lack of or contra dictional) Regulations, “I” for dominant Industrial culture and “P” for the aspects Politics, Press and Public.

Consequences of the risks are normally classified according to the Big 5-risk effects: (1) safety, (2) quality, (3) time, (4) finances and (5) reputation. Given the importance of political and social acceptance an additional effect will be considered: (6) environment (natural and social).

Risk step 3: Classify risks

In step 3 the probability of occurrence of every risk is determined, as well as the extent of the consequences, related to the objective. In other words: every risk gets classified.

The probability and consequences of occurrence of each risk are determined – if possible – geo-statistically, or – most likely – based on expert judgement. The expected accuracy of the calculations or expert judgements is made explicit. It will also be made explicit whether the classification of the risk is based on facts, interpretation of facts or assumptions.

A 4 x 3 risk matrix is used for the classification of the probability and consequences of occurrence of each risk. The 4 x 3 risk matrix consists of 4 probability classes and 3 consequence classes, see Figure 160, with the colours red, orange, and green standing for the “willingness to accept risks”.

4 x 3 Risk matrix		Consequence		
		1	2	3
Probability	3			
	2			
	1			
	0			

Figure 160. Risk Matrix.

- Red stands for large, unacceptable risks that have to be mitigated on short notice;

- Orange stands for moderate risks that will be addressed, if possible and necessary, with a medium-term time frame;
- Green stands for small, more or less "acceptable" risks that require no measures unless these are easy to incorporate and lead to further reduction of the consequences.

Risks with probability "0" represent a special category. These risks have a probability of occurrence that equals or approaches "0". For instance, as a result of physical barriers that contain the consequences of the risk, or when the probability of occurrence approaches "0", despite a large spread in assumptions. Such a classification needs to be substantiated with (a combination of) facts, interpretations of facts or, lacking both, assumptions. These interpretations and assumptions must be based upon thorough expert judgement. It is commonly accepted to classify the risks involved as extremely small / non-existing based upon state-of-the-art knowledge and experience.

Risks with probability "0" have no reasonable chance of occurrence. The consequences of these risks have to fall into the categories 1 to 3. If not, there is no risk at all.

Risk step 4: Dealing with risks

In step 4 it is decided whether or not, and if so which, measures must be taken to limit classified risks to an acceptable level or to keep them on that level. The "acceptable level" depends on the risk perception and risk willingness of the stakeholders. Furthermore, in step 4 it becomes clear if additional research is necessitated to better understand the (height of the) risk and the necessity of additional measures, preventive and/or corrective.

At the end of step 4 the risk assessment will be finalized with the determination of the residual risks, again displayed in a risk matrix.

Proposed structure for Phase 2

As discussed, in Phase 2 the risk assessment will be generic, not focussed on one specific site. This choice, though TNO recommended to select a specific site, was made by the KEM team. It was felt that more detailed information on the geology and the salt structures of "the specific site" was needed before a site-specific risk assessment could be carried out.

The risk assessment will be done only for the operational phase (the storage of the gas / liquid) as all other phases are political/social/financial (pre-execution phase) or related to the salt cavern itself (design, execution, decommissioning and post-abandonment monitoring). There is one exception: "*risks associated with surplus extraction (more than can be processed) of brine*". These risks are typical of the execution phase, the stage in which the salt cavern is developed.

For this specific risk we suggest to contact at least one, preferably several, members of the salt production industry primarily to establish if there actually is a risk of surplus extraction. At this moment the number of interested clients and their need for brine outnumbers the extracted quantity mainly due to the fact that the quality of the brine and the resulting salt in the Netherlands is excellent (*oral information salt industry, needs to be confirmed*).

The risk assessment itself will be done in several workshops, starting with a draft version of the template used for the risk assessment. This draft version, with a questionnaire, will be sent to all the experts who contribute in the KEM-28 project.

During Phase 2 the risk assessment will be filled in in 4 steps. In each step the experts of KEM-28 will participate. After each step the results will be processed and the form of the risk assessment will be filled gradually. The activities and results of each step are:

1. Determining all relevant stakeholders with their objectives. After step 1 all relevant stakeholders are recorded;
2. Identifying all important risks for each stakeholder. After step 2 all relevant combinations of stakeholders and risks are recorded and – preferably – classified;
3. Dealing with the risks. Determining the optional preventive and corrective measures to mitigate the risks. After step 3 all measures, preventive and corrective, are listed per addressed risk;
4. Determining the residual risks considering the measures. In the final meeting all risks and measures will be discussed, adjusted if needed, and the residual risks (quantified) will be determined.

After these steps the risk assessment has been filled and completed using the expertise of the team members and, preferably, the critical notes of the Ministry of EA&C.

Ideally the result of the assessment is discussed with representatives of each stakeholder to assure that their objectives have been formulated correctly and the risks that might influence their objectives have all been taken into account. However, with the concept of hydrogen storage in salt caverns still in – or even before – its pre-execution phase and the generic state of the risk assessment it is not possible or recommended to contact any stakeholders, other than the Ministry. The State Supervision of Mines will be contacted through the Ministry.

Bibliography

Van der Valk, K., Van Unen, M., Brunner, L., Groenenberg, R., 2020. Inventory of risks associated with underground storage of compressed air (CAES) and hydrogen (UHS), and qualitative comparison of risks of UHS vs. underground storage of natural gas (UGS) (No. TNO 2020 R12005). TNO, Utrecht.

CMEO, 1993. Milieu-effectrapport ondergrondse gasopslag te Norg.

DAGO, 2019. 20190903 DAGO Risico Matrix (QHSEP).

Evans, D.J., 2008. An appraisal of underground gas storage technologies and incidents, for the development of risk assessment methodology. Health and Safety Executive. RR605 Research Report.

Peterhead CCS project, 2016. Risk management plan & risk register. Doc No: PCCS00-PT-AA-5768-00001, Date of issue: 19/01/2016, DECC Ref No: 11.023.

E. Ruigrok, J. Spetzler, B. Dost, and L, Evers, 2019. Veendam event, 09-01-02019. Royal Netherlands Meteorological Institute (KNMI), Technical Report 373.

Van Unen, M., van der Valk, K., Koornneef, J., Brunner, L., & Koenen, M., 2020. HEATstore risk assessment approach ECW case Middenmeer. TNO report.

Eising, J., Brouwer, F., Andeweg, B., Van Gent, H.W. 2021. Risk analysis of worldwide salt cavern storage and its implications for the Dutch cavern storage industry. Thesis Vrije Universiteit and Staatstoezicht op de Mijnen.

Portarapillo, M., Di Benedetto, A., 2021. Risk Assessment of the Large-Scale Hydrogen Storage in Salt Caverns. Energies 2021, 14, 2856.

Van Staveren, M, 2015. Risicogestuurd werken in de praktijk.

Van Staveren, M, 2018. Risicoleiderschap, doelgericht omgaan met onzekerheden

Risk assessment of hydrogen storage in a conglomerate of salt caverns in the Netherlands

PART 2 – Geomechanical study

Reference: KEM-28 – Part 2

Summary

CHAPTER 1 GEOMECHANICAL ANALYSIS OF TYPICAL HYDROGEN-STORAGE CONFIGURATIONS

The literature review performed in Phase 1 shows that incidents related to salt caverns may have various causes. Several different mechanisms are involved. In some cases, local heterogeneities play a major role (Huntorf compressed-air-storage caverns); in other cases, dome-scale anomalies are to be incriminated (Big Hill oil-storage caverns); significant pressure changes might have been instrumental (Markham, Lille Torup gas-storage caverns). The geomechanical analysis that follows focuses mainly on potential mechanical stability problems related to hydrogen pressure and temperature variations.

A comprehensive geomechanical analysis of typical hydrogen-storage configurations has been performed.

The work was divided in six main tasks:

Task 1: Wellbore thermodynamics modelling
Task 2: Creation of parametrized 2D and 3D models of hydrogen caverns
Task 3: Numerical computations including sensitivity analysis
Task 4: Blowout modelling
Task 5: Workover modelling
Task 6: Analysis of the mechanical stability of a cluster of 9 caverns

Each of these tasks is briefly described below.

1. **Wellbore thermodynamics modelling**

The wellbore modelling is an important part for the full understanding of hydrogen cavern behaviour. A typical 9-⅝" production casing is considered. It is assumed that hydrogen caverns are loaded through a massic flowrate (in kg/s) set at the wellhead during injection and production phases. Wellbore modelling aims at calculating the evolutions of thermodynamic variables (pressure, temperature, velocity…) along the wellbore, and especially at cavern depth. The results of this task is used in the sensitivity analysis (task 3), it helps to better define optimal characteristics and operational patterns for future hydrogen caverns.

It is also assumed that hydrogen caverns will be operated through a cycling between the maximum and the minimum pressure, but the duration and pattern of each cycle depends on massic flowrates and is not well defined yet (it might also be site-specific). However, pressure and temperature variations are of upmost importance as cavern-pressure evolution determines stresses in the vicinity of the cavern and the possible onset of tensile stresses or rock-salt dilation. Several typical configurations are considered, including 3 casing-shoe depths (800, 1000 and 1200 m), 3 maximum cavern diameters (40, 60 and 80 m), and 3 cycling periods (1 month, 3 months and 1 year).

Computations were performed using the wellbore thermodynamic model embedded in the LOCAS software developed by Brouard Consulting. LOCAS has been used for a long time for many studies worldwide and successfully benchmarked against another commercial software (Kavpool+FLAC3D by ESK) as a part of the *Hypster* project[1].

[1] https://hypster-project.eu/

For each considered case, the following variables are calculated:

- cavern and wellhead pressure, pressure rate and temperature,
- hydrogen density and velocity,
- evolution of total wellbore pressure losses,
- evolution of convection heat flux at cavern depth,
- wellbore hydrogen properties vs. depth and time: pressure, temperature, density, velocity and
- heat flux.

Special attention is paid to the maximum hydrogen velocity along the wellbore which should remain smaller than 30 m/s. Higher velocities may create erosion and damage the production casing. Furthermore, high velocities may lead to large pressure losses and, thereby, reduce the overall efficiency.

2. Creation of parametrized 2D and 3D models of hydrogen caverns

Following the wellbore modelling, 2D finite-element parametrized models of typical caverns that could be used for hydrogen storage were designed. Creating meshes that are suitable for finite-elements computations with gas can be a difficult task. Meshing is especially important for gas caverns because computations require a very fine mesh at cavern wall (of the order of a few tens of cm maximum); this is especially true for hydrogen caverns submitted to high frequency cycling. The meshing process used in LOCAS involves several tools that check, correct, and optimize the generated meshes.

Creep properties are site specific. Furthermore, a creep law including transient creep is required when considering caverns that are submitted to rapid pressure changes (as this is the case in hydrogen storage). A typical set of parameters for the Munson-Dawson creep law was selected. A sensitivity analysis was performed considering a set exhibiting a faster creep rate.

3. Numerical computations including sensitivity analysis

The 2D finite-element models were used in a comprehensive stability analysis, coupling thermodynamics and rock-salt geomechanics, in order to determine the most important variables for the dimensioning of a storage.

Special attention was drawn to the contribution of the different mechanisms (thermoelasticity and viscoplasticity) to the stress distribution and to the possible onset of tensile effective stresses (possibility leading to hydrofracturing), and possible onset of salt dilation.

The mechanical stability of the cavern roof and last cemented casing shoe was analysed. Several damage and failure criteria were considered (tension, effective tension, dilatancy, casing stretching at cavern roof). The onset of salt dilation (also called dilatancy) was also assessed through a conservative criterion (RD criterion) that takes into account compressive and extensive state of stress.

A total of 54 calculation cases were computed and the results analysed with smartTectonics. Clustering and sorting of the simulation characteristics using a hierarchical clustering algorithm leads to define 7 classes that match well the overall sampling distribution. Some classes correspond to favourable parameter combinations, while others are much less favourable. It should be noted that, for a given geological configuration, there is generally a combination of parameters (cavern characteristics and/or mode of operation) that ensures acceptable mechanical stability.

4. Blowout modelling

A blowout is probably the most serious accident that could happen to an underground gas storage facility. During a blowout, thermo-dynamical behaviour of hydrogen in the cavern and hydrogen in the borehole are strongly coupled. Hydrogen temperature decreases in the cavern and in the borehole, with possible

serious consequences for the well. (Casing steel, cement and rock at the vicinity of the well experience large temperature changes, thermal contraction and development of tensile stresses.)

During the initial phase of the blowout, hydrogen flow is called *chocked*, it means that hydrogen velocity at the wellhead corresponds to the velocity of sound, which is large for hydrogen (>1200 m/s). During this phase, hydrogen pressure at the wellhead may be larger than atmospheric pressure. After some time, the gas flow becomes *normal* and wellhead pressure equals atmospheric pressure.

It must be mentioned that the duration of the blowout is not known in advance, it is a primary result of the coupled computations. A blowout simulator that includes full coupling between the cavern and the wellbore is embedded in LOCAS. This simulator includes a 2D finite element model for the cavern part. This LOCAS feature has been successfully benchmarked during a research study for the SMRI (Brouard Consulting and Respec, 2013) and also during *Hypster* project.

As for the analysis of cavern-pressure cycling, the mechanical stability of the cavern during the blowout was examined into details. It appears that the onset of dilation in a large zone around the cavern is the main subsurface consequence of a blowout.

5. Workover modelling

Workovers of hydrogen caverns may be needed from time to time. It is likely that cavern will be kept at atmospheric pressure for a few days or weeks during these workovers. Keeping cavern pressure at a low level for a long period of time may jeopardize cavern stability. The main question related to workovers is: how long a typical hydrogen cavern can safely be kept at atmospheric pressure?

A reference configuration as determined during the former sensitivity analysis was considered and a workover has been simulated. This workover consists in lowering cavern to atmospheric in a few days and to keep the pressure constant later on. Possible onset of dilation was analysed. As in the case of the blowout, low cavern pressure over a long period damages the salt by dilation over a thickness that can reach more than 20 metres if the cavern is kept at low pressure for a few months.

6. Analysis of the mechanical stability of a cluster of 9 caverns

The case of 'conglomerates' (large cavern clusters) has not been intensively studied in the literature, probably because it requires heavy computing resources. The design rules for the spacing of caverns on a site are generally based on an empirical model from the mining world, i.e., on an extraction ratio calculated for a network of chambers and pillars.

In the context of large-scale development of a hydrogen-based energy system, it could be necessary to create several dozen new caverns in the Netherlands. The aim of this task was to carry out a 3D sensibility analysis on the density of caverns on a site, in order to discuss the relevance of the rules of thumb for the spacing usually used.

A cluster of 9 caverns and extraction ratios between 5% and 30% were considered. Caverns with the same characteristics were considered, corresponding to the reference case in the 2D sensitivity study.

As previous studies had shown, the volume loss of each cavern is less than the volume loss of a single cavern. This is due to the fact that a large part of the vertical load above the cluster is progressively transferred to the abutment, which reduces the deviatoric stresses in the pillar that cause the loss of volume.

The differences between all the tested configurations, with or without pressure creep, remain small. The differences are most apparent during the first phase of hydrogen production, when the pressure has dropped to its minimum for the first time.

In the cases considered, the difference between an extraction ratio of 5% and 10% rate is small, for both cavern volume loss and maximum subsidence. By increasing the extraction ratio from 5% to 10%, the spacing between caverns is reduced by approximately 50 m (from 160 m to 110 m) and the surface area occupied by a cluster of 9 caverns is halved.

It should be noted that such a reduction in the size of the pillars between caverns does not generate any additional dilatant zone in the pillars.

CHAPTER 2 SEISMICITY: THERMOMECHANICAL MODELLING

As described in the literature section, the occurrence of induced seismicity can have several causes related to different aspects of cavern operations in rock salt. Here, we focus on estimating the potential of induced seismicity in the sedimentary rock adjacent to the salt dome by studying the influence of the hydrogen cavern field operation on the stress state and degree of induced brittle deformation in sedimentary rocks.

Seismicity is likely to occur on near-salt faults adjacent to the dome, as these are pre-existing weak zones in the overburden rock. From the detailed interpretation of 3D seismic reflection data, the typical radial orientation of the faults is well known. Although the near-salt radial faults reflect the brittle response of the overburden to the upwelling dynamics of the diapir throughout the halokinesis, precisely predicting the faults using geomechanical models is a complex task because, ideally, the entire geological evolution, including erosional and sedimentation processes as well as tectonic processes, should be taken into account. However, considering a geomechanical model of a present-day salt dome inferred from seismic data, the top salt surface acts as a tangential stress-free boundary and controls the stress state of the overburden and therefore determines the occurrence and orientation of the dominant near-salt faults. This allows us to employ state-of-the-art 3D thermomechanical models and derive the present-day 3D state of stress of a salt dome following the approach in KEM-17. Here, we start with a generic salt dome model geometry, calibrate the model and run a series of simulations and test different configurations with respect to the cavern field location in the salt dome and with respect to the uncertain rock salt creep rheology. The cavern field is implemented with cyclic loading pressure boundary conditions. We evaluate the scenarios by comparing them with sister simulations without an operational cavern field and focus on the changes in brittle deformation and the induced stress field. To compute the present-day state (Ist-Zustand) of the salt dome, we use an extended version of the thermo-mechanical simulation open-source software LaMEM (Lithosphere and Mantle Evolution Model).

The comparison showed that (1) the degree to which the stress field is perturbed depends on the creep rheology of the rock salt and the dome internal stratigraphy with distinct mechanical properties. (2) In terms of location, a cavern field in the centre of the dome has the least impact on the brittle deformation in the overburden, although the stress within a few hundred meters is significantly disturbed. (3) If the cavern field is located close to the salt-sediment interface and in the immediate vicinity of faults, induced brittle deformation can be observed in the pre-existing fault zones. (4) Several locations close to the dome flanks were tested and not all scenarios lead to the same level of stress perturbation, suggesting that general dome dynamics also play an important role. We suggest that it needs to be tested for site-specific conditions. The degree of brittle deformation in the overburden is also influenced by the uncertain creep rheology of the rock salt. It is expected that dynamic recrystallization in the rock salt (a process that is not yet accounted for in the models) takes place due to the induced load of the cavern field. Due to the reduction in grainsize, this would lead to more enhanced deformation in the near-field of the cavern cluster.

CHAPTER 3 DURABILITY: THE EFFECTIVE LONG-TERM CREEP PROPERTIES OF HETEROGENEOUS ROCK SALT

In the literature review we have shown that the Z2 *Kristallbrockensalz*, which is a common and main component of Dutch salt domes, has a complex rheology based on the very large grain size contrast even at the level of cores. The large halite crystals (mega grains) have a strong effect on creep behaviour, as fine-grained parts will be dominated by pressure solution and mega grains deform in a dislocation creep regime. Investigating creep behaviour with analogue creep tests is a challenge as the sample size is limited. In addition, the experiment is slowed down by the presence of megacrystals, i.e. their respective orientation in the sample and their volume fraction, so that the steady state can only be reached after very long waiting times, possibly only after 1.5 years or longer. However, thermomechanical cavern and dome-scale models rely on constitutive models that predict the upscaled creep deformation behaviour of the microstructure.

In this chapter, we therefore perform numerical creep tests with statistically generated heterogeneous rock salt samples on a representative element volume scale. We systematically investigate the role of megacrystals for the effective creep rheology. With the systematic numerical experiments on a data set of 420 synthetic models, we have tested this behaviour to determine appropriate constitutive relations for the thermo-hydromechanical simulations. We have established a general empirical constitutive law that parameterises the creep behaviour of Kristallbrockensalz, based on the applied stress, he known halite creep properties and its volume fraction. The results show that if the volume fraction of the halite matrix is above 80%, the creep properties of the halite matrix dominate the overall creep behaviour of the rock salt multi-phase aggregate. At halite matrix volume fractions below 80%, non-matrix phases (mega-grains and anhydrite) have a significant effect on creep behaviour at low stresses (1-3 orders of magnitude).

Machine-learning-assisted categorization of individual creep relations suggests that deviations in creep rate is strongest when non-matrix phases (mostly halite mega grains) form a skeleton-like structure throughout the entire model domain (2x2 meters). These structures stabilize the deformed samples, resulting in strain rates that converge toward pure dislocation creep because the mostly unconnected pockets of halite matrix cannot propagate the strain throughout the sample. It is likely that this behaviour occurs if the halite volume fraction is below 40%.

Furthermore, we established a general empirical constitutive law that parametrizes the strain rate of KB rock salt, based on the applied stress, known halite creep properties and its volume fraction. In the expected stress range and for the expected halite matrix volume fractions of natural salt domes, it can predict our synthetic dataset with an uncertainty of 20 %.

It is important to note that this only reflects the average creep behaviour of expert-knowledge curated but statistically derived KB rock salt models. The geometries of naturally occurring KB rock salt are, of course, more complex than the simplified statistical models generated in this study. Mapping the site-specific KB rock salt geometries, extrapolating these to representative scales and determining their creep behaviour is a highly interesting task for future studies.

However, the results and conclusions drawn in this study provide the basis to integrate creep of a highly heterogeneous multi-phase salt formation into dome-scale simulations, ultimately assisting risk assessments of underground hydrogen storage in salt caverns.

CHAPTER 4 DURABILITY: MICROSTRUCTURAL ANALYSES OF GEOCHEMICAL AND MICROBIAL PROCESSES

Understanding the extent and kinetics of reactions is crucial. Experimental work, along with microstructural analysis, is needed to determine input parameters for geochemical models related to

various reaction kinetics. Based on the findings of the literature review, we conducted experiments to study the kinetics of biotic and abiotic reactions involving H2, CO2, and H2S with anhydrite. This considered factors like bacterial growth, pressure, temperature, and anhydrite composition. These experiments aimed to reveal known and unknown processes affecting the stability of salt caverns during hydrogen storage at different scales, using microstructural analyses.

Anhydrite is significant in hydrogen storage within salt caverns for two main reasons: i) it is often found in layered structures and makes up a substantial part of the cavern's sump, and ii) it serves as a source of sulphate anions (SO_4^{2-}), which can lead to hydrogen sulphide (H2S) formation under certain conditions.

Even when bacterial sulphate reduction is absent and anhydrite layers are exposed during hydrogen storage, there are additional considerations. Anhydrite is soluble in water, and its hydration to gypsum is driven by water introduction. Various factors like temperature, pressure, water availability, surface area, depth, and impurity content influence this hydration process, affecting mechanical properties and hydrogeological behaviour of salt formations. While these reactions may be slow in a lab setting, microstructural investigations allow visualization of biological, chemical, and structural changes at submicron pore scales. This provides insights for upscaling processes and implementing preventive measures if needed. The knowledge gained from these experiments and literature reviews outlines the physical, biological, and chemical processes requiring further study to minimize potential risks during hydrogen storage in salt caverns.

In our initial step, we analysed anhydrite samples from the ISH 1 well in the Netherlands, using microanalytical techniques. The samples were artificially fractured to increase surface area. Experiments assessed biomass impact on hydraulic conductivity and bacterial sulphate reduction in anhydrite in the presence of hydrogen and carbondioxide. Post-experiment analysis included studying microbial activity, biofilm formation, and mineralogical changes.

The main findings of the study were as follows:

- Anhydrite can contain impurities or other minerals, affecting reaction kinetics. Grain size variation also influences reaction rates. High salt concentrations may impact sulphate-reducing bacteria, affecting H2S production.
- Although hydrate formation varied with temperature, further research is needed to assess implications on mechanical stability in typical cavern operating temperatures. The presence of brine together with the mobilization of fines can affect transport properties and surface accessibility for reactions during hydrogen storage.
- Microbes do not prefer specific surface and it was shown that dolomite formed through microbial activity in the presence of sulphate-reducing bacteria.
- Despite low porosity and permeability, anhydrite can allow the passage of aqueous solutions, increasing porosity. Competition between magnesium and calcium ions for carbonate ions can reduce calcium carbonate precipitation, elevating porosity.
- Microstructural examination of heterogeneous anhydrite samples aids in interpreting bulk measurements, particularly concerning hydrocarbons and impurities. Natural samples may differ from simplified models, emphasizing the importance of site-specific investigations to understand biological and chemical impacts during hydrogen storage in diverse salt formations.

Introduction

This part reports on the geomechanical study performed within the research phase of the project. The first chapter is a vast geomechanical analyses including wellbore thermodynamics modelling, creation of parametrized 2D and 3D models of hydrogen caverns, numerical computations including sensitivity analysis, blowout, and workover modelling of a generic case. Chapter 2 involves large scale 3D thermomechanical modelling and associated seismicity. The third chapter describes a study on the durability of salt rheology with respect to heterogeneities like *Kristallbrockensalz* and anhydrite. The final chapter reports on the durability in salt with respect to geochemical processes associated with second phases and microbes by using imaging.

In the following, we list the main author(s) of the relevant chapters:

- Chapter 1 Geomechanical analysis: Dr. Benoit Brouard and Dr. Vassily Zakharov
- Chapter 2 Seismicity: Thermomechanical modelling: Dr. Tobias Baumann and Dr. Anton Popov
- Chapter 3 Durability: The effective long-term creep properties of heterogeneous rock salt: Dr. Tobias Baumann, Dr. Maximilian Kottwitz and Dr. Anton Popov and Prof. Dr. Janos L. Urai
- Chapter 4 Durability: Microstructural analyses of geochemical and microbial processes: Dr. Joyce Schmatz

NB. Prof. Dr. Janos L. Urai also contributed to chapter 1 and 2 regarding discussions on the stratigraphy and internal structure to be used for the models as well as what constitutive law and damage model is best suited for the models. Unfortunately, due to his sudden death, he was unable to complete his tasks regarding chapter 3 on the evolving rheology, transport properties, damage, and healing of salt.

Nomenclature

Latin symbols

SYMBOL	DESCRIPTION	UNITS
A_{dc}	Prefactor for dislocation creep law	/MPa^n-yr
A_{nh}	Prefactor for Norton-Hoff creep law	/MPa^n-yr
A_{ps}	Prefactor for pressure solution creep law	K.mm^3/MPa-yr
C_w	Mass of water vapor in the cavern	kg
c	Parameter of Munson-Dawson creep law	—
c_p	Heat capacity of hydrogen at constant pressure	J/kg-K
c_v	Specific heat of hydrogen at constant volume	J/kg-K
D	Average grain size	mm
D_i	Cavern maximum diameter	m
D_{in}	Inner diameter of the production casing	mm
$\bar{D}_1, \bar{D}_2$	Parameters of the RD dilatation criterion	
f	Friction factor	—
E_{ent}	Cumulated additional enthalpy	MWh
E_{int}	Cavern internal energy	MWh
E_{mec}	Cumulated mechanical energy	MWh
E_{salt}	Young's modulus of rock salt	MPa
E_{th}	Cumulated heat flux through conduction	MWh
e	Extraction ratio	—
e_c	Hydrogen internal energy	J
G_{geo}^{cav}	Geothermal gradient in the cavern w/o convection	°C/m
G_i	Pressure gradient at the casing shoe	bar/m
g	Acceleration due to gravity	m/s²
h	Convective heat transfer coefficient	W/m²-K
H	Hydrogen enthalpy	J/kg
H_c	Enthalpy of hydrogen in the cavern	J
H_{inj}	Enthalpy of injected hydrogen	J
I_1	First invariant of the stress tensor	MPa
J_2	Second invariant of the stress tensor	MPa²
K_0	Parameters of Munson-Dawson creep law	—
k	Thermal conductivity of hydrogen	W/m-K
k_{salt}	Rock-salt thermal conductivity	W/m-K
k_{th}	Thermal conductivity of rocks	W/m-K
L	Length of the production casing	m
L_w	Phase change heat of water	J/kg
M	Mass of hydrogen in the cavern	kg
m	Parameter of Munson-Dawson creep law	—
n_{dc}	Exponent of dislocation creep law	—
n_{nh}	Exponent of Norton-Hoff creep law	—
P_c	Hydrogen pressure	bar

P_{ent}	Additional enthalpy rate (injection phases)	MW
P_h	Halmostatic pressure	bar
P_{int}	Total internal energy rate	MW
$P_{\max}$	Maximum pressure at the casing shoe	barg
P_{mec}	Mechanical power developed	MW
$P_{\min}$	Minimum pressure at the casing shoe	barg
P_{th}	Heat flux through conduction at cavern wall	MW
P_{∞}	Geostatic pressure	MPa
Q_{dc}	Activation energy for dislocation creep law	J/mol
Q_{geo}	Geothermal flux	mW/m²
Q_{nh}	Activation energy for Norton-Hoff creep law	J/mol
Q_{ps}	Activation energy for pressure solution creep	J/mol
q_{th}	Heat flux at the cavern wall	W/m²
q_m	Hydrogen massic flowrate	kg/s
R	Universal gas constant	J/mole-K
R_e	Reynold's number	—
r	Radius	m
S	Entropy	J/K
S_{cas}	Inner cross section of the production casing	m²
T	Absolute temperature	K
T_0	Unconfined tensile strength of rock salt	MPa
T_b	Brine temperature	°C
T_{inj}	Temperature of the injected hydrogen	°C
T_c	Hydrogen bulk temperature in the cavern	°C
T_{salt}	Rock-salt temperature	°C
T_{∞}	Geothermal temperature	°C
T_w	Cavern wall temperature	°C
t	Time	days
t_{sd}	Time of start of debrining	days
V	Hydrogen volume in the cavern	m^3
V_c	Total cavern volume (hydrogen + brine)	m^3
V_b	Brine volume in the cavern	m^3
u	Hydrogen velocity	m/s
v	Specific volume of hydrogen	m^3/kg
Z_{cs}	Casing-shoe depth	m
z	TVD Depth	m

Greek symbols

SYMBOL	DESCRIPTION	UNITS
α	Coefficient of thermal expansion of the hydrogen	/K
α_{salt}	Coefficient of thermal expansion of rock salt	/°C
α_w	Parameter of Munson-Dawson creep law	—
β	Coefficient of volume expansion of hydrogen	/bar
β_w	Parameter of Munson-Dawson creep law	—
Δ	Parameter of Munson-Dawson creep law	—
δ	Parameter of Munson-Dawson creep law	—
ζ	Internal variable of Munson-Dawson creep law	
ε	Inner rugosity of the production casing	mm
ε_{cr}	Creep strain	—
ε_{el}	Elastic strain	—
ε_{tot}	Total strain	—
$\dot{\varepsilon}_{cr}$	Creep strain rate	/s
ε_{ss}	Steady-state strain	/s
$\dot{\varepsilon}_{tr}$	Transient strain rate	/s
ε_{tr}^{*}	Transient strain limit	—
ε_{zz}	Vertical strain	—
μ	Dynamic viscosity of hydrogen	Pa.s
μ_{salt}	Shear modulus of rock salt	MPa
ν_{salt}	Poisson's ratio of rock salt	—
Φ	Relative humidity	%RH
ψ	Lode angle	°
ρ	Hydrogen density	kg/m^3
ρ_b	Saturated-brine density	kg/m^3
ρ_R	Rock density	kg/m^3
Σ	Cavern wall area	m²
σ	Deviatoric stress	MPa
σ_0	Dimensional constant	MPa
σ_e	Effective stress for Munson-Dawson creep law	MPa
σ_{eff}	Effective stress = $\sigma_{\max} + P_c$	MPa
$\sigma_{\max}$	Least compressive of the principal stresses	MPa

1 Geomechanical analysis

Authors: Benoit Brouard & Vassily Zakharov – Brouard Consulting

1.1 Introduction

This chapter is a relatively comprehensive geomechanical analysis of typical hydrogen storage configurations. A large body of literature has been devoted to the modelling of salt caverns. Several constitutive laws (see also KEM-17) and a number of software programs are available. The LOCAS software developed by Brouard Consulting is used here for modelling. LOCAS is a fully coupled 2D and 3D thermomechanical software (Brouard et al., 2020, 2021) that calculates both gas thermodynamics in the well and cavern, and rock mechanics. LOCAS can calculate pressure and temperature variations in the well and cavern resulting from gas injection and withdrawal and their consequences in terms of stresses and displacements in a rock mass; and compare stress distributions to dilation, effective stress, and tensile stress criteria.

1.1.1 Selection of a reference configuration

Section 1.2 describes the main characteristics of the model used for the calculations, including both the geometric characteristics, the geological configuration, and the rock properties. This model, although generic, attempts to represent a typical configuration for future hydrogen storage caverns in the Netherlands.

1.1.2 Cavern thermodynamics

The modelling of the wellbore and cavern is crucial for a comprehensive comprehension of hydrogen cavern behaviour. The LOCAS software includes a thermodynamic model of the wellbore, which has been effectively benchmarked as part of the HyPSTER initiative, designed for hydrogen projects and backed by the European Union's Horizon 2020 Research and Innovation programme (https://hypster-project.eu/).

Hydrogen caverns are expected to be loaded with a massic flowrate set at the wellhead during injection and production phases. The aim of wellbore modelling is to calculate the evolutions of thermodynamic variables, including pressure, temperature, and velocity, along the wellbore, specifically at the cavern depth. Variations in pressure and temperature are crucial as they determine stresses near the cavern and the potential occurrence of damage.

For simplicity's sake, this study assumes hydrogen caverns will undergo sinusoidal cycling between maximum and minimum pressure. However, the duration and pattern of each cycle depend on mass flow rates, and in reality, cycling patterns and durations may be more complex and site-specific.

The thermodynamic models used to simulate the behaviour of hydrogen in the well and in the cavern are described in Section 1.3. Through the modelling of wells and caverns and the implementation of a sensitivity analysis on key parameters, it is possible to establish more accurate definitions for the optimal features and operational techniques for forthcoming hydrogen caverns.

1.1.3 Rock-salt mechanical behaviour

Rock salt is a complex material that has been extensively researched, with ten conferences solely dedicated to its mechanical behaviour since the early 1980s. Its behaviour is highly non-linear and exhibits elastic-ductile qualities when undergoing short-term compression tests, and elastic-fragile behaviour when subjected to tensile tests. However, in the long term, salt behaves as a fluid, flowing even under small deviatoric stresses as soon as the state of stress is no longer purely isotropic. All caverns created through solution mining shrink gradually over time. It is important to note that steady-state creep, reached after several weeks or months of constant load, should be differentiated from transient creep,

which occurs during a period of several weeks after mechanical loading is applied or changed, as observed during laboratory tests.

The mechanical behaviour models considered in this generic study for rock salt and other rocks are described in section 1.4.

1.1.4 Mechanical stability of a salt cavern

The criteria for the mechanical stability of a cavern which are taken into account in this study are described in Section 1.5.

1.1.5 Wellbore modelling for the reference case

An example of modelling the behaviour of hydrogen in the well for a typical configuration is described in Section 1.6. This example highlights some of the indicators taken into account in the sensitivity study.

1.1.6 Creation of parametrized 2D finite element models of hydrogen caverns

The way in which the 2D finite element models were constructed for this study is described in Section 1.7. These models are parameterised, enabling the sensitivity study that follows to be carried out.

1.1.7 Cavern modelling for the reference case

An example of modelling the behaviour of hydrogen cavern for a typical configuration is described in Section 1.8. AS for the wellbore modelling, this example highlights some of the indicators taken into account in the sensitivity study.

1.1.8 Sensitivity analysis in 2D

A 2D finite element sensitivity study was carried out in Section 1.9, testing 54 different configurations, varying the diameter of the cavern, its depth, the frequency of pressure cycles to which the cavern will be subjected, and the pressure gradient corresponding to the minimum pressure in the cavern. The characteristics of these different configurations are described. 14 indicators of cavern stability and thermodynamic efficiency are given for each case considered.

An analysis of the calculation results is presented. This shows the most favourable configurations and those that should be avoided.

1.1.9 Worst case scenarios

1.1.9.1 Blowout

Blowout (wellhead failure leading to the loss of most or all the products) is an especially severe concern in the case of underground storages. The way in which a blowout can be modelled and an example in the reference case are presented in Section 1.11.

1.1.9.2 Workover

During the life of a gas storage cavern, it may be necessary to carry out maintenance operations requiring the pressure in the cavern to be lowered considerably and maintained at this low pressure for several weeks or more. A cavern maintained at low pressure rapidly loses volume, the deeper the cavern, and damage due to dilation can occur and increase over time as long as the pressure remains low. An example in the reference case is presented in Section 1.12.

1.1.10 Conglomerates

The case of ‘conglomerates’ (large cavern clusters) has not been intensively studied in the literature, probably because it requires heavy computing resources. The design rules for the spacing of caverns on a site are generally based on an empirical model from the mining world, i.e., on an extraction ratio calculated for a network of chambers and pillars.

In the context of large-scale development of a hydrogen-based energy system, it could be necessary to create several dozen new caverns in the Netherlands. The aim of Section 1.14 is to carry out a 3D sensibility analysis on the density of caverns on a site, in order to discuss the relevance of the rules of thumb for the spacing usually used.

1.2 Selection of a reference case (volume, geology, material parameters)

1.2.1 Introduction

This section describes the main characteristics of the model used for the calculations, including both the geometric characteristics, the geological configuration, and the rock properties.

1.2.2 Cavern volume and shape

For the purposes of this study, the volume of hydrogen in the cavern is assumed to be one million m^3 in all cases. Since the LOCAS model takes into account the residual brine at the bottom of the cavern (Figure 161), the total volume excavated is slightly higher than this value.

Given that good quality dome salt can be found in the Netherlands, this study considered caverns with the vertical cylindrical shape typical of existing caverns for gas storage or brine production at depths of between 500 and 2000 m. We have not considered low height, large diameter caverns because we know that this type of cavern has more problems with mechanical stability, so they will not be used for hydrogen storage.

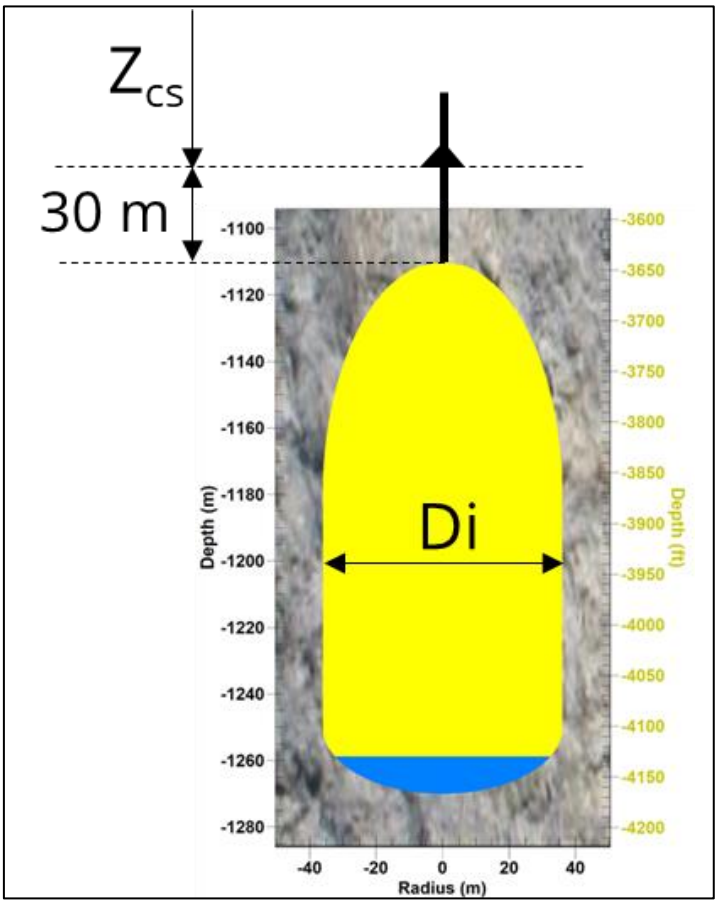

Figure 161. Shape considered for the cavern. The sensitivity study focuses in particular on the depth of the last cemented casing shoe (Z_{cs}) and the maximum diameter (D_i).

1.2.3 Selection a typical geological configuration for the Netherlands

It is difficult to define a typical geology for the salt domes of the Netherlands. 3D modelling must be considered at the scale of a site with several caverns, and this can only be site specific. For the generic study presented in this report, a simplified configuration of five tabular layers has been adopted, as shown in Figure 161. The top of salt is thought to be located at a depth of 548 m for all cases. The final layer, called "ZE" for Zechstein, corresponds to the rock-salt layer in which the cavern is located (Figure 162).

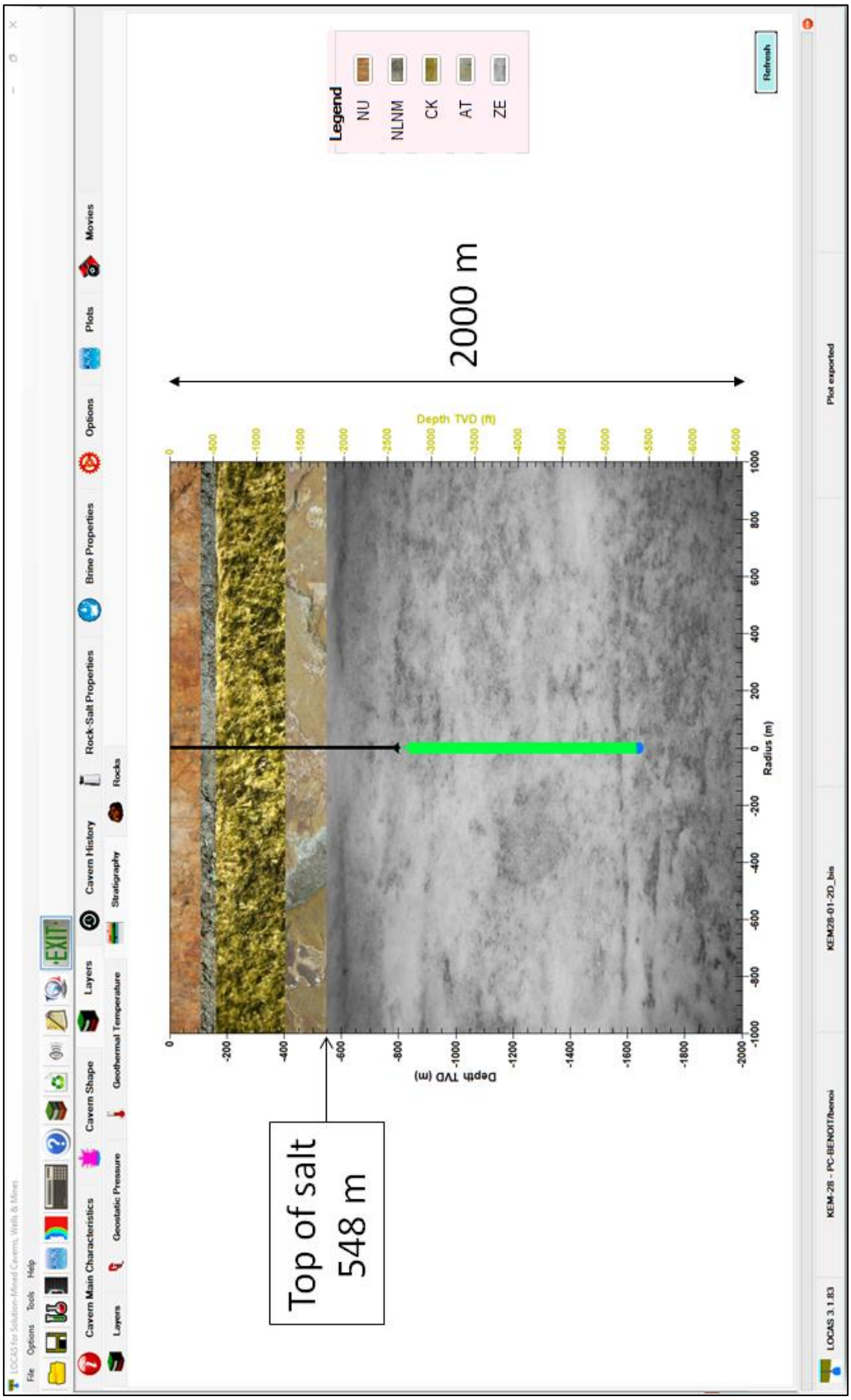

Figure 162. Simplified geology considered for the computations.

Table 10 gives the thicknesses of the different layers.

Table 10. Thickness of the different rock layers considered.

Layer	Thickness (m)	Depth range (m)
NU	108.1	0-108.1
NLNM	53.1	108.1-161.3
CK	242.3	161.3-403.6
AT	144.0	403.6-547.6
ZE	1452.5	547.6-2000

1.2.4 Selection of a depth for the last cemented casing shoe

It is assumed that a 30 m high chimney has been created between the shoe of the last cemented casing (LCCS) and the roof of the cavern (Figure 163) to limit overstretching of the cemented casing in its lower part (see Section 1.5.3). Three different depths are considered in the sensitivity analysis (Table 11).

Table 11. Casing-shoe depths considered for the sensitivity analysis.

Depth casing shoe Z_{cs}		
Z_1	Z_2	Z_3
800 m	**1000 m**	**1200 m**

1.2.5 Setting of cavern height and maximum radii

Three different cavern heights, corresponding to three different maximum diameters, are considered in the sensitivity analysis (Table 10 and Table 12). The shallowest cavern lies between 830 m and 1029 m, and the deepest between 1230 m and 2026 m.

Table 12. Considered cavern maximum diameters and corresponding heights.

Cavern Max. diameter	Cavern height
D_1 = 40 m	796 m
D_2 = 60 m	354 m
D_3 = 80 m	199 m

1.2.6 Selection of loading scenarios

For the sake of simplicity, it is assumed in this study that hydrogen caverns will be operated through a sinusoidal cycling between the maximum and the minimum pressure (Figure 164). In reality the actual cycling patterns and duration of each cycle will be probably much more complex and site-specific.

Maximum pressure

The maximum pressure is determined such that the pressure gradient at the last cemented casing shoe (LCCS) is 0.18 bar/m, which is a typical value in the Netherlands for the maximum allowable pressure in gas caverns.

Minimum pressure

The minimum pressure is usually less well defined. A 0.05 bar/min gradient at the LCCS is sometimes considered in the design studies. In the sensitivity study, we will compare the case of a minimum gradient of G_1 = 0.05 bar/m with that of a higher minimum gradient of G_2 = 0.1 bar/m.

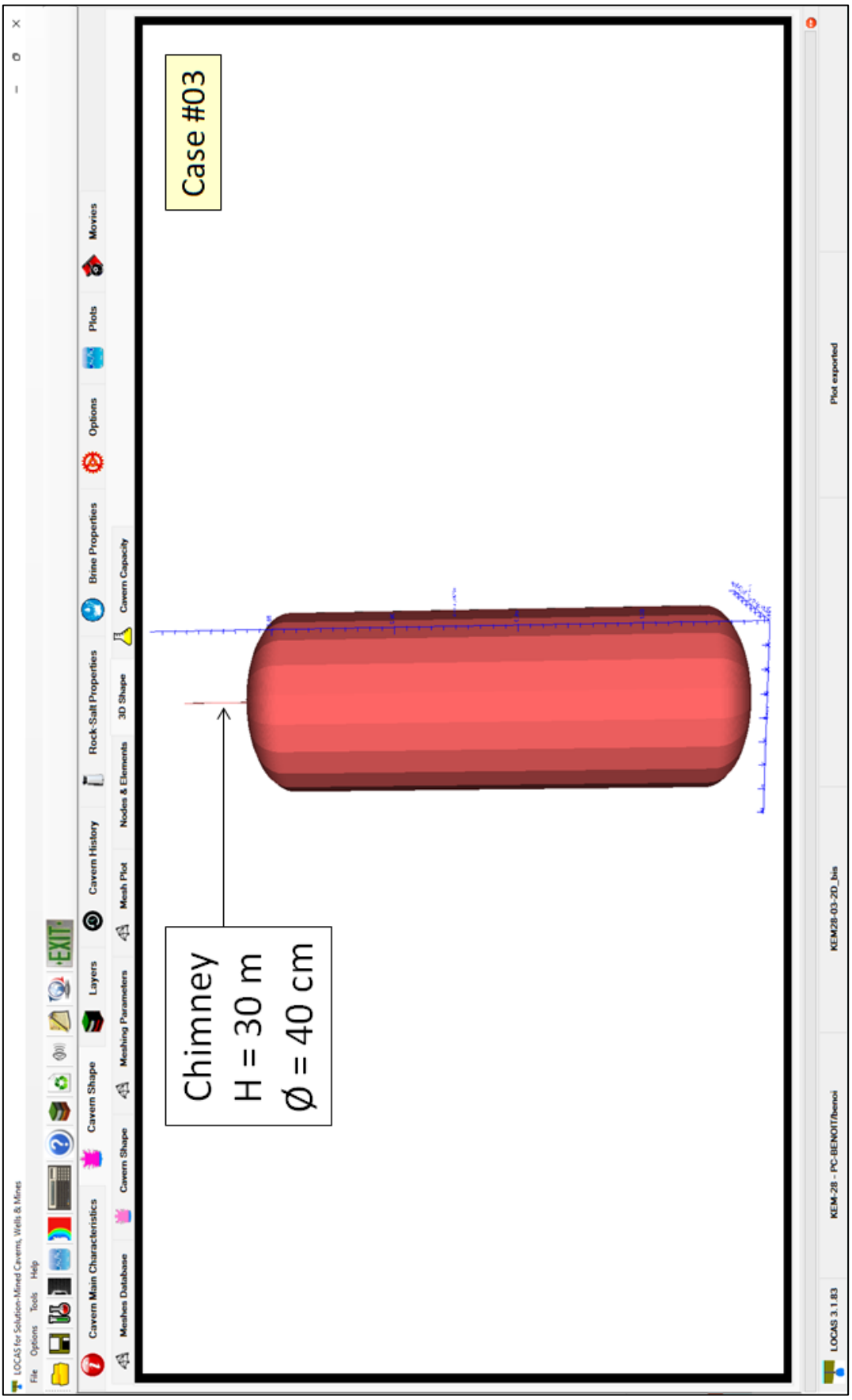

Figure 163. 3D view of one of the configurations considered (Case #03 of the sensitivity analysis.

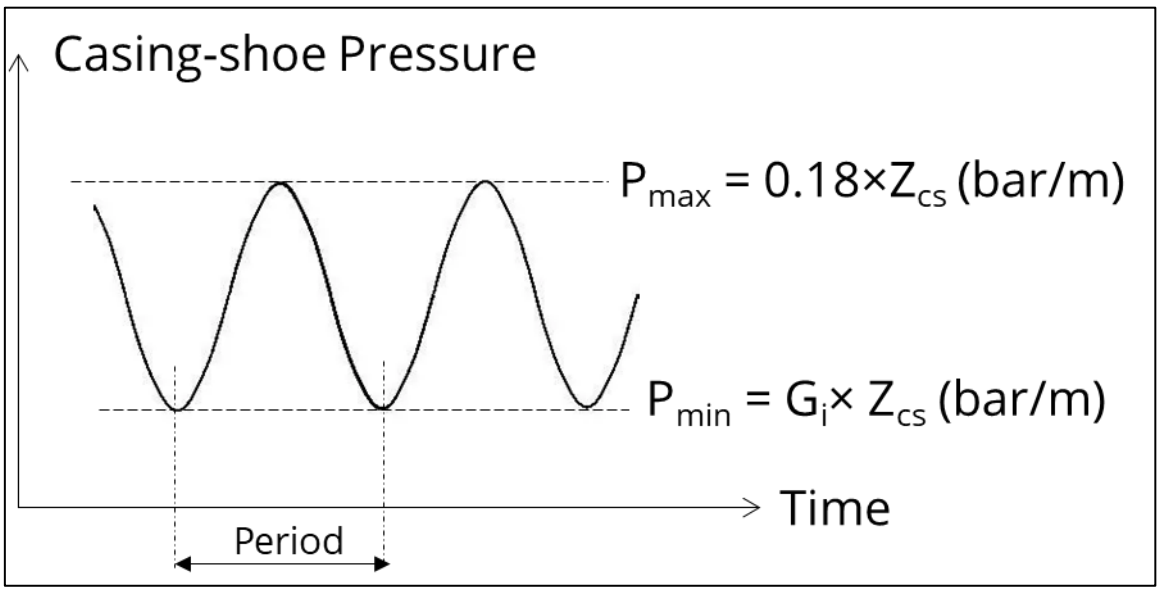

Figure 164. Sinusoidal cycling of cavern pressure (at casing shoe) between maximum and minimum pressure.

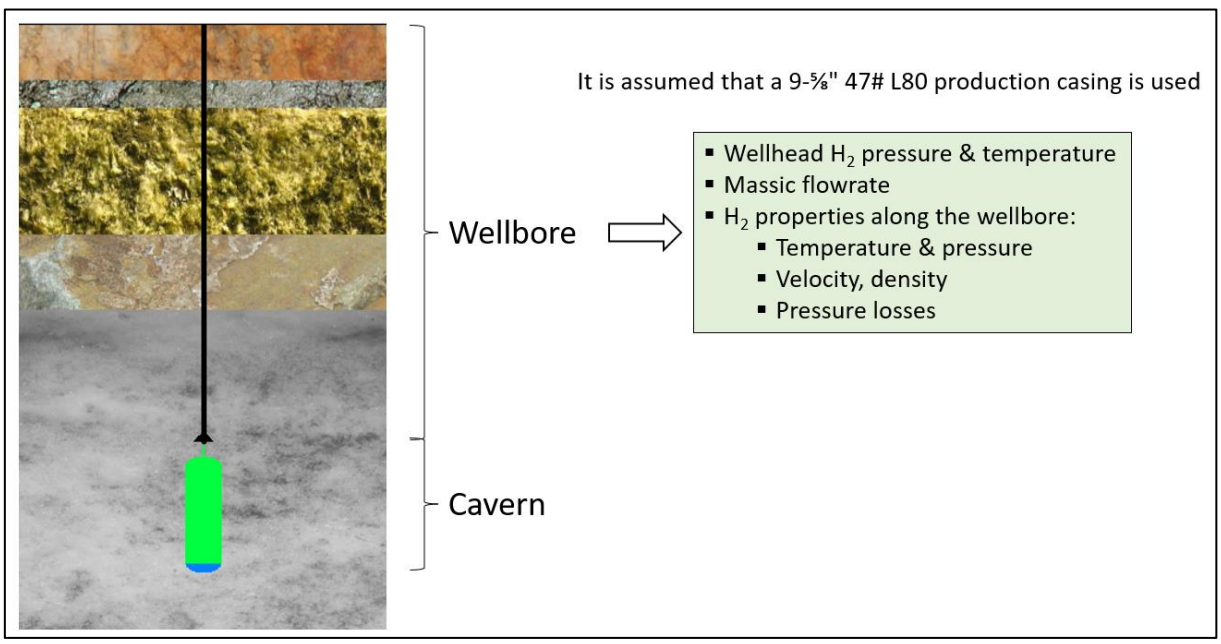

Figure 165. The purpose of wellbore modelling is to determine the hydrogen properties along the well as a function of time and depth during the cycling.

1.3 Wellbore/Cavern thermodynamics modelling

1.3.1 Introduction

This chapter describes the thermodynamic models used to model the behaviour of hydrogen in the well and in the cavern. The purpose of wellbore modelling is to determine the hydrogen properties along the well as a function of time and depth during the cycling (Figure 165).

1.3.2 Wellbore completion

For this generic study, it is assumed that a 9-⅝" 47# L80 production casing is used. This casing has an 8.681 inches (220-mm) inner diameter. The model does not take into account the existence of a safety valve inside the production casing, which can locally reduce its internal diameter.

1.3.3 Hydrogen thermodynamics properties

Calculation of hydrogen thermodynamic properties in LOCAS is based in particular on the state equation and the formulas provided in the report by Lemon & Leachman (2008). From our knowledge these formulas provide the most accurate estimation of hydrogen properties in the pressure and temperature range of interest.

- Heat capacities (c_v , c_p) are calculated using the Shomate equation given by Chase (1998).
- Hydrogen dynamic viscosity μ is calculated using formulas from Londono et al. (2002).
- Speed of sound, Joule-Thomson coefficient and isentropic index for Hydrogen are derived from the state equation provided by Lemon et al. (2008).

1.3.4 Pressure losses

The pressure losses due to hydrogen friction along the production casing when injecting or withdrawing hydrogen may not be negligible; it can be estimated through the following Darcy-Weisbach formula:

$$\Delta P = f \frac{L}{D_{in}} \frac{\rho u^2}{2} \tag{55}$$

where L is the length of the production casing, D_{in} is its inner diameter, ρ is hydrogen density (at the local current pressure and temperature conditions), u is hydrogen velocity and the friction factor, f, is calculated for turbulent flow assuming Colebrook's equation:

$$\frac{1}{\sqrt{f}} = -2\log_{10}\left(\frac{2.51}{\mathrm{Re}\sqrt{f}} + \frac{\varepsilon}{3.71 D_{in}}\right) \tag{56}$$

where ε is the inner roughness of the production casing and Re is Reynold's number (dimensionless). Reynold's number writes:

$$\mathrm{Re} = \frac{\rho q_m D_{in}}{\mu S_{cas}} \tag{57}$$

where μ is hydrogen dynamic viscosity, $S_{cas} = \pi D_{\mathrm{int}}^2 / 4$ is production casing inner cross-section and q_m is hydrogen massic flow rate.

All these variables vary with time and with the depth of the well. Formula (56) is implicit and therefore it must be solved at each time step to get the friction factor.

Inner roughness ε of the production casing must be considered for the calculation of pressure losses. Roughness varies whether it is a coated or non-coated steel pipe. A value of $\varepsilon = 0.0053\ \mathrm{mm}$ has been selected for the following computations.

1.3.5 Cavern thermodynamics

Salt-cavern thermodynamics is complex. There are several types of heat exchange between the cavern and the rock mass that need to be taken into account (Figure 166). Pressure-cycled gas caverns experience large temperature swings, especially when the cycling period is short. The thermodynamic behaviour of gas during cycles is not adiabatic, and the amplitude of the temperature changes strongly depends on the duration of the pressure change and the area-to-cavern volume ratio of the walls. Large pressure drops may generate net tensile stresses at cavern walls. However, the depth of penetration of thermal fractures seems to be relatively small (Bérest et al., 2016).

The upper part of a quiescent gas cavern is stirred by natural convection resulting from the geothermal gradient (Louvet et al., 2017). In most cases, a temperature-gradient inversion is observed in the lower part of the cavern, and heat or mass transfer is impeded above the brine sump except after a large temperature drop. It seems (Bérest and Louvet, 2020) that the brine sump in a frequently cycled cavern remains perennially cooler than the rock mass, as the gas cavern is a thermo-dynamic device: condensation (after a pressure drop) is spread in the entire gas body; and vaporization (after a pressure increase) takes place at the brine-gas interface. These mechanisms do not seem to raise a risk issue; they are important from the perspective of hydrogen purity, have not been discussed widely in the literature.

The kinetic energy of gas in a cavern can be neglected. The energy balance equation can be written:

$$M(\dot{e}_c + P_c\dot{v}) = q_{th} + < \dot{M} > \left(H_{inj} - H_c\right) + L_w\dot{C}_w \quad (58)$$

Where M is the mass of hydrogen in the cavern; $< \dot{M} >$ means that we only take into account positive variations, i.e., during hydrogen injection, while this term disappears for the production phases; P_c is hydrogen pressure in the cavern, v is the specific volume of hydrogen, e_c is the gas internal energy, and $\dot{e}_c + P_c\dot{v} = c_v\dot{T}_c + T_c(\partial P_c/\partial T_c)|_{v_c}\dot{v}$, where T_c is hydrogen temperature in the cavern and c_v is the heat capacity of the gas at constant volume. When hydrogen is injected in the cavern ($< \dot{M} >= \dot{M} > 0$), the difference between the enthalpy of the injected hydrogen (H_{inj}) and the enthalpy of the cavern hydrogen (H_c) must be taken into account. C_w is the mass of water vapor in the cavern, and L_w is the latent heat of water (from liquid phase to vapor phase).

Note that, for the sake of simplicity, humidity is not considered in the formulas.

1.3.6 Geothermal temperature

The vertical distribution of geothermal temperature T_∞ with depth z is determined from the geothermal flux Q_{geo} and thermal conductivity k_{th} of each rock layer:

$$Q_{geo} = k_{th}\frac{dT_\infty}{dz} \quad (59)$$

This heat flux can be considered as stationary and vertical in a 2D model. In a 3D model, the field may have a horizontal component depending on the geometry and conductivity of the layers it passes through.

In 2D the distribution of geothermal temperature with depth is piecewise linear, so the vertical temperature gradient in each layer must be inversely proportional to the thermal conductivity of the rock making up that layer. As the thermal conductivity of rock salt is much higher than that of other rocks (5.3 W/m-K in Table 14), the vertical temperature gradient in the rock salt (1.887 °C/100 m in Table 14) is lower than in the overburden.

Figure 167 shows a screenshot of an example of this distribution in LOCAS.

Figure 166. Heat exchanges between hydrogen, brine, and the rock mass. The possible exchange of heat between brine and hydrogen and the role of water vapour are neglected in the sensitivity study.

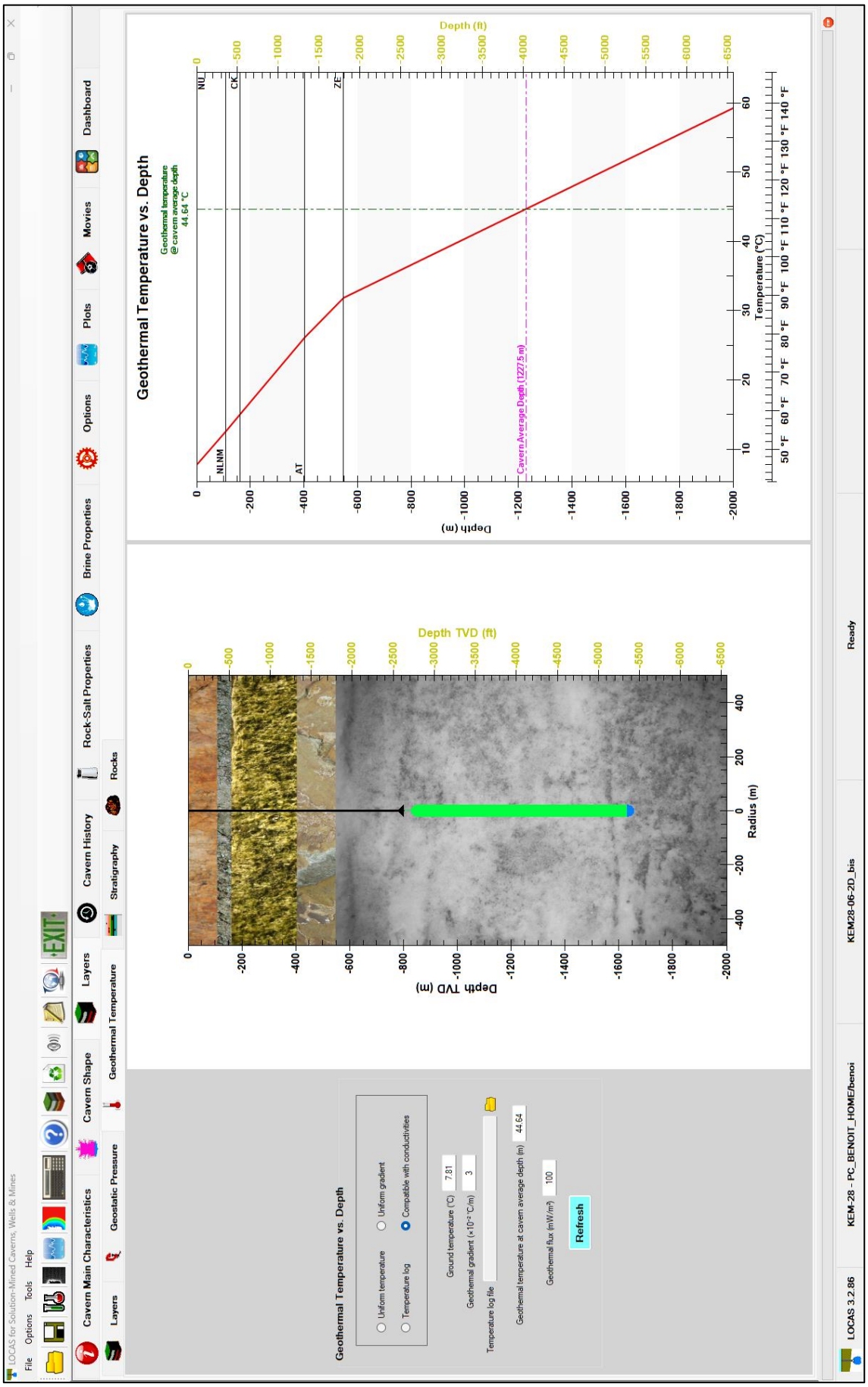

Figure 167. Geothermal temperature as a function of depth (LOCAS screenshot).

1.3.7 Onset of convection in a gas-filled cavern

An almost vertical temperature profile can be found in gas caverns, especially in the case of hydrogen and natural gas, as the adiabatic gradient, although larger than brine adiabatic gradient, is smaller the inferred geothermal gradient. The condition for onset of thermal convection in a gas cavern is:

$$\frac{\alpha T g}{c_p} < G_{geo}^{cav} \tag{60}$$

where G_{geo}^{cav} is the inferred geothermal gradient in the cavern should no convection take place (it is slightly smaller than the geothermal gradient in the rock); α is the coefficient of thermal expansion of the hydrogen, $\alpha T \simeq 1$, and the heat capacity of hydrogen at constant pressure, $c_p \approx 14600$ J/kg-K at 120 bar and 40 °C, is relatively large. Condition (60) is always met. There is a second condition for onset of natural convection: the Grasshof number must be sufficiently large, a condition also always met in a salt cavern.

In fact, this is not perfectly true, a temperature gradient inversion can be observed in some cases at cavern bottom, several dozens of meters above the hydrogen-brine interface (Figure 168). More details can be found in Bérest (2019).

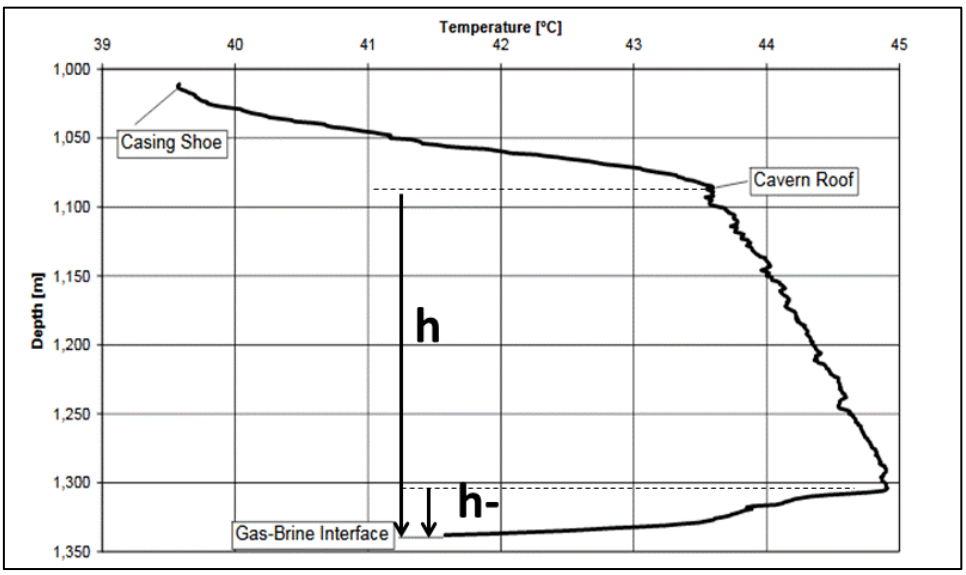

Figure 168. Temperature profile in an anonymous gas cavern: the temperature gradient in the upper part of the cavern is $G = 6$ °C/km; it is negative above the sump (After Berger et al., 2002).

1.3.8 Heat flux at cavern wall

During leaching and dewatering, the caverns fluids are assumed to be well mixed (Respec, 2004). The temperature is homogeneous in the hydrogen of the cavern because of the convective mixing. The natural convection is generated by the vertical temperature gradient in the salt. Note that, when the shape of the cavern is more complex, there may be several convection cells.

The cavern wall temperature (T_w) is equal to the bulk cavern temperature (T_c), and the heat flux into the cavern (q_{th}) at the cavern wall is described by:

$$q_{th} = k_{salt} \left.\frac{dT_{salt}}{dr}\right|_{wall} \tag{61}$$

Where k_{salt} is the thermal conductivity of salt and T_{salt} is salt temperature.

During hydrogen storage, when there is less turbulence in the cavern, the heat flux per area (W/m²) into the cavern at the cavern wall can be described by:

$$q_{th} = h(T_w, T_c) \tag{62}$$

Where h is the convective heat transfer coefficient. A single value of h is considered for the cavern. In the following computations, the convective heat transfer coefficient used in the cavern is based on the free convection for a vertical cylinder as provided by Kreith and Black (1980) and is given by:

$$h = 0.1\left[\frac{\beta g \rho^2 (T_w - T_c) c_p k^2}{\mu}\right]^{\frac{1}{3}} \tag{63}$$

where β is the coefficient of volume expansion of hydrogen, ρ is hydrogen density, g is the gravitational acceleration, c_p is the heat capacity of hydrogen at constant pressure and μ is the dynamic viscosity of hydrogen. For all computations when the heat transfer coefficient is considered, h is updated at each time step according to formula (63), and as h depends on the $T_w - T_c$ difference, it can change very quickly.

Note that a constant h =10-30 W/m²-K value can be found in some reports for natural gas. There is no easy way to calibrate the value of h from in situ measurements, cavern temperature would have to be measured continuously during large swings of its pressure/temperature. To our knowledge, there is no public data available for calibration, especially for hydrogen caverns.

Note that, for the sake of simplicity, this convective heat transfer coefficient is only considered in the computations made using the wellbore modeling part of this report (Section 1.6), and not in the 2D and 3D finite element (Sections 1.8 and 1.14.

1.3.9 Developed powers and energies

There are several contributions that can be considered when calculating the powers developed in the cavern during cycling:

- The mechanical energy developed during injection and production phases
- The heat flux that is exchanged at cavern wall between the cavern and the rock mass
- The additional enthalpy that is produced during injection phases.
- The heat flux that is exchanged at the interface between hydrogen and brine
- The heat generated by condensation or vaporization

In this report:

- The heat flux at the interface is neglected. This heat flux is probably small, and it depends on the sign of the difference between hydrogen temperature and brine temperature (Bérest, 2019).
- The effect of water vapor condensation or vaporization is not considered.
- Hydrogen temperature is assumed constant throughout the cavern (two symmetrical convection cells).

❖ **The heat flux through conduction** takes place in the rock mass, and the resulting heat flux through the cavern walls warms up or cools down the cavern hydrogen:

$$P_{th} = \int_{\partial V} -K_{salt} \frac{\partial T_{salt}}{\partial n} dA = q_{th} \Sigma \tag{64}$$

where k_{salt} and T_{salt} are rock-salt thermal conductivity and temperature respectively, and Σ is cavern wall area.

❖ **The mechanical power** developed during injection and production phases writes:

$$P_{mec} = (c_p - c_v) T q_m \tag{65}$$

where c_p and c_v are heat capacity of hydrogen at constant pressure and constant volume respectively; T is hydrogen temperature and $q_m$is hydrogen massic flowrate. P_{mec} is positive during injection phases as $q_m > 0$ and negative during production phases as $q_m < 0$.

- **The additional enthalpy rate** produced during injecting phases writes:

$$P_{ent} = c_p(T_{inj} - T_c)q_m \quad (66)$$

Where T_{inj} is the temperature of injected hydrogen. P_{ent} can be positive or negative depending on the sign of $T_{inj} - T_c$ which can be either positive or negative.

- **The total internal energy** of cavern is as follows:

$$E_{\text{int}} = c_v M T_c \quad (67)$$

Where M is the mass of hydrogen in the cavern and T_c is its absolute temperature.

The developed energies are calculated by the integration of the former powers over a given period, as for instance:

$$E_{t\ell}(t) = \int_{t_{sd}}^{t} P_{t\ell}(\tau)d\tau \quad (68)$$

Where t_{sd} is the time of the beginning of debrining.

1.3.10 Gas purity, the role of water vapor

In most gas caverns the temperature gradient is small, as natural convection stirs cavern gas and homogenizes its temperature. However, at cavern bottom but several dozens of meters above the interface between gas and the brine sump, a temperature gradient inversion is observed (Figure 169). Such an inversion can be expected short after debrining. The brine sump, which contains brine formed during solution-mining from circulating water originating from ground level, is still colder than the rock mass at sump depth (in sharp contrast with cavern gas, whose heat capacity is smaller than brine's, and swiftly reaches thermal equilibrium with the rock mass). However, this temperature difference is still present decades after debrining (Figure 170).

In this context, vapor content in the cavern is an important parameter during operation of a gas cavern. Field data suggest that, in the cavern, gas thermodynamic behaviour (its temperature, pressure and water content) is influenced by several coupled phenomena. During pressure cycles, temperature evolution is dictated by gas expansion-contraction and heat exchange with the rock mass. In addition, water vapor condenses in the entire gas body and evaporates at the brine-gas interface at the cavern bottom, an asymmetrical process leading to cooling of the brine sump, which remains perennially cooler than the rock mass, especially when cycles are frequent. The geothermal gradient generates natural convection in the upper part of the cavern; natural convection is impeded in the lower part of the cavern, above the brine sump, creating a buffer for water vapor diffusion in the cavern. These phenomena, which are important when the purity of the withdrawn gas is required (Bérest and Louvet, 2020) are not taken into account in the models for this study.

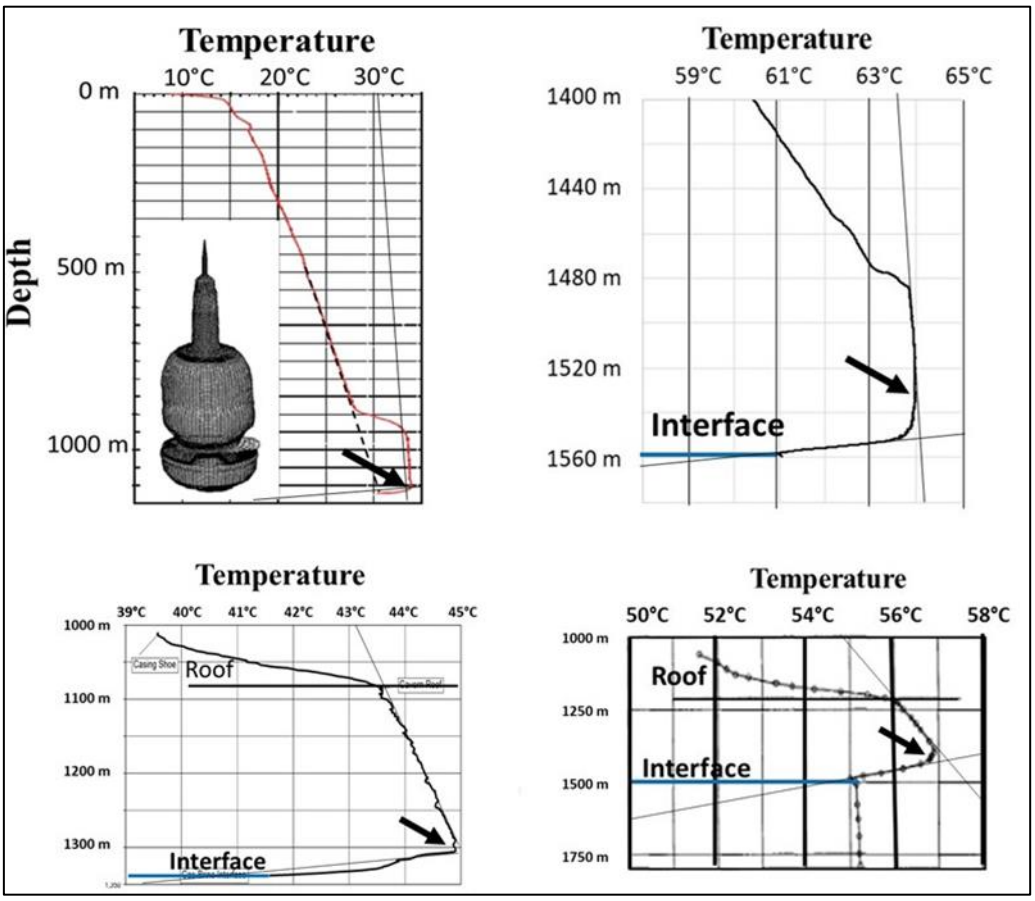

Figure 169. Vertical temperature profiles along the axes of symmetry of different gas storage caverns (Top left: Stassfurt S107 cavern [Klafki et al., 2003], top right: Storengy Tersanne cavern [Bérest and Louvet, 2020]; Bottom left: origin not mentioned [Berger et al., 2002]; Bottom right showing the temperature-gradient inversion at cavern mid-depth above the gas-brine interface (black arrow), from Thaule and Gentzsch, 1994).

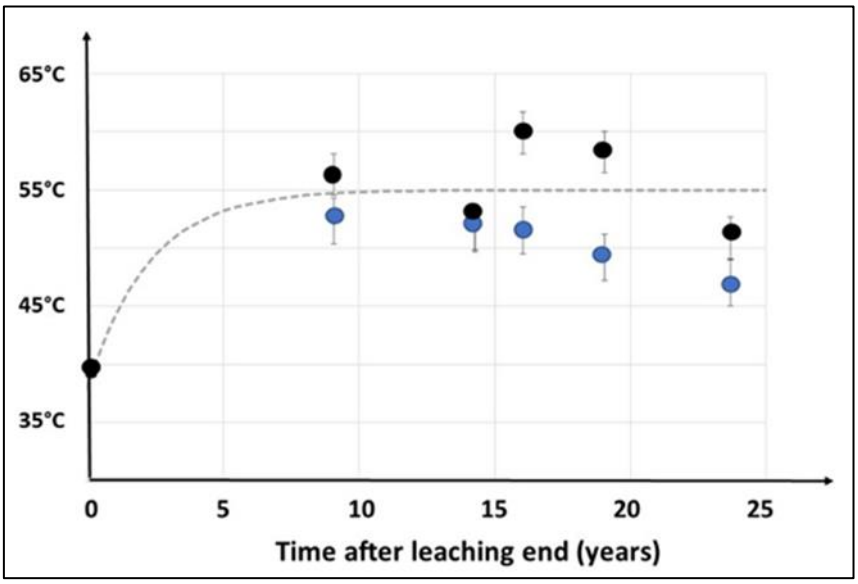

Figure 170. As-observed brine-sump temperature (blue dots), and average gas temperature (black dots) in a Storengy natural gas cavern. The dotted line is the computed brine-sump evolution when a 2.25-year characteristic time is assumed (Bérest and Louvet, 2020).

1.3.11 Selection of thermal parameters for the rocks

The selected thermal properties of rock salt and layers in the overburden are provided in Table 13. These parameters were selected by smartTectonics based on an analysis of the geological databases available in the Netherland, see Figure 162 for the position of various rock layers.

Table 13. Considered thermal properties of the rocks.

Rock	Heat capacity (J/kg-K)	Thermal conductivity (W/m-K)	Geothermal gradient (°C/100 m)
NU	950	2.3	4.348
NLNM	905	2.1	4.762
CK	780	2.2	4.545
AT	780	2.5	4.000
ZE	880	5.3	1.887

1.4 Geomechanical modelling

1.4.1 Introduction

This chapter describes the geomechanical model considered for rock salt and overlying layers.

1.4.2 Selection of mechanical for the rocks

1.4.2.1 Density and elasticity

Table 14 gives the considered density and elastic properties of the rocks. The layers forming the overburden over the salt are assumed to have a purely elastic behaviour while rock salt has an elasto-viscoplastic behaviour.

Table 14. Considered density and elastic properties of the rocks.

Rock	Thickness (m)	Depth (m)	Density (kg/m3)	Poisson's ratio	Young's modulus (MPa)
NU	108.14	0-108.14	1800	0.33	100
NLNM	53.12	108.14-161.26	2100	0.33	500
CK	242.32	161.26-403.58	2500	0.33	10000
AT	143.97	403.58-547.55	2600	0.33	15000
ZE	1452.45	547.28-2000	2160	0.27	33000

1.4.2.2 Mechanical behaviour of salt

Deviatoric stress (σ) in the vicinity of a salt cavern is usually smaller than the range of deviatoric stresses than can be tested at the laboratory ($\sigma > 5$ MPa). This is important because it has long been suspected (Spiers et al., 1990) that, in the small deviatoric stress domain, the governing mechanism for salt creep was pressure solution — rather than dislocation creep, which is measured in the laboratory. One consequence of this should be that creep rate in this domain is much faster (by several orders of magnitude) than that extrapolated from tests performed in the high-stress domain. In addition, creep rate should be a decreasing function of grain size: it should be a linear function of the applied stress, and the presence of a small amount of brine at the interfaces between grains should be a necessary condition for active creep. These statements were based on theoretical arguments, geological evidence and the results of tests performed on artificial salt. Uniaxial creep tests performed on salt samples in dead-end drifts of the Varangéville (France) and Altaussee (Austria) mines to take advantage of constant temperature and hygrometry. The applied loads were from 0.05 to 4.5 MPa, and these tests confirmed

the theoretical predictions (Bérest et al. 2022). Pressure-solution creep is important for problems such as cavern abandonment (Baumann et al., 2022a).

Generally speaking, it can be said that salt cavern behaviour exhibits both ductile (creep closure) and fragile (roof fall, block falls, cratering, fracturing) features.

Rock salt has an elasto-visco-plastic behaviour, its total strain rate can be written as the sum of five components:

$$\dot{\varepsilon}_{tot} = \dot{\varepsilon}_{el} + \dot{\varepsilon}_{ss} + \dot{\varepsilon}_{tr} + \dot{\varepsilon}_{ps} + \dot{\varepsilon}_{th} \tag{69}$$

i. $\dot{\varepsilon}_{el} = \frac{\dot{\sigma}}{E_{salt}}$ is the elastic part of the strain rate where E_{salt} is the Young's modulus or rock salt.

ii. $\dot{\varepsilon}_{ss}$ is the steady-state part of the dislocation-creep law. The Norton-Hoff is used widely:

$$\dot{\varepsilon}_{ss} = A_{dc}\, exp\left(\frac{-Q_{dc}}{RT_{salt}}\right)\sigma^{n_{dc}} \tag{70}$$

Where $A_{dc} = A_{dc}(\Phi)$ is a prefactor depending on the relative humidity Φ, Q_{dc} is the activation energy, R is the universal gas constant, T_{salt} is the absolute rock-salt temperature, and n_{dc} is the exponent of the creep law.

iii. $\dot{\varepsilon}_{tr}$ is the strain rate due to transient creep. It describes the rock viscoplastic behaviour before steady state is reached. Any change in applied loading or temperature triggers a transient creep response (Figure 171). Following a compressive load increase ("direct transient creep"), or $\sigma = \sigma_1$ when $t < t_{1\to2}$ and $\sigma = \sigma_2 > \sigma_1$ when $t > t_{1\to2}$, transient creep is characterized by faster initial strain rates compared to the steady-state strain rates. If the applied stress is kept constant after the stress change, the transient rate slowly decreases until the transient strain exhausts itself — i.e., the total strain rate becomes equal to the steady-state rate, and the transient strain reaches an asymptotic value defined as the transient strain limit $\varepsilon^*_{tr} = \varepsilon^*_{tr}(\sigma_2, T)$ that is a function of deviatoric stress and temperature. Several transient-creep laws can be found in the literature. Munson et al. (1984) proposed an internal variable, $\zeta(t)$, such that, during a creep test, $\dot{\varepsilon}_{tr} = \dot{\zeta}$, describes the evolution of the transient strain, which slowly increases to reach the transient strain limit $\varepsilon^*_{tr} = \varepsilon^*_{tr}(\sigma, T)$ when σ and T are kept constant. During a uniaxial creep test,

$$\begin{cases} \frac{\zeta}{\varepsilon^*_{tr}} < 1, \varepsilon^*_{tr} = K_0 e^{cT}\sigma^m \\ \frac{\dot{\zeta}}{\dot{\varepsilon}_{ss}} = \Phi(\zeta/\varepsilon^*_{tr}; \Delta) = exp\left[\Delta\left(1 - \frac{\zeta}{\varepsilon^*_{tr}}\right)^2\right] - 1 \end{cases} \tag{71}$$

where $K_0, c,$ and m are three material constants, and Δ is a function of σ:

$$\Delta = \alpha_w + \beta_w Log_{10}\left(\frac{\sigma}{\mu_{salt}}\right) \tag{72}$$

Where α_w and β_w are two material constants, and the shear modulus is $\mu_{salt} = \frac{E_{salt}}{2(1+\nu_{salt})}$.

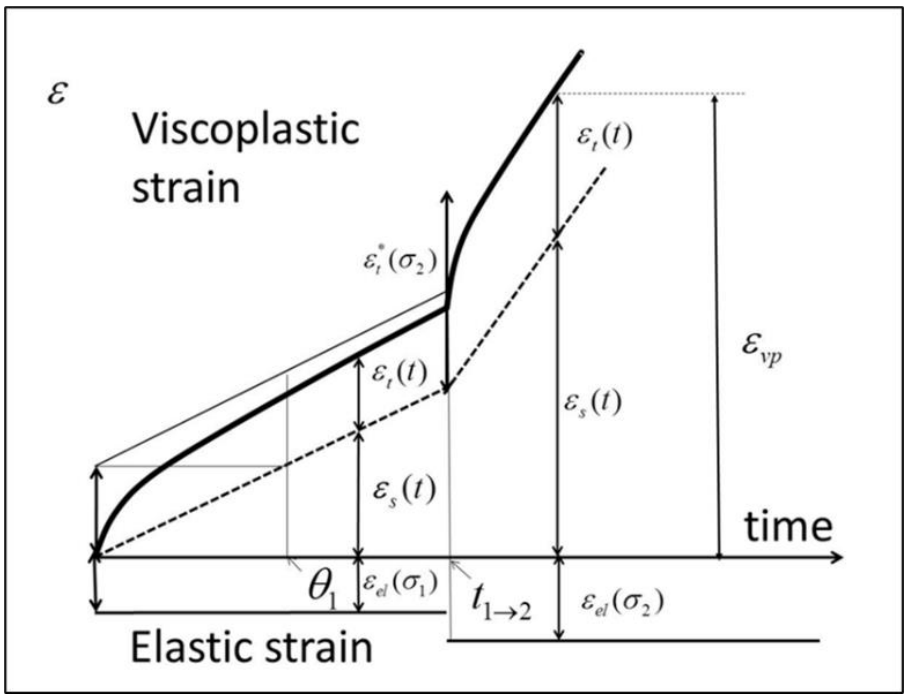

Figure 171. Schematic strain-stress curve during an isothermal uniaxial creep test. Increasing mechanical loading.

The 3D form of the law is given by

$$\dot{\varepsilon}_{ij}^{vp} = \frac{\partial \sigma_e}{\partial \sigma_{ij}} F \dot{\varepsilon}_{ss} \quad \begin{cases} F = e^{A\left(1-\frac{\zeta}{\varepsilon_{tr}^*}\right)^2} \text{ when } \zeta \le \varepsilon_{tr}^* \\ F = e^{-\delta\left(1-\frac{\zeta}{\varepsilon_{tr}^*}\right)^2} \text{ when } \zeta \ge \varepsilon_{tr}^* \end{cases} \tag{73}$$

where $\sigma = \sqrt{3J_2}$ is deviatoric, or "effective", stress, and δ is another material constant.

iv. $\dot{\varepsilon}_{ps}$ is the strain rate related to the pressure-solution mechanism:

$$\dot{\varepsilon}_{ps} = \frac{A_{ps}}{T_{salt} D^3} exp\left(\frac{-Q_{ps}}{R T_{salt}}\right) \sigma \tag{74}$$

where A_{ps} is a prefactor, D is the average grain size and Q_{ps} is the activation energy. Pressure solution is not taken into account in the 2D sensitivity analysis, but a sensitivity analysis in 3D is performed (see Section 1.14).

v. $\dot{\varepsilon}_{th} = \alpha_{salt} \dot{T}_{salt}$ is the thermoelastic strain rate following any temperature change, where $\alpha_{salt} \approx 4 \times 10^{-5}/°C$ is the coefficient of thermal expansion of salt.

Additionally, when the deviatoric stress applied on a salt sample is decreased abruptly and kept constant, steady-state creep rate will be reached again after a long period of time. This rate is slower than the steady-state rate when the load was higher, as $\dot{\varepsilon}_{ss}$ is an increasing function of σ. In fact, two kinds of behaviour can be observed. When the load decrease is small, the transient viscoplastic rate remains contractive (as it was before the load change). When the load decrease is large, the transient viscoplastic rate is expansive: over several weeks or months, sample height increases (Strain rate is negative.), although the applied axial stress is compressive. This phenomenon is called *reverse creep* and can be observed in salt caverns when the pressure is increased abruptly (Bérest et al., 2015).

At cavern scale, even without any transient component in the creep law, modelling shows that stresses are redistributed slowly around a cavern following any pressure change. The velocity of this redistribution depends on exponent *n* of the steady-state part of the law: the larger the exponent, the slower the redistribution. This phenomenon is called *geometric creep*.

In most cases, a complete set of creep parameters as described above is not available for a given site. Laboratory tests are quite expensive and not able to produce data for the pressure solution mechanism. However, calibration of thermal and creep parameters is also possible through simple in-situ tests performed on existing borehole or caverns (Brouard and Bérest, 2022).

Several creep laws can be found in the literature for dislocation creep (Figure 172). The two most commonly used laws that include both a stationary and a transient component are the Lubby2 and Munson-Dawson laws.

The Munson-Dawson law was chosen for this study because it has been shown to give the best account of transient creep when a cavern undergoes rapid changes in pressure (Brouard and Bérest, 2022).

The Munson-Dawson law has 3 parameters for its stationary part (A_{dc}, n_{dc}, Q_{dc}) and 6 parameters for its transient part ($K_0, m, \delta, \alpha_w, \beta_w, c$).

Salt constitutive behaviour is a site-dependent notion. The complete set of parameters selected for the Munson-Dawson creep law is provided in Table 15. The set of parameters for the steady-state part (dislocation creep, Norton-Hoff law) was determined by smartTectonics and can be considered realistic for the Dutch dome salt. No transient creep test was available to calibrate the transient creep parameters, so we chose to use the parameters provided by Munson himself for the Avery Island dome salt.

Table 15. Munson-Dawson parameters for dislocation creep.

	Parameter	Units	Value
Steady-state part	A_{dc}	/MPa^n-yr	17.95
	n_{dc}	–	4.86
	$\frac{Q_{dc}}{R}$	K	6495
Transient part	m	–	3
	α_w	–	-13.2
	β_w	–	-7.738
	K_0	–	7E-7
	δ	–	0.58
	c	/K	0.00902

Figure 172. Among the constitutive laws for rock-salt creep used to study the mechanical stability of salt caverns, the Munson-Dawson law is the one that best accounts for transient creep on a cavern scale

The set of parameters selected for the pressure solution creep law used in the 3D model is provided in Table 16.

Table 16. Parameters for pressure solution creep.

Parameter	Units	Value
$\boldsymbol{A_{ps}}$	/MPa-yr	896
$\boldsymbol{D}$	mm	2.7
$\boldsymbol{\frac{Q_{ps}}{R}}$	K	2910

1.4.3 Geostatic pressure

The vertical distribution of geostatic pressure P_∞ with depth z is calculated from the integration of rock densities ρ.

$$P_\infty(z) = \int_0^z \rho_R(x) g dx \tag{75}$$

Figure 173 shows a screenshot of an example of this distribution in LOCAS.

1.4.4 Coupling between hydrogen thermodynamics and rock-salt rock mechanics

The volume of the cavern ($V_c = V + V_b$, where V is hydrogen volume and V_b is brine volume in the sump) changes during cycling, mainly as a result of salt creep:

$$\dot{\varepsilon} = \frac{\dot{V}_c}{V_c} \tag{76}$$

Therefore rock-salt creep has the effect of modifying the specific volume of hydrogen ($v = \frac{1}{V}$) that appears in the equation (58). This is why a coupling between the thermodynamics of hydrogen and the mechanics of salt is necessary when the cavern undergoes significant variations in volume, which can be the case during the cycling of a gas storage cavern.

As shown in Figure 174, there is a full coupling between hydrogen thermodynamics and rock-salt rock mechanics in LOCAS.

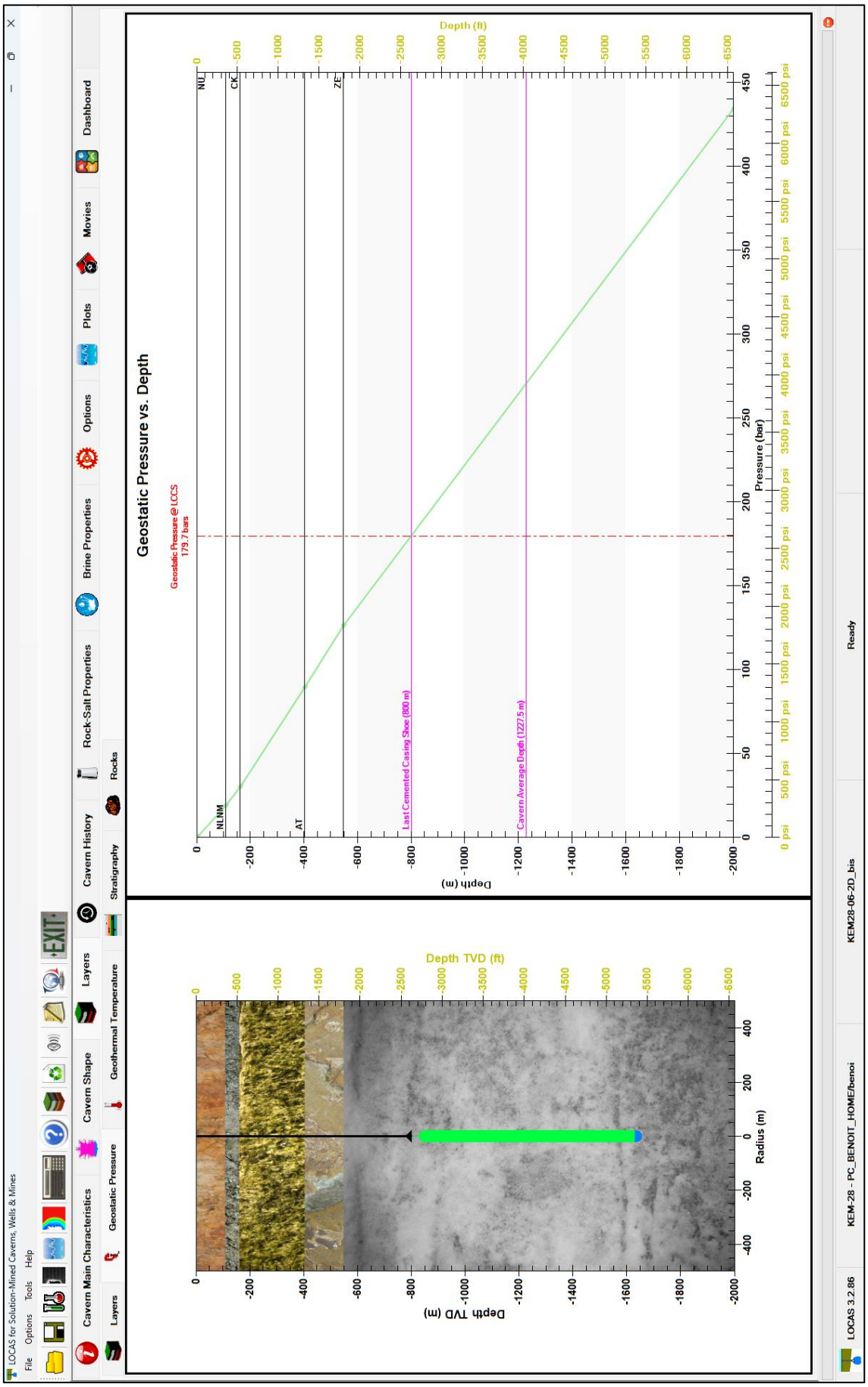

Figure 173. Geostatic pressure as a function of depth (LOCAS screenshot).

Figure 174. Coupling between thermodynamics and rock mechanics in LOCAS.

1.5 Cavern stability analysis

1.5.1 Introduction

When we are interested in the mechanical stability of a salt cavern, we need to look at a number of potential problems that are described in the following sections. Storing hydrogen does not seem to raise specific rock mechanics problems, except that its thermodynamic behaviour (hence, amplitude of the temperature swings) is slightly different from those of methane or compressed air and pressure cycles might be more frequent.

1.5.1.1 Maximum pressure

Typically, maximum pressure in gas storage cavern is a fraction of the overburden weight; in most cases it is close to 0.18 bar/m (Table 17). In a cavern whose pressure is increased rapidly to its maximum value after a long standby period at relatively low pressure, onset of tensile effective stresses can be feared (Bérest et al., 2020).

Table 17. Maximum pressure at the casing shoe for several facility worldwide (KEM-17 report).

Gas storage	Authors	CCS depth (m)	Pmax (bar)	Maximum gradient (bar/m)	Maximum gradient (psi/ft)
Aldbrough	Slingsby et al., 2011	1800	270	0.15	0.66
Carriço	Colcombet et al., 2008	1000	180	0.18	0.8
Etzel	Schweinsburg et al., 2010	1150	200	0.17	0.76
Holford	Fawthrop et al., 2013	≈ 550	100	0.18	0.8
Krummhörn	Rummel et al., 1996	≈1500	270	0.18	0.8
Nuttermoor	Bernhardt et al., 2013	≈ 1000	170	0.17	0.76
Teesside	Mullaly, 1982	≈ 350	45	0.13	0.58
Zuidwending	Hoelen et al., 2010	1000	180	0.18	0.8
Manosque	de Laguérie & Durup, 1994	1000	180	0.18	0.8
Stublach	Pellizzaro et al., 2011	≈ 550	100	0.18	0.8
Egan	Chabannes, 2005	1125	230	0.204	0.9
Kansas	Itsvan, 1998	NA	120		
China	Fansheng et al., 2010	≈ 2000	170	0.16-0.17	0.72
Aldbrough	McLeod et al., 2011	≈1500	270	0.155	0.66
Nüttermoor	Bernhardt et al., 2013	≈ 1020	170	0.17	0.8
Germany	Wagler et al., 2013	≈ 648	122	0.188	0.83
Torup	Johansen, 2010			0.184	0.81
Huai'an	Zhao et al., 2013	1493	260	0.175	0.77
Jintan (Xi-2#)	Yang et al., 2015	937	135 150	0.144 0.160	0.64 0.7
Jintan (PetroChina)	Hongling Ma, Institute of Soil and Rock Mechanics, Wuhan, pers.com. (May 2018)	≈1000	170 180	0.170 0.180	0.76 0.8
Jintan (Sinopec)		900	170	0.188	0.83
Qianjiang		1980	320	0.160	0.7

1.5.1.2 *Minimum gas pressure*

Rock-salt constitutive law is highly non-linear. At low hydrogen pressure, creep closure will be much higher than at high hydrogen pressure. Creep-closure rate and subsidence rate is maximum when cavern pressure is minimum. Furthermore, keeping the cavern pressure at a low level for a relatively long period of time can cause damage to the rock salt on the cavern wall due to dilation (Figure 175) and should therefore be avoided.

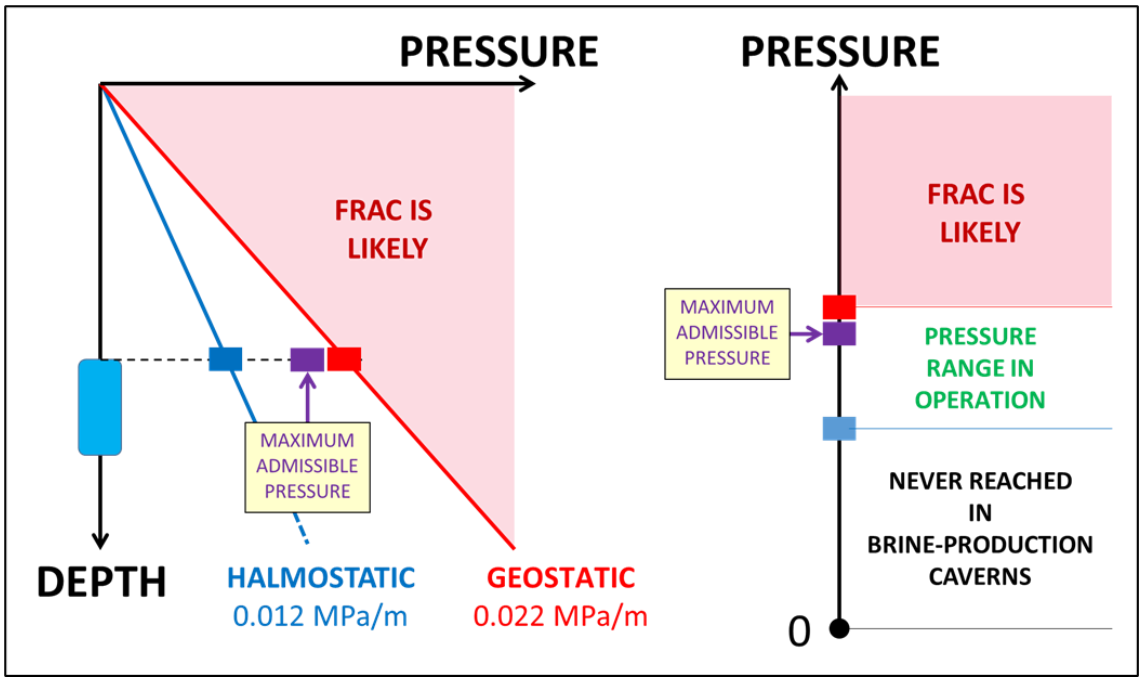

Figure 175. Operational domain for salt caverns (KEM-17 report).

1.5.2 Creep closure

All salt caverns shrink. The driving force for cavern volume loss is the gap between geostatic pressure and cavern fluid pressure. 1 %/yr is often considered as a maximum from an economic standpoint. Volume loss rate is a non-linear function of this gap. It is much faster in deeper caverns (for instance, a loss of volume by 60% in 37 years in the Tersanne gas storage site in France, Hévin et al., 2013, and by 3×10^{-5}/yr in a 250-m deep cavern at Gellenoncourt in France were measured, Brouard et al., 2017). Creep closure is significantly faster in a cavern whose pressure is cycled (rather than constant), Gordeliy and Bérest, 2022; volume loss rate is quite sensitive to the value of the minimum pressure. Volume loss rate strongly depend (several orders of magnitude) on the effective mechanical properties of the salt formations (Brouard and Bérest, 1998). Creep closure may lead to large volume losses, subsidence, casing overstretching, permeability increases at the anhydrite/salt interface.

1.5.3 Casing overstretching

Casing overstretching results from large cumulated strains at cavern roof when the steel casing, whose elastic limit is small, is not able to accommodate such strains, resulting in casing failure and gas leak. A couple of cases are known. The design of the cavern shape plays a major role for casing overstretch cases, as flat roofs, interlayered formations, large spans, and the absence of a cavern neck expose the cemented casings to large stains and increases the risk of casing overstretch. If it raises a concern (when cumulated strains in the salt roof where the casing is cemented to the salt formation are large after several decades) a special analysis would need to be performed.

1.5.4 Subsidence

Subsidence is a critical concern in the Netherlands, it is an unavoidable consequence of salt cavern creation and cavern creep closure. An abundant literature was dedicated to this topic. It is generally accepted that the volume of the subsidence bowl is close to the cavern volume loss. The maximum vertical subsidence is of the order of magnitude of the volume loss divided by the square of the cavern depth; however, the exact figure and, more generally, the shape of the subsidence bowl (the 'transfer function') are site-specific notions. Subsidence can be computed both through 2D or full 3D computations and more simply through a 'transfer function' method.

1.5.5 Onset of dilatancy

Dilatancy, also called dilation, can occur under certain compressive stress states. Dilatancy induces irreversible increase in salt volumetric strain which is due to micro-fracturing. Salt dilatancy must be avoided, as it may cause an increase in permeability and a reduction in salt strength. Compression and extension state of stress must be distinguished.

Several dilation criteria can be found in the literature, including the following two, which are undoubtedly the most widely used:

- The simple Ratigan/Van Sambeek dilation criterion:

$$\sqrt{J_2}_{dil} = -0.27 I_1 \tag{77}$$

- The RD dilation criterion:

$$\sqrt{J_2}_{dil} = \frac{D_1\left(\frac{I_1}{sign(I_1)\sigma_0}\right)^{\bar{m}} + T_0}{\left(\sqrt{3}\cos\psi - D_2 \sin\psi\right)} \tag{78}$$

Where J_2 is the second invariant of the stress tensor, I_1 is the first invariant of the stress tensor (compressive stresses are negative), i.e., the sum of the three principal stresses ($I_1 = tr\underline{\sigma}$), $\psi$is Lode angle, σ_0 is a dimensional constant, T_0 is the unconfined tensile strength, and $\bar{m}, D_1$, and D_2 are parameters specific to each salt formation.

A more complete description of these two criteria is given in Appendix B: Salt Dilation Criteria.

For all the considered dilation criteria, the **factor of safety** (FOS) is defined as

$$FOS = \frac{\sqrt{J_2}_{dil}}{\sqrt{J_2}} \tag{79}$$

where $\sqrt{J_2}$ is the computed deviatoric stress, and $\sqrt{J_2}_{dil}$ is the value of the dilatant deviatoric stress when the mean stress equals the computed value of the mean stress. Dilation develops when FOS < 1.

No generic set of parameters is available for Dutch salt. The set of parameters from Moss Bluff domal salt (Table 18) is considered in this study for the RD dilation criterion, as it is rather conservative (Brouard and Respec, 2004).

Table 18. RD dilation criterion parameter values for Moss Bluff salt.

Parameter	Value	Units
D_1	0.411	MPa
D_2	0.664	–
$\bar{T}_0$	1.351	MPa
m	0.85	–
σ_0	1.000	MPa

1.5.6 Stresses generated by creep closure and temperature changes

In the case of a pressure-cycled cavern, as it is expected for hydrogen caverns, creep closure is strongly coupled with thermomechanical effects (Bérest et al., 2014: Bérest et al., 2016; Brouard et al., 2018). For instance, a large pressure drop generates compressive tangential stresses at cavern wall, fast creep closure and in some cases formation of spalls at cavern wall (Rokahr et al., 2007). When pressure drop is swift, gas temperature also drops by several dozens of °C, generating large tensile stresses at cavern wall, Sicsic and Bérest, 2014 (1 MPa per °C is typical). In many cases, additional tensile stresses are larger than additional compressive stresses, possibly leading to the creation of fractures perpendicular to the cavern walls. However, when cycles period is small, the depth of penetration of fractures is small (dm). Conversely, following a fast and large pressure increase, effective tensile stresses can be generated at cavern wall, lessened by compressive stresses resulting from gas warming (Djizanne et al, 2014). Compared to a natural-gas cavern, the fast pressure cycling generates a state of stress which can be different from the state of stress resulting from seasonal storage.

Thermal computations must be performed assuming conductive heat transfer in the rock mass. The exact geometrical shape of the cavern must be considered, because the geometry of the cavern determines the heat flow and temperature distribution around it.

1.5.7 Onset of tensile stresses

stresses in the rock mass in most cases are compressive; tensile zones must be avoided, as the tensile strength of salt is low, of the order of 1-2 MPa. Large tensile stresses lead to the creation of fractures. Deep fractures may be the origin of roof or wall spalling. A 1.5 MPa tensile strength of rock-salt is assumed in the numerical computations.

1.5.8 Onset of tensile effective stresses

Effective stress is defined as the sum of the least compressive principal stress, σ_{max}, and cavern hydrogen pressure, P_c, at the same depth:

$$\sigma_{eff} = \sigma_{\max} + P_c \tag{80}$$

The principal stress and the pressure in the cavern are constantly changing. If the pressure decrease is rapid, additional thermoelastic stresses are created and the effective stress can become a tensile stress (Figure 176). Tensile effective stresses appear at the minimum pressure in some cases. When the effective stress is larger than rock tensile strength, micro-fracturing occurs, permeability increases drastically, and salt softens. In some cases, discrete fractures appear. Opening of a fracture is likely when effective stress is larger than the tensile strength of rock. Special attention is be paid to tensile effective stresses at cavern roof as vertical fractures may develop upward as the overburden weight decrease vertically and that would allow hydrogen to migrate upwards to a weaker shallow formation.

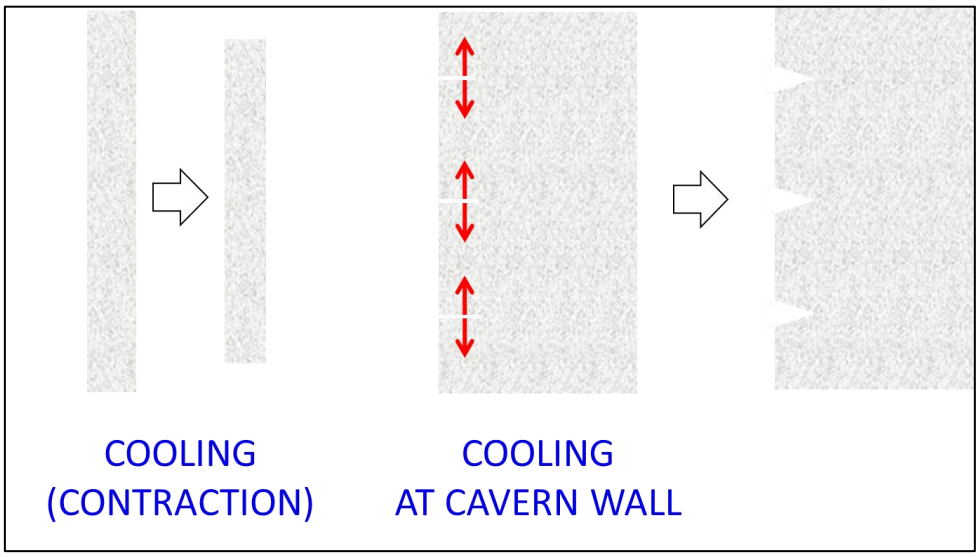

Figure 176. Rock-salt cooling at cavern wall can creates fractures.

1.5.9 Worst case scenarios

Accidents/incidents in salt caverns are exceedingly rare but can be sometimes spectacular. Some of the more or less serious problems that can occur are described below.

1.5.9.1 Roof falls

Roof falls are known to occur when cavern roof span is large, somewhat flat, and located in a stratified salt formation (Four cases are known from the literature). Large pressure drops are detrimental (Réveillère et al., 2021).

1.5.9.2 Block falls

Block falls from cavern wall is a mundane phenomenon and only major block falls are considered here (Seven cases have been described in the literature). Evidences include breaks or bending of hanging strings hit by falling blocks or strained by cavern bottom rise. Block falls are especially harmful during solution mining and, more generally, when the well is equipped with a string (Bérest et al., 2017), a circumstance which is less frequent in gas caverns than in oil caverns. Large block falls following an abrupt pressure drop occurred in Gulf Coast salt domes in which Anomalous Zones can be found. An example was described by Quast (1983) in a Huntorf cavern during debrining; its origin might be the change in Archimedes thrust during debrining (Djizanne et al., 2014), a mechanism which may be significant in an hydrogen storage.

1.5.9.3 Hydraulic connections

Hydraulic connections are created when pressure in a cavern is influenced by fluid pressure in another cavern, or by fluid pressure in a non-salt formation. Creation of a hydraulic connection — seven cases are known — may be due to the failure of a thin salt wall when fluid pressures applying on the two sides of the wall are (or were) significantly different. Hydraulic connection inside a massive salt body is more puzzling. Existence of a natural heterogeneity (a “weak”, “more porous and permeable”, “preferred-dissolution”, “anomalous” zone) crossing the salt formation and intersecting two neighbouring caverns often is invoked.

1.5.9.4 Cratering

Cratering is known to occur when a cavern is shallower than 500-600 m, when the diameter/depth ratio is not much smaller than two-thirds and when a thin salt roof is left above a cavern (Bérest, 2017). More

than thirty cases are well documented; however, no cratering case is known above hydrocarbon storage caverns.

1.5.9.5 Fracturing

Fracturing may occur in two circumstances: (1) after a large pressure and temperature drop when tensile tangential stresses develop at cavern wall (2) after a large pressure increase when (tangential) tensile effective stresses develop at cavern wall. In fact, in a cavern whose pressure is increased rapidly to its maximum value, onset of tensile effective stresses and cavern permeability increase can be feared (Bérest et al., 2020). Cavern abandonment raises the same kind of risk.

1.5.9.6 Blowout

Blowout (wellhead failure leading to the loss of most or all the products) is an especially severe concern in the case of underground storages. Only two natural gas blowouts from salt caverns are known. The first one is the Moss Bluff case in Texas, 2004 (Brouard Consulting and Respec, 2013) which led to the loss of the full natural gas inventory. In Europe (not in the US) it is mandatory to set an underground safety valve (SSSV) in a gas cavern well. Probability of a blowout is reduced by several orders of magnitude by this (no case is known when the cavern is equipped with such a valve). A blowout may last several hours or days depending on cavern size, wellbore diameter and on cavern initial pressure at the time of the blowout (Djizanne et al., 2014, 2022). During a blowout, thermo-dynamical behaviours of hydrogen in the cavern and hydrogen in the borehole are strongly coupled. Hydrogen temperature decreases in the cavern and in the borehole, with possible grave consequences for the well. (Casing steel, cement, and rock at the vicinity of the well experience large temperature changes, thermal contraction, and development of tensile stresses). The simulation of a blowout considering a typical configuration of a hydrogen cavern is presented in Section 1.10. As for the analysis of cavern-pressure cycling, the mechanical stability of the cavern (onset of dilation and tensile effective stresses) during the blowout is examined into details.

1.5.9.7 Workover

During the life of a gas storage cavern, it may be necessary to carry out maintenance operations requiring the pressure in the cavern to be lowered considerably and maintained at this low pressure for several weeks or more. This is the case, for example, when a cavern is initially full of gas and an equivalent volume of brine is not available to refill it with brine (known as “rebrining”). A cavern maintained at low pressure rapidly loses volume, the deeper the cavern, and damage due to dilation can occur and increase over time as long as the pressure remains low. The simulation of a workover is presented in Section 1.12.

1.6 Wellbore modeling – Reference case

1.6.1 Introduction

This section describes the results of wellbore modelling in the reference case, which is Case #07 in the sensitivity analysis (see Section 1.9). This case corresponds to a well where the shoe of the last cemented casing is at a depth of 800 m (Figure 177). The roof of the cavern is at 830 m and its bottom at 1655 m, i.e., the cavern height is 855 m. The diameter of the cavern in its main section is 40 m. The ratio of volume to surface area is 9.69 m. 90-day cycles are considered in this case and 10 cycles are calculated.

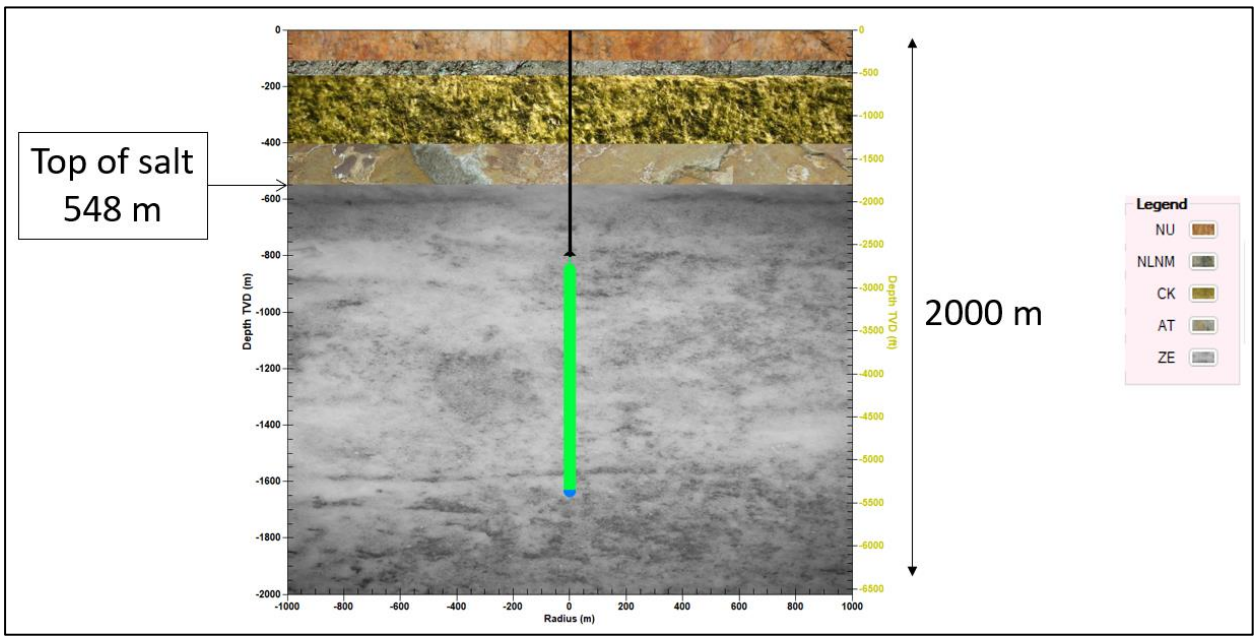

Figure 177. Configuration of the reference case.

1.6.2 Input for wellbore modelling: hydrogen inventory

For the wellbore modelling, for the sake of simplicity it is assumed that the mass of hydrogen stored in the cavern evolves sinusoidally. Figure 178 shows the evolution of hydrogen mass stored in the cavern. The maximum mass of hydrogen stored in this case is 10.4 Mkg. As the mass of the cushion gas is 6.5 Mkg (mass of hydrogen at the minimum pressure), the working gas mass is 3.9 Mkg. Figure 179 shows the corresponding flowrate of hydrogen injected or withdrawn. For these 90-day cycles, the maximum flowrate is ± 1.6 kg /s ≈ 138 tonnes/day.

1.6.3 Output: gas properties in the wellbore and in the cavern

Using the hydrogen mass flowrate imposed at the surface, LOCAS calculates changes in hydrogen properties both along the wellbore and in the cavern.

The computed hydrogen pressure at the wellhead is given in Figure 180. The evolution of wellbore pressure losses are shown in Figure 181. These pressure losses are very small because of the low density of hydrogen and its low velocity along the borehole (see Figure 188).

The rate of change of pressure at the shoe of the last cemented case is shown in Figure 182, with a maximum of around 2.2 bar/day in this case.

The evolution of hydrogen temperature at the LCCS and in the cavern are shown in Figure 183. The two temperatures are equal during the production phases, but not during the injection phases, because the hydrogen in the cavern has much more inertia. It should be noted that the trends fairly quickly reach a quasi-stationary regime, i.e., trends that are repeated from one cycle to the next.

Figure 184 shows the evolution of the temperature of the hydrogen at the wellhead, which is equal to 50°C during the injection phases (model assumption) and decreases between 40°C and 22°C between the beginning and end of the production phases.

The evolution of the heat flux q_{th} exchanged between hydrogen and salt at the cavern wall is shown in Figure 185. This heat flux varies between ± 17 W/m². Given that the surface area of the cavern is around 103,200 m², this corresponds to a maximum power of around 1.75 MW.

The evolution of the heat transfer coefficient h, which was considered in the wellbore model but not in the finite element models they are presented later in the report, is given on the Figure 186 and varies approximately between 0 and 46 W/m²-K. The minimums are reached towards the middle of the production phases, whereas the maximums are reached at the beginning and end of the production phases (which also corresponds to the beginning and end of the injection phases in this case).

The evolution of hydrogen density at the wellhead, at the casing shoe and in the cavern is shown in Figure 187. The amplitude of density variations is relatively small in this case, between 6 and 11 kg/m^3.

Figure 188 shows the evolution of the hydrogen velocity in the borehole. This velocity varies between -5.15 m/s and +5.25 m/s, which is far from the maximum value of 30 m/s sometimes considered for natural gas storages (to limit erosion of the production casing under the effect of friction).

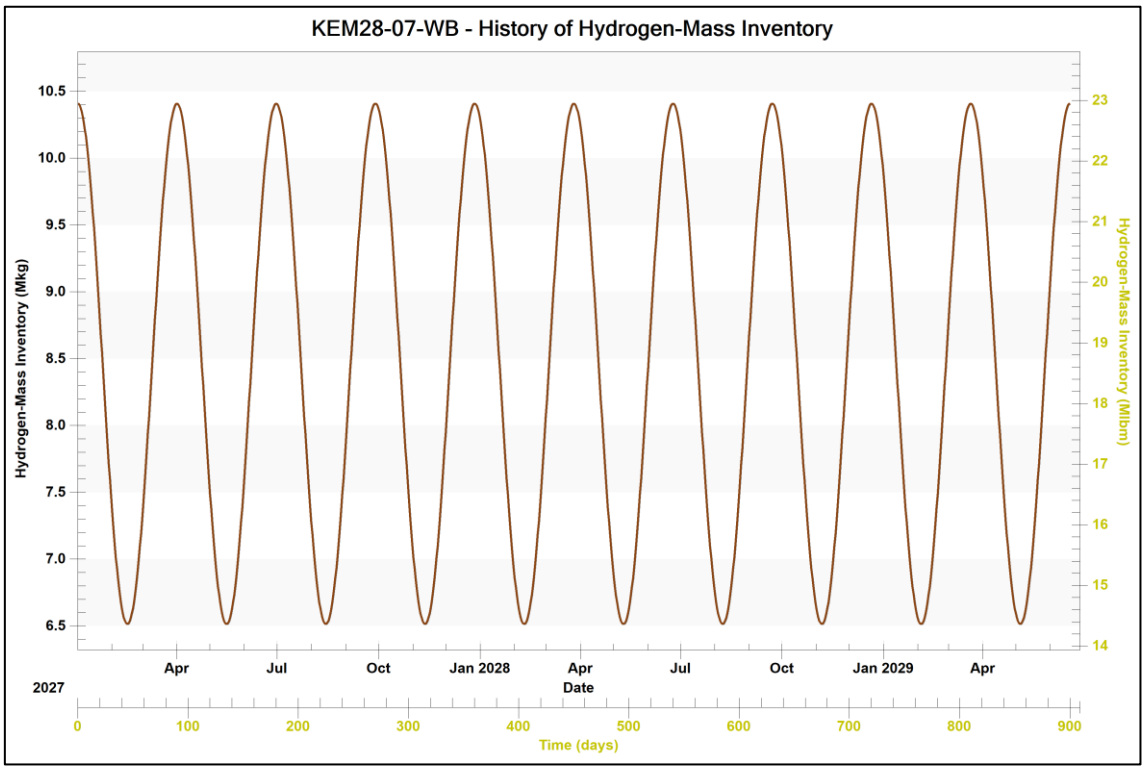

Figure 178. Wellbore modeling - Reference case - Evolution of hydrogen mass stored in the cavern.

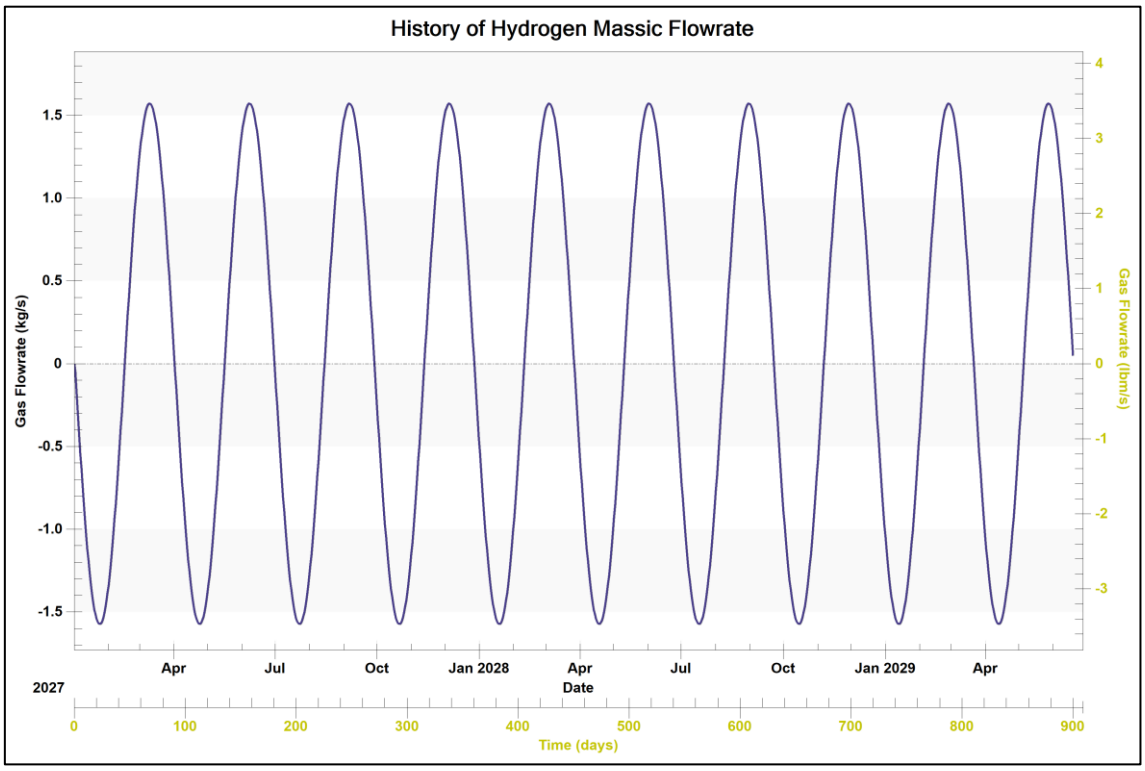

Figure 179. Wellbore modeling - Reference case - Evolution of hydrogen flowrate.

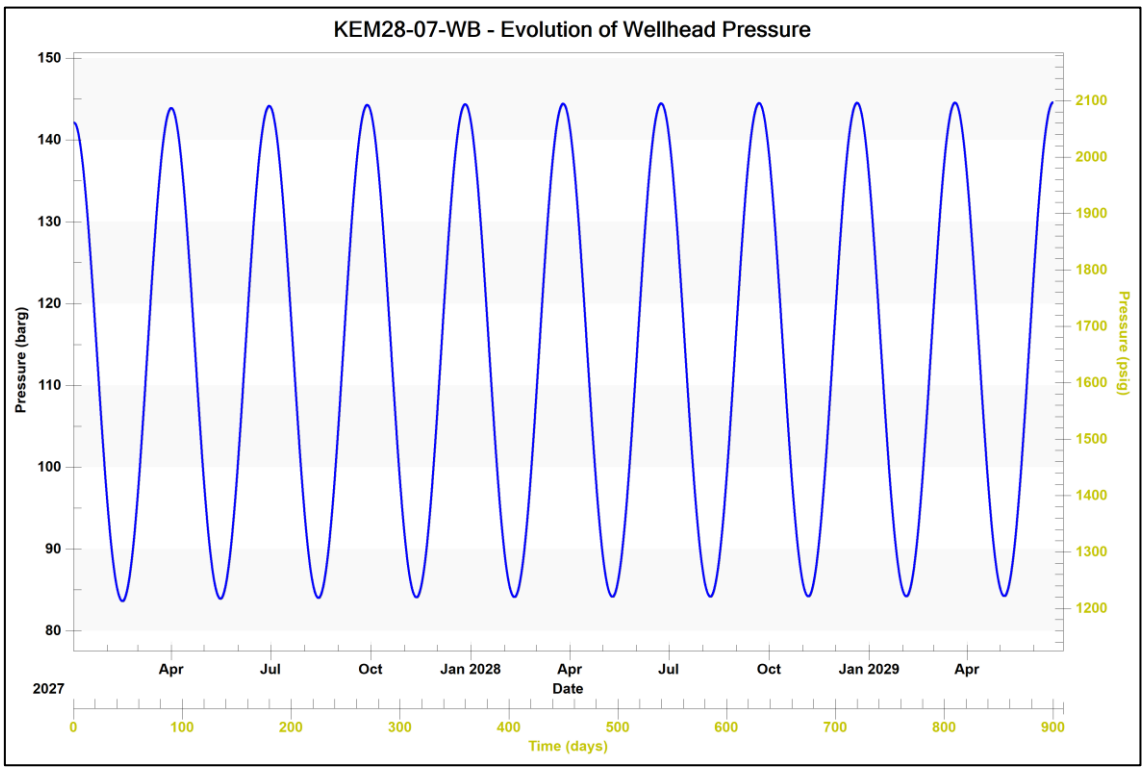

Figure 180. Wellbore modeling - Reference case - Evolution of wellhead hydrogen pressure.

Figure 181. Wellbore modeling - Reference Case – Evolution wellbore pressure losses.

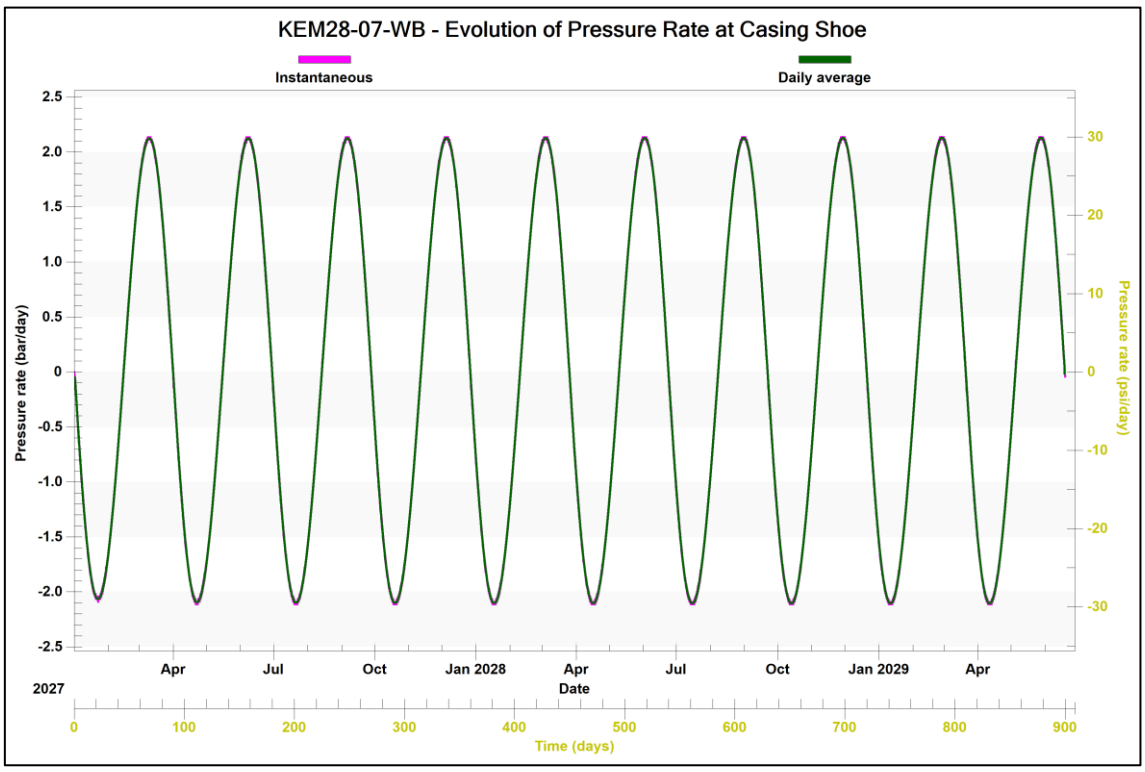

Figure 182. Wellbore modeling - Reference Case – Evolution of pressure rate at casing shoe.

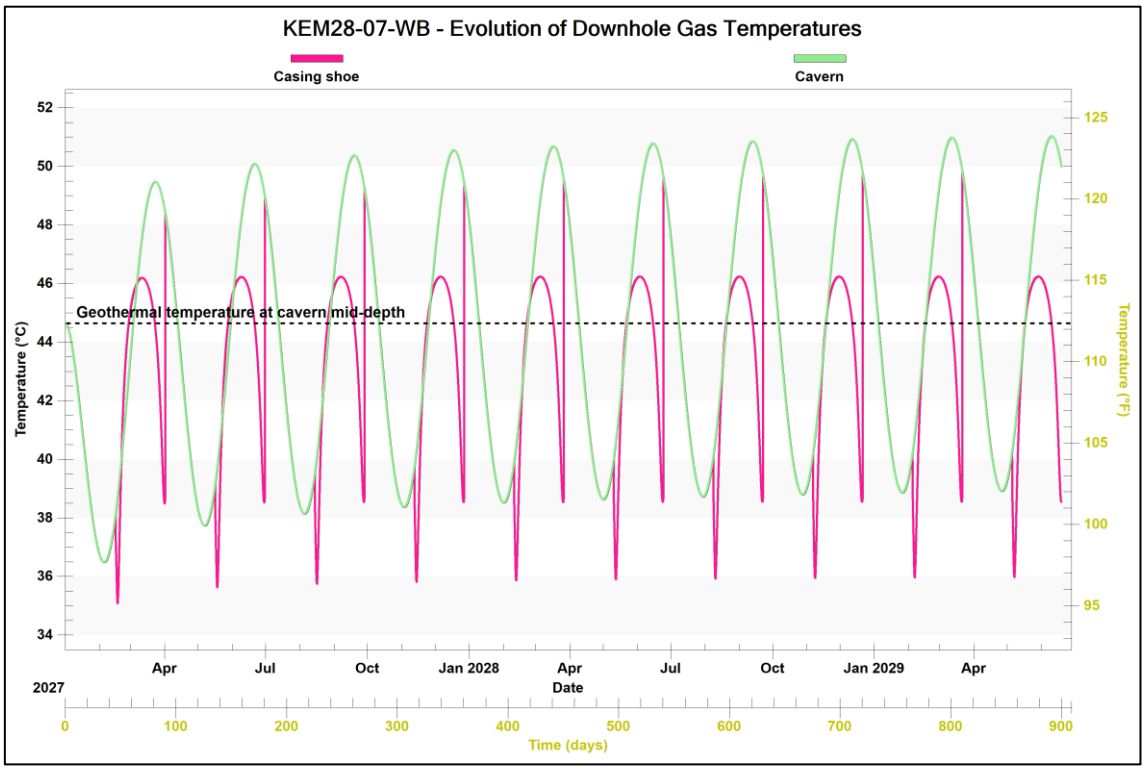

Figure 183. Wellbore modeling - Reference Case – Evolution of cavern and casing-shoe temperature.

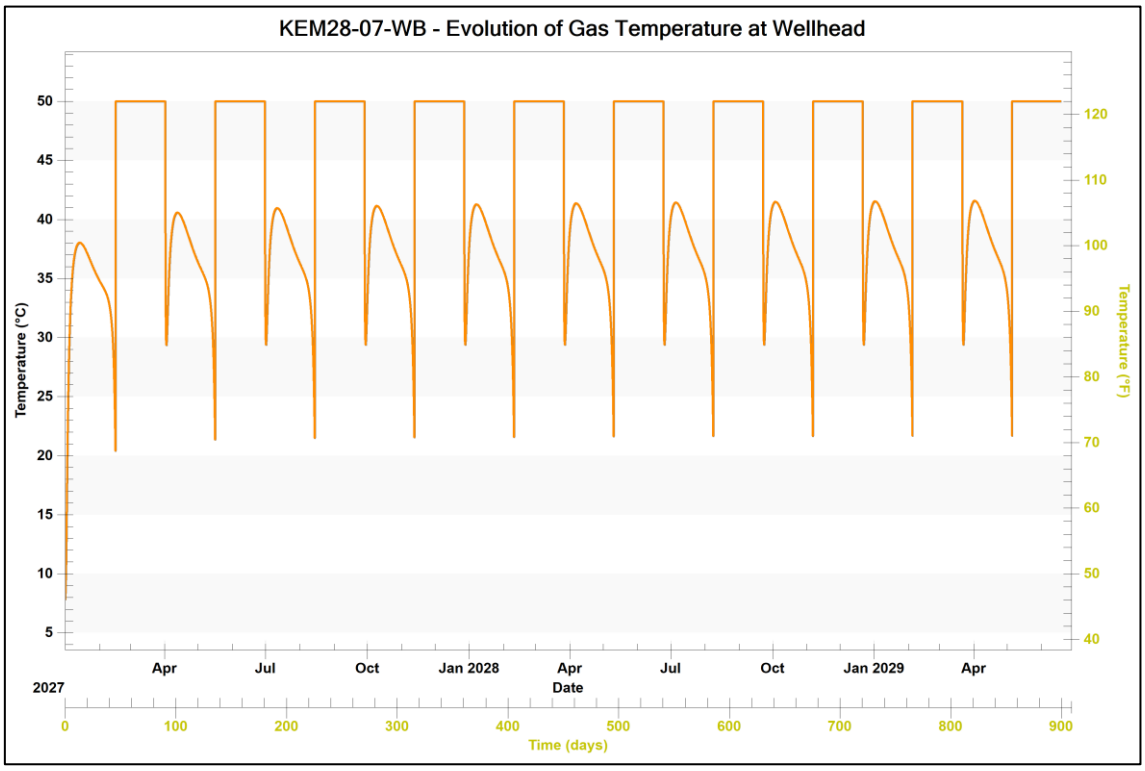

Figure 184. Wellbore modeling - Reference Case – Evolution of wellhead temperature.

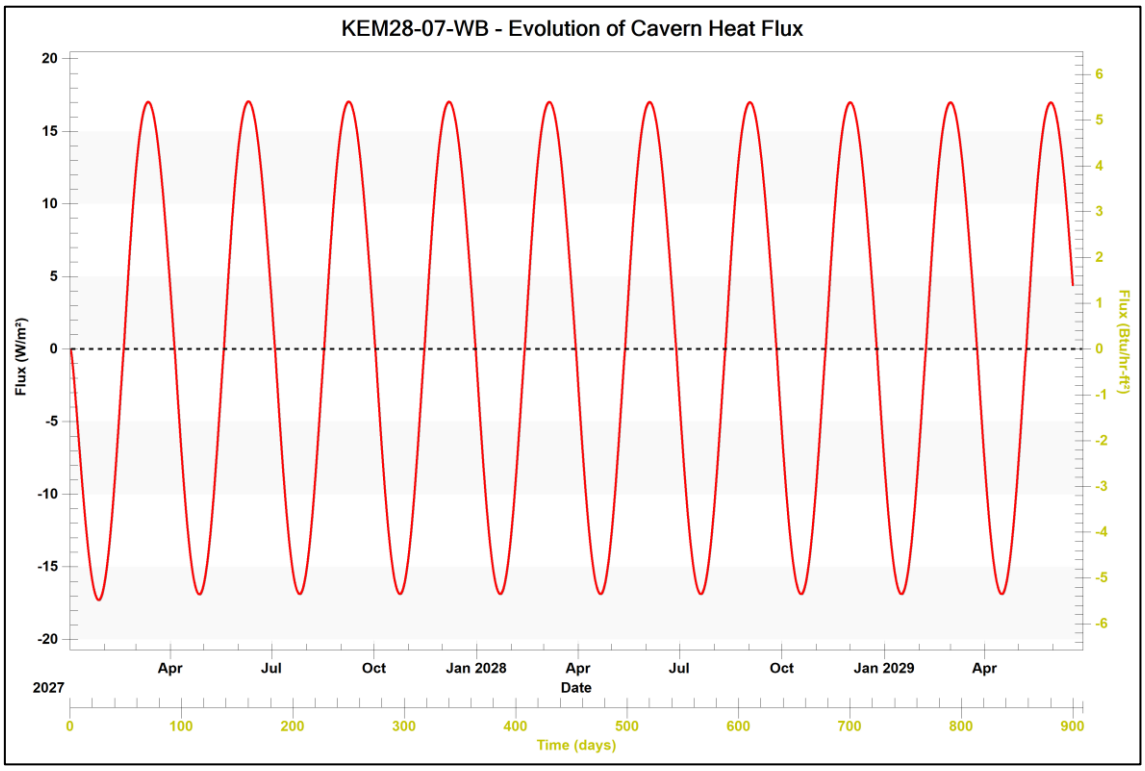

Figure 185. Wellbore modeling - Reference Case – Evolution of heat flux q_{th} at cavern wall.

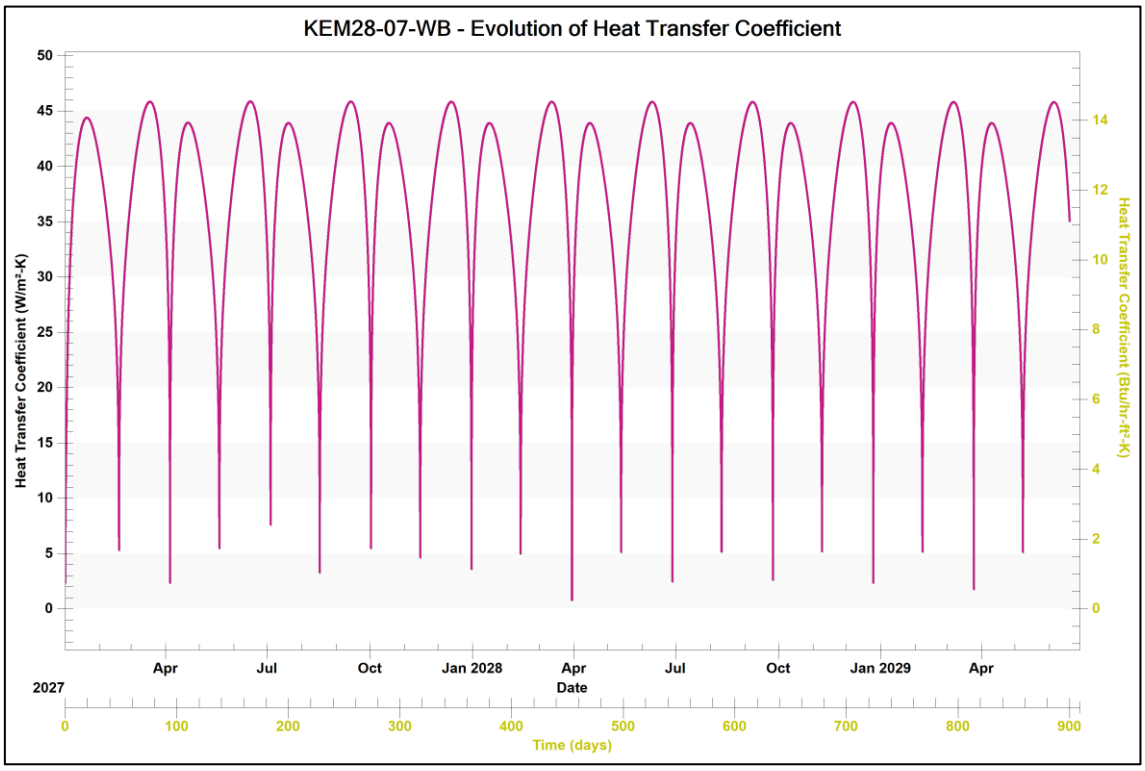

Figure 186. Wellbore modeling - Reference Case – Evolution of heat transfer coefficient h.

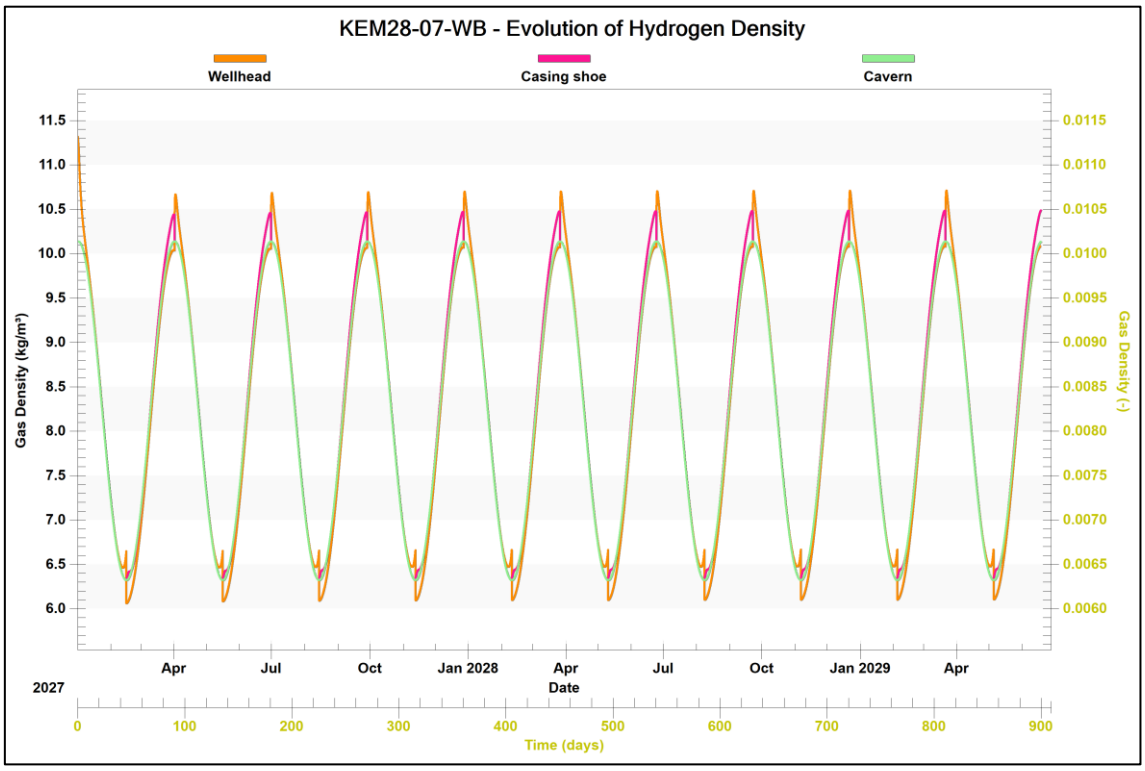

Figure 187. Wellbore modeling - Reference Case – Evolution hydrogen density at wellhead, at casing shoe and in the cavern.

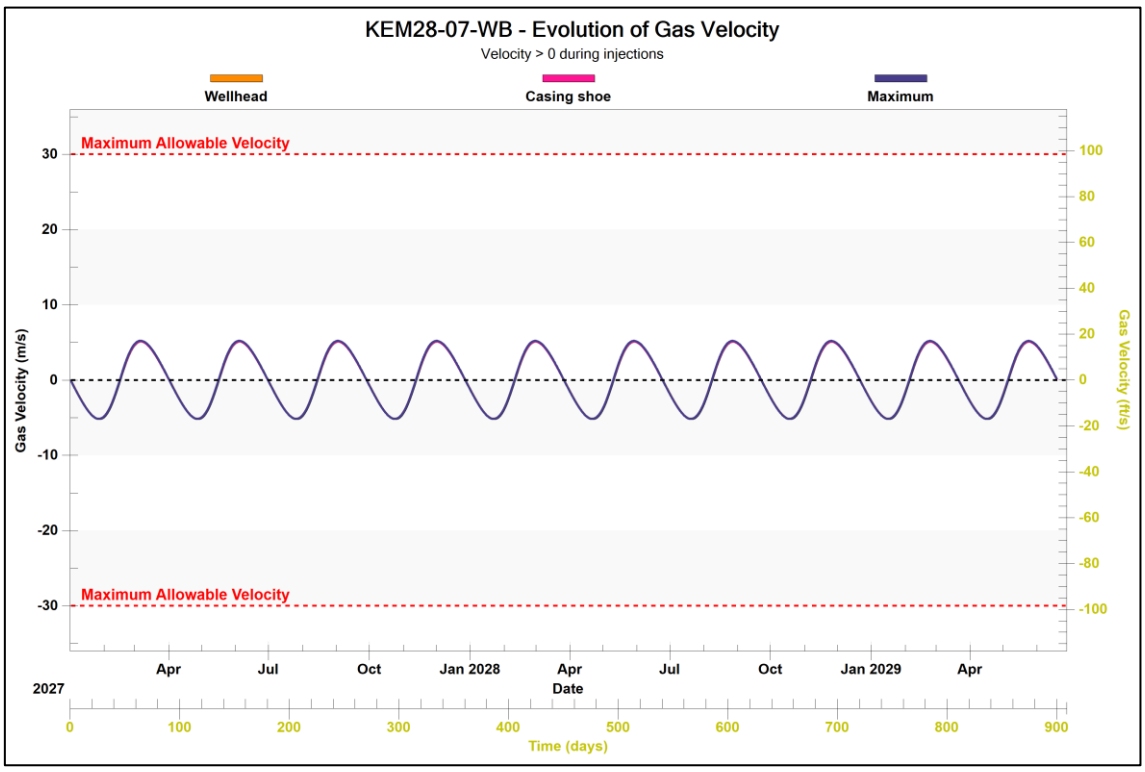

Figure 188. Wellbore modeling - Reference Case – Evolution hydrogen velocity in the wellbore. This velocity is still well below the 30 m/s limit often considered to limit the effects of erosion.

1.7 Creation of parametrized 2D finite element models of hydrogen caverns

1.7.1 Introduction

Various 2D axisymmetric finite element models of a cavern were created so that a sensitivity study could be carried out, focusing in particular on the geometric characteristics.

1.7.2 Boundary conditions

In the simulations carried out, isothermal boundaries are assumed for all outer boundaries of the model. Geostatic pressure is applied to each side of the model and vertical displacements are blocked at the bottom (Figure 189).

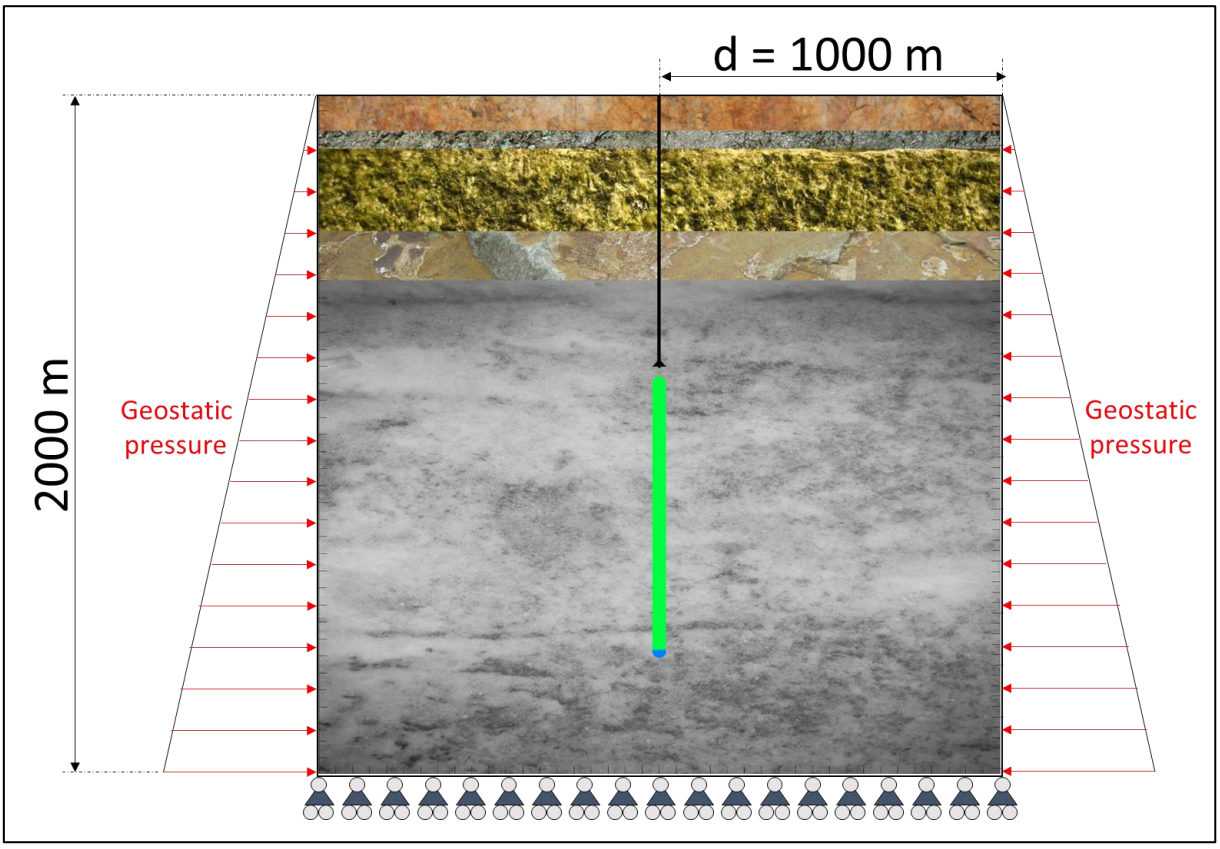

Figure 189. Boundary conditions. Geostatic pressure is applied to the lateral edges of the model and vertical displacement is blocked at the lower edge.

1.7.3 Meshing

For all 2D models, the edge of the mesh domain is located at a distance of 1 km from the cavern axis. Meshing is of upmost importance when performing numerical computations; it is very important to have small elements on the cavern wall, of the order of a few dozen cm maximum, because the temperature gradients can be large at this location, and we are trying to highlight skin effects (Brouard et al., 2011). This is why it is much easier to analyse the stability of the cavern wall in 2D, as a 3D mesh with very small elements is difficult to handle (mesh with too many elements and calculations can be extremely long).

Figure 190 to Figure 192 show the mesh used in the reference case (Case #07 of the sensitivity analysis). The maximum size of the elements is 20 cm, along the chimney (between the casing shoe and the roof of the cavern) and along the entire wall of the cavern.

1.7.4 Loading

In 2D finite element calculations, a cyclic evolution of the hydrogen pressure in the cavern is imposed and LOCAS calculates the evolution of temperatures and stresses.

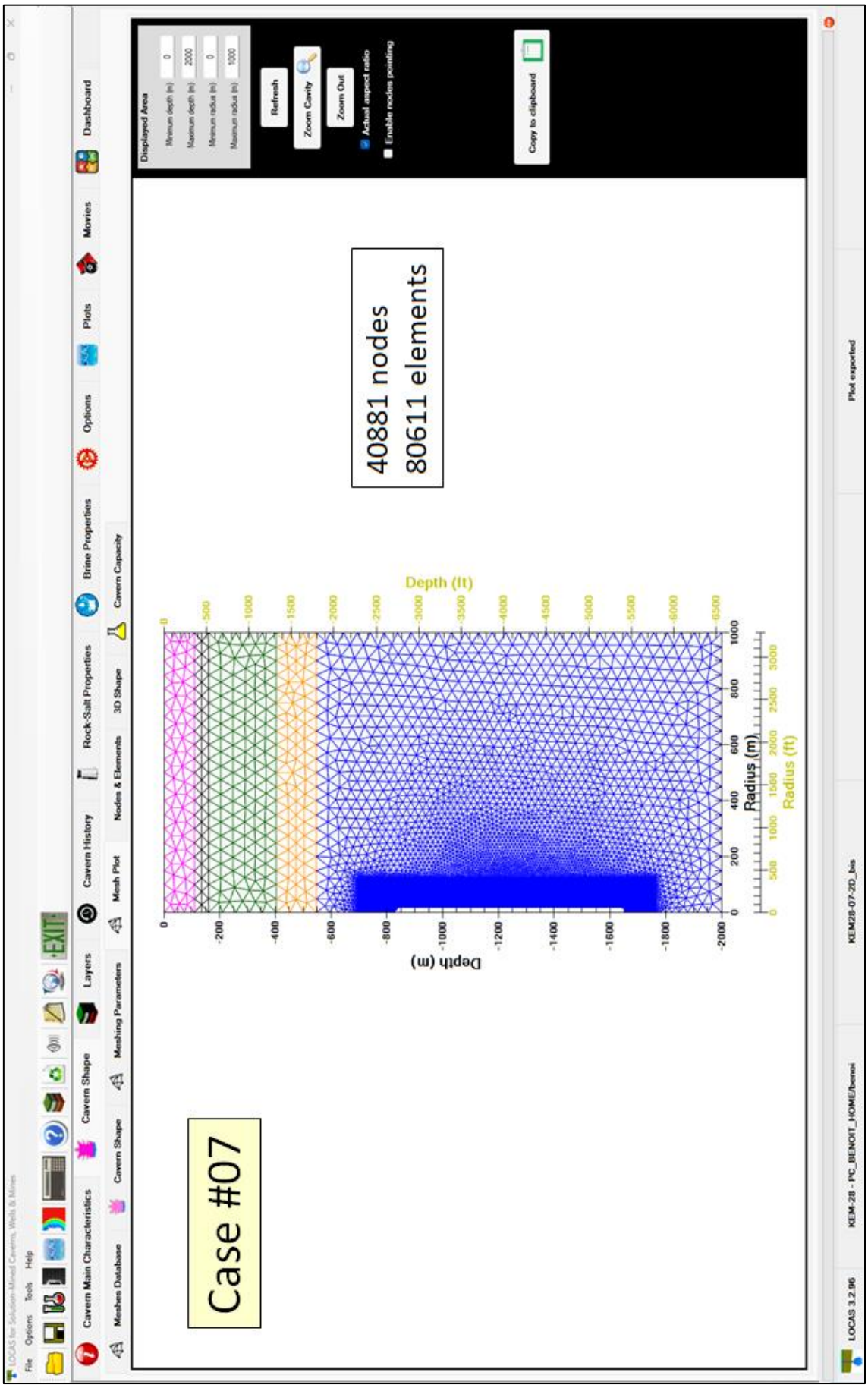

Figure 190. 2D Mesh for the reference case. It is necessary to use a very fine mesh for calculations involving gas storage caverns because the temperature and stress gradients are large at the wall.

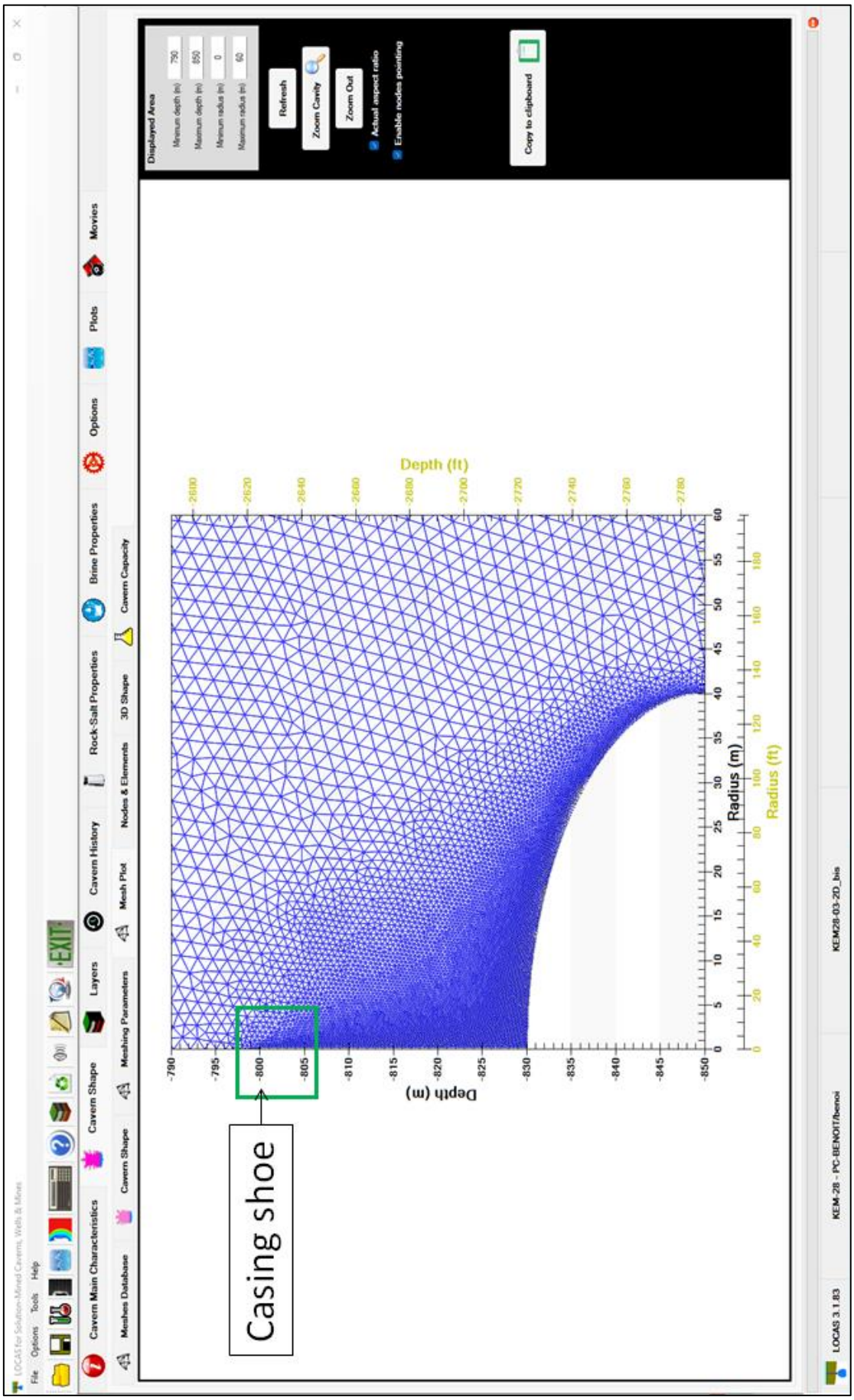

Figure 191. Mesh example, zoom near the cavern roof.

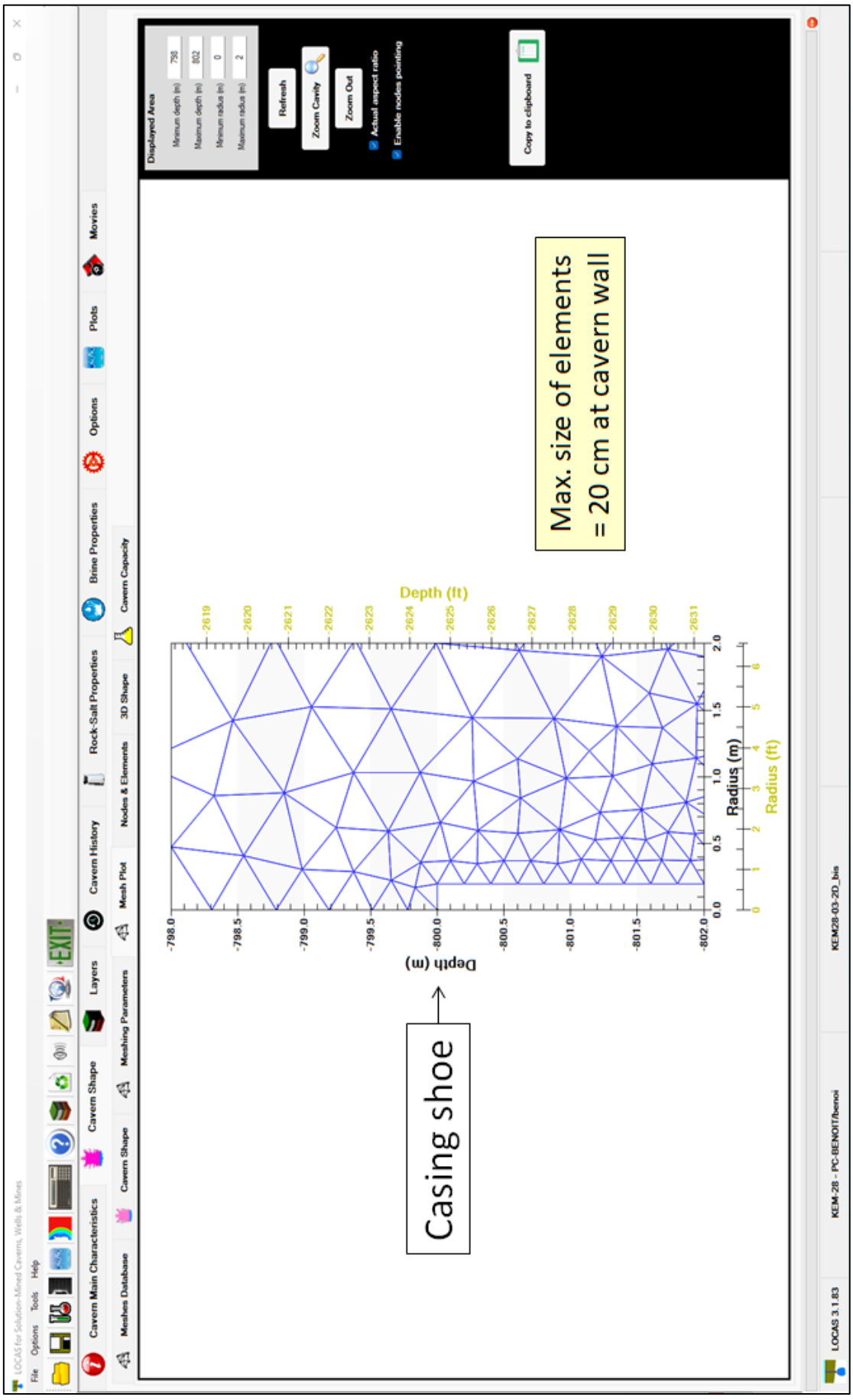

Figure 192. Mesh example, zoom at the top of the chimney. The maximum size of the elements on the wall is 20 cm.

1.7.5 Computation outcomes

Main outcomes of wellbore and cavern model computations are shown in Figure 193. The following is a list of the results that have been compiled for each of the cases in the sensitivity analysis.

❖ **From the wellbore modeling:**

Pressures

- Evolution of hydrogen pressure in the cavern (barg)
- Evolution of pressure and pressure gradient at casing shoe (barg and bar/m)
- Evolution of pressure losses along the production casing (bar)
- Evolution of hydrogen pressure at the wellhead (barg)
- Evolution of hydrogen-pressure rate at the casing shoe (bar/day)

Temperature and heat flux

- Evolution of hydrogen temperature in the cavern and at the casing shoe (°C)
- Evolution of hydrogen temperature at the wellhead (°C)
- Evolution of heat flux q_{th} (W/m²)
- Evolution of heat transfer coefficient$h$at cavern wall (W/m²-K)

Hydrogen properties

- Evolution of hydrogen mass (Mkg)
- Evolution of hydrogen density at wellhead, casing shoe and in the cavern (kg/m^3)
- Evolution of hydrogen velocity at wellhead, casing shoe and maximum along the casing (m/s)

❖ **From the 2D finite element cavern modelling:**

Pressures

- Evolution of pressure at casing shoe from the start of leaching (barg)
- Evolution of hydrogen and brine temperature in the cavern from the start of leaching (°C)

Creep closure and subsidence

- Evolution of cavern-volume loss after the end of leaching (m^3)
- Evolution of subsidence at ground level on cavern axis after the end of leaching (mm)

Powers and energies

- Evolution of heat flux through conduction to the cavern from the start of leaching (MW)
- Evolution of cumulated heat energy P_{th} after the start of debrining (MWh)
- Evolution of developed powers (P_{mec}, P_{ent}, P_{th}) after the start of debrining (MW)
- Evolution of cumulated energies ($E_{mec}, E_{ent}, E_{th}, E_{int}$) after the start of debrining (MWh)

1.7.6 Outputs

For all calculations, pressure is imposed and important moments in history (called “outputs”) are predefined for which LOCAS records the state of stress in order to plot contours and analyse mechanical stability. For example, Figure 194 shows the evolution of the pressure imposed in the reference case. Output #1 corresponds to the end of leaching, Output #3 is at the start of debrining, Output #4 is at the end of debrining. During cycling, outputs with an even number (from 4 to 24 in this case) correspond to the moment when the pressure is maximum, and outputs with an odd number (from 5 to 23 in this case) correspond to the moment when the pressure is minimum.

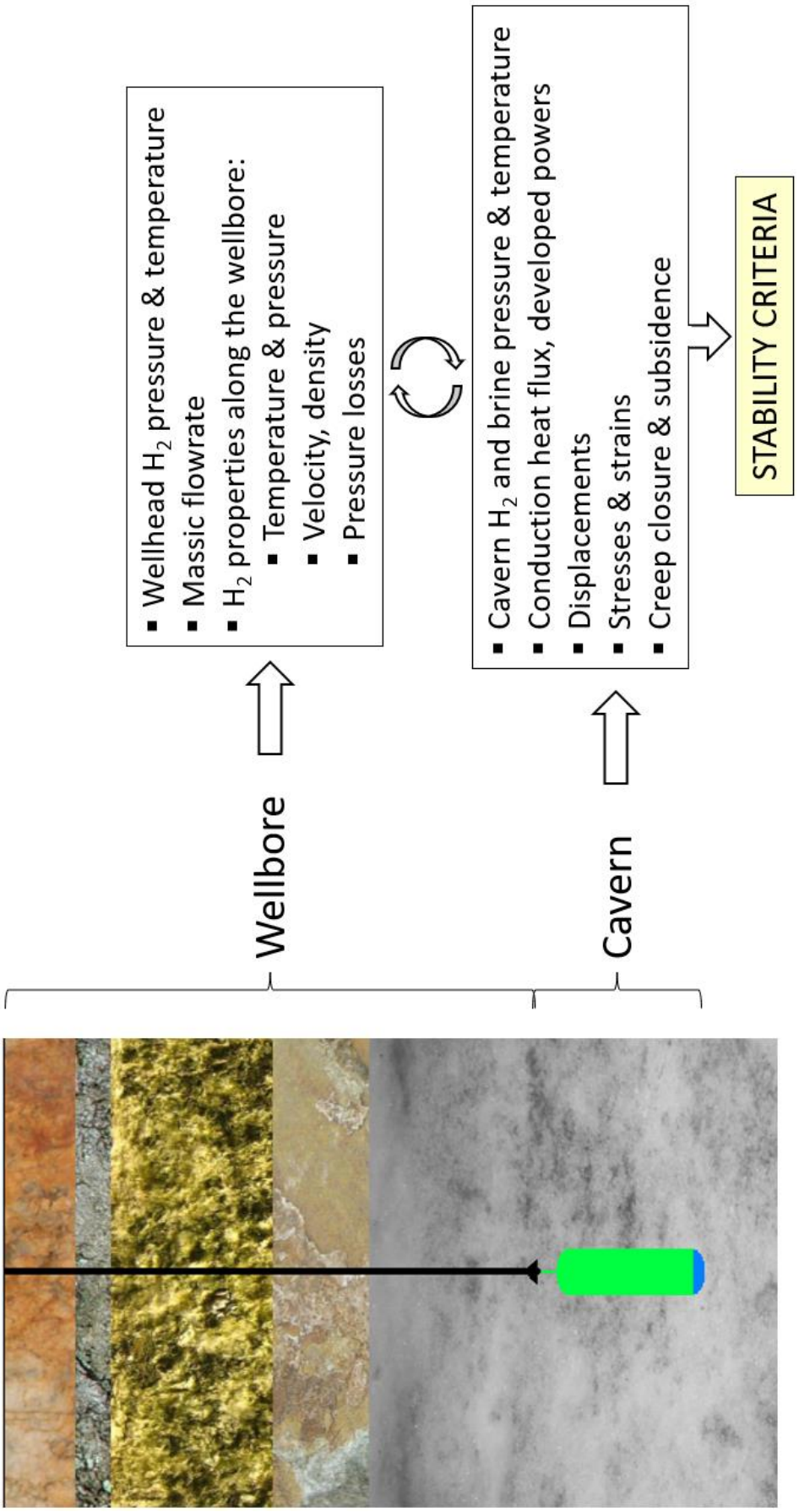

Figure 193. Outcomes from wellbore and cavern modelling. LOCAS can be used to calculate both the thermodynamic variables of hydrogen, in time and space, and also the temperature and stresses in the surrounding rock mass.

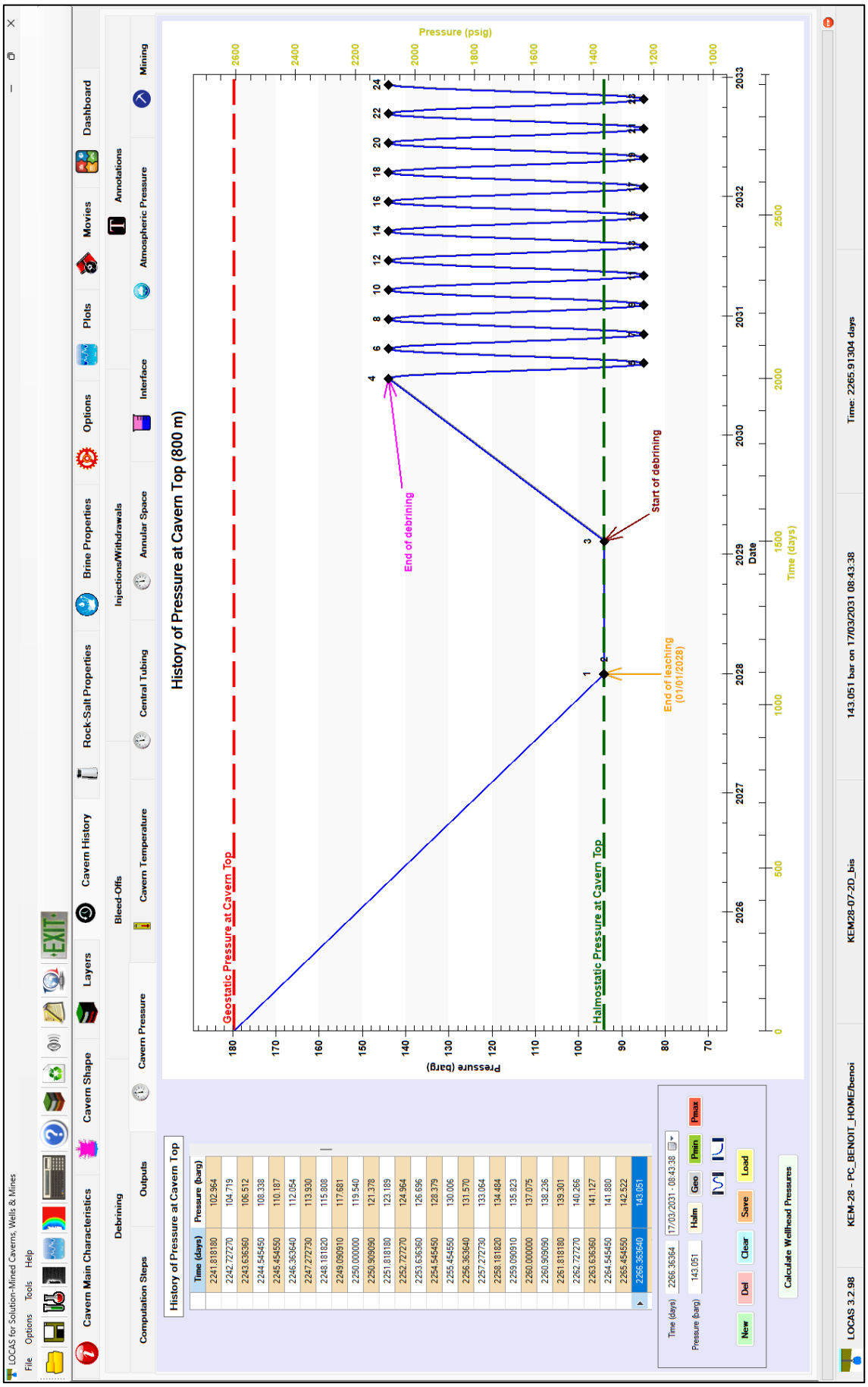

Figure 194. 2D finite element model. Evolution of cavern pressure, 24 outputs are predefined. A linear decrease in cavern pressure is considered during leaching, followed by a waiting phase at constant pressure (halmostatic), then the first filling with hydrogen (debrining) and the cyclic operations.

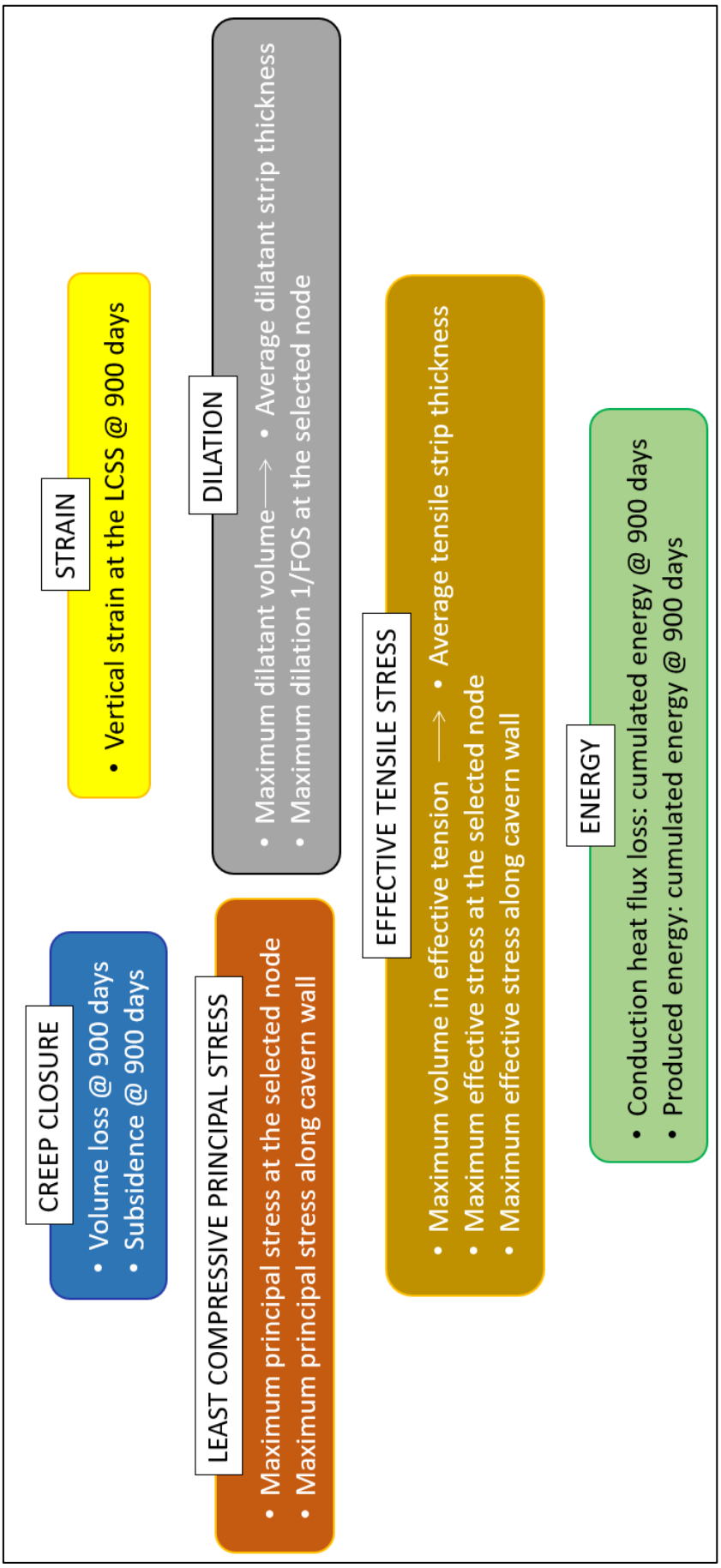

Figure 195. Indicators related to cavern stability. These indicators concern the loss of volume of the cavern, the vertical deformation at the shoe of the last cemented casing, the possible occurrence of effective tensile stresses or dilation, and also two indicators related to energy efficiency.

1.7.7 Evolution at a particular point on the wall

With LOCAS, it is possible to follow the evolution of parameters at a particular point; it is particularly interesting to select a point on the wall of the cavern (a node from the mesh) to better understand what is happening during cycling. We generally select a point on the wall located in the vertical part of the upper part of the cavern, below the arched section.

1.7.8 Evolution along the wall

At any time defined by the outputs, we can plot the stress distribution along the wall, starting at the casing shoe and extending along the axis to the bottom of the cavern.

1.7.9 Analysis of cavern stability

Figure 195 shows the indicators related to cavern stability that are considered in this study. There are 14 indicators divided into 6 groups, which are described in the following sections.

1.7.9.1 Creep closure

The progressive closure of the cavern under the effect of creep is an important indicator of cavern stability that should be minimised, as should the associated subsidence. In order to be able to compare the different cases taken into account in the sensitivity analysis (see Section 1.8), the loss of cavern volume and maximum subsidence after 900 days of cycling were considered.

1.7.9.2 Strain

With regard to the risk of overstretching, the vertical strain ε_{zz} at the LCCS after 900 days of cycling is considered as an indicator.

1.7.9.3 Least compressive principal stress

By plotting the Evolution of the least compressive principal stress (called σ_{max} for "Maximum principal stress" in this report) at the selected node, we select its maximum value as an indicator. For all outputs, the maximum value of σ_{max} along the wall is also considered as an indicator.

1.7.9.4 Effective tensile stress

As described in section 1.5.8, the effective stress is defined as the sum of the least compressive principal stress and the hydrogen pressure in the cavern at the same depth. As for the previous least compressive principal stress, one indicator corresponds to the maximum value reached during the cycling at the selected node, and another indicator corresponds to the maximum value reached along the wall for all the outputs considered (maximum and minimum hydrogen pressures). An additional indicator is defined by the total volume under effective tension around the cavern ($\sigma_{\max} + P_c > 0$). From this volume in tension, an “average tensile strip thickness” can be calculated by dividing the volume in tension by the surface area of the cavern wall.

1.7.9.5 Onset of dilation

The criterion for the occurrence of dilatancy depends essentially on the stress distribution at a given time. A rapid change in pressure in the cavern will instantly change the elastic distribution, as will any change in cavern temperature, which will create additional thermoelastic stresses near the cavern wall. The Respec criterion (RD Criterion) for the appearance of dilatancy is taken into account. This criterion has two branches depending on whether the state of stress is compressive or extensive (Figure 196). This criterion is described in more detail in Appendix B: Salt Dilation Criteria. As for the volume under effective tension, the total dilatant volume is considered as an indicator, and an “average dilatant strip thickness” is calculated. In addition, the maximum value of 1/FOS, where FOS is the *Factor of Safety*, reached during the cycling at the selected node at the cavern wall is another indicator.

1.7.9.6 Energy

The last two criteria relate to energy considerations. We will see that in all the cases considered in the sensitivity analysis, on average, heat is transferred from the cavern to the surrounding salt. A first energy indicator corresponds to the total heat lost after 900 days of cycling (a value that should be minimised). A second indicator corresponds to the cumulative energy after 900 days that was produced by the cavern during the production phases (hydrogen withdrawals).

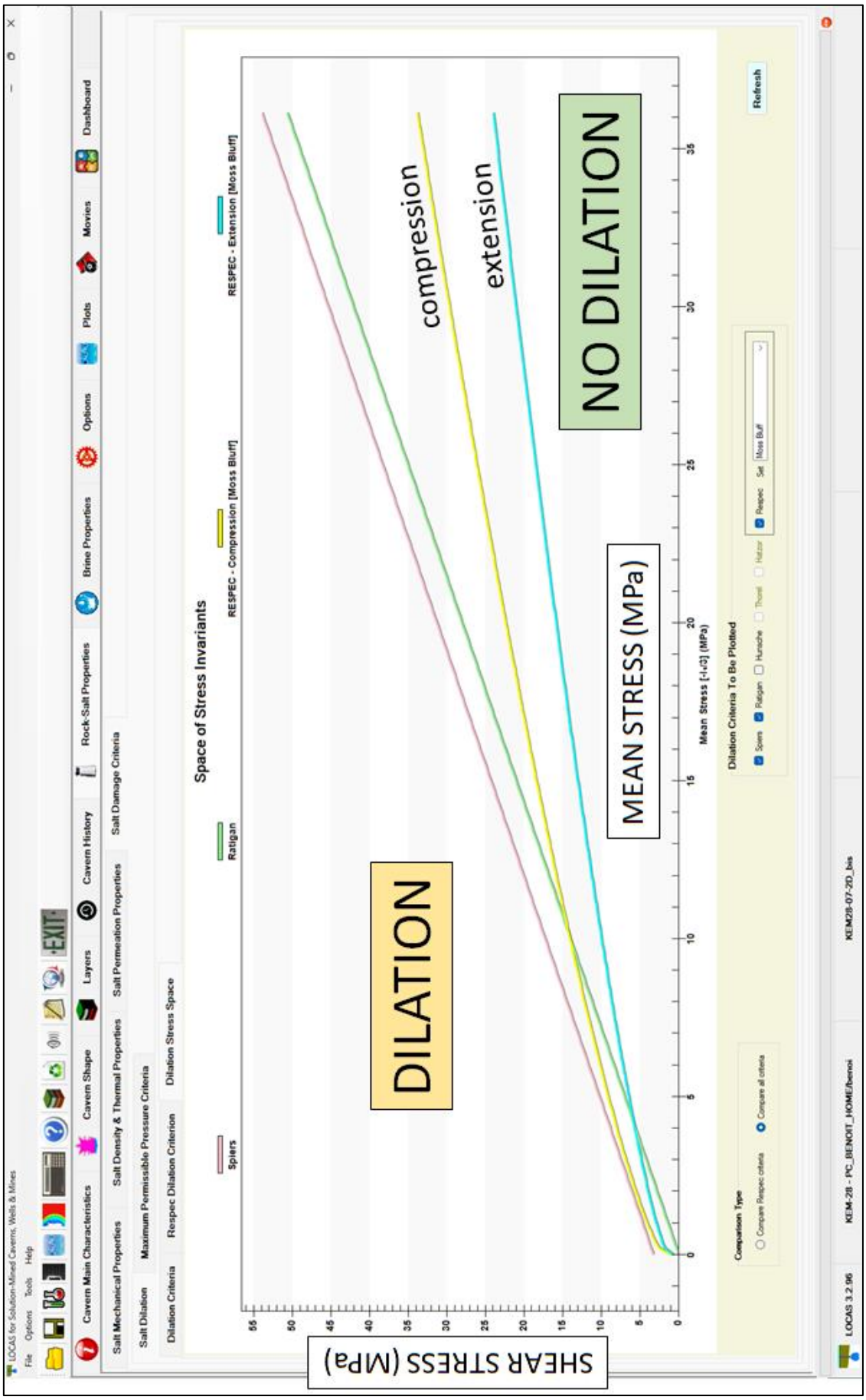

Figure 196. Dilation criteria in the space of stress invariants: shear stress as a function of mean stress. The salt can be damaged by dilation if the shear stress is high compared to the average stress. The selected RD criterion can be used to distinguish between compressive and extensive state of stress.

1.8 FEM cavern modelling – Reference case

1.8.1 Introduction

This chapter describes the results of the 2D finite element calculation carried out in the reference case (Case #07 in the sensitivity analysis presented later in this report).

1.8.2 Trends over time

Figure 197 shows the change in pressure at the shoe of the last cemented casing at a depth of 800 m. The leaching phase is expected to take 3 years to reach a final volume of just over 1 million m^3. This is followed by a standby phase of 400 days at constant pressure, corresponding to the time needed to set up the surface facilities and carry out preliminary integrity tests, before the first hydrogen fill. It was assumed that the first hydrogen filling would last 500 days, which is a long time compared to conventional natural gas first filling, but green hydrogen is supposed to be produced by renewable energy sources (solar panels, wind turbines) that cannot produce high flow rates continuously. The pressure in the cavern is then assumed to cycle between maximum and minimum pressure for 10 cycles of 90 days each.

Figure 198 shows the changes in the temperature of the hydrogen and the residual brine at the bottom of the cavern between the end of leaching and the end of the 10 cycles. It has been assumed that the temperature of the brine in the cavern is 30 °C at the end of the leaching process. The geothermal temperature at the average depth of the cavern (1227.5 m) is 44.6 °C, so the brine heats up gradually as soon as leaching is complete. This heating is slow because the cavern is very large. Oscillations in the temperature of the hydrogen during cycling have an amplitude of around twelve degrees. A drift can be observed that causes the average temperature to tend towards an intermediate temperature between the geothermal temperature at the average depth of the cavern (44.6 °C) and the hydrogen injection temperature (50 °C). It is interesting to note that the minimum/maximum temperature of hydrogen does not correspond to the minimum/maximum pressure, this is because the heat flux reverses before reaching the extremes.

Figure 199 shows the evolution of the heat flux exchanged between the cavern and the salt. The time lag between the heat flow and the minimum/maximum hydrogen pressure is clearly visible.

Figure 200 shows the cumulative heat lost to the salt formation since the start of debrining. In this case, the corresponding indicator for the sensitivity study is that the heat loss is 7900 MWh in 900 days.

The evolution of the mass of hydrogen in the cavern is shown in Figure 201.

The evolution of cavern volume loss and loss rate since the end of leaching is shown in Figure 202. In this case, the indicator for the volume loss after 900 days of cycling is 30 831 m^3 (loss calculated since the end of leaching). Figure 203 shows the displacement vectors in the vicinity of the selected node (100 m depth) at the last minimum pressure. The amplification coefficient is 10. Wall displacements are mainly radial at this vertical wall.

Figure 204 shows the changes in the various power levels developed during cycling (see Section 1.3.9 p°264). Figure 205 shows the corresponding energies (by integrating the previous powers with time).

Figure 206 shows the evolution of the energy produced by the cavern during the production phases. In this case, a cumulative total of 13.8 GWh was produced after the 10 cycles, giving an average power output of 0.64 MW.

Figure 207 shows the evolution of cushion gas, working gas and total storage capacity. In this case, the working hydrogen mass is 6100 tonnes, corresponding to the difference between the total storage capacity and the cushion gas capacity during the cycling period.

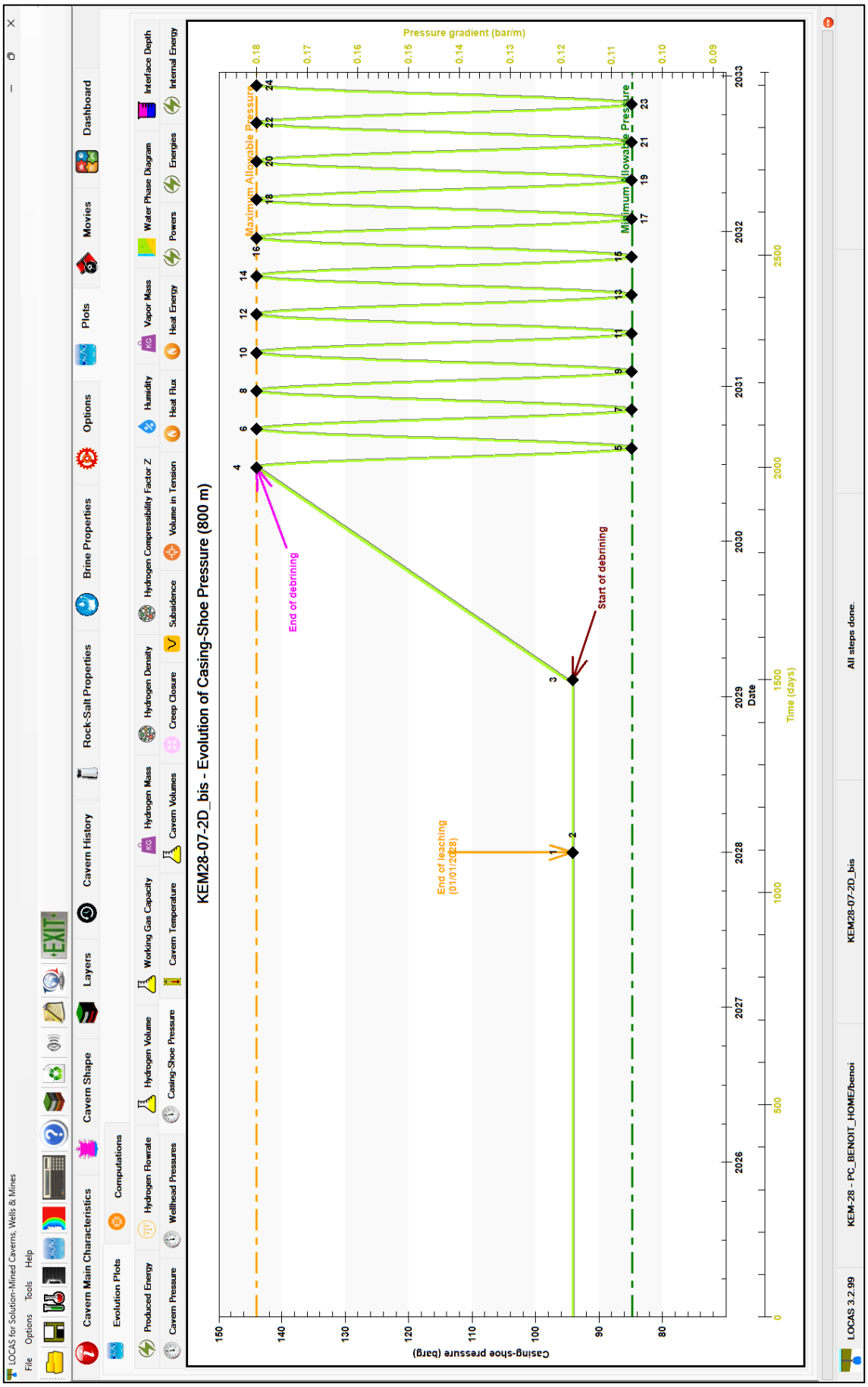

Figure 197. Reference Case – Evolution of pressure gradient at casing-shoe depth. We can check that the maximum pressure at the last cemented casing shoe corresponds to a gradient below the legal limit in the Netherlands of 0.18 bar/m.

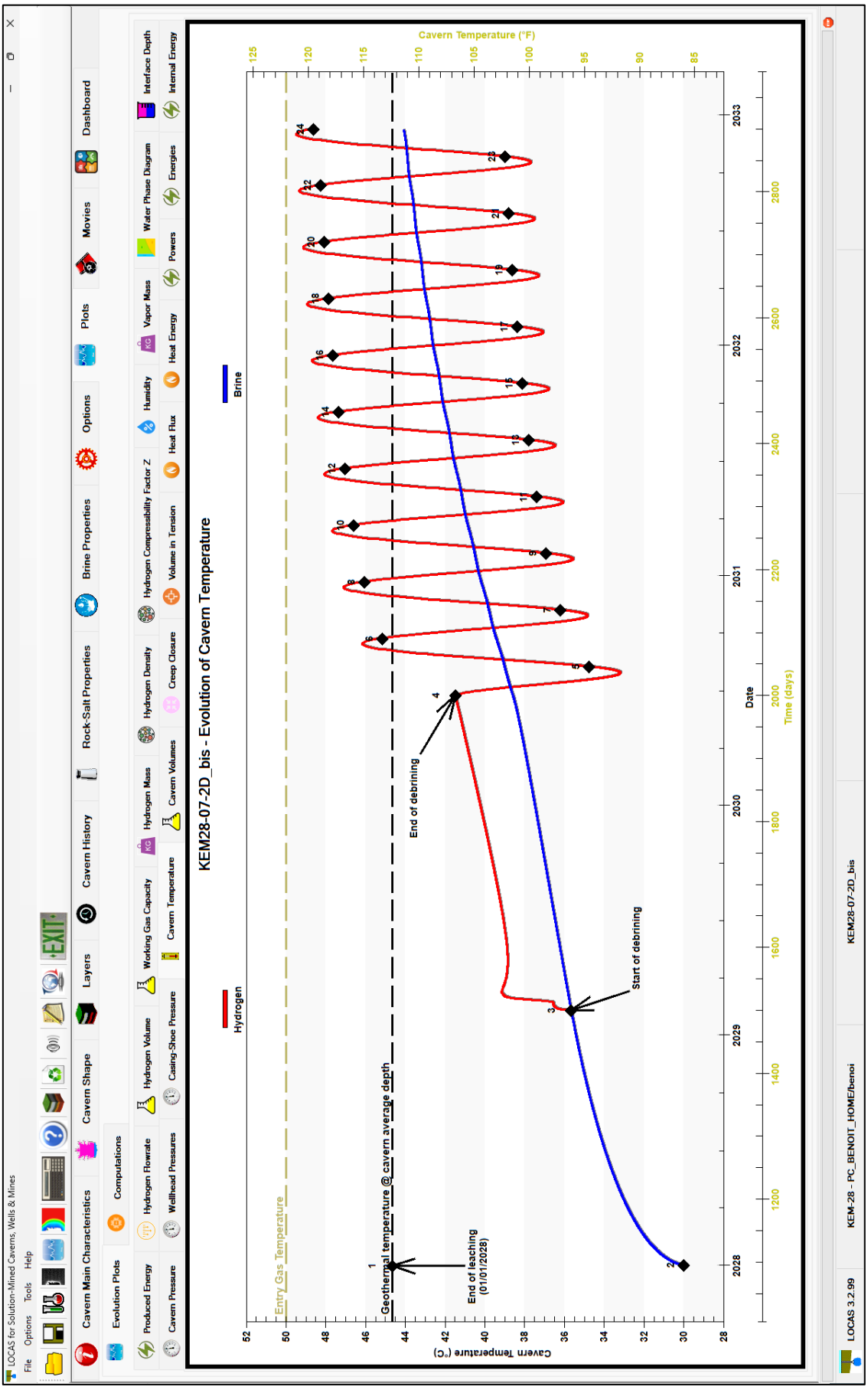

Figure 198. Reference Case – Evolution of hydrogen and brine temperature in the cavern. The temperature of the hydrogen varies by more than ten degrees during the cycles. The brine at the bottom of the cavern has a greater thermal inertia than hydrogen and, its long-term temperature tends to be intermediate between the geothermal temperature at mid-depth and the hydrogen injection temperature.

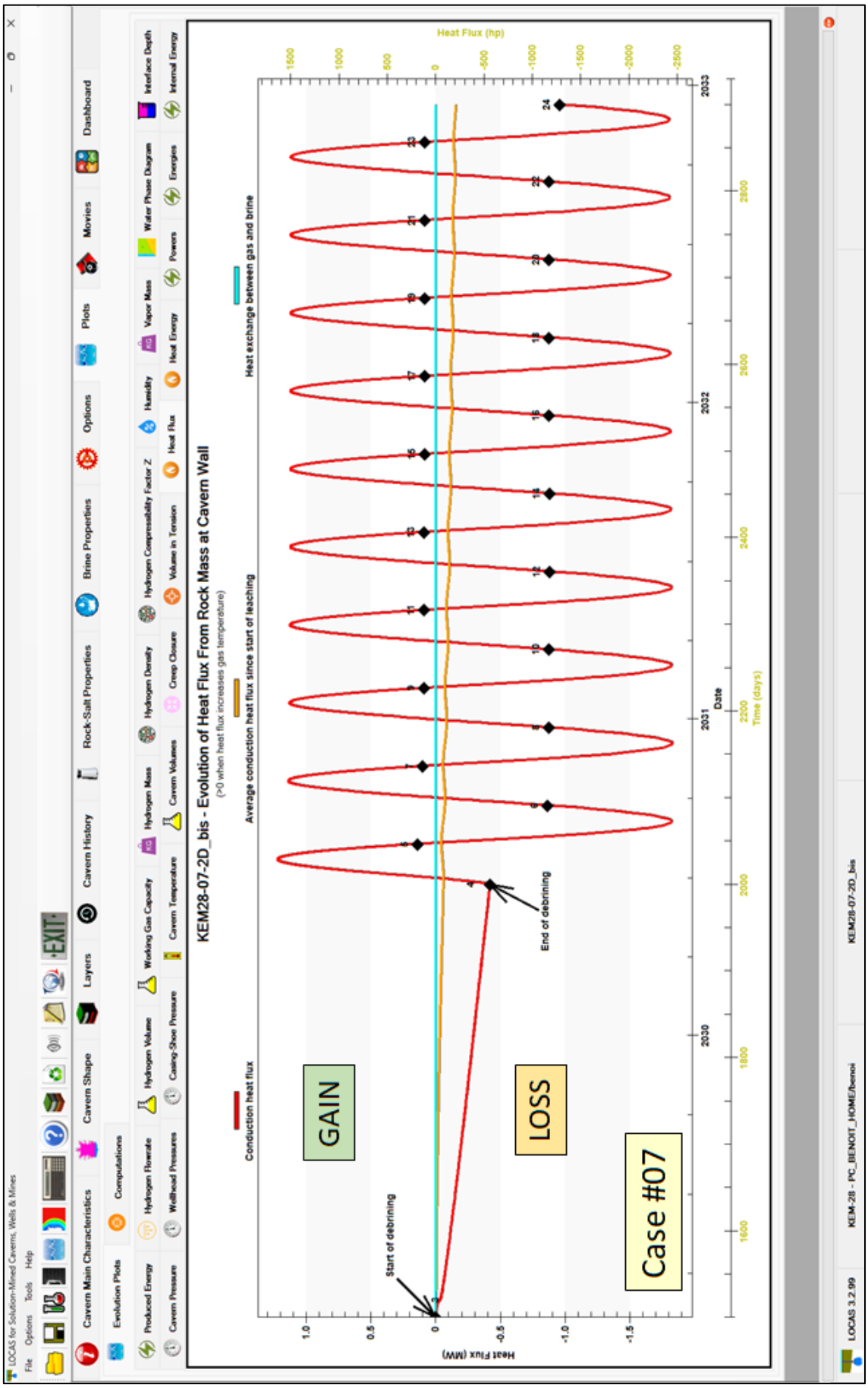

Figure 199. Reference Case – Evolution of the conduction heat flux at cavern wall. When the conduction flux is negative, this means that heat is transferred from the cavern to the salt because the temperature of the hydrogen is higher than that of the salt.

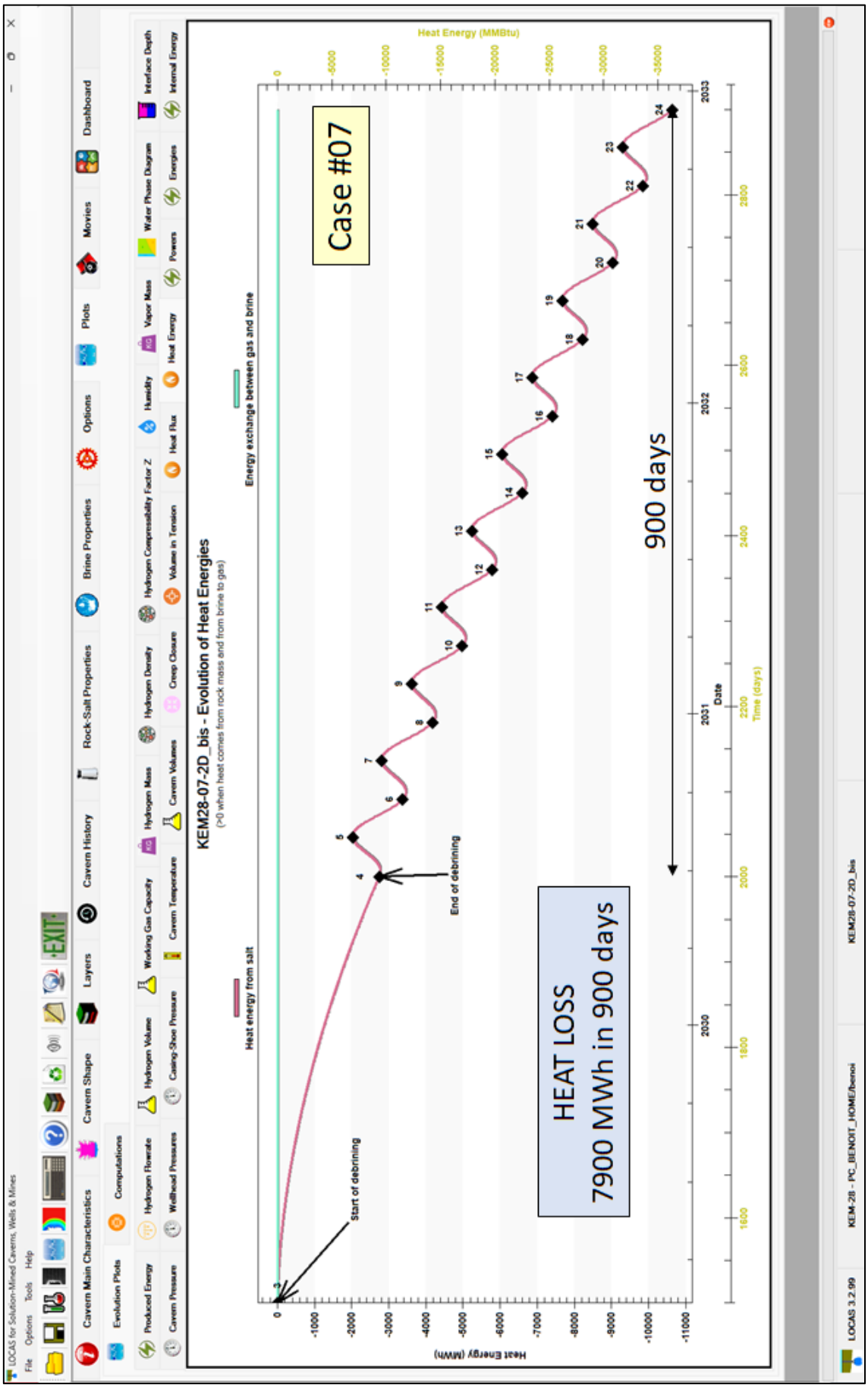

Figure 200. Reference Case – Evolution of the cumulated loss of heat since the start of debrining. Over the long term, heat is lost to the salt.

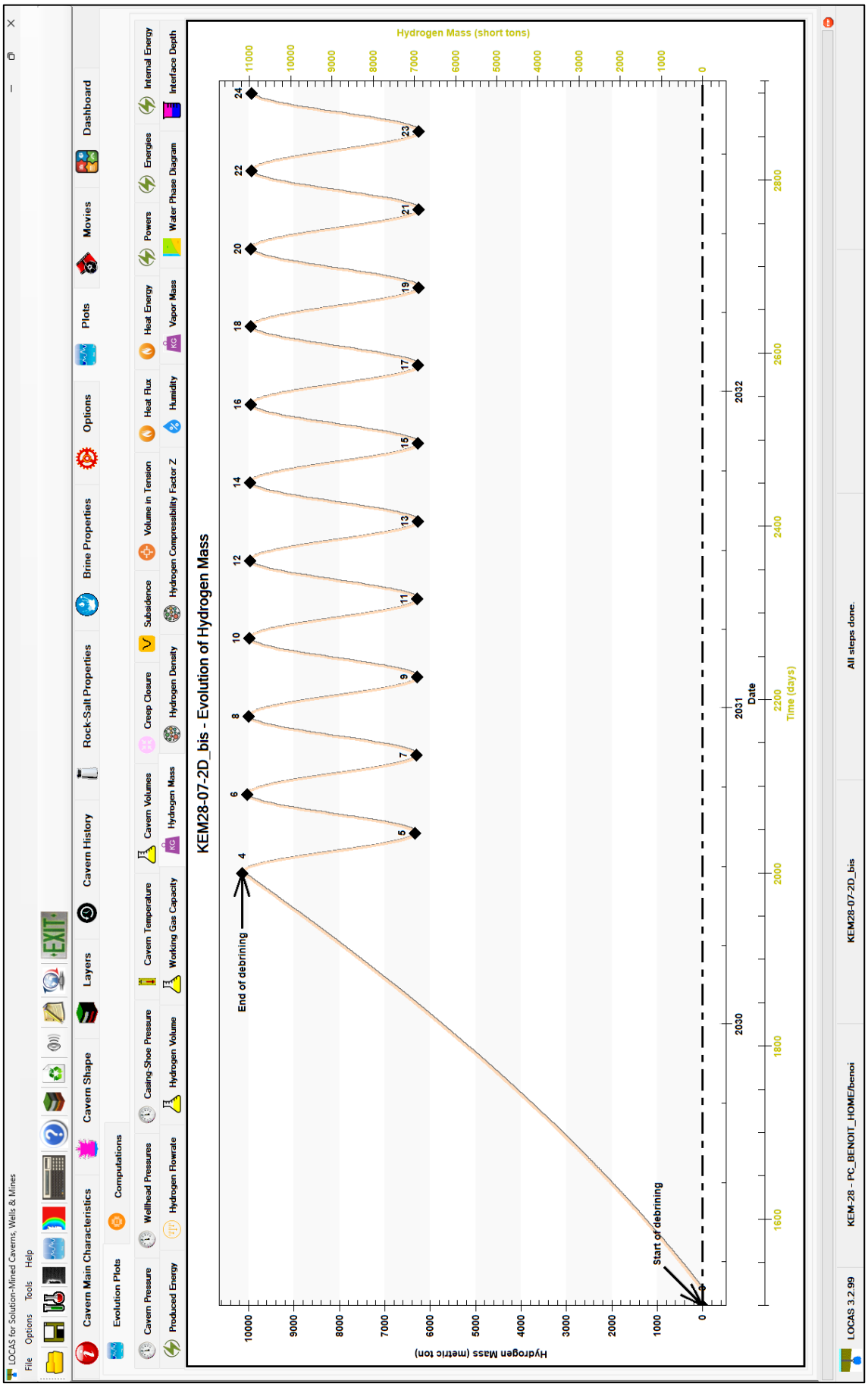

Figure 201. Reference Case – Evolution the mass of hydrogen in the cavern.

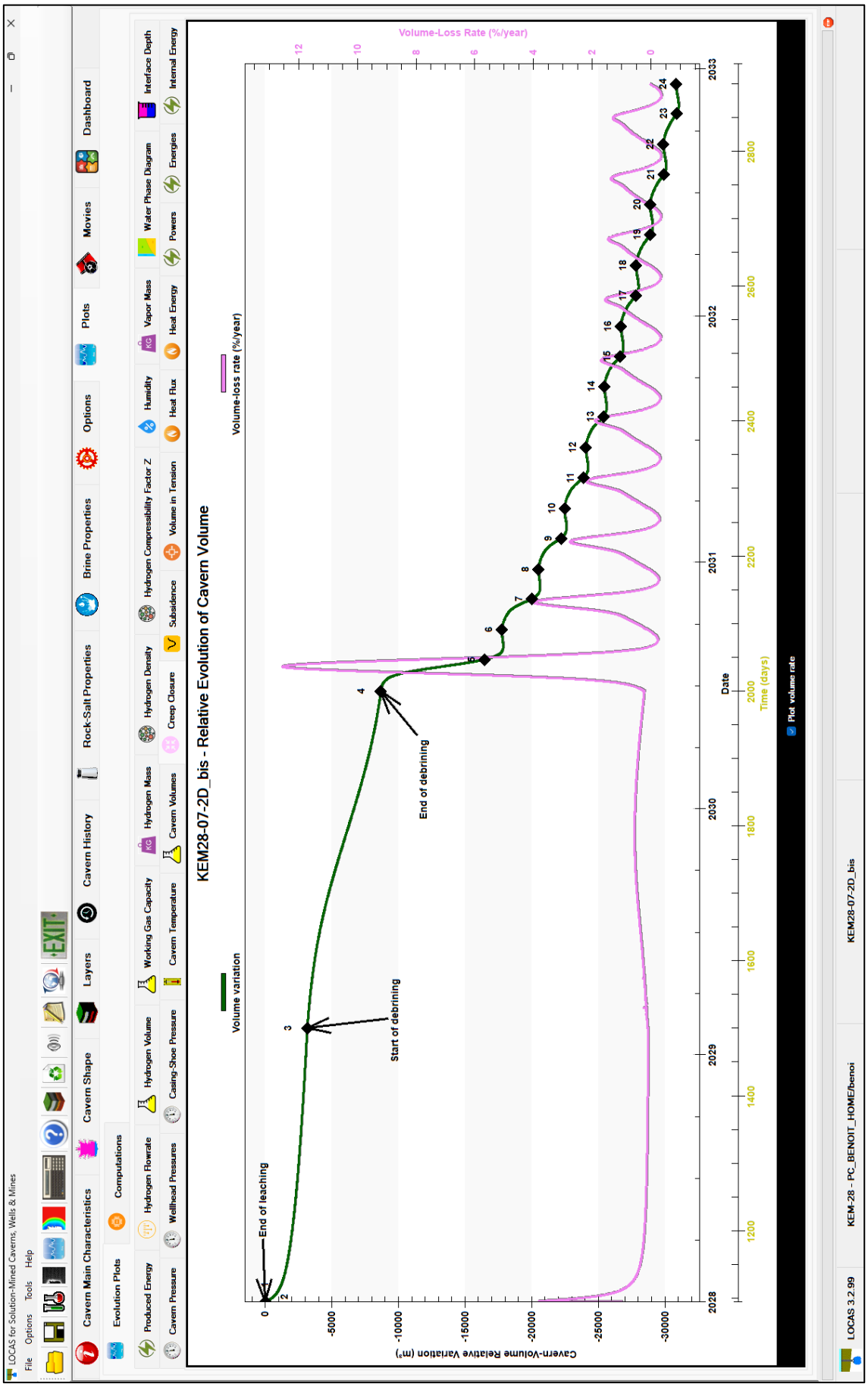

Figure 202. Reference Case – Evolution of cavern volume loss and loss rate since the end of leaching. A significant loss of volume occurs during the first production phase after debrining. Then rapidly a pseudo-stationary regime is reached with a relatively moderate rate of volume loss.

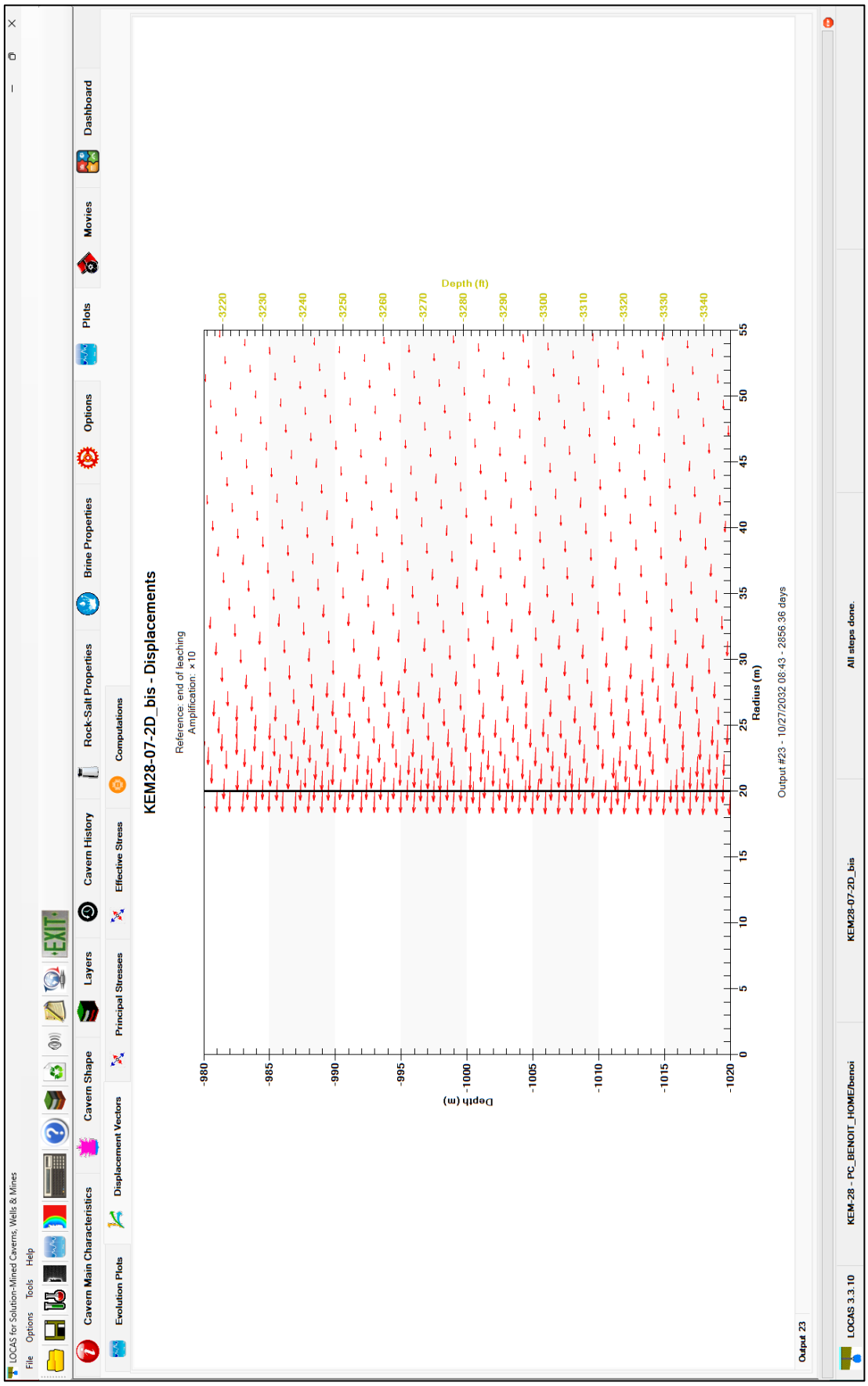

Figure 203. Displacement vectors in the vicinity of the selected node at the last minimum pressure (output #23) - The amplification coefficient is 10. On the vertical wall of the cavern, movement is mainly horizontal.

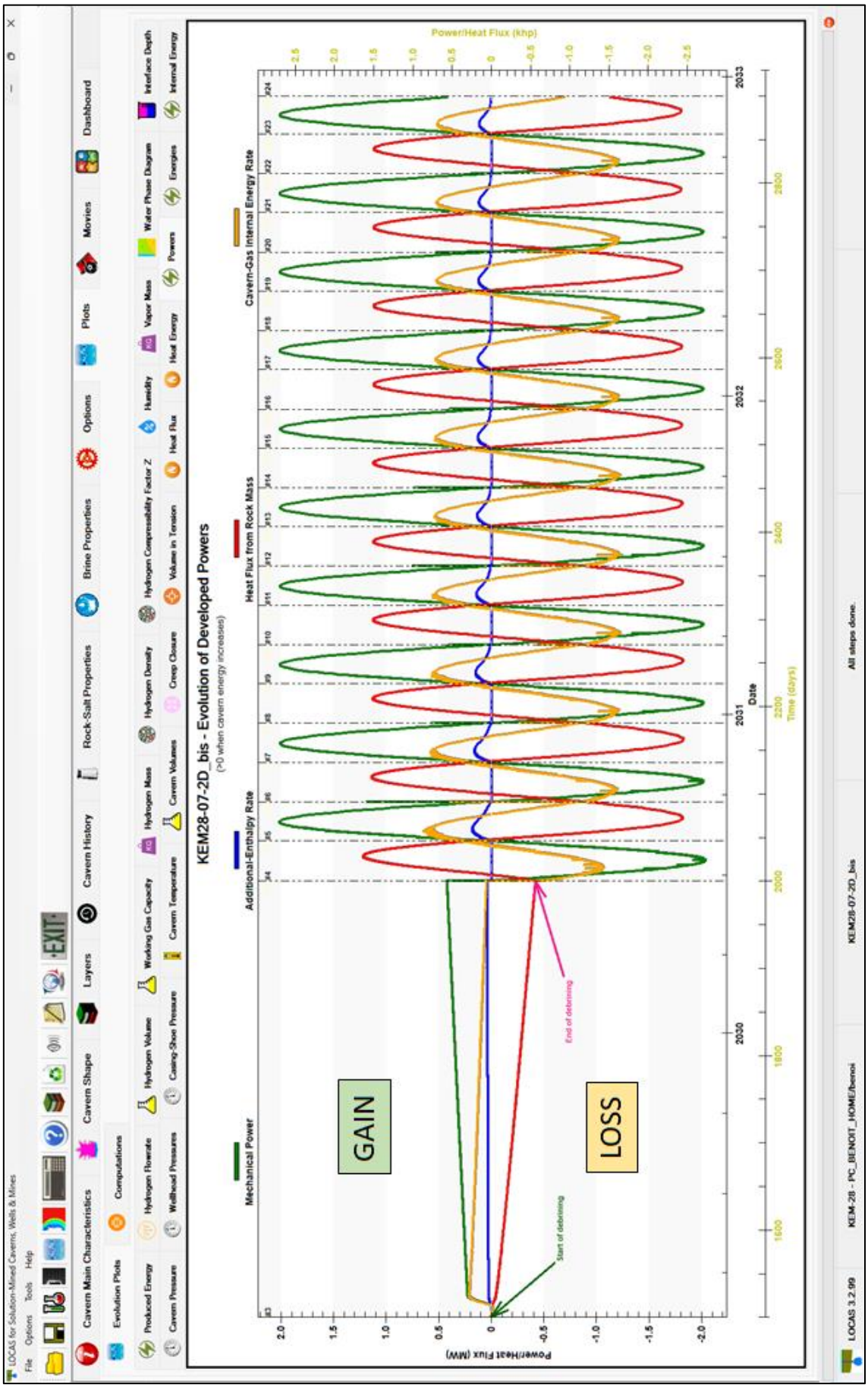

Figure 204. Reference Case – Evolution of the powers developed during the cycling. This corresponds to the power required to compress the gas during the injection phases and the mechanical power that is released during the production phases, also the heat supplied by the hot hydrogen during the injection phases, and the heat lost by conduction to the salt mass.

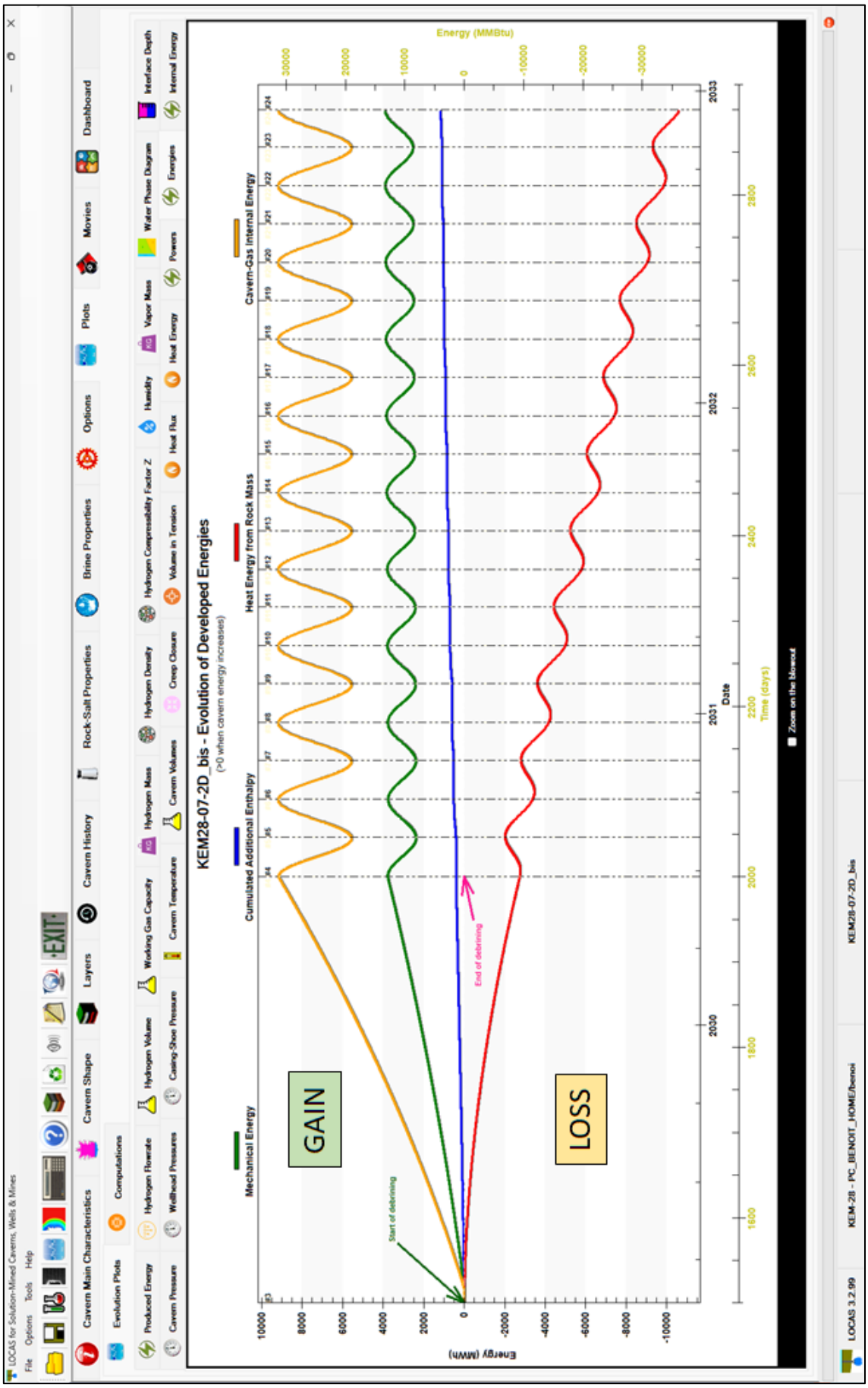

Figure 205. Reference Case – Evolution of the energies developed during the cycling. This corresponds to the integration over time of the powers plotted in the previous figure. The positive values correspond to the energy supplied to the cavern (compression, hot hydrogen) and the negative values to the loss by conduction to the rock mass.

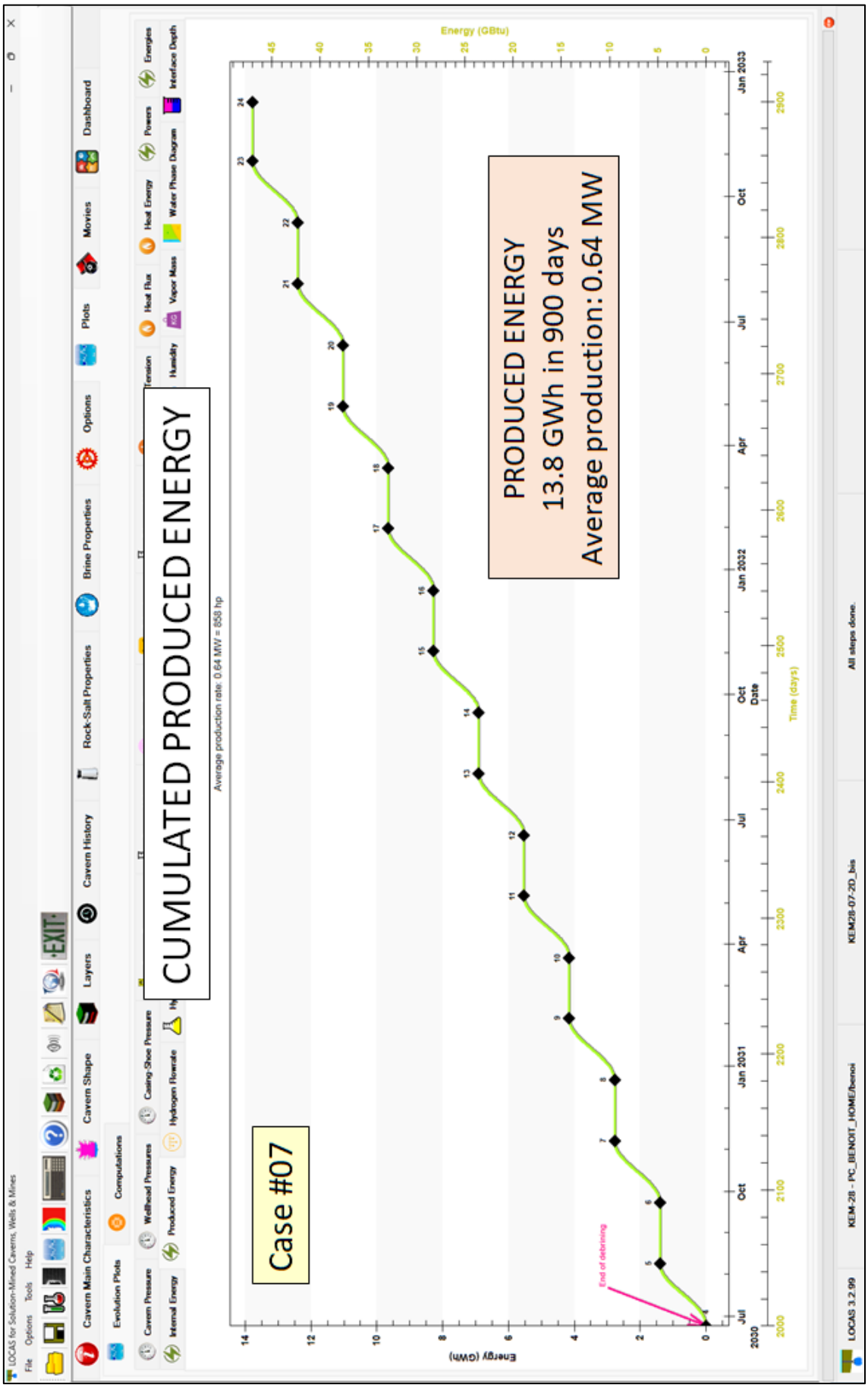

Figure 206. Reference Case – Evolution of the cumulated produced energy. This is the energy generated by the cavern during the production phases.

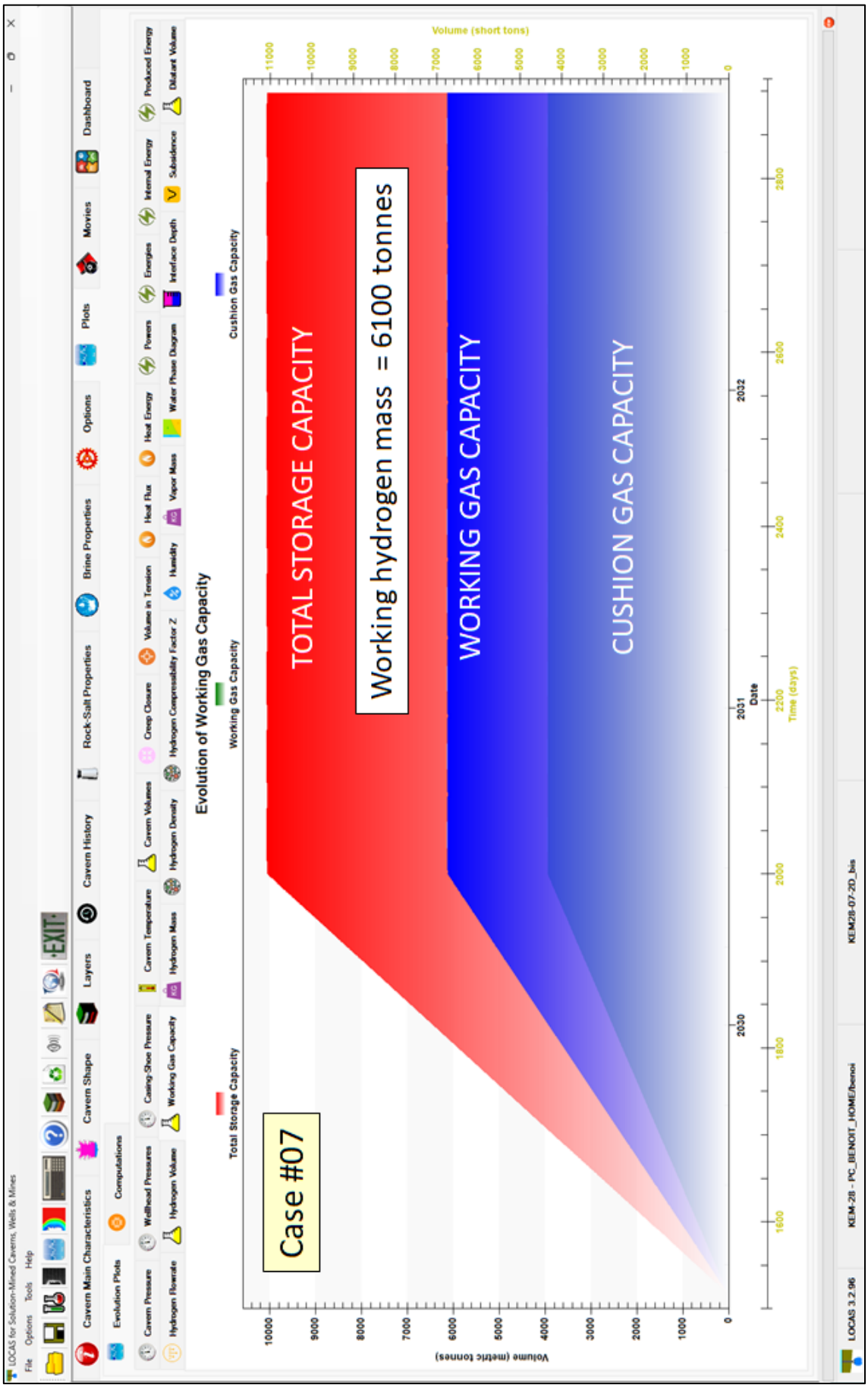

Figure 207. Reference Case – Evolution of cushion gas, working gas and total storage capacity.

Effective Tension

Figure 208 and Figure 209 show the Evolution of the least compressive principal stress σ_{max} and the effective stress σ_{eff} at the node selected at the wall, respectively. It is interesting to note that the least compressive principal stress is still compressive at this point, but the effective stress ($\sigma_{eff} = \sigma_{\max} + P_c$) reaches more than 8 MPa during the last cycle, a value much higher than the tensile strength of the salt, which can be estimated at around 1.5 MPa.

Figure 210 and Figure 211 show the effective stress contours in the vicinity of the selected node at the last minimum pressure. We can see that at the minimum pressure, a strip of salt on the wall of the cavern is in effective traction ($\sigma_{eff} > 0$). The maximum effective stress reached in this zone is 4.94 MPa, higher than the tensile strength of rock salt, which is estimated at around 1.5 MPa. Opening of a fracture is likely (see Section 1.5.8); we can estimate that a small series of small cracks will develop to a depth equal to the thickness of the zone in effective traction (thickness of the magenta zone on the Figure 210).

Effective stress at the cavern wall becomes compressive again at maximum pressure (Figure 212). Figure 213 and Figure 214 show the effective stress distribution along the cavern wall at the last minimum and maximum pressures, respectively. It can be seen that the maximum effective stress (6.38 MPa) at the minimum pressure is located at a depth of 870 m. At maximum pressure (Figure 214), none of the nodes on the wall are in effective tension, but it is possible that effective tensions exist at a short distance inside the salt (see example in Figure 215), which is the result of the succession of cycles.

Figure 216 shows the Evolution of the total volume in effective tension calculated all around the cavern at each output. It can be seen that, in this case, the volume in tension is already non-negligible at the end of leaching and increases progressively during cycling. Areas of effective traction are obtained at both minimum and maximum pressure, but they are greatest at minimum pressure. In this case, the effective tension zone reached 102 000 m^3 at the last minimum pressure, which represents an average thickness of approximately 1 m compared to the surface area of the cavern (103,713 m^2).

Figure 217 shows the orientation and magnitude of the principal stresses in the vicinity of the selected node at the last minimum pressure. The amplification coefficient is 0.1 m/MPa. All the arrows are blue, which means that all the main stresses are compressions. When the hydrogen pressure is added to the least compressive principal stress to obtain the effective stress ($\sigma_{eff} = \sigma_{\max} + P_c$), effective tensile stresses appear at the wall at the minimum pressure. The fractures that can then develop are horizontal at the level of the vertical wall at this depth (Figure 218).

Dilation

Figure 219 and Figure 220 show the FOS contours for the onset of dilation when the pressure in the cavern reaches the first minimum (output #5). Only a small, very narrow band of dilatant salt appears in the lower part of the cavern, where the hydrogen/brine interface is located.

Figure 221 shows the Evolution at the selected node of the inverse of the FOS for the onset of dilation. FOS decreases with each cycle (its inverse increases). Note that the minimums of the FOS (maximums of its inverse) are not synchronised with the minimum pressures but occurs during production phases before reaching the minimum pressure.

Figure 222 shows the Evolution of the total dilatant volume calculated at each output. It can be seen that, in this case, the calculated dilatant volume is at its maximum at the first pressure minimum (output #5) and is smaller for subsequent pressure minimums. The maximum dilatant volume is only 144 m^3, which in relation to the surface of the cavern in this case (103 713 m^2) represents a dilatant strip with an average thickness of only 1.4 mm.

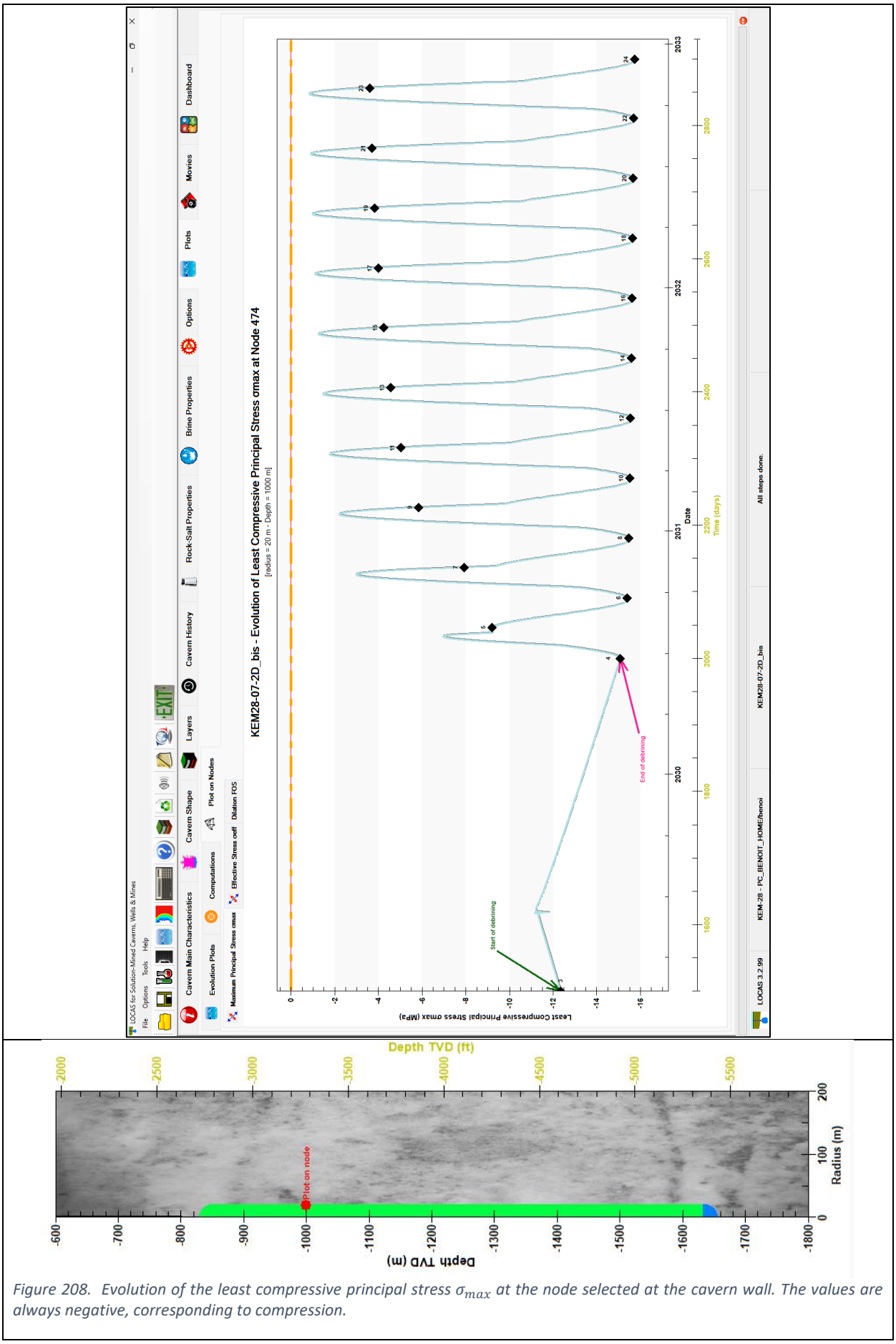

Figure 208. Evolution of the least compressive principal stress σ_{max} at the node selected at the cavern wall. The values are always negative, corresponding to compression.

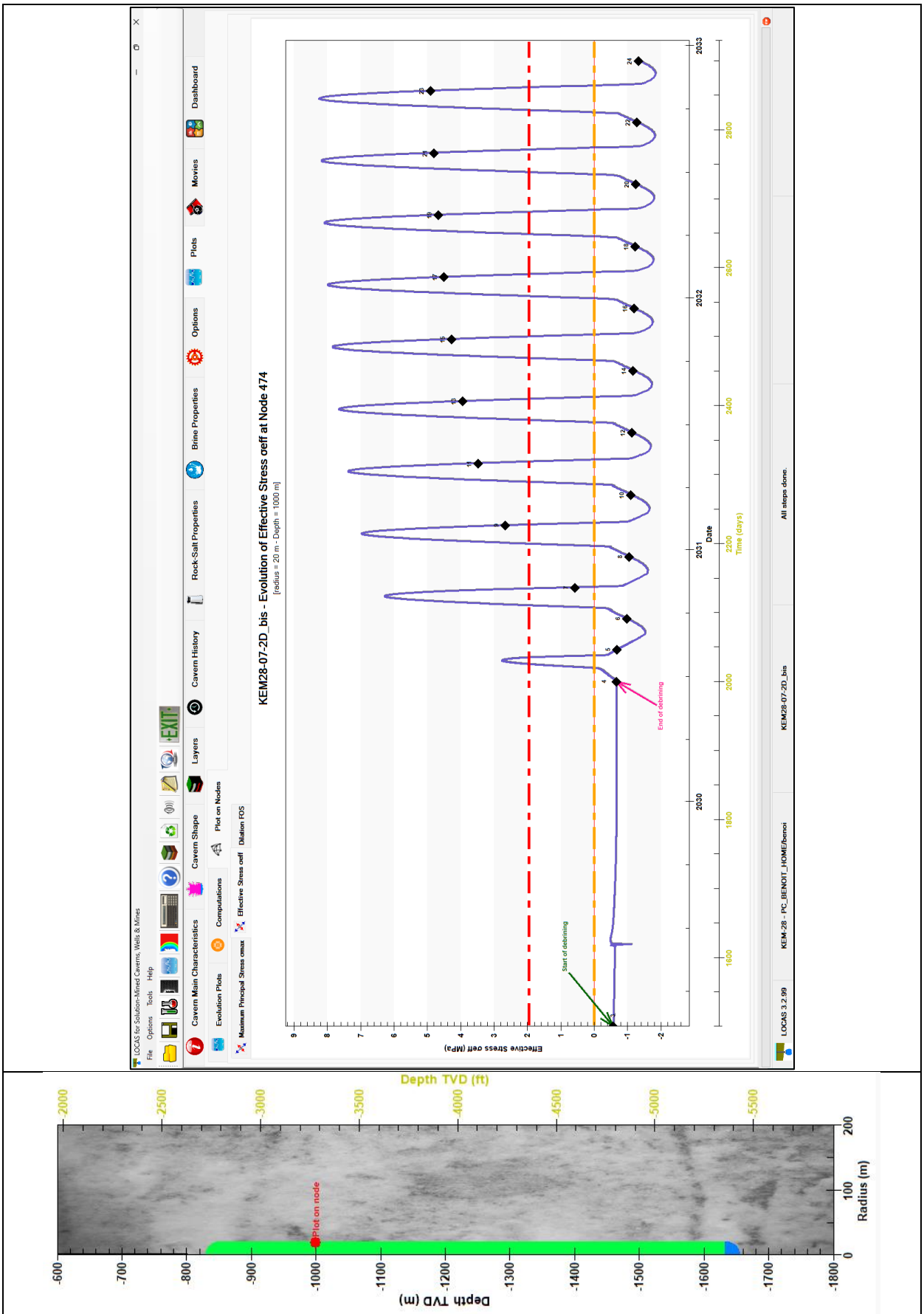

Figure 209. Evolution of the effective stress σ_{eff} at the node selected at the cavern wall. Values often exceed the salt's tensile strength (red line), which corresponds to tensile effective stress. The appearance of a fracture, or the re-opening of a fracture, in this location is likely.

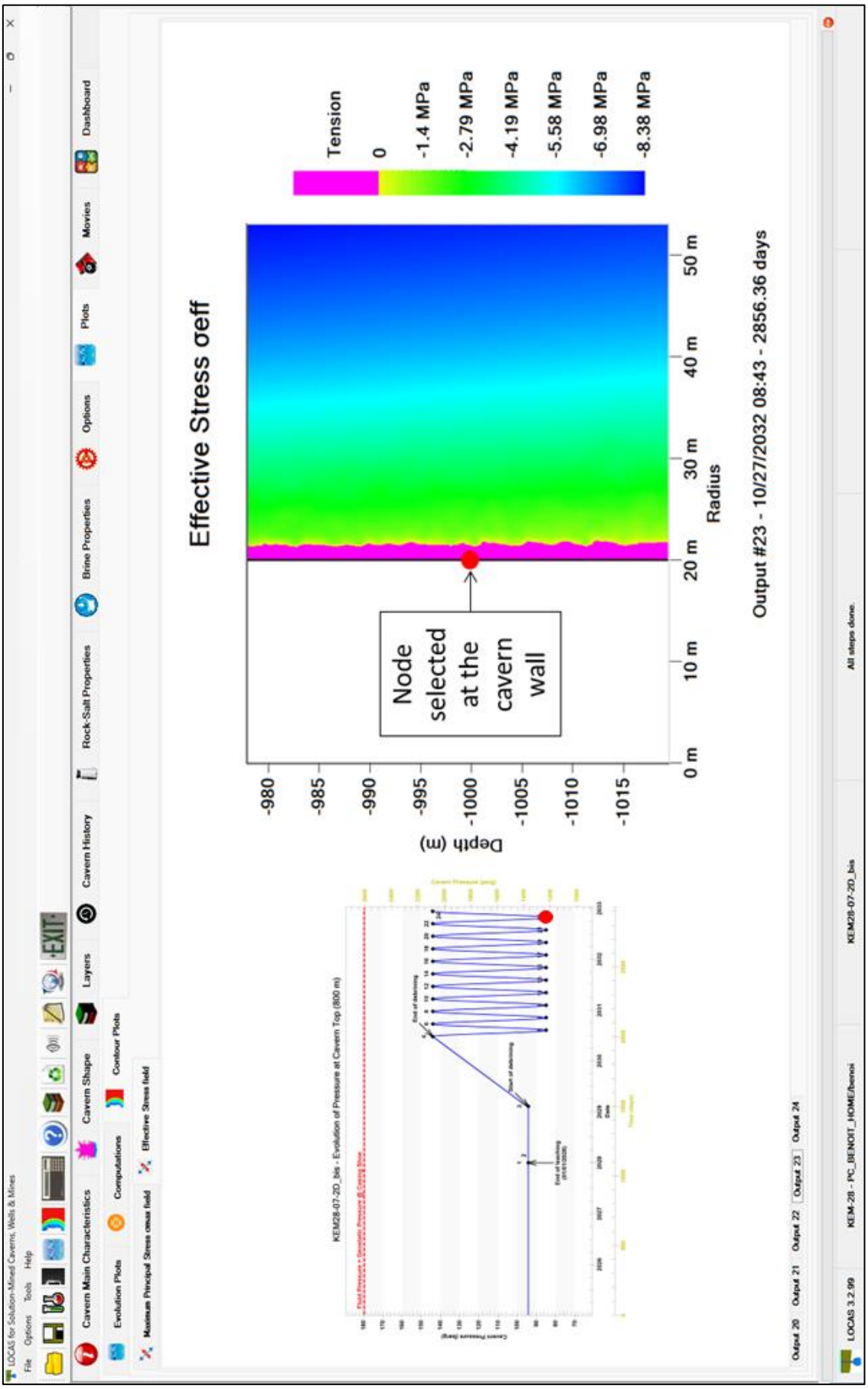

Figure 210. Contours of effective stress σ_{eff} in the vicinity of the selected node at the last minimum pressure (output #23). In this case, the zone of effective traction at the wall is around 2 m thick, which is the expected depth of the fractures.

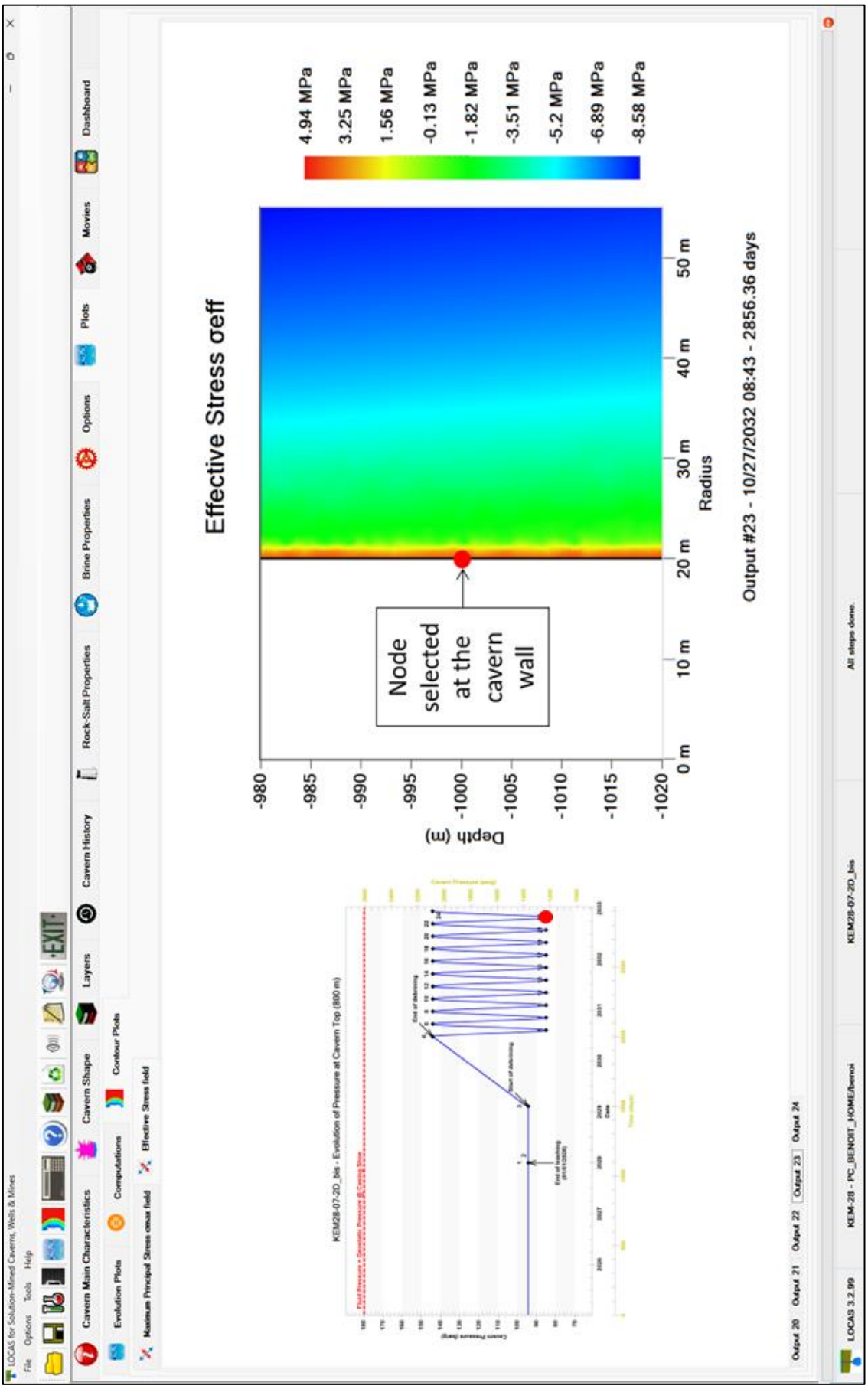

Figure 211. Contours of effective stress σ_{eff} in the vicinity of the selected node at the last minimum pressure (output #23). This is the same figure as above, but with a full colour scale between the minimum and maximum values of the effective stress.

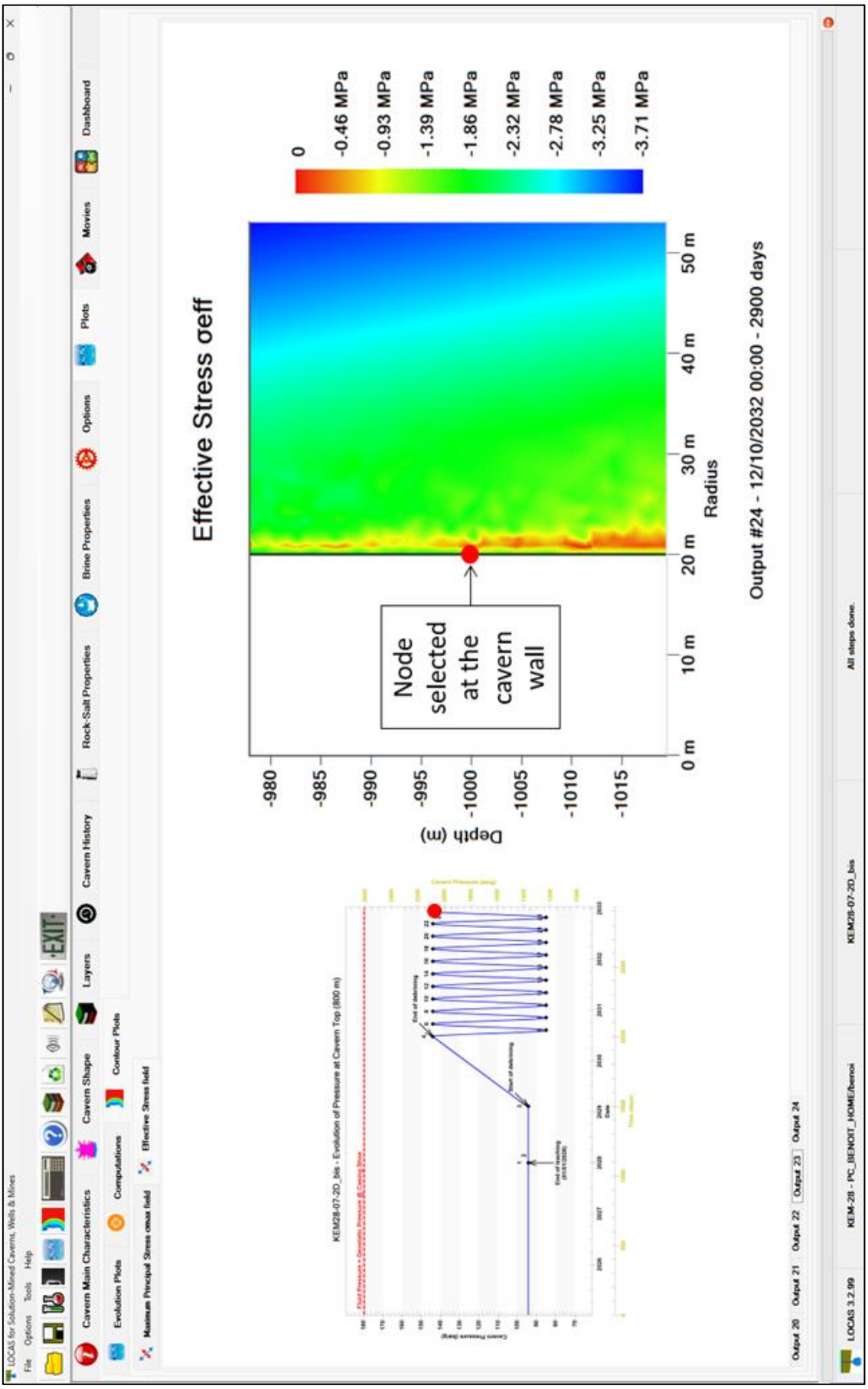

Figure 212. Contours of effective stress σ_{eff} in the vicinity of the selected node at the last maximum pressure (output #24). At maximum pressure, all the stresses are compressive at the wall, so we can imagine that the fractures that have opened previously are closing.

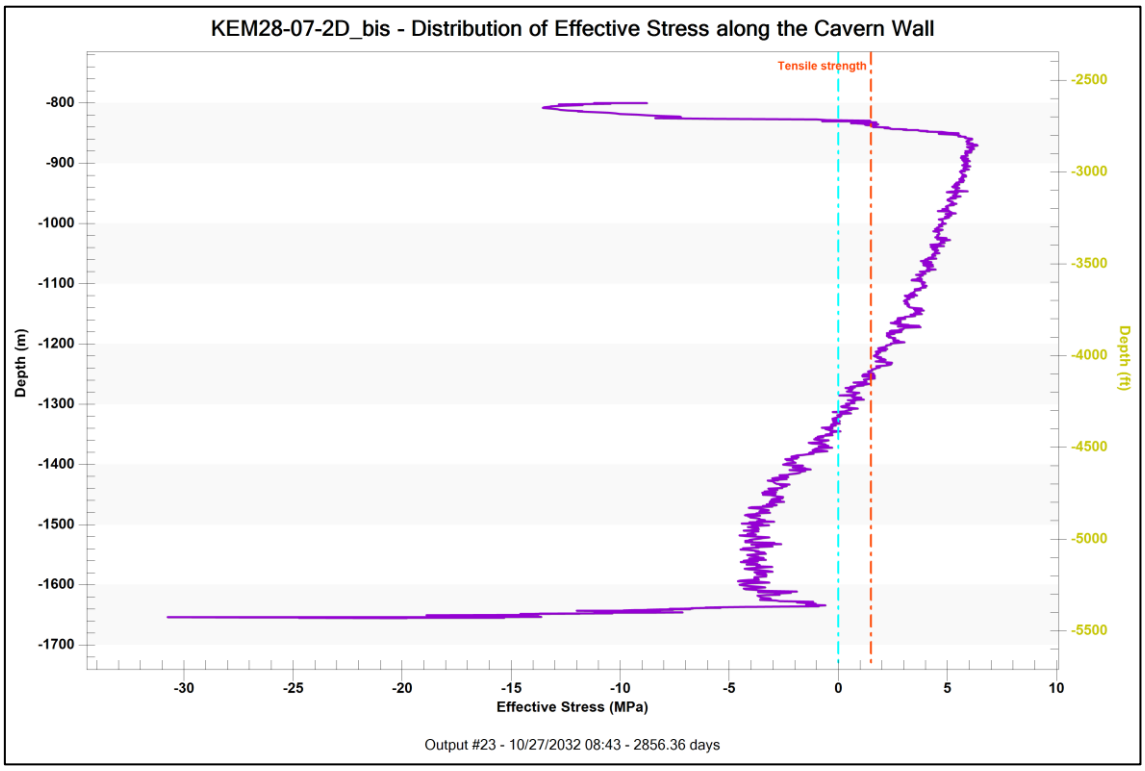

Figure 213. Reference Case –Effective stress distribution along the cavern wall (minimum pressure, output #23). The entire upper part of the cavern is under effective traction at this moment.

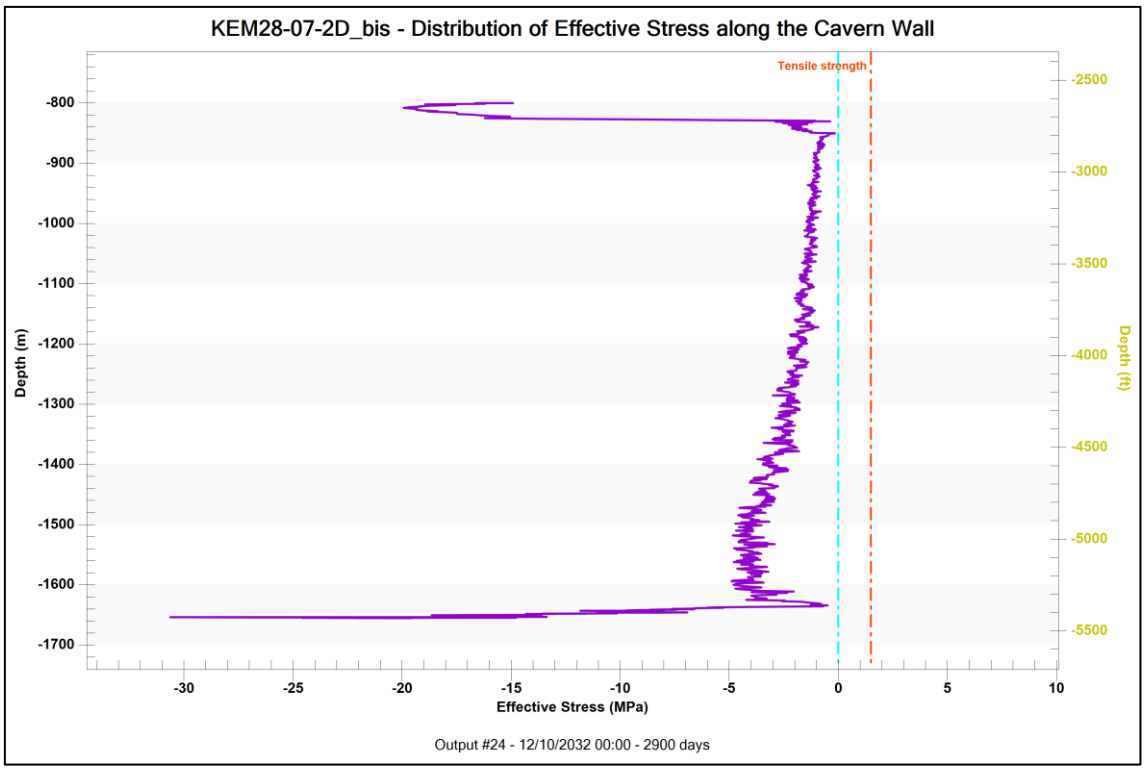

Figure 214. Reference Case –Effective stress distribution along the cavern wall (maximum pressure, output #24). The entire cavern wall is in a compressive state at this moment.

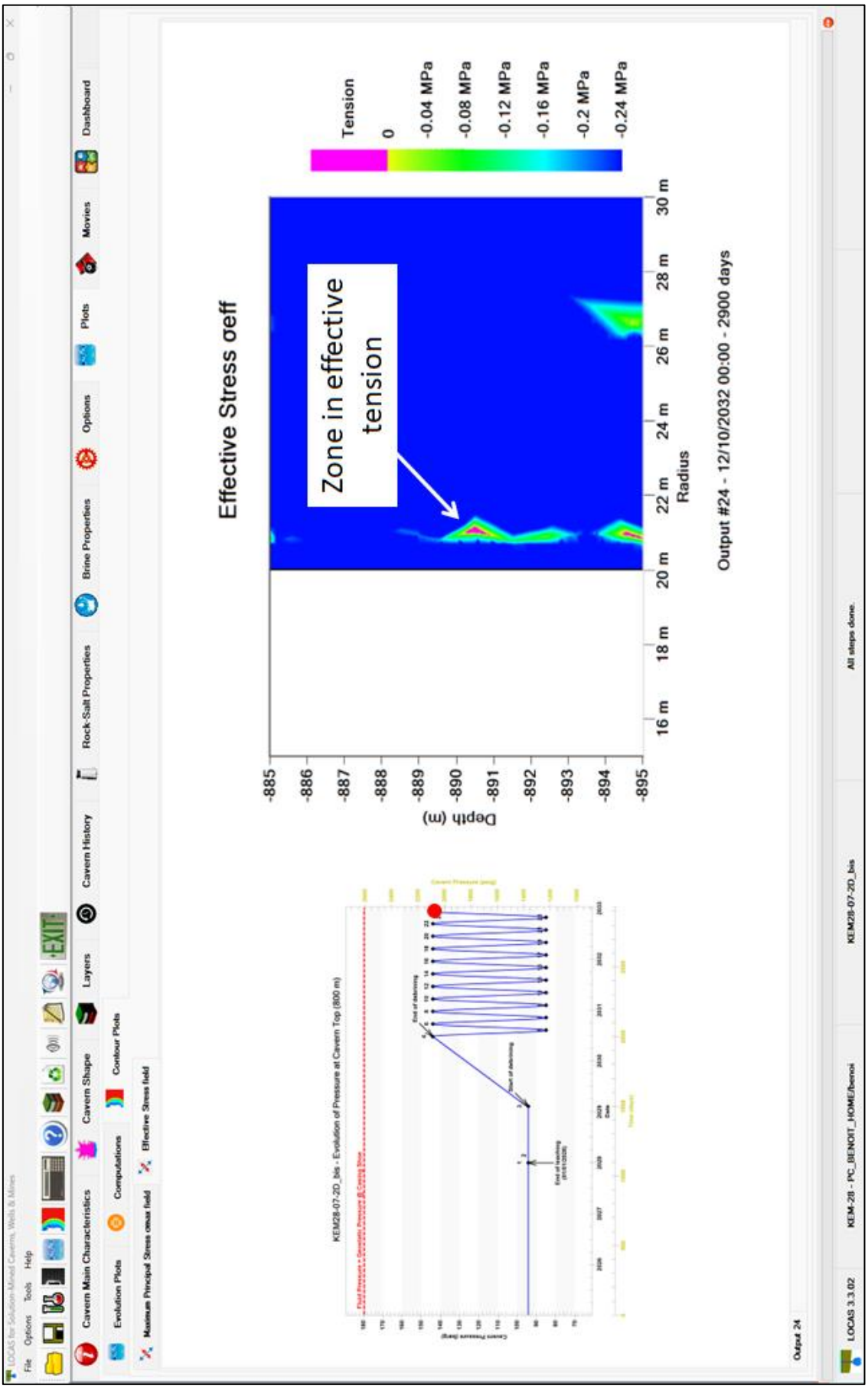

Figure 215. Contours of effective stress σ_{eff} in the vicinity of the selected node at the last maximum pressure (output #24). There are still areas of effective traction inside the salt, even if the wall itself is in a state of compression.

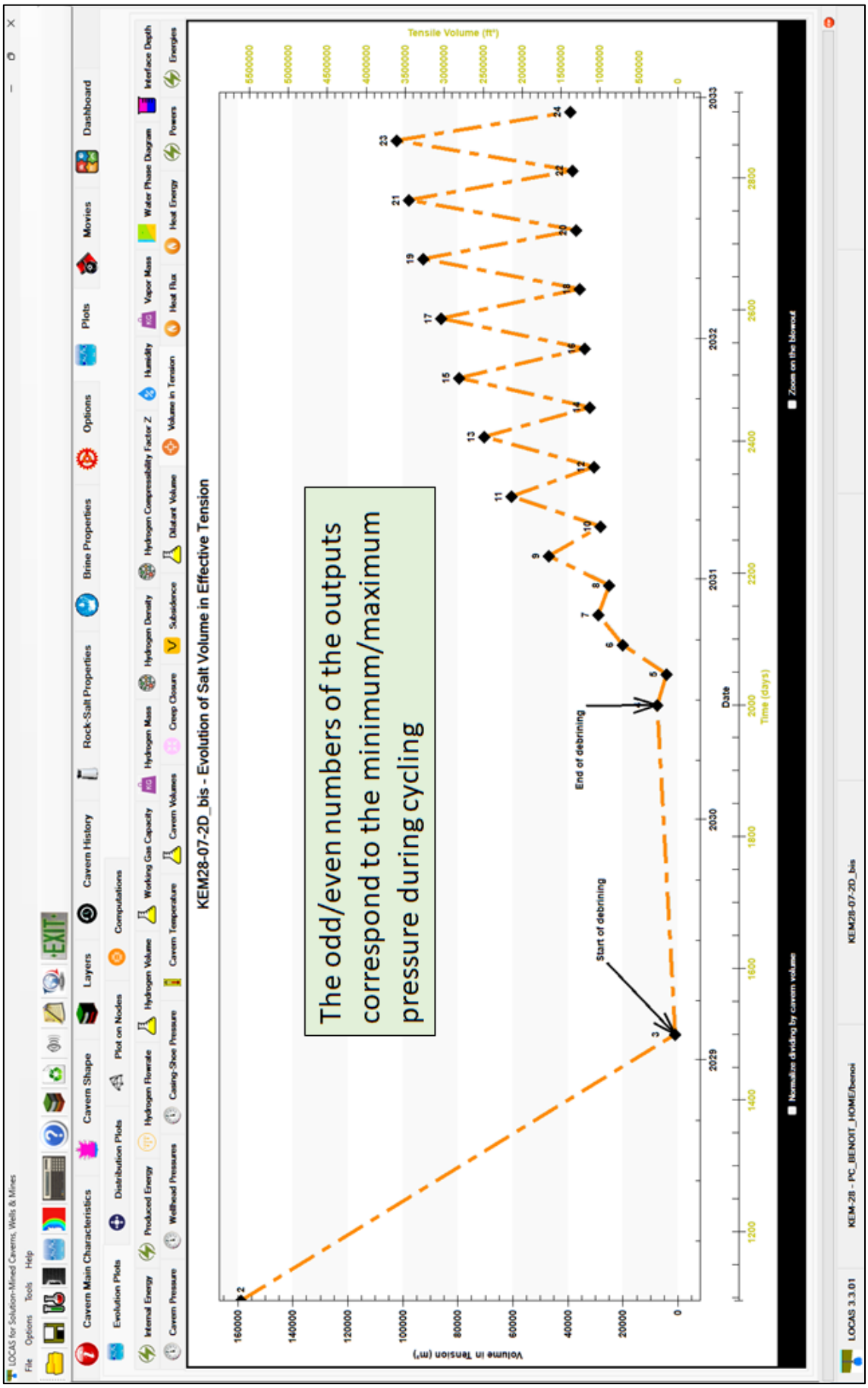

Figure 216. Reference Case – Evolution of the volume in effective tension calculated for each output. The extent of the volume in effective tension tends to increase with each cycle. The tensile zones are larger at minimum pressure, but they also remain at maximum pressure.

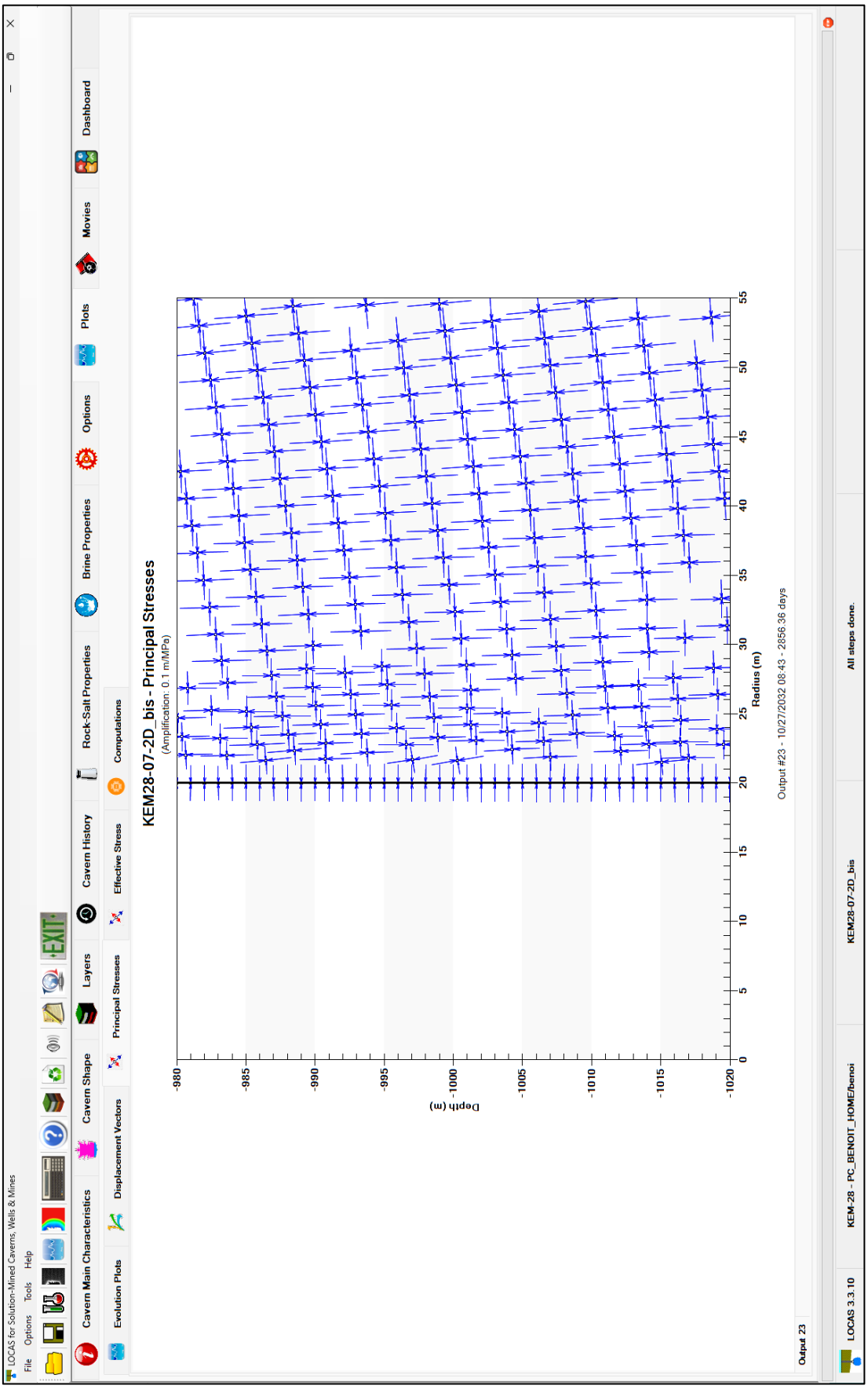

Figure 217. Orientation and magnitude of principal stresses in the vicinity of the selected node at the last minimum pressure (output #23) - The amplification coefficient is 0.1 m/MPa. In this case, all the arrows are blue, corresponding to compressions.

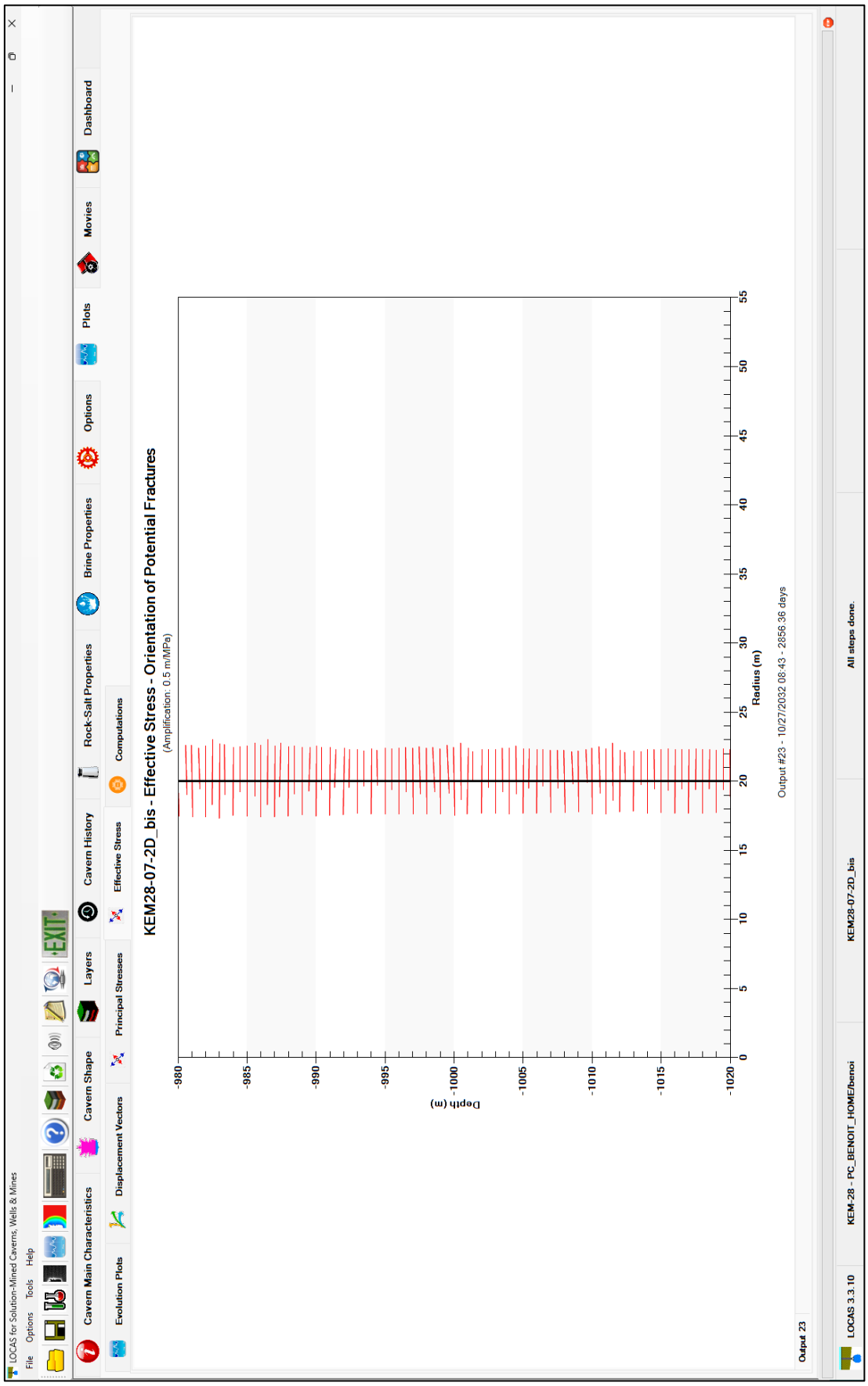

Figure 218. Orientation and magnitude of potential fracture in the vicinity of the selected node at the last minimum pressure (output #23) - The amplification coefficient is 0.5 m/MPa. On the vertical wall, the fractures that can open are horizontal.

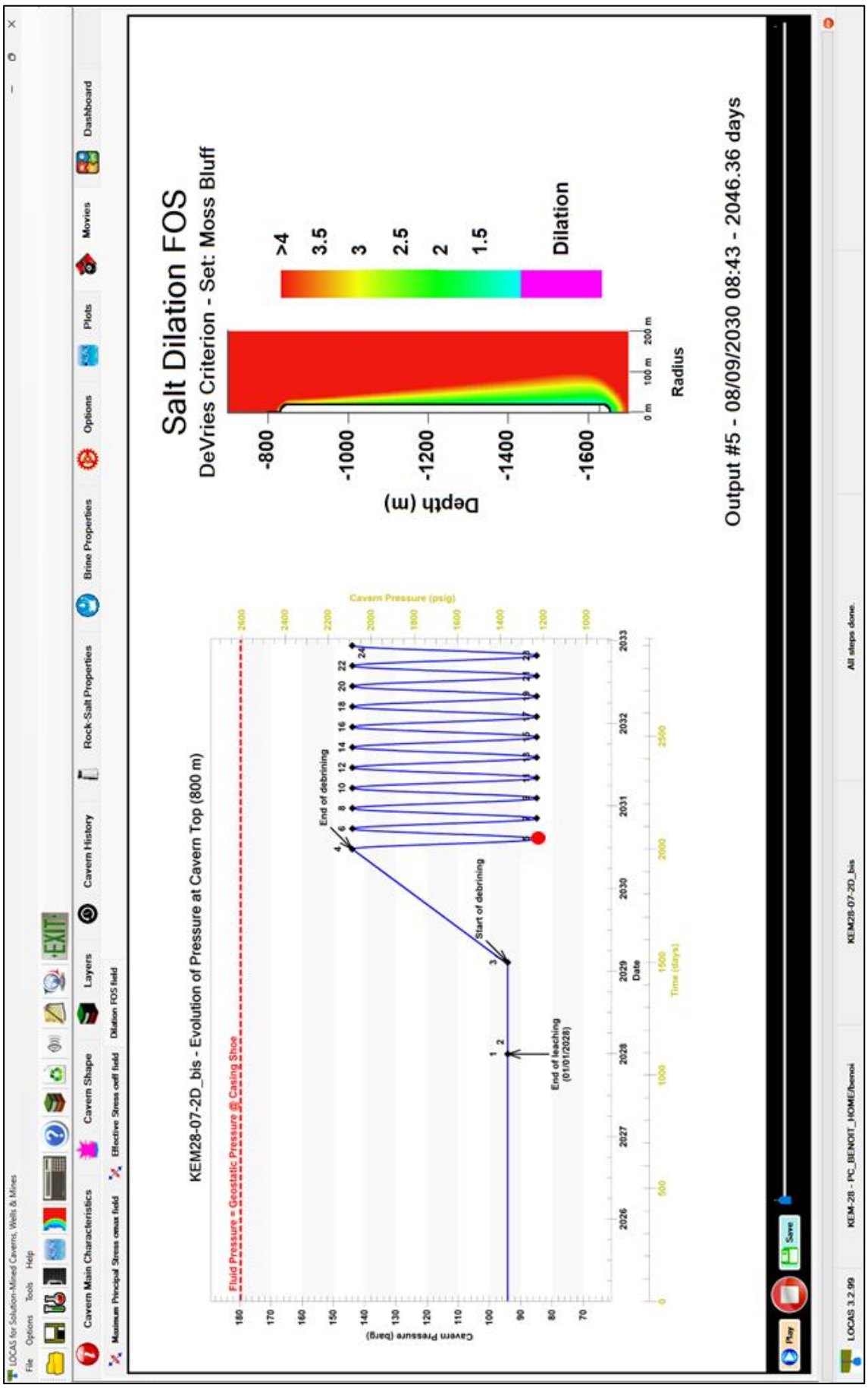

Figure 219. Reference Case – Contours of dilation FOS at the first minimum pressure (output #5). At this moment, there is no very significant dilatant zone at the wall of the cavern.

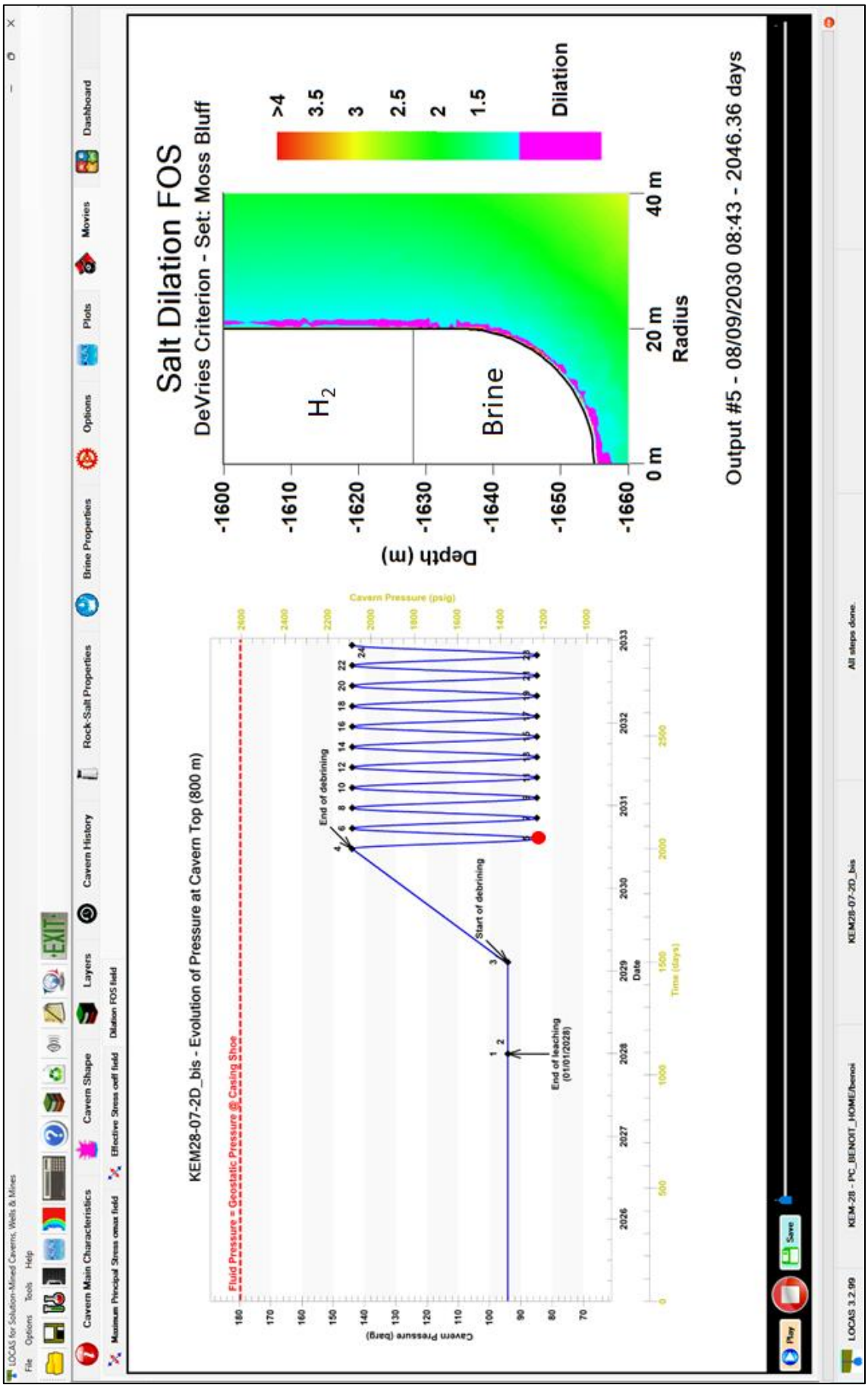

Figure 220. Reference Case – Contours of dilation FOS at the first minimum pressure (output #5) – Zoom at lower section. Small, inconsequential areas of dilation may be observed.

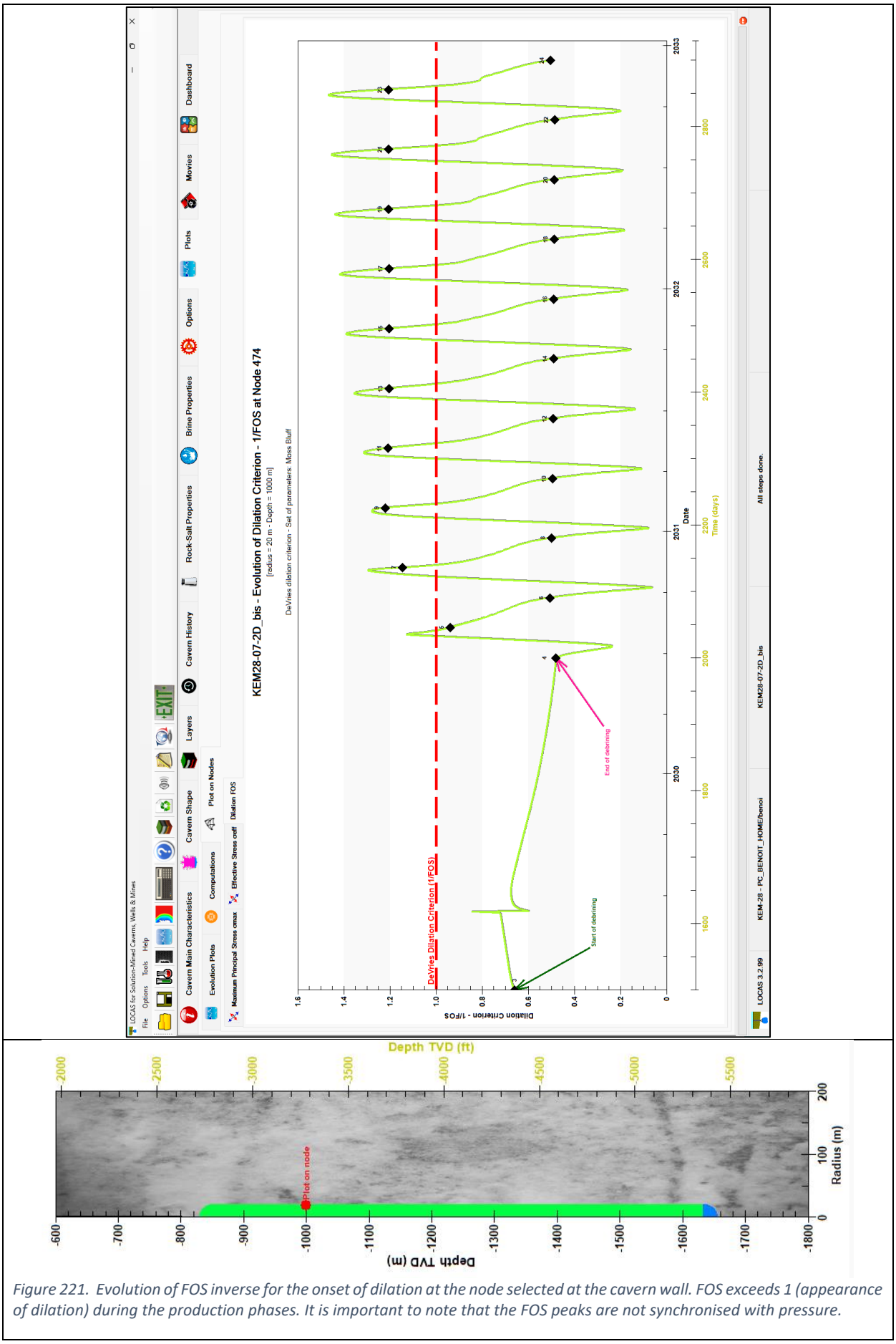

Figure 221. Evolution of FOS inverse for the onset of dilation at the node selected at the cavern wall. FOS exceeds 1 (appearance of dilation) during the production phases. It is important to note that the FOS peaks are not synchronised with pressure.

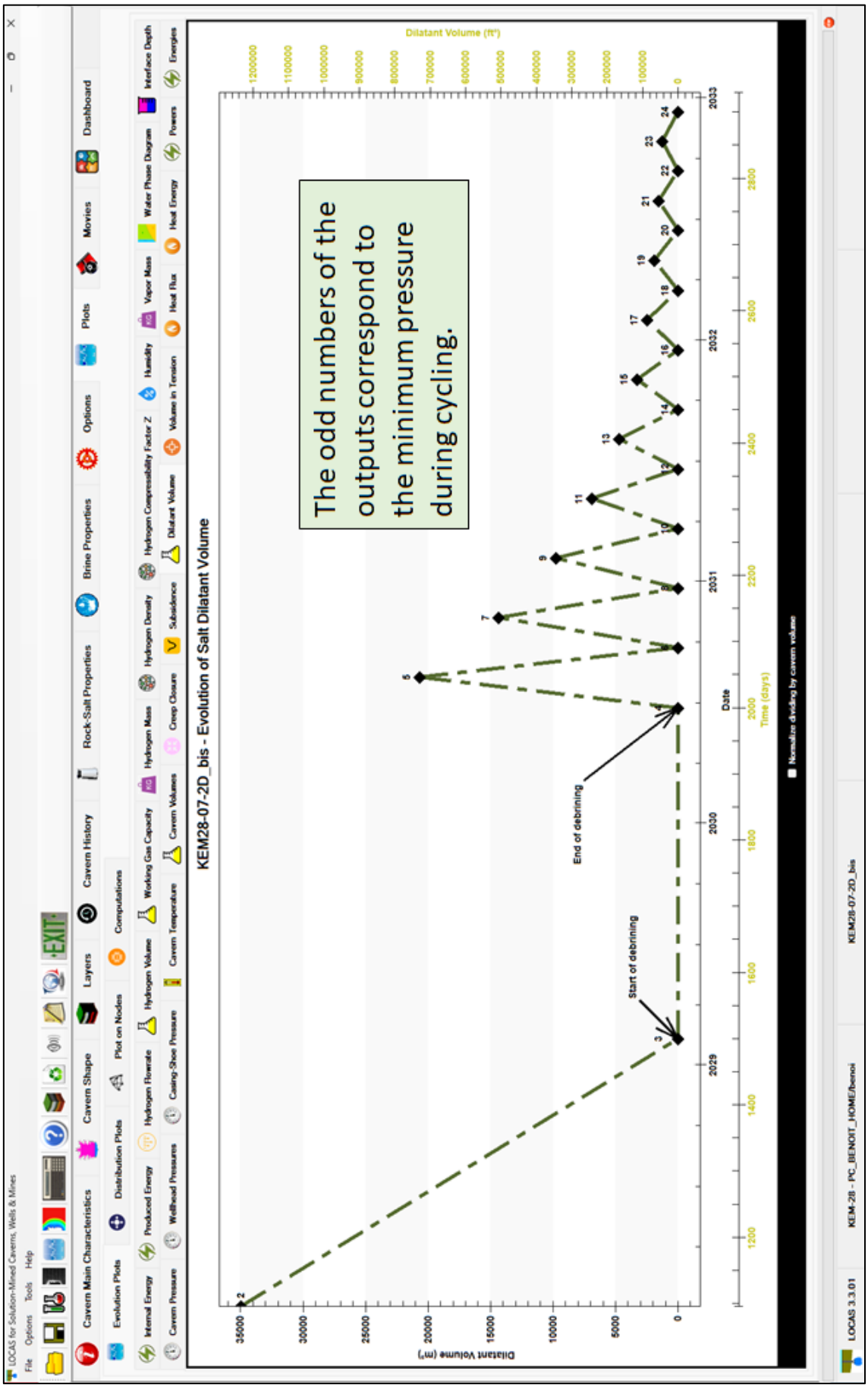

Figure 222. Reference Case – Evolution of the dilatant volume calculated for each output. The extent of the dilatant volume tends to increase with each cycle. The dilatant volume is zero at maximum pressure.

1.9 2D Numerical computations - Sensitivity analysis

1.9.1 Introduction

A sensitivity analysis was carried out using the 2D axisymmetric version of LOCAS. The aim of this study is to vary the main parameters in order to determine the most favourable and least favourable configurations from the point of view of mechanical stability. The results of these calculations were analysed in collaboration with smartTectonics.

The parameters considered are as follows:

- The depth of the last cemented casing shoe (LCCS)
- The maximum diameter of the cavern
- The pressure cycle period
- The pressure gradient corresponding to the minimum pressure

1.9.2 Selected combinations of parameters

The ranges considered for the various parameters in the sensitivity analysis are as follows:

- Three cavern depth and three cavern shapes are considered (Table 19 and Figure 223).
- We consider seasonal cycles (365-day period), quarterly cycles (90-day period) and monthly cycles (30-day period).
- A pressure gradient of 0.05 bar/m or 0.1 bar/m is assumed at the shoe of the last cemented casing.

Table 21 shows the characteristics of the 54 cases considered in the sensitivity analysis. These 54 cases cover two-thirds of the 81 possible combinations.

1.9.3 Calculation results

Table 22 shows the main results of the computations. As shown in Figure 195 (page 295), indicators are given for each case under consideration in Table 19.

Table 19.

Type	Indicator	Unit
Creep Closure	Volume loss after 900 days of cycling	m^3
	Subsidence on cavern axis after 900 days of cycling	mm
Strain	Vertical strain at the LCCS after 900 days of cycling	%
Least compressive principal stress	Maximum principal stress at the selected node	MPa
	Maximum principal stress along cavern wall	MPa
Effective tensile stress	Maximum volume in effective tension	m^3
	Average thickness of the tensile strip	m
	Maximum effective stress at the selected node	MPa
	Maximum effective stress along cavern wall	MPa
Dilation	Maximum dilatant volume	m^3
	Average thickness of the dilatant strip	m
	Maximum value of 1/FOS at the selected node	–
Energy	Cumulated heat loss after 900 days of cycling	MWh
	Cumulated produced energy after 900 days of cycling	GWh

Table 20. Characteristics of the cavern shapes considered in the sensitivity analysis.

Depth casing shoe			Cavern diameter		
Z1 (m)	Z2 (m)	Z3 (m)	D1 (m)	D2 (m)	D3 (m)
800	1000	1200	40	60	80

Depth cavern top (m)			Cavern height (m)		
830	1030	1230	796	354	199

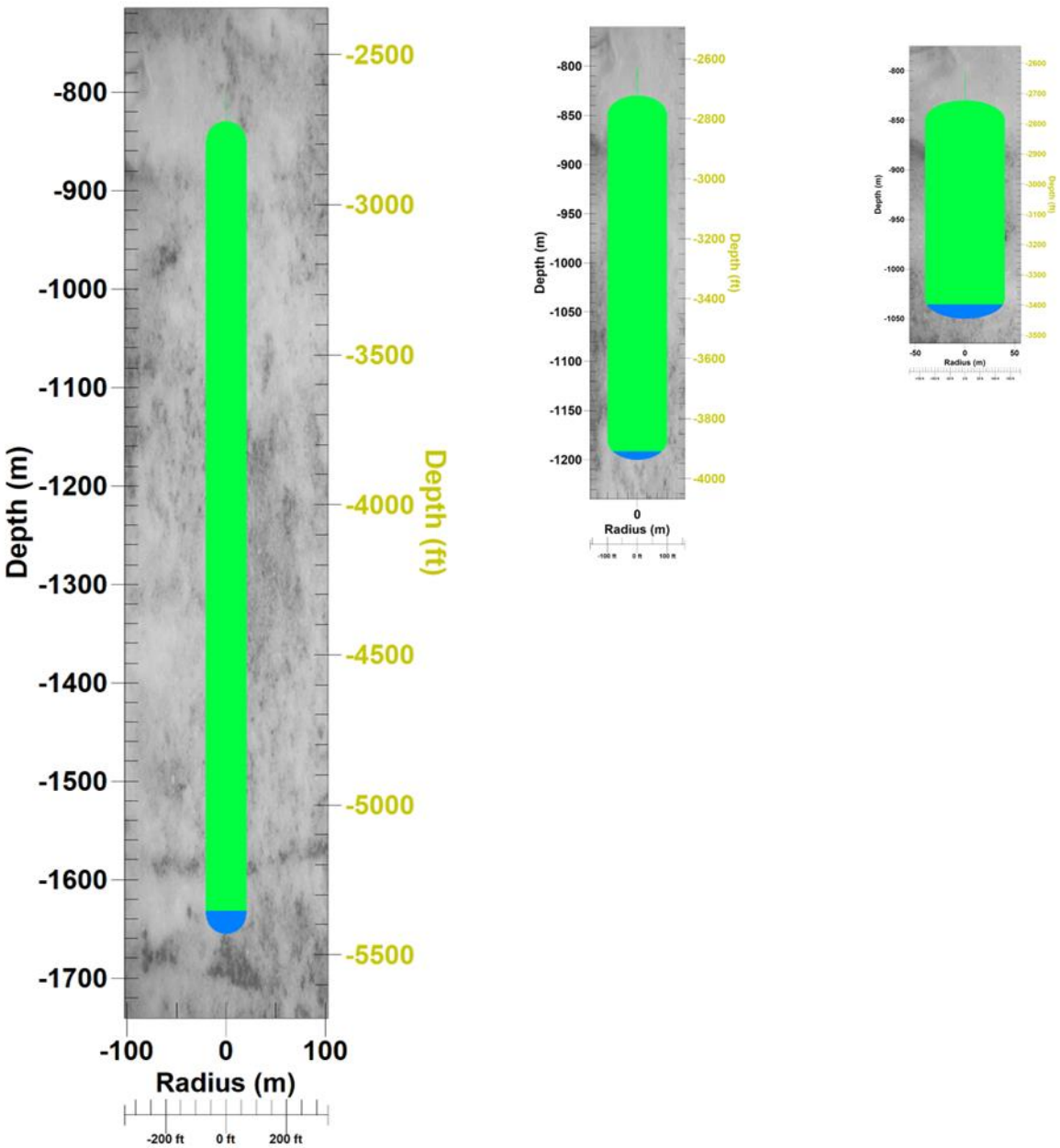

Figure 223. The three cavern shapes considered in the sensitivity analysis in 2D (case of a casing shoe at an 800-m depth).

Figure 224. Parameters for the sensitivity analysis in 2D. The geometry and depth of the cavern are varied, as are the frequency of cycles and the pressure gradient at minimum pressure.

Table 21. Characteristics of the 54 cases considered in the sensitivity analysis in 2D.

	Depth casing shoe			Cavern diameter			Cycling period			P_{min}	
Case	**Z1**	**Z2**	**Z3**	**D1**	**D2**	**D3**	**S**	**Q**	**M**	**G1**	**G2**
1	×			×			×			×	
2	×				×		×			×	
3	×					×	×			×	
4	×			×				×		×	
5	×			×					×	×	
6	×			×			×				×
7	×			×				×			×
8	×			×					×		×
9	×				×			×		×	
10	×				×				×	×	
11	×				×		×				×
12	×				×			×			×
13	×				×				×		×
14	×					×		×		×	
15	×					×			×	×	
16	×					×	×				×
17	×					×		×			×
18	×					×			×		×
19		×		×			×			×	
20		×			×		×			×	
21		×				×	×			×	
22		×		×				×		×	
23		×		×					×	×	
24		×		×			×				×
25		×		×				×			×
26		×		×					×		×
27		×			×			×		×	
28		×			×				×	×	
29		×			×		×				×
30		×			×			×			×
31		×			×				×		×
32		×				×		×		×	
33		×				×			×	×	
34		×				×	×				×
35		×				×		×			×
36		×				×			×		×
37			×	×			×			×	
38			×		×		×			×	
39			×			×	×			×	
40			×	×				×		×	
41			×	×					×	×	
42			×	×			×				×
43			×	×				×			×
44			×	×					×		×
45			×		×			×		×	
46			×		×				×	×	
47			×		×		×				×
48			×		×			×			×
49			×		×				×		×
50			×			×		×		×	
51			×			×			×	×	
52			×			×	×				×
53			×			×		×			×
54			×			×			×		×

Table 22. Main results of the 2D sensitivity study. The green cells correspond to favourable configurations, while the red cells correspond to unfavourable ones.

																								Selected Node						Along Cavern Wall			
		Depth casing shoe			Cavern diameter			Cycling period			P_{min}		Creep Closure (m^3)	Subsidence (mm)	Conduction Heat Flux Loss (MWh)	Produced Energy (GWh)	Surface Area (m^2)	Effective Tensile Stress			Dilation			Vertical Strain at CS (%)	Max.Principal Stress (MPa)		Max. Effective Stress (MPa)		Dilation		Max.Principal Stress (MPa)		Max. Effective Stress (MPa)	
																		Max. tensile volume		Av. tensile strip thickness (m)	Max. dilatant volume		Av. dilatant strip thickness (m)										
Case	Class	Z1	Z2	Z3	D1	D2	D3	S	Q	M	G1	G2	Volume loss @ 900 days	Subsidence @ 900 days	Cumulated energy @ 900 days	Cumulated energy @ 900 days		Value (m^3)	Date Output (Days)		Value (m^3)	Date Output (Days)		Strain @ 900 days (%)	Value (MPa)	Date (days)	Value (MPa)	Date (days)	Value 1/FOS	Date (days)	Value (MPa)	Date Output (Days)	Value (MPa)	Date Output (Days)
1	6	×			×			×			×		55 087	0.322	7 733	7.679	103 713	220	2733.69	0.00	28 792	2188.03	0.28	0.24	-0.64	2859.13	5.90	2844.25	1.17	2873.77	-4.26	2918.00	0.27	2733.69
2	3	×				×		×			×		19 389	0.791	4 112	7.582	71 151	49	2733.69	0.00	10 957	2188.03	0.15	0.35	5.43	2858.89	12.22	2837.30	5.29	2855.05	-3.36	2188.03	5.96	2368.69
3	3	×					×	×			×		13 232	1.109	2 931	7.471	59 163	160 994	2737.37	2.72	1 817	2188.03	0.03	0.44	5.72	2866.37	11.94	2844.56	6.74	2845.43	-3.37	2188.03	10.32	2737.37
4	5	×			×				×		×		59 576	0.326	12 457	24.908	103 713	13	2810.91	0.00	36 962	2046.36	0.36	0.33	7.96	2754.60	13.95	2748.68	8.45	2124.26	2.17	2856.36	6.21	2856.36
5	5	×			×					×	×		67 270	0.429	17 121	72.367	103 713	28 724	2885.46	0.28	53 998	2885.46	0.52	0.47	13.28	2882.07	18.97	2880.02	9.46	2517.88	9.01	2885.46	13.05	2885.46
6	1	×			×			×				×	29 307	0.069	8 334	4.266	103 713	3	2733.69	0.00	29	2188.03	0.00	0.15	-9.35	2176.98	0.40	2842.86	0.74	2175.46	-8.61	2553.03	0.16	2000.00
7	1	×			×				×			×	30 831	0.066	10 640	13.780	103 713	4	2810.91	0.00	144	2046.36	0.00	0.17	-0.83	2847.22	8.25	2844.77	1.13	2846.45	-2.13	2856.36	6.37	2856.36
8	1	×			×					×		×	33 596	0.089	12 982	39.804	103 713	3 879	2885.46	0.04	499	2015.46	0.00	0.20	3.87	2583.05	12.60	2402.40	2.49	2552.92	2.67	2885.46	11.20	2885.46
9	2	×				×			×		×		22 702	0.980	9 714	24.393	71 151	195 244	2810.91	2.74	102 755	2856.36	1.44	0.47	11.01	2844.53	16.80	2839.98	8.30	2740.13	1.25	2856.36	15.57	2540.91
10	2	×				×				×	×		25 779	1.112	14 751	70.619	71 151	302 830	2870.61	4.26	121 704	2645.46	1.71	0.46	17.60	2881.83	23.11	2880.62	9.43	2335.24	15.12	2885.46	24.50	2150.61
11	1	×				×		×				×	8 243	0.042	4 516	4.556	71 151	1	2733.69	0.00	0	1094.00	0.00	0.19	-0.97	2866.17	8.34	2851.48	1.07	2862.34	-5.43	2918.03	2.78	2000.00
12	3	×				×			×			×	9 615	0.038	7 569	14.595	71 151	89 609	2856.36	1.26	10 693	2856.36	0.15	0.28	4.15	2845.57	13.35	237.16	3.43	2845.57	0.00	2856.36	8.03	2856.36
13	4	×				×				×		×	10 770	0.045	10 591	41.957	71 151	90 416	2645.46	1.27	59 869	2885.46	0.84	0.34	9.24	2881.78	18.37	2879.94	8.97	2548.12	6.61	2885.46	14.63	2885.46
14	2	×					×		×		×		15 769	1.392	8 350	23.932	59 163	602 288	2811.82	10.18	133 633	2856.36	2.26	0.56	11.79	2845.37	17.42	2840.92	8.17	2828.74	5.05	2856.36	17.84	2451.82
15	2	×					×			×	×		17 330	1.441	12 603	69.253	59 163	681 610	2870.61	11.52	121 934	2495.46	2.06	0.54	18.61	2882.10	23.99	2880.62	8.81	2395.14	18.58	2885.46	27.70	2270.61
16	1	×					×	×				×	4 915	0.009	3 249	4.480	59 163	43 793	2918.03	0.74	0	1094.00	0.00	0.23	0.22	2866.44	9.56	2840.89	1.33	2862.95	-4.54	2918.03	3.48	2918.03
17	4	×					×		×			×	5 809	0.115	6 196	14.267	59 163	126 706	2856.36	2.14	41 887	2856.36	0.71	0.34	4.71	2846.12	13.81	2840.06	5.46	2846.57	1.54	2856.36	9.56	2856.36
18	4	×					×			×		×	6 380	0.089	8 889	40.974	59 163	98 122	2825.46	1.66	65 180	2615.46	1.10	0.38	10.11	2881.80	19.12	2880.61	9.15	2697.65	10.27	2885.46	18.13	2885.46
19	7		×		×			×			×		84 738	1.938	10 124	9.324	103 713	41	2737.37	0.00	36 318	2188.03	0.35	0.11	-1.93	2857.69	6.45	2840.75	1.14	2866.16	-5.16	2918.03	1.88	2737.37
20	6		×			×		×			×		31 529	1.527	6 056	9.186	71 151	271	2737.37	0.00	20 168	2188.03	0.28	0.52	4.24	2490.35	13.13	2468.14	2.67	2851.78	-3.99	2188.03	8.33	2372.37
21	3		×				×	×			×		21 763	1.172	4 632	9.034	59 163	454 811	2737.37	7.69	8 890	2188.03	0.15	0.59	5.14	2862.56	13.06	2843.81	4.32	2862.56	-4.16	2188.03	10.56	2737.37
22	5		×		×				×		×		90 548	1.924	15 099	30.113	103 713	80	2811.82	0.00	46 683	2046.36	0.45	0.14	7.24	2484.52	14.64	2209.11	7.36	2663.62	-0.35	2856.36	4.69	2856.36
23	5		×		×					×	×		101 501	2.182	19 206	87.271	103 713	20 494	2885.46	0.20	52 766	2015.46	0.51	0.17	12.42	2882.44	18.89	2880.59	10.83	2848.78	7.92	2885.46	12.97	2885.46
24	6		×		×			×				×	44 525	0.998	10 827	5.581	103 713	11	2737.37	0.00	217	1095.00	0.00	0.07	-10.79	2862.66	1.23	2840.63	0.75	2177.61	-10.12	2918.03	0.03	2737.37
25	6		×		×				×			×	46 787	0.974	13 351	17.943	103 713	16	2811.82	0.00	481	2046.36	0.00	0.07	-1.45	2846.45	9.39	2844.56	1.14	2846.33	-3.39	2856.36	6.64	2856.36
26	6		×		×					×		×	50 943	1.069	15 340	51.695	103 713	5 626	2885.46	0.05	1 008	2015.46	0.01	0.08	3.29	2793.03	13.80	2522.37	2.16	2793.03	2.11	2885.46	12.15	2885.46
27	2		×			×			×		×		36 197	1.693	12 002	29.430	71 151	393 483	2811.82	5.53	93 961	2856.36	1.32	0.60	10.56	2845.38	17.52	2840.82	9.42	2126.18	3.01	2856.36	15.89	2271.82
28	2		×			×				×	×		40 927	1.903	16 491	85.175	71 151	564 309	2870.61	7.93	121 006	2705.46	1.70	0.58	16.84	2882.10	23.41	2881.21	11.08	2043.29	12.72	2885.46	25.98	2210.61
29	1		×			×		×				×	12 215	0.385	6 576	5.512	71 151	4	2737.37	0.00	110	1095.00	0.00	0.30	-2.38	2862.53	9.41	2848.28	1.00	2858.83	-8.78	2918.03	1.39	2372.37
30	3		×			×			×			×	14 065	0.461	9 636	17.518	71 151	87 311	2856.36	1.23	3 428	2856.36	0.05	0.39	2.68	2846.40	13.97	2839.17	2.22	285.57	-2.01	2856.36	8.03	2856.36
31	4		×			×				×		×	15 561	0.507	12 259	50.256	71 151	89 569	2885.46	1.26	54 434	2885.46	0.77	0.42	7.44	2882.18	18.59	2879.68	9.83	2850.54	6.23	2885.46	16.25	2885.46
32	2		×				×		×		×		25 351	2.044	10 352	28.836	59 163	948 810	2811.82	16.04	113 848	2856.36	1.92	0.63	11.60	2846.33	18.36	2841.77	9.03	2563.77	0.27	2631.82	18.25	2631.82
33	2		×				×			×	×		27 536	2.174	14 061	83.395	59 163	1 189 253	2870.61	20.10	119 333	2645.46	2.02	0.61	18.69	2882.46	25.15	2881.20	10.81	2576.03	17.64	2885.46	25.96	2510.61
34	1		×				×	×				×	7 388	0.365	5 044	5.378	59 163	22 171	2918.03	0.37	67	1095.00	0.00	0.32	-1.38	2866.90	10.32	2840.98	1.13	2863.06	-7.82	2918.03	3.95	2372.37
35	3		×				×		×			×	8 568	0.473	8 055	17.076	59 163	181 087	2811.82	3.06	24 229	2856.36	0.41	0.41	3.31	2846.43	14.47	2840.01	2.65	2846.43	-1.15	2856.36	8.88	2856.36
36	4		×				×			×		×	9 197	0.480	10 339	49.033	59 163	241 628	2870.61	4.08	59 724	2855.46	1.01	0.41	8.71	2882.37	19.77	2880.65	10.24	2819.36	7.10	2885.46	17.14	2885.46
37	5			×	×			×			×		126 731	4.793	12 393	10.888	103 700	474	2737.37	0.00	43 019	2188.03	0.41	0.15	-8.45	2845.26	3.00	2831.17	1.04	2169.77	-6.77	2188.03	3.67	2737.37
38	7			×		×					×		48 942	2.711	7 892	10.708	71 151	2 963	2737.37	0.04	31 914	2188.03	0.45	0.37	2.39	2855.35	13.20	2464.63	1.85	2851.74	-4.88	2188.03	8.63	2372.37
39	3			×			×	×			×		34 673	2.739	6 231	10.510	59 163	754 530	2737.37	12.75	23 229	2188.03	0.39	0.52	4.28	2494.13	14.07	2475.45	2.71	2858.95	-4.97	2188.03	8.68	3095.00
40	5			×	×				×		×		133 784	4.663	17 359	35.016	103 700	609	2811.82	0.01	57 664	2046.36	0.56	0.16	4.13	2302.65	13.57	2209.77	2.30	2391.81	-3.83	2856.64	4.19	2271.82
41	5			×	×					×	×		148 156	5.169	20 628	101.332	103 700	7 113	2885.46	0.07	66 181	2015.46	0.64	0.19	10.71	2372.41	18.36	2281.22	12.10	2192.67	6.66	2885.46	12.71	2885.46
42	7			×	×			×				×	62 192	2.365	13 289	6.469	103 700	46	2737.37	0.00	625	1095.00	0.01	0.08	-14.66	2173.28	-1.01	2827.98	0.77	2173.71	-12.54	2188.03	0.34	2737.37
43	7			×	×				×			×	64 738	2.270	15 634	20.715	103 700	65	2811.82	0.00	625	1095.00	0.01	0.08	-5.78	2845.87	7.41	2843.68	0.90	2669.12	-5.79	2856.36	6.24	2856.36
44	7			×	×					×		×	69 814	2.446	16 853	59.613	103 700	1 208	2885.46	0.01	625	1095.00	0.01	0.08	-0.01	2643.05	12.51	2612.71	1.45	2823.05	0.44	2885.46	12.49	2885.46
45	2			×		×			×		×		55 202	2.892	13 944	34.187	71 151	604 458	2811.82	8.50	76 188	2856.36	1.07	0.36	10.06	2845.41	18.38	2840.09	10.91	2215.91	-4.81	2856.36	11.60	2091.82
46	2			×		×				×	×		62 458	3.243	17 716	98.772	71 151	857 792	2870.61	12.06	123 584	2885.46	1.74	0.33	16.89	2882.43	24.54	2881.18	12.05	2042.78	7.23	2885.46	14.93	2270.61
47	1			×		×		×				×	17 743	0.860	8 561	6.353	71 151	87	2737.37	0.00	264	1095.00	0.00	0.22	-4.12	2858.96	10.50	2839.33	0.93	2855.03	-11.30	2188.03	2.44	2372.37
48	1			×		×			×			×	20 229	0.956	11 581	20.155	71 151	89 745	2856.36	1.26	264	1095.00	0.00	0.23	1.24	2845.51	14.73	2840.00	1.78	2845.51	-4.66	2856.36	7.38	2856.36
49	4			×		×				×		×	22 313	1.052	13 542	57.833	71 151	171 553	2870.61	2.41	53 571	2885.46	0.75	0.21	6.23	2882.38	19.47	2880.32	5.02	2882.38	1.96	2885.46	14.00	2885.46
50	2			×			×		×		×		39 649	3.014	12 031	33.458	59 163	1 350 318	2811.82	22.82	88 180	2856.36	1.49	0.47	11.11	2846.36	18.99	2842.75	9.95	2746.81	-1.72	2856.36	11.11	2181.82
51	2			×			×			×	×		43 192	3.252	15 110	96.659	59 163	1 632 816	2870.61	27.60	116 045	2765.46	1.96	0.43	18.14	2882.73	25.54	2881.54	11.66	2757.23	12.72	2885.46	18.78	2885.46
52	1			×			×	×				×	11 039	0.701	6 748	6.218	59 163	31 130	2000.00	0.53	574	1095.00	0.01	0.28	-2.98	2862.88	11.20	2840.20	1.03	2859.39	-11.38	2553.03	4.65	2372.37
53	3			×			×		×			×	12 662	0.825	9 675	19.649	59 163	360 097	2811.82	6.09	7 508	2856.36	0.13	0.29	1.65	2847.35	14.89	2840.92	1.92	2846.43	-3.10	2856.36	8.93	2856.36
54	4			×			×			×		×	13 485	0.864	11 460	56.511	59 163	418 766	2870.61	7.08	53 410	2885.46	0.90	0.27	6.81	2882.70	19.89	2880.91	7.02	2882.70	4.04	2885.46	16.08	2885.46

1.9.4 Analysis of results by smartTectonics

The results shown in Table 22 were analysed by smartTectonics through the use of a hierarchical clustering algorithm. This allowed for the identification of 7 classes that correspond closely with the overall sampling distribution (Figure 225).

Computations results are sorted by classes in Table 23. Tables with configurations classified by depth, maximum diameter, etc. are given in Appendix C: Sensitivity Analysis Additional Tables.

Class 1 configurations appear to be the most favourable (Figure 226), whereas Class 0 and 5 (Figure 227) configurations are much less suitable. Classes 1 and 5 correspond respectively to cases with a minimum pressure gradient of 0.1 bar/m and cases with a minimum pressure of 0.05 bar/m (Figure 228). Class 5 appears less favourable than Class 1, i.e., we must prefer a minimum pressure that is not too low, which is obvious enough to limit the effects of creep.

Case #51 is an example of an unfavourable configuration (Figure 229), because for instance a very large zone of effective tension appears at the maximum pressure of the last cycle (Figure 230). It corresponds to the case of a relatively deep cavern (casing shoe at a 1200-m depth), with a wide diameter (80 m), subject to frequent cycles (period of 1 month) and with a low minimum pressure (0.05 bar/m or 60 barg at the last cemented casing shoe).

Case #16 is an example of a favourable configuration (Figure 231). It corresponds to the case of a relatively shallow cavern (casing shoe at a depth of 800 m), with a small diameter (40 m), subject to seasonal cycles (period of 1 year) and with a high minimum pressure (0.1 bar/m or 80 barg at the last cemented casing shoe).

For the following calculations in this report, case #7 has been taken as the reference case (Figure 232). This is a rather favourable configuration (Class 1), with a small diameter (which could make it possible to increase the density of the caverns in a cluster, see Section 1.14) and with a fairly rapid loading/unloading cycle (period of 90 days).

Generally speaking, we could say that deeper caverns, with a smaller maximum diameter and a higher average temperature, are more favourable than shallower caverns with a larger diameter, but this depends on the frequency of the cycles. For example, deep caverns with frequent cycles are less favourable because creep is faster.

Seasonal cycles, corresponding to the usual use of natural gas storage facilities, may appear more favourable than rapid cycles (Table 40), but there are exceptions.

Depending on the constraints at each site, for example the range of depths available for the caverns or the size of the pillars between caverns, a combination of parameters can be found that gives acceptable results.

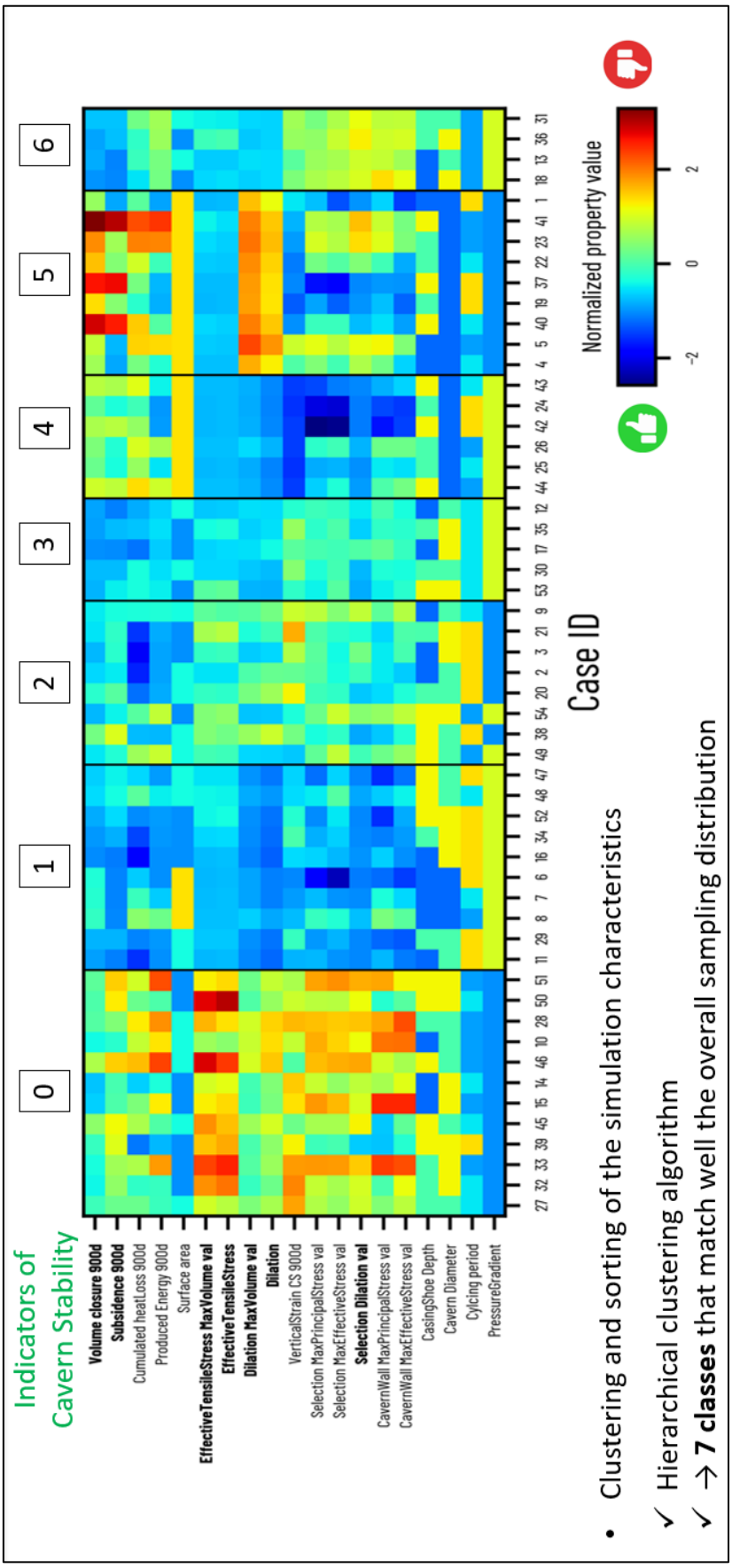

Figure 225. Analysis of the results of sensitivity calculations by smartTectonics. Determination of 7 main classes that match well the overall sampling distribution using a hierarchical clustering algorithm.

Table 23. List of cases sorted by class.

		Depth casing shoe			Cavern diameter			Cycling period					Creep Closure (m^3)	Subsidence (mm)	Conduction Heat Flux Loss (MWh)	Produced Energy (GWh)		Effective Tensile Stress				Dilation			Vertical Strain at CS (%)	Max.Principal Stress (MPa)		Max. Effective Stress (MPa)		Dilation		Max.Principal Stress (MPa)		Max. Effective Stress (MPa)	
Case	Class	Z1	Z2	Z3	D1	D2	D3	S	Q	M	P_{min} G1	G2	Volume loss @ 900 days	Subsidence @ 900 days	Cumulated energy @ 900 days	Cumulated energy @ 900 days	Surface Area (m^2)	Max. tensile volume		Av. tensile strip thickness (m)	Max. dilatant volume		Av. dilatant strip thickness (m)	Strain @ 900 days (%)	Value (MPa)	Date (days)	Value (MPa)	Date (days)	Value 1/FOS	Date (days)	Value (MPa)	Date Output (Days)	Value (MPa)	Date Output (Days)
																		Value (m^3)	Date Output (Days)		Value (m^3)	Date Output (Days)											
10	0	×				×				×	×		25 779	1.112	14 751	70.619	71 151	4 415 761	2870.61	62.06	330 734	2645.46	4.65	0.46	17.60	2881.83	23.11	2880.62	13.17	2335.24	15.12	2885.46	24.50	2150.61
14	0	×					×		×		×		15 769	1.392	8 350	23.932	59 163	5 668 992	2811.82	95.82	173 313	2856.36	2.93	0.56	11.79	2845.37	17.42	2840.92	11.35	2828.74	5.05	2856.36	17.84	2451.82
15	0	×					×		×		×		17 330	1.441	12 603	69.253	59 163	6 584 745	2870.61	111.30	169 031	2495.46	2.86	0.54	18.61	2882.10	23.99	2880.62	12.31	2395.14	18.58	2885.46	27.70	2270.61
27	0			×			×		×		×		36 197	1.693	12 002	29.483	71 151	5 618 184	2811.82	78.96	244 365	2046.36	3.43	0.60	10.56	2845.38	17.52	2840.82	11.92	2126.18	3.01	2856.36	15.89	2271.82
28	0		×			×			×		×		40 927	1.903	16 491	85.175	71 151	7 729 707	2870.61	108.64	340 677	2405.46	4.79	0.58	16.84	2882.10	23.41	2881.21	15.16	2043.29	12.72	2885.46	25.98	2210.61
32	0		×				×		×				25 351	2.044	10 352	28.836	59 163	8 515 558	2811.82	143.93	159 606	2856.36	2.70	0.63	11.60	2846.33	18.36	2841.77	12.17	2563.77	0.27	2631.82	18.25	2631.82
33	0		×			×			×		×		27 536	2.174	14 061	83.395	59 163	10 058 249	2870.61	170.01	192 424	2225.46	3.25	0.61	18.69	2882.46	25.15	2881.20	14.93	2576.03	17.64	2885.46	25.96	2510.61
39	0				×		×						34 673	2.739	6 231	10.510	59 163	7 455 414	2737.37	126.01	184 196	2188.03	3.11	0.52	4.28	2494.13	14.07	2475.45	3.32	2858.95	-4.97	2188.03	8.68	3095.00
45	0				×		×		×		×		55 202	2.892	13 944	34.187	71 151	8 513 798	2811.82	119.66	282 521	2046.36	3.97	0.36	10.06	2845.41	18.38	2840.09	13.54	2215.91	-4.81	2856.36	11.60	2091.82
46	0				×		×		×		×		62 458	3.243	17 716	98.772	71 151	11 551 325	2870.61	162.35	347 424	2555.46	4.88	0.33	16.89	2882.43	24.54	2881.18	16.13	2042.78	7.23	2885.46	14.93	2270.61
50	0			×			×	×		×			39 649	3.014	12 031	33.458	59 163	11 436 397	2811.82	193.30	191 364	2046.36	3.23	0.47	11.11	2846.36	18.99	2842.75	13.17	2746.81	-1.72	2856.36	11.11	2181.82
51	0			×			×		×		×		43 192	3.252	15 110	96.659	59 163	6 588 776	2870.61	111.37	224 283	2375.46	3.79	0.43	18.14	2882.73	25.54	2881.54	15.89	2757.23	12.72	2885.46	18.78	2885.46
6	1	×						×				×	29 307	0.069	8 334	4.266	103 713	500	2733.69	0.00	34 970	1095.00	0.34	0.15	-9.35	2176.98	0.40	2842.86	0.94	2175.46	-8.61	2553.03	0.16	2000.00
7	1	×						×				×	30 831	0.066	10 640	13.780	103 713	102 313	2856.36	0.99	34 970	1095.00	0.34	0.17	-0.83	2847.22	8.25	2844.77	1.47	2847.37	-2.13	2856.36	6.37	2856.36
8	1	×			×					×		×	33 596	0.089	12 982	39.804	103 713	130 394	2885.46	1.26	75 866	2885.46	0.73	0.20	3.87	2583.05	12.60	2402.40	3.05	2552.92	2.67	2885.46	11.20	2885.46
11	1	×				×		×				×	8 243	0.042	4 516	4.556	71 151	37 639	2918.03	0.53	8 118	1095.00	0.11	0.19	-0.97	2866.17	8.34	2851.48	1.34	2862.34	-5.43	2918.03	2.78	2000.00
16	1	×				×		×				×	4 915	0.009	3 249	4.480	59 163	105 428	2918.03	1.78	2 067	1095.00	0.03	0.23	0.22	2866.44	9.56	2840.89	1.64	2862.95	-4.54	2918.03	3.48	2918.03
29	1		×			×		×				×	12 215	0.385	6 576	5.512	71 151	276 144	2000.00	3.88	15 567	1095.00	0.22	0.30	-2.38	2862.53	9.41	2848.28	1.31	2523.01	-8.78	2918.03	1.39	2372.37
34	1		×				×	×	×			×	7 388	0.365	5 044	5.378	59 163	576 311	2000.00	9.74	9 642	1095.00	0.16	0.32	-1.38	2866.90	10.32	2840.98	1.39	2859.22	-7.82	2918.03	3.95	2372.37
47	1				×			×				×	17 743	0.860	8 561	6.353	71 151	837 825	2000.00	11.78	19 237	1095.00	0.27	0.22	-4.12	2858.96	10.50	2839.33	1.21	2519.04	-11.30	2188.03	2.44	2372.37
48	1			×			×		×			×	20 229	0.956	11 581	20.155	71 151	1 180 149	2811.82	16.59	41 291	2856.36	0.58	0.23	1.24	2845.51	14.73	2840.00	2.23	2844.59	-4.66	2856.36	7.38	2856.36
52	1			×			×		×			×	11 039	0.701	6 748	6.218	59 163	1 219 072	2000.00	20.61	13 136	1095.00	0.22	0.28	-2.98	2862.88	11.20	2840.20	1.26	2859.39	-11.38	2553.03	4.65	2372.37
2	2	×				×			×		×		19 389	0.791	4 112	7.582	71 151	811 624	2733.69	11.41	185 630	2188.03	2.61	0.35	5.43	2858.89	12.22	2837.30	6.47	2855.05	-3.36	2188.03	5.96	2368.69
3	2	×					×		×		×		13 232	1.109	2 931	7.471	59 163	1 967 344	2737.37	33.25	73 407	2188.03	1.24	0.44	5.72	2866.37	11.94	2844.56	8.54	2845.43	-3.37	2188.03	10.32	2737.37
9	2	×				×			×				22 702	0.980	9 714	24.393	71 151	2 986 703	2810.91	41.98	196 853	2046.36	2.77	0.47	11.01	2844.53	16.80	2839.98	11.43	2740.13	1.25	2856.36	15.57	2540.91
20	2		×			×			×		×		31 529	1.527	6 056	9.186	71 151	2 027 522	2737.37	28.50	235 616	2188.03	3.31	0.52	4.24	2490.35	13.13	2468.14	3.27	2851.78	-3.99	2188.03	8.33	2372.37
21	2		×				×		×		×		21 763	1.172	4 632	9.034	59 163	4 647 003	2737.37	78.55	127 887	2188.03	2.16	0.59	5.14	2862.56	13.06	2843.81	5.28	2862.56	-4.16	2188.03	10.56	2737.37
38	2					×		×					48 942	2.711	7 892	10.708	71 151	3 788 467	2737.37	53.25	275 139	2188.03	3.87	0.37	2.39	2855.35	13.20	2464.63	2.31	2486.68	-4.88	2188.03	8.63	2372.37
49	2			×		×				×			22 313	1.052	13 542	57.833	71 151	2 402 898	2870.61	33.77	84 727	2525.46	1.19	0.21	6.23	2882.38	19.47	2880.32	6.55	2882.38	1.96	2885.46	14.00	2885.46
54	2			×			×			×			13 485	0.864	11 460	56.511	59 163	3 746 265	2870.61	63.32	63 376	2405.46	1.07	0.27	6.81	2882.70	19.89	2880.91	9.26	2882.70	4.04	2885.46	16.08	2885.46
12	3	×					×			×			9 615	0.038	7 569	14.595	71 151	312 429	2810.91	4.39	91 326	2856.36	1.28	0.28	4.15	2845.57	13.35	2237.16	4.36	2845.57	0.00	2856.36	8.03	2856.36
17	3	×					×		×				5 809	0.115	6 196	14.267	59 163	544 514	2811.82	9.20	92 788	2856.36	1.57	0.34	4.71	2846.12	13.81	2840.06	7.22	2846.12	1.54	2856.36	9.56	2856.36
30	3		×			×			×				14 065	0.461	9 636	17.518	71 151	576 552	2811.82	8.10	67 418	2856.36	0.95	0.39	2.68	2846.40	13.97	2839.17	2.79	2845.29	-2.01	2856.36	8.03	2856.36
35	3		×				×	×					8 568	0.473	8 055	17.076	59 163	1 371 160	2811.82	23.18	77 572	2856.36	1.31	0.41	3.31	2846.43	14.47	2840.01	3.45	2846.43	-1.15	2856.36	8.88	2856.36
53	3						×		×				12 662	0.825	9 675	19.649	59 163	2 792 813	2811.82	47.21	48 151	2856.36	0.81	0.29	1.65	2847.35	14.89	2840.92	2.45	2846.43	-3.10	2856.36	8.93	2856.36
24	4		×		×				×				44 525	0.998	10 827	5.581	103 713	2 059	2737.37	0.02	41 566	1095.00	0.40	0.07	-10.79	2862.66	1.23	2840.63	0.96	2888.18	-10.12	2918.03	0.03	2737.37
25	4		×		×				×				46 787	0.974	13 351	17.943	103 713	46 060	2856.36	0.44	41 566	1095.00	0.40	0.07	-1.45	2846.45	9.39	2844.56	1.49	2847.34	-3.39	2856.36	6.64	2856.36
26	4		×		×					×			50 943	1.069	15 340	51.695	103 713	132 930	2885.46	1.28	88 496	2885.46	0.85	0.08	3.29	2793.03	13.80	2522.37	2.66	2793.03	2.11	2885.46	12.15	2885.46
42	4			×		×			×				62 192	2.365	13 289	6.469	103 700	11 064	2737.37	0.11	44 450	1095.00	0.43	0.08	-14.66	2173.28	-1.01	2827.98	0.93	2169.96	-12.54	2188.03	0.34	2737.37
43	4			×		×			×				64 738	2.270	15 634	20.715	103 700	56 735	2811.82	0.55	44 450	1095.00	0.43	0.08	-5.78	2845.87	7.41	2843.68	1.28	2309.51	-5.79	2856.36	6.24	2856.36
44	4			×		×				×			69 814	2.446	16 853	59.613	103 700	181 640	2870.61	1.75	49 031	2885.46	0.47	0.08	-0.01	2643.05	12.51	2612.71	1.88	2613.29	0.44	2885.46	12.49	2885.46
1	5	×					×			×			57 614	0.322	11 542	7.714	103 713	2 826	2733.69	0.03	441 662	2188.03	4.26	0.24	-0.64	2859.13	5.90	2844.25	1.66	2881.08	-4.26	2918.00	0.27	2733.69
4	5	×					×			×			59 576	0.326	12 457	24.908	103 713	193 007	2810.91	1.86	460 528	2046.36	4.44	0.33	7.96	2754.60	13.95	2748.68	10.70	2124.26	2.17	2856.36	6.21	2856.36
5	5	×					×			×			67 270	0.429	17 121	72.367	103 713	354 492	2870.30	3.42	565 436	2885.46	5.45	0.47	13.28	2882.07	18.97	2880.02	12.87	2517.88	9.01	2885.46	13.05	2885.46
19	5			×			×			×			84 738	1.938	10 124	9.324	103 713	10 992	2737.37	0.11	476 559	2188.03	4.59	0.11	-1.93	2857.69	6.45	2840.75	1.60	2870.04	-5.16	2918.03	1.88	2737.37
22	5		×				×			×			90 548	1.924	15 099	30.113	103 713	386 689	2811.82	3.73	495 593	2046.36	4.78	0.14	7.24	2484.52	14.64	2209.11	9.00	2663.62	-0.35	2856.36	4.69	2856.36
23	5		×				×			×			101 501	2.182	19 206	87.271	103 713	649 166	2870.61	6.26	520 511	2705.46	5.02	0.17	12.42	2882.44	18.89	2880.59	14.33	2073.13	7.92	2885.46	12.97	2885.46
37	5				×			×					126 731	4.793	12 393	10.888	103 700	68 943	2737.37	0.66	478 110	2188.03	4.61	0.15	-8.45	2845.26	3.00	2831.17	1.28	2169.66	-6.77	2188.03	3.67	2737.37
40	5			×			×			×			133 784	4.663	17 359	35.016	103 700	593 956	2811.82	5.73	508 236	2046.36	4.90	0.16	4.13	2302.65	13.57	2209.77	2.87	2301.96	-3.83	2856.64	4.19	2271.82
41	5			×			×			×			148 156	5.169	20 628	101.332	103 700	1 117 260	2870.61	10.77	507 637	2015.46	4.90	0.19	10.71	2372.41	18.36	2281.22	15.28	2192.67	6.66	2885.46	12.71	2885.46
13	6	×					×			×			10 770	0.045	10 591	41.957	71 151	367 183	2645.46	5.16	89 759	2885.46	1.26	0.34	9.24	2881.78	18.37	2879.94	11.90	2548.12	6.61	2885.46	14.63	2885.46
18	6	×					×			×			6 380	0.089	8 889	40.974	59 163	635 117	2870.61	10.74	74 764	2345.46	1.26	0.38	10.11	2881.80	19.12	2880.61	12.31	2697.65	10.27	2885.46	18.13	2885.46
31	6		×				×			×			15 561	0.507	12 259	50.256	71 151	1 080 031	2870.61	15.18	84 090	2375.46	1.18	0.42	7.44	2882.18	18.59	2879.68	13.01	2850.54	6.23	2885.46	16.25	2885.46
36	6		×				×			×			9 197	0.480	10 339	49.033	59 163	2 209 074	2870.61	37.34	69 985	2315.46	1.18	0.41	8.71	2882.37	19.77	2880.65	13.72	2819.36	7.10	2885.46	17.14	2885.46

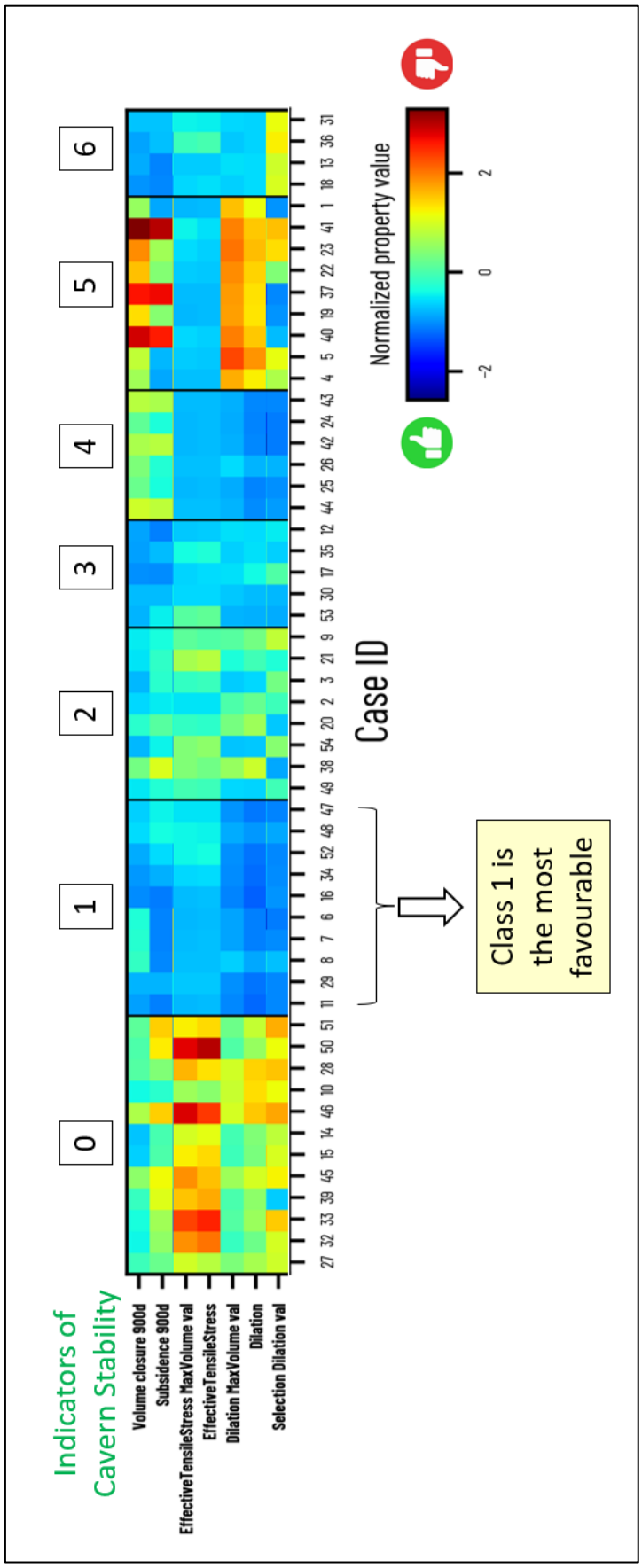

Figure 226. Class 1 configurations, mostly in blue, are the most favourable.

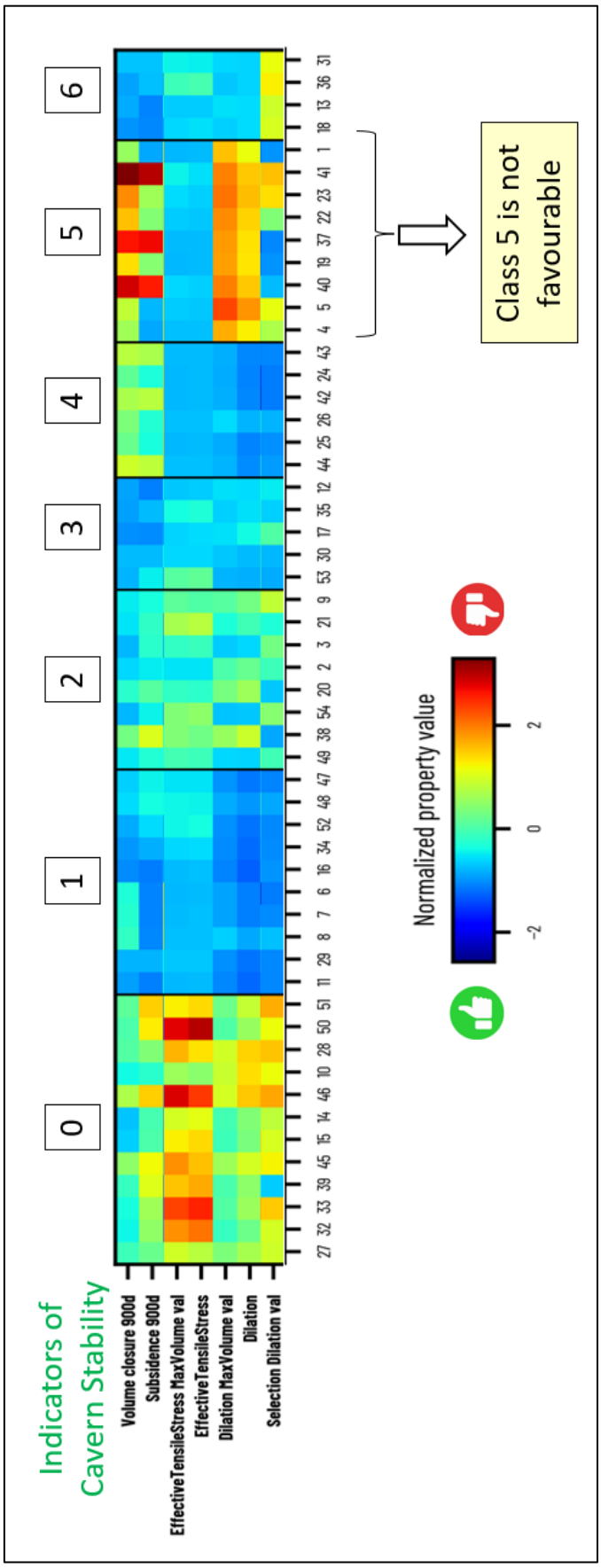

Figure 227. Class 5 configurations are not favourable.

		Depth casing shoe			Cavern diameter			Cycling period			P_{min}	
Case	Class	Z1	Z2	Z3	D1	D2	D3	S	Q	M	G1	G2
6	1	×			×			×				×
7	1	×			×				×			×
8	1	×			×					×		×
11	1	×				×		×				×
16	1	×					×	×				×
29	1		×			×		×				×
34	1		×				×	×				×
47	1			×		×		×				×
48	1			×		×			×			×
52	1			×			×	×				×

Class 1

High minimum pressure

		Depth casing shoe			Cavern diameter			Cycling period			P_{min}	
Case	Class	Z1	Z2	Z3	D1	D2	D3	S	Q	M	G1	G2
1	5	×			×			×			×	
4	5	×			×				×		×	
5	5	×			×					×	×	
19	5		×		×			×			×	
22	5		×		×				×		×	
23	5		×		×					×	×	
37	5			×	×			×			×	
40	5			×	×				×		×	
41	5			×	×					×	×	

Class 5

Low minimum pressure

Figure 228. Classes 1 and 5 correspond respectively to cases with a minimum pressure gradient of 0.1 bar/m and cases with a minimum pressure of 0.05 bar/m. Class 5 is not favourable compared to Class 1.

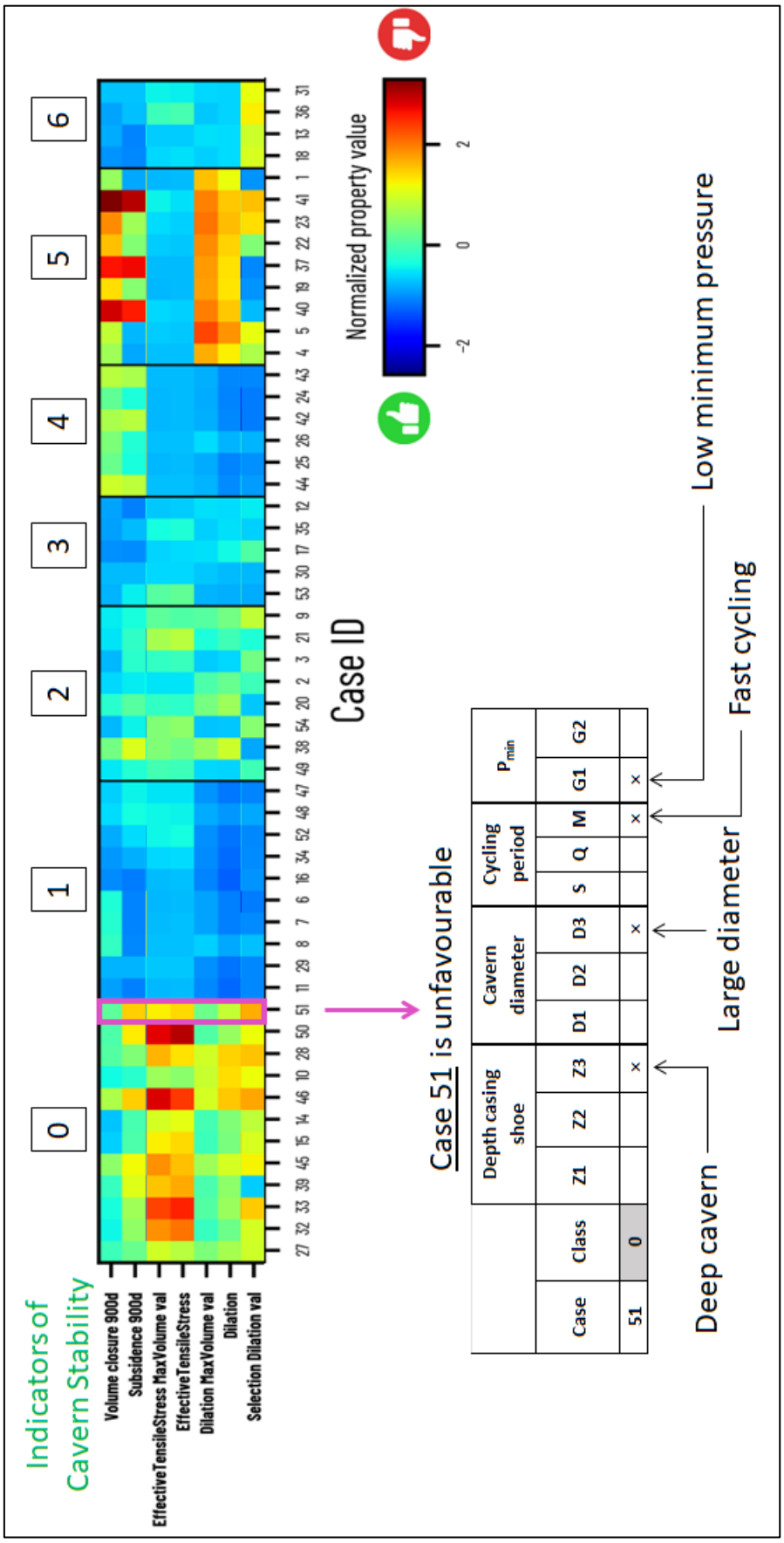

Figure 229. Example of a very unfavourable configuration (Case #51), this is the case of a deep cavern with a large diameter, operated with rapid cycles and low minimum pressure.

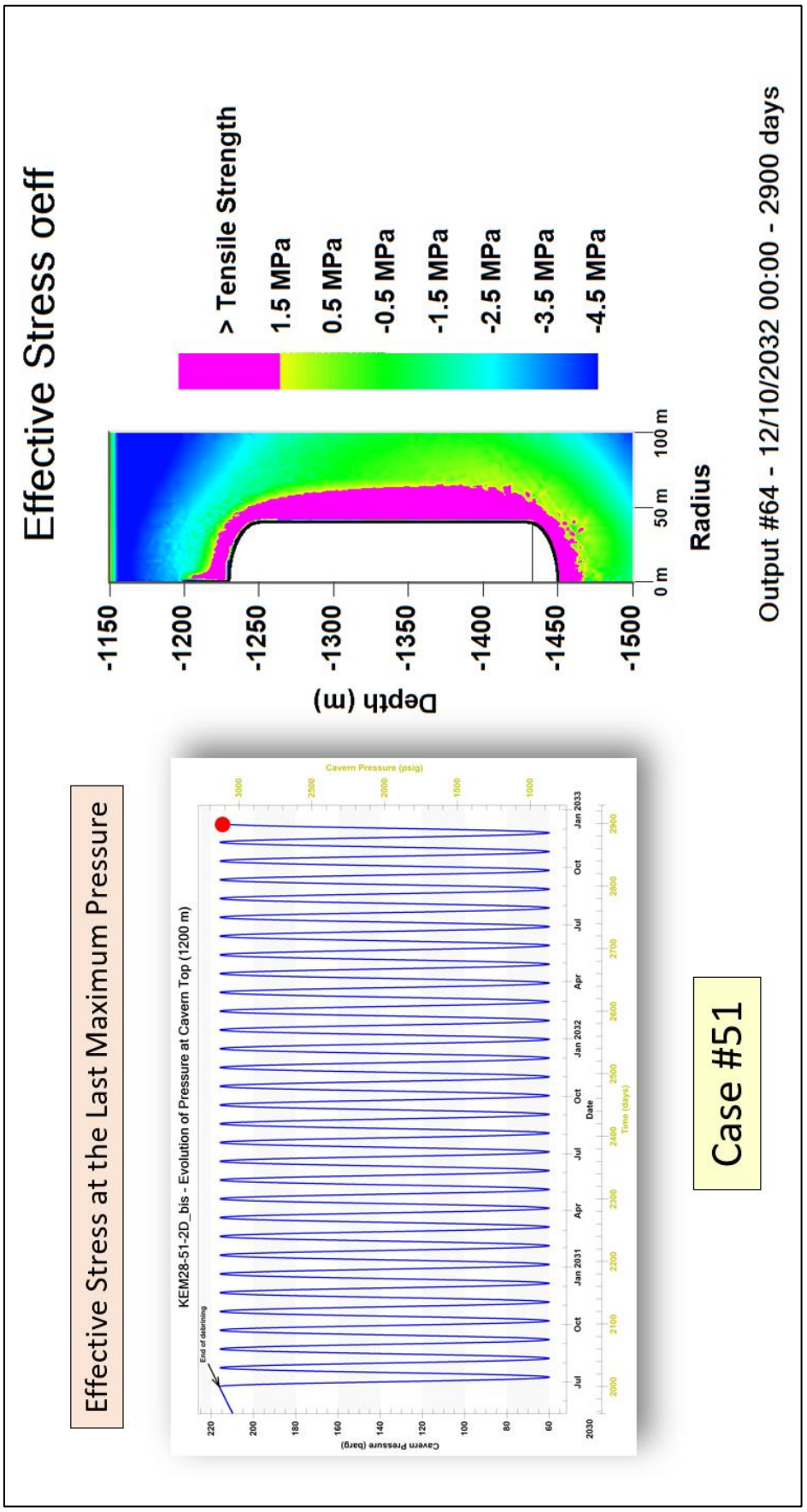

Figure 230. Unfavourable case: a very large zone of effective tension appears at the maximum pressure of the last cycle in case #51.

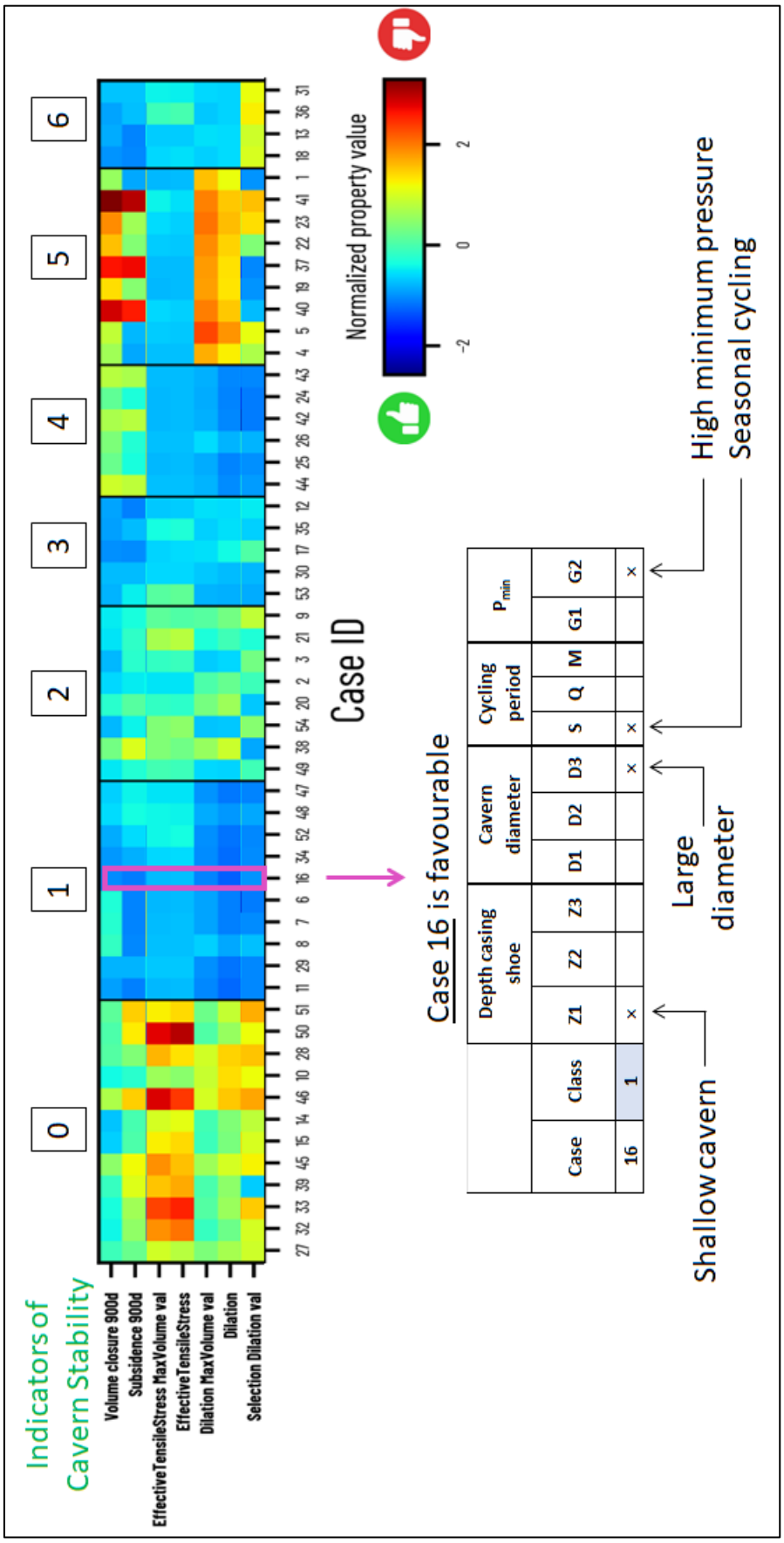

Figure 231. Example of a favourable configuration (Case 16), this is the case of a relatively shallow cavern with a large diameter, operated with yearly cycles and relatively high minimum pressure.

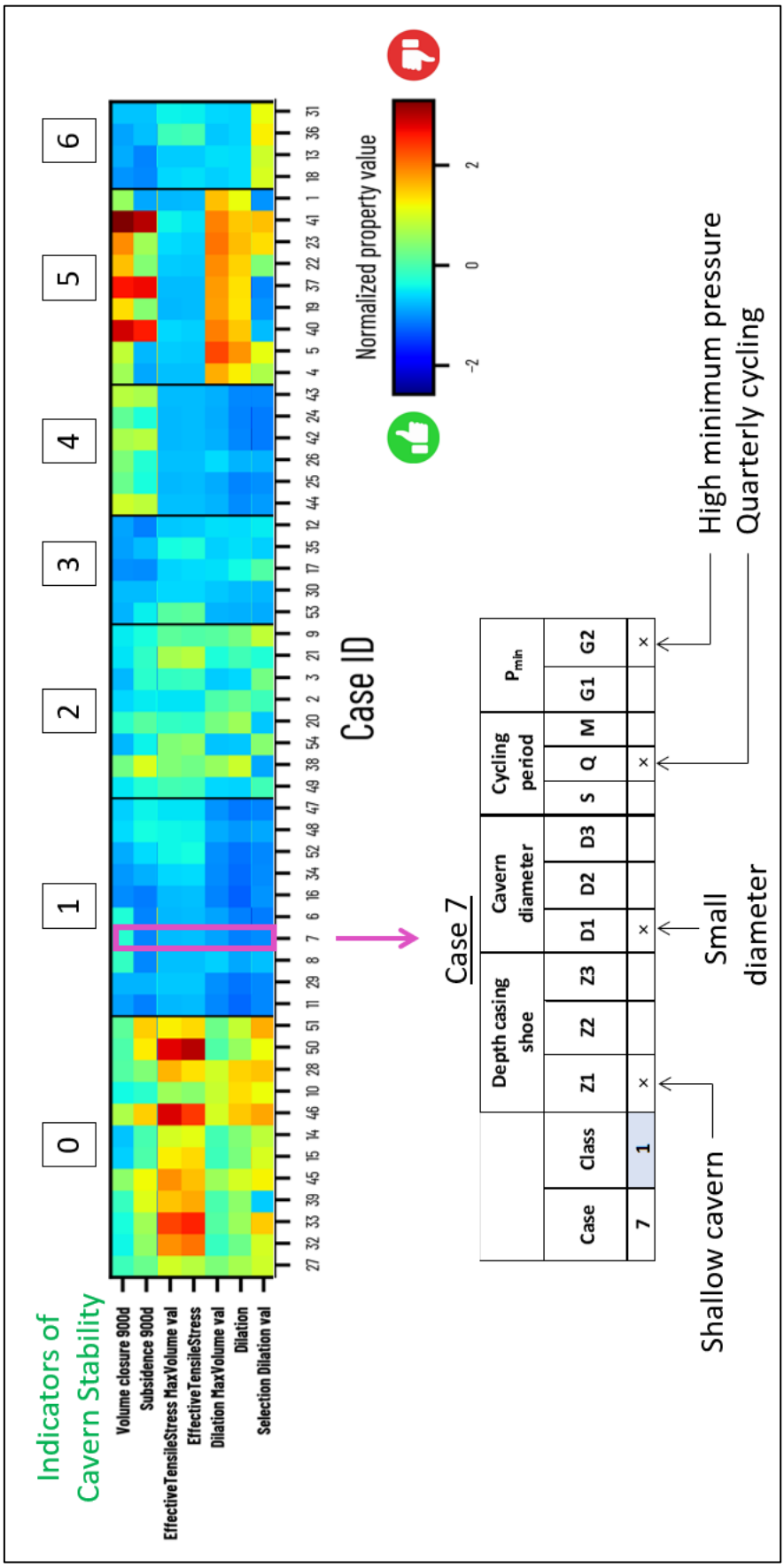

Figure 232. Example of a favourable configuration (Case 7 = reference case), this is the case of a relatively shallow cavern with a small diameter, operated with quarterly cycles and low minimum pressure

1.10 Additional sensitivity case: faster steady-state creep

1.10.1 Introduction

An additional variant has been realized by considering a much creep prone salt. The parameter set is the same as for the previous cases, except that prefactor A_{dc} of the steady-state dislocation creep is 50 times larger than for the previous cases (Table 24).

Table 24. Munson-Dawson parameters for faster dislocation creep.

	Parameter	Units	Value
Steady-state part	A_{dc}	/MPa^n-yr	900
	n_{dc}	–	4.86
	Q_{dc}/R	K	6495

1.10.2 Computation results

The evolution of the loss of cavern volume since the end of leaching is shown in Figure 233. The loss of volume is very large, 203 000 m^3 after 900 days of cycling, compared to 30 831 m^3 in the reference case (Case #07). It should be noted that the loss of volume is 6.6 times greater than in the reference case, while the prefactor of the steady-state dislocation creep prefactor is 50 times greater. This is because, in this configuration, most of the loss of cavern volume comes from the transient component of the dislocation creep.

The evolution of subsidence, more precisely the vertical displacement at the surface above the cavern, is shown on the Figure 234.

Figure 235 shows the effective stress and dilation FOS contours at the last minimum pressure and at the last maximum pressure. Small areas of effective tension appear at the roof of the cavern (Figure 236), at minimum and maximum pressure, but they are small in amplitude (of the order of the tensile strength of salt) and not very extensive.

There is almost no dilatation at the last minimum pressure and at the last maximum pressure in this case (FOS is larger than 1).

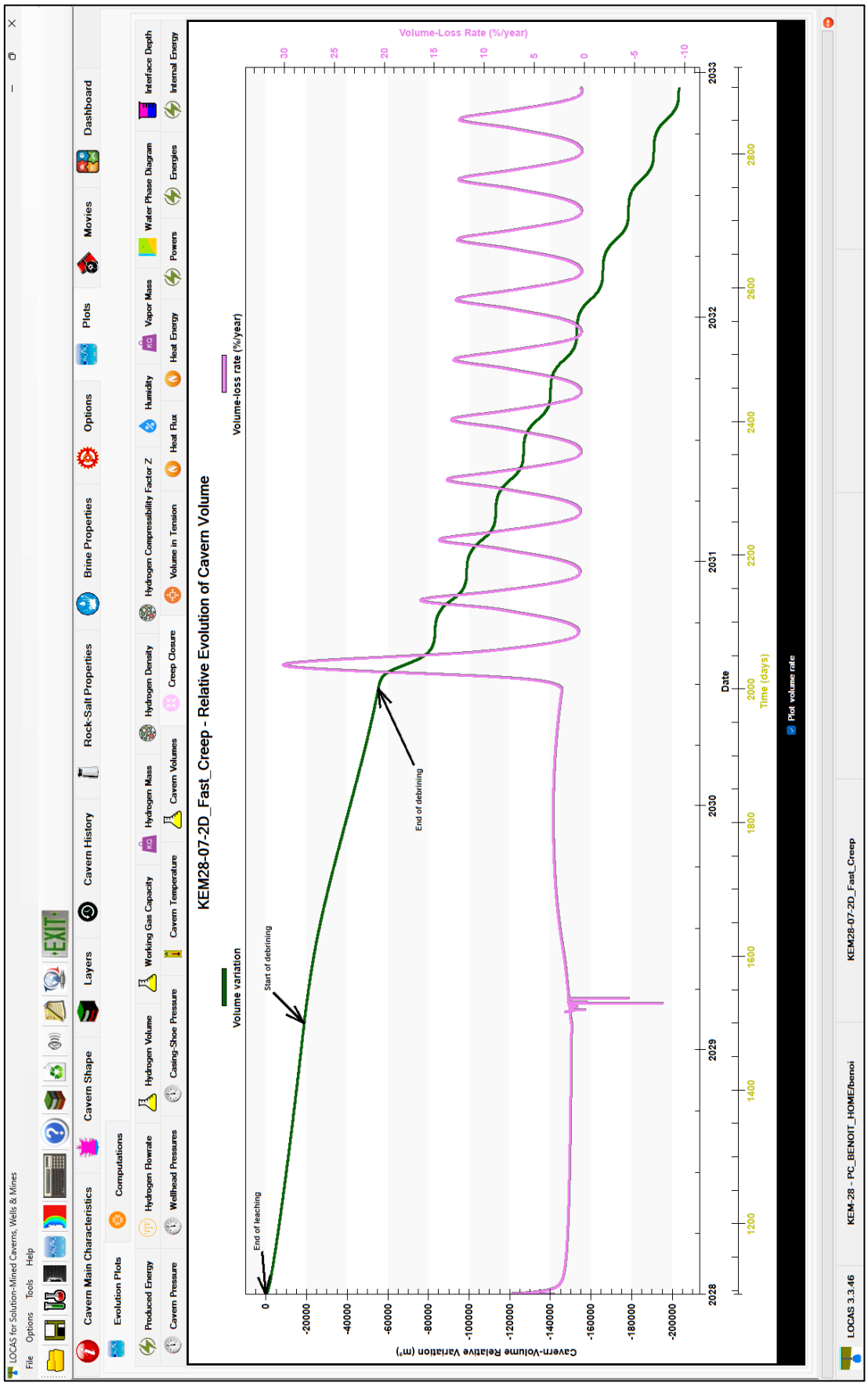

Figure 233. Fast creep – evolution of cavern volume loss and loss rate since the end of leaching. The average rate of volume loss is greater than 5%/year during pressure cycling.

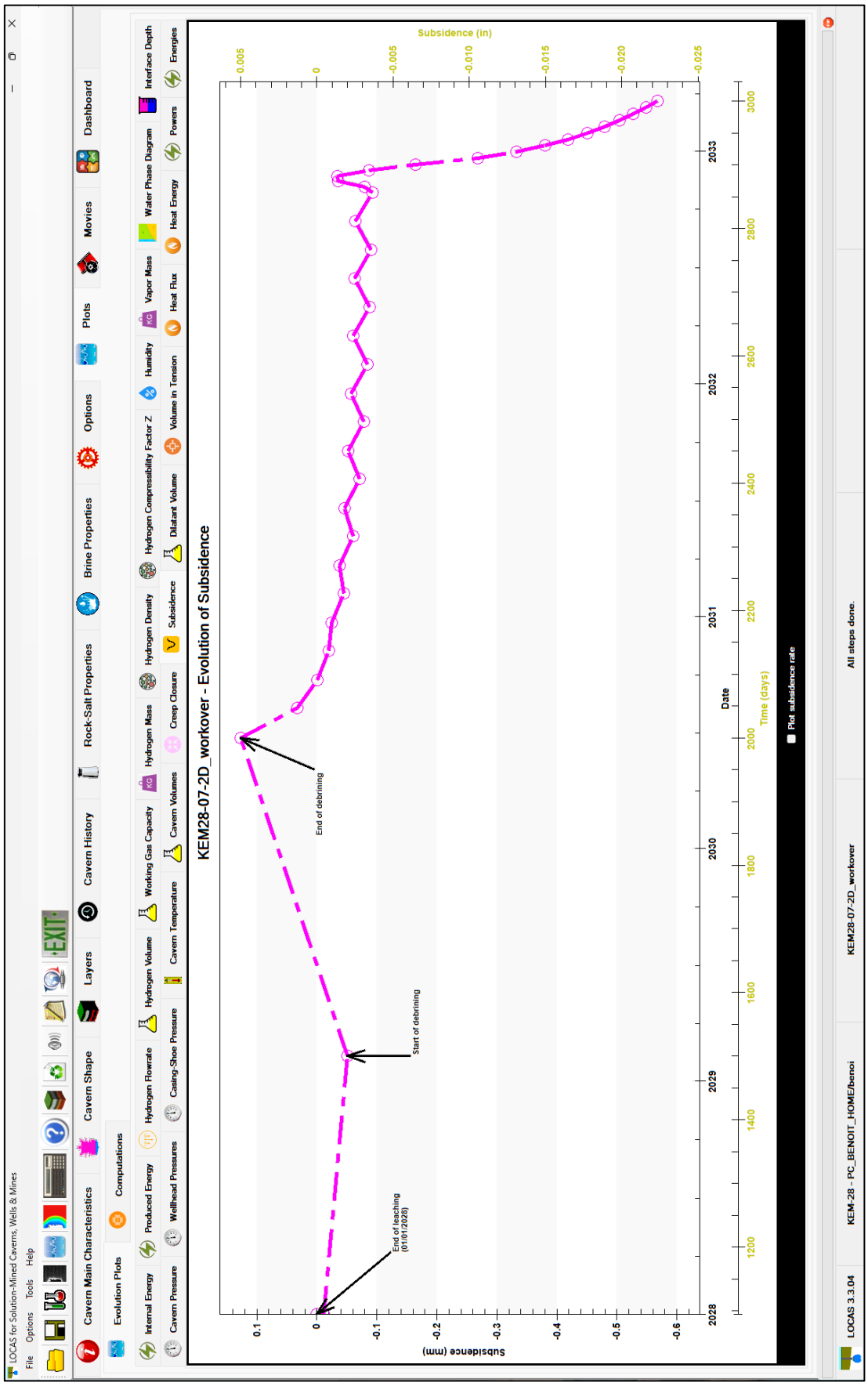

Figure 234. Fast creep – evolution of maximum subsidence from end of leaching to end of workover. Subsidence increases rapidly during workover but remains moderate (a fraction of a mm).

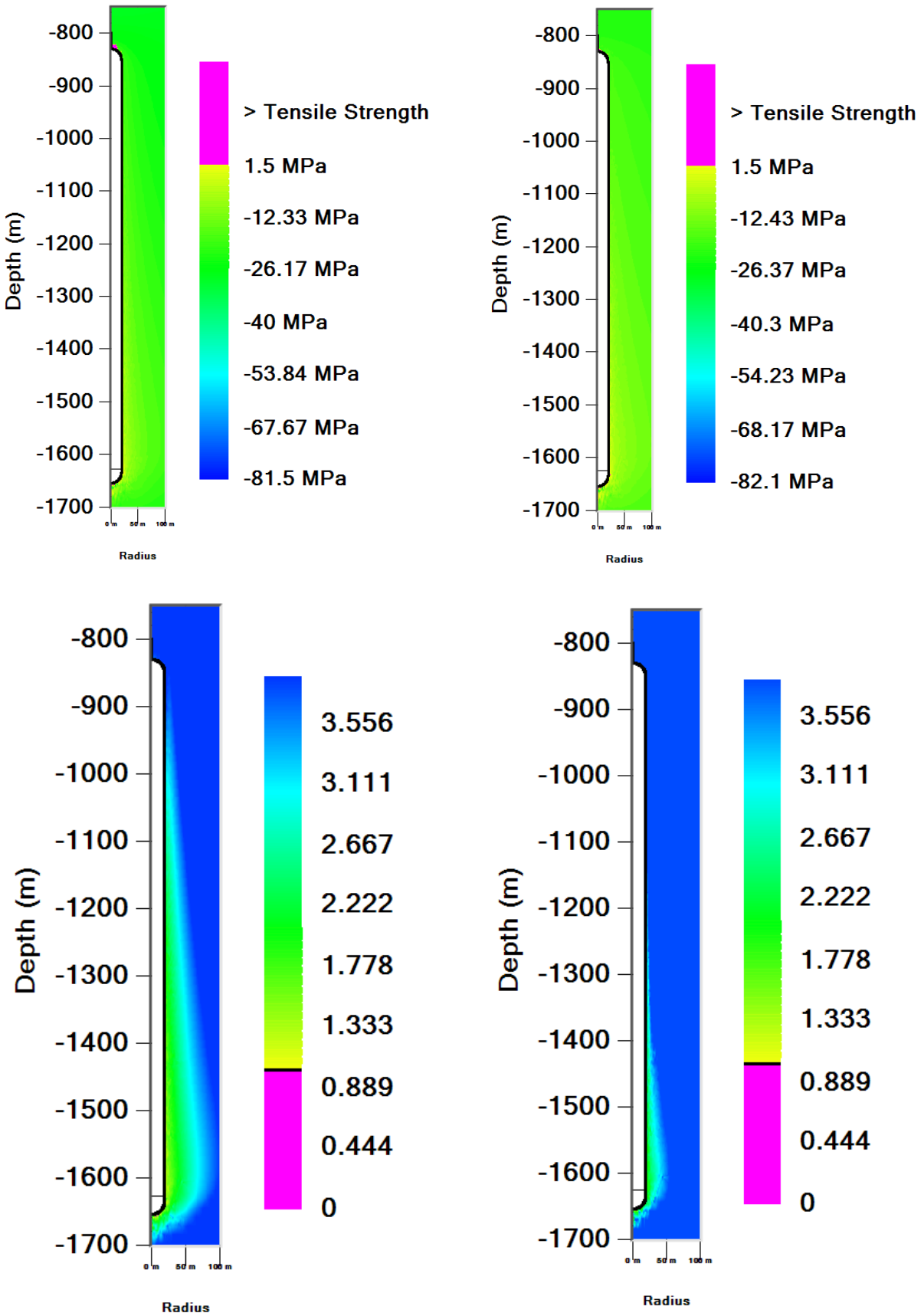

Figure 235. Fast creep –Effective stress (top) and dilation FOS (bottom) contours at the last minimum pressure (left) and at the last maximum pressure (right). There is no large damaged area.

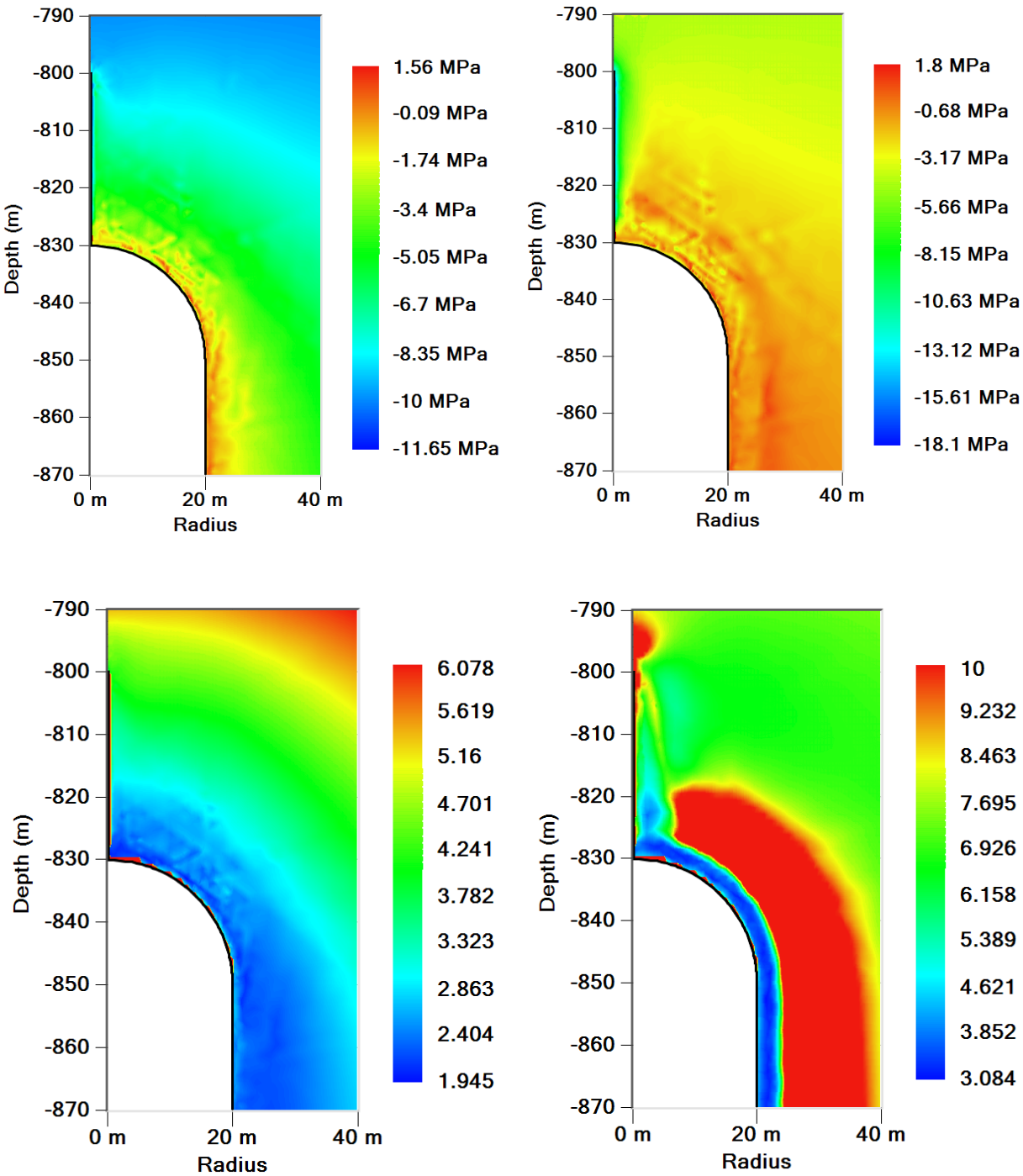

Figure 236. Fast creep – Effective stress (top) and dilation FOS (bottom) contours at the last minimum pressure (left) and at the last maximum pressure (right) - zoom in the vicinity of cavern roof. There is no damaged area.

1.11 Blowout modelling

1.11.1 Introduction

Blowout (wellhead failure leading to the loss of most or all the products) is an especially severe concern in the case of underground storages. Only two natural gas blowouts from salt caverns are known. The first one is the Moss Bluff case in Texas, 2004 (Brouard Consulting and Respec, 2013) which led to the loss of the full natural gas inventory. In Europe (not in the US) it is mandatory to set an underground safety valve (SSSV) in a gas cavern well. Probability of a blowout is lowered by several orders of magnitude by this (no case of a blowout is known when the cavern is equipped with such a valve).

Formation of a cloud in which flammability limit is reached is to be expected in the early times of the blowout. Its shape and height are a function of atmospheric conditions. Due to buoyancy and small density of hydrogen, this cloud vanishes rapidly.

1.11.2 Thermodynamics of a blowout

During a blowout, the gas velocity in a borehole typically is a couple hundreds of meters per second (more, when hydrogen is considered). In other words, only a few seconds are needed for gas to travel from the cavern top to ground level. Such a short period of time is insufficient for cavern pressure and temperature change significantly. Gas flow is adiabatic and turbulent, and the effects of friction are confined to a thin boundary layer at the steel casing wall (Djizanne et al., 2022). The gas flow, called *Fanno flow*, can be described by the following set of equations:

$$\begin{cases} \dot{m} = \dfrac{u(z)}{v(z)} = -\dfrac{V_0}{\Sigma}\dfrac{\dot{v}(z)}{v(z)} \\ \dfrac{\partial H}{\partial z} + u\dfrac{\partial u}{\partial z} + g = 0 \\ \dfrac{\partial P}{\partial z} + \rho u\dfrac{\partial u}{\partial z} + \rho g + \zeta\left(u,T\right) = 0 \\ T\dfrac{\partial S}{\partial z} = \dfrac{\partial H}{\partial z} - \dfrac{1}{\rho}\dfrac{\partial P}{\partial z} = \dfrac{\zeta\left(u,T\right)}{\rho} > 0 \end{cases} \tag{81}$$

The first equation is the mass conservation equation, where u is gas velocity, and $\frac{u(z)}{v(z)}$ is a constant in the well. The second equation is the energy equation where H is gas enthalpy. There is no heat transfer from the rock mass along the wellbore. The third equation is the momentum equation. Head losses per unit of length are described by $f > 0$, where f is the friction factor, which is a function of gas velocity, temperature, wellbore inner diameter, wall roughness, etc. The last equation is the condition of the positivity of entropy (S) change, which plays an important role. Closed-form solutions can be derived when some simplifications are considered, but complete numerical modelling is achievable and recommended.

The gas flow must remain subsonic in the wellbore. At the beginning of the blowout, the flow, which is sonic at ground level, is said to be a *choked flow*, and wellhead pressure is larger than atmospheric pressure. Conversely, when the cavern pressure becomes relatively small, the gas flow is said to be a *normal flow* and, even at ground level, the gas rate is significantly slower than the speed of sound, and wellhead pressure is equal to atmospheric pressure.

Very low temperatures can be reached in the cavern, along the wellbore and at the wellhead during the blowout (see example below). This can potentially affect the materials in the wellbore (cements, rubber, polymers, SSSV). In some cases, it can start to rain or even snow in the cavern depending on the initial gas-water content.

1.11.3 Modelling the blowout in the reference case

Figure 237 shows the evolution of casing-shoe pressure since the start of leaching. The blowout is assumed to occur at a very unfavourable moment, i.e., when the hydrogen pressure is at its maximum during the last cycle (Figure 238). The blowout lasts about a week, as shown in Figure 239. The pressure in the cavern decreases from maximum pressure to atmospheric pressure (plus the weight of the column of hydrogen in the well).

Figure 240 shows changes in the temperature of the hydrogen and brine in the cavern during the blowout. The temperature of the hydrogen in the cavern reached a minimum of -7°C after around two and a half days (Figure 241).

At the surface, the temperature of the hydrogen coming out of the well drops considerably, reaching a minimum of around -37°C after around two and a half days (Figure 242).

The evolution of the loss of cavern volume since the end of leaching is shown in Figure 243. We can see that the loss of volume caused by the blowout is very significant (in the order of 45 000 m^3) compared to the previous loss of volume.

The evolution of subsidence, more precisely the vertical displacement at the surface above the cavern, is shown on the Figure 244. The significant loss of volume in the cavern caused by the blowout is quickly reflected in the subsidence, which increases by around 0.5 mm in the quarter following the blowout. The cavern remains at atmospheric pressure for a fairly long period after the blowout before it can be re-pressurised by reinjecting brine.

Figure 245 shows the distribution of hydrogen velocity in the well at the start of the blowout. The hydrogen exits at the speed of sound at this point (nearly 1300 m/s during choked flow).

Figure 246 shows FOS (Factor of Safety) dilation contours at the end of the blowout (i.e., after one week). A dilatant zone with a maximum thickness of around 12 m appears in the lower part of the cavern (Figure 247).

Figure 248 and Figure 249 show that no significant effective tensile stress appears on the cavern wall at the end of the blowout, despite the significant drop in temperature.

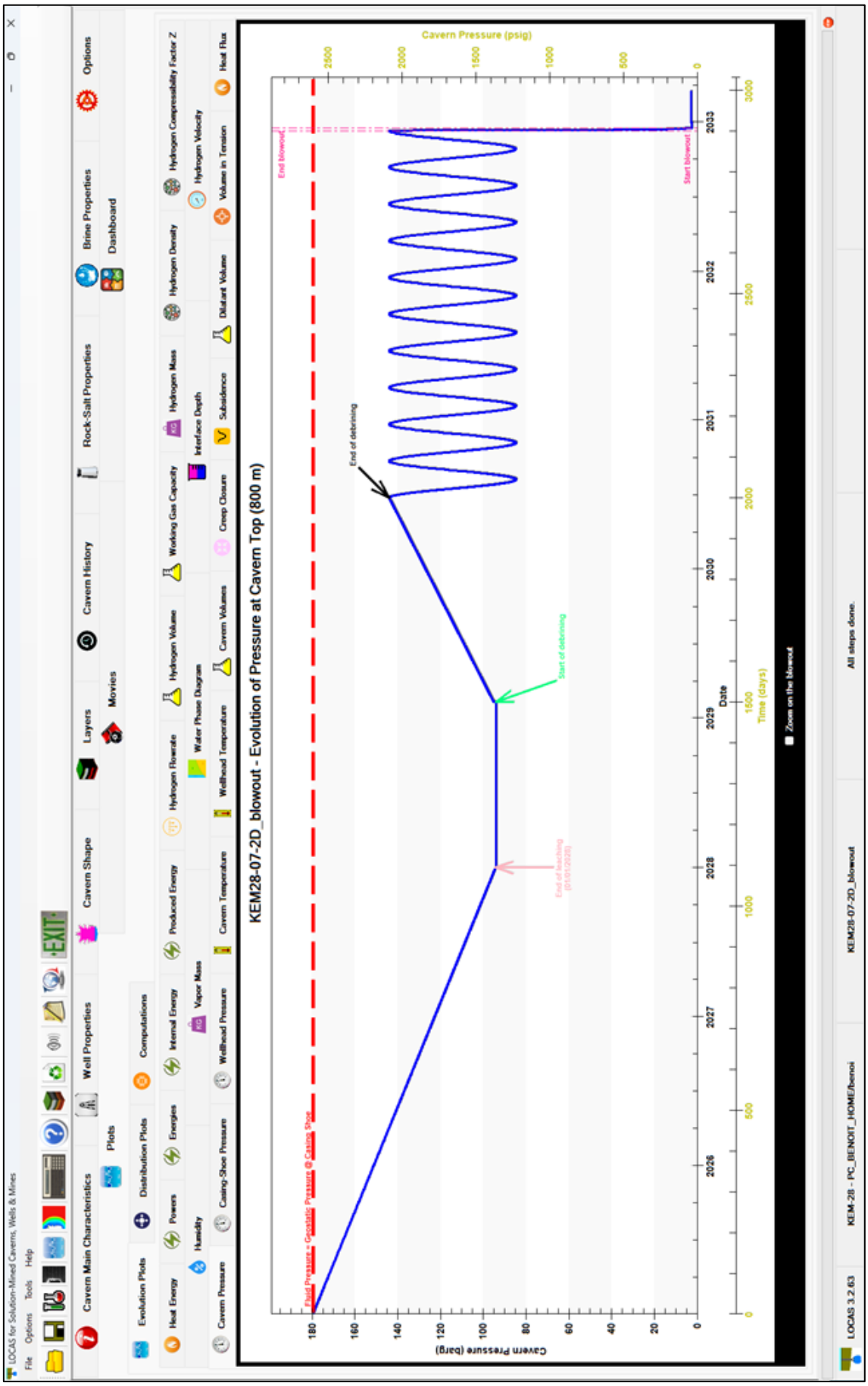

Figure 237. Pressure evolution in the cavern, the blowout is assumed to occur at the maximum pressure of the last cycle.

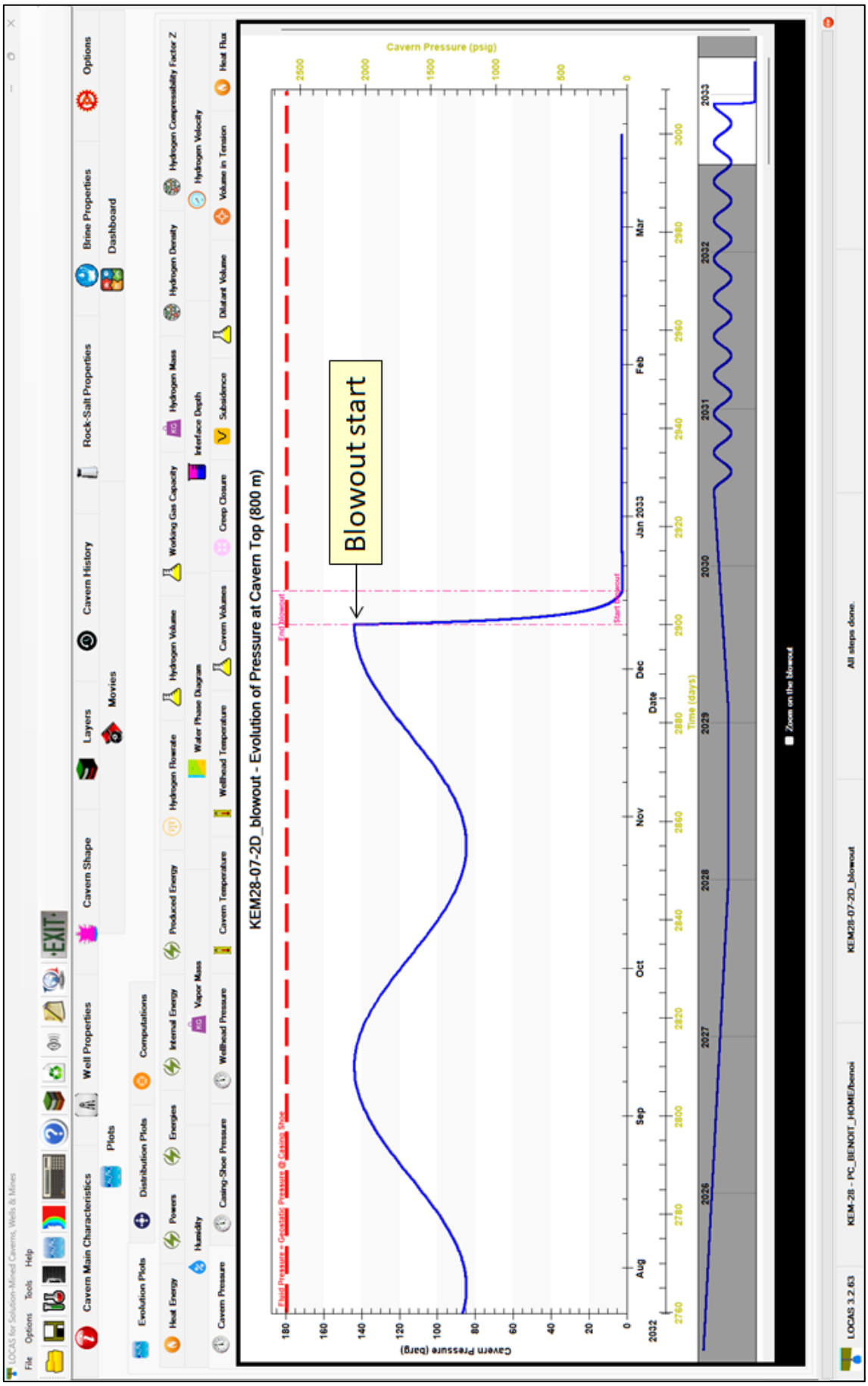

Figure 238. Pressure evolution in the cavern before and after the blowout. The pressure in the cavern decreases rapidly to atmospheric pressure in about a week.

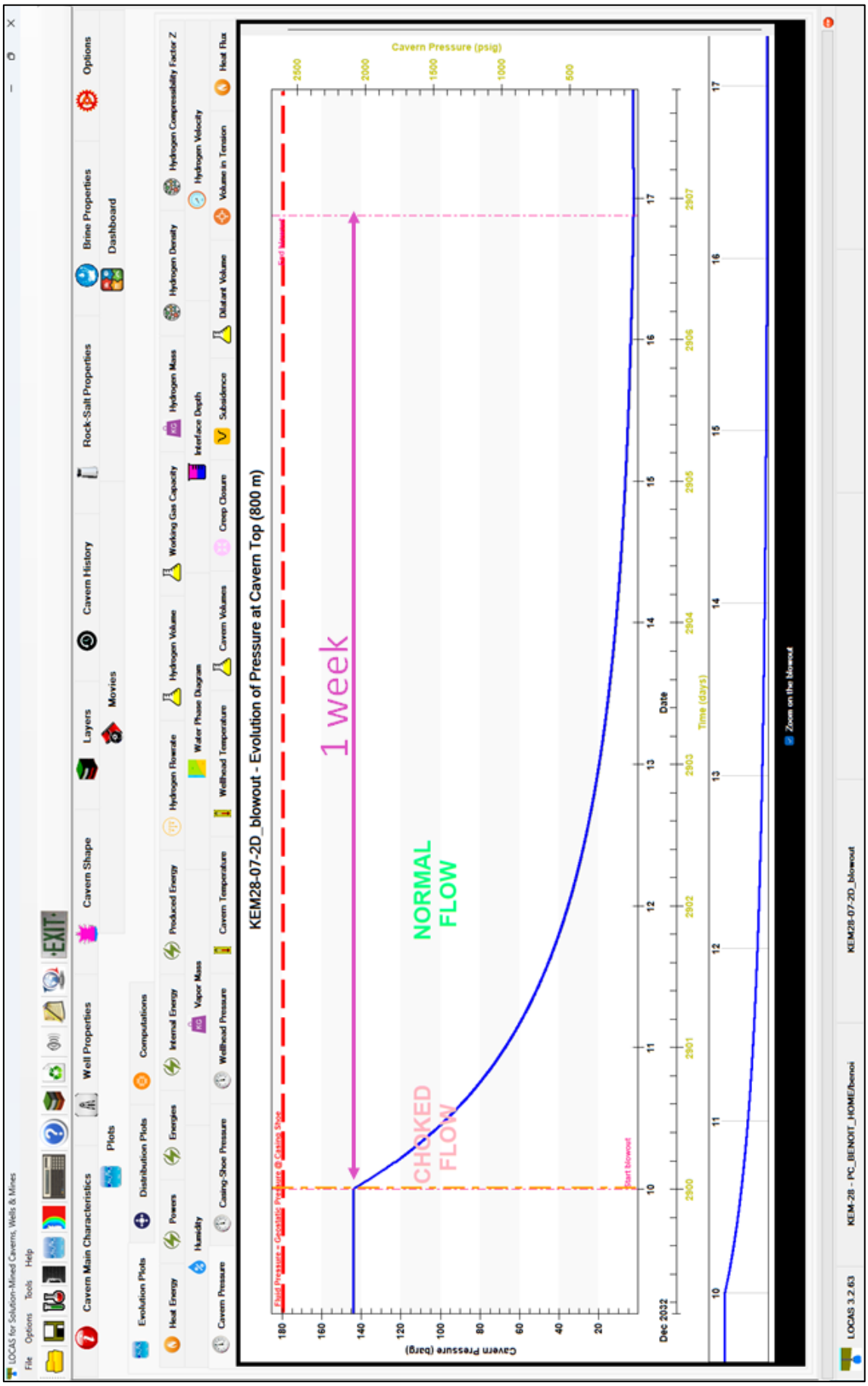

Figure 239. Pressure evolution in the cavern during the blowout, it lasts about one week.

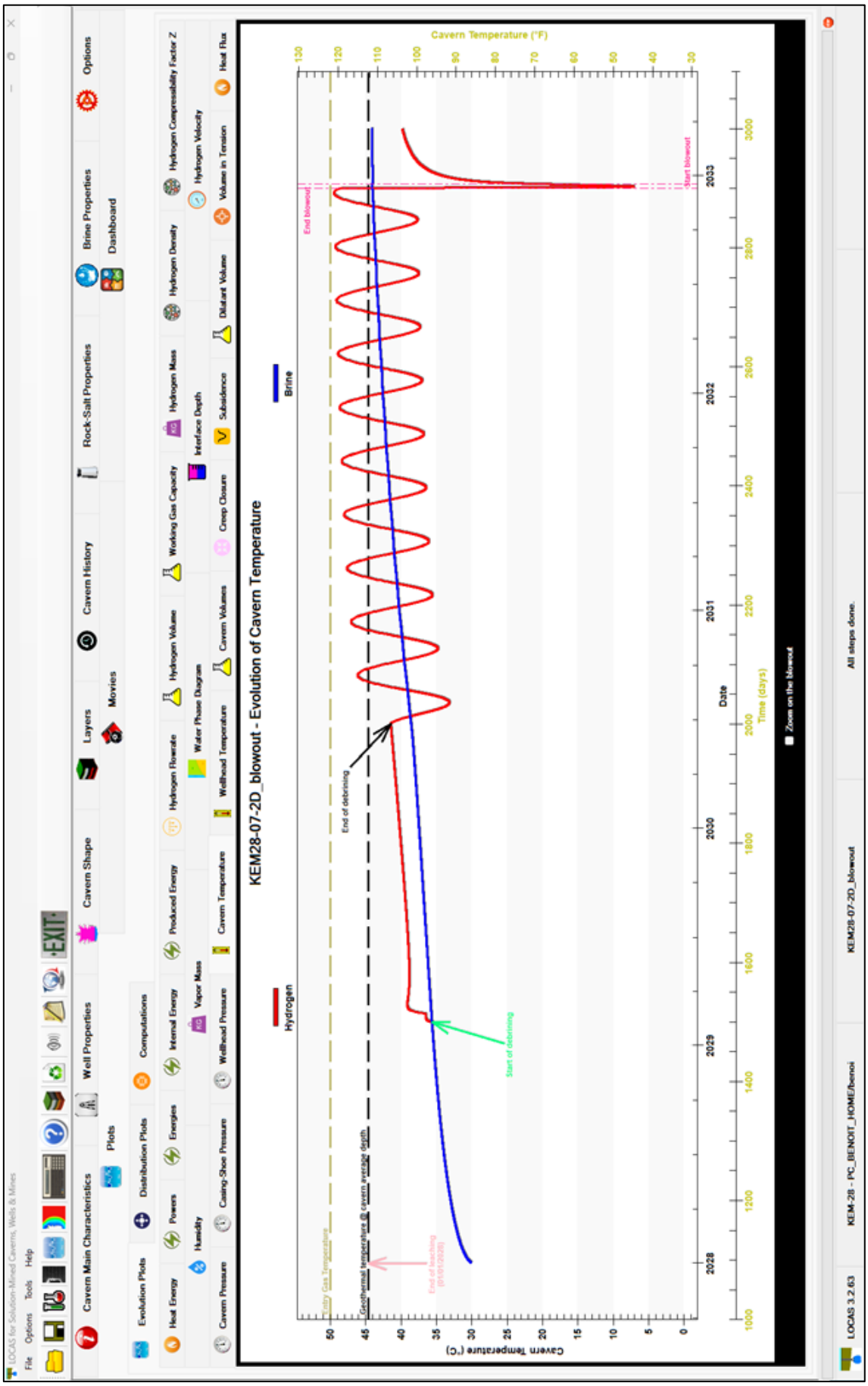

Figure 240. Temperature evolution in the cavern from the end of leaching to blowout. The temperature of the hydrogen in the cavern quickly decreases during the blowout.

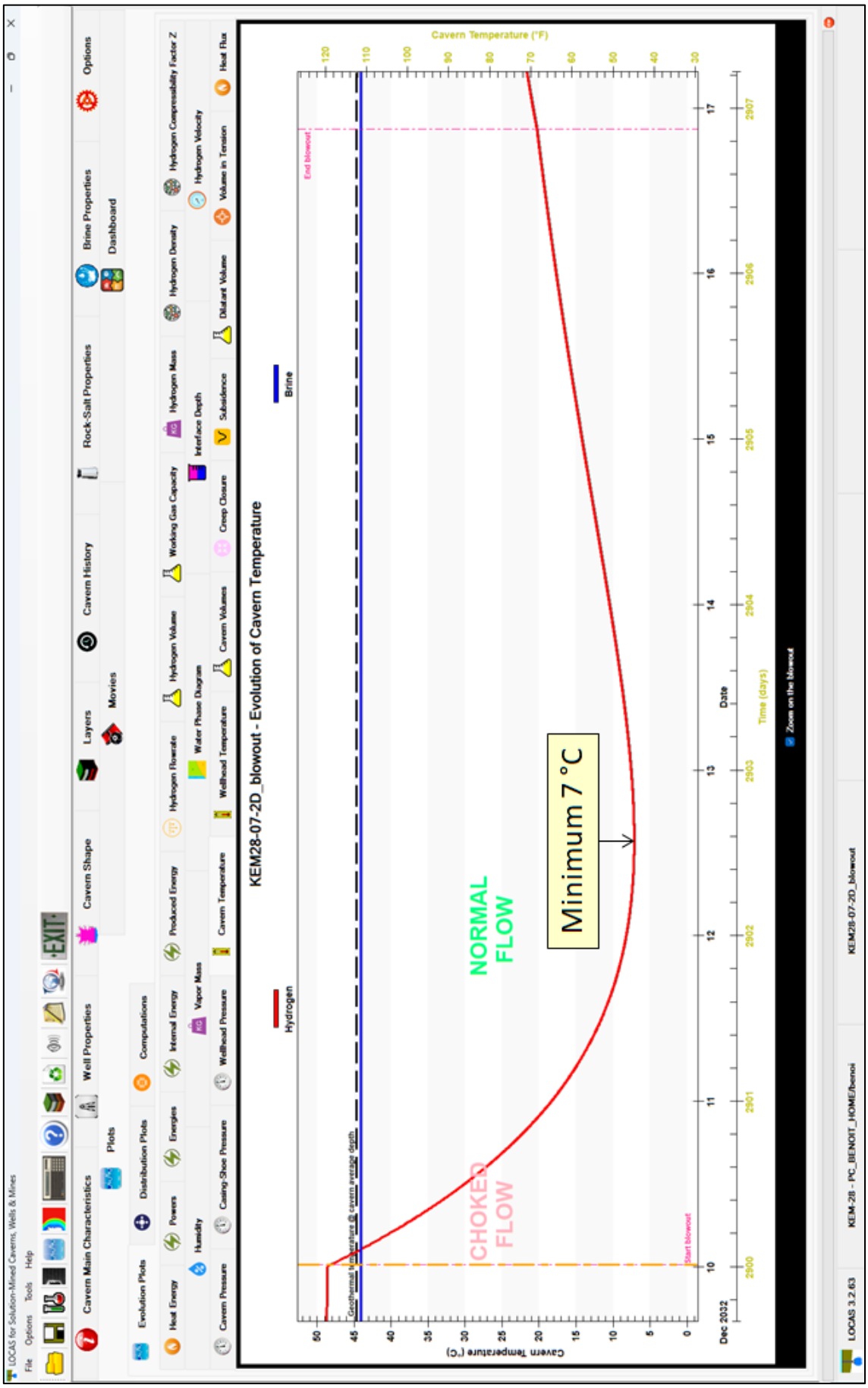

Figure 241. Hydrogen temperature evolution in the cavern during the blowout. The temperature of the hydrogen in the cavern reached a minimum of -7°C after around two and a half days.

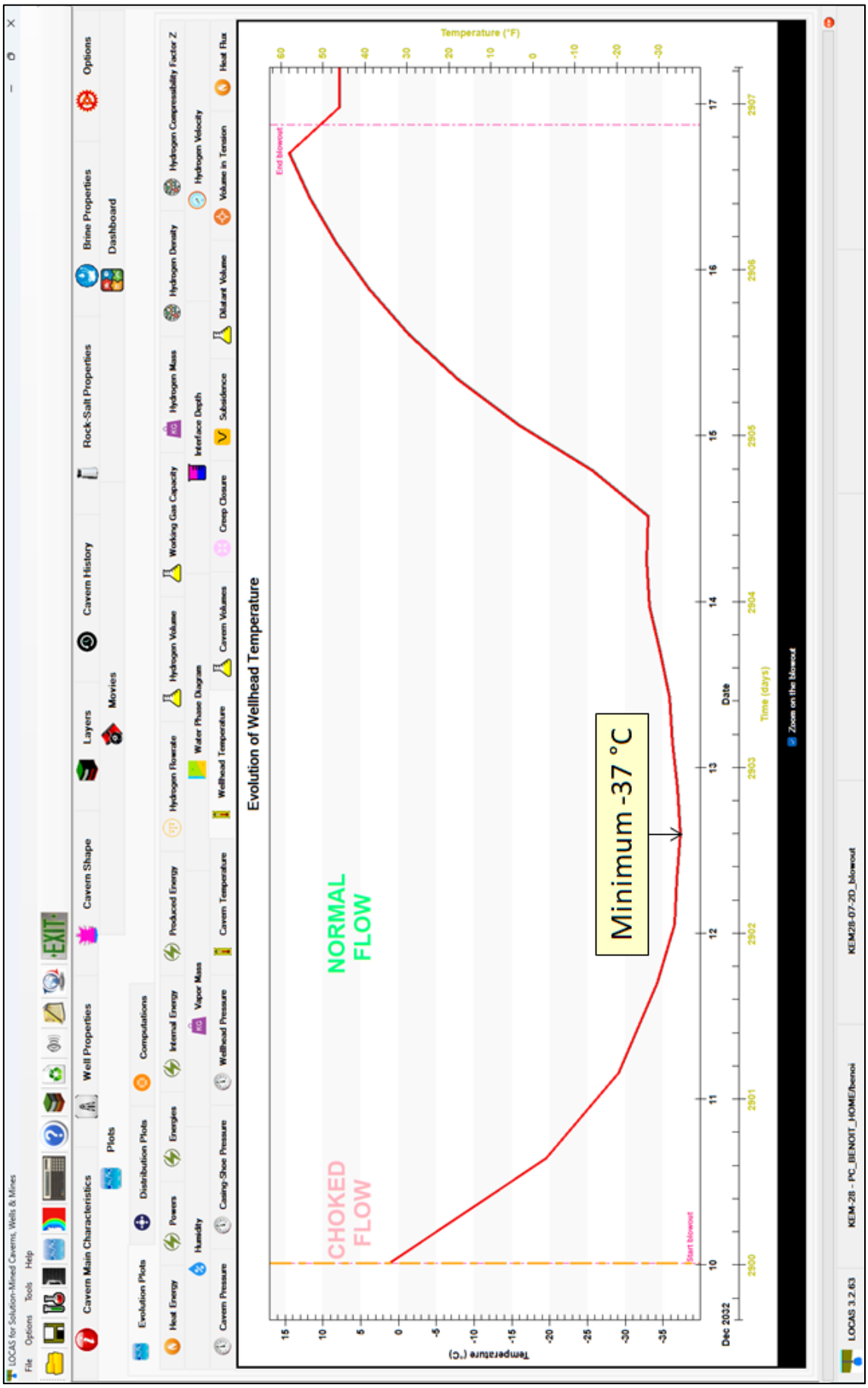

Figure 242. Hydrogen temperature evolution at the wellhead during the blowout. The temperature of the hydrogen at the wellhead reached a minimum of -37°C.

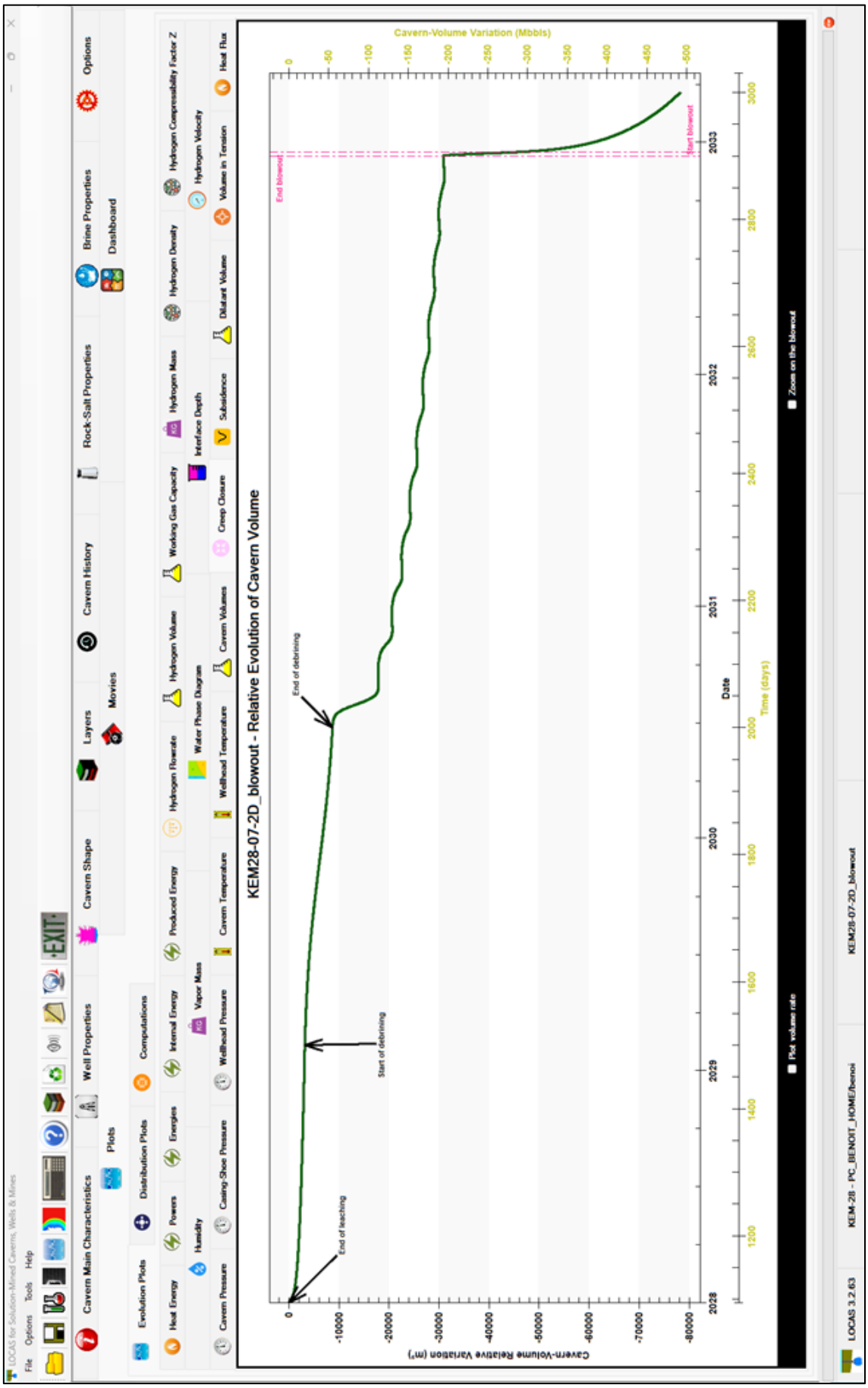

Figure 243. Evolution of cavern volume loss from the end of leaching to blowout. The loss of volume caused by the blowout is in the order of 45 000 m³.

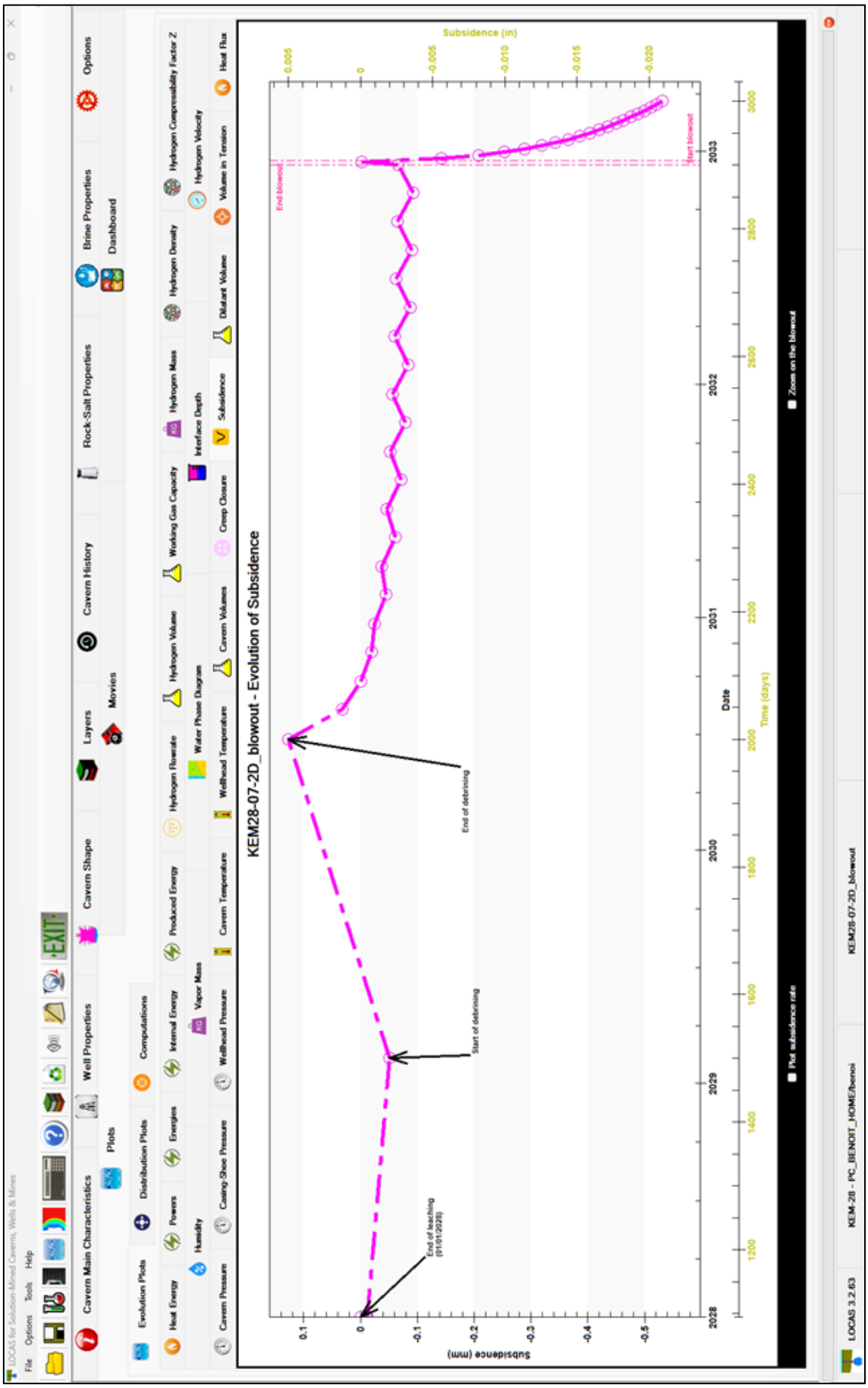

Figure 244. Evolution of maximum subsidence from the end of leaching to blowout.

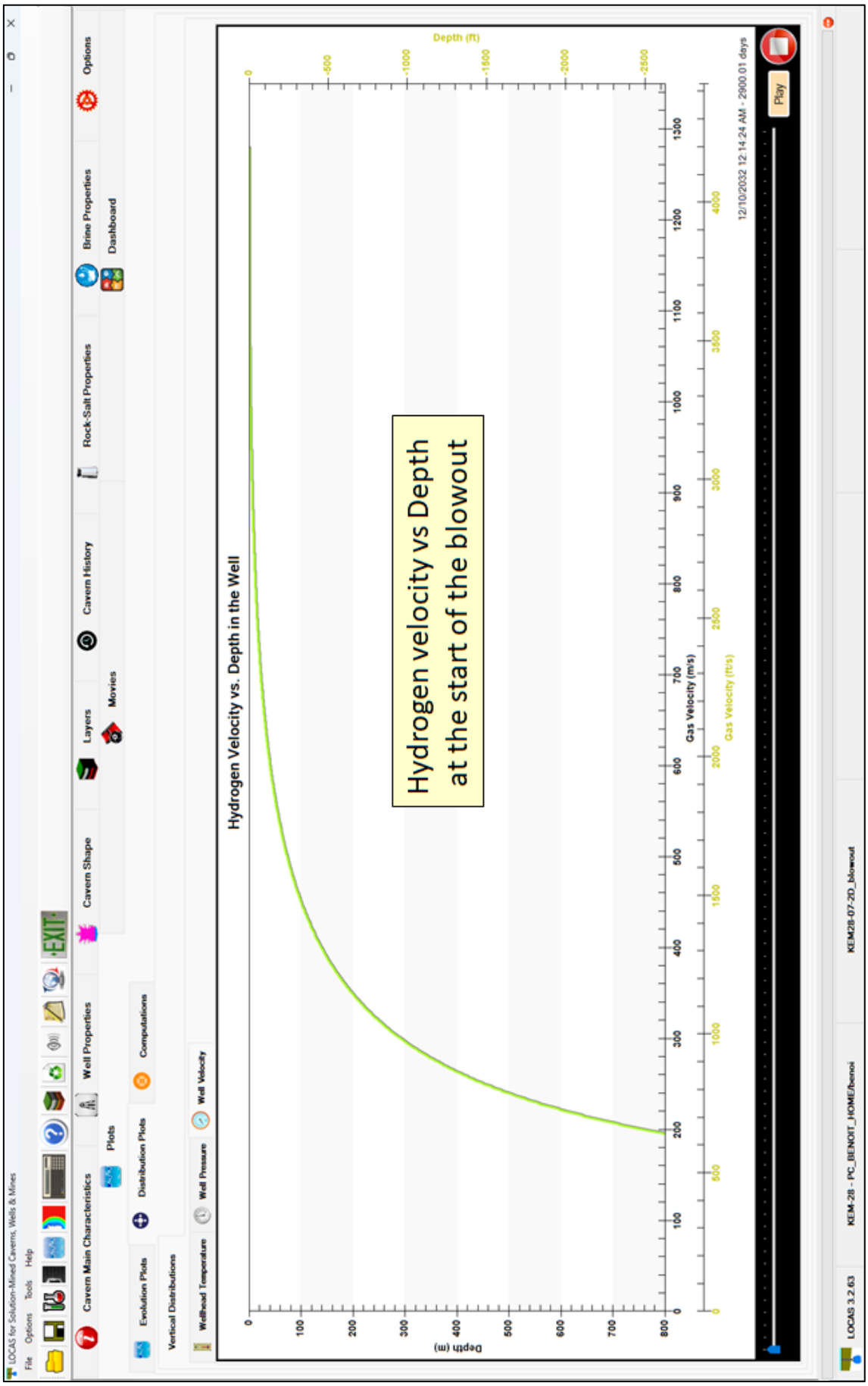

Figure 245. Hydrogen velocity distribution in the well at the start of the blowout. Hydrogen leaves the well at the speed of sound at the start of the blowout.

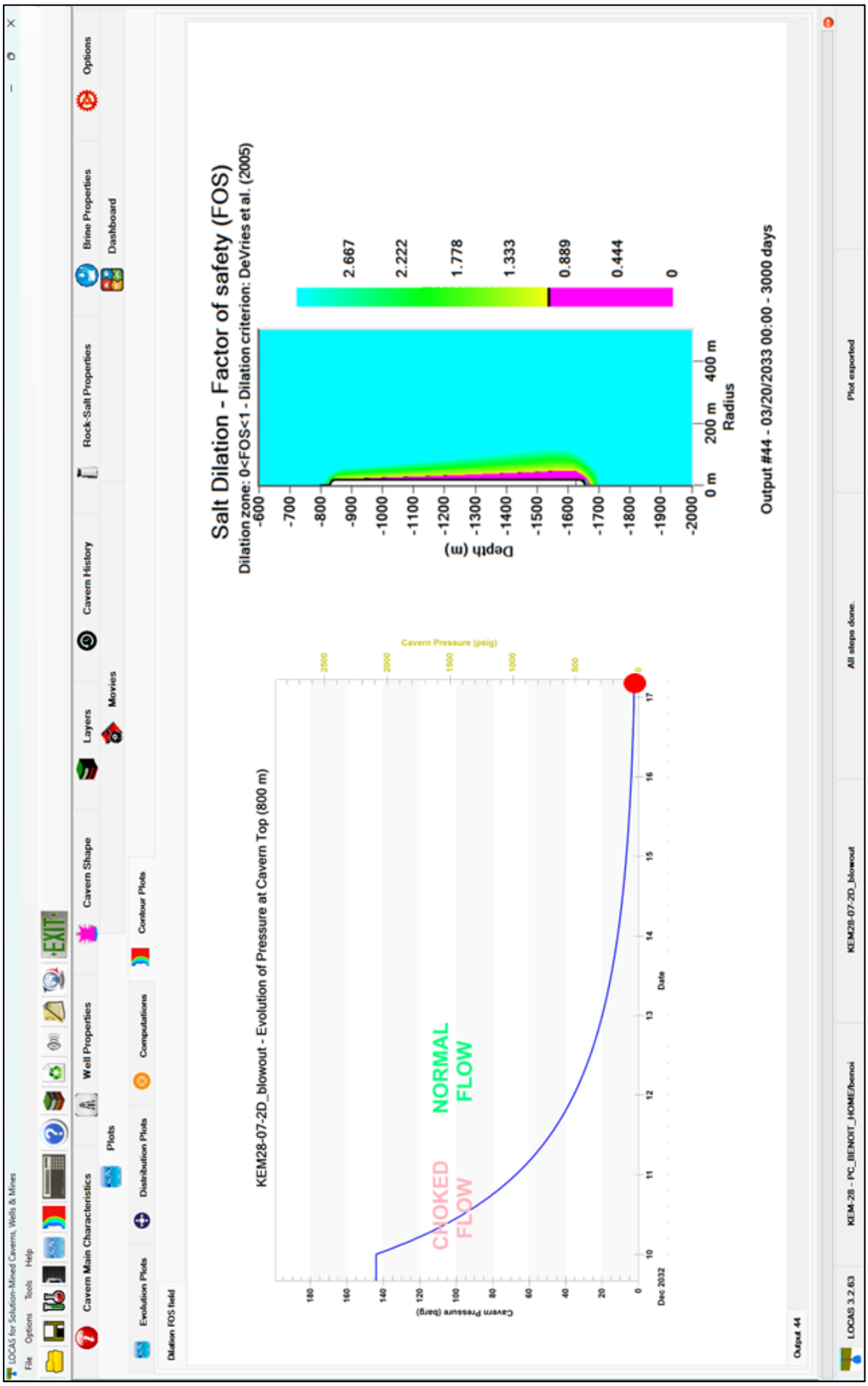

Figure 246. Contours of dilation Factor of Safety at the end of the blowout (dilatant zone in magenta). The damaged area is mainly located in the lower part of the cavern.

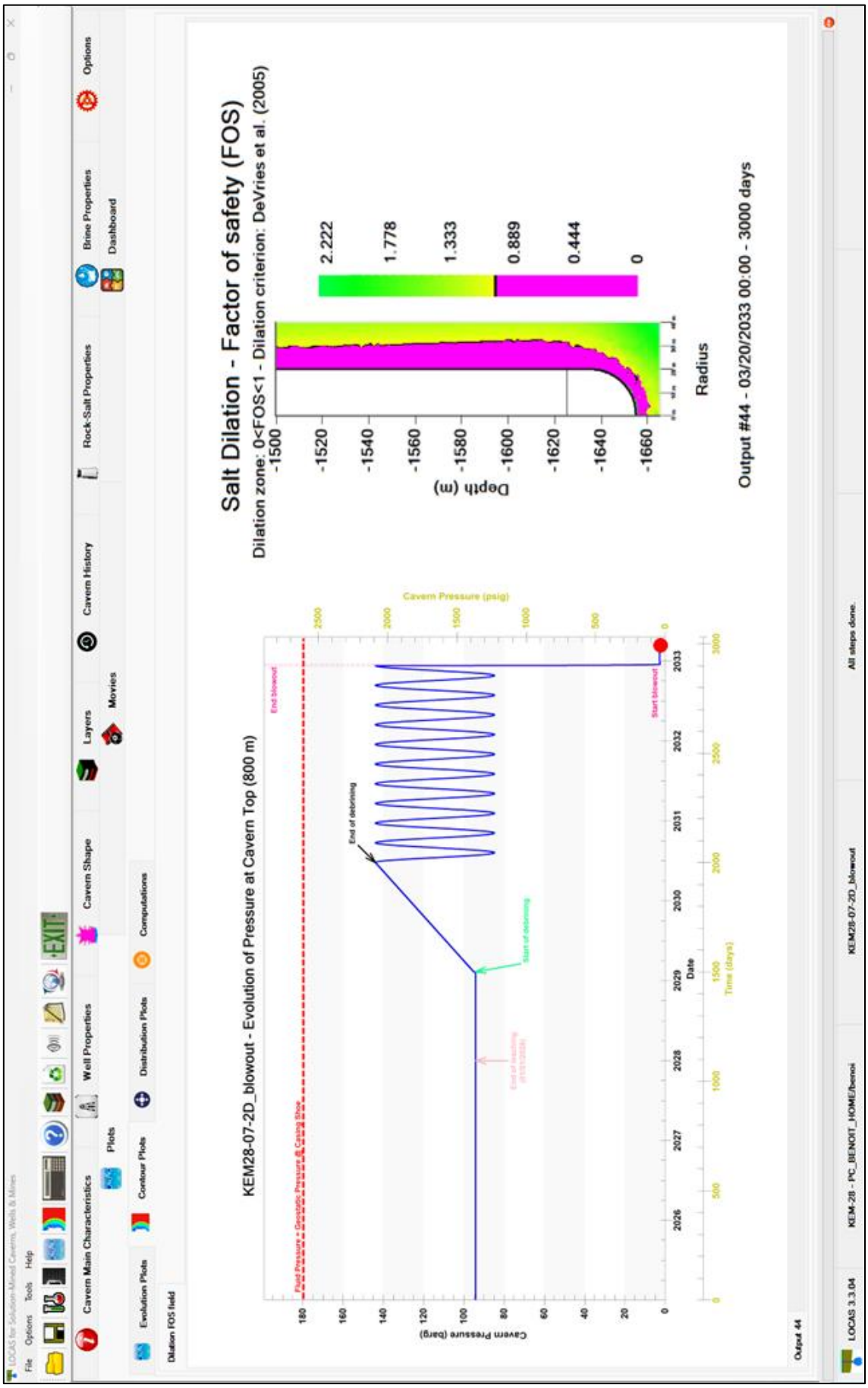

Figure 247. Contours of dilation Factor of Safety at the end of the blowout (zoom in on the lower section).

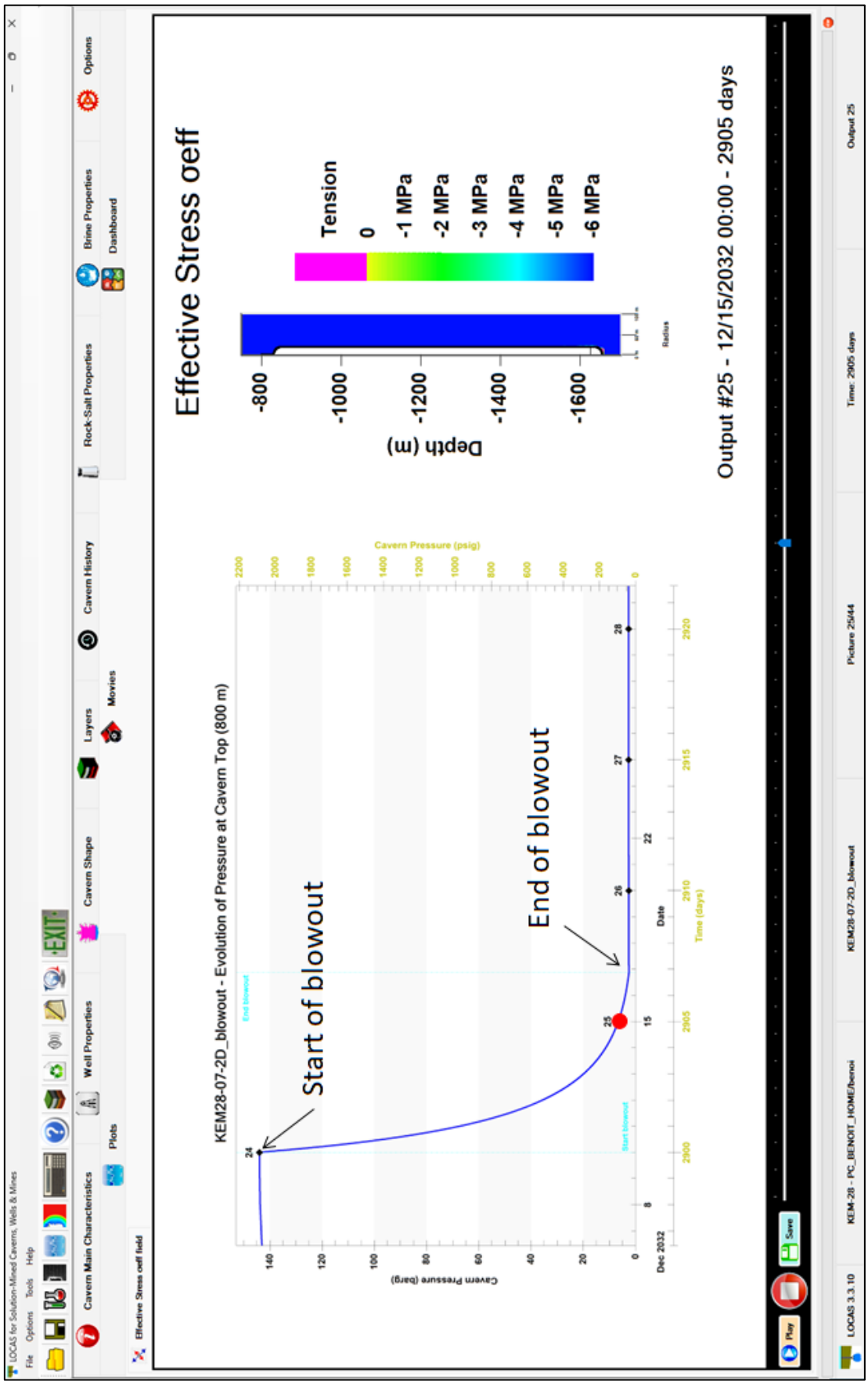

Figure 248. Contours of effective stress at the end of the blowout. No significant area in effective tension can be observed.

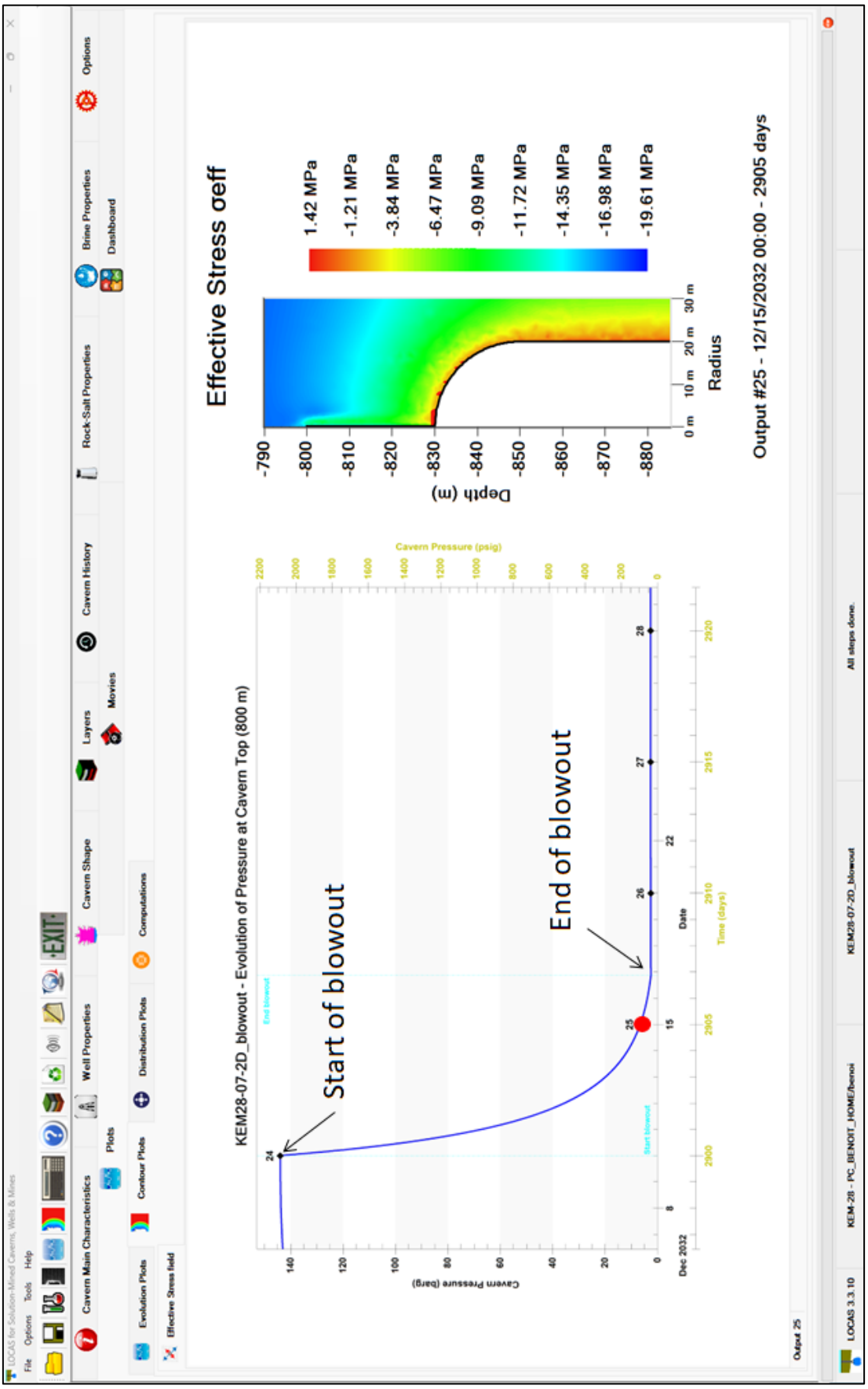

Figure 249. Contours of effective stress at the end of the blowout, zoom in the vicinity of cavern roof. No significant area in effective tension can be observed.

1.12 Workover modelling

1.12.1 Introduction

During the life of a gas storage cavern, it may be necessary to carry out maintenance operations requiring the pressure in the cavern to be lowered considerably and maintained at this low pressure for several weeks or more. This is the case, for example, when a cavern is initially full of gas and an equivalent volume of brine is not available to refill it with brine (known as “rebrining”). A cavern maintained at low pressure rapidly loses volume, the deeper the cavern, and damage due to dilation can occur and increase over time as long as the pressure remains low.

1.12.2 Modelling assumptions

The reference configuration is always considered, i.e., a cavern 40 m in diameter with a cavern shoe at a depth of 800 m, subjected to pressure cycles lasting 90 days.

It is assumed that the workover starts at the minimum pressure of the last cycle (Figure 250 and Figure 251). The hydrogen is withdrawn from the well in such a way as to reduce its pressure from 85 barg to 2 barg in approximately 44 days, giving an average rate of pressure reduction of just under 2 bar/day.

Figure 252 shows hydrogen and brine temperatures from end of leaching to end of the workover. Although decompression is relatively slow at the beginning of the workover, the temperature of the hydrogen decreases by around ten degrees (from 39.0 to 28.6°C).

The Evolution of the loss of cavern volume and loss rate since the end of leaching are shown in Figure 253. As for the blowout, the loss of volume is significant during the workover. The additional loss of cavern volume is in the order of 50 000 m^3 5 months after the start of the workover. After 5 months at low pressure, the rate of cavern closure is approximately 4.4 %/year.

During the 5 months of the workover, subsidence above the cavern increases by around 0.5 mm (Figure 254). After 5 months at low pressure, the rate of subsidence is approximately 0.06 mm/month.

Change in dilatant volume since the end of leaching is given in Figure 255. The dilatant volume increases considerably as the cavern decompresses, reaching 1 220 000 m^3 at the end of decompression, which represents an average thickness of 11.8 m when divided by the surface area of the cavern (103 713 m^2). The dilatant volume remains almost constant when the cavern pressure is kept subsequently low for a few months.

Figure 256 shows FOS dilation contours at the end of the workover (i.e., after 5 months). A dilatant zone with a maximum thickness of around 22 m appears in the lower part of the cavern.

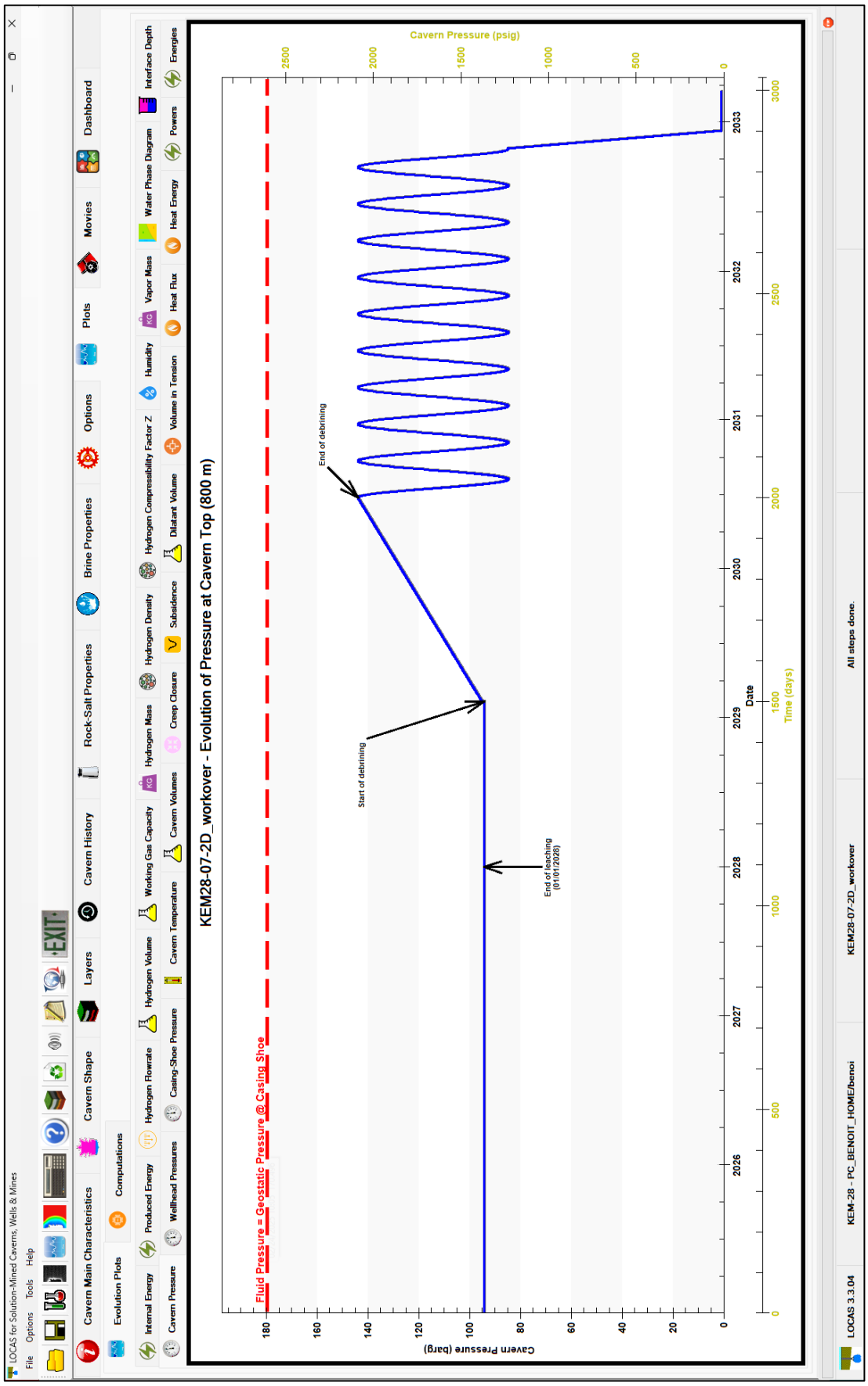

Figure 250. Pressure evolution in the cavern, the workover is assumed to occur at the minimum pressure of the last cycle.

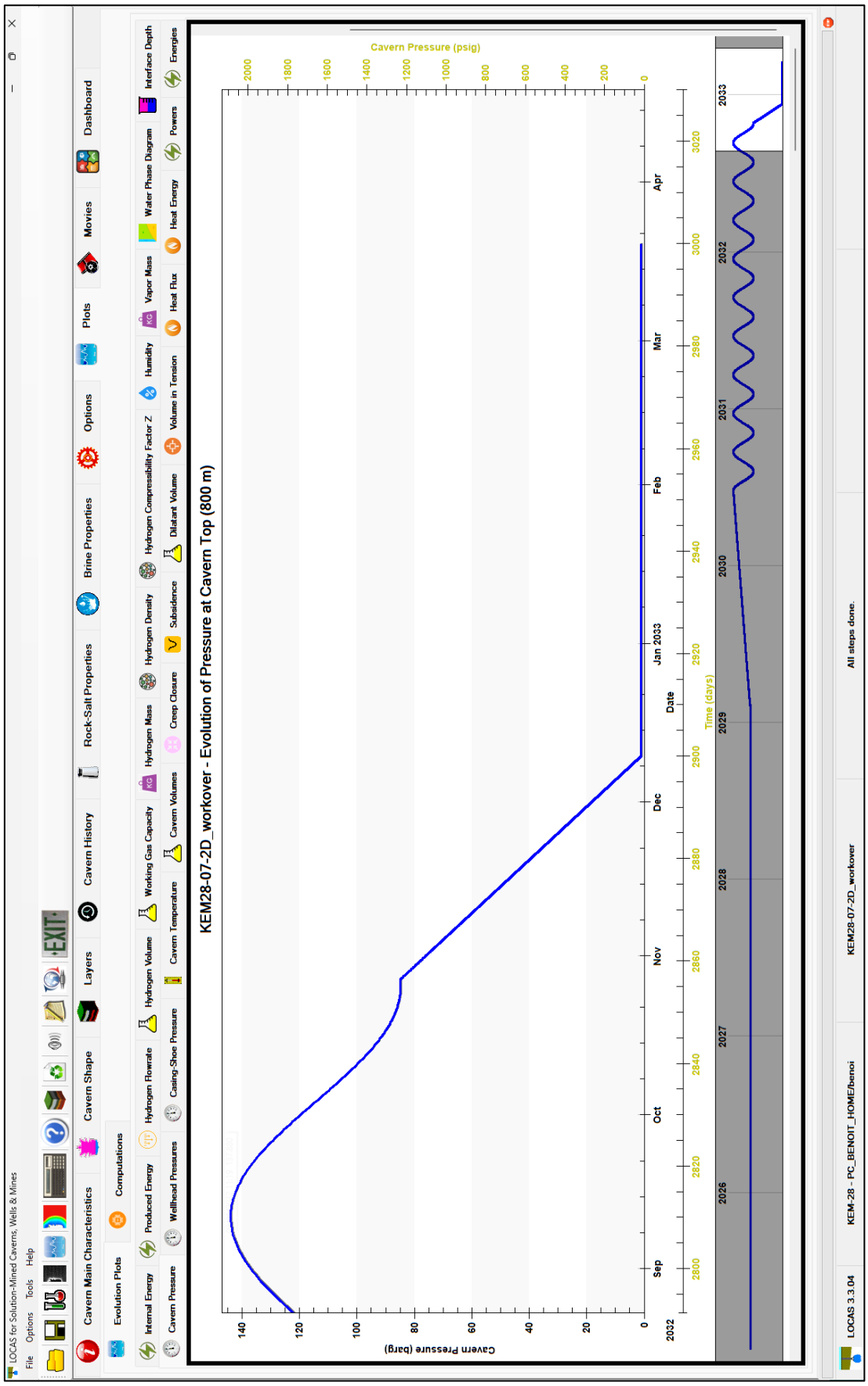

Figure 251. Cavern pressure evolution during before and during the workover. The workover starts when the pressure in the cavern is at a minimum (minimum stock of hydrogen).

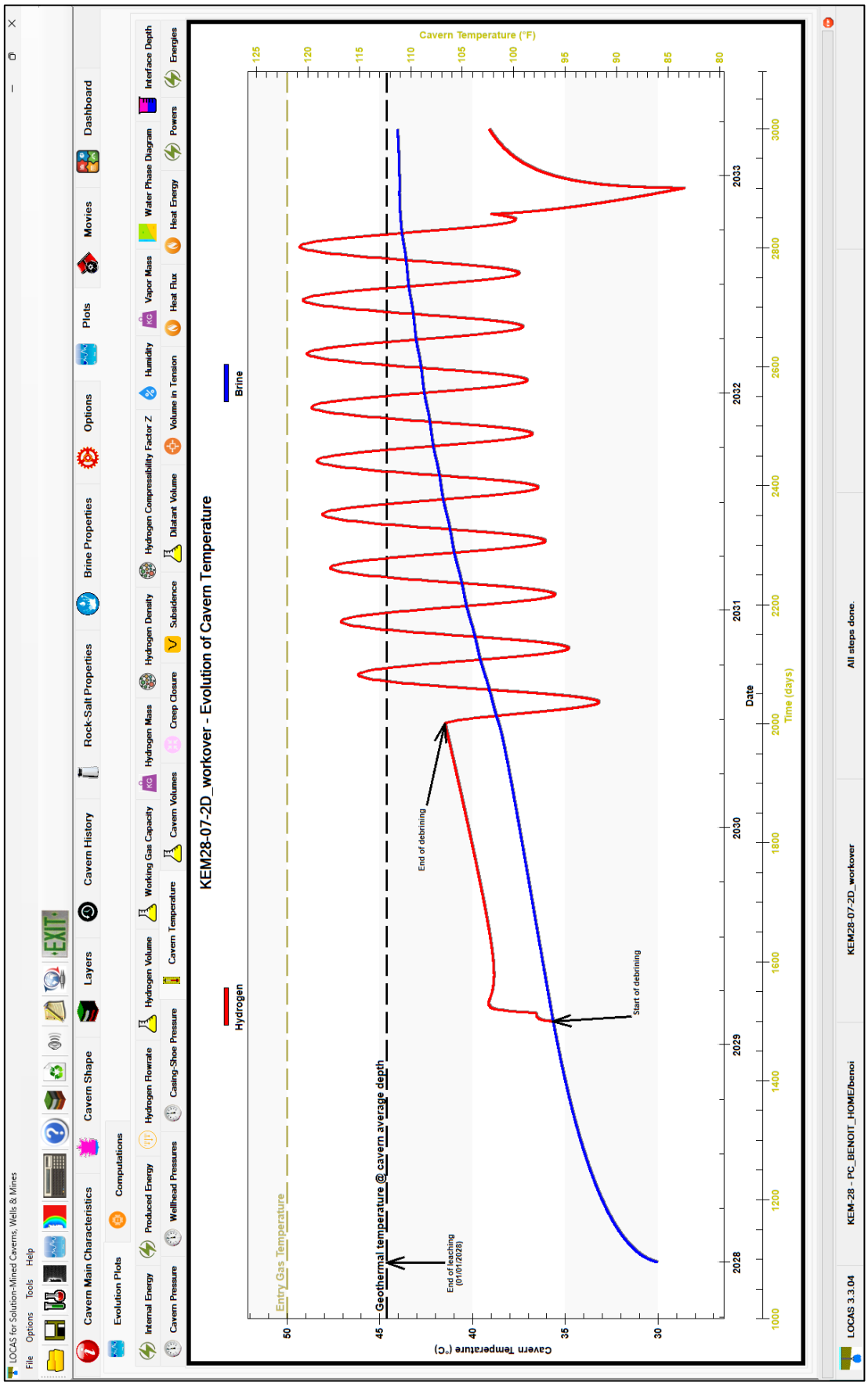

Figure 252. Cavern temperatures from end of leaching to end of the workover. Even a slow decompression of the cavern at the start of the workover is enough to cause the temperature in the cavern to drop by around 10 °C.

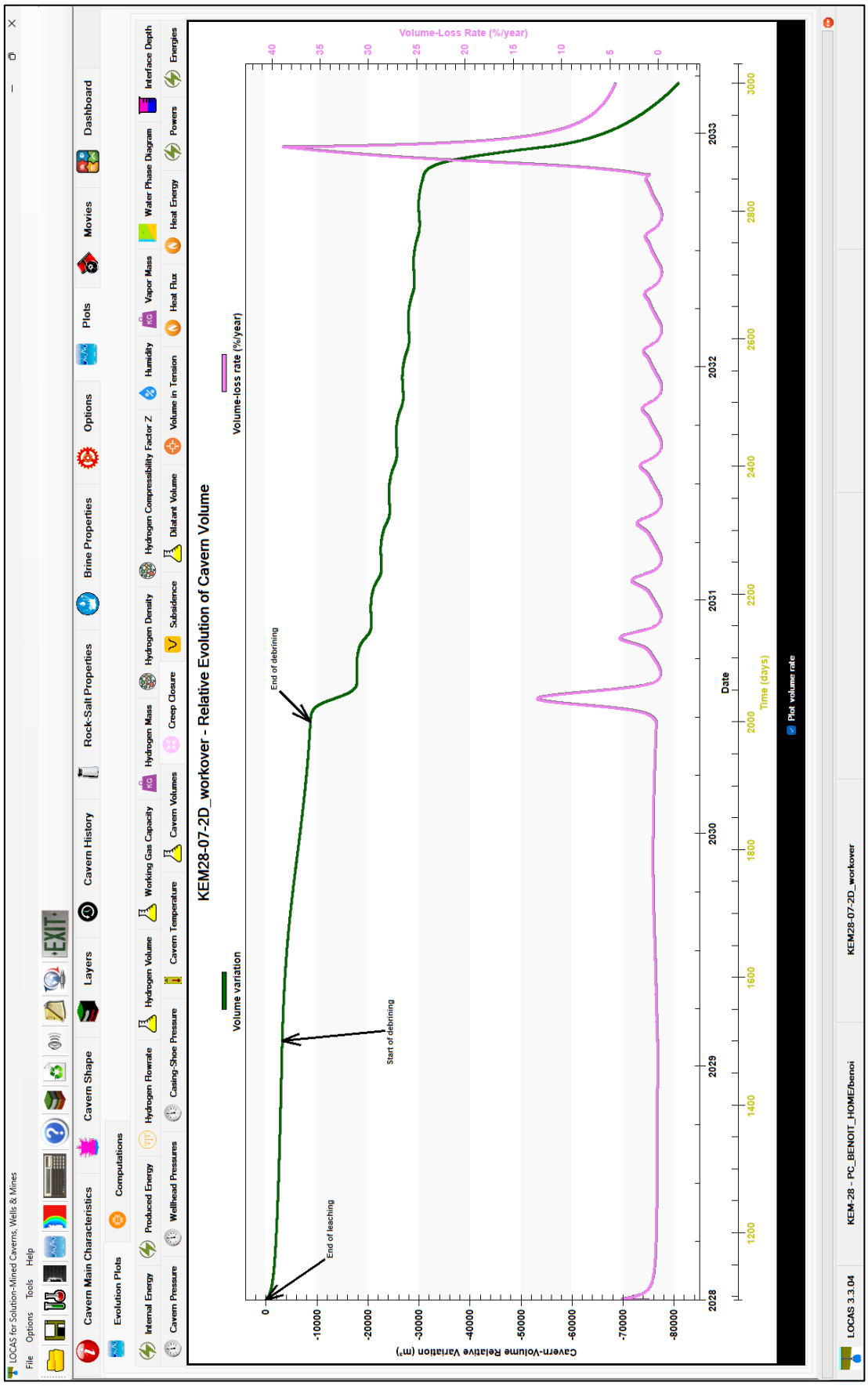

Figure 253. Evolution of cavern volume loss and loss rate from end of leaching to end of the workover. The additional loss of cavern volume is in the order of 50 000 m^3 5 months after the start of the workover. After 5 months at low pressure, the rate of cavern closure is approximately 4.4 %/year.

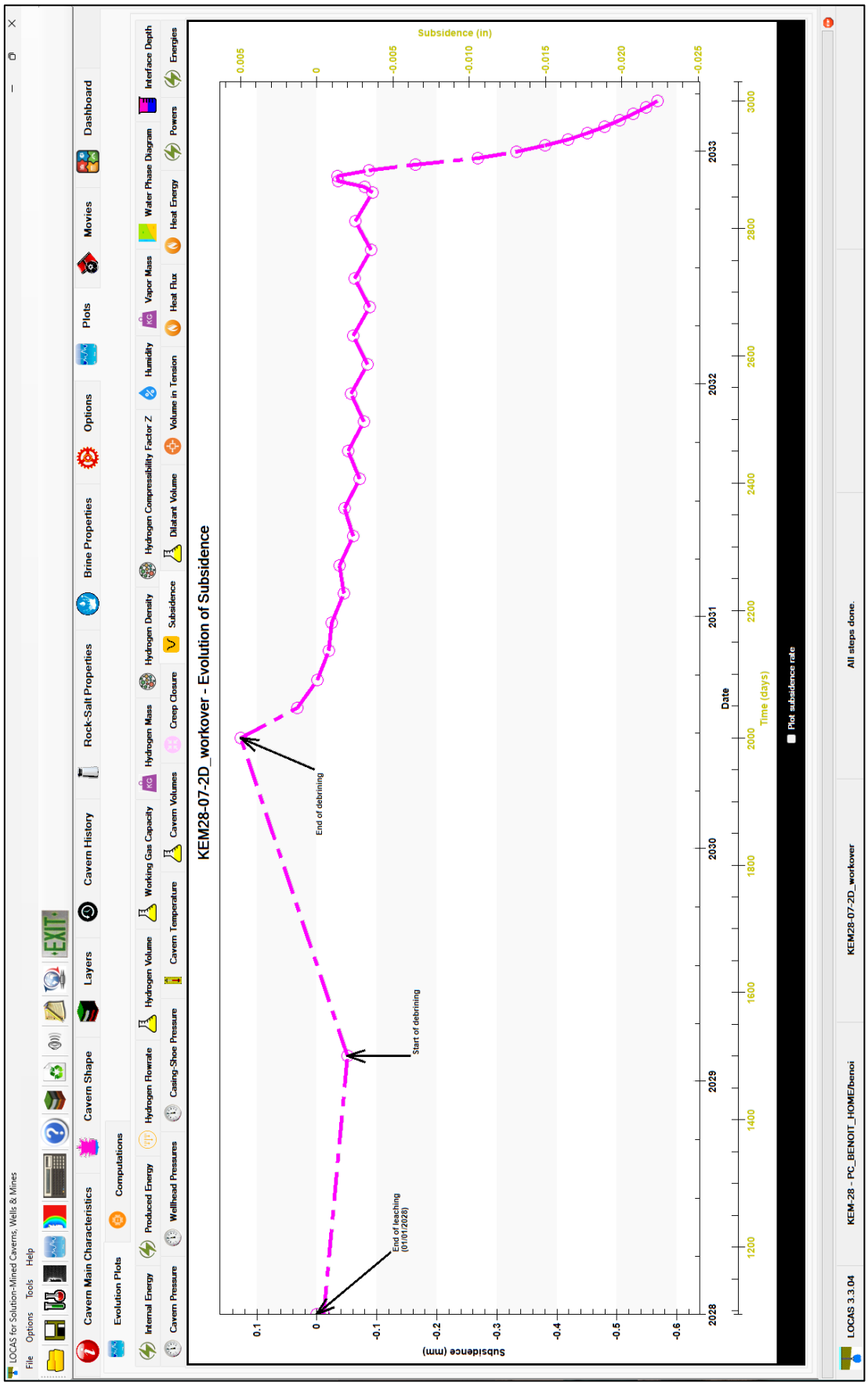

Figure 254. Evolution of maximum subsidence from end of leaching to end of workover. During the 5 months of the workover, subsidence above the cavern increases by around 0.5 mm. After 5 months at low pressure, the rate of subsidence is approximately 0.06 mm/month.

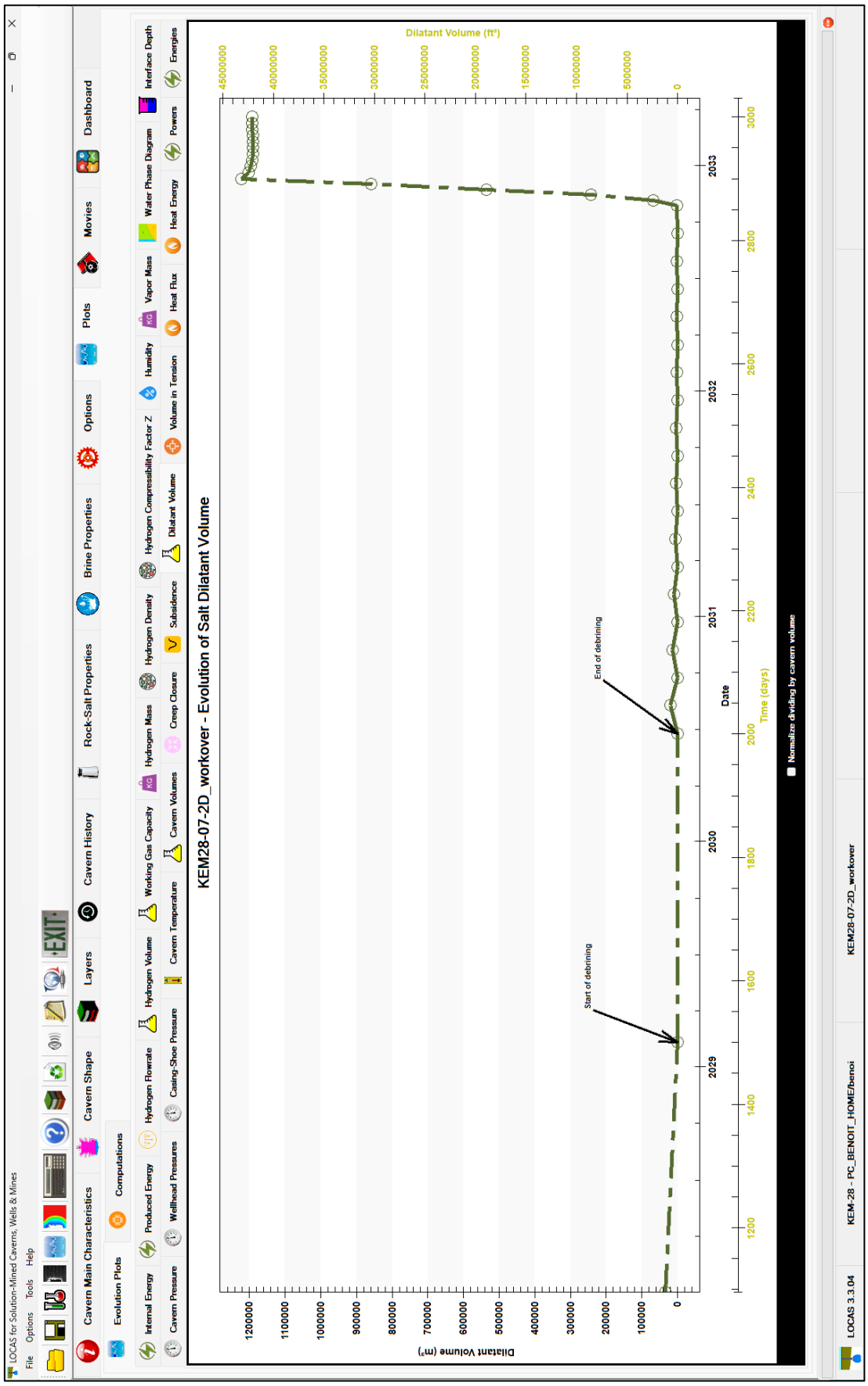

Figure 255. Change in dilatant volume since the end of leaching. The dilatant volume increases considerably as the cavern decompresses, reaching 1 220 000 m^3 at the end of decompression, which represents an average thickness of 11.8 m when divided by the surface area of the cavern (103 713 m^2). The dilatant volume remains almost constant when the cavern pressure is kept subsequently low for a few months.

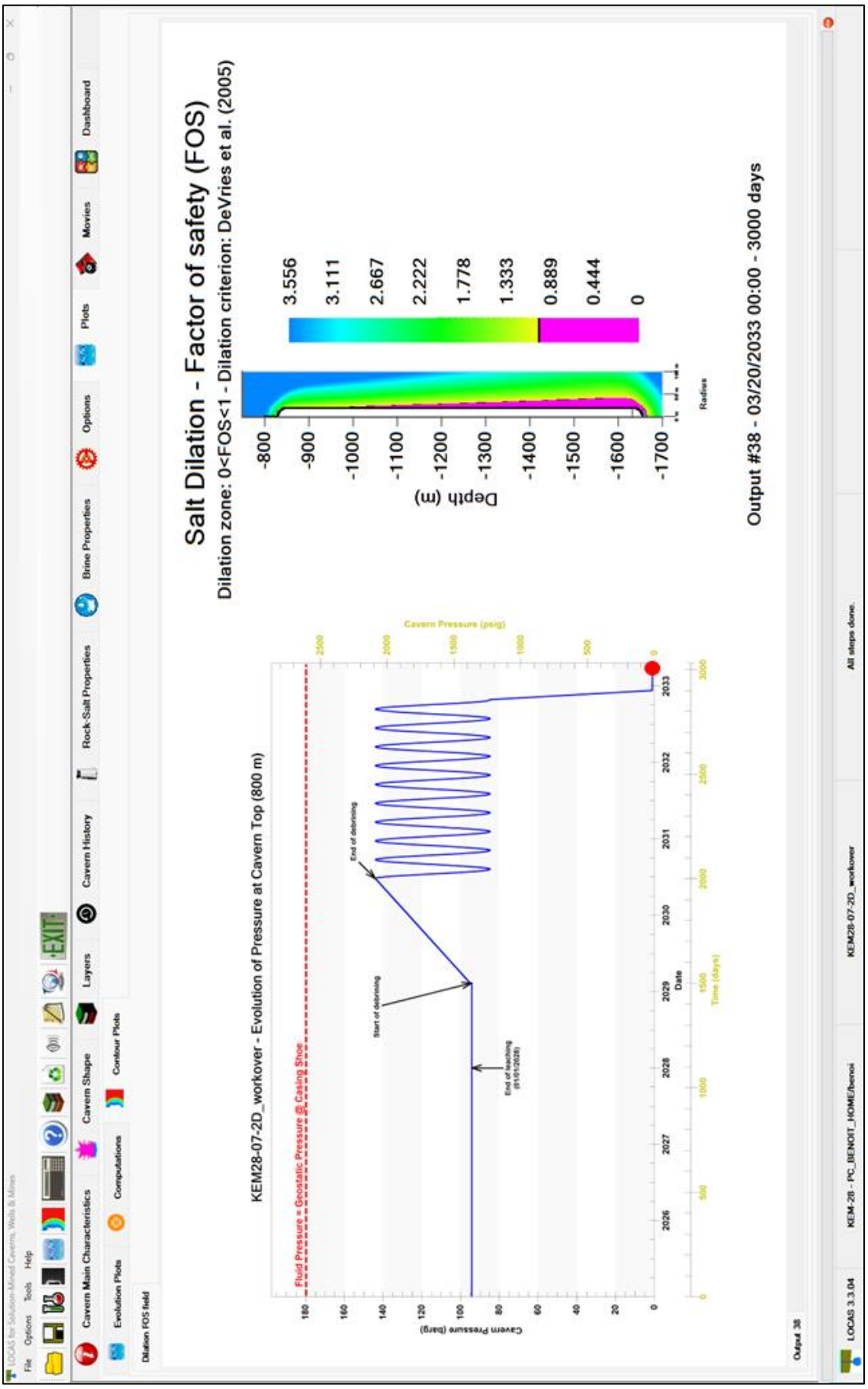

Figure 256. Contours of dilation Factor of Safety at the end of the workover (dilatant zone in magenta). A dilatant zone with a maximum thickness of around 22 m appears in the lower part of the cavern.

1.13 Non-halite layer intersecting the cavern

1.13.1 Introduction

Following an idea by Janos Urai, we considered here the case where an anhydrite layer intersects the cavern. This layer is assumed to have an elasto viscoplastic behaviour, but with a viscosity 50 times larger than the Zechstein salt around. The idea was that this heterogeneity of behaviour could create stress concentrations that were detrimental to the mechanical stability of the cavern.

1.13.2 Considered configuration

We considered the reference configuration used previously (Case #07) and a layer with a thickness of 30 m which intersects the cavern between 870 m and 900 m (Figure 257). It has been arbitrarily assumed that the anhydrite layer is stiffer than the salt layer and follows the Norton-Hoff creep law with a viscosity 50 times greater than the Zechstein. The thermal and elastic properties of this anhydrite layer are given in Table 25 and Table 26, respectively.

Table 25. Thermal properties of the anhydrite layer.

Rock	Heat capacity (J/kg-K)	Thermal conductivity (W/m-K)	Geothermal gradient (°C/100 m)
Anhydrite	880	5.3	1.887

Table 26. Considered density and elastic properties of the anhydrite layer.

Rock	Thickness (m)	Depth (m)	Density (kg/m3)	Poisson's ratio	Young's modulus (MPa)
Anhydrite	30	870-900	2160	0.27	40,000

Strain rate using Norton-Hoff's law can be written as:

$$\dot{\varepsilon} = A_{nh}\, exp\left(\frac{Q_{nh}}{R}\right)\sigma^{n} \tag{82}$$

The set of parameters selected for the Norton-Hoff creep law is provided in Table 27.

Table 27. Parameters for pressure solution creep.

Parameter	Units	Value
A_{nh}	/MPa-yr^{n}	0.4
n_{nh}	–	5
Q_{nh}/R	K	6495

In order not to introduce too many new changes with respect to the reference case, we have only modified the Young's modulus (stiffer intersected layer, 40 GPa vs. 30 GPa) and much smaller prefactor for stationary creep when comparing the behaviour of the salt and the anhydrite layer (50 times more viscous).

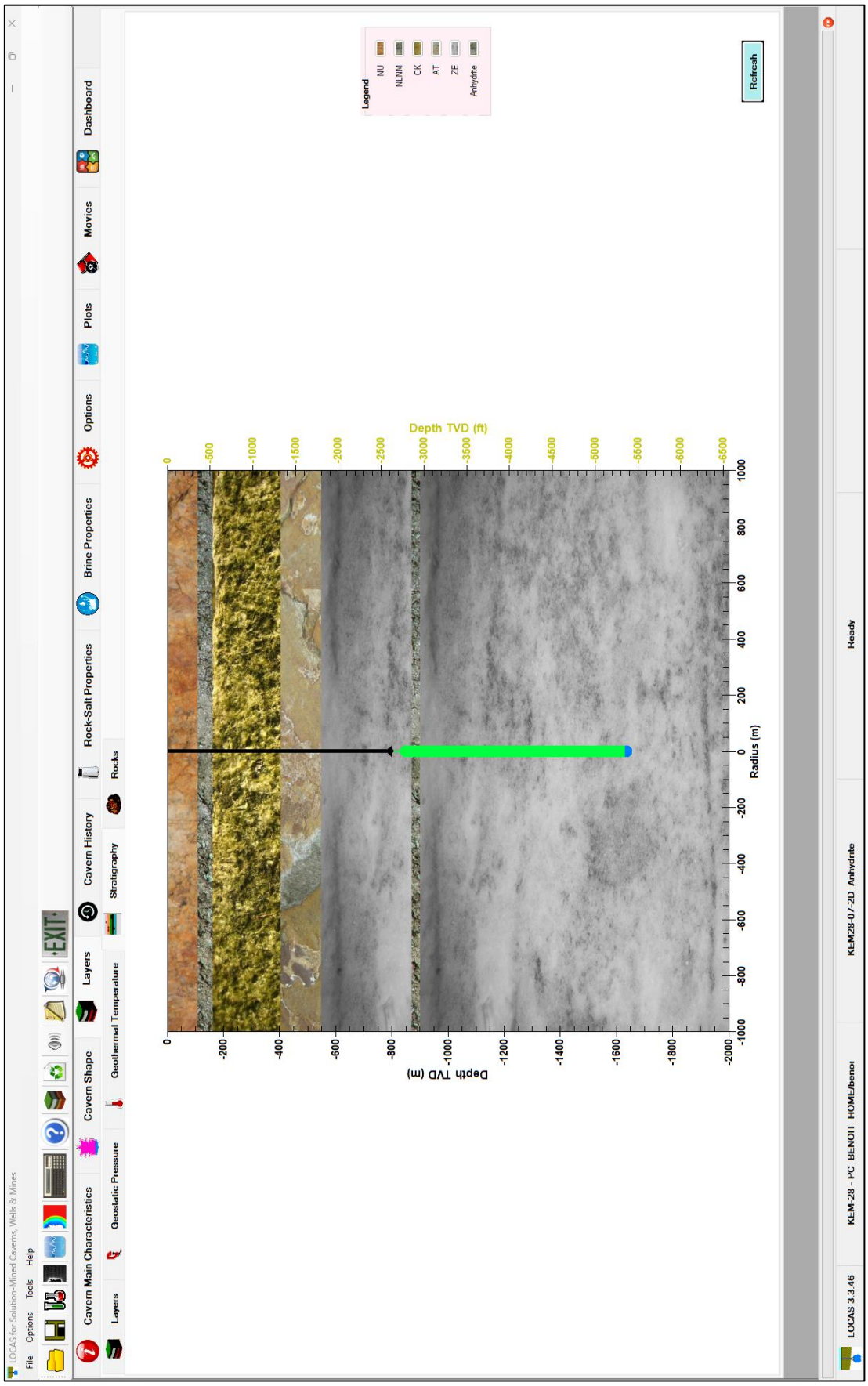

Figure 257. Considered configuration with an anhydrite layer intersecting the cavern.

Figure 258 and Figure 259 show contours of effective stress (σ_{eff}) at the last minimum pressure and the last maximum pressure respectively. A band in tension measuring 1.5 m in thickness is visible on the cavern wall, resembling the reference case (Figure 210). Tensile stresses also appear at the interface between the Zechstein and the anhydrite layer, both at minimum and maximum pressure. We can therefore conclude that the presence of a stiffer, more viscous layer intersecting the cavern creates more favourable conditions for the opening of a fracture at the interface between the two rocks.

Figure 260 shows that the effective stress reaches a value of nearly 8 MPa on the cavern wall at minimum pressure, and that the thickness of the band in effective tension is smaller on the wall of the anhydrite layer.

At the final maximum pressure, the band experiencing effective tension at the cavern wall has disappeared. However, there are still effective tensile stresses greater than 2 MPa present at the interface between the two rocks (Figure 261).

Figure 262 and Figure 263 display the effective stress distributions along the cavern wall, from the last cemented casing shoe to the cavern bottom, at the last minimum and maximum pressures, respectively. One can observe that the effective stress is lower at the wall in the stiffer and more viscous anhydrite layer.

Figure 264 shows the radial distribution of effective stress at a depth of 870 meters during the final minimum pressure. The effective stress reaches 4.9 MPa at a distance of about 50 cm from the cavern wall along the interface between the two rocks. It may be possible for this value to cause a fracture along the interface, but predicting the behaviour of the interface between the two rocks presents challenges as assumptions required for modelling may be difficult to confirm.

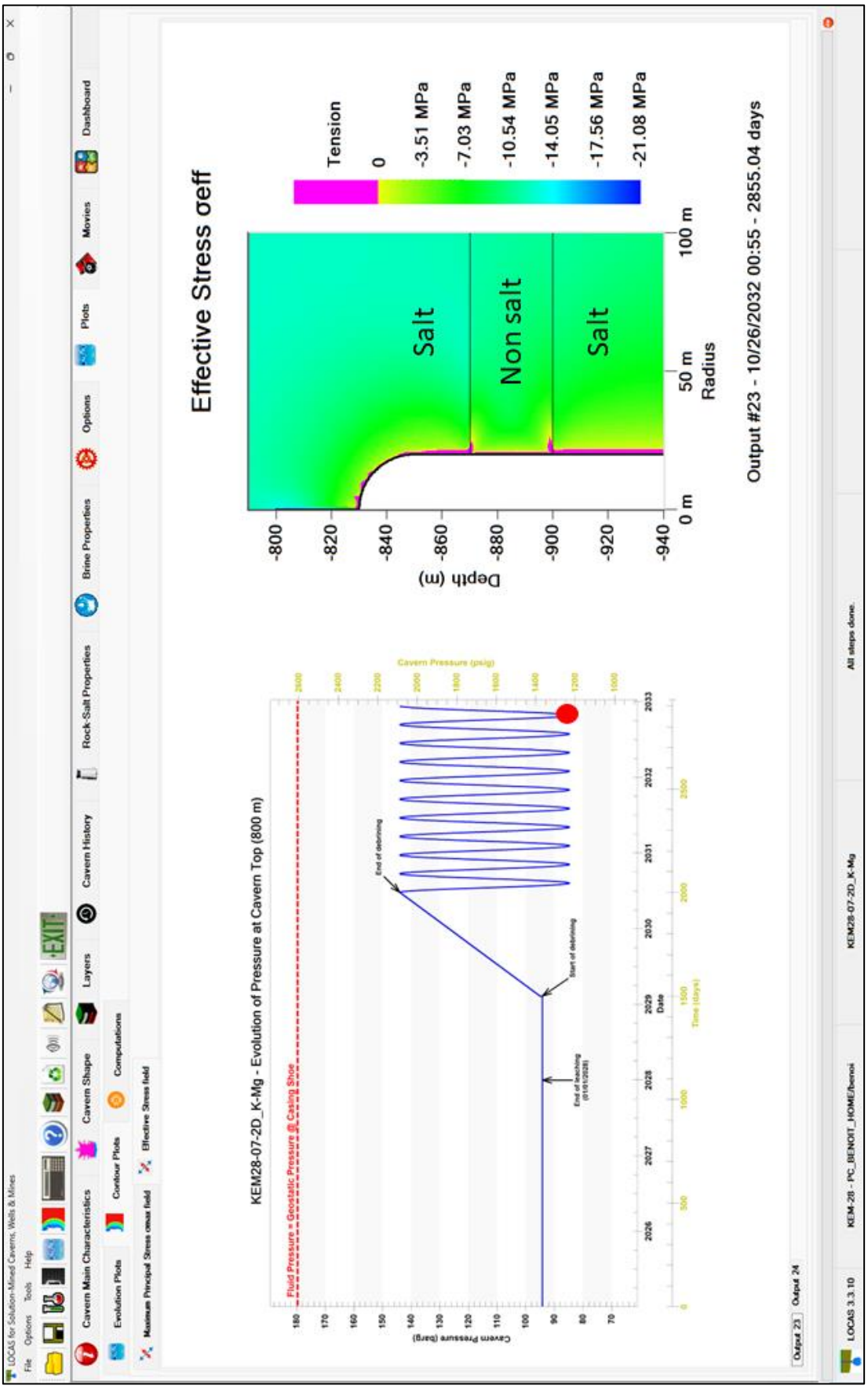

Figure 258. Contours of effective stress in the upper part of the cavern at the last minimum pressure (output #23). A band in tension measuring 1.5 m in thickness is visible on the cavern wall.

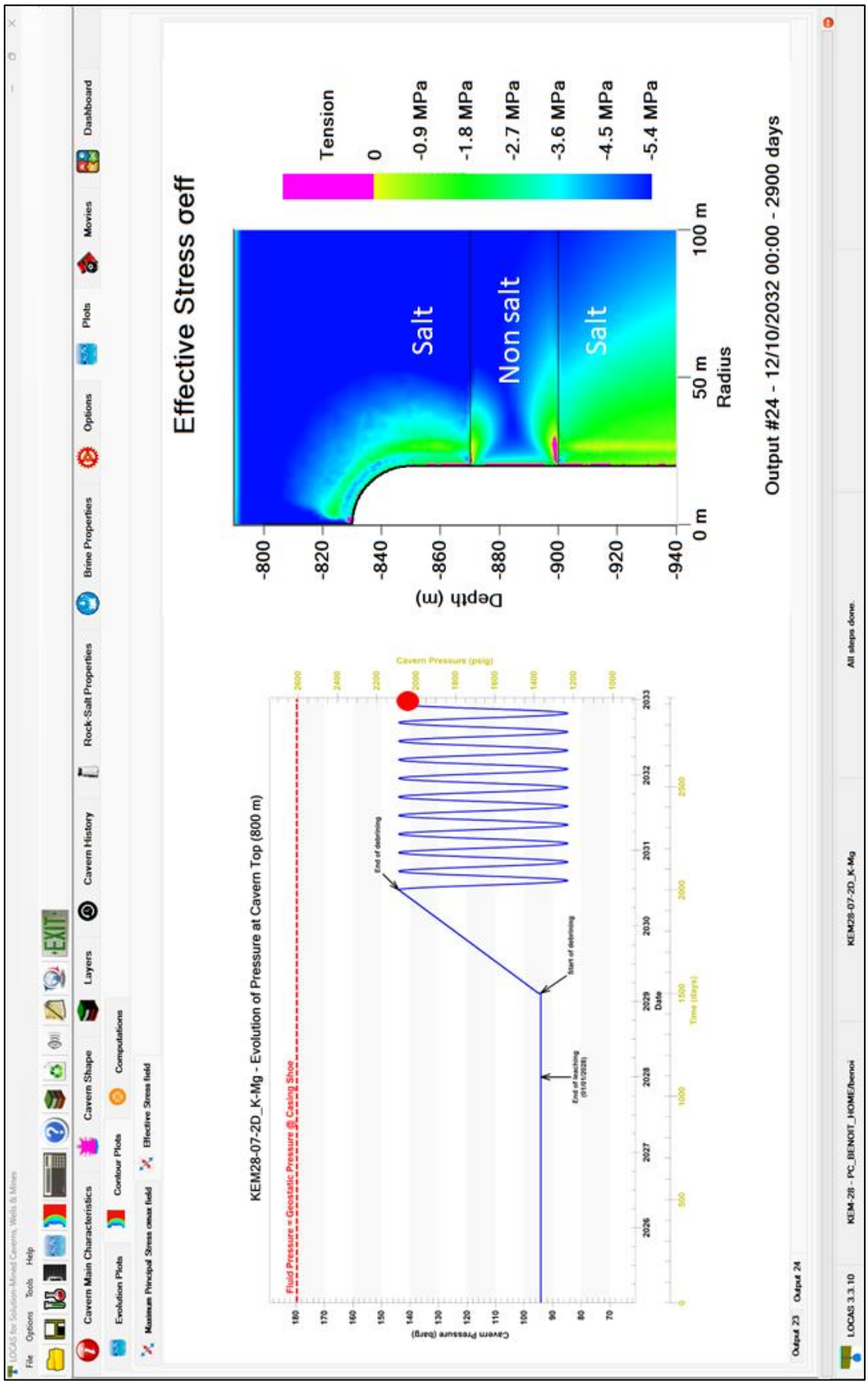

Figure 259. Contours of effective stress in the upper part of the cavern at the last maximum pressure (output #24).

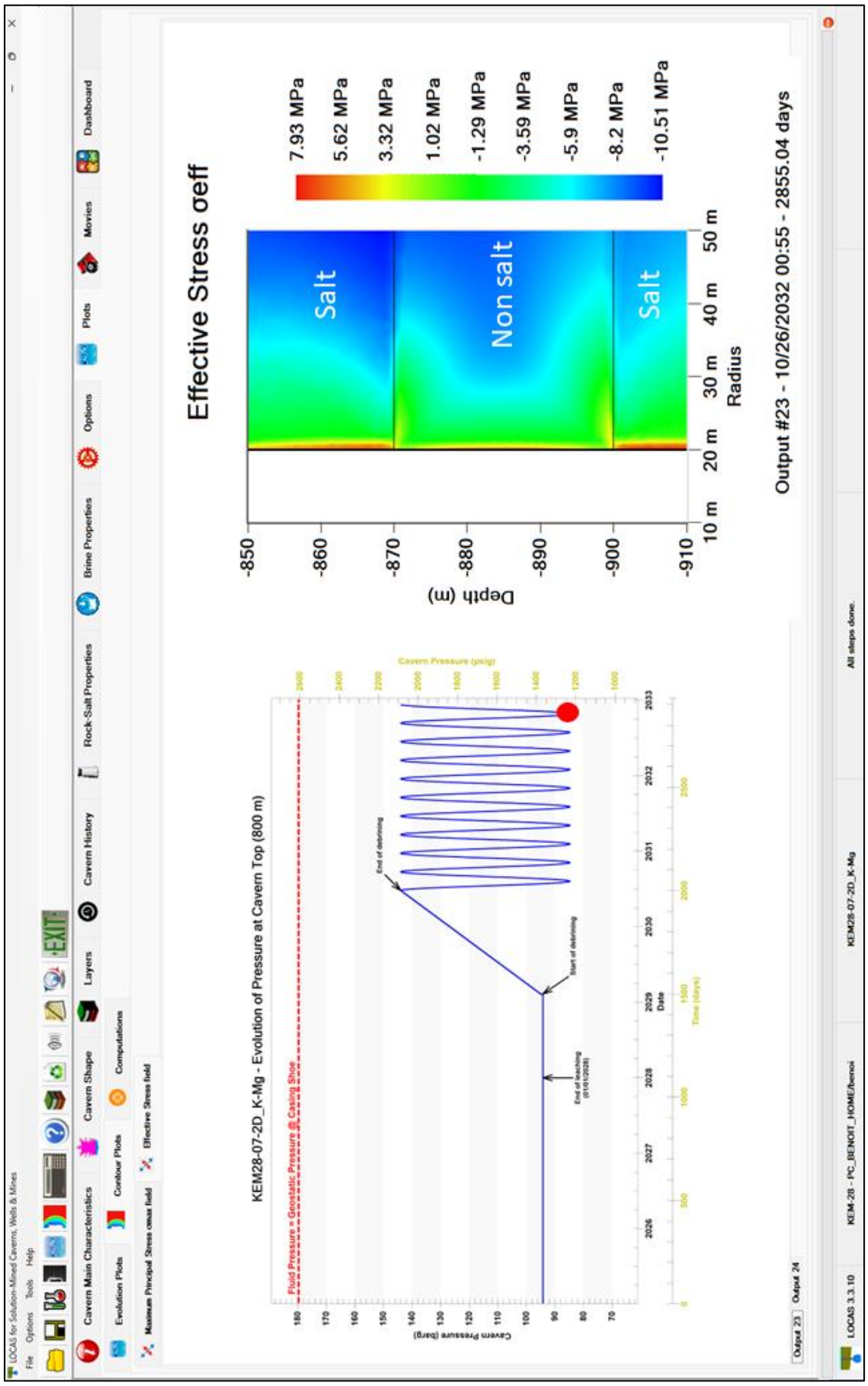

Figure 260. Contours of effective stress around the layer anhydrite at the last minimum pressure (output #23). The effective stress reaches a value of nearly 8 MPa on the cavern wall at minimum pressure, and that the thickness of the band in effective tension is smaller on the wall of the anhydrite layer.

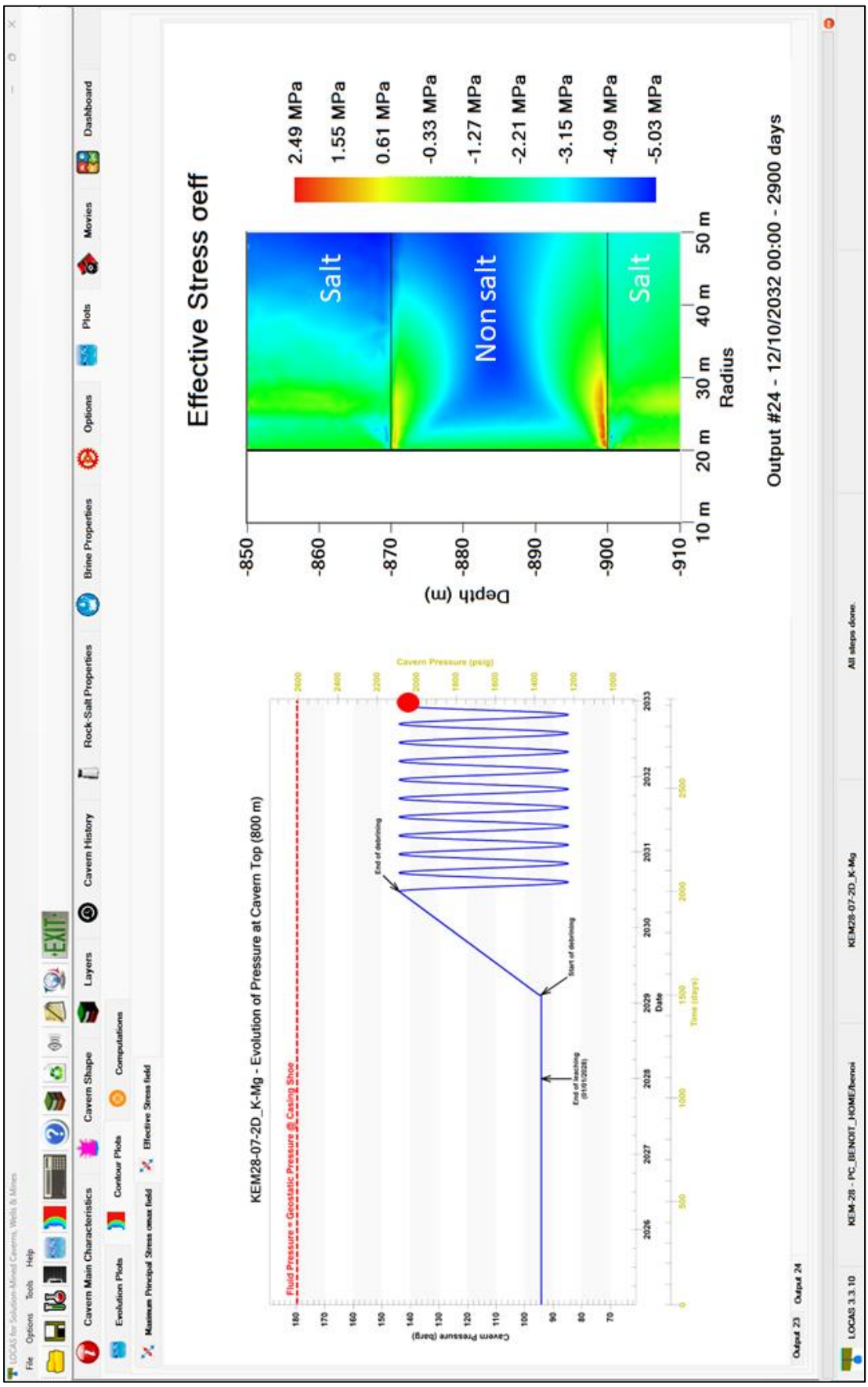

Figure 261. Contours of effective stress around the layer anhydrite at the last maximum pressure (output #24). The band experiencing effective tension at the cavern wall has disappeared. However, there are still effective tensile stresses greater than 2 MPa present at the interface between the two rocks.

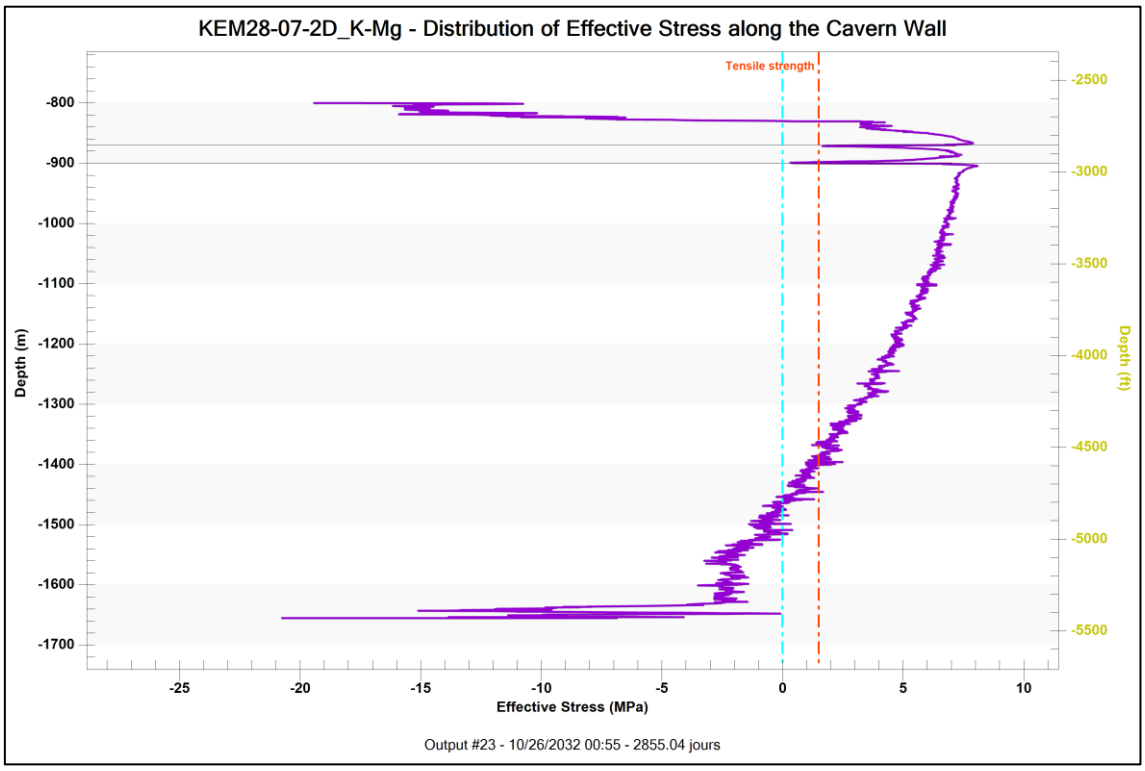

Figure 262. Effective stress distribution along the cavern wall (minimum pressure, output #23). The effective stress is lower at the wall in the stiffer and more viscous anhydrite layer.

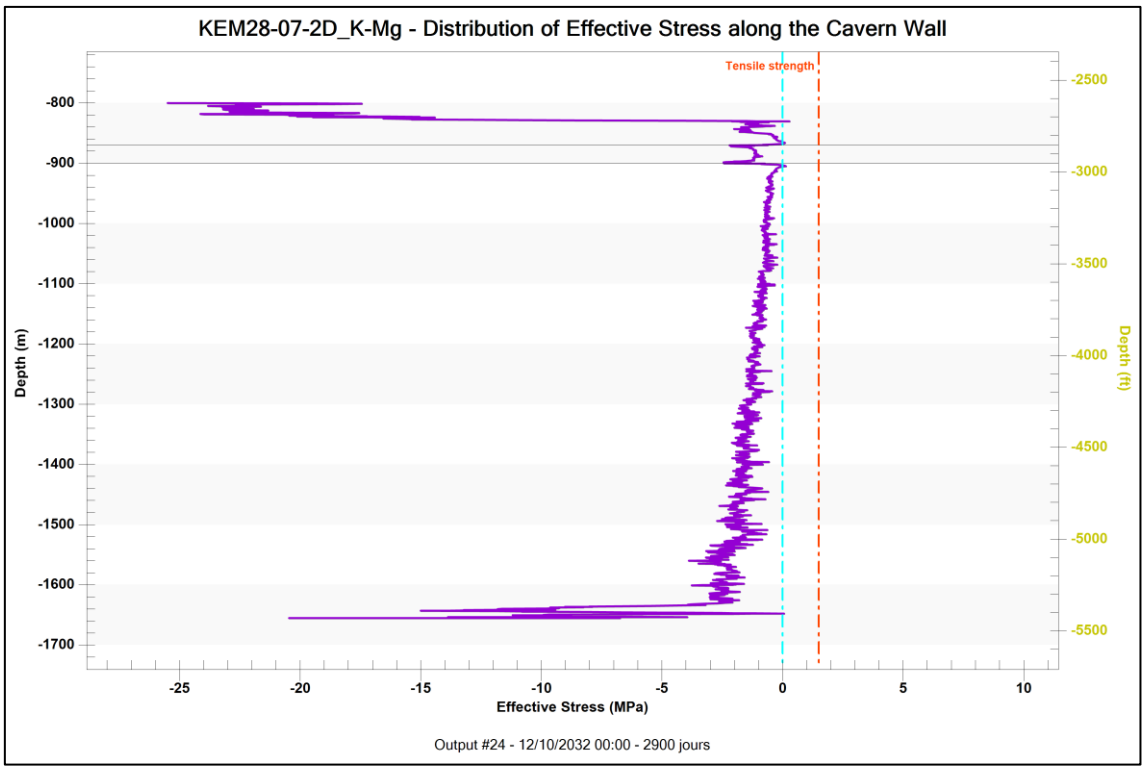

Figure 263. Effective stress distribution along the cavern wall (maximum pressure, output #24).

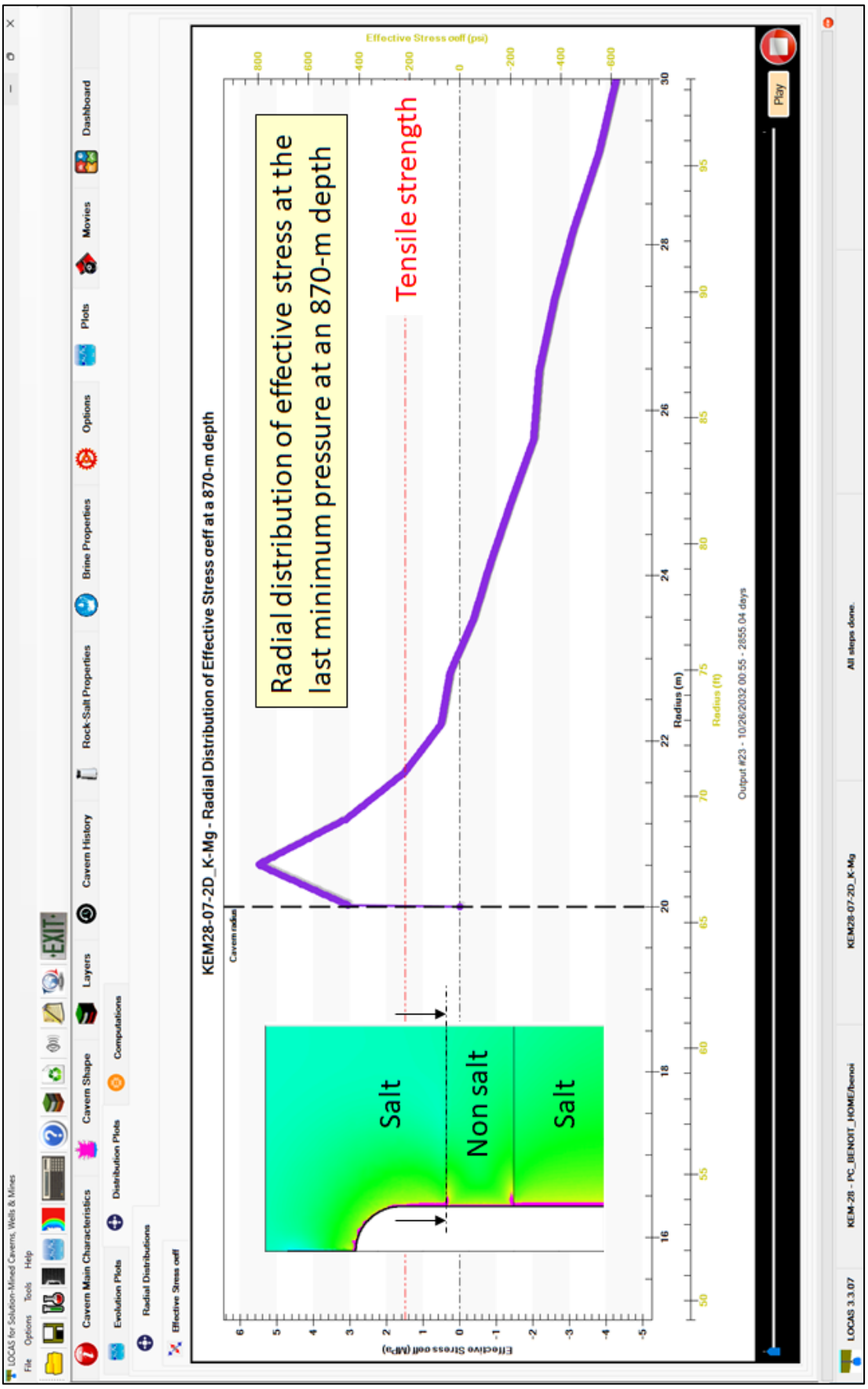

Figure 264. Radial distribution of effective stress at a depth of 870 meters during the final minimum pressure. The effective stress reaches 4.9 MPa at a distance of about 50 cm from the cavern wall along the interface between the two rocks. It may be possible for this value to cause a fracture along the interface.

1.14 3D Computations

1.14.1 Introduction

The design rules for the spacing of caverns on a site are generally based on an empirical model from the mining world, i.e., on an extraction ratio calculated for a network of chambers and pillars. The distance between each wellhead is often more than 200 m and the pillars, i.e., the minimum distance between each cavern, is usually more than 100 m, particularly in Northern Europe.

In the context of large-scale development of a hydrogen-based energy system, it could be necessary to create several dozen new caverns in the Netherlands. The aim of this chapter is to carry out a 3D sensibility analysis on the density of caverns on a site, in order to discuss the relevance of the rules of thumb for the spacing usually used.

1.14.2 Background

The behaviour of the salt pillar between 4 or 9 neighbouring caverns was discussed in Brouard et al., 2021a and Brouard et al., 2021b. The main results of these papers were recently confirmed by Ross et al. (2023).

The main results were as follows:

1. At the end of mining the central pillars are overloaded, but, a few years later, a large part of this overstress has been transferred outside the footprint of the cluster.

2. For elongated caverns, at cavern wall, vertical stress is less compressive than natural stress, this may induce tensile effective stresses and micro-cracks when cavern pressure is quickly increased, even at a cavern pressure significantly lower than geostatic pressure.

3. The average volume loss in a cluster is only slightly larger than the volume loss of a single cavern.

4. Rise of cavern bottom is faster than descent of cavern roof. The larger the extraction ratio, the larger the ratio between bottom rise and roof descent.

5. Computed maximum subsidence at ground level is sensitive to the selected boundary conditions (size of the meshed domain, etc.)

Performing such 3D heavy computations implies using a large amount of RAM in a high-performance computer (HPC). Computations generally last a few days or more depending on the size of the considered mesh and on the duration of the modelled period.

1.14.3 Considered configuration

Let's consider a cluster of 9 caverns as shown in Figure 265. Each cavern corresponds to the reference case (Case #07 in the 2D sensitivity analysis). The 3D model is composed of 5 tabular layers as in the 2D model (Table 10, page 256).

Extraction ratio

The extraction e is defined as:

$$e = \frac{\pi R_c^2}{l^2} \tag{83}$$

Where $2R_c$ is cavern maximum diameter and l is the distance between cavern axis.

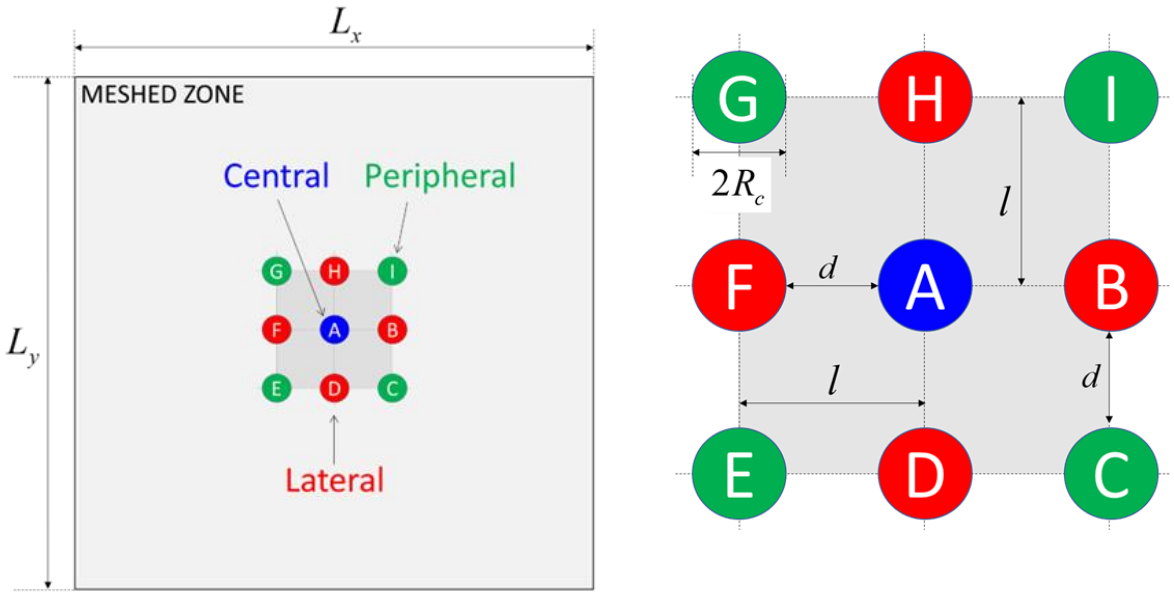

Figure 265. Analysis of a clusters of 9 caverns. For the sake of simplicity, it is assumed that the caverns are leached out simultaneously.

The mechanical stability of the cluster is analysed for different extraction ratios as shown in Table 28. The area occupied is calculated as $4\left(l+R_c\right)^2$.

Table 28. Geometric characteristics of the cases considered in the sensitivity analysis.

Extraction ratio e	Distance l (m)	Distance d (m)
5%	79.3	39.3
10%	64.7	24.7
20%	112.1	72.1
30%	158.5	118.5

Figure 266 and Figure 267 show an overview of the cluster in the case of a 20% extraction ratio. Figure 268 shows a diagonal vertical section along caverns G, A and C.

It is assumed that the nine caverns of the cluster are mined and operated simultaneously. All caverns are assumed to undergo synchronised 90-day cycles.

1.14.4 Meshing in 3D

The meshing process in 3D can be very complex and time consuming. In LOCAS several tools are used successively for meshing the modelled domain in 3D **(**Figure 269).

An example of a mesh in shown in Figure 270 and Figure 271 in the case of a 20% extraction ratio.

For all the considered meshes, the size of the meshed volume is 4000 m × 4000 m horizontally and 2500 m vertically. LOCAS can be used to check that the effective distance between the caverns in the mesh corresponds to the desired value Figure 272.

1.14.5 3D computations outcomes

3D calculations provide a wide range of different results. For this (relatively) limited study, we are only interested in the loss of cavern volume and the associated subsidence.

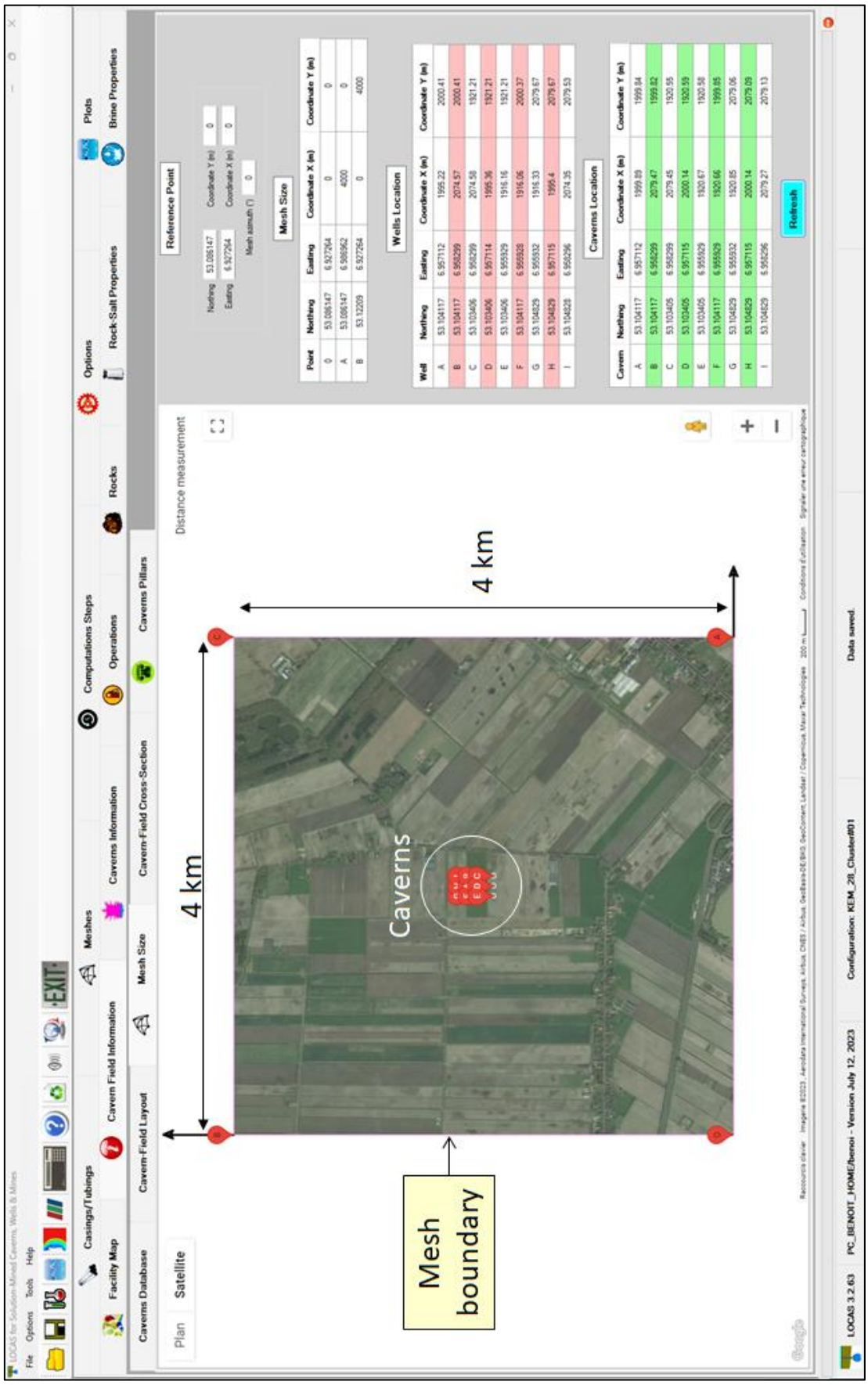

Figure 266. Meshed zone around the cluster (LOCAS screenshot). The edges of the mesh are located at a distance of 2 km from the centre of the cluster.

Figure 267. Example of a tested configuration (extraction ratio = 20%). For this extraction ratio, the distance between wells is 79.3 m.

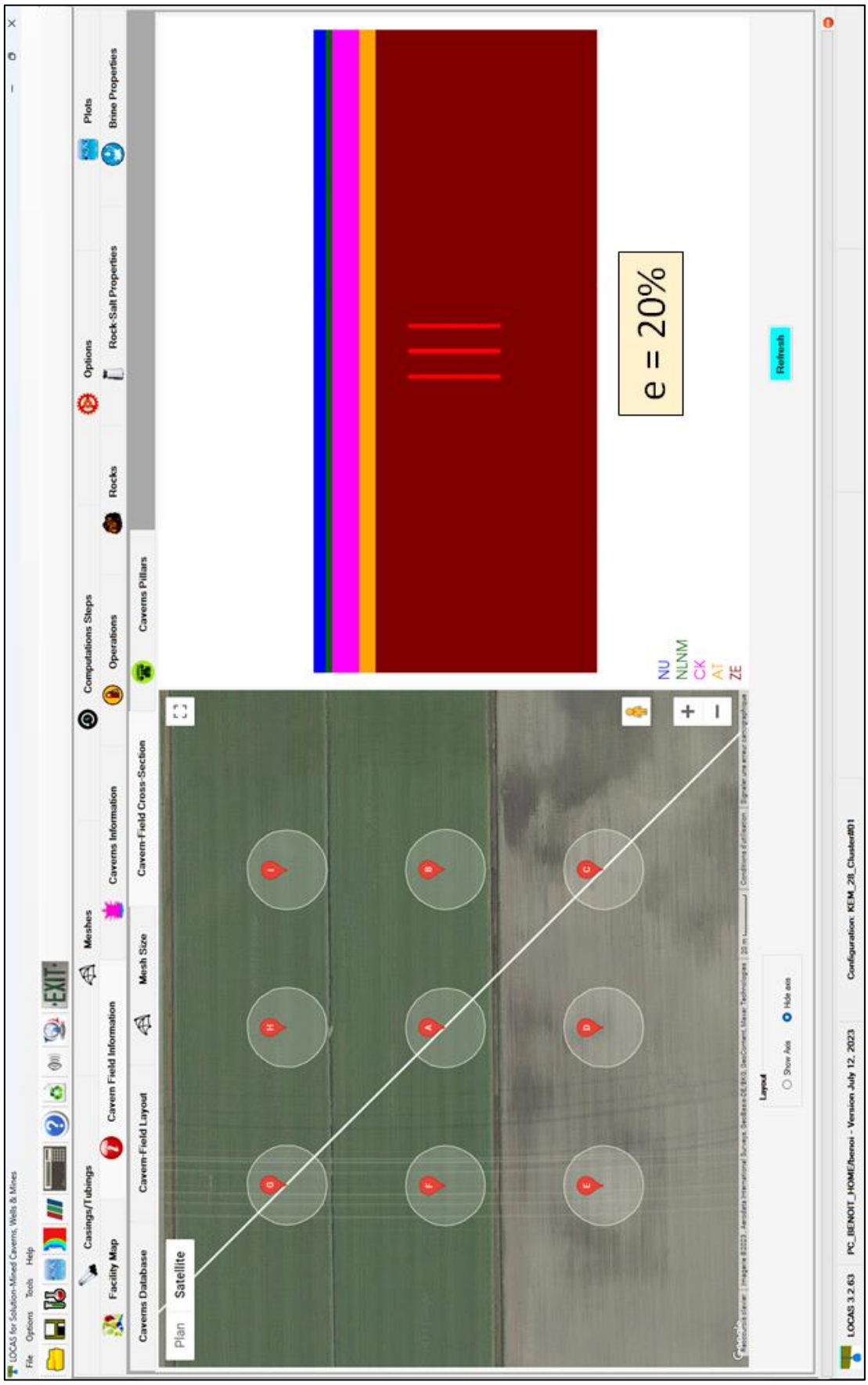

Figure 268. Vertical section along the axes of caverns G, A and C (e=20%, LOCAS screenshot).

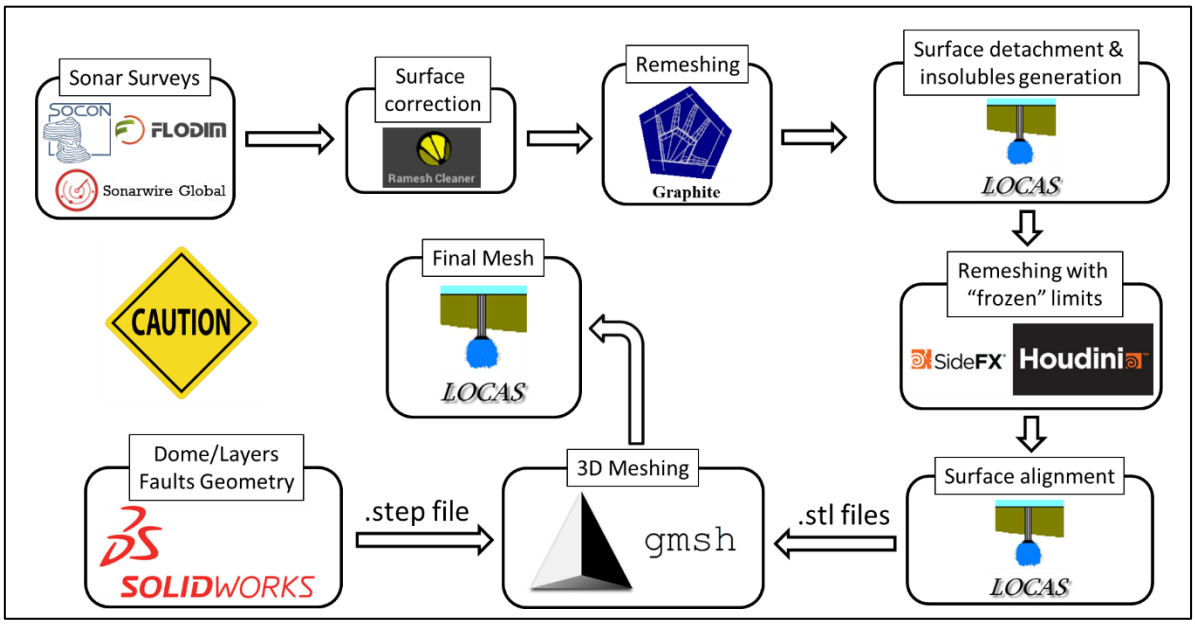

Figure 269. Complex 3D meshing workflow in LOCAS. Several tools are used sequentially to refine and check the quality of the mesh, in particular the absence of degenerate elements.

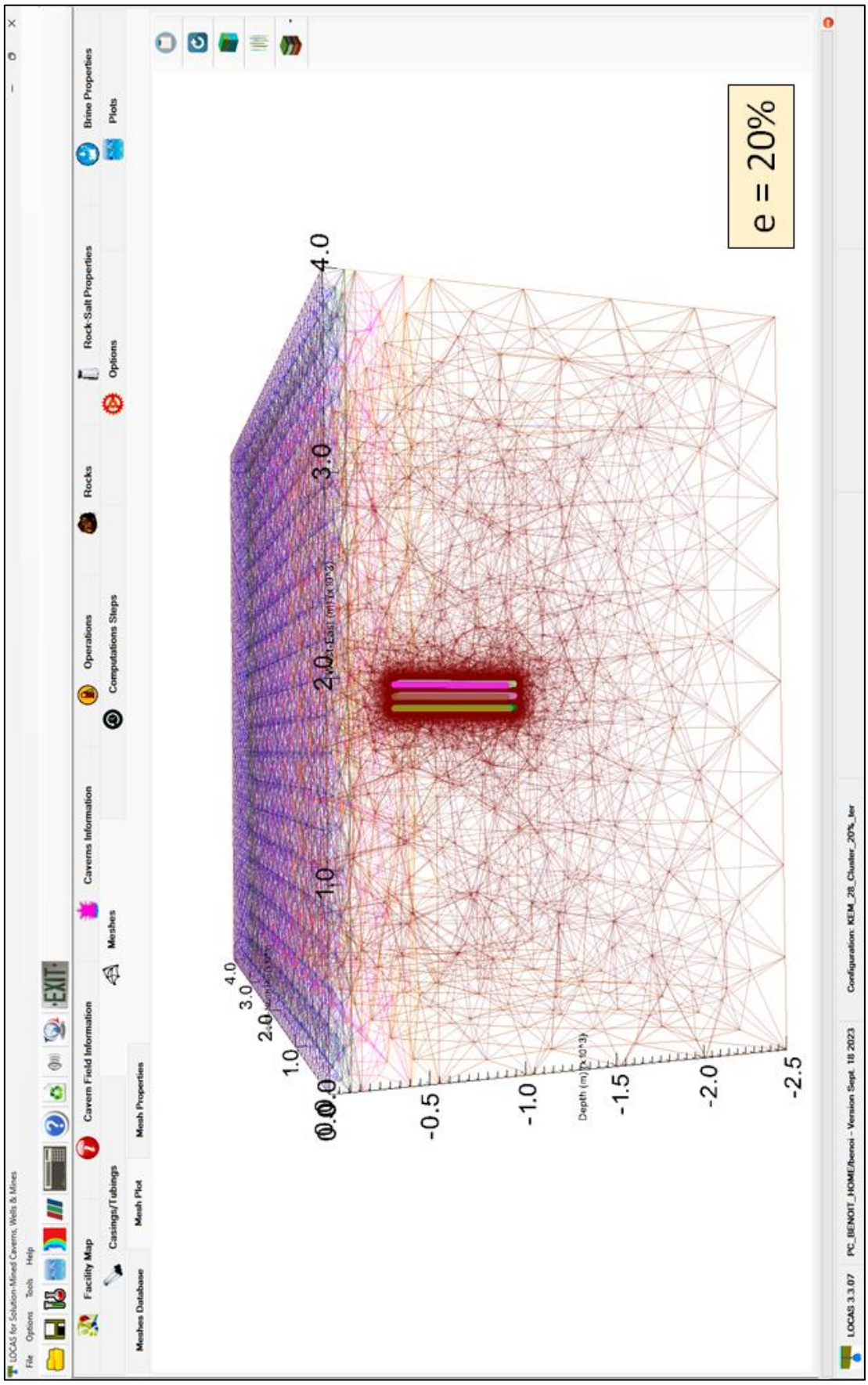

Figure 270. Example of a mesh, case extraction ratio = 20% (LOCAS screenshot).

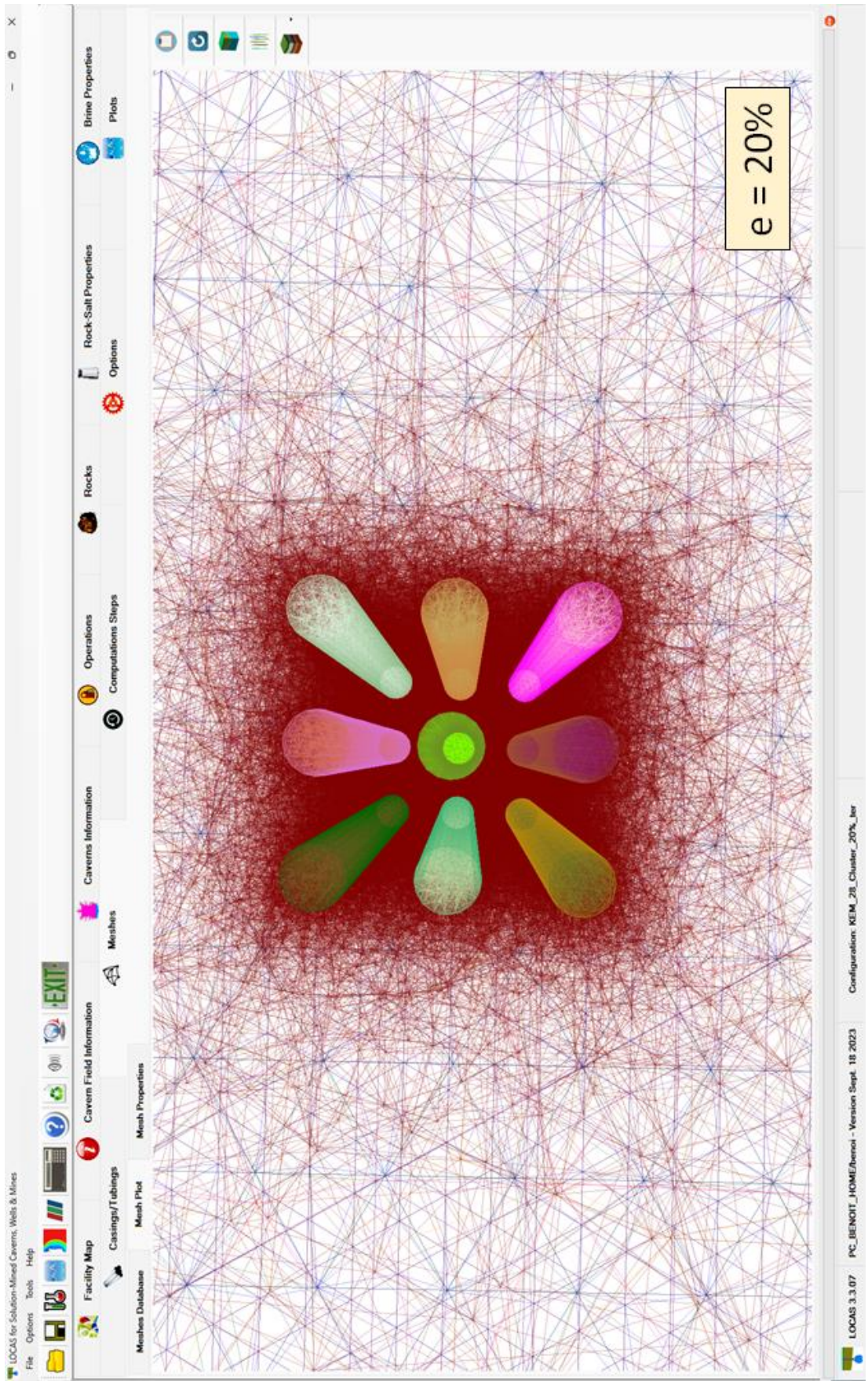

Figure 271. Top view of the mesh, case extraction ratio = 20% (LOCAS screenshot).

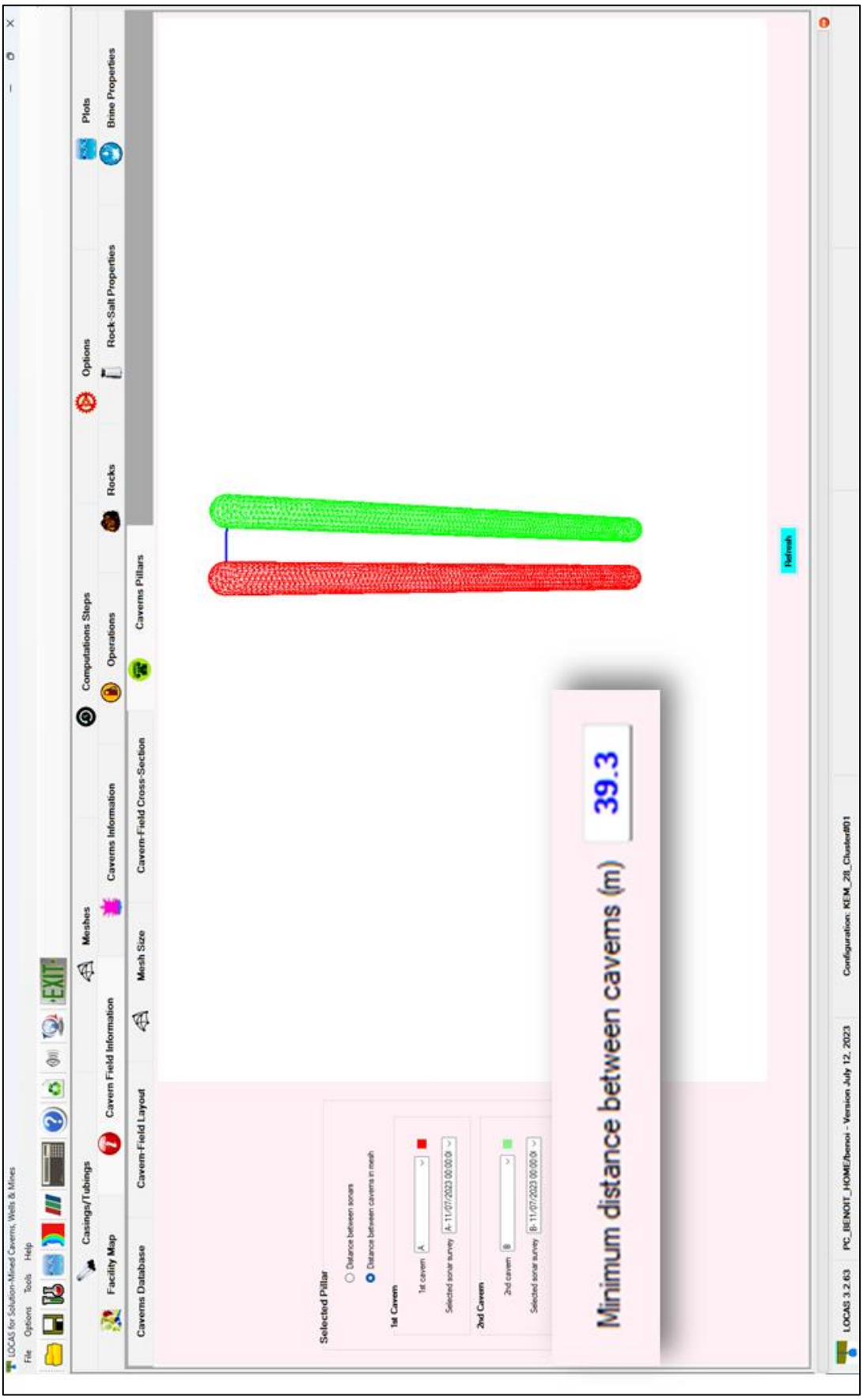

Figure 272. Checking the minimum distance between caverns in the mesh, case extraction ratio = 20% (LOCAS screenshot).

1.14.5.1 Cavern creep closure

The volume losses calculated after 900 days of cycling for an isolated cavern or cluster with an extraction ratio of 5% to 30%, taking into account both dislocation creep and pressure solution creep, are given in Table 29. We can see that the caverns in the cluster, whatever the extraction ratio between 5% and 30%, have a smaller loss of volume than an isolated cavern undergoing the same pressure history. This effect had already been observed in Brouard et al. (2021a, 2021b) and Ross et al. (2023). The pillar at the centre of the cluster is understressed. The larger the extraction ratio, the less compressive are vertical stresses in the pillar. A large part of the vertical load above the cluster is progressively transferred to the abutment, which reduces the deviatoric stresses in the pillar that cause the loss of volume.

It should be noted that the difference between all the configurations remains small; for example, the average loss of volume is 1.47%/year for an extraction ratio of 5% and 1.67%/year if the ratio is 30%, i.e., a difference of only 14%. However, the difference in size is quite large, 127,450 m² for a 5% extraction ratio and only 28,700 m² for a 30% extraction ratio (Table 28); i.e., more than four times less.

Whatever the extraction ratio, the central cavern (A) closes less quickly than the other caverns in the cluster. The caverns that close the fastest are those in the corners (CEGI). The higher the extraction ratio, the greater the difference between the central cavern and the other caverns.

Table 29. Volume loss and loss rate after 900 days of cycling (with pressure solution creep).

	Extraction ratio	Caverns	Volume loss after 900 days	Average Volume-loss rate
			m^3	%/year
Single Cavern	NA	**A**	43260	1.76
Cluster	**5%**	**A**	35783	1.45
		BDFH	35829	1.45
		CEGI	37204	1.51
		Average	36195	1.47
	10%	**A**	36909	1.50
		BDFH	37484	1.52
		CEGI	39881	1.62
		Average	38485	1.56
	20%	**A**	38527	1.56
		BDFH	39150	1.59
		CEGI	43207	1.75
		Average	40884	1.66
	30%	**A**	38423	1.56
		BDFH	38718	1.57
		CEGI	44034	1.79
		Average	41048	1.67

Table 30 gives the volume losses when the pressure solution creep mechanism is not taken into account. The loss of cavern volume is then around 30% smaller for all configurations (isolated cavern or cluster with different extraction ratios).

Table 30. Volume loss and loss rate after 900 days of cycling (without pressure solution creep).

	Extraction ratio	Caverns	Volume loss after 900 days m^3	Average Volume-loss rate $\times 10^{-4}$ /year
Single Cavern	NA	**A**	30713	1.25
Cluster	**5%**	**A**	25935	1.05
		BDFH	26159	1.06
		CEGI	27377	1.11
		Average	26675	1.08
	10%	**A**	26567	1.08
		BDFH	27080	1.10
		CEGI	28979	1.18
		Average	27867	1.13
	20%	**A**	27494	1.12
		BDFH	28007	1.14
		CEGI	31079	1.26
		Average	29315	1.19
	30%	**A**	27223	1.10
		BDFH	27525	1.12
		CEGI	31534	1.28
		Average	29273	1.19

Figure 273, Figure 274 and Figure 275 show the changes in cavern volume loss (counted since the end of leaching) for cavern A, caverns BDFH and CEGI respectively.

Figure 276, Figure 277, Figure 278 and Figure 279 show the changes in cavern volume loss with and without pressure solution creep for extraction ratios of 5%, 10%, 20% and 30% respectively. A lower extraction ratio results in a lower volume loss (of only a few thousand m^3) after the first production phase after the debrining, but thereafter the differences in the volume loss rate are small.

1.14.5.2 Cavern creep closure rate

Figure 280 to Figure 287 show the changes in volume loss rates for the different extraction ratios. Solid lines are when pressure solution is considered and dashed lines are when pressure solution is not considered. The differences remain small, and it is whether or not the pressure solution mechanism is taken into account that has the greatest effect.

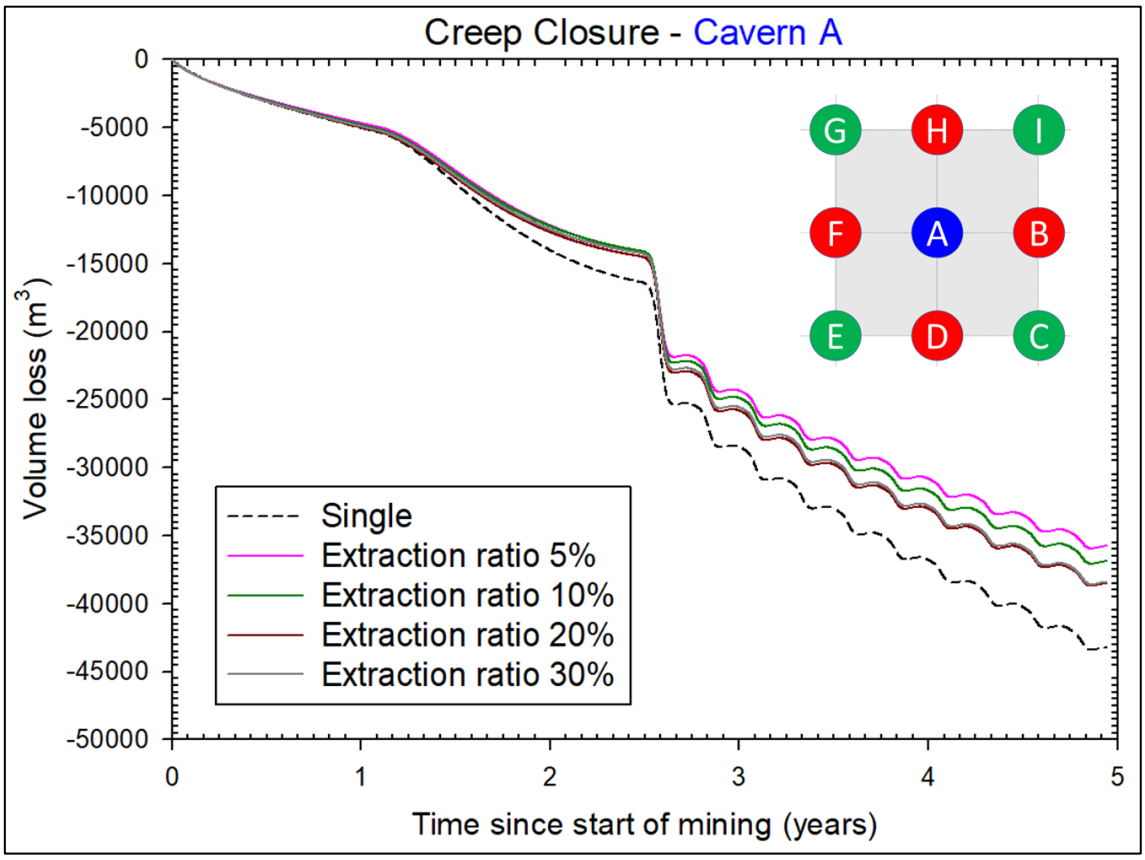

Figure 273. Evolution of cavern A volume loss since the start of mining (pressure solution included).

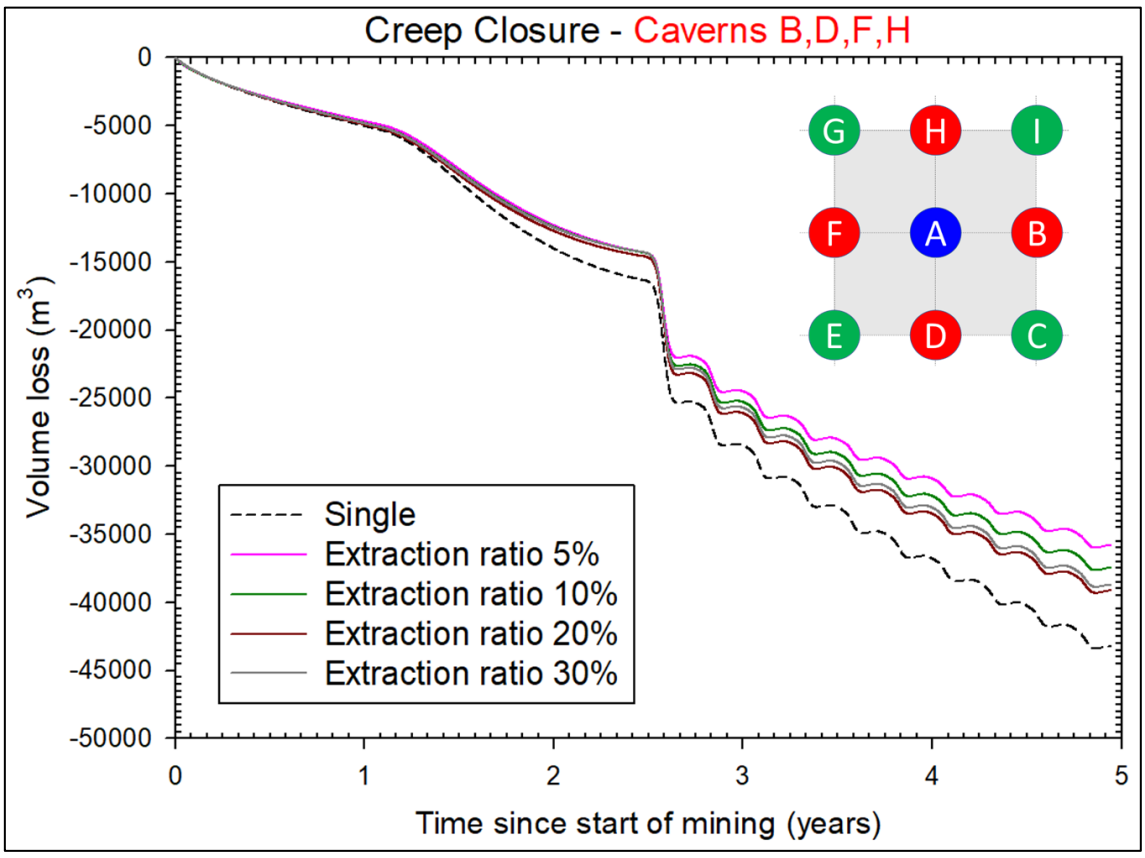

Figure 274. Evolution of caverns B,D,F,H volume loss since the start of mining (pressure solution included).

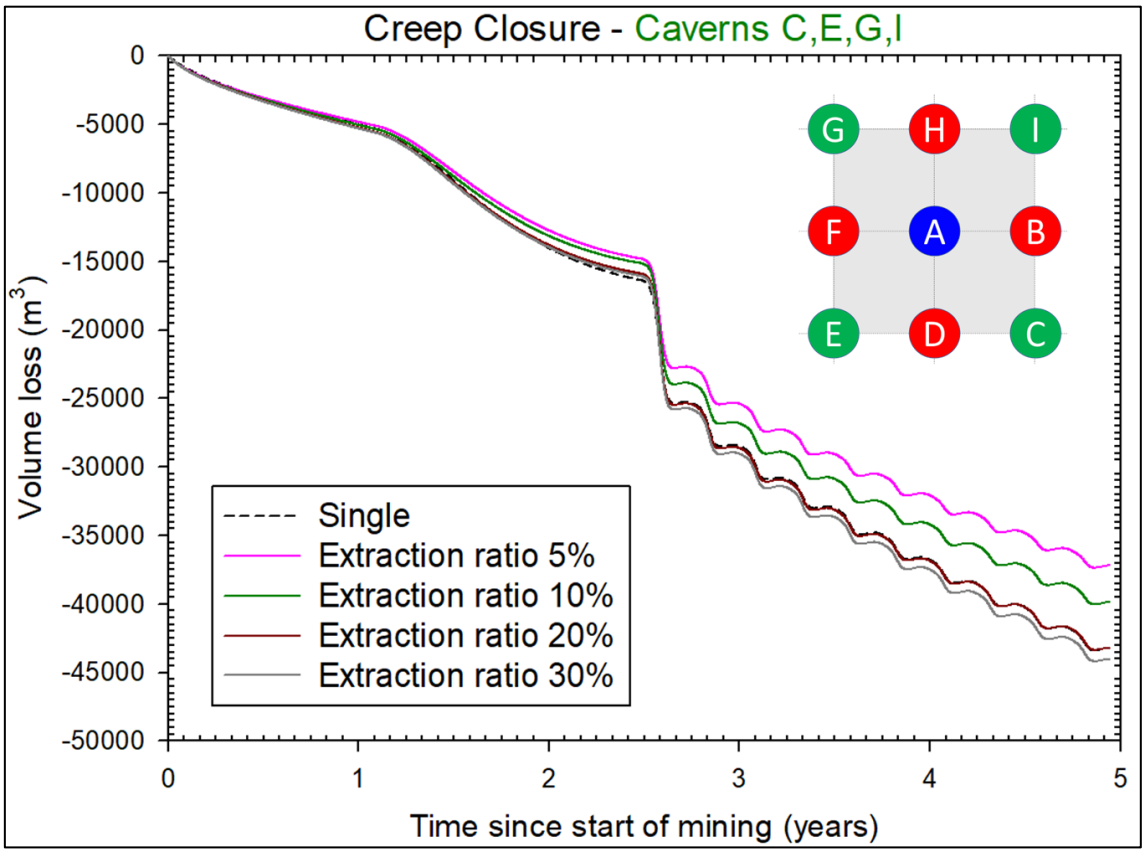

Figure 275. Evolution of caverns C,D,G,I volume loss since the start of mining (pressure solution included).

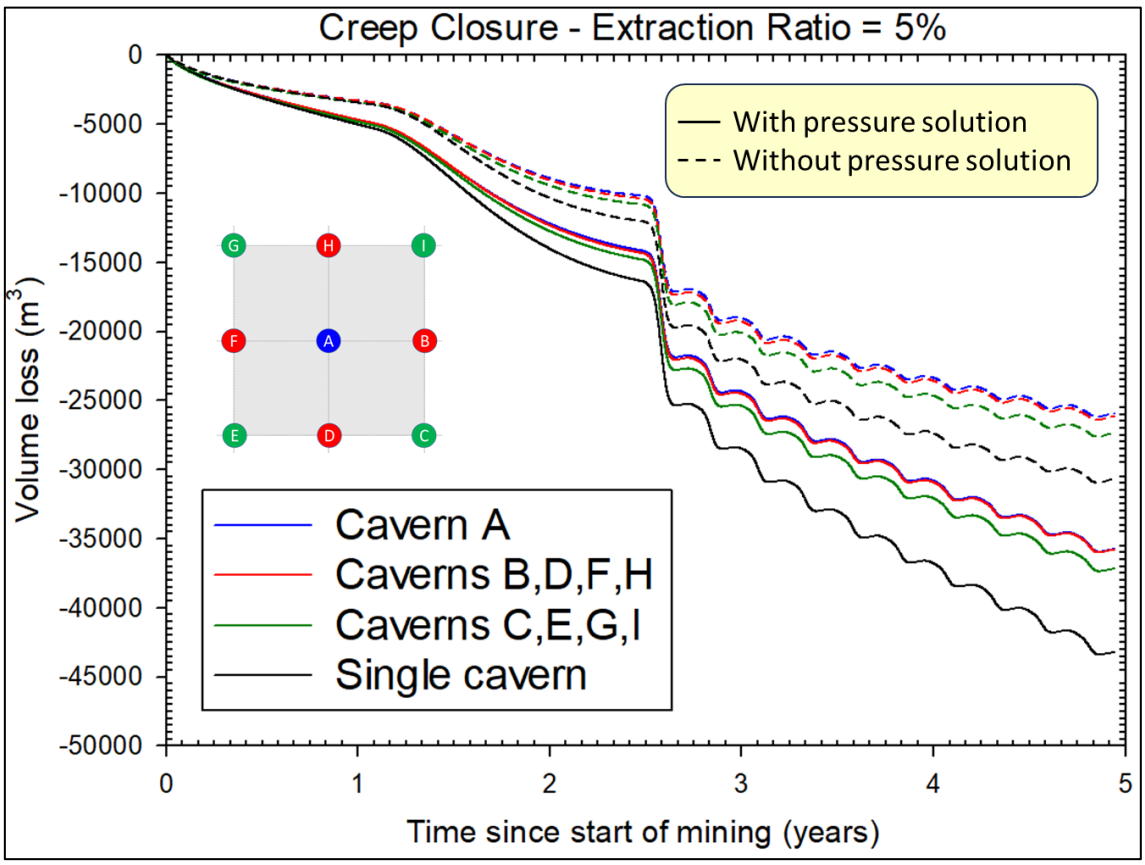

Figure 276. Evolution of caverns volume loss since the start of mining. Extraction ratio = 5%.

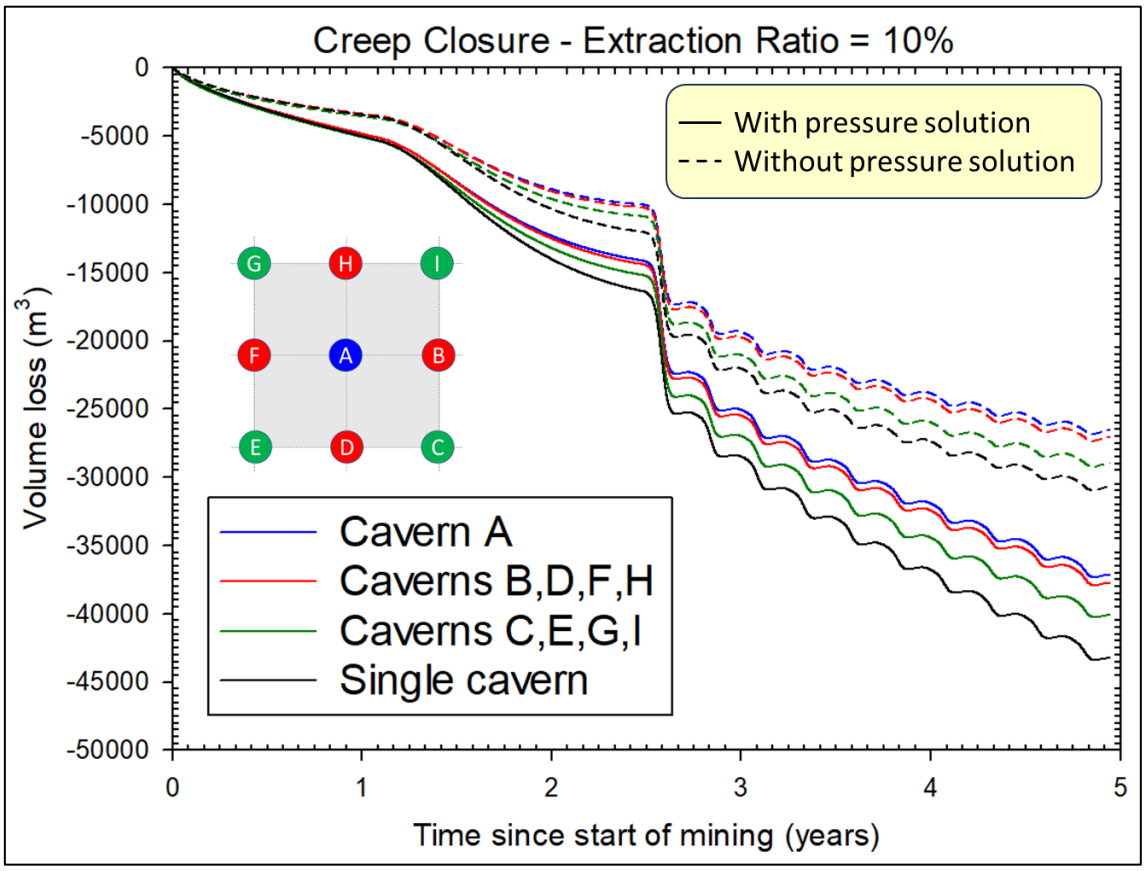

Figure 277. Evolution of caverns volume loss since the start of mining. Extraction ratio = 10%.

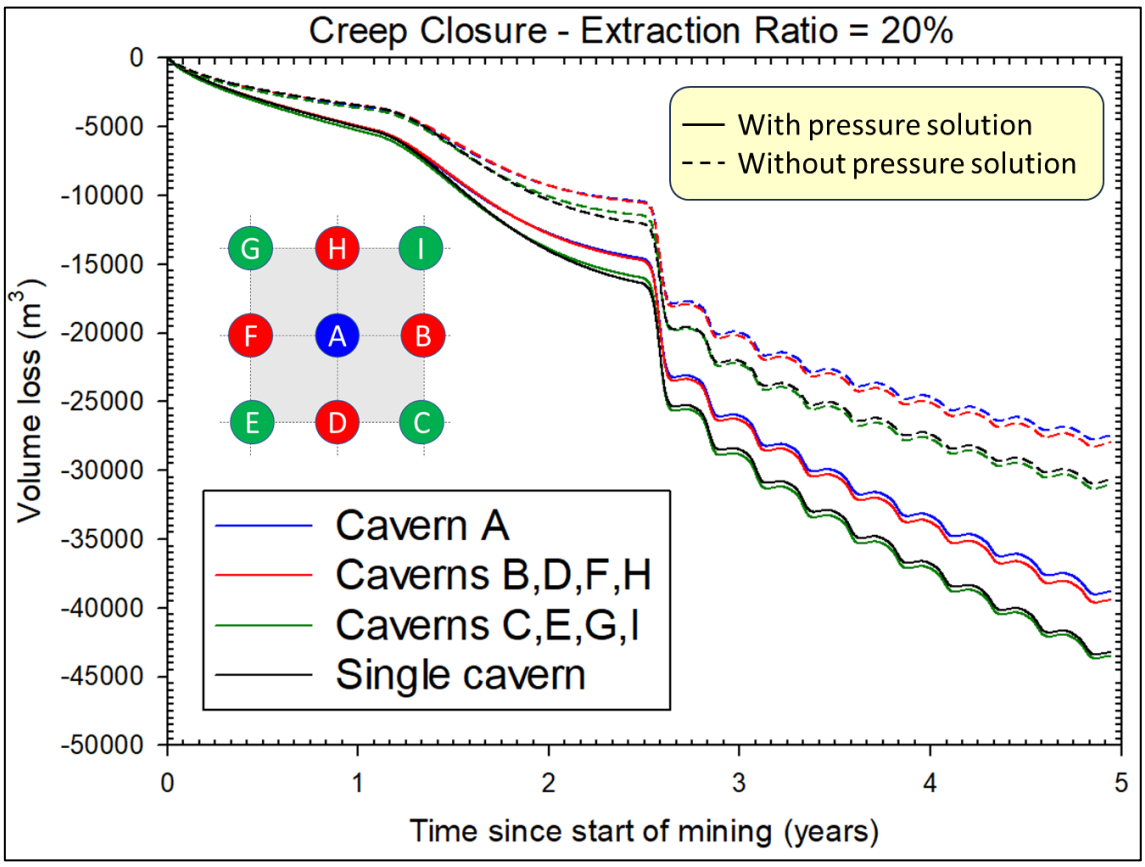

Figure 278. Evolution of caverns volume loss since the start of mining. Extraction ratio = 20%.

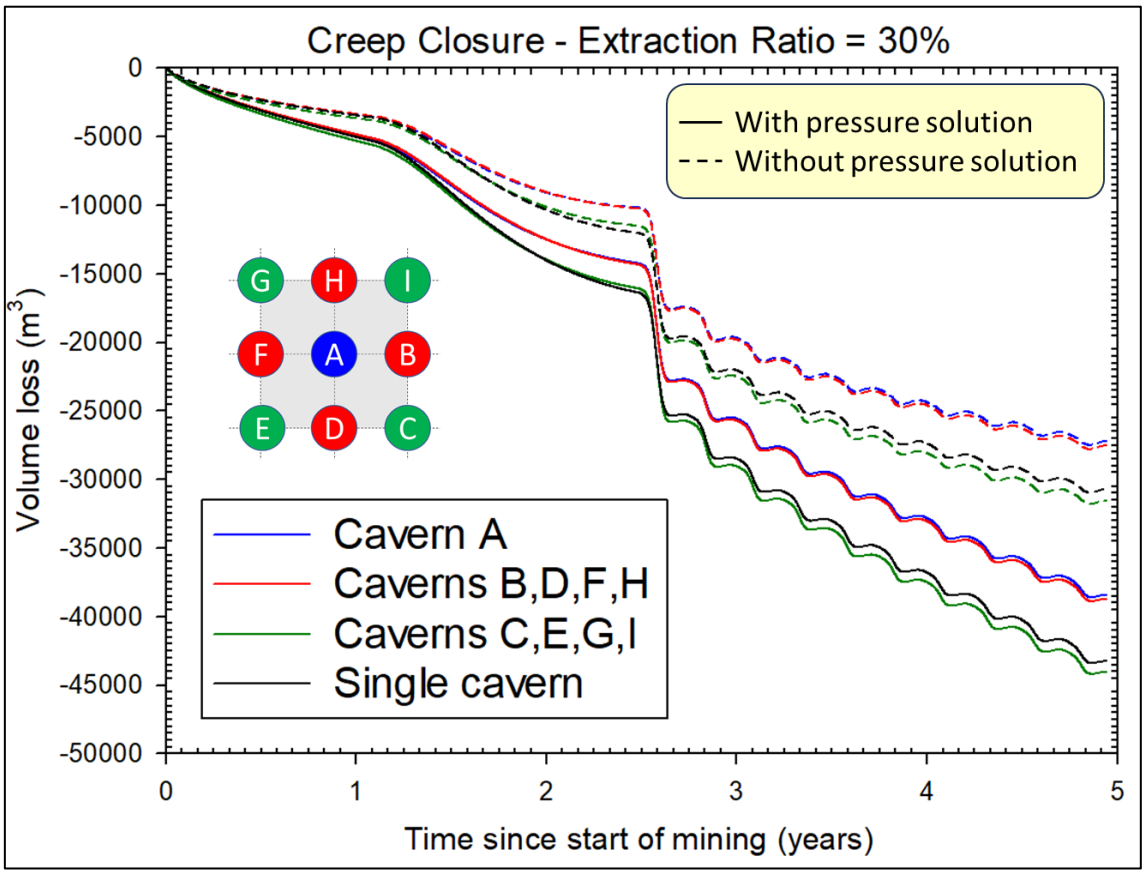

Figure 279. Evolution of caverns volume loss since the start of mining. Extraction ratio = 30%.

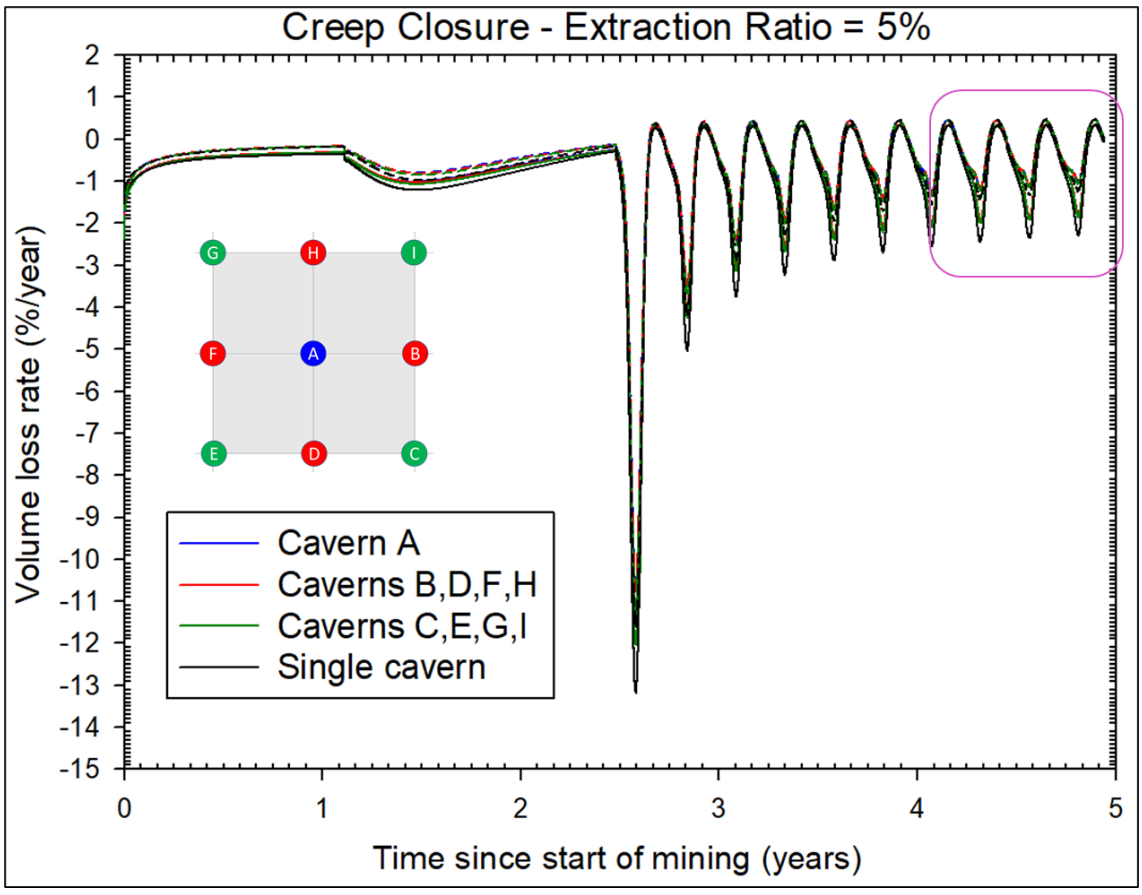

Figure 280. Evolution of caverns volume loss rate since the start of mining. Extraction ratio = 5%.

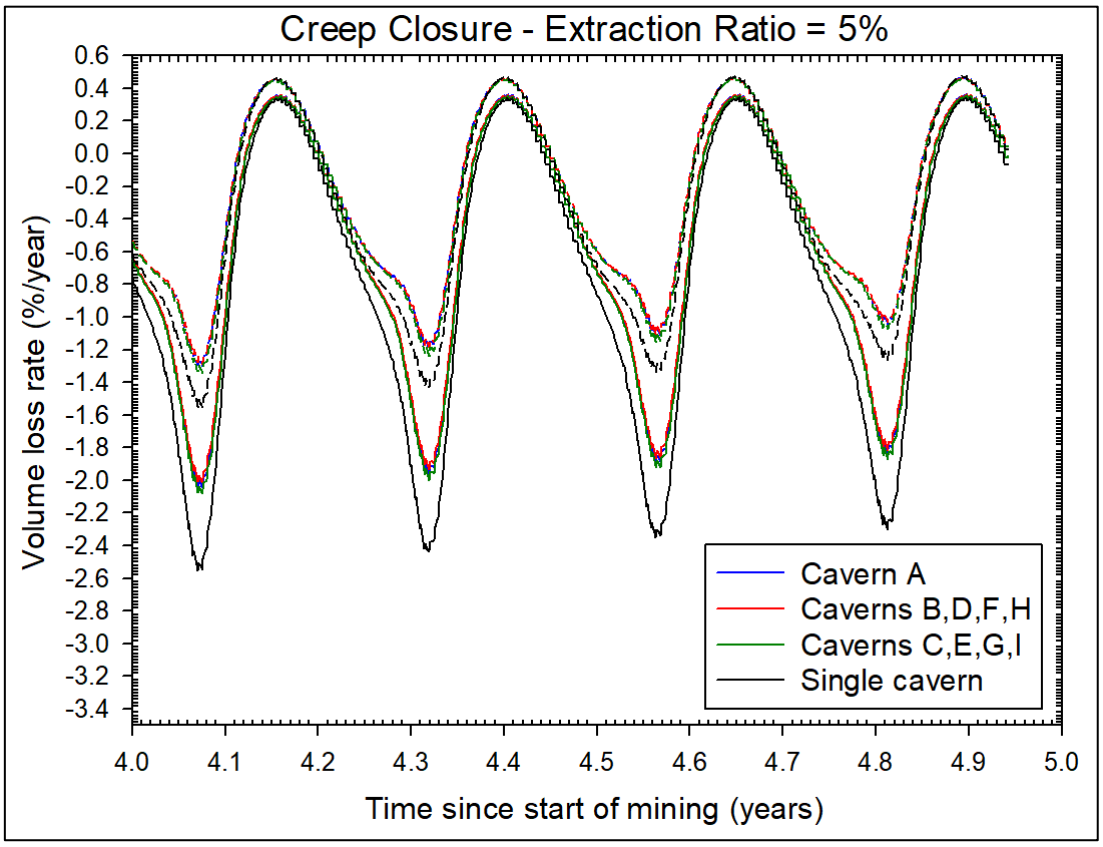

Figure 281. Evolution of caverns volume loss rate since the start of mining. Extraction ratio = 5% [Zoom].

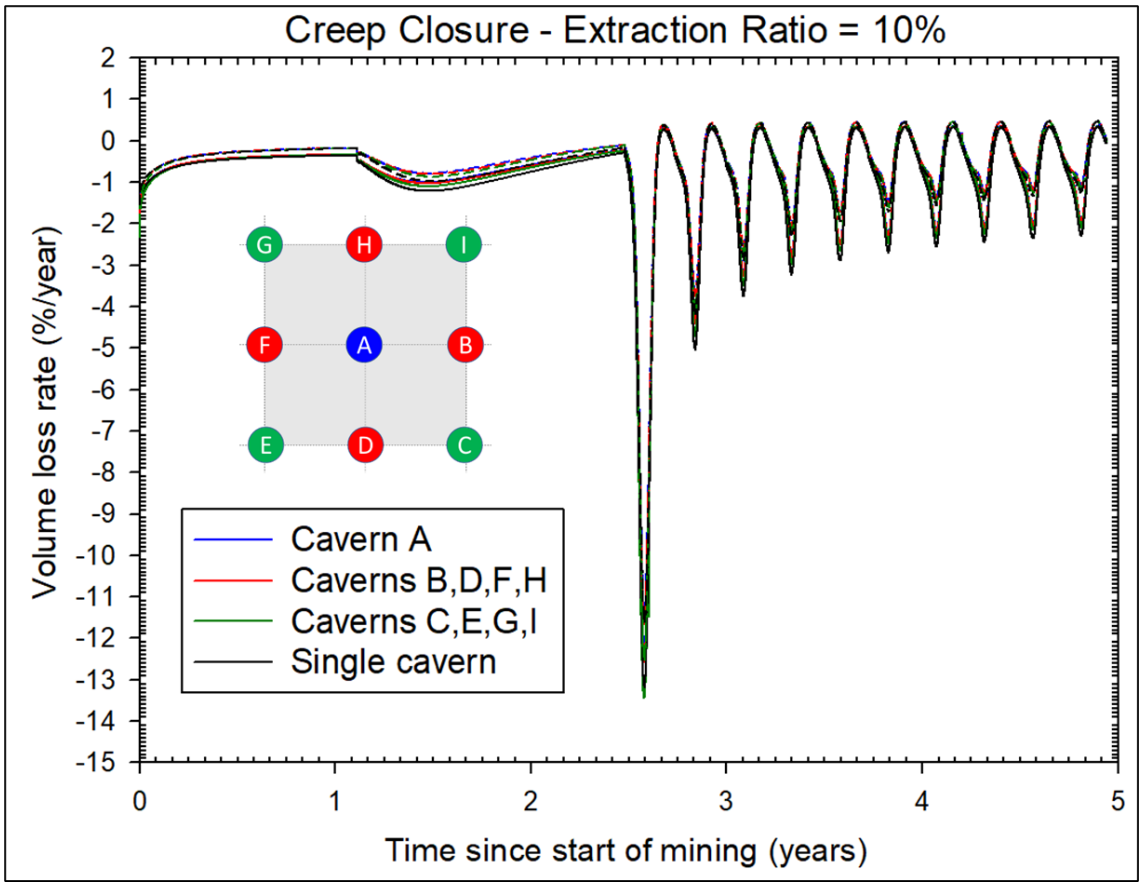

Figure 282. Evolution of caverns volume loss rate since the start of mining. Extraction ratio = 10%.

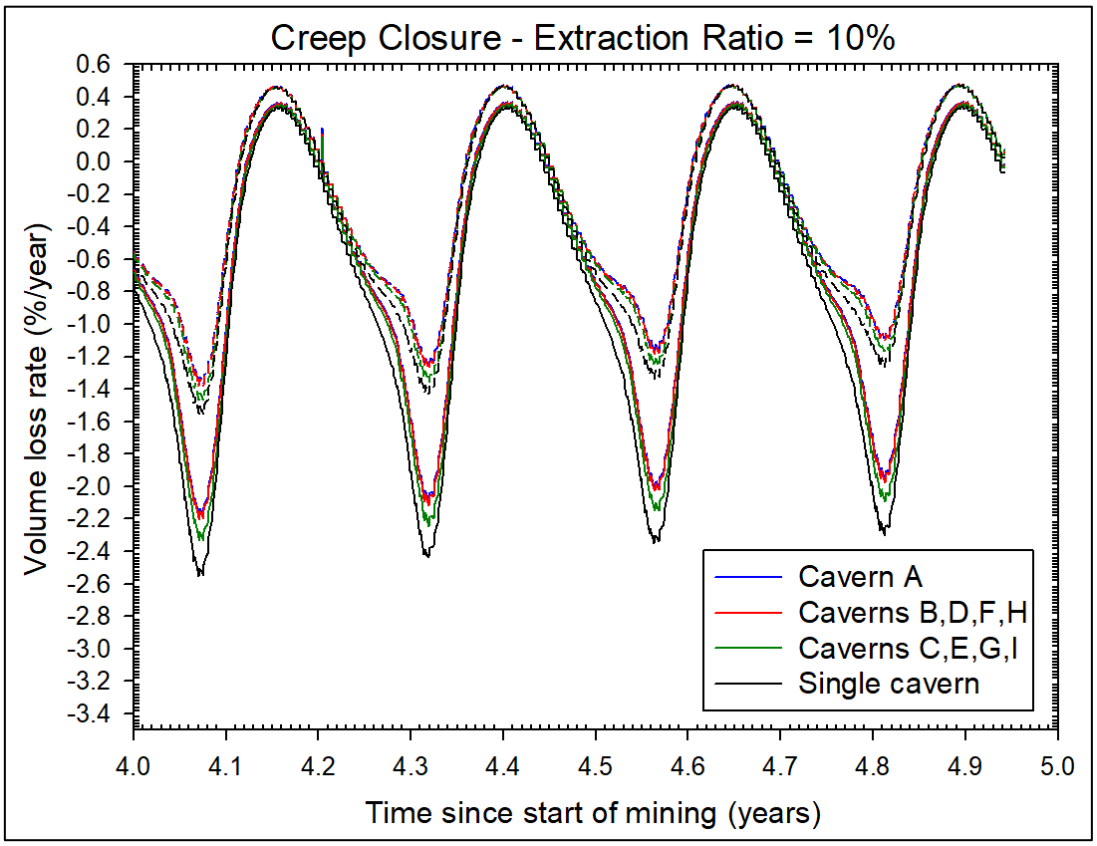

Figure 283. Evolution of caverns volume loss rate since the start of mining. Extraction ratio = 10% [Zoom].

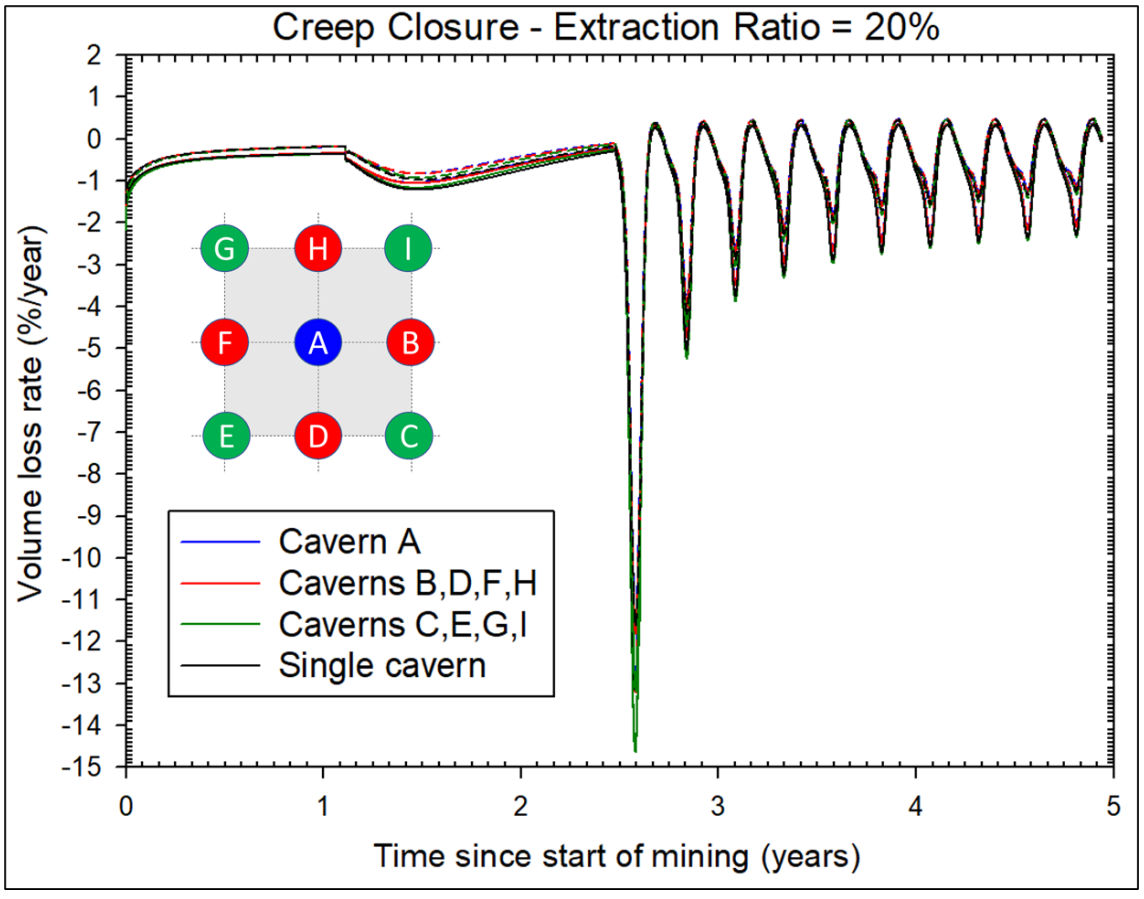

Figure 284. Evolution of caverns volume loss since the start of mining. Extraction ratio = 20%.

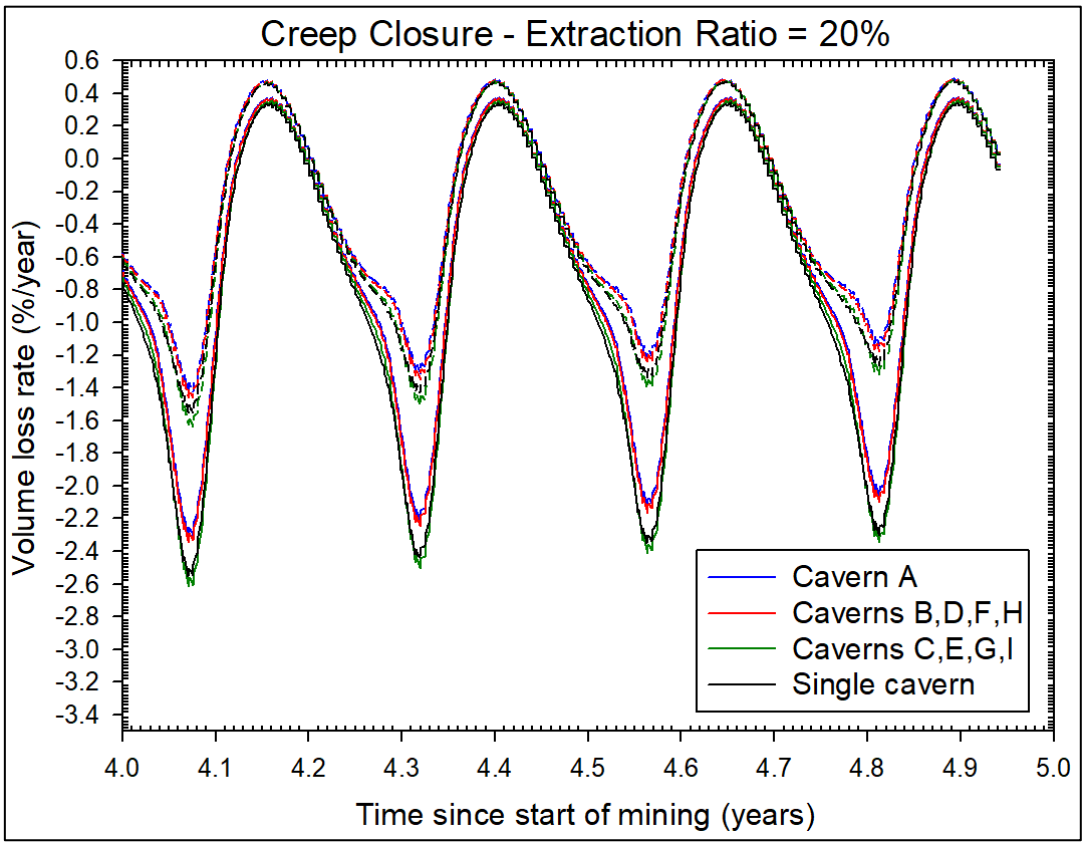

Figure 285. Evolution of caverns volume loss rate since the start of mining. Extraction ratio = 20% [Zoom].

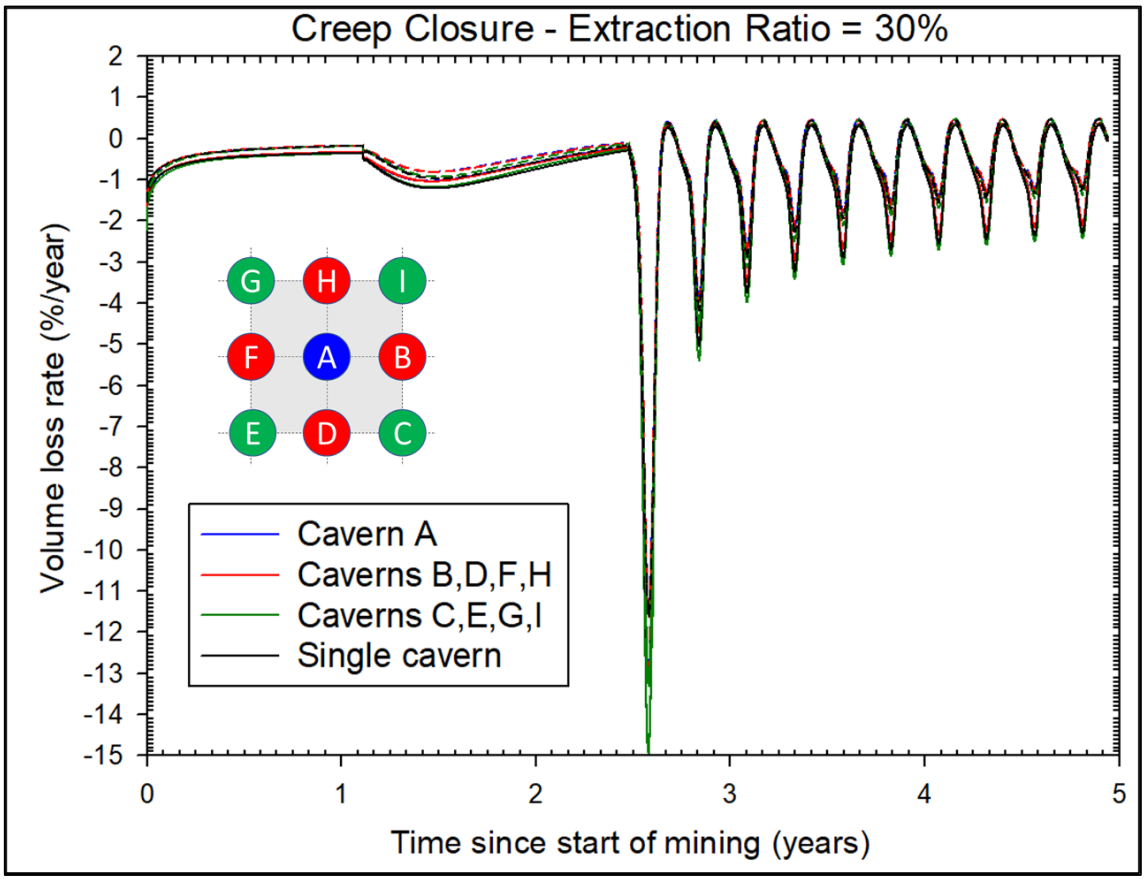

Figure 286. Evolution of caverns volume loss rate since the start of mining. Extraction ratio = 30%.

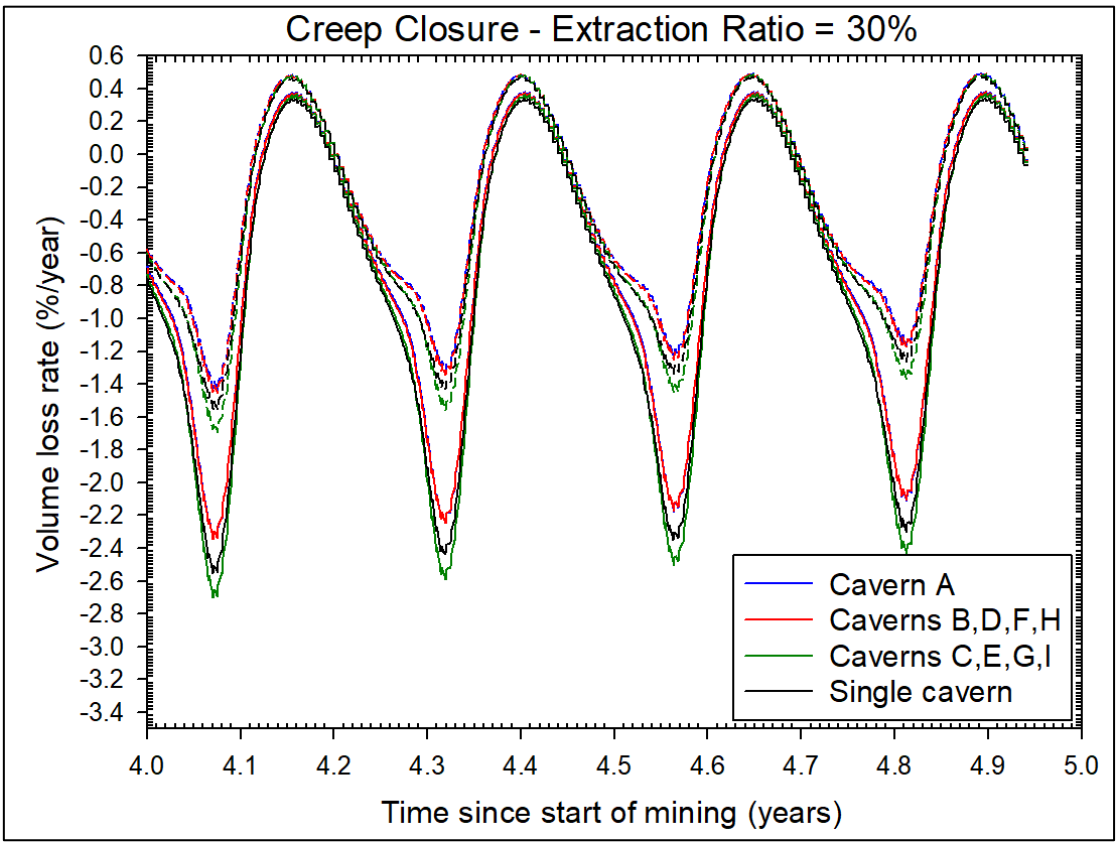

Figure 287. Evolution of caverns volume loss rate since the start of mining. Extraction ratio = 30% [Zoom].

1.14.5.3 Subsidence

Figure 288 shows the evolution of maximum subsidence (maximum vertical displacement at the surface) for the isolated cavern and for the clusters with different extraction ratios when pressure solution mechanism is taken into account. We can see that the subsidence created by the 9 caverns in a cluster is always less than 9 times the subsidence created by a single isolated cavern. As might be expected, maximum subsidence increases with the extraction ratio, being around 50% greater between a ratio of 5% and a ratio of 30%. We can also see that there is little difference between a ratio of 5% and a ratio of 10%, whereas the configuration with a ratio of 10% occupies an area 1.8 times smaller.

Figure 289 shows the evolution of maximum subsidence when pressure solution mechanism is not taken into account. When the pressure solution is not taken into account, the maximum subsidence is lower, but the difference is not significant for the clusters. The lower the extraction ratio, the wider the subsidence bowl.

1.14.5.4 Dilation

Figure 290 to Figure 293 show the contours of the Factor of Safety of the dilation criterion at the last minimum pressure for extraction ratios of 5 to 30%. It can be seen that the extraction rate has little effect in this configuration on the appearance of dilatation inside the pillars. The FOS is larger than 3 (yellow areas) in the centre of the pillars.

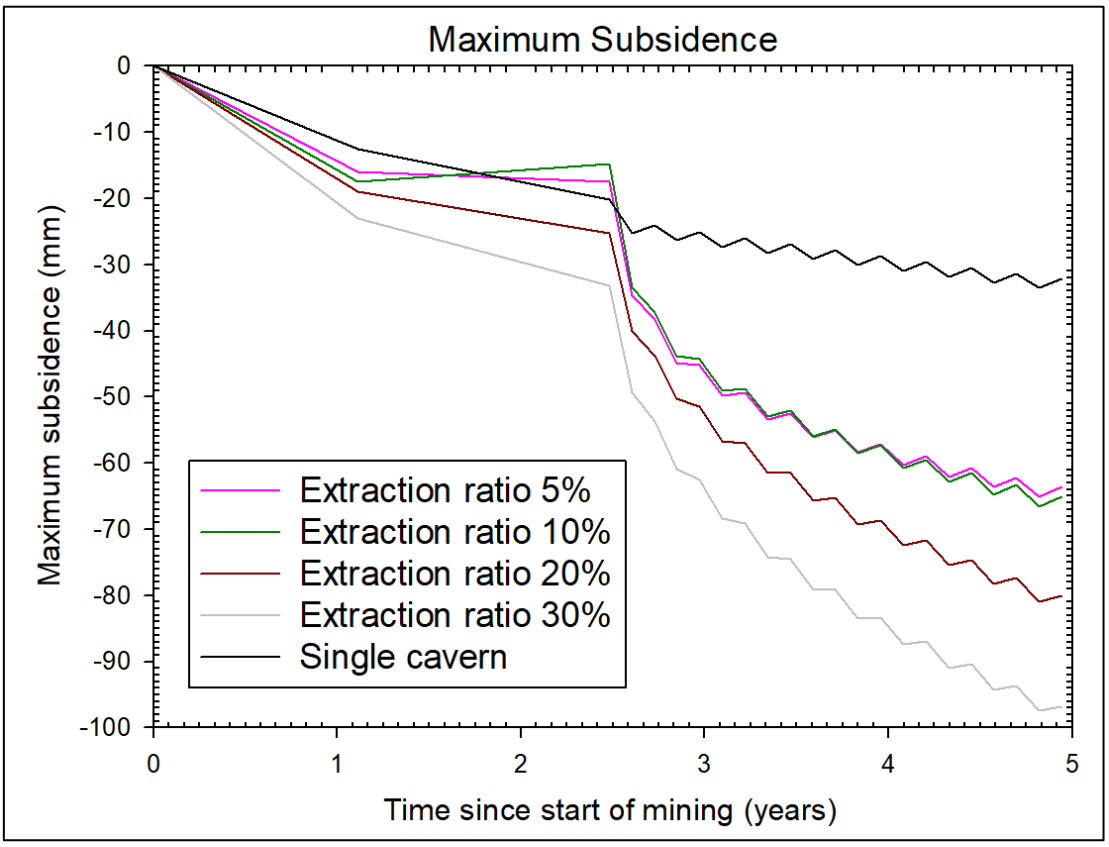

Figure 288. Evolution of maximum subsidence (pressure solution included).

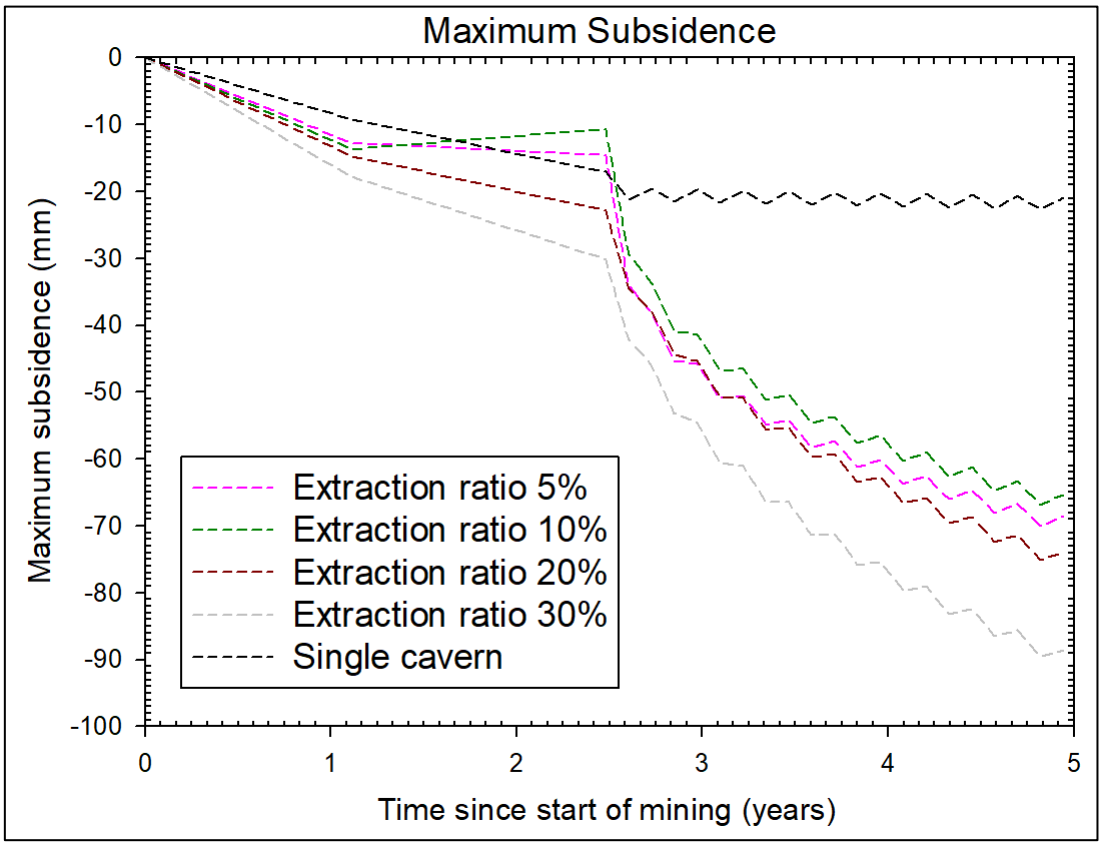

Figure 289. Evolution of maximum subsidence (pressure solution not included).

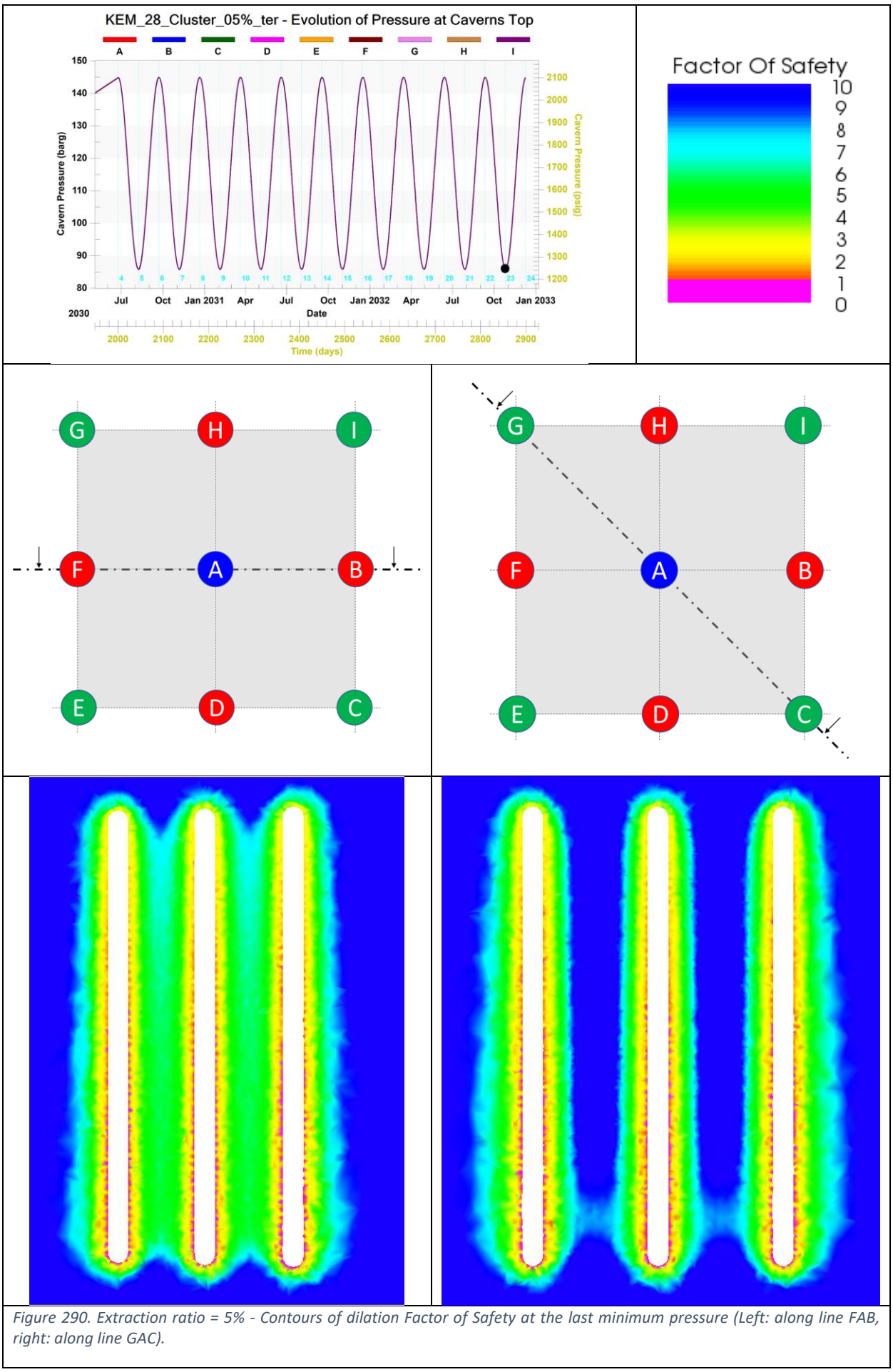

Figure 290. Extraction ratio = 5% - Contours of dilation Factor of Safety at the last minimum pressure (Left: along line FAB, right: along line GAC).

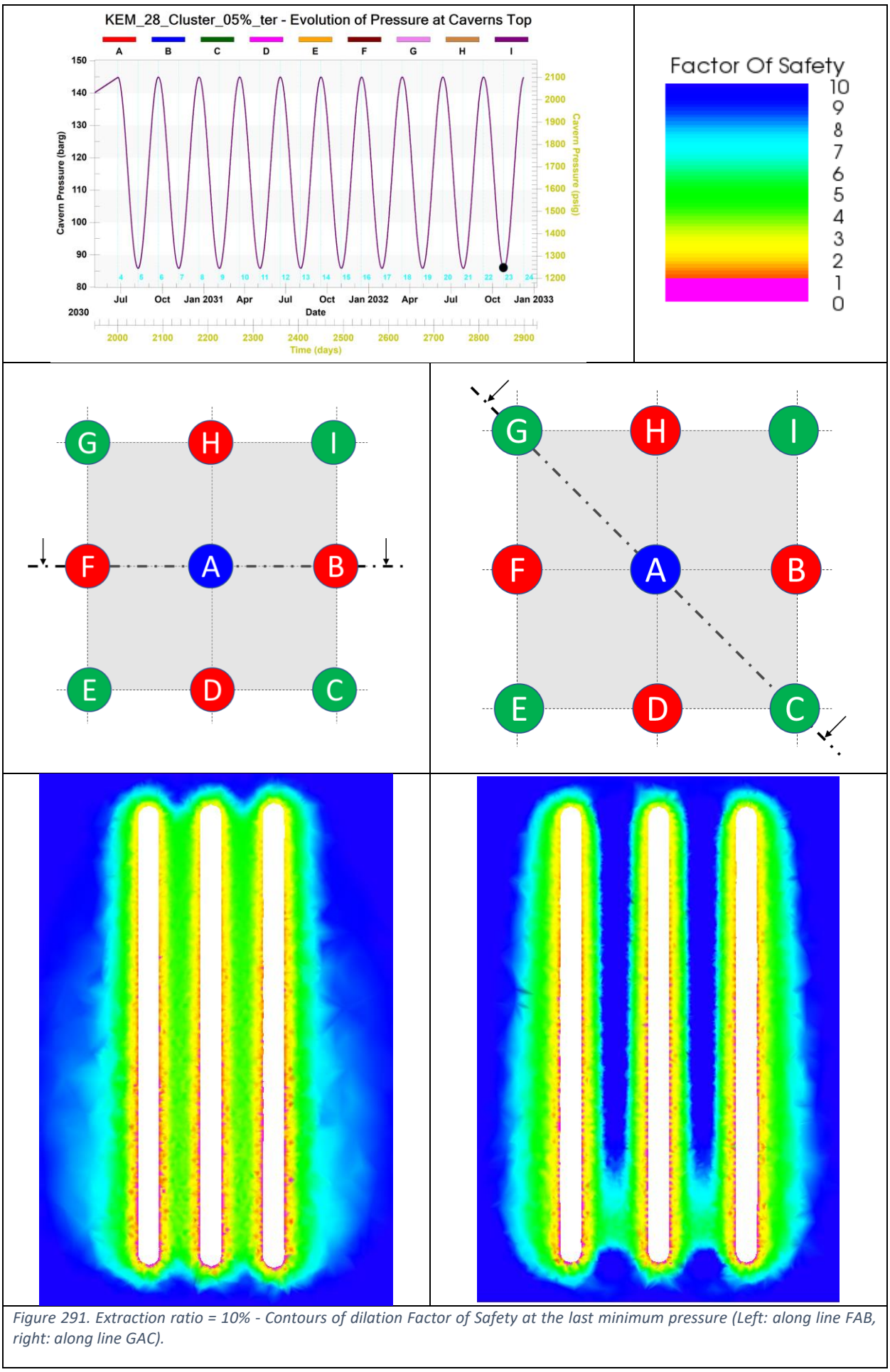

Figure 291. Extraction ratio = 10% - Contours of dilation Factor of Safety at the last minimum pressure (Left: along line FAB, right: along line GAC).

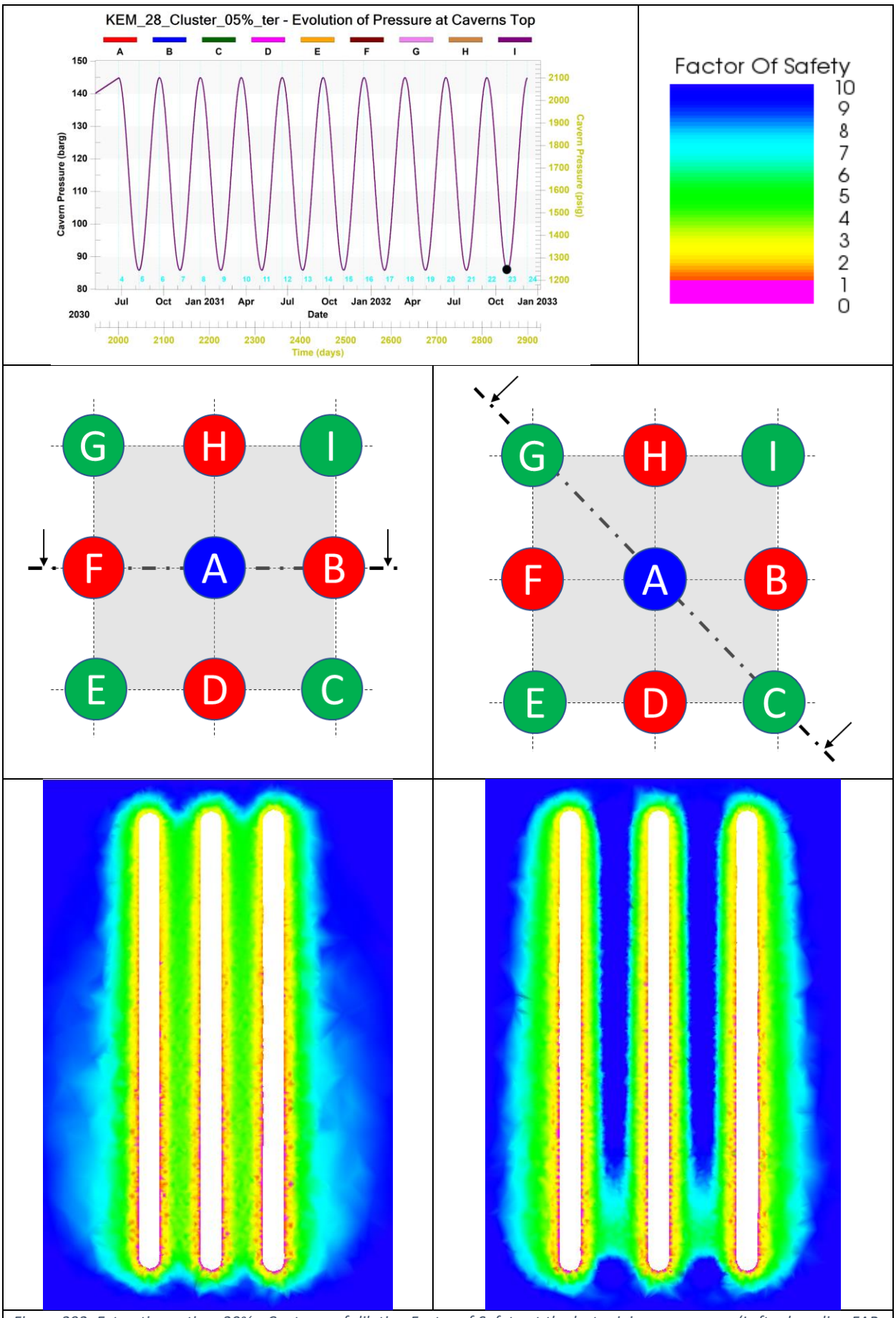

Figure 292. Extraction ratio = 20% - Contours of dilation Factor of Safety at the last minimum pressure (Left: along line FAB, right: along line GAC).

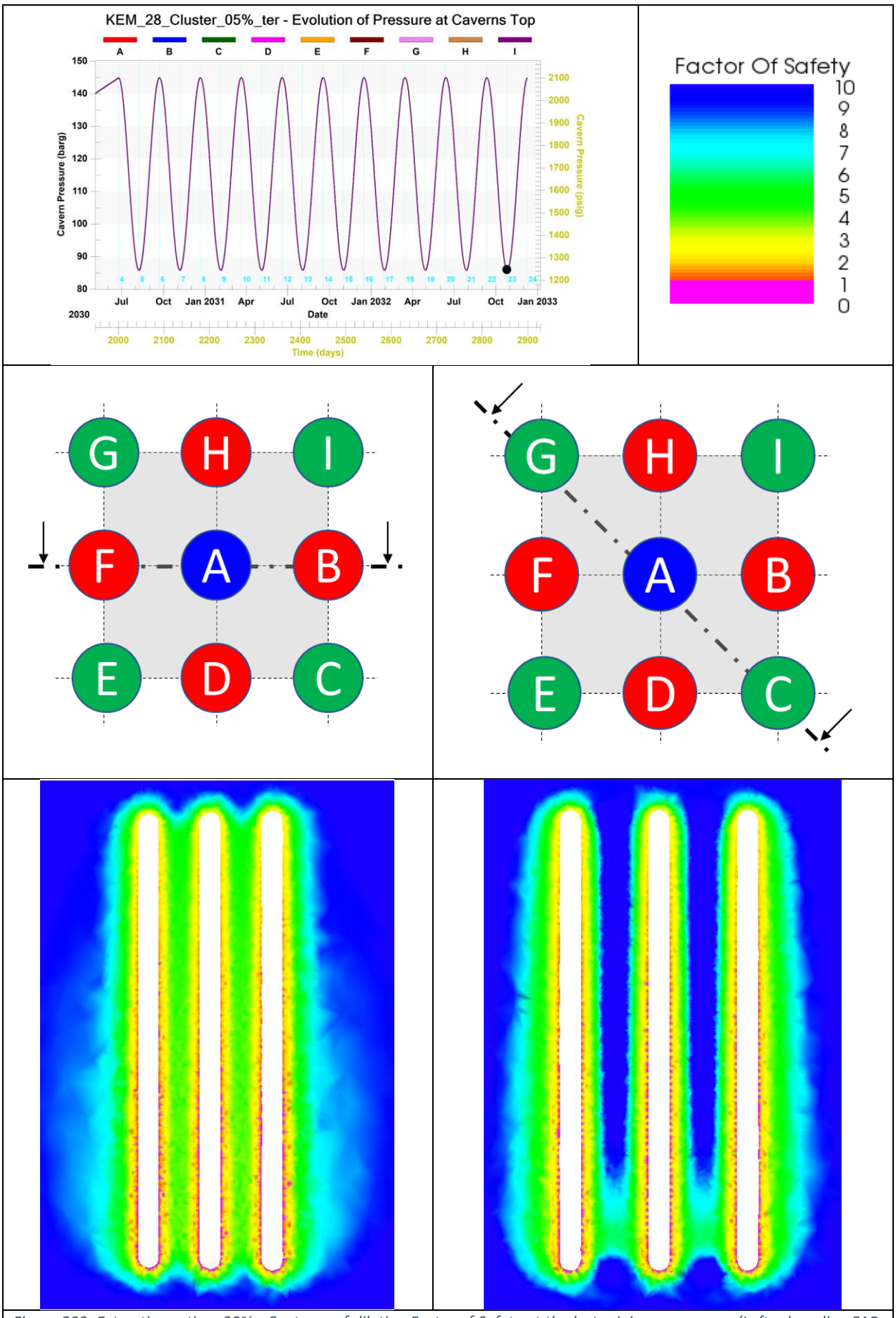

Figure 293. Extraction ratio = 30% - Contours of dilation Factor of Safety at the last minimum pressure (Left: along line FAB, right: along line GAC).

1.14.5.5 Case of a brine production cavern in a corner

We consider the case where a cavern in a corner (cavern G) is not filled with gas but remains at a constant pressure (halmostatic pressure corresponds to the weight of a column of saturated brine). Figure 294 shows the evolution of the volume loss of all the caverns in the cluster. The brine cavern G closes significantly more slowly than the hydrogen caverns. We can observe a small effect of the first phase of hydrogen production (descent from maximum to minimum pressure) on the cavern that remains in brine, but this effect is small, and cycling does not significantly affect the rate of volume loss in this cavern.

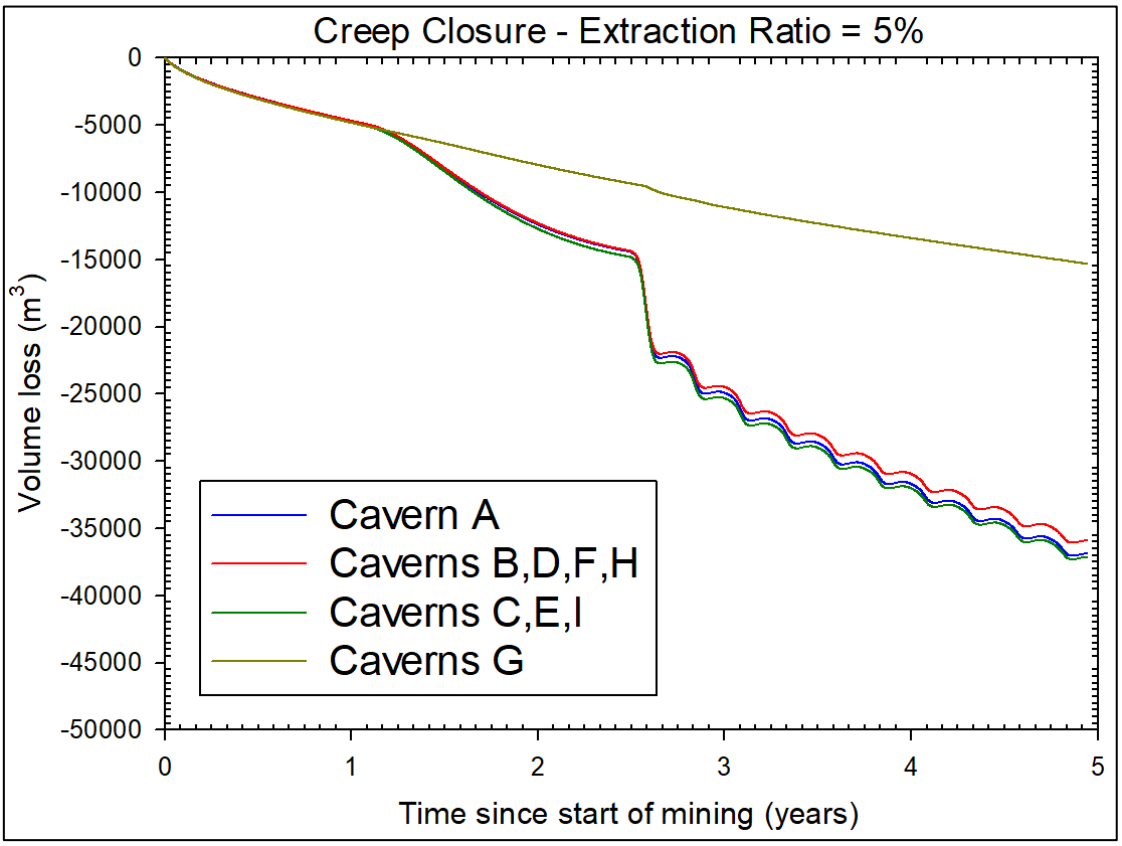

Figure 294. Case of brine cavern in a corner. Extraction ratio = 5%.

1.15 Conclusions

For this generic geomechanical study, a typical configuration of a hydrogen storage cavern in the Netherlands was defined. A total volume of 1 million m^3 of hydrogen in each cavern was considered.

Wellbore modeling and 2D computations

We modelled the flow of hydrogen into the well and the thermodynamic behaviour of the hydrogen and brine in the cavern. Coupled thermodynamic and rock mechanics calculations were carried out using LOCAS software. Parametric 2D finite element models were created so that numerous configurations could be tested.

The Munson-Dawson model for the mechanical behaviour of rock salt was considered because this model takes into account both stationary and transient creep and is the most suitable for calculations of cycling in gas caverns. It should be noted that the pressure solution creep mechanism was not taken into account in the 2D sensitivity study, but a sensitivity study on whether or not to take this mechanism into account was carried out in 3D.

A sensitivity study was carried out on more than 50 different configurations, varying the depth of the cavern, its maximum diameter, the cycling frequency, and the minimum pressure. We defined 14 indicators to compare the mechanical stability and energy efficiency of the cases considered. This sensitivity study highlighted 7 classes of configurations, some of which are very favourable to hydrogen storage, while others are much less so.

Using the results of all the calculations, we selected a reference case corresponding to a cavern with a small diameter (40 m), because this is probably more favourable from the point of view of subsidence (for instance, Shober et al., 1987), which is a serious concern in The Netherlands, and because a small diameter can optimise the spacing of caverns on a site (see 3D study). This case also corresponds to a cycling period of 90 days, which seems to correspond better than seasonal storage to what can be expected from hydrogen storage.

After selecting a reference case corresponding to a favourable configuration and fairly frequent cycling (period of 90 days), additional variants were carried out, such as taking into account faster stationary creep or the presence of a non-salt layer intersecting the cavern. We also studied the mechanical stability of the cavern during a blowout and a workover operation requiring the cavern to remain at very low pressure for a long period of time.

Blowout modeling

A blowout is probably the most serious accident that could happen to an underground gas storage facility. In the case modelled, the blowout lasts around a week and the temperature drops to 7 °C in the cavern and -37 °C at the wellhead. For the design of a real cavern, it will be necessary to check that the subsurface and surface installations are capable of withstanding both rapid variations in pressure and temperature.

At the end of the blowout, the pressure in the cavern is very low and remains so until the cavern is refilled with brine, which can take several weeks. This leads to the appearance of dilatation in the cavern wall; the thickness of the dilatation zone can reach more than twelve metres in the lower part of the cavern in this configuration. It is conceivable that this dilatant layer could disappear by dissolution if the cavern is filled with a brine that is not perfectly saturated.

It is interesting to note that the significant temperature drop in the cavity, which creates very high additional thermal stresses in the wall, does not result in significant effective tensile stresses in this configuration. This means that no deep fractures develop during the blowout.

Workover

During the life of a gas storage cavern, it may be necessary to carry out maintenance operations requiring the pressure in the cavern to be lowered considerably and maintained at this low pressure for several weeks or more. As in the case of the blowout, low pressure over a long period damages the salt by dilation over a thickness that can reach more than 20 metres if the cavern is kept at low pressure for 5 months.

3D computations

We carried out a small sensitivity study of the behaviour of a cluster of 9 caverns by varying the extraction ratio between 5% and 30%. Caverns with the same characteristics were considered, corresponding to the reference in the 2D sensitivity study.

As previous studies have shown, the volume loss of each cavern is less than the volume loss of a single cavern. This is due to the fact that a large part of the vertical load above the cluster is progressively transferred to the abutment, which reduces the deviatoric stresses in the pillar that cause the loss of volume.

The differences between all the tested configurations, with or without pressure creep, remain small. The differences are most apparent during the first phase of hydrogen production, when the pressure has dropped to its minimum for the first time.

In the cases considered, the difference between an extraction ratio of 5% and 10% rate is small, for both cavern volume loss and maximum subsidence. By increasing the extraction ratio from 5% to 10%, the spacing between wellhead is reduced by approximately 50 m (from 160 m to 110 m) and the surface area occupied by a cluster of 9 caverns is halved. Such a reduction in the size of the pillars between caverns does not generate any additional dilatant zone in the pillars.

A cavern full of brine, for example a brine production cavern at the end of production, in one corner of the cluster is practically unaffected by pressure cycling in the other caverns.

The case of a real project

It should be noted that the conclusions presented in this report are valid given the assumptions that have been made, both for the geometry and for the thermal and mechanical properties of the rocks.

This study is generic and not site specific. In the case of a real project, the geology and properties of the rocks will have to be precisely defined, both through studies on a microscopic scale (characterisation of the different types of salt and the average grain size, for example) and on a dome scale. Finally, realistic modelling on the scale of the caverns can be carried out to optimise the characteristics of the caverns, their positioning, and the operating method (minimum pressure, maximum rate of pressure change, etc.).

2 Seismicity: Thermomechanical modelling

Authors: Tobias Baumann and Anton Popov – smartTectonics GmbH

2.1 Introduction

As described in the literature section, the occurrence of induced seismicity can have several causes related to different aspects of cavern operations in rock salt (see section 5.2.1.3 and Figure 145). Here, we focus on estimating the potential of induced seismicity in the sedimentary rock adjacent to the salt dome by studying the influence of the hydrogen cavern field operation on the stress state and degree of induced brittle deformation in sedimentary rocks.

Seismicity is likely to occur on near-salt faults adjacent to the dome, as these are pre-existing weak zones in the overburden rock. From the detailed interpretation of 3D seismic reflection data, the typical radial orientation of the faults is well known (e.g., Carruthers et al., 2013; Coleman et al., 2018). Although it is clear that the near-salt radial faults reflect the brittle response of the overburden to the upwelling dynamics of the diapir throughout the halokinesis, precisely predicting the faults using geomechanical models is a complex task because, ideally, the entire geological evolution, including erosional and sedimentation processes as well as tectonic processes, should be taken into account. However, considering a geomechanical model of a present-day salt dome inferred from seismic data, the top salt surface acts as a tangential stress-free boundary and controls the stress state of the overburden (e.g., Baumann et al., 2022a, 2022b, 2019, 2018; Carruthers et al., 2013; Nikolinakou et al., 2014a, 2014b) and therefore determines the occurrence and orientation of the dominant near-salt faults (Baumann et al., 2022b; Spang et al., 2022). This allows us to employ state-of-the-art 3D thermomechanical models (Kaus et al., 2016) and derive the present-day 3D state of stress of a salt dome following the approach described in Baumann et al. (2022b, 2019, 2018). Here we start with a generic salt dome model geometry, calibrate the model and run a series of simulations and test the configuration with respect to the cavern field location in the salt dome and with respect to the uncertain rock salt creep rheology. Finally, we evaluate the scenarios by comparing them with sister simulations without an operational cavern field and focus on the changes in brittle deformation and the induced stress field under cyclic loading conditions.

2.2 Generic model of a 3D salt dome

2.2.1 Stratigraphy and model geometry

As a basis for the modelling work in the project, we decided to generate a generic, but realistic salt dome structure that is equipped with the typical geology present for the Netherlands.

For this purpose, a three-dimensional salt dome geometry was established based on the Dutch DGM-deep V5 model[1]. To mimic the internal Zechstein stratigraphy, we equipped the internal dome structure with two additional interfaces to match the first-order characteristics of a typical folding pattern (Figure 295). It should be noted that the folding patterns of such sub-vertical folds may be much more complex, especially on sub-seismic scales (e.g., Bräuer et al., 2011). Here it is important to account for the internal layering as each unit may have distinct microstructural characteristics that control the part of the expected creep mechanisms (e.g., Barabasch et al., 2023) and hence discontinuities in the 3D deformation field are to be expected.

[1] https://www.nlog.nl/details-dgm-diep-v5

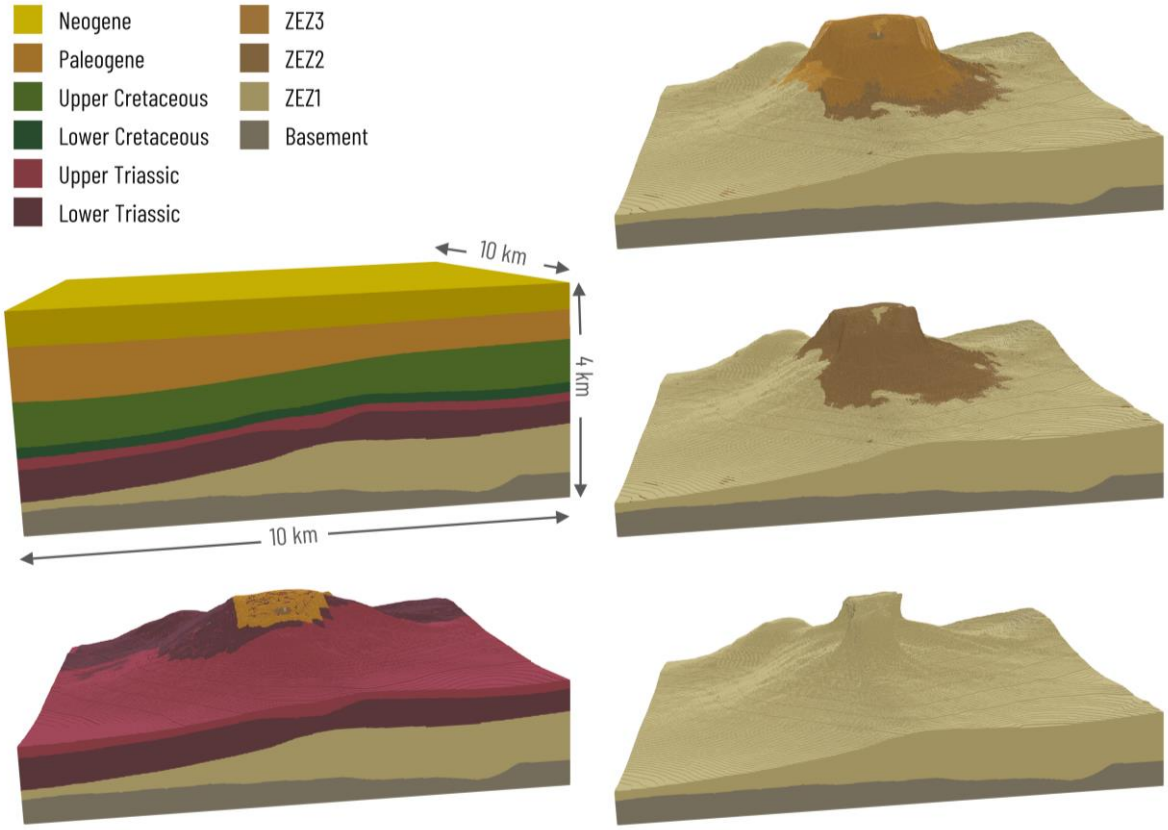

Figure 295. Three-dimensional model geometry of a generic salt dome. Based on the DGM-deep V5 model, a publicly available model of the Dutch surface (nlog.nl), a geometry of salt dome was selected, modified and equipped with a typical Zechstein stratigraphy for the internal structure. Each geological unit is equipped with a set of thermomechanical rock properties described in Table 31.

Table 31: Thermomechanical rock properties of the 3D generic salt dome model. EM1 and EM2 denote the two considered end-member rheologies of the outermost salt layer (i.e., "regular" vs. partly "depleted" grain boundaries).

	Density	Elastic		Brittle		Viscous						Thermal		
						Dislocation creep			Pressure solution creep					
Unit	ρ [kg m^{-1}]	E [GPa]	ν [ ]	c [MPa]	Φ [°]	$\log_{10}(A_{dc})$ [$MPa^{-n} yr^{-1}$]	Q_{dc}/R [K]	n_{dc} [ ]	A_{ps}/V_m [$K\ MPa^{n} yr^{-1}$]	Q_{ps}/R [K]	D_{ps} [mm]	α [K^{-1}]	C_p [$J\ Kg^{-1}\ K^{-1}$]	k [$Wm^{-1}\ K^{-1}$]
Neogene	1800	1	0.33	5	35							3.00E-05	950	2.3
Paleogene	2100	1	0.33	5	30							3.00E-05	905	2.1
Upper Cretaceous	2500	10	0.33	5	30							3.00E-05	780	2.2
Lower Cretaceous	2500	10	0.33	5	30							3.00E-05	780	2.2
Upper Triassic	2500	12	0.30	10	30							3.00E-05	860	3.8
Lower Triassic	2600	15	0.30	10	30							3.00E-05	860	3.0
ZEZ3 (EM1) ZEZ3 (EM2)	2165	25	0.25	10	30	2.39	6436.01	5.06	1.27	4352.76	3 30	3.00E-05	750	5.8
ZEZ2	2165	25	0.25	10	30	2.39	6436.01	5.06	1.27	4352.76	4	3.00E-05	750	5.8
ZEZ1	2165	25	0.25	10	30	2.39	6436.01	5.06	1.27	4352.76	2	3.00E-05	750	5.8
Basement	2700	*Non deforming, passive layer*										3.00E-05	835	3.0
R	8.31446	[$J\ K^{-1}\ mol^{-1}$]												
V_m	2.693e-5	[m^3]												

Each geological unit is equipped with a set of thermomechanical rock properties (Table 31) that are adjusted to match the expected situation in the Netherlands regarding vertical stress and temperature conditions. Temperature is initialized with the steady-state solution given the bottom heat flow and surface temperature as well as the assigned thermal conductivities (see Baumann et al. 2018, 2019).

2.2.2 Thermomechanical model and "Ist-Zustand"

To compute the present-day state (Ist-Zustand) of the salt dome, we use an extended version of the thermo-mechanical simulation open-source software LaMEM (Lithosphere and Mantle Evolution Model) that is actively developed at JGU Mainz (Kaus et al., 2016). The governing equations and the fundamental numerical description are described in Kaus et al. (2016) and Baumann et al. (2022a, 2018).

To allow the model to localize onsets of brittle faulting as a self-consistent and dynamic response to the prescribed salt dome geometry and associated mechanical properties, we employ a plasticity model with linear strain softening, where the physical friction is replaced with an effective friction with a linear dependence on accumulated brittle strain (Popov et al., 2012). This follows the approach of the KEM-17 dome-scale study (Baumann et al., 2019) where we determine the present-day state of stress ("Ist-Zustand") with a calibration phase to mimic the latest geological evolution of the dome and formation of brittle faults, consistent with the imposed salt dome geometry. We compute the present-day state before modelling the operational phase of the cavern field in all model scenarios to ensure realistic stress conditions of the dome before cavern leaching and operation. Moreover, reference scenarios without hydrogen caverns are computed with the same time and spatial resolution, allowing us to investigate accurate relative changes in our simulations. In the following section, we describe the details of the cavern boundary conditions that mimic the typical loading conditions during the storage of hydrogen.

2.3 3D THM dome-scale simulations to assess the potential for seismicity in the vicinity of a salt dome

2.3.1 Hydrogen cavern field boundary conditions

The geomechanical analysis in Chapter 1 shows that particular cavern designs are more likely to result in stable configurations than others. Based on these findings, we use the previously used cavern concept in our analysis and position the cavern field at different locations in the salt dome in order to further investigate the feedback with the salt dome structure and the adjacent overburden. We implement the hydrogen caverns as vertical cylinders of 40 m diameter with spherical caps, ranging from TVD = 830 m to 1655 m, and apply the typical loading scenario of a hydrogen cavern as proposed in Chapter 1. As presented in Section 1.14, the field design incorporates nine caverns organized in three rows and columns, as shown in Figure 296 and Figure 297 (see also Brouard et al., 2021a and Brouard et al., 2021b). The pre-defined pressure profile is synchronously applied to all caverns within the cavern field. The first three years of the profile represent the leaching phase of the cavern, followed by a 4.25-year waiting period before de-brining starts. Debrining is accompanied by a slow gas loading, where the cavern pressure increases continuously over 5.5 years. This gas filling is followed by a periodic loading cycle of 6 months' length, simulated for a duration of 25 years. It is important to note that this loading cycle was consistently applied throughout the simulation series, always with constant pressure minimum and maximum ($\mathrm{P}_{\min} \approx 15\ MPa, \mathrm{P}_{\min} \approx 7.5\ MPa$).

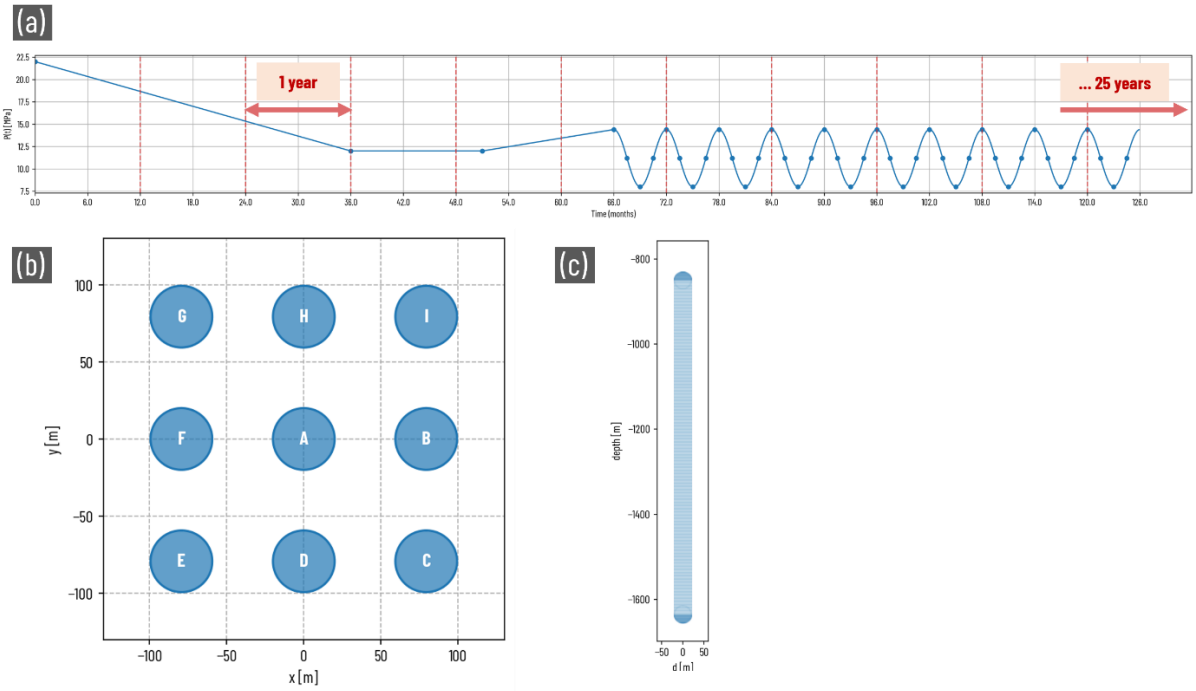

Figure 296. (a) Cyclic loading of a single hydrogen cavern superimposed as a pressure boundary condition to each cavern within the cavern field. Whereas the first three years of the pressure profile correspond to the leaching phase of the cavern, debrining is assumed to start after a 4.25-year waiting period. The debrining of the cavern goes along with a slow gas loading, which is modelled as a gentle linear increase in cavern pressure over a period of 5.5 years (see Chapter 1). After the initial gas filling, a periodic loading cycle of 6 months length is modelled over 25 years. The loading cycle shown here was applied throughout the simulation series. (b) Cavern field design as proposed in Chapter 1. Here, the cavern field is implemented in different locations within the salt dome to test the impact on the stress state and the deformation response of the adjacent rock mass. The distance between two neighbouring caverns symmetry axes is chosen to be 79.3 m following a 20% extraction ratio (see Chapter 1). (c) Corresponding cavern design used in this work.

In our analysis, we consider different locations of the cavern field in relation to the dome flanks and the existing fault zones. Figure 297(b) shows the scenario where the cavern field is located in the centre of the dome, with a relative distance to the nearest flank of about 960 m. In (c), the cavern field is moved closer to the flank (approx. 650 m distance). In (d), the centre of the cavern field is only 440 m away from the flank. (e) describes an alternative "flank" location on the opposite side of the dome. Here the cavern centre is even closer to the flank (340 m). (f) shows a specific scenario in which the cavern field is not only close to the dome flank, but also near a pre-existing fault zone in the overburden that is initiated during calibration.

All scenarios are computed with and without the loading conditions of the cavern field. In scenario (d) and (f) we also test the influence of the pressure solution creep mechanism. In order to simulate heterogeneous rock salt, we attenuate the pressure solution mechanism for the outermost Zechstein layer by increasing the apparent grain size associated to the geological unit to 3 cm. This could mimic an end-member situation where the fluids at the grain boundaries of the rock salt are partially depleted and pressure solution is only active at a few grain boundaries, so that actual conglomerates of grains participate in the pressure solution creep. It could also mimic a situation where the pressure solution creep rate is slowed down due to the presence of mega crystals or anhydrites (see Chapter 3).

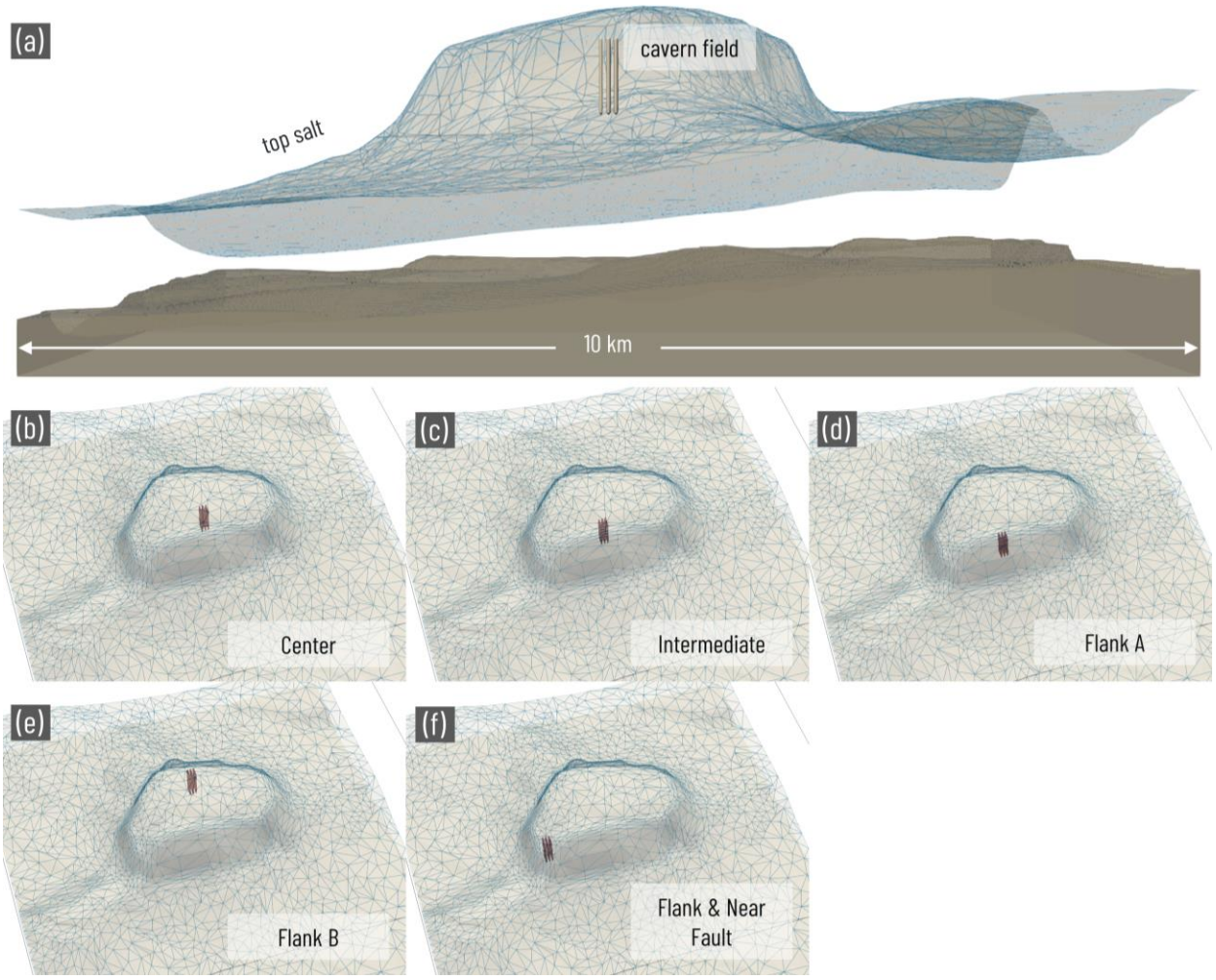

Figure 297. Scenarios considered with the 3D dome-scale simulations. (a) Side view with cavern field location in the centre of the dome. (b) Top view of the scenario with cavern field in the centre of the dome, (c) an intermediate case and (d) a scenario with cavern field at the flank. (e) is an alternative scenario at a different dome flank. (f) scenario with cavern field at the flank and in the vicinity of a pre-existing fault zone that is also present in the reference scenarios without cavern fields.

2.3.2 The influence of hydrogen cavern operation on the stress state of the salt dome and the degree of induced brittle deformation in the overburden.

The operating cavern field induces a cyclic load into the host rock. Here we consider the state of stress 25 years after initialisation of the cavern field and the preceding calibration phase. First, we look at the induced stress state within the salt dome due to cavern loading. Figure 298 shows how the induced stress is distributed in the salt dome. The contour surfaces show how the induced stress disturbance decreases radially over several hundred meters. Apart from a large-scale Zechstein stratification, we do not include other heterogeneities in the salt (e.g., anhydrite stringers etc. as in KEM-17) in this generic analysis, so the distribution of the induced stress is probably much less disturbed than in nature. However, we do gain insights into how the stress is affected by the transition of two Zechstein layers that are associated with different apparent grain sizes (see stress build-up at the layer interface in Figure 298). Since we have attributed a larger grain size to the younger Zechstein layer here, it accommodates higher differential stresses. Different elastic properties of the various Zechstein layers would of course also play a role here. However, we have deliberately kept these homogeneous in this parameter study.

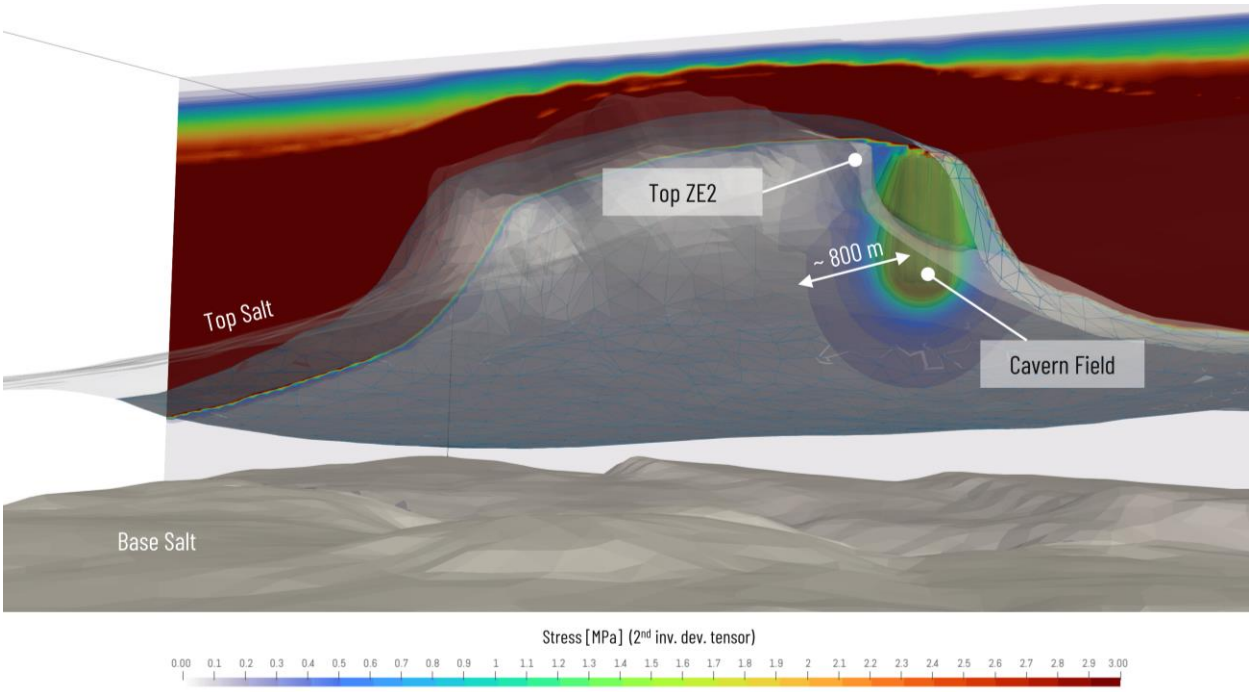

Figure 298. Stress distribution within the dome. The colour range is adjusted to the deviatoric stress obtained inside the salt dome. The stress field is perturbed by the induced stresses of the cavern field. The perturbation is visible up to a distance of 800m away from the cavern. Apart from the large-scale ZE stratification, the rock salt is homogeneous. However, the ZE interface is visible in the stress distribution as it reflects a contrast in grainsize and thus different creep rates.

The changes in differential stress in the overburden are small compared to Ist-Zustand situation. Figure 299 shows the maximum differential stress for all considered scenarios together with the 3D principal stress orientations after the 25 years operation period of the cavern field on a horizontal section at a depth of 900 m.

For a better understanding of the differences obtained, we provide a residual plot in Figure 300, in which we show the residual differential stress at 900 m depth, indicating the difference in differential stress for a scenario with and without the influence of the cavern field after 25 years of cyclic loading. The reference scenarios are computed with the exact same conditions and the same discretisation, with the exception of the cavern loading boundary conditions. Using the comparison, we make several observations. For the two cases with an operating cavern field in the centre of the dome (a) and an intermediate position to the dome flank (b), the residual plot clearly shows that the stress state outside the dome is not, or not significantly perturbed. Only the stress state in the rock salt is affected, which reflects the contrast in creep properties as one can see in (b) when the stress perturbation is distributed across multiple Zechstein layers. In all other scenarios (c-g), we find that differential stress is induced in the overburden.

Considering the scenario with the cavern field near the southern flank of the salt dome (c), there is a greater change in the differential stress in the overburden compared to the case where the cavern field is installed close to the northern flank of the dome (d), although the distance between the cavern field and the flank is around 100 m smaller compared to (c). The comparison of cases (a) - (d) shows that the distance to the dome flank always plays a role in the extent to which the thermomechanical influence of the cavern field affects the overburden. However, it must be considered that the salt dome is not symmetrical and is subject to the salt dome dynamics that are also influenced by the salt thickness below the dome.

In case (e), where the cavern field is located near the dome flank but also in the vicinity of a pre-existing fault zone in the adjacent sedimentary rocks, the induced stress in the overburden appears more distributed as it is also influenced by the more complex stress field around the fault zone.

The comparison with scenarios (f) and (g) in Figure 300 shows that a modified creep rheology of the younger ZEZ2 layer has a certain influence on the shape of the distribution of the induced stress. The induced stress changes appear more localized and larger, but the difference is small in comparison.

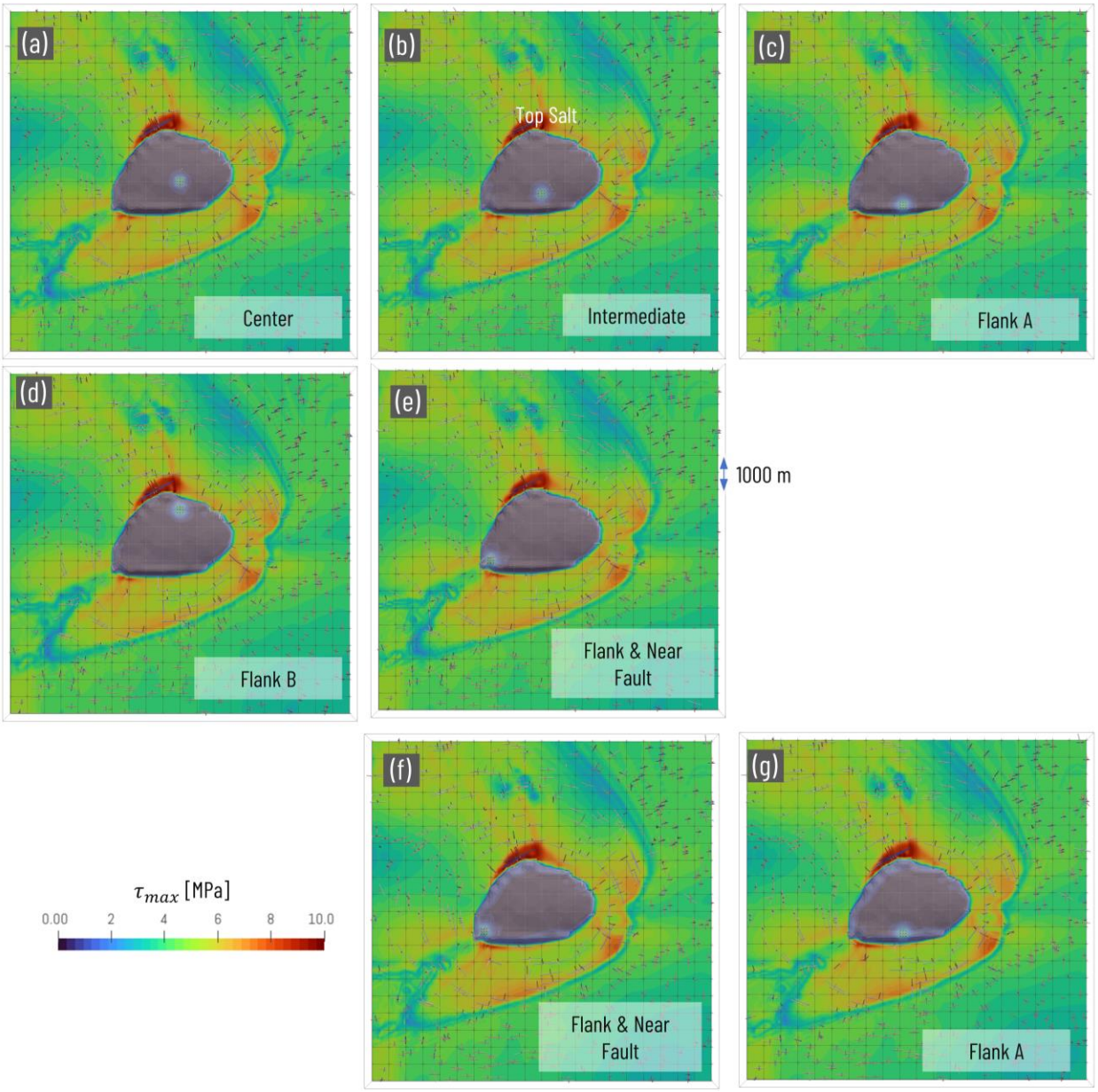

Figure 299. The distribution of the maximum differential stress around the salt dome at 900 m depth after 25 yrs of cavern operation. Markers indicate the principal stress components and orientation. The scenarios (a)-(e) correspond to the described in Figure 297. (f) and (g) have the same configuration are (c) and (f),but contain a larger grain size in the outermost Zechstein layer to test the influence of the pressure solution creep mechanism. In (f) and (g), pressure solution creep is dampened by increasing the effective grain size associated to 3 cm. Grid lines indicate 500 m distances in the model.

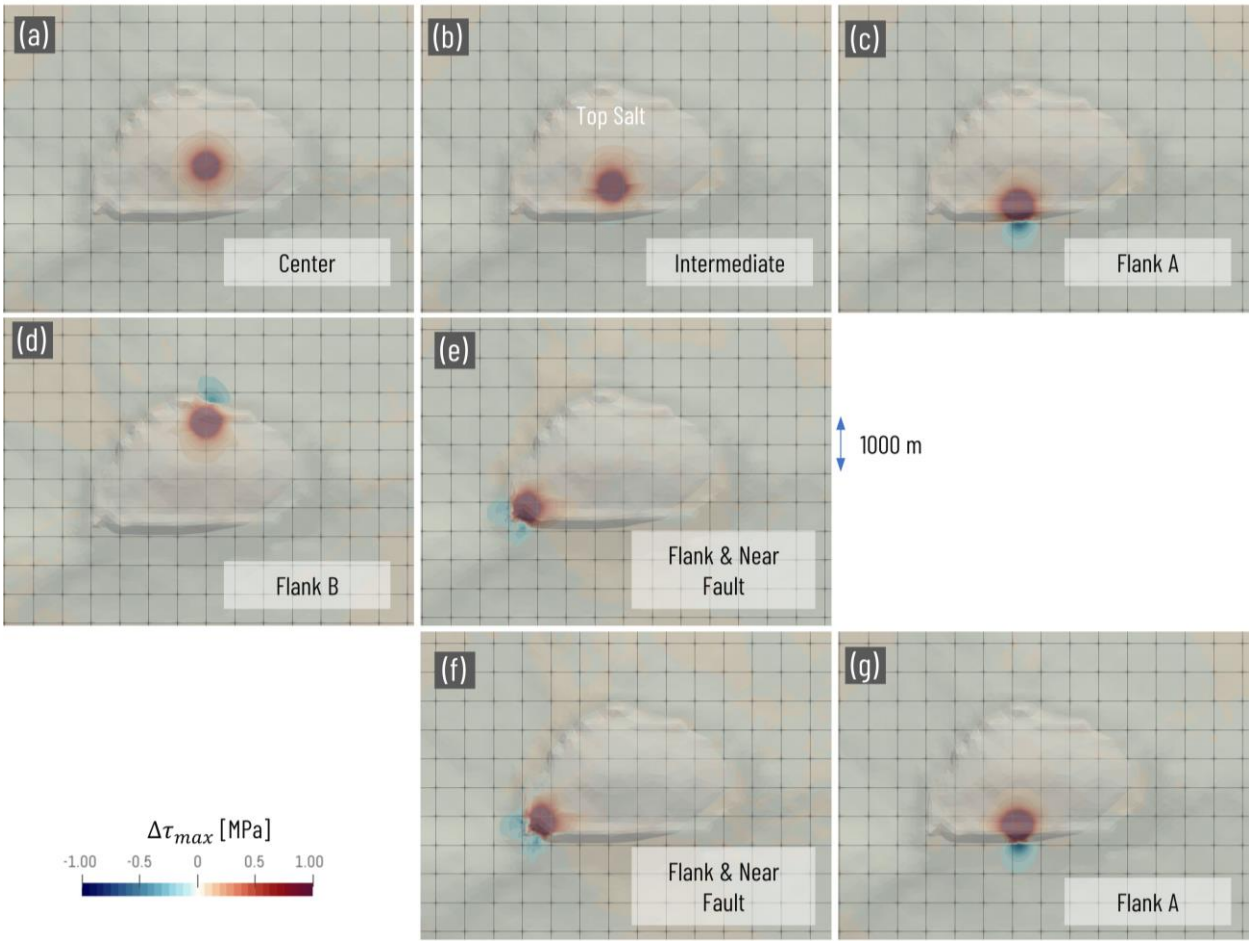

Figure 300. Difference in maximum differential stress comparing the scenario with and without cavern field at the end of the 25 yrs operational period. Grid cells are shown for reference and indicate 500 m distances in the model. The scenarios (a)-(e) correspond to the described cases in Figure 297. (f) and (g) have the same configuration are (c) and (f) but contain a larger grain size in the outermost Zechstein layer to test the influence of the pressure solution creep mechanism. In (f) and (g), pressure solution creep is attenuated by increasing the effective grain size associated to 3 cm.

In addition to the induced stress changes, we also consider the degree of brittle deformation in the overburden. Figure 301 shows an overview of the APS (accumulated plastic strain) on a horizontal section at a depth of 900 m for all cases considered. In order to get an idea of the corresponding three-dimensional distribution of APS, Figure 301 (h) provides an 3D example of case (b), where the cavern field has an intermediate distance to the salt dome flank.

When the cavern field is located at the southern flank of the dome (c), we see enhanced brittle strain compared with the scenarios where the cavern field is located at the intermediate or centre position. Interestingly, the APS is enhanced also at the pre-existing fault on the northern side of the dome. In contrast, in case (d), where the cavern field is located close to the northern flank of the dome, the APS is not enhanced as much as in (c). We have previously made a similar observation with the stress changes and explain the effect with the salt dome dynamics, which must be considered as a whole, since for example an induced stress change on one side may result in larger thermomechanical feedback with the overburden on the opposite side due to the associated flow dynamics within the dome. This explanation fits to the results of (f) and (g), where the flow rate is attenuated due to a larger apparent grainsize, which we attributed to the youngest rock salt layer in the outer parts of the dome. Both (f) and (g) show smaller APS magnitudes compared to their counterparts (e) and (c), where associated apparent grainsizes are smaller.

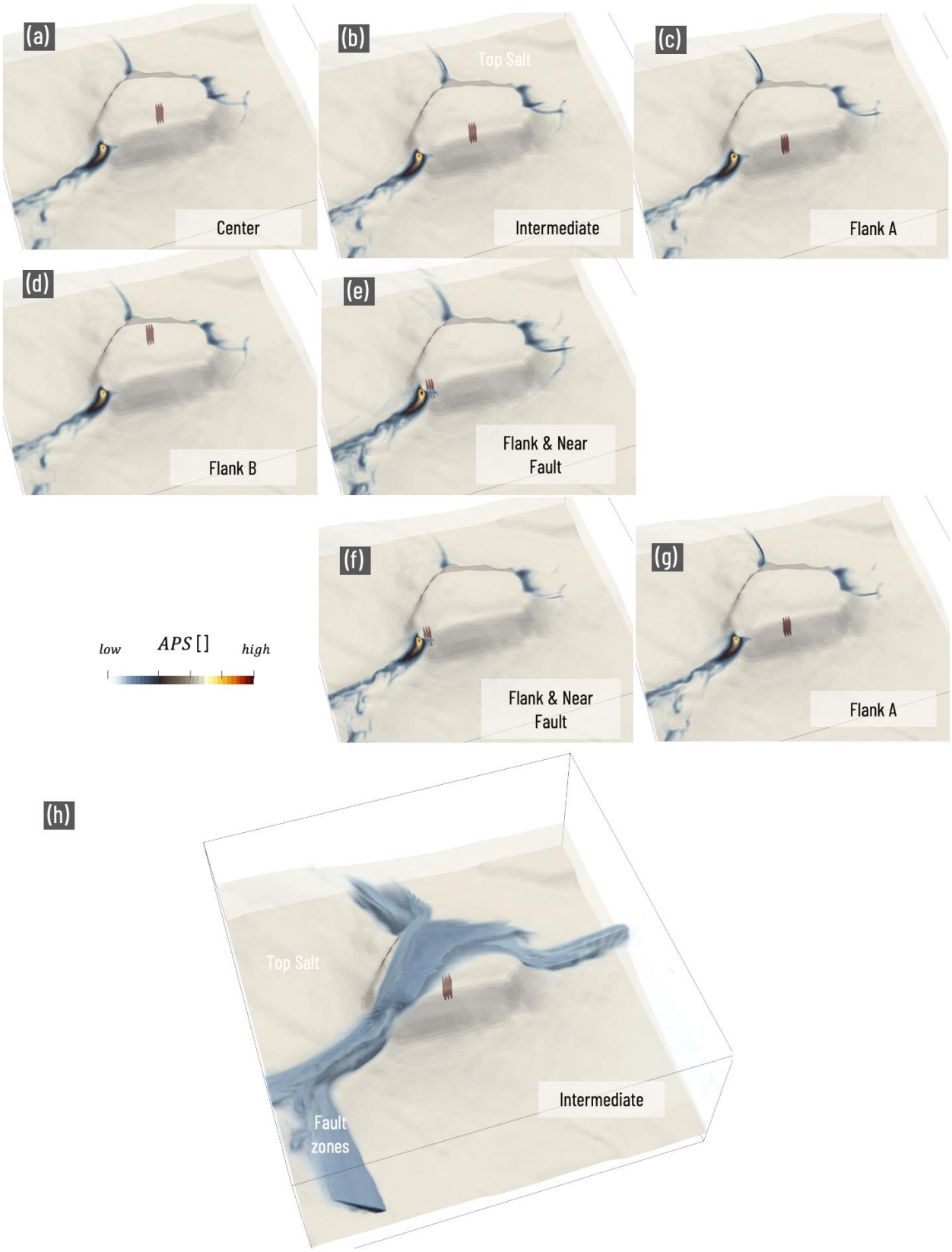

Figure 301. Accumulated brittle strain in the overburden at 900 m as a function of different loading scenarios, i.e., cavern field at different locations within the salt dome. The scenarios (a)-(e) correspond to the described cases in Figure 297. (f) and (g) have the same configuration are (c) and (f) but contain a larger grain size in the outermost Zechstein layer to test the influence of the pressure solution creep mechanism. In (f) and (g), pressure solution creep is attenuated by increasing the effective grain size associated to 3 cm. (h) shows the corresponding 3D distribution of localized brittle deformation as an example for the case of an intermediate distance of the cavern field from the flank of the salt dome (see b)

2.4 Conclusions

To investigate the potential for induced seismicity due to the operation of a hydrogen cavern field in a salt dome, we used state-of-the-art 3D thermomechanical models to examine the effects of a realistic, design-optimized nine-cavern hydrogen cavern field on the host and host rocks, focusing on the changes in the brittle deformation and the induced stress field under cyclic loading conditions. In our analysis, we tested five different locations of the cavern field within the dome, in the centre of the dome, at two different dome flanks, at intermediate distance to the flank and at a specific location that is at the flank and close to a pre-existing fault zone in the adjacent sedimentary rocks. In addition, we made simulations for two different sets of rock salt creep properties to account for the possible variability of salt creep.

The results confirm our expectations of the literature study, according to which we see enhanced geodynamics of the salt dome due to the induced stress of the cavern field. Whether or not this leads to feedback with the overburden depends on the location of the cavern field in the salt dome. The results suggest that a cavern field near the dome flanks is likely to affect the stress state of the overlying sedimentary rocks and may lead to brittle deformation of pre-existing faults. The comparison of different scenarios shows that also the distance between cavern field and pre-existing near-salt fault matters. Here, a cavern field in the centre of the dome with either 960 m or 650 m distance to the flanks does not affect the degree of brittle deformation in the overburden. A cavern field close to the flank influences the dynamics of the entire dome and we observe induced brittle deformation also on pre-existing faults on the opposite site of the dome, suggesting that the general dynamics of the salt dome is also an important factor. As the scenarios considered have shown, induced stress changes on certain dome flanks can have a greater influence on the overall dynamics of the salt dome than others. Therefore, the distance between the cavern field and the dome flank is important but is not necessarily crucial due to the overall dynamics of the salt dome. Factors that control the dome dynamics are the creep rheology, the geometry and the remaining salt below the dome. We therefore suggest performing site-specific 3D THM models that take into account those conditions.

The degree of brittle deformation in the overburden is also influenced by the uncertain creep rheology of the rock salt. This significantly determines both the natural dynamics of the salt dome and the dynamics induced by the cavern field in the form of increased deformation rates and differential stresses. The comparison of scenarios with active and attenuated pressure solution creep in the outer Zechstein layer of the dome shows that the grain size-dependent creep process has a visible influence on the salt dome dynamics, the stress state and the degree of induced brittle deformation in the overburden.

In addition, more complex creep mechanisms could also play an important role. For example, it is expected that dynamic recrystallization in the rock salt occurs due to the induced loading of the cavern field (a process that is not yet accounted for in the models). Due to the reduction in grainsize, this would lead to more enhanced deformation in the near field of the cavern cluster. This and other effects require more research.

3 Durability: The effective long-term creep properties of heterogeneous rock salt

Author: Tobias Baumann, Maximilian Kottwitz, Anton Popov – smartTectonics GmbH and [Janos Urai – GeoStructures Consultancy for Structural Geology and Geomechanics]

Durability: The evolving rheology, transport properties, damage and healing of salt **(after Urai 2022)[1]:** Not all is known of the near-cavern deformation and transport processes around a H2 cavern. This calls for a much better understanding of the processes in this complex damage zone over long periods. One can, for example, hypothesize of a self-propagating damage zone in the salt, being the product of stress changes due to cavern pressure, creation and destruction of porosity by microcracking, recrystallization, and fracture healing, the effect of effective pressure on deformation of salt and that of gas pressure gradients causing additional deformation. Little is known about these processes. Also, as we have argued in our proposal, the walls of H2 storage caverns will be covered with water during operation. However, little is known of the processes of damage, dissolution-precipitation and recrystallization in dilatant rock salt in the presence of water at the cavern walls. There is clearly the need for further research, for example to evaluate the hypothesis of self-propagating damage away from the cavern. For this, we will propose and discuss a series of novel laboratory experiments which will allow a first assessment of this (together with incorporating this lack of knowledge in the risk assessment).

Within the scope of the KEM 28 project, the durability work package should address the evolving properties of rock salt in terms creep and in terms of transport of fluids. Both are connected to microstructural processes and phenomena such as dynamic recrystallisation, grain size evolution, grain boundary activity. It seems likely that these processes may have significant influence on the thermomechanical response of the heterogeneous rock salt when caverns exert a cyclic stress in the presence of water. Comprehensive research should be carried out to address these topics. However, part of the complex behaviour of rock salt results from the heterogeneous structure and the uncertain mechanical properties associated to it. Therefore, a key aspect of this work was to quantify the effective long-term creep properties of "*Kristallbrockensalz*" (hereafter, KB rock salt), a prominent heterogeneous Zechstein unit hosting, amongst others, several cavern fields in the Netherlands.

3.1 Introduction

KB rock salt is a multi-phase aggregate salt rock found in the Zechstein 2 formation of the Permian Basin (Barabasch et al., 2023; Czapowski, 1987; Popp et al., 1999). It is classified as a tectonite and is characterized by the presence of large crystal porphyroclasts known as Kristallbrocken (or mega grains) within a fine recrystallized matrix (Barabasch et al., 2023; Küster et al., 2010; Urai et al., 2019). According to a recent publication of Barabasch et al. (2023), the formation of KB rock salt is believed to have occurred through sedimentation processes involving fine-grained matrix salt, layers of single crystalline halite, and thin anhydrite layers (Küster et al., 2011, 2009). The exact processes responsible for the formation of mega grains within KB rock salt are not fully understood. However, various models have been proposed, including post-sedimentary diagenetic grain growth or coalescence of fine-grained halite (Küster et al., 2011) as well as boudinage/rupturing of halite crystal layers during deformation with halite recrystallization in the boudin necks (Löffler, 1962).

Barabasch et al. (2023) write that the deformation of *KB rock salt* is evident at both macroscopic and microscopic scales. Macroscopically, KB rock salt exhibits an "*Augen-Gneiss*" structure, with the size of

[1] Internal communication. Due to sudden passing of Janos Urai his tasks on the formulation of hypotheses based on microphysical considerations and discussing implementation of novel constitutive equations in the cavern scale and dome scale models could not be completed. This text box describes the initial aim of his part of the study.

the mega grains decreasing with tectonic strain. This deformation is attributed to brittle deformation and dislocation glide, with a significant contrast in competence between the porphyroclastic *Kristallbrocken* crystals and the fine-grained mylonitic matrix halite (Küster et al., 2010; Urai et al., 2019). At the microscopic level, the intrinsic rock phases of KB rock salt deform individually. The deformation of the halite matrix involves two main mechanisms: solution-precipitation creep and dislocation creep (Bérest et al., 2019a; Urai et al., 2008). Pressure solution creep occurs primarily at low differential stresses (< 10 MPa) and involves the dissolution of grains at stressed boundary regions, causing intergranular sliding, recrystallization, and solution-precipitation-assisted mass diffusion (Spiers et al., 2003, 1990; Spiers and Schutjens, 1999). Higher brine contents increase the chance of grain boundary migration and dynamic recrystallization, resulting in a reduction of overall grain size which facilitates pressure solution creep (Peach et al., 2001; Schenk and Urai, 2004; J. H. Ter Heege et al., 2005; Urai et al., 1986). Dislocation creep becomes important at higher differential stress (> 10 – 20 MPa) and involves the movement of dislocations within the crystal lattice of halite grains, resulting in slip bands and subgrain formation within the grains (Carter et al., 1993). Dislocation creep is typically characterized by power law flow behaviour, with an exponent between 5 and 7, depending on temperature, differential stresses, and confining pressures (Carter et al., 1993; Hunsche and Hampel, 1999; Wawersik and Zeuch, 1986). We define the creep behaviour of the halite matrix as additive creep law (further referred to as SUM - Spiers-Urai-Model, e.g., Spiers et al., 1990; Urai et al., 1986; Urai and Spiers, 2017) as follows:

$$\dot{\varepsilon}_{ps} = A_{ps}\, e^{-\frac{Q_{ps}}{RT}} \left(\frac{{\sigma_d}^{n_{ps}}}{T {D_{ps}}^{m}} \right) \tag{1}$$

$$\dot{\varepsilon}_{dc} = A_{dc}\, e^{-\frac{Q_{dc}}{RT}} {\sigma_d}^{n_{dc}} \tag{2}$$

$$\dot{\varepsilon}_{tot} = \dot{\varepsilon}_{ps} + \dot{\varepsilon}_{dc} \tag{3}$$

Here, $\dot{\varepsilon}_{ps}$ is the pressure-solution and $\dot{\varepsilon}_{dc}$ the dislocation-creep contribution to the total strain-rate $\dot{\varepsilon}_{tot}$, A_{ps} and A_{dc} material-specific prefactors, Q_{ps} and Q_{dc} are the respective activation energies, T is the temperature and R the universal gas constant, σ_d the differential stress, D_{ps} the average grainsize of the halite matrix, m is the grainsize exponent, n_{ps} and n_{dc} are the stress exponents for pressure solution and dislocation creep, respectively (see Urai et al., 2008 and references therein for a compilation of parameters). In contrast to the relatively fine-grained halite matrix, the halite mega grains are considered to deform under dislocation creep conditions only (eq. (2)), even at low differential stresses (Barabasch et al., 2023).

The rheology of anhydrite is still under debate, but thought to be stronger and brittle in comparison to halite, based on short-term rock mechanics experiments, although observed ductile anhydrite fold structures in salt suggest that a viscous constitutive law governs the long-term deformation (e.g., Urai et al., 2019). Experimental data indicates that deformation of anhydrite is controlled by grain boundary diffusion (Pluymakers et al., 2014; Pluymakers and Spiers, 2015), similar to pure halite (e.g., Spiers et al., 1990; Urai et al., 1986). However, the rate of pressure solution creep in anhydrite is slower compared to pure halite, possibly due to differences in grain boundary structure between anhydrite and NaCl (Pluymakers et al., 2014). Thus, we model anhydrite creep rheology with a pressure solution model. To facilitate the approach, we employ the same pressure solution creep parameters as for halite but decrease the pre-factor to directly control the strain rate in an empirical sense.

Here, we will determine the effective creep rheology and associated uncertainties of KB rock salt. To achieve this, we conduct systematic numerical deformation experiments (Deubelbeiss et al., 2011, 2010; Deubelbeiss and Kaus, 2008; Schmalholz and Schmid, 2012) using synthetically generated representative

models of salt cores. From that, we derive a parameterised a constitutive model for the long-term creep rheology of KB rock salt that maps the variability of strain rates as a function of differential stress and degree of non-matrix phases.

3.2 Method: Numerical uniaxial deformation experiments

The assessment of the long-term creep properties of rock salt is commonly done through laboratory deformation experiments, typically by using tri- or uniaxial creep tests. In these tests, cylindrical specimens of rock salt are obtained from drill cores and placed in a triaxial deformation apparatus. A prescribed confining stress ($\sigma_2 = \sigma_3$) is applied to the outer cylindrical shell, while a normal load (σ_1) is applied to the top boundary. Here, $\sigma_{1,3}$ represent the principal stresses in ascending order and $\sigma_{\mathrm{d}} = \sigma_1 - \sigma_3$ represents the applied differential stress. During the experiment, vertical deformation is monitored to obtain a curve showing total strain versus time. This allows for calculating the strain rate. Ideally, the experiment continues until a steady-state strain rate is reached. However, non-matrix phases present in rock salt specimens (such as relatively stiff halite mega grains) can delay the achievement of steady-state. Depending on mega grain volume fractions, it could take several years or even longer.

Properly validated numerical deformation experiments have the advantage of providing quasi-instantaneous creep data without waiting months or even years compared to lab experiments. They can also operate on larger scales than typical lab setups with cylindrical sample diameters of around 10 cm. Also, the input data for numerical simulations can be easily acquired at low cost using segmented and meshed images of actual salt rocks or even synthetically generated models. These advantages make complementary numerical creep assessments extremely useful for quantifying uncertainties in determining creep parameters, as this typically requires large datasets, particularly for structurally heterogeneous salt rocks such as KB rock salt.

3.2.1 Mathematical model

We solve a coupled system of quasi-static equilibrium and continuity equations in a two-dimensional plane-strain formulation given by (assuming Einstein summation convention):

$$\begin{aligned} \frac{\partial \sigma_{ij}}{\partial x_j} + \rho g_i &= 0 \\ \dot{\theta} - \frac{1}{K}\frac{Dp}{Dt} &= 0\,, \end{aligned} \tag{4}$$

where x_i $(i = 1,2)$ are the spatial coordinates, σ_{ij} are the components of the Cauchy stress tensor (positive in extension), ρ is the density, g_i are the components of the gravity acceleration vector, $\dot{\theta}$ is the volumetric strain rate, K is the elastic bulk modulus, D/Dt is the material time derivative, and p is the mean stress, which is defined by volumetric-deviatoric decomposition of the Cauchy stress tensor:

$$\begin{aligned} \sigma_{ij} &= \tau_{ij} + p\,\delta_{ij} \\ p &= \frac{1}{3}\sigma_{kk}\,. \end{aligned} \tag{5}$$

Here τ_{ij} are the components of the Cauchy stress deviator, and δ_{ij} is the second-order unit tensor. Similarly, the volumetric-deviatoric decomposition of the strain rate tensor is defined as follows:

$$\begin{aligned} \dot{\varepsilon}_{ij} &= \frac{1}{2}\left(\frac{\partial v_i}{\partial x_j} + \frac{\partial v_j}{\partial x_i}\right) - \frac{1}{3}\frac{\partial v_k}{\partial x_k}\delta_{ij} \\ \dot{\theta} &= \frac{\partial v_k}{\partial x_k}. \end{aligned} \tag{6}$$

In the above equation $\dot{\varepsilon}_{ij}$ are the components of the deviatoric strain rate tensor, and v_i $(i = 1,2)$ are the velocity vector components. The elastic bulk and shear moduli (K and G) can be alternatively expressed in terms of the Young's modulus, and the Poisson's ratio (E and ν):

$$K = \frac{E}{3(1-2\nu)}, \quad G = \frac{E}{2(1+\nu)}. \tag{7}$$

The total deviatoric strain rate is assumed to be additively decomposed into the elastic, dislocation, and pressure solution creep component, respectively:

$$\dot{\varepsilon} = \dot{\varepsilon}_{el} + \dot{\varepsilon}_{dc} + \dot{\varepsilon}_{ps}\,. \tag{8}$$

Here the expressions for dislocation, and pressure solution long term creep mechanisms are given by (Urai et al., 2008), (Spiers et al., 1990):

$$\begin{aligned} \dot{\varepsilon}_{dc} &= A_{dc} \exp\left(-\frac{Q_{dc}}{RT}\right) \sigma_d^n \\ \dot{\varepsilon}_{ps} &= A_{ps} \exp\left(-\frac{Q_{ps}}{RT}\right) \frac{\sigma_d}{T\,D^3}, \end{aligned} \tag{9}$$

where A_{ps} and A_{dc} denote the corresponding pre-factors, Q_{ps} and Q_{dc} are the activation energies, R is the gas constant, T is the temperature, D is the grainsize, and σ_d is the differential stress. The above equations result form fitting the triaxial experiments and operate with scalar variables like axial strain rate and differential stress. Due to these limitations, they are not directly suitable for the numerical implementation. The deviatoric constitutive equation must be rewritten in the following tensor form:

$$\dot{\varepsilon}_{ij} = \frac{\dot{\tau}_{ij}}{2G} + B_{dc}(\tau_{II})^{n-1}\,\tau_{ij} + B_{ps}\,\tau_{ij}\,. \tag{10}$$

Here $\dot{\tau}_{ij}$ stands for the objective stress rate, τ_{II} is the effective deviatoric stress, given by:

$$\tau_{II} = \left(\frac{1}{2}\tau_{ij}\tau_{ij}\right)^{\frac{1}{2}}. \tag{11}$$

The combined creep pre-factors which include all effects, but the effect of stress can be written as:

$$\begin{aligned} B_{dc} &= \frac{3^{(n+1)/2}}{2} A_{dc} \exp\left(-\frac{Q_{dc}}{RT}\right) \\ B_{ps} &= \frac{3}{2} A_{ps} \exp\left(-\frac{Q_{ps}}{RT}\right) \frac{1}{T\,D^3}. \end{aligned} \tag{12}$$

It should be noted that these equations include the scaling factors that result from the discrepancy between the differential stress and the effective deviatoric stress in the triaxial test. For convenience we always assume that the input parameters of the creep mechanisms are defined in the stress-strain-rate space of the triaxial experiments. To comply with this assumption, we also rescale the results of the plane strain numerical experiments into the triaxial space before fitting the creep laws. For that purpose, the following expressions are employed:

$$\dot{\varepsilon}^{triax} = \frac{2}{\sqrt{3}}\,\dot{\varepsilon}^{plstr}$$
$$\sigma_d^{triax} = \frac{\sqrt{3}}{2}\,\sigma_d^{plstr}\,. \tag{13}$$

As the boundary conditions we use surface tractions (stresses) combined with the prescribed displacements. Special algorithm is invoked in case that displacement constraints are omitted (stress-only boundary conditions), since this generates singular stiffness matrices.

3.2.2 Numerical modeling scheme

The boundary value problem is discretized and solved using the finite element method (Zienkiewicz and Taylor, 2000). By applying the Galerkin procedure, the weak form of the equilibrium and continuity equations in the residual form is obtained:

$$\boldsymbol{r}_u = \int_V \boldsymbol{B}^T\,\boldsymbol{\sigma}\,dV - \int_V \boldsymbol{N}_u^T\,\boldsymbol{b}\,dV - \int_A \boldsymbol{N}_u^T\,\boldsymbol{t}\,dA = 0$$
$$\boldsymbol{r}_p = \int_V \boldsymbol{N}_p^T\left(\Delta\theta - \frac{\Delta p}{K}\right)dV = 0 \tag{14}$$

where $\boldsymbol{r_u}$ is the nodal force residual vector**,** $\boldsymbol{r_p}$ is the discretized continuity residual vector, N_u and N_p are the displacement and mean stress shape function matrices, respectively:

$$\boldsymbol{N}_p = \begin{bmatrix} N_{p1} & \dots \end{bmatrix}$$
$$\boldsymbol{N}_u = \begin{bmatrix} N_{u1} & 0 & \dots \\ 0 & N_{u1} & \dots \end{bmatrix}, \tag{15}$$

$\boldsymbol{B}$ is the differential operator matrix:

$$\boldsymbol{B} = \begin{bmatrix} \frac{\partial N_{u1}}{\partial x} & 0 & \cdots \\ 0 & \frac{\partial N_{u1}}{\partial y} & \cdots \\ 0 & 0 & \cdots \\ \frac{\partial N_{u1}}{\partial y} & \frac{\partial N_{u1}}{\partial x} & \cdots \end{bmatrix}, \tag{16}$$

t is the surface traction vector, V is the volume, and A is the surface area of the elements. The system of equilibrium and continuity equations is solved for the incremental displacements ($\Delta\mathbf{u}$) and incremental mean stresses ($\Delta\mathbf{p}$) as a primary variables:

$$\boldsymbol{p}_{n+1} = \boldsymbol{p}_n + \boldsymbol{\Delta p}$$
$$\boldsymbol{u}_{n+1} = \boldsymbol{u}_n + \boldsymbol{\Delta u}\,. \tag{17}$$

Here subscript indicates a time step index. The total Cauchy stresses in the integration point, and the volumetric strain increment are given by, respectively:

$$\boldsymbol{\sigma} = \boldsymbol{\tau} + p\,\boldsymbol{m}$$
$$\Delta\theta = \boldsymbol{m}^T\boldsymbol{B}\,\boldsymbol{\Delta u}\,, \tag{18}$$

where the volumetric projection matrix is defined as:

$$\boldsymbol{m}^T = [\,1 \qquad 1 \qquad 1 \qquad 0\,]. \tag{19}$$

The deviatoric stresses ($\boldsymbol{\tau}$) are computed by solving the scalar nonlinear equation that results from the time discretization of the deviatoric constitutive equation. The primary variables are iteratively updated on every time step by the Newton-Raphson algorithm, until the norm of the residual vectors is reduced to a small relative tolerance (typically 10^{-3}-10^{-4}):

$$\begin{bmatrix} \boldsymbol{\Delta u} \\ \boldsymbol{\Delta p} \end{bmatrix}_{k+1} = \begin{bmatrix} \boldsymbol{\Delta u} \\ \boldsymbol{\Delta p} \end{bmatrix}_{k} - \begin{bmatrix} \boldsymbol{K}_{uu} & \boldsymbol{K}_{up} \\ \boldsymbol{K}_{pu} & \boldsymbol{K}_{pp} \end{bmatrix}_{k}^{-1} \begin{bmatrix} \mathbf{r}_u \\ \mathbf{r}_p \end{bmatrix}_{k}. \tag{20}$$

Here the blocks of the tangent matrix are defined as follows:

$$\begin{aligned} \boldsymbol{K}_{uu} &= \int_V \boldsymbol{B}^T\, \boldsymbol{D}\, \boldsymbol{B}\, dV \\ \boldsymbol{K}_{up} &= \int_V \boldsymbol{B}^T\, \boldsymbol{m}\, \boldsymbol{N}_p\, dV \\ \boldsymbol{K}_{pu} &= \int_V \boldsymbol{N}_p^T\, \boldsymbol{m}^T\, \boldsymbol{B}\, dV \\ \boldsymbol{K}_{pp} &= -\int_V \boldsymbol{N}_p^T\, \frac{1}{K}\, \boldsymbol{N}_p\, dV. \end{aligned} \tag{21}$$

where $\boldsymbol{D}$ stands for the tangent operator, that linearizes the dependence of Cauchy stresses on the total strain increments.

To avoid the numerical instabilities resulting from the nearly incompressible viscous deformation, appropriate interpolation (shape) functions must be selected for the displacements and mean stresses. Here we use a seven-node triangular Crouzeix–Raviart finite element, shown in Figure 302, to discretize the weak form of the equilibrium and continuity equations over the domain. This element is completely free of instabilities, relatively simple, and performs robustly on practice. The quadratic shape functions enhanced with a cubic bubble function in the centre are used for the displacements. The linear discontinuous shape functions are employed for the mean stresses. It is also important to keep the edges of the element straight. Therefore, the linear shape functions are used to represent the geometry of the element. Coordinates are defined only in corner nodes, but not in the centres or on the edges. Hence the element is called sub-parametric, as opposed to the iso-parametric elements that uses the same shape functions for both displacements and coordinates. The stresses and all the material parameters are naturally defined in the integration points. Altogether 6 integration points are used to accurately evaluate the integrals over the element. Additionally, we assume that material parameters are constant within the element. For the output of stress results and visualization purposes, we interpolate the stress components and material parameters to the corner nodes. The high-resolution body-fitted triangular mesh is generated using the open-source two-dimensional quality mesh generator Triangle (Shewchuk, 1996).

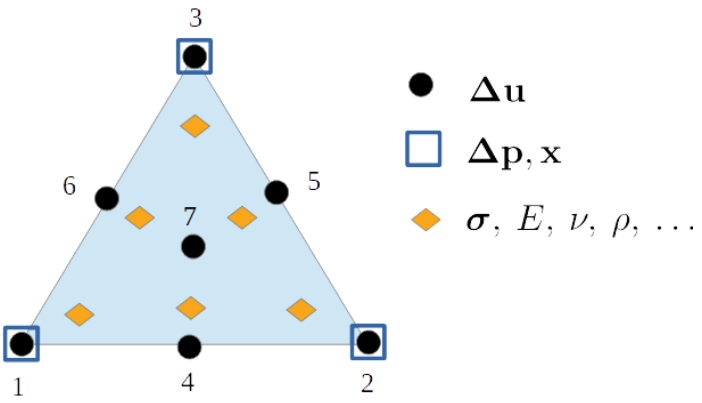

Figure 302. Schematic representation of the triangular seven-node Crouzeix–Raviart element. Displacements are interpolated by quadratic shape functions enhanced with a cubic bubble function in the centre. Mean stresses are discontinuous between the elements and interpolated by linear shape functions. Coordinates are represented in the corner nodes only. Edges remain straight (sub-parametric finite element). Material parameters and stresses are stored in 6 integration points. Material parameters are assumed to be constant within the element.

3.2.3 Workflow of numerical creep tests

Initially, a digital representation of the intrinsic phases of *KB rock salt* (e.g., images or synthetic model separating the halite matrix from individual halite megagrains and anhydrites, see Figure 303) are converted into a body-fitted mesh using our in-house meshing algorithms. This ensures that the numerical mesh is topologically consistent and highly resolved, while still preserving small-scale structural features. Next, different rheologies are assigned to each phase of the model, where pressure-solution-dislocation-creep is assigned to the halite matrix, dislocation-creep to the halite mega grains, and a reduced pressure-solution creep to the anhydrite (see Table 32).

With these assignments in place, a transient uniaxial deformation simulation is conducted. Boundary conditions applied during this simulation aim to mimic the boundary conditions of lab experiments. A constant confining pressure ($\sigma_2 = \sigma_3$ in 2D) is imposed at both left and right boundaries. The uniaxial load ($\sigma_1 > \sigma_3$) is enforced along the top boundary while no-slip conditions are set at the bottom boundary (see Figure 303). Dynamic time stepping schemes based on applied differential stress levels are implemented to ensure proper numerical convergence with minimal simulation time. Generally, larger normal loads result in smaller initial timesteps and slower relative timestep growth rates with a target of maintaining constant strain per timestep. After each timestep, we calculate volume-averaged strain rates of the whole sample and compare them with those from previous timesteps.

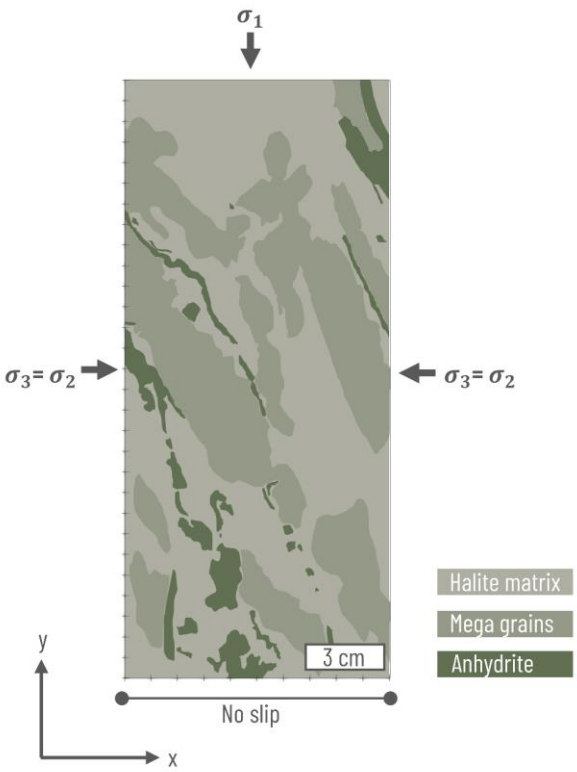

Figure 303. Numerical creep test on a digitized KB rock salt core sample (provided by MaP, KEM-17 Micro-scale report). Shown here are the three main mechanical phases of KB rock salt (halite matrix, halite mega grains, and anhydrite), segmented from a scanned core sample of about 10 by 30 cm in size. After applying a body-fitted mesh to the segmented phases, numerical uniaxial deformation tests with increasing loads are performed to estimate the sample's aggregate creep properties. The boundary conditions explained in the text are sketched in as well.

If there is less than a 0.1% relative change between consecutive timesteps' strain rates, it indicates that deformation has reached steady state (i.e., elastic stress relaxation has occurred, which results in purely viscous deformation characterized by constant strain rate) and we terminate the simulation. In the final step of our simulation procedure, we calculate the cumulative vertical displacement of the numerically deformed sample at each timestep. This allows us to obtain a curve showing the total vertical strain versus time, as well as displacement-based strain rates (see Figure 304).

This approach ensures comparability with typical physical deformation tests conducted in laboratory settings, which are interpreted in a similar manner. By repeating this experiment and systematically increasing the uniaxial load within a range of 0.01 to 50 MPa, we can establish a stress-strain-rate relationship specific to the sample being studied.

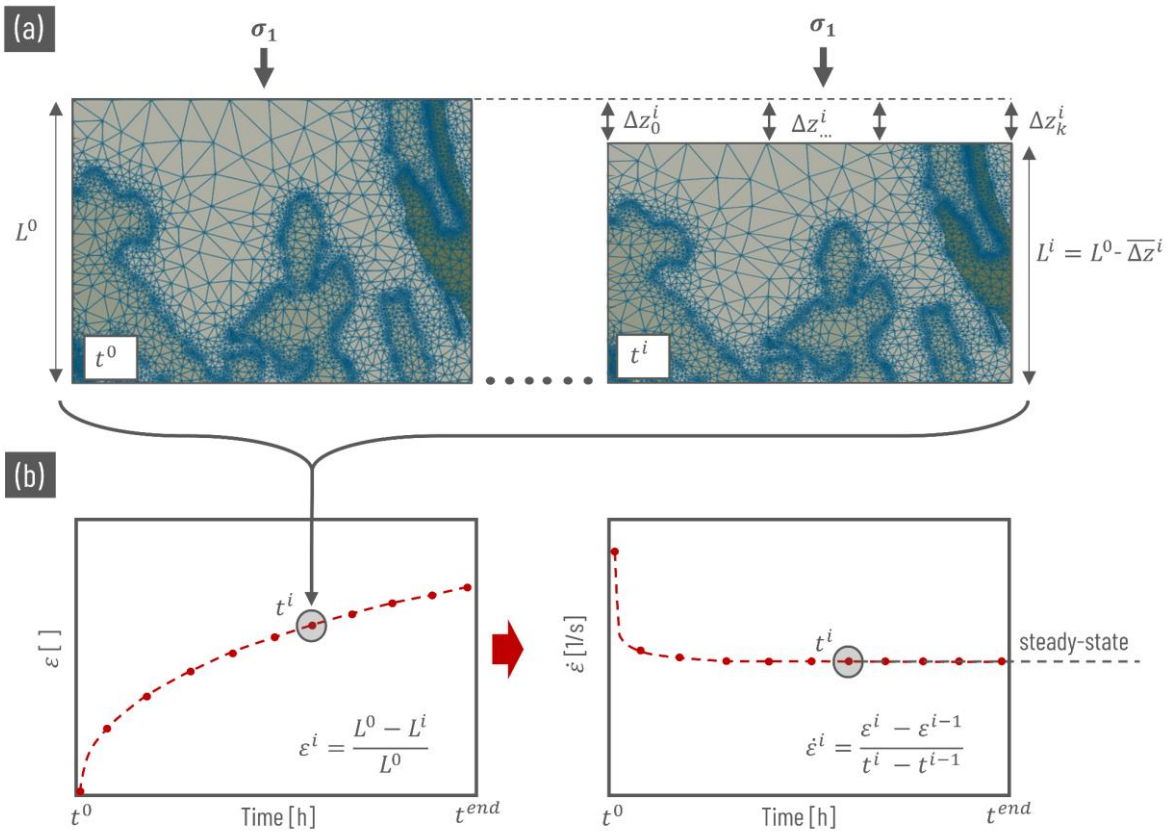

Figure 304. Sketch of workflow to compute displacement-based strain rate from numerical deformation experiments. In panel (a) we show how we extract a mean vertical displacement $\overline{\Delta z}^i$ at each timestep t^i by first computing the absolute difference at each node (index 0 to k, given in the subscript) at the top boundary from the current timestep (t^i) to the initial timestep (t^0) and then computing their mean value. From this, we can compute the current mean sample length L^i, from which the total strain of the current timestep ε^i can be computed according to the equation displayed in the lower right corner of the left plot in panel (b). The strain rate of the current timestep $\dot{\varepsilon}^i$ is defined by the slope of the strain vs. time curve from the left plot in panel (b), whereas the formula is given in the lower right corner in the right plot of panel (b).

3.2.4 Pure halite benchmark

To deliver a proof of concept of our numerical deformation experiments, we conducted several benchmark simulations. We used the method and workflow outlined above to deform a sample of pure halite over the full stress range. The mechanical input properties of the halite matrix are given in Table 32. By comparing the simulation results with the analytical creep equation (based on the SUM creep law, i.e., Eq. (*3*), we see that the expected pressure solution and dislocation creep behaviour at low and high stresses, respectively, is reproduced perfectly (Figure 305). With residuals below 0.1 % of the analytical solution, we demonstrate the validity of our numerical approach.

Table 32. Mechanical properties of KB rock salt intrinsic phases (halite matrix, mega grains and anhydrite. Symbols of viscous creep parameters correspond to the ones given in equations eq. (1) and eq. (2), whereas both activation energies (Q_{ps} and Q_{dc}) are normalized with the universal gas constant R and the pressure-solution prefactor A_{ps} is normalized by V_m, the molar volume of the solid phase (2.693E-05 m³, see (Spiers et al., 1990).

	Density	Elastic	Viscous						
			Dislocation creep			Pressure solution creep			
Symbol *[Unit]*	rho *[kgm^{-1}]*	E *[Pa]*	$\log_{10}(A_{dc})$ *[MPa^{-n}yr^{-1}]*	Q_{dc}/R *[K]*	n_{dc} *[ ]*	A_{ps}/V_m *[KMPa-nyr-1]*	Q_{ps}/R *[K]*	n_{ps} *[ ]*	D_{ps} *[mm]*
Halite matrix	2160	3,30E+10	3,87E-01	6494,71	5,0	2,93E-01	2886,54	1,0	2,0
Halite mega grain	2160	3,30E+10	3,87E-01	6494,71	5,0				
Anhydrite	2900	3,00E+10				2,93E-05	2886,54	1,0	2,0

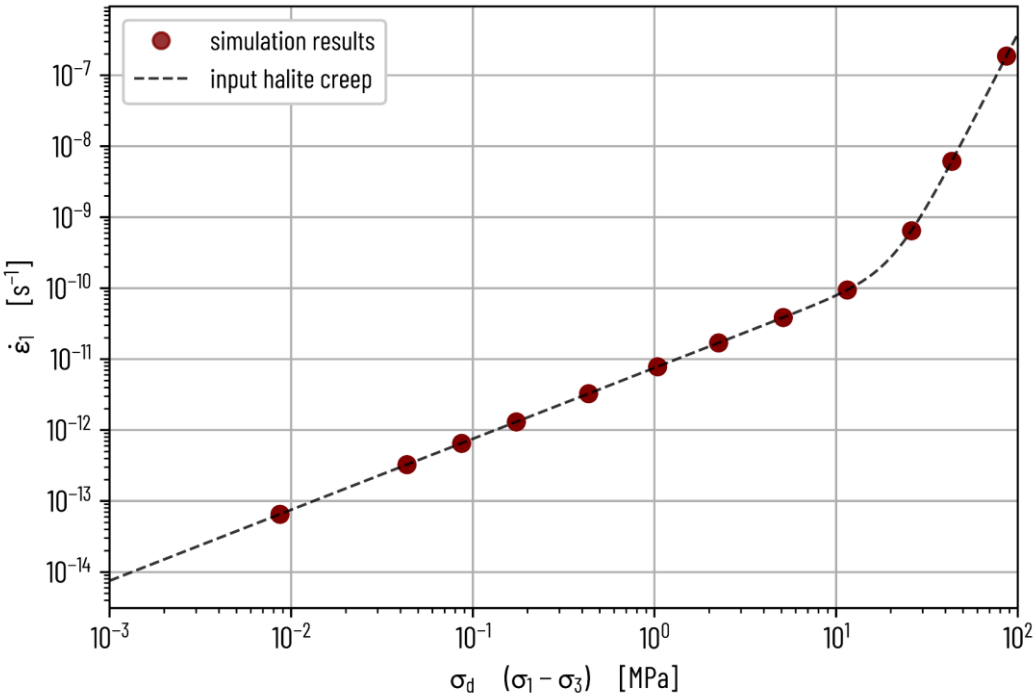

Figure 305. Halite creep benchmark computation. We compare the axial strain rate ($\dot{\varepsilon}_1$) of a numerically deformed synthetic model consisting of pure halite matrix at differential stresses (σ_d –obtained from the maximum and minimum principal stress components, σ_1 and σ_3, respectively) against the analytical input creep law (dashed black line).

3.3 Creep properties of *KB rock salt*

Heterogeneities and varying volume fractions of the *KB rock salt* intrinsic phases are thought to have a strong control on overall creep behaviour. To find a generally applicable, upscaled creep-law for *KB rock salt* that can be employed in dome-scale models, it needs to be determined at scales that are representative (i.e., much larger than typical sample sizes of 10 cm). Thus, we employ an upscaling workflow as follows. First, we utilize expert-knowledge determined grain statistics (orientation-, shape- and size-distributions) of the individual phases to generate synthetic 2D models of *KB rock salt* (grains are represented as ellipses) at scales we consider representative (i.e., larger than individual mega grains). Next, we determine effective creep properties from multiple synthetic *KB rock salt* model realisations with varying mega grain and anhydrite volume fractions by deforming them numerically over the full stress range. From this dataset, endmember rheologies for site-specific *KB rock salt* structures can be extracted. The following sections describe those individual steps in closer detail.

3.3.1 Synthetic 2D models

Having knowledge of the overall statistics regarding the crystalline structure of rocks allows us to generate synthetic microstructural models in a statistical manner using various approaches (Fullwood et al., 2008; Hart and Rimoli, 2020a; Torquato and Haslach, 2002). In this study, we utilize the open-source Python package MicroStructPy (Hart and Rimoli, 2020b) to generate different synthetic two-dimensional meshes that represent generic *KB rock salt* samples. MicroStructPy employs a Laguerre-Voronoi tessellation algorithm (Aurenhammer, 1987) on randomly distributed seeds of multi-phase geometric primitives such as circles (halite matrix) or ellipses (halite mega grains and anhydrites). These primitives have controlled overlap and prescribed statistical distributions for grain properties like volume fraction, size, shape, and orientation. The outcome is a gapless arrangement of Voronoi polygons which we discretize using our in-house meshing algorithm. This results in a high-quality body-fitted mesh that is suitable for use in our numerical deformation experiments. To generate synthetic models of *KB rock salt* that are representative for natural occurring *KB rock salt* in a quantitative manner, microstructural analysis should be employed

on thin sections of site-specific core samples to assess locally valid grain statistics. As the scope of this study is to provide general, non-site-specific recommendations for the long-term creep of *KB rock salt*, we utilize hypothetical, but expert-knowledge (KEM 17 micro-scale report Urai et al. (2019) and personal communication with J. Urai and MaP) approved grain statistics for shape, size and orientation of the mega grains and anhydrites in the synthetical *KB rock salt* models.

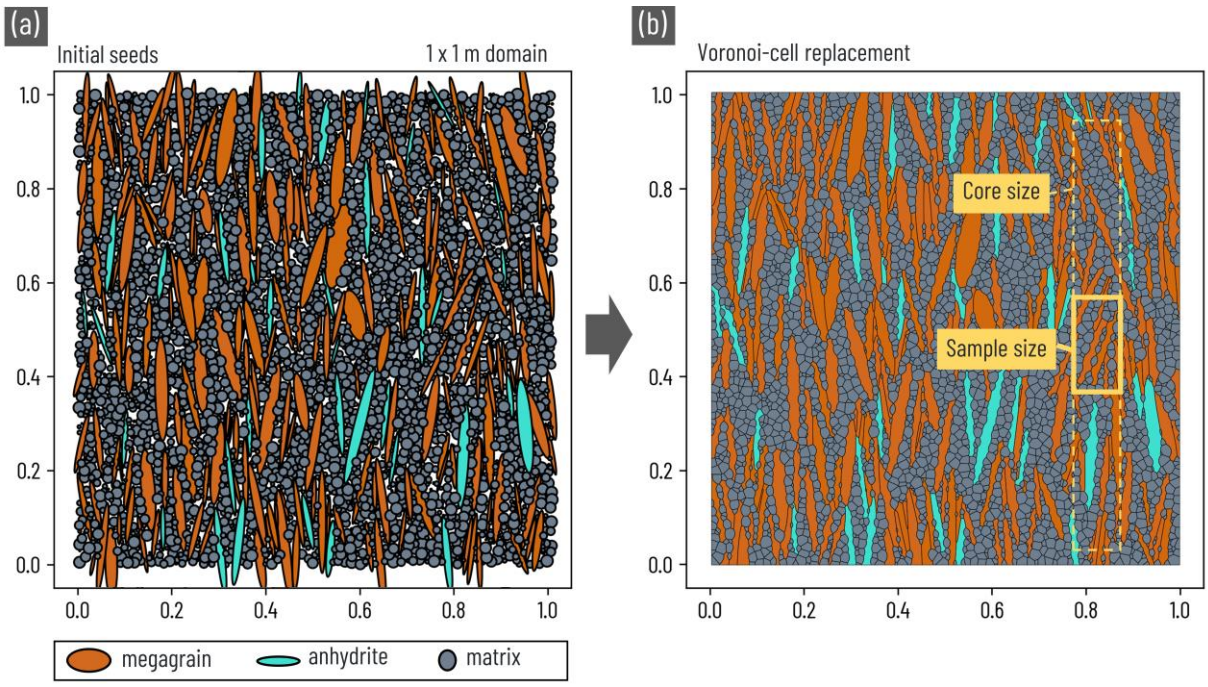

Figure 306. Synthetic KB rock salt model generation using MicroStructPy, which creates polycrystalline structures based on ellipses, representing grains with phase-specific distributions of size, aspect ratio and orientation. Panel (a) shows a domain of custom size (here 1 by 1 meter), that is populated by geometric primitives (circles for the halite matrix, ellipses for halite mega grains and anhydrites) while matching the predefined, phase-specific volume fractions. The resulting Laguerre-Voronoi tessellation is displayed in (b). The yellow dashed and solid boxes in (b) highlight the dimensions of conventional drill-cores and respective subsamples, which are used in lab-based, physical deformation tests.

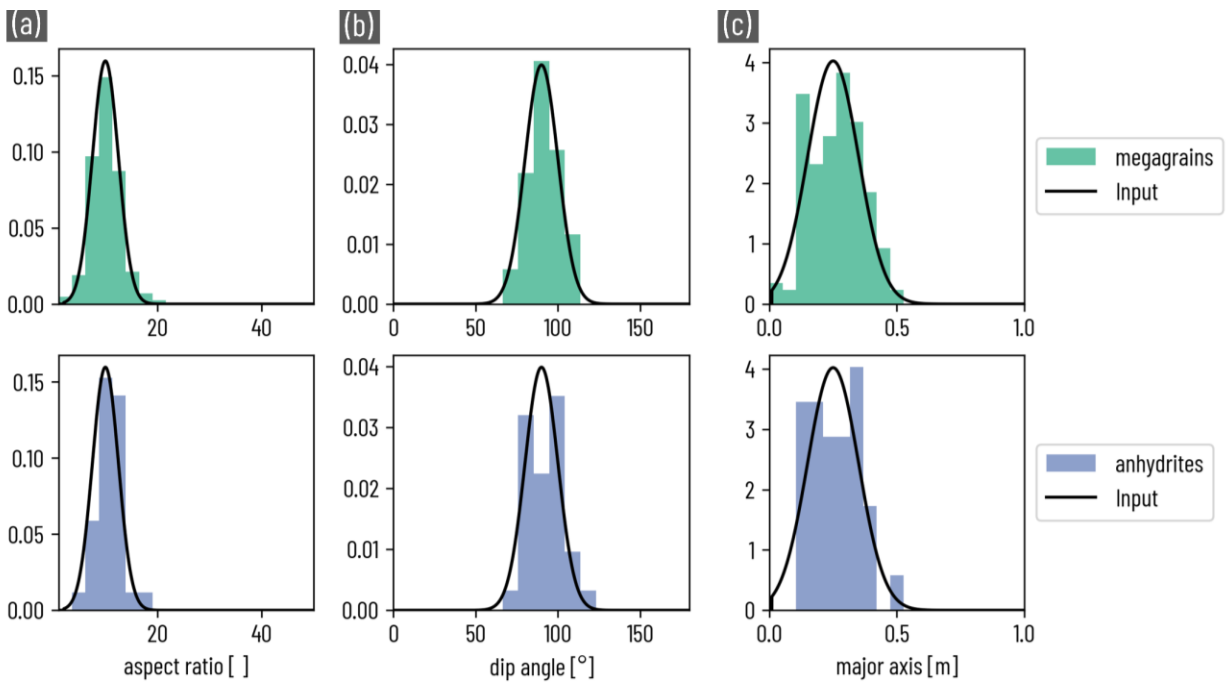

Figure 307. Properties of synthetically generated grains. The resulting histograms for the aspect ratio (a), orientation (b) and major axis length (c) obtained from a synthetic model are displayed row-wise for halite megagrains in green and anhydrites in blue, respectively. The input distributions outlined in the text are given in black, indicating good accordance to the generated data.

Here, for simplicity we use the same (truncated) normal distributions for both ellipse types, representing the mega grain and anhydrite phase. Their aspect ratios are normally distributed between 2 and 50 with a mean of 10 and a standard deviation of 2.5. By this we make sure that the individual grains are properly elongated, reflecting the sedimentary origin of the KB rock salt intrinsic phases. For the orientation we use a normal distribution of 90° with a standard deviation of 10°, which results in primarily vertically oriented grains. This corresponds to a KB rock salt formation that has went through bedding-parallel deformation (boudinage of *Kristallbrocken* layers). In contrast to that, strongly deformed and folded KB rock salt would result in more diffuse orientations, which, like the other properties, must be determined site-specifically. For the major axis of the ellipses, we again utilize truncated normal distributions between 0.01 and 1 m with a mean of 0.25 m and a standard deviation of 0.1 m. This ensures that we generate mega grains that on average are larger than a typical core sample (~0.1 m) and correspond to maximum lengths observable on drill cores (~1 m), reflecting H2C3-internal expert-knowledge. See Figure 307 for a comparison of input distributions and properties of the generated grains. Having the statistical distributions of the individual grains defined, we can now generate synthetic *KB rock salt* models with prescribed volume fractions for the matrix, mega grain, and anhydrite phase. For this study we generate a dataset with volume fraction combinations of 0, 10, 20, 30, 40, 50, 60 % mega grains and 0, 5, 15 % anhydrites, thus 21 different volume fraction configurations. For each configuration we generate 20 random realizations, resulting in a dataset of 420 KB rock salt models (see Figure 308 for a few examples). The model sizes are fixed to 2x2 m (twice the size of the maximum grain length of our models) to incorporate small and large grains in computational meshes feasible for numerical deformation experiments in a reasonable amount of time (12 stress increments between 0.01 and 50 MPa normal load are tested here, thus a total of 5040 simulations). By this, we ensure quantifying the long-term creep at scales we consider representative for the KB rock salt internal microstructure, while acknowledging its broad heterogeneity in a statistical manner.

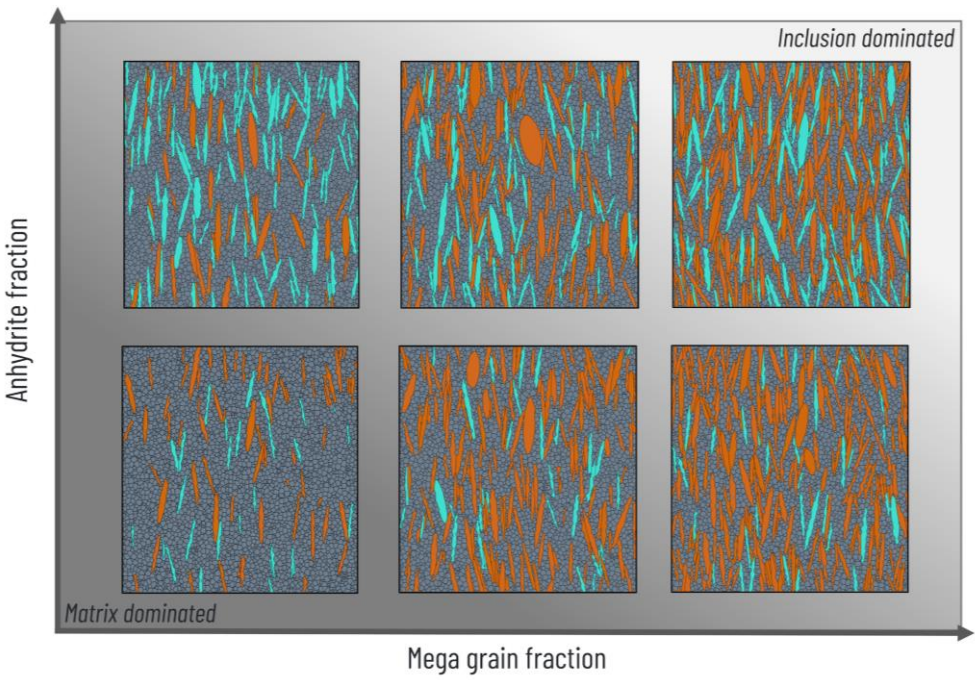

Figure 308. Chosen realizations of our synthetic KB rock salt model dataset for increasing mega grain and anhydrite volume fractions on the x- and y-axis, respectively. Input distributions for grainsize, orientation and shape are given in Figure 307, the model size is set to 2x2 meters.

3.3.2 Effective long term creep of KB rock salt

The 420 generated synthetic KB rock salt with 2 m side lengths generated according to the workflow outline above are numerically deformed over the full stress range from 0.01 to 50 MPa (see Table 32 for

the employed mechanical properties of each unit). In Figure 309, the resulting 420 stress-strain relationships of all synthetically generated models are displayed for varying overall mega grain (a), anhydrite (b) and halite matrix (c) volume fractions. A general visual inspection suggests that increasing volume fractions of halite mega grains cause significant deviations (up to 6 orders of magnitude) from pure halite creep behaviour, especially in the low-stress regime below 10 MPa differential stress with a generally visible trend of higher deviations for larger mega grain fractions. On the other hand, increasing volume fractions of anhydrite seem to cause deviations as well, but not in a clearly visual pattern as compared to the mega grain or halite fraction. The latter displays the clearest trend of deviation from pure halite creep with decreasing matrix fractions. Thus, the matrix volume fraction renders as primary variable for geometry quantification in the following interpretation approaches, as its inverse (the non-matrix fraction) combines mega grain and anhydrite fraction in one quantity.

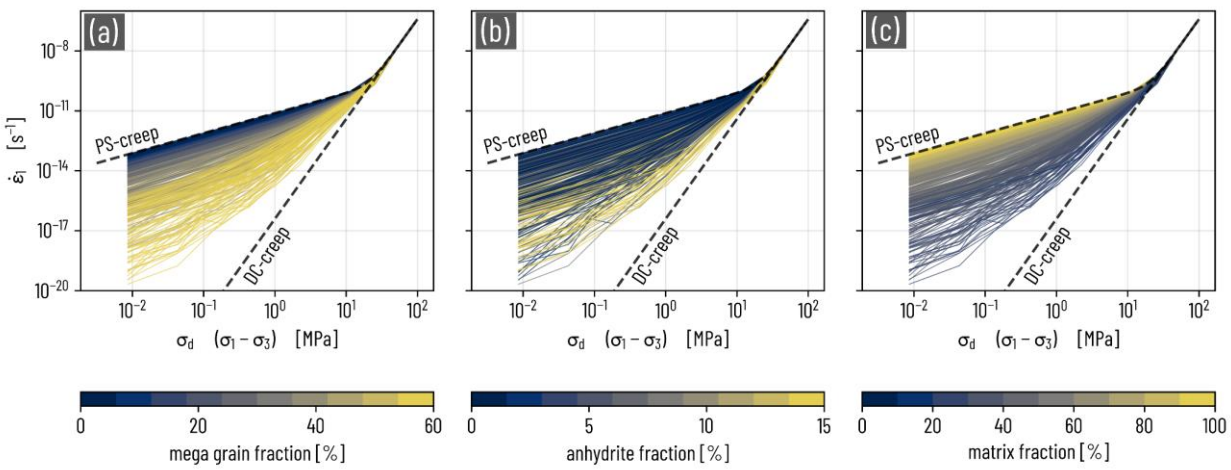

Figure 309. Numerically determined creep behaviour of synthetically generated 2D KB rock salt models at a representative scale of 2x2 m. From 21 different mega grain and anhydrite volume fraction configurations, we generated 420 synthetic KB rock salt models according to our workflow outline above and deform them numerically from 0.01 to 50 MPa (5040 simulations in total). The resulting creep-laws ($\dot{\varepsilon}_1$ – the uniaxial strainrate versus σ_d– the differential stress obtained from the maximum and minimum principal stress components, σ_1 and σ_3, respectively) are displayed in (a), (b) and (c), colored by halite megagrain, anhydrite and halite matrix fraction respectively. Dashed black lines depict input creep models of halite matrix (PS-creep, i.e., pressure-solution-dislocation creep) and pure dislocation creep (DC-creep, i.e., mega grain fraction of 1).

3.3.3 Analysis & interpretation

In addition, to a general visual inspection, we analyse the resulting stress-strain-rate relationships in more detail here. For that, we employ problem-tailored advanced data analysis methods to categorize our dataset. First, we employ the Uniform Manifold Approximation and Projection (UMAP) algorithm (see Sainburg et al., 2021), which enables us to simplify complex high-dimensional data by transforming it into a lower-dimensional space, while retaining its underlying structure. This allows us to distinguish similar and different simulation series in a quantitative manner. Here, we build a multi-dimensional input matrix from extracted strain rates at low-stress (0.01 to 5.11 MPa in 8 increments) for each simulation series, as this is where the largest rheological differences occur (i.e., 8-dimensional input data with 420 entries, see Figure 310). After employing the UMAP algorithm to embed our data into 2D space, we utilize the Hierarchical Density-Based Spatial Clustering of Applications with Noise (HDBSCAN) algorithm (McInnes et al., 2017) to effectively group similar lower-dimensional data points, each representing a unique KB rock salt rheology. This reveals meaningful clusters, even for heterogeneous data while accounting for its noise. Their creep properties and cluster-internal exemplary deformation patterns are displayed in Figure 311. Creep properties and example realizations of identified clusters. In panels a-e, the stress-strain-rate relationships pf all deformation series within the identified clusters are displayed on the left side, whereas cluster statistics w. r. t. mega grain (m) and anhydrite (a) volume fractions are indicated on the upper left

corner of the plot. Then, we extracted one exemplary realization of the cluster models (displayed on the right side of the figure) and visualized the strain rate in log10 space at 0.1 (pressure solution creep regime) and 30 MPa (dislocation creep regime) applied uniaxial load. Cluster IDs indicated in the top right of each panel correspond to the cluster IDs indicated in Figure 310.. The volume fraction statistics displayed in the upper left corner of the creep properties plot for each cluster confirm the hypothesis presented above that larger mega grain fractions cause significantly lower strain rates in the low-stress regime. This is expectable behaviour caused by the increased overall proportion of the chosen megagrain (dislocation creep only) rheology. However, the spatial arrangement of the mega grains at large volume fractions ($\gtrsim 45\,\%$) determines whether the strain rate reduction in the low-stress regime is in the order of two magnitudes (i.e., $c_{ID} = 2$) or up to six orders of magnitude (i.e., $c_{ID} = 3\ \&\ 4$). The example geometries from the clusters as well as the resulting strain rates in the low-stress regime at 0.1 MPa applied load (right plots in panels c, d, & e in Figure 311. Creep properties and example realizations of identified clusters. In panels a-e, the stress-strain-rate relationships pf all deformation series within the identified clusters are displayed on the left side, whereas cluster statistics w. r. t. mega grain (m) and anhydrite (a) volume fractions are indicated on the upper left corner of the plot. Then, we extracted one exemplary realization of the cluster models (displayed on the right side of the figure) and visualized the strain rate in log10 space at 0.1 (pressure solution creep regime) and 30 MPa (dislocation creep regime) applied uniaxial load. Cluster IDs indicated in the top right of each panel correspond to the cluster IDs indicated in Figure 310.) reveal, that this is the case if mega grains form a skeleton-like structure (i.e., large portions of mega grains are contacting and spanning the whole spatial extent of the sample, visible in panels d & e in Figure 311. Creep properties and example realizations of identified clusters. In panels a-e, the stress-strain-rate relationships pf all deformation series within the identified clusters are displayed on the left side, whereas cluster statistics w. r. t. mega grain (m) and anhydrite (a) volume fractions are indicated on the upper left corner of the plot. Then, we extracted one exemplary realization of the cluster models (displayed on the right side of the figure) and visualized the strain rate in log10 space at 0.1 (pressure solution creep regime) and 30 MPa (dislocation creep regime) applied uniaxial load. Cluster IDs indicated in the top right of each panel correspond to the cluster IDs indicated in Figure 310.). The presence of a skeleton-like geometry stabilizes the sample, which then predominantly deforms by dislocation creep. In clusters 1, and 2, the mega grains and anhydrite tend to “float” within the matrix, which accommodates most of the deformation. In contrast, in clusters 3, and 4, the remaining, largely unconnected “pockets” of halite matrix can no longer propagate the strain throughout the sample, which therefore deforms much more slowly.

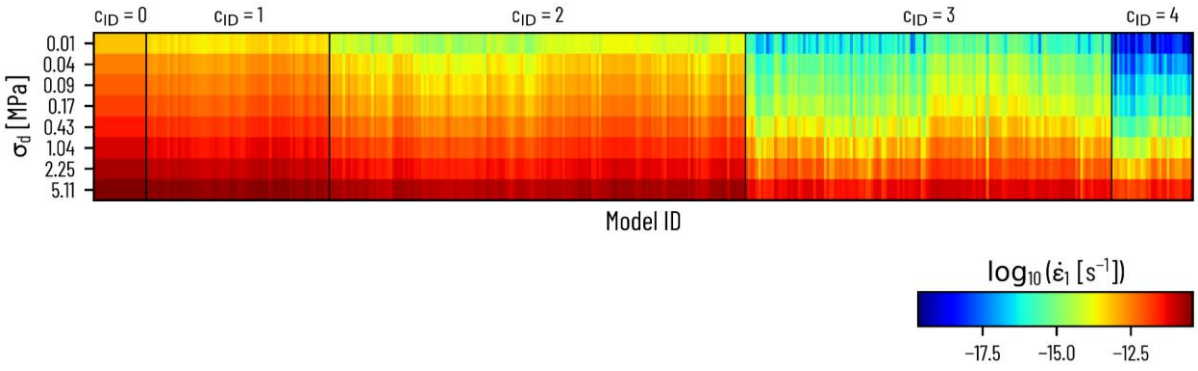

Figure 310. Reordered and categorized input data matrix of our dimensionality reduction (using UMAP) and clustering (using HDBSCAN) workflow. Each column represents the color-coded strain rates extracted at differential stress increments (indicated row-wise) for a unique numerical deformation series on a single synthetically generated KB rock salt sample. Black boxes outline categorized clusters, while the respective cluster ID c_{ID} is given above the black boxes. Note that clusters are ordered in ascending order, based on average strain rate per cluster.

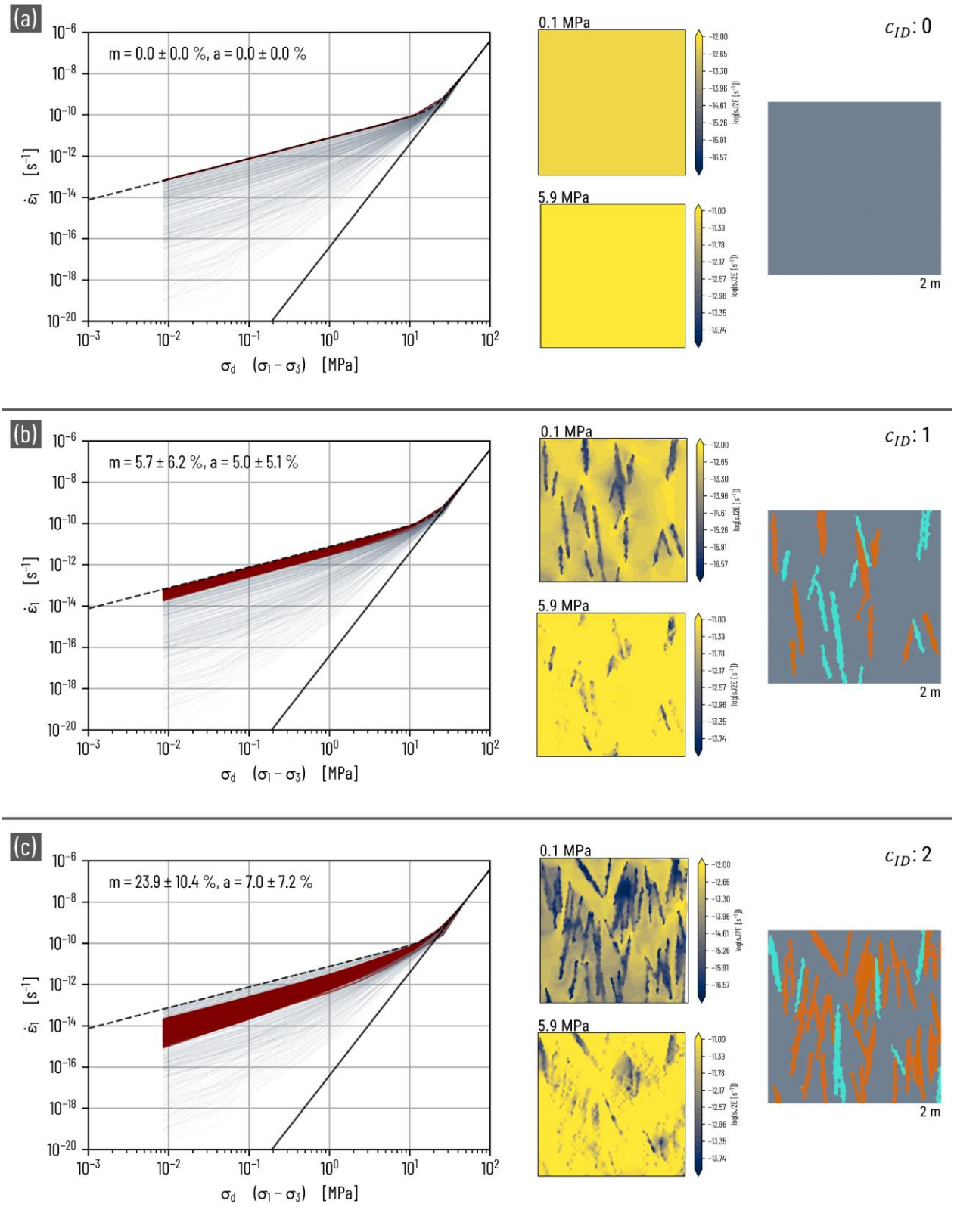

Figure continues on next page.

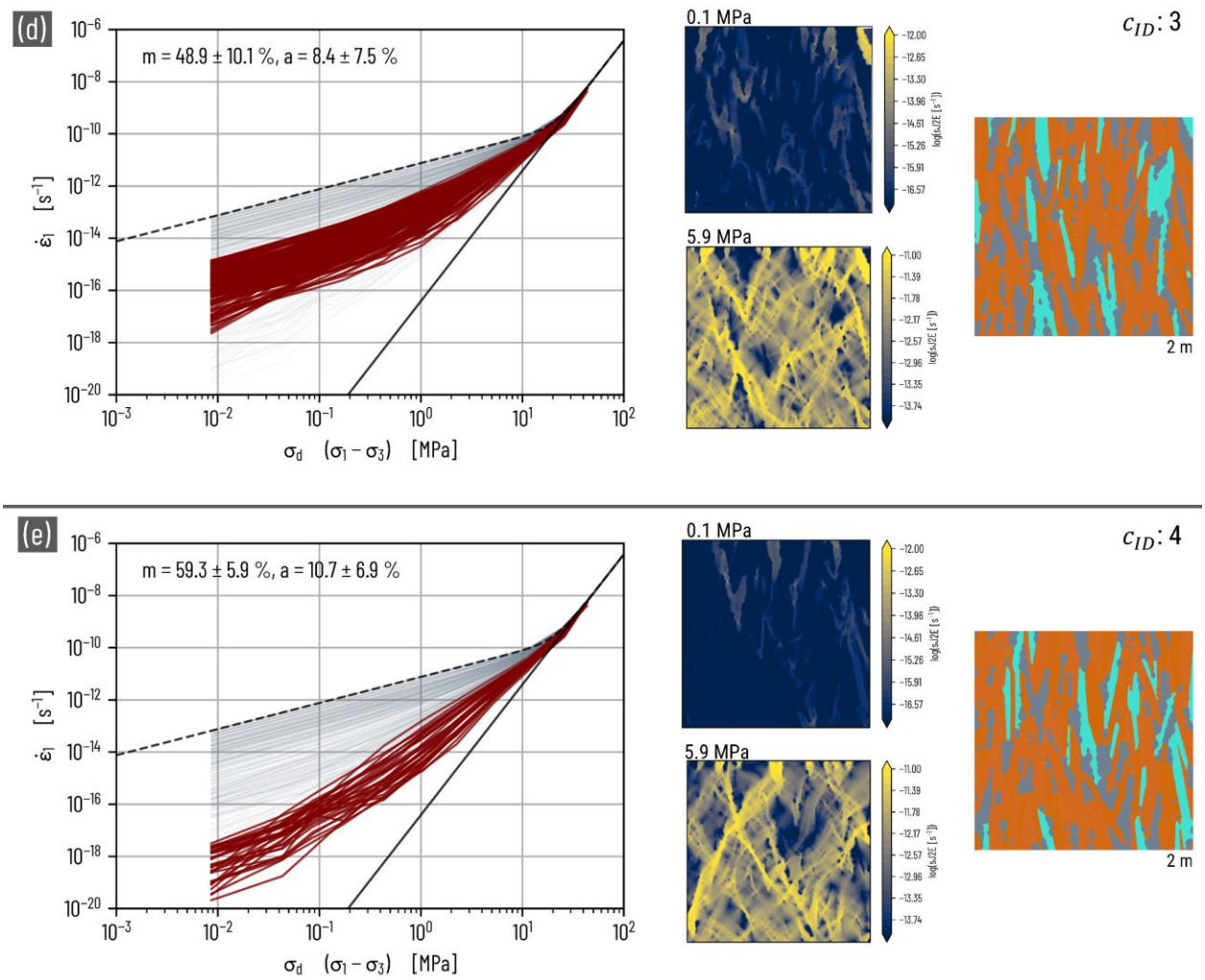

Figure 311. Creep properties and example realizations of identified clusters. In panels a-e, the stress-strain-rate relationships pf all deformation series within the identified clusters are displayed on the left side, whereas cluster statistics w. r. t. mega grain (m) and anhydrite (a) volume fractions are indicated on the upper left corner of the plot. Then, we extracted one exemplary realization of the cluster models (displayed on the right side of the figure) and visualized the strain rate in log10 space at 0.1 (pressure solution creep regime) and 30 MPa (dislocation creep regime) applied uniaxial load. Cluster IDs indicated in the top right of each panel correspond to the cluster IDs indicated in Figure 310.

3.3.4 General & site-specific recommendations

Findings from the previous section suggest that the effective creep of KB rock salt, even at scales considered to be representative, is strongly dependent on the volume fractions of the halite mega grains, especially at low stresses. Thus, as the macroscopic structure of KB rock salt is often unknown, an adequate creep law must account for these uncertainties, either in a probabilistic or mathematical manner. In general, the SUM-creep law (see Eq. 3) describes the steady-state viscous deformation behaviour of a single-phase rock salt without impurities. It represents a well-established, physics-based constitutive equation, benefiting from several decades of scientific research on the underlying mechanisms of halite deformation. Applying this constitutive equation to multi-phase, heterogeneous rock salts with impurities that commonly occur in nature is challenging. In fact, based on the results presented in the previous section, the SUM model should be further developed to take this into account. Doing this in an physics-based manner would require an enormous number of creep tests (analogue lab tests and numerical digital twin creep tests) of precisely quantified sample geometries, which is challenging. However, based on the results from the previous section, we derive an empirical relation that predicts the strain rates of KB rock salt as a function of applied stress (σ_d) and its halite matrix volume

fraction (φ_h). In our empirical model, we introduce an additional creep term next to the pressure solution and dislocation creep term as follows

$$\dot{\varepsilon}_{ps} = 10^{a}\ \varphi_h\ A_{ps}\ e^{-\frac{Q_{ps}}{RT}}\left(\frac{{\sigma_d}^{n_{ps}}}{TD_{ps}{}^{m}}\right), \tag{22}$$

$$\dot{\varepsilon}_{tr} = 10^{b}\ (1-\varphi_h)\ A_{ps}\ {\sigma_d}^{c}, \tag{23}$$

$$\dot{\varepsilon}_{dc} = A_{dc}\ e^{-\frac{Q_{dc}}{RT}}{\sigma_d}^{n_{dc}}, \tag{24}$$

$$\dot{\varepsilon}_{tot} = \dot{\varepsilon}_{ps} + \dot{\varepsilon}_{tr} + \dot{\varepsilon}_{dc}. \tag{25}$$

$\dot{\varepsilon}_{tr}$ describes a power-law creep to which we refer to as "transition creep" that dominates the transition between the endmember cases of pure pressure solution and dislocation creep at low and high stresses, respectively. The new parameters a and b are $\log_{10}$-spaced scaling coefficients for the pressure solution creep pre-factor A_{ps}, whereas c represents the power-law stress exponent of the transition creep term. Multiplying the $\log_{10}$-spaced scaling coefficients, a, and b with the halite matrix volume fraction φ_h and its complement $(1-\varphi_h)$, respectively, ensures the proper activation of the individual creep terms. For example, in case of a pure halite matrix, $(\varphi_h = 1)$, the transition creep term is switched off. We employed a constrained non-linear optimization algorithm on Eq. 25 for each of the 420 stress-strain-rate relationships shown in Figure 309 with halite creep parameters given in Table 32 as constraints to find values for a, b, and c (see Figure 312).

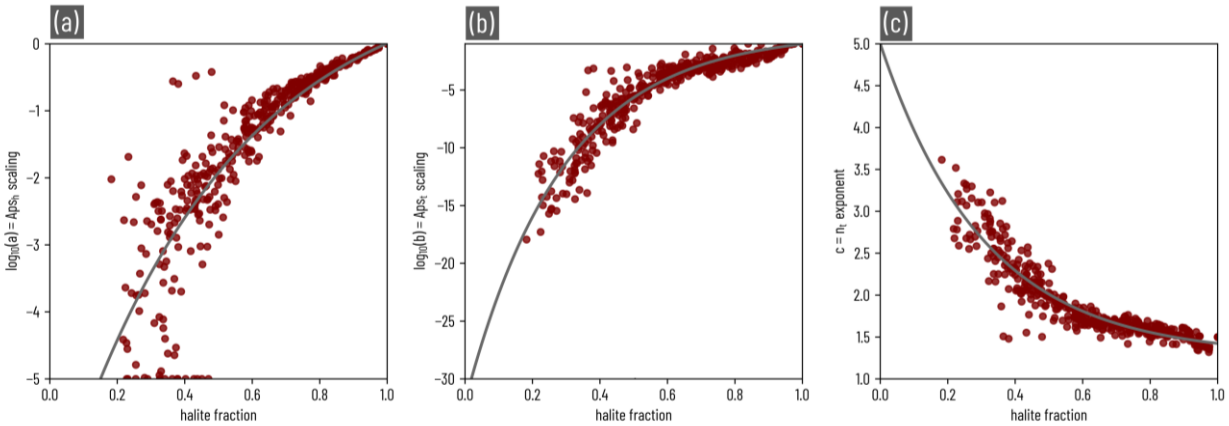

Figure 312. Log_{10}-spaced parameters a, b, and c, resulting from the optimization of Eq. 25 for all 420 stress-strain-rate relationships shown in Figure 309. The grey curves are exponential fits (Eq. 17) to the data, which are used to self-consistently parametrize a, b, and c in Eq. 16 as functions of the halite fraction V f_h. Fitting coefficients are given in Table 33.

We find that exponential functions of the form:

$$p(\varphi_h) = \alpha\ e^{-\beta\ \varphi_h} + \gamma \tag{23}$$

decently approximate these parameters as function of the halite matrix volume fraction φ_h with coefficients given in Table 33. In this way, our empirically derived constitutive law self-consistently maps the creep of KB rock salt based on known halite creep properties and its volume fraction. It serves as a quantitative framework that predicts the observed creep rates of general KB rock salt as described in this study. Figure 313 displays the empirical model in 3D and 2D in terms of its free parameters (i.e., applied stress and halite matrix volume fraction) as well as our raw simulation results, coloured by the residual of the model prediction. These residuals provide an impression of the variability of the modelled deformation behaviour of KB rock salt. In fact, we observe that for most of the space spanned by applied stress and halite fraction, the variability is below ~20 % and thus statistically quite reliable. We only notice increased variabilities for halite fractions below 60 % and stresses below 1 MPa. In this region, creep is

increasingly dominated by non-matrix, in our case represented by anhydrite and mega grains with endmember rheologies defined by reduced pressure solution (factor 1/10000) and dislocation creep, respectively (see Table 32).

Table 33. Coefficients for exponential functions in the form of Eq. 17 fitted to the newly introduced creep parameters as function of the halite matrix volume fractions displayed in Figure 312.

	coefficients		
parameter	α	β	γ
a	-8.2788	1.9872	1.1427
b	-31.9767	3.4780	-0.0351
c	3.7209	3.2519	1.2797

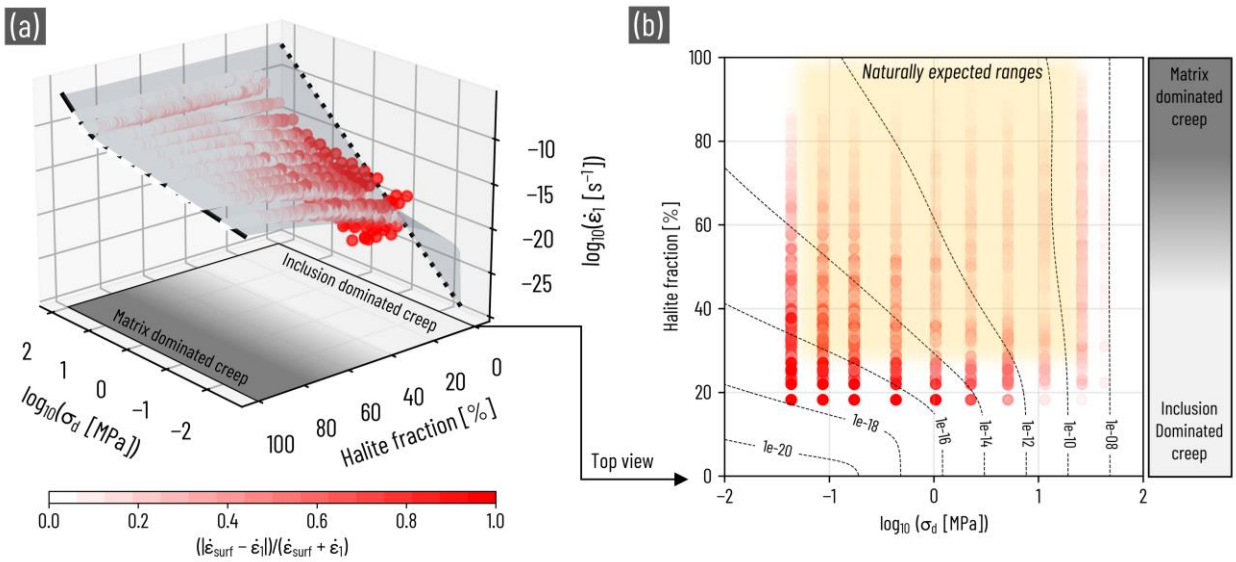

Figure 313. Data modelling of numerical creep test results. Every point in the 3D plot depicts the resulting uniaxial strain rate (z-axis) of a numerical deformation experiment at the applied stress indicated on the x-axis, whereas the halite volume fraction of the deformed sample is given on the y-axis. The colour of the points shows the relative residual to the interpolated 3D strain rate surface. A birds-eye view of the 3D data shown in a is given in panel b. The displayed contours indicate the strain rate obtained from the interpolated 3D surface shown in a. The yellow-transparent region focusses expert-knowledge defined parameter ranges, that are expected for naturally occurring KB rock salt in shallow salt domes.

However, since this increased variability only covers a small portion of the area spanned between expert-knowledge expected halite fractions for naturally occurring KB rock salt and typical differential stresses of a salt-dome (yellow-transparent area in panel b, Figure 313), we are confident that this model gives a good approximation of deformation in KB rock salt in general. From this model, we can extract the classical stress-strain-rate-relationship as shown in Figure 314, panel a, that comprehensively illustrates this deformation behaviour. If we examine the creep reduction factor related to the creep of pure halite creep, shown in panel b in the same figure, we can observe that KB rock salt deforms through dislocation creep above 10 MPa, regardless of its non-matrix content. Below this, we see drastic creep reductions by up to 6 orders of magnitude for increasing non-matrix content. Then, however, it is questionable whether the present formation still identifies as KB rock salt, or rather as separate endmembers (e.g., Kristall-Lagen or anhydrite layer) with individual rheologies.

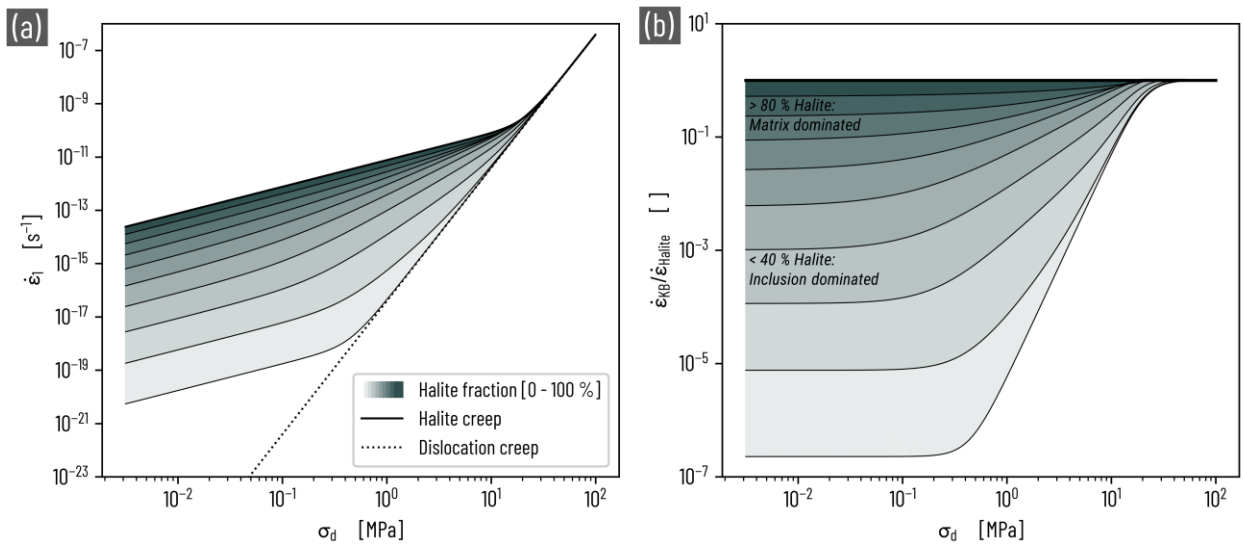

Figure 314. The stress-strain-rate relation of general KB rock salt for various fractions of anhydrite and mega grains is given in a. Filled (non-matrix fraction) and dashed contour lines (halite matrix fraction) are obtained from the interpolated surface shown in Figure 313, panel a. Panel b gives the creep rate reduction factor (using pure halite as reference, i.e., $\dot{\varepsilon}_{Halite}$ as denominator, and the halite matrix fraction contours shown in panel a, $\dot{\varepsilon}_{KB}$, as nominator) in log10 space for several halite matrix fractions.

Next to this general recommendation for the creep properties of KB rock salt, we also propose a strategy for determining a site-specific creep model. This requires micro- and macro-structural knowledge of the present rock salt formation, which needs to be assessed prior to engineering applications within the salt formation. One can then proceed by utilizing site-specific microstructural (i.e., grain size, -orientation and -shape distributions) and macroscopic formation knowledge (i.e., categorized specific units with individual volume fractions and geometric characteristics) to generate a dataset of synthetic models, which are numerically deformed over the stress range expected during the application case.

To obtain a first-order site-specific KB rock salt creep description, we can use the existing SUM creep model and treat the model parameters as effective parameters, utilizing the original model in an empirical sense. For example, when focusing on KB rock salt, the grain size parameter does not represent the grain size obtained from microstructural investigations, but rather the effective behaviour of the multi-phase rock salt. We, therefore, treat the grain size as apparent grain size and account for the observed difference in creep by increasing the grain size such that it reflects the observed first-order creep behaviour (see Figure 315 for an example). This procedure could be repeated to reflect the minimum and maximum possible creep rates with an adjusted apparent grainsize to incorporate fast- and slow-creeping endmembers.

Depending on the (usually sparse) available microstructural data, this approach is likely more feasible for spite-specific applications but tends to underestimate creep rates in the stress-range of pressure-solution to dislocation transition (around 1 MPa). Therefore, if a comprehensive microstructural database is available site-specifically, a large number of statistically representative synthetic KB rock salt models can be generated. Depending on the available computational resources for the numerical deformation experiments, we can thereby calculate a sufficiently large stress-strain rate catalogue to optimize Eq. 25 successfully and find suitable model parameters (a, b, and c) for the extended SUM creep model.

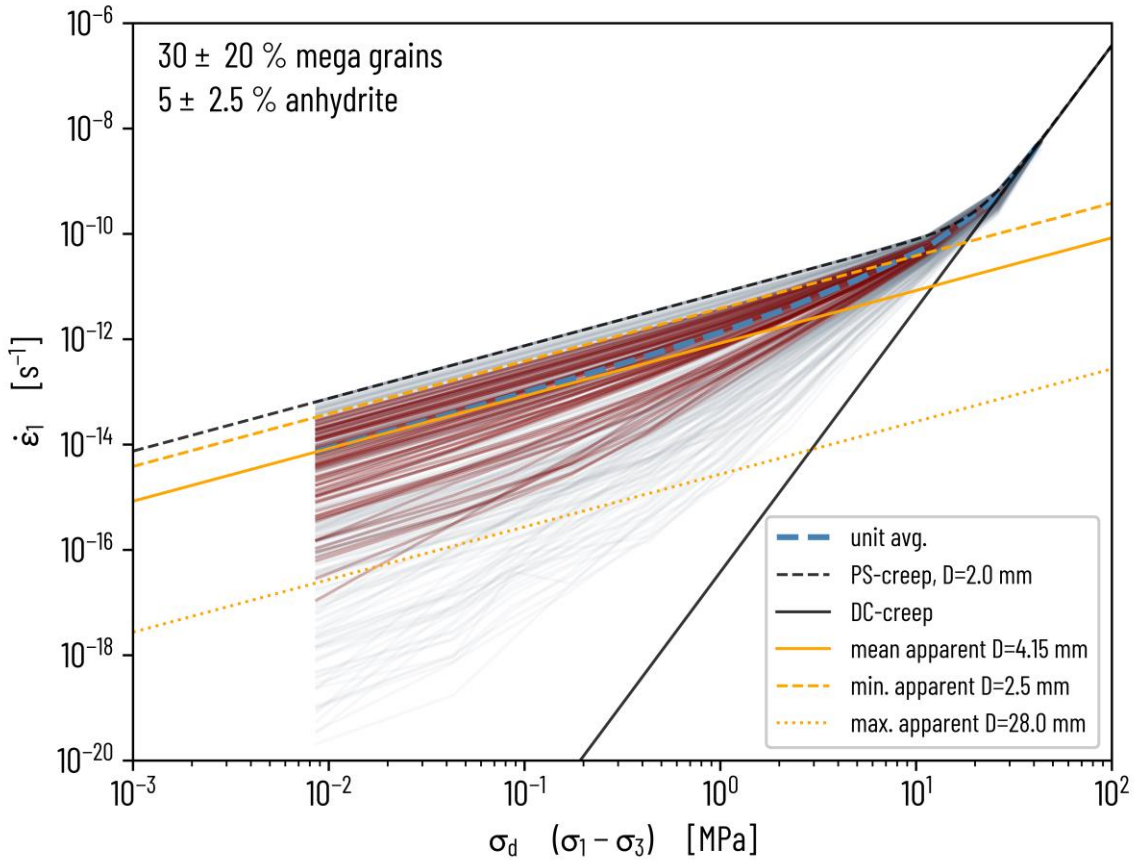

Figure 315. Example demonstration on how to determine the apparent grain size for the SUM model (eq. 3) of a hypothetical multi-phase rock salt formation with a mega grain fraction of 30 ±10 % and an anhydrite fraction of 5 ± 2.5 %. The apparent grain size is increased until it matches the unit average, obtained by first filtering the dataset presented in Figure 309 and then computing the average of all stress-strain-rate relationships.

3.4 Discussion: Influence of anhydrite rheology

The rheology of anhydrite is one major unknown, not only in this study, but also in the salt-tectonics community. Here, we have decided to follow the studies of Pluymakers et al. (2014) and Pluymakers & Spiers (2015), which propose pressure solution creep as primary deformation mechanism of anhydrite. They argue that, due to differences in the grain boundary structure of anhydrite and halite, pressure solution creep in anhydrite is slower compared to halite (Bérest et al., 2023). Thus, due to a lack of constraints, we assumed a similar grainsize of anhydrite and halite and modified the pre-factor in eq. 1 to model the anhydrites rheology. In our simulation series, we set the anhydrite prefactor to be 10000 smaller than the halite pre-factor. To assess the influence of this driven decision, we computed an additional series of simulations with six chosen synthetic KB rock salt geometries with different halite, anhydrite, and mega grain fractions. For each geometry, we considered eight different anhydrite rheologies with varying pre-factor ratios between 1/2 and 1/100000.

The results are shown in Figure 316. We observe no influence of anhydrite rheology on creep of KB rock salt for low anhydrite volume fractions (< 5 %, see panels a, c, and e in Figure 316), regardless of the chosen pre-factor ratio. For larger anhydrite fractions, the overall creep of KB rock salt is only slightly affected (about half a magnitude difference in the low-stress regime). However, for non-matrix phase dominated creep (halite matrix fractions $\lesssim$ 25 %), pre-factor ratios below or equal to 1/100 can cause an up to one order of magnitude increase in strain rate at stresses below 1 MPa (larger prefactor ratios result in larger strain rate increase). This is only the case for inclusion dominated geometries, where variabilities in the order of one magnitude are nonetheless present. Thus, we argue that the exact anhydrite creep plays a minor role in the effective KB rock salt creep and the chosen reference anhydrite rheology in this

study is reasonable, given that it is dominated by pressure solution creep in the considered stress ranges. Yet, this also highlights that more scientific work is needed with focus on anhydrite rheology.

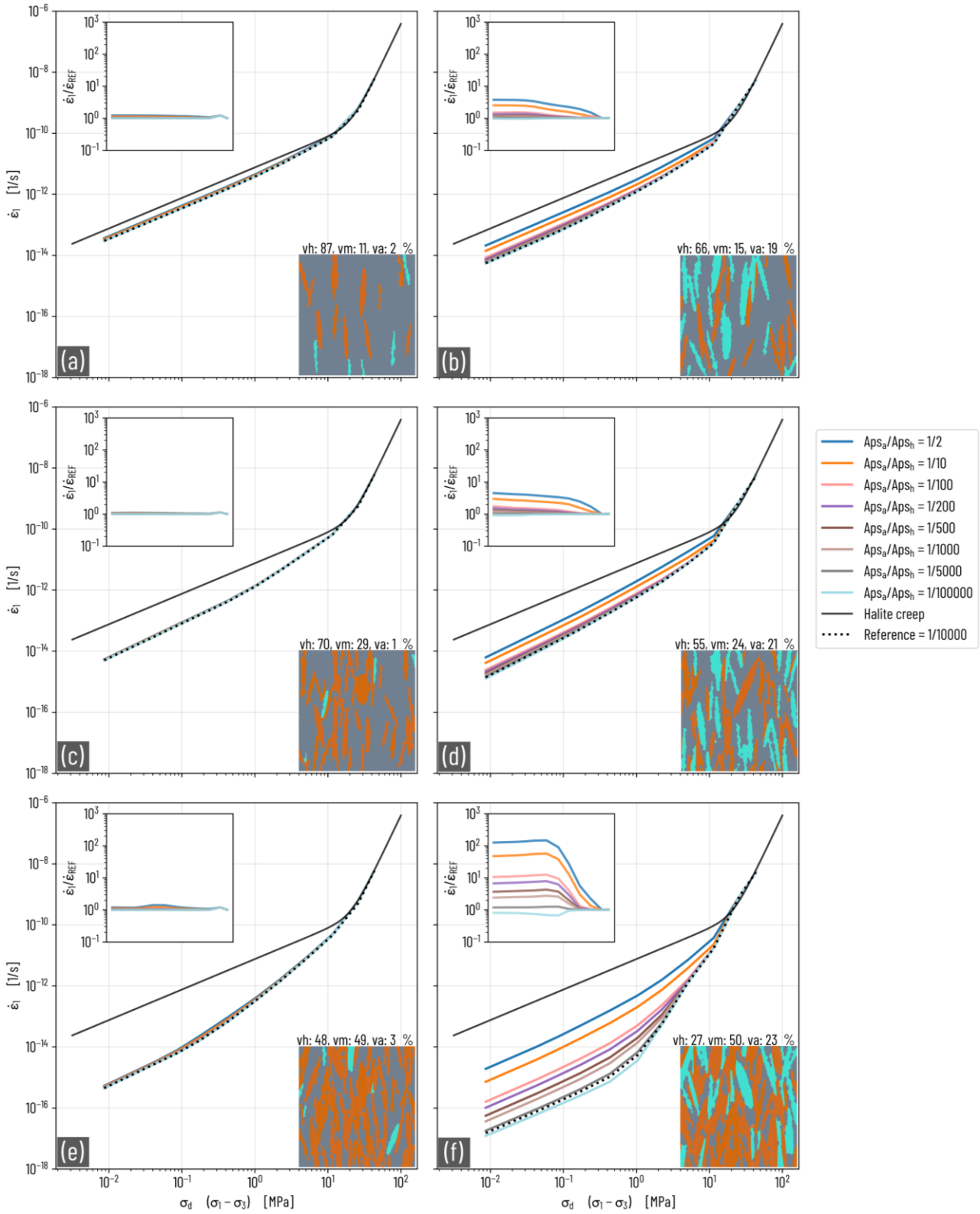

Figure 316. Results of anhydrite rheology test. Each panel gives the stress-strain-rate relations of numerical deformation experiments on the sample indicated in the lower right corner (volume fraction statistics given above) with various anhydrite rheologies. Inset plots in each panel compare the results of tested anhydrite rheologies with the reference rheology employed in our simulation series above (i.e., pressure solution pre-factor ratio of anhydrite to halite Aps_a/Aps_h of 1/10000).

3.5 Summary & conclusions

This study aimed to investigate the creep behaviour of a multi-phase aggregate of rock salt (*Kristallbrockensalz*) through 2D THM-coupled numerical deformation experiments on synthetically generated KB rock salt .We approached this by generating a dataset of 420 synthetic models with varying intrinsic rock phases of KB rock salt (i.e., halite matrix, halite mega grains and anhydrite), with individual grain statistics reflecting generally applicable microstructural properties of KB rock salt. After providing a proof-of-concept for our numerical digital-twin simulations of uniaxial deformation, this dataset is deformed at 0.01 to 50 MPa differential stress to obtain individual stress-strain rate relationships for each sample. This resulted in very heterogeneous strain rates below 10 MPa, which can be up to six orders of magnitude lower compared to the creep of pure halite.

There, the intensity of strain rate reduction notably depends on the volume fractions of the multi-phase aggregate. Generally visible trends suggest that decreasing halite matrix contents and increasing non-matrix content (halite mega grains and anhydrites) cause stronger deflections from pure halite creep behaviour.

The results show that if the volume fraction of the halite matrix is above 80%, the creep properties of the halite matrix dominate the overall creep behaviour of the rock salt multi-phase aggregate. At halite matrix volume fractions below 80%, non-matrix phases (mega-grains and anhydrite) have a significant effect on creep behaviour at low stresses (1-3 orders of magnitude).

Machine-learning-assisted categorization of individual creep relations suggests that deviations in creep rate is strongest when non-matrix phases (mostly halite mega grains) form a skeleton-like structure throughout the entire model domain (2x2 meters). These structures stabilize the deformed samples, resulting in strain rates that converge toward pure dislocation creep because the mostly unconnected pockets of halite matrix cannot propagate the strain throughout the sample. It is likely that this behaviour occurs if the halite volume fraction is below 40%.

Furthermore, we established a general empirical constitutive law that parametrizes the strain rate of KB rock salt, based on the applied stress, known halite creep properties and its volume fraction. In the expected stress range and for the expected halite matrix volume fractions of natural salt domes, it can predict our synthetic dataset with an uncertainty of 20 %.

It is important to note that this only reflects the average creep behaviour of expert-knowledge curated but statistically derived KB rock salt models. The geometries of naturally occurring KB rock salt are, of course, more complex than the simplified statistical models generated in this study. Mapping the site-specific KB rock salt geometries, extrapolating these to representative scales and determining their creep behaviour is a highly interesting task for future studies.

However, the results and conclusions drawn in this study provide the basis to integrate creep of a highly heterogeneous multi-phase salt formation into dome-scale simulations, ultimately assisting risk assessments of underground hydrogen storage in salt caverns.

4 Durability: Microstructural analyses of geochemical and microbial processes

Author: Joyce Schmatz – MaP – Microstructures and Pores GmbH

Disclaimer: The research described here has been conducted with generous support from the laboratories for petrophysics, microbiology, and cement chemistry at RWTH Aachen University. We extend our appreciation to the following individuals: Dr. G. Gaus and S. Khajooie, MSc. from the Institute for Geology and Geochemistry of Petroleum and Coal; Dr. H. Ballerstedt from the Chair of Applied Microbiology; and Dr. F. Georget from the Institute of Building Materials Research - Construction Materials.

4.1 Introduction

Hydrogen (H_2) is widely recognized as a highly reactive gas that serves as an energy source for numerous microorganisms. When exposed to aqueous sulphate, these microorganisms engage in bacterial sulphate reduction, a process that typically occurs within thermal regimes ranging from 0 to approximately 60-80°C (Machel, 2001). It is worth noting that sulphate is consistently present in salt formations to varying degrees, encompassing both anhydrite/polyhalite layers located adjacent to cavern walls and the insoluble sediment and brine sump, which can accumulate in substantial thicknesses at the cavern's base (Bérest and Brouard, 2003; Schwab et al., 2022).

Hydrogen gas becomes dissolved in the brine, and this dissolution occurs relatively rapidly due to the natural convection-driven stirring of the brine. Consequently, hydrogen sulphide (H_2S) can form, potentially interacting with the surrounding rock salt and second phase lithologies and thereby altering the composition of the stored gas. Of particular significance in this context are the extent, geometry, and physical attributes, particularly porosity (inclusive of fractures), as well as the connectivity and permeability of the insoluble or low-soluble layers. These characteristics play a critical role as they influence the surface area accessible to microorganisms, which in turn affects the formation of H_2S, among other contributing factors.

Furthermore, it is worth noting that there has been a limited number of studies to date that employ microstructural analyses to investigate the characteristics and impacts of various biotic and abiotic processes on Thermal-Hydrological-Mechanical-Chemical (THMC) properties and, consequently, on the integrity of storage media, including both rocks and casings (e.g., Flesch et al., 2018; Gloc et al., 2018). However, insights gained from research in the context of spatial-chemical relationships within porous media have highlighted the essential role of such analyses in enhancing our understanding and description of the processes governing reaction kinetics (e.g., Higgs et al., 2022; Jangda et al., 2022).

Modern analytical techniques, such as cryo-Scanning Electron Microscopy or µ- or nano-Computer Tomography, offer the capability to visualize these processes both ex-situ and in-situ during laboratory tests. These advanced methods hold the potential to provide valuable insights, enabling us to better constrain the processes that control rates during subsurface storage. This is particularly relevant concerning the rock phases involved, notably porous anhydrite, as well as casing materials like cement and steel (e.g., Bensing et al., 2022; Pötschke et al., 2022; Schmatz et al., 2015; Viani et al., 2019; Wetzel et al., 2021; Zingg et al., 2008).

Although a number of studies have been carried out, especially in recent years (e.g., Hemme and Van Berk, 2018), to evaluate the chemical-physical influences of hydrogen storage in underground salt caverns, many questions remain unresolved. Because of the lack of reliable data on the effect of hydrogen on permeability and mechanical integrity in the critical lithologies, such as anhydrites, sump sediments, or the casing cements, as well as information on the kinetics of abiotic geochemical and microbial

reactions in the corresponding pore fluids, predictions on the long-term behaviour of geological hydrogen storage are only possible to a limited extent.

4.2 Microbial induced microstructural changes anhydrite

Knowledge about the volumetric extent and kinetics of the reactions is essential and experimental work together with microstructural analyses is required to determine the input parameters for the geochemical models on the different reaction kinetics. Following Phase 1 findings, we conducted an experimental study on the kinetics of biotic and abiotic reactions involving H_2, CO_2, and H_2S with anhydrite. We considered factors such as the bacterial growth and reduction rate, the pressure and temperature, and in particular the variable composition of natural anhydrite, with the goal of visualizing the known but also the unknown processes occurring, which may affect the mechanical integrity of salt cavern during hydrogen storage at various scales, by microstructural analyses.

While it is challenging to constrain these reactions in laboratory experiments due to relatively slow rates, microstructural investigations enabled the visualisation of the onset of biological, chemical and structural changes in the sample material down to the submicron pore scale. This offers a foundation for upscaling these processes and assessing preventing measures, if required. Knowledge gained from these experiments and the literature review, shall outline the physical-biological-chemical processes and impacts that require further research to limit the potential risks of mechanical instabilities of the critical lithologies during hydrogen storage in salt caverns from a geochemical perspective.

In the first step the sample material, comprising different types of natural formed anhydrite originating from the ISH 1 well (Haaksbergen[1]) in the Netherlands was investigated using a range of established microanalytical techniques and methods enabling assessing the microstructure, pore space and mineralogy at high resolution and accuracy (e.g., Jiang et al., 2022; Klaver et al., 2015). Due to their inherently low porosity, the samples were artificially fractured to enhance surface area prior to placing them in a low-pressure reactor. These laboratory experiments were conducted and designed in collaboration with the H2_ReacT (Ostertag-Henning et al., 2021) team at the RWTH Aachen University, led by Dr. G. Gaus and S. Khajooie, MSc.. The bulk measurements were designed in a way, that they allow assessing microbial activity via mass spectrometry and pressure monitoring. After completion of the experiment, the presence of microorganisms, alterations in pore space due to biofilm formation as well as the mineralogical changes in the solid phases were investigated ex-situ by means of scanning electron microscopy on the fractured sample surfaces as well as on cross-sections polished with a Broad-Ion-Beam (Pötschke et al., 2022; Schmatz et al., 2015).

4.2.1 Problem statement microstructural changes anhydrite

Anhydrite plays an important role in the context of hydrogen storage within salt caverns for two primary reasons:

1. It is frequently found in layered structures, as fragments of layers, and constitutes a significant portion of the cavern's sump.
2. It serves as a source of sulphate anions (SO_4^{2-}). Under aqueous conditions, bacterial sulphate reduction leads to the formation of hydrogen sulphide (H_2S).

The overall bacterial sulphate reduction reaction can be simplified expressed as follows:

$$SO_4^{2-} + \text{Organic Electron Donor} \rightarrow H_2S + H_2O + \text{Organic Products} \quad (1)$$

[1] The sample selection was based on the availability of sample material from the Haaksbergen borehole. It is pointed out that this is not related to a potential H2 storage in the Haaksbergen formation.

In this reaction, sulphate (SO_4^{2-}) is reduced to hydrogen sulphide (H_2S), generating water (H_2O) and various organic by-products.

Moreover, also when bacterial sulphate reduction is absent and anhydrite layers are exposed to the cavern wall during hydrogen storage, there are additional considerations. This is particularly relevant as the storage conditions, including pressure cycling, may result in wet cavern walls. Anhydrite is soluble in water, and the hydration of anhydrite to gypsum is primarily driven by the introduction of water. The key chemical reactions involved are as follows:

When anhydrite comes into contact with water, it partially dissolves to form calcium ions (Ca^{2+}) and sulphate ions (SO_4^{2-}).

$$CaSO_4(s) + 2H_2O(l) \rightarrow Ca^{2+}(aq) + SO_4^{2-}(aq) + 2H_2O(l) \quad (2)$$

Subsequently, calcium ions and sulphate ions combine with water molecules to produce gypsum as a crystalline solid.

$$Ca^{2+}(aq) + SO_4^{2-}(aq) + 2H_2O(l) \rightarrow CaSO_4 \cdot 2H_2O(s) \quad (3)$$

Several factors influence the hydration process, including temperature, pressure, water availability, accessible surface area, and site-specific boundary conditions such as depth, temperature, and expected pressures. The associated volume change resulting from hydration has implications for the mechanical properties and is dependent on initial anhydrite characteristics, such as grain size, impurity content, and accessible pore space. The presence of porosity in anhydrite influences the hydrogeological behaviour of salt formations, affecting fluid migration, storage capacity, and overall salt repository stability. Understanding these factors is vital for geological assessments and industrial processes involving salt formations.

4.2.2 Materials and Methods anhydrite

4.2.2.1 Origin Anhydrite samples

The anhydrite samples origin from core material from the ISH-01 well of the Haaksbergen salt pillow. The anhydrite layers vary in thickness and distribution within the salt formation. Three samples were derived from core pieces originating from different depths: HK02 at 661 m, HK31 at 936 m, and HK40 at 974 m. HK02 and HK31 represent rather thin lamellae (layer thickness < 5 cm) within salt, while HK40 originates from a meter's thick layer of bulk anhydrite.

4.2.2.2 Bacteria

We used the microorganism Desulfovibrio Desulfuricans, obtained from the Leibniz Insitute DSMZ-German Collection of Microorganisms and Cell Cultures GmbH. This species of anaerobic sulphate-reducing bacteria (SRB) commonly found in various environments, including saline environments, and they adapt to a range of temperatures, although it is typically moderate temperature conditions between 20°C and 40°C. These bacteria are known for their ability to reduce sulphate ions ($SO4^{2-}$) to hydrogen sulphide (H_2S) as part of their metabolic processes. This specific SRB was chosen for the investigation because it has previously been utilized as a model organism for researching sulphate reduction and the

formation of carbonate minerals in freshwater and seawater (e.g., Atlas et al., 1988; Bosak and Newman, 2005, 2003; Han et al., 2016).

4.2.2.3 Sample preparation protocols

Our study comprises four different experimental setups allowing to iteratively study the chemical and microbial alteration of anhydrite in the presence of brine, brine and Desulfovibrio Desulfuricans, and brine and Desulfovibrio Desulfuricans in the presence of molecular hydrogen and carbon dioxide (Figure 317). Initially, a hydration test was performed to investigate potential hydration effects on the microstructure of anhydrite. The aim was to identify a representative microstructure resembling that of a gas cavern wall formed by solution mining. This "baseline" microstructure was then compared to changes observed after exposure to Desulfovibrio Desulfuricansand molecular hydrogen as well as carbon dioxide.

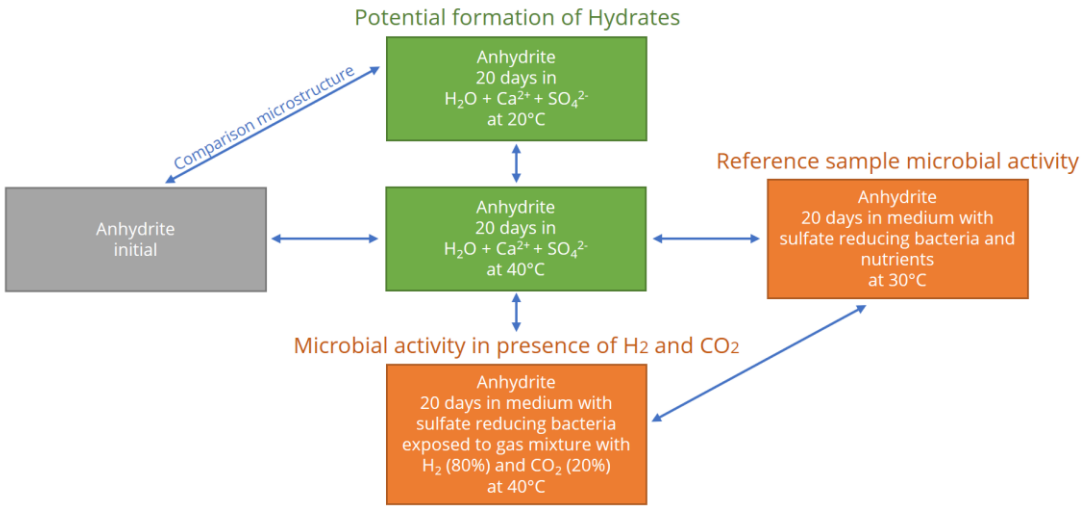

Figure 317 Overview experimental study microbial and chemical processes Anhydrite

4.2.2.4 Preparation initial samples

Due to the low permeability of the anhydrite/polyhalite samples, artificial fracturing was performed on them before assembly, prior to conducting the experiments, in order to increase the surface area. Additionally, a Broad-Ion-Beam (BIB) cross-section was prepared to facilitate the study of the microstructure within a 1 mm depth profile perpendicular to the fractured surface (Figure 318).

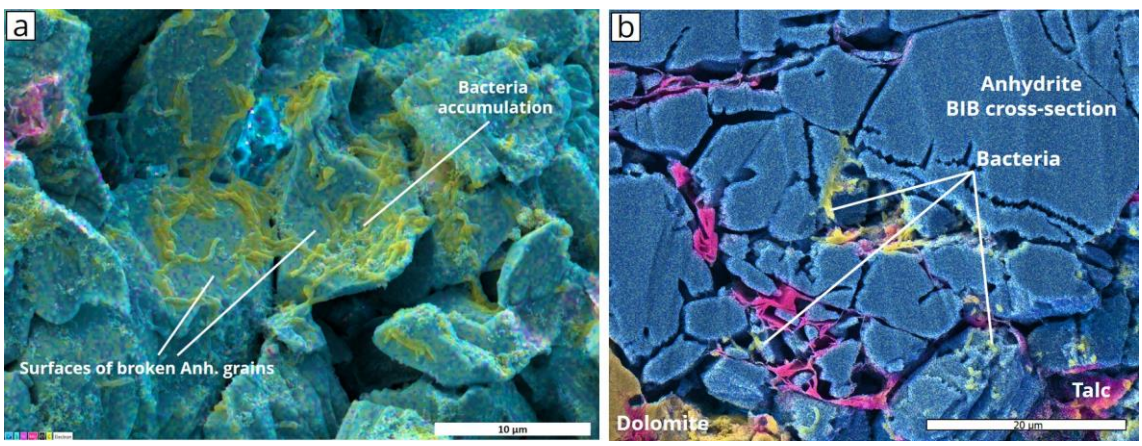

Figure 318 Microstructures were studied using SEM/EDS images of broken sample surfaces (a) together with SEM/EDS images of BIB cross-sections prepared perpendicular to the broken surface (b). In both setups allowed assessing the mineral composition together with the distribution of the microbes.

4.2.2.5 Preparation samples for hydration pre-test

The hydration experiment was conducted on all three anhydrite samples under ambient temperatures of 20°C and 40°C, respectively. To prevent anhydrite dissolution during the hydration test, the samples were submerged in brine saturated with Ca^{2+} and $SO4^{2-}$ ions for a period of 20 days. The pH of the brine was maintained at 6 throughout the experiment. Afterward, the samples were oven dried at 80°C for a duration of 3 days.

4.2.2.6 Experimental protocol microbial treatment

4.2.2.6.1 Reference samples

To investigate the influence of H_2 and CO_2, in conjunction with microbial activity on the microstructure, reference samples were prepared using the following procedure: Anhydrite pieces with one fractured surface were exposed to a brine solution containing a brine (growth medium A) comprising K_2HPO_4 (0.5 g), NH_4Cl (1.0 g), Na_2SO_4 (1.0 g), CaCl x $2H_2O$ (0.1 g), $MgSO_4$ x 7 H_2O (2.0 g), Na-DL-lactate (2.0 g), Yeast extract (1.0 g), Sodium resazurin (0.1% w/v, 0.5 g), and distilled water (980.0 g). These samples were then inoculated with microbes and kept at an optimal temperature of 30°C and under anaerobic conditions for a duration of 20 days. The lactate serves as an electron donor for sulphate reduction as a carbon source for growth of the microorganisms, however, both acetate and dissolved inorganic carbon are also required as carbon source when hydrogen serves as an electron donor for sulphate reduction (e.g., Li et al., 2009).

Following this incubation period, the samples were prepared for electron microscopy, adhering closely to the protocol proposed by Murtey et al. (2016) to ensure that the bacteria and biofilm were fixed in a manner that would preserve their integrity under high vacuum conditions and electron/ion bombardment throughout the BIB milling and the SEM investigation (Figure 318).

4.2.2.6.2 Samples exposed to SRB, H_2, and CO_2

We conducted an experimental investigation to assess the microbial activity of sulphate-reducing bacteria on anhydrite samples in the presence of H_2 and CO_2. The experimental setup included the three different fractured anhydrite samples, one sample of Bentheimer sandstone, and one bulk solution sample, all placed in individual low-pressure reactors, which were subsequently evacuated. We then introduced 20 ml of brine (growth medium B) into each bottle. The growth medium B employed for these experiments closely resembled the composition detailed in the previous section for the reference samples, with the exception that Na-DL-lactate was replaced by 5mM Na-Acetate. Furthermore, we adjusted the pH to 7.2 in the presence of N_2/CO_2 (80/20) by introducing crystalline $NaHCO_3$. Additionally, we injected 5 ml of bacteria into each reactor. We pressurized the reactors with approximately 2 bar (closed system) and monitored pressure decline with pressure transmitters and gas composition with mass spectroscopy.

4.2.2.7 SEM sample preparation

4.2.2.7.1 BIB cross-section

Broad Ion Beam milling (BIB, e.g., Klaver et al., 2015) is a preparation technique (Figure 319), which allows preparing smooth and dust-free sample surfaces, by removing some of the mechanical damage using Argon-ion sputtering. This way we are able to image microstructures using SEM that could be hidden or misinterpreted because of the mechanical damage caused by cutting and grinding. From the sub-samples, up to 100 µm of material was removed by using the JEOL BIB cross-section polisher (SM 09010). A titanium mask is put on the top of the sample, leaving about 100 µm of material uncovered which will be bombarded with Argon ions. The sample is oscillating during the ion milling to prevent curtaining of the polished section. Typically, the JEOL cross-section polisher produces a pseudo-Gaussian shaped polished surfaces covering an area of 1-2 mm^2 when operating for 8 hours at 6 kV and 150 µA. The BIB cross-section is a flat, planar surface with a minimum relief of +/- 5 nm over 1 μm^2.

All samples were BIB cross-sectioned perpendicular to the fractured surface in order to study the porosity (Klaver et al., 2015) and the mineral phase distribution (Jiang et al., 2022; Schmatz et al., 2022, 2017).

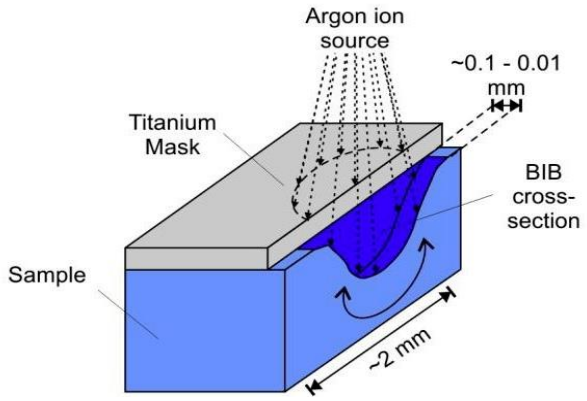

Figure 319. Sketch of BIB cross-section polishing in the JEOL BIB.

4.2.2.8 SEM imaging

Fractures surfaces and BIB cross sections of all samples were imaged using Scanning Electron Microscopy (SEM) using the Secondary Electron (SE2), Backscattered Electron (BSE), and Energy Dispersive Spectroscopy (EDS) detectors at 8-10 kV acceleration voltage simultaneously. For SE2/BSE the image dimension were 8192 x 6656 pixels with pixel resolutions of 7, 33, and 133 nm, covering areas of up to approximately 1mm^2. EDS maps were recorded at energy range of 10 keV with a pixel dwell time of 600 µs.

4.2.2.9 Image Analysis

To assess porosity, pore size distribution (PSD), and mineral phase distribution, we utilized a semi-automated image analysis approach on SEM/EDS image data obtained from the BIB cross-sections.

For pore space analysis, SE2 images with a pixel resolution of 133 nm were employed in conjunction with a trained AI model, as detailed by (Klaver et al., 2021). This AI model is structured based on a U-Net architecture and was continually enhanced through manual correction of the resulting pore segmentations, with the refined data being incorporated back into the AI model. A pixel size threshold for the practical pore resolution (Klaver et al., 2015) was set at 300nm.

We achieved precise pixel-level segmentation of distinct mineral phases through the application of superpixel algorithms, as demonstrated by Stutz et al. (2018) Yu et al. (2023), which were applied to both BSE images and EDS element maps. The automated labelling of mineral phases within the respective superpixels was executed using a customizable decision tree. This decision tree took into consideration the elemental composition of the mineral phases, as outlined by Jiang et al. (2022) and Schmatz et al. (2022). Furthermore, the decision tree was fine-tuned to accommodate the anticipated mineral phases present in the sample material and was calibrated through X-ray diffraction analysis.

4.2.3 Results and Discussion anhydrite

4.2.3.1 Composition and Microstructure initial samples

Based on the composition and fabric we distinguish three types of anhydrite (Figure 320):

Sample HK_02, classified as Type 1 anhydrite, exhibits a high degree of purity, featuring fine-grained, uniformly sized anhydrite crystals. Notably, spherical inclusions of dolomite or magnesite, measuring between 30 and 40 µm in diameter, sporadically dot the sample. The grain boundaries are tightly-packed, occasionally hosting small talc inclusions either along the grain boundaries or at grain triple junctions. When sawing and breaking the samples, a strong smell of hydrocarbons was detected. The porosity primarily comprises intergranular pore spaces, constituting 0.22% of the total area (Table 34). The pore

size distribution (PSD, Table 35, Figure 321) follows a log-normal pattern with a slight positive skew, revealing a median equivalent pore diameter of 368 nm.

Sample HK_31 (Type 2 anhydrite), displays a coarse-grained texture with significant porous talc regions located in between the anhydrite grains, while maintaining tight grain boundaries. Additionally, there are minor dolomite/magnesite inclusions present in the material. This sample type, different to the others, contains Sodium Chloride (NaCl) inclusions with sizes of up to 200µm (equivalent diameter). The primary porosity is found within the intergranular pore spaces within the talc inclusions, contributing to a total porosity of 0.38% of the area (Table 34). The PSD (Table 35, Figure 321), akin to Type 1, exhibits a log-normal distribution with a slight positive skew, with a median equivalent pore diameter of 424 nm.

Sample HK_40 (Type 3 anhydrite), has a coarse-grained texture, featuring an abundance of dolomite/magnesite inclusions with diameters ranging from 30 to 40 µm. The grain boundaries in this sample are tightly bound, with sporadic talc inclusions primarily located at grain triple junctions. The total porosity of this sample is relatively low, standing at 0.05% of the total area (Table 34), predominantly attributed to intergranular pore space within the dolomite/magnesite inclusions. The PSD (Table 35, Figure 321) follows a log-normal distribution with a slight positive skew, with a median equivalent pore diameter of 564 nm.

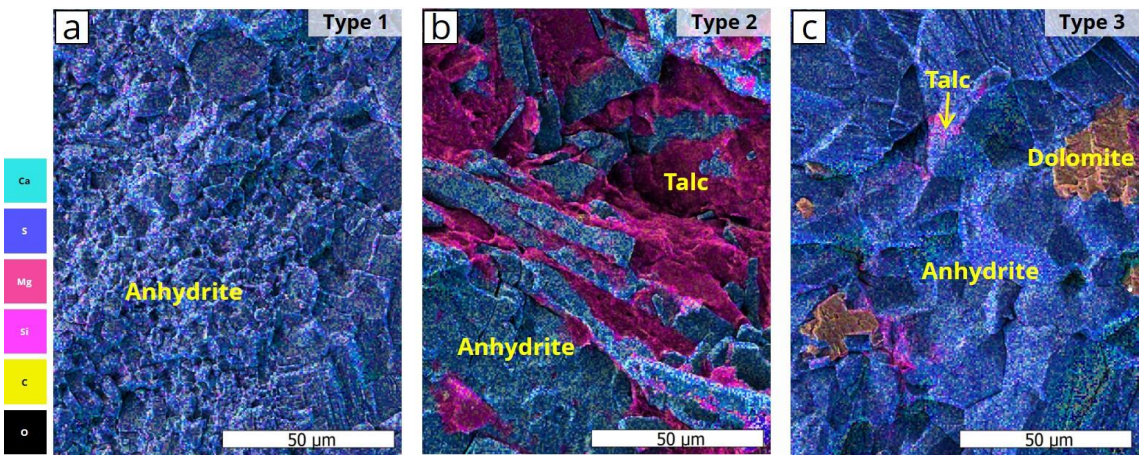

Figure 320. SE2/EDS micrographs showing the three different types of anhydrite used for the study: a) Type 1: predominantly pure, fine-grained Anhydrite, b) Type 2: coarse-grained Anhydrite containing a significant amount of Talc along the grain boundaries, c) Type 3: coarse-grained texture, featuring an abundance of dolomite/magnesite inclusions.

Table 34. Total porosity and mineral phase distribution segmented from SE2 micrographs of the BIB cross-sections.

		Total Porosity area [%]	Anhydrite area [%]	Calcium carbonate area [%]	Dolomite/Magnesite area [%]	Talc area [%]	Unknown area [%]	Sodium chlorite area [%]
Type 1	**initial**	0.22	97.00	0.00	0.00	1.00	1.00	0.00
	Brine, 20°C	0.10	96.00	0.00	2.00	1.00	1.00	0.00
	Brine, 40°C	0.25	90.00	1.00	5.00	3.00	0.00	0.00
	Medium, microbes, H2, CO2, close to surface	2.06	64.00	29.00	1.00	5.00	0.00	0.00
	Medium, microbes, H2, CO2		60.00	34.00	0.00	5.00	1.00	0.00
Type 2	**initial**	0.38	84.00	0.00	0.00	1.00	10.00	5.00
	Brine, 20°C	1.98	84.00	1.00	0.00	13.00	3.00	0.00
	Brine, 40°C	1.01	81.00	1.00	1.00	14.00	2.00	0.00
	Medium, microbes, H2, CO2		60.00	15.00	1.00	20.00	4.00	0.00
	Medium, microbes, H2, CO2, close to surface	2.82	71.00	12.00	0.00	9.00	8.00	0.00
Type 3	**initial**	0.05	96.00	0.00	2.00	1.00	0.00	0.00
	Brine, 20°C	6.18	96.00	0.00	2.00	1.00	1.00	0.00
	Brine, 40°C	2.26	95.00	0.00	2.00	2.00	0.00	0.00
	Medium, microbes, H2, CO2, close to surface	5.64	79.00	4.00	1.00	10.00	6.00	0.00
	Medium, microbes, H2, CO2		65.00	17.00	8.00	9.00	1.00	0.00

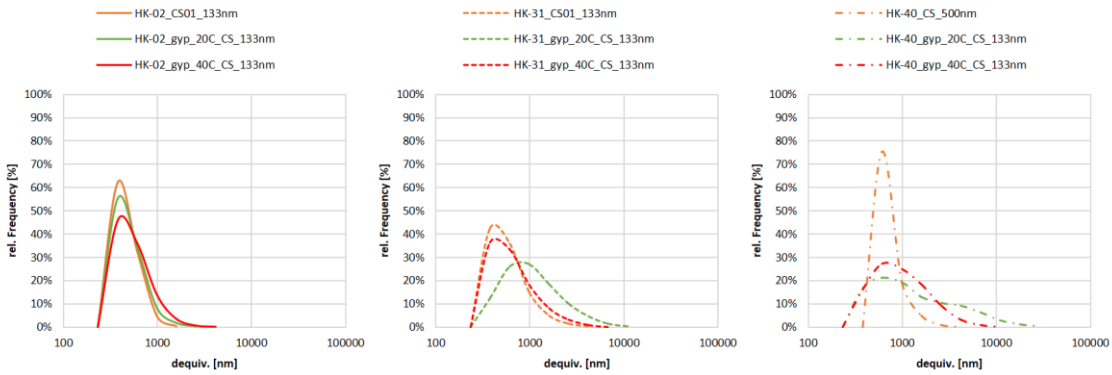

Figure 321. Histograms showing PSD of the initial samples, samples treated with brine at 20°C, and samples treated with brine at 40°C, distinguishing from left to right the three different types of anhydrites.

Table 35. Pore size statistics

	Type 1				Type 2				Type 3			
Sample	**initial**	**Brine, 20°C**	**Brine, 40°C**	**Medium, microbes, H_2, CO_2**	**initial**	**Brine, 20°C**	**Brine, 40°C**	**Medium, microbes, H_2, CO_2**	**initial**	**Brine, 20°C**	**Brine, 40°C**	**Medium, microbes, H_2, CO_2**
BIB cross-section	*HK-02_CS_133nm*	*HK-02_gyp_20C_CS_133nm*	*HK-02_gyp_40C_CS_133nm*	*HK-02_bac_H2_CS_133nm*	*HK-31_CS01_133nm*	*HK-31_gyp_20C_CS_133nm*	*HK-31_gyp_40C_CS_133nm*	*HK-31_bac_H2_CS_133nm*	*HK-40_CS_500nm*	*HK-40_gyp_20C_CS_133nm*	*HK-40_gyp_40C_CS_133nm*	*HK-40_bac_H2_CS_66nm*
Number	10901	3378	6937	43661	7078	12022	15611	11534	783	3427	6502	9066
Average $d_{equiv.}$ [nm]	391	427	477	618	520	1051	614	1091	663	1764	953	996
Std. Error $d_{equiv.}$ [nm]	1	3	3	2	4	9	4	13	8	40	10	10
Median $d_{equiv.}$ [nm]	368	368	397	475	424	735	450	654	564	808	688	653
Mode $d_{equiv.}$ [nm]	300	300	300	300	300	300	300	300	564	300	300	307
Std. Dev. $d_{equiv.}$ [nm]	123	185	238	446	329	955	485	1347	214	2348	844	930
Minimum $d_{equiv.}$ [nm]	300	300	300	300	300	300	300	300	564	300	300	307
Maximum $d_{equiv.}$ [nm]	4156	2236	3526	7866	5067	12470	9427	30467	2257	26117	12178	11469

4.2.3.2 Formation of secondary porosity due to anhydrite hydration and the mobilisation of fines

The result of the hydration test is shown in Figure 322. SEM imaging using secondary electrons allows studying the morphology of the anhydrite grains exposed to the fractured surfaces, which was used to identify morphological changes of the grains as result of the exposure to brine. In result, for all three sample types, there were no changes in the grain morphology for the experiments conducted at 40°C when compared to the fractured surfaces of the initial samples, while a few grains show disaggregation to porous aggregates composed of fibrous to prismatic grains, indicating hydration processes to gypsum for the experiments conducted at 20°C. Experimental data of previous work (e.g., Hardie, 1967; MacDonald, 1953) suggests that in a saline environment and at ambient pressures the hydration of anhydrite is unlikely at temperatures above 40°C. Measurements on the total porosity (Table 34) show only minor changes comparing the initial state (porosity is 0.2 area%) with the result of the hydration tests at 20°C (0.1 area%) and 40°C (0.3 area%), respectively, regarding the rather pure anhydrite sample type 1. For the rather impure anhydrite types 2 and 3, however, the total porosity changes after the

exposure to brine (Table 34) from initially <0.5 area% to up to 6.2 area% (Type 3, Brine, 40°C), which is thought to be related to the mobilisation of fines (talc), rather than to the formation of hydrates: from the SEM micrographs of the BIB cross-sections (Figure 323) we can distinguish the different mineral phases and pore space in a plane without morphology effects. This allows determining that new pore space formed after the exposure to brine in between the anhydrite grains at locations where also porous talc is present. At the interface of the anhydrite with talc these interfaces are often apertured, especially within anhydrite grain triple junctions. Next to the mobilisation of the talc, dissolution of anhydrite could be responsible for this feature. However, the fact that the brine was saturated with $SO4^{2-}$ and Ca^{2+} ions together with the observation that the anhydrite grain surfaces (Figure 322) of the initial samples are very similar to the samples that were exposed to brine, which show no dissolution structures, oppose this hypothesis.

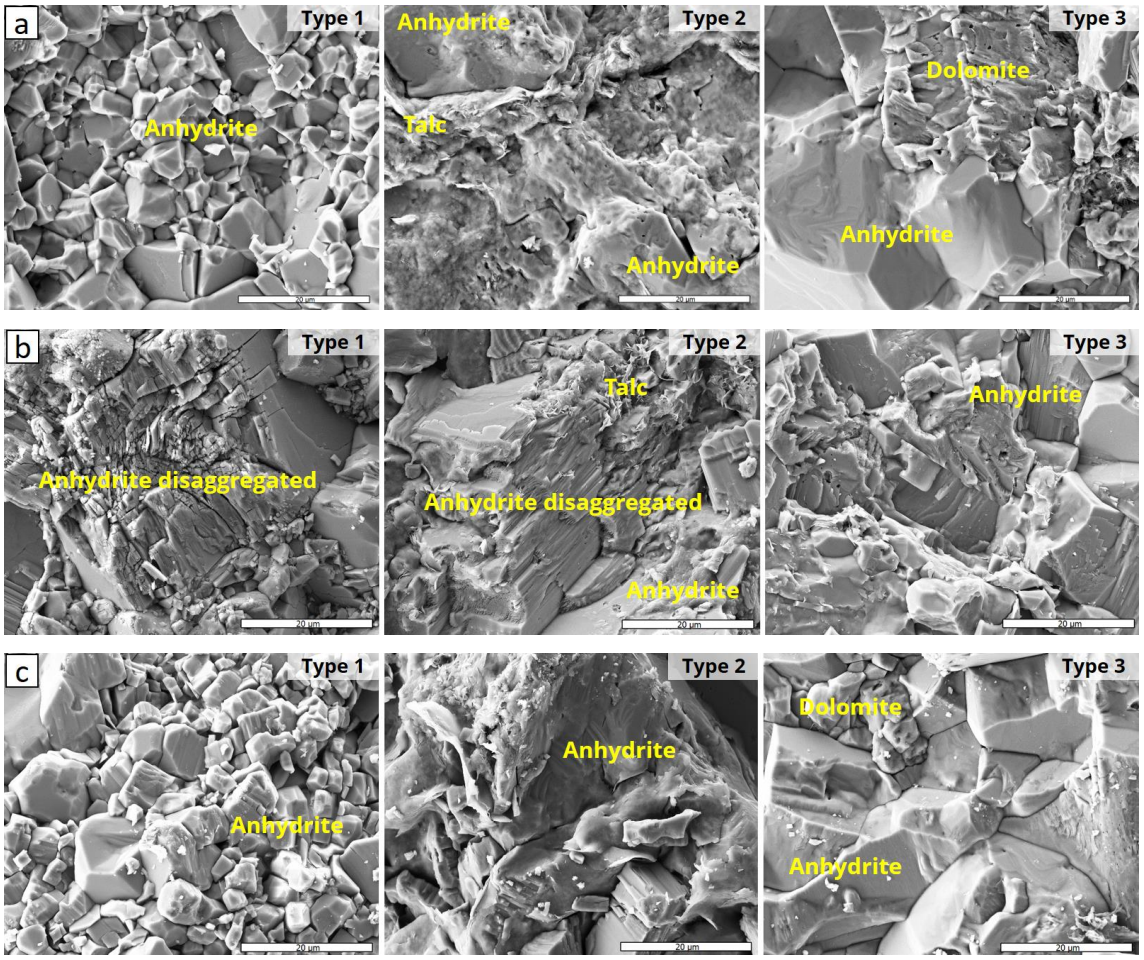

Figure 322. SE2 micrographs showing broken surfaces of the three anhydrite samples a) at the initial state, b) after exposure to brine saturated with $SO4^{-2}$(aq.) and Ca^{2+} (aq.) for 20 days at 20°C, and c) after exposure to brine saturated with SO4-2(aq.) and Ca2+ (aq.) for 20 days at 40°C. Formation of gypsum, shown in form of disaggregated anhydrite was mainly observed in Type 1 and Type 2 anhydrite exposed to the brine at 20°C.

4.2.3.3 Microstructural processes in presence of SRB, H_2 and CO_2

The three different anhydrite samples were individually subjected to SRB exposure, immersed in growth medium B, and exposed to a gas mixture of H_2 and CO_2 in a batch reactor. In such a complex, multi-component system, numerous interconnected chemical and microbiological processes are anticipated to unfold. To enhance the understanding of the results obtained from bulk measurements, which depict the evolution of pressure and gas composition over time (as shown in Figure 323 and Figure 324), post-mortem microstructural analysis was employed. The findings and interpretations of both bulk and microanalytical measurements are detailed in the subsequent sections.

As illustrated in Figure 323a, the pressure declines within the reactor, attributed to microbial activity (e.g., Khajooie et al., 2023; Strobel et al., 2023), predominantly characterizes the initial phase of the experiment. Consequently, elevated microbial activity can be associated with the first 80 hours of the experiment in anhydrite types 1 and 2. Beyond this point, a rise in pressure was detected in the reactor containing anhydrite type 1. In the reactor housing anhydrite type 2, another significant pressure drop occurred around the 150-hour mark. Conversely, in the reactor with anhydrite type 3, a substantial pressure drop was observed within the initial 20 hours. Subsequently, the pressure decreased at a very gradual rate, suggesting minimal microbial activity. In both, the anhydrite type 2 and type 3 reactors, a near-steady-state pressure level was achieved at approximately 360 hours.

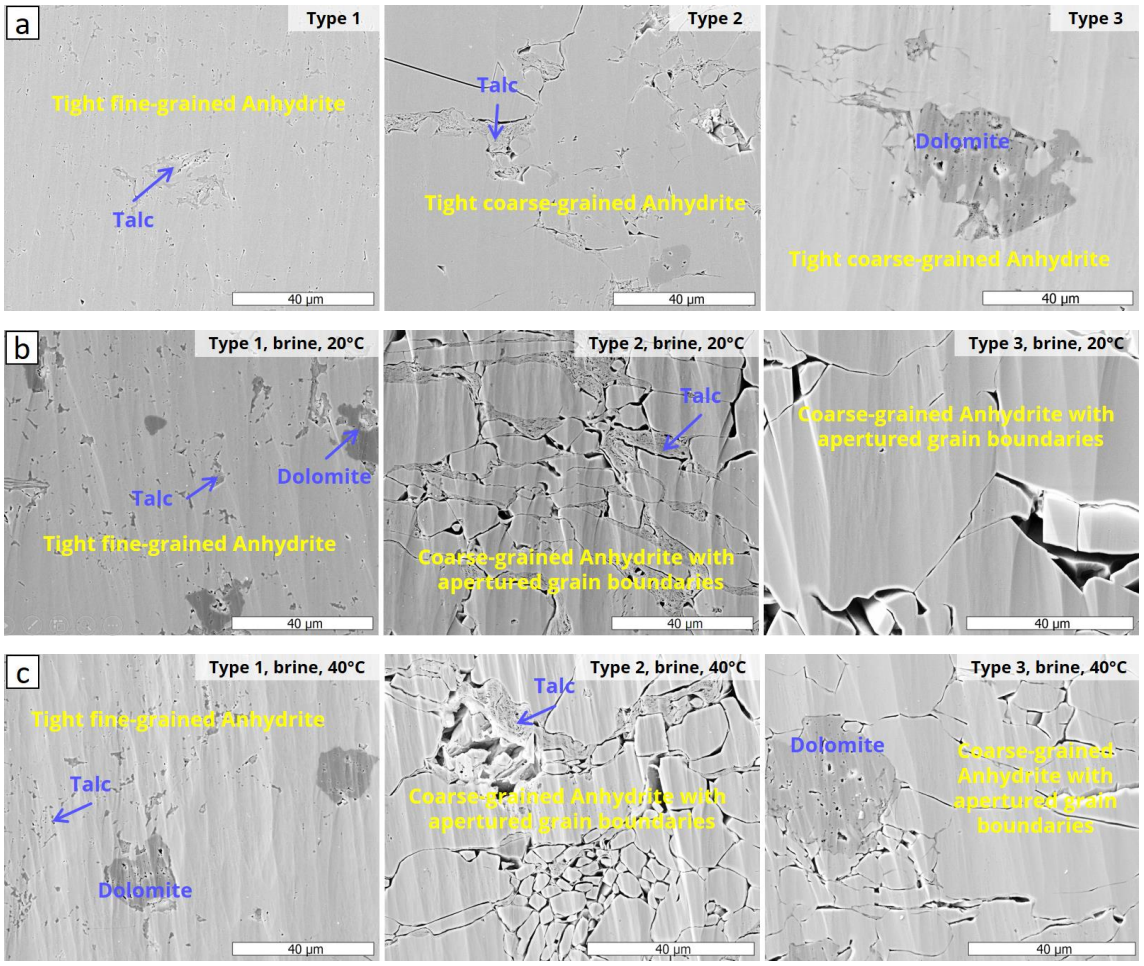

Figure 323. SE2 micrographs of BIB cross-sections of the three anhydrite samples a) at the initial state, b) after exposure to brine saturated with SO4-2(aq.) and Ca2+ (aq.) for 20 days at 20°C, and c) after exposure to brine saturated with SO4-2(aq.) and Ca2+ (aq.) for 20 days at 40°C, show illustrate the changes of microstructure after the sample exposure to the brine. Apertured grain boundaries were observed in Type 2 and Type 3 anhydrite.

Examining the temporal progression within the reactors (Figure 324 and Figure 325), it is discernible that the dissolution of CO2 occurs relatively rapidly within the initial < 2 hours, with the exception of anhydrite sample type 1 (HK02). Due to incomplete CO2 dissolution in this case, there is a corresponding reduction in the fraction of H2. Notably, sample HK02 exhibited an elevated level of CH4, substantiating the potential presence of natural hydrocarbons in this sample type.

The concentration of H2S in all samples remains below 0.1%, and an overall increasing trend is observed, ranging from 0.02% to 0.08% over the course of the testing period for all samples considered. The H2S values fall within the range of 100 to 1000 ppm, with concentrations of H2S at 100 ppm being regarded as immediately dangerous to life or health. Notably, in HK40 (Type 3 anhydrite), no H2S was generated. The highest concentrations of H2S are anticipated in the Bentheim sandstone, approaching 0.1%. The

consumption of H_2 and the corresponding production of H_2S in the reactor housing Type 2 anhydrite are notably subdued. Notably, Type 2 anhydrite is the only type that contains NaCl as a secondary phase. The presence of NaCl in the environment possesses the potential to exert an influence on microbial H_2S production due to its capacity to affect the growth and metabolic activity of these microorganisms, as elucidated by Martinez et al. (2023).

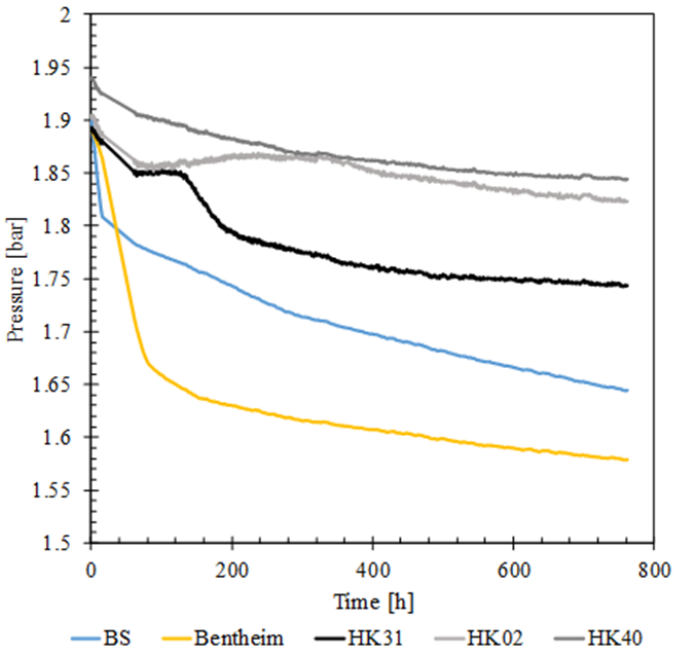

Figure 324. Diagrams showing the pressure monitored throughout the experiments for the bulk solution (BS) as reference, for Bentheimer sandstone as reference containing no sulphates, and for the type 1 (HK02), type 2 (HK31), and type 3 (HK40) anhydrite.

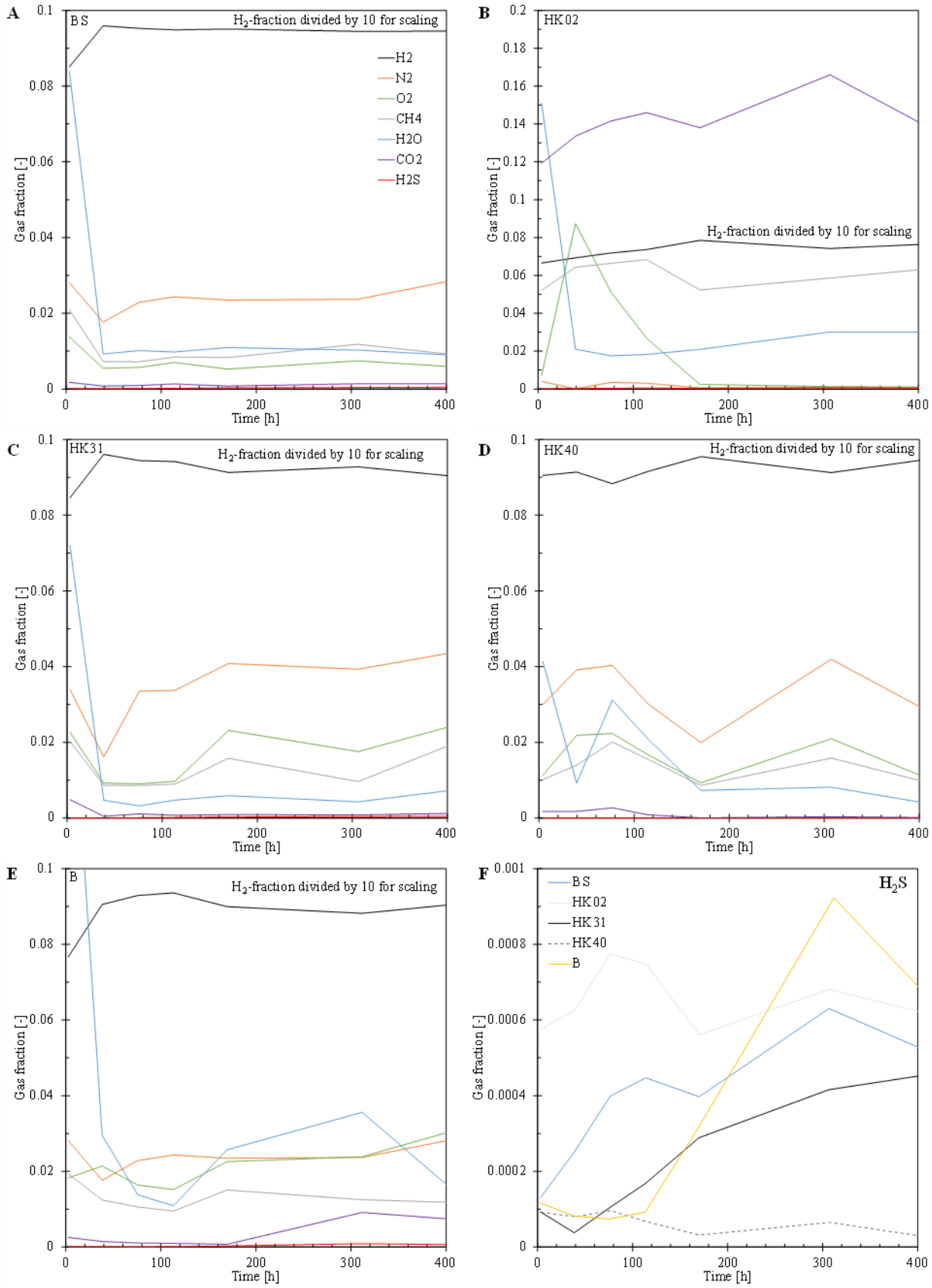

Figure 325. Diagrams showing the fractions of H_2, CO_2, N_2, O_2, CH_4, H_2O and H_2S monitored throughout the experiments for a) the bulk solution, b) anhydrite type 1 (HK02), c) type 2 (HK31), d) anhydrite type 3 (HK40) and e) Bentheim sandstone. H_2S generation as a function of time is shown for all samples in f).

4.2.3.3.1 Induced formation of mineral phases and biofilm

SEM/EDS examinations of fractured surfaces reveal the presence of biofilm formations on the mineral surfaces, as illustrated in Figure 326, Figure 327, and Figure 328. These biofilm accumulations are evident across all anhydrite samples. Interestingly, they exhibit no discernible preference for specific types of surfaces, such as particular mineral phases or surface roughness variations. The organisms manifest as individual bacterial bodies, typically measuring around 2 µm in length with a slight curvature, as well as clusters of bacterial bodies or as dense biofilm masses. However, regions covered by biofilm do not extend beyond areas larger than 30 µm x 30 µm. The thickness of the biofilm typically falls within the range of an individual bacterium's thickness, which is approximately 0.2 µm.

Redox reactions associated with respiration and growth of SRB can lead to mineral formation (Han et al., 2016 and authors therein). The formation of microbial induced dolomite is a common observation made for all three anhydrite types, visible as usually small (< 5µm in diameter), spherical crystals or crystal clusters, exposed on the fractured surfaces and occurring on all mineral surfaces that are present (Figure 326 and Figure 327). The occurrence in deeper levels inside the samples (BIB cross-sections) cannot be proven with the applied method because of the chemical similarities to the other mineral phases in combination with too low spatial resolution of the EDS. Microbial formation of dolomite is a process for instance occurring in sabkha environments induced by the microbial increase of pH and removal of SO_4, in which SO_4 is considered as an inhibitor for dolomite precipitation (Baker and Kastner, 1981; Bontognali, 2008; Vasconcelos and McKenzie, 1997).

The most prominent mineral phase formation observed encompasses the precipitation of calcium carbonate across all three sample variants. Notably, the anhydrite type 1 samples exhibited the highest quantities of calcium carbonate formation, both in terms of surface area and cross-sectional area. When studying the fractured surface of these samples, one can detect the development of columnar to prismatic aragonite structures (as shown in Figure 326), which extend to cover approximately 50% of the examined surface area, equivalent to about 0.5 cm^2. In contrast, sample type 3 also displayed columnar to prismatic aragonite (as illustrated in Figure 328), albeit in notably smaller proportions. Conversely, sample type 2 (Figure 327) sporadically displayed aragonite crystals on its surface.

These observations align impeccably with the findings detailed in Machel's (2001) study, as referenced below:

"By far the most common carbonate formed as a by-product of BSR (Bacterial Sulfate Reduction) is calcite, subordinately aragonite. In settings that have open void spaces, calcium carbonate often begins to form as acicular to columnar aragonite and/or calcite crystals (fig. 9) that later coalesce to larger masses. This type of carbonate, however, is volumetrically minor. Much more commonly, calcium carbonate replaces calcium , such that these two minerals are intimately intergrown with one another. At advanced stages of BSR, the calcium may be completely replaced by massive limestones up to the scale of entire outcrops (figs. 11 and 12), or larger."

Particular attention should be directed towards the concluding sentence in Marchel's (2001) statement, as a substantial-scale substitution of calcium sulphate with substantial limestone formations could conceivably induce significant alterations in the mechanical and transport characteristics of the original anhydrite layers.

Microstructural observations of the BIB cross-sections (Figure 329, Figure 330 and Figure 331) indicate that close to the surface, there is evidence of calcium carbonate precipitation occurring within the porous boundaries of anhydrite grains. In deeper layers, we observe the characteristic features of a mineral replacement process, as outlined by Putnis (2009). This process is marked by the gradual growth of $CaCO_3$ at the anhydrite solution interface. After conducting the experiments, it becomes apparent that the $CaCO_3$ rim, which has developed along the periphery of anhydrite grains, exhibits a maximum thickness in the

order of 0.5-1 µm. In the case of anhydrite type 1, characterized by a relatively pure anhydrite sample, the anhydrite cores, in conjunction with the $CaCO_3$ rims, have contributed to the formation of a dense, compact rock structure across all levels of the BIB cross-section. In the experiment a relatively high CO_2 concentration in the gas phase was observed throughout the experiment, opposing the observations made for the other samples. This could be related to the presence of hydrocarbons that was only determined for this sample type. Inorganic carbon can serve as a carbon source for SRB in the absence of suitable organic carbon, but it is generally less efficient compared to organic carbon.

Conversely, anhydrite types 2 and 3 display a multitude of porous boundaries between anhydrite grains (e.g., Figure 329d), accompanied by the incipient precipitation of $CaCO_3$. This observation is likely linked to the elevated availability of magnesium ions within these two sample types. The presence of magnesium ions can significantly decelerate the overall rate of calcium carbonate precipitation due to its interference with the growth and development of calcium carbonate crystals. This inhibitory effect is particularly pronounced at higher concentrations of magnesium within the solution, as demonstrated by previous research (Zhang and Dawe, 2000).

In the examination of the microstructural features within the fine-grained type 1 anhydrite as compared to the coarse-grained type 2 and 3 anhydrite, a marked distinction becomes apparent in the $CaSO_4$ to $CaCO_3$ ratio, as delineated in Table 34. Specifically, in type 1 anhydrite, roughly 30% of the anhydrite matrix has undergone substitution with $CaCO_3$, whereas this proportion is notably reduced to 20% in the case of Type 2 and 3 samples. This observation serves to expose the discernible influence of grain size on the overall reaction kinetics within the system.

This thickness of the observed $CaCO_3$ rims is approximately three orders of magnitude thinner than what was reported by Roncal-Herrero (2017) for a study involving anhydrite single crystals immersed in a 0.5 M Na_2CO_3 aqueous solution at 25°C. It is important to note that while their experimental methodology differs from the one employed in this study, the substantial difference in reaction kinetics is notable. This difference is influenced by various interconnected factors, including the availability of the different electron donors, which can either inhibit or accelerate the reaction, as well as the accessibility of surfaces, which is closely related to the effective porosity of the rock mass. This highlights the importance of recognizing that studying model systems can lead to overly simplified and inaccurate conclusions about reaction rates in natural systems, which are typically composed of heterogeneous rock masses.

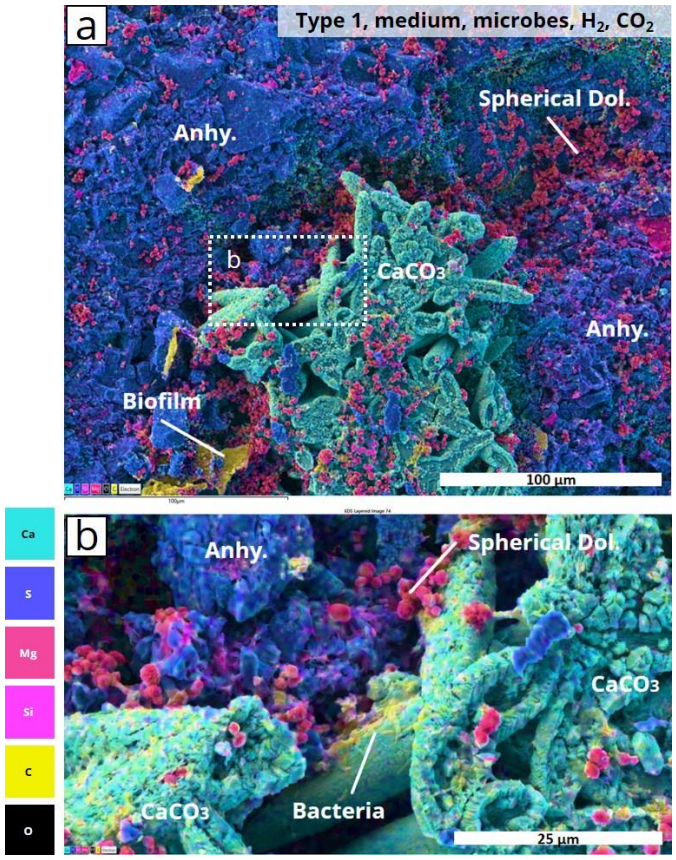

Figure 326. SE2/EDS micrographs showing fractured surfaces of type 1 anhydrite after exposure to SRB, H_2, and CO_2.

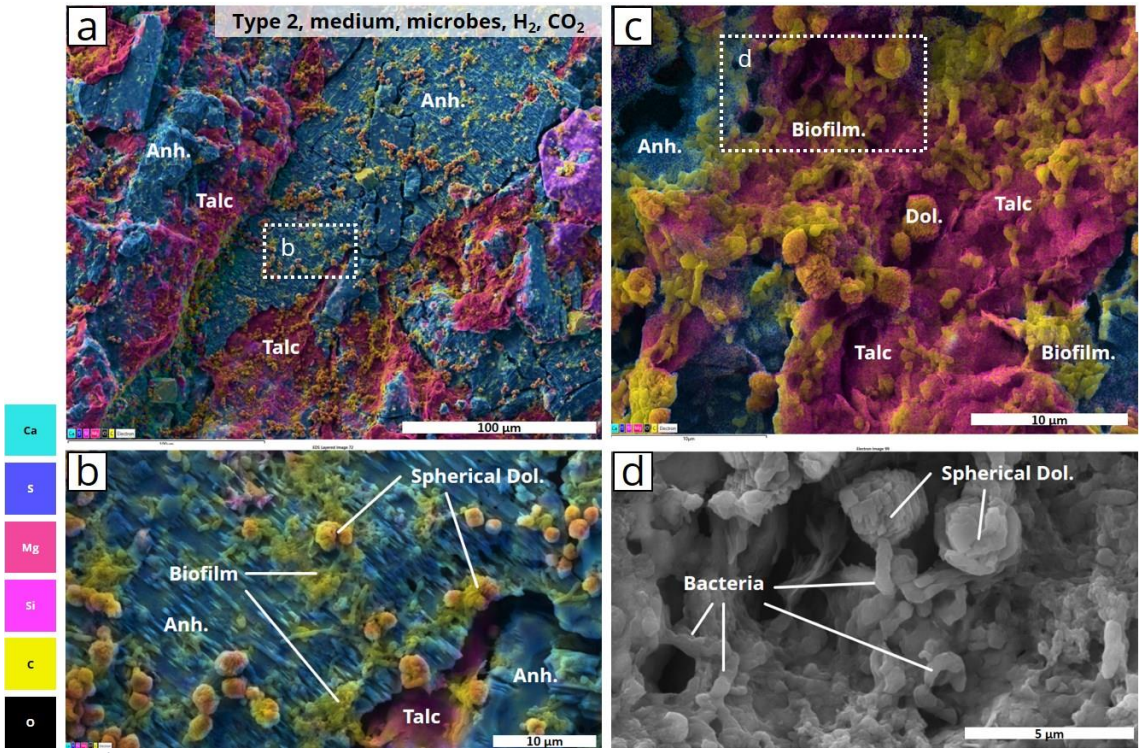

Figure 327. SE2/EDS micrographs showing fractured surfaces of type 2 anhydrite after exposure to SRB, H_2, and CO_2.

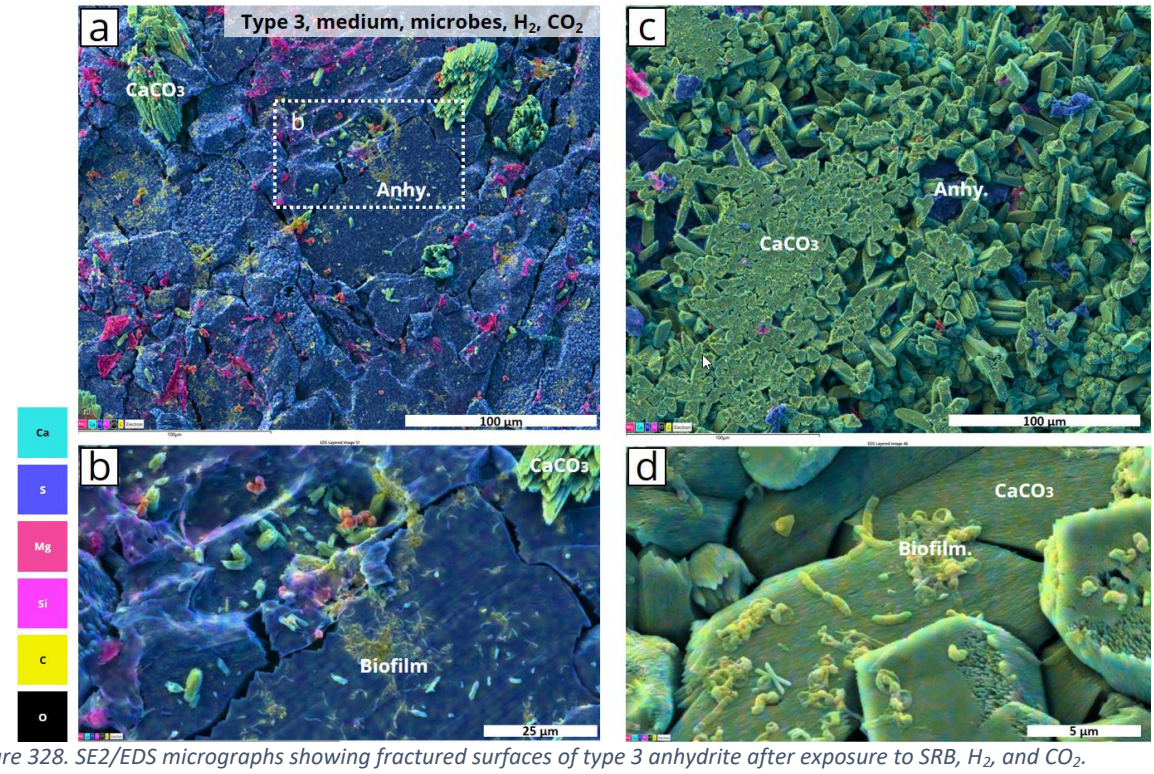

Figure 328. SE2/EDS micrographs showing fractured surfaces of type 3 anhydrite after exposure to SRB, H_2, and CO_2.

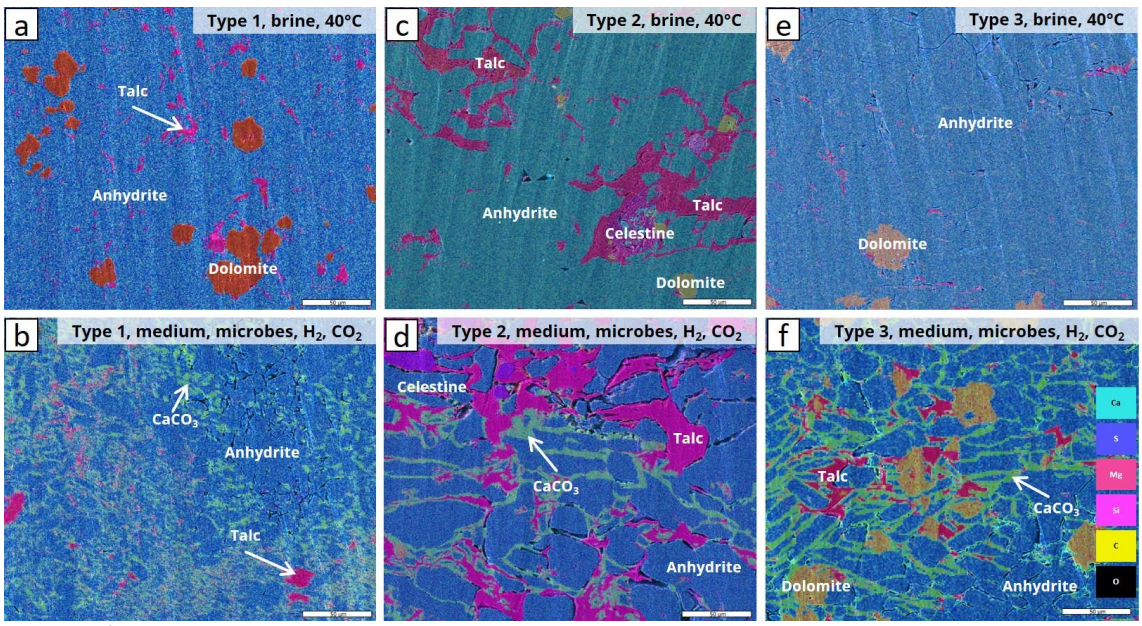

Figure 329. SE2/EDS micrographs showing BIB cross-sections of a) type 1, b) type 2, and c) type 3 anhydrite exposed to brine at 40°C in comparison to d) type 1, e) type 2), and f) type 3 anhydrite after exposure to SRB, H_2, and CO_2.

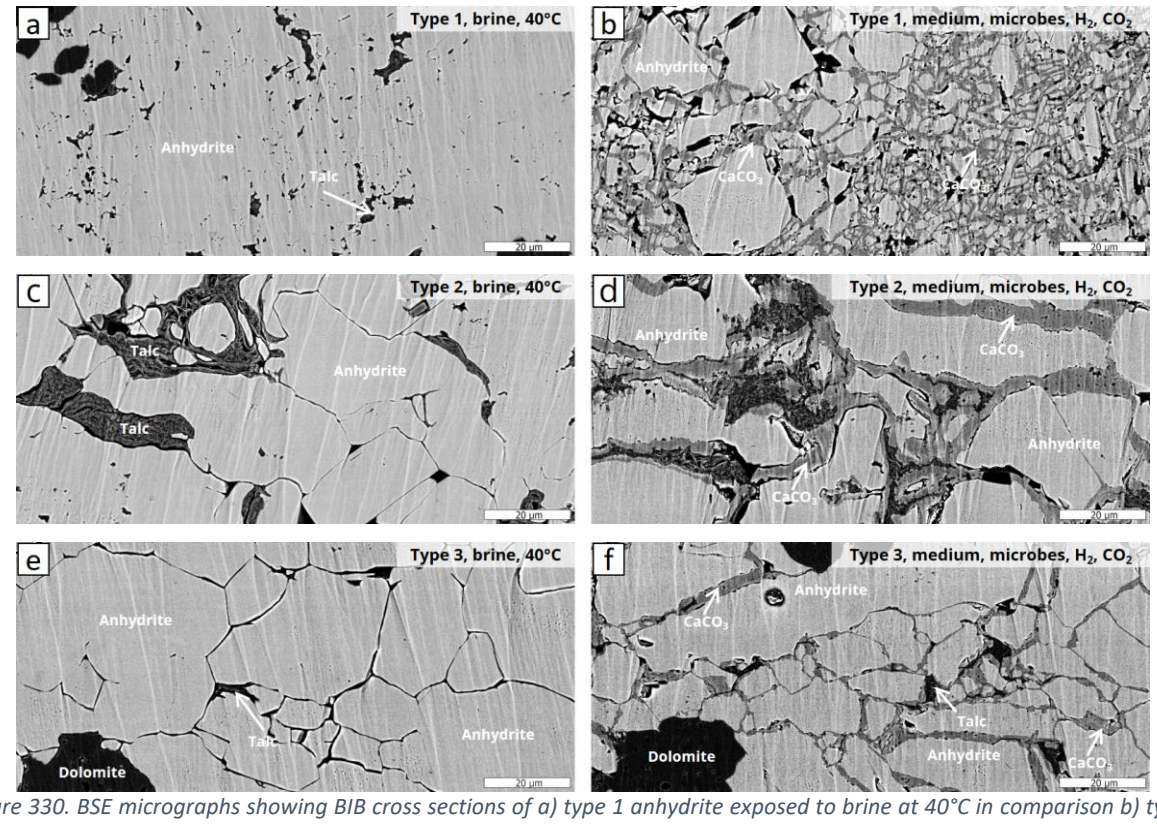

Figure 330. BSE micrographs showing BIB cross sections of a) type 1 anhydrite exposed to brine at 40°C in comparison b) type 1 anhydrite after exposure to SRB, H_2, and CO_2. The same is shown in c) and d) for type 2, and in e) and f) for type 3.

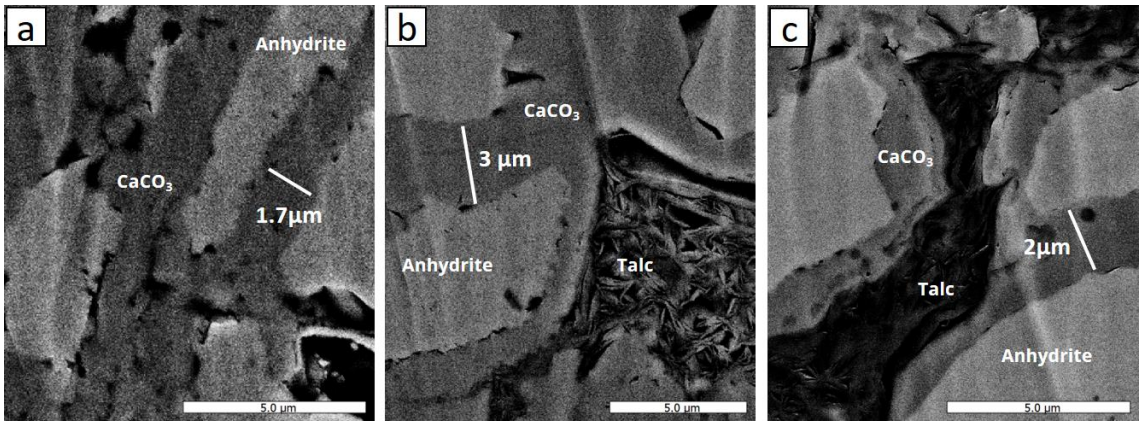

Figure 331. BSE Micrographs showing random measurement if thickness of CaCO3 formed at the anhydrite solution interface. a) type 1 anhydrite after exposure to SRB, H_2, and CO_2, b) type 2, and c) type 3.

4.2.3.3.2 Induced secondary porosity

Anhydrite has a larger molar volume than calcite. Consequently, carbonization of anhydrite is accompanied by the generation of porosity (Machel, 2001; Roncal-Herrero et al., 2017).

For all three anhydrite types, there is a notable increase in porosity when comparing the reference samples exposed to brine at 40°C with those subjected to microbial activity and a gas mixture at the same temperature (as indicated in Table 34). This increase in porosity can be reasonably attributed, to some extent, to carbonation processes, which caused compositional changes of up to 30 area% within the samples, as decribed above.

Further to the formation of secondary porosity by carbonization, dissolution of anhydrite induced by the SRB together with the inhibited precipitation of $CaCO_3$ due to the high availability of Mg^+ may play a role

in experiments conducted with anhydrite types 2 and 3. The H_2S produced by SRB can react with anhydrite ($CaSO_4$) in the surrounding environment. The reaction between H_2S and anhydrite results in the formation of calcium sulphide (CaS), water (H_2O), and sulphur dioxide (SO_2):

$$CaSO_4 + H2S \rightarrow CaS + H_2O + SO_2 \quad (4)$$

The formation of calcium sulphide (CaS) in the reaction contributes to the dissolution of anhydrite, as calcium sulphide is more soluble in water than anhydrite. This dissolution process leads to the release of calcium ions (Ca^{2+}) and sulphate ions (SO_4^{2-}) into the surrounding solution.

4.3 Concluding remarks anhydrite

Anhydrite can contain impurities or other minerals mixed in with the calcium sulphate. These impurities can vary greatly and depend on the specific geological conditions under which the anhydrite formed. Common impurities might include clay minerals, dolomite, halite, or various sulphate and sulphide minerals. The presence and amount of these impurities can significantly affect the reaction kinetic during bacterial sulphate reduction.

The grain size of anhydrite can vary as well. Anhydrite can form fine-grained to coarse-grained deposits, depending on factors like the rate of precipitation, temperature, and pressure during its formation. It was shown that a small grain size accelerates the overall reaction kinetics within the system with regard to the formation of $CaCO_3$.

It is important to note that the specific mechanisms by which NaCl affects sulphate-reducing bacteria require further investigation. It is possible that high salt concentrations disrupt cell membranes, affect enzyme activity, or alter the availability of sulphate ions, all of which could impact H_2S production.

In line with existing theories and prior experimental findings, we observed that no hydrates formed at a temperature of 40°C during exposure to brine, whereas they did form at 20°C. While it is important to note that storage caverns typically operate at temperatures outside these ranges, further research and site-specific investigations are indispensable for accurately assessing the implications of hydration and dissolution on the mechanical stability of the second-phase lithologies.

The presence of brine can lead to the occurrence of aperture-like grain boundaries, which can result from the mobilization of fine particles (talc). This phenomenon has the potential to influence both the transport properties and the accessibility of surfaces for chemical reactions during hydrogen storage.

Microbes exhibit no discernible preference for growth on particular types of surfaces, whether it be in terms of surface roughness or mineral composition

Dolomite formation through microbial activity was observed in the presence of sulphate-reducing bacteria SRB.

Despite the generally low porosity and permeability of anhydrite, it has been demonstrated that it can allow the passage of aqueous solutions, as evidenced by the formation of $CaCO_3$ at the edges of its grains involving an increase of porosity. Bacterial-induced mineral replacement processes, along with alterations in porosity, will impact the mechanical properties of the affected rock mass. Additional research is necessary to gain a more comprehensive understanding of the mechanical behaviour of a changing porous media, particularly in the context of hydrogen storage in salt caverns.

In the presence of magnesium ions within the aqueous solution, a competitive interaction arises between magnesium ions and calcium ions, competing for access to the available carbonate ions. This competition results in a diminished rate of precipitation for calcium carbonate crystals. Microscopic structural analyses have revealed that this phenomenon may additionally contribute to an elevation in porosity, particularly manifested in the form of grain boundary apertures.

The microstructural examination of heterogeneous anhydrite samples, conducted both prior to and subsequent to the bulk measurements, has substantially contributed to the interpretation of the bulk measurements. This contribution is particularly pronounced when considering the influence of hydrocarbons and impurities on the kinetics of the chemical reactions and the associated textural alterations in the samples.

Experimental findings obtained from natural samples often exhibit notable deviations from measurements conducted on simplified model systems. In light of this, it is wise to utilize site-specific investigations as a means to constrain the potential biological and chemical impacts that may occur during the storage of hydrogen in heterogeneous salt formations.

Risk assessment of hydrogen storage in a conglomerate of salt caverns in the Netherlands

PART 3 & 4 – Risk Analyses and recommended strategy for risk management and mitigation

Reference: KEM-28 – Part 3 & 4

Summary

Chapter 1 introduces the risk-based method. The first four steps are described in detail in the first paragraph followed by the reading guide and disclaimer, highlighting the extent and limitations of a generic situation. At the request of the Ministry of Economic Affairs and Climate (EZK) the current risk analysis is generic. A generic situation was preferred as this results in a (required) complete overview of risks compared to site specific elaboration. All site-specific information still needs to be gathered and subsequently processed in the actual risk assessment for any salt cavern planned for future H_2 storage. The results of the risk analysis will be used by EZK, SodM and their advisors to check and validate the risk analysis performed by operators. The results of the generic risk analysis represent a worst-case scenario, as all risks have to be taken into account without any specific knowledge of the use and the geology of the location.

The next two chapters list the most relevant stakeholders (risk step 1) and risks (risk step 2) that could be identified in a generic situation. Chapter 4 is the actual risk assessment analysis which includes classifying the risks (step 3) and dealing with risks (step 4) for hydrogen storage in salt caverns.

The total life-cycle of a salt cavern consists of several phases:

- the process of the design (pre-execution phase),
- the salt mining itself (execution phase),
- the storage of the gas / liquid (operation),
- the abandonment (decommissioning)
- and the monitoring afterwards (post abandonment monitoring).

The performed semi-quantitative[1] risk assessment focusses solely on the period of hydrogen storage, i.e., the operational phase (the storage of the gas / liquid). However, the results of the risk assessment in terms of research and measures do not solely apply to the operational phase, but also to the pre-execution and execution phase.

The final chapters of the report present the recommended strategy for risk management and mitigation following the Literature review (Part 1), Geomechanical study (Part 2) and the Risk analyses (Part 3). Chapter 5 details on all additional research and preventive and corrective measures necessary. These were identified in step 4 of the risk assessment to mitigate the risks and resulting mitigated risk matrix is shown in Figure 332. In general, these recommendations are based on a generic case and should be redefined and updated once a specific site has been selected as the stakeholders will change and new information will be available based on ongoing research.

[1] Semi-quantitative is the best way to describe the method of Risk-based working. The consequences or effects are classified 1, 2 or 3, in case of expected effects, or 0, in case no effect is expected. The numbers stand for ranges of costs, time etc instead of the hard figures in a geostatistical analysis. Furthermore, some of the effects can only be described and cannot be calculated, like quality or reputation

4*3 riskmatrix mitigated		Consequences		
		1	2	3
Chance	3	17.2; 18.2; 19.2; 20.2; 21.2	1.9; 2.2; 4.2; 5.2; 6.2; 7.2; 8.2; 9.2; 10.2; 11.2; 12.2; 13.2; 14.2; 23.2; 26.2; 27.2; 29.2; 30.2; 31.2; 32.2; 33.2; 34.2	
	2	10.4; 13.5; 15.3; 16.3; 20.5; 24.3 ; 29.1; 30.1; 30.3; 31.1; 31.3; 32.3; 33.1; 33.4; 34.8; 35.6	1.8; 1.12; 1.17; 1.18; 2.5; 3.2; 8.4; 8.6; 11.4; 12.5; 14.5; 22.1; 23.4; 23.6; 26.4; 27.5; 27.6; 28.1; 29.5; 34.6; 34.7; 35.4; 35.5	1.24; 9.6; 12.6; 13.6; 14.6; 23.8; 27.8
	1	1.2; 1.4; 1.10; 1.11; 1.15; 1.19 1.20; 1.21; 2.6; 8.5; 9.4; 10.1; 11,5; 11,6; 12.4; 13.4; 14.4; 18.3; 19.3; 21.3; 23.5; 26.5; 29.4; 34.4; 34.5; 35.3	1.1; 1.3; 1.5; 1.14; 1.16; 1.22; 1.23 ; 1.25; 2.7; 4.1; 4.3; 5.1; 5.3; 6.1; 6.3; 7.1; 7.3; 9.1; 9.5; 12.1; 13.1; 13.3; 14.1; 15.2; 16.2; 17.1; 17.3; 18.1; 19.1; 20.1; 20.3; 21.1; 22.2; 23.7; 24.2;	1.6; 1.7; 2.1; 2.3; 3.1; 8.1; 8.3; 9.3; 10.3; 11.1; 11.3; 12.3; 14.3; 15.1; 16.1; 23.1; 23.3; 24.1; 26.1; 26.3; 27.1; 27.3; 32.1; 34.1; 34.3; 35.1; 35.2
	0	1.13; 20.4; 21.4; 25.2; 29.3; 33.3		

Figure 332. The mitigated total risk matrix, the numbers refer to the risks for each stakeholder presented in Chapter 4 and Appendix D: Risk assessment.

The main recommendations from the risk assessment are described in Chapter 6 including the findings of the Geomechanical study resulting in a recommended strategy for cavern field development. Overall, after mitigation of the risks, hydrogen storage in a conglomerate of salt caverns in the Netherlands is technically feasible. Social acceptance of hydrogen storage is an important part of the success or failure of hydrogen storage and should receive attention from the government. Therefore, the development of a cavern field starts with selecting the right location and should be based on the geology and the minimum number of stakeholders in order to prevent more risks.

1 Introduction

In this introduction the method of Risk-based working used for the risk-based approach for Hydrogen Storage in salt caverns is described. Risk-based working has been used for the risk assessment that concludes the KEM 28 scientific study regarding the potential future storage of hydrogen in a cluster of salt caverns in the north-eastern part of The Netherlands.

We have chosen to perform a semi-quantitative analysis with categories of probabilities and effects / consequences. A quantitative analysis assumes the risks are all well-known and, by the occurrence of a significant amount of incidents, can be calculated by the law of large numbers. This enables a statistical analysis. In case of the storage of hydrogen in salt caverns the experience is limited to 4 existing salt caverns (UK and USA, first use in 1986 Clemence Dome Texas) that cannot be compared with the required operation of the future hydrogen storage in the Netherlands with respect to pressure changes within a short time span. The number is too small, incidents are unknown or at least publicly not available, and therefore a statistical analysis cannot be performed.

Furthermore, the ministry required a generic risk analysis which makes it even more difficult to perform a quantitative analysis as circumstances (with respect to the salt dome and the surroundings) are unknown.

1.1 General

The aim of the risk assessment is to get a clear view of the risks:

- by understanding nature and extent (probability of occurrence and consequences) of the risks with regard to the storage of hydrogen in a cluster of salt caverns
- by understanding purpose and extent of any investigation still to be carried out
- for coordination with the Ministry of EA&C (*Ministerie van Economische Zaken en Klimaat*) and future coordination with any stakeholders.

This working method or template is based upon the method of Risk-based Working, as described in the homonymous book (Van Staveren, 2015). This book is the practical version of the thesis “Risk, innovation & change: Design propositions for implementing risk management in organisations” (Van Staveren, 2009). The template has been developed based upon earlier experiences with salt caverns, specifically aimed at the potential development of deep soil contamination, the effect of fault propagation in hard-closed caverns and the effect of subsidence in and above salt caverns.

The template for “Risk based Working” consists of a structure of multiple steps of risk-based working. These risk steps are similar in each and every risk management approach. By going through these steps in an explicit and structured way for several possible arrangements of caverns used for the storage of hydrogen one gets (1) insight into the nature and extent of the risks and underlying uncertainties, and (2) insight into the necessity and possibilities for – whether or not – taking measures to contain these risks adequately. This is done in a transparent and therefore acceptable manner for all stakeholders.

Format

The template for “Risk based Working” consists of a structure of 6 steps of risk-based working.

When using Risk-based working unambiguous working definitions are needed for the key terms “uncertainty”, “risk” and “risk perception”. The following definitions are derived from the current definitions in the field of risk management and appear to work well.

- *Working definition “uncertainty”*

Uncertainty is incomplete certainty caused by (1) inevitable variation and/or (2) lack of information.

Inevitable variation, like the inherent variation in the composition of salt on a local scale, concerns an uncertainty that cannot be reduced. Lack of information in most cases concerns an uncertainty that can be reduced.

- *Working definition "risk"*

Risk is an uncertain event with causes, probability of occurrence and impact on objectives.

The definition implies that objectives are needed to determine risks. That means that for each and every stakeholder it must be completely clear what their objectives are in relation to the storage of H_2 in salt caverns. In other words, what is the desired or required situation with respect to H_2 storage.

In the following Figure 333 the relation between objective, risk, causes, consequences and constraining measures is displayed. The figure is based upon the well-known bow-tie scheme in which a risk is a result of causes leading to consequences.

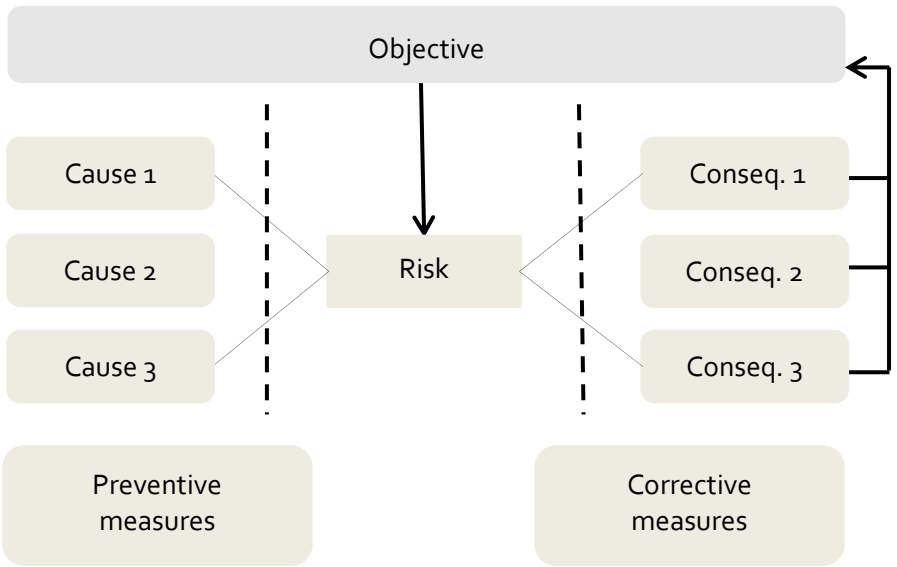

Figure 333. Relation between objective, risk, causes, consequences and constraining measures.

There are two types of measures that can be taken, preventive and corrective. Preventive measures aim at limiting or eliminating the causes, resulting in reduction of the risk itself. Corrective measures reduce or eliminate the consequences of risks. Both types of measures reduce the risk and with it the impact on the objectives.

- *Working definition "risk perception"*

Risk perception is the unique way in which a person assesses a risk.

Opportunities and consequences of risks often cannot be determined or calculated objectively. Furthermore, the way in which these opportunities and consequences are (un)acceptable - or:

the willingness to take risks - depends strongly on the position, interest and expectation of the stakeholder. Risk perception is not purely rational, emotions play an important part.

Six steps of Risk-based working

The method consists of 6 common risk steps:

- Risk step 1: Determine objectives
- Risk step 2: Identify risks
- Risk step 3: Classify risks
- Risk step 4: Dealing with risks
- Risk step 5: Evaluation of risk measures
- Risk step 6: Risk report

Steps 1 till 4 are explained underneath, steps 5 and 6 are placed further in time, when the cavern(s) are being or have been constructed. Steps 5 and 6 will therefore not be further elaborated in this stage.

In part 4 “Recommendations” steps 5 and 6 will be addressed as part of the total strategy.

Risk step 1: Determine objectives

Before starting a risk analysis, the objectives of the analysis must be perfectly clear for each and every stakeholder. This is a direct consequence of the working definition for “risk”. During this step all stakeholders and their main or multiple objective(s) will be determined. The objective of the stakeholders leads to the preferred or required end situation with respect to possible risks related to hydrogen storage in salt caverns.

Important focal points

(1) Describe the aims in a SMART way: Specific, Measurable, Achievable, Realistic, Time-based.
(2) Distinguish between objectives based on (a) assumptions, (b) facts and (c) interpretation of facts.

Risk step 2: Identify risks

Using the objectives of risk step 1 the risks related to hydrogen storage in salt caverns are identified. The risks are described in an unambiguous way as an uncertain event (not an existing problem!) with one or multiple causes and one or multiple consequences.

Causes are classified via HOT-RIP factors. “H” stands for Human cause, “O” for Organisational cause and “T” for Technical cause. The RIP factors may increase the impact of certain risks, with “R” standing for (lack of or contra dictional) Regulations, “I” for dominant Industrial culture and “P” for the aspects Politics, Press and Public. For the analysis of hydrogen storage an additional cause is added: “G” for Geological cause.

Consequences of the risks are normally classified according to the Big 5-risk effects: (1) safety, (2) quality, (3) time, (4) finances and (5) reputation.

Important focal points

(1) Describe each risk in an unambiguous way as an uncertain event or situation (not an existing problem) with causes and consequences for the specific objective.
(2) Describe whether the risk is identified based on (a) assumptions, (b) facts or factual information, or (c) interpretation of factual information.
(3) Describe the source(s) of information the risk identification is based upon.
(4) Describe whether the uncertain event (a) cannot or (b) can be minimized with additional information and describe (in case of (b)) which information is needed.
(5) Describe the type of causes (c) of the risk: [Tc] Technical, [Hc] Human, [Oc] Organisational, [Rc] Regulations, [Cc] Culture within the sector, [Pc] Politics press and public. It is possible to have several causes. Distinguish between (a) assumptions, (b) facts and (c) interpretation of facts.
(6) Describe the type of effects (e) of the risk for the objective: [Me] Money, [Te] Time, [Se] Safety, [Qe] Quality, [Re] Reputation. It is possible to have several effects. Distinguish between (a) assumptions, (b) facts and (c) interpretation of facts.

Risk step 3: Classify risks

In step 3 the probability of occurrence of every risk is determined, as well as the extent of the consequences, related to the objective. In other words: every risk gets classified.

The probability and consequences of occurrence of each risk are determined – if possible – geo-statistically, or – most likely – based on expert judgement. The expected accuracy of the calculations or expert judgements is made explicit. It will also be made explicit whether the classification of the risk is based on facts, interpretation of facts or assumptions.

During the classification systematic biases – distortion of risk perception – (like availability bias, optimism bias and confirmation bias) will be taken into account. The effect of biases can be limited by organising diversity in the expert team (and/or the group of "participating" stakeholders).

> The *availability bias* is the impact of one's most vivid experiences or memories on decision-making. It is a mental shortcut that allows people to easily connect ideas or decisions based on immediate or vivid examples.
>
> The *optimism bias* is a cognitive bias that causes one to believe that one him- or herself is less likely to experience a negative event. It is also known as unrealistic optimism or comparative optimism.
>
> The *confirmation bias* is the tendency to search for, interpret, favour, and recall information in a way that confirms or supports one's prior beliefs or values. People display this bias when selecting information that supports their views, ignoring contrary information.

A 4 x 3 risk matrix is used for the classification of the probability and consequences of occurrence of each risk (Figure 334). The 4 x 3 risk matrix consists of 4 probability classes and 3 consequence classes, see figure Y, with the colours red, orange and green standing for the "willingness to accept risks".

4 x 3 Risk matrix		Consequence/effect		
		1	2	3
Probability	3			
	2			
	1			
	0			

Figure 334. Risk Matrix.

- Red stands for large, unacceptable risks that have to be mitigated on short notice;
- Orange stands for moderate risks that will be addressed, if possible and necessary, with a medium-term time frame;
- Green stands for small, more or less “acceptable” risks that require no measures unless these are easy to incorporate and lead to further reduction of the consequences.

Risks with probability “0” represent a special category. These risks have a probability of occurrence that equals or approaches “0”. For instance, as a result of physical barriers that contain the consequences of the risk, or when the probability of occurrence approaches “0”, despite a large spread in assumptions. Such a classification needs to be substantiated with (a combination of) facts, interpretations of facts or, lacking both, assumptions. These interpretations and assumptions must be based upon thorough expert judgement. It is commonly accepted to classify the risks involved as extremely small / non-existing based upon state-of-the-art knowledge and experience.

Risks with probability “0” have no reasonable chance of occurrence. Furthermore, the consequences of any risk have to fall into the categories 1 to 3. If not, there is no risk at all.

The following tables contain specific criteria for the classification of the probability of occurrence and the consequences / effects of the risks as a result of the storage of hydrogen in salt caverns (values discussed and set by the participants of H2C3).

Classification probability of occurrence (frequency):	Classification effects: see below, specified per effect
0 = none = no cases known and not plausible, based on state-of-art knowledge and experience 1 = small = (less than) 1 case per 100 years 2 = limited = 1 case per 10 years 3 = large = (more than) 1 case per year	

Classification effects [Me] Money (in the form of necessary costs):	Classification effects [Te] Time (in the form of time required):
1 = less than 2 m€ 2 = more than/equal to 2 m€, less than 40 m€ 3 = more than 40 m€	1 = less than 2 months 2 = more than/equal to 2 months, less than 2 years 3 = more than 2 years
Classification effects [Se] Safety *: 1 = Minor physical injury with zero lost time 2 = Physical and/or psychological injury with lost time 3 = Serious or permanent injury and/or fatal incident	Classification effects [Qe] Quality#: 1 = (possible) visible effect without significant / measurable spread and impact 2 = (possible) visible effect, with limited distribution and without long-term impact 3 = significant effect, with wide distribution and permanent impact
Classification effects [Re] Reputation: 1 = publicly expressed attention for possible negative effects as a result of hydrogen storage in salt caverns 2 = local or national media attention for possible negative effects as a result of hydrogen storage in salt caverns 3 = international media attention for possible negative effects as a result of hydrogen storage in salt caverns	
*Physical and psychological safety of human beings	# Effects on environment and health

Please note: Risk classifications in grades for probability of occurrence and consequences / effects are inherently uncertain and – in most case – based on a collection of facts, assumptions and interpretations. The biases also contribute in this process. The risk classification is therefore primarily used for decision support in Risk step 4 about "Dealing with risks". The risk classification itself and the willingness to accept risks are fundamental for the decisions in Risk step 4 to, whether or not, contain the risks, for example with preventive or planned corrective measures.

Important focal points

(1) Classify the probability of occurrence as none (extremely small), small, limited or large with the classification 0, 1, 2, or 3 respectively of the risk matrix. Make use of the criteria of the 4 classifications. Indicate whether the classification is based on (a) (geostatistical) computations or (b) estimations based on expert judgement using (i) assumptions, (ii) facts and (iii) interpretation of facts.

(2) Classify the relevant effects of each risk for the objective – [Me] Money, [Te] Time, [Se] Safety, [Qe] Quality and [Re] Reputation – as small, limited or large with the score 1, 2 or 3 for "consequence / effect" in the risk matrix. Use the criteria for effect as mentioned in the table. Indicate whether the effect-classification is based on(a) (geostatistical) computations or (b) estimations based on expert judgement using (i) assumptions, (ii) facts and (iii) interpretation of facts.

(3) Describe the information used for the classification of probability and/or effect.

(4) Beware of the distortion of risk perception (bias): availability bias, optimism bias and confirmation bias.

Risk step 4: Dealing with risks

In step 4 it is decided whether or not, and if so which, measures must be taken to limit classified risks to an acceptable level or to keep them on that level. The "acceptable level" depends on the risk perception and risk willingness of the stakeholders. Furthermore, in step 4 it becomes clear if additional research is

necessitated to better understand the (height of the) risk and the necessity of additional measures. These measures can be preventive or corrective.

Preventive measures minimize or eliminate the probability of occurrence of a risk by addressing one or multiple causes of that specific risk. Corrective measures minimize or eliminate the consequences / effects of the occurring risks.

Two sub-steps in dealing with risks are (1) enumeration and selection of optimal measures needed because the risk is not acceptable and (2) the actual implementation of the selected measures. During the selection of the measures it is explicitly mentioned if they are chosen based on assumptions, facts or interpretation of facts.

At the end of step 4 the risk assessment will be finalized with the determination of the residual risks, again displayed in a risk matrix.

Important focal points

(1) Indicate if the implementation of measures can or have to be postponed due to necessary additional research to classify the risk more accurately. This may influence the decision whether or not to implement the measures. In case of additional research try to specify the content of the research (scope, analyses, measurements etc.)
(2) Distinguish between preventive and corrective measures.
(3) Describe the selected measures in a SMART way: Specific, Measurable, Achievable, Realistic, Time-based.
(4) Indicate if the desired effect of the measures is based upon (a) assumptions, (b) facts and (c) interpretation of facts.
(5) Describe and qualify the residual risk after the implementation of the measures. This must be done for the occurrence of each risk for both probability of occurrence and consequences / effects. Use the classification of step 3.

The actual process

The risk analysis was done and filled step-by-step. In each step the experts of KEM-28 have participated. After each step the results were processed and the form of the risk assessment was filled gradually.

1.2 Disclaimer

In the Risk based Working form, combined with the Template Risk based Working for Hydrogen storage in salt caverns, the risks associated with the storage of hydrogen in newly designed salt caverns have been assessed. This was done in a structured risk-based way using expert knowledge, experience and worldwide data. The potential consequences of Hydrogen Storage in salt caverns on a range of stakeholders with their own objectives is described in this form.

As discussed with the Ministry of Economic Affairs and Climate (EAC) the risk assessment was performed for a “generic situation”. A generic situation was preferred as this results in a (required) complete overview of risks compared to site specific elaboration. Furthermore, it was felt by the H2C3 team that, lacking more detailed information about geology, the salt structures, material characteristics etc., it was undoable to present a site-specific risk assessment.

Focus on storage

The earlier qualitative risk assessment of TNO (van der Valk et al., 2020) involves the total life-cycle:

- the process of the design (pre-execution phase),
- the salt mining itself (execution phase),
- the storage of the gas / liquid (operation),
- the abandonment (decommissioning)
- and the monitoring afterwards (post abandonment monitoring).

This semi-quantitative risk assessment focusses solely on the period of hydrogen storage and therefore was done only for the operational phase (the storage of the gas / liquid). All other phases are political/social/financial (pre-execution phase) or related to the salt cavern itself (design, execution, decommissioning and post-abandonment monitoring) and not referring to hydrogen storage. This includes the risk of not-matching supply and demand of hydrogen. There is one exception: “Risks associated with surplus extraction (more than can be processed) of brine”. These risks are typical of the execution phase, the stage in which the salt cavern is developed.

For this specific risk we have contacted members of the salt production industry primarily to establish if there actually is a risk of surplus extraction.

The method

By using the method of Risk based Working a gradual detailed assessment was performed for potentially involved and relevant stakeholders. The assessment describes the first 4 steps of Risk based Working. The process has been led and the form has been by René Vreugdenhil, the form has been filled in, by all experts of the H2C3 team, with occasional support of external experts like Eric van Oort. There has been no interview with any of the stakeholders.

NB: Due to the generic nature of the assessment a relevant part of the risks cannot be easily quantified as a result of lacking information. This results in the need for site specific risk assessments for each location or field – depending on the heterogeneity of the salt structure – its surroundings and differences in relevant stakeholders, see the next section, 1.3 Disclaimer, for further details. Additionally, the assessment has led to a large number of stakeholder-risk assessments, to increase readability the stakeholder risks of solely the, operator, SODM and Ministry of Economic Affairs and Climate are presented in the Chapter 4, the remaining stakeholders risk are presented in the Appendix D: Risk assessment.

In general, the common practices for salt solution mining as described by Pereira (2012) is considered as the base case for the risk assessment. As the current risk analysis is generic, an introduction for site specific application is necessary. In the following part the required information about the subsurface of the site itself, its direct surroundings and relevant stakeholders is summarized.

This listed required information is not meant to be exhaustive but solely gives an insight in the amount of data needed to make it site specific once the location is known. Additionally, as the exact number of caverns to be exploited remains unknown and the total number of accidents in gas storage caverns is relatively low, any statistical risk analysis is not straight forward (see also Database of (near-) accidents occurred), and therefore the probability of occurrence is approximated.

Site specific situation

For a site-specific risk assessment, the following information of each cavern is – at least – necessary:

> 3D geometry of geology, natural faults and folding, salt-internal structure, rheology, other rock properties and uncertainties, seismicity, salt cavern design (geometry and loading) or history (for the case of an existing cavern) and development, the probability of H_2S forming etc.

Apart from these also the direct surroundings need to be described and taken into account, both above and below the surface, like:

> the situation of the caverns in the direct vicinity (under development, used for storage of natural gas / hydrogen, used for CAES), infrastructure above and below ground level, distance to businesses and inhabitants, the use of the subsoil (e.g., geothermal energy, drinking water potential, oil or gas exploitation) etc. Models of hydrogen storage caverns affecting non-H_2

storage were included in the research phase as a reference study, however scenarios should be updated once locations are known.

Information concerning / related to stakeholders

For a site-specific risk assessment information of the surroundings is necessary, including:

locations of drinking water extraction and strategic drinking water supply, residential areas, areas of natural reserves, other underground activities.

2 List of stakeholders and their objectives

In risk step 1 all stakeholders and their main or multiple objective(s) related to hydrogen storage in salt caverns were determined. The objective of the stakeholders leads to the preferred or required end situation with respect to possible risks.

As the risk analysis is not site specific but has a general scope the number of possible stakeholders is quite large. The stakeholders are listed in categories, like Authorities and Companies, to make it more accessible and clearer.

Authorities

- National authorities:
  1. Ministry of Economic Affairs and Climate: climate neutral society with clean, reliable and affordable energy while respecting the balance between interests of producers and consumers
  2. State Supervision of Mines: protection of humanity and environment during energy production combined with protection and utilization of the subsoil, now and in future times
  3. Ministry of Infrastructure and Water Management (Rijkswaterstaat): managing and developing national roads and national waterways in a safe, liveable and accessible country
  4. Ministry of Agriculture, Nature and Food Quality ("Natuurnetwerk Nederland"): The Netherlands faces serious social and ecological challenges. We need to prevent depletion of soil, freshwater supplies and raw materials, halt the decline in biodiversity and fulfil our commitments to the Paris climate agreement

- Regional authorities (province(s)):
  5. provincial states:
     a. our organization is motivated, reliable and innovative. Our organization cooperates, links and joins in brainstorming in the search for solutions, keeping an eye on our province and the interests of environment and society including the agricultural industry
     b. our organization is responsible for the implementation and execution of the "management plan" for the Natura 2000 areas

- Local authorities (municipalities):
  6. municipalities: our municipality is a society with optimal development for our inhabitants and enterprises and cooperation based on self-initiation, strength and quality

Semi authorities

- National:
  7. Energie Beheer Nederland, 100 % daughter of Ministry of EAC: EBN is deploying value in the subsurface for the benefit of the future above ground

- Regional:
  8. Water Boards: we guarantee safety and clean and sufficient water at low cost
  9. Veiligheidsregio / safety region: we ensure that everyone can live and work in peace

Public companies:

- Owner/user of the salt caverns (hydrogen and other uses):
  10. Operator of the hydrogen storage (generic objectives): we store renewable ("green") energy as hydrogen gas in our own salt caverns. We are part of the energy transition and play an important role in the storage of renewable energy

11. Gasunie New Energy/ HyStock: New Energy is a daughter company of Gasunie dealing with business development in renewable energy. In developing projects, we look at technological, financial, economic and social aspects. New forms of energy must not only be sustainable, but also reliable and, of course, socially responsible
12. Gasunie Transport Services, owner of the cavern containing nitrogen gas (Heiligerlee): we offer gas transport services in a customer-orientated and transparent way. Safety, reliability, sustainability and cost-awareness are our priorities. We serve the public interest and operate professionally to create value for our stakeholders
13. Gasunie / Energystock, owner of the caverns containing natural gas (Zuidwending): we serve the public interest, offer integrated transport and infrastructure services to our customers and adhere to the highest safety and business standards. We focus on short- and long-term value creation for our shareholder(s), other stakeholders and the environment

- Drinking water company (restricted to the north-eastern part of the Netherlands):
  14. Water company Groningen ("Waterbedrijf Groningen"): as a social enterprise we want to secure the water interests in the region in a sustainable way. We are not just the supplier of drinking water but we also participate in matters such as public health, nature conservation, creation of sustainable sources … and innovation
  15. Water Company Drenthe ("Waterleiding Maatschappij Drenthe"): WMD provides impeccable drinking water at an acceptable cost for everyone in Drenthe, generation after generation

- Railway company:
  16. Railinfratrust / ProRail, owner of the rail infrastructure: we connect people, cities and companies by rail, now and in future times. We enable comfortable travelling and sustainable transport and ensure safety on and around the railway
  17. Railway companies using the railways (passenger trains): we want to connect people, cities and villages in a safe, reliable and sustainable way
  18. Railway companies using the railways (freight trains): we want a safe, reliable and sustainable way to transport all kind of goods by rail

- Vital energy infrastructure:
  19. Gasunie Transport Services, owner of the public gas network: we offer gas transport services in a customer-orientated and transparent way. Safety, reliability, sustainability and cost-awareness are our priorities. We serve the public interest and operate professionally to create value for our stakeholders
  20. TenneT, owner of all high-voltage lines and cables: we are driven by our mission to ensure the lights stay on and that power is available, at the flick of a switch, whenever and wherever you need it

Private companies:

- Companies in the direct vicinity of the salt caverns:
  21. NAM, Dutch exploration and production company: NAM is an innovative company that supplies energy to society and industry. We do this by exploring, developing and producing gas and oil from the Dutch subsoil. We strive to do this as safe and efficient as possible without damage to people and the environment
  22. Future CAES, CORRE energy: by storing surplus energy, we make a huge contribution to the energy transition by enabling the integration of large-scale renewable energy sources. With our technology, we can solve a vital piece of the energy transition puzzle and bring balance to the current energy landscape

- Water consuming companies:
  23. Water used for production: we want to ensure sustainable availability of sufficient (ground)water of excellent quality and contribute to efficient use of water
  24. Water used for cooling: we want to ensure the availability of suitable and sufficient groundwater for the purpose of cooling

- Salt producing company:
  25. Nobian:
      a. we excel in the safe and reliable supply of high-purity salt, chlor-alkali and chloromethanes…. we continue to innovate every day to become safer, more efficient and sustainable and to ensure the essential products of today will continue to enrich our lives tomorrow
      b. we are exploring how we can store green energy in our salt caverns. We're actively working to produce greener chemicals, including hydrogen, and are committed to stimulating and growing a circular economy

- Companies in the direct vicinity or effected by ground vibration, like
  26. Data storage facilities: the production of our company requires a safe and sound subsoil without disturbing vibrations

NGO's:

27. Greenpeace: Greenpeace is a global network of independent campaigning organizations that use peaceful protest and creative communication to expose global environmental problems and promote solutions that are essential to a green and peaceful future
28. Wadden Sea Association ("Waddenvereniging"): the organization strives for preservation, restoration and good management of nature, landscape and environment and the ecological and cultural-historical values of the Wadden area, including the northern sea clay-area and the North Sea as irreplaceable and unique nature reserves
29. Wadden Academy ("Waddenacademie"): The Wadden Academy aims to furnish the scientific foundations for an economically and ecologically responsible future in the Wadden Sea Region, a World Heritage Site

Population:

30. Private landowners, directly above the salt caverns:
    a. protection of private use of groundwater
    b. protection of private cattle and crops
    c. value retention of own property
31. Private landowners, in the direct vicinity of the salt caverns
    a. value retention of own property

3 List of risks

In risk step 2 all risks related to hydrogen storage in salt caverns were identified. For this we – all experts of the H2C3 team – started with the results from the literature review with respect to salt dome related accidents. Then we added the specific hydrogen related risks. Finally, we added all other possible risks, including risks coming from earlier salt related risk assessments ("Formulier – Template Risicosturing voor zoutwinveld Haaksbergen", versie 1.3, no reference [Vreugdenhil Milieuexpert, 2021]). All risks were discussed with the team.

1) Blowout / well control loss. Caused by:
   - catastrophic failure of the X-mas tree and subsurface safety valve
2) Well leaks / well integrity loss. Caused by (other related causes are treated separately e.g., risk 5):
   - leakage at the X-mas tree
3) Leakage in vertical tubing/casing. Caused by:
   - joint failure, corrosion, rupture, overstretching, failure at shoe
4) Pipeline integrity loss (rupture / leakage).
5) Casing overstretching.
6) Cavern breaches (tightness) / cavern integrity loss. Caused by:
   - Heterogeneous salt structure
7) Creep closure and subsidence.
8) Tensile failure (rock salt / cavern wall). Caused by:
   - thermal and mechanical stresses as a result of alternating pressure
9) Tensile failure (cement debonding). Caused by:
   - thermal and mechanical stresses as a result of alternating pressure in- and outside the casing/shoe
10) Tensile failure (materials like steel alloys, elastomers, etc.). Caused by:
    - thermal and mechanical stresses as a result of alternating pressure
11) Weakening of salt (cavern wall). Caused by:
    - interaction with hydrogen
12) Weakening of material (cement bonding and materials like steel alloys, elastomers, etc.). Caused by:
    - interaction with hydrogen
13) Cratering (overburden failure).
14) Roof fall.
15) Block falls.
16) Formation of H_2S beyond acceptable limits (required purity for industrial use and safety limit for employees and surroundings)
    - caused by: anhydrite and sump conditions
    - stimulated by: hydrocarbons like the blanket material or former methane storage
17) Registered induced seismicity. Caused by:
    - the operation (filling and emptying) of the cavern
18) Emergence of negative public opinion
19) Fire on site.
20) Natural disaster, e.g., flooding.
21) Terrorism.
22) IT failure.
23) Disputed responsibility due to stacked mining activities.
24) Threat for energy storage (Licence To Operate).
25) Risk of surplus extraction of brine

26) Political accountability.

Some of the risks have been grouped in the following assessment for stakeholders other than the operator. For the operator each risk needs to be elaborated to assure all important measures to be taken – preventive and corrective – will be considered. For all other stakeholders the effect(s) or consequence(s) are of main interest.

4 Risk assessment form

WHEN READING THE RISK ASSSESMENT, THE FOLLOWING IS OF IMPORTANCE:

1. **This form is based on the Template Risk based Working for Hydrogen storage in salt caverns (see Section 1.1). For the introduction, explanation and focal points of this specific form we explicitly refer to the introduction of this part of the report including the list of stakeholders and their objectives and the list of risks.**
2. **For practical reasons risk steps 1 till 4 are displayed for each individual stakeholder and each individual risk. In this way for each (stakeholder and) risk "risk maps" evolve with (1) the concrete objective/aim to which the risk relates, (2) the concrete description of the risk that may threaten the realisation of that particular objective/aim, (3) the classification of the probability of occurrence and consequences of the risk and (4) the optionally necessary measures to get or keep the risk at an acceptable level, related to the willingness to accept risks.**
3. **For the classification of the probability of occurrence and consequences of the risk a 4 x 3 risk matrix is used. In case of risks having more than one consequence the highest score will be decisive for the risk classification. The 4 x 3 risk matrix contains 4 probability or chance-classes and 3 consequence-classes, as shown in the introduction (**Figure 334**). As our expert knowledge is less extensive for some cases, we assumed a worst-case scenario and, therefore, a rather conservative consequence class.**
4. **For the operator all risks are treated individually while for the other stakeholders risks are grouped when appropriate. For these cases the main preventive and corrective measures are listed to avoid too much repetition, additionally we refer to the operator risks to see all measures.**
5. **Measures are implemented from the perspective of the activity / the operator. The aim is to reassure and/or satisfy the stakeholders.**

Note that probabilities are relatively high as we need to consider dozens of caverns (a cluster). The next pages present three risk assessments of three different stake holders. All other risk assessments, including all identified stakeholders and risks, are documented in Appendix D: Risk assessment.

4.1 Stakeholder: Operator

RISK Nr. 1.1 Blowout / well control loss

Risk step 1: Aim

Aim 1 for the Operator: "*We store renewable ("green") energy as hydrogen gas in our own salt caverns. We are part of the energy transition and play an important role in the storage of renewable energy*". Therefore, the aim is: no risk for all stakeholders, directly or indirectly involved, as a result of hydrogen storage in salt caverns.

Risk step 2: Risk identification

(1) *Risk:* Blowout / well control loss caused by catastrophic failure of the X-mas tree and subsurface safety valve
(2) *Risk based on:* Interpretation of facts
(3) *Source of information:* Literature review, example case histories[1][2]
(4) *Uncertainty:* Blow-out modelling e.g., as done by Brouard Consulting in Part 2 (1.11)
(5) *Type of causes*: [Tc][Hc][Gc][Oc][Rc]
(6) *Type of effects*: [Me][Te][Se][Qe][Re]

Risk step 3: Risk classification

(1) Classification probability class: 1 (c): interpretation of factual information
(2) Classification consequence class: [Me3][Te2][Se3][Qe2][Re3]

Risk step 4: Dealing with risks

(1) Additional research: modelling of Blow-out, safety study on the effect at the surface
(2) Preventive measures: highest quality of blowout preventer (BOP) and safety valves (H_2 certified material), larger diameter of the casing (decrease of blow-out duration), all equipment designed for low T, simulation of a blow-out (part of the permitting), four-eyes principle, regular maintenance and check, rapid response plan
(3) Corrective measures: actions according to rapid response plan, evacuation plan, fire extinguishing, damage control / repair, temporary partial shut-down and repair
(4) Description and classification residual risk considering the measures taken: taking the preventive and corrective measures into account the residual risk becomes: 1 (probability) and [Me2][Te2][Se1][Qe2][Re2] (consequences), **1/2**

[1] Fort Saskatchewan Ethane Blow-out and Fire, 2001 (2.3.2.1)

[2] Moss Bluff natural gas blow out and Fire, 2004 (2.3.2.2)

4.2 Stakeholder: SODM

RISK Nr. 2.2 Subsurface accident

Risk step 1: Aim

Aim 2 for State Supervision of Mines: "*Protection of humanity and environment during energy production combined with protection and utilization of the subsoil, now and in future times*". Therefore, the aim is: no risk for humans and environment as a result of hydrogen storage in salt caverns.

Risk step 2: Risk identification

(1) Risk: Subsurface accident (leakage vertical tubing/casing, casing overstretching, cavern breaches, tensile failure, weakening, falls) as a result of hydrogen storage
(2) Risk based on: Interpretation of facts / assumptions
(3) Source of information: Literature review[1][2][3][4][5], expert judgement
(4) Uncertainty: Additional research of the salt structure and rheology, the interaction with hydrogen, mechanical properties and damage evolution. Additional research of materials interacting with hydrogen.
(5) Type of causes: [Hc][Tc][Rc][Ic][Gc]
(6) Type of effects: [Me][Te][Se][Qe][Re]

Risk step 3: Risk classification

(1) Classification probability class: 3 (a/c): assumption based on expert judgement and interpretation of factual information
(2) Classification consequence class: [Me1][Te2][Se3][Qe3][Re2]

Risk step 4: Dealing with risks

(1) Additional research (5 main): creep research (grainsize) and durability of the salt, research of the salt dome internal structure, including anomalous zones (section 3.4.7.1.4), and rheology, additional research of the second phase rheology interacting with hydrogen, research on prevention of micro annuli at the casing / cement / rock interfaces, additional research of materials interacting with hydrogen, (see further research in risks 1.3, 1.5, 1.6, 1.8-1,12, 1.14 and 1.15)
(2) Preventive measures (5 main): minimum preconditions for H_2 storage cavern (well test), improved cavern design (avoid flat roof / interlayered formations / large diameter of the roof), periodic sonar measurements and cement bonding log (e.g., every 5 years), elastomers (no nitril) or self-healing material instead of cement, H_2 and H_2S certified material (including packers), (see further measures in risks 1.3, 1.5, 1.6, 1.8-1,12, 1.14 and 1.15)
(3) Corrective measures (5 main): controlled production / flaring of H_2, abandon cavern, adapt the pressures, (micro annuli and material) treatment with special materials (resins, silicates etc.,

[1] Magnolia, Louisiana, 2003 (2.2.3.2.10)
[2] Boling 1, 2, 4, Texas, USA, 2005 (3.3.2.1)
[3] Bayou Corne, Louisiana, 2012 (2.2.3.1.1)
[4] Eminence salt dome 1, 3, 4, Mississippi, 1972 (3.3.2.2)
[5] Jintan JK-A, China, 2015 (3.4.5.1.3)

biological treatment), use of deformable metals and casing expansion, (see further measures in risks 1.3, 1.5, 1.6, 1.8-1,12, 1.14 and 1.15)

(4) *Description and classification residual risk considering the measures taken:* taking the preventive and corrective measures into account the residual risk becomes: 3 (probability) and [Me1][Te2][Se1][Qe2][Re2] (consequences), **3/2**

4.3 Stakeholder: Ministry of Economic Affairs and Climate

RISK Nr. 3.3 Threat for (future) on-shore energy storage

Risk step 1: Aim

Aim 3 for Ministry of Economic Affairs and Climate: "*Climate neutral society with clean, reliable and affordable energy while respecting the balance between interests of producers and consumers*". Therefore, the aim is: no risk in the area of the hydrogen storage. No adverse consequences for social and political responsibility of the Ministry.

Risk step 2: Risk identification

(1) Risk: Threat to future energy storage in salt caverns (Licence to Operate) due to uncertainties about safety and consequences of the storage in salt caverns
(2) Risk based on: Assumption
(3) Source of information: public, press, politics
(4) Uncertainty: (generic and) Site-specific risk assessments, site-specific research on geology, rock-salt properties
(5) Type of causes: [Pc]
(6) Type of effects: [Me][Te][Qe][Re]

Risk step 3: Risk classification

(1) Classification probability class: 3 (a): assumption based on expert judgement
(2) Classification consequence class: [Me3][Te3][Se0][Qe3][Re3]

Risk step 4: Dealing with risks

(1) Additional research: (generic and) site-specific risk assessments, site-specific research on geology and rock-salt properties, first cavern for research purposes only
(2) Preventive measures (5 main): open pro-active communication with stakeholders (public, politics and press) and other operators, preferably use newly developed caverns (according to an optimal rock mechanical envelope), periodic leak tests (e.g., every 5 years), minimum preconditions for H_2 storage cavern, mandatory status-report (starting every year), see further measures in risk 1.24
(3) Corrective measures: open communication with stakeholders (public, politics and press) and other operators
(4) Description and classification residual risk considering the measures taken: taking the preventive and corrective measures into account the residual risk eventually becomes: 2 (probability) and [Me1][Te3][Se0][Qe0][Re2] (consequences), **2/3**

4.4 Bibliography

- Evo Energy Consulting, Qualitative Risk Assessment of long-term sealing behavior of materials and interfaces in boreholes, final report, reference KEM-18 (van Oort, 2022)
- DBI GmbH e.o., Leitfaden Planung, Genehmigung und Betrieb von Wasserstoff-Kavernenspeichern, Project Zwanzig20 – HYPOS – H2-UGS (DBI, 2022a)
- DBI Gut, Wasserstoff Speichern – Soviel ist sicher, reference G 201926 (DBI, 2022b)
- M.P. Laban, Hydrogen storage in salt caverns, chemical modelling and analysis of large-scale hydrogen storage in underground salt caverns, no reference, dated July 16 2020 (Laban, 2020)
- TECNA estudios, Sweetening technologies – a look at the whole picture, paper WGC, dated 2009
- Nouryon, Micro seismic network Heiligerlee & Zuidwending, observations Q3 2020, Powerpoint, no reference, no date
- NAM, Report "Instemmingsbesluit Norg", letter, no reference, dated December 3 2021
- Roland Berger, Zout impactstudie, het maatschappelijk en economisch belang van duurzame zoutwinning in Nederland, commissioned by Nobian, July 2022
- NAM, press information about leaking pipelines with production water, Twente, Drenthe, 2015
- D66, Motion referring to leakage in old salt pipelines, 2018
- Public opinion with respect to CO_2 storage underneath Barendrecht: "Stichting CO2isNEE", 2010
- Public opinion with respect to environmental problems and subsidence as a result of salt mining: "Stop Zoutwinning!", 2021
- Public opinion with respect to future salt extraction Municipality of Haaksbergen, 2023
- Public opinion with respect to underground discharge of production water, www.stopafvalwatertwente.nl
- Public opinion with respect to Nitrogen storage in Heiligerlee, www.mijnendijnbelang.nl
- Groenlinks, Stacked mining neglected in Nedmag-advice, 2019
- RTVOost, Growing frustration about mining, damage and new gas exploitation, January 2021
- N. Dopffel, Microbial impact on hydrogen storage, NORCE, 2nd International Summer School on UHS, dated July 2023
- C.A. Peters, Underground H_2 storage: Geochemistry Considerations, Princeton University, 2nd International Summer School on UHS, dated July 2023
- M. Portarapillo & A. di Benedetto, Risk assessment of the large-scale hydrogen storage in salt caverns, article in Energies 14 (Portarapillo and Di Benedetto, 2021)
- M. Panfilov, Underground and pipeline hydrogen storage, Compendium of Hydrogen Energy, pp 92-116, dated 2015 (Panfilov, 2016)
- Rapport parlementaire enquêtecommissie aardgaswinning Groningen, dated 24 februari 2023, https://www.tweedekamer.nl/Groningen/rapport

5 Risk management and mitigation

This chapter describes in more detail all additional research and preventive and corrective measures that were identified in step 4 following the risk assessment as presented in the previous chapter and Appendix D: Risk assessment to mitigate the risks.

5.1 Additional research

In this paragraph we aim to specify the content of the research (scope, analyses, measurements, etc.), and, where relevant, link to the research in Part 2 of this report. Ultimately, the additional research is essential to reduce uncertainties and to take appropriate measures. The identified additional research can be related to:

1. well integrity and materials;
2. geology and cavern integrity, and
3. generic research

and is grouped accordingly in the following sections. Both 5.1.1 and 5.1.2 conclude with a start on the required list of well and cavern acceptance criteria respectively. The required additional research will result in substantiated values for these criteria.

5.1.1 Well integrity and materials

The additional research topics on well integrity and materials are:

- Additional blow-out modelling to study the spatial (*x,y,z*) extent of the effect (temperature over time) at the surface using various cavern designs (sizes, depths and pressures) and weather conditions (i.e., wind, humidity etc.). The aim of this additional research is to define an aerial model that maps the spread of a gas cloud following a blowout and delineates danger zones for potential hazardous events as released hydrogen gas can cause fires and explosions, resulting in loss of life and environmental damage.
- Regarding the surface installations like pipelines, we advise to use the research carried out in the frame of KEM-29. Additional research should be carried out on the expected extreme temperature and pressure conditions and whether or not these remain within the safety limits of H_2 certified materials. Here, the outcome of the blow-out modelling should be taken into account in order to minimize the impact on surface installations.
- Further research (including desk studies, numerical modelling, lab experiments and field or pilot tests) on salt creep and integrity in the vicinity of the last cemented casing at local temperature and pressure conditions should be carried out, in particular over long time scales and during cyclic loading. The intention should be to better constrain the operational rules and chimney height in order to minimize the risk of casing overstretching.
- In line with the casing overstretching, maximum tensile stresses in all well materials for both casing and brine strings (including steel alloys, elastomers and seals) should be determined and tested using H_2 under cyclic temperature and pressure conditions. This should be done for “normal” conditions during operation and extreme conditions in case of a blow-out. According to DBI (2017), the API steel alloys typically used in UGS facilities are not tested specifically for the storage of H_2. Additionally, standards and rules for the selection of materials for underground storage of H_2 and operational experience seem not existing or available (DBI, 2022). Hence, a certification protocol for H_2 and salt-cavern-proof materials must be established.
- Following the risk analyses and KEM-18 (van Oort, 2022), the highest uncertainties regarding the well design are related to “Wells that have experienced significant cyclic loading leading to the formation of a micro-annulus, in the presence of corrosive gases and brines that can deteriorate

casing and cement". It seems unavoidable that micro annuli will form at the casing / cement / rock interfaces (especially when using ordinary cement) and thus research should be focused on how to prevent this and how to correct for these circumstances if they take place. Thus, alternative materials should be tested with H_2 and H_2S under cyclic temperature and pressure conditions. Again, this should be done for "normal" conditions during operation and extreme conditions in case of a blow-out. Preventive and corrective measures are presently known, though success cannot be guaranteed so further research is advised on micro annuli treated with special materials (resins, silicates etc., or biological treatment), use of deformable or self-healing materials (like salt) and casing expansion, see also KEM-18 (van Oort, 2022) for additional research.

- Specific research on the weakening of all well materials as a result of interaction with H_2 and/or H_2S should be continued, not only on the bulk properties but also on the microstructures (e.g., Part 2) to better understand the underlying processes over longer time scales. The ultimate goal should be to make a substantiated prediction of the changes in corrosion resistance and sealing effectiveness over a longer time period.

In general, the Authorities need to specify the maximum allowable leak rate of H_2 in kg/day. Roordink et al. (2022) and Buzogany and Meinecke (2023) considered a leak rate of ± 50 l/d at in situ conditions acceptable based on natural gas, but it is assumed that a test criterion adapted to hydrogen needs to be defined (Roordink et al., 2022). Furthermore, the question remains whether this leak rate is acceptable on the long run?

5.1.1.1 Well acceptance criteria

After a well is drilled it needs to pass certain acceptance criteria before mining the cavern. This will include specific research before drilling. The list below is a start and should be part of a subsequent study to set exact limits based on research. Finally, the opinion of an independent advisory committee of experts is required to define reasonable criteria based on best practices.

The main criteria are:

- Are all materials in place H_2 and H_2S certified?
- Has a double casing been set?
- A well integrity test has to be performed to assure the leakage rate is well below the permitted value (e.g., coMIT Roordink et al., 2022, and tests described in Lit Review)
- The leak test must be designed to provide the most accurate estimate of the possible leak. This requires a specific protocol for conducting and analysing the test, which must take into account the transient phenomena generated in the cavern by the large increase in pressure at the start of the test (Van Sambeek et al., 2005)
- Cement bonding tests have to be performed to assure a sound bonding between casing, cement and rock (assuming the composition of the cement is able to withstand large pressure and temperature variation and the presence of H_2 and H_2S)
- Installation of an underground automatic safety valve (designed and tested for H_2), see 2.3.4 Literature study), both in the production casing and in the protective annular filled with brine.
- …

Additionally, for existing wells, key risk factors regarding sealing behaviour of materials and interfaces in boreholes appear to be (KEM-18):

- Well age and type
- Working/cyclic load history
- Absolute in-situ temperature environment
- Geological, geomechanical and geochemical environment which the well is exposed to over time

- Wellbore deviation (only accept near vertical wells)

Obviously, these risk factors should be researched once a site is selected and resulting risks should be minimized, or, in case of unacceptable risk, existing wells should be avoided. Following up on the recommendations of KEM-18, it may be useful to re-enter and log the well using latest techniques (e.g., spectral noise logging) to investigate the flow behind the casing by default, and remediate any confirmed annular flow accordingly when flows exceed acceptable norms.

5.1.2 Geology and Cavern integrity

The additional research topics on geology and cavern integrity are mentioned below:

- A good understanding of the Zechstein salt in general and the large-scale internal structure of salt domes in the Netherlands is crucial, meaning the presence, fraction, thickness, extent and distribution of anomalous zones, (anhydrite stringers, carnallite layers). For this reason, it is recommended that seismic imaging techniques be improved to better resolve the internal structure of salt. Joint approaches with constraints from GPR, core analysis, and numerical modeling of the salt dome evolution may massively improve the robustness of the current imaging and interpretation techniques. Therefore, new research should be carried out to improve the existing methods.
- and collecting of new cores in salt domes should be encouraged to increase the knowledge base of the internal structure of Zechstein salt in the Netherlands.
- We also encourage a more systematic assessment of the second phase impurities and grain size characteristics of the Zechstein units as it has strong implications on the upscaled creep properties. The effect of heterogeneities should be taken into account in experiments, field tests and digital-twin simulations at all scales including change in rheology of the second phases due to interaction with H_2 and H_2S.
- To close the upscaling-gap between the creep properties obtained on sample and cavern scale, systematic creep tests on larger samples and calibrated, numerical creep test of digital twins may provide important constraints on intermediate scales next to creep tests and permeation tests in bore holes, and (small) caverns.
- Regarding the creep properties of rock salt, additional research is required related to recrystallization and grain-size reduction near the cavern wall due to temperature and stress changes affecting the (local) creep/rheology. This will improve the understanding of the damage evolution.
- The abiotic H_2S production in dry conditions should also be researched including the effect on the purity of H_2 (as a result of the mixing of H_2S and H_2 under normal and operational circumstances).
- The relation between microstructural evolution and permeation behaviour at operational conditions needs further research.

The knowledge gain regarding the above-mentioned research items (rheology, permeation, heterogeneity and internal structure) enables better-constrained generic geomechanical modeling scenarios and thus improved cavern designs (shape, distance, reaction surface, etc.). However, optimization of the cavern cluster design can only be performed once a site has been selected and detailed investigation of the local geology has been carried out.

Furthermore, the minimum and maximum expected required storage capacity over time has to be determined by additional research using scenario modelling in order to design the cavern cluster most efficiently (regarding size, capacity and timing of mining).

Combining the geological and geophysical constraints on the cavern cluster design enables further research like sensitivity analyses on characteristic locations in the salt dome prone to (micro)seismicity.

Obviously, models should be tested and validated by lab and field tests (see also 4.1 and 4.2, Part 1: literature review).

5.1.2.1 Cavern acceptance criteria

After a cavern has been developed according to the best salt mining practices and the required volume criteria the cavern must be tested by default before storing hydrogen by means of tightness and permeability tests. The list below is a start and should be part of a subsequent study to set exact limits based on research. Finally, the opinion of an independent advisory committee of experts is required to define reasonable criteria based on best practices.

- Quality control of the shape of the cavern
- Control of the exact location of the cavern with respect to the surrounding caverns (QC of the cavern cluster)
- Verification of the presence of heterogeneous layers, including thickness and composition
- Verification of the sump conditions with respect to the possibility of H_2S production and the suspected pace of the process

Additionally, for existing caverns, key risk factors appear to be:

- The age of the cavern and its shape
- The history of pressure in the cavern
- The absolute in-situ temperature environment
- The former use of the cavern. Has it been used for storage and might that lead to enhanced geochemical / microbial risks
- The geological, geomechanical and geochemical environment to which the cavern is and will be exposed to over time

5.1.3 Generic research

Part of the required research is not directly related to well or cavern integrity and is therefore characterized as “generic”. The main generic research topics are mentioned below:

- The risk analysis itself has to be repeated for each and every cavern (or at least cavern cluster) to assure that all relevant stakeholders with their own aims are included. This requires not just the risk analysis itself but also communication with all stakeholders concerned and a common agreement on the preventive and corrective measures beforehand.
- Additional research is needed to reduce uncertainties regarding the social embeddedness of underground activities in general and hydrogen energy storage in particular. This requires:
    - Proactive communication about risks, research and measures. (Too) late communication is bad communication.
    - Specific regulations, norms and standards for hydrogen energy storage must be developed based on proper research.
    - Good understanding of not just the physical but also the psychological safety of the public.
    - An open-minded discussion about the benefits related to the burdens for those involved.
    - A reversed burden of proof in case of negative consequences for a stakeholder.
- Directly related to both topics: (future) underground on-shore energy storage is depending on a transparency regarding (site specific) risks and measures taken, and positive social embeddedness.
- There should be no responsibility gap due to stacked mining. Therefore, scenario modelling of various critical scenarios to test regulations and determine duration of responsibilities should be researched based on real cases, especially if interaction with other underground storage facilities such as CAES, CO_2-storage and brine processing could take place once the site is selected.

- Finally, the risk of surplus extraction of brine has to be researched in more detail. An evaluation of salt production versus chlorine demand (in NL and EU) is required.

5.2 Preventive measures

In this paragraph we aim to specify the content of the preventive measures, and, where relevant, link to the specific parts in Part 2 of this report. The identified preventive measures can be related to:

1. well design;
2. cavern design, and
3. generic measures

and are grouped accordingly in the following sections. N.B.: An important part of the preventive measures is conditional as they depend on the results of the additional research that still must be performed.

5.2.1 Preventive measures regarding the well design to reduce risk

The preventive measures regarding well design are:

- The use of H_2 and H_2S certified material to guarantee the highest quality of BOP, pressure gauges and safety valves, X-mas tree, tubing/casing, pipeline and packers. Both gases are known to be (extremely) corrosive and all equipment has to be as persistent as possible, especially the parts that cannot be easily controlled / repaired or exchanged. The use of corrosion protection should also be considered, certified material however is a preferable solution.
- All equipment and materials must be designed for low temperatures (sub-zero temperatures can be reached in the well and cavern in the event of very rapid depressurization, as in the case of a blowout). The outflow of hydrogen and resulting decrease in pressure leads to a considerable decrease in temperature, especially when uncontrolled. This can be influenced by confining the flow of H_2 in normal conditions, however the material should be able to withstand the extreme conditions during a blow-out. The use of deformable metals might be considered for some parts.
- Obligatory materials quality control to ensure the most appropriate materials are used. The company responsible for the cavern production must record all information about all used materials, including maintenance. The materials must be in accordance with the norms and standards for hydrogen storage.
- The use of non-brittle containing replacement material for cementing the casing to ensure the well can cope with the (extreme) temperature fluctuations. Instead of normal (Portland) cement, (non-nitril) elastomers or self-healing materials (like natural salt or shale) should be used pending the results of additional research.
- The use of non-sulphur containing replacement material for cementing the casing. Instead of Portland cement, containing a considerable amount of sulphur, other materials should be used to ensure minimal (potential) production of H_2S.
- The introduction of a larger diameter of the casing to minimize the temperature fluctuations during normal (filling and emptying) circumstances. Furthermore, a larger diameter will decrease the duration of a blow-out and the thickness of the damaged zone at the cavern wall.
- Obligatory monitoring of the well consisting of:
    - H_2S monitoring system (beyond well site) to ensure safe working conditions for the operators and the surrounding area.
    - H_2 monitoring sensors in the X-mas tree, vertical tubing / casing and pipeline to monitor excess leakage of H_2
    - periodic monitoring of the integrity of the X-mas tree both visually and by using gamma ray equipment
    - both digital automated and analogue sensors.
- Obligatory periodic quality control of:

    - Casing wall thickness to verify the corroding effect of H_2 / H_2S and to ensure the casing still meets the requirements;
    - "Cement" bonding to verify the potential presence of micro annuli and to ensure the required tightness of the material (e.g., cement bonding log);
- Preferably avoid old wells and caverns (history of cavern pressure and used materials not well known). The progressive redistribution of stresses around caverns due to salt creep is such that fracturing is possible at lower pressure for an aged cavern than for a young cavern (Djizanne et al., 2014a). All existing caverns lack the required H_2 / H_2S certified material and do not comply with the determined preferred design.
- Double casing to reduce the risk and effect of casing overstretching and the effect of leakage in the vertical tubing / casing.
- Pressure gauges in the X-mas tree, vertical tubing / casing and pipeline. These gauges must be combined with automatic safety valves in case a maximum allowed figure (pressure, yield etc.) is exceeded.
- Overhanging blocks at the cavern wall (anhydrite stringers for instance) need to be removed, whenever possible, before the operation of H_2 storage starts. The presence of these blocks increases the risk of losing well integrity by roof and block falls (Fortier et al., 2006) as they might damage the production casing and lead to loss of control.
- The brine strings need to be removed before the operation of H_2 storage starts. The presence of brine strings increases the risk of losing well integrity by roof and block falls as they might damage the strings and lead to loss of control
- Pressure relief valve (PRV) for a worst-case scenario when pressure gets near lithostatic pressure at the casing shoe.
- Back-up system for the X-mas tree (mirrored system) and part of the partitioned pipeline system to ensure the continued production of the cavern.

5.2.2 Preventive measures regarding the cavern design to reduce risk

The preventive measures regarding cavern design are:

- Improved cavern design based on "good salt mining practice", eventually leading to a good rock mechanical envelope. The main aspects are:
    - avoid a flat roof to guarantee better rock mechanical properties
    - (try to) avoid interlayered formations as this will weaken the cavern and might give rise to increased production of H_2S
    - avoid a large diameter of the roof which fits the advice to construct small diameter caverns
    - the construction of a chimney (below the last cemented casing shoe, above the cavern roof) to minimize the risk for casing overstretching
- The modelling of the cavern design, including thermodynamical and geo-mechanical modelling, to ensure the best shape for hydrogen storage before the start of the construction
- Site specific creep model using the information from the exploratory drilling, introducing both the site-specific rheology and the operation (especially of loading and unloading, minimum and maximum pressure, work load and predicted flow)
- Field tests (permeability tests, pressure observation test [POT] and/or outflow test after drilling) and additional POTs after cavern leaching
- Preferably use newly developed caverns (according to an optimal rock mechanical envelope) instead of existing caverns with unknown history, including hydrocarbon source for microbes
- The determination of the minimum cavern pressure through numerical computations is required to limit cavern creep closure and related subsidence

- A solid understanding of the local stratigraphy for the exact depth decision, which might differ for each cavern and update accordingly when new data comes in
- Detection of heterogeneities like non-halite layers and if necessary, avoiding of these to minimize risk of roof and block falls and to avoid sulphate sources eventually leading to unwanted H_2S production
- The distance to the (expected) domes edge should be well guarded (no cavern close – at least 400 m – to the domes edge) by developing and maintaining an up-to-date geological model including uncertainties
- No storage activities in or near an active fault zone to minimize the possibility of induced seismicity
- Prevent contact of undersaturated brine with the roof during the operational phase to keep the roof in its best condition
- Periodic sonar survey to control the cavern shape and most vulnerable parts, specifically after a seismic event that might be classified as a rock fall
- Monitoring of subsidence by INSAR & surveying measurements before mining and during operation
- Seismic monitoring (natural and induced seismicity) including baseline measurements, seismic response plan and, furthermore, modelling of expected seismicity
- Stabilize the geochemical circumstances in the sump (in order to minimize the production of H_2S) by lowering the pH and increasing the iron content
- Avoid high temperatures (> 80 degrees) because of the abiotic sulphate reduction
- Avoid presence of hydrocarbons as they are perfect fuels for H_2S production. This will probably lead to no use of former hydrocarbon storage caverns
- Preventing undersaturated brine from coming into contact with the roof during operation, which would reduce the height of the chimney and increase the risk of overstretching the casing shoe.

5.2.3 Generic preventive measures to reduce risk (external source)

Part of the preventive measures is not directly related to well or cavern integrity and is therefore characterized as “generic”. The generic preventive measures are mentioned below:

- Four-eyes principle. The complete operation of hydrogen storage requires permanent quality control / quality assurance to compensate for the human factor
- Construction, quality control and maintenance protocols. The material used for the hydrogen storage, ranging from pipelines to casing and X-mas tree, is susceptible for degradation due to the corrosive nature of H_2 and H_2S. Protocols need to be developed and strictly followed during construction and operation
- Maintenance plan and regular maintenance and check, e.g., on the integrity of the well, surface systems and pipeline. The maintenance protocols must lead to obligatory maintenance plans
- Periodic leak test / tightness test (e.g., every 5 years). Leakage of H_2 can hardly be prevented but should be minimized. The allowable rate of leakage (amount per day) must be determined and afterwards periodically controlled and – if necessary – restored
- Monitoring of microbial activities, monitoring of geochemical composition. The conditions in the sump need to be monitored – preferably by continuous monitoring, otherwise by periodic sampling – to ensure that the production of H_2S is slowed own as much as possible
- Mandatory status-report (starting every year). Transparent report of the hydrogen storage with all information available (including production / accidents / incidents / leakages and taken measures). The information must be tailored to the knowledge and capacity of the stakeholders. Open communication and regular meetings with all operators involved (including independent chairman, e.g., SodM)

- Rapid response plan. Every hydrogen storage cavern requires its own rapid response plan for its specific circumstances. Furthermore, a rapid response plan should be practiced periodically
- Simulation of a blow-out (part of the permitting). Site specific (regarding the final design and the direct surroundings) model to simulate the effect of a blow-out and the consequences for the surroundings
- Regulations for all operators of underground activities regarding the arial extent and the duration of their responsibility with respect to damage. Special attention is required for stacked mining to ensure a potential responsibility gap is prevented. Another topic of attention: which party is taking over the responsibility in case of bankruptcy
- One overall geological model for all operators to assure all operators are aware of the activities around them (horizontally and vertically) and are aware of the possible effect of stacked mining
- Speed limitation on the flow rate (T-limit) / production rate to remain within temperature and pressure safety limits (flow restriction), e.g., by combining caverns during storage and production
- Transparent, pro-active and personal communication with all stakeholders (including public, politics and press) and other operators about e.g., the results of the test / first cavern, all taken preventive measures, any incidents and all taken corrective measures
- Try and find a possibility to compensate affected stakeholders by direct involvement (minority shareholders) or financial compensation ("both burdens and benefits")
- In case of accidents or damage implement the method of reversed burden of proof, shifting the responsibility of proving a fact from the affected stakeholder to the operator
- Assign the hydrogen storage and associated infrastructure as "vital infrastructure" and act accordingly. This will and/or might require:
    - a fended and secured area, including surveillance cameras
    - a no-fly zone and no local satellite footage
    - the location of critical infrastructure well above sea-level (surrounded by a dyke) or in a contained environment
- Avoid caverns near residential areas to minimize the number of stakeholders affected and to minimize the effect of – almost certain – negative public opinion
- Review the sensitivity of the intended location for all potential natural disasters
- Adhere to the general safety regulations and fire-prevention measurements for hydrogen installations and train local fire fighters for operations on site
- With respect to the operation have
    - (back-up by) remote-controlled operation via an internal network (no internet)
    - manual controls requiring double authorisation
    - analogue pressure and temperature gauges at critical locations (double system)
    - sufficient (vital) spare parts to ensure a high percentage of "up-time" and a direct active response to critical situations

With regards to the sole risk not directly connected with the operation phase – the risk of surplus extraction of brine during construction – the following preventive measures have to be taken:

- Salt production should preferably be combined with the construction of H_2 storage caverns. Any additional salt production will increase the volume of high-quality salt to the market
- Be one of the first appliers ("introducer") of H_2 storage in salt caverns in Europe. As H_2 storage is considered to have an important role in the (stability of the) future energy market the Netherlands is not the sole nation considering underground storage. Having an industry that is used to process a high volume of vacuum-salt is an advantage that should not be underestimated
- During salt mining the extracted brine should be re-used in existing salt caverns for optimal production. This will have an important effect on the quality and value of the extracted salt. It requires an advanced planning of salt solution mining

- As a last resort have temporary storage available like a terminal

5.3 Corrective measures

In this paragraph we aim to specify the content of the corrective measures, and, where relevant, link to the specific parts in Part 2 of this report. The identified corrective measures can be related to:

1. operational corrective measures;
2. organizational corrective measures;
3. repair and restoration, and
4. generic corrective measures

and are grouped accordingly in the following sections.

5.3.1 Corrective measures (operational)

The operational corrective measures are:

- change of the average cavern pressure (i.e., higher) to reduce the cavern creep closure and the rate of subsidence
- adapt the storage operations to minimize additional thermal stresses at the cavern wall, e.g., by reducing pressure rate during production phases.
- sweetening of the H_2 gas in an industrial sweetener to improve the quality of the H_2 according to the requirements
- restoring the preferred geochemical condition in the sump by correction of the pH and increase of the iron concentration (to immobilize the sulphur)
- automatic release of the pressure by controlled production of H_2 or even flaring of H_2 as a last resort
- temporary partial shut-down of the pipelines and repair the damaged part
- fire extinguishing according to the rapid response plan, partly automated (sprinkler), partly by the deployment of municipal and regional fire brigades
- replace the on-site normal operation by remote-controlled operation in case on-site operation is impossible to continue

5.3.2 Corrective measures (organizational)

The organizational corrective measures are:

- direct actions according to the rapid response plan, including fire alarm and an immediate evacuation when necessitated
- open and transparent communication with the municipal and regional fire departments for direct support
- transfer of the responsibility for the operation to remote-control operational room

5.3.3 Corrective measures (repair / restore)

The corrective measures with respect to repair / restore are:

- placement of a small liner directly followed by the injection of closing material
- treatment of the micro annuli behind the casing wall using special materials (resins, silicates etc., biological treatment) to restore the quality of the cement
- treatment of the cement and all other installation parts prone to or affected by H_2 / H_2S deterioration with special materials (resins/silicates, biological agents etc.)
- use of deformable or self-healing materials and casing expansion
- replacement of the production casing and the brine string (if any), or instead making use of a liner
- packer or plug the existing damaged (beyond repair) well and drill a new well

- temporary partial shut-down and repair of the pipeline

5.3.4 Generic corrective measures

Part of the corrective measures is not directly related to operations or organization, or requiring repair / restore activities and is therefore characterized as “generic”. The generic corrective measures are:

- transparent and personal communication about all taken corrective measures with all stakeholders involved (like public, politics and press and other operators)
- in extreme cases, abandon the cavern after producing all remaining H_2 and replacing it by brine to control the internal pressure, e.g., to minimize the creep closure and the subsidence
- financial compensation for any damage as a result of the hydrogen storage in salt caverns, based on reversed burden of proof, shifting the responsibility of proving a fact from the affected stakeholder to the operator
- mandatory insurance policy for all operators concerned to ensure the financial capability to compensate for any damage. This requires an adaptation in the Law.
- regulations for the take-over of the responsibilities in case of a bankruptcy of an operator. This may be a State-owned institute or commission specifically created for H_2 storage in salt caverns. This requires an adaptation in the Law
- in case of surplus extraction of brine replace the use of evaporation and rock salt (both of less quality) by the vacuum salt for food and road salt
- injection of brine in depleted gas reservoirs in case of surplus extracted volumes of brine and no commercial use possible

5.4 Description and classification residual risk matrix

Implementing all preventive and corrective measures results in significantly lower risks (see Figure 335) compared to unmitigated total risk matrix. However, there are still risks in the red zone which should not be present. These are all non-technical risks related to the uncertainties about safety and consequences of the storage in salt caverns threatening any (future) on-shore energy storage development, concerning the following stakeholders:

- The operator (1)
- Energie Beheer Nederland (9)
- Gasunie New Energy / Hystock (12)
- Gasunie Transport Services (nitrogen storage, 13)
- Gasunie / Energystock (14)
- CORRE Energy (future CAES, 23)
- Nobian Salt production (aim II, "*We are exploring how we can store green energy in our salt caverns. We're actively working to produce greener chemicals, including hydrogen, and are committed to stimulating and growing a circular economy*", 27)

Besides, there are still many risks in the orange zone, which should, preferably, be avoided.

These will likely reduce when a site-specific assessment will be performed, the number of stakeholders is minimized and specific research is carried out as depicted in 5.1.

4*3 riskmatrix mitigated		**Consequences**		
		1	**2**	**3**
Chance	**3**	17.2; 18.2; 19.2; 20.2; 21.2	1.9; 2.2; 4.2; 5.2; 6.2; 7.2; 8.2; 9.2; 10.2; 11.2; 12.2; 13.2; 14.2; 23.2; 26.2; 27.2; 29.2; 30.2; 31.2; 32.2; 33.2; 34.2	
	2	10.4; 13.5; 15.3; 16.3; 20.5; 24.3 ; 29.1; 30.1; 30.3; 31.1; 31.3; 32.3; 33.1; 33.4; 34.8; 35.6	1.8; 1.12; 1.17; 1.18; 2.5; 3.2; 8.4; 8.6; 11.4; 12.5; 14.5; 22.1; 23.4; 23.6; 26.4; 27.5; 27.6; 28.1; 29.5; 34.6; 34.7; 35.4; 35.5	1.24; 9.6; 12.6; 13.6; 14.6; 23.8; 27.8
	1	1.2; 1.4; 1.10; 1.11; 1.15; 1.19 1.20; 1.21; 2.6; 8.5; 9.4; 10.1; 11,5; 11,6; 12.4; 13.4; 14.4; 18.3; 19.3; 21.3; 23.5; 26.5; 29.4; 34.4; 34.5; 35.3	1.1; 1.3; 1.5; 1.14; 1.16; 1.22; 1.23 ; 1.25; 2.7; 4.1; 4.3; 5.1; 5.3; 6.1; 6.3; 7.1; 7.3; 9.1; 9.5; 12.1; 13.1; 13.3; 14.1; 15.2; 16.2; 17.1; 17.3; 18.1; 19.1; 20.1; 20.3; 21.1; 22.2; 23.7; 24.2;	1.6; 1.7; 2.1; 2.3; 3.1; 8.1; 8.3; 9.3; 10.3; 11.1; 11.3; 12.3; 14.3; 15.1; 16.1; 23.1; 23.3; 24.1; 26.1; 26.3; 27.1; 27.3; 32.1; 34.1; 34.3; 35.1; 35.2
	0	1.13; 20.4; 21.4; 25.2; 29.3; 33.3		

Figure 335. Mitigated risk matrix of all risks considered, the numbers refer to the risks for each stakeholder presented in Chapter 4 and Appendix D: Risk assessment.

6 Recommendations

6.1 General

The total life-cycle of a salt cavern consists of several phases:

- the process of the design (pre-execution phase),
- the salt mining itself (execution phase),
- the storage – cyclic injection and production – of the gas / liquid (operation),
- the abandonment (decommissioning)
- and the monitoring afterwards (post abandonment monitoring).

The performed semi-quantitative risk assessment focusses solely on the period of hydrogen storage, i.e., the operational phase (the storage of the gas / liquid). All other phases are political/social/financial (pre-execution phase) or related to the salt cavern itself (design, execution, decommissioning, and post-abandonment monitoring) and not directly referring to hydrogen storage.

This does not implicate that the results of the risk assessment solely apply to the operational phase. The necessary additional research and resulting preventive measures are primarily part of or affect the pre-execution ("Plan") and execution ("Do") phases. During the design process and the construction of the salt caverns planned for future H_2 storage all recommendations with respect to research and measures should be taken into account.

Cherry-picking in research and measures directly influences the result of the risk assessment. The residual risk after considering all reported measures is the cumulated effect of all measures, preventive, and corrective. In other words, if any of the measures is not implemented this might affect the risk assessment and the resulting residual risk, depending on the proverbial "weight of the measure".

6.2 Preferred location

At the request of the Ministry of EZK the current risk analysis is generic. As a result, all possible combinations of risks / stakeholders have been taken into account, situated on the least preferable location. the results therefore represent a worst-case scenario. All site-specific information still needs to be gathered and subsequently processed in the actual risk assessment for any salt cavern planned for future H_2 storage. Additionally, as mentioned in the introduction, the exact number of caverns to be exploited remains unknown, but 10s of caverns are projected (van Gessel et al., 2021c), while the total number of accidents in gas storage caverns is relatively low. This results in a risk assessment with an approximated probability of occurrence as any statistical risk analysis is not straight forward due to a lack of sufficient data.

The preference for a hydrogen storage cavern site is primarily determined by the presence of a suitable salt structure. Whether a salt structure is suitable depends on the results of site-specific research, see 6.2.1.

For the comparison of multiple suitable sites, the direct surroundings should be considered to determine the site with the least challenging activities nearby, see 6.2.2.

Last but not least, the number of affected stakeholders should be as low as possible, see 6.2.3.

6.2.1 Site specific research

In case of planned H_2 storage in a particular salt dome the following information needs to be gathered and/or elaborated:

- 3D geometry of the salt dome and overburden, natural faults, and the salt support below and adjacent to the dome,
- salt-internal structure and rheology,
- other rock properties and uncertainties,
- (natural) seismicity,
- salt cavern design (geometry, depth and anticipated loading),
- history in the case of an existing cavern,
- the H_2S forming potential.

6.2.2 Surroundings

Apart from the salt dome information also the direct surroundings need to be described and taken into account, both above and below the surface, like:

- the situation of the caverns in the direct vicinity (under development, used for storage of natural gas / hydrogen, used for CAES),
- infrastructure above and below ground level,
- distance to businesses and inhabitants,
- the use of the subsurface (e.g., geothermal energy, drinking water potential, oil or gas exploitation) etc.

Furthermore, models of hydrogen storage caverns affecting non-H_2 storage caverns were included in the research phase as a reference study, however scenarios should be updated once locations are known.

N.B.: This listed required information is not meant to be exhaustive but solely gives an insight in the amount of data needed to make the risk assessment site specific once the location is known.

6.2.3 Affected stakeholders

The main recommendation concerning stakeholders is that for the preferred location of the cavern(s) the number of affected stakeholders, or actually associated risks, should be as low as possible.

The main stakeholders with respect to residual risks (*the "threat for (future) on-shore energy storage in salt caverns" not taken into account*) that should be avoided, if possible, are:

- locations of drinking water extraction and strategic drinking water supply. The risks are depending on the distance between the site of the salt cavern and the boundary of the area of groundwater protection.
- locations of water extraction for industrial use in production. The risks are depending on the distance between the site of the salt cavern and the site of water extraction.
- residential areas with a high number of potentially affected inhabitants / landowners within a reasonable distance from the storage caverns.
- protected areas of natural reserves (Natura 2000[1] and NNN[2]).
- vital infrastructure both above and below the surface, like main energy lines, main water pipelines, highways and main waterways.

[1] Natura 2000 is an European network of protected natural reserves. In these reserves certain animals, vegetation and natural habitat are protected to preserve biodiversity.

[2] NNN stands for the Natural Network of the Netherlands, formerly known as EHS (Ecologische Hoofdstructuur = ecological main structure). It is a network in the Netherlands where nature takes precedence over other activities.

6.3 Main research topics and measures (preventive and corrective)

As we have generated a comprehensive generic risk assessment, the resulting number of research topics and measures – preventive and corrective – is large, maybe even overwhelming.

We therefore decided to rank the research topics and measures in the best way we could. We like to emphasize that all research and measures should be taken into account as the residual risk matrix is a result of all research topics and measures combined, see 5.4. Furthermore, we do want to emphasize that the top 5 lists might be (*or actually have been*) influenced by the bias of the scientific and geological background of (almost) all participants.

The main research topics:

- Research of the salt dome internal structure, including anomalous zones. This includes the improvement of specific tools for the investigation of internal salt stratigraphy and heterogeneity;
- Creep research (grainsize) and durability of the salt, including transport properties, damage and healing of salt;
- Research on prevention of micro annuli at the casing / cement / rock interfaces;
- Research of materials interacting with hydrogen and/or H_2S;
- Development of high-quality mechanical integrity tests (MIT) (to understanding the risks of fracturing induced by frequent cycles and or formation of micro-annuli)

The main preventive measures:

- Select the best location and configuration (shape and depth);
- Use of H_2 and H_2S certified material (including packers and valves);
- Minimum preconditions for H2 storage cavern (well test / acceptance criteria);
- Open, pro-active communication with stakeholders (public, politics and press) and other operators;
- Regular cavern and well tests, including sonar measurements, high quality MIT and cement bonding log (frequency to be determined) and safety valve tests (SSV);
- Implement strict regulations (e.g., with respect to stacked mining) and strengthen the role of the regulator;

The 5 main corrective measures:

- Actions according to the (to be developed and implemented) rapid response plan;
- Adaptation of the storage properties (e.g., pressures (min/max), max. yield);
- (micro annuli and material) treatment with special materials (resins, silicates etc., biological treatment);
- Controlled production / flaring of H_2;
- Open communication with stakeholders (public, politics and press) and other operators.

6.4 Specific recommendations following research Part 2

The vast 2D/3D geomechanical modelling and sensitivity study clearly indicate favourable over unfavourable configurations of salt caverns for hydrogen storage and should therefore be recommended once site is selected. Additionally, optimizing extraction ratio should be considered as it can minimize the impact on the surface. In the case of a real project, the geology and properties of the rocks will have to be precisely defined, both through studies on a microscopic scale (characterisation of the different types of salt and the average grain size, for example) and on a dome scale. Finally, realistic modelling on the scale of the caverns can be carried out to optimise the characteristics of the caverns, their positioning, and the operating method (minimum pressure, maximum rate of pressure change, etc.).

Additionally, there is a clear need for further research into: 1) calibration of transient creep law for Dutch salt, 2) Analysis of the stability of a cluster of caverns that could be leached asynchronously, and; 3) Validation of the existence of a heat exchange coefficient on the cavern wall and possible calibration of this parameter in the case of hydrogen.

Regarding geology, large-scale anomalous zones within salt domes can be partly assessed by the available cores and seismic data, however these are still limited. Therefore, further research should be carried out on seismic processing to improve the imaging of salt internal structure. The imaging task can be improved in a joint approach with GPR surveys from boreholes. Additionally, 3D geodynamic modelling of the formation of the salt dome offers powerful opportunities to better constrain possible interpretations of the of the salt dome's internal geometry and overall shape. It also helps to constrain dome dynamics and identify associated brittle zones in the side and overburden.

The question of whether a hydrogen cavern field with cyclic loading induces stresses in the adjacent sedimentary rocks of the dome and therefore could be a possible source of induced seismicity is primarily a location-dependent question. This study's research using dome-scale 3D thermo-mechanical modelling with a generic salt dome suggests that placing a cavern field in the centre of a dome does not affect overburden stress as much as a cavern field closer to the flank of the dome. However, it seems that it is not only the distance to the flank that matters, but also the general dynamics of the dome, which is also related to the volume of the salt source layer. Therefore it is recommended to (1) constrain the geometry and source layer of the salt dome as well as the internal heterogeneous structure and (2) perform site-specific 3D thermo-mechanical modelling to help constrain the natural dynamics of the salt dome in order to find an optimal location for the cavern field within the dome.

Our research shows that heterogeneous rock salt with mega grains and second phase impurities like anhydrite can exhibit significantly different creep behaviour compared to homogeneous rock salt. For example, a large volume fraction of halite mega grains causes a significant reduction in creep rate compared to pure halite. Given the implications for salt-cavern engineering, we recommend (1) quantifying the volume fractions of second phase impurities and halite mega grains at micro- (thin-sections or µ-CT) and macro-scales (cores or outcrops in salt mines); (2) conduct and validate digital twin simulations of creep experiments to facilitate the upscaling of the creep properties of multi-phase rock salt, (3) conduct more research on the creep properties of the individual heterogeneous rock salt phases (e.g., anhydrite) to gain a better understanding of the combined aggregate creep, and (4) to account for heterogeneous rock salt in THM-coupled numerical simulations at cavern- and dome-scales using halite volume fraction based parametrisations.

Concerning the geochemical processes, we recommend to: 1) Perform laboratory studies using analogues and case studies to simulate subsurface conditions under well-defined boundary conditions. These experiments should provide essential kinetic rate data; 3) Implement in-situ testing and monitoring during hydrogen storage to better understand the actual processes and reactions occurring in the subsurface. This can include measurements of geochemical, physical, and microbiological changes. 4) Incorporate advanced microstructural analysis techniques, such as cryo-Scanning Electron Microscopy or µ- or nano-Computer Tomography, into research efforts. Utilize these methods to visualize and study biotic and abiotic processes in rocks, casing materials (cement and steel), and other components of the storage system. These analyses will aid in understanding reaction kinetics and the impact on THMC (Thermo-Hydro-Mechanical-Chemical) properties. 5) Continue to develop and refine geochemical models to predict long-term behaviour, mineral dissolution, precipitation reactions, and transport dynamics during hydrogen storage. Utilize data obtained from laboratory experiments and in-situ monitoring to improve input parameters for these models. Consider employing pore network modeling approaches for a deeper understanding of transport processes within the reservoir.

6.5 Cavern field development and strategy

All operations in the subsurface are being regarded with utmost interest, both politically and publicly. Therefore, the development of H_2 storage in salt caverns needs to be as safe and least disturbing as possible. Any mitigation for foreseeable risks that can be taken, should be taken, as this will minimize the main remaining risk "threat for (future) underground on-shore energy storage".

Therefore, the development of the cavern field should be well considered. Our recommendations with respect to the cavern field development are:

- Location.
  It all starts with the location. As mentioned, the preferred location depends primarily on the geological circumstances, determined with site-specific research, see 6.2.1. Furthermore, the number of affected stakeholders should be minimized with special attention for the main influential stakeholders, see 6.2.3;
- New caverns.
  Preferably construct new caverns and avoid old wells and caverns. All existing caverns lack the required H_2 / H_2S certified material and might not comply with the determined preferred design. Furthermore, all existing caverns have, as far as we know, traces of remaining hydrocarbons which fuels the production of H_2S;
- Starting with small design.
  There are still many questions about the material, the design, the reaction of the salt etc., see 5.1. Therefore, it is recommended to start with a relatively small-scale cavern for which the results of storing and producing can still be reliably translated to a cavern of required dimensions;
- Starting with low frequency operation.
  There is no information available with respect to frequency of loading / producing, maximum flow or yield and the effect on the salt cavern itself, of the four H_2 storages that are being used right now. Starting with a low frequency gives the opportunity to do necessary research on all production related risks;
- Continuing research.
  Finally, a step-by-step approach enables the operator / the developer of the salt cavern to do continuous research on the development of and H_2 storage in salt caverns. As mentioned in 5.1 there are still many unknowns with considerable consequences if insufficient time remains to do proper research. Therefore, share results internationally, and encourage cooperation and sharing of results from other countries to learn from each other.

A last remark: the differences between methane storage and H_2 storage should not be underestimated. On almost all subjects H_2 storage has (significantly) increased risks and requires more mitigations than the well-known methane storage.

6.5.1 Continued risk assessment

The method of risk-based working consists of 6 steps, which are quite common in different risk assessment methods. The 6 risk steps are:

- Risk step 1: Determine objectives
- Risk step 2: Identify risks
- Risk step 3: Classify risks
- Risk step 4: Dealing with risks
- Risk step 5: Evaluation of risk measures
- Risk step 6: Risk report

Steps 1 till 4 are part of the generic risk assessment and are described in 1.1 Part 3. Steps 5 and 6 more or less close the PDCA loop, see Figure 336.

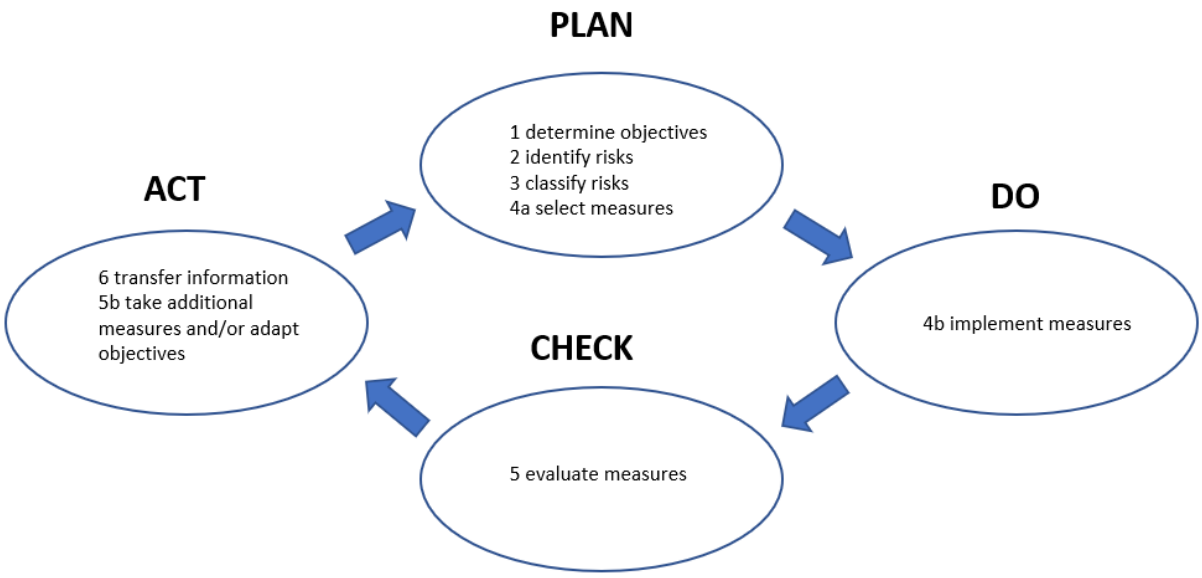

Figure 336. PDCA loop.

Risk step 5: Evaluate measures

In risk step 5 it will be made plausible whether the implemented measures have the intended result or not. This might require a monitoring program. In terms of time there might be months or even years between this step and the previous risk steps.

Based on the findings it could be necessary to take (additional) measures, for instance associated with a new monitoring system based on continuous sensors. Or some measures might be redundant and can be phased out. This also applies to monitoring.

Important focal points

(1) Distinguish between preventive measures [pm], that might reduce or remove altogether the probability of occurrence, and corrective measures [cm] to reduce or eliminate the consequences of occurring risks.

(2) Make an educated guess whether the intended effect of the measures is based upon (a) assumptions, (b) facts or (c) interpretation of facts.

(3) Evaluate the effect of the measures taken periodically, e.g., quarterly.

Risk step 6: transfer of information / risk file

During this risk step the relevant risk-information resulting from the previous risk steps are reported and transferred to the Authorities and other stakeholders involved. It is of utmost importance that the risk-information is adapted to the knowledge and needs of the different stakeholders. This means that the (differences in) risk perception and willingness to take risks should be taken into account and, for instance, uncertainties due to assumptions, lack of factual information and interpretations should be explicitly specified.

Important focal points

(1) Adapt the way to report the risk-information gathered in risk steps 1 till 4 to the knowledge and needs of the different stakeholders.

(2) Be aware of the (differences in) risk perception and willingness to take risks of the stakeholders involved.

(3) Specify explicitly whether the information is based upon (a) assumptions, (b) factual information, or (c) interpretation of factual information.

(4) Base the risk-information to be reported solely on the data gathered in the previous risk steps 1 till 4.

References

Ahmed, A., Soliman, A.M., Hesham El Naggar, M., Kamei, T., 2015. An assessment of geo-environmental properties for utilization of recycled gypsum in earthwork projects. Soils and Foundations, Special Issue on the Six International Symposium on Deformation Characteristics of Geomaterials IS-Buenos Aires2015 55, 1139–1147. https://doi.org/10.1016/j.sandf.2015.09.014

Alberta Energy and Utilities Board, 2002. BP Canada energy company ethane cavern well fires Fort Saskatchewan, Alberta August/September 2001: EUB Post-incident report April 2002. Calgary, Alberta.

Alkan, H., Pusch, G., 2002. Definition of the Dilatancy Boundary Based on Hydro-Mechanical Experiments and Acoustic Detection, in: Proceedings. Presented at the SMRI Fall Meeting 2002, SMRI, Bad Ischl, Austria, pp. 9–24.

Allen, K., 1972. Eminence Dome - Natural-Gas Storage In Salt Comes of Age. Journal of Petroleum Technology 24, 1299–1301. https://doi.org/10.2118/3433-PA

Allen, K., 1971. Eminence--natural gas storage in salt comes of age. American Institute Mining and Metallurgy Engineers Transactions 250, 276–279.

Allison, M.L., 2001. Hutchinson, Kansas: A Geologic Detective Story [WWW Document]. URL http://www.geotimes.org/oct01/feature_kansas.html (accessed 7.25.22).

Argüello, J.G., Rath, J.S., 2012. SIERRA mechanics for coupled multi-physics modeling of salt repositories: J. Guadalupe Argüello & Jonathan S. Rath, in: Mechanical Behavior of Salt VII - Proceedings of The. Presented at the 7th Conference on the Mechanical Behavior of Salt, Taylor & Francis, Paris, France, pp. 413–423.

Arnold, C., Hak, A.A., Feldrappe, H., 2014. Advanced exploration methods for dimensioning and optimizing of gas storage caverns at storage site Bernburg/Peissen (Central Germany), in: Proceedings. Presented at the SMRI Fall Meeting 2014, SMRI, Groningen, The Netherlands.

Arnold, C., Hanisch, P., Pischner, M., 2010. Long term development and extension of brine field and storage site Teutschenthal Bad Lauchstaedt in Central Germany, in: Proceedings. Presented at the SMRI Fall Conference 2010, SMRI, Leipzig, Germany, pp. 137–154.

Arnold, R.D., DeVries, K.L., Nieland, J.D., Tiruneh, H., 2011. Cyclic Fatigue Effects on the Mechanical Properties of Salt, in: Proceedings. Presented at the SMRI Spring Meeting 2011, Galveston, Texas, SMRI, pp. 51–64.

ATG Manual, 1985. Gas transport and distribution handbook (Manuel pour le transport et la distribution du gaz. Titre XIII, Stockages Souterrains de Gaz). Association Technique de l'Industrie du Gaz en France.

Atlas, R.M., Chowdhury, A.N., Gauri, K.L., 1988. Microbial calcification of gypsum-rock and sulfated marble. Studies in Conservation 33, 149–153. https://doi.org/10.1179/sic.1988.33.3.149

Aurenhammer, F., 1987. Power Diagrams: Properties, Algorithms and Applications. SIAM J. Comput. 16, 78–96. https://doi.org/10.1137/0216006

Baar, C.A., 1977. Applied Salt-rock Mechanics: The in-situ behavior of salt rocks. Developments in Geotechnical Engineering. Elsevier Scientific Publishing Company.

Baker, P.A., Kastner, M., 1981. Constraints on the Formation of Sedimentary Dolomite. Science 213, 214–216. https://doi.org/10.1126/science.213.4504.214

Balland, C., Billiotte, J., Tessier, B., Raingeard, A., Hertz, E., Hévin, G., 2016. Acoustic monitoring of thermo-mechanical tests in a salt mine, in: Proceedings. Presented at the SMRI Spring Meeting 2016, SMRI, Galveston, Texas, pp. 211–221.

Banach, A., Klafki, M., 2009. Stassfurt shallow cavern abandonment field test (Prepared for the Solution Mining Research Institute No. 2009–1). SMRI.

Barabasch, J., Schmatz, J., Klaver, J., Schwedt, A., Urai, J.L., 2023. Large grain-size-dependent rheology contrasts of halite at low differential stress: evidence from microstructural study of naturally deformed gneissic Zechstein 2 rock salt (Kristallbrockensalz) from the northern Netherlands. Solid Earth 14, 271–291. https://doi.org/10.5194/se-14-271-2023

Barabasch, J., Urai, J., Raith, A., de Jager, J., 2019. The early life of a salt giant: 3D seismic study on syntectonic Zechstein salt and stringer deposition on the Friesland Platform, Netherlands. Zeitschrift der Deutschen Gesellschaft für Geowissenschaften 170. https://doi.org/10.1127/zdgg/2019/0186

Bauer, S.J., Ehgartner, B.L., Neal, J.T., 2000. Geotechnical studies associated with decommissioning the strategic petroleum reserve facility at Weeks Island, Louisiana: A case history, in: Proceedings. Presented at the SMRI fall meeting 2000, SMRI, San Antonio, Texas, pp. 145–156.

Baumann, T.S., Bérest, P., Brouard, B., Braack, M. ter, Hartogh, M. den, Kaus, B.J.P., Klaver, J., Oonk, P.B.H., Popov, A., Schmatz, J., Urai, J.L., Wijermars, E.A.M., 2022a. CCC - integrated multiscale study of salt cavern abandonment in the Netherlands, in: Proceedings. Presented at the 10th Conference on the Mechanical Behavior of Salt, EarthArXiv, Utrecht University, Netherlands, p. 10. https://doi.org/10.31223/X5VP83

Baumann, T.S., Kaus, B., Popov, A., Urai, J., 2022b. Modeling of the 3D stress state of typical salt formations, in: The Mechanical Behavior of Salt X. CRC Press.

Baumann, T.S., Kaus, B.J., Popov, A.A., 2019. Over-pressured caverns and leakage mechanisms Part 3: Dome-scale analysis, KEM-17.

Baumann, T.S., Kaus, B.J., Popov, A.A., 2018. Deformation and stresses related to the Gorleben salt structure: insights from 3D numerical models. Mechanical Behavior of Salt, Saltmech IX 15–27.

Belzer, B.E., DeVries, K.L., 2017. Numerical Prediction of Tensile Casing Failure by Salt Creep for Evaluating the Integrity of Cemented Casings of Salt Caverns, in: Proceedings. Presented at the SMRI Spring Meeting 2017, SMRI, Albuquerque, New Mexico, p. 12p.

Bennett, W., 2009. Letter to Mr Joe S. Ball, Injection and Mining Division, Office of Conservation, Louisiana Department of Natural Resources, from Gulf South, dated November 10th 2009, requesting an extension to 2009 requirement for plugging and abandoning Gulf South Well #1.

Bensing, J.P., Misch, D., Skerbisch, L., Sachsenhofer, R.F., 2022. Hydrogen-induced calcite dissolution in Amaltheenton Formation claystones: Implications for underground hydrogen storage caprock integrity. International Journal of Hydrogen Energy 47, 30621–30626. https://doi.org/10.1016/j.ijhydene.2022.07.023

Bérest, P., 2019. Heat transfer in salt caverns. International Journal of Rock Mechanics and Mining Sciences 120, 82–95. https://doi.org/10.1016/j.ijrmms.2019.06.009

Bérest, P., 2017. Cases, causes and classifications of craters above salt caverns. International Journal of Rock Mechanics and Mining Sciences 100, 318–329. https://doi.org/10.1016/j.ijrmms.2017.10.025

Bérest, P., 2013. The mechanical behavior of salt and salt caverns, in: Kwaśniewski, M., Łydżba, D. (Eds.), Rock Mechanics for Resources, Energy and Environment. CRC Press/Balkema, Leiden, The Netherlands, pp. 17–29. https://doi.org/10.1201/b15683-5

Bérest, P., 2007. Questions On the Prediction of the Long-term Behaviour of Underground Openings. Presented at the 11th ISRM Congress, OnePetro.

Bérest, P., Antoine Blum, P., Pierre Charpentier, J., Gharbi, H., Valès, F., 2005. Very slow creep tests on rock samples. International Journal of Rock Mechanics and Mining Sciences 42, 569–576. https://doi.org/10.1016/j.ijrmms.2005.02.003

Bérest, P., Bergues, J., Brouard, B., 1999. Review of static and dynamic compressibility issues relating to deep underground salt caverns. International Journal of Rock Mechanics and Mining Sciences 36, 1031–1049. https://doi.org/10.1016/S0148-9062(99)00062-5

Bérest, P., Bergues, J., Brouard, B., Durup, J.G., Guerber, B., 2001a. A salt cavern abandonment test. International Journal of Rock Mechanics and Mining Sciences 38, 357–368. https://doi.org/10.1016/S1365-1609(01)00004-1

Bérest, P., Brouard, B., 2003. Safety of salt caverns used for underground storage: Blow out; mechanical instability; seepage; cavern abandonment. Oil & Gas Science and Technology 58, 361–384. https://doi.org/10.2516/ogst:2003023

Bérest, P., Brouard, B., Checkai, D., Gharbi, H., Hart, D., Zakharov, V., 2017. Salt-Fall Detection in Oil Storage Caverns, in: SMRI Fall Meeting. Presented at the SMRI Fall Meeting, Münster, Germany.

Bérest, P., Brouard, B., de Greef, V., 2001b. Salt Permeability Testing. The Influence of Permeability and stress on Hollow Salt Samples (Research Project Report No. 2001–8). SMRI.

Bérest, P., Brouard, B., de Greef, V., 2000. Salt permeability testing RFP 98-1: The influence of permeability and stress on spherical hollow salt samples: A brief account of tests 11,12,13 and 14 (Research Report). Laboratoire de M´ecanique des Solides (Ecole polytechnique), Paris, France.

Bérest, Pierre, Brouard, B., Durup, J.G., 2001. Tightness Tests in Salt-Cavern Wells. Oil & Gas Science and Technology - Rev. IFP 56, 451–469. https://doi.org/10.2516/ogst:2001037

Bérest, P., Brouard, B., Favret, F., Hévin, G., Karimi-Jafari, M., 2015. Maximum Pressure in Gas Storage Caverns, in: SMRI Spring Meeting. Presented at the SMRI Spring Meeting, Rochester, New York.

Bérest, P., Brouard, B., Feuga, B., Karimi-Jafari, M., 2008a. The 1873 collapse at the Varangéville salt mine (L'effondrement de 1873 à la mine de Varangéville), in: Actes Des Journées Nationales de Géotechnique et de Géologie de l'Ingénieur, JNGG'08. Presented at the Journées Nationales de Géotechnique et de Géologie de l'Ingénieur, JNGG'08, Nantes, France.

Bérest, P., Brouard, B., Feuga, B., Karimi-Jafari, M., 2008b. The 1873 collapse of the Saint-Maximilien panel at the Varangeville salt mine. International Journal of Rock Mechanics and Mining Sciences 45, 1025–1043. https://doi.org/10.1016/j.ijrmms.2007.10.007

Bérest, P., Brouard, B., Hévin, G., Réveillère, A., 2021a. Tightness of salt caverns used for hydrogen storage, in: 55th US Rock Mechanics/Geomechanics Symposium. Presented at the ARMA, American Rock Mechanics Association, Houston, Texas.

Bérest, P., Brouard, B., Hévin, G., Réveillère, A., 2021b. Tightness of salt caverns used for hydrogen storage, in: Proceedings. Presented at the SMRI Spring Meeting 2021, SMRI, Virtual Technical Conference.

Bérest, P., Brouard, B., Karimi-Jafari, M., Réveillère, A., 2020. Maximum admissible pressure in salt caverns used for brine production and hydrocarbon storage. Oil Gas Sci. Technol. – Rev. IFP Energies nouvelles 75, 76. https://doi.org/10.2516/ogst/2020068

Bérest, P., Djizanne, H., Brouard, B., Frangi, A., 2013. A Simplified Solution For Gas Flow During a Blow-out in an H2 or Air Storage Cavern, in: Proceedings of SMRI. Presented at the SMRI Spring Meeting, SMRI, Lafayette, USA.

Bérest, P., Djizanne, H., Brouard, B., Hévin, G., 2012. Rapid depressurizations: can they lead to irreversible damage?, in: Proceedings. Presented at the SMRI Fall Meeting 2012, SMRI, Regina, Saskatchewan, pp. 64–83.

Bérest, P., Gharbi, H., Blanco-Martín, L., Brouard, B., Brückner, D., DeVries, K.L., Hévin, G., Hofer, G., Spiers, C.J., Urai, J.L., 2023. Salt Creep: Transition Between the Low and High Stress Domains. Rock Mech Rock Eng. https://doi.org/10.1007/s00603-023-03485-y

Bérest, P., Gharbi, H., Brouard, B., Brückner, D., DeVries, K., Hévin, G., Hofer, G., Spiers, C., Urai, J., 2019a. Very Slow Creep Tests on Salt Samples. Rock Mech Rock Eng 52, 2917–2934. https://doi.org/10.1007/s00603-019-01778-9

Bérest, P., Gharbi, H., Gordeliy, L., Jehanno, D., Brouard, B., Blanco-Martin, L., Peach, C., 2022. Creep Tests on Salt Samples Performed at Very Small Stresses, in: Proceedings 56th US Rock Mechanics/Geomechanics Symposium. Presented at the ARMA 2022, Santa Fe, NM.

Bérest, P., Ghoreychi, M., Fauveau, M., Lebitoux, P., 1986. Mechanisms Of Creep In Gas Storage Caverns. Effect Of Gravity Forces. Presented at the The 27th U.S. Symposium on Rock Mechanics (USRMS), OnePetro, Tuscaloosa, Alabama, pp. 789–794.

Bérest, P., Louvet, F., 2020. Aspects of the thermodynamic behavior of salt caverns used for gas storage | Oil & Gas Science and Technology - Revue d'IFP Energies nouvelles. Oil & Gas Science and Technology - Rev. IFP Energies nouvelles 75, 10. https://doi.org/10.2516/ogst/2020040

Bérest, P., Réveillère, A., Evans, D., Stöwer, M., 2019b. Review and analysis of historical leakages from storage salt caverns wells. Oil Gas Sci. Technol. – Rev. IFP Energies nouvelles 74, 27. https://doi.org/10.2516/ogst/2018093

Bérest, P., Réveillère, A., Evans, D., Stöwer, M., 2019c. Review and analysis of historical leakages from storage salt caverns wells, in: Proceedings. Presented at the SMRI Spring Meeting 2019, SMRI, New Orleans, Louisiana.

Berger, H., Zündel, F., Walden, S., 2002. Water in Gas Storage Caverns – Problems and Solutions, in: Proceedings. Presented at the SMRI Fall Meeting 2002, SMRI, Bad Ischl, Austria.

Bernhardt, H., Steijn, J., 2013. Influence of tubing diameters on lifting methods during gas first fill of gas storage caverns – A practical example in the Nüttermoor Cavern Field, in: Proceedings. Presented at the SMRI Spring Meeting 2013, SMRI, La Fayette, Louisiana.

Bezirksregierung Arnsberg, 2014.

Bildstein, O., Worden, R.H., Brosse, E., 2001. Assessment of anhydrite dissolution as the rate-limiting step during thermochemical sulfate reduction. Chemical Geology 176, 173–189. https://doi.org/10.1016/S0009-2541(00)00398-3

Birnbaum, H.K., Wert, C.A., 1972. Diffusion of hydrogen in metals. Berichte der Bunsengesellschaft für physikalische Chemie 76, 806–816. https://doi.org/10.1002/bbpc.19720760835

Blanco Martín, L., Rutqvist, J., Birkholzer, J.T., 2015. Long-term modeling of the thermal–hydraulic–mechanical response of a generic salt repository for heat-generating nuclear waste. Engineering Geology 193, 198–211. https://doi.org/10.1016/j.enggeo.2015.04.014

Blue Ribbon Commission, 2014. Report on Bayou Corne sinkhole.

Boese, C.M., Wotherspoon, L., Alvarez, M., Malin, P., 2015. Analysis of anthropogenic and natural noise from multilevel borehole seismometers in an urban environment, Auckland, New Zealand. Bulletin of the seismological Society of America 105, 285–299.

Bonté, D., Wees, J.-D. van, Verweij, J.M., 2012. Subsurface temperature of the onshore Netherlands: new temperature dataset and modelling. Netherlands Journal of Geosciences 91, 491–515. https://doi.org/10.1017/S0016774600000354

Bontognali, T.R.R., 2008. Microbial dolomite formation within exopolymeric substances (Doctoral Thesis). ETH Zurich. https://doi.org/10.3929/ethz-a-005673286

Bosak, T., Newman, D.K., 2005. Microbial Kinetic Controls on Calcite Morphology in Supersaturated Solutions. Journal of Sedimentary Research 75, 190–199. https://doi.org/10.2110/jsr.2005.015

Bosak, T., Newman, D.K., 2003. Microbial nucleation of calcium carbonate in the Precambrian. Geology 31, 577–580. https://doi.org/10.1130/0091-7613(2003)031<0577:MNOCCI>2.0.CO;2

Bosq, H., Wijermars, E., Lubkowski, Z., 2020. Using continuous microseismic surveillance for the management of cavern fields, in: Proceedings. Presented at the SMRI Fall Virtual Technical Conference 2020.

Brace, W.F., 1980. Permeability of crystalline and argillaceous rocks. International Journal of Rock Mechanics and Mining Sciences & Geomechanics Abstracts 17, 241–251. https://doi.org/10.1016/0148-9062(80)90807-4

Branka, S., Mazur, M., Jasinski, Z., 2002. MIT in Gora underground cavern oil and fuel storage, in: Proceedings. Presented at the SMRI Fall Meeting 2002, SMRI, Bad Ischl, Austria, pp. 65–73.

Brasier, F.M., 1990. Assuring the integrity of solution mining operations, in: Proceedings. Presented at the SMRI Fall Meeting 1990, SMRI, Paris, France.

Bräuer, V., Eickemeier, R., Eisenburger, D., Grissemann, C., Hesser, J., Heusermann, S., Kaiser, D., Nipp, H., Nowak, T., Plischke, I., Schnier, H., Schulze, O., Soennke, J., Weber, J., 2011. Description of the Gorleben site Part 4 Geotechnical exploration of the Gorleben salt dome. Federal Institute for Geosciences and Natural Resources (BGR).

Brouard, B., Bérest, P., 2022. Calibration of Rock-Salt Thermal and Mechanical Parameters Based on Available Field Data, in: Proceedings SMRI Spring Meeting 2022. Presented at the SMRI Spring Meeting 2022, SMRI, Rapid City, SD.

Brouard, B., Bérest, P., 2019. Over-pressured caverns and leakage mechanisms Phase 2: Cavern scale, KEM-17. Brouard Consulting.

Brouard, B., Bérest, P., 1998. A tentative classification of salts according to their creep properties, in: Proceedings. Presented at the SMRI Spring Meeting 1998, SMRI, New Orleans, Louisiana, pp. 18–38.

Brouard, B., Bérest, P., Durup, J.G., 2001. In-situ salt permeability testing. Presented at the SMRI Fall Meeting 2001, SMRI, Albuquerque, New Mexico, pp. 1–18.

Brouard, B., Bérest, P., Hertz, E., Lheur, C., 2017. A cavern abandonment test at Gellenoncourt, Lorraine – An update, in: Proceedings of SMRI. Presented at the SMRI Fall Meeting, Münster, Germany.

Brouard, B., Bérest, P., Zakharov, V., 2021a. Assessment of Cavern Stability: Cavern Clusters Vs. Single Cavern. Presented at the SMRI Spring Meeting, Virtual Conference.

Brouard, B., Bérest, P., Zakharov, V., 2021b. Creep-Closure rate and induced subsidence in a cluster of salt caverns. Presented at the SMRI Fall Conference 2021, Galveston, Texas, USA.

Brouard, B., Karimi-Jafari, M., Bérest, P., 2007. Onset of tensile effective stresses in gas storage caverns, in: Proceedings. Presented at the SMRI Fall Meeting 2007, SMRI, Halifax, Canada, pp. 119–135.

Brouard Consulting, Institute für Unterirdishches Bauen (IUB), Ecole Polytechnique, Total E&P France, Géostock, 2006. Salt Cavern abandonment Field Test in Carresse (Final Report No. RFP 2003-2-B). SMRI.

Brouard Consulting, Respec, 2013. Analysis of Moss Bluff Cavern #1 Blow Out Data (Topical Report No. RSI-2013-01). The Solution Mining Research Institute.

Brückner, D., Lindert, A., Wiedemann, M., 2003. The Bernburg Test Cavern –A model study of cavern abandonment, in: Proceedings. Presented at the SMRI Fall Meeting 2003, Chester, United Kingdom.

Brückner, D., Minkley, W., Lindert, A., 2012. The improved IfG gas storage cavern design concept, in: Mechanical Behavior of Salt VII - Proceedings of The. Presented at the 7th Conference on the Mechanical Behavior of Salt, Taylor & Francis, Paris, France, pp. 391–398. https://doi.org/10.1201/b12041-52

Bruno, M.S., Dusseault, M.B., 2002. Geomechanical analysis of pressure limits for thin bedded salt caverns. Solution Mining Research Institute, Banff, Alberta, Canada, pp. 1–25.

Bryson, W.R., 1980. Leakage of liquefied petroleum gas from storage projects in bedded salt – An update, in: Proceedings. Presented at the SMRI Fall Meeting 1980, SMRI, Minneapolis, Minnesota.

Caglayan, D.G., Weber, N., Heinrichs, H.U., Linßen, J., Robinius, M., Kukla, P.A., Stolten, D., 2020. Technical potential of salt caverns for hydrogen storage in Europe. International Journal of Hydrogen Energy 45, 6793–6805. https://doi.org/10.1016/j.ijhydene.2019.12.161

Cała, M., Cyran, K., Kowalski, M., 2018. Influence of the Anhydrite Interbeds on a Stability of the Storage Caverns in the Mechelinki Salt Deposit (Northern Poland). Archives of Mining Sciences 63, 1007–1025. https://doi.org/10.24425/ams.2018.124990

Carosella, M.E., 1978. The Use of Salt Domes for the Strategic Petroleum Reserve, in: Coogan, A.H., Hauber, L. (Eds.), Proceedings 5th Symposium on Salt. Northern Ohio Geological Society Inc. Pub., pp. 69–75.

Carruthers, D., Cartwright, J., Jackson, M.P.A., Schutjens, P., 2013. Origin and timing of layer-bound radial faulting around North Sea salt stocks: New insights into the evolving stress state around rising diapirs. Marine and Petroleum Geology 48, 130–148. https://doi.org/10.1016/j.marpetgeo.2013.08.001

Carter, N.L., Horseman, S.T., Russell, J.E., Handin, J., 1993. Rheology of rocksalt. Journal of Structural Geology 15, 1257–1271. https://doi.org/10.1016/0191-8141(93)90168-A

Cartwright, M.J., Ratigan, J.L., 2005. Case history – Solution mining a cavern that intersects a plane of preferred dissolution, in: Proceedings. Presented at the SMRI Fall Meeting 2005, SMRI, Nancy, France.

CH2MHILL, Inc., 1995. Technical manual for external well mechanical integrity testing Class-III salt solution mining wells (Prepared for the Solution Mining Research Institute). SMRI.

Chabannes, C.R., 2005. Storage pressure limits – Egan facility, in: Ratigan, J. (Ed.), Proceedings Panel Discussion. Presented at the SMRI Spring Meeting 2005, SMRI, Syracuse, New York.

Chan, K.S., Munson, D.E., Bodner, S.R., Fossum, A.F., 1996. Cleavage and creep fracture of rock salt. Acta Materialia 44, 3553–3565. https://doi.org/10.1016/1359-6454(96)00004-3

Chow, Y.T.F., Maitland, G.C., Trusler, J.P.M., 2018. Interfacial tensions of (H2O + H2) and (H2O + CO2 + H2) systems at temperatures of (298–448) K and pressures up to 45 MPa. Fluid Phase Equilibria 475, 37–44. https://doi.org/10.1016/j.fluid.2018.07.022

Coates, G.K., Lee, C.A., McClain, W.C., Senseny, P.E., 1981. Failure of man-made cavities in salt and surface subsidence due to sulfur mining (Report No. SAND-81-7145). Sandia National Laboratories. https://doi.org/10.2172/5307825

Coates, G.K., Lee, C.A., McLain, W.C., Senseny, P.E., 1983. Closure and Collapse of Man-Made Cavities in Salt, in: Proc. 6th Int. Symp. Salt. pp. 139–157.

Colcombet, B., Guerreiro, V., Lúcio, J., 2008. An overview of the Carriço Gas Storage Project development, in: Proceedings. Presented at the SMRI Spring Meeting 2008, Porto, Portugal.

Colcombet, B., Nguyen, H.D., 2013. Well integrity management at the Geosel Manosque storage facility, in: Proceedings. Presented at the SMRI Fall Meeting 2013, SMRI, Avignon, France, pp. 221–230.

Coldewey, W.G., Wesche, D., 2015. Zusammenfassende Betrachtung der durchgeführten Untersuchungen sowie der geplanten Sanierungsmaßnahmen des Rohölschadens an der Kaverne S5 der Salzgewinnungsgesellschaft Westfalen mbH in Gronau-Epe unter besonderer Berücksichtigung der Geologie und Hydrogeologie, Bezirksregierung Arnsberg.

Cole, R., 2002. The long Term Effects of High Pressure Natural Gas Storage on Salt Caverns, in: Proceedings. Presented at the SMRI Spring Meeting 2002, Banff, Alberta, pp. 75–9.

Coleman, A.J., Jackson, C.A.-L., Duffy, O.B., Nikolinakou, M.A., 2018. How, where, and when do radial faults grow near salt diapirs? Geology 46, 655–658. https://doi.org/10.1130/G40338.1

Coleman Hale, R., Stroh, R., Osnes, J., 2015. The Effects of Interbedded Salt & Potash on Cemented Casing at Dewdney Field, in: Proceedings. Presented at the SMRI Fall Meeting 2015, SMRI, Santander, Spain.

Contrucci, I., Klein, E., Cao, N.-T., Daupley, X., Bigarré, P., 2011. Multi-parameter monitoring of a solution mining cavern collapse: First insight of precursors. Comptes Rendus Geoscience 343, 1–10. https://doi.org/10.1016/j.crte.2010.10.007

Cornet, J., Dabrowski, M., Schmid, D.W., 2017. Long-term cavity closure in non-linear rocks. Geophys J Int 210, 1231–1243. https://doi.org/10.1093/gji/ggx227

Cosenza, Ph., Ghoreychi, M., Chanchole, S., 2002. Effects of fluid-rock interaction on mechanical behavior of rock salt, in: Proceedings. Presented at the 5th Conference on Mechanical Behaviour of Salt 1999, CRC Press, Bucharest, Hungary, pp. 57–72.

Cristescu, N.D., Hunsche, U., 1998. Time effects in rock mechanics, Wiley series in materials, modelling and computation. John Wiley & Sons, Chichester, United Kingdom.

Cristescu, N.D., Paraschiv, I., 1996. Creep, damage and failure around large rectangular-like caverns and galleries. Mechanics of Cohesive-frictional Materials 1, 165–197. https://doi.org/10.1002/(SICI)1099-1484(199604)1:2<165::AID-CFM9>3.0.CO;2-4

Crossley, N.G., 1998. Sonar surveys used in gas-storage cavern analysis. Oil and Gas Journal 96.

Crossley, N.G., 1996. Salt cavern Integrity Evaluation Using Downhole Probes. A Transgas Perspective, in: Proceedings. Presented at the SMRI Fall Meeting 1996, SMRI, Cleveland, Ohio, pp. 21–54.

Crotogino, F., 1996. SMRI Reference for External Well Mechanical Integrity Testing/Performance, Data Evaluation and Assessment (Summary of the Final Project Report - SMRI Research Report 94-0001 No. 94– 0001). Houston, Texas.

Crotogino, F., Mohmeyer, K.-U., Scharf, R., 2001. Huntorf CAES: More than 20 Years of Successful Operation, in: Conference Proceedings. Presented at the Solution Mining Research Institute (SMRI) Spring Meeting, Orlando, Florida, USA, pp. 352–362.

Czapowski, G., 1987. Sedimentary facies in the Oldest Rock Salt (Na1) of the Leba elevation (northern Poland), in: Peryt, T.M. (Ed.), The Zechstein Facies in Europe, Lecture Notes in Earth Sciences. Springer, Berlin, Heidelberg, pp. 207–224. https://doi.org/10.1007/BFb0011380

DBI, G.U.G., 2022a. Leitfaden Planung, Genehmigung und Betrieb von Wasserstoff-Kavernenspeichern. BMBF, Projektträger Jülich.

DBI, G.U.G., 2022b. Wasserstoff Speichern – Soviel ist sicher (No. DVGW-Projekt-Nr. G 201926).

DBI, G.U.G., 2017. The effects of hydrogen injection in natural gas networks for the Dutch underground storages (Final Report, Commissioned by the ministry of Economic Affairs No. FLEXg16008). Netherlands Enterprise Agency (RVO.nl), Den Haag, Netherlands.

De Bresser, J., Ter Heege, J., Spiers, C., 2001. Grain size reduction by dynamic recrystallization: can it result in major rheological weakening? Int J Earth Sci 90, 28–45. https://doi.org/10.1007/s005310000149

De Bresser, J.H.P., Peach, C.J., Reijs, J.P.J., Spiers, C.J., 1998. On dynamic recrystallization during solid state flow: Effects of stress and temperature. Geophysical Research Letters 25, 3457–3460.

Denzau, H., Rudolph, F., 1997. Field test for determining the convergence of a gas storage cavern under load conditions frequently changing between maximum and minimum pressure and its finite element modelling, in: Proceedings. Presented at the SMRI Spring Meeting 1997, Cracow, Poland, pp. 71–84.

Deubelbeiss, Y., Kaus, B.J.P., 2008. Comparison of Eulerian and Lagrangian numerical techniques for the Stokes equations in the presence of strongly varying viscosity. Physics of the Earth and Planetary Interiors, Recent Advances in Computational Geodynamics: Theory, Numerics and Applications 171, 92–111. https://doi.org/10.1016/j.pepi.2008.06.023

Deubelbeiss, Y., Kaus, B.J.P., Connolly, J.A.D., 2010. Direct numerical simulation of two-phase flow: Effective rheology and flow patterns of particle suspensions. Earth and Planetary Science Letters 290, 1–12. https://doi.org/10.1016/j.epsl.2009.11.041

Deubelbeiss, Y., Kaus, B.J.P., Connolly, J.A.D., Caricchi, L., 2011. Potential causes for the non-Newtonian rheology of crystal-bearing magmas. Geochemistry, Geophysics, Geosystems 12. https://doi.org/10.1029/2010GC003485

DeVries, K.L., 2006. Geomechanical Analyses to Determine the Onset of Dilation Around Natural Gas Storage Caverns in Bedded Salt, in: Proceedings. Presented at the SMRI Spring Meeting 2006, SMRI, Brussels, Belgium, pp. 132–148.

DeVries, K.L., Mellegard, K.D., 2010. Effects of specimen preconditioning on salt dilation onset, in: Proceedings. Presented at the SMRI Fall Meeting, SMRI, Leipzig, Germany, pp. 60–65.

DeVries, K.L., Mellegard, K.D., Callahan, G.D., Goodman, W.M., 2005. Cavern roof stability for natural gas storage in bedded salt (Final Report No. RSI-1829). RESPEC, Rapid City, South Dakota, USA.

Diamond, H.W., 1989. The water-brine interface method—an alternative Mechanical Integrity Test for salt solution mining wells, in: Proceedings. Presented at the SMRI Fall Meeting 1989, SMRI, San Antonio, Texas.

Diamond, H.W., Bertram, B.M., French, P.S., Petrick, G.D., Schumacher, M.J., Smith, J.B., 1993. Detecting very small casing leaks using the waterbrine interface method, in: Proceedings. Presented at the 7th Symposium on Salt 1992, Elsevier, Kyoto, Japan, pp. 363–368.

Djizanne, H., Bérest, P., Brouard, B., 2014a. The Mechanical Stability of a Salt Cavern Used for Compressed Air Energy Storage (CAES). Presented at the SMRI Spring Meeting, Solution Minining Research Institute, San Antonio, TX, USA.

Djizanne, H., Bérest, P., Brouard, B., 2012. Tensile Effective Stresses in Hydrocarbon Storage Caverns, in: Proceedings. Presented at the SMRI Fall Meeting 2012, Bremen, Germany, pp. 223–240.

Djizanne, H., Bérest, P., Brouard, B., Frangi, A., 2014b. Blowout in Gas Storage Caverns. Oil & Gas Science and Technology 69, 1251–1267. https://doi.org/10.2516/ogst/2013208

Djizanne, H., Murillo Rueda, C., Brouard, B., Bérest, P., Hévin, G., 2022. Modeling of the Blowout of Hydrogen Underground Salt Cavern Storage, in: Proceedings. Presented at the SMRI Spring Meeting 2022, Rapid City, South Dakota.

Doe, Th., Osnes, J., 2006. In Situ Stress and Permeability Tests in the Hutchinson Salt and the Overlaying Shale, Kansas, in: Proceedings. Presented at the SMRI Fall Meeting 2006, SMRI, Rapid City, South Dakota, pp. 182–213.

Dopffel, N., Jansen, S., Gerritse, J., 2021. Microbial side effects of underground hydrogen storage – Knowledge gaps, risks and opportunities for successful implementation. International Journal of Hydrogen Energy 46, 8594–8606. https://doi.org/10.1016/j.ijhydene.2020.12.058

Dortland, S., 2003. The gravity effect of an upward migrating brine cavity in the Twenthe-Rijn concession area, East Netherlands (TNO-NITG rapport No. 03-149- B). TNO.

Dortland, S., Arts, R.J., Scheffers, B.C., 2005. The Gravity Effect of an Upward Migrating Brine Cavity in the Twenthe-Rijn Concession Area, East Netherlands. Presented at the 67th EAGE Conference & Exhibition, European Association of Geoscientists & Engineers, p. cp. https://doi.org/10.3997/2214-4609-pdb.1.P332

Dost, B., Haak, H.W., 2007. Natural and induced seismicity. Geology of the Netherlands 223–239.

Dreyer, W.E., 1978. Cold and cryogenic storage of petroleum products, in: Bergman, M. (Ed.), Storage in Excavated Rock Caverns: Rockstore 77. Pergamon, pp. 467–479. https://doi.org/10.1016/B978-1-4832-8406-4.50082-8

Duffy, O.B., Hudec, M., Peel, F., Apps, G., Bump, A., Moscardelli, L., Dooley, T., Bhattacharya, S., Wisian, K., Shuster, M., 2022. The Role of Salt Tectonics in the Energy Transition: An Overview and Future Challenges. In Review. https://doi.org/10.31223/X5363J

Duffy, O.B., Moscardelli, L., Hudec, M.R., Dooley, T.P., Peel, F., Apps, G., Shuster, M., Looff, K., In review. Potential controls on the origin, nature and distribution of shear zones in salt stocks: salt tectonic insights with a solution mining perspective. In review.

Durup, J.G., 1994a. Long term tests for tightness evaluations with brine and gas in salt, in: Proceedings. Presented at the SMRI Fall Meeting 1994, SMRI, Hannover, Germany.

Durup, J.G., 1994b. Long term tests for tightness evaluations with brine and gas in salt (Field test n°2 with gas) (Research Project Report No. 94– 002). SMRI.

Durup, J.G., 1990. Long term tests for tightness evaluations with brine and gas in salt (Field test n°1 with brine) (Research Project Report No. 90–2). SMRI.

Düsterloh, U., Lerche, S., Lux, K.H., 2012. Cyclic loading effects on the dilation and healing properties of rock salt from Avery Island Louisiana – 250 days cyclic loading tests and numerical back analysis, in: Proceedings. Presented at the SMRI Fall Meeting 2012, SMRI, Bremen, Germany, pp. 3–32.

Ebigbo, A., Golfier, F., Quintard, M., 2013. A coupled, pore-scale model for methanogenic microbial activity in underground hydrogen storage. Advances in Water Resources 61, 74–85. https://doi.org/10.1016/j.advwatres.2013.09.004

Edgar, 2005. Notes to unaudited condensed consolidated financial statements.

Edler, D., Scheler, R., Wiesner, F., 2003. Real time interpretation of tightness tests investigating the casing shoe region of final cemented casings in gas storage cavern wells, in: Proceedings. Presented at the SMRI Spring Meeting 2003, SMRI, Houston, Texas, pp. 251–9.

Ehgartner, B.L., 1997. Kinetics of a Rock Slab Falling in a Cavern. (Memo mentioned in Munson et al. 1998).

Ehgartner, B.L., Ballard, S., Tavares, M., Yeh, S., Hinkebein, T., Ostensen, R., 1995. A Predictive Model for Pressurization of SPR Caverns, in: Proceedings. Presented at the SMRI Fall Meeting 1995, SMRI, San Antonio, Texas.

EIA, 2006. U.S. underground natural gas storage developments: 1998–2005, Energy Information Administration (EIA). Office of Oil and Gas.

Eickemeier, R., 2005. A new model to predict subsidence above brine fields, in: Proceedings. Presented at the SMRI Fall Meeting 2005, SMRI, Nancy, France, pp. 250–269.

Eising, J., 2021. Risk analysis of worldwide salt cavern storage (rapport). VU University Amsterdam, Amsterdam, The Netherlands.

Fansheng, B., Guangjie, Y., Ruichen, S., 2010. Solution mining and injection-production technology of gas storage in deep salt cavern, in: Proceedings. Presented at the SMRI Fall Meeting, SMRI, Leipzig, Germany.

Fawthrope, R., Bonnier, N., Bublak, R., Schubert, J., Jackson, C., Robb, T., 2013. A first completion design in the UK to use welded completions for a new large onshore gas storage development in salt caverns, in: Proceedings. Presented at the SMRI Spring Meeting 2013, SMRI, La Fayette, Louisiana.

Fay, R.O., 1973a. The Elk City Blowout. Oklahoma Geol. Notes 33, 30–31.

Fay, R.O., 1973b. The Elk city blow-out – A chronology and analysis. Oklahoma Geol. Notes 33, 135–151.

Feuga, B., 2003. Old salt mine at Dieuze (France) revisited 150 years after being abandoned, in: Proceedings. Presented at the SMRI Fall Meeting 2003, Chester, United Kingdom, pp. 114–128.

Flesch, S., Pudlo, D., Albrecht, D., Jacob, A., Enzmann, F., 2018. Hydrogen underground storage—Petrographic and petrophysical variations in reservoir sandstones from laboratory experiments under simulated reservoir conditions. International Journal of Hydrogen Energy 43, 20822–20835. https://doi.org/10.1016/j.ijhydene.2018.09.112

Fokker, P., Smit, A.J., Barth, A., 2022. Field evidence of salt fracturing and healing in a MgCl2 cavern field, in: Mechanical Behavior of Salt X,. Presented at the 10th Conference on the Mechanical Behavior of Salt, Utrecht, The Netherlands.

Fokker, P.A., 1995. The behaviour of salt and salt caverns (Dissertation). Technical University Delft, Delft, The Netherlands.

Fokker, P.A., Bakker, T., Wilke, F.H., Barge, H.J., 2002. Aspects of deep salt mining by FrisiaZout B.V., in: Proceedings. Presented at the SMRI Fall Meeting 2002, Bad Ischl, Austria.

Fokker, P.A., in ’t Veld, C., Bakker, T.W., Jagt, M., 2004. 10 years’ experience in squeeze mining, in: Proceedings. Presented at the SMRI Fall Meeting 2004, SMRI, Berlin, Germany.

Fortier, E., Renoux, P.R., Maisons, C.M., 2006. Seismic Monitoring of Underground Storage in Salt Cavity in a Seismo-Tectonic Context. Presented at the First EAGE Passive Seismic Workshop - Exploration and Monitoring Applications, European Association of Geoscientists & Engineers, p. cp. https://doi.org/10.3997/2214-4609.201402590

Fu, Y., van Berk, W., Schulz, H.-M., 2016. Hydrogen sulfide formation, fate, and behavior in anhydrite-sealed carbonate gas reservoirs: A three-dimensional reactive mass transport modeling approach. AAPG Bulletin 100, 843–865. https://doi.org/10.1306/12111514206

Fullwood, D.T., Niezgoda, S.R., Kalidindi, S.R., 2008. Microstructure reconstructions from 2-point statistics using phase-recovery algorithms. Acta Materialia 56, 942–948. https://doi.org/10.1016/j.actamat.2007.10.044

G1, 2020. Dois anos após descoberta, cratera na Bahia chega a 110 metros de comprimento e moradores cobram explicações [WWW Document]. G1. URL https://g1.globo.com/ba/bahia/noticia/2020/05/29/dois-anos-apos-descoberta-cratera-na-bahia-chega-a-110-metros-de-comprimento-e-moradores-cobram-explicacoes.ghtml (accessed 7.29.22).

G1, 2019. Um ano após descoberta de cratera em Vera Cruz, MPF debate riscos de cavidade e possível aparecimento de outros buracos [WWW Document]. G1. URL https://g1.globo.com/ba/bahia/noticia/2019/05/29/um-ano-apos-descoberta-de-cratera-em-vera-cruz-mpf-debate-riscos-de-cavidade-e-possivel-aparecimento-de-outros-buracos.ghtml (accessed 7.29.22).

G1, 2018. A 1km de cratera gigante, moradores de vila de pescadores temem tragédia na BA: “A gente pode amanhecer morto” [WWW Document]. G1. URL https://g1.globo.com/ba/bahia/noticia/a-1km-de-cratera-gigante-moradores-de-vila-de-pescadores-temem-tragedia-na-ba-a-gente-pode-amanhecer-morto.ghtml (accessed 7.29.22).

Gabrielli, P., Poluzzi, A., Kramer, G.J., Spiers, C., Mazzotti, M., Gazzani, M., 2020. Seasonal energy storage for zero-emissions multi-energy systems via underground hydrogen storage. Renewable and Sustainable Energy Reviews 121, 109629. https://doi.org/10.1016/j.rser.2019.109629

Gebhardt, F., Eby, D., Barnett, D., 2001. Utilizing coiled tubing technology to control a liquid propane storage well fire, a case history, in: Proceedings. Presented at the SMRI Spring Meeting 2001, SMRI, Orlando, Florida, pp. 301–306.

Geluk, M., 2005. Stratigraphy and tectonics of Permo-Triassic basins in the Netherlands and surrounding areas.

Geluk, M.C., Paar, W.A., Fokker, P.A., 2007. Salt, in: Wong, T.E., Batjes, D.A.J., de Jager, J. (Eds.), Geology of the Netherlands. Royal Netherlands Academy of Arts and Sciences, Amsterdam, The Netherlands, pp. 283–294.

Gillhaus, A., 2007. Natural gas storage in salt caverns – Present status, developments and future trends in Europe, in: Proceedings. Presented at the SMRI Spring Meeting 2007, SMRI, Basel, Switzerland.

Gloc, M., Szwed, M., Zagórski, A., Mizera, J., 2018. Hydrogen Influence on Microstructure, Corrosion Resistance and Mechanical Properties of Low Alloy Steel and Explosively Cladded Steel Used for Hydrogen Storage Salt Caverns. Applied Mechanics and Materials 875, 47–52. https://doi.org/10.4028/www.scientific.net/AMM.875.47

Gordeliy, E., Bérest, P., 2022. Characteristic features of salt-cavern behavior. Submitted to International Journal of Rock Mechanics and Mining Sciences.

Gray, W.M., 1965. Surface spalling by thermal stresses in rocks, in: Proceedings of the Rock Mechanics Symposium Toronto. Department of Mines and Technical Surveys, Ottawa, pp. 85–106.

Groenenberg, R.M., Juez-Larre, J., Goncalves Machado, C., Wasch, L.J., Dijkstra, H.E., Wassing, B.B.T., Orlic, B., Brunner, L.G., van der Valk, K., Hajonides van der Meulen, T.C., Kranenburg-Bruinsma, K.J., 2020a. Techno-Economic Modelling of Large-Scale Energy Storage Systems (No. TNO 2020 R12004). TNO, Utrecht.

Groenenberg, R.M., Koornnef, J.M., Sijm, J.P.M., Janssen, G.J.M., Morales España, G.A., van Stralen, J., Hernandez-Serna, R., Smekens, K.E.L., Juez-Larre, J., Goncalves Machado, C., Wasch, L.J., Dijkstra, H.E., Wassing, B.B.L., Orlic, B., Brunner, L.G., van der Valk, K., van Unen, M., Hajonides van der Meulen, T.C., Kranenburg-Bruinsma, K.J., Winters, E., Puts, H., van Popering-Verkerk, J., Duijn, M., 2020b. Large-Scale Energy Storage in Salt Caverns and Depleted Fields (LSES) – Project Findings (No. TNO 2020 R12006). TNO, Utrecht, The Netherlands.

Groos, J.C., Ritter, J.R.R., 2009. Time domain classification and quantification of seismic noise in an urban environment. Geophysical Journal International 179, 1213–1231.

Guarascio, M., Delgado, G.F., Di Bella, C., 1999. Assessment of Sinkhole Formation Potential Above Brine Caverns, in: Proceedings. Presented at the SMRI Spring Meeting 1999, Las Vegas, Nevada.

Guimarães, J.T., Grissolia, E.M., Ferreira, J.C.S., Souza, J.L.M. de, Villar, P.M., Santiago, R., Sobrinho, V.S., 2018. Relatório preliminar: Ilha de Matarandiba, Bahia (Technical Report). CPRM.

Günther, R.-M., Salzer, K., 2012. Advanced strain-hardening approach: A powerful creep model for rock salt with dilatancy, strength and healing, in: Mechanical Behaviour of Salt VII. CRC Press, pp. 13–22.

Hampel, A., 2012. The CDM constitutive model for the mechanical behavior of rock salt: Recent developments and extensions, in: Mechanical Behaviour of Salt VII. CRC Press, pp. 45–56.

Han, X., Schultz, L., Zhang, W., Zhu, J., Meng, F., Geesey, G.G., 2016. Mineral formation during bacterial sulfate reduction in the presence of different electron donors and carbon sources. Chemical Geology 435, 49–59. https://doi.org/10.1016/j.chemgeo.2016.04.022

Hansen, F.D., Mellegard, K.D., Senseny, P.E., 1984. Elasticity and strength of ten natural rock salts, in: Proceedings. Presented at the 1st Conference Mechanical Behaviour of Salt, Trans Tech Publications, Pennsylvania State University, Pennsylvania, pp. 71–83.

Hardie, L.A., 1967. The Gypsum—anhydrite Equilibrium at One Atmosphere Pressure. American Mineralogist 52, 171–200.

Hart, K.A., Rimoli, J.J., 2020a. Generation of statistically representative microstructures with direct grain geometry control. Computer Methods in Applied Mechanics and Engineering 370, 113242. https://doi.org/10.1016/j.cma.2020.113242

Hart, K.A., Rimoli, J.J., 2020b. MicroStructPy: A statistical microstructure mesh generator in Python. SoftwareX 12. https://doi.org/10.1016/j.softx.2020.100595

Hashemi, L., Glerum, W., Farajzadeh, R., Hajibeygi, H., 2021. Contact angle measurement for hydrogen/brine/sandstone system using captive-bubble method relevant for underground hydrogen storage. Advances in Water Resources 154, 103964. https://doi.org/10.1016/j.advwatres.2021.103964

Hassannayebi, N., Azizmohammadi, S., De Lucia, M., Ott, H., 2019. Underground hydrogen storage: application of geochemical modelling in a case study in the Molasse Basin, Upper Austria. Environ Earth Sci 78, 177. https://doi.org/10.1007/s12665-019-8184-5

Hassannayebi, N., Jammernegg, B., Schritter, J., Arnold, P., Enzmann, F., Kersten, M., Loibner, A.P., Fernø, M., Ott, H., 2021. Relationship Between Microbial Growth and Hydraulic Properties at the Sub-Pore Scale. Transp Porous Med 139, 579–593. https://doi.org/10.1007/s11242-021-01680-5

Heinemann, N., Alcalde, J., Miocic, J.M., Hangx, S.J.T., Kallmeyer, J., Ostertag-Henning, C., Hassanpouryouzband, A., Thaysen, E.M., Strobel, G.J., Schmidt-Hattenberger, C., Edlmann, K., Wilkinson, M., Bentham, M., Haszeldine, R.S., Carbonell, R., Rudloff, A., 2021. Enabling large-scale hydrogen storage in porous media – the scientific challenges. Energy Environ. Sci. 14, 853–864. https://doi.org/10.1039/D0EE03536J

Heitman, N.A., 1987. Experience with cavern integrity testing using nitrogen gas, in: Proceedings. Presented at the SMRI Spring Meeting 1987, SMRI, Tulsa, Oklahoma.

Hemme, C., Van Berk, W., 2018. Hydrogeochemical Modeling to Identify Potential Risks of Underground Hydrogen Storage in Depleted Gas Fields. Applied Sciences 8, 2282. https://doi.org/10.3390/app8112282

Hemme, C., van Berk, W., 2017. Potential risk of H2S generation and release in salt cavern gas storage. Journal of Natural Gas Science and Engineering 47, 114–123. https://doi.org/10.1016/j.jngse.2017.09.007

Heusermann, S., Rolfs, O., Schmidt, U., 2003. Nonlinear finite-element analysis of solution mined storage caverns in rock salt using the LUBBY2 constitutive model. Computers & Structures, K.J Bathe 60th Anniversary Issue 81, 629–638. https://doi.org/10.1016/S0045-7949(02)00415-7

Higgs, S., Da Wang, Y., Sun, C., Ennis-King, J., Jackson, S.J., Armstrong, R.T., Mostaghimi, P., 2022. In-situ hydrogen wettability characterisation for underground hydrogen storage. International Journal of Hydrogen Energy 47, 13062–13075. https://doi.org/10.1016/j.ijhydene.2022.02.022

Hoelen, Q., Dijk, H., Wilke, F., Wippich, M., 2010. Gas storage in salt caverns Zuidwending – The Netherlands, in: Proceedings. Presented at the SMRI Fall Meeting 2010, SMRI, Leipzig, Germany.

Hopper, J.M., 2004. Gas Storage And Single-Point Failure Risk. Natural Gas, Hart Energy Publishing 4.

Horseman, S.T., 1988. Moisture content – A major uncertainty in storage cavity closure prediction, in: Proceedings. Presented at the 2nd Conference Mechanical Behaviour of Salt, Trans Tech Publications, Hannover, Germany, pp. 53–68.

Horváth, P.L., Schneider, G.-S., 2018. Update of SMRI´s Compilation of Worldwide Salt Deposits and Salt Cavern Fields.

Howarth, S.M., Peterson, E.W., Lagus, P.L., Lie, K.-H., Finley, S.J., Nowak, E.J., 1991. Interpretation of In-Situ Pressure and Flow Measurements of the Salado Formation at the Waste Isolation Pilot Plant. Presented at the Low Permeability Reservoirs Symposium, OnePetro. https://doi.org/10.2118/21840-MS

Hunfeld, L., Breunese, J., Wassing, B., 2022. The influence of a threshold stress for pressure solution creep on cavern convergence and subsidence behavior–An FEM study, in: Proceedings. Presented at the 10th Conference Mechanical Behavior of Salt (SaltMECH X), CRC Press, pp. 577–589.

Hunsche, U., 1984. Results and interpretation of creep experiments on rock salt, in: Proceedings. Presented at the 1st Conference Mechanical Behaviour of Salt 1981, Trans Tech Publications, Pennsylvania State University, Pennsylvania, pp. 159–167.

Hunsche, U., Hampel, A., 1999. Rock salt — the mechanical properties of the host rock material for a radioactive waste repository. Engineering Geology 52, 271–291. https://doi.org/10.1016/S0013-7952(99)00011-3

Hunsche, U., Schulze, O., 2002. Humidity induced creep and its relation to the dilatancy boundary, in: Proceedings. Presented at the 5th Conference Mechanical Behaviour of Salt 1999, CRC Press, Bucharest, Hungary, pp. 73–87.

Hunsche, U., Schulze, O., 1996. Effect of humidity & confining pressure on creep of rock salt, in: Proceedings. Presented at the 3rd Conference Mechanical behavior of salt 1993, Trans Tech Publications, Palaiseau, France, pp. 237–248.

Iglauer, S., 2022. Optimum geological storage depths for structural H2 geo-storage. Journal of Petroleum Science and Engineering 212, 109498. https://doi.org/10.1016/j.petrol.2021.109498

Igoshin, A., Kazaryan, V., Khloptsov, V., Novenkov, Y., Salokhin, V., 2010. Design, technology and experience of cavern construction at Kaliningrad UGS in Russia, in: Proceedings. Presented at the SMRI Fall Meeting, SMRI, Leipzig, Germany.

Istvan, J.A., 1998. Potential for Storage of Natural Gas in the Hutchinson Salt Member of the Wellington Formation of South-Central Kansas, in: Proceedings. Presented at the SMRI Fall Meeting 1998, SMRI, Roma, Italy, pp. 245–268.

Istvan, J.A., Evans, L.J., Weber, J.H., Devine, C., 1997. Rock mechanics for gas storage in bedded salt caverns. International Journal of Rock Mechanics and Mining Sciences 34, 142. https://doi.org/10.1016/S1365-1609(97)00108-1

Jackson, M.P., Hudec, M.R., 2017. Salt tectonics: Principles and practice. Cambridge University Press.

Jallais, S., 2018. Enjeux du stockage et vecteurs fluides énergétiques.

Jangda, Z., Menke, H., Busch, A., Geiger, S., Bultreys, T., Lewis, H., Singh, K., 2022. Pore-Scale Visualization of Hydrogen Storage in a Sandstone at Subsurface Pressure and Temperature Conditions: Trapping, Dissolution and Wettability. https://doi.org/10.48550/arXiv.2207.04128

Jensen, H.S., Nielsen, A.H., Hvitved-Jacobsen, T., Vollertsen, J., 2009. Modeling of Hydrogen Sulfide Oxidation in Concrete Corrosion Products from Sewer Pipes. Water Environment Research 81, 365–373. https://doi.org/10.2175/106143008X357110

Jiang, M., Rößler, C., Wellmann, E., Klaver, J., Kleiner, F., Schmatz, J., 2022. Workflow for high-resolution phase segmentation of cement clinker from combined BSE image and EDX spectral data. Journal of Microscopy 286, 85–91.

Joekar-Niasar, V., Hassanizadeh, S.M., 2012. Analysis of Fundamentals of Two-Phase Flow in Porous Media Using Dynamic Pore-Network Models: A Review. Critical Reviews in Environmental Science and Technology 42, 1895–1976. https://doi.org/10.1080/10643389.2011.574101

Johansen, J.I., 2010. 25 years of lifetime history for seven Energinet.dk gas caverns in the L.I. Torup Zechstein salt dome in Jutland, Denmark, in: Proceedings. Presented at the SMRI Spring Meeting 2010, SMRI, Grand Junction, Colorado.

Johnson, C., Hoffine, S., 2004. Update on fugitive NGL issues in the Conway area – Assessment and monitoring, in: Proceedings. Presented at the SMRI Spring Meeting 2004, SMRI, Wichita, Kansas, pp. 199–226.

Johnson, D.O., 2003. Regulatory response to unanticipated geo-mechanical events effecting gas storage cavern operations in Texas, in: Proceedings. Presented at the SMRI Spring Meeting 2003, SMRI, Houston, Texas.

Johnson, W., 2002. KDHE unveils gas storage rules. Hutchinson News,.

Juez-Larré, J., Gessel, S. van, Dalman, R., Remmelts, G., Groenenberg, R., 2019. Assessment of underground energy storage potential to support the energy transition in the Netherlands. First Break 37, 57–66. https://doi.org/10.3997/1365-2397.n0039

Kamlot, P., Günther, R.M., Stockmann, N., Gärtner, G., 2007. Modeling of strain softening and dilatancy in the mining system of the southern flank of the Asse II salt mine, in: Wallner, M., Lux, K.-H., Minkley, W., Hardy, H.R. (Eds.), The Mechanical Behavior of Salt – Understanding of THMC Processes in Salt Proceedings. Presented at the 6th Conference Mechanical Behavior of Salt, CRC Press, Hannover, Germany, pp. 327–336.

Kansas Geological Survey, 2001a. KGS--Hutchinson Response--General Geology [WWW Document]. URL https://www.kgs.ku.edu/Hydro/Hutch/GeneralGeology/index.html (accessed 7.25.22).

Kansas Geological Survey, 2001b. KGS--Hutchinson Response--References [WWW Document]. URL https://www.kgs.ku.edu/Hydro/Hutch/references.html (accessed 7.25.22).

Karimi-Jafari, M., Bérest, P., Brouard, B., 2007. Thermal Effects in Salt Caverns, in: Proceedings. Presented at the SMRI Spring Meeting 2007, SMRI, Basel, Switzerland, pp. 167–177.

Katzung, G., Krull, P., Kühn, F., 1996. Havarie einer Rohrtour der UGS-Sonde Lauchstädt 5 im Jahr 1988 - Auswirkungen und geologische Bedingungen. Zeitschrift für Angewandte Geologie 42, 19–26.

Kaus, B.J.P., Popov, A.A., Baumann, T.S., Pusok, A.E., Bauville, A., Fernandez, N., Collignon, M., 2016. Forward and Inverse Modelling of Lithospheric Deformation on Geological Timescales, in: NIC Symposium 2016, NIC Series. Forschungszentrum Julich GmbH, Zentralbibliothek, Julich, pp. 299–307.

KEM-17, 2019. Conclusions and recommendations of the over-pressured caverns and leakage mechanisms project (KEM-17), KEM-17. Brouard Consulting.

Kenter, C.J., Doig, S.J., Rogaar, H.P., Fokker, P.A., Davies, D.R., 1990. Diffusion of brine through rock salt roof of caverns, in: Proceedings. Presented at the SMRI Fall Meeting 1990, SMRI, Paris, France.

Khajooie, S., Gaus, G., Dohrmann, A.B., Krüger, M., Littke, R., 2023. Methanogenic conversion of hydrogen to methane in reservoir rocks: An experimental study of microbial activity in water-filled pore space. International Journal of Hydrogen Energy. https://doi.org/10.1016/j.ijhydene.2023.07.065

Khaledi, K., Mahmoudi, E., Datcheva, M., Schanz, T., 2016. Stability and serviceability of underground energy storage caverns in rock salt subjected to mechanical cyclic loading. International Journal of Rock Mechanics and Mining Sciences 86, 115–131. https://doi.org/10.1016/j.ijrmms.2016.04.010

Kinscher, J., Bernard, P., Contrucci, I., Mangeney, A., Piguet, J.P., Bigarre, P., 2015. Location of microseismic swarms induced by salt solution mining. Geophysical Journal International 200, 337–362. https://doi.org/10.1093/gji/ggu396

Kirmic, A., Rałowicz, B., 2003. The selected cases of surveying salt caverns geometry in Turquish Arabali Field made by Echosonda-Chemkop, in: Proceedings. Presented at the SMRI Fall Meeting 2003, SMRI, Chester, UK.

Klafki, M., Bannach, A., Wagler, T., Pusch, G., Meyn, V., 2003a. State of the Art Review of Hydrate Formation Potential Associated with Natural Gas Storage Operations in Salt Caverns (Prepared for the Solution Mining Research Institute No. Report 2003-1). SMRI.

Klafki, M., Wagler, T., Grosswig, S., Kneer, A., 2003b. Long-Term Down Hole Fibre Optic Temperature Measurements and CFD-Modeling for Investigation of Different Gas Operating Modes. Presented at the Solution Mining Research Institute (SMRI), Fall 2003 Meeting, Chester, United Kingdom, pp. 179–189. https://doi.org/10.13140/RG.2.1.1149.6484

Klaver, J., Desbois, G., Littke, R., Urai, J.L., 2015. BIB-SEM characterization of pore space morphology and distribution in postmature to overmature samples from the Haynesville and Bossier Shales. Marine and Petroleum Geology 59, 451–466. https://doi.org/10.1016/j.marpetgeo.2014.09.020

Klaver, J., Schmatz, J., Wang, R., Jiang, M., Kleipool, L.M., Cilona, A., Urai, J.L., 2021. Automated Carbonate Reservoir Pore and Fracture Classification by Multiscale Imaging and Deep Learning. Presented at the 82nd EAGE Annual Conference & Exhibition, European Association of Geoscientists & Engineers, pp. 1–5. https://doi.org/10.3997/2214-4609.202011981

Köhler, N., Spies, T., Dahm, T., 2009. Seismicity patterns and variation of the frequency-magnitude distribution of microcracks in salt. Geophysical Journal International 179, 489–499. https://doi.org/10.1111/j.1365-246X.2009.04303.x

Koopmans, T., Groenenberg, R., Pinkse, T., 2014. 21st century gas oil storage in Twente, The Netherlands. State-of-the art, multiple-barrier design based on a novel risk management approach, in: Proceedings. Presented at the SMRI Fall Meeting 2014, SMRI, Groningen, The Netherlands, pp. 31–44.

Krieter, M., Gotthardt, K., 2015. The in-situ Sampling of Gas in Caverns and the Development of Software to avoid Hydrates and reduce the Admixture of Inhibitors, in: Proceedings. Presented at the SMRI Fall Meeting 2015, SMRI, Santander, Spain, pp. 187–196.

Kukla, P., Urai, J., Raith, A., Li, S., Barabasch, J., Strozyk, F., 2019. The European Zechstein Salt Giant-Trusheim and Beyond, in: Proceedings of the 37th Annual GCSSEPM Foundation Perkins-Rosen Research Conference. Presented at the Salt Tectonics, Associated Processes, and Exploration Potential, Houston, Texas.

Kukla, P.A., Urai, J.L., 2015. Ölaustritte an der Erdoberfläche infolge einer Leckage an der Verrohrung der Kavernenbohrung Epe S5: Zusammenfassender Bericht zu den Ursachen der Ölaustritte und deren Verbreitung (Summary Report No. Bezirksregierung Arnsberg). RWTH Aachen University, Aachen, Germany.

Kupfer, D.H., 1990. Anomalous features in the Five Islands Salt Stocks, Louisiana. Trans. Gulf Coast Assoc. Geo. Soc. XL 425–437.

Kushnir, R., Dayan, A., Ullmann, A., 2012. Temperature and pressure variations within compressed air energy storage caverns. International Journal of Heat and Mass Transfer 55, 5616–5630. https://doi.org/10.1016/j.ijheatmasstransfer.2012.05.055

Küster, Y., Leiss, B., Schramm, M., 2010. Structural characteristics of the halite fabric type 'Kristallbrocken' from the Zechstein Basin with regard to its development. International Journal of Earth Sciences 99, 505–526. https://doi.org/10.1007/s00531-008-0399-8

Küster, Y., Schramm, M., Bornemann, O., Leiss, B., 2009. Bromide distribution characteristics of different Zechstein 2 rock salt sequences of the Southern Permian Basin: a comparison between bedded and domal salts. Sedimentology 56, 1368–1391. https://doi.org/10.1111/j.1365-3091.2008.01038.x

Küster, Y., Schramm, M., Leiss, B., 2011. Compositional and microstructural characterisation of solid inclusions in the laminated halite type “Kristallbrocken” with regard to its formation in the Central European Zechstein Basin. Zeitschrift der Deutschen Gesellschaft für Geowissenschaften 162, 277–294. https://doi.org/10.1127/1860-1804/2011/0162-0277

Laban, M.P., 2020. Hydrogen Storage in Salt Caverns: Chemical modelling and analysis of large-scale hydrogen storage in underground salt caverns. (Master’s Thesis). Technical University Delft, Delft, The Netherlands.

Lampe, B., Ratigan, J.L., 2014. Pitfalls of a Nitrogen-Brine interface Mechanical Integrity Test, in: Proceedings. Presented at the SMRI Spring Meeting 2014, SMRI, San Antonio, Texas, pp. 19–30.

Landau, L., Lifchitz, E., 1971. Mécanique Des Fluides, Physique Théorique. Èditions Mir, Moscow.

Langlinais, J., Moran, T., 2008. Using a Downhole Camera to Monitor the Nitrogen Interface During an MIT, in: Proceedings. Presented at the SMRI Fall Meeting 2008, SMRI, Galveston, Texas.

Le Cléac’h, J.M., Ghazali, A., Deveughele, M., Brulhet, J., 1996. Experimental study of the role of humidity on the thermomechanical behaviour of various halitic rocks, in: Proceedings. Presented at the 3rd Conference Mechanical behavior of salt 1993, Trans Tech Publications, Palaiseau, France, pp. 231–236.

Lee, C.F., Tsui, K.K., Tsai, A., 1982. Thermomechanical Response Of A Disposal Vault In A High Horizontal Stress Field. Presented at the ISRM International Symposium, Balkema, pp. 961–969.

Li, S.-Y., Urai, J.L., 2016. Numerical modeling of gravitational sinking of anhydrite stringers in salt (at rest). Bollettino di Geofisica Teorica ed Applicata 57, 233–246. https://doi.org/10.4430/bgta0178

Li, X., Luo, Q., Wofford, N.Q., Keller, K.L., McInerney, M.J., Wall, J.D., Krumholz, L.R., 2009. A Molybdopterin Oxidoreductase Is Involved in H2 Oxidation in Desulfovibrio desulfuricans G20. Journal of Bacteriology 191, 2675–2682. https://doi.org/10.1128/jb.01814-08

Liquide, A., 2022. Air Liquide Gas Encyclopedia [WWW Document]. Air Liquide Gas Encyclopedia. URL https://encyclopedia.airliquide.com/ (accessed 7.25.22).

Liu, X., Hunsche, U., 1988. Creep behavior of salt under true triaxial stress, in: Proceedings. Presented at the 2nd Conference Mechanical Behaviour of Salt 1984, Trans Tech Publications, Hanover, Germany, pp. 235–243.

Löitler, J., 1962. Zur Genese der Augensalze im Zechstein der Deutschen Demokratischen Republik, in: Zur Genese der Augensalze im Zechstein der Deutschen Demokratischen Republik. De Gruyter, pp. 583–589. https://doi.org/10.1515/9783112558201-006

Long, J.C.S., Birkholzer, J.T., Mace, A.J., Brady, S.E., 2018. Long-Term Viability of Underground Natural Gas Storage in California: An Independent Review of Scientific and Technical Information.

Looff, K., 2017. The Impact of Anomalous Salt and Boundary Shear Zones on Salt Cavern Geometry, Cavern Operations, and Cavern Integrity. Presented at the American Gas Association Operations Conference, Orlando, Florida, USA.

Looff, Karl M., Looff, Kurt M., 1998. Geologic evaluation for domal salt storage projects - an overview. SMRI, New Orleans, Louisiana, USA, pp. 182–209.

Looff, Kurt M., Looff, Karl M., Rautman, C., 2010a. Inferring the geologic significance and potential impact of salt fabric and anomalous salt on the development and long-term operation of salt storage caverns on Gulf Coast salt domes, in: Proceedings. Presented at the SMRI Spring Technical Conference, SMRI, Grand Junction, Colorado, USA, pp. 1–25.

Looff, Kurt M., Looff, K.M., Rautman, C.A., 2010b. Salt Spines, Boundary Shear Zones and Anomalous Salts: Their Characteristics, Detection and Influence on Salt Dome Storage Caverns, in: Proceedings. Presented at the SMRI Spring Technical Conference 2010, SMRI, Grand Junction, Colorado, p. 23.

Lord, A.S., Rautman, C.A., Looff, K.M., 2006. Geologic technical assessment of the Stratton Ridge salt dome, Texas, for potential expansion of the U.S. strategic petroleum reserve. (No. SAND2006-7159). Sandia National Laboratories (SNL), Albuquerque, NM, and Livermore, CA (United States). https://doi.org/10.2172/899080

Louvet, F., Charnavel, Y., Hévin, G., 2017. Thermodynamic studies of hydrogen storage in salt caverns, in: Proceedings. Presented at the SMRI Spring Meeting 2017, SMRI, Albuquerque, New Mexico, USA, pp. 38–352.

Lux, K.-H., 1984. Gebirgsmechanischer Entwurf und Felderfahrungen im Salzkavernenbau: ein Beitrag zur Entwicklung von Prognosemodellen für den Hohlraumbau im duktilen Salzgebirge. Enke, Stuttgart.

Lux, K.-H., Dresen, R., 2012. Design of salt caverns for high frequency cycling of storage gas, in: Proceedings. Presented at the Mechanical Behavoir of Salt VII, Paris, France.

Lux, K.H., Wolters, R., Pan, T.J., 2019. Load-Bearing Behaviour of Steel Casing as Well as Annulus Cementation Regarding Salt Cavern Wells Subjected to Long-Term Operation – A Contribution to Integrity Analysis. Presented at the 53rd U.S. Rock Mechanics/Geomechanics Symposium, OnePetro, New York City, New York.

Lysyy, M., Ersland, G., Fernø, M., 2022. Pore-scale dynamics for underground porous media hydrogen storage. Advances in Water Resources 163, 104167. https://doi.org/10.1016/j.advwatres.2022.104167

MacDonald, G.J.F., 1953. Anhydrite-gypsum equilibrium relations. American Journal of Science 251, 884–898. https://doi.org/10.2475/ajs.251.12.884

Machel, H.G., 2001. Bacterial and thermochemical sulfate reduction in diagenetic settings — old and new insights. Sedimentary Geology 140, 143–175. https://doi.org/10.1016/S0037-0738(00)00176-7

Maciel, S.T.R., Rocha, M.P., Schimmel, M., 2021. Urban seismic monitoring in Brasília, Brazil. Plos one 16, e0253610.

Manivannan, S., Bérest, P., Brouard, B., 2015. Effects of changes in the pressure and temperature of the testing fluid during a liquid-liquid MIT, in: SMRI Fall Meeting. Presented at the SMRI Fall Meeting 2015, SMRI, Santander, Spain, pp. 3–19.

Manthei, G., Plenkers, K., 2018. Review on in situ acoustic emission monitoring in the context of structural health monitoring in mines. Applied Sciences 8, 1595.

Marketos, G., Spiers, C.J., Govers, R., 2016. Impact of rock salt creep law choice on subsidence calculations for hydrocarbon reservoirs overlain by evaporite caprocks: ROCK SALT FLOW AND SUBSIDENCE OVER GAS FIELDS. J. Geophys. Res. Solid Earth 121, 4249–4267. https://doi.org/10.1002/2016JB012892

Marlow, R.S., 1989. Cement Bonding Characteristics in Gas Wells. Journal of Petroleum Technology 41, 1146–1153. https://doi.org/10.2118/17121-PA

Martínez, C., Viedma, P., Cárdenas, F., Cotoras, D., 2023. Biogenic Hydrogen Sulfide Production Using Elemental Sulfur and Low-Cost Organic Substrates to Remove Metal Ions from Mining Effluents. Mining 3, 241–260. https://doi.org/10.3390/mining3020015

Maruyama, T., 1964. Statical elastic dislocations in an infinite and semi-infinite medium. Bulletin of the Earthquake Research Institute 42, 289–368.

McCauley, T.V., Ratigan, J.L., Sydansk, R.D., Wilson, S.D., 1998. Characterization of the brine loss zone and development of a polymer gel plugging agent to repair Louisiana Offshore Oil Port (LOOP) Cavern 14, in: Proceedings. Presented at the SMRI Fall Meeting 1998, SMRI, Roma, Italy.

McInnes, L., Healy, J., Astels, S., 2017. hdbscan: Hierarchical density based clustering. Journal of Open Source Software 2, 205. https://doi.org/10.21105/joss.00205

McLeod, R., Cooke, D., Slingsby, J., 2011. The repair of a gas storage cavern well after failure of a pre-operational Mechanical Integrity Test, in: Proceedings. Presented at the SMRI Fall Meeting 2011, SMRI, York, UK.

Meinecke, I., Walter, M., Kruck, O., 2013. A Hydraulic Mechanical Integrity Test of an Oil Cavern using the SoMIT Method, in: Proceedings. Presented at the SMRI Fall Meeting 2013, SMRI, Avignon, France.

Mellegard, K.D., DeVries, K.L., Callahan, G.D., 2007. Lode angle effects on the creep of salt, in: The Mechanical Behavior of Salt – Understanding of THMC Processes in Salt. CRC Press.

Mensen, A.J.H., Paar, W.A., 2002. Modelleren van bodemdaling bij zoutwinning, in: Barends, F.B.J., Kenselaar, F., Schröder, F.H. (Eds.), Bodemdaling meten in Nederland. Hoe precies moet het? Hoe moet het precies? NCG Nederlandse Commissie voor Geodesie, Delft, The Netherlands, pp. 63–77.

Menzel, W., Schreiner, W., 1985. Results of rock mechanical investigations for establishing storage cavern in salt formations, in: Proceedings. Presented at the 6th Symposium on Salt 1983, Salt Institute, Toronto, Ontario, pp. 501–510.

Mercerat, E.D., Driad-Lebeau, L., Bernard, P., 2010. Induced seismicity monitoring of an underground salt cavern prone to collapse. Pure and Applied Geophysics 167, 5–25.

Minkley, W., Menzel, W., 1996. Local Instability and System Instability of Room and Pillar Fields in Potash Mining, in: Proceedings. Presented at the 3rd Conference Mechanical Behaviour of Salt, Trans Tech Publications, pp. 497–510.

Miyazaki, B., 2009. Well integrity: An overlooked source of risk and liability for underground natural gas storage. Lessons learned from incidents in the USA. Geological Society, London, Special Publications 313, 163–172. https://doi.org/10.1144/SP313.11

Mohr, M., Kukla, P.A., Urai, J.L., Bresser, G., 2005. Multiphase salt tectonic evolution in NW Germany: Seismic interpretation and retro-deformation. International Journal of Earth Sciences 94, 917–940. https://doi.org/10.1007/s00531-005-0039-5

Muhammed, N.S., Haq, B., Al Shehri, D., Al-Ahmed, A., Rahman, M.M., Zaman, E., 2022. A review on underground hydrogen storage: Insight into geological sites, influencing factors and future outlook. Energy Reports 8, 461–499. https://doi.org/10.1016/j.egyr.2021.12.002

Munson, D.E., 2008. Bryan Mound Storage Caverns Features and the Internal Structure of the Dome, in: Proceedings. Presented at the SMRI Fall 2008 Technical Conference, SMRI, Galveston, Texas, p. 26.

Munson, D.E., 1998. Analysis of Multistage and Other Creep Data for Domal Salts (No. SAND98-2276). Sandia National Laboratories (SNL), Albuquerque, NM, and Livermore, CA (United States). https://doi.org/10.2172/1897

Munson, D.E., 1997. Constitutive model of creep in rock salt applied to underground room closure. International Journal of Rock Mechanics and Mining Sciences 34, 233–247. https://doi.org/10.1016/S0148-9062(96)00047-2

Munson, D.E., Dawson, P.R., 1984. Salt-constitutive modeling using mechanism maps, in: Proceedings. Presented at the 1st Conference Mechanical Behaviour of Salt, Trans Tech Publications, Pennsylvania State University, Pennsylvania, pp. 717–737.

Munson, D.E., DeVries, K.L., Schiermeister, D.M., DeYonge, W.F., Jones, R.L., 1992. Measured and calculated closures of open and brine filled shafts and deep vertical boreholes in salt, in: Proceedings. Presented at the The 33rd U.S. Symposium on Rock Mechanics (USRMS), OnePetro, Santa Fe, New Mexico.

Munson, D.E., Ehgartner, B., Bauer, S., Rautman, C., Myers, R., 2004. Analysis of a Salt Fall in Big Hill Cavern 103, and A Preliminary Concept of Salt Dome Structure, in: Proceedings. Presented at the SMRI Spring Meeting 2004, SMRI, Wichita, Kansas, p. 15.

Munson, D.E., Molecke, M.A., Myers, R.E., 1998. Interior cavern conditions and salt fall potential, in: Proceedings. Presented at the SMRI Spring Meeting 1998, SMRI, New Orleans, Louisiana. https://doi.org/10.2172/650136

Muntendam-Bos, A.G., Hoedeman, G., Polychronopoulou, K., Draganov, D., Weemstra, C., Zee, W. van der, Bakker, R.R., Roest, H., 2022. An overview of induced seismicity in the Netherlands. Netherlands Journal of Geosciences 101, 20. https://doi.org/10.1017/njg.2021.14

Murtey, M.D., Ramasamy, P., Murtey, M.D., Ramasamy, P., 2016. Retracted: Sample Preparations for Scanning Electron Microscopy – Life Sciences, in: Modern Electron Microscopy in Physical and Life Sciences. IntechOpen. https://doi.org/10.5772/61720

Nations, J.D., 2005. Report to Arizona Oil and Gas Commission on safety at gas storage facilities. Arizona Oil and Gas Conservation Commission, Tucson, Arizona.

Neal, J.T., Bauer, S.J., Ehgartner, B.L., 1995. Sinkhole progression at the Weeks Island, Louisiana, Strategic Petroleum Reserve (SPR) site, in: Proceedings. Presented at the SMRI Fall Meeting 1995, SMRI, San Antonio, Texas, p. 20.

Neal, J.T., Magorian, T.R., Ahmad, S., 1994. Strategic Petroleum Reserve (SPR) additional geologic site characterization studies, Bryan Mound Salt Dome, Texas (Sandia report No. SAND94-2331). Sandia National Laboratories. https://doi.org/10.2172/10196809

Nelson, P.E., van Sambeek, L.L., 2003. State-of-the-art review and new techniques for Mechanical Integrity Tests of (gas-filled) natural gas storage caverns (SMRI research project report No. 2001–4). SMRI.

Nguyen Minh, D., Maïtournam, H., Braham, S., Durup, J.G., 1993. A tentative interpretation of Long-Term subsidence Measurements over a solution-Mined Cavern Field, in: Proceedings. Presented at the 7th Symposium on Salt 1992, Elsevier, Kyoto, Japan, pp. 441–450.

Nicot, J.-P., 2009. A survey of oil and gas wells in the Texas Gulf Coast, USA, and implications for geological sequestration of CO2. Environ Geol 57, 1625–1638. https://doi.org/10.1007/s00254-008-1444-4

Nieland, J.D., 2008. Salt cavern thermodynamics–Comparison between hydrogen, natural gas, and air storage, in: Proceedings. Presented at the SMRI Fall Meeting 2008, SMRI, Austin, Texas, pp. 215–234.

Nikolinakou, M.A., Flemings, P.B., Hudec, M.R., 2014a. Modeling stress evolution around a rising salt diapir. Marine and Petroleum Geology 51, 230–238. https://doi.org/10.1016/j.marpetgeo.2013.11.021

Nikolinakou, M.A., Hudec, M.R., Flemings, P.B., 2014b. Comparison of evolutionary and static modeling of stresses around a salt diapir. Marine and Petroleum Geology 57, 537–545. https://doi.org/10.1016/j.marpetgeo.2014.07.002

Omosebi, O.A., Sharma, M., Ahmed, R.M., Shah, S.N., Saasen, A., Osisanya, S.O., 2017. Cement Degradation in CO2 - H2S Environment under High Pressure-High Temperature Conditions. Presented at the SPE Bergen One Day Seminar, OnePetro. https://doi.org/10.2118/185932-MS

Osnes, J.D., DeVries, K.L., Ratigan, J.L., Meece, M.W., Thompson, M., Spencer, G.W., 2007. A case history of the threaded coupling production casing failure in gas caverns – Part 1: detection and geomechanical analysis, in: Proceedings. Presented at the SMRI Fall Meeting 2007, SMRI, Halifax, Nova Scotia, p. 29p.

Ostertag-Henning, C., Alperman, T., Krüger, M., Dohrmann, A., Keller, S., Stanjek, H., Thüns, N., Krooss, B.M., Amann-Hildenbrand, A., Gaus, G., Zieger, L., Pilz, P., Hierold, J., Schmidt-Hattenberger, C., Strauch, B., 2021. Transport of hydrogen in rocks considering abiotic chemical and microbial redox reactions: The H2_ReacT research projects. Presented at the 2nd Geoscience & Engineering in Energy Transition Conference, European Association of Geoscientists & Engineers, pp. 1–5. https://doi.org/10.3997/2214-4609.202121064

Pan, B., Yin, X., Iglauer, S., 2021. Rock-fluid interfacial tension at subsurface conditions: Implications for H2, CO2 and natural gas geo-storage. International Journal of Hydrogen Energy 46, 25578–25585. https://doi.org/10.1016/j.ijhydene.2021.05.067

Panfilov, M., 2016. 4 - Underground and pipeline hydrogen storage, in: Gupta, R.B., Basile, A., Veziroğlu, T.N. (Eds.), Compendium of Hydrogen Energy, Woodhead Publishing Series in Energy. Woodhead Publishing, pp. 91–115. https://doi.org/10.1016/B978-1-78242-362-1.00004-3

Park, B.-Y., Ehgartner, B.L., Lee, M.Y., Sobolik, S.R., Herrick, C.G., 2006. Numerical Simulation Evaluating the Structural Integrity of SPR Caverns in the Big Hill Salt Dome. Presented at the Golden Rocks 2006, The 41st U.S. Symposium on Rock Mechanics (USRMS), OnePetro.

Peach, C.J., 1991. Influence of deformation on the fluid transport properties of salt rocks (Dissertation). Geologica Ultraiectina. Faculteit Aardwetenschappen der Rijksuniversiteit te Utrecht, University Utrecht.

Peach, C.J., Spiers, C.J., Trimby, P.W., 2001. Effect of confining pressure on dilatation, recrystallization, and flow of rock salt at 150°C. Journal of Geophysical Research: Solid Earth 106, 13315–13328. https://doi.org/10.1029/2000JB900300

Pellizzaro, C., Bergeret, G., Leadbetter, A., Charnavel, Y., 2011. Thermomechanical behavior of Stublach gas storage caverns, in: Proceedings. Presented at the SMRI Fall Meeting 2011, SMRI, York, UK, pp. 161–178.

Pereira, J.C, 2012. Common practices – gas cavern site characterization, design, construction, maintenance, and operation (MRI Project Report No. RR2012- 03). SMRI.

Pereira, José C., 2012. Common Practices – Gas Cavern Site Characterization, Design, Construction, Maintenance, and Operation (No. RR2012- 03_SMRI). SMRI.

Pfeiffer, W.T., Bauer, S., 2015. Subsurface Porous Media Hydrogen Storage – Scenario Development and Simulation. Energy Procedia, European Geosciences Union General Assembly 2015 - Division Energy, Resources and Environment, EGU 2015 76, 565–572. https://doi.org/10.1016/j.egypro.2015.07.872

Pfeifle, T.W., Hurtado, L.D., 2000. Effect of pore pressure on damage accumulation in salt, in: Geertman, R.M. (Ed.), Proceedings 8th World Salt Symposium. Elsevier, pp. 307–312.

Pichat, A., 2022. Stratigraphy, Paleogeography and Depositional Setting of the K–Mg Salts in the Zechstein Group of Netherlands—Implications for the Development of Salt Caverns. Minerals 12, 486. https://doi.org/10.3390/min12040486

Pirkle, R.J., 1986. Near Surface Geochemical Monitoring of Underground Gas Storage Facilities. Chicago, Illinois.

Pluymakers, A.M.H., Peach, C.J., Spiers, C.J., 2014. Diagenetic compaction experiments on simulated anhydrite fault gouge under static conditions. Journal of Geophysical Research: Solid Earth 119, 4123–4148. https://doi.org/10.1002/2014JB011073

Pluymakers, A.M.H., Spiers, C.J., 2015. Compaction creep of simulated anhydrite fault gouge by pressure solution: theory v. experiments and implications for fault sealing. Geological Society, London, Special Publications 409, 107–124. https://doi.org/10.1144/SP409.6

Popov, A.A., Sobolev, S.V., Zoback, M.D., 2012. Modeling evolution of the San Andreas Fault system in northern and central California. Geochemistry, Geophysics, Geosystems 13. https://doi.org/10.1029/2012GC004086

Popp, T., Kern, H., Schulze, O., 2002. Permeation and development of dilatancy in rock salt, in: Proceedings. Presented at the 5th Conference Mechanical Behaviour of Salt, CRC Press.

Popp, T., Kern, H., Schulze, O., 1999. Lithologische Variabilität der petrophysikalischen und mineralogisch-gefügekundlichen Eigenschaften des älteren Steinsalzes (z2) aus dem Salzstock Gorleben. Meyniana 51, 55–75.

Popp, T., Minkley, W., Salzer, O., Schulze, K., 2012. Gas transport properties of rock salt—synoptic view, in: Proceedings. Presented at the 7th Conference Mechanical Behaviour of Salt, Taylor & Francis, pp. 143–153.

Popp, T., Wiedemann, M., Kansy, A., Pusch, G., 2007. Gas transport in dry rock salt – implications from laboratory investigations and field studies, in: Proceedings. Presented at the 6th Conference Mechanical Behaviour of Salt, Taylor & Francis, pp. 17–26. https://doi.org/10.1201/9781315106502-3

Portarapillo, M., Di Benedetto, A., 2021. Risk Assessment of the Large-Scale Hydrogen Storage in Salt Caverns. Energies 14, 2856. https://doi.org/10.3390/en14102856

Pötschke, L., Huber, P., Stegschuster, G., Schriever, S., Kroppen, N., Schmatz, J., Gries, T., Blank, L.M., Farber, P., Rosenbaum, M.A., 2022. Customized Woven Carbon Fiber Electrodes for Bioelectrochemical Systems—A Study of Structural Parameters. Frontiers in Chemical Engineering 4.

Poyer, C., Cochran, M., 2003. Kansas underground storage regulations, in: Proceedings. Presented at the SMRI Spring Meeting 2003, SMRI, Houston, Texas.

Pratt, H.R., Hustrulid, W.A., Stephenson, D.E., 1978. Earthquake damage to underground facilities (PREPARED FOR THE U. S. DEPARTMENT OF ENERGY UNDER CONTRACT AT(07-2)-1 No. DP-1513). E. 1. DU PONT DE NEMOURS AND COMPANY SAVANNAH RIVER LABORATORY, Aiken, South Carolina.

Pudewills, A., 2012. Numerical simulation of coupled Thermo-Hydro-Mechanical processes in rock salt, in: Proceedings. Presented at the 7th Conference Mechancial Behaviour of Salt, Taylor & Francis.

Pusch, G., Alkan, H., 2002. Gas Permeation Models Related to Dilatancy Development Under Deviatoric Stress conditions, in: Proceedings. Presented at the SMRI Fall Meeting 2002, SMRI, Bad Ischl, Austria, pp. 213–232.

Putnis, A., 2009. Mineral Replacement Reactions. Reviews in Mineralogy and Geochemistry 70, 87–124. https://doi.org/10.2138/rmg.2009.70.3

Quast, P., 1983. L'installation de Huntorf : Plus de trois années de fonctionnement de cavernes à air comprimé. Annales des Mines 5, 93–102.

Quintanilha de Menezes, J.E., Guerreiro, V.N., Lúcio, J.M., 2001. Natural gas underground storage at Carriço in Portugal, in: Proceedings. Presented at the SMRI Fall Meeting 2001, SMRI, Albuquerque, New Mexico.

Rahbari, A., Brenkman, J., Hens, R., Ramdin, M., van den Broeke, L.J.P., Schoon, R., Henkes, R., Moultos, O.A., Vlugt, T.J.H., 2019. Solubility of Water in Hydrogen at High Pressures: A Molecular Simulation Study. J. Chem. Eng. Data 64, 4103–4115. https://doi.org/10.1021/acs.jced.9b00513

Raith, A.F., Strozyk, F., Visser, J., Urai, J.L., 2016. Evolution of rheologically heterogeneous salt structures: A case study from the NE Netherlands. Solid Earth 7, 67–82. https://doi.org/10.5194/se-7-67-2016

Raith, A.F., Urai, J.L., Visser, J., 2017. Structural and microstructural analysis of K–Mg salt layers in the Zechstein 3 of the Veendam Pillow, NE Netherlands: Development of a tectonic mélange during salt flow. Netherlands Journal of Geosciences 96, 331–351. https://doi.org/10.1017/njg.2017.31

Ramesh Kumar, K., Makhmutov, A., Spiers, C.J., Hajibeygi, H., 2021. Geomechanical simulation of energy storage in salt formations. Sci Rep 11, 19640. https://doi.org/10.1038/s41598-021-99161-8

Ratigan, J., 2003. The SMRI Cavern Sealing & Abandonment Research Program Summary, in: Proceedings. Presented at the SMRI Spring Meeting 2003, SMRI, Houston, Texas, pp. 141–164.

Ratigan, J.L., 2014. Examples of Surface Subsidence Induced by Salt Caverns, in: Proceedings. Presented at the SMRI Fall Meeting 2014, SMRI, Groningen, The Netherlands.

Ratigan, J.L., 2009. Liquefied petroleum gas storage at Mont Belvieu, Texas, USA, in: In: Sha Zuoliang (Ed.), Proc. Presented at the 9th World Salt Symposium, Gold Wall Press, Beijing, China, pp. 449–456.

Ratigan, J.L., 2001. Testimony before the Kansas Senate Utilities Committee, Topeka, Kansas.

Ratigan, J.L., 1991. Subsidence at Mont Belvieu, in: Proceedings. Presented at the SMRI Spring Meeting 1991, SMRI, Atlanta, Georgia.

Ratigan, J.L., McClain, A., Nichols, J., Hoffine, S., 2002. Fugitive NGL at the Williams midstream natural gas liquids Conway underground storage facility – Geologic and hydrogeologic studies, Cavern well testing and NGL recovery plans. Presented at the SMRI Spring Meeting 2002, SMRI, Banff, Alberta, pp. 339–362.

Rautman, C.A., Stein, J.S., 2003. Three-dimensional representations of salt-dome margins at four active strategic petroleum reserve sites. (Sandia report No. SAND2003-3300). Sandia National Laboratories (SNL), Albuquerque, NM, and Livermore, CA (United States). https://doi.org/10.2172/876351

Reitze, A., 2000. Prediction of ground movements above salt caverns using influence functions, in: Proceedings. Presented at the SMRI Fall Meeting 2000, SMRI, San Antonio,Texas.

Remizov, V.V., Pozdnyakov, A.G., Igoshin, A.I., 2000. Examination of rock salt underground cavern testing for leak-tightness by pressure alteration, in: Proceedings. Presented at the SMRI Fall Meeting 2000, SMRI, San Antonio, Texas, pp. 55–64.

Remmelts, G., 2011. Mogelijke alternatieven voor onder-grondse opslag van gas in de zoutkoepel Pieterburen (No. TNO-060-UT-2011-00725). TNO, Utrecht, The Netherlands.

Réveillère, A., 2017. Examples of historical incidents on storage salt caverns, SMRI Fall 2017 Technical Class. SMRI, Münster, Germany.

Réveillère, A., Azimi, B., Arnold, C., 2016. Prevention of stored gas humidification: lessons learnt and review of possibilities. Presented at the Solution Mining Research Institute Spring 2016 Technical Conference, Galveston, Texas, USA.

Réveillère, A., Bérest, P., Evans, D.J., Stöwer, M., Chabannes, C., Koopmans, T., Bolt, R., 2017. Past Salt Caverns Incidents Database Part 1: Leakage, Overfilling and Blow-out (Research Report No. RR2017-2). SMRI, Clarks Summit.

Réveillère, A., Bérest, P., Jeronimo, R., 2021. Past Salt Caverns Incidents Database Part 2: Sinkholes, Major Block Falls, Roof Falls, Casing Overstretch, Hydraulic Connections and Unexpectedly Fast Creep (Research Report No. RR2021-3). SMRI.

Rittenhour, T.P., Heath, S.A., 2012. Moss Bluff Cavern 1 Blowout, in: Proceedings. Presented at the SMRI Fall Technical Conference 2012, SMRI, Bremen, Germany, pp. 119–130.

Rohr, H.U., 1974. Mechanical behavior of a gas storage cavern in evaporitic rocks, in: Proceedings. Presented at the 4th Symposium on Salt, Salt Institute, pp. 93–100.

Rokahr, R., Staudtmeister, K., Schiebenhöfer, D., Johansen, J.I., 2007. In-situ Test with a Gas Storage Cavern as a Basis for Optimization, in: Proceedings. Presented at the SMRI Spring Meeting 2007, SMRI, Basel, Switzerland, pp. 84–97.

Rokahr, R., Staudtmeister, K., Zander-Schiebenhöfer, D., 2003. High pressure cavern analysis, in: Proceedings. Presented at the SMRI Spring Meeting 2003, SMRI, Houston, Texas, USA, pp. 88–113.

Rokahr, R., Staudtmeister, K., Zapf, D., 2011. Rock mechanical design for a planned gas cavern field in the Preesall Project Area, Lancashire, UK, in: Proceedings. Presented at the SMRI Fall Meeting 2011, SMRI, York, UK, pp. 189–204.

Rokahr, R.B., Hauck, R., Staudtmeister, K., Zander-Schiebenhöfer, D., 2000. The results of the pressure build-up test in the brine filled cavern Etzel K102, in: Proceedings. Presented at the SMRI Fall Meeting 2000, SMRI, San Antonio, Texas, pp. 89–100.

Roncal-Herrero, T., Astilleros, J.M., Bots, P., Rodríguez-Blanco, J.D., Prieto, M., Benning, L.G., Fernández-Díaz, L., 2017. Reaction pathways and textural aspects of the replacement of anhydrite by calcite at 25 °C. American Mineralogist 102, 1270–1278. https://doi.org/10.2138/am-2017-5963CCBY

Rowan, M.G., Urai, J.L., Fiduk, J.C., Kukla, P.A., 2019. Deformation of intrasalt competent layers in different modes of salt tectonics. Solid Earth 10, 987–1013. https://doi.org/10.5194/se-2019-49

Ruigrok, E., Spetzler, J., Dost, B., Evers, L., 2019. KNMI, Dept. R&D Seismology and Acoustics 14.

Ruigrok, E., Spetzler, J., Dost, B., Evers, L., 2018. KNMI, Dept. R&D Seismology and Acoustics 27.

Rummel, F., Benke, K., Denzau, H., 1996. Hydraulic fracturing stress measurements in the Krummhörn gas storage field, northwestern Germany, in: Proceedings. Presented at the SMRI Spring Meeting 1996, SMRI, Houston, Texas.

Sainburg, T., McInnes, L., Gentner, T.Q., 2021. Parametric UMAP Embeddings for Representation and Semisupervised Learning. Neural Computation 1–27. https://doi.org/10.1162/neco_a_01434

SaskEnergy, 2016a. Media release, available online 26/10/2016.

SaskEnergy, 2016b. SaskEnergy completes investigation into Prud'homme cavern wellhead fire; decommissions affected underground storage cavern [WWW Document]. SaskEnergy. URL https://www.saskenergy.com/about-us/newsroom/saskenergy-completes-investigation-prudhomme-cavern-wellhead-fire-decommissions (accessed 7.27.22).

SaskEnergy, 2015. Media release, available online 26/10/2016.

Schenk, O., Urai, J.L., 2004. Microstructural evolution and grain boundary structure during static recrystallization in synthetic polycrystals of sodium chloride containing saturated brine. Contributions to Mineralogy and Petrology 146, 671–682. https://doi.org/10.1007/s00410-003-0522-6

Schlichtenmayer, M., Bannach, A., Amro, M., Freese, C., 2015. Renewable Energy Storage in Salt Caverns – A comparison of Thermodynamics and Permeability between Natural Gas, Air and Hydrogen (Report prepared for the Solution Mining Research Institute No. 2015–1). SMRI.

Schmalholz, S.M., Schmid, D.W., 2012. Folding in power-law viscous multi-layers. Philos Trans A Math Phys Eng Sci 370, 1798–1826. https://doi.org/10.1098/rsta.2011.0421

Schmatz, J., Klaver, J., Jiang, M., Urai, J.L., 2017. Nanoscale morphology of brine/oil/mineral contacts in connected pores of carbonate reservoirs: Insights on wettability from cryo-BIB-SEM. SPE Journal 22, 1374–1384. https://doi.org/10.2118/180049-PA

Schmatz, J., Klaver, J., Wellmann, E., Jiang, M., Kraus, W., Freitag, S., Hoffmann, A., Deckert, H., 2022. Prediction of Fault Rock Permeability With Deep Learning: Training Data from Transfer Samples of Fault Cores. Presented at the 83rd EAGE Annual Conference & Exhibition, European Association of Geoscientists & Engineers, pp. 1–5. https://doi.org/10.3997/2214-4609.202210764

Schmatz, J., Urai, J.L., Berg, S., Ott, H., 2015. Nanoscale imaging of pore-scale fluid-fluid-solid contacts in sandstone. Geophysical Research Letters 42, 2189–2195. https://doi.org/10.1002/2015GL063354

Schreiner, W., Jäpel, G., Popp, T., 2004. Pneumatic fracture tests and numerical modeling for evaluation of the maximum gas pressure capacity and the effective stress conditions in the leaching horizon of storage caverns in salt diapirs, in: SMRI Fall Conference.

Schreiner, W., Lindert, A., Brückner, D., 2010. IfG Cavern design concept. Rock mechanical aspects for the development and operation of rock salt caverns, in: Proceedings. Presented at the SMRI Fall Meeting 2010, SMRI, Leipzig, Germany.

Schultze, O., 2007. Investigations on damage and healing in rocks, in: Proceedings. Presented at the 6th Conference Mechanical Behaviour of Salt, Taylor & Francis, pp. 33–44.

Schultz-Ela, D., Jackson, M., Vendeville, B., 1993. Mechanics of Active Diapirism. Tectonophysics 228, 275–312. https://doi.org/10.1016/0040-1951(93)90345-K

Schultz-Ela, D.D., Jackson, M.P.A., 1996. Relation of subsalt structures to suprasalt structures during extension. AAPG bulletin 80, 1896–1924.

Schwab, L., Popp, D., Nowack, G., Bombach, P., Vogt, C., Richnow, H.H., 2022. Structural analysis of microbiomes from salt caverns used for underground gas storage. International Journal of Hydrogen Energy 47, 20684–20694. https://doi.org/10.1016/j.ijhydene.2022.04.170

Schweinsburg, H.J., Schneider, R., 2010. Etzel Cavern storage Rock mechanical and solution mining aspects relating to cavern field expansion, in: Proceedings. Presented at the SMRI Spring Meeting 2010, Grand Junction, Colorado.

Serata, S., Cundey, T.E., 1979. Design Variables in Solution Cavities for Storage of Solids, Liquids and Gases, in: Proc. 5th Symposium on Salt. The Northern Ohio Geological Society Inc. Pub., pp. 161–170.

Serata, S., Fuenkajorn, K., 1993. Formulation of a Constitutive Equation for Salt, in: Proceedings. Presented at the 7th Symposium on Salt, Elsevier, pp. 483–488.

Shewchuk, J.R., 1996. Triangle: Engineering a 2D Quality Mesh Generator and Delaunay Triangulator, in: Lin, M.C., Manocha, D. (Eds.), Applied Computational Geometry: Towards Geometric Engineering, Lecture Notes in Computer Science. Springer-Verlag, pp. 203–222.

Shober, F., Sroka, A., Hartmann, A., 1987. Ein Konzept zur Senkungs vor ausberech nungûber Kavernen feldern. Kali und Steinsalz 9, 374–379.

Sicsic, P., Bérest, P., 2014. Thermal cracking following a blowout in a gas-storage cavern. International Journal of Rock Mechanics and Mining Sciences 71, 320–329. https://doi.org/10.1016/j.ijrmms.2014.07.014

Sijm, J.P.M., Janssen, G.J.M., Morales España, G.A., van Stralen, J., Hernandez-Serna, R., Smekens, K.E.L., 2020. The role of large-scale energy storage in the energy systems of the Netherlands 2030-2050 (No. TNO 2020 P11106). TNO, Petten.

Skaug, N., Ratigan, J.L., Lampe, B.C., 2011. A critical look at the Nitrogen/Brine Interface Mechanical Integrity Test, in: Proceedings. Presented at the SMRI Fall Meeting 2011, SMRI, York, UK, pp. 324–332.

Smit, A.J., 2019. Sudden pressure drop in Nedmag cavern cluster, in: Proceedings. Presented at the SMRI Fall Meeting 2019, SMRI, Berlin, Germany.

Smith, C.L., Barrett, M., Bell, K., Cosgrove, P., Eames, P., Garvey, S., Metcalfe, I., Muskett, M., Nayak-Luke, R., Rhys, J., Roulstone, T., Shah, N., Shearing, P., Valera-Medina, A., 2023. Large-scale electricity storage. The Royal Society, London, United Kingdom.

Sobolik, S.R., Ehgartner, B.L., 2012. Analyzing large pressure changes on the stability of large-diameter caverns using the M-D model, in: Proceedings. Presented at the Mechanical Behavoir of Salt VII, Taylor & Francis Group, Paris, France, pp. 321–329.

Sobolik, S.R., Ehgartner, B.L., 2009. Analysis of Cavern Stability at the Bryan Mound SPR Site (Sandia report No. SAND2009-1986). Sandia National Laboratories, Albuquerque, New Mexico 87185 and Livermore, California 94550.

Spang, A., Baumann, T.S., Kaus, B.J.P., 2022. Geodynamic Modeling With Uncertain Initial Geometries. Geochemistry, Geophysics, Geosystems 23, e2021GC010265. https://doi.org/10.1029/2021GC010265

Spiers, C.J., de Meer, S., Niemeijer, A.R., Zhang, X., 2003. Kinetics of rock deformation by pressure solution and the role of thin aqueous films, in: Physicochemistry of Water in Geological and Biological Systems - Structures and Properties of Thin Aqueous Films. Universal Academy Press, Tokyo, Japan, pp. 129–158.

Spiers, C.J., Schutjens, P.M.T.M., 1999. Intergranular Pressure Solution in Nacl: Grain-To-Grain Contact Experiments under the Optical Microscope. Oil & Gas Science and Technology - Rev. IFP 54, 729–750. https://doi.org/10.2516/ogst:1999062

Spiers, C.J., Schutjens, P.M.T.M., Brzesowsky, R.H., Peach, C.J., Liezenberg, J.L., Zwart, H.J., 1990. Experimental determination of constitutive parameters governing creep of rocksalt by pressure solution. Geological Society, London, Special Publications 54, 215–227. https://doi.org/10.1144/GSL.SP.1990.054.01.21

State of Louisiana, 2017. Oil Insurance Limited versus Dow Chemical Company, Dow Hydrocarbons and Resources Inc., Frank's Casing Crew Rental Tools inc. and Grey Wolf Drilling Company, State of Louisiana Court of Appeal, First Circuit, 2007 CA 0418. Judgment Rendered, November 2nd, 2007.

Staudtmeister, K., Zapf, D., Leuger, B., 2011. The influence of different loading scenarios on the thermo-mechanical behavior of a gas storage cavern, in: Proceedings. Presented at the SMRI Spring Meeting 2011, SMRI, Galveston Texas, pp. 83–97.

Staudtmeister, K., Zapf, D., Leuger, B., Elend, M., 2017. Temperature Induced Fracturing of Rock Salt Mass. Procedia Engineering 191, 967–974. https://doi.org/10.1016/j.proeng.2017.05.268

Stormont, J.C., Daemen, J.J.K., 1992. Laboratory study of gas permeability changes in rock salt during deformation. International Journal of Rock Mechanics and Mining Sciences & Geomechanics Abstracts 29, 325–342. https://doi.org/10.1016/0148-9062(92)90510-7

Strobel, G., Hagemann, B., Lüddeke, C.T., Ganzer, L., 2023. Coupled model for microbial growth and phase mass transfer in pressurized batch reactors in the context of underground hydrogen storage. Frontiers in Microbiology 14.

Strozyk, F., Urai, J.L., van Gent, H., de Keijzer, M., Kukla, P.A., 2014. Regional variations in the structure of the Permian Zechstein 3 intrasalt stringer in the northern Netherlands: 3D seismic interpretation and implications for salt tectonic evolution. Interpretation 2, SM101–SM117. https://doi.org/10.1190/INT-2014-0037.1

Strozyk, F., Van Gent, H., Urai, J.L., Kukla, P.A., 2012. 3D seismic study of complex intra-salt deformation: An example from the Upper Permian Zechstein 3 stringer, western Dutch offshore. Geological Society, London, Special Publications 363, 489–501. https://doi.org/10.1144/SP363.23

Stutz, D., Hermans, A., Leibe, B., 2018. Superpixels: An evaluation of the state-of-the-art. Computer Vision and Image Understanding 166, 1–27. https://doi.org/10.1016/j.cviu.2017.03.007

Ter Heege, J.H., De Bresser, J.H.P., Spiers, C.J., 2005. Dynamic recrystallization of wet synthetic polycrystalline halite: dependence of grain size distribution on flow stress, temperature and strain. Tectonophysics 396, 35–57. https://doi.org/10.1016/j.tecto.2004.10.002

Ter Heege, J. H., de Bresser, J.H.P., Spiers, C.J., 2005. Rheological behaviour of synthetic rocksalt: the interplay between water, dynamic recrystallization and deformation mechanisms. Journal of Structural Geology 27, 948–963. https://doi.org/10.1016/j.jsg.2005.04.008

Thaule, S.B., Gentzsch, L., 1994. Experience with Thermophysical Modelling of Gas Cavern Operations in Etzel, in: Proceedings. Presented at the SMRI Fall Meeting 1994, SMRI, Hannover, Germany.

Thiel, W.R., 1993. Precision Methods for testing the integrity of solution mined underground storage caverns, in: Proceedings. Presented at the 7th Symposium on Salt 1992, Elsevier, Kyoto, Japan, pp. 377–383.

Thiel, W.R., Russel, J.M., 2004. Pressure observation testing solution mined underground storage caverns in Kansas, in: Proceedings. Presented at the SMRI spring meeting 2004, SMRI, Wichita, Kansas, pp. 186–98.

Thompson, M., Spencer, G.W., Meece, M.W., Blair, R.W., Ratigan, J.L., 2007. A Case History of the Threaded Coupling Production Casing Failure in Gas Caverns — Part 2: Well Repair, Testing, and Return to Service, in: Proceedings. Presented at the SMRI Fall Meeting 2007, SMRI, Halifax, Nova Scotia, p. 14p.

Thoms, R.L., Gehle, R.M., 1983. Borehole tests to predict cavern performance, in: Proceedings. Presented at the SMRI Spring Meeting 1983, Toronto, Canada.

Thoms, R.L., Neal, J.T., 1992. Effects of anomalous features on solution mining of storage caverns in domal salt, in: Proceedings. Presented at the SMRI Fall Meeting 1992, SMRI, Houston, Texas.

Thorel, L., Ghoreychi, M., 1993. Rock salt damage. Experimental results and interpretation, in: Proceedings. Presented at the 3rd Conference Mechanical Behaviour of Salt, Taylor & Francis, pp. 97–106.

Tijani, M., Hadj-Hassen, F., Rouabhi, A., Gatelier, J.S.& N., 2012. Effect of insoluble materials on salt behavior during creep tests, in: Proceedings. Presented at the 7th Conference Mechanical Behaviour of Salt, CRC Press, p. 8.

Tijani, M., Hassen, F.H., Gatelier, N., 2009. Improvement of Lemaitre's creep law to assess the salt mechanical behavior for a large range of the deviatoric stress, in: Proceedings. Presented at the 9th International Symposium on Salt, Beijing, China, p. 135.

Torquato, S.,. Author, Haslach, HW ,. Jr, 2002. Random Heterogeneous Materials: Microstructure and Macroscopic Properties. Applied Mechanics Reviews 55, B62–B63. https://doi.org/10.1115/1.1483342

Toth, J., 1990. Gas is being burned off after mishap near Clute. Houston Chronicle 1.

Toth, J., 1989a. Search ruled out for chemical lost in Clute. Houston Chronicle, Section: B 1.

Toth, J., 1989b. Firm backtracks, plans to drill well to find missing ethylene. Houston Chronicle 1.

Trautmann, A., Mori, G., Loder, B., 2021. Hydrogen Embrittlement of Steels in High Pressure H2 Gas and Acidified H2S-saturated Aqueous Brine Solution. Berg Huettenmaenn Monatsh 166, 450–457. https://doi.org/10.1007/s00501-021-01143-w

Truche, L., Berger, G., Destrigneville, C., Guillaume, D., Giffaut, E., 2010. Kinetics of pyrite to pyrrhotite reduction by hydrogen in calcite buffered solutions between 90 and 180°C: Implications for nuclear waste disposal. Geochimica et Cosmochimica Acta 74, 2894–2914. https://doi.org/10.1016/j.gca.2010.02.027

Trusheim, F., 1957. Über Halokinese und ihre Bedeutung für die strukturelle Entwicklung Norddeutschlands. Zeitschrift der Deutschen Geologischen Gesellschaft 111–151. https://doi.org/10.1127/zdgg/109/1957/111

Ugarte, E.R., Salehi, S., 2021. A Review on Well Integrity Issues for Underground Hydrogen Storage. Journal of Energy Resources Technology 144. https://doi.org/10.1115/1.4052626

Urai, J., Schléder, Z., Spiers, C., Kukla, P., 2008. Flow and Transport Properties of Salt Rocks, in: Dynamics of Complex Intracontinental Basins: The Central European Basin System. Springer, Berlin, Germany, pp. 277–290.

Urai, J.L., Schmatz, J., Klaver, J., 2019. Over-pressured salt solution mining caverns and leakage mechanisms, phase 1: micro-scale processes, KEM-17.

Urai, J.L., Spiers, C.J., 2017. The effect of grain boundary water on deformation mechanisms and rheology of rocksalt during long-term deformation, in: Wallner, M., Lux, K.-H., Minkley, W., Hardy, H.R. (Eds.), The Mechanical Behavior of Salt – Understanding of THMC Processes in Salt. CRC Press, pp. 149–158. https://doi.org/10.1201/9781315106502-17

Urai, J.L., Spiers, C.J., 2007. The effect of grain boundary water on deformation mechanisms and rheology of rocksalt during long-term deformation [WWW Document]. The Mechanical Behavior of Salt – Understanding of THMC Processes in Salt. https://doi.org/10.1201/9781315106502-17

Urai, J.L., Spiers, C.J., Zwart, H.J., Lister, G.S., 1986. Weakening of rock salt by water during long-term creep. Nature 324, 554–557. https://doi.org/10.1038/324554a0

van der Valk, K., van Unen, M., Brunner, L.G., Groenenberg, R.M., 2020. Inventory of risks associated with underground storage of compressed air (CAES) and hydrogen (UHS), and qualitative comparison of risks of UHS vs. underground storage of natural gas (UGS) (No. TNO 2020 R12005). TNO, Utrecht.

van Fossan, N.E., 1985. The characterization of mechanical integrity for cased boreholes entering solution caverns, in: Proceedings. Presented at the 6th International Symposium on Salt 1983, Salt Institute, Toronto, Ontario, pp. 111–120.

van Fossan, N.E., Whelply, F.V., 1985. Nitrogen as a testing medium for proving the mechanical integrity of wells, in: Proceedings. Presented at the SMRI fall meeting 1985, SMRI, Houston, Texas.

van Gent, H.W., Urai, J.L., de Keijzer, M., 2011. The internal geometry of salt structures – A first look using 3D seismic data from the Zechstein of the Netherlands. Journal of Structural Geology, Flow of Rocks 33, 292–311. https://doi.org/10.1016/j.jsg.2010.07.005

van Gessel, S., Huijskes, T., Juez-Larré, J., Dalman, R., 2021a. Ondergrondse Energieopslag in Nederland 2030 – 2050: Technische evaluatie van vraag en aanbod (No. TNO2021 R11125). TNO and EBN, Utrecht, The Netherlands.

van Gessel, S., Huijskes, T., Juez-Larré, J., Dalman, R., 2021b. Ondergrondse Energieopslag in Nederland 2030 – 2050: Ontwikkelpaden en aanbevelingen (No. TNO2021 R11147). TNO and EBN, Utrecht, The Netherlands.

van Gessel, S., Huijskes, T., Schroot, B., Dalman, R., 2021c. Ondergrondse energieopslag noodzakelijk voor toekomstig energiesysteem: Opslag garandeert leveringszekerheid en flexibiliteit.

van Gessel, S.F., Breunese, J.N., Juez-Larre, J., Huijskes, T.D., Remmelts, G., 2018. Ondergrondse opslag in Nederland - Technische verkenning (No. TNO 2018 R11372). TNO, Utrecht.

van Heekeren, H., Bakker, T., Duquesnoy, T., de Ruiter, V., 2009. Abandonment of an extremely deep Cavern at Frisia Salt, in: Proceedings. Presented at the SMRI Fall Meeting 2009, SMRI, Krakow, Poland, pp. 1–13.

van Noort, R., Visser, H.J., Spiers, C.J., 2008. Influence of grain boundary structure on dissolution controlled pressure solution and retarding effects of grain boundary healing. Journal of Geophysical Research: Solid Earth 113.

van Oort, E., 2022. Qualitative Risk Assessment of Long-Term Sealing Behavior of Materials and Interfaces in Boreholes KEM-18 – Final Report (No. KEM-18).

Van Oosterhout, B.G.A., Hangx, S.J.T., Spiers, C.J., 2022. A threshold stress for pressure solution creep in rock salt: Model predictions vs. observations, in: Proceedings. Presented at the 10th Conference on the Mechanical Behavior of Salt (SaltMech X), CRC Press, Utrecht University, The Netherlands, pp. 57–67.

van Rooijen, W., Hashemi, L., Boon, M., Farajzadeh, R., Hajibeygi, H., 2022. Microfluidics-based analysis of dynamic contact angles relevant for underground hydrogen storage. Advances in Water Resources 164, 104221. https://doi.org/10.1016/j.advwatres.2022.104221

van Sambeek, L., 2009. Natural compressed air storage: a catastrophe at a Kansas salt mine, in: Zuoliang Sha (Ed.), Proc. 9th Int. Symp. on Salt. Beijing, China, pp. 621–632.

van Sambeek, L., 2000. Subsidence Modeling and the use of the SMRI SALT_SUB SID Software, in: Proceedings. Presented at the SMRI Fall Meeting 2000, SMRI, San Antonio, Texas, pp. 11–22.

van Sambeek, L., Thoms, R., 2000. Pre- and Post-Flooding Surface Subsidence Rates at the Retsof, Belle Isle, Jefferson Island Salt Mines, in: Proceedings. Presented at the SMRI Fall Meeting 2000, SMRI, San Antonio, Texas, pp. 75–85.

van Sambeek, L.L., 2012. Measurements of humidity-enhanced salt creep in salt mines: Proving the Joffe effect, in: Proceedings. Presented at the 7th Conference on the Mechanical Behavior of Salt, Taylor & Francis, pp. 179–184.

van Sambeek, L.L., Bérest, P., Brouard, B., 2005. Improvements in Mechanical Integrity Tests for solution-mined caverns used for mineral production or liquid-product storage (SMRI research project report No. 2005–1). SMRI.

van Sambeek, L.L., Ratigan, J.L., Hansen, F.D., 1993. Dilatancy of rock salt in laboratory tests. International Journal of Rock Mechanics and Mining Sciences & Geomechanics Abstracts 30, 735–738. https://doi.org/10.1016/0148-9062(93)90015-6

Vasconcelos, C., McKenzie, J.A., 1997. Microbial mediation of modern dolomite precipitation and diagenesis under anoxic conditions (Lagoa Vermelha, Rio de Janeiro, Brazil). Journal of Sedimentary Research 67, 378–390. https://doi.org/10.1306/D4268577-2B26-11D7-8648000102C1865D

Vassileva, M., Al-Halbouni, D., Motagh, M., Walter, T.R., Dahm, T., Wetzel, H.-U., 2021. A decade-long silent ground subsidence hazard culminating in a metropolitan disaster in Maceió, Brazil. Sci Rep 11, 7704. https://doi.org/10.1038/s41598-021-87033-0

Viani, A., Sotiriadis, K., Lanzafame, G., Mancini, L., 2019. 3D microstructure of magnesium potassium phosphate ceramics from X-ray tomography: new insights into the reaction mechanisms. J Mater Sci 54, 3748–3760. https://doi.org/10.1007/s10853-018-3113-7

von Vogel, P., Marx, C., 1985. Berechnung von Blowoutraten in Erdgassonden. Erdoel-Erdgas 101.Jg, 311–316.

Vrakas, J.J., 1988. Cavern Integrity Testing on the SPR Program, in: Proceedings. Presented at the SMRI Spring Meeting 1988, SMRI, Mobile, Alabama.

Wagler, T., Draijer, A., 2013. Nitrogen buffer for large scale conditioning of H- to L-Gas. How to fit an existing cavern to capacity and performance requirements?, in: Proceedings. Presented at the SMRI Fall Meeting, SMRI, Avignon, France.

Wallner, M., 1988. Frac-Pressure risk for cavities in rock salt, in: Proceedings. Presented at the 2nd Conference Mechanical Behaviour Salt, Trans Tech Publications, pp. 645–658.

Wallner, M., 1984. Analysis of thermomechanical problems related to the storage of heat producing radioactive wastes, in: Proceedings. Presented at the 1st Conference Mechanical Behaviour of Salt, Trans Tech Publications, pp. 739–763.

Wallner, M., Eickemeier, R., 2001. Subsidence and Fractures Caused by Thermo-Mechanical Effects, in: Proceedings. Presented at the SMRI Spring Meeting 2001, SMRI, Orlando, Florida, pp. 363–371.

Wallner, M., Paar, W.A., 1997. Risk of progressive pressure build up in a sealed cavity, in: Proceedings. Presented at the SMRI Fall Meeting 1997, SMRI, El Paso, Texas, pp. 177–188.

Wang, L., Bérest, P., Brouard, B., 2015. Mechanical Behavior of Salt Caverns: Closed-Form Solutions vs Numerical Computations. Rock Mechanics and Rock Engineering 48, 2369–2382. https://doi.org/10.1007/s00603-014-0699-1

Wang, T., Yang, C., Chen, J., Daemen, J.J.K., 2018. Geomechanical investigation of roof failure of China's first gas storage salt cavern. Engineering Geology 243, 59–69. https://doi.org/10.1016/j.enggeo.2018.06.013

Wang, T., Yang, C., Li, Jianjun, Li, Jinlong, Shi, X., Ma, H., 2017. Failure analysis of overhanging blocks in the walls of a gas storage salt cavern: A case study. Rock Mechanics and Rock Engineering 50, 125–137. https://doi.org/10.1007/s00603-016-1102-1

Warnecke, M., Röhling, S., 2021. Untertägige Speicherung von Wasserstoff – Status quo. Zeitschrift der Deutschen Gesellschaft für Geowissenschaften 172, 641–659. https://doi.org/10.1127/zdgg/2021/0295

Warren, J.K., 2017. Salt usually seals, but sometimes leaks: Implications for mine and cavern stabilities in the short and long term. Earth-Science Reviews 165, 302–341. https://doi.org/10.1016/j.earscirev.2016.11.008

Warren, J.K., 2006. Solution mining and cavern use, in: Evaporites: Sediments, Resources and Hydrocarbons. Springer Berlin Heidelberg, Berlin, Heidelberg, pp. 893–943. https://doi.org/10.1007/3-540-32344-9_12

Watson, T.L., Bachu, S., 2009. Evaluation of the Potential for Gas and CO2 Leakage Along Wellbores. SPE Drilling & Completion 24, 115–126. https://doi.org/10.2118/106817-PA

Wawersik, W.R., Stone, C.M., 1989. A characterization of pressure records in inelastic rock demonstrated by hydraulic fracturing measurements in salt. International Journal of Rock Mechanics and Mining Sciences & Geomechanics Abstracts 26, 613–627. https://doi.org/10.1016/0148-9062(89)91442-3

Wawersik, W.R., Zeuch, D.H., 1986. Modeling and mechanistic interpretation of creep of rock salt below 200°C. Tectonophysics 121, 125–152. https://doi.org/10.1016/0040-1951(86)90040-5

Wellinghoff, J., Moeller, P.D., Norris, J.R., LaFleur, C.A., 2013. Order approving abandonment, amending certificate authority, and granting clarification, United States of America Federal Energy Regulatory Commission (FERC) decision relating to Transcontinental Gas Pipeline Company.

Wetzel, M., Kempka, T., Kühn, M., 2021. Diagenetic Trends of Synthetic Reservoir Sandstone Properties Assessed by Digital Rock Physics. Minerals 11, 151. https://doi.org/10.3390/min11020151

Winters, E., Puts, H., van Popering-Verkerk, J., Duijn, M., 2020. Legal and societal embeddedness of large-scale energy storage (No. TNO 2020 R11116). TNO, Den Haag.

Wolters, R., Lux, K.H., Düsterloh, U., 2012. Evaluation of rock salt barriers with respect to tightness: influence of thermomechanical damage, fluid infiltration and sealing/healing, in: Proceedings. Presented at the 7th Mechanical behaviour of Salt, Taylor & Francis, pp. 425–434.

Woodward, J.L., Cook, J., Papadourakis, A., 1995. Modeling and validation of a dispersing aerosol jet. Journal of Hazardous Materials, Consequence Modeling for Plant Safety and Environmental Impact 44, 185–207. https://doi.org/10.1016/0304-3894(95)00054-X

Yekta, A.E., Manceau, J.-C., Gaboreau, S., Pichavant, M., Audigane, P., 2018. Determination of Hydrogen–Water Relative Permeability and Capillary Pressure in Sandstone: Application to Underground Hydrogen Injection in Sedimentary Formations. Transp Porous Med 122, 333–356. https://doi.org/10.1007/s11242-018-1004-7

Yu, J., Wellmann, F., Virgo, S., von Domarus, M., Jiang, M., Schmatz, J., Leibe, B., 2023. Superpixel segmentations for thin sections: Evaluation of methods to enable the generation of machine learning training data sets. Computers & Geosciences 170, 105232. https://doi.org/10.1016/j.cageo.2022.105232

Zapf, D., Staudtmeister, K., Rokahr, R.B., 2012. Analysis of thermal induced fractures in salt, in: Proceedings. Presented at the SMRI Spring Meeting 2012, SMRI, Regina, Saskatchewan, pp. 47–62.

Zhang, Y., Dawe, R.A., 2000. Influence of Mg2+ on the kinetics of calcite precipitation and calcite crystal morphology. Chemical Geology 163, 129–138. https://doi.org/10.1016/S0009-2541(99)00097-2

Zienkiewicz, O.C., Taylor, R.L., 2000. Finite Element Method: Volume 1 - The Basis, 5th ed. Butterworth-Heinemann, Oxford.

Zingg, A., Holzer, L., Kaech, A., Winnefeld, F., Pakusch, J., Becker, S., Gauckler, L., 2008. The microstructure of dispersed and non-dispersed fresh cement pastes — New insight by cryo-microscopy. Cement and Concrete Research 38, 522–529. https://doi.org/10.1016/j.cemconres.2007.11.007

Appendix A: Munson-Dawson Creep Law

A.1 Munson-Dawson Creep Law

The Munson-Dawson (M-D) model comprises two differential equations: (1) the strain-rate equations that give the viscoplastic strain rates [Eq. (84)]; and (2) the evolutionary equation that gives the rate of change of an internal variable [Eq. (85)]. The three-dimensional form of the M-D model is given below:

$$\dot{\varepsilon}_{ij}^{vp} = \frac{\partial \sigma_e}{\partial \sigma_{ij}} F \, \dot{\varepsilon}_s \tag{84}$$

$$\dot{\varsigma} = \left(F - 1\right)\dot{\varepsilon}_s \tag{85}$$

where

$$\dot{\varepsilon}_s = \sum_{i=1}^{3} \dot{\varepsilon}_{s_i} \tag{86}$$

($\dot{\varepsilon}_{s_i}$ = steady-state strain rate for mechanism i)

$$\dot{\varepsilon}_{s_1} = A_1 \exp\left(-Q_1/RT\right)\left(\sigma_e/\mu\right)^{n_1} \tag{87}$$

$$\dot{\varepsilon}_{s_2} = A_2 \exp\left(-Q_2/RT\right)\left(\sigma_e/\mu\right)^{n_2} \tag{88}$$

$$\dot{\varepsilon}_{s_3} = \left[B_1 \exp\left(-Q_1/RT\right) + B_2 \exp\left(-Q_2/RT\right)\right] \cdot \sinh\left[q\left(\sigma_e - \sigma_o\right)/\mu\right] H\left(\sigma_e - \sigma_o\right) \tag{89}$$

$$F = \begin{cases} \exp\left[\Delta\left(1 - \dfrac{\varsigma}{\varepsilon_t^*}\right)^2\right] & \text{for } \varsigma < \varepsilon_t^* \\ 1 & \text{for } \varsigma = \varepsilon_t^* \\ \exp\left[-\delta\left(1 - \dfrac{\varsigma}{\varepsilon_t^*}\right)^2\right] & \text{for } \varsigma > \varepsilon_t^* \end{cases} \tag{90}$$

$$\varepsilon_t^* = K_o \exp\left(c_{MD} T\right)\left(\sigma_e/\mu_{MD}\right)^{m_{MD}} \tag{91}$$

$$\Delta = \alpha_w + \beta_w \log\left(\sigma_e/\mu_{MD}\right) \tag{92}$$

where

$\dot{\varepsilon}_{ij}^{vp} =$ viscoplastic strain-rate tensor

$\sigma_e =$ $\sqrt{3J_2}$ (effective stress)

$J_2 = \frac{1}{2} s_{ij} s_{ji}$

$s_{ij} =$ $\sigma_{ij} - \delta_{ij}\sigma_m$ (deviatoric stress tensor)

$\sigma_m = \frac{1}{3}\sigma_{kk}$ (mean stress)

$\sigma_{ij} =$ stress tensor

$\delta_{ij} =$ Kronecker delta

$\varsigma =$ internal variable

$T =$ absolute temperature

$H(x) =$ Heaviside function

$\mu_{MD} =$ a normalizing constant equal to the shear modulus (1.7985×10^6 psi = 12.4 GPa)

Terms $A_1, A_2, B_1, B_2, Q_1, Q2, n_1, n_2, q, \sigma_0, \delta, K_0, c, m, \alpha_w$ and β_w are experimentally determined parameters. As indicated by Eq. (86), the steady-state creep rate ($\dot{\varepsilon}_{ss}$) based on the M-D model is composed of three terms. Each term is associated with a different creep mechanism. The first, second and third mechanisms are dislocation climb, cross-slip, and dislocation glide, respectively.

The formulation of the M-D model is implemented into LOCAS. Dislocation climb (first mechanism) and dislocation glide (third mechanism) are not considered, because they contribute little to the strain rate of the salt surrounding most salt caverns. The dislocation-climb mechanism is important for very high temperature (> 250 °F = 120 °C), and the dislocation-glide mechanism is important for very high deviatoric stresses (> 300 psi = 20 MPa). The contribution of each steady-state mechanism to the total steady-state creep rate is illustrated in Figure 337 for a temperature of 120 °F (48.9 °C).

The trend seems to introduce a fourth mechanism, pressure-solution, in the small deviatoric stress domain. However, a general agreement has not yet been reached on the parameters of this law.

A.2 Munson-Dawson Creep Law Parameters

Table 36 provides the set of parameters for Munson-Dawson when considering Avery Island salt.

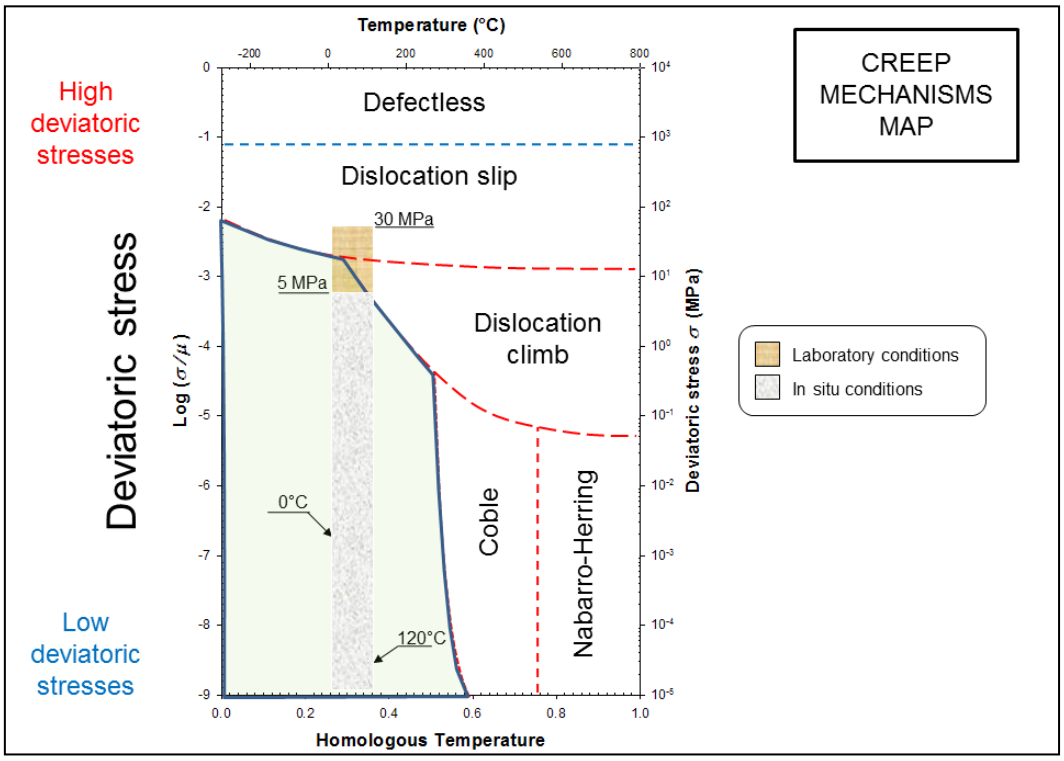

Figure 337. Mechanism Map (after Munson and Dawson, 1984).

Table 36 - Munson-Dawson parameters for Avery Island salt.

Parameter	U.S. Units		SI Units	
	Unit	Value	Unit	Value
A_1	year^{-1}	7.63×10^{28}	year^{-1}	7.63×10^{28}
n_1	—	5.5	—	5.5
A_2	year^{-1}	4.14×10^{16}	year^{-1}	4.14×10^{16}
n_2	—	3.14	—	3.14
$\frac{Q_1}{R}$	°R	22,734	K	12,630
Q_2/R	°R	11,736	K	6520
B_1	year^{-1}	2.17×10^{13}	year^{-1}	2.17×10^{13}
B_2	year^{-1}	6.89×10^{5}	year^{-1}	6.89×10^{5}
q	—	3.33×10^{3}	—	3.33×10^{3}
σ_0	psi	1280	MPa	8.83
K_0	—	2.52×10^{4}	—	2.52×10^{4}
m_{MD}	—	2.54	—	2.54
c_{MD}	°R^{-1}	0.017	K^{-1}	9.20×10^{-3}
α_w	—	-8.83	—	-8.83
β_w	—	-5.05	—	-5.05
δ	—	0.242	—	0.242
μ_{MD}	psi	1.40×10^{6}	MPa	9,619

Appendix B: Salt Dilation Criteria

B.1 Introduction

An increase in salt volume may occur under certain stress states. This volume increase is due to micro-fracturing in the salt, a phenomenon called dilation. Salt dilation must be avoided, as it may cause an increase in permeability and a reduction in salt strength. Table 37 gives the two dilation criteria that usually are considered.

Table 37. Salt-dilation criteria.

DILATION CRITERIA	REFERENCE	FORMULA
Criterion #1	Van Sambeek et al. (1993)	$\sqrt{J_2} = -0.27 I_1$
Criterion #2	DeVries (2006)	$\sqrt{J_2} = \frac{D_1 \left(\frac{I_1}{sgn(I_1)\,\sigma_0} \right)^{\bar{m}} + T_0}{\left(\sqrt{3}\cos\psi - D_2 \sin\psi \right)}$

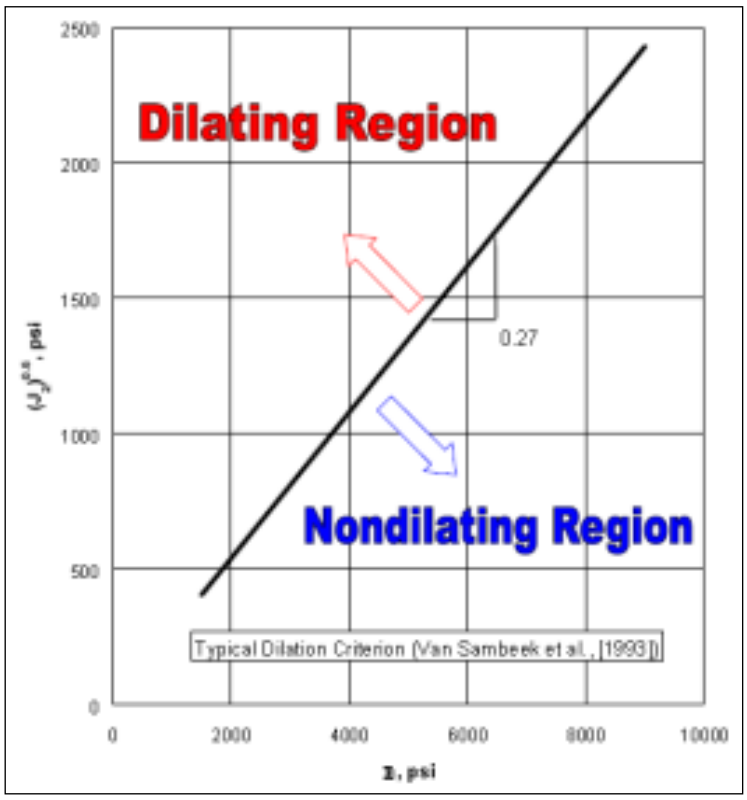

Figure 338. Van Sambeek dilation criterion (After DeVries et al., 2003).

B.2 Dilation Criterion #1 (Ratigan criterion)

Ratigan et al. (1991) and, later, Van Sambeek et al. (1993), suggested a simple linear criterion in the form

$$\sqrt{J_2}_{dil} = -0.27 I_1 \tag{93}$$

where I_1 ($I_1 < 0$) is equal to three times the mean stress ($I_1 = 3\sigma_m$), and J_2 are the first and second invariants of the stress tensor, respectively, which are defined as follows:

$$I_1 = \sigma_1 + \sigma_2 + \sigma_3 \tag{94}$$

$$J_2 = \frac{1}{6}[(\sigma_1 - \sigma_2)^2 + (\sigma_1 - \sigma_3)^2 + (\sigma_2 - \sigma_3)^2] \tag{95}$$

where σ_1, σ_2 and σ_3 are the principal stresses. (Compressive stresses are negative.) Figure 338 shows a sketch of dilating and non-dilating regions.

A Factor of Safety (FOS) can be defined from this Ratigan criterion:

$$FOS = \frac{\sqrt{J_2}_{dil}}{\sqrt{J_2}} \tag{96}$$

Dilation may appear when the FOS is lower than 1.

B.3 Dilation Criterion #2 (DeVries or RD criterion)

The dilatancy criterion developed by RE/SPEC (DeVries et al., 2003) is referred to as the RE/SPEC Dilation criterion.[1] The criterion is based on a Mohr-Coulomb-type failure criterion to represent salt failure as a function of shear stress, mean stress, and lode angle. The dilation limit of the criterion is defined as

$$\sqrt{J_2}_{dil} = \frac{D_1\left(\frac{I_1}{sign(I_1)\sigma_0}\right)^{\bar{m}} + T_0}{(\sqrt{3}\cos\psi - D_2 \sin\psi)} \tag{97}$$

where the lode angle (ψ) describes the relation between the principal stresses and ranges between – 30° and + 30°, σ_0 is a dimensional constant equal to 1 MPa (145 psi), T_0 is the unconfined tensile strength, and $\bar{m}$, D_1, and D_2 are parameters that must be determined for each salt formation. The RD criterion can predict both linear and nonlinear relations for the dilation boundary in the $\sqrt{J_2}$ and I_1 stress spaces.

[1] The RD criterion, also called the "DeVries criterion" in LOCAS, is based on whether the stress state is one that results in dilation (micro- or macro-fracturing associated with increases in porosity and permeability).

Appendix C: Sensitivity Analysis Additional Tables

Table 38 to Table 44 provides tables with configurations classified by depth, maximum diameter, etc.

Table 38. Sensitivity analysis in 2D. List of cases classified according to by cavern depth.

		Depth casing shoe			Cavern diameter			Cycling period			P_{min}		Creep Closure (m^3)	Subsidence (mm)	Conduction Heat Flux Loss (MWh)	Produced Energy (GWh)	Surface Area (m^2)	Effective Tensile Stress			Dilation			Vertical Strain at CS (%)	Max.Principal Stress (MPa)		Max. Effective Stress (MPa)		Dilation		Max.Principal Stress (MPa)		Max. Effective Stress (MPa)	
																		Max. tensile volume		Av. tensile strip thickness (m)	Max. dilatant volume		Av. dilatant strip thickness (m)	Strain @ 900 days (%)	Value (MPa)	Date (days)	Value (MPa)	Date (days)	Value 1/FOS	Date (days)	Value (MPa)	Date Output (Days)	Value (MPa)	Date Output (Days)
Case	Class	Z1	Z2	Z3	D1	D2	D3	S	Q	M	G1	G2	Volume loss @ 900 days	Subsidence @ 900 days	Cumulated energy @ 900 days	Cumulated energy @ 900 days		Value (m^3)	Date Output (Days)		Value	Date Output (Days)												
10	0	×				×					×		25 779	1.112	14 751	70.619	71 151	4 415 761	2870.61	62.06	330 734	2645.46	4.65	0.46	17.60	2881.83	23.11	2880.62	13.17	2335.24	15.12	2885.46	24.50	2150.61
14	0	×					×		×				15 769	1.392	8 350	23.932	59 163	5 668 992	2811.82	95.82	173 313	2856.36	2.93	0.56	11.79	2845.37	17.42	2840.92	11.35	2828.74	5.05	2856.36	17.84	2451.82
15	0	×					×			×	×		17 330	1.441	12 603	69.253	59 163	6 584 745	2870.61	111.30	169 031	2495.46	2.86	0.54	18.61	2882.10	23.99	2880.62	12.31	2395.14	18.58	2885.46	27.70	2270.61
6	1	×			×			×				×	29 307	0.069	8 334	4.266	103 713	500	2733.69	0.00	34 970	1095.00	0.34	0.15	-9.35	2176.98	0.40	2842.86	0.94	2175.46	-8.61	2553.03	0.16	2000.00
7	1	×			×				×			×	30 831	0.066	10 640	13.780	103 713	102 313	2856.36	0.99	34 970	1095.00	0.34	0.17	-0.83	2847.22	8.25	2844.77	1.47	2847.37	-2.13	2856.36	6.37	2856.36
8	1	×			×					×		×	33 596	0.089	12 982	39.804	103 713	130 394	2885.46	1.26	75 866	2885.46	0.73	0.20	3.87	2583.05	12.60	2402.40	3.05	2552.92	2.67	2885.46	11.20	2885.46
11	1	×					×	×				×	8 243	0.042	4 516	4.556	71 151	37 639	2918.03	0.53	8 118	1095.00	0.11	0.19	-0.97	2866.17	8.34	2851.48	1.34	2862.34	-5.43	2918.03	2.78	2000.00
16	1	×					×	×				×	4 915	0.009	3 249	4.480	59 163	105 428	2918.03	1.78	2 067	1095.00	0.03	0.22	0.22	2866.44	9.56	2840.89	1.64	2862.95	-4.54	2918.03	3.48	2918.03
2	2	×				×			×			×	19 389	0.791	4 112	7.582	71 151	811 624	2733.69	11.41	185 630	2188.03	2.61	0.35	5.43	2858.89	12.22	2837.30	6.47	2855.05	-3.36	2188.03	5.96	2368.69
3	2	×				×		×			×		13 232	1.109	2 931	7.471	59 163	1 967 344	2737.37	33.25	73 407	2188.03	1.24	0.44	5.72	2866.37	11.94	2844.56	8.54	2845.43	-3.37	2188.03	10.32	2737.37
9	2	×					×		×		×		22 702	0.980	9 714	24.393	71 151	2 986 703	2810.91	41.98	196 853	2046.36	2.77	0.47	11.01	2844.53	16.80	2839.98	11.43	2740.13	1.25	2856.36	15.57	2540.91
12	3	×					×		×			×	9 615	0.038	7 569	14.595	71 151	312 429	2810.91	4.39	91 326	2856.36	1.28	0.28	4.15	2845.57	13.35	237.16	4.36	2845.57	0.00	2856.36	8.03	2856.36
17	3	×				×		×				×	5 809	0.115	6 196	14.267	59 163	544 514	2811.82	9.20	92 788	2856.36	1.57	0.34	4.71	2846.12	13.81	2840.06	7.22	2846.12	1.54	2856.36	9.56	2856.36
1	5	×			×					×			57 614	0.322	11 542	7.714	103 713	2 826	2733.69	0.03	441 662	2188.03	4.26	0.24	-0.64	2859.13	5.90	2844.25	1.66	2881.08	-4.26	2918.03	0.27	2733.69
4	5	×			×				×		×		59 576	0.326	12 457	24.908	103 713	193 007	2810.91	1.86	460 528	2046.36	4.44	0.33	7.96	2754.60	13.95	2748.68	10.70	2124.26	2.17	2856.36	6.21	2856.36
5	5	×			×					×	×		67 270	0.429	17 121	72.367	103 713	354 492	2870.30	3.42	565 436	2885.46	5.45	0.47	13.28	2882.07	18.97	2880.02	12.87	2517.88	9.01	2885.46	13.05	2885.46
13	6	×				×				×		×	10 770	0.045	10 591	41.957	71 151	367 183	2645.46	5.16	89 759	2885.46	1.26	0.34	9.24	2881.78	18.37	2879.94	11.90	2548.12	6.61	2885.46	14.63	2885.46
18	6	×					×			×		×	6 380	0.089	8 889	40.974	59 163	635 117	2870.61	10.74	74 764	2345.46	1.26	0.38	10.11	2881.80	19.12	2880.61	12.31	2697.65	10.27	2885.46	18.13	2885.46
27	0		×			×			×		×		36 197	1.693	12 002	29.483	71 151	5 618 184	2811.82	78.96	244 365	2046.36	3.43	0.60	10.56	2845.38	17.52	2840.82	11.92	2126.18	3.01	2856.36	15.89	2271.82
28	0		×				×			×	×		40 927	1.903	16 491	85.175	71 151	7 729 707	2870.61	108.64	340 677	2405.46	4.79	0.58	16.84	2882.10	23.41	2881.21	15.16	2043.29	12.72	2885.46	25.98	2210.61
32	0			×				×			×		25 351	2.044	10 352	28.836	59 163	8 515 558	2811.82	143.93	159 606	2856.36	2.70	0.63	11.60	2846.33	18.36	2841.77	12.17	2563.77	0.27	2631.82	18.25	2631.82
33	0			×				×			×		27 536	2.174	14 061	83.395	59 163	10 058 249	2870.61	170.01	192 424	2225.46	3.25	0.61	18.69	2882.46	25.15	2881.20	14.93	2576.03	17.64	2885.46	25.96	2510.61
29	1		×				×			×		×	12 215	0.385	6 576	5.512	71 151	276 144	2000.00	3.88	15 567	1095.00	0.22	0.30	-2.38	2862.53	9.41	2848.28	1.31	2523.01	-8.78	2918.03	1.39	2372.37
34	1		×				×			×		×	7 388	0.365	5 044	5.378	59 163	576 311	2000.00	9.74	9 642	1095.00	0.16	0.32	-1.38	2866.90	10.32	2840.98	1.39	2859.22	-7.82	2918.03	3.95	2372.37
20	2		×				×			×		×	31 529	1.527	6 056	9.186	71 151	2 027 522	2737.37	28.50	235 616	2188.03	3.31	0.52	4.24	2490.35	13.13	2468.14	3.27	2851.78	-3.99	2188.03	8.33	2372.37
21	2		×				×			×		×	21 763	1.172	4 632	9.034	59 163	4 647 003	2737.37	78.55	127 887	2188.03	2.16	0.59	5.14	2862.56	13.06	2843.81	5.28	2862.56	-4.16	2188.03	10.56	2737.37
30	3		×				×			×		×	14 065	0.461	9 636	17.518	71 151	576 552	2811.82	8.10	67 418	2856.36	0.95	0.39	2.68	2846.40	13.97	2839.17	2.79	2845.29	-2.01	2856.36	8.03	2856.36
35	3		×				×			×		×	8 568	0.473	8 055	17.076	59 163	1 371 160	2811.82	23.18	77 572	2856.36	1.31	0.41	3.31	2846.43	14.47	2840.01	3.45	2846.43	-1.15	2856.36	8.88	2856.36
24	4		×		×				×			×	44 525	0.998	10 827	5.581	103 713	2 059	2737.37	0.02	41 566	1095.00	0.40	0.07	-10.79	2862.66	1.23	2840.63	0.96	2888.18	-10.12	2918.03	0.03	2737.37
25	4		×		×				×			×	46 787	0.974	13 351	17.943	103 713	46 060	2856.36	0.44	41 566	1095.00	0.40	0.07	-1.45	2846.45	9.39	2844.56	1.49	2847.34	-3.39	2856.36	6.64	2856.36
26	4		×		×				×			×	50 943	1.069	15 340	51.695	103 713	132 930	2885.46	1.28	88 496	2885.46	0.85	0.08	3.29	2793.03	13.80	2522.37	2.66	2793.03	2.11	2885.46	12.15	2885.46
19	5		×		×				×			×	84 738	1.938	10 124	9.324	103 713	10 992	2737.37	0.11	476 559	2188.03	4.59	0.11	-1.93	2857.69	6.45	2840.75	1.60	2870.04	-5.16	2918.03	1.88	2737.37
22	5		×		×				×			×	90 548	1.924	15 099	30.113	103 713	386 689	2811.82	3.73	495 593	2046.36	4.78	0.14	7.24	2484.52	14.64	2209.11	9.00	2663.62	-0.35	2856.36	4.69	2856.36
23	5		×		×					×	×		101 501	2.182	19 206	87.271	103 713	649 166	2870.61	6.26	520 511	2705.46	5.02	0.17	12.42	2882.44	18.89	2880.59	14.33	2073.13	7.92	2885.46	12.97	2885.46
31	6		×				×			×		×	15 561	0.507	12 259	50.256	71 151	1 080 031	2870.61	15.18	84 090	2375.46	1.18	0.42	7.44	2882.18	18.59	2879.68	13.01	2850.54	6.23	2885.46	16.25	2885.46
36	6		×				×			×		×	9 197	0.480	10 339	49.033	59 163	2 209 074	2870.61	37.34	69 985	2315.46	1.18	0.41	8.71	2882.37	19.77	2880.65	13.72	2819.36	7.10	2885.46	17.14	2885.46
39	0			×			×			×		×	34 673	2.739	6 231	10.510	59 163	7 455 414	2737.37	126.01	184 196	2188.03	3.11	0.52	4.28	2494.13	14.07	2475.45	3.32	2858.95	-4.97	2188.03	8.68	3095.00
45	0			×			×			×		×	55 202	2.892	13 944	34.187	71 151	8 513 798	2811.82	119.66	282 521	2046.36	3.97	0.36	10.06	2845.41	18.38	2840.09	13.54	2215.91	-4.81	2856.36	11.60	2091.82
46	0			×			×			×		×	62 458	3.243	17 716	98.772	71 151	11 551 325	2870.61	162.35	347 424	2555.46	4.88	0.33	16.89	2882.43	24.54	2881.18	16.13	2042.78	7.23	2885.46	14.93	2270.61
50	0			×			×			×		×	39 649	3.014	12 031	33.458	59 163	11 436 397	2811.82	193.30	191 364	2046.36	3.23	0.47	11.11	2846.36	18.99	2842.75	13.17	2746.81	-1.72	2856.36	11.11	2181.82
51	0			×			×			×		×	43 192	3.252	15 110	96.659	59 163	6 588 776	2870.61	111.37	224 283	2375.46	3.79	0.43	18.14	2882.73	25.54	2881.54	15.89	2757.23	12.72	2885.46	18.78	2885.46
47	1			×			×			×		×	17 743	0.860	8 561	6.353	71 151	837 825	2000.00	11.78	19 237	1095.00	0.27	0.22	-4.12	2858.96	10.50	2839.33	1.21	2519.04	-11.30	2188.03	2.44	2372.37
48	1			×			×			×		×	20 229	0.956	11 581	20.155	71 151	1 180 149	2811.82	16.59	41 291	2856.36	0.58	0.23	1.24	2845.51	14.73	2840.00	2.23	2844.59	-4.66	2856.36	7.38	2856.36
52	1			×			×			×		×	11 039	0.701	6 748	6.218	59 163	1 219 072	2000.00	20.61	13 136	1095.00	0.22	0.28	-2.98	2862.88	11.20	2840.20	1.26	2859.39	-11.38	2553.03	4.65	2372.37
38	2			×			×			×		×	48 942	2.711	7 892	10.708	71 151	3 788 467	2737.37	53.25	275 139	2188.03	3.87	0.37	2.39	2855.35	13.20	2464.63	2.31	2486.68	-4.88	2188.03	8.63	2372.37
49	2			×			×			×		×	22 313	1.052	13 542	57.833	71 151	2 402 898	2870.61	33.77	84 727	2525.46	1.19	0.21	6.23	2882.38	19.47	2880.32	6.55	2882.38	1.96	2885.46	14.00	2885.46
54	2			×			×			×		×	13 485	0.864	11 460	56.511	59 163	3 746 265	2870.61	63.32	63 376	2405.46	1.07	0.27	6.81	2882.70	19.89	2880.91	9.26	2882.70	4.04	2885.46	16.08	2885.46
53	3			×			×			×		×	12 662	0.825	9 675	19.649	59 163	2 792 813	2811.82	47.21	48 151	2856.36	0.81	0.29	1.65	2847.35	14.89	2840.92	2.45	2846.43	-3.10	2856.36	8.93	2856.36
42	4			×			×			×		×	62 192	2.365	13 289	6.469	103 700	11 064	2737.37	0.11	44 450	1095.00	0.43	0.08	-14.66	2173.28	-1.01	2827.98	0.93	2169.96	-12.54	2188.03	0.34	2737.37
43	4			×			×			×		×	69 814	2.270	15 634	20.715	103 700	56 735	2811.82	0.55	44 450	1095.00	0.43	0.08	-5.78	2845.87	7.41	2843.68	1.28	2309.51	-5.79	2856.36	6.24	2856.36
44	4			×			×			×		×	69 814	2.446	16 853	59.613	103 700	181 640	2870.61	1.75	49 031	2885.46	0.47	0.08	-0.01	2643.05	12.51	2612.71	1.88	2613.29	0.44	2885.46	12.49	2885.46
37	5			×			×			×		×	126 731	4.793	12 393	10.888	103 700	68 943	2737.37	0.66	478 110	2188.03	4.61	0.15	-8.45	2845.26	3.00	2831.17	1.28	2169.66	-6.77	2188.03	3.67	2737.37
40	5			×			×			×		×	133 784	4.663	17 359	35.016	103 700	593 956	2811.82	5.73	508 236	2046.36	4.90	0.16	4.13	2302.65	13.57	2209.77	2.87	2301.96	-3.83	2856.64	4.19	2271.82
41	5			×			×			×		×	148 156	5.169	20 628	101.332	103 700	1 117 260	2870.61	10.77	507 637	2015.46	4.90	0.19	10.71	2372.41	18.36	2281.22	15.28	2192.67	6.66	2885.46	12.71	2885.46

Table 39. Sensitivity analysis in 2D. List of cases classified according to cavern maximum diameter.

		Depth casing shoe			Cavern diameter			Cycling period			P_{min}		Creep Closure (m^3)	Subsidence (mm)	Conduction Heat Flux Loss (MWh)	Produced Energy (GWh)	Surface Area (m^2)	Effective Tensile Stress				Dilation		Vertical Strain at CS (%)	Max.Principal Stress (MPa)		Max. Effective Stress (MPa)		Dilation		Max.Principal Stress (MPa)		Max. Effective Stress (MPa)	
																		Max. tensile volume		Av. tensile strip thickness (m)	Max. dilatant volume		Av. dilatant strip thickness (m)	Strain @ 900 days (%)									
Case	Class	Z1	Z2	Z3	D1	D2	D3	S	Q	M	G1	G2	Volume loss @ 900 days	Subsidence @ 900 days	Cumulated energy @ 900 days	Cumulated energy @ 900 days		Value (m^3)	Date Output (Days)		Value (m^3)	Date Output (Days)		Value (MPa)	Date (days)	Value (MPa)	Date (days)	Value	Date (days)	Value (MPa)	Date Output (Days)	Value (MPa)	Date Output (Days)
1	5	×			×				×		×		57 614	0.322	11 542	7.714	103 713	2 826	2733.69	0.03	441 662	2188.03	4.26	-0.64	2859.13	5.90	2844.25	1.66	2881.08	-4.26	2918.00	0.27	2733.69
4	5	×			×			×			×		59 576	0.326	12 457	24.908	103 713	193 007	2810.91	1.86	460 528	2046.36	4.44	0.33	7.96	2754.60	13.95	2748.68	10.70	2124.26	2.17	2856.36	6.21	2856.36
5	5	×			×					×	×		67 270	0.429	17 121	72.367	103 713	354 492	2870.30	3.42	565 436	2885.46	5.45	0.47	13.28	2882.07	18.97	2880.02	12.87	2517.88	9.01	2885.46	13.05	2885.46
6	1	×			×			×				×	29 307	0.069	8 334	4.266	103 713	500	2733.69	0.00	34 970	1095.00	0.34	0.15	-9.35	2176.98	0.40	2842.86	0.94	2175.46	-8.61	2553.03	0.16	2000.00
7	1	×			×			×			×		30 831	0.066	10 640	13.780	103 713	102 313	2856.36	0.99	34 970	1095.00	0.34	0.17	-0.83	2847.22	8.25	2844.77	1.47	2847.37	-2.13	2856.36	6.37	2856.36
8	1	×			×				×		×		33 596	0.089	12 982	39.804	103 713	130 394	2885.46	1.26	75 866	2885.46	0.73	0.20	3.87	2583.05	12.60	2402.40	3.05	2552.92	2.67	2885.46	11.20	2885.46
19	5		×		×					×	×		84 738	1.938	10 124	9.324	103 713	10 992	2737.37	0.11	476 559	2188.03	4.59	0.11	-1.93	2857.69	6.45	2840.75	1.60	2870.04	-5.16	2918.03	1.88	2737.37
22	5		×		×			×			×		90 548	1.924	15 099	30.113	103 713	386 689	2811.82	3.73	495 593	2046.36	4.78	0.14	7.24	2484.52	14.64	2209.11	9.00	2663.62	-0.35	2856.36	4.69	2856.36
23	5		×		×					×	×		101 501	2.182	19 206	87.271	103 713	649 166	2870.61	6.26	520 511	2705.46	5.02	0.17	12.42	2882.44	18.89	2880.59	14.33	2073.13	7.92	2885.46	12.97	2885.46
24	4		×		×				×		×		44 525	0.998	10 827	5.581	103 713	2 059	2737.37	0.02	41 566	1095.00	0.40	0.07	-10.79	2862.66	1.23	2840.63	0.96	2888.18	-10.12	2918.03	0.03	2737.37
25	4	×			×				×		×		46 787	0.974	13 351	17.943	103 713	46 060	2856.36	0.44	41 566	1095.00	0.40	0.07	-1.45	2846.45	9.39	2844.56	1.49	2847.34	-3.39	2856.36	6.64	2856.36
26	4		×		×					×	×		50 943	1.069	15 340	51.695	103 713	132 930	2885.46	1.28	88 496	2885.46	0.85	0.08	3.29	2793.03	13.80	2522.37	2.66	2793.03	2.11	2885.46	12.15	2885.46
37	5					×	×		×			×	126 731	4.793	12 393	10.888	103 700	68 943	2737.37	0.66	478 110	2188.03	4.61	0.15	-8.45	2845.26	3.00	2831.17	1.28	2169.66	-6.77	2188.03	3.67	2737.37
40	5					×	×			×	×		133 784	4.663	17 359	35.016	103 700	593 956	2811.82	5.73	508 236	2046.36	4.90	0.16	4.13	2302.65	13.57	2209.77	2.87	2301.96	-3.83	2856.64	4.19	2271.82
41	5					×	×			×		×	148 156	5.169	20 628	101.332	103 700	1 117 260	2870.61	10.77	507 637	2015.46	4.90	0.19	10.71	2372.41	18.36	2281.22	15.28	2192.67	6.66	2885.46	12.71	2885.46
42	4			×		×	×		×			×	62 192	2.365	13 289	6.469	103 700	11 064	2737.37	0.11	44 450	1095.00	0.43	0.08	-14.66	2173.28	-1.01	2827.98	0.93	2169.96	-12.54	2188.03	0.34	2737.37
43	4			×		×	×		×			×	64 738	2.270	15 634	20.715	103 700	56 735	2811.82	0.55	44 450	1095.00	0.43	0.08	-5.78	2845.05	7.41	2843.68	1.28	2309.51	-5.79	2856.36	6.24	2856.36
44	4			×		×	×		×			×	69 814	2.446	16 853	59.613	103 700	181 640	2870.61	1.75	49 031	2885.46	0.47	0.08	-0.01	2643.05	12.51	2612.71	1.88	2613.29	0.44	2885.46	12.49	2885.46
2	2	×					×		×		×		19 389	0.791	4 112	7.582	71 151	811 624	2733.69	11.41	185 630	2188.03	2.61	0.35	5.43	2858.89	12.22	2837.30	6.47	2855.05	-3.36	2188.03	5.96	2368.69
9	2	×					×		×		×		22 702	0.980	9 714	24.393	71 151	2 986 703	2810.91	41.98	196 853	2046.36	2.77	0.47	11.01	2844.53	16.80	2839.98	11.43	2740.13	1.25	2856.36	15.57	2540.91
10	0	×			×		×			×	×		25 779	1.112	14 751	70.619	71 151	4 415 761	2870.61	62.06	330 734	2645.46	4.65	0.46	17.60	2881.83	23.11	2880.62	13.17	2335.24	15.12	2885.46	24.50	2150.61
11	1	×					×		×			×	8 243	0.042	4 516	4.556	71 151	37 639	2918.03	0.53	8 118	1095.00	0.11	0.19	-0.97	2866.17	8.34	2851.48	1.34	2862.34	-5.43	2918.03	2.78	2000.00
12	3	×					×		×			×	9 615	0.038	7 569	14.595	71 151	312 429	2810.91	4.39	91 326	2856.36	1.28	0.28	4.15	2845.57	13.35	237.16	4.36	2845.57	0.00	2856.36	8.03	2856.36
13	6	×					×			×		×	10 770	0.045	10 591	41.957	71 151	367 183	2645.46	5.16	89 759	2885.46	1.26	0.34	9.24	2881.78	18.37	2879.94	11.90	2548.12	6.61	2885.46	14.63	2885.46
20	2			×			×		×			×	31 529	1.527	6 056	9.186	71 151	2 027 522	2737.37	28.50	235 616	2188.03	3.31	0.52	4.24	2490.35	13.13	2468.14	3.27	2851.78	-3.99	2188.03	8.33	2372.37
27	0		×		×		×		×		×		36 197	1.693	12 002	29.483	71 151	5 618 184	2811.82	78.96	244 365	2046.36	3.43	0.60	10.56	2845.38	17.52	2840.82	11.92	2126.18	3.01	2856.36	15.89	2271.82
28	0		×		×		×			×	×		40 927	1.903	16 491	85.175	71 151	7 729 707	2870.61	108.64	340 677	2405.46	4.79	0.58	16.84	2882.10	23.41	2881.21	15.16	2043.29	12.72	2885.46	25.98	2210.61
29	1			×			×		×			×	12 215	0.385	6 576	5.512	71 151	276 144	2000.00	3.88	15 567	1095.00	0.22	0.30	-2.38	2862.53	9.41	2848.28	1.31	2523.01	-8.78	2918.03	1.39	2372.37
30	3		×			×			×			×	14 065	0.461	9 636	17.518	71 151	576 552	2811.82	8.10	67 418	2856.36	0.95	0.39	2.68	2846.40	13.97	2839.17	2.79	2845.29	-2.01	2856.36	8.03	2856.36
31	6		×			×				×		×	15 561	0.507	12 259	50.256	71 151	1 080 031	2870.61	15.18	84 090	2375.46	1.18	0.42	7.44	2882.18	18.59	2879.68	13.01	2850.54	6.23	2885.46	16.25	2885.46
38	2			×		×			×			×	48 942	2.711	7 892	10.708	71 151	3 788 467	2737.37	53.25	275 139	2188.03	3.87	0.37	2.39	2855.35	13.20	2464.63	2.31	2486.68	-4.88	2188.03	8.63	2372.37
45	0			×		×			×			×	55 202	2.892	13 944	34.187	71 151	8 513 798	2811.82	119.66	282 521	2046.36	3.97	0.36	10.06	2845.41	18.38	2840.09	13.54	2215.91	-4.81	2856.36	11.60	2091.82
46	0			×		×			×			×	62 458	3.243	17 716	98.772	71 151	11 551 325	2870.61	162.35	347 424	2555.46	4.88	0.33	16.89	2882.43	24.54	2881.18	16.13	2042.78	7.23	2885.46	14.93	2270.61
47	1			×		×		×				×	17 743	0.860	8 561	6.353	71 151	837 825	2000.00	11.78	19 237	1095.00	0.27	0.22	-4.12	2858.96	10.50	2839.33	1.21	2519.04	-11.30	2188.03	2.44	2372.37
48	1			×		×			×			×	20 229	0.956	11 581	20.155	71 151	1 180 149	2811.82	16.59	41 291	2856.36	0.58	0.23	1.24	2845.51	14.73	2840.00	2.23	2844.59	-4.66	2856.36	7.38	2856.36
49	2			×		×				×		×	22 313	1.052	13 542	57.833	71 151	2 402 898	2870.61	33.77	84 727	2525.46	1.19	0.21	6.23	2882.38	19.47	2880.32	6.55	2882.38	1.96	2885.46	14.00	2885.46
3	2	×						×	×			×	13 232	1.109	2 931	7.471	59 163	1 967 344	2737.37	33.25	73 407	2188.03	1.24	0.44	5.72	2866.37	11.94	2844.56	8.54	2845.43	-3.37	2188.03	10.32	2737.37
14	0	×					×		×			×	15 769	1.392	8 350	23.932	59 163	5 668 992	2811.82	95.82	173 313	2856.36	2.93	0.56	11.79	2845.37	17.42	2840.92	11.35	2828.74	5.05	2856.36	17.84	2451.82
15	0	×					×		×			×	17 330	1.441	12 603	69.253	59 163	6 584 745	2870.61	111.30	169 031	2495.46	2.86	0.54	18.61	2882.10	23.99	2880.62	12.31	2395.14	18.58	2885.46	27.70	2270.61
16	1	×					×	×				×	4 915	0.009	3 249	4.480	59 163	105 428	2918.03	1.78	2 067	1095.00	0.03	0.23	0.22	2866.44	9.56	2840.89	1.64	2862.95	-4.54	2918.03	3.48	2918.03
17	3	×					×	×				×	5 809	0.115	6 196	14.267	59 163	544 514	2811.82	9.20	92 788	2856.36	1.57	0.34	4.71	2846.12	13.81	2840.06	7.22	2846.12	1.54	2856.36	9.56	2856.36
18	6	×					×		×			×	6 380	0.089	8 889	40.974	59 163	635 117	2870.61	10.74	74 764	2345.46	1.26	0.38	10.11	2881.80	19.12	2880.61	12.31	2697.65	10.27	2885.46	18.13	2885.46
21	2		×				×		×			×	21 763	1.172	4 632	9.034	59 163	4 647 003	2737.37	78.55	127 887	2188.03	2.16	0.59	5.14	2862.56	13.06	2843.81	5.28	2862.56	-4.16	2188.03	10.56	2737.37
32	0		×			×			×			×	25 351	2.044	10 352	28.836	59 163	8 515 558	2811.82	143.93	159 606	2856.36	2.70	0.63	11.60	2846.33	18.36	2841.77	12.17	2563.77	0.27	2631.82	18.25	2631.82
33	0		×			×			×			×	27 536	2.174	14 061	83.395	59 163	10 058 249	2870.61	170.01	192 424	2225.46	3.25	0.61	18.69	2882.46	25.15	2881.20	14.93	2576.03	17.64	2885.46	25.96	2510.61
34	1		×			×			×			×	7 388	0.365	5 044	5.378	59 163	576 311	2000.00	9.74	9 642	1095.00	0.16	0.32	-1.38	2866.90	10.32	2840.98	1.39	2859.22	-7.82	2918.03	3.95	2372.37
35	3		×			×			×			×	8 568	0.473	8 055	17.076	59 163	1 371 160	2811.82	23.18	77 572	2856.36	1.31	0.41	3.31	2846.43	14.47	2840.01	3.45	2846.43	-1.15	2856.36	8.88	2856.36
36	6		×			×			×			×	9 197	0.480	10 339	49.033	59 163	2 209 074	2870.61	37.34	69 985	2315.46	1.18	0.41	8.71	2882.37	19.77	2880.65	13.72	2819.36	7.10	2885.46	17.14	2885.46
39	0			×			×			×		×	34 673	2.739	6 231	10.510	59 163	7 455 414	2737.37	126.01	184 196	2188.03	3.11	0.52	4.28	2494.13	14.07	2475.45	3.32	2858.95	-4.97	2188.03	8.68	3095.00
50	0			×			×			×		×	39 649	3.014	12 031	33.458	59 163	11 436 397	2811.82	193.30	191 364	2046.36	3.23	0.47	18.14	2882.75	25.54	2881.54	15.89	2757.23	12.72	2885.46	18.78	2885.46
51	0			×			×			×		×	43 192	3.252	15 110	96.659	59 163	6 588 776	2870.61	111.37	224 283	2375.46	3.79	0.43	18.14	2882.73	25.54	2881.54	15.89	2757.23	12.72	2885.46	18.78	2885.46
52	1			×			×			×		×	11 039	0.701	6 748	6.218	59 163	1 219 072	2000.00	20.61	13 136	1095.00	0.22	0.28	-2.98	2862.88	11.20	2840.20	1.26	2859.39	-11.38	2553.03	4.65	2372.37
53	3			×			×		×			×	12 662	0.825	9 675	19.649	59 163	2 792 813	2811.82	47.21	48 151	2856.36	0.81	0.29	1.65	2847.35	14.89	2840.92	2.45	2846.43	-3.10	2856.36	8.93	2856.36
54	2			×			×			×		×	13 485	0.864	11 460	56.511	59 163	3 746 265	2870.61	63.32	63 376	2405.46	1.07	0.27	6.81	2882.70	19.89	2880.91	9.26	2882.70	4.04	2885.46	16.08	2885.46

Table 40. Sensitivity analysis in 2D. List of cases classified according to cycling period.

		Depth casing shoe			Cavern diameter			Cycling period			P_{min}		Creep Closure (m^3)	Subsidence (mm)	Conduction Heat Flux Loss (MWh)	Produced Energy (GWh)	Surface Area (m^2)	Effective Tensile Stress				Dilation		Vertical Strain at CS (%)	Max.Principal Stress (MPa)		Max. Effective Stress (MPa)		Dilation		Max.Principal Stress (MPa)		Max. Effective Stress (MPa)	
																		Max. tensile volume		Av. tensile strip thickness (m)	Max. dilatant volume		Av. dilatant strip thickness (m)	Strain @ 900 days (%)									
Case	Class	Z1	Z2	Z3	D1	D2	D3	S	Q	M	G1	G2	Volume loss @ 900 days	Subsidence @ 900 days	Cumulated energy @ 900 days	Cumulated energy @ 900 days		Value (m^3)	Date Output (Days)		Value (m^3)	Date Output (Days)		Value (MPa)	Date (days)	Value (MPa)	Date (days)	Value T/FOS	Date (days)	Value (MPa)	Date Output (Days)	Value (MPa)	Date Output (Days)
1	5	×			×				×		×		57 614	0.322	11 542	7.714	103 713	2 826	2733.69	0.03	441 662	2188.03	4.26	-0.64	2859.13	5.90	2844.25	1.66	2881.08	-4.26	2918.00	0.27	2733.69
2	2	×				×			×			×	19 389	0.791	4 112	7.582	71 151	811 624	2733.69	11.41	185 630	2188.03	2.61	5.43	2858.89	12.22	2837.30	6.47	2855.05	-3.36	2188.03	5.96	2368.69
3	2	×					×		×		×		13 232	1.109	2 931	7.471	59 163	1 967 344	2737.37	33.25	73 407	2188.03	1.24	5.72	2866.37	11.94	2844.56	8.54	2845.43	-3.37	2188.03	10.32	2737.37
6	1	×			×					×		×	29 307	0.069	8 334	4.266	103 713	500	2733.69	0.00	34 970	1095.00	0.34	-9.35	2176.98	0.40	2842.86	0.94	2175.46	-8.61	2553.03	0.16	2000.00
11	1	×				×		×				×	8 243	0.042	4 516	4.556	71 151	37 639	2918.03	0.53	8 118	1095.00	0.11	-0.97	2866.17	8.34	2851.48	1.34	2862.34	-5.43	2918.03	2.78	2000.00
16	1	×					×	×				×	4 915	0.009	3 249	4.480	59 163	105 428	2918.03	1.78	2 067	1095.00	0.03	0.22	2866.44	9.56	2840.89	1.64	2862.95	-4.54	2918.03	3.48	2918.03
19	5		×		×			×			×		84 738	1.938	10 124	9.324	103 713	10 992	2737.37	0.11	476 559	2188.03	4.59	-1.93	2857.69	6.45	2840.75	1.60	2870.04	-5.16	2918.03	1.88	2737.37
20	2		×			×		×			×		31 529	1.527	6 056	9.186	71 151	2 027 522	2737.37	28.50	235 616	2188.03	3.31	4.24	2490.35	13.13	2468.14	3.27	2851.78	-3.99	2188.03	8.33	2737.37
21	2		×				×	×			×		21 763	1.172	4 632	9.034	59 163	4 647 003	2737.37	78.55	127 887	2188.03	2.16	5.14	2862.56	13.06	2843.81	5.28	2862.56	-4.16	2188.03	10.56	2737.37
24	4		×		×			×			×		44 525	0.998	10 827	5.581	103 713	2 059	2737.37	0.02	41 566	1095.00	0.40	-10.79	2862.66	1.23	2840.63	0.96	2888.18	-10.12	2918.03	0.03	2737.37
29	1		×			×			×			×	12 215	0.385	6 576	5.512	71 151	276 144	2000.00	3.88	15 567	1095.00	0.22	-2.38	2862.53	9.41	2848.28	1.31	2523.01	-8.78	2918.03	1.39	2372.37
34	1		×			×			×			×	7 388	0.365	5 044	5.378	59 163	576 311	2000.00	9.74	9 642	1095.00	0.16	-1.38	2866.90	10.32	2840.98	1.39	2859.22	-7.82	2918.03	3.95	2372.37
37	5			×	×			×			×		126 731	4.793	12 393	10.888	103 700	68 943	2737.37	0.66	478 110	2188.03	4.61	-8.45	2845.26	3.00	2831.17	1.28	2169.66	-6.77	2188.03	3.67	2737.37
38	2			×		×		×			×		48 942	2.711	7 892	10.708	71 151	3 788 467	2737.37	53.25	275 139	2188.03	3.87	0.37	2.39	2855.35	13.20	2464.63	2.31	2486.68	-4.88	2188.03	8.63	2372.37
39	0			×			×	×			×		34 673	2.739	6 231	10.510	59 163	7 455 414	2737.37	126.01	184 196	2188.03	3.11	0.52	4.28	2494.13	14.07	2475.45	3.32	2858.95	-4.97	2188.03	8.68	3095.00
42	4			×	×			×			×		62 192	2.365	13 289	6.469	103 700	11 064	2737.37	0.11	44 450	1095.00	0.43	0.08	-14.66	2173.28	-1.01	2827.98	0.93	2169.96	-12.54	2188.03	0.34	2737.37
47	1			×	×						×		17 743	0.860	8 561	6.353	71 151	837 825	2000.00	11.78	19 237	1095.00	0.27	0.22	-4.12	2858.96	10.50	2839.33	1.21	2519.04	-11.30	2188.03	2.44	2372.37
52	1			×		×					×		11 039	0.701	6 748	6.218	59 163	1 219 072	2000.00	20.61	13 136	1095.00	0.22	0.28	-2.98	2862.88	11.20	2840.20	1.26	2859.39	-11.38	2553.03	4.65	2372.37
4	5	×			×				×		×		59 576	0.326	12 457	24.908	103 713	193 007	2810.91	1.86	460 528	2046.36	4.44	7.96	2754.60	13.95	2748.68	10.70	2124.26	2.17	2856.36	6.21	2856.36
7	1	×					×		×			×	30 831	0.066	10 640	13.780	103 713	102 313	2856.36	0.99	34 970	1095.00	0.34	0.17	-0.83	2847.22	8.25	2844.77	1.47	2847.37	-2.13	2856.36	6.37	2856.36
9	2	×					×	×				×	22 702	0.980	9 714	24.393	71 151	2 986 703	2810.91	41.98	196 853	2046.36	2.77	0.47	11.01	2844.53	16.80	2839.98	11.43	2740.13	1.25	2856.36	15.57	2540.91
12	3	×					×	×				×	9 615	0.038	7 569	14.595	71 151	312 429	2810.91	4.39	91 326	2856.36	1.28	0.28	4.15	2845.57	13.35	237.16	4.36	2845.57	0.00	2856.36	8.03	2856.36
14	0	×						×	×		×		15 769	1.392	8 350	23.932	59 163	5 668 992	2811.82	95.82	173 313	2856.36	2.93	0.56	11.79	2845.37	17.42	2840.92	11.35	2828.74	5.05	2856.36	17.84	2451.82
17	3	×					×	×			×		5 809	0.115	6 196	14.267	59 163	544 514	2811.82	9.20	92 788	2856.36	1.57	0.34	4.71	2846.12	13.81	2840.06	7.22	2846.12	1.54	2856.36	9.56	2856.36
22	5		×		×			×	×		×		90 548	1.924	15 099	30.113	103 713	386 689	2811.82	3.73	495 593	2046.36	4.78	0.14	7.24	2484.52	14.64	2209.11	9.00	2663.62	-0.35	2856.36	4.69	2856.36
25	4		×		×			×	×		×		46 787	0.974	13 351	17.943	103 713	46 060	2856.36	0.44	41 566	1095.00	0.40	0.07	-1.45	2846.45	9.39	2844.56	1.49	2847.34	-3.39	2856.36	6.64	2856.36
27	0		×			×			×		×		36 197	1.693	12 002	29.483	71 151	5 618 184	2811.82	78.96	244 365	2046.36	3.43	0.60	10.56	2845.38	17.52	2840.82	11.92	2126.18	3.01	2856.36	15.89	2271.82
30	3												14 065	0.461	9 636	17.518	71 151	576 552	2811.82	8.10	67 418	2856.36	0.95	0.39	2.68	2846.40	13.97	2839.17	2.79	2845.29	-2.01	2856.36	8.03	2856.36
32	0		×			×			×			×	25 351	2.044	10 352	28.836	59 163	8 515 558	2811.82	143.93	159 606	2856.36	2.70	0.63	11.60	2846.33	18.36	2841.77	12.17	2563.77	0.27	2631.82	18.25	2631.82
35	3		×			×			×			×	8 568	0.473	8 055	17.076	59 163	1 371 160	2811.82	23.18	77 572	2856.36	1.31	0.41	3.31	2846.43	14.47	2840.01	3.45	2846.43	-1.15	2856.36	8.88	2856.36
40	5			×			×		×		×		133 784	4.663	17 359	35.016	103 700	593 956	2811.82	5.73	508 236	2046.36	4.90	0.16	4.13	2302.65	13.57	2209.77	2.87	2301.96	-3.83	2856.64	4.19	2271.82
43	4			×			×		×		×		64 738	2.270	15 634	20.715	103 700	56 735	2811.82	0.55	44 450	1095.00	0.43	0.08	-5.78	2845.87	7.41	2843.68	1.28	2309.51	-5.79	2856.36	6.24	2856.36
45	0			×		×			×		×		55 202	2.892	13 944	34.187	71 151	8 513 798	2811.82	119.66	282 521	2046.36	3.97	0.36	10.06	2845.41	18.38	2840.09	13.54	2215.91	-4.81	2856.36	11.60	2091.82
48	1			×		×			×			×	20 229	0.956	11 581	20.155	71 151	1 180 149	2811.82	16.59	41 291	2856.36	0.58	0.23	1.24	2845.51	14.73	2840.00	2.23	2844.59	-4.66	2856.36	7.38	2856.36
50	0			×			×		×		×		39 649	3.014	12 031	33.458	59 163	11 436 397	2811.82	193.30	191 364	2046.36	3.23	0.47	11.11	2846.36	18.99	2842.75	13.17	2746.81	-1.72	2856.36	11.11	2181.82
53	3			×			×						12 662	0.825	9 675	19.649	59 163	2 792 813	2811.82	47.21	48 151	2856.36	0.81	0.29	1.65	2847.35	14.89	2840.92	2.45	2846.43	-3.10	2856.36	8.93	2856.36
5	5	×							×		×		67 270	0.429	17 121	72.367	103 713	354 492	2870.30	3.42	565 436	2885.46	5.45	0.47	13.28	2882.07	18.97	2880.02	12.87	2517.88	9.01	2885.46	13.05	2885.46
8	1	×							×		×		33 596	0.089	12 982	39.804	103 713	130 394	2885.46	1.26	75 866	2885.46	0.73	0.20	3.87	2583.05	12.60	2402.40	3.05	2552.92	2.67	2885.46	11.20	2885.46
10	0	×							×		×		25 779	1.112	14 751	70.619	71 151	4 415 761	2870.61	62.06	330 734	2645.46	4.65	0.46	17.60	2881.83	23.11	2880.62	13.17	2335.24	15.12	2885.46	24.50	2150.61
13	6	×							×		×		10 770	0.045	10 591	41.957	71 151	367 183	2645.46	5.16	89 759	2885.46	1.26	0.34	9.24	2881.78	18.37	2879.94	11.90	2548.12	6.61	2885.46	14.63	2885.46
15	0	×							×		×		17 330	1.441	12 603	69.253	59 163	6 584 745	2870.61	111.30	169 031	2495.46	2.86	0.54	18.61	2882.10	23.99	2880.62	12.31	2395.14	18.58	2870.61	27.70	2270.61
18	6	×							×		×		6 380	0.089	8 889	40.974	59 163	635 117	2870.61	10.74	74 764	2345.46	1.26	0.38	10.11	2881.80	19.12	2880.61	12.31	2697.65	10.27	2885.46	18.13	2885.46
23	5		×		×			×			×		101 501	2.182	19 206	87.271	103 713	649 166	2870.61	6.26	520 511	2705.46	5.02	0.17	12.42	2882.44	18.89	2880.59	14.33	2073.13	7.92	2885.46	12.97	2885.46
26	4		×		×			×			×		50 943	1.069	15 340	51.695	103 713	132 930	2885.46	1.28	88 496	2885.46	0.85	0.08	3.29	2793.03	13.80	2522.37	2.66	2793.03	2.11	2885.46	12.15	2885.46
28	0		×			×			×		×		40 927	1.903	16 491	85.175	71 151	7 729 707	2870.61	108.64	340 677	2405.46	4.79	0.58	16.84	2882.10	23.41	2881.21	15.16	2043.29	12.72	2885.46	25.98	2210.61
31	6		×			×			×		×		15 561	0.507	12 259	50.256	71 151	1 080 031	2870.61	15.18	84 090	2375.46	1.18	0.42	7.44	2882.18	18.59	2879.68	13.01	2850.54	6.23	2885.46	16.25	2885.46
33	0		×				×			×	×		27 536	2.174	14 061	83.395	59 163	10 058 249	2870.61	170.01	192 424	2225.46	3.25	0.61	18.69	2882.46	25.15	2881.20	14.93	2576.03	17.64	2885.46	25.96	2510.61
36	6		×			×			×		×		9 197	0.480	10 339	49.033	59 163	2 209 074	2870.61	37.34	69 985	2315.46	1.18	0.41	8.71	2882.37	19.77	2880.65	13.72	2819.36	7.10	2885.46	17.14	2885.46
41	5		×				×			×	×		148 156	5.169	20 628	101.332	103 700	1 117 260	2870.61	10.77	507 637	2015.46	4.90	0.19	10.71	2372.41	18.36	2281.22	15.28	2192.67	6.66	2885.46	12.71	2885.46
44	4			×			×			×	×		69 814	2.446	16 853	59.613	103 700	181 640	2870.61	1.75	49 031	2885.46	0.47	0.08	-0.01	2643.05	12.51	2612.71	1.88	2613.29	0.44	2885.46	12.49	2885.46
46	0			×			×			×	×		62 458	3.243	17 716	98.772	71 151	11 551 325	2870.61	162.35	347 424	2555.46	4.88	0.33	16.89	2882.43	24.54	2881.18	16.13	2042.78	7.23	2885.46	14.93	2270.61
49	2			×			×			×			22 313	1.052	13 542	57.833	71 151	2 402 898	2870.61	33.77	84 727	2525.46	1.19	0.21	6.23	2882.38	19.47	2880.32	6.55	2882.38	1.96	2885.46	14.00	2885.46
51	0			×			×			×	×		43 192	3.252	15 110	96.659	59 163	6 588 776	2870.61	111.37	224 283	2375.46	3.79	0.43	18.14	2882.73	25.54	2881.54	15.89	2757.23	12.72	2885.46	18.78	2885.46
54	2			×			×			×			13 485	0.864	11 460	56.511	59 163	3 746 265	2870.61	63.32	63 376	2405.46	1.07	0.27	6.81	2882.70	19.89	2880.91	9.26	2882.70	4.04	2885.46	16.08	2885.46

Table 41. Sensitivity analysis in 2D. List of cases classified according to minimum pressure gradient.

		Depth casing shoe			Cavern diameter			Cycling period			P_{min}		Creep Closure (m^3)	Subsidence (mm)	Conduction Heat Flux Loss (MWh)	Produced Energy (GWh)	Surface Area (m^2)	Effective Tensile Stress				Dilation		Vertical Strain at CS (%)	Max.Principal Stress (MPa)		Max. Effective Stress (MPa)		Dilation		Max.Principal Stress (MPa)		Max. Effective Stress (MPa)	
																		Max. tensile volume		Av. tensile strip thickness (m)	Max. dilatant volume		Av. dilatant strip thickness (m)									
Case	Class	Z1	Z2	Z3	D1	D2	D3	S	Q	M	G1	G2	Volume loss @ 900 days	Subsidence @ 900 days	Cumulated energy @ 900 days	Cumulated energy @ 900 days		Value (m^3)	Date Output (Days)		Value (m^3)	Date Output (Days)		Strain @ 900 days (%)	Value (MPa)	Date (days)	Value (MPa)	Date (days)	Value 1/FOS	Date (days)	Value (MPa)	Date Output (Days)	Value (MPa)	Date Output (Days)
1	5	×			×			×			×		57 614	0.322	11 542	7.714	103 713	2 826	2733.69	0.03	441 662	2188.03	4.26	0.24	-0.64	2859.13	5.90	2844.25	1.66	2881.08	-4.26	2918.00	0.27	2733.69
2	2	×				×			×		×		19 389	0.791	4 112	7.582	71 151	811 624	2733.69	11.41	185 630	2188.03	2.61	0.35	5.43	2858.89	12.22	2837.30	6.47	2855.05	-3.36	2188.03	5.96	2368.69
3	2	×					×		×		×		13 232	1.109	2 931	7.471	59 163	1 967 344	2737.37	33.25	73 407	2188.03	1.24	0.44	5.72	2866.37	11.94	2844.56	8.54	2845.43	-3.37	2188.03	10.32	2737.37
4	5	×				×			×		×		59 576	0.326	12 457	24.908	103 713	193 007	2810.91	1.86	460 528	2046.36	4.44	0.33	7.96	2754.60	13.95	2748.68	10.70	2124.26	2.17	2856.36	6.21	2856.36
5	5	×				×				×		×	67 270	0.429	17 121	72.367	103 713	354 492	2870.30	3.42	565 436	2885.46	5.45	0.47	13.28	2882.07	18.97	2880.02	12.87	2517.88	9.01	2885.46	13.05	2885.46
9	2	×					×		×			×	22 702	0.980	9 714	24.393	71 151	2 986 703	2810.91	41.98	196 853	2046.36	2.77	0.47	11.01	2844.53	16.80	2839.98	11.43	2740.13	1.25	2856.36	15.57	2540.91
10	0	×					×			×		×	25 779	1.112	14 751	70.619	71 151	4 415 761	2870.61	62.06	330 734	2645.46	4.65	0.46	17.60	2881.83	23.11	2880.62	13.17	2335.24	15.12	2885.46	24.50	2150.61
14	0	×						×			×		15 769	1.392	8 350	23.932	59 163	5 668 992	2811.82	95.82	173 313	2856.36	2.93	0.56	11.79	2845.37	17.42	2840.92	11.35	2828.74	5.05	2856.36	17.84	2451.82
15	0	×					×			×		×	17 330	1.441	12 603	69.253	59 163	6 584 745	2870.61	111.30	169 031	2495.46	2.86	0.54	18.61	2882.10	23.99	2880.62	12.31	2395.14	18.58	2885.46	27.70	2270.61
19	5		×		×			×			×		84 738	1.938	10 124	9.324	103 713	10 992	2737.37	0.11	476 559	2188.03	4.59	0.11	-1.93	2857.69	6.45	2840.75	1.60	2870.04	-5.16	2918.03	1.88	2737.37
20	2		×			×		×			×		31 529	1.527	6 056	9.186	71 151	2 027 522	2737.37	28.50	235 616	2188.03	3.31	0.52	4.24	2490.35	13.13	2468.14	3.27	2851.78	-3.99	2188.03	8.33	2372.37
21	2		×			×		×			×		21 763	1.172	4 632	9.034	59 163	4 647 003	2737.37	78.55	127 887	2188.03	2.16	0.59	5.14	2862.56	13.06	2843.81	5.28	2862.56	-4.16	2188.03	10.56	2737.37
22	5		×		×				×		×		90 548	1.924	15 099	30.113	103 713	386 689	2811.82	3.73	495 593	2046.36	4.78	0.14	7.24	2484.52	14.64	2209.11	9.00	2663.62	-0.35	2856.36	4.69	2856.36
23	5		×		×					×	×		101 501	2.182	19 206	87.271	103 713	649 166	2870.61	6.26	520 511	2705.46	5.02	0.17	12.42	2882.44	18.89	2880.59	14.33	2073.13	7.92	2885.46	12.97	2885.46
27	0		×			×			×		×		36 197	1.693	12 002	29.483	71 151	5 618 184	2811.82	78.96	244 365	2046.36	3.43	0.60	10.56	2845.38	17.52	2840.82	11.92	2126.18	3.01	2856.36	15.89	2271.82
28	0		×			×				×	×		40 927	1.903	16 491	85.175	71 151	7 729 707	2870.61	108.64	340 677	2405.46	4.79	0.58	16.84	2882.10	23.41	2881.21	15.16	2043.29	12.72	2885.46	25.98	2210.61
32	0		×				×			×	×		25 351	2.044	10 352	28.836	59 163	8 515 558	2811.82	143.93	159 606	2856.36	2.70	0.63	11.60	2846.33	18.36	2841.77	12.17	2563.77	0.27	2631.82	18.25	2631.82
33	0		×			×				×	×		27 536	2.174	14 061	83.395	59 163	10 058 249	2870.61	170.01	192 424	2225.46	3.25	0.61	18.69	2882.46	25.15	2881.20	14.93	2576.03	17.64	2885.46	25.96	2510.61
37	5			×	×				×		×		126 731	4.793	12 393	10.888	103 700	68 943	2737.37	0.66	478 110	2188.03	4.61	0.15	-8.45	2845.26	3.00	2831.17	1.28	2169.66	-6.77	2188.03	3.67	2737.37
38	2			×		×			×		×		48 942	2.711	7 892	10.708	71 151	3 788 467	2737.37	53.25	275 139	2188.03	3.87	0.37	2.39	2855.35	13.20	2464.63	2.31	2486.68	-4.88	2188.03	8.63	2372.37
39	0			×			×			×		×	34 673	2.739	6 231	10.510	59 163	7 455 414	2737.37	126.01	184 196	2188.03	3.11	0.52	4.28	2494.13	14.07	2475.45	3.32	2858.95	-4.97	2188.03	8.68	3095.00
40	5			×			×		×			×	133 784	4.663	17 359	35.016	103 700	593 956	2811.82	5.73	508 236	2046.36	4.90	0.16	4.13	2302.65	13.57	2209.77	2.87	2301.96	-3.83	2856.64	4.19	2271.82
41	5			×			×			×		×	148 156	5.169	20 628	101.332	103 700	1 117 260	2870.61	10.77	507 637	2015.46	4.90	0.19	10.71	2372.41	18.36	2281.22	15.28	2192.67	6.66	2885.46	12.71	2885.46
45	0			×			×		×			×	55 202	2.892	13 944	34.187	71 151	8 513 798	2811.82	119.66	282 521	2046.36	3.97	0.36	10.06	2845.41	18.38	2840.09	13.54	2215.91	-4.81	2856.36	11.60	2091.82
46	0			×			×			×		×	62 458	3.243	17 716	98.772	71 151	11 551 325	2870.61	162.35	347 424	2555.46	4.88	0.33	16.89	2882.43	24.54	2881.18	16.13	2042.78	7.23	2885.46	14.93	2270.61
50	0			×			×		×			×	39 649	3.014	12 031	33.458	59 163	11 436 397	2811.82	193.30	191 364	2046.36	3.23	0.47	11.11	2846.36	18.99	2842.75	13.17	2746.81	-1.72	2856.36	11.11	2181.82
51	0			×			×		×			×	43 192	3.252	15 110	96.659	59 163	6 588 776	2870.61	111.37	224 283	2375.46	3.79	0.43	18.14	2882.73	25.54	2881.54	15.89	2757.23	12.72	2885.46	18.78	2885.46
6	1	×					×			×		×	29 307	0.069	8 334	4.266	103 713	500	2733.69	0.00	34 970	1095.00	0.34	0.15	-9.35	2176.98	0.40	2842.86	0.94	2175.46	-8.61	2553.03	0.16	2000.00
7	1	×					×		×			×	30 831	0.066	10 640	13.780	103 713	102 313	2856.36	0.99	34 970	1095.00	0.34	0.17	-0.83	2847.22	8.25	2844.77	1.47	2847.37	-2.13	2856.36	6.37	2856.36
8	1	×					×			×		×	33 596	0.089	12 982	39.804	103 713	130 394	2885.46	1.26	75 866	2885.46	0.73	0.20	3.87	2583.05	12.60	2402.40	3.05	2552.92	2.67	2885.46	11.20	2885.46
11	1	×					×			×		×	8 243	0.042	4 516	4.556	71 151	37 639	2918.03	0.53	8 118	1095.00	0.11	0.19	-0.97	2866.17	8.34	2851.48	1.34	2862.34	-5.43	2918.03	2.78	2000.00
12	3	×					×			×		×	9 615	0.038	7 569	14.595	71 151	312 429	2810.91	4.39	91 326	2856.36	1.28	0.28	4.15	2845.57	13.35	237.16	4.36	2845.57	0.00	2856.36	8.03	2856.36
13	6	×					×			×		×	10 770	0.045	10 591	41.957	71 151	367 183	2645.46	5.16	89 759	2885.46	1.26	0.34	9.24	2881.78	18.37	2879.94	11.90	2548.12	6.61	2885.46	14.63	2885.46
16	1	×					×	×				×	4 915	0.009	3 249	4.480	59 163	105 428	2918.03	1.78	2 067	1095.00	0.03	0.23	0.22	2866.44	9.56	2840.89	1.64	2862.95	-4.54	2918.03	3.48	2918.03
17	3	×					×		×			×	5 809	0.115	6 196	14.267	59 163	544 514	2811.82	9.20	92 788	2856.36	1.57	0.34	4.71	2846.12	13.81	2840.06	7.22	2846.12	1.54	2856.36	9.56	2856.36
18	6	×					×		×			×	6 380	0.089	8 889	40.974	59 163	635 117	2870.61	10.74	74 764	2345.46	1.26	0.38	10.11	2881.80	19.12	2880.61	12.31	2697.65	10.27	2885.46	18.13	2885.46
24	4		×		×				×		×		44 525	0.998	10 827	5.581	103 713	2 059	2737.37	0.02	41 566	1095.00	0.40	0.07	-10.79	2862.66	1.23	2840.63	0.96	2888.18	-10.12	2918.03	0.03	2737.37
25	4		×		×				×		×		46 787	0.974	13 351	17.943	103 713	46 060	2856.36	0.44	41 566	1095.00	0.40	0.07	-1.45	2846.45	9.39	2844.56	1.49	2847.34	-3.39	2856.36	6.64	2856.36
26	4		×		×				×		×		50 943	1.069	15 340	51.695	103 713	132 930	2885.46	1.28	88 496	2885.46	0.85	0.08	3.29	2793.03	13.80	2522.37	2.66	2793.03	2.11	2885.46	12.15	2885.46
29	1		×				×					×	12 215	0.385	6 576	5.512	71 151	276 144	2000.00	3.88	15 567	1095.00	0.22	0.30	-2.38	2862.53	9.41	2848.28	1.31	2523.01	-8.78	2918.03	1.39	2372.37
30	3		×				×		×			×	14 065	0.461	9 636	17.518	71 151	576 552	2811.82	8.10	67 418	2856.36	0.95	0.39	2.68	2846.40	13.97	2839.17	2.79	2845.29	-2.01	2856.36	8.03	2856.36
31	6		×				×		×			×	15 561	0.507	12 259	50.256	71 151	1 080 031	2870.61	15.18	84 090	2375.46	1.18	0.42	7.44	2882.18	18.59	2879.68	13.01	2850.54	6.23	2885.46	16.25	2885.46
34	1		×					×	×			×	7 388	0.365	5 044	5.378	59 163	576 311	2000.00	9.74	9 642	1095.00	0.16	0.32	-1.38	2866.90	10.32	2840.98	1.39	2859.22	-7.82	2918.03	3.95	2372.37
35	3		×					×		×		×	8 568	0.473	8 055	17.076	59 163	1 371 160	2811.82	23.18	77 572	2856.36	1.31	0.41	3.31	2846.43	14.47	2840.01	3.45	2846.43	-1.15	2856.36	8.88	2856.36
36	6		×				×			×		×	9 197	0.480	10 339	49.033	59 163	2 209 074	2870.61	37.34	69 985	2315.46	1.18	0.41	8.71	2882.37	19.77	2880.65	13.72	2819.36	7.10	2885.46	17.14	2885.46
42	4			×	×				×		×		62 192	2.365	13 289	6.469	103 700	11 064	2737.37	0.11	44 450	1095.00	0.43	0.08	-14.66	2173.28	-1.01	2827.98	0.93	2169.96	-12.54	2188.03	0.34	2737.37
43	4			×	×				×		×		64 738	2.270	15 634	20.715	103 700	56 735	2811.82	0.55	44 450	1095.00	0.43	0.08	-5.78	2845.87	7.41	2843.68	1.28	2309.51	-5.79	2856.36	6.24	2856.36
44	4			×	×				×		×		69 814	2.446	16 853	59.613	103 700	181 640	2870.61	1.75	49 031	2885.46	0.47	0.08	-0.01	2643.05	12.51	2612.71	1.88	2613.29	0.44	2885.46	12.49	2885.46
47	1		×			×		×			×		17 743	0.860	8 561	6.353	71 151	837 825	2000.00	11.78	19 237	1095.00	0.27	0.22	-4.12	2858.96	10.50	2839.33	1.21	2519.04	-11.30	2188.03	2.44	2372.37
48	1		×			×			×		×		20 229	0.956	11 581	20.155	71 151	1 180 149	2811.82	16.59	41 291	2856.36	0.58	0.23	1.24	2845.51	14.73	2840.00	2.23	2844.59	-4.66	2856.36	7.38	2856.36
49	2		×			×				×	×		22 313	1.052	13 542	57.833	71 151	2 402 898	2870.61	33.77	84 727	2525.46	1.19	0.21	6.23	2882.38	19.47	2880.32	6.55	2882.38	1.96	2885.46	14.00	2885.46
52	1		×			×				×	×		11 039	0.701	6 748	6.218	59 163	1 219 072	2000.00	20.61	13 136	1095.00	0.22	0.28	-2.98	2862.88	11.20	2840.20	1.26	2859.39	-11.38	2553.03	4.65	2372.37
53	3		×			×			×		×		12 662	0.825	9 675	19.649	59 163	2 792 813	2811.82	47.21	48 151	2856.36	0.81	0.29	1.65	2847.35	14.89	2840.92	2.45	2846.43	-3.10	2856.36	8.93	2856.36
54	2		×			×			×		×		13 485	0.864	11 460	56.511	59 163	3 746 265	2870.61	63.32	63 376	2405.46	1.07	0.27	6.81	2882.70	19.89	2880.91	9.26	2882.70	4.04	2885.46	16.08	2885.46

Table 42. Sensitivity analysis in 2D. List of cases classified according to subsidence.

		Depth casing shoe			Cavern diameter			Cycling period			P_{min}		Creep Closure (m^3)	Subsidence (mm)	Conduction Heat Flux Loss (MWh)	Produced Energy (GWh)	Surface Area (m^2)	Effective Tensile Stress: Max. tensile volume		Effective Tensile Stress: Av. tensile strip thickness (m)	Dilation: Max. dilatant volume		Dilation: Av. dilatant strip thickness (m)	Vertical Strain at CS (%)	Max.Principal Stress (MPa)		Max. Effective Stress (MPa)		Dilation		Max.Principal Stress (MPa)		Max. Effective Stress (MPa)	
Case	Class	Z1	Z2	Z3	D1	D2	D3	S	Q	M	G1	G2	Volume loss @ 900 days	Subsidence @ 900 days	Cumulated energy @ 900 days	Cumulated energy @ 900 days		Value (m^3)	Date Output (Days)		Value (m^3)	Date Output (Days)		Strain @ 900 days (%)	Value (MPa)	Date (days)	Value (MPa)	Date (days)	Value 1/FOS	Date (days)	Value (MPa)	Date Output (Days)	Value (MPa)	Date Output (Days)
16	1	×					×	×				×	4 915	0.009	3 249	4.480	59 163	105 428	2918.03	1.78	2 067	1095.00	0.03	0.23	0.22	2866.44	9.56	2840.89	1.64	2862.95	-4.54	2918.03	3.48	2918.03
12	3	×				×			×			×	9 615	0.038	7 569	14.595	71 151	312 429	2810.91	4.39	91 326	2856.36	1.28	0.28	4.15	2845.57	13.35	237.16	4.36	2845.57	0.00	2856.36	8.03	2856.36
11	1	×				×		×				×	8 243	0.042	4 516	4.556	71 151	37 639	2918.03	0.53	8 118	1095.00	0.11	0.19	-0.97	2866.17	8.34	2851.48	1.34	2862.34	-5.43	2918.03	2.78	2000.00
13	6	×				×				×		×	10 770	0.045	10 591	41.957	71 151	367 183	2645.46	5.16	89 759	2885.46	1.26	0.34	9.24	2881.78	18.37	2879.94	11.90	2548.12	6.61	2885.46	14.63	2885.46
7	1	×			×				×			×	30 831	0.066	10 640	13.780	103 713	102 313	2856.36	0.99	34 970	1095.00	0.34	0.17	-0.83	2847.22	8.25	2844.77	1.47	2847.37	-2.13	2856.36	6.37	2856.36
6	1	×			×			×				×	29 307	0.069	8 334	4.266	103 713	500	2733.69	0.00	34 970	1095.00	0.34	0.15	-9.35	2176.98	0.40	2842.86	0.94	2175.46	-8.61	2553.03	0.16	2000.00
8	1	×			×					×		×	33 596	0.089	12 982	39.804	103 713	130 394	2885.46	1.26	75 866	2885.46	0.73	0.20	3.87	2583.05	12.60	2402.40	3.05	2552.92	2.67	2885.46	11.20	2885.46
18	6	×					×			×		×	6 380	0.089	8 889	40.974	59 163	635 117	2870.61	10.74	74 764	2345.46	1.26	0.38	10.11	2881.80	19.12	2880.61	12.31	2697.65	10.27	2885.46	18.13	2885.46
17	3	×					×		×			×	5 809	0.115	6 196	14.267	59 163	544 514	2811.82	9.20	92 788	2856.36	1.57	0.34	4.71	2846.12	13.81	2840.06	7.22	2846.12	1.54	2856.36	9.56	2856.36
1	5	×			×			×			×		57 614	0.322	11 542	7.714	103 713	2 826	2733.69	0.03	441 662	2188.03	4.26	0.24	-0.64	2859.13	5.90	2844.25	1.66	2881.08	-4.26	2918.00	0.27	2733.69
4	5	×			×				×		×		59 576	0.326	12 457	24.908	103 713	193 007	2810.91	1.86	460 528	2046.36	4.44	0.33	7.96	2754.60	13.95	2748.68	10.70	2124.26	2.17	2856.36	6.21	2856.36
34	1		×				×	×				×	7 388	0.365	5 044	5.378	59 163	576 311	2000.00	9.74	9 642	1095.00	0.16	0.32	-1.38	2866.90	10.32	2840.98	1.39	2859.22	-7.82	2918.03	3.95	2372.37
29	1		×			×		×				×	12 215	0.385	6 576	5.512	71 151	276 144	2000.00	3.88	15 567	1095.00	0.22	0.30	-2.38	2862.53	9.41	2848.28	1.31	2523.01	-8.78	2918.03	1.39	2372.37
5	5	×			×					×	×		67 270	0.429	17 121	72.367	103 713	354 492	2870.30	3.42	565 436	2885.46	5.45	0.47	13.28	2882.07	18.97	2880.02	12.87	2517.88	9.01	2885.46	13.05	2885.46
30	3		×			×			×			×	14 065	0.461	9 636	17.518	71 151	576 552	2811.82	8.10	67 418	2856.36	0.95	0.39	2.68	2846.40	13.97	2839.17	2.79	2845.29	-2.01	2856.36	8.03	2856.36
35	3		×				×		×			×	8 568	0.473	8 055	17.076	59 163	1 371 160	2811.82	23.18	77 572	2856.36	1.31	0.41	3.31	2846.43	14.47	2840.01	3.45	2846.43	-1.15	2856.36	8.88	2856.36
36	6		×				×			×		×	9 197	0.480	10 339	49.033	59 163	2 209 074	2870.61	37.34	69 985	2315.46	1.18	0.41	8.71	2882.37	19.77	2880.65	13.72	2819.36	7.10	2885.46	17.14	2885.46
31	6		×			×				×		×	15 561	0.507	12 259	50.256	71 151	1 080 031	2870.61	15.18	84 090	2375.46	1.18	0.42	7.44	2882.18	18.59	2879.68	13.01	2850.54	6.23	2885.46	16.25	2885.46
52	1			×			×	×				×	11 039	0.701	6 748	6.218	59 163	1 219 072	2000.00	20.61	13 136	1095.00	0.22	0.28	-2.98	2862.88	11.20	2840.20	1.26	2859.39	-11.38	2553.03	4.65	2372.37
2	2	×				×		×			×		19 389	0.791	4 112	7.582	71 151	811 624	2733.69	11.41	185 630	2188.03	2.61	0.35	5.43	2858.89	12.22	2837.30	6.47	2855.05	-3.36	2188.03	5.96	2368.69
53	3			×			×		×			×	12 662	0.825	9 675	19.649	59 163	2 792 813	2811.82	47.21	48 151	2856.36	0.81	0.29	1.65	2847.35	14.89	2840.92	2.45	2846.43	-3.10	2856.36	8.93	2856.36
47	1			×		×		×				×	17 743	0.860	8 561	6.353	71 151	837 825	2000.00	11.78	19 237	1095.00	0.27	0.22	-4.12	2858.96	10.50	2839.33	1.21	2519.04	-11.30	2188.03	2.44	2372.37
54	2			×			×			×		×	13 485	0.864	11 460	56.511	59 163	3 746 265	2870.61	63.32	63 376	2405.46	1.07	0.27	6.81	2882.70	19.89	2880.91	9.26	2882.70	4.04	2885.46	16.08	2885.46
48	1			×		×			×			×	20 229	0.956	11 581	20.155	71 151	1 180 149	2811.82	16.59	41 291	2856.36	0.58	0.23	1.24	2845.51	14.73	2840.00	2.23	2844.59	-4.66	2856.36	7.38	2856.36
25	4		×		×				×			×	46 787	0.974	13 351	17.943	103 713	46 060	2856.36	0.44	41 566	1095.00	0.40	0.07	-1.45	2846.45	9.39	2844.56	1.49	2847.34	-3.39	2856.36	6.64	2856.36
9	2	×				×			×		×		22 702	0.980	9 714	24.393	71 151	2 986 703	2810.91	41.98	196 853	2046.36	2.77	0.47	11.01	2844.53	16.80	2839.98	11.43	2740.13	1.25	2856.36	15.57	2540.91
24	4		×		×			×				×	44 525	0.998	10 827	5.581	103 713	2 059	2737.37	0.02	41 566	1095.00	0.40	0.07	-10.79	2862.66	1.23	2840.63	0.96	2888.18	-10.12	2918.03	0.03	2737.37
49	2			×		×				×		×	22 313	1.052	13 542	57.833	71 151	2 402 898	2870.61	33.77	84 727	2525.46	1.19	0.21	6.23	2882.38	19.47	2880.32	6.55	2882.38	1.96	2885.46	14.00	2885.46
26	4		×		×					×		×	50 943	1.069	15 340	51.695	103 713	132 930	2885.46	1.28	88 496	2885.46	0.85	0.08	3.29	2793.03	13.80	2522.37	2.66	2793.03	2.11	2885.46	12.15	2885.46
3	2	×					×	×			×		13 232	1.109	2 931	7.471	59 163	1 967 344	2737.37	33.25	73 407	2188.03	1.24	0.44	5.72	2866.37	11.94	2844.56	8.54	2845.43	-3.37	2188.03	10.32	2737.37
10	0	×				×				×	×		25 779	1.112	14 751	70.619	71 151	4 415 761	2870.61	62.06	330 734	2645.46	4.65	0.46	17.60	2881.83	23.11	2880.62	13.17	2335.24	15.12	2885.46	24.50	2150.61
21	2		×				×	×			×		21 763	1.172	4 632	9.034	59 163	4 647 003	2737.37	78.55	127 887	2188.03	2.16	0.59	5.14	2862.56	13.06	2843.81	5.28	2862.56	-4.16	2188.03	10.56	2737.37
14	0	×					×		×		×		15 769	1.392	8 350	23.932	59 163	5 668 992	2811.82	95.82	173 313	2856.36	2.93	0.56	11.79	2845.37	17.42	2840.92	11.35	2828.74	5.05	2856.36	17.84	2451.82
15	0	×					×			×	×		17 330	1.441	12 603	69.253	59 163	6 584 745	2870.61	111.30	169 031	2495.46	2.86	0.54	18.61	2882.10	23.99	2880.62	12.31	2395.14	18.58	2885.46	27.70	2270.61
20	2		×			×		×			×		31 529	1.527	6 056	9.186	71 151	2 027 522	2737.37	28.50	235 616	2188.03	3.31	0.52	4.24	2490.35	13.13	2468.14	3.27	2851.78	-3.99	2188.03	8.33	2372.37
27	0		×			×			×		×		36 197	1.693	12 002	29.483	71 151	5 618 184	2811.82	78.96	244 365	2046.36	3.43	0.60	10.56	2845.38	17.52	2840.82	11.92	2126.18	3.01	2856.36	15.89	2271.82
28	0		×			×				×	×		40 927	1.903	16 491	85.175	71 151	7 729 707	2870.61	108.64	340 677	2405.46	4.79	0.58	16.84	2882.10	23.41	2881.21	15.16	2043.29	12.72	2885.46	25.98	2210.61
22	5		×		×				×		×		90 548	1.924	15 099	30.113	103 713	386 689	2811.82	3.73	495 593	2046.36	4.78	0.14	7.24	2484.52	14.64	2209.11	9.00	2663.62	-0.35	2856.36	4.69	2856.36
19	5		×		×			×			×		84 738	1.938	10 124	9.324	103 713	10 992	2737.37	0.11	476 559	2188.03	4.59	0.11	-1.93	2857.69	6.45	2840.75	1.60	2870.04	-5.16	2918.03	1.88	2737.37
32	0		×				×		×		×		25 351	2.044	10 352	28.836	59 163	8 515 558	2811.82	143.93	159 606	2856.36	2.70	0.63	11.60	2846.33	18.36	2841.77	12.17	2563.77	0.27	2631.82	18.25	2631.82
33	0		×				×			×	×		27 536	2.174	14 061	83.395	59 163	10 058 249	2870.61	170.01	192 424	2225.46	3.25	0.61	18.69	2882.46	25.15	2881.20	14.93	2576.03	17.64	2885.46	25.96	2510.61
23	5		×		×					×	×		101 501	2.182	19 206	87.271	103 713	649 166	2870.61	6.26	520 511	2705.46	5.02	0.17	12.42	2882.44	18.89	2880.59	14.33	2073.13	7.92	2885.46	12.97	2885.46
43	4			×	×				×			×	64 738	2.270	15 634	20.715	103 700	56 735	2811.82	0.55	44 450	1095.00	0.43	0.08	-5.78	2845.87	7.41	2843.68	1.28	2309.51	-5.79	2856.36	6.24	2856.36
42	4			×	×			×				×	62 192	2.365	13 289	6.469	103 700	11 064	2737.37	0.11	44 450	1095.00	0.43	0.08	-14.66	2173.28	-1.01	2827.98	0.93	2169.96	-12.54	2188.03	0.34	2737.37
44	4			×	×					×		×	69 814	2.446	16 853	59.613	103 700	181 640	2870.61	1.75	49 031	2885.46	0.47	0.08	-0.01	2643.05	12.51	2612.71	1.88	2613.29	0.44	2885.46	12.49	2885.46
38	2			×		×		×			×		48 942	2.711	7 892	10.708	71 151	3 788 467	2737.37	53.25	275 139	2188.03	3.87	0.37	2.39	2855.35	13.20	2464.63	2.31	2486.68	-4.88	2188.03	8.63	2372.37
39	0			×			×	×			×		34 673	2.739	6 231	10.510	59 163	7 455 414	2737.37	126.01	184 196	2188.03	3.11	0.52	4.28	2494.13	14.07	2475.45	3.32	2858.95	-4.97	2188.03	8.68	3095.00
45	0			×		×			×		×		55 202	2.892	13 944	34.187	71 151	8 513 798	2811.82	119.66	282 521	2046.36	3.97	0.36	10.06	2845.41	18.38	2840.09	13.54	2215.91	-4.81	2856.36	11.60	2091.82
50	0			×			×		×		×		39 649	3.014	12 031	33.458	59 163	11 436 397	2811.82	193.30	191 364	2046.36	3.23	0.47	11.11	2846.36	18.99	2842.75	13.17	2746.81	-1.72	2856.36	11.11	2181.82
46	0			×		×				×	×		62 458	3.243	17 716	98.772	71 151	11 551 325	2870.61	162.35	347 424	2555.46	4.88	0.33	16.89	2882.43	24.54	2881.18	16.13	2042.78	7.23	2885.46	14.93	2270.61
51	0			×			×			×	×		43 192	3.252	15 110	96.659	59 163	6 588 776	2870.61	111.37	224 283	2375.46	3.79	0.43	18.14	2882.73	25.54	2881.54	15.89	2757.23	12.72	2885.46	18.78	2885.46
40	5			×	×				×		×		133 784	4.663	17 359	35.016	103 700	593 956	2811.82	5.73	508 236	2046.36	4.90	0.16	4.13	2302.65	13.57	2209.77	2.87	2301.96	-3.83	2856.64	4.19	2271.82
37	5			×	×			×			×		126 731	4.793	12 393	10.888	103 700	68 943	2737.37	0.66	478 110	2188.03	4.61	0.15	-8.45	2845.26	3.00	2831.17	1.28	2169.66	-6.77	2188.03	3.67	2737.37
41	5			×	×					×	×		148 156	5.169	20 628	101.332	103 700	1 117 260	2870.61	10.77	507 637	2015.46	4.90	0.19	10.71	2372.41	18.36	2281.22	15.28	2192.67	6.66	2885.46	12.71	2885.46

Table 43. Sensitivity analysis in 2D. List of cases classified according to average tensile strip thickness

		Depth casing shoe			Cavern diameter			Cycling period			P_{min}		Creep Closure (m^3)	Subsidence (mm)	Conduction Heat Flux Loss (MWh)	Produced Energy (GWh)		Effective Tensile Stress				Dilation		Vertical Strain at CS (%)	Max.Principal Stress (MPa)		Max. Effective Stress (MPa)		Dilation		Max.Principal Stress (MPa)		Max. Effective Stress (MPa)	
Case	Class	Z1	Z2	Z3	D1	D2	D3	S	Q	M	G1	G2	Volume loss @ 900 days	Subsidence @ 900 days	Cumulated energy @ 900 days	Cumulated energy @ 900 days	Surface Area (m^2)	Max. tensile volume		Av. tensile strip thickness (m)	Max. dilatant volume		Av. dilatant strip thickness (m)	Strain @ 900 days (%)	Value (MPa)	Date (days)	Value (MPa)	Date (days)	Value 1/FOS	Date (days)	Value (MPa)	Date Output (Days)	Value (MPa)	Date Output (Days)
																		Value (m^3)	Date Output (Days)		Value (m^3)	Date Output (Days)											
6	1	×				×			×			×	29 307	0.069	8 334	4.266	103 713	500	2733.69	0.00	34 970	1095.00	0.34	0.15	-9.35	2176.98	0.40	2842.86	0.94	2175.46	-8.61	2553.03	0.16	2000.00
24	4		×		×				×			×	44 525	0.998	10 827	5.581	103 713	2 059	2737.37	0.02	41 566	1095.00	0.40	0.07	-10.79	2862.66	1.23	2840.63	0.96	2888.18	-10.12	2918.03	0.03	2737.37
1	5	×			×			×			×		57 614	0.322	11 542	7.714	103 713	2 826	2733.69	0.03	441 662	2188.03	4.26	0.24	-0.64	2859.13	5.90	2844.25	1.66	2881.08	-4.26	2918.00	0.27	2733.69
19	5		×		×			×			×		84 738	1.938	10 124	9.324	103 713	10 992	2737.37	0.11	476 559	2188.03	4.59	0.11	-1.93	2857.69	6.45	2840.75	1.60	2870.04	-5.16	2918.03	1.88	2737.37
42	4			×	×			×				×	62 192	2.365	13 289	6.469	103 700	11 064	2737.37	0.11	44 450	1095.00	0.43	0.08	-14.66	2173.28	-1.01	2827.98	0.93	2169.96	-12.54	2188.03	0.34	2737.37
25	4		×		×				×			×	46 787	0.974	13 351	17.943	103 713	46 060	2856.36	0.44	41 566	1095.00	0.40	0.07	-1.45	2846.45	9.39	2844.56	1.49	2847.34	-3.39	2856.36	6.64	2856.36
11	1	×				×		×				×	8 243	0.042	4 516	4.556	71 151	37 639	2918.03	0.53	8 118	1095.00	0.11	0.19	-0.97	2866.17	8.34	2851.48	1.34	2862.34	-5.43	2918.03	2.78	2000.00
43	4				×			×				×	64 738	2.270	15 634	20.715	103 700	56 735	2811.82	0.55	44 450	1095.00	0.43	0.08	-5.78	2845.87	7.41	2843.68	1.28	2309.51	-5.79	2856.36	6.24	2856.36
37	5			×	×			×			×		126 731	4.793	12 393	10.888	103 700	68 943	2737.37	0.66	478 110	2188.03	4.61	0.15	-8.45	2845.26	3.00	2831.17	1.28	2169.66	-6.77	2188.03	3.67	2737.37
7	1	×			×				×		×		30 831	0.066	10 640	13.780	103 713	102 313	2856.36	0.99	34 970	1095.00	0.34	0.17	-0.83	2847.22	8.25	2844.77	1.47	2847.37	-2.13	2856.36	6.37	2856.36
8	1	×			×					×		×	33 596	0.089	12 982	39.804	103 713	130 394	2885.46	1.26	75 866	2885.46	0.73	0.20	3.87	2583.05	12.60	2402.40	3.05	2552.92	2.67	2885.46	11.20	2885.46
26	4		×		×				×		×		50 943	1.069	15 340	51.695	103 713	132 930	2885.46	1.28	88 496	2885.46	0.85	0.08	3.29	2793.03	13.80	2522.37	2.66	2793.03	2.11	2885.46	12.15	2885.46
44	4				×				×		×		69 814	2.446	16 853	59.613	103 700	181 640	2870.61	1.75	49 031	2885.46	0.47	0.08	-0.01	2643.05	12.51	2612.71	1.88	2613.29	0.44	2885.46	12.49	2885.46
16	1	×					×	×					4 915	0.009	3 249	4.480	59 163	105 428	2918.03	1.78	2 067	1095.00	0.03	0.23	-2.38	2862.53	9.41	2848.28	1.31	2523.01	-8.78	2918.03	1.39	2372.37
4	5	×			×				×		×		59 576	0.326	12 457	24.908	103 713	193 007	2810.91	1.86	460 528	2046.36	4.44	0.33	7.96	2754.60	13.95	2748.68	10.70	2124.26	2.17	2856.36	6.21	2856.36
5	5	×			×					×	×		67 270	0.429	17 121	72.367	103 713	354 492	2870.30	3.42	565 436	2885.46	5.45	0.47	13.28	2882.07	18.97	2880.02	12.87	2517.88	9.01	2885.46	13.05	2885.46
22	5		×		×				×		×		90 548	1.924	15 099	30.113	103 713	386 689	2811.82	3.73	495 593	2046.36	4.78	0.14	7.24	2494.52	14.64	2209.11	9.00	2663.62	-0.35	2856.36	4.69	2856.36
29	1	×				×						×	12 215	0.385	6 576	5.512	71 151	276 144	2000.00	3.88	15 567	1095.00	0.22	0.30	-2.38	2862.53	9.41	2848.28	1.31	2523.01	-8.78	2918.03	1.39	2372.37
12	3	×					×		×				9 615	0.038	7 569	14.595	71 151	312 429	2810.91	4.39	91 326	2856.36	1.28	0.28	4.15	2845.57	13.35	237.16	4.36	2845.57	0.00	2856.36	8.03	2856.36
13	6	×					×			×			10 770	0.045	10 591	41.957	71 151	367 183	2645.46	5.16	89 759	2885.46	1.26	0.34	9.24	2881.78	18.37	2879.94	11.90	2548.12	6.61	2885.46	14.63	2885.46
40	5			×			×		×		×		133 784	4.663	17 359	35.016	103 700	593 956	2811.82	5.73	508 236	2046.36	4.90	0.16	4.13	2302.65	13.57	2209.77	2.87	2301.96	-3.83	2856.64	4.19	2271.82
23	5			×			×			×	×		101 501	2.182	19 206	87.271	103 713	649 166	2870.61	6.26	520 511	2705.46	5.02	0.17	12.42	2882.44	18.89	2880.59	14.33	2073.13	7.92	2885.46	12.97	2885.46
30	3		×			×			×			×	14 065	0.461	9 636	17.518	71 151	576 552	2811.82	8.10	67 418	2856.36	0.95	0.39	2.68	2846.40	13.97	2839.17	2.79	2845.29	-2.01	2856.36	8.03	2856.36
17	3	×					×	×					5 809	0.115	6 196	14.267	59 163	544 514	2811.82	9.20	92 788	2856.36	1.57	0.34	4.71	2846.12	13.81	2840.06	7.22	2846.12	1.54	2856.36	9.56	2856.36
34	1		×				×	×					7 388	0.365	5 044	5.378	59 163	576 311	2000.00	9.74	9 642	1095.00	0.16	0.32	-1.38	2866.90	10.32	2840.98	1.39	2859.22	-7.82	2918.03	3.95	2372.37
18	6	×					×			×			6 380	0.089	8 889	40.974	59 163	635 117	2870.61	10.74	74 764	2345.46	1.26	0.38	10.11	2881.80	19.12	2880.61	12.31	2697.65	10.27	2885.46	18.13	2885.46
41	5			×						×	×		148 156	5.169	20 628	101.332	103 700	1 117 260	2870.61	10.77	507 637	2015.46	4.90	0.19	10.71	2372.41	18.36	2281.22	15.28	2192.67	6.66	2885.46	12.71	2885.46
2	2	×				×			×				19 389	0.791	4 112	7.582	71 151	811 624	2733.69	11.41	185 630	2188.03	2.61	0.35	5.43	2858.89	12.22	2837.30	6.47	2855.05	-3.36	2188.03	5.96	2368.69
47	1			×			×	×					17 743	0.860	8 561	6.353	71 151	837 825	2000.00	11.78	19 237	1095.00	0.27	0.22	-4.12	2858.96	10.50	2839.33	1.21	2519.04	-11.30	2188.03	2.44	2372.37
31	6		×			×				×			15 561	0.507	12 259	50.256	71 151	1 080 031	2870.61	15.18	84 090	2375.46	1.18	0.42	7.44	2882.18	18.59	2879.68	13.01	2850.54	6.23	2885.46	16.25	2885.46
48	1			×			×		×				20 229	0.956	11 581	20.155	71 151	1 180 149	2811.82	16.59	41 291	2846.36	0.58	0.23	1.24	2845.51	14.73	2840.00	2.23	2844.59	-4.66	2856.36	7.38	2856.36
52	1			×			×	×			×		11 039	0.701	6 748	6.218	59 163	1 219 072	2000.00	20.61	13 136	1095.00	0.22	0.28	-2.98	2862.88	11.20	2840.20	1.26	2859.39	-11.38	2553.03	4.65	2372.37
35	3		×			×		×			×		8 568	0.473	8 055	17.076	59 163	1 371 160	2811.82	23.18	77 572	2856.36	1.31	0.41	3.31	2846.43	14.47	2840.01	3.45	2846.43	-1.15	2856.36	8.88	2856.36
20	2		×			×			×				31 529	1.527	6 056	9.186	71 151	2 027 522	2737.37	28.50	235 616	2188.03	3.31	0.52	4.24	2490.35	13.13	2468.14	3.27	2851.78	-3.99	2188.03	8.33	2372.37
3	2	×					×	×					13 232	1.109	2 931	7.471	59 163	1 967 344	2737.37	33.25	73 407	2188.03	1.24	0.44	5.72	2866.37	11.94	2844.56	8.54	2845.43	-3.37	2188.03	10.32	2737.37
49	2			×		×				×			22 313	1.052	13 542	57.833	71 151	2 402 898	2870.61	33.77	84 727	2525.46	1.19	0.21	6.23	2882.38	19.47	2880.32	6.55	2882.38	1.96	2885.46	14.00	2885.46
36	6		×				×			×			9 197	0.480	10 339	49.033	59 163	2 209 074	2870.61	37.34	69 985	2315.46	1.18	0.41	8.71	2882.37	19.77	2880.65	13.72	2819.36	7.10	2885.46	17.14	2885.46
9	2	×				×			×				22 702	0.980	9 714	24.393	71 151	2 986 703	2810.91	41.98	196 853	2046.36	2.77	0.47	11.01	2844.53	16.80	2839.98	11.43	2740.13	1.25	2856.36	15.57	2540.91
53	3			×			×		×				12 662	0.825	9 675	19.649	59 163	2 792 813	2811.82	47.21	48 151	2856.36	0.81	0.29	1.65	2847.35	14.89	2840.92	2.45	2846.43	-3.10	2856.36	8.93	2856.36
38	2			×		×				×			48 942	2.711	7 892	10.708	71 151	3 788 467	2737.37	53.25	275 139	2188.03	3.87	0.37	2.39	2855.35	13.20	2464.63	2.31	2486.68	-4.88	2188.03	8.63	2372.37
10	0		×			×				×			25 779	1.112	14 751	70.619	71 151	4 415 761	2870.61	62.06	330 734	2645.46	4.65	0.46	17.60	2881.83	23.11	2880.62	13.17	2335.24	15.12	2885.46	24.50	2150.61
54	2			×			×			×			13 485	0.864	11 460	56.511	59 163	3 746 265	2870.61	63.32	63 376	2405.46	1.07	0.27	6.81	2882.70	19.89	2880.91	9.26	2882.70	4.04	2885.46	16.08	2885.46
21	2												21 763	1.172	4 632	9.034	59 163	4 647 003	2737.37	78.55	127 887	2188.03	2.16	0.59	5.14	2862.56	13.06	2843.81	5.28	2862.56	-4.16	2188.03	10.56	2737.37
27	0		×				×			×			36 197	1.693	12 002	29.483	71 151	5 618 184	2811.82	78.96	244 365	2046.36	3.43	0.60	10.56	2845.38	17.52	2840.82	11.92	2126.18	3.01	2856.36	15.89	2271.82
14	0	×					×			×			15 769	1.392	8 350	23.932	59 163	5 668 992	2811.82	95.82	173 313	2856.36	2.93	0.56	11.79	2845.37	17.42	2840.92	11.35	2828.74	5.05	2856.36	17.84	2451.82
28	0		×			×				×			40 927	1.903	16 491	85.175	71 151	7 729 707	2870.61	108.64	340 677	2405.46	4.79	0.58	16.84	2882.10	23.41	2881.21	15.16	2043.29	12.72	2885.46	25.98	2210.61
15	0	×					×			×			17 330	1.441	12 603	69.253	59 163	6 584 745	2870.61	111.30	169 031	2495.46	2.86	0.54	18.61	2882.10	23.99	2880.62	12.31	2395.14	18.58	2885.46	27.70	2270.61
51	0												43 192	3.252	15 110	96.659	59 163	6 588 776	2870.61	111.37	224 283	2375.46	3.79	0.43	18.14	2882.73	25.54	2881.54	15.89	2757.23	12.72	2885.46	18.78	2885.46
45	0			×			×			×			55 202	2.892	13 944	34.187	71 151	8 513 798	2811.82	119.66	282 521	2046.36	3.97	0.36	10.06	2845.41	18.38	2840.09	13.54	2215.91	-4.81	2856.36	11.60	2091.82
39	0			×			×		×				34 673	2.739	6 231	10.510	59 163	7 455 414	2737.37	126.01	184 196	2188.03	3.11	0.52	4.28	2494.13	14.07	2475.45	3.32	2858.95	-4.97	2188.03	8.68	3095.00
32	0		×			×			×				25 351	2.044	10 352	28.836	59 163	8 515 558	2811.82	143.93	159 606	2856.36	2.70	0.63	11.60	2846.33	18.36	2841.77	12.17	2563.77	0.27	2631.82	18.25	2631.82
46	0			×			×			×			62 458	3.243	17 716	98.772	71 151	11 551 325	2870.61	162.35	347 424	2555.46	4.88	0.33	16.89	2882.43	24.54	2881.18	16.13	2042.78	7.23	2885.46	14.93	2270.61
33	0		×				×		×				27 536	2.174	14 061	83.395	59 163	10 058 249	2870.61	170.01	192 424	2225.46	3.25	0.61	18.69	2882.46	25.15	2881.20	14.93	2576.03	17.64	2885.46	25.96	2510.61
50	0			×			×			×			39 649	3.014	12 031	33.458	59 163	11 436 397	2811.82	193.30	191 364	2046.36	3.23	0.47	11.11	2846.36	18.99	2842.75	13.17	2746.81	-1.72	2856.36	11.11	2181.82

Table 44. Sensitivity analysis in 2D. List of cases classified according to average dilatant strip thickness.

		Depth casing shoe			Cavern diameter			Cycling period			P_{min}	Creep Closure (m^3)	Subsidence (mm)	Conduction Heat Flux Loss (MWh)	Produced Energy (GWh)		Effective Tensile Stress				Dilation		Vertical Strain at CS (%)	Max.Principal Stress (MPa)		Max. Effective Stress (MPa)		Dilation		Max.Principal Stress (MPa)		Max. Effective Stress (MPa)	
																	Max. tensile volume		Av. tensile strip thickness (m)	Max. dilatant volume		Av. dilatant strip thickness (m)	Strain @ 900 days (%)									
Case	Class	Z1	Z2	Z3	D1	D2	D3	S	Q	M	G1	G2	Volume loss @ 900 days	Subsidence @ 900 days	Cumulated energy @ 900 days	Cumulated energy @ 900 days	Surface Area (m^2)	Value (m^3)	Date Output (Days)		Value (m^3)	Date Output (Days)		Value (MPa)	Date (days)	Value (MPa)	Date (days)	Value	Date (days)	Value (MPa)	Date Output (Days)	Value (MPa)	Date Output (Days)
16	1	×					×					×	4 915	0.009	3 249	4.480	105 428	2918.03	1.78	2 067	1095.00	0.03	0.23	0.22	2866.44	9.56	2840.89	1.64	2862.95	-4.54	2918.03	3.48	2918.03
11	1	×				×		×				×	8 243	0.042	4 516	4.556	71 151	37 639	0.53	8 118	1095.00	0.11	0.19	-0.97	2866.17	8.34	2851.48	1.34	2862.34	-5.43	2918.03	2.78	2000.00
34	1		×				×	×				×	7 388	0.365	5 044	5.378	59 163	576 311	2000.00	9.74	9 642	1095.00	0.16	0.32	-1.38	2866.90	10.32	2840.98	1.39	2859.22	-7.82	2918.03	3.95	2372.37
29	1		×			×		×				×	12 215	0.385	6 576	5.512	71 151	276 144	2000.00	3.88	15 567	1095.00	0.22	0.30	-2.38	2862.53	9.41	2848.28	1.31	2523.01	-8.78	2918.03	1.39	2372.37
52	1				×			×				×	11 039	0.701	6 748	6.218	59 163	1 219 072	2000.00	20.61	13 136	1095.00	0.22	0.28	-2.98	2862.88	11.20	2840.20	1.26	2859.39	-11.38	2553.03	4.65	2372.37
47	1												17 743	0.860	8 561	6.353	71 151	837 825	2000.00	11.78	19 237	1095.00	0.27	0.22	-4.12	2858.96	10.50	2839.33	1.21	2519.04	-11.30	2188.03	2.44	2372.37
6	1	×											29 307	0.069	8 334	4.266	103 713	500	2733.69	0.00	34 970	1095.00	0.34	0.15	-9.35	2176.98	0.40	2842.86	0.94	2175.46	-8.61	2553.03	0.16	2000.00
7	1	×			×			×				×	30 831	0.066	10 640	13.780	103 713	102 313	2856.36	0.99	34 970	1095.00	0.34	0.17	-0.83	2847.22	8.25	2844.77	1.47	2847.37	-2.13	2856.36	6.37	2856.36
24	4		×		×			×				×	44 525	0.998	10 827	5.581	103 713	2 059	2737.37	0.02	41 566	1095.00	0.40	0.07	-10.79	2862.66	1.23	2840.63	0.96	2888.18	-10.12	2918.03	0.03	2737.37
25	4		×		×				×				46 787	0.974	13 351	17.943	103 713	46 060	2856.36	0.44	41 566	1095.00	0.40	0.07	-1.45	2846.45	9.39	2844.56	1.49	2847.34	-3.39	2856.36	6.64	2856.36
42	4				×	×		×				×	62 192	2.365	13 289	6.469	103 700	11 064	2737.37	0.11	44 450	1095.00	0.43	0.08	-14.66	2173.28	-1.01	2827.98	0.93	2169.96	-12.54	2188.03	0.34	2737.37
43	4				×	×			×				64 738	2.270	15 634	20.715	103 700	56 735	2811.82	0.55	44 450	1095.00	0.43	0.08	-5.78	2845.87	7.41	2843.68	1.28	2309.51	-5.79	2856.36	6.24	2856.36
44	4				×	×				×			69 814	2.446	16 853	59.613	103 700	181 640	2870.61	1.75	49 031	2885.46	0.47	0.08	-0.01	2643.05	12.51	2612.71	1.88	2613.29	0.44	2885.46	12.49	2885.46
48	1			×			×						20 229	0.956	11 581	20.155	71 151	1 180 149	2811.82	16.59	41 291	2856.36	0.58	0.23	1.24	2845.51	14.73	2840.00	2.23	2844.59	-4.66	2856.36	7.38	2856.36
8	1	×			×								33 596	0.089	12 982	39.804	103 713	130 394	2885.46	1.26	75 866	2885.46	0.73	0.20	3.87	2583.05	12.60	2402.40	3.05	2552.92	2.67	2885.46	11.20	2885.46
53	3			×			×		×				12 662	0.825	9 675	19.649	59 163	2 792 813	2811.82	47.21	48 151	2856.36	0.81	0.29	1.65	2847.35	14.89	2840.92	2.45	2846.43	-3.10	2856.36	8.93	2856.36
26	4			×						×			50 943	1.069	15 340	51.695	103 713	132 930	2885.46	1.28	88 496	2885.46	0.85	0.08	3.29	2793.03	13.80	2522.37	2.66	2793.03	2.11	2885.46	12.15	2885.46
30	3		×				×		×				14 065	0.461	9 636	17.518	71 151	576 552	2811.82	8.10	67 418	2856.36	0.95	0.39	2.68	2846.40	13.97	2839.17	2.79	2845.29	-2.01	2856.36	8.03	2856.36
54	2			×			×			×			13 485	0.864	11 460	56.511	59 163	3 746 265	2870.61	63.32	63 376	2405.46	1.07	0.27	6.81	2882.70	19.89	2880.91	9.26	2882.70	4.04	2885.46	16.08	2885.46
31	6		×			×				×			15 561	0.507	12 259	50.256	71 151	1 080 031	2870.61	15.18	84 090	2375.46	1.18	0.42	7.44	2882.18	18.59	2879.68	13.01	2850.54	6.23	2885.46	16.25	2885.46
36	6		×				×		×				9 197	0.480	10 339	49.033	59 163	2 209 074	2870.61	37.34	69 985	2315.46	1.18	0.41	8.71	2882.37	19.77	2880.65	13.72	2819.36	7.10	2885.46	17.14	2885.46
49	2					×				×			22 313	1.052	13 542	57.833	71 151	2 402 898	2870.61	33.77	84 727	2525.46	1.19	0.21	6.23	2882.38	19.47	2880.32	6.55	2882.38	1.96	2885.46	14.00	2885.46
3	2	×					×	×			×		13 232	1.109	2 931	7.471	59 163	1 967 344	2737.37	33.25	73 407	2188.03	1.24	0.44	5.72	2866.37	11.94	2844.56	8.54	2845.43	-3.37	2188.03	10.32	2737.37
13	6	×					×	×			×		10 770	0.045	10 591	41.957	71 151	367 183	2645.46	5.16	89 759	2885.46	1.26	0.34	9.24	2881.78	18.37	2879.94	11.90	2548.12	6.61	2885.46	14.63	2885.46
18	6	×					×	×			×		6 380	0.089	8 889	40.974	59 163	635 117	2870.61	10.74	74 764	2345.46	1.26	0.38	10.11	2881.80	19.12	2880.61	12.31	2697.65	10.27	2885.46	18.13	2885.46
12	3	×					×		×				9 615	0.038	7 569	14.595	71 151	312 429	2810.91	4.39	91 326	2856.36	1.28	0.28	4.15	2845.57	13.35	237.16	4.36	2845.57	0.00	2856.36	8.03	2856.36
35	3			×			×		×				8 568	0.473	8 055	17.076	59 163	1 371 160	2811.82	23.18	77 572	2856.36	1.31	0.41	3.31	2846.43	14.47	2840.01	3.45	2846.43	-1.15	2856.36	8.88	2856.36
17	3	×					×		×				5 809	0.115	6 196	14.267	59 163	544 514	2811.82	9.20	92 788	2856.36	1.57	0.34	4.71	2846.12	13.81	2840.06	7.22	2846.12	1.54	2856.36	9.56	2856.36
21	2		×				×	×			×		21 763	1.172	4 632	9.034	59 163	4 647 003	2737.37	78.55	127 887	2188.03	2.16	0.59	5.14	2862.56	13.06	2843.81	5.28	2862.56	-4.16	2188.03	10.56	2737.37
2	2	×				×			×				19 389	0.791	4 112	7.582	71 151	811 624	2733.69	11.41	185 630	2188.03	2.61	0.35	5.43	2858.89	12.22	2837.30	6.47	2855.05	-3.36	2188.03	5.96	2368.69
32	0			×			×		×				25 351	2.044	10 352	28.836	59 163	8 515 558	2811.82	143.93	159 606	2856.36	2.70	0.63	11.60	2846.33	18.36	2841.77	12.17	2563.77	0.27	2631.82	18.25	2631.82
9	2	×				×			×				22 702	0.980	9 714	24.393	71 151	2 986 703	2810.91	41.98	196 853	2046.36	2.77	0.47	11.01	2844.53	16.80	2839.98	11.43	2740.13	1.25	2856.36	15.57	2540.91
15	0	×					×			×	×		17 330	1.441	12 603	69.253	59 163	6 584 745	2870.61	111.30	169 031	2495.46	2.86	0.54	18.61	2882.10	23.99	2880.62	12.31	2395.14	18.58	2885.46	27.70	2270.61
14	0	×					×		×		×		15 769	1.392	8 350	23.932	59 163	5 668 992	2811.82	95.82	173 313	2856.36	2.93	0.56	11.79	2845.37	17.42	2840.92	11.35	2828.74	5.05	2856.36	17.84	2451.82
39	0				×		×		×		×		34 673	2.739	6 231	10.510	59 163	7 455 414	2737.37	126.01	184 196	2188.03	3.11	0.52	4.28	2494.13	14.07	2475.45	3.32	2858.95	-4.97	2188.03	8.68	3095.00
50	0			×			×		×		×		39 649	3.014	12 031	33.458	59 163	11 436 397	2811.82	193.30	191 364	2046.36	3.23	0.47	11.11	2846.36	18.99	2842.75	13.17	2746.81	-1.72	2856.36	11.11	2181.82
33	0						×		×		×		27 536	2.174	14 061	83.395	59 163	10 058 249	2870.61	170.01	192 424	2225.46	3.25	0.61	18.69	2882.46	25.15	2881.20	14.93	2576.03	17.64	2885.46	25.96	2510.61
20	2		×								×		31 529	1.527	6 056	9.186	71 151	2 027 522	2737.37	28.50	235 616	2188.03	3.31	0.52	4.24	2490.35	13.13	2468.14	3.27	2851.78	-3.99	2188.03	8.33	2372.37
27	0		×				×		×		×		36 197	1.693	12 002	29.483	71 151	5 618 184	2811.82	78.96	244 365	2046.36	3.43	0.60	10.56	2845.38	17.52	2840.82	11.92	2126.18	3.01	2856.36	15.89	2271.82
51	0					×				×	×		43 192	3.252	15 110	96.659	59 163	6 588 776	2870.61	111.37	224 283	2375.46	3.79	0.43	18.14	2882.73	25.54	2881.54	15.89	2757.23	12.72	2885.46	18.78	2885.46
38	2			×		×			×		×		48 942	2.711	7 892	10.708	71 151	3 788 467	2737.37	53.25	275 139	2188.03	3.87	0.37	2.39	2855.35	13.20	2464.63	2.31	2486.68	-4.88	2188.03	8.63	2372.37
45	0			×		×			×		×		55 202	2.892	13 944	34.187	71 151	8 513 798	2811.82	119.66	282 521	2046.36	3.97	0.36	10.06	2845.41	18.38	2840.09	13.54	2215.91	-4.81	2856.36	11.60	2091.82
1	5	×					×			×	×		57 614	0.322	11 542	7.714	103 713	2 826	2733.69	0.03	441 662	2188.03	4.26	0.24	-0.64	2859.13	5.90	2844.25	1.66	2881.08	-4.26	2918.00	0.27	2733.69
4	5	×					×			×	×		59 576	0.326	12 457	24.908	103 713	193 007	2810.91	1.86	460 528	2046.36	4.44	0.33	7.96	2754.60	13.95	2748.68	10.70	2124.26	2.17	2856.36	6.21	2856.36
19	5						×			×	×		84 738	1.938	10 124	9.324	103 713	10 992	2737.37	0.11	476 559	2188.03	4.59	0.11	-1.93	2857.69	6.45	2840.75	1.60	2870.04	-5.16	2918.03	1.88	2737.37
37	5						×			×	×		126 731	4.793	12 393	10.888	103 700	68 943	2737.37	0.66	478 110	2188.03	4.61	0.15	-8.45	2845.26	3.00	2831.17	1.28	2169.66	-6.77	2188.03	3.67	2737.37
10	0	×					×			×			25 779	1.112	14 751	70.619	71 151	4 415 761	2870.61	62.06	330 734	2645.46	4.65	0.46	17.60	2881.83	23.11	2880.62	13.17	2335.24	15.12	2885.46	24.50	2150.61
22	5		×			×			×				90 548	1.924	15 099	30.113	103 713	386 689	2811.82	3.73	495 593	2046.36	4.78	0.14	7.24	2484.52	14.64	2209.11	9.00	2663.62	-0.35	2856.36	4.69	2856.36
28	0		×				×			×	×		40 927	1.903	16 491	85.175	71 151	7 729 707	2870.61	108.64	340 677	2405.46	4.79	0.58	16.84	2882.10	23.41	2881.21	15.16	2043.29	12.72	2885.46	25.98	2210.61
46	0					×				×	×		62 458	3.243	17 716	98.772	71 151	11 551 325	2870.61	162.35	347 424	2555.46	4.88	0.33	16.89	2882.43	24.54	2881.18	16.13	2042.78	7.23	2885.46	14.93	2270.61
41	5			×			×			×			148 156	5.169	20 628	101.332	103 700	1 117 260	2870.61	10.77	507 637	2015.46	4.90	0.19	10.71	2372.41	18.36	2281.22	15.28	2192.67	6.66	2885.46	12.71	2885.46
40	5			×			×			×			133 784	4.663	17 359	35.016	103 700	593 956	2811.82	5.73	508 236	2046.36	4.90	0.16	4.13	2302.65	13.57	2209.77	2.87	2301.96	-3.83	2856.64	4.19	2271.82
23	5		×				×			×			101 501	2.182	19 206	87.271	103 713	649 166	2870.61	6.26	520 511	2705.46	5.02	0.17	12.42	2882.44	18.89	2880.59	14.33	2073.13	7.92	2885.46	12.97	2885.46
5	5	×					×			×			67 270	0.429	17 121	72.367	103 713	354 492	2870.30	3.42	565 436	2885.46	5.45	0.47	13.28	2882.07	18.97	2880.02	12.87	2517.88	9.01	2885.46	13.05	2885.46

Appendix D: Risk assessment

D.1 Stakeholder: Operator

RISK Nr. 1.2 Well integrity loss (X-mas Tree)

Risk step 1: Aim

Aim 1 for the Operator: "*We store renewable ("green") energy as hydrogen gas in our own salt caverns. We are part of the energy transition and play an important role in the storage of renewable energy*". Therefore, the aim is: no risk for all stakeholders, directly or indirectly involved, as a result of hydrogen storage in salt caverns.

Risk step 2: Risk identification

(1) Risk: Well integrity loss caused by leakage at the X-mas tree
(2) Risk based on: Assumption
(3) Source of information: Expert judgement
(4) Uncertainty: Cannot be reduced
(5) Type of causes: [Tc][Hc][Oc][Rc]
(6) Type of effects: [Me][Te][Qe][Re]

Risk step 3: Risk classification

(1) Classification probability class: 2 (a): assumption based on expert judgement
(2) Classification consequence class: [Me1][Te2][Se0][Qe1][Re1]

Risk step 4: Dealing with risks

(1) Additional research: -
(2) Preventive measures: monitoring integrity X-mas tree, pressure gauges, H_2 certified material (steel), sensors at the well site, maintenance plan, mirroring the production tree, accident report obligation
(3) Corrective measures: damage control / repair
(4) Description and classification residual risk considering the measures taken: taking the preventive and corrective measures into account the residual risk becomes: 1 (probability) and [Me0][Te1][Se0][Qe0][Re0] (consequences), **1/1**

RISK Nr. 1.3 Leakage in vertical tubing / casing

Risk step 1: Aim

Aim 1 for the Operator: "*We store renewable ("green") energy as hydrogen gas in our own salt caverns. We are part of the energy transition and play an important role in the storage of renewable energy*". Therefore, the aim is: no risk for all stakeholders, directly or indirectly involved, as a result of hydrogen storage in salt caverns.

Risk step 2: Risk identification

(1) Risk: Leakage in vertical casing and tubing caused by joint failure, corrosion, rupture, failure at shoe
(2) Risk based on: Interpretation of facts
(3) Source of information: Literature review (12 cases described in Paragraph 2.2.3.2), example case histories[1][2]
(4) Uncertainty: Cannot be reduced
(5) Type of causes: [Tc][Oc][Ic]
(6) Type of effects: [Me][Te][Se][Qe][Re]

Risk step 3: Risk classification

(1) Classification probability class: 2 (c): interpretation of factual information
(2) Classification consequence class: [Me2][Te2][Se3][Qe2][Re3]

Risk step 4: Dealing with risks

(1) Additional research: -
(2) Preventive measures: H_2 certified material, corrosion protection, pressure gauges, periodic well control (gamma ray), speed limitation on the flow rate (T-limit), H_2S monitor system (beyond well site), minimum preconditions for H_2 storage cavern, double casing, preferably use newly developed caverns (according to an optimal rock mechanical envelope)
(3) Corrective measures: replace casing and tubing, use liner, packer or plug and drill new well, controlled production / flaring of H_2
(4) Description and classification residual risk considering the measures taken: taking the preventive and corrective measures into account the residual risk becomes: 1 (probability) and [Me2][Te1][Se1][Qe2][Re1] (consequences), **1/2**

[1] Magnolia, Louisiana, 2003 (2.2.3.2.10)

[2] Teutschenthal/Bad Lauchstädt, Germany, 1988 (2.2.3.2.6)

RISK Nr. 1.4 Pipeline integrity loss

Risk step 1: Aim

Aim 1 for the Operator: "*We store renewable ("green") energy as hydrogen gas in our own salt caverns. We are part of the energy transition and play an important role in the storage of renewable energy*". Therefore, the aim is: no risk for all stakeholders, directly or indirectly involved, as a result of hydrogen storage in salt caverns.

Risk step 2: Risk identification

(1) Risk: Pipeline integrity loss caused by rupture / leakage
(2) Risk based on: Interpretation of facts
(3) Source of information: public, press[3][4], politics[5], case histories[6][7] from literature review
(4) Uncertainty: Experience within the industry with hydrogen pipelines
(5) Type of causes: [Tc][Hc][Oc][Ic]
(6) Type of effects: [Me][Te][Se][Qe][Re]

Risk step 3: Risk classification

(1) Classification probability class: 2 (c): interpretation of factual information
(2) Classification consequence class: [Me1][Te1][Se3][Qe1][Re2]

Risk step 4: Dealing with risks

(1) Additional research: Literature research hydrogen infrastructure KEM 29 (research in progress)[8]
(2) Preventive measures: H_2 certified material, monitoring of integrity, construction and maintenance protocols, automatic valves, pressure gauges, partitioned piping, fended area, surveillance cameras, KLIC, sufficient spare parts, back-up system, H_2 monitoring sensors
(3) Corrective measures: temporary partial shut-down and repair
(4) Description and classification residual risk considering the measures taken: taking the preventive and corrective measures into account the residual risk becomes: 1 (probability) and [Me0][Te1][Se1][Qe1][Re1] (consequences), **1/1**

[3] Several publications referring to accidents with underground Natural Gas pipelines
[4] NAM, press information about leaking pipelines with production water, Twente, Drenthe, 2015
[5] D66, Motion referring to leakage in old salt pipelines, 2018
[6] Viriat, France, 1986, gas leak and cloud due to failure of compressor unit (Database of (near-) accidents occurred)
[7] Fort Saskatchewan (2.3.2.1)
[8] https://kemprogramma.nl/

RISK Nr. 1.5 Casing overstretching

Risk step 1: Aim

Aim 1 for the Operator: "*We store renewable ("green") energy as hydrogen gas in our own salt caverns. We are part of the energy transition and play an important role in the storage of renewable energy*". Therefore, the aim is: no risk for all stakeholders, directly or indirectly involved, as a result of hydrogen storage in salt caverns.

Risk step 2: Risk identification

(1) Risk: Casing overstretching
(2) Risk based on: Interpretation of facts
(3) Source of information: Literature review (section 3.3), example case histories[9][10][11]
(4) Uncertainty: Creep research, durability of the salt
(5) Type of causes: [Oc][Tc][Rc][Ic][Gc][Pc]
(6) Type of effects: [Me][Te][Qe][Re]

Risk step 3: Risk classification

(1) Classification probability class: 2 (c): interpretation of factual information
(2) Classification consequence class: [Me2][Te2][Se0][Qe2][Re1]

Risk step 4: Dealing with risks

(1) Additional research: creep research (grainsize), durability of the salt, site specific cavern behavior / design, R&D on optimal roof design / construction
(2) Preventive measures: chimney (below the shoe, above the cavern roof), prevent contact undersaturated brine with chimney, double casing, improved cavern design (avoid flat roof / interlayered formations / large diameter of the roof), site specific creep model combined with rheology and operation, periodic logging (H_2 certified logging material)
(3) Corrective measures: small liner, injection of closing material
(4) Description and classification residual risk considering the measures taken: taking the preventive and corrective measures into account the residual risk becomes: 1 (probability) and [Me1][Te2][Se0][Qe1][Re0] (consequences), **1/2**

[9] Boling 1, 2, 4, Texas, USA, 2005 (3.3.2.1)
[10] Dewdney Field, Saskatchewan, Canada, 2015 (3.3.2.3)
[11] Eminence salt dome 1, 3, 4, Mississippi, 1972 (3.3.2.2)

RISK Nr. 1.6 Cavern breaches / cavern integrity loss

Risk step 1: Aim

Aim 1 for the Operator: "*We store renewable ("green") energy as hydrogen gas in our own salt caverns. We are part of the energy transition and play an important role in the storage of renewable energy*". Therefore, the aim is: no risk for all stakeholders, directly or indirectly involved, as a result of hydrogen storage in salt caverns.

Risk step 2: Risk identification

(1) Risk: Cavern breaches (tightness) / cavern integrity loss
(2) Risk based on: Interpretation of facts
(3) Source of information: Literature review (7 cases described in section 2.2.3.1), example case histories[12][13]
(4) Uncertainty: Additional research of the salt structure and rheology, cavern design
(5) Type of causes: [Tc][Rc][Gc][Oc][Ic]
(6) Type of effects: [Me][Te][Se][Qe][Re]

Risk step 3: Risk classification

(1) Classification probability class: 2 (c): interpretation of factual information
(2) Classification consequence class: [Me2][Te2][Se2][Qe3][Re2]

Risk step 4: Dealing with risks

(1) Additional research: research of the salt dome internal structure, including anomalous zones (section 3.4.7.1.4), and rheology, cavern design
(2) Preventive measures: periodic leak tests (e.g., every 5 years), open communication with other operators, sonar surveys, GPR (radar), minimum preconditions for H_2 storage cavern, detection of heterogeneities, enough distance to the domes edge, tightness test, prevent responsibility gap, leakage report obligation, preferably use newly developed caverns (according to an optimal rock mechanical envelope)
(3) Corrective measures: abandon cavern
(4) Description and classification residual risk considering the measures taken: taking the preventive and corrective measures into account the residual risk becomes: 1 (probability) and [Me2][Te2][Se2][Qe3][Re2] (consequences), **1/3**

[12] Bayou Corne, Louisiana, 2012 (2.2.3.1.1)
[13] Clovelly salt dome, Louisiana, 1992 (2.2.3.1.4)

RISK Nr. 1.7 Creep closure and subsidence

Risk step 1: Aim

Aim 1 for the Operator: "*We store renewable ("green") energy as hydrogen gas in our own salt caverns. We are part of the energy transition and play an important role in the storage of renewable energy*". Therefore, the aim is: no risk for all stakeholders, directly or indirectly involved, as a result of hydrogen storage in salt caverns.

Risk step 2: Risk identification

(1) Risk: Subsidence (beyond predicted limits)
(2) Risk based on: Interpretation of facts
(3) Source of information: Literature review, example case histories[14][15]
(4) Uncertainty: Additional research of the salt structure and rheology, cavern design
(5) Type of causes: [Rc][Ic][Gc][Oc][Tc][Pc]
(6) Type of effects: [Me][Te][Se][Qe][Re]

Risk step 3: Risk classification

(1) Classification probability class: 2 (c): interpretation of factual information
(2) Classification consequence class: [Me2][Te3][Se1][Qe1][Re2]

Risk step 4: Dealing with risks

(1) Additional research: research of the salt structure and rheology, cavern design, geo-mechanical modelling
(2) Preventive measures: monitoring of subsidence by INSAR & surveying measurements, field tests (pressure observation test POT after well drill), updated cavern design, additional POT after cavern design, geo-mechanical modelling, sonar, determination of the minimum cavern pressure
(3) Corrective measures: change of the average cavern pressure (higher), minimizing the subsidence by controlled abandonment
(4) Description and classification residual risk considering the measures taken: taking the preventive and corrective measures into account the residual risk becomes: 1 (probability) and [Me2][Te3][Se1][Qe1][Re2] (consequences), **1/3**

[14] Subsidence at Maceió, Brazil, 2021 (3.2.3.4)
[15] Subsidence at Bernburg, Germany (3.2.3.2)

RISK Nr. 1.8 Tensile failure (rock salt / cavern wall) as a result of alternating pressure

Risk step 1: Aim

Aim 1 for the Operator: "*We store renewable ("green") energy as hydrogen gas in our own salt caverns. We are part of the energy transition and play an important role in the storage of renewable energy*". Therefore, the aim is: no risk for all stakeholders, directly or indirectly involved, as a result of hydrogen storage in salt caverns.

Risk step 2: Risk identification

(1) Risk: Tensile failure (rock salt / cavern wall) caused by thermal and mechanical stresses as a result of alternating pressure
(2) Risk based on: Interpretation of facts
(3) Source of information: Literature review, example case histories[16][17]
(4) Uncertainty: Research in mechanical properties, damage evolution
(5) Type of causes: [Hc][Rc][Ic][Gc][Tc]
(6) Type of effects: [Me][Te]

Risk step 3: Risk classification

(1) Classification probability class: 3 (c): interpretation of factual information
(2) Classification consequence class: [Me2][Te1][Se0][Qe0][Re0]

Risk step 4: Dealing with risks

(1) Additional research: research in mechanical properties, damage evolution, modelling of localized stress at anhydrite layers, mechanical properties of anhydrite, interphase of anhydrite and rocksalt
(2) Preventive measures: periodic sonar measurements (e.g., every 5 years), good salt mining practice, good rock mechanical envelope, minimum preconditions for H_2 storage cavern (well test), limitation of the production rate, preferably use newly developed caverns (according to an optimal rock mechanical envelope)
(3) Corrective measures: adapt the pressures
(4) Description and classification residual risk considering the measures taken: taking the preventive and corrective measures into account the residual risk becomes: 2 (probability) and [Me2][Te1][Se0][Qe0][Re0] (consequences), **2/2**

[16] Mine ventilation shaft in the Gorleben mine (3.4.3.2.4)

[17] Test in a salt mine, Varangéville France, 2015 (3.4.3.2.3)

RISK Nr. 1.9 Tensile failure (cement debonding) as a result of alternating pressure and temperature

Risk step 1: Aim

Aim 1 for the Operator: "*We store renewable ("green") energy as hydrogen gas in our own salt caverns. We are part of the energy transition and play an important role in the storage of renewable energy*". Therefore, the aim is: no risk for all stakeholders, directly or indirectly involved, as a result of hydrogen storage in salt caverns.

Risk step 2: Risk identification

(1) *Risk:* Tensile failure (cement debonding) caused by thermal and mechanical stresses as a result of alternating pressure in- and outside casing/shoe
(2) *Risk based on:* Assumption / interpretation of facts
(3) *Source of information:* Expert judgement[18], report KEM 18[19]
(4) *Uncertainty:* Research on prevention of micro annuli, research on temperature and pressure safety limits
(5) *Type of causes*: [Tc][Rc][Ic][Gc]
(6) *Type of effects*: [Me][Te][Se][Qe]

Risk step 3: Risk classification

(1) *Classification probability class:* 3 (a/c): assumption based on expert judgement and interpretation of facts
(2) *Classification consequence class:* [Me2][Te1][Se3][Qe2][Re3]

Risk step 4: Dealing with risks

(1) *Additional research:* research on prevention of micro annuli at the casing / cement / rock interfaces, research on temperature and pressure safety limits, research on use of self-healing materials
(2) *Preventive measures:* elastomers instead of cement, preferably avoid old wells (*use of cement, no known history with respect to loading cycles, temperature changes, wellbore deviation*), periodic well test, periodic "cement" bonding log, use of deformable metals, use of self-healing materials (like natural salt or shale), remain within temperature and pressure safety limits (flow restriction)
(3) *Corrective measures:* micro annuli treated with special materials (resins, silicates etc., biological treatment), use of deformable or self-healing materials and casing expansion, smaller pressure difference
(4) *Description and classification residual risk considering the measures taken:* taking the preventive and corrective measures into account the residual risk becomes: 3 (probability) and [Me2][Te1][Se2][Qe2][Re2] (consequences), **3/2**

[18] Interview with Eric van Oort

[19] Evo Energy Consulting, Qualitative Risk Assessment of long-term sealing behavior of materials and interfaces in boreholes, final report, reference KEM-18, dated January 20 2022 (van Oort, 2022)

RISK Nr. 1.10 Tensile failure (other materials) as a result of alternating pressure and temperature

Risk step 1: Aim

Aim 1 for the Operator: "*We store renewable ("green") energy as hydrogen gas in our own salt caverns. We are part of the energy transition and play an important role in the storage of renewable energy*". Therefore, the aim is: no risk for all stakeholders, directly or indirectly involved, as a result of hydrogen storage in salt caverns.

Risk step 2: Risk identification

(1) Risk: Tensile failure (materials like steel alloys, elastomers, etc.) caused by thermal and mechanical stresses as a result of alternating pressure
(2) Risk based on: Interpretation of facts / assumptions
(3) Source of information: Expert judgement and literature[20]
(4) Uncertainty: additional research for certification of H_2-proof material
(5) Type of causes: [Tc][Rc][Ic][Gc]
(6) Type of effects: [Me][Te][Se][Qe]

Risk step 3: Risk classification

(1) Classification probability class: 3 (a/c): assumption based on expert judgement and interpretation of facts
(2) Classification consequence class: [Me1][Te1][Se3][Qe2][Re3]

Risk step 4: Dealing with risks

(1) Additional research: additional research on the sealing effectiveness of all materials used for completion (steel alloys, elastomers and seals), no H_2-certified material available (low T, high p)
(2) Preventive measures: avoid nitril elastomers, preferably avoid old wells (*no known history with respect to loading cycles, temperature changes, wellbore deviation, used materials*), periodic well test, materials quality control, use of deformable metals, remain within pressure and temperature safety limits (e.g., by combining caverns during storage and production)
(3) Corrective measures: treatment with special materials (resins/silicates, biological agents etc.)
(4) Description and classification residual risk considering the measures taken: taking the preventive and corrective measures into account the residual risk becomes: 1 (probability) and [Me1][Te1][Se1][Qe0][Re0] (consequences), **1/1**

[20] DBI GmbH e.o., Leitfaden Planung, Genehmigung und Betrieb von Wasserstoff-Kavernenspeichern, Project Zwanzig20 – HYPOS – H2-UGS (DBI, 2022a)

RISK Nr. 1.11 Weakening of salt (cavern wall) only due to interaction with hydrogen

Risk step 1: Aim

Aim 1 for the Operator: "*We store renewable ("green") energy as hydrogen gas in our own salt caverns. We are part of the energy transition and play an important role in the storage of renewable energy*". Therefore, the aim is: no risk for all stakeholders, directly or indirectly involved, as a result of hydrogen storage in salt caverns.

Risk step 2: Risk identification

(1) Risk: Weakening of salt (cavern wall) caused by interaction with hydrogen
(2) Risk based on: Assumption
(3) Source of information: Expert judgement, literature[21]
(4) Uncertainty: Additional research of the second phases interacting with hydrogen
(5) Type of causes: [Gc][Rc]
(6) Type of effects: [Me][Te]

Risk step 3: Risk classification

(1) Classification probability class: 1 (a): assumption based on expert judgement
(2) Classification consequence class: [Me1][Te1][Se0][Qe0][Re0]

Risk step 4: Dealing with risks

(1) Additional research: additional research of the second phase rheology interacting with hydrogen, model abiotic H_2S production in dry conditions
(2) Preventive measures: -
(3) Corrective measures: -
(4) Description and classification residual risk considering the measures taken: Both probability and consequence classes have not been reduced and remain: **1/1**, in more detail [Me1][Te1][Se0][Qe0][Re0]

[21] DBI GmbH e.o., Leitfaden Planung, Genehmigung und Betrieb von Wasserstoff-Kavernenspeichern, Project Zwanzig20 – HYPOS – H2-UGS (DBI, 2022a)

RISK Nr. 1.12 Weakening of material (cement bonding and other materials) only due to interaction with hydrogen

Risk step 1: Aim

Aim 1 for the Operator: "*We store renewable ("green") energy as hydrogen gas in our own salt caverns. We are part of the energy transition and play an important role in the storage of renewable energy*". Therefore, the aim is: no risk for all stakeholders, directly or indirectly involved, as a result of hydrogen storage in salt caverns.

Risk step 2: Risk identification

(1) Risk: Weakening of material (cement and materials like steel alloys, elastomers, etc.) caused by interaction with hydrogen
(2) Risk based on: Interpretation of facts / assumptions
(3) Source of information: Expert judgement, literature[22][23]
(4) Uncertainty: Additional research of materials interacting with hydrogen
(5) Type of causes: [Tc][Rc][Ic]
(6) Type of effects: [Me][Te][Se][Qe]

Risk step 3: Risk classification

(1) Classification probability class: 3 (a/c): assumption based on expert judgement and interpretation of facts
(2) Classification consequence class: [Me2][Te1][Se2][Qe2][Re0]

Risk step 4: Dealing with risks

(1) Additional research: additional research on the sealing effectiveness and corrosion resistance of all materials used for completion (steel alloys, elastomers and seals)
(2) Preventive measures: H_2 and H_2S certified material (including packers), materials quality control (monitoring and wall thickness surveys), specific properties for steel[24], use of elastomers, avoid sulphur-rich cement
(3) Corrective measures: treatment with special materials (resins/silicates, biological agents etc.)
(4) Description and classification residual risk considering the measures taken: taking the preventive and corrective measures into account the residual risk becomes: 2 (probability) and [Me2][Te1][Se0][Qe2][Re0] (consequences), **2/2**

[22] DBI GmbH e.o., Leitfaden Planung, Genehmigung und Betrieb von Wasserstoff-Kavernenspeichern, Project Zwanzig20 – HYPOS – H2-UGS, (DBI, 2022a)

[23] DBI Gut, Wasserstoff Speichern – Soviel ist sicher, reference G 201926 (DBI, 2022b)

[24] DBI Gut, Wasserstoff Speichern – Soviel ist sicher, reference G 201926, paragraph 3.5.2 (DBI, 2022b)

RISK Nr. 1.13 Cratering

Risk step 1: Aim

Aim 1 for the Operator: "*We store renewable ("green") energy as hydrogen gas in our own salt caverns. We are part of the energy transition and play an important role in the storage of renewable energy*". Therefore, the aim is: no risk for all stakeholders, directly or indirectly involved, as a result of hydrogen storage in salt caverns.

Risk step 2: Risk identification

(1) Risk: Cratering (overburden failure)
(2) Risk based on: Interpretation of facts
(3) Source of information: Literature review (section 3.4.4), example case histories[25][26]
(4) Uncertainty: Additional regulations regarding shape, volume and depth of cavern
(5) Type of causes: [Rc][Ic][Gc]
(6) Type of effects: [Me][Te][Se][Qe][Re]

Risk step 3: Risk classification

(1) Classification probability class: 1[27] (c): interpretation of factual information
(2) Classification consequence class: [Me3][Te3][Se3][Qe3][Re3]

Risk step 4: Dealing with risks

(1) Additional research: research on additional regulations regarding shape, volume, diameter and depth of cavern, research on the acceptable depth of the roof and aspect ratio of the cavern
(2) Preventive measures: no cavern close to the salt dome edge, modelling of the cavern design
(3) Corrective measures: -
(4) Description and classification residual risk considering the measures taken: taking the preventive measures into account the residual risk becomes: 0 (probability), **0**

[25] Matarandiba Island, Brazil, 2018 (3.4.4.2)
[26] Bayou Corne, Louisiana, 2012 (3.4.4.1)
[27] Brouard Consulting, Over-pressured salt solution mining caverns and leakage mechanisms, Phase 2: Cavern scale, reference KEM-17, dated November 4 2019 (Brouard and Bérest, 2019)

RISK Nr. 1.14 Roof fall

Risk step 1: Aim

Aim 1 for the Operator: "*We store renewable ("green") energy as hydrogen gas in our own salt caverns. We are part of the energy transition and play an important role in the storage of renewable energy*". Therefore, the aim is: no risk for all stakeholders, directly or indirectly involved, as a result of hydrogen storage in salt caverns.

Risk step 2: Risk identification

(1) Risk: Roof fall
(2) Risk based on: Interpretation of facts
(3) Source of information: Literature review (section 3.4.5.1), example case histories[28][29]
(4) Uncertainty: Cannot be reduced
(5) Type of causes: [Rc][Ic][Gc]
(6) Type of effects: [Me][Te]

Risk step 3: Risk classification

(1) Classification probability class: 3 (c): interpretation of factual information
(2) Classification consequence class: [Me3][Te2][Se3][Qe2][Re3][30]

Risk step 4: Dealing with risks

(1) Additional research: -
(2) Preventive measures: no brine strings left behind, avoid non-halite layers in the roof, improved cavern design (avoid flat roof / large diameter of the roof), prevent contact undersaturated brine with roof, preferably use newly developed caverns (according to an optimal rock mechanical envelope)
(3) Corrective measures: -
(4) Description and classification residual risk considering the measures taken: taking the preventive measures into account the residual risk becomes: 1 (probability) and [Me2][Te1][Se0][Qe1][Re0] (consequences), **1/2**

[28] Regina South No. 5, Saskatchewan, Canada, 1989 (3.4.5.1.2)
[29] Jintan JK-A, China, 2015 (3.4.5.1.3)
[30] The classification is based on a blow-out as ultimate result

RISK Nr. 1.15 Block falls

Risk step 1: Aim

Aim 1 for the Operator: "*We store renewable ("green") energy as hydrogen gas in our own salt caverns. We are part of the energy transition and play an important role in the storage of renewable energy*". Therefore, the aim is: no risk for all stakeholders, directly or indirectly involved, as a result of hydrogen storage in salt caverns.

Risk step 2: Risk identification

(1) Risk: Block falls
(2) Risk based on: Interpretation of facts
(3) Source of information: Literature review (section 3.4.7.1), example case histories[31][32]
(4) Uncertainty: Cannot be reduced
(5) Type of causes: [Rc][Ic][Gc]
(6) Type of effects: [Me][Te]

Risk step 3: Risk classification

(1) Classification probability class: 3 (c): interpretation of factual information
(2) Classification consequence class: [Me1][Te1][Se0][Qe1][Re0]

Risk step 4: Dealing with risks

(1) Additional research: -
(2) Preventive measures: no brine strings left behind, avoid massive anhydrite layers, good understanding of stratigraphy (depth decision), sonar survey, preferably use newly developed caverns (according to an optimal rock mechanical envelope)
(3) Corrective measures: -
(4) Description and classification residual risk considering the measures taken: taking the preventive measures into account the residual risk becomes: 1 (probability) and [Me1][Te1][Se0][Qe0][Re0] (consequences), **1/1**

[31] Jintan JJKK-D cavern, China, 2015 (3.4.7.1.3)
[32] Huntorf, Germany, 1980 (3.4.7.1.2)

RISK Nr. 1.16 Formation of H_2S beyond acceptable limits

Risk step 1: Aim

Aim 1 for the Operator: "*We store renewable ("green") energy as hydrogen gas in our own salt caverns. We are part of the energy transition and play an important role in the storage of renewable energy*". Therefore, the aim is: no risk for all stakeholders, directly or indirectly involved, as a result of hydrogen storage in salt caverns.

Risk step 2: Risk identification

(1) Risk: Formation of H_2S beyond acceptable limits caused by anhydrite and other second phases (like carbonates), accelerated by contaminated brine or residual organic (blanket) material
(2) Risk based on: Assumption
(3) Source of information: Literature review (section 5.4) and research[3334353637]
(4) Uncertainty: Additional research on the circumstances leading to the formation of H_2S
(5) Type of causes: [Tc][Gc]
(6) Type of effects: [Me][Te][Se][Qe]

Risk step 3: Risk classification

(1) Classification probability class: 3 (a): assumption based on expert judgement
(2) Classification consequence class: [Me3][38][Te3][Se1][Qe3][Re0]

Risk step 4: Dealing with risks

(1) Additional research: additional research on the circumstances leading to the formation of H_2S, characterize sulphur oxidation state in addition to sulphur abundance, research on the effect on the purity of produced H_2, research on the mix of H_2 and H_2S, research on optimal dimensions of the cavern (reduce reaction surface)
(2) Preventive measures: pH correction, avoid sulphate sources, avoid CO_2 cushion gas, increase iron concentration (preferably Fe II, binding of sulphate), monitoring of microbial activities, avoid high temperatures (> 80 degrees) because of the abiotic sulphate reduction, avoid presence of hydrocarbons (preferably no use of existing caverns), monitoring of geochemical composition
(3) Corrective measures: sweetening of the H_2 gas, pH correction, increase iron concentration

[33] M.P.Laban, Hydrogen storage in salt caverns, chemical modelling and analysis of large-scale hydrogen storage in underground salt caverns, no reference, dated July 16 2020
[34] N. Dopffel, Microbial impact on hydrogen storage, NORCE, 2nd International Summer School on UHS, dated July 2023
[35] C.A. Peters, Underground H_2 storage: Geochemistry Considerations, Princeton University, 2nd International Summer School on UHS, dated July 2023
[36] M. Portarapillo & A. di Benedetto, Risk assessment of the large-scale hydrogen storage in salt caverns, article in Energies 14, dated 2021
[37] M. Panfilov, Underground and pipeline hydrogen storage, Compendium of Hydrogen Energy, pp 92-116, dated 2015
[38] TECNA estudios, Sweetening technologies – a look at the whole picture, paper WGC, dated 2009

(4) *Description and classification residual risk considering the measures taken:* taking the preventive and corrective measures into account the residual risk becomes: 1 (probability) and [Me2][Te2][Se1][Qe1][Re0] (consequences), **1/2**

RISK Nr. 1.17 Registered induced seismicity

Risk step 1: Aim

Aim 1 for the Operator: "*We store renewable ("green") energy as hydrogen gas in our own salt caverns. We are part of the energy transition and play an important role in the storage of renewable energy*". Therefore, the aim is: no risk for all stakeholders, directly or indirectly involved, as a result of hydrogen storage in salt caverns.

Risk step 2: Risk identification

(1) Risk: Registered induced seismicity caused by the operation (filling and emptying) of the cavern
(2) Risk based on: Interpretation of facts / assumption
(3) Source of information: Monitoring plans of underground Natural Gas and Nitrogen storage[39][40], literature review (section 5.2)
(4) Uncertainty: Research on characteristic locations in the salt dome sensitive to (micro)seismicity
(5) Type of causes: [Rc][Gc]
(6) Type of effects: [Te][Re]

Risk step 3: Risk classification

(1) Classification probability class: 3 (a/c): assumption based on expert judgement and interpretation of facts
(2) Classification consequence class: [Me0][Te2][Se0][Qe0][Re3]

Risk step 4: Dealing with risks

(1) Additional research: research on characteristic locations in the salt dome sensitive to (micro)seismicity
(2) Preventive measures: seismic monitoring (natural and induced seismicity), modelling of expected seismicity, no storage activities in or near an active fault zone, transparency and open communication, baseline measurement, transparency regarding seismic data
(3) Corrective measures: adapt storage properties to reduce stress near the cavern
(4) Description and classification residual risk considering the measures taken: taking the preventive measures into account the residual risk becomes: 2 (probability) and [Me0][Te1][Se0][Qe0][Re1] (consequences), **2/1**

[39] Nouryon, Micro seismic network Heiligerlee & Zuidwending, observations Q3 2020, Powerpoint, no reference, no date

[40] NAM, Report "Instemmingsbesluit Norg", letter, no reference, dated December 3 2021

RISK Nr. 1.18 Emergence of negative public opinion

Risk step 1: Aim

Aim 1 for the Operator: "*We store renewable ("green") energy as hydrogen gas in our own salt caverns. We are part of the energy transition and play an important role in the storage of renewable energy*". Therefore, the aim is: no risk for all stakeholders, directly or indirectly involved, as a result of hydrogen storage in salt caverns.

Risk step 2: Risk identification

(1) *Risk:* Emergence of negative public opinion, e.g., triggered by regional or national media
(2) *Risk based on:* Interpretation of facts
(3) *Source of information:* public opinion[41][42][43][44][45]
(4) *Uncertainty:* complete stakeholder analysis per location, risk analysis discussion with all stakeholders (separately)
(5) *Type of causes*: [Pc]
(6) *Type of effects*: [Me][Te][Se][Re]

Risk step 3: Risk classification

(1) *Classification probability class:* 3 (c): interpretation of factual information
(2) *Classification consequence class:* [Me2][Te3][Se1][Qe0][Re3]

Risk step 4: Dealing with risks

(1) *Additional research:* complete stakeholder analysis per location, risk analysis discussion with all stakeholders (separately)
(2) *Preventive measures:* transparent, pro-active and personal communication, direct involvement (shareholders), financial compensation ("burdens and benefits"), transparency with respect to all taken preventive measures (other risks), transparent communication regarding results test cavern
(3) *Corrective measures:* transparent and personal communication, financial compensation (based on reversed burden of proof), transparency with respect to all taken corrective measures (other risks)
(4) *Description and classification residual risk considering the measures taken:* taking the preventive and corrective measures into account the residual risk eventually becomes: 2 (probability) and [Me1][Te2][Se1][Qe0][Re1] (consequences), **2/2**

[41] Public opinion with respect to CO_2 storage underneath Barendrecht: "Stichting CO2isNEE", 2010
[42] Public opinion with respect to environmental problems and subsidence as a result of salt mining: "Stop Zoutwinning!", 2021
[43] Public opinion with respect to future salt extraction Municipality of Haaksbergen, 2023
[44] Public opinion with respect to underground discharge of production water, www.stopafvalwatertwente.nl
[45] Public opinion with respect to Nitrogen storage in Heiligerlee, www.mijnendijnbelang.nl

RISK Nr. 1.19 Fire on site

Risk step 1: Aim

Aim 1 for the Operator: "*We store renewable ("green") energy as hydrogen gas in our own salt caverns. We are part of the energy transition and play an important role in the storage of renewable energy*". Therefore, the aim is: no risk for all stakeholders, directly or indirectly involved, as a result of hydrogen storage in salt caverns.

Risk step 2: Risk identification

(1) Risk: Fire on site
(2) Risk based on: Assumption
(3) Source of information: Expert Judgement
(4) Uncertainty: Cannot be reduced
(5) Type of causes: [Hc][Oc][Tc][Rc][Ic]
(6) Type of effects: [Me][Te][Se][Qe][Re]

Risk step 3: Risk classification

(1) Classification probability class: 1 (a): assumption based on expert judgement
(2) Classification consequence class: [Me2][Te2][Se3][Qe3][Re3]

Risk step 4: Dealing with risks

(1) Additional research: research on preventive measures regarding leakage potential (materials)
(2) Preventive measures: adhere to the general safety regulations and fire-prevention measurements for hydrogen installations, train local fire fighters for operations on site, monitoring system for H_2 leakage, sprinkler installation
(3) Corrective measures: rapid response plan, fire alarm and extinguishing
(4) Description and classification residual risk considering the measures taken: taking the preventive and corrective measures into account the residual risk eventually becomes: 1 (probability) and [Me1][Te1][Se1][Qe0][Re0] (consequences), **1/1**

RISK Nr. 1.20 Natural disaster

Risk step 1: Aim

Aim 1 for the Operator: "*We store renewable ("green") energy as hydrogen gas in our own salt caverns. We are part of the energy transition and play an important role in the storage of renewable energy*". Therefore, the aim is: no risk for all stakeholders, directly or indirectly involved, as a result of hydrogen storage in salt caverns.

Risk step 2: Risk identification

(1) Risk: Natural disaster, e.g., flooding
(2) Risk based on: Assumption
(3) Source of information: Expert Judgement
(4) Uncertainty: Cannot be reduced
(5) Type of causes: [Tc][Rc]
(6) Type of effects: [Me][Te][Se][Qe][Re]

Risk step 3: Risk classification

(1) Classification probability class: 1 (a): assumption based on expert judgement
(2) Classification consequence class: [Me2][Te2][Se1][Qe3][Re1]

Risk step 4: Dealing with risks

(1) Additional research: -
(2) Preventive measures: build a dyke around the site, locate critical infrastructure well above sea-level or in contained environment, back-up by remote-controlled operation, review sensitivity for all potential natural disasters, assign as "vital infrastructure" and act accordingly
(3) Corrective measures: remote-controlled operation
(4) Description and classification residual risk considering the measures taken: taking the preventive and corrective measures into account the residual risk eventually becomes: 1 (probability) and [Me1][Te1][Se0][Qe1][Re0] (consequences), **1/1**

RISK Nr. 1.21 Terrorism

Risk step 1: Aim

Aim 1 for the Operator: "*We store renewable ("green") energy as hydrogen gas in our own salt caverns. We are part of the energy transition and play an important role in the storage of renewable energy*". Therefore, the aim is: no risk for all stakeholders, directly or indirectly involved, as a result of hydrogen storage in salt caverns.

Risk step 2: Risk identification

(1) Risk: Terrorism
(2) Risk based on: Assumption
(3) Source of information: Expert Judgement
(4) Uncertainty: Cannot be reduced
(5) Type of causes: [Hc]
(6) Type of effects: [Me][Te][Se][Qe][Re]

Risk step 3: Risk classification

(1) Classification probability class: 1 (a): assumption based on expert judgement
(2) Classification consequence class: [Me2][Te2][Se3][Qe3][Re1]

Risk step 4: Dealing with risks

(1) Additional research: -
(2) Preventive measures: no-fly zone, no local satellite footage, camera security, fenced and secured area, assign as "vital infrastructure" and act accordingly, review information release from scratch
(3) Corrective measures: -
(4) Description and classification residual risk considering the measures taken: taking the preventive measures into account the residual risk eventually becomes: 1 (probability) and [Me1][Te1][Se0][Qe1][Re0] (consequences), **1/1**

RISK Nr. 1.22 IT failure

Risk step 1: Aim

Aim 1 for the Operator: "*We store renewable ("green") energy as hydrogen gas in our own salt caverns. We are part of the energy transition and play an important role in the storage of renewable energy*". Therefore, the aim is: no risk for all stakeholders, directly or indirectly involved, as a result of hydrogen storage in salt caverns.

Risk step 2: Risk identification

(1) Risk: IT failure
(2) Risk based on: Assumption
(3) Source of information: Expert Judgement
(4) Uncertainty: Cannot be reduced
(5) Type of causes: [Hc][Oc][Tc][Rc]
(6) Type of effects: [Me][Te][Se][Qe][Re]

Risk step 3: Risk classification

(1) Classification probability class: 2 (a): assumption based on expert judgement
(2) Classification consequence class: [Me2][Te1][Se1][Qe1][Re1]

Risk step 4: Dealing with risks

(1) Additional research: -
(2) Preventive measures: remote-controlled operation via internal network (no internet), manual controls requiring double authorisation, analogue pressure and temperature gauges at critical locations (double system), pressure relief valve (PRV) for worst case when pressure gets near lithostatic pressure at casing shoe, assign as "vital infrastructure" and act accordingly
(3) Corrective measures: automatic release of pressure
(4) Description and classification residual risk considering the measures taken: taking the preventive and corrective measures into account the residual risk eventually becomes: 1 (probability) and [Me2][Te1][Se0][Qe0][Re0] (consequences), **1/2**

RISK Nr. 1.23 Disputed responsibility due to stacked mining activities

Risk step 1: Aim

Aim 1 for the Operator: "*We store renewable ("green") energy as hydrogen gas in our own salt caverns. We are part of the energy transition and play an important role in the storage of renewable energy*". Therefore, the aim is: no risk for all stakeholders, directly or indirectly involved, as a result of hydrogen storage in salt caverns.

Risk step 2: Risk identification

(1) Risk: Disputed responsibility due to stacked mining activities
(2) Risk based on: Assumption
(3) Source of information: Political discussions[46], public[47]
(4) Uncertainty: Scenario modelling of various critical scenarios to test regulations
(5) Type of causes: [Rc]
(6) Type of effects: [Me][Te][Re]

Risk step 3: Risk classification

(1) Classification probability class: 3 (a): assumption based on expert judgement
(2) Classification consequence class: [Me2][Te3][Se0][Qe0][Re2]

Risk step 4: Dealing with risks

(1) Additional research: scenario modelling of various critical scenarios to test regulations and determine duration of responsibilities
(2) Preventive measures: regulations for operators regarding arial extent and duration of responsibility, seismic monitoring system, monitoring of subsidence by INSAR & surveying measurements before mining and during storage, mandatory report of incidents, regular meetings with all operators involved (including independent chairman, e.g., SodM), one overall geological model for all operators
(3) Corrective measures: mandatory insurance policy for all operators concerned, regulations for take-over of responsibilities in case of bankruptcy operator
(4) Description and classification residual risk considering the measures taken: taking the preventive and corrective measures into account the residual risk eventually becomes: 1 (probability) and [Me1][Te2][Se0][Qe0][Re0] (consequences), **1/2**

[46] Groenlinks, Stacked mining neglected in Nedmag-advice, 2019

[47] RTVOost, Growing frustration about mining, damage and new gas exploitation, January 2021

RISK Nr. 1.24 Threat for (future) underground on-shore energy storage

Risk step 1: Aim

Aim 1 for the Operator: "*We store renewable ("green") energy as hydrogen gas in our own salt caverns. We are part of the energy transition and play an important role in the storage of renewable energy*". Therefore, the aim is: no risk for all stakeholders, directly or indirectly involved, as a result of hydrogen storage in salt caverns.

Risk step 2: Risk identification

(1) Risk: Threat to future hydrogen storage in salt caverns (Licence to Operate) due to uncertainties about safety and consequences of the storage in salt caverns
(2) Risk based on: Assumption
(3) Source of information: Public, press, politics
(4) Uncertainty: (generic and) Site-specific risk assessments, site-specific research on geology, rock-salt properties
(5) Type of causes: [Pc]
(6) Type of effects: [Me][Te][Qe][Re]

Risk step 3: Risk classification

(1) Classification probability class: 3 (a): assumption based on expert judgement
(2) Classification consequence class: [Me3][Te3][Se0][Qe3][Re3]

Risk step 4: Dealing with risks

(1) Additional research: (generic and) site-specific risk assessments, site-specific research on geology and rock-salt properties
(2) Preventive measures: open pro-active communication with stakeholders (public, politics and press) and other operators, financial compensation ("burdens and benefits"), reversed burden of proof, preferably use newly developed caverns (according to an optimal rock mechanical envelope), improved cavern design (avoid flat roof / interlayered formations / large diameter of the roof), periodic leak tests (e.g., every 5 years), sonar surveys, GPR (radar), minimum preconditions for H_2 storage cavern, minimize chance of H_2S formation, mandatory status-report (starting every year), avoid caverns near residential areas
(3) Corrective measures: open communication with stakeholders (public, politics and press) and other operators

Description and classification residual risk considering the measures taken: taking the preventive and corrective measures into account the residual risk eventually becomes: 2 (probability) and [Me1][Te3][Se0][Qe0][Re2] (consequences), **2/3**

RISK Nr. 1.25 Risk of surplus extraction of brine

Risk step 1: Aim

Aim 1 for the Operator: "*We store renewable ("green") energy as hydrogen gas in our own salt caverns. We are part of the energy transition and play an important role in the storage of renewable energy*". Therefore, the aim is: no risk for all stakeholders, directly or indirectly involved, as a result of hydrogen storage in salt caverns.

Risk step 2: Risk identification

(1) *Risk:* Risk of surplus extraction (more than can be processed) of brine
(2) *Risk based on:* Assumption
(3) *Source of information:* Expert judgement[48] and literature[49]
(4) *Uncertainty:* Evaluation of salt production versus chlorine demand (NL and EU)
(5) *Type of causes*: [Oc][Rc][Pc]
(6) *Type of effects*: [Me][Te][Qe][Re]

Risk step 3: Risk classification

(1) *Classification probability class:* 1 (a): assumption based on expert judgement
(2) *Classification consequence class:* [Me2][Te3][Se0][Qe3][Re2]

Risk step 4: Dealing with risks

(1) *Additional research:* Evaluation of salt production versus chlorine demand (NL and EU)
(2) *Preventive measures:* salt production preferred for H_2 storage caverns, extracted brine re-used in existing salt caverns for optimal production, temporary storage available (terminal), first applier ("introducer") of H_2 storage, advanced planning of salt solution mining
(3) *Corrective measures:* additional use of vacuum salt for food and road salt (replacement of evaporation and rock salt), injection in depleted gas reservoirs
(4) *Description and classification residual risk considering the measures taken:* taking the preventive and corrective measures into account the residual risk eventually becomes: 1 (probability) and [Me1][Te2][Se0][Qe1][Re0] (consequences), **1/2**

[48] At this moment the number of interested clients and their need for brine outnumbers the extracted quantity mainly due to the fact that the quality of the brine and the resulting salt in the Netherlands is assumed to be excellent

[49] Roland Berger, Zout impactstudie, het maatschappelijk en economisch belang van duurzame zoutwinning in Nederland, commissioned by Nobian, July 2022

Stakeholder: Operator

Unmitigated risk matrix

4 x 3 Risk matrix		Consequence		
		1	2	3
Chance	3	1.15	1.8; 1.12	1.9; 1.10; 1.14; 1.16; 1.17; 1.18; 1.23; 1.24
	2		1.2; 1.5; 1.22	1.3; 1.4; 1.6; 1.7
	1	1.11		1.1; 1.13; 1.19; 1.20; 1.21; 1.25
	0			

Residual (mitigated) risk matrix

4 x 3 Risk matrix		Consequence		
		1	2	3
Chance	3		1.9	
	2	1,17	1.8; 1.12; 1.18	1.24
	1	1.2; 1.4; 1.10; 1.11; 1.15 1.19; 1.20; 1.21	1.1; 1.3; 1.5; 1.14; 1.16; 1.22; 1.23; 1.25	1.6; 1.7
	0	1.13		

D.2 Stakeholder: SODM

RISK Nr. 2.1 Accident at the surface

Risk step 1: Aim

Aim 2 for State Supervision of Mines: "*Protection of humanity and environment during energy production combined with protection and utilization of the subsoil, now and in future times*". Therefore, the aim is: no risk for humans and environment as a result of hydrogen storage in salt caverns.

Risk step 2: Risk identification

(1) Risk: Accident at the surface (blow-out, well leak, pipeline integrity loss) as a result of hydrogen storage
(2) Risk based on: Interpretation of facts / assumptions
(3) Source of information: Literature review[1][2], expert judgement
(4) Uncertainty: Blow-out modelling done by Brouard Consulting, experience within the industry with hydrogen pipelines
(5) Type of causes: [Tc][Hc][Gc][Oc][Rc][Ic]
(6) Type of effects: [Me][Te][Se][Qe][Re]

Risk step 3: Risk classification

(1) Classification probability class: 2 (a/c): assumption based on expert judgement and interpretation of factual information
(2) Classification consequence class: [Me1][Te2][Se3][Qe2][Re2]

Risk step 4: Dealing with risks

(1) Additional research: modelling of Blow-out, safety study on the effect at the surface, literature research hydrogen infrastructure KEM 29 (research in progress)
(2) Preventive measures (5 main): highest quality of BOP and safety valves / pressure gauges (H_2 certified material), all equipment designed for low T, rapid response plan, H_2-certified material (steel), construction / maintenance and monitoring protocols, (see further measures in risks 1.1, 1.2 and 1.4)
(3) Corrective measures: actions according to rapid response plan. evacuation plan, fire extinguishing, damage control / repair, temporary partial shut-down and repair

Description and classification residual risk considering the measures taken: taking the preventive and corrective measures into account the residual risk becomes: 1 (probability) and [Me1][Te2][Se3][Qe2][Re2] (consequences), **1/3**

[1] Fort Saskatchewan Ethane Blow-out and Fire, 2001 (2.3.2.1)

[2] Moss Bluff natural gas blow out and Fire, 2004 (2.3.2.2)

RISK Nr. 2.3 Creep closure and subsidence

Risk step 1: Aim

Aim 2 for State Supervision of Mines: "*Protection of humanity and environment during energy production combined with protection and utilization of the subsoil, now and in future times*". Therefore, the aim is: no risk for humans and environment as a result of hydrogen storage in salt caverns.

Risk step 2: Risk identification

(1) Risk: Subsidence (beyond predicted limits)
(2) Risk based on: Interpretation of facts
(3) Source of information: Literature review[3][4]
(4) Uncertainty: Additional research of the salt structure and rheology, cavern design
(5) Type of causes: [Rc][Ic][Gc][Oc][Tc][Pc]
(6) Type of effects: [Me][Te][Re]

Risk step 3: Risk classification

(1) Classification probability class: 2 (c): interpretation of factual information
(2) Classification consequence class: [Me1][Te3][Se0][Qe0][Re2]

Risk step 4: Dealing with risks

(1) Additional research: research of the salt structure and rheology, cavern design, geomechanical modelling
(2) Preventive measures: monitoring of subsidence by INSAR & surveying measurements, field tests (pressure observation test POT after well drill), updated cavern design, geomechanical modelling, determination of the minimum cavern pressure (see further measures in risk 1.7)
(3) Corrective measures: change of the average cavern pressure (higher), minimizing the subsidence by controlled abandonment
(4) Description and classification residual risk considering the measures taken: taking the preventive and corrective measures into account the residual risk becomes: 1 (probability) and [Me1][Te3][Se0][Qe0][Re2] (consequences), **1/3**

[3] Subsidence at Maceió, Brazil, 2021 (3.2.3.4)
[4] Subsidence at Bernburg, Germany (3.2.3.2)

RISK Nr. 2.4 Registered induced seismicity

Risk step 1: Aim

Aim 2 for State Supervision of Mines: "*Protection of humanity and environment during energy production combined with protection and utilization of the subsoil, now and in future times*". Therefore, the aim is: no risk for humans and environment as a result of hydrogen storage in salt caverns.

Risk step 2: Risk identification

(1) Risk: Registered induced seismicity caused by the operation (filling and emptying) of the cavern
(2) Risk based on: Interpretation of facts / assumption
(3) Source of information: Monitoring plans of underground Natural Gas and Nitrogen storage[5][6], literature review (section 5.2)
(4) Uncertainty: Research on characteristic locations in the salt dome sensitive to (micro)seismicity
(5) Type of causes: [Rc][Gc]
(6) Type of effects: [Te][Re]

Risk step 3: Risk classification

(1) Classification probability class: 3 (a/c): assumption based on expert judgement and interpretation of facts
(2) Classification consequence class: [Me0][Te2][Se0][Qe0][Re2]

Risk step 4: Dealing with risks

(1) Additional research: research on characteristic locations in the salt dome sensitive to (micro)seismicity
(2) Preventive measures: seismic monitoring (natural and induced seismicity), modelling of expected seismicity, no storage activities in or near an active fault zone, transparency and open communication, baseline measurement, transparency regarding seismic data
(3) Corrective measures: -
(4) Description and classification residual risk considering the measures taken: taking the preventive measures into account the residual risk becomes: 2 (probability) and [Me0][Te2][Se0][Qe0][Re1] (consequences), **2/2**

[5] Nouryon, Micro seismic network Heiligerlee & Zuidwending, observations Q3 2020, Powerpoint, no reference, no date

[6] NAM, Report "Instemmingsbesluit Norg", letter, no reference, dated December 3 2021

RISK Nr. 2.5 Emergence of negative public opinion

Risk step 1: Aim

Aim 2 for State Supervision of Mines: "*Protection of humanity and environment during energy production combined with protection and utilization of the subsoil, now and in future times*". Therefore, the aim is: no risk for humans and environment as a result of hydrogen storage in salt caverns.

Risk step 2: Risk identification

(1) Risk: Emergence of negative public opinion resulting in discussions about measures taken / actions by the operator and supervision by SodM ultimately leading to political questions for the Minister of EAC
(2) Risk based on: Interpretation of facts
(3) Source of information: public opinion[7][8][9][10][11]
(4) Uncertainty: complete stakeholder analysis per location, risk analysis discussion with all stakeholders (separately)
(5) Type of causes: [Pc]
(6) Type of effects: [Me][Te][Re]

Risk step 3: Risk classification

(1) Classification probability class: 3 (c): interpretation of factual information
(2) Classification consequence class: [Me1][Te3][Se0][Qe0][Re2]

Risk step 4: Dealing with risks

(1) Additional research: complete stakeholder analysis per location, risk analysis discussion with all stakeholders (separately)
(2) Preventive measures: transparent, pro-active and personal communication, direct involvement (shareholders), financial compensation ("burdens and benefits"), transparency with respect to all taken preventive measures (other risks)
(3) Corrective measures: transparent and personal communication, financial compensation (based on reversed burden of proof), transparency with respect to all taken corrective measures (other risks)
(4) Description and classification residual risk considering the measures taken: taking the preventive and corrective measures into account the residual risk eventually becomes: 2 (probability) and [Me1][Te2][Se1][Qe0][Re1] (consequences), **2/2**

[7] Public opinion with respect to CO_2 storage underneath Barendrecht: "Stichting CO2isNEE", 2010
[8] Public opinion with respect to environmental problems and subsidence as a result of salt mining: "Stop Zoutwinning!", 2021
[9] Public opinion with respect to future salt extraction Municipality of Haaksbergen, 2023
[10] Public opinion with respect to underground discharge of production water, www.stopafvalwatertwente.nl
[11] Public opinion with respect to Nitrogen storage in Heiligerlee, www.mijnendijnbelang.nl

RISK Nr. 2.6 Failure of the storage system

Risk step 1: Aim

Aim 2 for State Supervision of Mines: "*Protection of humanity and environment during energy production combined with protection and utilization of the subsoil, now and in future times*". Therefore, the aim is: no risk for humans and environment as a result of hydrogen storage in salt caverns.

Risk step 2: Risk identification

(1) Risk: Failure of the storage system (due to fire, natural disaster, terrorism or IT-failure)
(2) Risk based on: Assumptions
(3) Source of information: Expert judgement
(4) Uncertainty: Cannot be reduced
(5) Type of causes: [Hc][Oc][Tc][Rc][Ic]
(6) Type of effects: [Me][Te][Se][Qe][Re]

Risk step 3: Risk classification

(1) Classification probability class: 2 (a): assumption based on expert judgement
(2) Classification consequence class: [Me2][Te2][Se3][Qe3][Re2]

Risk step 4: Dealing with risks

(1) Additional research: -
(2) Preventive measures (5 main): adhere to the general safety regulations and fire-prevention measurements for hydrogen installations, back-up by remote-controlled operation, manual controls requiring double authorisation, analogue pressure and temperature gauges at critical locations (double system), assign as "vital infrastructure" and act accordingly (see further measures in risks 1.19 – 1.22)
(3) Corrective measures: actions according to rapid response plan, fire alarm and fire extinguishing, remote-controlled operation, pressure relief valve (PRV) for worst case when pressure gets near lithostatic pressure at casing shoe, automatic release of pressure
(4) Description and classification residual risk considering the measures taken: taking the preventive and corrective measures into account the residual risk eventually becomes: 1 (probability) and [Me1][Te1][Se0][Qe1][Re0] (consequences), **1/1**

RISK Nr. 2.7 Disputed responsibility due to stacked mining activities

Risk step 1: Aim

Aim 2 for State Supervision of Mines: "*Protection of humanity and environment during energy production combined with protection and utilization of the subsoil, now and in future times*". Therefore, the aim is: no risk for humans and environment as a result of hydrogen storage in salt caverns.

Risk step 2: Risk identification

(1) Risk: Disputed responsibility due to stacked mining activities
(2) Risk based on: Assumption
(3) Source of information: Political discussions[12], public[13]
(4) Uncertainty: Scenario modelling of various critical scenarios to test regulations
(5) Type of causes: [Rc]
(6) Type of effects: [Me][Te][Re]

Risk step 3: Risk classification

(1) Classification probability class: 3 (a): assumption based on expert judgement
(2) Classification consequence class: [Me1][Te3][Se0][Qe0][Re2]

Risk step 4: Dealing with risks

(1) Additional research: scenario modelling of various critical scenarios to test regulations
(2) Preventive measures: regulations for operators regarding arial extent and duration of responsibility, seismic monitoring system, monitoring of subsidence by INSAR & surveying measurements before mining and during storage, mandatory report of incidents, regular meetings with all operators involved (including independent chairman, e.g., SodM), one overall geological model for all operators
(3) Corrective measures: mandatory insurance policy for all operators concerned, regulations for take-over of responsibilities in case of bankruptcy operator
(4) Description and classification residual risk considering the measures taken: taking the preventive and corrective measures into account the residual risk eventually becomes: 1 (probability) and [Me1][Te2][Se0][Qe0][Re0] (consequences), **1/2**

[12] Groenlinks, Stacked mining neglected in Nedmag-advice, 2019

[13] RTVOost, Growing frustration about mining, damage and new gas exploitation, January 2021

Stakeholder: SodM

Unmitigated risk matrix

4 x 3 Risk matrix		Consequence		
		1	2	3
Chance	3		2.4	2.2; 2.5; 2.7
	2			2.1; 2.3; 2.6
	1			
	0			

Residual (mitigated) risk matrix

4 x 3 Risk matrix		Consequence		
		1	2	3
Chance	3		2.2	
	2		2.4; 2.5	
	1	2.6	2.7	2.1; 2.3
	0			

D.3 Stakeholder: Ministry of Economic Affairs and Climate

RISK Nr. 3.1 Political accountability

Risk step 1: Aim

Aim 3 for Ministry of Economic Affairs and Climate: "*Climate neutral society with clean, reliable and affordable energy while respecting the balance between interests of producers and consumers*". Therefore, the aim is: no risk in the area of the energy security and safety. No adverse consequences for social and political responsibility of the Ministry.

Risk step 2: Risk identification

(1) Risk: Political accountability for the occurrence of health damage and/or energy shortage due to accumulated risks of hydrogen storage (risks 1.1, 1.3, 1.4, 1.9, 1.10, 1.13, 1.14, 1.19 and 1.21)
(2) Risk based on: Interpretation of facts / assumption
(3) Source of information: Literature review[1][2][3], politics[4], expert judgement
(4) Uncertainty: Cannot be reduced
(5) Type of causes: [Hc][Tc][Rc][Gc]
(6) Type of effects: [Me][Te][Se][Qe][Re]

Risk step 3: Risk classification

(1) Classification probability class: 2 (a/c): assumption based on expert judgement and interpretation of factual information
(2) Classification consequence class: [Me3][Te3][Se0][Qe2][Re3]

Risk step 4: Dealing with risks

(1) Additional research: modelling of Blow-out, safety study on the effect at the surface, literature research hydrogen infrastructure KEM 29 (research in progress), research on prevention of micro annuli at the casing / cement / rock interfaces, incorporate KEM-18 including the recommendations for research R&D swelling elastomers and geopolymers
(2) Preventive measures:
   a. Generic: provide information for open discussion about the burdens and benefits of underground H_2 storage in salt caverns, highest quality of BOP, safety valves and pressure gauges (H_2 certified material), larger diameter of the casing (decrease of blow-out duration), all equipment designed for low T, simulation of a blow-out (part of the permitting), four-eyes principle, regular maintenance and check, rapid response plan, corrosion protection, speed limitation on the flow rate (T-limit), periodic work-over, H_2S monitor system (beyond well site), minimum preconditions for H_2 storage cavern (well test), double casing, monitoring of integrity, construction and maintenance protocols, automatic valves, ,partitioned piping, KLIC, sufficient spare parts, back-up system,

[1] Magnolia, Louisiana, 2003 (2.2.3.2.10)
[2] Eminence salt dome 1, 3, 4, Mississippi, 1972 (3.3.2.2)
[3] Fort Saskatchewan Ethane Blow-out and Fire, 2001 (2.3.2.1)
[4] Rapport parlementaire enquêtecommissie aardgaswinning Groningen, https://www.tweedekamer.nl/Groningen/rapport

elastomers instead of cement, avoid old wells[5] (no known history with respect to loading cycles, temperature changes, wellbore deviation), periodic cement bonding log and well test, use of deformable metals, materials quality control, no brine strings left behind, avoid non-halite layers in the roof, improved cavern design (avoid flat roof / large diameter of the roof), prevent contact undersaturated brine with roof, adhere to the general safety regulations and fire-prevention measurements for hydrogen installations, train local fire fighters on site, no-fly zone, no local satellite footage, camera security, fenced and secured area

b. Specific: strengthen the role of the inspection /regulator (SodM), total independency

(3) Corrective measures: actions according to rapid response plan. evacuation plan, fire extinguishing, liner, packer or plug and drill new well, controlled production / flaring of H_2, temporary partial shut-down and repair, micro annuli treated with special materials (resins, silicates etc., biological treatment), use of deformable metals and casing expansion, smaller pressure difference, restoration of the sump conditions, fire alarm, sprinkler installation

(4) Description and classification residual risk considering the measures taken: taking the preventive and corrective measures into account the residual risk eventually becomes: 1 (probability) and [Me2][Te2][Se0][Qe2][Re3] (consequences), **1/3**

[5] Evo Energy Consulting, Qualitative Risk Assessment of long-term sealing behavior of materials and interfaces in boreholes, paragraph 3.2, final report, reference KEM-18, dated January 20 2022 (van Oort, 2022)

RISK Nr. 3.2 Emergence of negative public opinion

Risk step 1: Aim

Aim 3 for Ministry of Economic Affairs and Climate: "*Climate neutral society with clean, reliable and affordable energy while respecting the balance between interests of producers and consumers*". Therefore, the aim is: no risk in the area of the hydrogen storage. No adverse consequences for social and political responsibility of the Ministry.

Risk step 2: Risk identification

(1) Risk: Emergence of negative public opinion resulting in parliamentary discussion ultimately leading to political questions for the Minister of EAC
(2) Risk based on: Interpretation of facts
(3) Source of information: public opinion[6][7][8][9][10]
(4) Uncertainty: complete stakeholder analysis per location, risk analysis discussion with all stakeholders (separately)
(5) Type of causes: [Pc]
(6) Type of effects: [Me][Te][Re]

Risk step 3: Risk classification

(1) Classification probability class: 3 (c): interpretation of factual information
(2) Classification consequence class: [Me2][Te3][Se0][Qe0][Re3]

Risk step 4: Dealing with risks

(1) Additional research: complete stakeholder analysis per location, risk analysis discussion with all stakeholders (separately)
(2) Preventive measures: transparent, pro-active and personal communication, direct involvement (shareholders), financial compensation ("burdens and benefits"), transparency with respect to all taken preventive measures (other risks)
(3) Corrective measures: transparent and personal communication, financial compensation (based on reversed burden of proof), transparency with respect to all taken corrective measures (other risks)

Description and classification residual risk considering the measures taken: taking the preventive and corrective measures into account the residual risk eventually becomes: 2 (probability) and [Me1][Te2][Se1][Qe0][Re1] (consequences), **2/2**

[6] Public opinion with respect to CO_2 storage underneath Barendrecht: "Stichting CO2isNEE", 2010
[7] Public opinion with respect to environmental problems and subsidence as a result of salt mining: "Stop Zoutwinning!", 2021
[8] Public opinion with respect to future salt extraction Municipality of Haaksbergen, 2023
[9] Public opinion with respect to underground discharge of production water, www.stopafvalwatertwente.nl
[10] Public opinion with respect to Nitrogen storage in Heiligerlee, www.mijnendijnbelang.nl

Stakeholder: Ministry of EZK

Unmitigated risk matrix

4 x 3 Risk matrix		Consequence		
		1	2	3
Chance	3			3.2; 3.3
	2			3.1
	1			
	0			

Residual (mitigated) risk matrix

4 x 3 Risk matrix		Consequence		
		1	2	3
Chance	3			
	2		3.2	3.3
	1			3.1
	0			

D.4 Stakeholder: Ministry of Infrastructure and Water Management (Rijkswaterstaat)

RISK Nr. 4.1 Accident at the surface

Risk step 1: Aim

Aim 4 for Ministry of Infrastructure and Water Management (Rijkswaterstaat): "*Managing and developing national roads and national waterways in a safe, liveable and accessible country*". Therefore, the aim is: no risk for the national infrastructure (roads, waterways) in the area of the hydrogen storage.

Risk step 2: Risk identification

(1) Risk: Accident at the surface (blow-out, well leak, pipeline integrity loss) as a result of hydrogen storage causing damage to national infrastructure
(2) Risk based on: Interpretation of facts / assumptions
(3) Source of information: Literature review[12], expert judgement
(4) Uncertainty: Blow-out modelling done by Brouard Consulting, experience within the industry with hydrogen pipelines
(5) Type of causes: [Tc][Hc][Gc][Oc][Rc][Ic]
(6) Type of effects: [Me][Te][Se][Qe][Re]

Risk step 3: Risk classification

(1) Classification probability class: 2 (a/c): assumption based on expert judgement and interpretation of factual information
(2) Classification consequence class: [Me2][Te2][Se2][Qe2][Re2]

Risk step 4: Dealing with risks

(1) Additional research: modelling of Blow-out, safety study on the effect at the surface, literature research hydrogen infrastructure KEM 29 (research in progress)
(2) Preventive measures (5 main): highest quality of BOP and safety valves / pressure gauges (H_2 certified material), all equipment designed for low T, rapid response plan, H_2-certified material (steel), construction and maintenance protocols, (see further measures in risks 1.1, 1.2 and 1.4)
(3) Corrective measures: actions according to rapid response plan, evacuation plan, fire extinguishing, damage control / repair, temporary partial shut-down and repair
(4) Description and classification residual risk considering the measures taken: taking the preventive and corrective measures into account the residual risk becomes: 1 (probability) and[Me2][Te2][Se2][Qe2][Re2] (consequences), **1/2**

[1] Fort Saskatchewan Ethane Blow-out and Fire (2001)
[2] Moss Bluff natural gas blow out and Fire (2004)

RISK Nr. 4.2 Subsurface accident

Risk step 1: Aim

Aim 4 for Ministry of Infrastructure and Water Management (Rijkswaterstaat): "*Managing and developing national roads and national waterways in a safe, liveable and accessible country*". Therefore, the aim is: no risk for the national infrastructure (roads, waterways) in the area of the hydrogen storage.

Risk step 2: Risk identification

(1) Risk: Subsurface accident (leakage vertical tubing/casing, casing overstretching, cavern breaches, tensile failure, falls) as a result of hydrogen storage causing damage to national infrastructure
(2) Risk based on: Interpretation of facts / assumptions
(3) Source of information: Literature review[3][4][5][6][7], expert judgement
(4) Uncertainty: Additional research of the salt structure and rheology, the interaction with hydrogen, mechanical properties and damage evolution. Additional research of materials interacting with hydrogen
(5) Type of causes: [Hc][Tc][Rc][Ic][Gc]
(6) Type of effects: [Me][Te][Qe][Re]

Risk step 3: Risk classification

(1) Classification probability class: 3 (a/c): assumption based on expert judgement and interpretation of factual information
(2) Classification consequence class: [Me1][Te2][Se0][Qe1][Re1]

Risk step 4: Dealing with risks

(1) Additional research (5 main): creep research (grainsize) and durability of the salt, research of the salt dome internal structure, including anomalous zones (section 3.4.7.1.4), and rheology, additional research of the second phase rheology interacting with hydrogen, research on prevention of micro annuli at the casing / cement / rock interfaces, additional research of materials interacting with hydrogen, (see further research topics in risks 1.3, 1.5, 1.6, 1.8-1,12, 1.14 and 1.15)
(2) Preventive measures (5 main): minimum preconditions for H_2 storage cavern (well test), improved cavern design (avoid flat roof / interlayered formations / large diameter of the roof), periodic sonar measurements and cement bonding log (e.g., every 5 years), elastomers (no nitril) or self-healing material instead of cement, H_2 and H_2S certified material (including packers), (see further measures in risks 1.3, 1.5, 1.6, 1.8-1,12, 1.14 and 1.15)
(3) Corrective measures (5 main): controlled production / flaring of H_2, abandon cavern, adapt the pressures, (micro annuli and material) treatment with special materials (resins, silicates etc., biological treatment), use of deformable metals and casing expansion, (see further measures in risks 1.3, 1.5, 1.6, 1.8-1,12, 1.14 and 1.15)

[3] Magnolia, Louisiana, 2003
[4] Boling 1, 2, 4, Texas, USA, 2005
[5] Bayou Corne, Louisiana, 2012
[6] Eminence salt dome 1, 3, 4, Mississippi, 1972
[7] Jintan JK-A, China, 2015

(4) *Description and classification residual risk considering the measures taken:* Both probability and consequence classes have not been reduced and remain: **3/2**, in more detail 3 (probability) and [Me1][Te2][Se0][Qe1][Re0] (consequences)

RISK Nr. 4.3 Creep closure and subsidence

Risk step 1: Aim

Aim 4 for Ministry of Infrastructure and Water Management (Rijkswaterstaat): "*Managing and developing national roads and national waterways in a safe, liveable and accessible country*". Therefore, the aim is: no risk for the national infrastructure (roads, waterways) in the area of the hydrogen storage.

Risk step 2: Risk identification

(1) Risk: Subsidence (beyond predicted limits) causing damage to national infrastructure
(2) Risk based on: Interpretation of facts
(3) Source of information: Literature review (sections 3.1.5.1 and 3.2.3) [8][9]
(4) Uncertainty: Additional research of the salt structure and rheology, cavern design
(5) Type of causes: [Rc][Ic][Gc][Oc][Tc][Pc]
(6) Type of effects: [Me][Te][Qe]

Risk step 3: Risk classification

(1) Classification probability class: 2 ©: interpretation of factual information
(2) Classification consequence class: [Me1][Te1][Se0][Qe2][Re0]

Risk step 4: Dealing with risks

(1) Additional research: research of the salt structure and rheology, cavern design, geomechanical modelling
(2) Preventive measures: monitoring of subsidence by INSAR & surveying measurements, field tests (pressure observation test POT after well drill), updated cavern design, geomechanical modelling, determination of the minimum cavern pressure (see further measures in risk 1.7)
(3) Corrective measures: change of the average cavern pressure (higher), minimizing the subsidence by controlled abandonment
(4) *Description and classification residual risk considering the measures taken:* taking the preventive and corrective measures into account the residual risk becomes: 1 (probability) and [Me1][Te1][Se0][Qe2][Re0] (consequences), **1/2**

[8] Subsidence at Maceió, Brazil, 2021 [9] Matarandiba Island, Brazil, 2018

Stakeholder: Ministry of IWM

Unmitigated risk matrix

4 x 3 Risk matrix		Consequence		
		1	2	3
Chance	3		4.2	
	2		4.1 4.3	
	1			
	0			

Residual (mitigated) risk matrix

4 x 3 Risk matrix		Consequence		
		1	2	3
Chance	3		4.2	
	2			
	1		4.1 4.3	
	0			

D.5 Stakeholder: Ministry of Agriculture, Nature and Food Quality (Natuurnetwerk)

RISK Nr. 5.1 Accident at the surface

Risk step 1: Aim

Aim 5 for Ministry of Agriculture, Nature and Food Quality (Natuurnetwerk): "*The Netherlands faces serious social and ecological challenges. We need to prevent depletion of soil, freshwater supplies and raw materials, halt the decline in biodiversity and fulfil our commitments to the Paris climate agreement*". Therefore, the aim is: no risk for, and preservation and protection of, natural values in the area of the hydrogen storage.

Risk step 2: Risk identification

(1) Risk: Accident at the surface (blow-out, well leak, pipeline integrity loss) as a result of hydrogen storage causing damage to natural values
(2) Risk based on: Interpretation of facts / assumptions, assumptions
(3) Source of information: Literature review[1][2], expert judgement
(4) Uncertainty: Blow-out modelling done by Brouard Consulting, experience within the industry with hydrogen pipelines
(5) Type of causes: [Tc][Hc][Gc][Oc][Rc][Ic]
(6) Type of effects: [Me][Te][Qe][Re]

Risk step 3: Risk classification

(1) Classification probability class: 2 (a/c): assumption based on expert judgement and interpretation of factual information
(2) Classification consequence class: [Me1][Te2][Se0][Qe2][Re1]

Risk step 4: Dealing with risks

(1) Additional research: modelling of Blow-out, safety study on the effect at the surface, literature research hydrogen infrastructure KEM 29 (research in progress)
(2) Preventive measures (5 main): highest quality of BOP and safety valves / pressure gauges (H_2 certified material), all equipment designed for low T, rapid response plan, H_2-certified material (steel), construction and maintenance protocols, (see further measures in risks 1.1, 1.2 and 1.4)
(3) Corrective measures: actions according to rapid response plan, evacuation plan, fire extinguishing, damage control / repair, temporary partial shut-down and repair
(4) Description and classification residual risk considering the measures taken: taking the preventive and corrective measures into account the residual risk becomes: 1 (probability) and [Me1][Te2][Se0][Qe2][Re1] (consequences), **1/2**

[1] Fort Saskatchewan Ethane Blow-out and Fire (2001) [2] Moss Bluff natural gas blow out and Fire (2004)

RISK Nr. 5.2 Subsurface accident

Risk step 1: Aim

Aim 5 for Ministry of Agriculture, Nature and Food Quality (Natuurnetwerk): "*The Netherlands faces serious social and ecological challenges. We need to prevent depletion of soil, freshwater supplies and raw materials, halt the decline in biodiversity and fulfil our commitments to the Paris climate agreement*". Therefore, the aim is: no risk for, and preservation and protection of, natural values in the area of the hydrogen storage.

Risk step 2: Risk identification

(1) *Risk:* Subsurface accident (leakage vertical tubing/casing, casing overstretching, cavern breaches, tensile failure, falls) as a result of hydrogen storage causing damage to natural values
(2) *Risk based on:* Interpretation of facts / assumptions
(3) *Source of information:* Literature review[3][4][5][6][7], expert judgement
(4) *Uncertainty:* Additional research of the salt structure and rheology, the interaction with hydrogen, mechanical properties and damage evolution. Additional research of materials interacting with hydrogen
(5) *Type of causes*: [Hc][Tc][Rc][Ic][Gc]
(6) *Type of effects*: [Me][Te][Qe]

Risk step 3: Risk classification

(1) *Classification probability class:* 3 (a/c): assumption based on expert judgement and interpretation of factual information
(2) *Classification consequence class:* [Me1][Te2][Se0][Qe1][Re0]

Risk step 4: Dealing with risks

(1) *Additional research (5 main):* creep research (grainsize) and durability of the salt, research of the salt dome internal structure, including anomalous zones (section 3.4.7.1.4), and rheology, additional research of the second phase rheology interacting with hydrogen, research on prevention of micro annuli at the casing / cement / rock interfaces, additional research of materials interacting with hydrogen, (see further research topics in risks 1.3, 1.5, 1.6, 1.8-1,12, 1.14 and 1.15)
(2) *Preventive measures (5 main):* minimum preconditions for H_2 storage cavern (well test), improved cavern design (avoid flat roof / interlayered formations / large diameter of the roof), periodic sonar measurements and cement bonding log (e.g., every 5 years), elastomers (no nitril) or self-healing material instead of cement, H_2 and H_2S certified material (including packers), (see further measures in risks 1.3, 1.5, 1.6, 1.8-1,12, 1.14 and 1.15)
(3) *Corrective measures:* controlled production / flaring of H_2, abandon cavern, adapt the pressures, (micro annuli and material) treatment with special materials (resins, silicates etc., biological

[3] Magnolia, Louisiana, 2003
[4] Boling 1, 2, 4, Texas, USA, 2005
[5] Bayou Corne, Louisiana, 2012
[6] Eminence salt dome 1, 3, 4, Mississippi, 1972
[7] Jintan JK-A, China, 2015

treatment), use of deformable metals and casing expansion, (see further measures in risks 1.3, 1.5, 1.6, 1.8-1,12, 1.14 and 1.15)

(4) Description and classification residual risk considering the measures taken: Both probability and consequence classes have not been reduced and remain: **3/2**, in more detail 3 (probability) and [Me1][Te2][Se0][Qe1][Re0] (consequences)

RISK Nr. 5.3 Creep closure and subsidence

Risk step 1: Aim

Aim 5 for Ministry of Agriculture, Nature and Food Quality (Natuurnetwerk): "*The Netherlands faces serious social and ecological challenges. We need to prevent depletion of soil, freshwater supplies and raw materials, halt the decline in biodiversity and fulfil our commitments to the Paris climate agreement*". Therefore, the aim is: no risk for, and preservation and protection of, natural values in the area of the hydrogen storage.

Risk step 2: Risk identification

(1) Risk: Subsidence (beyond predicted limits) causing damage to natural values
(2) Risk based on: Case histories[8][9]
(3) Source of information: Literature review (sections 3.1.5.1 and 3.2.3)
(4) Uncertainty: Additional research of the salt structure and rheology, cavern design
(5) Type of causes: [Rc][Ic][Gc][Oc][Tc][Pc]
(6) Type of effects: [Te][Qe]

Risk step 3: Risk classification

(1) Classification probability class: 2 (c): interpretation of factual information
(2) Classification consequence class: [Me0][Te1][Se0][Qe2][Re0]

Risk step 4: Dealing with risks

(1) Additional research: research of the salt structure and rheology, cavern design, geomechanical modelling
(2) Preventive measures: monitoring of subsidence by INSAR & surveying measurements, field tests (pressure observation test POT after well drill), updated cavern design, geomechanical modelling, determination of the minimum cavern pressure (see further measures in risk 1.7)
(3) Corrective measures: change of the average cavern pressure (higher), minimizing the subsidence by controlled abandonment
(4) Description and classification residual risk considering the measures taken: taking the preventive and corrective measures into account the residual risk becomes: 1 (probability) and [Me0][Te1][Se0][Qe2][Re0] (consequences), **1/2**

[8] Subsidence at Maceió, Brazil, 2021 [9] Matarandiba Island, Brazil, 2018

Stakeholder: Ministry of ANFQ

Unmitigated risk matrix

4 x 3 Risk matrix		Consequence		
		1	2	3
Chance	3		5.2	
	2		5.1 5.3	
	1			
	0			

Residual (mitigated) risk matrix

4 x 3 Risk matrix		Consequence		
		1	2	3
Chance	3		5.2	
	2			
	1		5.1 5.3	
	0			

D.6 Stakeholder: Provincial states (I)

RISK Nr. 6.1 Accident at the surface

Risk step 1: Aim

Aim 6 for Provincial states: "*Our organization is motivated, reliable and innovative. Our organization cooperates, links and joins in brainstorming in the search for solutions, keeping an eye on our province and the interests of environment and society including the agricultural industry*". Therefore, the aim is: no risk for and protection of the agricultural industry in the area of the hydrogen storage.

Risk step 2: Risk identification

(1) Risk: Accident at the surface (blow-out, well leak, pipeline integrity loss) as a result of hydrogen storage causing damage to the agricultural industry
(2) Risk based on: Interpretation of facts / assumptions
(3) Source of information: Literature review[1][2], expert judgement
(4) Uncertainty: Blow-out modelling done by Brouard Consulting, experience within the industry with hydrogen pipelines
(5) Type of causes: [Tc][Hc][Gc][Oc][Rc][Ic]
(6) Type of effects: [Me][Te][Qe]

Risk step 3: Risk classification

(1) Classification probability class: 2 (a/c): assumption based on expert judgement and interpretation of factual information
(2) Classification consequence class: [Me1][Te2][Se0][Qe2][Re0]

Risk step 4: Dealing with risks

(1) Additional research: modelling of blow-out, safety study on the effect at the surface, literature research hydrogen infrastructure KEM 29 (research in progress)
(2) Preventive measures (5 main): highest quality of BOP and safety valves / pressure gauges (H_2 certified material), all equipment designed for low T, rapid response plan, H_2-certified material (steel), construction and maintenance protocols, (see further measures in risks 1.1, 1.2 and 1.4)
(3) Corrective measures: actions according to rapid response plan, evacuation plan, fire extinguishing, damage control / repair, temporary partial shut-down and repair
(4) Description and classification residual risk considering the measures taken: taking the preventive and corrective measures into account the residual risk becomes: 1 (probability) and [Me1][Te2][Se0][Qe2][Re0] (consequences), **1/2**

[1] Fort Saskatchewan Ethane Blow-out and Fire (2001)

[2] Moss Bluff natural gas blow out and Fire (2004)

RISK Nr. 6.2 Subsurface accident

Risk step 1: Aim

Aim 6 for Provincial states: "*Our organization is motivated, reliable and innovative. Our organization cooperates, links and joins in brainstorming in the search for solutions, keeping an eye on our province and the interests of environment and society including the agricultural industry*". Therefore, the aim is: no risk for and protection of the agricultural industry in the area of the hydrogen storage.

Risk step 2: Risk identification

(1) Risk: Subsurface accident (leakage vertical tubing/casing, casing overstretching, cavern breaches, tensile failure, falls) as a result of hydrogen storage causing damage to the agricultural industry
(2) Risk based on: Interpretation of facts / assumptions
(3) Source of information: Literature review[3][4][5][6][7], expert judgement
(4) Uncertainty: Additional research of the salt structure and rheology, the interaction with hydrogen, mechanical properties and damage evolution. Additional research of materials interacting with hydrogen
(5) Type of causes: [Hc][Tc][Rc][Ic][Gc]
(6) Type of effects: [Me][Te][Qe]

Risk step 3: Risk classification

(1) Classification probability class: 3 (a/c): assumption based on expert judgement and interpretation of factual information
(2) Classification consequence class: [Me1][Te2][Se0][Qe1][Re0]

Risk step 4: Dealing with risks

(1) Additional research (5 main): creep research (grainsize) and durability of the salt, research of the salt dome internal structure, including anomalous zones (section 3.4.7.1.4), and rheology, additional research of the second phase rheology interacting with hydrogen, research on prevention of micro annuli at the casing / cement / rock interfaces, additional research of materials interacting with hydrogen, (see further research topics in risks 1.3, 1.5, 1.6, 1.8-1,12, 1.14 and 1.15)
(2) Preventive measures (5 main): minimum preconditions for H_2 storage cavern (well test), improved cavern design (avoid flat roof / interlayered formations / large diameter of the roof), periodic sonar measurements and cement bonding log (e.g., every 5 years), elastomers (no nitril) or self-healing material instead of cement, H_2 and H_2S certified material (including packers), (see further measures in risks 1.3, 1.5, 1.6, 1.8-1,12, 1.14 and 1.15)
(3) Corrective measures (5 main): controlled production / flaring of H_2, abandon cavern, adapt the pressures, (micro annuli and material) treatment with special materials (resins, silicates etc.,

[3] Magnolia, Louisiana, 2003
[4] Boling 1, 2, 4, Texas, USA, 2005
[5] Bayou Corne, Louisiana, 2012
[6] Eminence salt dome 1, 3, 4, Mississippi, 1972
[7] Jintan JK-A, China, 2015

biological treatment), use of deformable metals and casing expansion, (see further measures in risks 1.3, 1.5, 1.6, 1.8-1,12, 1.14 and 1.15)

(4) Description and classification residual risk considering the measures taken: Both probability and consequence classes have not been reduced and remain: **3/2**, in more detail 3 (probability) and [Me1][Te2][Se0][Qe1][Re0] (consequences)

RISK Nr. 6.3 Creep closure and subsidence

Risk step 1: Aim

Aim 6 for Provincial states: "*Our organization is motivated, reliable and innovative. Our organization cooperates, links and joins in brainstorming in the search for solutions, keeping an eye on our province and the interests of environment and society including the agricultural industry*". Therefore, the aim is: no risk for and protection of the agricultural industry in the area of the hydrogen storage.

Risk step 2: Risk identification

(1) Risk: Subsidence (beyond predicted limits) causing damage to the agricultural industry
(2) Risk based on: Interpretation of facts
(3) Source of information: Literature review (sections 3.1.5.1 and 3.2.3) [8][9]
(4) Uncertainty: Additional research of the salt structure and rheology, cavern design
(5) Type of causes: [Rc][Ic][Gc][Oc][Tc][Pc]
(6) Type of effects: [Te][Qe]

Risk step 3: Risk classification

(1) Classification probability class: 2 (c): interpretation of factual information
(2) Classification consequence class: [Me0][Te2][Se0][Qe1][Re0]

Risk step 4: Dealing with risks

(1) Additional research: research of the salt structure and rheology, cavern design, geomechanical modelling
(2) Preventive measures: monitoring of subsidence by INSAR & surveying measurements, field tests (pressure observation test POT after well drill), updated cavern design, geomechanical modelling, determination of the minimum cavern pressure (see further measures in risk 1.7)
(3) Corrective measures: change of the average cavern pressure (higher), minimizing the subsidence by controlled abandonment
(4) Description and classification residual risk considering the measures taken: taking the preventive and corrective measures into account the residual risk becomes: 1 (probability) and [Me0][Te2][Se0][Qe1][Re0] (consequences), **1/2**

[8] Subsidence at Maceió, Brazil, 2021

[9] Matarandiba Island, Brazil, 2018

Stakeholder: Provincial States (agriculture)

Unmitigated risk matrix

4 x 3 Risk matrix		Consequence		
		1	2	3
Chance	3		6.2	
	2		6.1 6.3	
	1			
	0			

Residual (mitigated) risk matrix

4 x 3 Risk matrix		Consequence		
		1	2	3
Chance	3		6.2	
	2			
	1		6.1 6.3	
	0			

D.7 Stakeholder: Provincial states (II)

RISK Nr. 7.1 Accident at the surface

Risk step 1: Aim

Aim 7 for Provincial states: "*Our organisation is responsible for the implementation and execution of the "management plan" for the Natura 2000 areas*". Therefore, the aim is: no risk for, and preservation and protection of, natural values in the area of the hydrogen storage.

Risk step 2: Risk identification

(1) Risk: Accident at the surface (blow-out, well leak, pipeline integrity loss) as a result of hydrogen storage causing damage to natural values
(2) Risk based on: Interpretation of facts / assumptions
(3) Source of information: Literature review[1][2], expert judgement
(4) Uncertainty: Blow-out modelling done by Brouard Consulting, experience within the industry with hydrogen pipelines
(5) Type of causes: [Tc][Hc][Gc][Oc][Rc][Ic]
(6) Type of effects: [Te][Qe]

Risk step 3: Risk classification

(1) Classification probability class: 2 (a/c): assumption based on expert judgement and interpretation of factual information
(2) Classification consequence class: [Me0][Te2][Se0][Qe2][Re0]

Risk step 4: Dealing with risks

(1) Additional research: modelling of Blow-out, safety study on the effect at the surface, literature research hydrogen infrastructure KEM 29 (research in progress)
(2) Preventive measures (5 main): highest quality of BOP and safety valves / pressure gauges (H_2 certified material), all equipment designed for low T, rapid response plan, H_2-certified material (steel), construction and maintenance protocols, (see further measures in risks 1.1, 1.2 and 1.4)
(3) Corrective measures: actions according to rapid response plan, evacuation plan, fire extinguishing, damage control / repair, temporary partial shut-down and repair
(4) Description and classification residual risk considering the measures taken: taking the preventive and corrective measures into account the residual risk becomes: 1 (probability) and [Me0][Te2][Se0][Qe2][Re0] (consequences), **1/2**

[1] Fort Saskatchewan Ethane Blow-out and Fire (2001)

[2] Moss Bluff natural gas blow out and Fire (2004)

RISK Nr. 7.2 Subsurface accident

Risk step 1: Aim

Aim 7 for Provincial states: "*Our organisation is responsible for the implementation and execution of the "management plan" for the Natura 2000 areas*". Therefore, the aim is: no risk for, and preservation and protection of, natural values in the area of the hydrogen storage.

Risk step 2: Risk identification

(1) Risk: Subsurface accident (leakage vertical tubing/casing, casing overstretching, cavern breaches, tensile failure, falls) as a result of hydrogen storage causing damage to natural values
(2) Risk based on: Interpretation of facts / assumptions
(3) Source of information: Literature review[3][4][5][6][7], expert judgement
(4) Uncertainty: Additional research of the salt structure and rheology, the interaction with hydrogen, mechanical properties and damage evolution. Additional research of materials interacting with hydrogen
(5) Type of causes: [Hc][Tc][Rc][Ic][Gc]
(6) Type of effects: [Te][Qe]

Risk step 3: Risk classification

(1) Classification probability class: 3 (a/c): assumption based on expert judgement and interpretation of factual information
(2) Classification consequence class: [Me0][Te2][Se0][Qe1][Re0]

Risk step 4: Dealing with risks

(1) Additional research (5 main): creep research (grainsize) and durability of the salt, research of the salt dome internal structure, including anomalous zones (section 3.4.7.1.4), and rheology, additional research of the second phase rheology interacting with hydrogen, research on prevention of micro annuli at the casing / cement / rock interfaces, additional research of materials interacting with hydrogen, (see further research topics in risks 1.3, 1.5, 1.6, 1.8-1,12, 1.14 and 1.15)
(2) Preventive measures (5 main): minimum preconditions for H_2 storage cavern (well test), improved cavern design (avoid flat roof / interlayered formations / large diameter of the roof), periodic sonar measurements and cement bonding log (e.g., every 5 years), elastomers (no nitril) or self-healing material instead of cement, H_2 and H_2S certified material (including packers), (see further measures in risks 1.3, 1.5, 1.6, 1.8-1,12, 1.14 and 1.15)
(3) Corrective measures (5 main): controlled production / flaring of H_2, abandon cavern, adapt the pressures, (micro annuli and material) treatment with special materials (resins, silicates etc., biological treatment), use of deformable metals and casing expansion, (see further measures in risks 1.3, 1.5, 1.6, 1.8-1,12, 1.14 and 1.15)

[3] Magnolia, Louisiana, 2003
[4] Boling 1, 2, 4, Texas, USA, 2005
[5] Bayou Corne, Louisiana, 2012
[6] Eminence salt dome 1, 3, 4, Mississippi, 1972
[7] Jintan JK-A, China, 2015

(4) *Description and classification residual risk considering the measures taken:* Both probability and consequence classes have not been reduced and remain: **3/2**, in more detail 3 (probability) and [Me0][Te2][Se0][Qe1][Re0] (consequences)

RISK Nr. 7.3 Creep closure and subsidence

Risk step 1: Aim

Aim 7 for Provincial states: "*Our organisation is responsible for the implementation and execution of the "management plan" for the Natura 2000 areas*". Therefore, the aim is: no risk for, and preservation and protection of, natural values in the area of the hydrogen storage.

Risk step 2: Risk identification

(1) Risk: Subsidence (beyond predicted limits) causing damage to natural values
(2) Risk based on: Interpretation of facts
(3) Source of information: Literature review (sections 3.1.5.1 and 3.2.3) [8][9]
(4) Uncertainty: Additional research of the salt structure and rheology, cavern design
(5) Type of causes: [Rc][Ic][Gc][Oc][Tc][Pc]
(6) Type of effects: [Te][Qe]

Risk step 3: Risk classification

(1) Classification probability class: 2 (c): interpretation of factual information
(2) Classification consequence class: [Me0][Te2][Se0][Qe1][Re0]

Risk step 4: Dealing with risks

(1) Additional research: research of the salt structure and rheology, cavern design, geomechanical modelling
(2) Preventive measures: monitoring of subsidence by INSAR & surveying measurements, field tests (pressure observation test POT after well drill), updated cavern design, geomechanical modelling, determination of the minimum cavern pressure (see further measures in risk 1.7)
(3) Corrective measures: change of the average cavern pressure (higher), minimizing the subsidence by controlled abandonment
(4) Description and classification residual risk considering the measures taken: taking the preventive and corrective measures into account the residual risk becomes: 1 (probability) and [Me0][Te2][Se0][Qe1][Re0] (consequences), **1/2**

[8] Subsidence at Maceió, Brazil, 2021
[9] Matarandiba Island, Brazil, 2018

Stakeholder: Provincial States (Natura 2000)

Unmitigated risk matrix

4 x 3 Risk matrix		Consequence		
		1	2	3
Chance	3		7.2	
	2		7.1 7.3	
	1			
	0			

Residual (mitigated) risk matrix

4 x 3 Risk matrix		Consequence		
		1	2	3
Chance	3		7.2	
	2			
	1		7.1 7.3	
	0			

D.8 Stakeholder: Municipalities

RISK Nr. 8.1 Accident at the surface

Risk step 1: Aim

Aim 8 for municipalities: "*Our municipality is a society with optimal development for our inhabitants and enterprises and cooperation based on self-initiation, strength and quality*". Therefore, the aim is: no risk for the inhabitants and the direct surroundings as a result of hydrogen storage in salt caverns.

Risk step 2: Risk identification

(1) Risk: Accident at the surface (blow-out, well leak, pipeline integrity loss) as a result of hydrogen storage threatens inhabitants and direct surroundings
(2) Risk based on: Interpretation of facts / assumptions
(3) Source of information: Literature review[1][2], expert judgement
(4) Uncertainty: Blow-out modelling done by Brouard Consulting, experience within the industry with hydrogen pipelines
(5) Type of causes: [Tc][Hc][Gc][Oc][Rc][Ic]
(6) Type of effects: [Me][Te][Se][Qe][Re]

Risk step 3: Risk classification

(1) Classification probability class: 2 (a/c): assumption based on expert judgement and interpretation of factual information
(2) Classification consequence class: [Me1][Te2][Se3][Qe2][Re2]

Risk step 4: Dealing with risks

(1) Additional research: modelling of Blow-out, safety study on the effect at the surface, literature research hydrogen infrastructure KEM 29 (research in progress)
(2) Preventive measures (5 main): highest quality of BOP and safety valves / pressure gauges (H_2 certified material), all equipment designed for low T, rapid response plan, H_2-certified material (steel), construction and maintenance protocols, (see further measures in risks 1.1, 1.2 and 1.4)
(3) Corrective measures: actions according to rapid response plan, evacuation plan, fire extinguishing, damage control / repair, temporary partial shut-down and repair
(4) Description and classification residual risk considering the measures taken: taking the preventive and corrective measures into account the residual risk becomes: 1 (probability) and [Me1][Te2][Se3][Qe2][Re2] (consequences), **1/3**

[1] Fort Saskatchewan Ethane Blow-out and Fire (2001)

[2] Moss Bluff natural gas blow out and Fire (2004)

RISK Nr. 8.2 Subsurface accident

Risk step 1: Aim

Aim 8 for municipalities: "*Our municipality is a society with optimal development for our inhabitants and enterprises and cooperation based on self-initiation, strength and quality*". Therefore, the aim is: no risk for the inhabitants and the direct surroundings as a result of hydrogen storage in salt caverns.

Risk step 2: Risk identification

(1) Risk: Subsurface accident (leakage vertical tubing/casing, casing overstretching, cavern breaches, tensile failure, falls) as a result of hydrogen storage threatens inhabitants and direct surroundings
(2) Risk based on: Interpretation of facts / assumptions
(3) Source of information: Literature review[3][4][5][6][7], expert judgement
(4) Uncertainty: Additional research of the salt structure and rheology, the interaction with hydrogen, mechanical properties and damage evolution. Additional research of materials interacting with hydrogen
(5) Type of causes: [Hc][Tc][Rc][Ic][Gc]
(6) Type of effects: [Me][Te][Se][Qe][Re]

Risk step 3: Risk classification

(1) Classification probability class: 3 (a/c): assumption based on expert judgement and interpretation of factual information
(2) Classification consequence class: [Me1][Te2][Se3][Qe2][Re2]

Risk step 4: Dealing with risks

(1) Additional research (5 main): creep research (grainsize) and durability of the salt, research of the salt dome internal structure, including anomalous zones (section 3.4.7.1.4), and rheology, additional research of the second phase rheology interacting with hydrogen, research on prevention of micro annuli at the casing / cement / rock interfaces, additional research of materials interacting with hydrogen, (see further research topics in risks 1.3, 1.5, 1.6, 1.8-1,12, 1.14 and 1.15)
(2) Preventive measures (5 main): minimum preconditions for H_2 storage cavern (well test), improved cavern design (avoid flat roof / interlayered formations / large diameter of the roof), periodic sonar measurements and cement bonding log (e.g., every 5 years), elastomers (no nitril) or self-healing material instead of cement, H_2 and H_2S certified material (including packers), (see further measures in risks 1.3, 1.5, 1.6, 1.8-1,12, 1.14 and 1.15)
(3) Corrective measures: controlled production / flaring of H_2, abandon cavern, adapt the pressures, (micro annuli and material) treatment with special materials (resins, silicates etc., biological

[3] Magnolia, Louisiana, 2003
[4] Boling 1, 2, 4, Texas, USA, 2005
[5] Bayou Corne, Louisiana, 2012
[6] Eminence salt dome 1, 3, 4, Mississippi, 1972
[7] Jintan JK-A, China, 2015

treatment), use of deformable metals and casing expansion, (see further measures in risks 1.3, 1.5, 1.6, 1.8-1,12, 1.14 and 1.15)

(4) Description and classification residual risk considering the measures taken: taking the preventive and corrective measures into account the residual risk becomes: 3 (probability) and [Me1][Te2][Se1][Qe2][Re2] (consequences), **3/2**

RISK Nr. 8.3 Creep closure and subsidence

Risk step 1: Aim

Aim 8 for municipalities: "*Our municipality is a society with optimal development for our inhabitants and enterprises and cooperation based on self-initiation, strength and quality*". Therefore, the aim is: no risk for the inhabitants and the direct surroundings as a result of hydrogen storage in salt caverns.

Risk step 2: Risk identification

(1) Risk: Subsidence (beyond predicted limits) threatens inhabitants and direct surroundings
(2) Risk based on: Interpretation of facts
(3) Source of information: Literature review (sections 3.1.5.1 and 3.2.3) [8][9]
(4) Uncertainty: Additional research of the salt structure and rheology, cavern design
(5) Type of causes: [Rc][Ic][Gc][Oc][Tc][Pc]
(6) Type of effects: [Me][Te][Se][Qe]

Risk step 3: Risk classification

(1) Classification probability class: 2 (c): interpretation of factual information
(2) Classification consequence class: [Me1][Te3][Se1][Qe1][Re0]

Risk step 4: Dealing with risks

(1) Additional research: research of the salt structure and rheology, cavern design, geomechanical modelling
(2) Preventive measures: monitoring of subsidence by INSAR & surveying measurements, field tests (pressure observation test POT after well drill), updated cavern design, geomechanical modelling, determination of the minimum cavern pressure (see further measures in risk 1.7)
(3) Corrective measures: change of the average cavern pressure (higher), minimizing the subsidence by controlled abandonment
(4) Description and classification residual risk considering the measures taken: taking the preventive and corrective measures into account the residual risk becomes: 1 (probability) and [Me1][Te3][Se1][Qe1][Re0] (consequences), **1/3**

[8] Subsidence at Maceió, Brazil, 2021

[9] Matarandiba Island, Brazil, 2018

RISK Nr. 8.4 Registered induced seismicity

Risk step 1: Aim

Aim 8 for municipalities: "*Our municipality is a society with optimal development for our inhabitants and enterprises and cooperation based on self-initiation, strength and quality*". Therefore, the aim is: no risk for the inhabitants and the direct surroundings as a result of hydrogen storage in salt caverns.

Risk step 2: Risk identification

(1) Risk: Registered induced seismicity caused by the operation (filling and emptying) of the cavern disturbs inhabitants and direct surroundings
(2) Risk based on: Interpretation of facts / assumption
(3) Source of information: Monitoring plans of underground Natural Gas and Nitrogen storage[10][11], literature review (section 5.2)
(4) Uncertainty: Research on characteristic locations in the salt dome sensitive to (micro)seismicity
(5) Type of causes: [Rc][Gc]
(6) Type of effects: [Te][Re]

Risk step 3: Risk classification

(1) Classification probability class: 3 (a/c): assumption based on expert judgement and interpretation of facts
(2) Classification consequence class: [Me0][Te2][Se0][Qe0][Re1]

Risk step 4: Dealing with risks

(1) Additional research: research on characteristic locations in the salt dome sensitive to (micro)seismicity
(2) Preventive measures: seismic monitoring (natural and induced seismicity), modelling of expected seismicity, no storage activities in or near an active fault zone, transparency and open communication, baseline measurement, transparency regarding seismic data
(3) Corrective measures: -
(4) Description and classification residual risk considering the measures taken: taking the preventive measures into account the residual risk becomes: 2 (probability) and [Me0][Te2][Se0][Qe0][Re1] (consequences), **2/2**

[10] Nouryon, Micro seismic network Heiligerlee & Zuidwending, observations Q3 2020, Powerpoint, no reference, no date

[11] NAM, Report "Instemmingsbesluit Norg", letter, no reference, dated December 3 2021

RISK Nr. 8.5 Failure of the storage system

Risk step 1: Aim

Aim 8 for municipalities: "*Our municipality is a society with optimal development for our inhabitants and enterprises and cooperation based on self-initiation, strength and quality*". Therefore, the aim is: no risk for the inhabitants and the direct surroundings as a result of hydrogen storage in salt caverns.

Risk step 2: Risk identification

(1) Risk: Failure of the storage system (due to fire, natural disaster, terrorism or IT-failure) threatens inhabitants and direct surroundings
(2) Risk based on: Assumptions
(3) Source of information: Expert judgement
(4) Uncertainty: Cannot be reduced
(5) Type of causes: [Hc][Oc][Tc][Rc][Ic]
(6) Type of effects: [Me][Te][Se][Qe][Re]

Risk step 3: Risk classification

(1) Classification probability class: 2 (a): assumption based on expert judgement
(2) Classification consequence class: [Me1][Te2][Se3][Qe3][Re2]

Risk step 4: Dealing with risks

(1) Additional research: -
(2) Preventive measures (5 main): adhere to the general safety regulations and fire-prevention measurements for hydrogen installations, back-up by remote-controlled operation, assign as "vital infrastructure" and act accordingly, manual controls requiring double authorisation, analogue pressure and temperature gauges at critical locations (double system) (see further measures in risks 1.19 – 1.22)
(3) Corrective measures: actions according to rapid response plan, fire alarm and fire extinguishing, remote-controlled operation, pressure relief valve (PRV) for worst case when pressure gets near lithostatic pressure at casing shoe, automatic release of pressure
(4) Description and classification residual risk considering the measures taken: taking the preventive and corrective measures into account the residual risk eventually becomes: 1 (probability) and [Me0][Te1][Se0][Qe1][Re0] (consequences), **1/1**

RISK Nr. 8.6 Emergence of negative public opinion

Risk step 1: Aim

Aim 8 for municipalities: "*Our municipality is a society with optimal development for our inhabitants and enterprises and cooperation based on self-initiation, strength and quality*". Therefore, the aim is: no risk for the inhabitants and the direct surroundings as a result of hydrogen storage in salt caverns.

Risk step 2: Risk identification

(1) Risk: Emergence of negative public opinion, e.g., triggered by regional or national media
(2) Risk based on: Interpretation of facts
(3) Source of information: public opinion[12][13][14][15][16]
(4) Uncertainty: complete stakeholder analysis per location, risk analysis discussion with all stakeholders (separately)
(5) Type of causes: [Pc]
(6) Type of effects: [Me][Te][Se][Re]

Risk step 3: Risk classification

(1) Classification probability class: 3 (c): interpretation of factual information
(2) Classification consequence class: [Me1][Te3][Se1][Qe0][Re2]

Risk step 4: Dealing with risks

(1) Additional research: complete stakeholder analysis per location, risk analysis discussion with all stakeholders (separately)
(2) Preventive measures: transparent, pro-active and personal communication, direct involvement (shareholders), financial compensation ("burdens and benefits"), transparency with respect to all taken preventive measures (other risks)
(3) Corrective measures: transparent and personal communication, financial compensation (based on reversed burden of proof), transparency with respect to all taken corrective measures (other risks)
(4) Description and classification residual risk considering the measures taken: taking the preventive and corrective measures into account the residual risk eventually becomes: 2 (probability) and [Me1][Te2][Se1][Qe0][Re1] (consequences), **2/2**

[12] Public opinion with respect to CO_2 storage underneath Barendrecht: "Stichting CO2isNEE", 2010
[13] Public opinion with respect to environmental problems and subsidence as a result of salt mining: "Stop Zoutwinning!", 2021
[14] Public opinion with respect to future salt extraction Municipality of Haaksbergen, 2023
[15] Public opinion with respect to underground discharge of production water, www.stopafvalwatertwente.nl
[16] Public opinion with respect to Nitrogen storage in Heiligerlee, www.mijnendijnbelang.nl

Stakeholder: Municipalities

Unmitigated risk matrix

4 x 3 Risk matrix		Consequence		
		1	2	3
Chance	3		8.4	8.2 8.6
	2			8.1 8.3 8.5
	1			
	0			

Residual (mitigated) risk matrix

4 x 3 Risk matrix		Consequence		
		1	2	3
Chance	3		8.2	
	2		8.4 8.6	
	1	8.5		8.1 8.3
	0			

D.9 Stakeholder: Energie Beheer Nederland

RISK Nr. 9.1 Accident at the surface

Risk step 1: Aim

Aim 9 for Energie Beheer Nederland: "*EBN is deploying value in the subsurface for the benefit of the future above ground*". Therefore, the aim is: no risk in the area of the hydrogen storage at the surface and in the subsurface. No adverse consequences for (future) use of the subsurface in general and hydrogen storage in salt caverns more specifically.

Risk step 2: Risk identification

(1) Risk: Accident at the surface (blow-out, well leak, pipeline integrity loss) as a result of hydrogen storage
(2) Risk based on: Interpretation of facts / assumptions
(3) Source of information: Literature review[1][2], expert judgement
(4) Uncertainty: Blow-out modelling done by Brouard Consulting, experience within the industry with hydrogen pipelines
(5) Type of causes: [Tc][Hc][Gc][Oc][Rc][Ic]
(6) Type of effects: [Me][Te][Qe]

Risk step 3: Risk classification

(1) Classification probability class: 2 (a/c): assumption based on expert judgement and interpretation of factual information
(2) Classification consequence class: [Me1][Te2][Se0][Qe2][Re0]

Risk step 4: Dealing with risks

(1) Additional research: modelling of Blow-out, safety study on the effect at the surface, literature research hydrogen infrastructure KEM 29 (research in progress)
(2) Preventive measures (5 main): highest quality of BOP and safety valves / pressure gauges (H_2 certified material), all equipment designed for low T, rapid response plan, H_2-certified material (steel), construction and maintenance protocols, (see further measures in risks 1.1, 1.2 and 1.4)
(3) Corrective measures: actions according to rapid response plan, evacuation plan, fire extinguishing, damage control / repair, temporary partial shut-down and repair
(4) Description and classification residual risk considering the measures taken: taking the preventive and corrective measures into account the residual risk becomes: 1 (probability) and [Me1][Te2][Se0][Qe2][Re0] (consequences), **1/2**

[1] Fort Saskatchewan Ethane Blow-out and Fire (2001)

[2] Moss Bluff natural gas blow out and Fire (2004)

RISK Nr. 9.2 Subsurface accident

Risk step 1: Aim

Aim 9 for Energie Beheer Nederland: "*EBN is deploying value in the subsurface for the benefit of the future above ground*". Therefore, the aim is: no risk in the area of the hydrogen storage at the surface and in the subsurface. No adverse consequences for (future) use of the subsurface in general and hydrogen storage in salt caverns more specifically.

Risk step 2: Risk identification

(1) Risk: Subsurface accident (leakage vertical tubing/casing, casing overstretching, cavern breaches, tensile failure, falls) as a result of hydrogen storage
(2) Risk based on: Interpretation of facts / assumptions
(3) Source of information: Literature review[3][4][5][6][7], expert judgement
(4) Uncertainty: Additional research of the salt structure and rheology, the interaction with hydrogen, mechanical properties and damage evolution. Additional research of materials interacting with hydrogen
(5) Type of causes: [Hc][Tc][Rc][Ic][Gc]
(6) Type of effects: [Me][Te][Qe]

Risk step 3: Risk classification

(1) Classification probability class: 3 (a/c): assumption based on expert judgement and interpretation of factual information
(2) Classification consequence class: [Me1][Te2][Se0][Qe3][Re0]

Risk step 4: Dealing with risks

(1) Additional research (5 main): creep research (grainsize) and durability of the salt, research of the salt dome internal structure, including anomalous zones (section 3.4.7.1.4), and rheology, additional research of the second phase rheology interacting with hydrogen, research on prevention of micro annuli at the casing / cement / rock interfaces, additional research of materials interacting with hydrogen, (see further research topics in risks 1.3, 1.5, 1.6, 1.8-1,12, 1.14 and 1.15)
(2) Preventive measures (5 main): minimum preconditions for H_2 storage cavern (well test), improved cavern design (avoid flat roof / interlayered formations / large diameter of the roof), periodic sonar measurements and cement bonding log (e.g., every 5 years), elastomers (no nitril) or self-healing material instead of cement, H_2 and H_2S certified material (including packers), (see further measures in risks 1.3, 1.5, 1.6, 1.8-1,12, 1.14 and 1.15)
(3) Corrective measures (5 main): controlled production / flaring of H_2, abandon cavern, adapt the pressures, (micro annuli and material) treatment with special materials (resins, silicates etc.,

[3] Magnolia, Louisiana, 2003
[4] Boling 1, 2, 4, Texas, USA, 2005
[5] Bayou Corne, Louisiana, 2012
[6] Eminence salt dome 1, 3, 4, Mississippi, 1972
[7] Jintan JK-A, China, 2015

biological treatment), use of deformable metals and casing expansion, (see further measures in risks 1.3, 1.5, 1.6, 1.8-1,12, 1.14 and 1.15)

(4) Description and classification residual risk considering the measures taken: taking the preventive and corrective measures into account the residual risk becomes: **3/2**, in more detail 3 (probability) and [Me1][Te2][Se0][Qe2][Re0] (consequences)

RISK Nr. 9.3 Creep closure and subsidence

Risk step 1: Aim

Aim 9 for Energie Beheer Nederland: "*EBN is deploying value in the subsurface for the benefit of the future above ground*". Therefore, the aim is: no risk in the area of the hydrogen storage at the surface and in the subsurface. No adverse consequences for (future) use of the subsurface in general and hydrogen storage in salt caverns more specifically.

Risk step 2: Risk identification

(1) Risk: Subsidence (beyond predicted limits)
(2) Risk based on: Interpretation of facts
(3) Source of information: Literature review (sections 3.1.5.1 and 3.2.3) [8][9]
(4) Uncertainty: Additional research of the salt structure and rheology, cavern design
(5) Type of causes: [Rc][Ic][Gc][Oc][Tc][Pc]
(6) Type of effects: [Te][Qe]

Risk step 3: Risk classification

(1) Classification probability class: 2 (c): interpretation of factual information
(2) Classification consequence class: [Me0][Te3][Se0][Qe1][Re0]

Risk step 4: Dealing with risks

(1) Additional research: research of the salt structure and rheology, cavern design, geomechanical modelling
(2) Preventive measures: monitoring of subsidence by INSAR & surveying measurements, field tests (pressure observation test POT after well drill), updated cavern design, geomechanical modelling, determination of the minimum cavern pressure (see further measures in risk 1.7)
(3) Corrective measures: change of the average cavern pressure (higher), minimizing the subsidence by controlled abandonment
(4) Description and classification residual risk considering the measures taken: taking the preventive and corrective measures into account the residual risk becomes: 1 (probability) and [Me0][Te3][Se0][Qe1][Re0] (consequences), **1/3**

[8] Subsidence at Maceió, Brazil, 2021

[9] Matarandiba Island, Brazil, 2018

RISK Nr. 9.4 Failure of the storage system

Risk step 1: Aim

Aim 9 for Energie Beheer Nederland: "*EBN is deploying value in the subsurface for the benefit of the future above ground*". Therefore, the aim is: no risk in the area of the hydrogen storage at the surface and in the subsurface. No adverse consequences for (future) use of the subsurface in general and hydrogen storage in salt caverns more specifically.

Risk step 2: Risk identification

(1) Risk: Failure of the storage system (due to fire, natural disaster, terrorism or IT-failure)
(2) Risk based on: Assumptions
(3) Source of information: Expert judgement
(4) Uncertainty: Cannot be reduced
(5) Type of causes: [Hc][Oc][Tc][Rc][Ic]
(6) Type of effects: [Me][Te][Qe]

Risk step 3: Risk classification

(1) Classification probability class: 2 (a): assumption based on expert judgement
(2) Classification consequence class: [Me1][Te2][Se0][Qe3][Re0]

Risk step 4: Dealing with risks

(1) Additional research: -
(2) Preventive measures (5 main): adhere to the general safety regulations and fire-prevention measurements for hydrogen installations, back-up by remote-controlled operation, assign as "vital infrastructure" and act accordingly, manual controls requiring double authorisation, analogue pressure and temperature gauges at critical locations (double system) (see further measures in risks 1.19 – 1.22)
(3) Corrective measures: actions according to rapid response plan, fire alarm and fire extinguishing, remote-controlled operation, pressure relief valve (PRV) for worst case when pressure gets near lithostatic pressure at casing shoe, automatic release of pressure
(4) Description and classification residual risk considering the measures taken: taking the preventive and corrective measures into account the residual risk eventually becomes: 1 (probability) and [Me0][Te1][Se0][Qe1][Re0] (consequences), **1/1**

RISK Nr. 9.5 Disputed responsibility due to stacked mining activities

Risk step 1: Aim

Aim 9 for Energie Beheer Nederland: "*EBN is deploying value in the subsurface for the benefit of the future above ground*". Therefore, the aim is: no risk in the area of the hydrogen storage at the surface and in the subsurface. No adverse consequences for (future) use of the subsurface in general and hydrogen storage in salt caverns more specifically.

Risk step 2: Risk identification

(1) Risk: Disputed responsibility due to stacked mining activities
(2) Risk based on: Assumption
(3) Source of information: Political discussions[10], public[11]
(4) Uncertainty: Scenario modelling of various critical scenarios to test regulations
(5) Type of causes: [Rc]
(6) Type of effects: [Te]

Risk step 3: Risk classification

(1) Classification probability class: 3 (a): assumption based on expert judgement
(2) Classification consequence class: [Me0][Te3][Se0][Qe0][Re0]

Risk step 4: Dealing with risks

(1) Additional research: scenario modelling of various critical scenarios to test regulations
(2) Preventive measures: regulations for operators regarding arial extent and duration of responsibility, seismic monitoring system, monitoring of subsidence by INSAR & surveying measurements before mining and during storage, mandatory report of incidents, regular meetings with all operators involved (including independent chairman, e.g., SodM), one overall geological model for all operators
(3) Corrective measures: mandatory insurance policy for all operators concerned, regulations for take-over of responsibilities in case of bankruptcy operator
(4) Description and classification residual risk considering the measures taken: taking the preventive and corrective measures into account the residual risk eventually becomes: 1 (probability) and [Me0][Te2][Se0][Qe0][Re0] (consequences), **1/2**

[10] Groenlinks, Stacked mining neglected in Nedmag-advice, 2019

[11] RTVOost, Growing frustration about mining, damage and new gas exploitation, January 2021

RISK Nr. 9.6 Threat for (future) on-shore energy storage

Risk step 1: Aim

Aim 9 for Energie Beheer Nederland: "*EBN is deploying value in the subsurface for the benefit of the future above ground*". Therefore, the aim is: no risk in the area of the hydrogen storage at the surface and in the subsurface. No adverse consequences for (future) use of the subsurface in general and hydrogen storage in salt caverns more specifically.

Risk step 2: Risk identification

(1) Risk: Threat to future energy storage in salt caverns (Licence to Operate) due to uncertainties about safety and consequences of the storage in salt caverns
(2) Risk based on: Assumption
(3) Source of information: Public, press, politics
(4) Uncertainty: (generic and) Site-specific risk assessments, site-specific research on geology, rock-salt properties
(5) Type of causes: [Pc]
(6) Type of effects: [Me][Te][Qe]

Risk step 3: Risk classification

(1) Classification probability class: 3 (a): assumption based on expert judgement
(2) Classification consequence class: [Me3][Te3][Se0][Qe3][Re0]

Risk step 4: Dealing with risks

(1) Additional research: (generic and) site-specific risk assessments, site-specific research on geology and rock-salt properties
(2) Preventive measures(5 main): open pro-active communication with stakeholders (public, politics and press) and other operators, preferably use newly developed caverns (according to an optimal rock mechanical envelope), periodic leak tests (e.g., every 5 years), minimum preconditions for H_2 storage cavern, mandatory status-report (starting every year) (see further measures in risk 1.24)
(3) Corrective measures: open communication with stakeholders (public, politics and press) and other operators
(4) Description and classification residual risk considering the measures taken: taking the preventive and corrective measures into account the residual risk eventually becomes: 2 (probability) and [Me1][Te3][Se0][Qe0][Re0] (consequences), **2/3**

Stakeholder: EBN

Unmitigated risk matrix

4 x 3 Risk matrix		Consequence		
		1	2	3
Chance	3			9,2 9.5 9.6
	2		9.1	9.3 9.4
	1			
	0			

Residual (mitigated) risk matrix

4 x 3 Risk matrix		Consequence		
		1	2	3
Chance	3		9.2	
	2			9.6
	1	9.4	9.1 9.5	9.3
	0			

D.10 Stakeholder: Water Boards

RISK Nr. 10.1 Accident at the surface

Risk step 1: Aim

Aim 10 for Water Boards: "*We guarantee safety and clean and sufficient water at low cost*". Therefore, the aim is: no risk, that is protection of the surface water system (water and dykes) for which the Water Board is responsible, at all time.

Risk step 2: Risk identification

(1) Risk: Accident at the surface (blow-out, well leak, pipeline integrity loss) as a result of hydrogen storage
(2) Risk based on: Interpretation of facts / assumptions
(3) Source of information: Literature review[1][2], expert judgement
(4) Uncertainty: Blow-out modelling done by Brouard Consulting, experience within the industry with hydrogen pipelines
(5) Type of causes: [Tc][Hc][Gc][Oc][Rc][Ic]
(6) Type of effects: [Me][Te][Qe]

Risk step 3: Risk classification

(1) Classification probability class: 2 (a/c): assumption based on expert judgement and interpretation of factual information
(2) Classification consequence class: [Me1][Te1][Se0][Qe1][Re0]

Risk step 4: Dealing with risks

(1) Additional research: modelling of Blow-out, safety study on the effect at the surface, literature research hydrogen infrastructure KEM 29 (research in progress)
(2) Preventive measures (5 main): highest quality of BOP and safety valves / pressure gauges (H_2 certified material), all equipment designed for low T, rapid response plan, H_2-certified material (steel), construction and maintenance protocols (see further measures in risks 1.1, 1.2 and 1.4)
(3) Corrective measures: actions according to rapid response plan, evacuation plan, fire extinguishing, damage control / repair, temporary partial shut-down and repair
(4) Description and classification residual risk considering the measures taken: taking the preventive and corrective measures into account the residual risk becomes: 1 (probability) and [Me1][Te1][Se0][Qe1][Re0] (consequences), **1/1**

[1] Fort Saskatchewan Ethane Blow-out and Fire (2001)

[2] Moss Bluff natural gas blow out and Fire (2004)

RISK Nr. 10.2 Subsurface accident

Risk step 1: Aim

Aim 10 for Water Boards: "*We guarantee safety and clean and sufficient water at low cost*". Therefore, the aim is: no risk, that is protection of the surface water system (water and dykes) for which the Water Board is responsible, at all time.

Risk step 2: Risk identification

(1) Risk: Subsurface accident (leakage vertical tubing/casing, casing overstretching, cavern breaches, tensile failure, falls) as a result of hydrogen storage
(2) Risk based on: Interpretation of facts / assumptions
(3) Source of information: Literature review[3][4][5][6][7], expert judgement
(4) Uncertainty: Additional research of the salt structure and rheology, the interaction with hydrogen, mechanical properties and damage evolution. Additional research of materials interacting with hydrogen
(5) Type of causes: [Hc][Tc][Rc][Ic][Gc]
(6) Type of effects: [Me][Te][Qe]

Risk step 3: Risk classification

(1) Classification probability class: 3 (a/c): assumption based on expert judgement and interpretation of factual information
(2) Classification consequence class: [Me1][Te2][Se0][Qe1][Re0]

Risk step 4: Dealing with risks

(1) Additional research (5 main): creep research (grainsize) and durability of the salt, research of the salt dome internal structure, including anomalous zones (section 3.4.7.1.4), and rheology, additional research of the second phase rheology interacting with hydrogen, research on prevention of micro annuli at the casing / cement / rock interfaces, additional research of materials interacting with hydrogen, (see further research topics in risks 1.3, 1.5, 1.6, 1.8-1,12, 1.14 and 1.15)
(2) Preventive measures (5 main): minimum preconditions for H_2 storage cavern (well test), improved cavern design (avoid flat roof / interlayered formations / large diameter of the roof), periodic sonar measurements and cement bonding log (e.g., every 5 years), elastomers (no nitril) or self-healing material instead of cement, H_2 and H_2S certified material (including packers), (see further measures in risks 1.3, 1.5, 1.6, 1.8-1,12, 1.14 and 1.15)
(3) Corrective measures (5 main): controlled production / flaring of H_2, abandon cavern, adapt the pressures, (micro annuli and material) treatment with special materials (resins, silicates etc., biological treatment), use of deformable metals and casing expansion, (see further measures in risks 1.3, 1.5, 1.6, 1.8-1,12, 1.14 and 1.15)

[3] Magnolia, Louisiana, 2003
[4] Boling 1, 2, 4, Texas, USA, 2005
[5] Bayou Corne, Louisiana, 2012
[6] Eminence salt dome 1, 3, 4, Mississippi, 1972
[7] Jintan JK-A, China, 2015

(4) *Description and classification residual risk considering the measures taken:* Both probability and consequence classes have not been reduced and remain: **3/2**, in more detail 3 (probability) and [Me1][Te2][Se0][Qe1][Re0] (consequences)

RISK Nr. 10.3 Creep closure and subsidence

Risk step 1: Aim

Aim 10 for Water Boards: "*We guarantee safety and clean and sufficient water at low cost*". Therefore, the aim is: no risk, that is protection of the surface water system (water and dykes) for which the Water Board is responsible, at all time.

Risk step 2: Risk identification

(1) Risk: Subsidence (beyond predicted limits)
(2) Risk based on: Interpretation of facts
(3) Source of information: Literature review (sections 3.1.5.1 and 3.2.3) [8][9]
(4) Uncertainty: Additional research of the salt structure and rheology, cavern design
(5) Type of causes: [Rc][Ic][Gc][Oc][Tc][Pc]
(6) Type of effects: [Me][Te][Qe]

Risk step 3: Risk classification

(1) Classification probability class: 2 (c): interpretation of factual information
(2) Classification consequence class: [Me1][Te3][Se0][Qe2][Re0]

Risk step 4: Dealing with risks

(1) Additional research: research of the salt structure and rheology, cavern design, geomechanical modelling
(2) Preventive measures: monitoring of subsidence by INSAR & surveying measurements, field tests (pressure observation test POT after well drill), updated cavern design, geomechanical modelling, determination of the minimum cavern pressure (see further measures in risk 1.7)
(3) Corrective measures: change of the average cavern pressure (higher), minimizing the subsidence by controlled abandonment
(4) Description and classification residual risk considering the measures taken: taking the preventive and corrective measures into account the residual risk becomes: 1 (probability) and [Me1][Te3][Se0][Qe2][Re0] (consequences), **1/3**

[8] Subsidence at Maceió, Brazil, 2021

[9] Matarandiba Island, Brazil, 2018

RISK Nr. 10.4 Emergence of negative public opinion

Risk step 1: Aim

Aim 10 for Water Boards: "*We guarantee safety and clean and sufficient water at low cost*". Therefore, the aim is: no risk, that is protection of the surface water system (water and dykes) for which the Water Board is responsible, at all time.

Risk step 2: Risk identification

(1) Risk: Emergence of negative public opinion, e.g., triggered by regional or national media, threatening the public image of the Water Board
(2) Risk based on: Interpretation of facts
(3) Source of information: public opinion[10][11][12][13][14]
(4) Uncertainty: complete stakeholder analysis per location, risk analysis discussion with all stakeholders (separately)
(5) Type of causes: [Pc]
(6) Type of effects: [Me][Te][Se][Re]

Risk step 3: Risk classification

(1) Classification probability class: 3 (c): interpretation of factual information
(2) Classification consequence class: [Me0][Te2][Se0][Qe0][Re1]

Risk step 4: Dealing with risks

(1) Additional research: complete stakeholder analysis per location, risk analysis discussion with all stakeholders (separately)
(2) Preventive measures: transparent, pro-active and personal communication, direct involvement (shareholders), financial compensation ("burdens and benefits"), transparency with respect to all taken preventive measures (other risks)
(3) Corrective measures: transparent and personal communication, financial compensation (based on reversed burden of proof), transparency with respect to all taken corrective measures (other risks)
(4) Description and classification residual risk considering the measures taken: taking the preventive and corrective measures into account the residual risk eventually becomes: 2 (probability) and [Me0][Te1][Se0][Qe0][Re1] (consequences), **2/1**

[10] Public opinion with respect to CO_2 storage underneath Barendrecht: "Stichting CO2isNEE", 2010
[11] Public opinion with respect to environmental problems and subsidence as a result of salt mining: "Stop Zoutwinning!", 2021
[12] Public opinion with respect to future salt extraction Municipality of Haaksbergen, 2023
[13] Public opinion with respect to underground discharge of production water, www.stopafvalwatertwente.nl
[14] Public opinion with respect to Nitrogen storage in Heiligerlee, www.mijnendijnbelang.nl

Stakeholder: Waterboards

Unmitigated risk matrix

4 x 3 Risk matrix		Consequence		
		1	2	3
Chance	3		10.2 10.4	
	2	10.1		10.3
	1			
	0			

Residual (mitigated) risk matrix

4 x 3 Risk matrix		Consequence		
		1	2	3
Chance	3		10.2	
	2	10.4		
	1	10.1		10.3
	0			

D.11 Stakeholder: Safety region (Veiligheidsregio)

RISK Nr. 11.1 Accident at the surface

Risk step 1: Aim

Aim 11 for Safety Region ("Veiligheidsregio"): "*We ensure that everyone can live and work in peace and space*". Therefore, the aim is: no risk or disruption due to hydrogen storage in salt caverns for the population, at all time.

Risk step 2: Risk identification

(1) *Risk:* Accident at the surface (blow-out, well leak, pipeline integrity loss) as a result of hydrogen storage
(2) *Risk based on:* Interpretation of facts / assumptions
(3) *Source of information:* Literature review[1][2], expert judgement
(4) *Uncertainty:* Blow-out modelling done by Brouard Consulting, experience within the industry with hydrogen pipelines
(5) *Type of causes*: [Tc][Hc][Gc][Oc][Rc][Ic]
(6) *Type of effects*: [Te][Se][Qe][Re]

Risk step 3: Risk classification

(1) *Classification probability class:* 2 (a/c): assumption based on expert judgement and interpretation of factual information
(2) *Classification consequence class:* [Me0][Te2][Se3][Qe2][Re2]

Risk step 4: Dealing with risks

(1) *Additional research:* modelling of Blow-out, safety study on the effect at the surface, literature research hydrogen infrastructure KEM 29 (research in progress)
(2) *Preventive measures (5 main):* highest quality of BOP and safety valves / pressure gauges (H_2 certified material), all equipment designed for low T, rapid response plan, H_2-certified material (steel), construction and maintenance protocols (see further measures in risks 1.1, 1.2 and 1.4)
(3) *Corrective measures:* actions according to rapid response plan, evacuation plan, fire extinguishing, damage control / repair, temporary partial shut-down and repair
(4) *Description and classification residual risk considering the measures taken:* taking the preventive and corrective measures into account the residual risk becomes: 1 (probability) and [Me0][Te2][Se3][Qe2][Re2] (consequences), **1/3**

[1] Fort Saskatchewan Ethane Blow-out and Fire (2001)

[2] Moss Bluff natural gas blow out and Fire (2004)

RISK Nr. 11.2 Subsurface accident

Risk step 1: Aim

Aim 11 for Safety Region ("Veiligheidsregio"): "*We ensure that everyone can live and work in peace and space*". Therefore, the aim is: no risk or disruption due to hydrogen storage in salt caverns for the population, at all time.

Risk step 2: Risk identification

(1) Risk: Subsurface accident (leakage vertical tubing/casing, casing overstretching, cavern breaches, tensile failure, falls) as a result of hydrogen storage
(2) Risk based on: Interpretation of facts / assumptions
(3) Source of information: Literature review[3][4][5][6][7], expert judgement
(4) Uncertainty: Additional research of the salt structure and rheology, the interaction with hydrogen, mechanical properties and damage evolution. Additional research of materials interacting with hydrogen
(5) Type of causes: [Hc][Tc][Rc][Ic][Gc]
(6) Type of effects: [Te][Se][Qe][Re]

Risk step 3: Risk classification

(1) Classification probability class: 3 (a/c): assumption based on expert judgement and interpretation of factual information
(2) Classification consequence class: [Me0][Te2][Se3][Qe2][Re2]

Risk step 4: Dealing with risks

(1) Additional research (5 main): creep research (grainsize) and durability of the salt, research of the salt dome internal structure, including anomalous zones (section 3.4.7.1.4), and rheology, additional research of the second phase rheology interacting with hydrogen, research on prevention of micro annuli at the casing / cement / rock interfaces, additional research of materials interacting with hydrogen, (see further research topics in risks 1.3, 1.5, 1.6, 1.8-1,12, 1.14 and 1.15)
(2) Preventive measures (5 main): minimum preconditions for H_2 storage cavern (well test), improved cavern design (avoid flat roof / interlayered formations / large diameter of the roof), periodic sonar measurements and cement bonding log (e.g., every 5 years), elastomers (no nitril) or self-healing material instead of cement, H_2 and H_2S certified material (including packers), (see further measures in risks 1.3, 1.5, 1.6, 1.8-1,12, 1.14 and 1.15)
(3) Corrective measures (5 main): controlled production / flaring of H_2, abandon cavern, adapt the pressures, (micro annuli and material) treatment with special materials (resins, silicates etc., biological treatment), use of deformable metals and casing expansion, (see further measures in risks 1.3, 1.5, 1.6, 1.8-1,12, 1.14 and 1.15)

[3] Magnolia, Louisiana, 2003
[4] Boling 1, 2, 4, Texas, USA, 2005
[5] Bayou Corne, Louisiana, 2012
[6] Eminence salt dome 1, 3, 4, Mississippi, 1972
[7] Jintan JK-A, China, 2015

(4) *Description and classification residual risk considering the measures taken:* taking the preventive and corrective measures into account the residual risk becomes: 3 (probability) and [Me1][Te2][Se2][Qe2][Re2] (consequences), **3/2**

RISK Nr. 11.3 Creep closure and subsidence

Risk step 1: Aim

Aim 11 for Safety Region ("Veiligheidsregio"): "*We ensure that everyone can live and work in peace and space*". Therefore, the aim is: no risk or disruption due to hydrogen storage in salt caverns for the population, at all time.

Risk step 2: Risk identification

(1) Risk: Subsidence (beyond predicted limits)
(2) Risk based on: Interpretation of facts
(3) Source of information: Literature review (sections 3.1.5.1 and 3.2.3) [8][9]
(4) Uncertainty: Additional research of the salt structure and rheology, cavern design
(5) Type of causes: [Rc][Ic][Gc][Oc][Tc][Pc]
(6) Type of effects: [Te][Qe][Re]

Risk step 3: Risk classification

(1) Classification probability class: 2 (c): interpretation of factual information
(2) Classification consequence class: [Me0][Te3][Se0][Qe1][Re2]

Risk step 4: Dealing with risks

(1) Additional research: research of the salt structure and rheology, cavern design, geomechanical modelling
(2) Preventive measures: monitoring of subsidence by INSAR & surveying measurements, field tests (pressure observation test POT after well drill), updated cavern design, geomechanical modelling, determination of the minimum cavern pressure (see further measures in risk 1.7)
(3) Corrective measures: change of the average cavern pressure (higher), minimizing the subsidence by controlled abandonment
(4) Description and classification residual risk considering the measures taken: taking the preventive and corrective measures into account the residual risk becomes: 1 (probability) and [Me0][Te3][Se0][Qe1][Re2] (consequences), **1/3**

[8] Subsidence at Maceió, Brazil, 2021
[9] Matarandiba Island, Brazil, 2018

RISK Nr. 11.4 Registered induced seismicity

Risk step 1: Aim

Aim 11 for Safety Region ("Veiligheidsregio"): "*We ensure that everyone can live and work in peace and space*". Therefore, the aim is: no risk or disruption due to hydrogen storage in salt caverns for the population, at all time.

Risk step 2: Risk identification

(1) Risk: Registered induced seismicity caused by the operation (filling and emptying) of the cavern
(2) Risk based on: Interpretation of facts / assumption
(3) Source of information: Monitoring plans of underground Natural Gas and Nitrogen storage[10][11], literature review (section 5.2)
(4) Uncertainty: Research on characteristic locations in the salt dome sensitive to (micro)seismicity
(5) Type of causes: [Rc][Gc]
(6) Type of effects: [Te][Re]

Risk step 3: Risk classification

(1) Classification probability class: 3 (a/c): assumption based on expert judgement and interpretation of facts
(2) Classification consequence class: [Me0][Te2][Se0][Qe0][Re2]

Risk step 4: Dealing with risks

(1) Additional research: research on characteristic locations in the salt dome sensitive to (micro)seismicity
(2) Preventive measures: seismic monitoring (natural and induced seismicity), modelling of expected seismicity, no storage activities in or near an active fault zone, transparency and open communication, baseline measurement, transparency regarding seismic data
(3) Corrective measures: -
(4) Description and classification residual risk considering the measures taken: taking the preventive measures into account the residual risk becomes: 2 (probability) and [Me0][Te2][Se0][Qe0][Re1] (consequences), **2/2**

[10] Nouryon, Micro seismic network Heiligerlee & Zuidwending, observations Q3 2020, Powerpoint, no reference, no date

[11] NAM, Report "Instemmingsbesluit Norg", letter, no reference, dated December 3 2021

RISK Nr. 11.5 Formation of H_2S beyond acceptable limits

Risk step 1: Aim

Aim 11 for Safety Region ("Veiligheidsregio"): "*We ensure that everyone can live and work in peace and space*". Therefore, the aim is: no risk or disruption due to hydrogen storage in salt caverns for the population, at all time.

Risk step 2: Risk identification

(1) Risk: Formation of H_2S beyond acceptable limits caused by anhydrite and other second phases (like carbonates), accelerated by contaminated brine or residual organic (blanket material)
(2) Risk based on: Assumption
(3) Source of information: Literature review (section 5.4)[12] and research[13][14][15][16]
(4) Uncertainty: Additional research on the circumstances leading to the formation of H_2S
(5) Type of causes: [Tc][Gc]
(6) Type of effects: [Me][Te]

Risk step 3: Risk classification

(1) Classification probability class: 3 (a): assumption based on expert judgement
(2) Classification consequence class: [Me1][Te2][Se0][Qe0][Re0]

Risk step 4: Dealing with risks

(1) Additional research: additional research on the circumstances leading to the formation of H_2S, characterize sulphur oxidation state in addition to sulphur abundance, research on the effect on the purity of produced H_2, research on the mix of H_2 and H_2S, research on optimal dimensions of the cavern (reduce reaction surface)
(2) Preventive measures: pH correction, avoid sulphate sources, avoid CO_2 cushion gas, increase iron concentration (binding of sulphate), monitoring of microbial activities, avoid high temperatures (> 80 degrees) because of the abiotic sulphate reduction, avoid presence of hydrocarbons (no use of existing caverns), monitoring of geochemical composition, periodic restoration of sump conditions (see further measures in risk 1.16)
(3) Corrective measures: sweetening of the H_2 gas, pH correction, increase iron concentration, restoration of the sump conditions

[12] M.P.Laban, Hydrogen storage in salt caverns, chemical modelling and analysis of large-scale hydrogen storage in underground salt caverns, no reference, dated July 16 2020
[13] N. Dopffel, Microbial impact on hydrogen storage, NORCE, 2nd International Summer School on UHS, dated July 2023
[14] C.A. Peters, Underground H_2 storage: Geochemistry Considerations, Princeton University, 2nd International Summer School on UHS, dated July 2023
[15] M. Portarapillo & A. di Benedetto, Risk assessment of the large-scale hydrogen storage in salt caverns, article in Energies 14, dated 2021
[16] M. Panfilov, Underground and pipeline hydrogen storage, Compendium of Hydrogen Energy, pp 92-116, dated 2015

(4) *Description and classification residual risk considering the measures taken:* taking the preventive and corrective measures into account the residual risk becomes: 1 (probability) and [Me1][Te1][Se0][Qe0][Re0] (consequences), **1/1**

RISK Nr. 11.6 Failure of the storage system

Risk step 1: Aim

Aim 11 for Safety Region ("Veiligheidsregio"): "*We ensure that everyone can live and work in peace and space*". Therefore, the aim is: no risk or disruption due to hydrogen storage in salt caverns for the population, at all time.

Risk step 2: Risk identification

(1) Risk: Failure of the storage system (due to fire, natural disaster, terrorism or IT-failure)
(2) Risk based on: Assumptions
(3) Source of information: Expert judgement
(4) Uncertainty: Cannot be reduced
(5) Type of causes: [Hc][Oc][Tc][Rc][Ic]
(6) Type of effects: [Me][Te][Se][Qe]

Risk step 3: Risk classification

(1) Classification probability class: 2 (a): assumption based on expert judgement
(2) Classification consequence class: [Me1][Te2][Se3][Qe3][Re2]

Risk step 4: Dealing with risks

(1) Additional research: -
(2) Preventive measures (5 main): adhere to the general safety regulations and fire-prevention measurements for hydrogen installations, back-up by remote-controlled operation, assign as "vital infrastructure" and act accordingly, manual controls requiring double authorisation, analogue pressure and temperature gauges at critical locations (double system) (see further measures in risks 1.19 – 1.22)
(3) Corrective measures: actions according to rapid response plan, fire alarm and fire extinguishing, remote-controlled operation, pressure relief valve (PRV) for worst case when pressure gets near lithostatic pressure at casing shoe, automatic release of pressure
(4) Description and classification residual risk considering the measures taken: taking the preventive and corrective measures into account the residual risk eventually becomes: 1 (probability) and [Me0][Te1][Se0][Qe1][Re1] (consequences), **1/1**

Stakeholder: Safety Region

Unmitigated risk matrix

4 x 3 Risk matrix		Consequence		
		1	2	3
Chance	3		11.2 11.4 11.5	
	2			11.1 11.3 11.6
	1			
	0			

Residual (mitigated) risk matrix

4 x 3 Risk matrix		Consequence		
		1	2	3
Chance	3		11.2	
	2		11.4	
	1	11.5 11.6		11.1 11.3
	0			

D.12 Stakeholder: Gasunie New Energy / Hystock

RISK Nr. 12.1 Accident at the surface

Risk step 1: Aim

Aim 12 for Gasunie New Energy/ HyStock: "*New Energy is a daughter company of Gasunie dealing with business development in renewable energy. In developing projects, we look at technological, financial, economic and social aspects. New forms of energy must not only be sustainable, but also reliable and, of course, socially responsible*". Therefore, the aim is: no risk or disruption due to hydrogen storage in salt caverns for our own operations, at all time.

Risk step 2: Risk identification

(1) Risk: Accident at the surface (blow-out, well leak, pipeline integrity loss) as a result of hydrogen storage
(2) Risk based on: Interpretation of facts / assumptions
(3) Source of information: Literature review[1][2], expert judgement
(4) Uncertainty: Blow-out modelling done by Brouard Consulting, experience within the industry with hydrogen pipelines
(5) Type of causes: [Tc][Hc][Gc][Oc][Rc][Ic]
(6) Type of effects: [Me][Te][Se][Qe][Re]

Risk step 3: Risk classification

(1) Classification probability class: 2 (a/c): assumption based on expert judgement and interpretation of factual information
(2) Classification consequence class: [Me2][Te2][Se1][Qe2][Re2]

Risk step 4: Dealing with risks

(1) Additional research: modelling of Blow-out, safety study on the effect at the surface, literature research hydrogen infrastructure KEM 29 (research in progress)
(2) Preventive measures (5 main): highest quality of BOP and safety valves / pressure gauges (H_2 certified material), all equipment designed for low T, rapid response plan, H_2-certified material (steel), construction and maintenance protocols (see further measures in risks 1.1, 1.2 and 1.4)
(3) Corrective measures: actions according to rapid response plan, evacuation plan, fire extinguishing, damage control / repair, temporary partial shut-down and repair
(4) Description and classification residual risk considering the measures taken: taking the preventive and corrective measures into account the residual risk becomes: 1 (probability) and [Me2][Te2][Se1][Qe2][Re2] (consequences), **1/2**

[1] Fort Saskatchewan Ethane Blow-out and Fire (2001)

[2] Moss Bluff natural gas blow out and Fire (2004)

RISK Nr. 12.2 Subsurface accident

Risk step 1: Aim

Aim 12 for Gasunie New Energy/ HyStock: "*New Energy is a daughter company of Gasunie dealing with business development in renewable energy. In developing projects, we look at technological, financial, economic and social aspects. New forms of energy must not only be sustainable, but also reliable and, of course, socially responsible*". Therefore, the aim is: no risk or disruption due to hydrogen storage in salt caverns for our own operations, at all time.

Risk step 2: Risk identification

(1) *Risk:* Subsurface accident (leakage vertical tubing/casing, casing overstretching, cavern breaches, tensile failure, falls) as a result of hydrogen storage
(2) *Risk based on:* Interpretation of facts / assumptions
(3) *Source of information:* Literature review[3][4][5][6][7], expert judgement
(4) *Uncertainty:* Additional research of the salt structure and rheology, the interaction with hydrogen, mechanical properties and damage evolution. Additional research of materials interacting with hydrogen
(5) *Type of causes*: [Hc][Tc][Rc][Ic][Gc]
(6) *Type of effects*: [Me][Te][Se][Qe][Re]

Risk step 3: Risk classification

(1) *Classification probability class:* 3 (a/c): assumption based on expert judgement and interpretation of factual information
(2) *Classification consequence class:* [Me2][Te2][Se1][Qe3][Re2]

Risk step 4: Dealing with risks

(1) *Additional research (5 main):* creep research (grainsize) and durability of the salt, research of the salt dome internal structure, including anomalous zones (section 3.4.7.1.4), and rheology, additional research of the second phase rheology interacting with hydrogen, research on prevention of micro annuli at the casing / cement / rock interfaces, additional research of materials interacting with hydrogen, (see further research topics in risks 1.3, 1.5, 1.6, 1.8-1,12, 1.14 and 1.15)
(2) *Preventive measures (5 main):* minimum preconditions for H_2 storage cavern (well test), improved cavern design (avoid flat roof / interlayered formations / large diameter of the roof), periodic sonar measurements and cement bonding log, elastomers (no nitril) or self-healing material instead of cement, H_2 and H_2S certified material (including packers), (see further measures in risks 1.3, 1.5, 1.6, 1.8-1,12, 1.14 and 1.15)
(3) *Corrective measures (5 main):* controlled production / flaring of H_2, abandon cavern, adapt the pressures, (micro annuli and material) treatment with special materials (resins, silicates etc.,

[3] Magnolia, Louisiana, 2003
[4] Boling 1, 2, 4, Texas, USA, 2005
[5] Bayou Corne, Louisiana, 2012
[6] Eminence salt dome 1, 3, 4, Mississippi, 1972
[7] Jintan JK-A, China, 2015

biological treatment), use of deformable metals and casing expansion, (see further measures in risks 1.3, 1.5, 1.6, 1.8-1,12, 1.14 and 1.15)

(4) Description and classification residual risk considering the measures taken: taking the preventive and corrective measures into account the residual risk becomes: 3 (probability) and [Me1][Te2][Se2][Qe2][Re2] (consequences), **3/2**

RISK Nr. 12.3 Creep closure and subsidence

Risk step 1: Aim

Aim 12 for Gasunie New Energy/ HyStock: "*New Energy is a daughter company of Gasunie dealing with business development in renewable energy. In developing projects, we look at technological, financial, economic and social aspects. New forms of energy must not only be sustainable, but also reliable and, of course, socially responsible*". Therefore, the aim is: no risk or disruption due to hydrogen storage in salt caverns for our own operations, at all time.

Risk step 2: Risk identification

(1) Risk: Subsidence (beyond predicted limits)
(2) Risk based on: Interpretation of facts
(3) Source of information: Literature review (sections 3.1.5.1 and 3.2.3) [8][9]
(4) Uncertainty: Additional research of the salt structure and rheology, cavern design
(5) Type of causes: [Rc][Ic][Gc][Oc][Tc][Pc]
(6) Type of effects: [Me][Te][Se][Qe][Re]

Risk step 3: Risk classification

(1) Classification probability class: 2 (c): interpretation of factual information
(2) Classification consequence class: [Me2][Te3][Se0][Qe1][Re2]

Risk step 4: Dealing with risks

(1) Additional research: research of the salt structure and rheology, cavern design, geomechanical modelling
(2) Preventive measures: monitoring of subsidence by INSAR & surveying measurements, field tests (pressure observation test POT after well drill), updated cavern design, geomechanical modelling, determination of the minimum cavern pressure (see further measures in risk 1.7)
(3) Corrective measures: change of the average cavern pressure (higher), minimizing the subsidence by controlled abandonment
(4) Description and classification residual risk considering the measures taken: taking the preventive and corrective measures into account the residual risk becomes: 1 (probability) and [Me2][Te3][Se0][Qe1][Re2] (consequences), **1/3**

[8] Subsidence at Maceió, Brazil, 2021

[9] Matarandiba Island, Brazil, 2018

RISK Nr. 12.4 Failure of the storage system

Risk step 1: Aim

Aim 12 for Gasunie New Energy/ HyStock: "*New Energy is a daughter company of Gasunie dealing with business development in renewable energy. In developing projects, we look at technological, financial, economic and social aspects. New forms of energy must not only be sustainable, but also reliable and, of course, socially responsible*". Therefore, the aim is: no risk or disruption due to hydrogen storage in salt caverns for our own operations, at all time.

Risk step 2: Risk identification

(1) Risk: Failure of the storage system (due to fire, natural disaster, terrorism or IT-failure)
(2) Risk based on: Assumptions
(3) Source of information: Expert judgement
(4) Uncertainty: Cannot be reduced
(5) Type of causes: [Hc][Oc][Tc][Rc][Ic]
(6) Type of effects: [Me][Te][Se][Qe][Re]

Risk step 3: Risk classification

(1) Classification probability class: 2 (a): assumption based on expert judgement
(2) Classification consequence class: [Me2][Te2][Se1][Qe3][Re2]

Risk step 4: Dealing with risks

(1) Additional research: -
(2) Preventive measures (5 main): adhere to the general safety regulations and fire-prevention measurements for hydrogen installations, back-up by remote-controlled operation, assign as "vital infrastructure" and act accordingly, manual controls requiring double authorisation, analogue pressure and temperature gauges at critical locations (double system) (see further measures in risks 1.19 – 1.22)
(3) Corrective measures: actions according to rapid response plan, fire alarm and fire extinguishing, remote-controlled operation, pressure relief valve (PRV) for worst case when pressure gets near lithostatic pressure at casing shoe, automatic release of pressure
(4) Description and classification residual risk considering the measures taken: taking the preventive and corrective measures into account the residual risk eventually becomes: 1 (probability) and [Me1][Te1][Se0][Qe1][Re0] (consequences), **1/1**

RISK Nr. 12.5 Emergence of negative public opinion

Risk step 1: Aim

Aim 12 for Gasunie New Energy/ HyStock: "*New Energy is a daughter company of Gasunie dealing with business development in renewable energy. In developing projects, we look at technological, financial, economic and social aspects. New forms of energy must not only be sustainable, but also reliable and, of course, socially responsible*". Therefore, the aim is: no risk or disruption due to hydrogen storage in salt caverns for our own operations, at all time.

Risk step 2: Risk identification

(1) *Risk:* Emergence of negative public opinion, e.g., triggered by regional or national media, threatening the support for the operation of HyStock
(2) *Risk based on:* Interpretation of facts
(3) *Source of information:* public opinion[10][11][12][13][14]
(4) *Uncertainty:* complete stakeholder analysis per location, risk analysis discussion with all stakeholders (separately)
(5) *Type of causes*: [Pc]
(6) *Type of effects*: [Me][Te][Se][Re]

Risk step 3: Risk classification

(1) *Classification probability class:* 3 (c): interpretation of factual information
(2) *Classification consequence class:* [Me2][Te3][Se1][Qe0][Re3]

Risk step 4: Dealing with risks

(1) *Additional research:* complete stakeholder analysis per location, risk analysis discussion with all stakeholders (separately)
(2) *Preventive measures:* transparent, pro-active and personal communication, direct involvement (shareholders), financial compensation ("burdens and benefits"), transparency with respect to all taken preventive measures (other risks)
(3) *Corrective measures:* transparent and personal communication, financial compensation (based on reversed burden of proof), transparency with respect to all taken corrective measures (other risks)
(4) *Description and classification residual risk considering the measures taken:* taking the preventive and corrective measures into account the residual risk eventually becomes: 2 (probability) and [Me1][Te2][Se1][Qe0][Re1] (consequences), **2/2**

[10] Public opinion with respect to CO_2 storage underneath Barendrecht: "Stichting CO2isNEE", 2010
[11] Public opinion with respect to environmental problems and subsidence as a result of salt mining: "Stop Zoutwinning!", 2021
[12] Public opinion with respect to future salt extraction Municipality of Haaksbergen, 2023
[13] Public opinion with respect to underground discharge of production water, www.stopafvalwatertwente.nl
[14] Public opinion with respect to Nitrogen storage in Heiligerlee, www.mijnendijnbelang.nl

RISK Nr. 12.6 Threat for (future) on-shore energy storage

Risk step 1: Aim

Aim 12 for Gasunie New Energy/ HyStock: "*New Energy is a daughter company of Gasunie dealing with business development in renewable energy. In developing projects, we look at technological, financial, economic and social aspects. New forms of energy must not only be sustainable, but also reliable and, of course, socially responsible*". Therefore, the aim is: no risk or disruption due to hydrogen storage in salt caverns for our own operations, at all time.

Risk step 2: Risk identification

(1) Risk: Threat to future hydrogen storage in salt caverns (Licence to Operate) due to uncertainties about safety and consequences of the storage in salt caverns
(2) Risk based on: Assumption
(3) Source of information: Public, press, politics
(4) Uncertainty: (generic and) Site-specific risk assessments, site-specific research on geology, rock-salt properties
(5) Type of causes: [Pc]
(6) Type of effects: [Me][Te][Qe][Re]

Risk step 3: Risk classification

(1) Classification probability class: 3 (a): assumption based on expert judgement
(2) Classification consequence class: [Me3][Te3][Se0][Qe3][Re3]

Risk step 4: Dealing with risks

(1) Additional research: (generic and) site-specific risk assessments, site-specific research on geology and rock-salt properties
(2) Preventive measures (5 main): open pro-active communication with stakeholders (public, politics and press) and other operators, preferably use newly developed caverns (according to an optimal rock mechanical envelope), periodic leak tests, minimum preconditions for H_2 storage cavern, mandatory status-report (starting every year) (see further measures in risk 1.24)
(3) Corrective measures: open communication with stakeholders (public, politics and press) and other operators
(4) Description and classification residual risk considering the measures taken: taking the preventive and corrective measures into account the residual risk eventually becomes: 2 (probability) and [Me1][Te3][Se0][Qe0][Re2] (consequences), **2/3**

Stakeholder: Gasunie New Energy/ HyStock

Unmitigated risk matrix

4 x 3 Risk matrix		Consequence		
		1	2	3
Chance	3		12.2	12.5 12.6
	2		12.1	12.3 12.4
	1			
	0			

Residual (mitigated) risk matrix

4 x 3 Risk matrix		Consequence		
		1	2	3
Chance	3		12.2	
	2		12.5	12.6
	1	12.4	12.1	12.3
	0			

D.13 Stakeholder: Gasunie Transport Services (nitrogen storage)

RISK Nr. 13.1 Accident at the surface

Risk step 1: Aim

Aim 13 for Gasunie Transport Services, owner and operator of the cavern containing nitrogen gas (GTS Heiligerlee): "*We offer gas transport services in a customer-orientated and transparent way. Safety, reliability, sustainability and cost-awareness are our priorities. We serve the public interest and operate professionally to create value for our stakeholders*". Therefore, the aim is: no risk or disruption due to hydrogen storage in salt caverns for our own operations, at all time.

Risk step 2: Risk identification

(1) Risk: Accident at the surface (blow-out, well leak, pipeline integrity loss) as a result of hydrogen storage
(2) Risk based on: Interpretation of facts / assumptions
(3) Source of information: Literature review[1][2], expert judgement
(4) Uncertainty: Blow-out modelling done by Brouard Consulting, experience within the industry with hydrogen pipelines
(5) Type of causes: [Tc][Hc][Gc][Oc][Rc][Ic]
(6) Type of effects: [Me][Te][Re]

Risk step 3: Risk classification

(1) Classification probability class: 2 (a/c): assumption based on expert judgement and interpretation of factual information
(2) Classification consequence class: [Me1][Te2][Se0][Qe0][Re1]

Risk step 4: Dealing with risks

(1) Additional research: modelling of Blow-out, safety study on the effect at the surface, literature research hydrogen infrastructure KEM 29 (research in progress)
(2) Preventive measures (5 main): highest quality of BOP and safety valves / pressure gauges (H_2 certified material), all equipment designed for low T, rapid response plan, H_2-certified material (steel), construction and maintenance protocols (see further measures in risks 1.1, 1.2 and 1.4)
(3) Corrective measures: actions according to rapid response plan, evacuation plan, fire extinguishing, damage control / repair, temporary partial shut-down and repair
(4) Description and classification residual risk considering the measures taken: taking the preventive and corrective measures into account the residual risk becomes: 1 (probability) and [Me1][Te2][Se0][Qe0][Re1] (consequences), **1/2**

[1] Fort Saskatchewan Ethane Blow-out and Fire (2001)

[2] Moss Bluff natural gas blow out and Fire (2004)

RISK Nr. 13.2 Subsurface accident

Risk step 1: Aim

Aim 13 for Gasunie Transport Services, owner and operator of the cavern containing nitrogen gas (GTS Heiligerlee): "*We offer gas transport services in a customer-orientated and transparent way. Safety, reliability, sustainability and cost-awareness are our priorities. We serve the public interest and operate professionally to create value for our stakeholders*". Therefore, the aim is: no risk or disruption due to hydrogen storage in salt caverns for our own operations, at all time.

Risk step 2: Risk identification

(1) *Risk:* Subsurface accident (leakage vertical tubing/casing, casing overstretching, cavern breaches, tensile failure, falls) as a result of hydrogen storage
(2) *Risk based on:* Interpretation of facts / assumptions
(3) *Source of information:* Literature review[3][4][5][6][7], expert judgement
(4) *Uncertainty:* Additional research of the salt structure and rheology, the interaction with hydrogen, mechanical properties and damage evolution. Additional research of materials interacting with hydrogen
(5) *Type of causes*: [Hc][Tc][Rc][Ic][Gc]
(6) *Type of effects*: [Me][Te][Re]

Risk step 3: Risk classification

(1) *Classification probability class:* 3 (a/c): assumption based on expert judgement and interpretation of factual information
(2) *Classification consequence class:* [Me1][Te2][Se0][Qe0][Re1]

Risk step 4: Dealing with risks

(1) *Additional research (5 main):* creep research (grainsize) and durability of the salt, research of the salt dome internal structure, including anomalous zones (section 3.4.7.1.4), and rheology, additional research of the second phase rheology interacting with hydrogen, research on prevention of micro annuli at the casing / cement / rock interfaces, additional research of materials interacting with hydrogen, (see further research topics in risks 1.3, 1.5, 1.6, 1.8-1,12, 1.14 and 1.15)
(2) *Preventive measures (5 main):* minimum preconditions for H_2 storage cavern (well test), improved cavern design (avoid flat roof / interlayered formations / large diameter of the roof), periodic sonar measurements and cement bonding log, elastomers (no nitril) or self-healing material instead of cement, H_2 and H_2S certified material (including packers), (see further measures in risks 1.3, 1.5, 1.6, 1.8-1,12, 1.14 and 1.15)
(3) *Corrective measures (5 main):* controlled production / flaring of H_2, abandon cavern, adapt the pressures, (micro annuli and material) treatment with special materials (resins, silicates etc.,

[3] Magnolia, Louisiana, 2003
[4] Boling 1, 2, 4, Texas, USA, 2005
[5] Bayou Corne, Louisiana, 2012
[6] Eminence salt dome 1, 3, 4, Mississippi, 1972
[7] Jintan JK-A, China, 2015

biological treatment), use of deformable metals and casing expansion, (see further measures in risks 1.3, 1.5, 1.6, 1.8-1,12, 1.14 and 1.15)

(4) Description and classification residual risk considering the measures taken: Both probability and consequence classes have not been reduced and remain: **3/2**, in more detail 3 (probability) and [Me1][Te2][Se0][Qe0][Re1] (consequences)

RISK Nr. 13.3 Creep closure and subsidence

Risk step 1: Aim

Aim 13 for Gasunie Transport Services, owner and operator of the cavern containing nitrogen gas (GTS Heiligerlee): "*We offer gas transport services in a customer-orientated and transparent way. Safety, reliability, sustainability and cost-awareness are our priorities. We serve the public interest and operate professionally to create value for our stakeholders*". Therefore, the aim is: no risk or disruption due to hydrogen storage in salt caverns for our own operations, at all time.

Risk step 2: Risk identification

(1) Risk: Subsidence (beyond predicted limits)
(2) Risk based on: Interpretation of facts
(3) Source of information: Literature review (sections 3.1.5.1 and 3.2.3) [8][9]
(4) Uncertainty: Additional research of the salt structure and rheology, cavern design
(5) Type of causes: [Rc][Ic][Gc][Oc][Tc][Pc]
(6) Type of effects: [Qe][Re]

Risk step 3: Risk classification

(1) Classification probability class: 2 (c): interpretation of factual information
(2) Classification consequence class: [Me0][Te0][Se0][Qe1][Re2]

Risk step 4: Dealing with risks

(1) Additional research: research of the salt structure and rheology, cavern design, geomechanical modelling
(2) Preventive measures: monitoring of subsidence by INSAR & surveying measurements, field tests (pressure observation test POT after well drill), updated cavern design, geomechanical modelling, determination of the minimum cavern pressure (see further measures in risk 1.7)
(3) Corrective measures: change of the average cavern pressure (higher), minimizing the subsidence by controlled abandonment
(4) Description and classification residual risk considering the measures taken: taking the preventive and corrective measures into account the residual risk becomes: 1 (probability) and [Me0][Te0][Se0][Qe1][Re2] (consequences), **1/2**

[8] Subsidence at Maceió, Brazil, 2021

[9] Matarandiba Island, Brazil, 2018

RISK Nr. 13.4 Failure of the storage system

Risk step 1: Aim

Aim 13 for Gasunie Transport Services, owner and operator of the cavern containing nitrogen gas (GTS Heiligerlee): "*We offer gas transport services in a customer-orientated and transparent way. Safety, reliability, sustainability and cost-awareness are our priorities. We serve the public interest and operate professionally to create value for our stakeholders*". Therefore, the aim is: no risk or disruption due to hydrogen storage in salt caverns for our own operations, at all time.

Risk step 2: Risk identification

(1) Risk: Failure of the storage system (due to fire, natural disaster, terrorism or IT-failure)
(2) Risk based on: Assumptions
(3) Source of information: Expert judgement
(4) Uncertainty: Cannot be reduced
(5) Type of causes: [Hc][Oc][Tc][Rc][Ic]
(6) Type of effects: [Me][Te][Se][Qe][Re]

Risk step 3: Risk classification

(1) Classification probability class: 2 (a): assumption based on expert judgement
(2) Classification consequence class: [Me1][Te2][Se0][Qe3][Re1]

Risk step 4: Dealing with risks

(1) Additional research: -
(2) Preventive measures (5 main): adhere to the general safety regulations and fire-prevention measurements for hydrogen installations, back-up by remote-controlled operation, assign as "vital infrastructure" and act accordingly, manual controls requiring double authorisation, analogue pressure and temperature gauges at critical locations (double system) (see further measures in risks 1.19 – 1.22)
(3) Corrective measures: actions according to rapid response plan, fire alarm and fire extinguishing, remote-controlled operation, pressure relief valve (PRV) for worst case when pressure gets near lithostatic pressure at casing shoe, automatic release of pressure
(4) Description and classification residual risk considering the measures taken: taking the preventive and corrective measures into account the residual risk eventually becomes: 1 (probability) and [Me0][Te1][Se0][Qe1][Re0] (consequences), **1/1**

RISK Nr. 13.5 Emergence of negative public opinion

Risk step 1: Aim

Aim 13 for Gasunie Transport Services, owner and operator of the cavern containing nitrogen gas (GTS Heiligerlee): "*We offer gas transport services in a customer-orientated and transparent way. Safety, reliability, sustainability and cost-awareness are our priorities. We serve the public interest and operate professionally to create value for our stakeholders*". Therefore, the aim is: no risk or disruption due to hydrogen storage in salt caverns for our own operations, at all time.

Risk step 2: Risk identification

(1) Risk: Emergence of negative public opinion, e.g., triggered by regional or national media, threatening the support for storage of nitrogen by GTS
(2) Risk based on: Interpretation of facts
(3) Source of information: public opinion[10][11][12][13][14]
(4) Uncertainty: complete stakeholder analysis per location, risk analysis discussion with all stakeholders (separately)
(5) Type of causes: [Pc]
(6) Type of effects: [Te][Re]

Risk step 3: Risk classification

(1) Classification probability class: 3 (c): interpretation of factual information
(2) Classification consequence class: [Me0][Te2][Se0][Qe0][Re2]

Risk step 4: Dealing with risks

(1) Additional research: complete stakeholder analysis per location, risk analysis discussion with all stakeholders (separately)
(2) Preventive measures: transparent, pro-active and personal communication, direct involvement (shareholders), financial compensation ("burdens and benefits"), transparency with respect to all taken preventive measures (other risks)
(3) Corrective measures: transparent and personal communication, financial compensation (based on reversed burden of proof), transparency with respect to all taken corrective measures (other risks)
(4) *Description and classification residual risk considering the measures taken:* taking the preventive and corrective measures into account the residual risk eventually becomes: 2 (probability) and [Me0][Te1][Se0][Qe0][Re1] (consequences), **2/1**

[10] Public opinion with respect to CO_2 storage underneath Barendrecht: "Stichting CO2isNEE", 2010
[11] Public opinion with respect to environmental problems and subsidence as a result of salt mining: "Stop Zoutwinning!", 2021
[12] Public opinion with respect to future salt extraction Municipality of Haaksbergen, 2023
[13] Public opinion with respect to underground discharge of production water, www.stopafvalwatertwente.nl
[14] Public opinion with respect to Nitrogen storage in Heiligerlee, www.mijnendijnbelang.nl

RISK Nr. 13.6 Threat for (future) on-shore energy storage

Risk step 1: Aim

Aim 13 for Gasunie Transport Services, owner and operator of the cavern containing nitrogen gas (GTS Heiligerlee): "*We offer gas transport services in a customer-orientated and transparent way. Safety, reliability, sustainability and cost-awareness are our priorities. We serve the public interest and operate professionally to create value for our stakeholders*". Therefore, the aim is: no risk or disruption due to hydrogen storage in salt caverns for our own operations, at all time.

Risk step 2: Risk identification

(1) Risk: Threat to future nitrogen storage in salt caverns (Licence to Operate) due to uncertainties about safety and consequences of the storage in salt caverns
(2) Risk based on: Assumption
(3) Source of information: Public, press, politics
(4) Uncertainty: (generic and) Site-specific risk assessments, site-specific research on geology, rock-salt properties
(5) Type of causes: [Pc]
(6) Type of effects: [Me][Te][Qe][Re]

Risk step 3: Risk classification

(1) Classification probability class: 3 (a): assumption based on expert judgement
(2) Classification consequence class: [Me2][Te3][Se0][Qe3][Re3]

Risk step 4: Dealing with risks

(1) Additional research: (generic and) site-specific risk assessments, site-specific research on geology and rock-salt properties
(2) Preventive measures (5 main): open pro-active communication with stakeholders (public, politics and press) and other operators, preferably use newly developed caverns (according to an optimal rock mechanical envelope), periodic leak tests, minimum preconditions for H_2 storage cavern, mandatory status-report (starting every year) (see further measures in risk 1.24)
(3) Corrective measures: open communication with stakeholders (public, politics and press) and other operators
(4) Description and classification residual risk considering the measures taken: taking the preventive and corrective measures into account the residual risk eventually becomes: 2 (probability) and [Me1][Te3][Se0][Qe0][Re2] (consequences), **2/3**

Stakeholder: Gasunie Transport Services (nitrogen storage)

Unmitigated risk matrix

4 x 3 Risk matrix		Consequence		
		1	2	3
Chance	3		13.2 13.5	13.6
	2		13.1 13.3	13.4
	1			
	0			

Residual (mitigated) risk matrix

4 x 3 Risk matrix		Consequence		
		1	2	3
Chance	3		13.2	
	2	13.5		13.6
	1	13.4	13.1 13.3	
	0			

D.14 Stakeholder: Gasunie / Energystock

RISK Nr. 14.1 Accident at the surface

Risk step 1: Aim

Aim 14 for Gasunie / Energystock, of the caverns containing natural gas (Zuidwending): "*We serve the public interest, offer integrated transport and infrastructure services to our customers and adhere to the highest safety and business standards. We focus on short and long term value creation for our shareholder(s), other stakeholders and the environment*". Therefore, the aim is: no risk or disruption due to hydrogen storage in salt caverns for our own operations, at all time.

Risk step 2: Risk identification

(1) Risk: Accident at the surface (blow-out, well leak, pipeline integrity loss) as a result of hydrogen storage
(2) Risk based on: Interpretation of facts / assumptions
(3) Source of information: Literature review[1][2], expert judgement
(4) Uncertainty: Blow-out modelling done by Brouard Consulting, experience within the industry with hydrogen pipelines
(5) Type of causes: [Tc][Hc][Gc][Oc][Rc][Ic]
(6) Type of effects: [Me][Te][Se][Qe][Re]

Risk step 3: Risk classification

(1) Classification probability class: 2 (a/c): assumption based on expert judgement and interpretation of factual information
(2) Classification consequence class: [Me2][Te2][Se1][Qe2][Re2]

Risk step 4: Dealing with risks

(1) Additional research: modelling of Blow-out, safety study on the effect at the surface, literature research hydrogen infrastructure KEM 29 (research in progress)
(2) Preventive measures (5 main): highest quality of BOP and safety valves / pressure gauges (H_2 certified material), all equipment designed for low T, rapid response plan, H_2-certified material (steel), construction and maintenance protocols (see further measures in risks 1.1, 1.2 and 1.4)
(3) Corrective measures: actions according to rapid response plan, evacuation plan, fire extinguishing, damage control / repair, temporary partial shut-down and repair
(4) Description and classification residual risk considering the measures taken: taking the preventive and corrective measures into account the residual risk becomes: 1 (probability) and [Me2][Te2][Se1][Qe2][Re2] (consequences), **1/2**

[1] Fort Saskatchewan Ethane Blow-out and Fire (2001)

[2] Moss Bluff natural gas blow out and Fire (2004)

RISK Nr. 14.2 Subsurface accident

Risk step 1: Aim

Aim 14 for Gasunie / Energystock, of the caverns containing natural gas (Zuidwending): "*We serve the public interest, offer integrated transport and infrastructure services to our customers and adhere to the highest safety and business standards. We focus on short and long term value creation for our shareholder(s), other stakeholders and the environment*". Therefore, the aim is: no risk or disruption due to hydrogen storage in salt caverns for our own operations, at all time.

Risk step 2: Risk identification

(1) Risk: Subsurface accident (leakage vertical tubing/casing, casing overstretching, cavern breaches, tensile failure, falls) as a result of hydrogen storage
(2) Risk based on: Interpretation of facts / assumptions
(3) Source of information: Literature review[3][4][5][6][7], expert judgement
(4) Uncertainty: Additional research of the salt structure and rheology, the interaction with hydrogen, mechanical properties and damage evolution. Additional research of materials interacting with hydrogen
(5) Type of causes: [Hc][Tc][Rc][Ic][Gc]
(6) Type of effects: [Me][Te][Qe][Re]

Risk step 3: Risk classification

(1) Classification probability class: 3 (a/c): assumption based on expert judgement and interpretation of factual information
(2) Classification consequence class: [Me2][Te2][Se0][Qe1][Re2]

Risk step 4: Dealing with risks

(1) Additional research (5 main): creep research (grainsize) and durability of the salt, research of the salt dome internal structure, including anomalous zones (section 3.4.7.1.4), and rheology, additional research of the second phase rheology interacting with hydrogen, research on prevention of micro annuli at the casing / cement / rock interfaces, additional research of materials interacting with hydrogen, (see further research topics in risks 1.3, 1.5, 1.6, 1.8-1,12, 1.14 and 1.15)
(2) Preventive measures (5 main): minimum preconditions for H_2 storage cavern (well test), improved cavern design (avoid flat roof / interlayered formations / large diameter of the roof), periodic sonar measurements and cement bonding log, elastomers (no nitril) or self-healing material instead of cement, H_2 and H_2S certified material (including packers), (see further measures in risks 1.3, 1.5, 1.6, 1.8-1,12, 1.14 and 1.15)
(3) Corrective measures (5 main): controlled production / flaring of H_2, abandon cavern, adapt the pressures, (micro annuli and material) treatment with special materials (resins, silicates etc.,

[3] Magnolia, Louisiana, 2003
[4] Boling 1, 2, 4, Texas, USA, 2005
[5] Bayou Corne, Louisiana, 2012
[6] Eminence salt dome 1, 3, 4, Mississippi, 1972
[7] Jintan JK-A, China, 2015

biological treatment), use of deformable metals and casing expansion, (see further measures in risks 1.3, 1.5, 1.6, 1.8-1,12, 1.14 and 1.15)

(4) Description and classification residual risk considering the measures taken: Both probability and consequence classes have not been reduced and remain: **3/2**, in more detail 3 (probability) and [Me1][Te2][Se0][Qe1][Re2] (consequences)

RISK Nr. 14.3 Creep closure and subsidence

Risk step 1: Aim

Aim 14 for Gasunie / Energystock, of the caverns containing natural gas (Zuidwending): "*We serve the public interest, offer integrated transport and infrastructure services to our customers and adhere to the highest safety and business standards. We focus on short and long term value creation for our shareholder(s), other stakeholders and the environment*". Therefore, the aim is: no risk or disruption due to hydrogen storage in salt caverns for our own operations, at all time.

Risk step 2: Risk identification

(1) Risk: Subsidence (beyond predicted limits)
(2) Risk based on: Interpretation of facts
(3) Source of information: Literature review (sections 3.1.5.1 and 3.2.3) [8][9]
(4) Uncertainty: Additional research of the salt structure and rheology, cavern design
(5) Type of causes: [Rc][Ic][Gc][Oc][Tc][Pc]
(6) Type of effects: [Me][Te][Qe][Re]

Risk step 3: Risk classification

(1) Classification probability class: 2 (c): interpretation of factual information
(2) Classification consequence class: [Me1][Te3][Se0][Qe1][Re1]

Risk step 4: Dealing with risks

(1) Additional research: research of the salt structure and rheology, cavern design, geomechanical modelling
(2) Preventive measures: monitoring of subsidence by INSAR & surveying measurements, field tests (pressure observation test POT after well drill), updated cavern design, geomechanical modelling, determination of the minimum cavern pressure (see further measures in risk 1.7)
(3) Corrective measures: change of the average cavern pressure (higher), minimizing the subsidence by controlled abandonment
(4) Description and classification residual risk considering the measures taken: taking the preventive and corrective measures into account the residual risk becomes: 1 (probability) and [Me1][Te3][Se0][Qe1][Re1] (consequences), **1/3**

[8] Subsidence at Maceió, Brazil, 2021
[9] Matarandiba Island, Brazil, 2018

RISK Nr. 14.4 Failure of the storage system

Risk step 1: Aim

Aim 14 for Gasunie / Energystock, of the caverns containing natural gas (Zuidwending): "*We serve the public interest, offer integrated transport and infrastructure services to our customers and adhere to the highest safety and business standards. We focus on short and long term value creation for our shareholder(s), other stakeholders and the environment*". Therefore, the aim is: no risk or disruption due to hydrogen storage in salt caverns for our own operations, at all time.

Risk step 2: Risk identification

(1) Risk: Failure of the storage system (due to fire, natural disaster, terrorism or IT-failure)
(2) Risk based on: Assumptions
(3) Source of information: Expert judgement
(4) Uncertainty: Cannot be reduced
(5) Type of causes: [Hc][Oc][Tc][Rc][Ic]
(6) Type of effects: [Me][Te][Qe][Re]

Risk step 3: Risk classification

(1) Classification probability class: 2 (a): assumption based on expert judgement
(2) Classification consequence class: [Me1][Te2][Se0][Qe3][Re1]

Risk step 4: Dealing with risks

(1) Additional research: -
(2) Preventive measures (5 main): adhere to the general safety regulations and fire-prevention measurements for hydrogen installations, back-up by remote-controlled operation, assign as "vital infrastructure" and act accordingly, manual controls requiring double authorisation, analogue pressure and temperature gauges at critical locations (double system) (see further measures in risks 1.19 – 1.22)
(3) Corrective measures: actions according to rapid response plan, fire alarm and fire extinguishing, remote-controlled operation, pressure relief valve (PRV) for worst case when pressure gets near lithostatic pressure at casing shoe, automatic release of pressure
(4) Description and classification residual risk considering the measures taken: taking the preventive and corrective measures into account the residual risk eventually becomes: 1 (probability) and [Me0][Te1][Se0][Qe1][Re0] (consequences), **1/1**

RISK Nr. 14.5 Emergence of negative public opinion

Risk step 1: Aim

Aim 14 for Gasunie / Energystock, of the caverns containing natural gas (Zuidwending): "*We serve the public interest, offer integrated transport and infrastructure services to our customers and adhere to the highest safety and business standards. We focus on short and long term value creation for our shareholder(s), other stakeholders and the environment*". Therefore, the aim is: no risk or disruption due to hydrogen storage in salt caverns for our own operations, at all time.

Risk step 2: Risk identification

(1) *Risk:* Emergence of negative public opinion, e.g., triggered by regional or national media, threatening the support for the operation of Energystock
(2) *Risk based on:* Interpretation of facts
(3) *Source of information:* public opinion[10][11][12][13][14]
(4) *Uncertainty:* complete stakeholder analysis per location, risk analysis discussion with all stakeholders (separately)
(5) *Type of causes*: [Pc]
(6) *Type of effects*: [Te][Re]

Risk step 3: Risk classification

(1) *Classification probability class:* 3 (c): interpretation of factual information
(2) *Classification consequence class:* [Me0][Te3][Se0][Qe0][Re2]

Risk step 4: Dealing with risks

(1) *Additional research:* complete stakeholder analysis per location, risk analysis discussion with all stakeholders (separately)
(2) *Preventive measures:* transparent, pro-active and personal communication, direct involvement (shareholders), financial compensation ("burdens and benefits"), transparency with respect to all taken preventive measures (other risks)
(3) *Corrective measures:* transparent and personal communication, financial compensation (based on reversed burden of proof), transparency with respect to all taken corrective measures (other risks)
(4) *Description and classification residual risk considering the measures taken:* taking the preventive and corrective measures into account the residual risk eventually becomes: 2 (probability) and [Me0][Te2][Se0][Qe0][Re1] (consequences), **2/2**

[10] Public opinion with respect to CO_2 storage underneath Barendrecht: "Stichting CO2isNEE", 2010
[11] Public opinion with respect to environmental problems and subsidence as a result of salt mining: "Stop Zoutwinning!", 2021
[12] Public opinion with respect to future salt extraction Municipality of Haaksbergen, 2023
[13] Public opinion with respect to underground discharge of production water, www.stopafvalwatertwente.nl
[14] Public opinion with respect to Nitrogen storage in Heiligerlee, www.mijnendijnbelang.nl

RISK Nr. 14.6 Threat for (future) on-shore energy storage

Risk step 1: Aim

Aim 14 for Gasunie / Energystock, of the caverns containing natural gas (Zuidwending): "*We serve the public interest, offer integrated transport and infrastructure services to our customers and adhere to the highest safety and business standards. We focus on short and long term value creation for our shareholder(s), other stakeholders and the environment*". Therefore, the aim is: no risk or disruption due to hydrogen storage in salt caverns for our own operations, at all time.

Risk step 2: Risk identification

(1) Risk: Threat to future natural gas storage in salt caverns (Licence to Operate) due to uncertainties about safety and consequences of the storage in salt caverns
(2) Risk based on: Assumption
(3) Source of information: Public, press, politics
(4) Uncertainty: (generic and) Site-specific risk assessments, site-specific research on geology, rock-salt properties
(5) Type of causes: [Pc]
(6) Type of effects: [Me][Te][Qe][Re]

Risk step 3: Risk classification

(1) Classification probability class: 3 (a): assumption based on expert judgement
(2) Classification consequence class: [Me2][Te3][Se0][Qe3][Re3]

Risk step 4: Dealing with risks

(1) Additional research: (generic and) site-specific risk assessments, site-specific research on geology and rock-salt properties
(2) Preventive measures (5 main): open pro-active communication with stakeholders (public, politics and press) and other operators, preferably use newly developed caverns (according to an optimal rock mechanical envelope), periodic leak tests, minimum preconditions for H_2 storage cavern, mandatory status-report (starting every year) (see further measures in risk 1.24)
(3) Corrective measures: open communication with stakeholders (public, politics and press) and other operators
(4) Description and classification residual risk considering the measures taken: taking the preventive and corrective measures into account the residual risk eventually becomes: 2 (probability) and [Me0][Te3][Se0][Qe0][Re2] (consequences), **2/3**

Stakeholder: Gasunie New Energy/ HyStock

Unmitigated risk matrix

4 x 3 Risk matrix		Consequence		
		1	2	3
Chance	3		14.2	14.5 14.6
	2		14.1	14.3 14.4
	1			
	0			

Residual (mitigated) risk matrix

4 x 3 Risk matrix		Consequence		
		1	2	3
Chance	3		14.2	
	2		14.5	14.6
	1	14.4	14.1	14.3
	0			

D.15 Stakeholder: Water Company Groningen

RISK Nr. 15.1 Cavern integrity loss

Risk step 1: Aim

Aim 15 for Water Company Groningen ("Waterbedrijf Groningen"): "*As a social enterprise we want to secure the water interests in the region in a sustainable way. We are not just the supplier of drinking water but we also participate in matters such as public health, nature conservation, creation of sustainable sources … and innovation*". Therefore, the aim is: no risk as a result of hydrogen storage in salt caverns, that is protection of the groundwater protection area of WCG being a reliable supplier.

Risk step 2: Risk identification

(1) Risk: Cavern breaches (tightness) / cavern integrity loss
(2) Risk based on: Interpretation of facts
(3) Source of information: Literature review (7 cases described in section 2.2.3.1) [1][2]
(4) Uncertainty: Additional research of the salt structure and rheology, cavern design
(5) Type of causes: [Tc][Rc][Gc][Oc][Ic]
(6) Type of effects: [Me][Te][Se][Qe][Re]

Risk step 3: Risk classification

(1) Classification probability class: 2 ©: interpretation of factual information
(2) Classification consequence class: [Me1][Te2][Se0][Qe3][Re2]

Risk step 4: Dealing with risks

(1) Additional research: research of the salt dome internal structure, including anomalous zones (section 3.4.7.1.4), and rheology, cavern design
(2) Preventive measures: periodic leak tests, open communication with other operators, sonar surveys, GPR (radar), minimum preconditions for H_2 storage cavern, detection of heterogeneities, enough distance to the domes edge, tightness test, prevent responsibility gap, leakage report obligation, preferably use newly developed caverns (according to an optimal rock mechanical envelope) (see further measures in risk 1.6)
(3) Corrective measures: abandon cavern
(4) Description and classification residual risk considering the measures taken: taking the preventive and corrective measures into account the residual risk becomes: 1 (probability) and [Me1][Te2][Se0][Qe3][Re2] (consequences), **1/3**

[1] Bayou Corne, Louisiana, 2012

[2] Clovelly salt dome, Louisiana, 1992

RISK Nr. 15.2 Formation of H_2S beyond acceptable limits

Risk step 1: Aim

Aim 15 for Water Company Groningen ("Waterbedrijf Groningen"): "*As a social enterprise we want to secure the water interests in the region in a sustainable way. We are not just the supplier of drinking water but we also participate in matters such as public health, nature conservation, creation of sustainable sources … and innovation*". Therefore, the aim is: no risk as a result of hydrogen storage in salt caverns, that is protection of the groundwater protection area of WCG being a reliable supplier.

Risk step 2: Risk identification

(1) Risk: Formation of H_2S leading to contamination of the groundwater due to leakage
(2) Risk based on: Assumption
(3) Source of information: Literature review (section 5.4)[3] and research[4][5][6][7]
(4) Uncertainty: Additional research on the circumstances leading to the formation of H_2S
(5) Type of causes: [Tc][Gc]
(6) Type of effects: [Me][Te][Qe]

Risk step 3: Risk classification

(1) Classification probability class: 3 (a): assumption based on expert judgement
(2) Classification consequence class: [Me1][Te2][Se0][Qe2][Re0]

Risk step 4: Dealing with risks

(1) Additional research: additional research on the circumstances leading to the formation of H_2S, characterize sulphur oxidation state in addition to sulphur abundance, research on the effect on the purity of produced H_2, research on the mix of H_2 and H_2S, research on optimal dimensions of the cavern (reduce reaction surface)
(2) Preventive measures: avoid sulphate sources, monitoring of microbial activities, avoid presence of hydrocarbons (no use of existing caverns), monitoring of geochemical composition, periodic restoration of sump conditions (see further measures in risk 1.16)
(3) Corrective measures: pH correction, increase iron concentration, restoration of sump conditions
(4) Description and classification residual risk considering the measures taken: taking the preventive and corrective measures into account the residual risk becomes: 1 (probability) and [Me1][Te2][Se0][Qe1][Re0] (consequences), **1/2**

[3] M.P.Laban, Hydrogen storage in salt caverns, chemical modelling and analysis of large-scale hydrogen storage in underground salt caverns, no reference, dated July 16 2020
[4] N. Dopffel, Microbial impact on hydrogen storage, NORCE, 2nd International Summer School on UHS, dated July 2023
[5] C.A. Peters, Underground H_2 storage: Geochemistry Considerations, Princeton University, 2nd International Summer School on UHS, dated July 2023
[6] M. Portarapillo & A. di Benedetto, Risk assessment of the large-scale hydrogen storage in salt caverns, article in Energies 14, dated 2021
[7] M. Panfilov, Underground and pipeline hydrogen storage, Compendium of Hydrogen Energy, pp 92-116, dated 2015

RISK Nr. 15.3 Emergence of negative public opinion

Risk step 1: Aim

Aim 15 for Water Company Groningen ("Waterbedrijf Groningen"): "*As a social enterprise we want to secure the water interests in the region in a sustainable way. We are not just the supplier of drinking water but we also participate in matters such as public health, nature conservation, creation of sustainable sources … and innovation*". Therefore, the aim is: no risk as a result of hydrogen storage in salt caverns, that is protection of the groundwater protection area of WCG being a reliable supplier.

Risk step 2: Risk identification

(1) *Risk:* Emergence of negative public opinion, e.g., triggered by regional or national media, threatening the public image of the Water Company
(2) *Risk based on:* Interpretation of facts
(3) *Source of information:* public opinion[8][9][10][11][12]
(4) *Uncertainty:* complete stakeholder analysis per location, risk analysis discussion with all stakeholders (separately)
(5) *Type of causes*: [Pc]
(6) *Type of effects*: [Te][Re]

Risk step 3: Risk classification

(1) *Classification probability class:* 3 ©: interpretation of factual information
(2) *Classification consequence class:* [Me0][Te2][Se0][Qe0][Re1]

Risk step 4: Dealing with risks

(1) *Additional research:* complete stakeholder analysis per location, risk analysis discussion with all stakeholders (separately)
(2) *Preventive measures:* transparent, pro-active and personal communication, direct involvement (shareholders), financial compensation ("burdens and benefits"), transparency with respect to all taken preventive measures (other risks)
(3) *Corrective measures:* transparent and personal communication, financial compensation (based on reversed burden of proof), transparency with respect to all taken corrective measures (other risks)
(4) *Description and classification residual risk considering the measures taken:* taking the preventive and corrective measures into account the residual risk eventually becomes: 2 (probability) and [Me0][Te1][Se0][Qe0][Re0] (consequences), **2/1**

[8] Public opinion with respect to CO_2 storage underneath Barendrecht: "Stichting CO2isNEE", 2010
[9] Public opinion with respect to environmental problems and subsidence as a result of salt mining: "Stop Zoutwinning!", 2021
[10] Public opinion with respect to future salt extraction Municipality of Haaksbergen, 2023
[11] Public opinion with respect to underground discharge of production water, www.stopafvalwatertwente.nl
[12] Public opinion with respect to Nitrogen storage in Heiligerlee, www.mijnendijnbelang.nl

Stakeholder: Water Company Groningen

Unmitigated risk matrix

4 x 3 Risk matrix		Consequence		
		1	2	3
Chance	3		15.2 15.3	
	2			15.1
	1			
	0			

Residual (mitigated) risk matrix

4 x 3 Risk matrix		Consequence		
		1	2	3
Chance	3			
	2	15.3		
	1		15.2	15.1
	0			

D.16 Stakeholder: Water Company Drenthe

RISK Nr. 16.1 Cavern integrity loss

Risk step 1: Aim

Aim 16 for Water Company Drenthe ("Waterleiding Maatschappij Drenthe"): "*WMD provides impeccable drinking water at an acceptable cost for everyone in Drenthe, generation after generation*". Therefore, the aim is: no risk as a result of hydrogen storage in salt caverns, that is protection of the groundwater protection area of WCD being a reliable supplier.

Risk step 2: Risk identification

(1) Risk: Cavern breaches (tightness) / cavern integrity loss
(2) Risk based on: Interpretation of facts
(3) Source of information: Literature review (7 cases described in section 2.2.3.1) [1][2]
(4) Uncertainty: Additional research of the salt structure and rheology, cavern design
(5) Type of causes: [Tc][Rc][Gc][Oc][Ic]
(6) Type of effects: [Me][Te][Se][Qe][Re]

Risk step 3: Risk classification

(1) Classification probability class: 2 (c): interpretation of factual information
(2) Classification consequence class: [Me1][Te2][Se0][Qe3][Re2]

Risk step 4: Dealing with risks

(1) Additional research: research of the salt dome internal structure, including anomalous zones (section 3.4.7.1.4), and rheology, cavern design
(2) Preventive measures: open communication with other operators, minimum preconditions for H_2 storage cavern, detection of heterogeneities, enough distance to the domes edge, preferably use newly developed caverns (according to an optimal rock mechanical envelope) (see further measures in risk 1.6)
(3) Corrective measures: abandon cavern
(4) Description and classification residual risk considering the measures taken: taking the preventive and corrective measures into account the residual risk becomes: 1 (probability) and [Me1][Te2][Se0][Qe3][Re2] (consequences), **1/3**

[1] Bayou Corne, Louisiana, 2012

[2] Clovelly salt dome, Louisiana, 1992

RISK Nr. 16.2 Formation of H_2S beyond acceptable limits

Risk step 1: Aim

Aim 16 for Water Company Drenthe ("Waterleiding Maatschappij Drenthe"): "*WMD provides impeccable drinking water at an acceptable cost for everyone in Drenthe, generation after generation*". Therefore, the aim is: no risk as a result of hydrogen storage in salt caverns, that is protection of the groundwater protection area of WCD being a reliable supplier.

Risk step 2: Risk identification

(1) Risk: Formation of H_2S leading to contamination of the groundwater due to leakage
(2) Risk based on: Assumption
(3) Source of information: Literature review (section 5.4)[3] and research[4][5][6][7]
(4) Uncertainty: Additional research on the circumstances leading to the formation of H_2S
(5) Type of causes: [Tc][Gc]
(6) Type of effects: [Me][Te][Se][Qe]

Risk step 3: Risk classification

(1) Classification probability class: 3 (a): assumption based on expert judgement
(2) Classification consequence class: [Me1][Te2][Se0][Qe2][Re0]

Risk step 4: Dealing with risks

(1) Additional research: additional research on the circumstances leading to the formation of H_2S, characterize sulphur oxidation state in addition to sulphur abundance, research on the effect on the purity of produced H_2, research on the mix of H_2 and H_2S, research on optimal dimensions of the cavern (reduce reaction surface)
(2) Preventive measures: avoid sulphate sources, monitoring of microbial activities, avoid presence of hydrocarbons (no use of existing caverns), monitoring of geochemical composition, periodic restoration of sump conditions (see further measures in risk 1.16)
(3) Corrective measures: pH correction, increase iron concentration, restoration of sump conditions
(4) Description and classification residual risk considering the measures taken: taking the preventive and corrective measures into account the residual risk becomes: 1 (probability) and [Me1][Te2][Se0][Qe1][Re0] (consequences), **1/2**

[3] M.P.Laban, Hydrogen storage in salt caverns, chemical modelling and analysis of large-scale hydrogen storage in underground salt caverns, no reference, dated July 16 2020
[4] N. Dopffel, Microbial impact on hydrogen storage, NORCE, 2nd International Summer School on UHS, dated July 2023
[5] C.A. Peters, Underground H_2 storage: Geochemistry Considerations, Princeton University, 2nd International Summer School on UHS, dated July 2023
[6] M. Portarapillo & A. di Benedetto, Risk assessment of the large-scale hydrogen storage in salt caverns, article in Energies 14, dated 2021
[7] M. Panfilov, Underground and pipeline hydrogen storage, Compendium of Hydrogen Energy, pp 92-116, dated 2015

RISK Nr. 16.3 Emergence of negative public opinion

Risk step 1: Aim

Aim 16 for Water Company Drenthe ("Waterleiding Maatschappij Drenthe"): "*WMD provides impeccable drinking water at an acceptable cost for everyone in Drenthe, generation after generation*". Therefore, the aim is: no risk as a result of hydrogen storage in salt caverns, that is protection of the groundwater protection area of WCD being a reliable supplier.

Risk step 2: Risk identification

(1) Risk: Emergence of negative public opinion, e.g., triggered by regional or national media, threatening the public image of the Water Company
(2) Risk based on: Interpretation of facts
(3) Source of information: public opinion[8][9][10][11][12]
(4) Uncertainty: complete stakeholder analysis per location, risk analysis discussion with all stakeholders (separately)
(5) Type of causes: [Pc]
(6) Type of effects: [Te][Re]

Risk step 3: Risk classification

(1) Classification probability class: 3 (c): interpretation of factual information
(2) Classification consequence class: [Me0][Te2][Se0][Qe0][Re1]

Risk step 4: Dealing with risks

(1) Additional research: complete stakeholder analysis per location, risk analysis discussion with all stakeholders (separately)
(2) Preventive measures: transparent, pro-active and personal communication, direct involvement (shareholders), financial compensation ("burdens and benefits"), transparency with respect to all taken preventive measures (other risks)
(3) Corrective measures: transparent and personal communication, financial compensation (based on reversed burden of proof), transparency with respect to all taken corrective measures (other risks)
(4) Description and classification residual risk considering the measures taken: taking the preventive and corrective measures into account the residual risk eventually becomes: 2 (probability) and [Me0][Te1][Se0][Qe0][Re0] (consequences), **2/1**

[8] Public opinion with respect to CO_2 storage underneath Barendrecht: "Stichting CO2isNEE", 2010
[9] Public opinion with respect to environmental problems and subsidence as a result of salt mining: "Stop Zoutwinning!", 2021
[10] Public opinion with respect to future salt extraction Municipality of Haaksbergen, 2023
[11] Public opinion with respect to underground discharge of production water, www.stopafvalwatertwente.nl
[12] Public opinion with respect to Nitrogen storage in Heiligerlee, www.mijnendijnbelang.nl

Stakeholder: Water Company Drenthe

Unmitigated risk matrix

4 x 3 Risk matrix		Consequence		
		1	2	3
Chance	3		16.2 16.3	
	2			16.1
	1			
	0			

Residual (mitigated) risk matrix

4 x 3 Risk matrix		Consequence		
		1	2	3
Chance	3			
	2	16.3		
	1		16.2	16.1
	0			

D.17 Stakeholder: Railinfratrust / ProRail

RISK Nr. 17.1 Accident at the surface

Risk step 1: Aim

Aim 17 for Railinfratrust / ProRail, owner of the rail infrastructure: "*We connect people, cities and companies by rail, now and in future times. We enable comfortable travelling and sustainable transport and ensure safety on and around the railway*". Therefore, the aim is: no risk for the railway infrastructure in the area of the hydrogen storage.

Risk step 2: Risk identification

(1) Risk: Accident at the surface (blow-out, well leak, pipeline integrity loss) as a result of hydrogen storage
(2) Risk based on: Interpretation of facts / assumptions
(3) Source of information: Literature review[1][2], expert judgement
(4) Uncertainty: Blow-out modelling done by Brouard Consulting, experience within the industry with hydrogen pipelines
(5) Type of causes: [Tc][Hc][Gc][Oc][Rc][Ic]
(6) Type of effects: [Me][Te][Qe][Re]

Risk step 3: Risk classification

(1) Classification probability class: 2 (a/c): assumption based on expert judgement and interpretation of factual information
(2) Classification consequence class: [Me1][Te1][Se0][Qe2][Re1]

Risk step 4: Dealing with risks

(1) Additional research: modelling of Blow-out, safety study on the effect at the surface, literature research hydrogen infrastructure KEM 29 (research in progress)
(2) Preventive measures (5 main): highest quality of BOP and safety valves / pressure gauges (H_2 certified material), all equipment designed for low T, rapid response plan, H_2-certified material (steel), construction and maintenance protocols (see further measures in risks 1.1, 1.2 and 1.4)
(3) Corrective measures: actions according to rapid response plan, evacuation plan, fire extinguishing, damage control / repair, temporary partial shut-down and repair
(4) Description and classification residual risk considering the measures taken: taking the preventive and corrective measures into account the residual risk becomes: 1 (probability) and [Me1][Te1][Se0][Qe2][Re1] (consequences), **1/2**

[1] Fort Saskatchewan Ethane Blow-out and Fire (2001)

[2] Moss Bluff natural gas blow out and Fire (2004)

RISK Nr. 17.2 Subsurface accident

Risk step 1: Aim

Aim 17 for Railinfratrust / ProRail, owner of the rail infrastructure: "*We connect people, cities and companies by rail, now and in future times. We enable comfortable travelling and sustainable transport and ensure safety on and around the railway*". Therefore, the aim is: no risk for the railway infrastructure in the area of the hydrogen storage.

Risk step 2: Risk identification

(1) Risk: Subsurface accident (leakage vertical tubing/casing, casing overstretching, cavern breaches, tensile failure, falls) as a result of hydrogen storage
(2) Risk based on: Interpretation of facts / assumptions
(3) Source of information: Literature review[3][4][5][6][7], expert judgement
(4) Uncertainty: Additional research of the salt structure and rheology, the interaction with hydrogen, mechanical properties and damage evolution. Additional research of materials interacting with hydrogen
(5) Type of causes: [Hc][Tc][Rc][Ic][Gc]
(6) Type of effects: [Me][Te][Qe][Re]

Risk step 3: Risk classification

(1) Classification probability class: 3 (a/c): assumption based on expert judgement and interpretation of factual information
(2) Classification consequence class: [Me1][Te1][Se0][Qe1][Re1]

Risk step 4: Dealing with risks

(1) Additional research (5 main): creep research (grainsize) and durability of the salt, research of the salt dome internal structure, including anomalous zones (section 3.4.7.1.4), and rheology, additional research of the second phase rheology interacting with hydrogen, research on prevention of micro annuli at the casing / cement / rock interfaces, additional research of materials interacting with hydrogen, (see further research topics in risks 1.3, 1.5, 1.6, 1.8-1,12, 1.14 and 1.15)
(2) Preventive measures (5 main): minimum preconditions for H_2 storage cavern (well test), improved cavern design (avoid flat roof / interlayered formations / large diameter of the roof), periodic sonar measurements and cement bonding log, elastomers (no nitril) or self-healing material instead of cement, H_2 and H_2S certified material (including packers), (see further measures in risks 1.3, 1.5, 1.6, 1.8-1,12, 1.14 and 1.15)
(3) Corrective measures (5 main): controlled production / flaring of H_2, abandon cavern, adapt the pressures, (micro annuli and material) treatment with special materials (resins, silicates etc.,

[3] Magnolia, Louisiana, 2003
[4] Boling 1, 2, 4, Texas, USA, 2005
[5] Bayou Corne, Louisiana, 2012
[6] Eminence salt dome 1, 3, 4, Mississippi, 1972
[7] Jintan JK-A, China, 2015

biological treatment), use of deformable metals and casing expansion, (see further measures in risks 1.3, 1.5, 1.6, 1.8-1,12, 1.14 and 1.15)

(4) Description and classification residual risk considering the measures taken: Both probability and consequence classes have not been reduced and remain: **3/1**, in more detail 3 (probability) and [Me1][Te1][Se0][Qe1][Re1] (consequences)

RISK Nr. 17.3 Creep closure and subsidence

Risk step 1: Aim

Aim 17 for Railinfratrust / ProRail, owner of the rail infrastructure: "*We connect people, cities and companies by rail, now and in future times. We enable comfortable travelling and sustainable transport and ensure safety on and around the railway*". Therefore, the aim is: no risk for the railway infrastructure in the area of the hydrogen storage.

Risk step 2: Risk identification

(1) Risk: Subsidence (beyond predicted limits)
(2) Risk based on: Interpretation of facts
(3) Source of information: Literature review (sections 3.1.5.1 and 3.2.3) [8][9]
(4) Uncertainty: Additional research of the salt structure and rheology, cavern design
(5) Type of causes: [Rc][Ic][Gc][Oc][Tc][Pc]
(6) Type of effects: [Me][Te][Qe][Re]

Risk step 3: Risk classification

(1) Classification probability class: 2 (c): interpretation of factual information
(2) Classification consequence class: [Me1][Te2][Se0][Qe1][Re1]

Risk step 4: Dealing with risks

(1) Additional research: research of the salt structure and rheology, cavern design, geomechanical modelling
(2) Preventive measures: monitoring of subsidence by INSAR & surveying measurements, field tests (pressure observation test POT after well drill), updated cavern design, geomechanical modelling, determination of the minimum cavern pressure (see further measures in risk 1.7)
(3) Corrective measures: change of the average cavern pressure (higher), minimizing the subsidence by controlled abandonment
(4) Description and classification residual risk considering the measures taken: taking the preventive and corrective measures into account the residual risk becomes: 1 (probability) and [Me1][Te2][Se0][Qe1][Re1] (consequences), **1/2**

[8] Subsidence at Maceió, Brazil, 2021 [9] Matarandiba Island, Brazil, 2018

Stakeholder: Railinfratrust / ProRail

Unmitigated risk matrix

4 x 3 Risk matrix		Consequence		
		1	2	3
Chance	3	17.2		
	2		17.1 17.3	
	1			
	0			

Residual (mitigated) risk matrix

4 x 3 Risk matrix		Consequence		
		1	2	3
Chance	3	17.2		
	2			
	1		17.1 17.3	
	0			

D.18 Stakeholder: Railway companies (passengers)

RISK Nr. 18.1 Accident at the surface

Risk step 1: Aim

Aim 18 for Railway companies (passengers): "*We want to connect people, cities and villages in a safe, reliable and sustainable way*". Therefore, the aim is: no risk for the railway passenger transport in the area of the hydrogen storage.

Risk step 2: Risk identification

(1) Risk: Accident at the surface (blow-out, well leak, pipeline integrity loss) as a result of hydrogen storage
(2) Risk based on: Interpretation of facts / assumptions
(3) Source of information: Literature review[12], expert judgement
(4) Uncertainty: Blow-out modelling done by Brouard Consulting, experience within the industry with hydrogen pipelines
(5) Type of causes: [Tc][Hc][Gc][Oc][Rc][Ic]
(6) Type of effects: [Me][Te][Se][Qe][Re]

Risk step 3: Risk classification

(1) Classification probability class: 2 (a/c): assumption based on expert judgement and interpretation of factual information
(2) Classification consequence class: [Me1][Te1][Se1][Qe2][Re1]

Risk step 4: Dealing with risks

(1) Additional research: modelling of Blow-out, safety study on the effect at the surface, literature research hydrogen infrastructure KEM 29 (research in progress)
(2) Preventive measures (5 main): highest quality of BOP and safety valves / pressure gauges (H_2 certified material), all equipment designed for low T, rapid response plan, H_2-certified material (steel), construction and maintenance protocols (see further measures in risks 1.1, 1.2 and 1.4)
(3) Corrective measures: actions according to rapid response plan, evacuation plan, fire extinguishing, damage control / repair, temporary partial shut-down and repair
(4) Description and classification residual risk considering the measures taken: taking the preventive and corrective measures into account the residual risk becomes: 1 (probability) and [Me1][Te1][Se1][Qe2][Re1] (consequences), **1/2**

[1] Fort Saskatchewan Ethane Blow-out and Fire (2001)
[2] Moss Bluff natural gas blow out and Fire (2004)

RISK Nr. 18.2 Subsurface accident

Risk step 1: Aim

Aim 18 for Railway companies (passengers): "*We want to connect people, cities and villages in a safe, reliable and sustainable way*". Therefore, the aim is: no risk for the railway passenger transport in the area of the hydrogen storage.

Risk step 2: Risk identification

(1) Risk: Subsurface accident (leakage vertical tubing/casing, casing overstretching, cavern breaches, tensile failure, falls) as a result of hydrogen storage
(2) Risk based on: Interpretation of facts / assumptions
(3) Source of information: Literature review[3][4][5][6][7], expert judgement
(4) Uncertainty: Additional research of the salt structure and rheology, the interaction with hydrogen, mechanical properties and damage evolution. Additional research of materials interacting with hydrogen
(5) Type of causes: [Hc][Tc][Rc][Ic][Gc]
(6) Type of effects: [Te][Qe][Re]

Risk step 3: Risk classification

(1) Classification probability class: 3 (a/c): assumption based on expert judgement and interpretation of factual information
(2) Classification consequence class: [Me0][Te1][Se0][Qe1][Re1]

Risk step 4: Dealing with risks

(1) Additional research (5 main): creep research (grainsize) and durability of the salt, research of the salt dome internal structure, including anomalous zones (section 3.4.7.1.4), and rheology, additional research of the second phase rheology interacting with hydrogen, research on prevention of micro annuli at the casing / cement / rock interfaces, additional research of materials interacting with hydrogen, (see further research topics in risks 1.3, 1.5, 1.6, 1.8-1,12, 1.14 and 1.15)
(2) Preventive measures (5 main): minimum preconditions for H_2 storage cavern (well test), improved cavern design (avoid flat roof / interlayered formations / large diameter of the roof), periodic sonar measurements and cement bonding log, elastomers (no nitril) or self-healing material instead of cement, H_2 and H_2S certified material (including packers), (see further measures in risks 1.3, 1.5, 1.6, 1.8-1,12, 1.14 and 1.15)
(3) Corrective measures (5 main): controlled production / flaring of H_2, abandon cavern, adapt the pressures, (micro annuli and material) treatment with special materials (resins, silicates etc., biological treatment), use of deformable metals and casing expansion, (see further measures in risks 1.3, 1.5, 1.6, 1.8-1,12, 1.14 and 1.15)

[3] Magnolia, Louisiana, 2003
[4] Boling 1, 2, 4, Texas, USA, 2005
[5] Bayou Corne, Louisiana, 2012
[6] Eminence salt dome 1, 3, 4, Mississippi, 1972
[7] Jintan JK-A, China, 2015

(4) *Description and classification residual risk considering the measures taken:* Both probability and consequence classes have not been reduced and remain: **3/1**, in more detail 3 (probability) and [Me0][Te1][Se0][Qe1][Re1] (consequences)

RISK Nr. 18.3 Creep closure and subsidence

Risk step 1: Aim

Aim 18 for Railway companies (passengers): "*We want to connect people, cities and villages in a safe, reliable and sustainable way*". Therefore, the aim is: no risk for the railway passenger transport in the area of the hydrogen storage.

Risk step 2: Risk identification

(1) Risk: Subsidence (beyond predicted limits)
(2) Risk based on: Interpretation of facts
(3) Source of information: Literature review (sections 3.1.5.1 and 3.2.3) [8][9]
(4) Uncertainty: Additional research of the salt structure and rheology, cavern design
(5) Type of causes: [Rc][Ic][Gc][Oc][Tc][Pc]
(6) Type of effects: [Te][Qe][Re]

Risk step 3: Risk classification

(1) Classification probability class: 2 (c): interpretation of factual information
(2) Classification consequence class: [Me0][Te1][Se0][Qe1][Re1]

Risk step 4: Dealing with risks

(1) Additional research: research of the salt structure and rheology, cavern design, geomechanical modelling
(2) Preventive measures: monitoring of subsidence by INSAR & surveying measurements, field tests (pressure observation test POT after well drill), updated cavern design, geomechanical modelling, determination of the minimum cavern pressure (see further measures in risk 1.7)
(3) Corrective measures: change of the average cavern pressure (higher), minimizing the subsidence by controlled abandonment
(4) Description and classification residual risk considering the measures taken: taking the preventive and corrective measures into account the residual risk becomes: 1 (probability) and [Me0][Te1][Se0][Qe1][Re1] (consequences), **1/1**

[8] Subsidence at Maceió, Brazil, 2021

[9] Matarandiba Island, Brazil, 2018

Stakeholder: Railway companies (passengers)

Unmitigated risk matrix

4 x 3 Risk matrix		Consequence		
		1	2	3
Chance	3	18.2		
	2	18.3	18.1	
	1			
	0			

Residual (mitigated) risk matrix

4 x 3 Risk matrix		Consequence		
		1	2	3
Chance	3	18.2		
	2			
	1	18.3	18.1	
	0			

D.19 Stakeholder: Railway companies (freight)

RISK Nr. 19.1 Accident at the surface

Risk step 1: Aim

Aim 19 for Railway companies (freight): "*We want a safe, reliable and sustainable way to transport all kind of goods by rail*". Therefore, the aim is: no risk for the railway freight transport in the area of the hydrogen storage.

Risk step 2: Risk identification

(1) Risk: Accident at the surface (blow-out, well leak, pipeline integrity loss) as a result of hydrogen storage
(2) Risk based on: Interpretation of facts / assumptions
(3) Source of information: Literature review[1][2], expert judgement
(4) Uncertainty: Blow-out modelling done by Brouard Consulting, experience within the industry with hydrogen pipelines
(5) Type of causes: [Tc][Hc][Gc][Oc][Rc][Ic]
(6) Type of effects: [Me][Te][Qe]

Risk step 3: Risk classification

(1) Classification probability class: 2 (a/c): assumption based on expert judgement and interpretation of factual information
(2) Classification consequence class: [Me1][Te1][Se0][Qe2][Re0]

Risk step 4: Dealing with risks

(1) Additional research: modelling of Blow-out, safety study on the effect at the surface, literature research hydrogen infrastructure KEM 29 (research in progress)
(2) Preventive measures (5 main): highest quality of BOP and safety valves / pressure gauges (H_2 certified material), all equipment designed for low T, rapid response plan, H_2-certified material (steel), construction and maintenance protocols (see further measures in risks 1.1, 1.2 and 1.4)
(3) Corrective measures: actions according to rapid response plan, evacuation plan, fire extinguishing, damage control / repair, temporary partial shut-down and repair
(4) Description and classification residual risk considering the measures taken: taking the preventive and corrective measures into account the residual risk becomes: 1 (probability) and [Me1][Te1][Se0][Qe2][Re0] (consequences), **1/2**

[1] Fort Saskatchewan Ethane Blow-out and Fire (2001) [2] Moss Bluff natural gas blow out and Fire (2004)

RISK Nr. 19.2 Subsurface accident

Risk step 1: Aim

Aim 19 for Railway companies (freight): "*We want a safe, reliable and sustainable way to transport all kind of goods by rail*". Therefore, the aim is: no risk for the railway freight transport in the area of the hydrogen storage.

Risk step 2: Risk identification

(1) Risk: Subsurface accident (leakage vertical tubing/casing, casing overstretching, cavern breaches, tensile failure, falls) as a result of hydrogen storage
(2) Risk based on: Interpretation of facts / assumptions
(3) Source of information: Literature review[3][4][5][6][7], expert judgement
(4) Uncertainty: Additional research of the salt structure and rheology, the interaction with hydrogen, mechanical properties and damage evolution. Additional research of materials interacting with hydrogen
(5) Type of causes: [Hc][Tc][Rc][Ic][Gc]
(6) Type of effects: [Te][Qe]

Risk step 3: Risk classification

(1) Classification probability class: 3 (a/c): assumption based on expert judgement and interpretation of factual information
(2) Classification consequence class: [Me0][Te1][Se0][Qe1][Re0]

Risk step 4: Dealing with risks

(1) Additional research (5 main): creep research (grainsize) and durability of the salt, research of the salt dome internal structure, including anomalous zones (section 3.4.7.1.4), and rheology, additional research of the second phase rheology interacting with hydrogen, research on prevention of micro annuli at the casing / cement / rock interfaces, additional research of materials interacting with hydrogen, (see further research topics in risks 1.3, 1.5, 1.6, 1.8-1,12, 1.14 and 1.15)
(2) Preventive measures (5 main): minimum preconditions for H_2 storage cavern (well test), improved cavern design (avoid flat roof / interlayered formations / large diameter of the roof), periodic sonar measurements and cement bonding log, elastomers (no nitril) or self-healing material instead of cement, H_2 and H_2S certified material (including packers), (see further measures in risks 1.3, 1.5, 1.6, 1.8-1,12, 1.14 and 1.15)
(3) Corrective measures (5 main): controlled production / flaring of H_2, abandon cavern, adapt the pressures, (micro annuli and material) treatment with special materials (resins, silicates etc., biological treatment), use of deformable metals and casing expansion, (see further measures in risks 1.3, 1.5, 1.6, 1.8-1,12, 1.14 and 1.15)

[3] Magnolia, Louisiana, 2003
[4] Boling 1, 2, 4, Texas, USA, 2005
[5] Bayou Corne, Louisiana, 2012
[6] Eminence salt dome 1, 3, 4, Mississippi, 1972
[7] Jintan JK-A, China, 2015

(4) *Description and classification residual risk considering the measures taken:* Both probability and consequence classes have not been reduced and remain: **3/1**, in more detail 3 (probability) and [Me0][Te1][Se0][Qe1][Re0] (consequences)

RISK Nr. 19.3 Creep closure and subsidence

Risk step 1: Aim

Aim 19 for Railway companies (freight): "*We want a safe, reliable and sustainable way to transport all kind of goods by rail*". Therefore, the aim is: no risk for the railway freight transport in the area of the hydrogen storage.

Risk step 2: Risk identification

(1) Risk: Subsidence (beyond predicted limits)
(2) Risk based on: Interpretation of facts
(3) Source of information: Literature review (sections 3.1.5.1 and 3.2.3) [8][9]
(4) Uncertainty: Additional research of the salt structure and rheology, cavern design
(5) Type of causes: [Rc][Ic][Gc][Oc][Tc][Pc]
(6) Type of effects: [Te][Qe]

Risk step 3: Risk classification

(1) Classification probability class: 2 (c): interpretation of factual information
(2) Classification consequence class: [Me0][Te1][Se0][Qe1][Re0]

Risk step 4: Dealing with risks

(1) Additional research: research of the salt structure and rheology, cavern design, geomechanical modelling
(2) Preventive measures: monitoring of subsidence by INSAR & surveying measurements, field tests (pressure observation test POT after well drill), updated cavern design, geomechanical modelling, determination of the minimum cavern pressure (see further measures in risk 1.7)
(3) Corrective measures: change of the average cavern pressure (higher), minimizing the subsidence by controlled abandonment
(4) Description and classification residual risk considering the measures taken: taking the preventive and corrective measures into account the residual risk becomes: 1 (probability) and [Me0][Te1][Se0][Qe1][Re0] (consequences), **1/1**

[8] Subsidence at Maceió, Brazil, 2021

[9] Matarandiba Island, Brazil, 2018

Stakeholder: Railway companies (freight)

Unmitigated risk matrix

4 x 3 Risk matrix		Consequence		
		1	2	3
Chance	3	19.2		
	2	19.3	19.1	
	1			
	0			

Residual (mitigated) risk matrix

4 x 3 Risk matrix		Consequence		
		1	2	3
Chance	3	19.2		
	2			
	1	19.3	19.1	
	0			

D.20 Stakeholder: Gasunie Transport Services (gas network)

RISK Nr. 20.1 Accident at the surface

Risk step 1: Aim

Aim 20 for Gasunie Transport Services, owner and operator of the national gas network: "*We offer gas transport services in a customer-orientated and transparent way. Safety, reliability, sustainability and cost-awareness are our priorities. We serve the public interest and operate professionally to create value for our stakeholders*". Therefore, the aim is: no risk or disruption due to hydrogen storage in salt caverns for our network, at all time.

Risk step 2: Risk identification

(1) Risk: Accident at the surface (blow-out, well leak, pipeline integrity loss) as a result of hydrogen storage
(2) Risk based on: Interpretation of facts / assumptions
(3) Source of information: Literature review[1][2], expert judgement
(4) Uncertainty: Blow-out modelling done by Brouard Consulting, experience within the industry with hydrogen pipelines
(5) Type of causes: [Tc][Hc][Gc][Oc][Rc][Ic]
(6) Type of effects: [Me][Te][Qe]

Risk step 3: Risk classification

(1) Classification probability class: 2 (a/c): assumption based on expert judgement and interpretation of factual information
(2) Classification consequence class: [Me1][Te1][Se0][Qe2][Re0]

Risk step 4: Dealing with risks

(1) Additional research: modelling of Blow-out, safety study on the effect at the surface, literature research hydrogen infrastructure KEM 29 (research in progress)
(2) Preventive measures (5 main): highest quality of BOP and safety valves / pressure gauges (H_2 certified material), all equipment designed for low T, rapid response plan, H_2-certified material (steel), construction and maintenance protocols (see further measures in risks 1.1, 1.2 and 1.4)
(3) Corrective measures: actions according to rapid response plan, evacuation plan, fire extinguishing, damage control / repair, temporary partial shut-down and repair
(4) Description and classification residual risk considering the measures taken: taking the preventive and corrective measures into account the residual risk becomes: 1 (probability) and [Me1][Te1][Se0][Qe2][Re0] (consequences), **1/2**

[1] Fort Saskatchewan Ethane Blow-out and Fire (2001)

[2] Moss Bluff natural gas blow out and Fire (2004)

RISK Nr. 20.2 Subsurface accident

Risk step 1: Aim

Aim 20 for Gasunie Transport Services, owner and operator of the national gas network: "*We offer gas transport services in a customer-orientated and transparent way. Safety, reliability, sustainability and cost-awareness are our priorities. We serve the public interest and operate professionally to create value for our stakeholders*". Therefore, the aim is: no risk or disruption due to hydrogen storage in salt caverns for our network, at all time.

Risk step 2: Risk identification

(1) *Risk:* Subsurface accident (leakage vertical tubing/casing, casing overstretching, cavern breaches, tensile failure, falls) as a result of hydrogen storage
(2) *Risk based on:* Interpretation of facts / assumptions
(3) *Source of information:* Literature review[3][4][5][6][7], expert judgement
(4) *Uncertainty:* Additional research of the salt structure and rheology, the interaction with hydrogen, mechanical properties and damage evolution. Additional research of materials interacting with hydrogen
(5) *Type of causes*: [Hc][Tc][Rc][Ic][Gc]
(6) *Type of effects*: [Me][Te][Qe]

Risk step 3: Risk classification

(1) *Classification probability class:* 3 (a/c): assumption based on expert judgement and interpretation of factual information
(2) *Classification consequence class:* [Me1][Te1][Se0][Qe1][Re0]

Risk step 4: Dealing with risks

(1) *Additional research (5 main):* creep research (grainsize) and durability of the salt, research of the salt dome internal structure, including anomalous zones (section 3.4.7.1.4), and rheology, additional research of the second phase rheology interacting with hydrogen, research on prevention of micro annuli at the casing / cement / rock interfaces, additional research of materials interacting with hydrogen, (see further research topics in risks 1.3, 1.5, 1.6, 1.8-1,12, 1.14 and 1.15)
(2) *Preventive measures (5 main):* minimum preconditions for H_2 storage cavern (well test), improved cavern design (avoid flat roof / interlayered formations / large diameter of the roof), periodic sonar measurements and cement bonding log, elastomers (no nitril) or self-healing material instead of cement, H_2 and H_2S certified material (including packers), (see further measures in risks 1.3, 1.5, 1.6, 1.8-1,12, 1.14 and 1.15)
(3) *Corrective measures:* controlled production / flaring of H_2, abandon cavern, adapt the pressures, (micro annuli and material) treatment with special materials (resins, silicates etc., biological

[3] Magnolia, Louisiana, 2003
[4] Boling 1, 2, 4, Texas, USA, 2005
[5] Bayou Corne, Louisiana, 2012
[6] Eminence salt dome 1, 3, 4, Mississippi, 1972
[7] Jintan JK-A, China, 2015

treatment), use of deformable metals and casing expansion, (see further measures in risks 1.3, 1.5, 1.6, 1.8-1,12, 1.14 and 1.15)

(4) Description and classification residual risk considering the measures taken: Both probability and consequence classes have not been reduced and remain: **3/1**, in more detail 3 (probability) and [Me1][Te1][Se0][Qe1][Re0] (consequences)

RISK Nr. 20.3 Creep closure and subsidence

Risk step 1: Aim

Aim 20 for Gasunie Transport Services, owner and operator of the national gas network: "*We offer gas transport services in a customer-orientated and transparent way. Safety, reliability, sustainability and cost-awareness are our priorities. We serve the public interest and operate professionally to create value for our stakeholders*". Therefore, the aim is: no risk or disruption due to hydrogen storage in salt caverns for our network, at all time.

Risk step 2: Risk identification

(1) Risk: Subsidence (beyond predicted limits)
(2) Risk based on: Interpretation of facts
(3) Source of information: Literature review (sections 3.1.5.1 and 3.2.3) [8][9]
(4) Uncertainty: Additional research of the salt structure and rheology, cavern design
(5) Type of causes: [Rc][Ic][Gc][Oc][Tc][Pc]
(6) Type of effects: [Me][Te][Qe]

Risk step 3: Risk classification

(1) Classification probability class: 2 (c): interpretation of factual information
(2) Classification consequence class: [Me1][Te2][Se0][Qe1][Re0]

Risk step 4: Dealing with risks

(1) Additional research: research of the salt structure and rheology, cavern design, geomechanical modelling
(2) Preventive measures (5 main): monitoring of subsidence by INSAR & surveying measurements, field tests (pressure observation test POT after well drill), updated cavern design, geomechanical modelling, determination of the minimum cavern pressure (see further measures in risk 1.7)
(3) Corrective measures: change of the average cavern pressure (higher), minimizing the subsidence by controlled abandonment
(4) Description and classification residual risk considering the measures taken: taking the preventive and corrective measures into account the residual risk becomes: 1 (probability) and [Me1][Te2][Se0][Qe1][Re0] (consequences), **1/2**

[8] Subsidence at Maceió, Brazil, 2021
[9] Matarandiba Island, Brazil, 2018

RISK Nr. 20.4 Failure of the storage system

Risk step 1: Aim

Aim 20 for Gasunie Transport Services, owner and operator of the national gas network: "*We offer gas transport services in a customer-orientated and transparent way. Safety, reliability, sustainability and cost-awareness are our priorities. We serve the public interest and operate professionally to create value for our stakeholders*". Therefore, the aim is: no risk or disruption due to hydrogen storage in salt caverns for our network, at all time.

Risk step 2: Risk identification

(1) Risk: Failure of the storage system (due to fire, natural disaster, terrorism or IT-failure)
(2) Risk based on: Assumptions
(3) Source of information: Expert judgement
(4) Uncertainty: Cannot be reduced
(5) Type of causes: [Hc][Oc][Tc][Rc][Ic]
(6) Type of effects: [Me][Te][Qe]

Risk step 3: Risk classification

(1) Classification probability class: 2 (a): assumption based on expert judgement
(2) Classification consequence class: [Me1][Te1][Se0][Qe1][Re0]

Risk step 4: Dealing with risks

(1) Additional research: -
(2) Preventive measures (5 main): adhere to the general safety regulations and fire-prevention measurements for hydrogen installations, back-up by remote-controlled operation, assign as "vital infrastructure" and act accordingly, manual controls requiring double authorisation, analogue pressure and temperature gauges at critical locations (double system) (see further measures in risks 1.19 – 1.22)
(3) Corrective measures: actions according to rapid response plan, fire alarm and fire extinguishing, remote-controlled operation, pressure relief valve (PRV) for worst case when pressure gets near lithostatic pressure at casing shoe, automatic release of pressure
(4) Description and classification residual risk considering the measures taken: taking the preventive and corrective measures into account the residual risk eventually becomes: 1 (probability) and [Me0][Te0][Se0][Qe0][Re0] (consequences), **0**

RISK Nr. 20.5 Emergence of negative public opinion

Risk step 1: Aim

Aim 20 for Gasunie Transport Services, owner and operator of the national gas network: "*We offer gas transport services in a customer-orientated and transparent way. Safety, reliability, sustainability and cost-awareness are our priorities. We serve the public interest and operate professionally to create value for our stakeholders*". Therefore, the aim is: no risk or disruption due to hydrogen storage in salt caverns for our network, at all time.

Risk step 2: Risk identification

(1) *Risk:* Emergence of negative public opinion, e.g., triggered by regional or national media, threatening the public image of Gasunie
(2) *Risk based on:* Interpretation of facts
(3) *Source of information:* public opinion[10][11][12][13][14]
(4) *Uncertainty:* complete stakeholder analysis per location, risk analysis discussion with all stakeholders (separately)
(5) *Type of causes*: [Pc]
(6) *Type of effects*: [Me][Te][Se][Re]

Risk step 3: Risk classification

(1) *Classification probability class:* 3 (c): interpretation of factual information
(2) *Classification consequence class:* [Me1][Te2][Se0][Qe0][Re0]

Risk step 4: Dealing with risks

(1) *Additional research:* complete stakeholder analysis per location, risk analysis discussion with all stakeholders (separately)
(2) *Preventive measures:* transparent, pro-active and personal communication, direct involvement (shareholders), financial compensation ("burdens and benefits"), transparency with respect to all taken preventive measures (other risks)
(3) *Corrective measures:* transparent and personal communication, financial compensation (based on reversed burden of proof), transparency with respect to all taken corrective measures (other risks)
(4) *Description and classification residual risk considering the measures taken:* taking the preventive and corrective measures into account the residual risk eventually becomes: 2 (probability) and [Me0][Te1][Se0][Qe0][Re0] (consequences), **2/1**

[10] Public opinion with respect to CO_2 storage underneath Barendrecht: "Stichting CO2isNEE", 2010
[11] Public opinion with respect to environmental problems and subsidence as a result of salt mining: "Stop Zoutwinning!", 2021
[12] Public opinion with respect to future salt extraction Municipality of Haaksbergen, 2023
[13] Public opinion with respect to underground discharge of production water, www.stopafvalwatertwente.nl
[14] Public opinion with respect to Nitrogen storage in Heiligerlee, www.mijnendijnbelang.nl

Stakeholder: Gasunie Transport Services (gas network)

Unmitigated risk matrix

4 x 3 Risk matrix		Consequence		
		1	2	3
Chance	3	20.2 20.4	20.5	
	2		20.1 20.3	
	1			
	0			

Residual (mitigated) risk matrix

4 x 3 Risk matrix		Consequence		
		1	2	3
Chance	3	20.2		
	2	20.5		
	1		20.1 20.3	
	0	20.4		

D.21 Stakeholder: TenneT

RISK Nr. 21.1 Accident at the surface

Risk step 1: Aim

Aim 21 for TenneT, owner and operator of the national network of high-voltage lines and cables: "*We are driven by our mission to ensure the lights stay on and that power is available, at the flick of a switch, whenever and wherever you need it*". Therefore, the aim is: no risk or disruption due to hydrogen storage in salt caverns for our network, at all time.

Risk step 2: Risk identification

(1) Risk: Accident at the surface (blow-out, well leak, pipeline integrity loss) as a result of hydrogen storage
(2) Risk based on: Interpretation of facts / assumptions
(3) Source of information: Literature review[1][2], expert judgement
(4) Uncertainty: Blow-out modelling done by Brouard Consulting, experience within the industry with hydrogen pipelines
(5) Type of causes: [Tc][Hc][Gc][Oc][Rc][Ic]
(6) Type of effects: [Me][Te][Qe]

Risk step 3: Risk classification

(1) Classification probability class: 2 (a/c): assumption based on expert judgement and interpretation of factual information
(2) Classification consequence class: [Me1][Te1][Se0][Qe2][Re0]

Risk step 4: Dealing with risks

(1) Additional research: modelling of Blow-out, safety study on the effect at the surface, literature research hydrogen infrastructure KEM 29 (research in progress)
(2) Preventive measures (5 main): highest quality of BOP and safety valves / pressure gauges (H_2 certified material), all equipment designed for low T, rapid response plan, H_2-certified material (steel), construction and maintenance protocols (see further measures in risks 1.1, 1.2 and 1.4)
(3) Corrective measures: actions according to rapid response plan, evacuation plan, fire extinguishing, damage control / repair, temporary partial shut-down and repair
(4) Description and classification residual risk considering the measures taken: taking the preventive and corrective measures into account the residual risk becomes: 1 (probability) and [Me1][Te1][Se0][Qe2][Re0] (consequences), **1/2**

[1] Fort Saskatchewan Ethane Blow-out and Fire (2001)

[2] Moss Bluff natural gas blow out and Fire (2004)

RISK Nr. 21.2 Subsurface accident

Risk step 1: Aim

Aim 21 for TenneT, owner and operator of the national network of high-voltage lines and cables: "*We are driven by our mission to ensure the lights stay on and that power is available, at the flick of a switch, whenever and wherever you need it*". Therefore, the aim is: no risk or disruption due to hydrogen storage in salt caverns for our network, at all time.

Risk step 2: Risk identification

(1) Risk: Subsurface accident (leakage vertical tubing/casing, casing overstretching, cavern breaches, tensile failure, falls) as a result of hydrogen storage
(2) Risk based on: Interpretation of facts / assumptions
(3) Source of information: Literature review[3][4][5][6][7], expert judgement
(4) Uncertainty: Additional research of the salt structure and rheology, the interaction with hydrogen, mechanical properties and damage evolution. Additional research of materials interacting with hydrogen
(5) Type of causes: [Hc][Tc][Rc][Ic][Gc]
(6) Type of effects: [Te][Qe]

Risk step 3: Risk classification

(1) Classification probability class: 3 (a/c): assumption based on expert judgement and interpretation of factual information
(2) Classification consequence class: [Me0][Te1][Se0][Qe1][Re0]

Risk step 4: Dealing with risks

(1) Additional research (5 main): creep research (grainsize) and durability of the salt, research of the salt dome internal structure, including anomalous zones (section 3.4.7.1.4), and rheology, additional research of the second phase rheology interacting with hydrogen, research on prevention of micro annuli at the casing / cement / rock interfaces, additional research of materials interacting with hydrogen, (see further research topics in risks 1.3, 1.5, 1.6, 1.8-1,12, 1.14 and 1.15)
(2) Preventive measures (5 main): minimum preconditions for H_2 storage cavern (well test), improved cavern design (avoid flat roof / interlayered formations / large diameter of the roof), periodic sonar measurements and cement bonding log, elastomers (no nitril) or self-healing material instead of cement, H_2 and H_2S certified material (including packers), (see further measures in risks 1.3, 1.5, 1.6, 1.8-1,12, 1.14 and 1.15)
(3) Corrective measures (5 main): controlled production / flaring of H_2, abandon cavern, adapt the pressures, (micro annuli and material) treatment with special materials (resins, silicates etc.,

[3] Magnolia, Louisiana, 2003
[4] Boling 1, 2, 4, Texas, USA, 2005
[5] Bayou Corne, Louisiana, 2012
[6] Eminence salt dome 1, 3, 4, Mississippi, 1972
[7] Jintan JK-A, China, 2015

biological treatment), use of deformable metals and casing expansion, (see further measures in risks 1.3, 1.5, 1.6, 1.8-1,12, 1.14 and 1.15)

(4) Description and classification residual risk considering the measures taken: Both probability and consequence classes have not been reduced and remain: **3/1**, in more detail 3 (probability) and [Me0][Te1][Se0][Qe1][Re0] (consequences)

RISK Nr. 21.3 Creep closure and subsidence

Risk step 1: Aim

Aim 21 for TenneT, owner and operator of the national network of high-voltage lines and cables: "*We are driven by our mission to ensure the lights stay on and that power is available, at the flick of a switch, whenever and wherever you need it*". Therefore, the aim is: no risk or disruption due to hydrogen storage in salt caverns for our network, at all time.

Risk step 2: Risk identification

(1) Risk: Subsidence (beyond predicted limits)
(2) Risk based on: Interpretation of facts
(3) Source of information: Literature review (sections 3.1.5.1 and 3.2.3) [8][9]
(4) Uncertainty: Additional research of the salt structure and rheology, cavern design
(5) Type of causes: [Rc][Ic][Gc][Oc][Tc][Pc]
(6) Type of effects: [Me][Te][Qe]

Risk step 3: Risk classification

(1) Classification probability class: 2 (c): interpretation of factual information
(2) Classification consequence class: [Me1][Te1][Se0][Qe1][Re0]

Risk step 4: Dealing with risks

(1) Additional research: research of the salt structure and rheology, cavern design, geomechanical modelling
(2) Preventive measures: monitoring of subsidence by INSAR & surveying measurements, field tests (pressure observation test POT after well drill), updated cavern design, geomechanical modelling, determination of the minimum cavern pressure (see further measures in risk 1.7)
(3) Corrective measures: change of the average cavern pressure (higher), minimizing the subsidence by controlled abandonment
(4) Description and classification residual risk considering the measures taken: taking the preventive and corrective measures into account the residual risk becomes: 1 (probability) and [Me1][Te1][Se0][Qe1][Re0] (consequences), **1/1**

[8] Subsidence at Maceió, Brazil, 2021

[9] Matarandiba Island, Brazil, 2018

RISK Nr. 21.4 Failure of the storage system

Risk step 1: Aim

Aim 21 for TenneT, owner and operator of the national network of high-voltage lines and cables: "*We are driven by our mission to ensure the lights stay on and that power is available, at the flick of a switch, whenever and wherever you need it*". Therefore, the aim is: no risk or disruption due to hydrogen storage in salt caverns for our network, at all time.

Risk step 2: Risk identification

(1) Risk: Failure of the storage system (due to fire, natural disaster, terrorism or IT-failure)
(2) Risk based on: Assumptions
(3) Source of information: Expert judgement
(4) Uncertainty: Cannot be reduced
(5) Type of causes: [Hc][Oc][Tc][Rc][Ic]
(6) Type of effects: [Me][Te][Qe]

Risk step 3: Risk classification

(1) Classification probability class: 2 (a): assumption based on expert judgement
(2) Classification consequence class: [Me1][Te1][Se0][Qe2][Re0]

Risk step 4: Dealing with risks

(1) Additional research: -
(2) Preventive measures (5 main): adhere to the general safety regulations and fire-prevention measurements for hydrogen installations, back-up by remote-controlled operation, assign as "vital infrastructure" and act accordingly, manual controls requiring double authorisation, analogue pressure and temperature gauges at critical locations (double system) (see further measures in risks 1.19 – 1.22)
(3) Corrective measures: actions according to rapid response plan, fire alarm and fire extinguishing, remote-controlled operation, pressure relief valve (PRV) for worst case when pressure gets near lithostatic pressure at casing shoe, automatic release of pressure
(4) Description and classification residual risk considering the measures taken: taking the preventive and corrective measures into account the residual risk eventually becomes: 1 (probability) and [Me0][Te0][Se0][Qe0][Re0] (consequences), **0**

Stakeholder: TenneT

Unmitigated risk matrix

4 x 3 Risk matrix		Consequence		
		1	2	3
Chance	3	21.2		
	2	21.3	21.1 21.4	
	1			
	0			

Residual (mitigated) risk matrix

4 x 3 Risk matrix		Consequence		
		1	2	3
Chance	3	21.2		
	2			
	1	21.3	21.1	
	0	21.4		

D.22 Stakeholder: NAM

RISK Nr. 22.1 Registered induced seismicity

Risk step 1: Aim

Aim 22 for NAM, Dutch exploration and production company: "*NAM is an innovative company that supplies energy to society and industry. We do this by exploring, developing and producing gas and oil from the Dutch subsoil. We strive to do this as safe and efficient as possible without damage to people and the environment*". Therefore, the aim is: no risk for the present gas extraction or for future claims as a result of hydrogen storage in salt caverns.

Risk step 2: Risk identification

(1) Risk: Registered induced seismicity caused by the operation (filling and emptying) of the cavern
(2) Risk based on: Interpretation of facts / assumption
(3) Source of information: Monitoring plans of underground Natural Gas and Nitrogen storage[1][2], literature review (section 5.2)
(4) Uncertainty: Research on characteristic locations in the salt dome sensitive to (micro)seismicity
(5) Type of causes: [Rc][Gc]
(6) Type of effects: [Te][Re]

Risk step 3: Risk classification

(1) Classification probability class: 3 (a/c): assumption based on expert judgement and interpretation of facts
(2) Classification consequence class: [Me0][Te2][Se0][Qe0][Re3]

Risk step 4: Dealing with risks

(1) Additional research: research on characteristic locations in the salt dome sensitive to (micro)seismicity
(2) Preventive measures: seismic monitoring (natural and induced seismicity), modelling of expected seismicity, no storage activities in or near an active fault zone, transparency and open communication, baseline measurement, transparency regarding seismic data
(3) Corrective measures: -
(4) Description and classification residual risk considering the measures taken: taking the preventive measures into account the residual risk becomes: 2 (probability) and [Me0][Te2][Se0][Qe0][Re1] (consequences), **2/2**

[1] Nouryon, Micro seismic network Heiligerlee & Zuidwending, observations Q3 2020, Powerpoint, no reference, no date

[2] NAM, Report "Instemmingsbesluit Norg", letter, no reference, dated December 3 2021

RISK Nr. 22.2 Disputed responsibility due to stacked mining activities

Risk step 1: Aim

Aim 22 for NAM, Dutch exploration and production company: "*NAM is an innovative company that supplies energy to society and industry. We do this by exploring, developing and producing gas and oil from the Dutch subsoil. We strive to do this as safe and efficient as possible without damage to people and the environment*". Therefore, the aim is: no risk for the present gas extraction or for future claims as a result of hydrogen storage in salt caverns.

Risk step 2: Risk identification

(1) Risk: Disputed responsibility due to stacked mining activities
(2) Risk based on: Assumption
(3) Source of information: Political discussions[3], public[4]
(4) Uncertainty: Scenario modelling of various critical scenarios to test regulations
(5) Type of causes: [Rc]
(6) Type of effects: [Me][Te][Re]

Risk step 3: Risk classification

(1) Classification probability class: 3 (a): assumption based on expert judgement
(2) Classification consequence class: [Me2][Te3][Se0][Qe0][Re2]

Risk step 4: Dealing with risks

(1) Additional research: scenario modelling of various critical scenarios to test regulations
(2) Preventive measures: regulations for operators regarding arial extent and duration of responsibility, seismic monitoring system, monitoring of subsidence by INSAR & surveying measurements before mining and during storage, mandatory report of incidents, regular meetings with all operators involved (including independent chairman, e.g., SodM), one overall geological model for all operators
(3) Corrective measures: mandatory insurance policy for all operators concerned, regulations for take-over of responsibilities in case of bankruptcy operator
(4) Description and classification residual risk considering the measures taken: taking the preventive and corrective measures into account the residual risk eventually becomes: 1 (probability) and [Me1][Te2][Se0][Qe0][Re0] (consequences), **1/2**

[3] Groenlinks, Stacked mining neglected in Nedmag-advice, 2019

[4] RTVOost, Growing frustration about mining, damage and new gas exploitation, January 2021

Stakeholder: NAM

Unmitigated risk matrix

4 x 3 Risk matrix		Consequence		
		1	2	3
Chance	3			22.1 22.2
	2			
	1			
	0			

Residual (mitigated) risk matrix

4 x 3 Risk matrix		Consequence		
		1	2	3
Chance	3			
	2		22.1	
	1		22.2	
	0			

D.23 Stakeholder: Corre Energy (CAES)

RISK Nr. 23.1 Accident at the surface

Risk step 1: Aim

Aim 23 for CORRE Energy (future CAES): "*By storing surplus energy, we make a huge contribution to the energy transition by enabling the integration of large scale renewable energy sources. With our technology, we can solve a vital piece of the energy transition puzzle and bring balance to the current energy landscape*". Therefore, the aim is: no risk for the use of salt caverns for our own operations as a result of hydrogen storage in salt caverns, at all time.

Risk step 2: Risk identification

(1) Risk: Accident at the surface (blow-out, well leak, pipeline integrity loss) as a result of hydrogen storage
(2) Risk based on: Interpretation of facts / assumptions
(3) Source of information: Literature review[1][2], expert judgement
(4) Uncertainty: Blow-out modelling done by Brouard Consulting, experience within the industry with hydrogen pipelines
(5) Type of causes: [Tc][Hc][Gc][Oc][Rc][Ic]
(6) Type of effects: [Me][Te][Se][Qe][Re]

Risk step 3: Risk classification

(1) Classification probability class: 2 (a/c): assumption based on expert judgement and interpretation of factual information
(2) Classification consequence class: [Me2][Te2][Se3][Qe3][Re2]

Risk step 4: Dealing with risks

(1) Additional research: modelling of Blow-out, safety study on the effect at the surface, literature research hydrogen infrastructure KEM 29 (research in progress)
(2) Preventive measures (5 main): highest quality of BOP and safety valves / pressure gauges (H_2 certified material), all equipment designed for low T, rapid response plan, H_2-certified material (steel), construction and maintenance protocols (see further measures in risks 1.1, 1.2 and 1.4)
(3) Corrective measures: actions according to rapid response plan, evacuation plan, fire extinguishing, damage control / repair, temporary partial shut-down and repair
(4) Description and classification residual risk considering the measures taken: taking the preventive and corrective measures into account the residual risk becomes: 1 (probability) and [Me2][Te2][Se3][Qe3][Re2] (consequences), **1/3**

[1] Fort Saskatchewan Ethane Blow-out and Fire (2001)

[2] Moss Bluff natural gas blow out and Fire (2004)

RISK Nr. 23.2 Subsurface accident

Risk step 1: Aim

Aim 23 for CORRE Energy (future CAES): "*By storing surplus energy, we make a huge contribution to the energy transition by enabling the integration of large scale renewable energy sources. With our technology, we can solve a vital piece of the energy transition puzzle and bring balance to the current energy landscape*". Therefore, the aim is: no risk for the use of salt caverns for our own operations as a result of hydrogen storage in salt caverns, at all time.

Risk step 2: Risk identification

(1) Risk: Subsurface accident (leakage vertical tubing/casing, casing overstretching, cavern breaches, tensile failure, falls) as a result of hydrogen storage
(2) Risk based on: Interpretation of facts / assumptions
(3) Source of information: Literature review[3][4][5][6][7], expert judgement
(4) Uncertainty: Additional research of the salt structure and rheology, the interaction with hydrogen, mechanical properties and damage evolution. Additional research of materials interacting with hydrogen
(5) Type of causes: [Hc][Tc][Rc][Ic][Gc]
(6) Type of effects: [Me][Te][Se][Qe][Re]

Risk step 3: Risk classification

(1) Classification probability class: 3 (a/c): assumption based on expert judgement and interpretation of factual information
(2) Classification consequence class: [Me2][Te2][Se3][Qe2][Re2]

Risk step 4: Dealing with risks

(1) Additional research (5 main): creep research (grainsize) and durability of the salt, research of the salt dome internal structure, including anomalous zones (section 3.4.7.1.4), and rheology, additional research of the second phase rheology interacting with hydrogen, research on prevention of micro annuli at the casing / cement / rock interfaces, additional research of materials interacting with hydrogen, (see further research topics in risks 1.3, 1.5, 1.6, 1.8-1,12, 1.14 and 1.15)
(2) Preventive measures (5 main): minimum preconditions for H_2 storage cavern (well test), improved cavern design (avoid flat roof / interlayered formations / large diameter of the roof), periodic sonar measurements and cement bonding log, elastomers (no nitril) or self-healing material instead of cement, H_2 and H_2S certified material (including packers), (see further measures in risks 1.3, 1.5, 1.6, 1.8-1,12, 1.14 and 1.15)
(3) Corrective measures (5 main): controlled production / flaring of H_2, abandon cavern, adapt the pressures, (micro annuli and material) treatment with special materials (resins, silicates etc.,

[3] Magnolia, Louisiana, 2003
[4] Boling 1, 2, 4, Texas, USA, 2005
[5] Bayou Corne, Louisiana, 2012
[6] Eminence salt dome 1, 3, 4, Mississippi, 1972
[7] Jintan JK-A, China, 2015

biological treatment), use of deformable metals and casing expansion, (see further measures in risks 1.3, 1.5, 1.6, 1.8-1,12, 1.14 and 1.15)

(4) *Description and classification residual risk considering the measures taken:* taking the preventive and corrective measures into account the residual risk becomes: 3 (probability) and [Me1][Te2][Se1][Qe2][Re2] (consequences), **3/2**

RISK Nr. 23.3 Creep closure and subsidence

Risk step 1: Aim

Aim 23 for CORRE Energy (future CAES): "*By storing surplus energy, we make a huge contribution to the energy transition by enabling the integration of large scale renewable energy sources. With our technology, we can solve a vital piece of the energy transition puzzle and bring balance to the current energy landscape*". Therefore, the aim is: no risk for the use of salt caverns for our own operations as a result of hydrogen storage in salt caverns, at all time.

Risk step 2: Risk identification

(1) Risk: Subsidence (beyond predicted limits)
(2) Risk based on: Interpretation of facts
(3) Source of information: Literature review (sections 3.1.5.1 and 3.2.3) [8][9]
(4) Uncertainty: Additional research of the salt structure and rheology, cavern design
(5) Type of causes: [Rc][Ic][Gc][Oc][Tc][Pc]
(6) Type of effects: [Me][Te][Qe][Re]

Risk step 3: Risk classification

(1) Classification probability class: 2 (c): interpretation of factual information
(2) Classification consequence class: [Me2][Te3][Se0][Qe1][Re2]

Risk step 4: Dealing with risks

(1) Additional research: research of the salt structure and rheology, cavern design, geomechanical modelling
(2) Preventive measures: monitoring of subsidence by INSAR & surveying measurements, field tests (pressure observation test POT after well drill), updated cavern design, geomechanical modelling, determination of the minimum cavern pressure (see further measures in risk 1.7)
(3) Corrective measures: change of the average cavern pressure (higher), minimizing the subsidence by controlled abandonment
(4) Description and classification residual risk considering the measures taken: taking the preventive and corrective measures into account the residual risk becomes: 1 (probability) and [Me2][Te3][Se0][Qe1][Re2] (consequences), **1/3**

[8] Subsidence at Maceió, Brazil, 2021

[9] Matarandiba Island, Brazil, 2018

RISK Nr. 23.4 Registered induced seismicity

Risk step 1: Aim

Aim 23 for CORRE Energy (future CAES): "*By storing surplus energy, we make a huge contribution to the energy transition by enabling the integration of large scale renewable energy sources. With our technology, we can solve a vital piece of the energy transition puzzle and bring balance to the current energy landscape*". Therefore, the aim is: no risk for the use of salt caverns for our own operations as a result of hydrogen storage in salt caverns, at all time.

Risk step 2: Risk identification

(1) Risk: Registered induced seismicity caused by the operation (filling and emptying) of the cavern
(2) Risk based on: Interpretation of facts /assumption
(3) Source of information: Monitoring plans of underground Natural Gas and Nitrogen storage[10][11], literature review (section 5.2)
(4) Uncertainty: Research on characteristic locations in the salt dome sensitive to (micro)seismicity
(5) Type of causes: [Rc][Gc]
(6) Type of effects: [Te][Re]

Risk step 3: Risk classification

(1) Classification probability class: 3 (a/c): assumption based on expert judgement and interpretation of facts
(2) Classification consequence class: [Me0][Te2][Se0][Qe0][Re3]

Risk step 4: Dealing with risks

(1) Additional research: research on characteristic locations in the salt dome sensitive to (micro)seismicity
(2) Preventive measures: seismic monitoring (natural and induced seismicity), modelling of expected seismicity, no storage activities in or near an active fault zone, transparency and open communication, baseline measurement, transparency regarding seismic data
(3) Corrective measures: -
(4) Description and classification residual risk considering the measures taken: taking the preventive measures into account the residual risk becomes: 2 (probability) and [Me0][Te2][Se0][Qe0][Re1] (consequences), **2/2**

[10] Nouryon, Micro seismic network Heiligerlee & Zuidwending, observations Q3 2020, Powerpoint, no reference, no date

[11] NAM, Report "Instemmingsbesluit Norg", letter, no reference, dated December 3 2021

RISK Nr. 23.5 Failure of the storage system

Risk step 1: Aim

Aim 23 for CORRE Energy (future CAES): "*By storing surplus energy, we make a huge contribution to the energy transition by enabling the integration of large scale renewable energy sources. With our technology, we can solve a vital piece of the energy transition puzzle and bring balance to the current energy landscape*". Therefore, the aim is: no risk for the use of salt caverns for our own operations as a result of hydrogen storage in salt caverns, at all time.

Risk step 2: Risk identification

(1) Risk: Failure of the storage system (due to fire, natural disaster, terrorism or IT-failure)
(2) Risk based on: Assumptions
(3) Source of information: Expert judgement
(4) Uncertainty: Cannot be reduced
(5) Type of causes: [Hc][Oc][Tc][Rc][Ic]
(6) Type of effects: [Me][Te][Se][Qe][Re]

Risk step 3: Risk classification

(1) Classification probability class: 2 (a): assumption based on expert judgement
(2) Classification consequence class: [Me2][Te2][Se3][Qe3][Re2]

Risk step 4: Dealing with risks

(1) Additional research: -
(2) Preventive measures (5 main): adhere to the general safety regulations and fire-prevention measurements for hydrogen installations, back-up by remote-controlled operation, assign as "vital infrastructure" and act accordingly, manual controls requiring double authorisation, analogue pressure and temperature gauges at critical locations (double system) (see further measures in risks 1.19 – 1.22)
(3) Corrective measures: actions according to rapid response plan, fire alarm and fire extinguishing, remote-controlled operation, pressure relief valve (PRV) for worst case when pressure gets near lithostatic pressure at casing shoe, automatic release of pressure
(4) Description and classification residual risk considering the measures taken: taking the preventive and corrective measures into account the residual risk eventually becomes: 1 (probability) and [Me1][Te1][Se0][Qe1][Re0] (consequences), **1/1**

RISK Nr. 23.6 Emergence of negative public opinion

Risk step 1: Aim

Aim 23 for CORRE Energy (future CAES): "*By storing surplus energy, we make a huge contribution to the energy transition by enabling the integration of large scale renewable energy sources. With our technology, we can solve a vital piece of the energy transition puzzle and bring balance to the current energy landscape*". Therefore, the aim is: no risk for the use of salt caverns for our own operations as a result of hydrogen storage in salt caverns, at all time.

Risk step 2: Risk identification

(1) *Risk:* Emergence of negative public opinion, e.g., triggered by regional or national media, threatening the support for the operation of CORRE Energy
(2) *Risk based on:* Interpretation of facts
(3) *Source of information:* public opinion[12][13][14][15][16]
(4) *Uncertainty:* complete stakeholder analysis per location, risk analysis discussion with all stakeholders (separately)
(5) *Type of causes*: [Pc]
(6) *Type of effects*: [Me][Te][Se][Re]

Risk step 3: Risk classification

(1) *Classification probability class:* 3 (c): interpretation of factual information
(2) *Classification consequence class:* [Me2][Te3][Se1][Qe0][Re2]

Risk step 4: Dealing with risks

(1) *Additional research:* complete stakeholder analysis per location, risk analysis discussion with all stakeholders (separately)
(2) *Preventive measures:* transparent, pro-active and personal communication, direct involvement (shareholders), financial compensation ("burdens and benefits"), transparency with respect to all taken preventive measures (other risks)
(3) *Corrective measures:* transparent and personal communication, financial compensation (based on reversed burden of proof), transparency with respect to all taken corrective measures (other risks)
(4) *Description and classification residual risk considering the measures taken:* taking the preventive and corrective measures into account the residual risk eventually becomes: 2 (probability) and [Me1][Te2][Se1][Qe0][Re1] (consequences), **2/2**

[12] Public opinion with respect to CO_2 storage underneath Barendrecht: "Stichting CO2isNEE", 2010
[13] Public opinion with respect to environmental problems and subsidence as a result of salt mining: "Stop Zoutwinning!", 2021
[14] Public opinion with respect to future salt extraction Municipality of Haaksbergen, 2023
[15] Public opinion with respect to underground discharge of production water, www.stopafvalwatertwente.nl
[16] Public opinion with respect to Nitrogen storage in Heiligerlee, www.mijnendijnbelang.nl

RISK Nr. 23.7 Disputed responsibility due to stacked mining activities

Risk step 1: Aim

Aim 23 for CORRE Energy (future CAES): "*By storing surplus energy, we make a huge contribution to the energy transition by enabling the integration of large scale renewable energy sources. With our technology, we can solve a vital piece of the energy transition puzzle and bring balance to the current energy landscape*". Therefore, the aim is: no risk for the use of salt caverns for our own operations as a result of hydrogen storage in salt caverns, at all time.

Risk step 2: Risk identification

(1) Risk: Disputed responsibility due to stacked mining activities
(2) Risk based on: Assumption
(3) Source of information: Political discussions[17], public[18]
(4) Uncertainty: Scenario modelling of various critical scenarios to test regulations
(5) Type of causes: [Rc]
(6) Type of effects: [Me][Te][Re]

Risk step 3: Risk classification

(1) Classification probability class: 3 (a): assumption based on expert judgement
(2) Classification consequence class: [Me2][Te3][Se0][Qe0][Re2]

Risk step 4: Dealing with risks

(1) Additional research: scenario modelling of various critical scenarios to test regulations
(2) Preventive measures: regulations for operators regarding arial extent and duration of responsibility, seismic monitoring system, monitoring of subsidence by INSAR & surveying measurements before mining and during storage, mandatory report of incidents, regular meetings with all operators involved (including independent chairman, e.g., SodM), one overall geological model for all operators
(3) Corrective measures: mandatory insurance policy for all operators concerned, regulations for take-over of responsibilities in case of bankruptcy operator
(4) Description and classification residual risk considering the measures taken: taking the preventive and corrective measures into account the residual risk eventually becomes: 1 (probability) and [Me1][Te2][Se0][Qe0][Re0] (consequences), **1/2**

[17] Groenlinks, Stacked mining neglected in Nedmag-advice, 2019

[18] RTVOost, Growing frustration about mining, damage and new gas exploitation, January 2021

RISK Nr. 23.8 Threat for (future) on-shore energy storage

Risk step 1: Aim

Aim 23 for CORRE Energy (future CAES): "*By storing surplus energy, we make a huge contribution to the energy transition by enabling the integration of large scale renewable energy sources. With our technology, we can solve a vital piece of the energy transition puzzle and bring balance to the current energy landscape*". Therefore, the aim is: no risk for the use of salt caverns for our own operations as a result of hydrogen storage in salt caverns, at all time.

Risk step 2: Risk identification

(1) Risk: Threat to future energy storage in salt caverns (Licence to Operate) due to uncertainties about safety and consequences of the storage in salt caverns
(2) Risk based on: Assumption
(3) Source of information: Public, press, politics
(4) Uncertainty: (generic and) Site-specific risk assessments, site-specific research on geology, rock-salt properties
(5) Type of causes: [Pc]
(6) Type of effects: [Me][Te][Qe][Re]

Risk step 3: Risk classification

(1) Classification probability class: 3 (a): assumption based on expert judgement
(2) Classification consequence class: [Me3][Te3][Se0][Qe3][Re3]

Risk step 4: Dealing with risks

(1) Additional research: (generic and) site-specific risk assessments, site-specific research on geology and rock-salt properties
(2) Preventive measures (5 main): open pro-active communication with stakeholders (public, politics and press) and other operators, preferably use newly developed caverns (according to an optimal rock mechanical envelope), periodic leak tests, minimum preconditions for H_2 storage cavern, mandatory status-report (starting every year) (see further measures in risk 1.24)
(3) Corrective measures: open communication with stakeholders (public, politics and press) and other operators
(4) Description and classification residual risk considering the measures taken: taking the preventive and corrective measures into account the residual risk eventually becomes: 2 (probability) and [Me1][Te3][Se0][Qe0][Re2] (consequences), **2/3**

Stakeholder: Corre Energy (CAES)

Unmitigated risk matrix

4 x 3 Risk matrix		Consequence		
		1	2	3
Chance	3			23.2 23.4 23.6 23.7 23.8
	2			23.1 23.3 23.5
	1			
	0			

Residual (mitigated) risk matrix

4 x 3 Risk matrix		Consequence		
		1	2	3
Chance	3		23.2	
	2		23.4 23.6	23.8
	1	23.5	23.7	23.1 23.3
	0			

D.24 Stakeholder: Water consuming companies (production)

RISK Nr. 24.1 Cavern integrity loss

Risk step 1: Aim

Aim 24 for Water consuming companies (production): "*we want to ensure sustainable availability of sufficient (ground)water of excellent quality and contribute to efficient use of water*". Therefore, the aim is: no risk as a result of hydrogen storage in salt caverns for the quality of the extracted groundwater.

Risk step 2: Risk identification

(1) Risk: Cavern breaches (tightness) / cavern integrity loss
(2) Risk based on: Interpretation of facts
(3) Source of information: Literature review (7 cases described in section 2.2.3.1)[1][2]
(4) Uncertainty: Additional research of the salt structure and rheology, cavern design
(5) Type of causes: [Tc][Rc][Gc][Oc][Ic]
(6) Type of effects: [Me][Te][Se][Qe][Re]

Risk step 3: Risk classification

(1) Classification probability class: 2 (c): interpretation of factual information
(2) Classification consequence class: [Me1][Te2][Se0][Qe3][Re2]

Risk step 4: Dealing with risks

(1) Additional research: research of the salt dome internal structure, including anomalous zones (section 3.4.7.1.4), and rheology, cavern design
(2) Preventive measures: open communication with other operators, minimum preconditions for H_2 storage cavern, detection of heterogeneities, enough distance to the domes edge, preferably use newly developed caverns (according to an optimal rock mechanical envelope) (see further measures in risk 1.6)
(3) Corrective measures: abandon cavern
(4) Description and classification residual risk considering the measures taken: taking the preventive and corrective measures into account the residual risk becomes: 1 (probability) and [Me2][Te2][Se0][Qe3][Re2] (consequences), **1/3**

[1] Bayou Corne, Louisiana, 2012

[2] Clovelly salt dome, Louisiana, 1992

RISK Nr. 24.2 Formation of H_2S beyond acceptable limits

Risk step 1: Aim

Aim 24 for Water consuming companies (production): "*we want to ensure sustainable availability of sufficient (ground)water of excellent quality and contribute to efficient use of water*". Therefore, the aim is: no risk as a result of hydrogen storage in salt caverns for the quality of the extracted groundwater.

Risk step 2: Risk identification

(1) Risk: Formation of H_2S leading to contamination of the groundwater due to leakage
(2) Risk based on: Assumption
(3) Source of information: Literature review (section 5.4)[3] and research[4][5][6][7]
(4) Uncertainty: Additional research on the circumstances leading to the formation of H_2S
(5) Type of causes: [Tc][Gc]
(6) Type of effects: [Me][Te][Qe]

Risk step 3: Risk classification

(1) Classification probability class: 3 (a): assumption based on expert judgement
(2) Classification consequence class: [Me1][Te2][Se0][Qe2][Re0]

Risk step 4: Dealing with risks

(1) Additional research: additional research on the circumstances leading to the formation of H_2S, characterize sulphur oxidation state in addition to sulphur abundance, research on the effect on the purity of produced H_2, research on the mix of H_2 and H_2S, research on optimal dimensions of the cavern (reduce reaction surface)
(2) Preventive measures: avoid sulphate sources, monitoring of microbial activities, avoid presence of hydrocarbons (no use of existing caverns), monitoring of geochemical composition, periodic restoration of sump conditions (see further measures in risk 1.16)
(3) Corrective measures: pH correction, increase iron concentration, restoration of sump conditions
(4) Description and classification residual risk considering the measures taken: taking the preventive and corrective measures into account the residual risk becomes: 1 (probability) and [Me1][Te2][Se0][Qe1][Re0] (consequences), **1/2**

[3] M.P.Laban, Hydrogen storage in salt caverns, chemical modelling and analysis of large-scale hydrogen storage in underground salt caverns, no reference, dated July 16 2020
[4] N. Dopffel, Microbial impact on hydrogen storage, NORCE, 2nd International Summer School on UHS, dated July 2023
[5] C.A. Peters, Underground H_2 storage: Geochemistry Considerations, Princeton University, 2nd International Summer School on UHS, dated July 2023
[6] M. Portarapillo & A. di Benedetto, Risk assessment of the large-scale hydrogen storage in salt caverns, article in Energies 14, dated 2021
[7] M. Panfilov, Underground and pipeline hydrogen storage, Compendium of Hydrogen Energy, pp 92-116, dated 2015

RISK Nr. 24.3 Emergence of negative public opinion

Risk step 1: Aim

Aim 24 for Water consuming companies (production): "*we want to ensure sustainable availability of sufficient (ground)water of excellent quality and contribute to efficient use of water*". Therefore, the aim is: no risk as a result of hydrogen storage in salt caverns for the quality of the extracted groundwater.

Risk step 2: Risk identification

(1) Risk: Emergence of negative public opinion, e.g., triggered by regional or national media, threatening the public image of the company using groundwater for their products
(2) Risk based on: Interpretation of facts
(3) Source of information: public opinion[8][9][10][11][12]
(4) Uncertainty: complete stakeholder analysis per location, risk analysis discussion with all stakeholders (separately)
(5) Type of causes: [Pc]
(6) Type of effects: [Te][Re]

Risk step 3: Risk classification

(1) Classification probability class: 3 (c): interpretation of factual information
(2) Classification consequence class: [Me0][Te2][Se0][Qe0][Re2]

Risk step 4: Dealing with risks

(1) Additional research: complete stakeholder analysis per location, risk analysis discussion with all stakeholders (separately)
(2) Preventive measures: transparent, pro-active and personal communication, direct involvement (shareholders), financial compensation ("burdens and benefits"), transparency with respect to all taken preventive measures (other risks)
(3) Corrective measures: transparent and personal communication, financial compensation (based on reversed burden of proof), transparency with respect to all taken corrective measures (other risks)
(4) Description and classification residual risk considering the measures taken: taking the preventive and corrective measures into account the residual risk eventually becomes: 2 (probability) and [Me0][Te1][Se0][Qe0][Re1] (consequences), **2/1**

[8] Public opinion with respect to CO_2 storage underneath Barendrecht: "Stichting CO2isNEE", 2010
[9] Public opinion with respect to environmental problems and subsidence as a result of salt mining: "Stop Zoutwinning!", 2021
[10] Public opinion with respect to future salt extraction Municipality of Haaksbergen, 2023
[11] Public opinion with respect to underground discharge of production water, www.stopafvalwatertwente.nl
[12] Public opinion with respect to Nitrogen storage in Heiligerlee, www.mijnendijnbelang.nl

Stakeholder: Water consuming companies (production)

Unmitigated risk matrix

4 x 3 Risk matrix		Consequence		
		1	2	3
Chance	3		24.2 24.3	
	2			24.1
	1			
	0			

Residual (mitigated) risk matrix

4 x 3 Risk matrix		Consequence		
		1	2	3
Chance	3			
	2	24.3		
	1		24.2	24.1
	0			

D.25 Stakeholder: Water consuming companies (cooling)

RISK Nr. 25.1 Cavern integrity loss

Risk step 1: Aim

Aim 25 for Water consuming companies (cooling): "*we want to ensure the availability of suitable and sufficient groundwater for the purpose of cooling*". Therefore, the aim is: no risk as a result of hydrogen storage in salt caverns for the extraction of groundwater for cooling.

Risk step 2: Risk identification

(1) Risk: Cavern breaches (tightness) / cavern integrity loss
(2) Risk based on: Interpretation of facts
(3) Source of information: Literature review (7 cases described in section 2.2.3.1) [1][2]
(4) Uncertainty: Additional research of the salt structure and rheology, cavern design
(5) Type of causes: [Tc][Rc][Gc][Oc][Ic]
(6) Type of effects: [Me][Te][Se][Qe][Re]

Risk step 3: Risk classification

(1) Classification probability class: 2 (c): interpretation of factual information
(2) Classification consequence class: [Me0][Te2][Se0][Qe1][Re0]

Risk step 4: Dealing with risks

(1) Additional research: research of the salt dome internal structure, including anomalous zones (section 3.4.7.1.4), and rheology, cavern design
(2) Preventive measures: open communication with other operators, minimum preconditions for H_2 storage cavern, detection of heterogeneities, enough distance to the domes edge, preferably use newly developed caverns (according to an optimal rock mechanical envelope) (see further measures in risk 1.6)
(3) Corrective measures: abandon cavern
(4) Description and classification residual risk considering the measures taken: taking the preventive and corrective measures into account the residual risk becomes: 1 (probability) and [Me0][Te2][Se0][Qe1][Re0] (consequences), **1/2**

[1] Bayou Corne, Louisiana, 2012

[2] Clovelly salt dome, Louisiana, 1992

RISK Nr. 25.2 Formation of H_2S beyond acceptable limits

Risk step 1: Aim

Aim 25 for Water consuming companies (cooling): "*we want to ensure the availability of suitable and sufficient groundwater for the purpose of cooling*". Therefore, the aim is: no risk as a result of hydrogen storage in salt caverns for the extraction of groundwater for cooling.

Risk step 2: Risk identification

(1) Risk: Formation of H_2S leading to contamination of the groundwater due to leakage
(2) Risk based on: Assumption
(3) Source of information: Literature review (section 5.4)[3] and research[4][5][6][7]
(4) Uncertainty: Additional research on the circumstances leading to the formation of H_2S
(5) Type of causes: [Tc][Gc]
(6) Type of effects: [Te][Qe]

Risk step 3: Risk classification

(1) Classification probability class: 3 (a): assumption based on expert judgement
(2) Classification consequence class: [Me0][Te1][Se0][Qe1][Re0]

Risk step 4: Dealing with risks

(1) Additional research: additional research on the circumstances leading to the formation of H_2S, characterize sulphur oxidation state in addition to sulphur abundance, research on the effect on the purity of produced H_2, research on the mix of H_2 and H_2S, research on optimal dimensions of the cavern (reduce reaction surface)
(2) Preventive measures: avoid sulphate sources, monitoring of microbial activities, avoid presence of hydrocarbons (no use of existing caverns), monitoring of geochemical composition, periodic restoration of sump conditions (see further measures in risk 1.16)
(3) Corrective measures: pH correction, increase iron concentration, restoration of sump conditions
(4) Description and classification residual risk considering the measures taken: taking the preventive and corrective measures into account the residual risk becomes: 1 (probability) and [Me0][Te0][Se0][Qe0][Re0] (consequences), **0**

[3] M.P.Laban, Hydrogen storage in salt caverns, chemical modelling and analysis of large-scale hydrogen storage in underground salt caverns, no reference, dated July 16 2020
[4] N. Dopffel, Microbial impact on hydrogen storage, NORCE, 2nd International Summer School on UHS, dated July 2023
[5] C.A. Peters, Underground H_2 storage: Geochemistry Considerations, Princeton University, 2nd International Summer School on UHS, dated July 2023
[6] M. Portarapillo & A. di Benedetto, Risk assessment of the large-scale hydrogen storage in salt caverns, article in Energies 14, dated 2021
[7] M. Panfilov, Underground and pipeline hydrogen storage, Compendium of Hydrogen Energy, pp 92-116, dated 2015

Stakeholder: Water consuming companies (cooling)

Unmitigated risk matrix

4 x 3 Risk matrix		Consequence		
		1	2	3
Chance	3	25.2		
	2		25.1	
	1			
	0			

Residual (mitigated) risk matrix

4 x 3 Risk matrix		Consequence		
		1	2	3
Chance	3			
	2			
	1		25.1	
	0	25.2		

D.26 Stakeholder: Nobian salt production (I)

RISK Nr. 26.1 Accident at the surface

Risk step 1: Aim

Aim 26 for Nobian salt production (I): "*We excel in the safe and reliable supply of high-purity salt, chlor-alkali and chloromethanes…. we continue to innovate every day to become safer, more efficient and sustainable and to ensure the essential products of today will continue to enrich our lives tomorrow*". Therefore, the aim is: no risk for salt mining in general and our own operations as a result of hydrogen storage in salt caverns, at all time.

Risk step 2: Risk identification

(1) Risk: Accident at the surface (blow-out, well leak) as a result of hydrogen storage
(2) Risk based on: Interpretation of facts / assumptions
(3) Source of information: Literature review[1][2], expert judgement
(4) Uncertainty: Blow-out modelling done by Brouard Consulting
(5) Type of causes: [Tc][Hc][Gc][Oc][Rc]
(6) Type of effects: [Me][Te][Qe][Re]

Risk step 3: Risk classification

(1) Classification probability class: 2 (a/c): assumption based on expert judgement and interpretation of factual information
(2) Classification consequence class: [Me2][Te2][Se0][Qe3][Re2]

Risk step 4: Dealing with risks

(1) Additional research: modelling of Blow-out, safety study on the effect at the surface
(2) Preventive measures (5 main): highest quality of BOP and safety valves / pressure gauges (H_2 certified material), all equipment designed for low T, rapid response plan, H_2-certified material (steel), construction and maintenance protocols (see further measures in risks 1.1 and 1.2)
(3) Corrective measures: actions according to rapid response plan, evacuation plan, fire extinguishing, damage control / repair, temporary partial shut-down and repair
(4) Description and classification residual risk considering the measures taken: taking the preventive and corrective measures into account the residual risk becomes: 1 (probability) and [Me2][Te2][Se0][Qe3][Re2] (consequences), **1/3**

[1] Fort Saskatchewan Ethane Blow-out and Fire (2001)

[2] Moss Bluff natural gas blow out and Fire (2004)

RISK Nr. 26.2 Subsurface accident

Risk step 1: Aim

Aim 26 for Nobian salt production (I): "*We excel in the safe and reliable supply of high-purity salt, chlor-alkali and chloromethanes…. we continue to innovate every day to become safer, more efficient and sustainable and to ensure the essential products of today will continue to enrich our lives tomorrow*". Therefore, the aim is: no risk for salt mining in general and our own operations as a result of hydrogen storage in salt caverns, at all time.

Risk step 2: Risk identification

(1) Risk: Subsurface accident (leakage vertical tubing/casing, casing overstretching, cavern breaches, falls) as a result of hydrogen storage
(2) Risk based on: Interpretation of facts / assumptions
(3) Source of information: Literature review[3][4][5][6][7], expert judgement
(4) Uncertainty: Additional research of the salt structure and rheology, the interaction with hydrogen, mechanical properties and damage evolution. Additional research of materials interacting with hydrogen
(5) Type of causes: [Hc][Tc][Rc][Ic][Gc]
(6) Type of effects: [Me][Te][Qe][Re]

Risk step 3: Risk classification

(1) Classification probability class: 3 (a/c): assumption based on expert judgement and interpretation of factual information
(2) Classification consequence class: [Me1][Te2][Se0][Qe3][Re2]

Risk step 4: Dealing with risks

(1) Additional research (5 main): creep research (grainsize) and durability of the salt, research of the salt dome internal structure, including anomalous zones (section 3.4.7.1.4), and rheology, additional research of the second phase rheology interacting with hydrogen, research on prevention of micro annuli at the casing / cement / rock interfaces, additional research of materials interacting with hydrogen, (see further research topics in risks 1.3, 1.5, 1.6, 1.8-1,12, 1.14 and 1.15)
(2) Preventive measures (5 main): minimum preconditions for H_2 storage cavern (well test), improved cavern design (avoid flat roof / interlayered formations / large diameter of the roof), periodic sonar measurements and cement bonding log (e.g., every 5 years), elastomers (no nitril) or self-healing material instead of cement, H_2 and H_2S certified material (including packers), (see further measures in risks 1.3, 1.5, 1.6, 1.8-1,12, 1.14 and 1.15)
(3) Corrective measures (5 main): controlled production / flaring of H_2, abandon cavern, adapt the pressures, (micro annuli and material) treatment with special materials (resins, silicates etc.,

[3] Magnolia, Louisiana, 2003
[4] Boling 1, 2, 4, Texas, USA, 2005
[5] Bayou Corne, Louisiana, 2012
[6] Eminence salt dome 1, 3, 4, Mississippi, 1972
[7] Jintan JK-A, China, 2015

biological treatment), use of deformable metals and casing expansion, (see further measures in risks 1.3, 1.5, 1.6, 1.8-1,12, 1.14 and 1.15)

(4) *Description and classification residual risk considering the measures taken:* taking the preventive and corrective measures into account the residual risk becomes: 3 (probability) and [Me1][Te2][Se0][Qe2][Re2] (consequences), **3/2**

RISK Nr. 26.3 Creep closure and subsidence

Risk step 1: Aim

Aim 26 for Nobian salt production (I): "*We excel in the safe and reliable supply of high-purity salt, chlor-alkali and chloromethanes…. we continue to innovate every day to become safer, more efficient and sustainable and to ensure the essential products of today will continue to enrich our lives tomorrow*". Therefore, the aim is: no risk for salt mining in general and our own operations as a result of hydrogen storage in salt caverns, at all time.

Risk step 2: Risk identification

(1) Risk: Subsidence (beyond predicted limits)
(2) Risk based on: Interpretation of facts
(3) Source of information: Literature review (sections 3.1.5.1 and 3.2.3) [8][9]
(4) Uncertainty: Additional research of the salt structure and rheology, cavern design
(5) Type of causes: [Rc][Ic][Gc][Oc][Tc][Pc]
(6) Type of effects: [Me][Te][Qe][Re]

Risk step 3: Risk classification

(1) Classification probability class: 2 (c): interpretation of factual information
(2) Classification consequence class: [Me1][Te3][Se0][Qe1][Re2]

Risk step 4: Dealing with risks

(1) Additional research: research of the salt structure and rheology, cavern design, geomechanical modelling
(2) Preventive measures: monitoring of subsidence by INSAR & surveying measurements, field tests (pressure observation test POT after well drill), updated cavern design, geomechanical modelling, determination of the minimum cavern pressure (see further measures in risk 1.7)
(3) Corrective measures: change of the average cavern pressure (higher), minimizing the subsidence by controlled abandonment
(4) Description and classification residual risk considering the measures taken: taking the preventive and corrective measures into account the residual risk becomes: 1 (probability) and [Me1][Te3][Se0][Qe1][Re2] (consequences), **1/3**

[8] Subsidence at Maceió, Brazil, 2021

[9] Matarandiba Island, Brazil, 2018

RISK Nr. 26.4 Emergence of negative public opinion

Risk step 1: Aim

Aim 26 for Nobian salt production (I): "*We excel in the safe and reliable supply of high-purity salt, chlor-alkali and chloromethanes…. we continue to innovate every day to become safer, more efficient and sustainable and to ensure the essential products of today will continue to enrich our lives tomorrow*". Therefore, the aim is: no risk for salt mining in general and our own operations as a result of hydrogen storage in salt caverns, at all time.

Risk step 2: Risk identification

(1) *Risk:* Emergence of negative public opinion, e.g., triggered by regional or national media, threatening the salt mining operation of Nobian
(2) *Risk based on:* Interpretation of facts
(3) *Source of information:* public opinion[10][11][12][13][14]
(4) *Uncertainty:* complete stakeholder analysis per location, risk analysis discussion with all stakeholders (separately)
(5) *Type of causes*: [Pc]
(6) *Type of effects*: [Me][Te][Se][Re]

Risk step 3: Risk classification

(1) *Classification probability class:* 3 (c): interpretation of factual information
(2) *Classification consequence class:* [Me2][Te3][Se1][Qe0][Re2]

Risk step 4: Dealing with risks

(1) *Additional research:* complete stakeholder analysis per location, risk analysis discussion with all stakeholders (separately)
(2) *Preventive measures:* transparent, pro-active and personal communication, direct involvement (shareholders), financial compensation ("burdens and benefits"), transparency with respect to all taken preventive measures (other risks)
(3) *Corrective measures:* transparent and personal communication, financial compensation (based on reversed burden of proof), transparency with respect to all taken corrective measures (other risks)
(4) *Description and classification residual risk considering the measures taken:* taking the preventive and corrective measures into account the residual risk eventually becomes: 2 (probability) and [Me1][Te2][Se0][Qe0][Re1] (consequences), **2/2**

[10] Public opinion with respect to CO_2 storage underneath Barendrecht: "Stichting CO2isNEE", 2010
[11] Public opinion with respect to environmental problems and subsidence as a result of salt mining: "Stop Zoutwinning!", 2021
[12] Public opinion with respect to future salt extraction Municipality of Haaksbergen, 2023
[13] Public opinion with respect to underground discharge of production water, www.stopafvalwatertwente.nl
[14] Public opinion with respect to Nitrogen storage in Heiligerlee, www.mijnendijnbelang.nl

RISK Nr. 26.5 Disputed responsibility due to stacked mining activities

Risk step 1: Aim

Aim 26 for Nobian salt production (I): "*We excel in the safe and reliable supply of high-purity salt, chlor-alkali and chloromethanes…. we continue to innovate every day to become safer, more efficient and sustainable and to ensure the essential products of today will continue to enrich our lives tomorrow*". Therefore, the aim is: no risk for salt mining in general and our own operations as a result of hydrogen storage in salt caverns, at all time.

Risk step 2: Risk identification

(1) Risk: Disputed responsibility due to stacked mining activities
(2) Risk based on: Assumption
(3) Source of information: Political discussions[15], public[16]
(4) Uncertainty: Scenario modelling of various critical scenarios to test regulations
(5) Type of causes: [Rc]
(6) Type of effects: [Me][Te][Re]

Risk step 3: Risk classification

(1) Classification probability class: 3 (a): assumption based on expert judgement
(2) Classification consequence class: [Me1][Te2][Se0][Qe0][Re2]

Risk step 4: Dealing with risks

(1) Additional research: scenario modelling of various critical scenarios to test regulations
(2) Preventive measures: regulations for operators regarding arial extent and duration of responsibility, seismic monitoring system, monitoring of subsidence by INSAR & surveying measurements before mining and during storage, mandatory report of incidents, regular meetings with all operators involved (including independent chairman, e.g., SodM), one overall geological model for all operators
(3) Corrective measures: mandatory insurance policy for all operators concerned, regulations for take-over of responsibilities in case of bankruptcy operator
(4) Description and classification residual risk considering the measures taken: taking the preventive and corrective measures into account the residual risk eventually becomes: 1 (probability) and [Me0][Te1][Se0][Qe0][Re0] (consequences), **1/1**

[15] Groenlinks, Stacked mining neglected in Nedmag-advice, 2019

[16] RTVOost, Growing frustration about mining, damage and new gas exploitation, January 2021

Stakeholder: Nobian salt production (I)

Unmitigated risk matrix

4 x 3 Risk matrix		Consequence		
		1	2	3
Chance	3		26.5	26.2 26.4
	2			26.1 26.3
	1			
	0			

Residual (mitigated) risk matrix

4 x 3 Risk matrix		Consequence		
		1	2	3
Chance	3		26.2	
	2		26.4	
	1	26.5		26.1 26.3
	0			

D.27 Stakeholder: Nobian salt production (II)

RISK Nr. 27.1 Accident at the surface

Risk step 1: Aim

Aim 27 for Nobian salt production (II): "*We are exploring how we can store green energy in our salt caverns. We're actively working to produce greener chemicals, including hydrogen, and are committed to stimulating and growing a circular economy*". Therefore, the aim is: no risk for salt mining in general and our own operations as a result of hydrogen storage in salt caverns, at all time.

Risk step 2: Risk identification

(1) Risk: Accident at the surface (blow-out, well leak) as a result of hydrogen storage
(2) Risk based on: Interpretation of facts / assumptions
(3) Source of information: Literature review[1][2], expert judgement
(4) Uncertainty: Blow-out modelling done by Brouard Consulting
(5) Type of causes: [Tc][Hc][Gc][Oc][Rc]
(6) Type of effects: [Me][Te][Se][Qe][Re]

Risk step 3: Risk classification

(1) Classification probability class: 2 (a/c): assumption based on expert judgement and interpretation of factual information
(2) Classification consequence class: [Me2][Te2][Se1][Qe3][Re2]

Risk step 4: Dealing with risks

(1) Additional research: modelling of Blow-out, safety study on the effect at the surface
(2) Preventive measures (5 main): highest quality of BOP and safety valves / pressure gauges (H_2 certified material), all equipment designed for low T, rapid response plan, H_2-certified material (steel), construction and maintenance protocols (see further measures in risks 1.1 and 1.2)
(3) Corrective measures: actions according to rapid response plan, evacuation plan, fire extinguishing, damage control / repair, temporary partial shut-down and repair
(4) Description and classification residual risk considering the measures taken: taking the preventive and corrective measures into account the residual risk becomes: 1 (probability) and [Me2][Te2][Se1][Qe3][Re2] (consequences), **1/3**

[1] Fort Saskatchewan Ethane Blow-out and Fire (2001)

[2] Moss Bluff natural gas blow out and Fire (2004)

RISK Nr. 27.2 Subsurface accident

Risk step 1: Aim

Aim 27 for Nobian salt production (II): "*We are exploring how we can store green energy in our salt caverns. We're actively working to produce greener chemicals, including hydrogen, and are committed to stimulating and growing a circular economy*". Therefore, the aim is: no risk for salt mining in general and our own operations as a result of hydrogen storage in salt caverns, at all time.

Risk step 2: Risk identification

(1) Risk: Subsurface accident (leakage vertical tubing/casing, casing overstretching, cavern breaches, tensile failures, falls) as a result of hydrogen storage
(2) Risk based on: Interpretation of facts / assumptions
(3) Source of information: Literature review[3][4][5][6][7], expert judgement
(4) Uncertainty: Additional research of the salt structure and rheology, the interaction with hydrogen, mechanical properties and damage evolution. Additional research of materials interacting with hydrogen
(5) Type of causes: [Hc][Tc][Rc][Ic][Gc]
(6) Type of effects: [Me][Te][Se][Qe][Re]

Risk step 3: Risk classification

(1) Classification probability class: 3 (a/c): assumption based on expert judgement and interpretation of factual information
(2) Classification consequence class: [Me2][Te2][Se1][Qe3][Re3]

Risk step 4: Dealing with risks

(1) Additional research (5 main): creep research (grainsize) and durability of the salt, research of the salt dome internal structure, including anomalous zones (section 3.4.7.1.4), and rheology, additional research of the second phase rheology interacting with hydrogen, research on prevention of micro annuli at the casing / cement / rock interfaces, additional research of materials interacting with hydrogen, (see further research topics in risks 1.3, 1.5, 1.6, 1.8-1,12, 1.14 and 1.15)
(2) Preventive measures (5 main): minimum preconditions for H_2 storage cavern (well test), improved cavern design (avoid flat roof / interlayered formations / large diameter of the roof), periodic sonar measurements and cement bonding log, elastomers (no nitril) or self-healing material instead of cement, H_2 and H_2S certified material (including packers), (see further measures in risks 1.3, 1.5, 1.6, 1.8-1,12, 1.14 and 1.15)
(3) Corrective measures (5 main): controlled production / flaring of H_2, abandon cavern, adapt the pressures, (micro annuli and material) treatment with special materials (resins, silicates etc.,

[3] Magnolia, Louisiana, 2003
[4] Boling 1, 2, 4, Texas, USA, 2005
[5] Bayou Corne, Louisiana, 2012
[6] Eminence salt dome 1, 3, 4, Mississippi, 1972
[7] Jintan JK-A, China, 2015

biological treatment), use of deformable metals and casing expansion, (see further measures in risks 1.3, 1.5, 1.6, 1.8-1,12, 1.14 and 1.15)

(4) *Description and classification residual risk considering the measures taken:* taking the preventive and corrective measures into account the residual risk becomes: 3 (probability) and [Me1][Te2][Se2][Qe2][Re2] (consequences), **3/2**

RISK Nr. 27.3 Creep closure and subsidence

Risk step 1: Aim

Aim 27 for Nobian salt production (II): "*We are exploring how we can store green energy in our salt caverns. We're actively working to produce greener chemicals, including hydrogen, and are committed to stimulating and growing a circular economy*". Therefore, the aim is: no risk for salt mining in general and our own operations as a result of hydrogen storage in salt caverns, at all time.

Risk step 2: Risk identification

(1) Risk: Subsidence (beyond predicted limits)
(2) Risk based on: Interpretation of facts
(3) Source of information: Literature review (sections 3.1.5.1 and 3.2.3) [8][9]
(4) Uncertainty: Additional research of the salt structure and rheology, cavern design
(5) Type of causes: [Rc][Ic][Gc][Oc][Tc][Pc]
(6) Type of effects: [Me][Te][Qe][Re]

Risk step 3: Risk classification

(1) Classification probability class: 2 (c): interpretation of factual information
(2) Classification consequence class: [Me2][Te3][Se0][Qe1][Re2]

Risk step 4: Dealing with risks

(1) Additional research: research of the salt structure and rheology, cavern design, geomechanical modelling
(2) Preventive measures: monitoring of subsidence by INSAR & surveying measurements, field tests (pressure observation test POT after well drill), updated cavern design, geomechanical modelling, determination of the minimum cavern pressure (see further measures in risk 1.7)
(3) Corrective measures: change of the average cavern pressure (higher), minimizing the subsidence by controlled abandonment
(4) Description and classification residual risk considering the measures taken: taking the preventive and corrective measures into account the residual risk becomes: 1 (probability) and [Me2][Te3][Se0][Qe1][Re2] (consequences), **1/3**

[8] Subsidence at Maceió, Brazil, 2021

[9] Matarandiba Island, Brazil, 2018

RISK Nr. 27.4 Formation of H_2S beyond acceptable limits

Risk step 1: Aim

Aim 27 for Nobian salt production (II): "*We are exploring how we can store green energy in our salt caverns. We're actively working to produce greener chemicals, including hydrogen, and are committed to stimulating and growing a circular economy*". Therefore, the aim is: no risk for salt mining in general and our own operations as a result of hydrogen storage in salt caverns, at all time.

Risk step 2: Risk identification

(1) Risk: Formation of H_2S beyond acceptable limits caused by anhydrite and other second phases (like carbonates), accelerated by contaminated brine or residual organic (blanket) material
(2) Risk based on: Assumption
(3) Source of information: Literature review (section 5.4)[10] and research[11][12][13][14]
(4) Uncertainty: Additional research on the circumstances leading to the formation of H_2S
(5) Type of causes: [Tc][Gc]
(6) Type of effects: [Me][Te][Qe]

Risk step 3: Risk classification

(1) Classification probability class: 3 (a): assumption based on expert judgement
(2) Classification consequence class: [Me1][Te2][Se0][Qe2][Re0]

Risk step 4: Dealing with risks

(1) Additional research: additional research on the circumstances leading to the formation of H_2S, characterize sulphur oxidation state in addition to sulphur abundance, research on the effect on the purity of produced H_2, research on the mix of H_2 and H_2S, research on optimal dimensions of the cavern (reduce reaction surface)
(2) Preventive measures: avoid sulphate sources, monitoring of microbial activities, avoid presence of hydrocarbons (no use of existing caverns), monitoring of geochemical composition, periodic restoration of sump conditions (see further measures in risk 1.16)
(3) Corrective measures: sweetening of the H_2 gas, pH correction, increase iron concentration, restoration of sump conditions
(4) Description and classification residual risk considering the measures taken: taking the preventive and corrective measures into account the residual risk becomes: 1 (probability) and [Me1][Te2][Se0][Qe1][Re0] (consequences), **1/2**

[10] M.P.Laban, Hydrogen storage in salt caverns, chemical modelling and analysis of large-scale hydrogen storage in underground salt caverns, no reference, dated July 16 2020
[11] N. Dopffel, Microbial impact on hydrogen storage, NORCE, 2nd International Summer School on UHS, dated July 2023
[12] C.A. Peters, Underground H_2 storage: Geochemistry Considerations, Princeton University, 2nd International Summer School on UHS, dated July 2023
[13] M. Portarapillo & A. di Benedetto, Risk assessment of the large-scale hydrogen storage in salt caverns, article in Energies 14, dated 2021
[14] M. Panfilov, Underground and pipeline hydrogen storage, Compendium of Hydrogen Energy, pp 92-116, dated 2015

RISK Nr. 27.5 Registered induced seismicity

Risk step 1: Aim

Aim 27 for Nobian salt production (II): "*We are exploring how we can store green energy in our salt caverns. We're actively working to produce greener chemicals, including hydrogen, and are committed to stimulating and growing a circular economy*". Therefore, the aim is: no risk for salt mining in general and our own operations as a result of hydrogen storage in salt caverns, at all time.

Risk step 2: Risk identification

(1) Risk: Registered induced seismicity caused by the operation (filling and emptying) of the cavern
(2) Risk based on: Interpretation of facts / assumption
(3) Source of information: Monitoring plans of underground Natural Gas and Nitrogen storage[15][16], literature review (section 5.2)
(4) Uncertainty: Research on characteristic locations in the salt dome sensitive to (micro)seismicity
(5) Type of causes: [Rc][Gc]
(6) Type of effects: [Te][Re]

Risk step 3: Risk classification

(1) Classification probability class: 3 (a/c): assumption based on expert judgement and interpretation of facts
(2) Classification consequence class: [Me0][Te2][Se0][Qe0][Re1]

Risk step 4: Dealing with risks

(1) Additional research: research on characteristic locations in the salt dome sensitive to (micro)seismicity
(2) Preventive measures: seismic monitoring (natural and induced seismicity), modelling of expected seismicity, no storage activities in or near an active fault zone, transparency and open communication, baseline measurement, transparency regarding seismic data
(3) Corrective measures: -
(4) Description and classification residual risk considering the measures taken: taking the preventive measures into account the residual risk becomes: 2 (probability) and [Me0][Te2][Se0][Qe0][Re1] (consequences), **2/2**

[15] Nouryon, Micro seismic network Heiligerlee & Zuidwending, observations Q3 2020, Powerpoint, no reference, no date

[16] NAM, Report "Instemmingsbesluit Norg", letter, no reference, dated December 3 2021

RISK Nr. 27.6 Emergence of negative public opinion

Risk step 1: Aim

Aim 27 for Nobian salt production (II): "*We are exploring how we can store green energy in our salt caverns. We're actively working to produce greener chemicals, including hydrogen, and are committed to stimulating and growing a circular economy*". Therefore, the aim is: no risk for salt mining in general and our own operations as a result of hydrogen storage in salt caverns, at all time.

Risk step 2: Risk identification

(1) Risk: Emergence of negative public opinion, e.g., triggered by regional or national media, threatening the secondary use of Nobian caverns
(2) Risk based on: Interpretation of facts
(3) Source of information: public opinion[17][18][19][20][21]
(4) Uncertainty: complete stakeholder analysis per location, risk analysis discussion with all stakeholders (separately)
(5) Type of causes: [Pc]
(6) Type of effects: [Me][Te][Re]

Risk step 3: Risk classification

(1) Classification probability class: 3 (c): interpretation of factual information
(2) Classification consequence class: [Me2][Te3][Se0][Qe0][Re2]

Risk step 4: Dealing with risks

(1) Additional research: complete stakeholder analysis per location, risk analysis discussion with all stakeholders (separately)
(2) Preventive measures: transparent, pro-active and personal communication, direct involvement (shareholders), financial compensation ("burdens and benefits"), transparency with respect to all taken preventive measures (other risks)
(3) Corrective measures: transparent and personal communication, financial compensation (based on reversed burden of proof), transparency with respect to all taken corrective measures (other risks)
(4) Description and classification residual risk considering the measures taken: taking the preventive and corrective measures into account the residual risk eventually becomes: 2 (probability) and [Me1][Te2][Se0][Qe0][Re1] (consequences), **2/2**

[17] Public opinion with respect to CO_2 storage underneath Barendrecht: "Stichting CO2isNEE", 2010
[18] Public opinion with respect to environmental problems and subsidence as a result of salt mining: "Stop Zoutwinning!", 2021
[19] Public opinion with respect to future salt extraction Municipality of Haaksbergen, 2023
[20] Public opinion with respect to underground discharge of production water, www.stopafvalwatertwente.nl
[21] Public opinion with respect to Nitrogen storage in Heiligerlee, www.mijnendijnbelang.nl

RISK Nr. 27.7 Disputed responsibility due to stacked mining activities

Risk step 1: Aim

Aim 27 for Nobian salt production (II): "*We are exploring how we can store green energy in our salt caverns. We're actively working to produce greener chemicals, including hydrogen, and are committed to stimulating and growing a circular economy*". Therefore, the aim is: no risk for salt mining in general and our own operations as a result of hydrogen storage in salt caverns, at all time.

Risk step 2: Risk identification

(1) Risk: Disputed responsibility due to stacked mining activities
(2) Risk based on: Assumption
(3) Source of information: Political discussions[22], public[23]
(4) Uncertainty: Scenario modelling of various critical scenarios to test regulations
(5) Type of causes: [Rc]
(6) Type of effects: [Me][Te][Re]

Risk step 3: Risk classification

(1) Classification probability class: 3 (a): assumption based on expert judgement
(2) Classification consequence class: [Me2][Te3][Se0][Qe0][Re2]

Risk step 4: Dealing with risks

(1) Additional research: scenario modelling of various critical scenarios to test regulations
(2) Preventive measures: regulations for operators regarding arial extent and duration of responsibility, seismic monitoring system, monitoring of subsidence by INSAR & surveying measurements before mining and during storage, mandatory report of incidents, regular meetings with all operators involved (including independent chairman, e.g., SodM), one overall geological model for all operators
(3) Corrective measures: mandatory insurance policy for all operators concerned, regulations for take-over of responsibilities in case of bankruptcy operator
(4) Description and classification residual risk considering the measures taken: taking the preventive and corrective measures into account the residual risk eventually becomes: 1 (probability) and [Me1][Te2][Se0][Qe0][Re0] (consequences), **1/2**

[22] Groenlinks, Stacked mining neglected in Nedmag-advice, 2019

[23] RTVOost, Growing frustration about mining, damage and new gas exploitation, January 2021

RISK Nr. 27.8 Threat for (future) on-shore energy storage

Risk step 1: Aim

Aim 27 for Nobian salt production (II): "*We are exploring how we can store green energy in our salt caverns. We're actively working to produce greener chemicals, including hydrogen, and are committed to stimulating and growing a circular economy*". Therefore, the aim is: no risk for salt mining in general and our own operations as a result of hydrogen storage in salt caverns, at all time.

Risk step 2: Risk identification

(1) Risk: Threat to future green energy storage in salt caverns (Licence to Operate) due to uncertainties about safety and consequences of the storage in salt caverns
(2) Risk based on: Assumption
(3) Source of information: Public, press, politics
(4) Uncertainty: (generic and) Site-specific risk assessments, site-specific research on geology, rock-salt properties
(5) Type of causes: [Pc]
(6) Type of effects: [Me][Te][Qe][Re]

Risk step 3: Risk classification

(1) Classification probability class: 3 (a): assumption based on expert judgement
(2) Classification consequence class: [Me3][Te3][Se0][Qe3][Re3]

Risk step 4: Dealing with risks

(1) Additional research: (generic and) site-specific risk assessments, site-specific research on geology and rock-salt properties
(2) Preventive measures (5 main): open pro-active communication with stakeholders (public, politics and press) and other operators, preferably use newly developed caverns (according to an optimal rock mechanical envelope), periodic leak tests, minimum preconditions for H_2 storage cavern, mandatory status-report (starting every year) (see further measures in risk 1.24)
(3) Corrective measures: open communication with stakeholders (public, politics and press) and other operators
(4) Description and classification residual risk considering the measures taken: taking the preventive and corrective measures into account the residual risk eventually becomes: 2 (probability) and [Me1][Te3][Se0][Qe0][Re2] (consequences), **2/3**

Stakeholder: Nobian salt production (II)

Unmitigated risk matrix

4 x 3 Risk matrix		Consequence		
		1	2	3
Chance	3		27.4 27.5	27.2 27.6 27.7 27.8
	2			27.1 27.3
	1			
	0			

Residual (mitigated) risk matrix

4 x 3 Risk matrix		Consequence		
		1	2	3
Chance	3		27.2	
	2		27.5 27.6	27.8
	1		27.4 27.7	27.1 27.3
	0			

D.28 Stakeholder: Data storage facilities (effected by ground vibrations)

RISK Nr. 28.1 Registered induced seismicity

Risk step 1: Aim

Aim 28 for Data storage facilities (effected by ground vibrations): "*The production of our company requires a safe and sound subsoil without disturbing vibrations*". Therefore, the aim is: no risk for our own operations as a result of hydrogen storage in salt caverns, at all time.

Risk step 2: Risk identification

(1) Risk: Registered induced seismicity caused by the operation (filling and emptying) of the cavern
(2) Risk based on: Interpretation of facts / assumption
(3) Source of information: Monitoring plans of underground Natural Gas and Nitrogen storage[1,2], literature review (section 5.2)
(4) Uncertainty: Research on characteristic locations in the salt dome sensitive to (micro)seismicity
(5) Type of causes: [Rc][Gc]
(6) Type of effects: [Me][Te]

Risk step 3: Risk classification

(1) Classification probability class: 3 (a/c): assumption based on expert judgement and interpretation of facts
(2) Classification consequence class: [Me1][Te2][Se0][Qe0][Re0]

Risk step 4: Dealing with risks

(1) Additional research: research on characteristic locations in the salt dome sensitive to (micro)seismicity
(2) Preventive measures: seismic monitoring (natural and induced seismicity), modelling of expected seismicity, no storage activities in or near an active fault zone, transparency and open communication, baseline measurement, transparency regarding seismic data
(3) Corrective measures: -
(4) Description and classification residual risk considering the measures taken: taking the preventive measures into account the residual risk becomes: 2 (probability) and [Me1][Te2][Se0][Qe0][Re0] (consequences), **2/2**

[1] Nouryon, Micro seismic network Heiligerlee & Zuidwending, observations Q3 2020, Powerpoint, no reference, no date

[2] NAM, Report "Instemmingsbesluit Norg", letter, no reference, dated December 3 2021

Stakeholder: Data storage facilities

Unmitigated risk matrix

4 x 3 Risk matrix		Consequence		
		1	2	3
Chance	3		28.1	
	2			
	1			
	0			

Residual (mitigated) risk matrix

4 x 3 Risk matrix		Consequence		
		1	2	3
Chance	3			
	2		28.1	
	1			
	0			

D.29 Stakeholder: Greenpeace

RISK Nr. 29.1 Accident at the surface

Risk step 1: Aim

Aim 29 for Greenpeace: "*Greenpeace is a global network of independent campaigning organizations that use peaceful protest and creative communication to expose global environmental problems and promote solutions that are essential to a green and peaceful future*". Therefore, the aim is: no risk for a green and peaceful future as a result of hydrogen storage in salt caverns, at all time.

Risk step 2: Risk identification

(1) Risk: Accident at the surface (blow-out, well leak, pipeline integrity) as a result of hydrogen storage
(2) Risk based on: Interpretation of facts / assumptions
(3) Source of information: Literature review[1][2], expert judgement
(4) Uncertainty: Blow-out modelling done by Brouard Consulting, experience within the industry with hydrogen pipelines
(5) Type of causes: [Tc][Hc][Gc][Oc][Rc][Ic]
(6) Type of effects: [Te][Qe]

Risk step 3: Risk classification

(1) Classification probability class: 2 (a/c): assumption based on expert judgement and interpretation of factual information
(2) Classification consequence class: [Me0][Te2][Se0][Qe1][Re0]

Risk step 4: Dealing with risks

(1) Additional research: modelling of Blow-out, safety study on the effect at the surface, literature research hydrogen infrastructure KEM 29 (research in progress)
(2) Preventive measures (5 main): highest quality of BOP and safety valves / pressure gauges (H_2 certified material), all equipment designed for low T, rapid response plan, H_2-certified material (steel), construction and maintenance protocols, (see further measures in risks 1.1, 1.2 and 1.4)
(3) Corrective measures: actions according to rapid response plan, evacuation plan, fire extinguishing, damage control / repair, temporary partial shut-down and repair
(4) Description and classification residual risk considering the measures taken: taking the preventive and corrective measures into account the residual risk becomes: 1 (probability) and [Me0][Te2][Se0][Qe1][Re02] (consequences), **1/2**

[1] Fort Saskatchewan Ethane Blow-out and Fire (2001)

[2] Moss Bluff natural gas blow out and Fire (2004)

RISK Nr. 29.2 Subsurface accident

Risk step 1: Aim

Aim 29 for Greenpeace: "*Greenpeace is a global network of independent campaigning organizations that use peaceful protest and creative communication to expose global environmental problems and promote solutions that are essential to a green and peaceful future*". Therefore, the aim is: no risk for a green and peaceful future as a result of hydrogen storage in salt caverns, at all time.

Risk step 2: Risk identification

(1) Risk: Subsurface accident (leakage vertical tubing/casing, casing overstretching, cavern breaches, tensile failures, falls) as a result of hydrogen storage
(2) Risk based on: Interpretation of facts / assumptions
(3) Source of information: Literature review[3][4][5][6][7], expert judgement
(4) Uncertainty: Additional research of the salt structure and rheology, the interaction with hydrogen, mechanical properties and damage evolution. Additional research of materials interacting with hydrogen
(5) Type of causes: [Hc][Tc][Rc][Ic][Gc]
(6) Type of effects: [Te][Qe]

Risk step 3: Risk classification

(1) Classification probability class: 3 (a/c): assumption based on expert judgement and interpretation of factual information
(2) Classification consequence class: [Me0][Te2][Se0][Qe1][Re0]

Risk step 4: Dealing with risks

(1) Additional research (5 main): creep research (grainsize) and durability of the salt, research of the salt dome internal structure, including anomalous zones (section 3.4.7.1.4), and rheology, additional research of the second phase rheology interacting with hydrogen, research on prevention of micro annuli at the casing / cement / rock interfaces, additional research of materials interacting with hydrogen, (see further research topics in risks 1.3, 1.5, 1.6, 1.8-1,12, 1.14 and 1.15)
(2) Preventive measures (5 main): minimum preconditions for H_2 storage cavern (well test), improved cavern design (avoid flat roof / interlayered formations / large diameter of the roof), periodic sonar measurements and cement bonding log (e.g., every 5 years), elastomers (no nitril) or self-healing material instead of cement, H_2 and H_2S certified material (including packers), (see further measures in risks 1.3, 1.5, 1.6, 1.8-1,12, 1.14 and 1.15)
(3) Corrective measures (5 main): controlled production / flaring of H_2, abandon cavern, adapt the pressures, (micro annuli and material) treatment with special materials (resins, silicates etc.,

[3] Magnolia, Louisiana, 2003
[4] Boling 1, 2, 4, Texas, USA, 2005
[5] Bayou Corne, Louisiana, 2012
[6] Eminence salt dome 1, 3, 4, Mississippi, 1972
[7] Jintan JK-A, China, 2015

biological treatment), use of deformable metals and casing expansion, (see further measures in risks 1.3, 1.5, 1.6, 1.8-1,12, 1.14 and 1.15)

(4) Description and classification residual risk considering the measures taken: Both probability and consequence classes have not been reduced and remain: **3/2**, in more detail 3 (probability) and [Me0][Te2][Se0][Qe1][Re0] (consequences)

RISK Nr. 29.3 Failure of the storage system

Risk step 1: Aim

Aim 29 for Greenpeace: "*Greenpeace is a global network of independent campaigning organizations that use peaceful protest and creative communication to expose global environmental problems and promote solutions that are essential to a green and peaceful future*". Therefore, the aim is: no risk for a green and peaceful future as a result of hydrogen storage in salt caverns, at all time.

Risk step 2: Risk identification

(1) Risk: Failure of the storage system (due to fire, natural disaster, terrorism or IT-failure)
(2) Risk based on: Assumptions
(3) Source of information: Expert judgement
(4) Uncertainty: Cannot be reduced
(5) Type of causes: [Hc][Oc][Tc][Rc][Ic]
(6) Type of effects: [Te][Qe]

Risk step 3: Risk classification

(1) Classification probability class: 2 (a): assumption based on expert judgement
(2) Classification consequence class: [Me0][Te2][Se0][Qe1][Re0]

Risk step 4: Dealing with risks

(1) Additional research: -
(2) Preventive measures (5 main): adhere to the general safety regulations and fire-prevention measurements for hydrogen installations, back-up by remote-controlled operation, assign as "vital infrastructure" and act accordingly, manual controls requiring double authorisation, analogue pressure and temperature gauges at critical locations (double system) (see further measures in risks 1.19 – 1.22)
(3) Corrective measures: actions according to rapid response plan, fire alarm and fire extinguishing, remote-controlled operation, pressure relief valve (PRV) for worst case when pressure gets near lithostatic pressure at casing shoe, automatic release of pressure
(4) Description and classification residual risk considering the measures taken: taking the preventive and corrective measures into account the residual risk eventually becomes: 1 (probability) and [Me0][Te0][Se0][Qe0][Re0] (consequences), **0**

RISK Nr. 29.4 Formation of H_2S beyond acceptable limits

Risk step 1: Aim

Aim 29 for Greenpeace: "*Greenpeace is a global network of independent campaigning organizations that use peaceful protest and creative communication to expose global environmental problems and promote solutions that are essential to a green and peaceful future*". Therefore, the aim is: no risk for a green and peaceful future as a result of hydrogen storage in salt caverns, at all time.

Risk step 2: Risk identification

(1) Risk: Formation of H_2S leading to contamination of the environment due to leakage
(2) Risk based on: Assumption
(3) Source of information: Literature review (section 5.4)[8] and research[9][10][11][12]
(4) Uncertainty: Additional research on the circumstances leading to the formation of H_2S
(5) Type of causes: [Tc][Gc]
(6) Type of effects: [Te]

Risk step 3: Risk classification

(1) Classification probability class: 3 (a): assumption based on expert judgement
(2) Classification consequence class: [Me0][Te2][Se0][Qe0][Re0]

Risk step 4: Dealing with risks

(1) Additional research: additional research on the circumstances leading to the formation of H_2S, characterize sulphur oxidation state in addition to sulphur abundance, research on the effect on the purity of produced H_2, research on the mix of H_2 and H_2S, research on optimal dimensions of the cavern (reduce reaction surface)
(2) Preventive measures: avoid sulphate sources, monitoring of microbial activities, avoid presence of hydrocarbons (no use of existing caverns), monitoring of geochemical composition, periodic restoration of sump conditions (see further measures in risk 1.16)
(3) Corrective measures: pH correction, increase iron concentration, restoration of sump conditions
(4) Description and classification residual risk considering the measures taken: taking the preventive and corrective measures into account the residual risk becomes: 1 (probability) and [Me0][Te1][Se0][Qe0][Re0] (consequences), **1/1**

[8] M.P.Laban, Hydrogen storage in salt caverns, chemical modelling and analysis of large-scale hydrogen storage in underground salt caverns, no reference, dated July 16 2020
[9] N. Dopffel, Microbial impact on hydrogen storage, NORCE, 2nd International Summer School on UHS, dated July 2023
[10] C.A. Peters, Underground H_2 storage: Geochemistry Considerations, Princeton University, 2nd International Summer School on UHS, dated July 2023
[11] M. Portarapillo & A. di Benedetto, Risk assessment of the large-scale hydrogen storage in salt caverns, article in Energies 14, dated 2021
[12] M. Panfilov, Underground and pipeline hydrogen storage, Compendium of Hydrogen Energy, pp 92-116, dated 2015

RISK Nr. 29.5 Registered induced seismicity

Risk step 1: Aim

Aim 29 for Greenpeace: "*Greenpeace is a global network of independent campaigning organizations that use peaceful protest and creative communication to expose global environmental problems and promote solutions that are essential to a green and peaceful future*". Therefore, the aim is: no risk for a green and peaceful future as a result of hydrogen storage in salt caverns, at all time.

Risk step 2: Risk identification

(1) Risk: Registered induced seismicity caused by the operation (filling and emptying) of the cavern
(2) Risk based on: Interpretation of facts / assumption
(3) Source of information: Monitoring plans of underground Natural Gas and Nitrogen storage[13][14], literature review (section 5.2)
(4) Uncertainty: Research on characteristic locations in the salt dome sensitive to (micro)seismicity
(5) Type of causes: [Rc][Gc]
(6) Type of effects: [Te]

Risk step 3: Risk classification

(1) Classification probability class: 3 (a/c): assumption based on expert judgement and interpretation of facts
(2) Classification consequence class: [Me0][Te2][Se0][Qe0][Re0]

Risk step 4: Dealing with risks

(1) Additional research: research on characteristic locations in the salt dome sensitive to (micro)seismicity
(2) Preventive measures: seismic monitoring (natural and induced seismicity), modelling of expected seismicity, no storage activities in or near an active fault zone, transparency and open communication, baseline measurement, transparency regarding seismic data
(3) Corrective measures: -
(4) Description and classification residual risk considering the measures taken: taking the preventive measures into account the residual risk becomes: 2 (probability) and [Me0][Te2][Se0][Qe0][Re0] (consequences), **2/2**

[13] Nouryon, Micro seismic network Heiligerlee & Zuidwending, observations Q3 2020, Powerpoint, no reference, no date

[14] NAM, Report "Instemmingsbesluit Norg", letter, no reference, dated December 3 2021

Stakeholder: Greenpeace

Unmitigated risk matrix

4 x 3 Risk matrix		Consequence		
		1	2	3
Chance	3		29.2 29.4 29.5	
	2		29.1 29.3	
	1			
	0			

Residual (mitigated) risk matrix

4 x 3 Risk matrix		Consequence		
		1	2	3
Chance	3		29.2	
	2		29.5	
	1	29.4	29.1	
	0	29.3		

D.30 Stakeholder: Wadden Sea Association ("Waddenvereniging")

RISK Nr. 30.1 Accident at the surface

Risk step 1: Aim

Aim 30 for Wadden Sea Association ("Waddenvereniging"): "*The organization strives for preservation, restoration and good management of nature, landscape and environment and the ecological and cultural-historical values of the Wadden area, including the northern sea clay-area and the North Sea as irreplaceable and unique nature reserves*". Therefore, the aim is: no risk for the nature reserves within the Wadden area, including the northern sea clay-area and the North Sea, as a result of the hydrogen storage.

Risk step 2: Risk identification

(1) Risk: Accident at the surface (blow-out, well leak, pipeline integrity loss) as a result of hydrogen storage
(2) Risk based on: Interpretation of facts / assumptions
(3) Source of information: Literature review[1][2], expert judgement
(4) Uncertainty: Blow-out modelling done by Brouard Consulting, experience within the industry with hydrogen pipelines
(5) Type of causes: [Tc][Hc][Gc][Oc][Rc][Ic]
(6) Type of effects: [Te][Qe]

Risk step 3: Risk classification

(1) Classification probability class: 2 (a/c): assumption based on expert judgement and interpretation of factual information
(2) Classification consequence class: [Me0][Te2][Se0][Qe1][Re0]

Risk step 4: Dealing with risks

(1) Additional research: modelling of Blow-out, safety study on the effect at the surface, literature research hydrogen infrastructure KEM 29 (research in progress)
(2) Preventive measures (5 main): highest quality of BOP and safety valves / pressure gauges (H_2 certified material), all equipment designed for low T, rapid response plan, H_2-certified material (steel), construction and maintenance protocols (see further measures in risks 1.1, 1.2 and 1.4)
(3) Corrective measures: actions according to rapid response plan, evacuation plan, fire extinguishing, damage control / repair, temporary partial shut-down and repair
(4) Description and classification residual risk considering the measures taken: taking the preventive and corrective measures into account the residual risk becomes: 1 (probability) and [Me0][Te2][Se0][Qe1][Re02] (consequences), **1/2**

[1] Fort Saskatchewan Ethane Blow-out and Fire (2001)
[2] Moss Bluff natural gas blow out and Fire (2004)

RISK Nr. 30.2 Subsurface accident

Risk step 1: Aim

Aim 30 for Wadden Sea Association ("Waddenvereniging"): "*The organization strives for preservation, restoration and good management of nature, landscape and environment and the ecological and cultural-historical values of the Wadden area, including the northern sea clay-area and the North Sea as irreplaceable and unique nature reserves*". Therefore, the aim is: no risk for the nature reserves within the Wadden area, including the northern sea clay-area and the North Sea, as a result of the hydrogen storage.

Risk step 2: Risk identification

(1) Risk: Subsurface accident (leakage vertical tubing/casing, casing overstretching, cavern breaches, tensile failure, falls) as a result of hydrogen storage
(2) Risk based on: Interpretation of facts / assumptions
(3) Source of information: Literature review[3][4][5][6][7], expert judgement
(4) Uncertainty: Additional research of the salt structure and rheology, the interaction with hydrogen, mechanical properties and damage evolution. Additional research of materials interacting with hydrogen
(5) Type of causes: [Hc][Tc][Rc][Ic][Gc]
(6) Type of effects: [Te][Qe]

Risk step 3: Risk classification

(1) Classification probability class: 3 (a/c): assumption based on expert judgement and interpretation of factual information
(2) Classification consequence class: [Me0][Te2][Se0][Qe1][Re0]

Risk step 4: Dealing with risks

(1) Additional research (5 main): creep research (grainsize) and durability of the salt, research of the salt dome internal structure, including anomalous zones (section 3.4.7.1.4), and rheology, additional research of the second phase rheology interacting with hydrogen, research on prevention of micro annuli at the casing / cement / rock interfaces, additional research of materials interacting with hydrogen, (see further research topics in risks 1.3, 1.5, 1.6, 1.8-1,12, 1.14 and 1.15)
(2) Preventive measures (5 main): minimum preconditions for H_2 storage cavern (well test), improved cavern design (avoid flat roof / interlayered formations / large diameter of the roof), periodic sonar measurements and cement bonding log, elastomers (no nitril) or self-healing material instead of cement, H_2 and H_2S certified material (including packers), (see further measures in risks 1.3, 1.5, 1.6, 1.8-1,12, 1.14 and 1.15)

[3] Magnolia, Louisiana, 2003
[4] Boling 1, 2, 4, Texas, USA, 2005
[5] Bayou Corne, Louisiana, 2012
[6] Eminence salt dome 1, 3, 4, Mississippi, 1972
[7] Jintan JK-A, China, 2015

(3) *Corrective measures (5 main):* controlled production / flaring of H_2, abandon cavern, adapt the pressures, (micro annuli and material) treatment with special materials (resins, silicates etc., biological treatment), use of deformable metals and casing expansion, (see further measures in risks 1.3, 1.5, 1.6, 1.8-1,12, 1.14 and 1.15)

(4) *Description and classification residual risk considering the measures taken:* Both probability and consequence classes have not been reduced and remain: **3/2**, in more detail 3 (probability) and [Me0][Te2][Se0][Qe1][Re0] (consequences)

RISK Nr. 30.3 Creep closure and subsidence

Risk step 1: Aim

Aim 30 for Wadden Sea Association ("Waddenvereniging"): "*The organization strives for preservation, restoration and good management of nature, landscape and environment and the ecological and cultural-historical values of the Wadden area, including the northern sea clay-area and the North Sea as irreplaceable and unique nature reserves*". Therefore, the aim is: no risk for the nature reserves within the Wadden area, including the northern sea clay-area and the North Sea, as a result of the hydrogen storage.

Risk step 2: Risk identification

(1) Risk: Subsidence (beyond predicted limits)
(2) Risk based on: Interpretation of facts
(3) Source of information: Literature review (sections 3.1.5.1 and 3.2.3) [8][9]
(4) Uncertainty: Additional research of the salt structure and rheology, cavern design
(5) Type of causes: [Rc][Ic][Gc][Oc][Tc][Pc]
(6) Type of effects: [Te]

Risk step 3: Risk classification

(1) Classification probability class: 2 (c): interpretation of factual information
(2) Classification consequence class: [Me0][Te2][Se0][Qe0][Re0]

Risk step 4: Dealing with risks

(1) Additional research: research of the salt structure and rheology, cavern design, geomechanical modelling
(2) Preventive measures: monitoring of subsidence by INSAR & surveying measurements, field tests (pressure observation test POT after well drill), updated cavern design, additional POT after cavern design, geomechanical modelling, sonar, determination of the minimum cavern pressure
(3) Corrective measures: change of the average cavern pressure (higher), minimizing the subsidence by controlled abandonment
(4) Description and classification residual risk considering the measures taken: taking the preventive and corrective measures into account the residual risk becomes: 1 (probability) and [Me0][Te2][Se0][Qe0][Re0] (consequences), **1/2**

[8] Subsidence at Maceió, Brazil, 2021

[9] Matarandiba Island, Brazil, 2018

Stakeholder: Wadden Sea Association ("Waddenvereniging")

Unmitigated risk matrix

4 x 3 Risk matrix		Consequence		
		1	2	3
Chance	3		30.2	
	2		30.1 30.3	
	1			
	0			

Residual (mitigated) risk matrix

4 x 3 Risk matrix		Consequence		
		1	2	3
Chance	3		30.2	
	2			
	1		30.1 30.3	
	0			

D.31 Stakeholder: Wadden Academy

RISK Nr. 31.1 Accident at the surface

Risk step 1: Aim

Aim 31 for Wadden Academy: "*The Wadden Academy aims to furnish the scientific foundations for an economically and ecologically responsible future in the Wadden Sea Region, a World Heritage Site*". Therefore, the aim is: no risk for the World Heritage Site, the Wadden Sea Region, as a result of the hydrogen storage.

Risk step 2: Risk identification

(1) Risk: Accident at the surface (blow-out, well leak, pipeline integrity loss) as a result of hydrogen storage
(2) Risk based on: Interpretation of facts / assumptions
(3) Source of information: Literature review[1][2], expert judgement
(4) Uncertainty: Blow-out modelling done by Brouard Consulting, experience within the industry with hydrogen pipelines
(5) Type of causes: [Tc][Hc][Gc][Oc][Rc][Ic]
(6) Type of effects: [Te][Qe]

Risk step 3: Risk classification

(1) Classification probability class: 2 (a/c): assumption based on expert judgement and interpretation of factual information
(2) Classification consequence class: [Me0][Te2][Se0][Qe1][Re0]

Risk step 4: Dealing with risks

(1) Additional research: modelling of Blow-out, safety study on the effect at the surface, literature research hydrogen infrastructure KEM 29 (research in progress)
(2) Preventive measures (5 main): highest quality of BOP and safety valves / pressure gauges (H_2 certified material), all equipment designed for low T, rapid response plan, H_2-certified material (steel), construction and maintenance protocols (see further measures in risks 1.1, 1.2 and 1.4)
(3) Corrective measures: actions according to rapid response plan, evacuation plan, fire extinguishing, damage control / repair, temporary partial shut-down and repair
(4) Description and classification residual risk considering the measures taken: taking the preventive and corrective measures into account the residual risk becomes: 1 (probability) and [Me0][Te2][Se0][Qe1][Re0] (consequences), **1/2**

[1] Fort Saskatchewan Ethane Blow-out and Fire (2001)
[2] Moss Bluff natural gas blow out and Fire (2004)

RISK Nr. 31.2 Subsurface accident

Risk step 1: Aim

Aim 31 for Wadden Academy: "*The Wadden Academy aims to furnish the scientific foundations for an economically and ecologically responsible future in the Wadden Sea Region, a World Heritage Site*". Therefore, the aim is: no risk for the World Heritage Site, the Wadden Sea Region, as a result of the hydrogen storage.

Risk step 2: Risk identification

(1) Risk: Subsurface accident (leakage vertical tubing/casing, casing overstretching, cavern breaches, tensile failure, falls) as a result of hydrogen storage
(2) Risk based on: Interpretation of facts / assumptions
(3) Source of information: Literature review[3][4][5][6][7], expert judgement
(4) Uncertainty: Additional research of the salt structure and rheology, the interaction with hydrogen, mechanical properties and damage evolution. Additional research of materials interacting with hydrogen
(5) Type of causes: [Hc][Tc][Rc][Ic][Gc]
(6) Type of effects: [Te][Qe]

Risk step 3: Risk classification

(1) Classification probability class: 3 (a/c): assumption based on expert judgement and interpretation of factual information
(2) Classification consequence class: [Me0][Te2][Se0][Qe1][Re0]

Risk step 4: Dealing with risks

(1) Additional research (5 main): creep research (grainsize) and durability of the salt, research of the salt dome internal structure, including anomalous zones (section 3.4.7.1.4), and rheology, additional research of the second phase rheology interacting with hydrogen, research on prevention of micro annuli at the casing / cement / rock interfaces, additional research of materials interacting with hydrogen, (see further research topics in risks 1.3, 1.5, 1.6, 1.8-1,12, 1.14 and 1.15)
(2) Preventive measures (5 main): minimum preconditions for H_2 storage cavern (well test), improved cavern design (avoid flat roof / interlayered formations / large diameter of the roof), periodic sonar measurements and cement bonding log, elastomers (no nitril) or self-healing material instead of cement, H_2 and H_2S certified material (including packers), (see further measures in risks 1.3, 1.5, 1.6, 1.8-1,12, 1.14 and 1.15)
(3) Corrective measures: controlled production / flaring of H_2, abandon cavern, adapt the pressures, (micro annuli and material) treatment with special materials (resins, silicates etc., biological

[3] Magnolia, Louisiana, 2003
[4] Boling 1, 2, 4, Texas, USA, 2005
[5] Bayou Corne, Louisiana, 2012
[6] Eminence salt dome 1, 3, 4, Mississippi, 1972
[7] Jintan JK-A, China, 2015

treatment), use of deformable metals and casing expansion, (see further measures in risks 1.3, 1.5, 1.6, 1.8-1,12, 1.14 and 1.15)

(4) Description and classification residual risk considering the measures taken: Both probability and consequence classes have not been reduced and remain: **3/2**, in more detail 3 (probability) and [Me0][Te2][Se0][Qe1][Re0] (consequences)

RISK Nr. 31.3 Creep closure and subsidence

Risk step 1: Aim

Aim 31 for Wadden Academy: "*The Wadden Academy aims to furnish the scientific foundations for an economically and ecologically responsible future in the Wadden Sea Region, a World Heritage Site*". Therefore, the aim is: no risk for the World Heritage Site, the Wadden Sea Region, as a result of the hydrogen storage.

Risk step 2: Risk identification

(1) Risk: Subsidence (beyond predicted limits)
(2) Risk based on: Interpretation of facts
(3) Source of information: Literature review (sections 3.1.5.1 and 3.2.3) [8][9]
(4) Uncertainty: Additional research of the salt structure and rheology, cavern design
(5) Type of causes: [Rc][Ic][Gc][Oc][Tc][Pc]
(6) Type of effects: [Te]

Risk step 3: Risk classification

(1) Classification probability class: 2 (c): interpretation of factual information
(2) Classification consequence class: [Me0][Te2][Se0][Qe0][Re0]

Risk step 4: Dealing with risks

(1) Additional research: research of the salt structure and rheology, cavern design, geomechanical modelling
(2) Preventive measures: monitoring of subsidence by INSAR & surveying measurements, field tests (pressure observation test POT after well drill), updated cavern design, additional POT after cavern design, geomechanical modelling, sonar, determination of the minimum cavern pressure
(3) Corrective measures: change of the average cavern pressure (higher), minimizing the subsidence by controlled abandonment
(4) Description and classification residual risk considering the measures taken: taking the preventive and corrective measures into account the residual risk becomes: 1 (probability) and [Me0][Te2][Se0][Qe0][Re0] (consequences), **1/2**

[8] Subsidence at Maceió, Brazil, 2021
[9] Matarandiba Island, Brazil, 2018

Stakeholder: Wadden Academy

Unmitigated risk matrix

4 x 3 Risk matrix		Consequence		
		1	2	3
Chance	3		31.2	
	2		31.1 31.3	
	1			
	0			

Residual (mitigated) risk matrix

4 x 3 Risk matrix		Consequence		
		1	2	3
Chance	3		31.2	
	2			
	1		31.1 31.3	
	0			

D.32 Stakeholder: Private landowner above/close to salt caverns (I)

RISK Nr. 32.1 Accident at the surface

Risk step 1: Aim

Aim 32 for Private landowner above/close to salt caverns (I): "*Protection of private use of groundwater*". Therefore, the aim is: no risk for the quality of the private well(s) as a result of the hydrogen storage.

Risk step 2: Risk identification

(1) Risk: Accident at the surface (blow-out, well leak, pipeline integrity loss) as a result of hydrogen storage
(2) Risk based on: Interpretation of facts / assumptions
(3) Source of information: Literature review[12], expert judgement
(4) Uncertainty: Blow-out modelling done by Brouard Consulting, experience within the industry with hydrogen pipelines
(5) Type of causes: [Tc][Hc][Gc][Oc][Rc][Ic]
(6) Type of effects: [Me][Te][Qe]

Risk step 3: Risk classification

(1) Classification probability class: 2 (a/c): assumption based on expert judgement and interpretation of factual information
(2) Classification consequence class: [Me1][Te2][Se0][Qe3][Re0]

Risk step 4: Dealing with risks

(1) Additional research: modelling of Blow-out, safety study on the effect at the surface, literature research hydrogen infrastructure KEM 29 (research in progress)
(2) Preventive measures (5 main): highest quality of BOP and safety valves / pressure gauges (H_2 certified material), all equipment designed for low T, rapid response plan, H_2-certified material (steel), construction and maintenance protocols (see further measures in risks 1.1, 1.2 and 1.4)
(3) Corrective measures: actions according to rapid response plan, evacuation plan, fire extinguishing, damage control / repair, temporary partial shut-down and repair
(4) Description and classification residual risk considering the measures taken: taking the preventive and corrective measures into account the residual risk becomes: 1 (probability) and [Me1][Te2][Se0][Qe3][Re0] (consequences), **1/3**

[1] Fort Saskatchewan Ethane Blow-out and Fire (2001)
[2] Moss Bluff natural gas blow out and Fire (2004)

RISK Nr. 32.2 Subsurface accident

Risk step 1: Aim

Aim 32 for Private landowner above/close to salt caverns (I): "*Protection of private use of groundwater*". Therefore, the aim is: no risk for the quality of the private well(s) as a result of the hydrogen storage.

Risk step 2: Risk identification

(1) Risk: Subsurface accident (leakage vertical tubing/casing, casing overstretching, cavern breaches, tensile failure, falls) as a result of hydrogen storage
(2) Risk based on: Interpretation of facts / assumptions
(3) Source of information: Literature review[3][4][5][6][7], expert judgement
(4) Uncertainty: Additional research of the salt structure and rheology, the interaction with hydrogen, mechanical properties and damage evolution. Additional research of materials interacting with hydrogen
(5) Type of causes: [Hc][Tc][Rc][Ic][Gc]
(6) Type of effects: [Me][Te][Qe]

Risk step 3: Risk classification

(1) Classification probability class: 3 (a/c): assumption based on expert judgement and interpretation of factual information
(2) Classification consequence class: [Me1][Te3][Se0][Qe3][Re0]

Risk step 4: Dealing with risks

(1) Additional research (5 main): creep research (grainsize) and durability of the salt, research of the salt dome internal structure, including anomalous zones (section 3.4.7.1.4), and rheology, additional research of the second phase rheology interacting with hydrogen, research on prevention of micro annuli at the casing / cement / rock interfaces, additional research of materials interacting with hydrogen, (see further research topics in risks 1.3, 1.5, 1.6, 1.8-1,12, 1.14 and 1.15)
(2) Preventive measures (5 main): minimum preconditions for H_2 storage cavern (well test), improved cavern design (avoid flat roof / interlayered formations / large diameter of the roof), periodic sonar measurements and cement bonding log, elastomers (no nitril) or self-healing material instead of cement, H_2 and H_2S certified material (including packers), (see further measures in risks 1.3, 1.5, 1.6, 1.8-1,12, 1.14 and 1.15)
(3) Corrective measures (5 main): controlled production / flaring of H_2, abandon cavern, adapt the pressures, (micro annuli and material) treatment with special materials (resins, silicates etc., biological treatment), use of deformable metals and casing expansion, (see further measures in risks 1.3, 1.5, 1.6, 1.8-1,12, 1.14 and 1.15)

[3] Magnolia, Louisiana, 2003
[4] Boling 1, 2, 4, Texas, USA, 2005
[5] Bayou Corne, Louisiana, 2012
[6] Eminence salt dome 1, 3, 4, Mississippi, 1972
[7] Jintan JK-A, China, 2015

(4) *Description and classification residual risk considering the measures taken:* taking the preventive and corrective measures into account the residual risk becomes: 3 (probability) and [Me1][Te2][Se0][Qe2][Re0] (consequences), **3/2**

RISK Nr. 32.3 Formation of H_2S beyond acceptable limits

Risk step 1: Aim

Aim 32 for Private landowner above/close to salt caverns (I): "*Protection of private use of groundwater*". Therefore, the aim is: no risk for the quality of the private well(s) as a result of the hydrogen storage.

Risk step 2: Risk identification

(1) Risk: Formation of H_2S leading to contamination of the groundwater due to leakage
(2) Risk based on: Assumption
(3) Source of information: Literature review (section 5.4)[8] and research[9][10][11][12]
(4) Uncertainty: Additional research on the circumstances leading to the formation of H_2S
(5) Type of causes: [Tc][Gc]
(6) Type of effects: [Te][Se][Qe]

Risk step 3: Risk classification

(1) Classification probability class: 3 (a): assumption based on expert judgement
(2) Classification consequence class: [Me0][Te2][Se1][Qe3][Re0]

Risk step 4: Dealing with risks

(1) Additional research: additional research on the circumstances leading to the formation of H_2S, characterize sulphur oxidation state in addition to sulphur abundance, research on the effect on the purity of produced H_2, research on the mix of H_2 and H_2S, research on optimal dimensions of the cavern (reduce reaction surface)
(2) Preventive measures: avoid sulphate sources, monitoring of microbial activities, avoid presence of hydrocarbons (no use of existing caverns), monitoring of geochemical composition, periodic restoration of sump conditions (see further measures in risk 1.16)
(3) Corrective measures: pH correction, increase iron concentration, restoration of sump conditions, alternative water source (drinking water)
(4) Description and classification residual risk considering the measures taken: taking the preventive and corrective measures into account the residual risk becomes: 1 (probability) and [Me0][Te1][Se0][Qe2][Re0] (consequences), **1/2**

[8] M.P.Laban, Hydrogen storage in salt caverns, chemical modelling and analysis of large-scale hydrogen storage in underground salt caverns, no reference, dated July 16 2020
[9] N. Dopffel, Microbial impact on hydrogen storage, NORCE, 2nd International Summer School on UHS, dated July 2023
[10] C.A. Peters, Underground H_2 storage: Geochemistry Considerations, Princeton University, 2nd International Summer School on UHS, dated July 2023
[11] M. Portarapillo & A. di Benedetto, Risk assessment of the large-scale hydrogen storage in salt caverns, article in Energies 14, dated 2021
[12] M. Panfilov, Underground and pipeline hydrogen storage, Compendium of Hydrogen Energy, pp 92-116, dated 2015

Stakeholder: Private landowner above/close to salt caverns (I)

Unmitigated risk matrix

4 x 3 Risk matrix		Consequence		
		1	2	3
Chance	3			32.2 32.3
	2			32.1
	1			
	0			

Residual (mitigated) risk matrix

4 x 3 Risk matrix		Consequence		
		1	2	3
Chance	3		32.2	
	2			
	1		32.3	32.1
	0			

D.33 Stakeholder: Private landowner above/close to salt caverns (II)

RISK Nr. 33.1 Accident at the surface

Risk step 1: Aim

Aim 33 for Private landowner above/close to salt caverns (II): "*Protection of private cattle and crops*". Therefore, the aim is: no risk for the private cattle and crops as a result of the hydrogen storage.

Risk step 2: Risk identification

(1) Risk: Accident at the surface (blow-out, well leak, pipeline integrity loss) as a result of hydrogen storage
(2) Risk based on: Interpretation of facts / assumptions
(3) Source of information: Literature review[1][2], expert judgement
(4) Uncertainty: Blow-out modelling done by Brouard Consulting, experience within the industry with hydrogen pipelines
(5) Type of causes: [Tc][Hc][Gc][Oc][Rc][Ic]
(6) Type of effects: [Me][Te][Qe][Re]

Risk step 3: Risk classification

(1) Classification probability class: 2 (a/c): assumption based on expert judgement and interpretation of factual information
(2) Classification consequence class: [Me1][Te2][Se0][Qe2][Re2]

Risk step 4: Dealing with risks

(1) Additional research: modelling of Blow-out, safety study on the effect at the surface, literature research hydrogen infrastructure KEM 29 (research in progress)
(2) Preventive measures (5 main): highest quality of BOP and safety valves / pressure gauges (H_2 certified material), all equipment designed for low T, rapid response plan, H_2-certified material (steel), construction and maintenance protocols (see further measures in risks 1.1, 1.2 and 1.4)
(3) Corrective measures: actions according to rapid response plan, evacuation plan, fire extinguishing, damage control / repair, temporary partial shut-down and repair
(4) Description and classification residual risk considering the measures taken: taking the preventive and corrective measures into account the residual risk becomes: 1 (probability) and [Me1][Te2][Se0][Qe2][Re2] (consequences), **1/2**

[1] Fort Saskatchewan Ethane Blow-out and Fire (2001)

[2] Moss Bluff natural gas blow out and Fire (2004)

RISK Nr. 33.2 Subsurface accident

Risk step 1: Aim

Aim 33 for Private landowner above/close to salt caverns (II): "*Protection of private cattle and crops*". Therefore, the aim is: no risk for the private cattle and crops as a result of the hydrogen storage.

Risk step 2: Risk identification

(1) Risk: Subsurface accident (leakage vertical tubing/casing, casing overstretching, cavern breaches, tensile failure, falls) as a result of hydrogen storage
(2) Risk based on: Interpretation of facts / assumptions
(3) Source of information: Literature review[3][4][5][6][7], expert judgement
(4) Uncertainty: Additional research of the salt structure and rheology, the interaction with hydrogen, mechanical properties and damage evolution. Additional research of materials interacting with hydrogen
(5) Type of causes: [Hc][Tc][Rc][Ic][Gc]
(6) Type of effects: [Te][Qe][Re]

Risk step 3: Risk classification

(1) Classification probability class: 3 (a/c): assumption based on expert judgement and interpretation of factual information
(2) Classification consequence class: [Me0][Te2][Se0][Qe2][Re2]

Risk step 4: Dealing with risks

(1) Additional research (5 main): creep research (grainsize) and durability of the salt, research of the salt dome internal structure, including anomalous zones (section 3.4.7.1.4), and rheology, additional research of the second phase rheology interacting with hydrogen, research on prevention of micro annuli at the casing / cement / rock interfaces, additional research of materials interacting with hydrogen, (see further research topics in risks 1.3, 1.5, 1.6, 1.8-1,12, 1.14 and 1.15)
(2) Preventive measures (5 main): minimum preconditions for H_2 storage cavern (well test), improved cavern design (avoid flat roof / interlayered formations / large diameter of the roof), periodic sonar measurements and cement bonding log (e.g., every 5 years), elastomers (no nitril) or self-healing material instead of cement, H_2 and H_2S certified material (including packers), (see further measures in risks 1.3, 1.5, 1.6, 1.8-1,12, 1.14 and 1.15)
(3) Corrective measures (5 main): controlled production / flaring of H_2, abandon cavern, adapt the pressures, (micro annuli and material) treatment with special materials (resins, silicates etc., biological treatment), use of deformable metals and casing expansion, (see further measures in risks 1.3, 1.5, 1.6, 1.8-1,12, 1.14 and 1.15)

[3] Magnolia, Louisiana, 2003
[4] Boling 1, 2, 4, Texas, USA, 2005
[5] Bayou Corne, Louisiana, 2012
[6] Eminence salt dome 1, 3, 4, Mississippi, 1972
[7] Jintan JK-A, China, 2015

(4) *Description and classification residual risk considering the measures taken:* Both probability and consequence classes have not been reduced and remain: **3/2**, in more detail 3 (probability) and [Me0][Te2][Se0][Qe2][Re2] (consequences)

RISK Nr. 33.3 Failure of the storage system

Risk step 1: Aim

Aim 33 for Private landowner above/close to salt caverns (II): "*Protection of private cattle and crops*". Therefore, the aim is: no risk for the private cattle and crops as a result of the hydrogen storage.

Risk step 2: Risk identification

(1) Risk: Failure of the storage system (due to fire, natural disaster, terrorism or IT-failure)
(2) Risk based on: Assumptions
(3) Source of information: Expert judgement
(4) Uncertainty: Cannot be reduced
(5) Type of causes: [Hc][Oc][Tc][Rc][Ic]
(6) Type of effects: [Me][Te][Qe]

Risk step 3: Risk classification

(1) Classification probability class: 2 (a): assumption based on expert judgement
(2) Classification consequence class: [Me1][Te2][Se0][Qe3][Re0]

Risk step 4: Dealing with risks

(1) Additional research: -
(2) Preventive measures (5 main): adhere to the general safety regulations and fire-prevention measurements for hydrogen installations, back-up by remote-controlled operation, assign as "vital infrastructure" and act accordingly, manual controls requiring double authorisation, analogue pressure and temperature gauges at critical locations (double system) (see further measures in risks 1.19 – 1.22)
(3) Corrective measures: actions according to rapid response plan, fire alarm and fire extinguishing, remote-controlled operation, pressure relief valve (PRV) for worst case when pressure gets near lithostatic pressure at casing shoe, automatic release of pressure
(4) Description and classification residual risk considering the measures taken: taking the preventive and corrective measures into account the residual risk eventually becomes: 1 (probability) and [Me0][Te0][Se0][Qe0][Re0] (consequences), **0**

RISK Nr. 33.4 Formation of H_2S beyond acceptable limits

Risk step 1: Aim

Aim 33 for Private landowner above/close to salt caverns (II): "*Protection of private cattle and crops*". Therefore, the aim is: no risk for the private cattle and crops as a result of the hydrogen storage.

Risk step 2: Risk identification

(1) Risk: Formation of H_2S leading to contamination of the groundwater due to leakage
(2) Risk based on: Assumption
(3) Source of information: Literature review (section 5.4)[8] and research[9][10][11][12]
(4) Uncertainty: Additional research on the circumstances leading to the formation of H_2S
(5) Type of causes: [Tc][Gc]
(6) Type of effects: [Me][Te][Se][Qe]

Risk step 3: Risk classification

(1) Classification probability class: 3 (a): assumption based on expert judgement
(2) Classification consequence class: [Me0][Te2][Se1][Qe3][Re0]

Risk step 4: Dealing with risks

(1) Additional research: additional research on the circumstances leading to the formation of H_2S, characterize sulphur oxidation state in addition to sulphur abundance, research on the effect on the purity of produced H_2, research on the mix of H_2 and H_2S, research on optimal dimensions of the cavern (reduce reaction surface)
(2) Preventive measures: avoid sulphate sources, monitoring of microbial activities, avoid presence of hydrocarbons (no use of existing caverns), monitoring of geochemical composition, periodic restoration of sump conditions (see further measures in risk 1.16)
(3) Corrective measures: pH correction, increase iron concentration, restoration of sump conditions, alternative water source (drinking water)
(4) Description and classification residual risk considering the measures taken: taking the preventive and corrective measures into account the residual risk becomes: 1 (probability) and [Me0][Te1][Se0][Qe2][Re0] (consequences), **1/2**

[8] M.P.Laban, Hydrogen storage in salt caverns, chemical modelling and analysis of large-scale hydrogen storage in underground salt caverns, no reference, dated July 16 2020
[9] N. Dopffel, Microbial impact on hydrogen storage, NORCE, 2nd International Summer School on UHS, dated July 2023
[10] C.A. Peters, Underground H_2 storage: Geochemistry Considerations, Princeton University, 2nd International Summer School on UHS, dated July 2023
[11] M. Portarapillo & A. di Benedetto, Risk assessment of the large-scale hydrogen storage in salt caverns, article in Energies 14, dated 2021
[12] M. Panfilov, Underground and pipeline hydrogen storage, Compendium of Hydrogen Energy, pp 92-116, dated 2015

Stakeholder: Private landowner above/close to salt caverns (II)

Unmitigated risk matrix

4 x 3 Risk matrix		Consequence		
		1	2	3
Chance	3		33.2	33.4
	2		33.1	33.3
	1			
	0			

Residual (mitigated) risk matrix

4 x 3 Risk matrix		Consequence		
		1	2	3
Chance	3		33.2	
	2			
	1		33.1 33.4	
	0	33.3		

D.34 Stakeholder: Private landowner above/close to salt caverns (III)

RISK Nr. 34.1 Accident at the surface

Risk step 1: Aim

Aim 34 for Private landowner above/close to salt caverns (III): "*Value retention of own property*". Therefore, the aim is: no risk for the own property (buildings, terrain) as a result of the hydrogen storage.

Risk step 2: Risk identification

(1) Risk: Accident at the surface (blow-out, well leak, pipeline integrity loss) as a result of hydrogen storage
(2) Risk based on: Interpretation of facts / assumptions
(3) Source of information: Literature review[1][2], expert judgement
(4) Uncertainty: Blow-out modelling done by Brouard Consulting, experience within the industry with hydrogen pipelines
(5) Type of causes: [Tc][Hc][Gc][Oc][Rc][Ic]
(6) Type of effects: [Me][Te][Se][Qe]

Risk step 3: Risk classification

(1) Classification probability class: 2 (a/c): assumption based on expert judgement and interpretation of factual information
(2) Classification consequence class: [Me1][Te3][Se3][Qe3][Re0]

Risk step 4: Dealing with risks

(1) Additional research: modelling of Blow-out, safety study on the effect at the surface, literature research hydrogen infrastructure KEM 29 (research in progress)
(2) Preventive measures (5 main): highest quality of BOP and safety valves / pressure gauges (H_2 certified material), all equipment designed for low T, rapid response plan, H_2-certified material (steel), construction and maintenance protocols, (see further measures in risks 1.1, 1.2 and 1.4)
(3) Corrective measures: actions according to rapid response plan, evacuation plan, fire extinguishing, damage control / repair, temporary partial shut-down and repair
(4) Description and classification residual risk considering the measures taken: taking the preventive and corrective measures into account the residual risk becomes: 1 (probability) and [Me1][Te3][Se3][Qe3][Re0] (consequences), **1/3**

[1] Fort Saskatchewan Ethane Blow-out and Fire (2001)

[2] Moss Bluff natural gas blow out and Fire (2004)

RISK Nr. 34.2 Subsurface accident

Risk step 1: Aim

Aim 34 for Private landowner above/close to salt caverns (III): "*Value retention of own property*". Therefore, the aim is: no risk for the own property (buildings, terrain) as a result of the hydrogen storage.

Risk step 2: Risk identification

(1) Risk: Subsurface accident (leakage vertical tubing/casing, casing overstretching, cavern breaches, tensile failure, falls) as a result of hydrogen storage
(2) Risk based on: Interpretation of facts / assumptions
(3) Source of information: Literature review[3][4][5][6][7], expert judgement
(4) Uncertainty: Additional research of the salt structure and rheology, the interaction with hydrogen, mechanical properties and damage evolution. Additional research of materials interacting with hydrogen
(5) Type of causes: [Hc][Tc][Rc][Ic][Gc]
(6) Type of effects: [Me][Te][Se][Qe]

Risk step 3: Risk classification

(1) Classification probability class: 3 (a/c): assumption based on expert judgement and interpretation of factual information
(2) Classification consequence class: [Me1][Te3][Se3][Qe3][Re0]

Risk step 4: Dealing with risks

(1) Additional research (5 main): creep research (grainsize) and durability of the salt, research of the salt dome internal structure, including anomalous zones (section 3.4.7.1.4), and rheology, additional research of the second phase rheology interacting with hydrogen, research on prevention of micro annuli at the casing / cement / rock interfaces, additional research of materials interacting with hydrogen, (see further research topics in risks 1.3, 1.5, 1.6, 1.8-1,12, 1.14 and 1.15)
(2) Preventive measures (5 main): minimum preconditions for H_2 storage cavern (well test), improved cavern design (avoid flat roof / interlayered formations / large diameter of the roof), periodic sonar measurements and cement bonding log (e.g., every 5 years), elastomers (no nitril) or self-healing material instead of cement, H_2 and H_2S certified material (including packers), (see further measures in risks 1.3, 1.5, 1.6, 1.8-1,12, 1.14 and 1.15)
(3) Corrective measures (5 main): controlled production / flaring of H_2, abandon cavern, adapt the pressures, (micro annuli and material) treatment with special materials (resins, silicates etc., biological treatment), use of deformable metals and casing expansion, (see further measures in risks 1.3, 1.5, 1.6, 1.8-1,12, 1.14 and 1.15)

[3] Magnolia, Louisiana, 2003
[4] Boling 1, 2, 4, Texas, USA, 2005
[5] Bayou Corne, Louisiana, 2012
[6] Eminence salt dome 1, 3, 4, Mississippi, 1972
[7] Jintan JK-A, China, 2015

(4) *Description and classification residual risk considering the measures taken:* taking the preventive and corrective measures into account the residual risk becomes: 3 (probability) and [Me1][Te2][Se1][Qe2][Re0] (consequences), **3/2**

RISK Nr. 34.3 Creep closure and subsidence

Risk step 1: Aim

Aim 34 for Private landowner above/close to salt caverns (III): "*Value retention of own property*". Therefore, the aim is: no risk for the own property (buildings, terrain) as a result of the hydrogen storage.

Risk step 2: Risk identification

(1) Risk: Subsidence (beyond predicted limits)
(2) Risk based on: Interpretation of facts
(3) Source of information: Literature review (sections 3.1.5.1 and 3.2.3) [8][9]
(4) Uncertainty: Additional research of the salt structure and rheology, cavern design
(5) Type of causes: [Rc][Ic][Gc][Oc][Tc][Pc]
(6) Type of effects: [Me][Te][Se][Qe]

Risk step 3: Risk classification

(1) Classification probability class: 2 (c): interpretation of factual information
(2) Classification consequence class: [Me1][Te3][Se1][Qe3][Re0]

Risk step 4: Dealing with risks

(1) Additional research: research of the salt structure and rheology, cavern design, geomechanical modelling
(2) Preventive measures: monitoring of subsidence by INSAR & surveying measurements, field tests (pressure observation test POT after well drill), updated cavern design, geomechanical modelling, determination of the minimum cavern pressure (see further measures in risk 1.7)
(3) Corrective measures: change of the average cavern pressure (higher), minimizing the subsidence by controlled abandonment
(4) Description and classification residual risk considering the measures taken: taking the preventive and corrective measures into account the residual risk becomes: 1 (probability) and [Me1][Te3][Se1][Qe3][Re0] (consequences), **1/3**

[8] Subsidence at Maceió, Brazil, 2021

[9] Matarandiba Island, Brazil, 2018

RISK Nr. 34.4 Failure of the storage system

Risk step 1: Aim

Aim 34 for Private landowner above/close to salt caverns (III): "*Value retention of own property*". Therefore, the aim is: no risk for the own property (buildings, terrain) as a result of the hydrogen storage.

Risk step 2: Risk identification

(1) Risk: Failure of the storage system (due to fire, natural disaster, terrorism or IT-failure)
(2) Risk based on: Assumptions
(3) Source of information: Expert judgement
(4) Uncertainty: Cannot be reduced
(5) Type of causes: [Hc][Oc][Tc][Rc][Ic]
(6) Type of effects: [Me][Te][Se][Qe]

Risk step 3: Risk classification

(1) Classification probability class: 2 (a): assumption based on expert judgement
(2) Classification consequence class: [Me1][Te2][Se3][Qe3][Re0]

Risk step 4: Dealing with risks

(1) Additional research: -
(2) Preventive measures (5 main): adhere to the general safety regulations and fire-prevention measurements for hydrogen installations, back-up by remote-controlled operation, assign as "vital infrastructure" and act accordingly, manual controls requiring double authorisation, analogue pressure and temperature gauges at critical locations (double system) (see further measures in risks 1.19 – 1.22)
(3) Corrective measures: actions according to rapid response plan, fire alarm and fire extinguishing, remote-controlled operation, pressure relief valve (PRV) for worst case when pressure gets near lithostatic pressure at casing shoe, automatic release of pressure
(4) Description and classification residual risk considering the measures taken: taking the preventive and corrective measures into account the residual risk eventually becomes: 1 (probability) and [Me0][Te1][Se0][Qe1][Re0] (consequences), **1/1**

RISK Nr. 34.5 Formation of H_2S beyond acceptable limits

Risk step 1: Aim

Aim 34 for Private landowner above/close to salt caverns (III): "*Value retention of own property*". Therefore, the aim is: no risk for the own property (buildings, terrain) as a result of the hydrogen storage.

Risk step 2: Risk identification

(1) Risk: Formation of H_2S leading to contamination of the groundwater due to leakage
(2) Risk based on: Assumption
(3) Source of information: Literature review (section 5.4)[10] and research[11][12][13][14]
(4) Uncertainty: Additional research on the circumstances leading to the formation of H_2S
(5) Type of causes: [Tc][Gc]
(6) Type of effects: [Me][Te][Se][Qe]

Risk step 3: Risk classification

(1) Classification probability class: 3 (a): assumption based on expert judgement
(2) Classification consequence class: [Me0][Te2][Se1][Qe0][Re0]

Risk step 4: Dealing with risks

(1) Additional research: additional research on the circumstances leading to the formation of H_2S, characterize sulphur oxidation state in addition to sulphur abundance, research on the effect on the purity of produced H_2, research on the mix of H_2 and H_2S, research on optimal dimensions of the cavern (reduce reaction surface)
(2) Preventive measures: avoid sulphate sources, monitoring of microbial activities, avoid presence of hydrocarbons (no use of existing caverns), monitoring of geochemical composition, periodic restoration of sump conditions (see further measures in risk 1.16)
(3) Corrective measures: pH correction, increase iron concentration, restoration of sump conditions
(4) Description and classification residual risk considering the measures taken: taking the preventive and corrective measures into account the residual risk becomes: 1 (probability) and [Me0][Te1][Se0][Qe1][Re0] (consequences), **1/1**

[10] M.P.Laban, Hydrogen storage in salt caverns, chemical modelling and analysis of large-scale hydrogen storage in underground salt caverns, no reference, dated July 16 2020
[11] N. Dopffel, Microbial impact on hydrogen storage, NORCE, 2nd International Summer School on UHS, dated July 2023
[12] C.A. Peters, Underground H_2 storage: Geochemistry Considerations, Princeton University, 2nd International Summer School on UHS, dated July 2023
[13] M. Portarapillo & A. di Benedetto, Risk assessment of the large-scale hydrogen storage in salt caverns, article in Energies 14, dated 2021
[14] M. Panfilov, Underground and pipeline hydrogen storage, Compendium of Hydrogen Energy, pp 92-116, dated 2015

RISK Nr. 34.6 Registered induced seismicity

Risk step 1: Aim

Aim 34 for Private landowner above/close to salt caverns (III): "*Value retention of own property*". Therefore, the aim is: no risk for the own property (buildings, terrain) as a result of the hydrogen storage.

Risk step 2: Risk identification

(1) Risk: Registered induced seismicity caused by the operation (filling and emptying) of the cavern
(2) Risk based on: Interpretation of facts / assumption
(3) Source of information: Monitoring plans of underground Natural Gas and Nitrogen storage[15][16], literature review (section 5.2)
(4) Uncertainty: Research on characteristic locations in the salt dome sensitive to (micro)seismicity
(5) Type of causes: [Rc][Gc]
(6) Type of effects: [Te][Se]

Risk step 3: Risk classification

(1) Classification probability class: 3 (a/c): assumption based on expert judgement and interpretation of facts
(2) Classification consequence class: [Me0][Te2][Se1][Qe0][Re0]

Risk step 4: Dealing with risks

(1) Additional research: research on characteristic locations in the salt dome sensitive to (micro)seismicity
(2) Preventive measures: seismic monitoring (natural and induced seismicity), modelling of expected seismicity, no storage activities in or near an active fault zone, transparency and open communication, baseline measurement, transparency regarding seismic data
(3) Corrective measures: -
(4) Description and classification residual risk considering the measures taken: taking the preventive measures into account the residual risk becomes: 2 (probability) and [Me0][Te2][Se1][Qe0][Re0] (consequences), **2/2**

[15] Nouryon, Micro seismic network Heiligerlee & Zuidwending, observations Q3 2020, Powerpoint, no reference, no date

[16] NAM, Report "Instemmingsbesluit Norg", letter, no reference, dated December 3 2021

RISK Nr. 34.7 Emergence of negative public opinion

Risk step 1: Aim

Aim 34 for Private landowner above/close to salt caverns (III): "*Value retention of own property*". Therefore, the aim is: no risk for the own property (buildings, terrain) as a result of the hydrogen storage.

Risk step 2: Risk identification

(1) Risk: Emergence of negative public opinion, e.g., triggered by regional or national media
(2) Risk based on: Interpretation of facts
(3) Source of information: public opinion[17][18][19][20][21]
(4) Uncertainty: complete stakeholder analysis per location, risk analysis discussion with all stakeholders (separately)
(5) Type of causes: [Pc]
(6) Type of effects: [Te][Se][Re]

Risk step 3: Risk classification

(1) Classification probability class: 3 (c): interpretation of factual information
(2) Classification consequence class: [Me0][Te3][Se1][Qe0][Re2]

Risk step 4: Dealing with risks

(1) Additional research: complete stakeholder analysis per location, risk analysis discussion with all stakeholders (separately)
(2) Preventive measures: transparent, pro-active and personal communication, direct involvement (shareholders), financial compensation ("burdens and benefits"), transparency with respect to all taken preventive measures (other risks)
(3) Corrective measures: transparent and personal communication, financial compensation (based on reversed burden of proof), transparency with respect to all taken corrective measures (other risks)
(4) Description and classification residual risk considering the measures taken: taking the preventive and corrective measures into account the residual risk eventually becomes: 2 (probability) and [Me0][Te2][Se1][Qe0][Re0] (consequences), **2/2**

[17] Public opinion with respect to CO_2 storage underneath Barendrecht: "Stichting CO2isNEE", 2010
[18] Public opinion with respect to environmental problems and subsidence as a result of salt mining: "Stop Zoutwinning!", 2021
[19] Public opinion with respect to future salt extraction Municipality of Haaksbergen, 2023
[20] Public opinion with respect to underground discharge of production water, www.stopafvalwatertwente.nl
[21] Public opinion with respect to Nitrogen storage in Heiligerlee, www.mijnendijnbelang.nl

RISK Nr. 34.8 Disputed responsibility due to stacked mining activities

Risk step 1: Aim

Aim 34 for Private landowner above/close to salt caverns (III): "*Value retention of own property*". Therefore, the aim is: no risk for the own property (buildings, terrain) as a result of the hydrogen storage.

Risk step 2: Risk identification

(1) Risk: Disputed responsibility due to stacked mining activities
(2) Risk based on: Assumption
(3) Source of information: Political discussions[22], public[23]
(4) Uncertainty: Scenario modelling of various critical scenarios to test regulations
(5) Type of causes: [Rc]
(6) Type of effects: [Te][Se]

Risk step 3: Risk classification

(1) Classification probability class: 3 (a): assumption based on expert judgement
(2) Classification consequence class: [Me0][Te3][Se1][Qe0][Re0]

Risk step 4: Dealing with risks

(1) Additional research: scenario modelling of various critical scenarios to test regulations
(2) Preventive measures: regulations for operators regarding arial extent and duration of responsibility, seismic monitoring system, monitoring of subsidence by INSAR & surveying measurements before mining and during storage, mandatory report of incidents, regular meetings with all operators involved (including independent chairman, e.g., SodM), one overall geological model for all operators
(3) Corrective measures: mandatory insurance policy for all operators concerned, regulations for take-over of responsibilities in case of bankruptcy operator
(4) Description and classification residual risk considering the measures taken: taking the preventive and corrective measures into account the residual risk eventually becomes: 1 (probability) and [Me0][Te2][Se0][Qe0][Re0] (consequences), **1/2**

[22] Groenlinks, Stacked mining neglected in Nedmag-advice, 2019

[23] RTVOost, Growing frustration about mining, damage and new gas exploitation, January 2021

Stakeholder: Private landowner above/close to salt caverns (III)

Unmitigated risk matrix

4 x 3 Risk matrix		Consequence		
		1	2	3
Chance	3		34.5 34.6	34.2 34.7 34.8
	2			34.1 34.3 34.4
	1			
	0			

Residual (mitigated) risk matrix

4 x 3 Risk matrix		Consequence		
		1	2	3
Chance	3		34.2	
	2		34.6 34.7	
	1	34.4 34.5	34.8	34.1 34.3
	0			

D.35 Stakeholder: Private landowner in the vicinity

RISK Nr. 35.1 Accident at the surface

Risk step 1: Aim

Aim 35 for Private landowner in the vicinity: "*Value retention of own property*". Therefore, the aim is: no risk for the own property (buildings, terrain) as a result of the hydrogen storage.

Risk step 2: Risk identification

(1) Risk: Accident at the surface (blow-out, well leak, pipeline integrity loss) as a result of hydrogen storage
(2) Risk based on: Interpretation of facts / assumptions
(3) Source of information: Literature review[1][2], expert judgement
(4) Uncertainty: Blow-out modelling done by Brouard Consulting, experience within the industry with hydrogen pipelines
(5) Type of causes: [Tc][Hc][Gc][Oc][Rc][Ic]
(6) Type of effects: [Me][Te][Se][Qe]

Risk step 3: Risk classification

(1) Classification probability class: 2 (a/c): assumption based on expert judgement and interpretation of factual information
(2) Classification consequence class: [Me1][Te3][Se1][Qe2][Re0]

Risk step 4: Dealing with risks

(1) Additional research: modelling of Blow-out, safety study on the effect at the surface, literature research hydrogen infrastructure KEM 29 (research in progress)
(2) Preventive measures (5 main): highest quality of BOP and safety valves / pressure gauges (H_2 certified material), all equipment designed for low T, rapid response plan, H_2-certified material (steel), construction and maintenance protocols (see further measures in risks 1.1, 1.2 and 1.4)
(3) Corrective measures: actions according to rapid response plan, evacuation plan, fire extinguishing, damage control / repair, temporary partial shut-down and repair
(4) Description and classification residual risk considering the measures taken: taking the preventive and corrective measures into account the residual risk becomes: 1 (probability) and [Me1][Te3][Se1][Qe2][Re0] (consequences), **1/3**

[1] Fort Saskatchewan Ethane Blow-out and Fire (2001)

[2] Moss Bluff natural gas blow out and Fire (2004)

RISK Nr. 35.2 Creep closure and subsidence

Risk step 1: Aim

Aim 35 for Private landowner in the vicinity: "*Value retention of own property*". Therefore, the aim is: no risk for the own property (buildings, terrain) as a result of the hydrogen storage.

Risk step 2: Risk identification

(1) Risk: Subsidence (beyond predicted limits)
(2) Risk based on: Interpretation of facts
(3) Source of information: Literature review (sections 3.1.5.1 and 3.2.3) [3][4]
(4) Uncertainty: Additional research of the salt structure and rheology, cavern design
(5) Type of causes: [Rc][Ic][Gc][Oc][Tc][Pc]
(6) Type of effects: [Me][Te][Se][Qe]

Risk step 3: Risk classification

(1) Classification probability class: 2 (c): interpretation of factual information
(2) Classification consequence class: [Me1][Te3][Se1][Qe2][Re0]

Risk step 4: Dealing with risks

(1) Additional research: research of the salt structure and rheology, cavern design, geomechanical modelling
(2) Preventive measures: monitoring of subsidence by INSAR & surveying measurements, field tests (pressure observation test POT after well drill), updated cavern design, geomechanical modelling, determination of the minimum cavern pressure (see further measures in risk 1.7)
(3) Corrective measures: change of the average cavern pressure (higher), minimizing the subsidence by controlled abandonment
(4) Description and classification residual risk considering the measures taken: taking the preventive and corrective measures into account the residual risk becomes: 1 (probability) and [Me1][Te3][Se1][Qe2][Re0] (consequences), **1/3**

[3] Eminence salt dome 1, 3, 4, Mississippi, 1972 [4] Subsidence at Maceió, Brazil, 2021

RISK Nr. 35.3 Formation of H_2S beyond acceptable limits

Risk step 1: Aim

Aim 35 for Private landowner in the vicinity: "*Value retention of own property*". Therefore, the aim is: no risk for the own property (buildings, terrain) as a result of the hydrogen storage.

Risk step 2: Risk identification

(1) Risk: Formation of H_2S leading to contamination of the groundwater due to leakage
(2) Risk based on: Assumption
(3) Source of information: Literature review (section 5.4)[5] and research[6][7][8][9]
(4) Uncertainty: Additional research on the circumstances leading to the formation of H_2S
(5) Type of causes: [Tc][Gc]
(6) Type of effects: [Me][Te][Se][Qe]

Risk step 3: Risk classification

(1) Classification probability class: 3 (a): assumption based on expert judgement
(2) Classification consequence class: [Me0][Te2][Se1][Qe0][Re0]

Risk step 4: Dealing with risks

(1) Additional research: additional research on the circumstances leading to the formation of H_2S, characterize sulphur oxidation state in addition to sulphur abundance, research on the effect on the purity of produced H_2, research on the mix of H_2 and H_2S, research on optimal dimensions of the cavern (reduce reaction surface)
(2) Preventive measures: avoid sulphate sources, monitoring of microbial activities, avoid presence of hydrocarbons (no use of existing caverns), monitoring of geochemical composition, periodic restoration of sump conditions (see further measures in risk 1.16)
(3) Corrective measures: sweetening of the H_2 gas, pH correction, increase iron concentration
(4) Description and classification residual risk considering the measures taken: taking the preventive and corrective measures into account the residual risk becomes: 1 (probability) and [Me0][Te1][Se0][Qe0][Re0] (consequences), **1/1**

[5] M.P.Laban, Hydrogen storage in salt caverns, chemical modelling and analysis of large-scale hydrogen storage in underground salt caverns, no reference, dated July 16 2020
[6] N. Dopffel, Microbial impact on hydrogen storage, NORCE, 2nd International Summer School on UHS, dated July 2023
[7] C.A. Peters, Underground H_2 storage: Geochemistry Considerations, Princeton University, 2nd International Summer School on UHS, dated July 2023
[8] M. Portarapillo & A. di Benedetto, Risk assessment of the large-scale hydrogen storage in salt caverns, article in Energies 14, dated 2021
[9] M. Panfilov, Underground and pipeline hydrogen storage, Compendium of Hydrogen Energy, pp 92-116, dated 2015

RISK Nr. 35.4 Registered induced seismicity

Risk step 1: Aim

Aim 35 for Private landowner in the vicinity: "*Value retention of own property*". Therefore, the aim is: no risk for the own property (buildings, terrain) as a result of the hydrogen storage.

Risk step 2: Risk identification

(1) Risk: Registered induced seismicity caused by the operation (filling and emptying) of the cavern
(2) Risk based on: Interpretation of facts / assumption
(3) Source of information: Monitoring plans of underground Natural Gas and Nitrogen storage[10][11], literature review (section 5.2)
(4) Uncertainty: Research on characteristic locations in the salt dome sensitive to (micro)seismicity
(5) Type of causes: [Rc][Gc]
(6) Type of effects: [Te][Se]

Risk step 3: Risk classification

(1) Classification probability class: 3 (a/c): assumption based on expert judgement and interpretation of facts
(2) Classification consequence class: [Me0][Te2][Se1][Qe0][Re0]

Risk step 4: Dealing with risks

(1) Additional research: research on characteristic locations in the salt dome sensitive to (micro)seismicity
(2) Preventive measures: seismic monitoring (natural and induced seismicity), modelling of expected seismicity, no storage activities in or near an active fault zone, transparency and open communication, baseline measurement, transparency regarding seismic data
(3) Corrective measures: -
(4) Description and classification residual risk considering the measures taken: taking the preventive measures into account the residual risk becomes: 2 (probability) and [Me0][Te2][Se1][Qe0][Re0] (consequences), **2/2**

[10] Nouryon, Micro seismic network Heiligerlee & Zuidwending, observations Q3 2020, Powerpoint, no reference, no date

[11] NAM, Report "Instemmingsbesluit Norg", letter, no reference, dated December 3 2021

RISK Nr. 35.5 Emergence of negative public opinion

Risk step 1: Aim

Aim 35 for Private landowner in the vicinity: "*Value retention of own property*". Therefore, the aim is: no risk for the own property (buildings, terrain) as a result of the hydrogen storage.

Risk step 2: Risk identification

(1) Risk: Emergence of negative public opinion, e.g., triggered by regional or national media
(2) Risk based on: Interpretation of facts
(3) Source of information: public opinion[12][13][14][15][16]
(4) Uncertainty: complete stakeholder analysis per location, risk analysis discussion with all stakeholders (separately)
(5) Type of causes: [Pc]
(6) Type of effects: [Te][Se][Re]

Risk step 3: Risk classification

(1) Classification probability class: 3 (c): interpretation of factual information
(2) Classification consequence class: [Me0][Te3][Se1][Qe0][Re2]

Risk step 4: Dealing with risks

(1) Additional research: complete stakeholder analysis per location, risk analysis discussion with all stakeholders (separately)
(2) Preventive measures: transparent, pro-active and personal communication, direct involvement (shareholders), financial compensation ("burdens and benefits"), transparency with respect to all taken preventive measures (other risks)
(3) Corrective measures: transparent and personal communication, financial compensation (based on reversed burden of proof), transparency with respect to all taken corrective measures (other risks)
(4) Description and classification residual risk considering the measures taken: taking the preventive and corrective measures into account the residual risk eventually becomes: 2 (probability) and [Me0][Te2][Se1][Qe0][Re0] (consequences), **2/2**

[12] Public opinion with respect to CO_2 storage underneath Barendrecht: "Stichting CO2isNEE", 2010
[13] Public opinion with respect to environmental problems and subsidence as a result of salt mining: "Stop Zoutwinning!", 2021
[14] Public opinion with respect to future salt extraction Municipality of Haaksbergen, 2023
[15] Public opinion with respect to underground discharge of production water, www.stopafvalwatertwente.nl
[16] Public opinion with respect to Nitrogen storage in Heiligerlee, www.mijnendijnbelang.nl

RISK Nr. 35.6 Disputed responsibility due to stacked mining activities

Risk step 1: Aim

Aim 35 for Private landowner in the vicinity: "*Value retention of own property*". Therefore, the aim is: no risk for the own property (buildings, terrain) as a result of the hydrogen storage.

Risk step 2: Risk identification

(1) Risk: Disputed responsibility due to stacked mining activities
(2) Risk based on: Assumption
(3) Source of information: Political discussions[17], public[18]
(4) Uncertainty: Scenario modelling of various critical scenarios to test regulations
(5) Type of causes: [Rc]
(6) Type of effects: [Te][Se]

Risk step 3: Risk classification

(1) Classification probability class: 3 (a): assumption based on expert judgement
(2) Classification consequence class: [Me0][Te3][Se1][Qe0][Re0]

Risk step 4: Dealing with risks

(1) Additional research: scenario modelling of various critical scenarios to test regulations
(2) Preventive measures: regulations for operators regarding arial extent and duration of responsibility, seismic monitoring system, monitoring of subsidence by INSAR & surveying measurements before mining and during storage, mandatory report of incidents, regular meetings with all operators involved (including independent chairman, e.g., SodM), one overall geological model for all operators
(3) Corrective measures: mandatory insurance policy for all operators concerned, regulations for take-over of responsibilities in case of bankruptcy operator
(4) Description and classification residual risk considering the measures taken: taking the preventive and corrective measures into account the residual risk eventually becomes: 1 (probability) and [Me0][Te2][Se0][Qe0][Re0] (consequences), **1/2**

[17] Groenlinks, Stacked mining neglected in Nedmag-advice, 2019

[18] RTVOost, Growing frustration about mining, damage and new gas exploitation, January 2021

Stakeholder: Private landowner in the vicinity

Unmitigated risk matrix

4 x 3 Risk matrix		Consequence		
		1	2	3
Chance	3		35·3 35·4	35·5 35·6
	2			35·1 35·2
	1			
	0			

Residual (mitigated) risk matrix

4 x 3 Risk matrix		Consequence		
		1	2	3
Chance	3			
	2		34·4 34·5	
	1	34·3	34·6	34·1 34·2
	0			